

NASA SP-288

**CASE FILE
COPY**

VIBRATION OF SHELLS

LEISSA



NATIONAL AERONAUTICS AND SPACE ADMINISTRATION

VIBRATION OF SHELLS

Arthur W. Leissa

**Ohio State University
Columbus, Ohio**



Scientific and Technical Information Office

NATIONAL AERONAUTICS AND SPACE ADMINISTRATION

Washington, D.C.

1973

For sale by the Superintendent of Documents,
U.S. Government Printing Office, Washington, D.C. 20402
Price \$5.20 domestic postpaid or \$4.75 GPO Bookstore
Stock Number 3300-0422
Library of Congress Catalogue Card Number 77-186367

Preface

This monograph is the second in a series dedicated to the organization and summarization of knowledge existing in the field of continuum vibrations. The first monograph, entitled *Vibration of Plates*, was published in 1969, also by the National Aeronautics and Space Administration.

The objectives of the present work are the same as those of the previous one, namely, to provide

(1) A comprehensive presentation of available results for free vibration frequencies and mode shapes which can be used by the design or development engineer.

(2) A summary of known results for the researcher, facilitating comparison of future theoretical and experimental results, and delineating by implication those problems which need further study.

The scope of the present monograph is also the same as that of the previous one in that

(1) Materials are assumed to be linearly elastic.

(2) Structures were not included in this study, although some attention has been given to the accuracy of representing a stiffened shell as an orthotropic shell for purposes of vibration analysis.

The key to a comprehensive monograph such as this is organization. Careful organization not only makes the completed work more understandable and useful to the reader, but also facilitates the writing. Although much of the organization can be seen from the Contents, I will attempt to explain it further below.

Shells have all the characteristics of plates along with an additional one—curvature. Thus we have cylindrical (noncircular, as well as circular), conical, spherical, ellipsoidal, paraboloidal, toroidal, and hyperbolic paraboloidal shells as practical examples of various curvatures. The plate, on the other hand, is the special limiting case of a shell having no curvature. So called “curved plates” found in the literature are, in reality, shells. Thus, the primary classifier of the field of shell vibrations is chosen to be curvature. For a given curvature (say circular cylindrical, for example) the available literature is divided as to whether complicating effects such as anisotropy, initial stresses, variable thickness, large deflections, nonhomogeneity, shear deformation and rotary inertia, and the effects of surrounding media are present or not. The next subdivision of organization is boundary shape. Thus, a circular cylindrical shell can be open or closed, have boundaries which are parallel to the principal coordinates or not, and have cut-outs or not. Once the boundary shape is determined, attention is given to the possible types of fixity that can exist along each edge (i.e., the boundary conditions). Finally, attention is given to such special considerations as point supports or added point masses. Thus, for each type of curvature, the organization of the previous monograph *Vibration of Plates* is followed.

In addition to having the added complexity of curvature, shells are more complicated than plates because their bending cannot, in general, be separated from their stretching. Thus, a "classical" bending theory of shells is governed by an eighth order system of governing partial differential equations of motion, while a corresponding plate bending theory is only of the fourth order. This added complexity enters into the problem not only by means of more complex equations of motion, but through the boundary conditions as well. The classical bending theory of plates requires only two conditions to be specified along an edge, while a corresponding shell theory requires four specified conditions.

To demonstrate the significance of the latter point, consider a flat panel (i.e., a plate) which is simply supported along two of its opposite edges. The number of possible problems which can then arise, considering all combinations of "simple" boundary conditions which can exist on the remaining two edges, is 10. For a cylindrically curved panel (i.e., a shell) the corresponding number is 136!

To complicate matters further, whereas all academicians will agree on the form of the classical, fourth order equations of motion for a plate, such agreement does not exist in shell theory. Numerous different shell theories have been derived and are used. Thus, if analytical results for frequencies and mode shapes of a given shell configuration are presented, strictly speaking, the shell theory used in the calculations must be specified. For the sake of separating and defining clearly the various shell theories commonly found in the shell vibration literature, chapter 1 is devoted to their derivation, with special emphasis being given to the identification of points in the derivation where the different assumptions are made which give rise to the different theories.

Statements are found in the literature which imply the equivalence of all eighth order shell theories. The accuracy of such statements is examined carefully in chapter 2 on a problem for which exact solutions exist—the closed circular cylindrical shell supported at both ends by shear diaphragms. Extensive comparisons of results from the various shell theories are made with those from the exact, three dimensional elasticity theory.

In addition to the differences in theories, simplifications are often made in the resulting equations of motion or the characteristic (frequency) equations. These simplifications include, among others: neglecting certain (hopefully) small terms in the equations of motion, neglect of the tangential inertia terms, linearization of the characteristic equations, and assuming that the wave length in one direction is considerably longer than in the other. Comparisons of the effects of these simplifications are also made in chapter 2.

Comparing plate and shell vibrations, it is found that shell frequencies are more closely spaced and less easily identified, both analytically and experimentally. Furthermore, the fundamental (lowest frequency) mode for a shell is generally not all obvious, whereas for a plate it usually is.

There are more parameters required to define the shell vibration problem. For example, consider a rectangular plate simply supported on all its edges. The complete frequency spectrum is determined by varying one parameter—the length-to-width ratio. For the cylindrically curved panel having the same edge conditions, however, three *additional* parameters can be independently varied—the thickness-to-radius ratio, the length-to-radius ratio, and Poisson's ratio.

The present monograph contains approximately 1000 references. Of these, more than half deal with circular cylindrical shells. Therefore, two chapters were devoted to this voluminous topic. Chapter 2 deals with the results of classical

theory while complicating effects are studied in chapter 3. By contrast, very little work has been done with noncircular cylindrical shells, and these results are summarized in chapter 4. Chapter 5 is devoted to circular conical shells.

Because of the complexity of the field of shell vibrations as described above, and because of my own limitations in time and organizational capability, the following sacrifices had to be made in the present monograph:

(1) There are undoubtedly more relevant references which have been unknowingly omitted from this work than in the previous one. This is mainly due to the comparative recentness of the shell vibrations literature.

(2) Chapter 6 is only a bibliography for the vibrations of spherical and other shells.

(3) Numerous forms of nondimensional frequency parameters as given in the literature are used directly without conversion to a common parameter.

For these shortcomings I sincerely apologize to all my readers.

The support of the National Aeronautics and Space Administration is gratefully acknowledged, particularly that of Mr. Douglas Michel, who sees the value of devoting time and effort to making available research results *useful* to mankind, as well as to the creation of new knowledge. I wish to thank Messrs. S. G. Sampath, Adel Kadi, and Ting-hwa Wang, three of my doctoral students, for their devotion to this work. Without their help in supervising the procurement of the relevant literature, in providing analytical help (particularly in chapters 1 and 2), and in editing the manuscript, this monograph would not have been possible—indeed, I would not have undertaken it. I also wish to thank Drs. Robert Fulton, Francis Niedenfuhr, Herbert Reismann, and Carl Popelar for their technical advice. Finally, the enormous editorial assistance of Mr. Chester Ball, and Mrs. Ada Simon is gratefully acknowledged.

ARTHUR W. LEISSA
The Ohio State University

Page intentionally left blank

Contents

CHAPTER		PAGE
1	Fundamental Equations of Thin Shell Theory.....	1
1.1	Brief Outline of the Theory of Surfaces.....	2
1.2	Shell Coordinates and the Fundamental Shell Element.....	5
1.3	Love's First Approximation.....	6
1.4	Strain-Displacement Equation.....	7
1.5	Force and Moment Resultants.....	13
1.6	Equations of Motion.....	21
1.7	Synthesis of Equations.....	25
1.8	Boundary Conditions.....	26
1.9	Shallow Shell Theory.....	27
	References for Chapter 1.....	28
2	Thin Circular Cylindrical Shells.....	31
2.1	Equations of Motion.....	31
2.2	Shells of Infinite Length.....	37
2.3	Closed Shells—Shear Diaphragms at Both Ends.....	43
2.4	Other Simple Edge Conditions.....	83
2.5	Elastic Supports.....	146
2.6	Added Mass.....	149
2.7	Noncircular Boundaries and Cutouts.....	151
2.8	Open Circular Cylindrical Shells.....	157
	References for Chapter 2.....	175
3	Complicating Effects in Circular Cylindrical Shells.....	185
3.1	Anisotropy.....	185
3.2	Variable Thickness.....	218
3.3	Large (Nonlinear) Displacements.....	219
3.4	Initial Stress.....	231
3.5	Other Complicating Effects in Circular Cylindrical Shells...	289
	References for Chapter 3.....	308
4	Noncircular Cylindrical Shells.....	321
4.1	Equations of Motion.....	321
4.2	Elliptical Cylindrical.....	322
4.3	Oval Cylindrical.....	326
4.4	Open Shells.....	328
	References for Chapter 4.....	329

5	Conical Shells.....	331
5.1	Equations of Motion.....	332
5.2	Complete Cone.....	334
5.3	Frustum of a Cone.....	344
5.4	Open Conical Shells.....	387
5.5	Anisotropy.....	387
5.6	Large Displacements.....	389
5.7	Initial Stress.....	389
5.8	Other Effects.....	393
	References for Chapter 5.....	397
6	Spherical and Other Shells (Bibliographies).....	403
6.1	Spherical Shells.....	404
6.2	Ellipsoidal (or Spheroidal) Shells.....	410
6.3	Paraboloidal Shells.....	410
6.4	Toroidal Shells.....	411
6.5	Other Shells of Revolution.....	411
6.6	Others.....	412
	Appendix: Solution of the Three Dimensional Equations of Motion for Cylinders.....	413
A.1	Equations of Motion.....	413
A.2	End Conditions.....	414
A.3	Displacement Potential Functions.....	414
A.4	Solution of the Equations of Motion.....	414
A.5	Expressions for Stresses.....	416
A.6	Frequency Equation.....	417
	References for Appendix.....	418
	Author Index.....	419
	Subject Index.....	425

Fundamental Equations of Thin Shell Theory

A thin shell is a three-dimensional body which is bounded by two closely spaced curved surfaces, the distance between the surfaces being small in comparison with the other dimensions. The locus of points which lie midway between these surfaces is called the middle surface of the shell.

The distance between the surfaces measured along the normal to the middle surface is the thickness of the shell at that point. The thickness need not be constant in the formulation of a suitable theory of deformation, but constant thickness results in governing equations which are easier to solve; furthermore, certain manufacturing processes naturally yield shells of essentially constant thickness.

Shells may be regarded as generalizations of a flat plate; conversely, a flat plate is a special case of a shell having no curvature. The terminology "curved plate" is used occasionally in the literature—usually referring to a shell having small changes in slope of the undeformed middle surface. In this work the "shallow shell" will be used to describe this type of shell.

This chapter presents the fundamental equations of thin shell theory in their most simple, consistent form. Thus the material is assumed to be linearly elastic, isotropic, and homogeneous; displacements are assumed to be small, thereby yielding linear equations; shear deformation and rotary inertia effects are neglected; and the thickness is taken to be constant. Inasmuch as this work is aimed at the vibration of shells, it should also be said that the vibration results predicted analytically are assumed to be for a shell in a vacuum (although experimental results will generally be given in air) and that vibrations will occur with respect to zero values of static initial stress in the shell. These complicating features will be discussed (in those cases for which information is available) in subsequent

chapters dealing with special configurations of shells.

A large number of differing sets of equations have been arrived at by various academicians, all purporting to describe the motion of a given shell. This state of affairs is in contrast with the thin plate theory, wherein a single fourth order differential equation of motion is universally agreed upon.

Furthermore, there is considerable argument in the literature as to whether the differences between the various thin shell theories are significant or not (cf., refs. 1.1 through 1.8). In chapter 2 some attempt will be made to compare the results for free vibration frequencies and mode shapes arising from various thin shell theories in the case of circular cylindrical shells, especially for one particular set of boundary conditions.

The main purpose of this chapter is to present straightforward derivations of the sets of equations of various thin shell theories. It will be seen that differences in the theories result from slight differences in simplifying assumptions and/or the exact point in a derivation where a given assumption is used. Only those theories which are obtainable from Love's postulates (see sec. 1.3) by using a differential element of the middle surface, have been derived for shells of arbitrary curvature, and which have been applied in the literature to shell vibration problems will be considered in this chapter. Among the thin shell theories which will be derived in this chapter are those attributed to Donnell (refs. 1.9 and 1.10), Mushtari (refs. 1.11 and 1.12), Love (refs. 1.13 and 1.14), Timoshenko (ref. 1.15), Reissner (ref. 1.16), Naghdi and Berry (ref. 1.17), Vlasov (refs. 1.18 and 1.19), Sanders (ref. 1.20), Byrne (ref. 1.21), Flügge (refs. 1.22 and 1.23), Goldenveizer (ref. 1.24), Lur'ye (ref. 1.25),

and Novozhilov (ref. 1.26). However, not all of the theories listed above are independent. Many of the theories use certain sets of equations in common, and some are generalizations or duplications of another. Numerous other theories are available in the literature. Some are derived by expansion of the displacements and stresses in power series in the thickness coordinate z . Others are derived by asymptotic integration. The following authors have originated some of the general theories for arbitrary curvature not included in this chapter: Aron (ref. 1.27), Basset (ref. 1.28), Epstein (ref. 1.29), Trefftz (ref. 1.30), Synge and Chien (refs. 1.31 and 1.32), Lamb (ref. 1.33), Osgood and Joseph (ref. 1.34), Haywood and Wilson (ref. 1.35), Koiter (ref. 1.36), Cohen (refs. 1.37 and 1.38), and Knowles and Reissner (refs. 1.39 and 1.40). Writings which are particularly good from the standpoint of comparison of various thin shell theories include references 1.1, 1.4, 1.7, 1.17, and 1.41 through 1.47.

1.1 BRIEF OUTLINE OF THE THEORY OF SURFACES

The deformation of a thin shell will be completely determined by the displacements of its middle surface. Certain relationships relating to the behavior of a surface will be summarized in this section. More useful information can be found in the numerous texts dealing with differential geometry, the theory of surfaces, and shell theory (cf., refs. 1.19, 1.24–1.26, and 1.42).

1.1.1 Coordinate System

Let the equation of the undeformed middle surface be given in terms of two independent parameters α and β by the radius vector

$$\vec{r} = \vec{r}(\alpha, \beta) \quad (1.1)$$

Equation (1.1) determines the geometric properties of the surface and yields a method for finding points on the surface. Suppose that the parameter α is kept at a fixed value α_0 , while β changes. In this case equation (1.1) determines a space curve on the surface. Such curves are called β curves, and the set of all values α_0 within a given interval corresponds to a family of β curves. In an analogous manner one can introduce the concept of α curves (fig. 1.1).

Assume that the parameters α and β always vary within a definite region, and that a one-to-one correspondence exists between the points of this region and points on the portion of the surface of interest. Denote

$$\left. \begin{aligned} \vec{r}_{,\alpha} &= \frac{\partial \vec{r}}{\partial \alpha} \\ \vec{r}_{,\beta} &= \frac{\partial \vec{r}}{\partial \beta} \end{aligned} \right\} \quad (1.2)$$

The vectors $\vec{r}_{,\alpha}$ and $\vec{r}_{,\beta}$ are tangent to the α and β curves, respectively. The length of these vectors will be denoted by

$$\left. \begin{aligned} |\vec{r}_{,\alpha}| &= A \\ |\vec{r}_{,\beta}| &= B \end{aligned} \right\} \quad (1.3)$$

Consequently it follows that $\vec{r}_{,\alpha}/A$ and $\vec{r}_{,\beta}/B$ are unit vectors tangent to the coordinate curves. If the angle between the coordinate curves is denoted by χ then

$$\frac{\vec{r}_{,\alpha}}{A} \cdot \frac{\vec{r}_{,\beta}}{B} = \cos \chi \quad (1.4)$$

Denoting

$$\frac{\vec{r}_{,\alpha}}{A} = \hat{i}_\alpha \quad \frac{\vec{r}_{,\beta}}{B} = \hat{i}_\beta \quad \hat{i}_n = \frac{\hat{i}_\alpha \times \hat{i}_\beta}{\sin \chi} \quad (1.5)$$

where \hat{i}_n is the unit vector of the normal to the surface and is orthogonal to the vectors \hat{i}_α and \hat{i}_β .

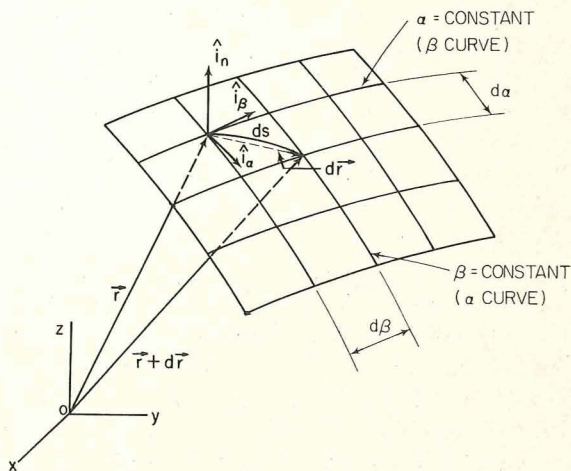


FIGURE 1.1.—Middle surface coordinates.

The unit vectors \hat{i}_α , \hat{i}_β and \hat{i}_n are usually called the basic vectors of the surface.

1.1.2 First Quadratic Form

Let there be given two points (α, β) and $(\alpha + d\alpha, \beta + d\beta)$ arbitrarily near to each other and both lying on the surface. The increment of the vector \vec{r} in moving from the first point to the second point is

$$d\vec{r} = \vec{r}_{,\alpha} d\alpha + \vec{r}_{,\beta} d\beta \quad (1.6)$$

From equations (1.3), (1.4), (1.5) and (1.6) the square of the differential of the arc length on the surface is

$$d\vec{r} \cdot d\vec{r} = ds^2 = A^2 d\alpha^2 + 2AB \cos \chi d\alpha d\beta + B^2 d\beta^2 \quad (1.7)$$

The right-hand side of equation (1.7) is the "first quadratic form of the surface." This form determines the infinitesimal lengths, the angle between the curves; and the area on the surface, i.e., the intrinsic geometry of the surface. However, the first quadratic form does not determine a surface by itself. The terms A^2 , $AB \cos \chi$, and B^2 are called the "first fundamental quantities."

1.1.3 Second Quadratic Form

The concept of the second quadratic form arises when one considers the problem of finding the curvature of a curve which lies on the surface. Let $\vec{r} = \vec{r}(s)$ be the vectorial equation of a curve on the surface (s is the arc length from a certain origin). Denoting the unit vector along the tangent to the curve by $\hat{\tau}$, then

$$\hat{\tau} = \frac{d\vec{r}}{ds} = \vec{r}_{,\alpha} \frac{d\alpha}{ds} + \vec{r}_{,\beta} \frac{d\beta}{ds} \quad (1.8)$$

According to Frenet's formula (ref. 1.48), the derivative of this vector is

$$\frac{d\hat{\tau}}{ds} = \frac{\hat{N}}{\rho} \quad (1.9)$$

where $1/\rho$ is the curvature of the curve, and \hat{N} is the unit vector of the principal normal to the curve.

Substituting for $\hat{\tau}$ from equation (1.8) into equation (1.9) one obtains

$$\begin{aligned} \frac{\hat{N}}{\rho} = & \vec{r}_{,\alpha\alpha} \left(\frac{d\alpha}{ds} \right)^2 + 2\vec{r}_{,\alpha\beta} \left(\frac{d\alpha}{ds} \right) \left(\frac{d\beta}{ds} \right) \\ & + \vec{r}_{,\beta\beta} \left(\frac{d\beta}{ds} \right)^2 + \vec{r}_{,\alpha} \frac{d^2\alpha}{ds^2} + \vec{r}_{,\beta} \frac{d^2\beta}{ds^2} \end{aligned} \quad (1.10)$$

where

$$\vec{r}_{,ij} = \frac{\partial^2 \vec{r}}{\partial i \partial j}, \quad \begin{cases} i = \alpha, \beta \\ j = \alpha, \beta \end{cases}$$

Let φ be the angle between the normal to the surface \hat{i}_n and the principal normal to the curve under consideration \hat{N} ; then

$$\cos \varphi = \hat{i}_n \cdot \hat{N} \quad (1.11)$$

If both sides of equation (1.10) are scalar-multiplied by \hat{i}_n , one obtains

$$\frac{\cos \varphi}{\rho} = \frac{L d\alpha^2 + 2M d\alpha d\beta + N d\beta^2}{ds^2} \quad (1.12)$$

where

$$\left. \begin{aligned} L &= \vec{r}_{,\alpha\alpha} \cdot \hat{i}_n \\ M &= \vec{r}_{,\alpha\beta} \cdot \hat{i}_n = \vec{r}_{,\beta\alpha} \cdot \hat{i}_n \\ N &= \vec{r}_{,\beta\beta} \cdot \hat{i}_n \end{aligned} \right\} \quad (1.13)$$

The expression $(L d\alpha^2 + 2M d\alpha d\beta + N d\beta^2)$ is called the "second quadratic form" of the surface and the quantities L , M , and N are the coefficients of the form. The second quadratic form is thus related to the curvatures of the curves on the surface.

From equation (1.12) one can obtain the normal curvatures of the surface; i.e., the curvatures of the curves obtained by intersecting the surface with normal planes. For the curve generated by a normal plane, \hat{i}_n and \hat{N} are either parallel ($\varphi = 0$) or have opposite directions ($\varphi = \pi$). Since a "plane" curve always leaves its tangent in the direction of vector \hat{N} and if one takes its outer normal as the positive normal to the surface, $\varphi = \pi$ results. Thus from equations (1.7) and (1.12) the normal curvature is

$$\frac{1}{R} = - \frac{L d\alpha^2 + 2M d\alpha d\beta + N d\beta^2}{A^2 d\alpha^2 + 2AB \cos \chi d\alpha d\beta + B^2 d\beta^2} \quad (1.14)$$

To obtain the curvatures of the α curves and the β curves take $\beta = \text{constant}$ and $\alpha = \text{constant}$ respectively, thus

$$\left. \begin{aligned} \frac{1}{R_\alpha} &= -\frac{L}{A^2} \\ \frac{1}{R_\beta} &= -\frac{N}{B^2} \end{aligned} \right\} \quad (1.15)$$

1.1.4 Gauss Derivative Formulas

At this point assume that the curves $\alpha = \text{constant}$ and $\beta = \text{constant}$ are lines of principal curvature of the undeformed middle surface. The coordinates α, β are then called principal coordinates. Weatherburn (ref. 1.49) shows that the necessary and sufficient conditions for the parametric curves to be lines of principal curvature on a surface are that

$$\cos \chi = 0 \quad (1.16a)$$

$$M = 0 \quad (1.16b)$$

The condition given by equation (1.16a) is that of orthogonality satisfied by all lines of principal curvature, while $M = 0$ is the necessary and sufficient condition that the parametric curves form a conjugate system (i.e., through each point on the surface passes a unique curve of each family of curves).

The second derivatives of \vec{r} with respect to the parameters may be expressed in terms of $\vec{r}_{,\alpha}, \vec{r}_{,\beta}$ and \hat{i}_n . Remembering that L, M , and N are the normal components of $\vec{r}_{,\alpha\alpha}, \vec{r}_{,\alpha\beta}$ and $\vec{r}_{,\beta\beta}$, one may write

$$\left. \begin{aligned} \vec{r}_{,\alpha\alpha} &= \Gamma_{11}^1 \vec{r}_{,\alpha} + \Gamma_{11}^2 \vec{r}_{,\beta} + L \hat{i}_n \\ \vec{r}_{,\alpha\beta} &= \Gamma_{12}^1 \vec{r}_{,\alpha} + \Gamma_{12}^2 \vec{r}_{,\beta} + M \hat{i}_n \\ \vec{r}_{,\beta\beta} &= \Gamma_{22}^1 \vec{r}_{,\alpha} + \Gamma_{22}^2 \vec{r}_{,\beta} + N \hat{i}_n \end{aligned} \right\} \quad (1.17)$$

where Γ_{jk}^i ($i, j, k = 1, 2$) are the Christoffel symbols which can be expressed in terms of the coefficients of the first principal quadratic form as follows (ref. 1.24):

$$\left. \begin{aligned} \Gamma_{11}^1 &= \frac{1}{A} \frac{\partial A}{\partial \alpha} \\ \Gamma_{11}^2 &= -\frac{A}{B^2} \frac{\partial A}{\partial \beta} \\ \Gamma_{12}^1 &= \frac{1}{A} \frac{\partial A}{\partial \beta} \end{aligned} \right\} \quad (1.18)$$

$$\left. \begin{aligned} \Gamma_{12}^2 &= \frac{1}{B} \frac{\partial B}{\partial \alpha} \\ \Gamma_{22}^1 &= -\frac{B}{A^2} \frac{\partial B}{\partial \alpha} \\ \Gamma_{22}^2 &= \frac{1}{B^2} \frac{\partial B}{\partial \beta} \end{aligned} \right\} \quad (1.18)$$

1.1.5 Derivatives of the Basic Vectors

Making use of equations (1.17) and (1.18) and the fact that $\hat{i}_n \cdot \hat{i}_n = 1$ one obtains the following expressions for the derivatives of the basic vectors (ref. 1.42)

$$\left. \begin{aligned} \hat{i}_{n,\alpha} &= \frac{A}{R_\alpha} \hat{i}_\alpha \\ \hat{i}_{n,\beta} &= \frac{B}{R_\beta} \hat{i}_\beta \\ \hat{i}_{\alpha,\alpha} &= -\frac{1}{B} \frac{\partial A}{\partial \beta} \hat{i}_\beta - \frac{A}{R_\alpha} \hat{i}_n \\ \hat{i}_{\alpha,\beta} &= \frac{1}{A} \frac{\partial B}{\partial \alpha} \hat{i}_\beta \\ \hat{i}_{\beta,\alpha} &= \frac{1}{B} \frac{\partial A}{\partial \beta} \hat{i}_\alpha \\ \hat{i}_{\beta,\beta} &= -\frac{1}{A} \frac{\partial B}{\partial \alpha} \hat{i}_\alpha - \frac{B}{R_\beta} \hat{i}_n \end{aligned} \right\} \quad (1.19)$$

1.1.6 Gauss Characteristic Equation

The four fundamental quantities for principal coordinates A, B, L , and N are not functionally independent, but are connected by three differential relations. One of these, due to Gauss, is an expression for (LN) in terms of A and B and their derivatives, and may be deduced from either of the following equations:

$$(\hat{i}_{\alpha,\alpha})_{,\beta} = (\hat{i}_{\alpha,\beta})_{,\alpha} \quad (1.20a)$$

$$(\hat{i}_{\beta,\alpha})_{,\beta} = (\hat{i}_{\beta,\beta})_{,\alpha} \quad (1.20b)$$

Substituting for the derivatives of basic vectors from equations (1.19) into equations (1.20) one obtains for principal coordinates

$$\frac{\partial}{\partial \alpha} \left(\frac{1}{A} \frac{\partial B}{\partial \alpha} \right) + \frac{\partial}{\partial \beta} \left(\frac{1}{B} \frac{\partial A}{\partial \beta} \right) = -\frac{AB}{K} = -\frac{LN}{AB} \quad (1.21)$$

where $1/K = 1/R_\alpha R_\beta$ and is called the Gaussian curvature. Since the Gaussian curvature is expressible in terms of the coefficients of the first fundamental form and their derivatives, one can conclude that surfaces which have the same first fundamental quantities have the same Gaussian curvature.

1.1.7 Mainardi-Codazzi Relations

In addition to the Gauss characteristic equation, there are two other independent relations. These may be established from the following equation:

$$(\hat{i}_n, \alpha)_{,\beta} = (\hat{i}_n, \beta)_{,\alpha} \quad (1.22)$$

Substituting for derivatives of the basic vectors from equations (1.19) into equations (1.22)

$$\left[\frac{\partial}{\partial \beta} \left(\frac{A}{R_\alpha} \right) - \frac{1}{R_\beta} \frac{\partial A}{\partial \beta} \right] \hat{i}_\alpha + \left[\frac{1}{R_\alpha} \frac{\partial B}{\partial \alpha} - \frac{\partial}{\partial \alpha} \left(\frac{B}{R_\beta} \right) \right] \hat{i}_\beta = 0 \quad (1.23)$$

Equation (1.23) is satisfied if

$$\left\{ \begin{aligned} \frac{\partial}{\partial \beta} \left(\frac{A}{R_\alpha} \right) &= \frac{1}{R_\beta} \frac{\partial A}{\partial \beta} \\ \frac{\partial}{\partial \alpha} \left(\frac{B}{R_\beta} \right) &= \frac{1}{R_\alpha} \frac{\partial B}{\partial \alpha} \end{aligned} \right\} \quad (1.24)$$

The formulas given by equations (1.24) are the Mainardi-Codazzi relations. It is worthwhile noting that Bonnet (ref. 1.49) has proved the theorem: When A , B , R_α , and R_β are given, satisfying the Gauss characteristic equation and the Mainardi-Codazzi relations, they determine a surface uniquely, except to position and orientation in space.

1.2 SHELL COORDINATES AND THE FUNDAMENTAL SHELL ELEMENT

To describe the location of an arbitrary point in the space occupied by a thin shell, the position vector is defined as

$$\vec{R}(\alpha, \beta, z) = \vec{r}(\alpha, \beta) + z \hat{i}_n \quad (1.25)$$

where z measures the distance of the point from the corresponding point on the middle surface along \hat{i}_n and varies over the thickness

$$(-h/2 \leq z \leq h/2)$$

The magnitude of an arbitrary infinitesimal change in the vector $\vec{R}(\alpha, \beta, z)$ is determined by

$$(ds)^2 = d\vec{R} \cdot d\vec{R} = (d\vec{r} + z d\hat{i}_n + \hat{i}_n dz) \cdot (d\vec{r} + z d\hat{i}_n + \hat{i}_n dz) \quad (1.26a)$$

Remembering the orthogonality of the coordinate system, then from equations (1.5), (1.6), and (1.19) and the chain rule

$$d\hat{i}_n = \frac{\partial \hat{i}_n}{\partial \alpha} d\alpha + \frac{\partial \hat{i}_n}{\partial \beta} d\beta \quad (1.26b)$$

one obtains

$$(ds)^2 = g_1 d\alpha^2 + g_2 d\beta^2 + g_3 dz^2 \quad (1.27)$$

where

$$\left. \begin{aligned} g_1 &= \left[A \left(1 + \frac{z}{R_\alpha} \right) \right]^2 \\ g_2 &= \left[B \left(1 + \frac{z}{R_\beta} \right) \right]^2 \\ g_3 &= 1 \end{aligned} \right\} \quad (1.28)$$

The quantities g_1 , g_2 , g_3 , A , B , R_α , and R_β are connected by the equations of Lamb (cf., ref. 1.18), since the three-dimensional space (the space in which the three independent variables α , β , z vary) is a Euclidean space.

$$\begin{aligned} & \frac{\partial}{\partial \alpha} \left\{ \frac{1}{A(1+z/R_\alpha)} \frac{\partial}{\partial \alpha} \left[B \left(1 + \frac{z}{R_\beta} \right) \right] \right\} \\ & + \frac{\partial}{\partial \beta} \left\{ \frac{1}{B(1+z/R_\beta)} \frac{\partial}{\partial \beta} \left[A \left(1 + \frac{z}{R_\alpha} \right) \right] \right\} = \frac{AB}{R_\alpha R_\beta} \end{aligned} \quad (1.29a)$$

$$\begin{aligned} & \frac{1}{A(1+z/R_\alpha)} \frac{\partial}{\partial \alpha} \left[B \left(1 + \frac{z}{R_\beta} \right) \right] \frac{\partial}{\partial z} \left[A \left(1 + \frac{z}{R_\alpha} \right) \right] \\ & = \frac{\partial^2}{\partial \alpha \partial z} \left[B \left(1 + \frac{z}{R_\beta} \right) \right] \end{aligned} \quad (1.29b)$$

$$\begin{aligned} & \frac{1}{B(1+z/R_\beta)} \frac{\partial}{\partial \beta} \left[A \left(1 + \frac{z}{R_\alpha} \right) \right] \frac{\partial}{\partial z} \left[B \left(1 + \frac{z}{R_\beta} \right) \right] \\ & = \frac{\partial^2}{\partial \beta \partial z} \left[A \left(1 + \frac{z}{R_\alpha} \right) \right] \end{aligned} \quad (1.29c)$$

which are the Gauss equation (1.21) and the Mainardi-Codazzi equations (1.24) generalized for a surface at a distance z from the middle surface. Using equations (1.24) equations (1.29b) and (1.29c) can be transformed to

$$\left. \begin{aligned} \frac{\partial}{\partial \alpha} \left[B \left(1 + \frac{z}{R_\beta} \right) \right] &= \left(1 + \frac{z}{R_\alpha} \right) \frac{\partial B}{\partial \alpha} \\ \frac{\partial}{\partial \beta} \left[A \left(1 + \frac{z}{R_\alpha} \right) \right] &= \left(1 + \frac{z}{R_\beta} \right) \frac{\partial A}{\partial \beta} \end{aligned} \right\} \quad (1.30)$$

Having established the coordinate system of the shell space, the fundamental three-dimensional element of a thin shell will be defined next. The fundamental shell element is the differential element bounded by two surfaces dz apart at a distance z from the middle surface and four ruled surfaces whose generators are the normals to the middle surface along the parametric curves $\alpha = \alpha_0$, $\alpha = \alpha_0 + d\alpha$, $\beta = \beta_0$ and $\beta = \beta_0 + d\beta$. The assumption that the parametric curves are lines of principal curvature ensures that the ruled surfaces will be plane surfaces and, furthermore, that these planes intersect each other at right angles. The lengths of the edges of this fundamental element are according to equation (1.27) (see fig. 1.2)

$$\left. \begin{aligned} ds_\alpha^{(z)} &= A(1+z/R_\alpha) d\alpha \\ ds_\beta^{(z)} &= B(1+z/R_\beta) d\beta \end{aligned} \right\} \quad (1.31)$$

the differential areas of the edge faces of the fundamental element are

$$\left. \begin{aligned} dA_\alpha^{(z)} &= A(1+z/R_\alpha) d\alpha dz \\ dA_\beta^{(z)} &= B(1+z/R_\beta) d\beta dz \end{aligned} \right\} \quad (1.32)$$

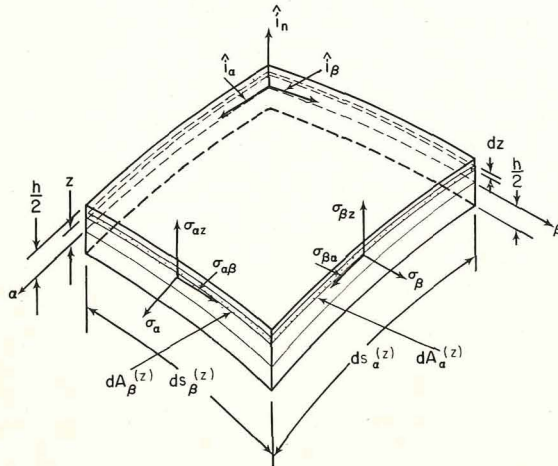


FIGURE 1.2.—Notation and positive directions of stress in shell coordinates.

while the volume of the fundamental element is

$$dV^{(z)} = [A(1+z/R_\alpha)][B(1+z/R_\beta)] d\alpha d\beta dz \quad (1.33)$$

1.3 LOVE'S FIRST APPROXIMATION

In the classical theory of small displacements of thin shells the following assumptions were made by Love (ref. 1.13)

(1) The thickness of the shell is small compared with the other dimensions, for example, the smallest radius of curvature of the middle surface of the shell.

(2) Strains and displacements are sufficiently small so that the quantities of second- and higher-order magnitude in the strain-displacement relations may be neglected in comparison with the first-order terms (ref. 1.43).

(3) The transverse normal stress is small compared with the other normal stress components and may be neglected.

(4) Normals to the undeformed middle surface remain straight and normal to the deformed middle surface and suffer no extension.

These four assumptions taken together give rise to what Love called his "first approximation" shell theory. These approximations are almost universally accepted by others in the derivation of thin shell theories.

The first assumption defines what is meant by "thin shells" and sets the stage for the entire theory. Denoting the thickness of the shell by h and the smallest radius of curvature by R , then it will be convenient at various places in the subsequent derivation of shell theories to neglect higher powers of z/R or h/R in comparison with unity. The second assumption permits one to refer all calculations to the original configuration of the shell and ensures that the differential equations will be linear. The fourth assumption is known as Kirchhoff's hypothesis and categorizes the shell theories that will be discussed in this chapter. As a consequence of this geometric assumption

$$\left. \begin{aligned} \gamma_{\alpha z} &= 0 \\ \gamma_{\beta z} &= 0 \\ e_z &= 0 \end{aligned} \right\} \quad (1.34)$$

and therefore the transverse shear stresses

$$\sigma_{\alpha z} = \sigma_{\beta z} = 0$$

from Hooke's law. In the following section, non-vanishing shear resultants Q_α and Q_β will be defined as integrals of the transverse shearing stresses, and the transverse shearing stresses can be expressed in terms of the shear resultants and the surface loads (cf., ref. 1.42). However, the vanishing of transverse shearing strains is inconsistent with the presence of transverse shearing stresses. Thus, transverse shearing strains must exist. Adding to that geometric assumption the static assumption that σ_z is negligible, another inconsistency is introduced; i.e., the vanishing of e_z and σ_z simultaneously.

The third and fourth assumptions deal with the constitutive equations of thin elastic shells and assume the shell to behave like a material having a special type of orthotropy wherein $E_z = G_{\alpha z} = G_{\beta z} = \infty$, and $\nu_{\alpha z} = \nu_{\beta z} = 0$ (ref. 1.41).

1.4 STRAIN-DISPLACEMENT EQUATION

The well-known strain-displacement equations of the three-dimensional theory of elasticity in orthogonal curvilinear coordinates are (cf., ref. 1.50, pp. 179–180)

$$\left. \begin{aligned} e_i &= \frac{\partial}{\partial \alpha_i} \left(\frac{U_i}{\sqrt{g_i}} \right) + \frac{1}{2g_i} \sum_{k=1}^3 \frac{\partial g_i}{\partial \alpha_k} \frac{U_k}{\sqrt{g_k}}, & i=1,2,3 \\ \gamma_{ij} &= \frac{1}{\sqrt{g_i g_j}} \left[g_i \frac{\partial}{\partial \alpha_j} \left(\frac{U_i}{\sqrt{g_i}} \right) + g_j \frac{\partial}{\partial \alpha_i} \left(\frac{U_j}{\sqrt{g_j}} \right) \right], & i,j=1,2,3 \\ & & i \neq j \end{aligned} \right\} \quad (1.35)$$

where the e_i , γ_{ij} , and U_i are normal strains, shear strains, and displacement components, respectively, at an arbitrary point. In the shell coordinates the indices 1, 2, and 3 are replaced by α , β , and z , respectively, except for the displacements U_1 , U_2 , and U_3 , which are replaced by U , V , and W , respectively, and the coefficients of the metric tensor are given by equations (1.28), thus yielding

$$e_\alpha = \frac{1}{(1+z/R_\alpha)} \left(\frac{1}{A} \frac{\partial U}{\partial \alpha} + \frac{V}{AB} \frac{\partial A}{\partial \beta} + \frac{W}{R_\alpha} \right) \quad (1.36a)$$

$$e_\beta = \frac{1}{(1+z/R_\beta)} \left(\frac{U}{AB} \frac{\partial B}{\partial \alpha} + \frac{1}{B} \frac{\partial V}{\partial \beta} + \frac{W}{R_\beta} \right) \quad (1.36b)$$

$$e_z = \frac{\partial W}{\partial z} \quad (1.36c)$$

$$\gamma_{\alpha\beta} = \frac{A(1+z/R_\alpha)}{B(1+z/R_\beta)} \frac{\partial}{\partial \beta} \left[\frac{U}{A(1+z/R_\alpha)} \right] + \frac{B(1+z/R_\beta)}{A(1+z/R_\alpha)} \frac{\partial}{\partial \alpha} \left[\frac{V}{B(1+z/R_\beta)} \right] \quad (1.36d)$$

$$\gamma_{\alpha z} = \frac{1}{A(1+z/R_\alpha)} \frac{\partial W}{\partial \alpha} + A(1+z/R_\alpha) \frac{\partial}{\partial z} \left[\frac{U}{A(1+z/R_\alpha)} \right] \quad (1.36e)$$

$$\gamma_{\beta z} = \frac{1}{B(1+z/R_\beta)} \frac{\partial W}{\partial \beta} + B(1+z/R_\beta) \frac{\partial}{\partial z} \left[\frac{V}{B(1+z/R_\beta)} \right] \quad (1.36f)$$

Now in order to satisfy the Kirchhoff hypothesis, the class of displacements is restricted to the following linear relationships:

$$U(\alpha, \beta, z) = u(\alpha, \beta) + z\theta_\alpha(\alpha, \beta) \quad (1.37a)$$

$$V(\alpha, \beta, z) = v(\alpha, \beta) + z\theta_\beta(\alpha, \beta) \quad (1.37b)$$

$$W(\alpha, \beta, z) = w(\alpha, \beta) \quad (1.37c)$$

where u , v , and w are the components of displacement at the middle surface in the α , β , and normal directions, respectively, and θ_α and θ_β are the rotations of the normal to the middle surface during deformation about the β and α axes, respectively; i.e.,

$$\left. \begin{aligned} \theta_\alpha &= \frac{\partial U(\alpha, \beta, z)}{\partial z} \\ \theta_\beta &= \frac{\partial V(\alpha, \beta, z)}{\partial z} \end{aligned} \right\} \quad (1.38)$$

The third of equations (1.34) is satisfied by using equation (1.37c) with equation (1.36c); i.e., W is independent of z and is completely defined by the middle surface component w . Substituting equations (1.37) into equations (1.36e) and (1.36f), the first two of equations (1.34) are satisfied provided that

$$\theta_\alpha = \frac{u}{R_\alpha} - \frac{1}{A} \frac{\partial w}{\partial \alpha} \quad \theta_\beta = \frac{v}{R_\beta} - \frac{1}{B} \frac{\partial w}{\partial \beta} \quad (1.39)$$

1.4.1 Equations of Byrne, Flügge, Goldenveizer, Lur'ye and Novozhilov

Substituting equations (1.37) into equations (1.36a, b, and d) yields

$$e_\alpha = \frac{1}{(1+z/R_\alpha)}(\epsilon_\alpha + z\kappa_\alpha) \quad (1.40a)$$

$$e_\beta = \frac{1}{(1+z/R_\beta)}(\epsilon_\beta + z\kappa_\beta) \quad (1.40b)$$

$$\gamma_{\alpha\beta} = \frac{1}{(1+z/R_\alpha)(1+z/R_\beta)} \left[\left(1 - \frac{z^2}{R_\alpha R_\beta}\right) \epsilon_{\alpha\beta} + z \left(1 + \frac{z}{2R_\alpha} + \frac{z}{2R_\beta}\right) \tau \right] \quad (1.40c)$$

where ϵ_α , ϵ_β , and $\epsilon_{\alpha\beta}$ are the normal and shear strains in the middle surface ($z=0$) given by

$$\left. \begin{aligned} \epsilon_\alpha &= \frac{1}{A} \frac{\partial u}{\partial \alpha} + \frac{v}{AB} \frac{\partial A}{\partial \beta} + \frac{v}{R_\alpha} \\ \epsilon_\beta &= \frac{u}{AB} \frac{\partial B}{\partial \alpha} + \frac{1}{B} \frac{\partial v}{\partial \beta} + \frac{v}{R_\beta} \\ \epsilon_{\alpha\beta} &= \frac{A}{B} \frac{\partial}{\partial \beta} \left(\frac{u}{A} \right) + \frac{B}{A} \frac{\partial}{\partial \alpha} \left(\frac{v}{B} \right) \end{aligned} \right\} \quad (1.41)$$

and κ_α and κ_β are the midsurface changes in curvature and τ the midsurface twist, given by

$$\kappa_\alpha = \frac{1}{A} \frac{\partial \theta_\alpha}{\partial \alpha} + \frac{\theta_\beta}{AB} \frac{\partial A}{\partial \beta} \quad (1.42a)$$

$$\kappa_\beta = \frac{\theta_\alpha}{AB} \frac{\partial B}{\partial \alpha} + \frac{1}{B} \frac{\partial \theta_\beta}{\partial \beta} \quad (1.42b)$$

$$\tau = \frac{A}{B} \frac{\partial}{\partial \beta} \left(\frac{\theta_\alpha}{A} \right) + \frac{B}{A} \frac{\partial}{\partial \alpha} \left(\frac{\theta_\beta}{B} \right) + \frac{1}{R_\alpha} \left(\frac{1}{B} \frac{\partial u}{\partial \beta} - \frac{v}{AB} \frac{\partial B}{\partial \alpha} \right) + \frac{1}{R_\beta} \left(\frac{1}{A} \frac{\partial v}{\partial \alpha} - \frac{u}{AB} \frac{\partial A}{\partial \beta} \right) \quad (1.42c)$$

These are the strain-displacement equations used by Byrne, Flügge, Goldenveizer, Lur'ye, and Novozhilov.

1.4.2 Equations of Love and Timoshenko

If in equations (1.40) one neglects the terms z/R_α and z/R_β and their products as being small in comparison with unity one obtains

$$e_\alpha = \epsilon_\alpha + z\kappa_\alpha \quad e_\beta = \epsilon_\beta + z\kappa_\beta \quad \gamma_{\alpha\beta} = \epsilon_{\alpha\beta} + z\tau \quad (1.43)$$

with $\epsilon_\alpha, \dots, \tau$ still given by equations (1.41) and (1.42). These are the strain-displacement equations which represent the theories of Love and Timoshenko.

1.4.3 Equations of Reissner, Naghdi, and Berry

If one chooses to make the simplification of Love and Timoshenko (i.e., z/R_α and $z/R_\beta \ll 1$) earlier in the derivation, then doing so in equations (1.36a, b, and d) reduces them to

$$\left. \begin{aligned} e_\alpha &= \frac{1}{A} \frac{\partial U}{\partial \alpha} + \frac{V}{AB} \frac{\partial A}{\partial \beta} + \frac{W}{R_\alpha} \\ e_\beta &= \frac{U}{AB} \frac{\partial B}{\partial \alpha} + \frac{1}{B} \frac{\partial V}{\partial \beta} + \frac{W}{R_\beta} \\ \gamma_{\alpha\beta} &= \frac{A}{B} \frac{\partial}{\partial \beta} \left(\frac{U}{A} \right) + \frac{B}{A} \frac{\partial}{\partial \alpha} \left(\frac{V}{B} \right) \end{aligned} \right\} \quad (1.44)$$

Then substituting equations (1.37) into equations (1.44) the total strains can again be represented as the sum of the stretching and bending strains as in equations (1.43) with equations (1.41) and (1.42) still applying, except that equation (1.42c) changes to become

$$\tau = \frac{A}{B} \frac{\partial}{\partial \beta} \left(\frac{\theta_\alpha}{A} \right) + \frac{B}{A} \frac{\partial}{\partial \alpha} \left(\frac{\theta_\beta}{B} \right) \quad (1.45)$$

1.4.4 Equations of Vlasov

Recognizing that for a shell z/R_i ($i=\alpha, \beta$) is less than unity, then one can expand the quotient $1/(1+z/R_i)$ into a well-known geometric series by simple division; i.e.,

$$\frac{1}{1+z/R_i} = \sum_{n=0}^{\infty} \left(-\frac{z}{R_i} \right)^n, \quad i=\alpha, \beta \quad (1.46)$$

Substituting equations (1.37) and (1.46) into equations (1.36a, b, and d) gives

$$\left. \begin{aligned} e_\alpha &= (\epsilon_\alpha + z\kappa_\alpha) \sum_{n=0}^{\infty} \left(-\frac{z}{R_\alpha} \right)^n \\ e_\beta &= (\epsilon_\beta + z\kappa_\beta) \sum_{n=0}^{\infty} \left(-\frac{z}{R_\beta} \right)^n \end{aligned} \right\} \quad (1.47)$$

$$\left. \begin{aligned} \gamma_{\alpha\beta} = & \frac{A}{B} \left(1 + \frac{z}{R_\alpha} \right) \sum_{n=0}^{\infty} \left\{ \left(-\frac{z}{R_\beta} \right)^n \frac{\partial}{\partial \beta} \right. \\ & \left. \left[\frac{(u+z\theta_\alpha)}{A} \sum_{n=0}^{\infty} \left(-\frac{z}{R_\alpha} \right)^n \right] \right\} \\ & + \frac{B}{A} \left(1 + \frac{z}{R_\beta} \right) \sum_{n=0}^{\infty} \left\{ \left(-\frac{z}{R_\alpha} \right)^n \frac{\partial}{\partial \alpha} \right. \\ & \left. \left[\frac{(v+z\theta_\beta)}{B} \sum_{n=0}^{\infty} \left(-\frac{z}{R_\beta} \right)^n \right] \right\} \end{aligned} \right\} \quad (1.47)$$

with ϵ_α , ϵ_β , κ_α , and κ_β given by equations (1.41) and (1.42). Equations (1.47) can be rearranged as

$$\left. \begin{aligned} \epsilon_\alpha &= \epsilon_\alpha + \sum_{n=1}^{\infty} \kappa_{\alpha n} z^n \\ \epsilon_\beta &= \epsilon_\beta + \sum_{n=1}^{\infty} \kappa_{\beta n} z^n \\ \gamma_{\alpha\beta} &= \epsilon_{\alpha\beta} + \sum_{n=1}^{\infty} \tau_n z^n \end{aligned} \right\} \quad (1.48)$$

where

$$\left. \begin{aligned} \kappa_{\alpha n} &= \left(-\frac{1}{R_\alpha} \right)^{n-1} \left(\kappa_\alpha - \frac{\epsilon_\alpha}{R_\alpha} \right) \\ \kappa_{\beta n} &= \left(-\frac{1}{R_\beta} \right)^{n-1} \left(\kappa_\beta - \frac{\epsilon_\beta}{R_\beta} \right) \\ \tau_n &= (-1)^n \left\{ \left(\frac{1}{R_\alpha} - \frac{1}{R_\beta} \right) \right. \\ & \quad \left[\left(\frac{1}{R_\beta} \right)^{n-1} \frac{A}{B} \frac{\partial}{\partial \beta} \left(\frac{u}{A} \right) \right. \\ & \quad \left. \left. - \left(\frac{1}{R_\alpha} \right)^{n-1} \frac{B}{A} \frac{\partial}{\partial \alpha} \left(\frac{v}{B} \right) \right] \right. \\ & \quad \left. - \frac{1}{AB} \left[\left(\frac{1}{R_\alpha} \right)^{n-1} + \left(\frac{1}{R_\beta} \right)^{n-1} \right] \right. \\ & \quad \left. \left(\frac{\partial^2 w}{\partial \alpha \partial \beta} - \frac{1}{B} \frac{\partial B}{\partial \alpha} \frac{\partial w}{\partial \beta} - \frac{1}{A} \frac{\partial A}{\partial \beta} \frac{\partial w}{\partial \alpha} \right) \right\} \end{aligned} \right\} \quad (1.49)$$

and where $\epsilon_{\alpha\beta}$ is that of equations (1.41). If now the series contained in equations (1.48) are truncated after $n=1$ to provide linear relationships in z , then equations (1.49) simplify to

$$\left. \begin{aligned} \kappa_{\alpha 1} &= \kappa_\alpha - \frac{\epsilon_\alpha}{R_\alpha} \\ \kappa_{\beta 1} &= \kappa_\beta - \frac{\epsilon_\beta}{R_\beta} \\ \tau_1 &= \left(\frac{1}{R_\alpha} - \frac{1}{R_\beta} \right) \left[\frac{A}{B} \frac{\partial}{\partial \beta} \left(\frac{u}{A} \right) - \frac{B}{A} \frac{\partial}{\partial \alpha} \left(\frac{v}{B} \right) \right] \\ & \quad - \frac{2}{AB} \left(\frac{\partial^2 w}{\partial \alpha \partial \beta} - \frac{1}{B} \frac{\partial B}{\partial \alpha} \frac{\partial w}{\partial \beta} - \frac{1}{A} \frac{\partial A}{\partial \beta} \frac{\partial w}{\partial \alpha} \right) \end{aligned} \right\} \quad (1.50)$$

which are the middle surface curvature relationships of Vlasov's theory.

1.4.5 Equations of Sanders

Sanders (ref. 1.20) developed an eighth order shell theory from the principle of virtual work. The principle is written as

$$\begin{aligned} \int_{\alpha} \int_{\beta} \left[\left(\frac{\partial B N_\alpha}{\partial \alpha} + \frac{\partial A N_{\beta\alpha}}{\partial \beta} + N_{\alpha\beta} \frac{\partial A}{\partial \beta} \right. \right. \\ \left. \left. - N_\beta \frac{\partial B}{\partial \alpha} + Q_\alpha \frac{AB}{R_\alpha} \right) \delta u \right. \\ \left. + \left(\frac{\partial A N_\beta}{\partial \beta} + \frac{\partial B N_{\alpha\beta}}{\partial \alpha} + N_{\beta\alpha} \frac{\partial B}{\partial \alpha} \right. \right. \\ \left. \left. - N_\alpha \frac{\partial A}{\partial \beta} + Q_\beta \frac{AB}{R_\beta} \right) \delta v \right. \\ \left. + \left(-N_\alpha \frac{AB}{R_\alpha} - N_\beta \frac{AB}{R_\beta} \right. \right. \\ \left. \left. + \frac{\partial B Q_\alpha}{\partial \alpha} + \frac{\partial A Q_\beta}{\partial \beta} \right) \delta w \right. \\ \left. + \left(\frac{\partial B M_\alpha}{\partial \alpha} + \frac{\partial A M_{\beta\alpha}}{\partial \beta} + M_{\alpha\beta} \frac{\partial A}{\partial \beta} \right. \right. \\ \left. \left. - M_\beta \frac{\partial B}{\partial \alpha} - AB Q_\alpha \right) \delta \theta_\alpha \right. \\ \left. + \left(\frac{\partial A M_\beta}{\partial \beta} + \frac{\partial B M_{\alpha\beta}}{\partial \alpha} + M_{\beta\alpha} \frac{\partial B}{\partial \alpha} \right. \right. \\ \left. \left. - M_\alpha \frac{\partial A}{\partial \beta} - AB Q_\beta \right) \delta \theta_\beta \right. \\ \left. + AB \left(N_{\alpha\beta} - N_{\beta\alpha} + \frac{M_{\alpha\beta}}{R_\alpha} \right. \right. \\ \left. \left. - \frac{M_{\beta\alpha}}{R_\beta} \right) \delta \theta_n \right] d\alpha d\beta = 0 \quad (1.51) \end{aligned}$$

where the "generalized displacements" include the displacement components u , v , and w and the rotations θ_α , θ_β , and θ_n about the β , α , and n directions, respectively, and δu , for example, is the variation of u . The six quantities in parenthe-

ses represent the "generalized forces" associated with the generalized displacements as obtained from a "generally accepted" set of equations of equilibrium (cf., eqs. (1.112) and (1.115)) neglecting body forces and moments and surface loads. Integrating equation (1.51) by parts yields

$$\begin{aligned} \int_{\alpha} \int_{\beta} \left[N_{\alpha} \delta \left(B \frac{\partial u}{\partial \alpha} + v \frac{\partial A}{\partial \beta} + \frac{AB}{R_{\alpha}} w \right) \right. \\ + N_{\alpha\beta} \delta \left(-u \frac{\partial A}{\partial \beta} + B \frac{\partial v}{\partial \alpha} - AB \theta_n \right) \\ + N_{\beta\alpha} \delta \left(A \frac{\partial u}{\partial \beta} - v \frac{\partial B}{\partial \alpha} + AB \theta_n \right) \\ + N_{\beta} \delta \left(u \frac{\partial B}{\partial \alpha} + A \frac{\partial v}{\partial \beta} + \frac{AB}{R_{\beta}} w \right) \\ + Q_{\alpha} \delta \left(B \frac{\partial w}{\partial \alpha} - u \frac{AB}{R_{\alpha}} + AB \theta_{\alpha} \right) \\ + Q_{\beta} \delta \left(A \frac{\partial w}{\partial \beta} - v \frac{AB}{R_{\beta}} + AB \theta_{\beta} \right) \\ + M_{\alpha} \delta \left(B \frac{\partial \theta_{\alpha}}{\partial \alpha} + \theta_{\beta} \frac{\partial A}{\partial \beta} \right) \\ + M_{\alpha\beta} \delta \left(B \frac{\partial \theta_{\beta}}{\partial \alpha} - \theta_{\alpha} \frac{\partial A}{\partial \beta} - \theta_n \frac{AB}{R_{\alpha}} \right) \\ + M_{\beta\alpha} \delta \left(A \frac{\partial \theta_{\alpha}}{\partial \beta} - \theta_{\beta} \frac{\partial B}{\partial \alpha} + \theta_n \frac{AB}{R_{\beta}} \right) \\ + M_{\beta} \delta \left(A \frac{\partial \theta_{\beta}}{\partial \beta} + \theta_{\alpha} \frac{\partial B}{\partial \alpha} \right) \Big] d\alpha d\beta \\ - \oint_C [(N_{\alpha} \delta u + N_{\alpha\beta} \delta v + Q_{\alpha} \delta w \\ + M_{\alpha} \delta \theta_{\alpha} + M_{\alpha\beta} \delta \theta_{\beta}) B d\beta \\ - (N_{\beta\alpha} \delta u + N_{\beta} \delta v + Q_{\beta} \delta w \\ + M_{\beta\alpha} \delta \theta_{\alpha} + M_{\beta} \delta \theta_{\beta}) A d\alpha] = 0 \quad (1.52) \end{aligned}$$

where the double integral extends over the region of the middle surface of the shell enclosed by the curve C . The double integral represents the virtual change in strain energy within C and the line integral represents the virtual work of the boundary forces. The quantities within the parentheses can now be regarded as the strains corresponding to the ten components of "generalized resultants," N_{α} , . . . , M_{β} , thereby yielding the following strain-displacement relations:

$$\epsilon_{\alpha} = \frac{1}{A} \frac{\partial u}{\partial \alpha} + \frac{v}{AB} \frac{\partial A}{\partial \beta} + \frac{w}{R_{\alpha}} \quad (1.53a)$$

$$\epsilon_{\beta} = \frac{u}{AB} \frac{\partial B}{\partial \alpha} + \frac{1}{B} \frac{\partial v}{\partial \beta} + \frac{w}{R_{\beta}} \quad (1.53b)$$

$$\gamma_{\alpha} = -\frac{u}{AB} \frac{\partial A}{\partial \beta} + \frac{1}{A} \frac{\partial v}{\partial \alpha} - \theta_n \quad (1.53c)$$

$$\gamma_{\beta} = \frac{1}{B} \frac{\partial u}{\partial \beta} - \frac{v}{AB} \frac{\partial B}{\partial \alpha} + \theta_n \quad (1.53d)$$

$$\kappa_{\alpha} = \frac{1}{A} \frac{\partial \theta_{\alpha}}{\partial \alpha} + \frac{\theta_{\beta}}{AB} \frac{\partial A}{\partial \beta} \quad (1.53e)$$

$$\kappa_{\beta} = \frac{\theta_{\alpha}}{AB} \frac{\partial B}{\partial \alpha} + \frac{1}{B} \frac{\partial \theta_{\beta}}{\partial \beta} \quad (1.53f)$$

$$\kappa_{\alpha\beta} = -\frac{\theta_{\alpha}}{AB} \frac{\partial A}{\partial \beta} + \frac{1}{A} \frac{\partial \theta_{\beta}}{\partial \alpha} - \frac{\theta_n}{R_{\alpha}} \quad (1.53g)$$

$$\kappa_{\beta\alpha} = \frac{1}{B} \frac{\partial \theta_{\alpha}}{\partial \beta} - \frac{\theta_{\beta}}{AB} \frac{\partial B}{\partial \alpha} + \frac{\theta_n}{R_{\beta}} \quad (1.53h)$$

$$\gamma_{\alpha z} = \frac{1}{A} \frac{\partial w}{\partial \alpha} - \frac{u}{R_{\alpha}} + \theta_{\alpha} \quad (1.53i)$$

$$\gamma_{\beta z} = \frac{1}{B} \frac{\partial w}{\partial \beta} - \frac{v}{R_{\beta}} + \theta_{\beta} \quad (1.53j)$$

where γ_{α} and γ_{β} are the tangential shear strains corresponding to the force resultants $N_{\alpha\beta}$ and $N_{\beta\alpha}$, respectively, and where $\gamma_{\alpha z}$ and $\gamma_{\beta z}$ are the transverse shear strains corresponding to the transverse shear force resultants Q_{α} and Q_{β} . Using Kirchhoff's hypothesis, $\gamma_{\alpha z} = \gamma_{\beta z} = 0$; therefore, equations (1.53i and j) yield the same expressions for the rotations of the normal, θ_{α} and θ_{β} , as were obtained previously in equations (1.39).

The rotation about the normal, θ_n , may be calculated in terms of u and v by taking the normal component of the surface curl of the total displacement vector (cf., ref. 1.51) giving

$$\theta_n = \frac{1}{2AB} \left(\frac{\partial Bv}{\partial \alpha} - \frac{\partial Au}{\partial \beta} \right) \quad (1.54)$$

and substituting equation (1.54) into equations (1.53c and d) shows that

$$\gamma_{\alpha} = \gamma_{\beta} \quad (1.55)$$

Furthermore, using equations (1.53c, d, g and h), (1.39), (1.54), and the Mainardi-Codazzi equations (1.24), the following identity holds:

$$\kappa_{\alpha\beta} - \kappa_{\beta\alpha} = \frac{1}{2} \left(\frac{1}{R_{\beta}} - \frac{1}{R_{\alpha}} \right) (\gamma_{\alpha} + \gamma_{\beta}) \quad (1.56)$$

Now define

$$\epsilon_{\alpha\beta} = \gamma_{\alpha} + \gamma_{\beta} \quad (1.57)$$

$$\tau = \kappa_{\alpha\beta} + \kappa_{\beta\alpha} \quad (1.58)$$

$$S = \frac{1}{2}(N_{\alpha\beta} + N_{\beta\alpha}) + \frac{1}{4}\left(\frac{1}{R_\beta} - \frac{1}{R_\alpha}\right)(M_{\alpha\beta} - M_{\beta\alpha}) \quad (1.59)$$

$$H = \frac{1}{2}(M_{\alpha\beta} + M_{\beta\alpha}) \quad (1.60)$$

Using equations (1.54) through (1.60), then equation (1.52) can be written as

$$\begin{aligned} & \int_{\alpha} \int_{\beta} (N_{\alpha} \delta \epsilon_{\alpha} + S \delta \epsilon_{\alpha\beta} + N_{\beta} \delta \epsilon_{\beta} + M_{\alpha} \delta \kappa_{\alpha} + H \delta \tau \\ & + M_{\beta} \delta \kappa_{\beta}) AB d\alpha d\beta - \oint_C [(N_{\alpha} \delta u + N_{\alpha\beta} \delta v + Q_{\alpha} \delta w \\ & + M_{\alpha} \delta \theta_{\alpha} + M_{\alpha\beta} \delta \theta_{\beta}) B d\beta - (N_{\beta\alpha} \delta u + N_{\beta} \delta v \\ & + Q_{\beta} \delta w + M_{\beta\alpha} \delta \theta_{\alpha} + M_{\beta} \delta \theta_{\beta}) A d\alpha] = 0 \quad (1.61) \end{aligned}$$

From the double integral in equation (1.61) which represents the virtual change in strain energy the generalized strains $\epsilon_{\alpha\beta}$ and τ correspond to the resulting S and H . Hence, it is observed that the strain-displacement equations of the Sanders theory are given by equations (1.41), (1.42a and b), and

$$\begin{aligned} \tau = & \frac{A}{B} \frac{\partial}{\partial \beta} \left(\frac{\theta_{\alpha}}{A} \right) + \frac{B}{A} \frac{\partial}{\partial \alpha} \left(\frac{\theta_{\beta}}{B} \right) \\ & + \frac{1}{2AB} \left(\frac{1}{R_{\beta}} - \frac{1}{R_{\alpha}} \right) \left(\frac{\partial B v}{\partial \alpha} - \frac{\partial A u}{\partial \beta} \right) \quad (1.62) \end{aligned}$$

1.4.6 Equations of Donnell and Mushtari

If one neglects the tangential displacements and their derivatives in equations (1.42) for the midsurface changes in curvature and twist, they simplify to

$$\left. \begin{aligned} \kappa_{\alpha} &= -\frac{1}{A} \frac{\partial}{\partial \alpha} \left(\frac{1}{A} \frac{\partial w}{\partial \alpha} \right) - \frac{1}{AB^2} \frac{\partial A}{\partial \beta} \frac{\partial w}{\partial \beta} \\ \kappa_{\beta} &= -\frac{1}{B} \frac{\partial}{\partial \beta} \left(\frac{1}{B} \frac{\partial w}{\partial \beta} \right) - \frac{1}{A^2 B} \frac{\partial B}{\partial \alpha} \frac{\partial w}{\partial \alpha} \\ \tau &= -\frac{B}{A} \frac{\partial}{\partial \alpha} \left(\frac{1}{B^2} \frac{\partial w}{\partial \beta} \right) - \frac{A}{B} \frac{\partial}{\partial \beta} \left(\frac{1}{A^2} \frac{\partial w}{\partial \alpha} \right) \end{aligned} \right\} \quad (1.63)$$

The strains at any point in the shell are then given for the Donnell-Mushtari theory by equations (1.43) where ϵ_{α} , ϵ_{β} , and $\epsilon_{\alpha\beta}$ are given by equations (1.41) and κ_{α} , κ_{β} , and τ are given by equations (1.63).

1.4.7 Remarks on the Strain-Displacement Equations

From the preceding section it can be seen that the total strains at any point (according to all the theories considered here) can be represented as the sum of two parts—one due to stretching and the other due to bending. In the theories considered three types of expressions were found to represent the total strain. These are summarized in table 1.1. The expressions of Byrne et al. are the

TABLE 1.1.—Total Strains at Any Point in a Shell

Theory	e_{α}, e_{β}	$\gamma_{\alpha\beta}$
Byrne, Flügge, Goldenveizer, Lur'ye, Novozhilov	$\frac{1}{(1+z/R_{\alpha})}(\epsilon_{\alpha} + z\kappa_{\alpha})$ $\frac{1}{(1+z/R_{\beta})}(\epsilon_{\beta} + z\kappa_{\beta})$	$\frac{1}{(1+z/R_{\alpha})(1+z/R_{\beta})} \left[\left(1 - \frac{z^2}{R_{\alpha}R_{\beta}} \right) \epsilon_{\alpha\beta} + z \left(1 + \frac{z}{2R_{\alpha}} + \frac{z}{2R_{\beta}} \right) \tau \right]$
Love, Timoshenko, Reissner, Naghdi, Berry, Sanders, Donnell, Mushtari	$\epsilon_{\alpha} + z\kappa_{\alpha}$ $\epsilon_{\beta} + z\kappa_{\beta}$	$\epsilon_{\alpha\beta} + z\tau$
Generalized Vlasov	$\epsilon_{\alpha} + \sum_{n=1}^{\infty} \kappa_{\alpha n} z^n$ $\epsilon_{\beta} + \sum_{n=1}^{\infty} \kappa_{\beta n} z^n$	$\epsilon_{\alpha\beta} + \sum_{n=1}^{\infty} \tau_n z^n$

most general of the three types, with the other types being special cases of these. The expressions of Byrne et al. are the direct result of the application of the Kirchhoff hypothesis to the strain-displacement relationships of the three-dimensional theory of elasticity. The expressions of Love et al. were arrived at by neglecting z/R_α and z/R_β in comparison with unity, as is seen in table 1.1. A milder approximation is that of Vlasov who represented a quotient of the type $1/(1+z/R_\alpha)$ by its geometric series expansion; the accuracy of the approximation then depends upon the number of terms retained in the series. The expressions ascribed to Vlasov in table 1.1 are the generalized forms arrived at before truncation of the series. However, it will be seen in section 1.5.3 that the series will be truncated

after $n=2$ for the subsequent development of the Vlasov theory.

The expressions for the middle surface strains ϵ_α , ϵ_β and $\epsilon_{\alpha\beta}$ are the same according to all the theories considered here. They are given by equations (1.41).

There is general agreement among the theories for the expressions of the middle surface curvature changes, κ_α and κ_β , as can be seen in table 1.2. If one considers only the linear terms ($n=1$) of the series expansions for the strains according to the Vlasov theory (i.e., eq. (1.50)), then Vlasov's κ_α , for example, differs from those of the other theories by the term ϵ_α/R_α . This difference arose due to replacing $1/(1+z/R_\alpha)$ by its series expansion in the derivation. The Donnell-

TABLE 1.2.—*Change in Curvature of the Middle Surface*

Theory	κ_α	κ_β
Byrne, Flügge, Goldenveizer, Lur'ye, Novozhilov, Love, Timoshenko, Reissner, Naghdi, Berry, Sanders	$\frac{1}{A} \frac{\partial \theta_\alpha}{\partial \alpha} + \frac{\theta_\beta}{AB} \frac{\partial A}{\partial \beta}$	$\frac{1}{B} \frac{\partial \theta_\beta}{\partial \beta} + \frac{\theta_\alpha}{AB} \frac{\partial B}{\partial \alpha}$
Vlasov ^a	$\frac{1}{A} \frac{\partial \theta_\alpha}{\partial \alpha} + \frac{\theta_\beta}{AB} \frac{\partial A}{\partial \beta} - \frac{1}{R_\alpha} \left(\frac{1}{A} \frac{\partial u}{\partial \alpha} + \frac{v}{AB} \frac{\partial A}{\partial \beta} + \frac{w}{R_\alpha} \right)$	$\frac{1}{B} \frac{\partial \theta_\beta}{\partial \beta} + \frac{\theta_\alpha}{AB} \frac{\partial B}{\partial \alpha} - \frac{1}{R_\beta} \left(\frac{u}{AB} \frac{\partial B}{\partial \alpha} + \frac{1}{B} \frac{\partial v}{\partial \beta} + \frac{w}{R_\beta} \right)$
Donnell, Mushtari	$-\frac{1}{A} \frac{\partial}{\partial \alpha} \left(\frac{1}{A} \frac{\partial w}{\partial \alpha} \right) - \frac{1}{AB^2} \frac{\partial A}{\partial \beta} \frac{\partial w}{\partial \beta}$	$-\frac{1}{B} \frac{\partial}{\partial \beta} \left(\frac{1}{B} \frac{\partial w}{\partial \beta} \right) - \frac{1}{A^2 B} \frac{\partial B}{\partial \alpha} \frac{\partial w}{\partial \alpha}$

^a Terms given for the Vlasov theory correspond only to the linear ($n=1$) terms of table 1.1.

TABLE 1.3.—*Change in Twist (τ) of the Middle Surface*

Byrne, Flügge, Lur'ye, Goldenveizer, Novozhilov, Timoshenko, Love	$\frac{A}{B} \frac{\partial}{\partial \beta} \left(\frac{\theta_\alpha}{A} \right) + \frac{B}{A} \frac{\partial}{\partial \alpha} \left(\frac{\theta_\beta}{B} \right) + \frac{1}{R_\alpha} \left(\frac{1}{B} \frac{\partial u}{\partial \beta} - \frac{v}{AB} \frac{\partial B}{\partial \alpha} \right) + \frac{1}{R_\beta} \left(\frac{1}{A} \frac{\partial v}{\partial \alpha} - \frac{u}{AB} \frac{\partial A}{\partial \beta} \right)$
Reissner, Berry, Naghdi	$\frac{A}{B} \frac{\partial}{\partial \beta} \left(\frac{\theta_\alpha}{A} \right) + \frac{B}{A} \frac{\partial}{\partial \alpha} \left(\frac{\theta_\beta}{B} \right)$
Vlasov ^a	$\left(\frac{1}{R_\alpha} - \frac{1}{R_\beta} \right) \left[\frac{A}{B} \frac{\partial}{\partial \beta} \left(\frac{u}{A} \right) - \frac{B}{A} \frac{\partial}{\partial \alpha} \left(\frac{v}{B} \right) \right] - \frac{B}{A} \frac{\partial}{\partial \alpha} \left(\frac{1}{B^2} \frac{\partial w}{\partial \beta} \right) - \frac{A}{B} \frac{\partial}{\partial \beta} \left(\frac{1}{A^2} \frac{\partial w}{\partial \alpha} \right)$
Sanders	$\frac{A}{B} \frac{\partial}{\partial \beta} \left(\frac{\theta_\alpha}{A} \right) + \frac{B}{A} \frac{\partial}{\partial \alpha} \left(\frac{\theta_\beta}{B} \right) + \frac{1}{2AB} \left(\frac{1}{R_\beta} - \frac{1}{R_\alpha} \right) \left(\frac{\partial B v}{\partial \alpha} - \frac{\partial A u}{\partial \beta} \right)$
Mushtari-Donnell	$-\frac{B}{A} \frac{\partial}{\partial \alpha} \left(\frac{1}{B^2} \frac{\partial w}{\partial \beta} \right) - \frac{A}{B} \frac{\partial}{\partial \beta} \left(\frac{1}{A^2} \frac{\partial w}{\partial \alpha} \right)$

^a Terms given for the Vlasov theory correspond only to the linear ($n=1$) terms of table 1.1.

Mushtari expressions in table 1.2 are simplifications of the others obtained by neglecting terms containing the tangential displacements u and v .

However, there is widespread disagreement among academicians concerning the proper form for the middle surface change in twist, τ . These disagreements are summarized in table 1.3. The differences in the expressions of Vlasov and of Donnell and Mushtari from that of Byrne et al. are due to the same reasons discussed in the previous paragraph for κ_α . The τ of Reissner et al. differs from that of Byrne et al. because the neglect of z/R_α and z/R_β in comparison with unity, and doing so at an earlier stage in the derivation than in the Love-Timoshenko formulation. Sanders' expression can best be described as one having a correction factor added to that of Reissner et al., as will be seen in the next paragraph.

Let a shell be subjected to a rigid body translation denoted by the vector

$$\vec{\delta} = \delta_\alpha \hat{t}_\alpha + \delta_\beta \hat{t}_\beta + \delta_n \hat{t}_n \quad (1.64)$$

and a rigid body rotation by the vector

$$\vec{\Omega} = -\Omega_\beta \hat{t}_\alpha + \Omega_\alpha \hat{t}_\beta + \Omega_n \hat{t}_n \quad (1.65)$$

Then the displacement vector of a point on the middle surface is given by

$$\vec{u} = \vec{\delta} + (\vec{\Omega} \times \vec{r}) \quad (1.66)$$

where \vec{r} is the position vector locating the middle surface as described in section 1.1. Of course, if a shell is given a rigid body motion, then substituting the displacement of a typical point as given in equation (1.66) into the strain-displacement equations should result in no strains. Sanders (ref. 1.20) showed that his strain-displacement equations are consistent from this standpoint, but that the twist does not vanish in the Reissner-Naghdi-Berry theory. For the latter theory the twist becomes (ref. 1.20)

$$\tau = \left(\frac{1}{R_\alpha} - \frac{1}{R_\beta} \right) \Omega_n \quad (1.67)$$

which vanishes only for a spherical shell, a flat plate, or an axisymmetrically loaded shell of revolution. If the rotation Ω_n is large it can lead to significant errors, as found by Cohen (ref. 1.38) on helicoidal shells. Thus if the correction

factor $[(1/R_\alpha) - (1/R_\beta)]\theta_n$ is arbitrarily added (with θ_n given by eq. (1.54)) to the expression of Reissner et al. in table 1.3, the inconsistency discussed above is eliminated and the τ of the Sanders theory results. Kraus (ref. 1.42, p. 68) showed that the strain-displacement equations of Byrne, Flügge, Goldenveizer, Lur'ye, and Novozhilov have no inconsistencies with regard to rigid body motions. Kadi (ref. 1.44) found that the equations of Love, Timoshenko, and Vlasov are also free from this inconsistency, but the Donnell-Mushtari theory gives curvature changes

$$\left. \begin{aligned} \kappa_\alpha &= -\frac{\delta_\alpha}{A} \frac{\partial}{\partial \alpha} \left(\frac{1}{R_\alpha} \right) \\ &\quad + \left(\frac{1}{R_\alpha} - \frac{1}{R_\beta} \right) \frac{\delta_\beta}{AB} \frac{\partial A}{\partial \beta} + \frac{\delta_n}{R_\alpha^2} \\ \kappa_\beta &= -\frac{\delta_\beta}{B} \frac{\partial}{\partial \beta} \left(\frac{1}{R_\beta} \right) \\ &\quad + \left(\frac{1}{R_\beta} - \frac{1}{R_\alpha} \right) \frac{\delta_\alpha}{AB} \frac{\partial B}{\partial \alpha} + \frac{\delta_n}{R_\beta^2} \\ \tau &= \left(\frac{1}{R_\alpha} - \frac{1}{R_\beta} \right) \left[\frac{A}{B} \frac{\partial}{\partial \beta} \left(\frac{\delta_\alpha}{A} \right) - \frac{B}{A} \frac{\partial}{\partial \alpha} \left(\frac{\delta_\beta}{B} \right) \right] \end{aligned} \right\} \quad (1.68)$$

due to rigid body translations δ_α , δ_β , and δ_n in the u , v , and w directions, respectively.

1.5 FORCE AND MOMENT RESULTANTS

As shown in the previous section one result of the Kirchhoff hypothesis is to restrict the displacements u and v to those which vary linearly through the thickness (cf., eqs. (1.37a and b)). Consequently, for the theories of Love, Timoshenko, Vlasov, Reissner, Naghdi, Berry, Sanders, Donnell, and Mushtari, as shown in table 1.1, the resulting strains e_α , e_β , and $\gamma_{\alpha\beta}$ also vary linearly with z . For the other theories the strain variation is more complicated, but nevertheless, completely defined with respect to z . Thus, if the relationships between stresses and strains are defined (as, for example, in Hooke's Law), the resulting stresses can be integrated over the shell thickness. The resultants of the integrals will be termed "force resultants" and "moment resultants" in this work. Other terminologies for these quantities used variously in the literature of shells include "stress resultants" and "forces," corresponding to our force resul-

tants, and "stress couples," "couples," "couple resultants," and "moments," corresponding to our moment resultants. The force and moment resultants are components of second order tensors, and hence they are not true forces and moments. The force and moment resultants will have dimensions of force per unit length and moment per unit length, respectively.

Proceeding along the path laid out in the previous paragraph, Hooke's Law will first be assumed as the constitutive law to be followed. This limits all shells considered in this monograph to be made from materials which are linearly elastic. Furthermore, in this chapter devoted to deriving shell theories in their most simple forms, the materials will be limited to those which are isotropic. The effects of orthotropy and its generalization, anisotropy, will be seen in subsequent chapters. Hooke's Law is written in its well-known three-dimensional form as

$$e_\alpha = \frac{1}{E}[\sigma_\alpha - \nu(\sigma_\beta + \sigma_z)] \quad (1.69a)$$

$$e_\beta = \frac{1}{E}[\sigma_\beta - \nu(\sigma_z + \sigma_\alpha)] \quad (1.69b)$$

$$e_z = \frac{1}{E}[\sigma_z - \nu(\sigma_\alpha + \sigma_\beta)] \quad (1.69c)$$

$$\gamma_{\alpha\beta} = \frac{2(1+\nu)}{E}\sigma_{\alpha\beta} \quad (1.69d)$$

$$\gamma_{\alpha z} = \frac{2(1+\nu)}{E}\sigma_{\alpha z} \quad (1.69e)$$

$$\gamma_{\beta z} = \frac{2(1+\nu)}{E}\sigma_{\beta z} \quad (1.69f)$$

where, in accordance with the shell element shown in figure 1.2, σ_α and σ_β are the normal stresses and $\sigma_{\alpha\beta}$ and $\sigma_{\beta\alpha}$ are the shear stresses in the tangential (α and β) directions and $\sigma_{\alpha z}$ and $\sigma_{\beta z}$ are the transverse (i.e., in the z direction) shear stresses, all acting upon the transverse faces of a shell element; E is Young's modulus, and ν is Poisson's ratio. Assuming the symmetry of the stress tensor (neglecting body couples), then $\sigma_{\alpha\beta} = \sigma_{\beta\alpha}$. It is pointed out that the strains are also assumed to be independent of temperature because temperature has no explicit effect upon the free vibration case being considered

in this monograph. Temperature can enter the problem implicitly through its influence upon *initial* stresses or upon the elastic moduli—two complicating effects which will be discussed in subsequent chapters.

The Kirchhoff hypothesis, as discussed in section 1.3, yields $e_z = \gamma_{\alpha z} = \gamma_{\beta z} = 0$, whence, by equations (1.69c, e, and f), $\sigma_{\alpha z} = \sigma_{\beta z} = 0$ and $\sigma_z = \nu(\sigma_\alpha + \sigma_\beta)$. But Love's third assumption is that σ_z is negligibly small, which is one unavoidable contradiction in the order of shell theory being considered here. Another contradiction is that $\sigma_{\alpha z}$ and $\sigma_{\beta z}$ are clearly not zero, since their integrals must supply the transverse shearing forces needed for equilibrium; but they are usually small in comparison with σ_α , σ_β , and $\sigma_{\alpha\beta}$. Retaining the assumption that σ_z is negligibly small reduces the problem to one of plane stress; that is, equations (1.69) reduce to

$$\left. \begin{aligned} e_\alpha &= \frac{1}{E}(\sigma_\alpha - \nu\sigma_\beta) \\ e_\beta &= \frac{1}{E}(\sigma_\beta - \nu\sigma_\alpha) \\ \gamma_{\alpha\beta} &= \frac{2(1+\nu)}{E}\sigma_{\alpha\beta} \end{aligned} \right\} \quad (1.70)$$

which, when inverted, give

$$\sigma_\alpha = \frac{E}{1-\nu^2}(e_\alpha + \nu e_\beta) \quad (1.71a)$$

$$\sigma_\beta = \frac{E}{1-\nu^2}(e_\beta + \nu e_\alpha) \quad (1.71b)$$

$$\sigma_{\alpha\beta} = \frac{E}{2(1+\nu)}\gamma_{\alpha\beta} \quad (1.71c)$$

Consider the face of the element in figure 1.2 that is perpendicular to the α -axis (i.e., the face for which α is constant). On that face the stresses σ_α , $\sigma_{\alpha\beta}$, and $\sigma_{\alpha z}$ act. The arc length of the intercept of the middle surface with the face is $ds_\beta = B d\beta$, and the arc lengths of intercepts of parallel surfaces are $ds_\beta^{(z)} = B(1+z/R_\beta) d\beta$, as discussed in section 1.2. The infinitesimal force for example, acting upon the elemental area of thickness dz on the face is then given by $\sigma_\alpha ds_\beta^{(z)} dz$. Integrating such forces over the thickness of the shell and dividing by $B d\beta$ yield the force resultant N_α , expressed in units of force per

unit length of middle surface. Thus, the force resultants acting on this face can be expressed as

$$\begin{Bmatrix} N_\alpha \\ N_{\alpha\beta} \\ Q_\alpha \end{Bmatrix} = \int_{-h/2}^{h/2} \begin{Bmatrix} \sigma_\alpha \\ \sigma_{\alpha\beta} \\ \sigma_{\alpha z} \end{Bmatrix} \left(1 + \frac{z}{R_\beta}\right) dz \quad (1.72)$$

and, similarly, the force resultants on the face perpendicular to the β -axis will be

$$\begin{Bmatrix} N_\beta \\ N_{\beta\alpha} \\ Q_\beta \end{Bmatrix} = \int_{-h/2}^{h/2} \begin{Bmatrix} \sigma_\beta \\ \sigma_{\beta\alpha} \\ \sigma_{\beta z} \end{Bmatrix} \left(1 + \frac{z}{R_\alpha}\right) dz \quad (1.73)$$

The positive directions of the force resultants are shown in figure 1.3.

Similarly, the moment of the infinitesimal force $\sigma_\alpha ds_\beta^{(z)} dz$ about the β -line is simply $z\sigma_\alpha ds_\beta^{(z)} dz$ and the moment resultant M_α is obtained by dividing the total integrated moment over the thickness by $B d\beta$. Thus, the moment resultants are given by

$$\begin{Bmatrix} M_\alpha \\ M_{\alpha\beta} \end{Bmatrix} = \int_{-h/2}^{h/2} \begin{Bmatrix} \sigma_\alpha \\ \sigma_{\alpha\beta} \end{Bmatrix} \left(1 + \frac{z}{R_\beta}\right) z dz \quad (1.74)$$

$$\begin{Bmatrix} M_\beta \\ M_{\beta\alpha} \end{Bmatrix} = \int_{-h/2}^{h/2} \begin{Bmatrix} \sigma_\beta \\ \sigma_{\beta\alpha} \end{Bmatrix} \left(1 + \frac{z}{R_\alpha}\right) z dz$$

and, consequently, have dimensions of moment per unit length of middle surface. The positive directions of the moment resultants are shown in figure 1.4.

It is worthy to note that although $\sigma_{\alpha\beta} = \sigma_{\beta\alpha}$ from the symmetry of the stress tensor, it is obvious from equations (1.72), (1.73), and (1.74) that $N_{\alpha\beta} \neq N_{\beta\alpha}$ and $M_{\alpha\beta} \neq M_{\beta\alpha}$ unless $R_\alpha = R_\beta$.

At this point the assumption will be made that the shell material is *homogeneous*; in particular, that the elastic constants E and ν are independent of z . Thus, if equations (1.71) are substituted into equations (1.72), (1.73), and (1.74) and the integrations over z are carried out, E and ν will be treated as constants. The procedure for a heterogeneous material will be discussed in subsequent chapters.

1.5.1 Equations of Love, Timoshenko, Reissner, Naghdi, Berry, Sanders, Mushtari, and Donnell

If one neglects z/R_α and z/R_β in comparison to unity, then equations (1.72), (1.73), and (1.74) can be rewritten as

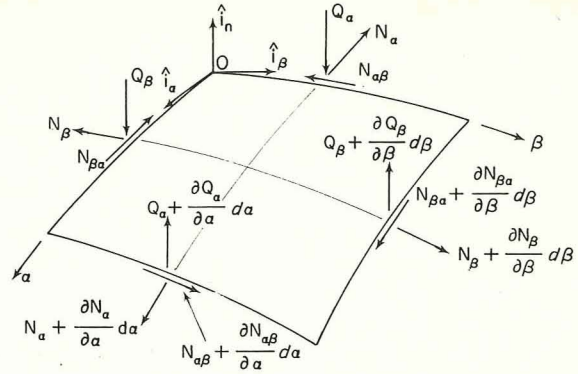


FIGURE 1.3.—Notation and positive directions of force resultants in shell coordinates.

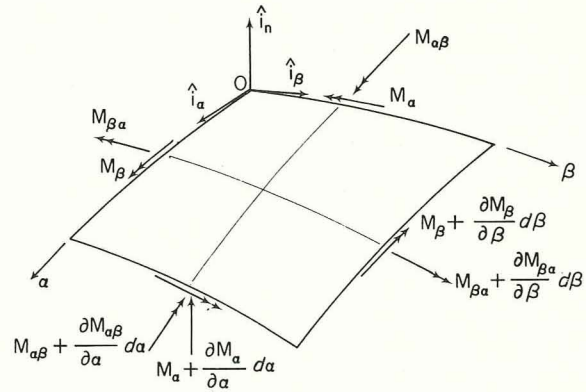


FIGURE 1.4.—Notation and positive directions of moment resultants in shell coordinates.

$$\begin{Bmatrix} N_\alpha \\ M_\alpha \end{Bmatrix} = \frac{E}{1-\nu^2} \int_{-h/2}^{h/2} \begin{Bmatrix} 1 \\ z \end{Bmatrix} (e_\alpha + \nu e_\beta) dz \quad (1.75a)$$

$$\begin{Bmatrix} N_\beta \\ M_\beta \end{Bmatrix} = \frac{E}{1-\nu^2} \int_{-h/2}^{h/2} \begin{Bmatrix} 1 \\ z \end{Bmatrix} (e_\beta + \nu e_\alpha) dz \quad (1.75b)$$

$$\begin{Bmatrix} N_{\alpha\beta} = N_{\beta\alpha} \\ M_{\alpha\beta} = M_{\beta\alpha} \end{Bmatrix} = \frac{E}{2(1+\nu)} \int_{-h/2}^{h/2} \begin{Bmatrix} 1 \\ z \end{Bmatrix} \gamma_{\alpha\beta} dz \quad (1.75c)$$

where the stress strain equations (1.71) have been used and where the transverse force resultants have been omitted. Substituting the expressions for the total strains according to Love, Timoshenko, Vlasov, Reissner, Naghdi, Berry, Sanders, Donnell, and Mushtari as given in table 1.1, equations (1.75) become

$$N_\alpha = \frac{Eh}{(1-\nu^2)} (\epsilon_\alpha + \nu \epsilon_\beta) \quad (1.76a)$$

$$N_\beta = \frac{Eh}{(1-\nu^2)}(\epsilon_\beta + \nu\epsilon_\alpha) \quad (1.76b)$$

$$N_{\alpha\beta} = N_{\beta\alpha} = \frac{Eh}{2(1+\nu)}\epsilon_{\alpha\beta} \quad (1.76c)$$

$$M_\alpha = \frac{Eh^3}{12(1-\nu^2)}(\kappa_\alpha + \nu\kappa_\beta) \quad (1.76d)$$

$$M_\beta = \frac{Eh^3}{12(1-\nu^2)}(\kappa_\beta + \nu\kappa_\alpha) \quad (1.76e)$$

$$M_{\alpha\beta} = M_{\beta\alpha} = \frac{Eh^3}{24(1+\nu)}\tau \quad (1.76f)$$

To obtain force and moment resultants in terms of the displacement u , v , and w it would now be necessary to substitute the expressions for ϵ_α , ϵ_β , and $\epsilon_{\alpha\beta}$ from equations (1.41) and the various expressions for κ_α , κ_β , and τ (according to the various theories) from tables 1.2 and 1.3.

1.5.2 Equations of Byrne, Flügge, and Lur'ye

If the strain expressions of Byrne, Flügge, and Lur'ye from table 1.1 are substituted into equations (1.72), (1.73) and (1.74), along with equations (1.71), the results are as given in eq. 1.77. Now utilizing the fact that z/R_α and z/R_β are less than unity, quotients of the type $1/(1+z/R_i)$ can be replaced by their geometric series equivalents, as indicated previously by equation (1.46). Then for sufficiently small z/R_i , the series of equation (1.46) is truncated after terms of the third degree and is substituted into equations (1.77). The integrands are then expanded, terms of degree greater than three are discarded, and the integrations are carried out, giving

$$N_\alpha = \frac{Eh}{1-\nu^2} \left[\epsilon_\alpha + \nu\epsilon_\beta - \frac{h^2}{12} \left(\frac{1}{R_\alpha} - \frac{1}{R_\beta} \right) \left(\kappa_\alpha - \frac{\epsilon_\alpha}{R_\alpha} \right) \right] \quad (1.78a)$$

$$N_\beta = \frac{Eh}{1-\nu^2} \left[\epsilon_\beta + \nu\epsilon_\alpha - \frac{h^2}{12} \left(\frac{1}{R_\beta} - \frac{1}{R_\alpha} \right) \left(\kappa_\beta - \frac{\epsilon_\beta}{R_\beta} \right) \right] \quad (1.78b)$$

$$N_{\alpha\beta} = \frac{Eh}{2(1+\nu)} \left[\epsilon_{\alpha\beta} - \frac{h^2}{12} \left(\frac{1}{R_\alpha} - \frac{1}{R_\beta} \right) \left(\frac{\tau}{2} - \frac{\epsilon_{\alpha\beta}}{R_\alpha} \right) \right] \quad (1.78c)$$

$$N_{\beta\alpha} = \frac{Eh}{2(1+\nu)} \left[\epsilon_{\alpha\beta} - \frac{h^2}{12} \left(\frac{1}{R_\beta} - \frac{1}{R_\alpha} \right) \left(\frac{\tau}{2} - \frac{\epsilon_{\alpha\beta}}{R_\beta} \right) \right] \quad (1.78d)$$

$$M_\alpha = \frac{Eh^3}{12(1-\nu^2)} \left[\kappa_\alpha + \nu\kappa_\beta - \left(\frac{1}{R_\alpha} - \frac{1}{R_\beta} \right) \epsilon_\alpha \right] \quad (1.79a)$$

$$M_\beta = \frac{Eh^3}{12(1-\nu^2)} \left[\kappa_\beta + \nu\kappa_\alpha - \left(\frac{1}{R_\beta} - \frac{1}{R_\alpha} \right) \epsilon_\beta \right] \quad (1.79b)$$

$$M_{\alpha\beta} = \frac{Eh^3}{24(1+\nu)} \left(\tau - \frac{\epsilon_{\alpha\beta}}{R_\alpha} \right) \quad (1.79c)$$

$$M_{\beta\alpha} = \frac{Eh^3}{24(1+\nu)} \left(\tau - \frac{\epsilon_{\alpha\beta}}{R_\beta} \right) \quad (1.79d)$$

1.5.3 Equations of Vlasov

To obtain force and moment resultants, Vlasov retained two terms of the series expansions for the total strains given in table 1.1; i.e.,

$$\left. \begin{aligned} e_\alpha &= \epsilon_\alpha + z\kappa_{\alpha 1} + z^2\kappa_{\alpha 2} \\ e_\beta &= \epsilon_\beta + z\kappa_{\beta 1} + z^2\kappa_{\beta 2} \\ \tau &= \epsilon_{\alpha\beta} + z\tau_1 + z^2\tau_2 \end{aligned} \right\} \quad (1.80)$$

with $\kappa_{\alpha n}$, $\kappa_{\beta n}$, and τ_n defined by equations (1.49). Substituting equations (1.80) into equations (1.75), integrating, and disregarding terms which contain powers of h greater than three, one obtains the force and moment resultants of Vlasov (ref. 1.19, p. 284).

$$\left. \begin{aligned} \left\{ \begin{aligned} N_\alpha \\ M_\alpha \end{aligned} \right\} &= \frac{E}{1-\nu^2} \int_{-h/2}^{h/2} \left\{ \begin{aligned} 1 \\ z \end{aligned} \right\} \left[\left(1 + \frac{z}{R_\beta} \right) \left(1 + \frac{z}{R_\alpha} \right)^{-1} (\epsilon_\alpha + z\kappa_\alpha) + \nu (\epsilon_\beta + z\kappa_\beta) \right] dz \\ \left\{ \begin{aligned} N_\beta \\ M_\beta \end{aligned} \right\} &= \frac{E}{1-\nu^2} \int_{-h/2}^{h/2} \left\{ \begin{aligned} 1 \\ z \end{aligned} \right\} \left[\left(1 + \frac{z}{R_\alpha} \right) \left(1 + \frac{z}{R_\beta} \right)^{-1} (\epsilon_\beta + z\kappa_\beta) + \nu (\epsilon_\alpha + z\kappa_\alpha) \right] dz \\ \left\{ \begin{aligned} N_{\alpha\beta} \\ M_{\alpha\beta} \end{aligned} \right\} &= \frac{E}{2(1+\nu)} \int_{-h/2}^{h/2} \left\{ \begin{aligned} 1 \\ z \end{aligned} \right\} \left(1 + \frac{z}{R_\alpha} \right)^{-1} \left[\left(1 - \frac{z^2}{R_\alpha R_\beta} \right) \epsilon_{\alpha\beta} + z \left(1 + \frac{z}{2R_\alpha} + \frac{z}{2R_\beta} \right) \tau \right] dz \\ \left\{ \begin{aligned} N_{\beta\alpha} \\ M_{\beta\alpha} \end{aligned} \right\} &= \frac{E}{2(1+\nu)} \int_{-h/2}^{h/2} \left\{ \begin{aligned} 1 \\ z \end{aligned} \right\} \left(1 + \frac{z}{R_\beta} \right)^{-1} \left[\left(1 - \frac{z^2}{R_\alpha R_\beta} \right) \epsilon_{\alpha\beta} + z \left(1 + \frac{z}{2R_\alpha} + \frac{z}{2R_\beta} \right) \tau \right] dz \end{aligned} \right\} \quad (1.77)$$

$$\left. \begin{aligned}
 N_\alpha &= \frac{Eh}{1-\nu^2} \left[\epsilon_\alpha + \nu \epsilon_\beta - \frac{h^2}{12} \left(\frac{1}{R_\alpha} - \frac{1}{R_\beta} \right) \left(\kappa_\alpha - \frac{\epsilon_\alpha}{R_\alpha} \right) \right] \\
 N_\beta &= \frac{Eh}{1-\nu^2} \left[\epsilon_\beta + \nu \epsilon_\alpha - \frac{h^2}{12} \left(\frac{1}{R_\beta} - \frac{1}{R_\alpha} \right) \left(\kappa_\beta - \frac{\epsilon_\beta}{R_\beta} \right) \right] \\
 N_{\alpha\beta} &= \frac{Eh}{2(1+\nu)} \left[\epsilon_{\alpha\beta} - \frac{h^2}{24} \left(\frac{1}{R_\alpha} - \frac{1}{R_\beta} \right) \tau \right] \\
 N_{\beta\alpha} &= \frac{Eh}{2(1+\nu)} \left[\epsilon_{\alpha\beta} - \frac{h^2}{24} \left(\frac{1}{R_\beta} - \frac{1}{R_\alpha} \right) \tau \right] \\
 M_\alpha &= \frac{Eh^3}{12(1-\nu^2)} \left[\kappa_\alpha + \nu \kappa_\beta - \left(\frac{1}{R_\alpha} - \frac{1}{R_\beta} \right) \epsilon_\alpha \right] \\
 M_\beta &= \frac{Eh^3}{12(1-\nu^2)} \left[\kappa_\beta + \nu \kappa_\alpha - \left(\frac{1}{R_\beta} - \frac{1}{R_\alpha} \right) \epsilon_\beta \right] \\
 M_{\alpha\beta} &= \frac{Eh^3}{24(1+\nu)} \left(\tau + \frac{\epsilon_{\alpha\beta}}{R_\beta} \right) \\
 M_{\beta\alpha} &= \frac{Eh^3}{24(1+\nu)} \left(\tau + \frac{\epsilon_{\alpha\beta}}{R_\alpha} \right)
 \end{aligned} \right\} \quad (1.81)$$

$$\left. \begin{aligned}
 M_\alpha &= \frac{Eh^3}{12(1-\nu^2)} \left[\kappa_\alpha + \nu \kappa_\beta - \left(\frac{1}{R_\alpha} - \frac{1}{R_\beta} \right) \epsilon_\alpha \right] \\
 M_\beta &= \frac{Eh^3}{12(1-\nu^2)} \left[\kappa_\beta + \nu \kappa_\alpha - \left(\frac{1}{R_\beta} - \frac{1}{R_\alpha} \right) \epsilon_\beta \right] \\
 M_{\alpha\beta} &= \frac{Eh^3}{24(1+\nu)} \left(\tau + \frac{\epsilon_{\alpha\beta}}{R_\beta} \right) \\
 M_{\beta\alpha} &= \frac{Eh^3}{24(1+\nu)} \left(\tau + \frac{\epsilon_{\alpha\beta}}{R_\alpha} \right)
 \end{aligned} \right\} \quad (1.82)$$

1.5.4 Equations of Goldenveizer and Novozhilov

From the theory of elasticity the well-known expression for the strain energy stored in a body during elastic deformation is

$$U = \frac{1}{2} \int_V (\sigma_\alpha \epsilon_\alpha + \sigma_\beta \epsilon_\beta + \sigma_n \epsilon_n + \sigma_{\alpha\beta} \gamma_{\alpha\beta} + \sigma_{\alpha z} \gamma_{\alpha z} + \sigma_{\beta z} \gamma_{\beta z}) dV \quad (1.83)$$

where dV is the element of volume which, expressed in shell coordinates, is (see eq. (1.33))

$$dV = \left(1 + \frac{z}{R_\alpha} \right) \left(1 + \frac{z}{R_\beta} \right) AB d\alpha d\beta dz$$

Applying the Kirchhoff hypothesis of thin shells reduces equation (1.83) to

$$U = \frac{1}{2} \int_V (\sigma_\alpha \epsilon_\alpha + \sigma_\beta \epsilon_\beta + \sigma_{\alpha\beta} \gamma_{\alpha\beta}) dV \quad (1.84)$$

Substituting equations (1.71) into equation (1.84) yields

$$U = \frac{E}{2(1-\nu^2)} \int_V \left[e_\alpha^2 + e_\beta^2 + 2\nu e_\alpha e_\beta + \frac{(1-\nu)}{2} \gamma_{\alpha\beta}^2 \right] dV \quad (1.85)$$

Substituting further the expressions for the total strains in terms of the middle surface strains and changes in curvature given in table 1.1, equation (1.85) becomes

$$U = \frac{E}{2(1-\nu^2)} \int_V \left\{ \left(1 + \frac{z}{R_\beta} \right) \left(1 + \frac{z}{R_\alpha} \right)^{-1} (\epsilon_\alpha + z\kappa_\alpha)^2 + \left(1 + \frac{z}{R_\alpha} \right) \left(1 + \frac{z}{R_\beta} \right)^{-1} (\epsilon_\beta + z\kappa_\beta)^2 + 2\nu (\epsilon_\alpha + z\kappa_\alpha) (\epsilon_\beta + z\kappa_\beta) + \frac{(1-\nu)}{2} \left[\left(1 - \frac{z^2}{R_\alpha R_\beta} \right) \epsilon_{\alpha\beta} + z \left(1 + \frac{z}{2R_\alpha} + \frac{z}{2R_\beta} \right) \tau \right]^2 \right\} AB d\alpha d\beta dz \quad (1.86)$$

Replacing $(1+z/R_i)^{-1}$ in equation (1.86) by its series expansion given in equation (1.46) and neglecting terms raised to powers of z greater than two in the integrand one obtains

$$U = \frac{E}{2(1-\nu^2)} \int_V (Q_0 + zQ_1 + z^2Q_2) AB d\alpha d\beta dz \quad (1.87)$$

where Q_0 , Q_1 , and Q_2 are defined by (ref. 1.26)

$$Q_0 = (\epsilon_\alpha + \epsilon_\beta)^2 - 2(1-\nu) \left(\epsilon_\alpha \epsilon_\beta - \frac{\epsilon_{\alpha\beta}^2}{4} \right) \quad (1.88a)$$

$$Q_1 = 2(\epsilon_\alpha \kappa_\alpha + \epsilon_\beta \kappa_\beta) + 2\nu (\epsilon_\alpha \kappa_\beta + \epsilon_\beta \kappa_\alpha) + (1-\nu) \epsilon_{\alpha\beta} \tau - \left(\frac{1}{R_\alpha} - \frac{1}{R_\beta} \right) (\epsilon_\alpha^2 - \epsilon_\beta^2) \quad (1.88b)$$

$$Q_2 = (\kappa_\alpha + \kappa_\beta)^2 - 2(1-\nu) \left(\kappa_\alpha \kappa_\beta - \frac{\tau^2}{4} \right) - 2 \left(\frac{1}{R_\alpha} - \frac{1}{R_\beta} \right) (\epsilon_\alpha \kappa_\alpha - \epsilon_\beta \kappa_\beta) - \frac{1-\nu}{2} \left(\frac{1}{R_\alpha} + \frac{1}{R_\beta} \right) \epsilon_{\alpha\beta} \tau + \left(\frac{1}{R_\alpha} - \frac{1}{R_\beta} \right) \left(\frac{\epsilon_\alpha^2}{R_\alpha} - \frac{\epsilon_\beta^2}{R_\beta} \right) + \frac{(1-\nu)}{2} \left(\frac{1}{R_\alpha^2} - \frac{1}{R_\alpha R_\beta} + \frac{1}{R_\beta^2} \right) \epsilon_{\alpha\beta}^2 \quad (1.88c)$$

Carrying out the integration of equation (1.87) over the thickness (taken to be constant) between limits $z = -h/2$ and $z = +h/2$ gives

$$U = \frac{Eh}{2(1-\nu^2)} \int_{\alpha} \int_{\beta} \left(Q_0 + \frac{h^2}{12} Q_2 \right) AB \, d\alpha \, d\beta \quad (1.89)$$

where the integral of the term in equation (1.87) containing Q_1 disappears because of symmetric limits.

Novozhilov (ref. 1.26, p. 45) argued that because the use of the Kirchhoff hypothesis in replacing the strain energy integral given in equation (1.83) by that of equation (1.84) introduces errors of the order h/R in comparison to unity, then terms of this order cannot be arbitrarily rejected in equation (1.89), but must be examined carefully to determine whether they are to be retained or rejected. First the curvature changes and twist are replaced by dimensionless quantities defined by

$$\left. \begin{aligned} \epsilon_{\alpha}' &= \frac{h}{2} \kappa_{\alpha} \\ \epsilon_{\beta}' &= \frac{h}{2} \kappa_{\beta} \\ \epsilon_{\alpha\beta}' &= h\tau \end{aligned} \right\} \quad (1.90)$$

where ϵ_{α}' , ϵ_{β}' , and $\epsilon_{\alpha\beta}'$ can be physically interpreted as the strains in the extreme fibers of the shell resulting from κ_{α} , κ_{β} , and τ , respectively. Substituting equations (1.88a and c) and (1.90) into equation (1.89), equation (1.89) can be rewritten as

$$U = \frac{E}{2(1-\nu^2)} \int_{\alpha} \int_{\beta} (I_1 + I_2 + I_3) AB \, d\alpha \, d\beta \quad (1.91)$$

where

$$\left. \begin{aligned} I_1 &= (\epsilon_{\alpha} + \epsilon_{\beta})^2 - 2(1-\nu) \left(\epsilon_{\alpha}\epsilon_{\beta} - \frac{\epsilon_{\alpha\beta}^2}{4} \right) \\ &\quad + \frac{1}{3} [(\epsilon_{\alpha}' + \epsilon_{\beta}')^2 \\ &\quad - 2(1-\nu) \left(\epsilon_{\alpha}'\epsilon_{\beta}' - \frac{\epsilon_{\alpha\beta}'^2}{16} \right)] \\ I_2 &= -\frac{1}{3} \left(\frac{h}{R_{\alpha}} - \frac{h}{R_{\beta}} \right) (\epsilon_{\alpha}\epsilon_{\alpha}' - \epsilon_{\beta}\epsilon_{\beta}') \\ &\quad - \frac{(1-\nu)}{24} \left(\frac{h}{R_{\alpha}} + \frac{h}{R_{\beta}} \right) (\epsilon_{\alpha\beta}\epsilon_{\alpha\beta}') \end{aligned} \right\} \quad (1.92)$$

$$I_3 = \frac{1}{12} \left(\frac{h}{R_{\alpha}} - \frac{h}{R_{\beta}} \right) \left(\frac{h}{R_{\alpha}} \epsilon_{\alpha}^2 - \frac{h}{R_{\beta}} \epsilon_{\beta}^2 \right) + \frac{(1-\nu)}{24} \left(\frac{h^2}{R_{\alpha}^2} - \frac{h^2}{R_{\alpha}R_{\beta}} + \frac{h^2}{R_{\beta}^2} \right) \epsilon_{\alpha\beta}^2$$

It can now be seen that I_2 and I_3 are now of the orders (h/R_i) and $(h/R_i)^2$, respectively, with respect to unity; hence, I_2 and I_3 were neglected by Novozhilov in comparison with I_1 , giving for equation (1.89):

$$U = \frac{Eh}{2(1-\nu^2)} \int_{\alpha} \int_{\beta} \left\{ (\epsilon_{\alpha} + \epsilon_{\beta})^2 - 2(1-\nu) \left(\epsilon_{\alpha}\epsilon_{\beta} - \frac{\epsilon_{\alpha\beta}^2}{4} \right) + \frac{h^2}{12} (\kappa_{\alpha} + \kappa_{\beta})^2 - 2(1-\nu) \left(\kappa_{\alpha}\kappa_{\beta} - \frac{\tau^2}{4} \right) \right\} AB \, d\alpha \, d\beta \quad (1.93)$$

This is the same as Love's (ref. 1.13) strain energy expression, wherein stretching and bending portions are uncoupled.

Returning to the strain energy functional given by equation (1.84) and taking its variation gives:

$$\delta U = \int_V (\sigma_{\alpha} \delta e_{\alpha} + \sigma_{\beta} \delta e_{\beta} + \sigma_{\alpha\beta} \delta \gamma_{\alpha\beta}) \, dV \quad (1.94)$$

Substituting the expressions for the total strains from table 1.1 gives

$$\begin{aligned} \delta U &= \int_{\alpha} \int_{\beta} \int_z \left[\sigma_{\alpha} \left(1 + \frac{z}{R_{\beta}} \right) (\delta \epsilon_{\alpha} + z \delta \kappa_{\alpha}) \right. \\ &\quad + \sigma_{\beta} \left(1 + \frac{z}{R_{\alpha}} \right) (\delta \epsilon_{\beta} + z \delta \kappa_{\beta}) \\ &\quad + \sigma_{\alpha\beta} \left(1 - \frac{z^2}{R_{\alpha}R_{\beta}} \right) \delta \epsilon_{\alpha\beta} \\ &\quad \left. + z \sigma_{\alpha\beta} \left(1 + \frac{z}{2R_{\alpha}} + \frac{z}{2R_{\beta}} \right) \delta \tau \right] AB \, d\alpha \, d\beta \, dz \end{aligned} \quad (1.95)$$

Making use of the definitions of force and moment resultants given by equations (1.72), (1.73), and (1.74), equation (1.95) can be rewritten as

$$\delta U = \int_{\alpha} \int_{\beta} (N_{\alpha} \delta \epsilon_{\alpha} + N_{\beta} \delta \epsilon_{\beta} + S \delta \epsilon_{\alpha\beta} + M_{\alpha} \delta \kappa_{\alpha} + M_{\beta} \delta \kappa_{\beta} + H \delta \tau) AB \, d\alpha \, d\beta \quad (1.96)$$

where

$$S = N_{\alpha\beta} - \frac{M_{\beta\alpha}}{R_{\beta}} = N_{\beta\alpha} - \frac{1}{R_{\alpha}} M_{\alpha\beta} \quad (1.97a)$$

$$H = \frac{1}{2}(M_{\alpha\beta} + M_{\beta\alpha}) \quad (1.97b)$$

Taking the variation of equation (1.93) yields

$$\begin{aligned} \delta U = & \frac{Eh}{(1-\nu^2)} \int_{\alpha} \int_{\beta} \left\{ \left[(\epsilon_{\alpha} + \nu\epsilon_{\beta}) \delta\epsilon_{\alpha} + (\epsilon_{\beta} + \nu\epsilon_{\alpha}) \delta\epsilon_{\beta} \right. \right. \\ & \left. \left. + \frac{(1-\nu)}{2} \epsilon_{\alpha\beta} \delta\epsilon_{\alpha\beta} \right] \right. \\ & \left. + \frac{h^2}{12} \left[(\kappa_{\alpha} + \nu\kappa_{\beta}) \delta\kappa_{\alpha} + (\kappa_{\beta} + \nu\kappa_{\alpha}) \delta\kappa_{\beta} \right. \right. \\ & \left. \left. + \frac{(1-\nu)}{2} \tau \delta\tau \right] \right\} AB d\alpha d\beta \quad (1.98) \end{aligned}$$

Comparing equations (1.96) and (1.98) leads one to the following relationships:

$$N_{\alpha} = \frac{Eh}{(1-\nu^2)} (\epsilon_{\alpha} + \nu\epsilon_{\beta}) \quad (1.99a)$$

$$N_{\beta} = \frac{Eh}{(1-\nu^2)} (\epsilon_{\beta} + \nu\epsilon_{\alpha}) \quad (1.99b)$$

$$S = \frac{Eh}{2(1+\nu)} \epsilon_{\alpha\beta} \quad (1.99c)$$

$$M_{\alpha} = \frac{Eh^3}{12(1-\nu^2)} (\kappa_{\alpha} + \nu\kappa_{\beta}) \quad (1.99d)$$

$$M_{\beta} = \frac{Eh^3}{12(1-\nu^2)} (\kappa_{\beta} + \nu\kappa_{\alpha}) \quad (1.99e)$$

$$H = \frac{Eh^3}{24(1+\nu)} \tau \quad (1.99f)$$

These are the force and moment relationships given by Novozhilov (ref. 1.26, p. 48).

To obtain relationships for $N_{\alpha\beta}$, $N_{\beta\alpha}$, $M_{\alpha\beta}$, and $M_{\beta\alpha}$ instead of those for S and H given in equations (1.99), some further manipulation is necessary. Define a function φ by

$$\varphi = \frac{1}{2}(M_{\alpha\beta} - M_{\beta\alpha}) \quad (1.100)$$

Adding equations (1.97b) and (1.100) and substituting equation (1.99f) gives

$$M_{\alpha\beta} = \frac{Eh^3}{24(1+\nu)} \tau + \varphi \quad (1.101)$$

Substituting equations (1.97b) and (1.100) similarly leads to

$$M_{\beta\alpha} = \frac{Eh^3}{24(1+\nu)} \tau - \varphi \quad (1.102)$$

Substituting the definitions of the moment resultants given in equations (1.74) into equation (1.100) (remembering $\sigma_{\alpha\beta} = \sigma_{\beta\alpha}$) yields

$$\varphi = \frac{1}{2} \left(\frac{1}{R_{\beta}} - \frac{1}{R_{\alpha}} \right) \int_{-h/2}^{h/2} \sigma_{\alpha\beta} z dz \quad (1.103)$$

and using equation (1.71c) gives further

$$\begin{aligned} \varphi = & \frac{E}{4(1+\nu)} \left(\frac{1}{R_{\beta}} - \frac{1}{R_{\alpha}} \right) \int_{-h/2}^{h/2} z^2 \left(1 + \frac{z}{R_{\alpha}} \right)^{-1} \\ & \left(1 + \frac{z}{R_{\beta}} \right)^{-1} \left[\left(1 - \frac{z^2}{R_{\alpha}R_{\beta}} \right) \epsilon_{\alpha\beta} \right. \\ & \left. + z \left(1 + \frac{z}{2R_{\alpha}} + \frac{z}{2R_{\beta}} \right) \tau \right] dz \quad (1.104) \end{aligned}$$

Integrating equation (1.104) and neglecting terms containing h raised to powers greater than three (actually neglecting powers of h/R_i greater than three with respect to unity, if the equations are put into nondimensional form as was done earlier in this section) yields

$$\varphi = \frac{Eh^3}{48} \left(\frac{1}{R_{\alpha}} - \frac{1}{R_{\beta}} \right) \epsilon_{\alpha\beta} \quad (1.105)$$

Inserting equation (1.105) into equations (1.101) and (1.102) and using the nondimensional form of the twist given by equation (1.90c), one can see that the function φ is of order h/R_i in comparison with unity and, hence, can be neglected. Thus, a consistent set of force and moment relationships for $N_{\alpha\beta}$, $N_{\beta\alpha}$, $M_{\alpha\beta}$, and $M_{\beta\alpha}$ by this theory is, from equations (1.101), (1.102), (1.97a), (1.99f), and (1.99c),

$$\left. \begin{aligned} N_{\alpha\beta} &= \frac{Eh}{2(1+\nu)} \left(\epsilon_{\alpha\beta} + \frac{h^2}{12R_{\beta}} \tau \right) \\ N_{\beta\alpha} &= \frac{Eh}{2(1+\nu)} \left(\epsilon_{\alpha\beta} + \frac{h^2}{12R_{\alpha}} \tau \right) \\ M_{\alpha\beta} &= M_{\beta\alpha} = \frac{Eh^3}{24(1+\nu)} \tau \end{aligned} \right\} \quad (1.106)$$

The force and moment resultant equations given above as derived by Novozhilov (ref. 1.26) (and independently by Balabukh (ref. 1.52) at the same time) are also those which were adopted by Goldenveizer (cf., ref. 1.24, pp. 83, 84, and 230).

1.5.5 Remarks on the Force and Moment Resultant Equations

Essentially three different procedures have been followed in obtaining the force and moment resultant equations given in the preceding sections. Beginning with the defining equations (1.72), (1.73), and (1.74) for the forces and moments, after the stress-strain equations (1.71) are introduced, equations (1.75) corresponding to the theories of Love, Timoshenko, Reissner, Naghdi, Berry, Sanders, Mushtari, and Donnell are arrived at by indiscriminantly neglecting z/R_i ($i = \alpha, \beta$) in comparison with unity. On the other hand, integration of the unsimplified equations (cf., eqs. (1.77)) over the thickness is extremely cumbersome. The theory of Byrne, Flügge, and Lur'ye simplifies the integration and at the same time attempts a more careful discard of terms of higher order by using the series expansion of quotients of the type $1/(1+z/R_i)$. The Vlasov theory does likewise, following a slightly different algebraic manipulation.

Consider now a rationale which could be used to reduce equation (1.78a) of the Byrne-Flügge-Lur'ye theory to the corresponding equation (1.76a) of Love et al. Equation (1.78a) is first rewritten as

$$N_\alpha = \frac{Eh}{(1-\nu^2)} \left\{ \left[1 + \frac{h^2}{12} \left(\frac{1}{R_\alpha^2} - \frac{1}{R_\alpha R_\beta} \right) \right] \epsilon_\alpha + \nu \epsilon_\beta - \frac{h^2}{12} \left(\frac{1}{R_\alpha} - \frac{1}{R_\beta} \right) \kappa_\alpha \right\} \quad (1.107)$$

For a thin shell, it is reasonable to neglect the term $h^2[(1/R_\alpha^2) - (1/R_\alpha R_\beta)]/12$ in equation (1.107) with respect to unity. The second step required to reduce equation (1.107) would be to neglect $h^2[(1/R_\alpha) - (1/R_\beta)]\kappa_\alpha/12$ with respect to $(\epsilon_\alpha + \nu\epsilon_\beta)$. Introducing the nondimensional curvature ϵ'_α given by equation (1.90a), it is seen that the second assumption is valid provided that the strains due to bending are small compared to those due to stretching.

On the other hand, consider the analogous procedure to reduce equation (1.79c) for the twisting moment $M_{\alpha\beta}$ to the corresponding expression of Love et al., equation (1.76f). To do so, it is necessary to neglect the term $\epsilon_{\alpha\beta}/R_\alpha$ in comparison with τ . But substituting equations (1.39) into equation (1.42c) and using equations (1.41), the resulting expanded form for τ contains $\epsilon_{\alpha\beta}/R_\alpha$ as an explicit, non-negligible term. It is therefore inconsistent to neglect $\epsilon_{\alpha\beta}/R_\alpha$ in comparison with τ .

The third procedure, leading to the equations used by Novozhilov and Goldenveizer, avoided inconsistencies of the type described above by taking variations of the strain energy functional and carefully discarding terms.

The force and moment resultant equations arising from the various theories are summarized in tables 1.4 and 1.5.

TABLE 1.4.—Force Resultants According to the Various Theories

Theory	$(1-\nu^2)N_\alpha/Eh$	$(1-\nu^2)N_\beta/Eh$	$2(1+\nu)N_{\alpha\beta}/Eh$	$2(1+\nu)N_{\beta\alpha}/Eh$
Byrne, Flügge, Lur'ye	$\epsilon_\alpha + \nu\epsilon_\beta - \frac{h^2}{12} \left(\frac{1}{R_\alpha} - \frac{1}{R_\beta} \right) \left(\kappa_\alpha - \frac{\epsilon_\alpha}{R_\alpha} \right)$	$\epsilon_\beta + \nu\epsilon_\alpha - \frac{h^2}{12} \left(\frac{1}{R_\beta} - \frac{1}{R_\alpha} \right) \left(\kappa_\beta - \frac{\epsilon_\beta}{R_\beta} \right)$	$\epsilon_{\alpha\beta} - \frac{h^2}{12} \left(\frac{1}{R_\alpha} - \frac{1}{R_\beta} \right) \left(\frac{\tau}{2} - \frac{\epsilon_{\alpha\beta}}{R_\alpha} \right)$	$\epsilon_{\alpha\beta} - \frac{h^2}{12} \left(\frac{1}{R_\beta} - \frac{1}{R_\alpha} \right) \left(\frac{\tau}{2} - \frac{\epsilon_{\alpha\beta}}{R_\beta} \right)$
Goldenveizer, Novozhilov	$\epsilon_\alpha + \nu\epsilon_\beta$	$\epsilon_\beta + \nu\epsilon_\alpha$	$\epsilon_{\alpha\beta} + \frac{h^2}{12R_\beta} \tau$	$\epsilon_{\alpha\beta} + \frac{h^2}{12R_\alpha} \tau$
Love, Timoshenko, Reissner, Berry, Naghdi, Mushtari, Donnell, Sanders	$\epsilon_\alpha + \nu\epsilon_\beta$	$\epsilon_\beta + \nu\epsilon_\alpha$	$\epsilon_{\alpha\beta}$	$\epsilon_{\alpha\beta}$
Vlasov	Same as Byrne, Flügge, Lur'ye	Same as Byrne, Flügge, Lur'ye	$\epsilon_{\alpha\beta} - \frac{h^2}{24} \left(\frac{1}{R_\alpha} - \frac{1}{R_\beta} \right) \tau$	$\epsilon_{\alpha\beta} - \frac{h^2}{24} \left(\frac{1}{R_\beta} - \frac{1}{R_\alpha} \right) \tau$

TABLE 1.5.—*Moment Resultants According to the Various Theories*

Theory	$12(1-\nu^2)M_\alpha/Eh^3$	$12(1-\nu^2)M_\beta/Eh^3$	$24(1+\nu)M_{\alpha\beta}/Eh^3$	$24(1+\nu)M_{\beta\alpha}/Eh^3$
Byrne, Flügge, Lur'ye	$\kappa_\alpha + \nu\kappa_\beta - \left(\frac{1}{R_\alpha} - \frac{1}{R_\beta}\right)\epsilon_\alpha$	$\kappa_\beta + \nu\kappa_\alpha - \left(\frac{1}{R_\beta} - \frac{1}{R_\alpha}\right)\epsilon_\beta$	$\tau - \frac{\epsilon_{\alpha\beta}}{R_\alpha}$	$\tau - \frac{\epsilon_{\alpha\beta}}{R_\beta}$
Goldeneveizer, Novozhilov, Love, Timoshenko, Reissner, Naghdi, Berry, Mushtari, Donnell, Sanders	$\kappa_\alpha + \nu\kappa_\beta$	$\kappa_\beta + \nu\kappa_\alpha$	τ	τ
Vlasov	Same as Flügge, Byrne, Lur'ye	Same as Byrne, Flügge, Lur'ye	$\tau + \frac{\epsilon_{\alpha\beta}}{R_\beta}$	$\tau + \frac{\epsilon_{\alpha\beta}}{R_\alpha}$

1.6 EQUATIONS OF MOTION

At least three distinct methods are used in the literature for obtaining equations of motion, all depending upon the results obtained in the previous sections. The first method is the one most widely used and, hence, is the "standard one." It simply applies Newton's laws by summing forces and moments which act upon a shell element of thickness h . An excellent derivation based on this approach is given in Novozhilov's monograph (ref. 1.26, p. 33). The second method, exemplified by the derivation in section 1.6.2, begins with the equations of motion of an infinitesimal element of the three-dimensional theory of elasticity and integrates them over the thickness to obtain the equations of motion for a shell element. The third method is actually a class of variational methods. One derivation of the variational type depending upon Hamilton's principle was made by Kraus (ref. 1.42, p. 40). Sander's equations derived in section 1.6.4 are also an example of the third method.

In the derivations which follow, for simplicity the equations of motion are derived in the static case, yielding equations which govern the equilibrium of a shell element. However, the equilibrium equations will include body force and body moment terms which are readily capable of representing inertial terms by applying D'Alembert's principle at a later stage.

1.6.1 The Standard Derivation

Consider the equilibrium of the shell element of thickness h shown in figure 1.2 under the

influence of internal force and moment resultants as shown in figures 1.3 and 1.4 and externally applied body forces and moments and surface loads. The total external force intensity vector \vec{q} is the sum of all such effects and can be written as

$$\vec{q} = q_\alpha \hat{l}_\alpha + q_\beta \hat{l}_\beta + q_n \hat{l}_n \quad (1.108)$$

In general, \vec{q} has components in all three directions as indicated, is considered to be acting at the middle surface, and must be multiplied by the area of the middle surface ($AB d\alpha d\beta$) to obtain a true force. Thus, q has the dimensions of force per unit area. In practice it may arise due to externally applied pressures or external fields (gravitational, accelerative, magnetic, etc., see eqs. (1.118) for the integrals defining q_α , q_β , and q_n). Similarly, the moment intensity due to these external fields is given by

$$\vec{m} = m_\alpha \hat{l}_\alpha + m_\beta \hat{l}_\beta + m_n \hat{l}_n \quad (1.109)$$

and has dimensions of moment per unit area.

Let the total forces acting upon the faces defined by $\alpha = \text{constant}$ and by $\beta = \text{constant}$ be denoted by \vec{F}_α and \vec{F}_β , respectively, where

$$\left. \begin{aligned} \vec{F}_\alpha &= (N_\alpha \hat{l}_\alpha + N_{\alpha\beta} \hat{l}_\beta + Q_\alpha \hat{l}_n) B d\beta \\ \vec{F}_\beta &= (N_\beta \hat{l}_\alpha + N_{\beta\alpha} \hat{l}_\beta + Q_\beta \hat{l}_n) A d\alpha \end{aligned} \right\} \quad (1.110)$$

as shown in figure 1.3. Love's second postulate that the deflections are sufficiently small allows

one to refer equations (1.110), which are written naturally in terms of the deformed middle surface, to the undeformed middle surface instead. On the other two faces of the shell element the corresponding forces are $\vec{F}_\alpha + (\partial \vec{F}_\alpha / \partial \alpha) d\alpha$ and $\vec{F}_\beta + (\partial \vec{F}_\beta / \partial \beta) d\beta$. Thus, the vector equation of force equilibrium for the shell element is given by

$$\frac{\partial \vec{F}_\alpha}{\partial \alpha} d\alpha + \frac{\partial \vec{F}_\beta}{\partial \beta} d\beta + \vec{q} AB d\alpha d\beta = 0 \quad (1.111)$$

Substituting equations (1.108) and (1.110) into equation (1.111) and utilizing the rules for differentiation of unit vectors given by equations (1.19), the vector equation can be expanded into its three scalar components as follows:

$$\frac{\partial}{\partial \alpha}(BN_\alpha) + \frac{\partial}{\partial \beta}(AN_{\beta\alpha}) + \frac{\partial A}{\partial \beta}N_{\alpha\beta} - \frac{\partial B}{\partial \alpha}N_\beta + \frac{AB}{R_\alpha}Q_\alpha + ABq_\alpha = 0 \quad (1.112a)$$

$$\frac{\partial}{\partial \beta}(AN_\beta) + \frac{\partial}{\partial \alpha}(BN_{\alpha\beta}) + \frac{\partial B}{\partial \alpha}N_{\beta\alpha} - \frac{\partial A}{\partial \beta}N_\alpha + \frac{AB}{R_\beta}Q_\beta + ABq_\beta = 0 \quad (1.112b)$$

$$-\frac{AB}{R_\alpha}N_\alpha - \frac{AB}{R_\beta}N_\beta + \frac{\partial}{\partial \alpha}(BQ_\alpha) + \frac{\partial}{\partial \beta}(AQ_\beta) + ABq_n = 0 \quad (1.112c)$$

Let the total moments acting upon the faces defined by $\alpha = \text{constant}$ and by $\beta = \text{constant}$ be denoted by $\vec{\mathfrak{M}}_\alpha$ and $\vec{\mathfrak{M}}_\beta$, respectively, where

$$\vec{\mathfrak{M}}_\alpha = (-M_{\alpha\beta}\hat{i}_\alpha + M_\alpha\hat{i}_\beta)B d\beta \quad (1.113a)$$

$$\vec{\mathfrak{M}}_\beta = (-M_\beta\hat{i}_\alpha + M_{\beta\alpha}\hat{i}_\beta)A d\alpha \quad (1.113b)$$

as shown in figure 1.4. On the other two faces of the element the corresponding moments are $\vec{\mathfrak{M}}_\alpha + (\partial \vec{\mathfrak{M}}_\alpha / \partial \alpha) d\alpha$ and $\vec{\mathfrak{M}}_\beta + (\partial \vec{\mathfrak{M}}_\beta / \partial \beta) d\beta$. Thus, the vector equation of moment equilibrium for the shell element is given by

$$\begin{aligned} \frac{\partial \vec{\mathfrak{M}}_\alpha}{\partial \alpha} d\alpha + \frac{\partial \vec{\mathfrak{M}}_\beta}{\partial \beta} d\beta - (\vec{F}_\alpha \times \hat{i}_\beta) \frac{ds_\beta}{2} - (\vec{F}_\beta \times \hat{i}_\alpha) \frac{ds_\alpha}{2} + \left(\vec{F}_\alpha + \frac{\partial \vec{F}_\alpha}{\partial \alpha} d\alpha \right) \times \left(ds_\alpha \hat{i}_\alpha + \frac{ds_\beta}{2} \hat{i}_\beta \right) + \left(\vec{F}_\beta + \frac{\partial \vec{F}_\beta}{\partial \beta} d\beta \right) \\ \times \left(ds_\beta \hat{i}_\beta + \frac{ds_\alpha}{2} \hat{i}_\alpha \right) + \vec{m} AB d\alpha d\beta = 0 \end{aligned} \quad (1.114)$$

where the point 0 has been used as the reference origin for the moments; where the term $(\vec{F}_\alpha \times \hat{i}_\beta) ds_\beta / 2$, for example, represents the moment of the force F_α located by the position vector $(ds_\beta / 2) \hat{i}_\beta$ with respect to 0; and where $ds_\alpha = A d\alpha$ and $ds_\beta = B d\beta$. Substituting equations (1.109), (1.110), and (1.113) into equation (1.114), performing the indicated vector cross products, and utilizing equations (1.19), the vector equation can be expanded into its three scalar components as follows:

$$\frac{\partial}{\partial \alpha}(BM_\alpha) + \frac{\partial}{\partial \beta}(AM_{\beta\alpha}) + \frac{\partial A}{\partial \beta}M_{\alpha\beta} - \frac{\partial B}{\partial \alpha}M_\beta - ABQ_\alpha + ABm_\beta = 0 \quad (1.115a)$$

$$\frac{\partial}{\partial \beta}(AM_\beta) + \frac{\partial}{\partial \alpha}(BM_{\alpha\beta}) + \frac{\partial B}{\partial \alpha}M_{\beta\alpha} - \frac{\partial A}{\partial \beta}M_\alpha - ABQ_\beta + ABm_\alpha = 0 \quad (1.115b)$$

$$N_{\alpha\beta} - N_{\beta\alpha} + \frac{M_{\alpha\beta}}{R_\alpha} - \frac{M_{\beta\alpha}}{R_\beta} = 0 \quad (1.115c)$$

Equations (1.112) and (1.115) form the set of equations of equilibrium used by most authors in shell theory.

1.6.2 An Alternative Derivation

The three-dimensional equations of equilibrium in a set of orthogonal, curvilinear coordinates are given by (cf., ref. 1.50, p. 181)

$$\sum_{j=1}^3 \left[\frac{\partial}{\partial \alpha_j} \left(\frac{g g_{ij}}{\sqrt{g_i g_j}} \right) - \frac{1}{2} \frac{g_{ij}}{g_j} \frac{\partial g_j}{\partial \alpha_i} \right] + q_i^* g \sqrt{g_i} = 0 \quad i=1,2,3 \quad (1.116)$$

where $g = \sqrt{g_1 g_2 g_3}$ and q_i^* is the body force intensity per unit volume. In shell coordinates the indices 1, 2, 3 are replaced by α , β , and z , respectively, and the coefficients of the metric tensor are given by equations (1.28), thus yielding (ref. 1.41)

$$\frac{\partial}{\partial \alpha} (\sqrt{g_\beta} \sigma_\alpha) - \frac{\partial \sqrt{g_\beta}}{\partial \alpha} \sigma_\beta + \frac{\partial}{\partial \beta} (\sqrt{g_\alpha} \sigma_{\alpha\beta}) + \frac{\partial \sqrt{g_\alpha}}{\partial \beta} \sigma_{\alpha\beta} + \frac{\partial}{\partial z} (\sqrt{g_\alpha g_\beta} \sigma_{\alpha z}) + \frac{A \sqrt{g_\beta}}{R_\alpha} \sigma_{\alpha z} + \sqrt{g_\alpha g_\beta} q_\alpha^* = 0 \quad (1.117a)$$

$$\frac{\partial}{\partial \beta} (\sqrt{g_\alpha} \sigma_\beta) - \frac{\partial \sqrt{g_\alpha}}{\partial \beta} \sigma_\alpha + \frac{\partial}{\partial \alpha} (\sqrt{g_\beta} \sigma_{\alpha\beta}) + \frac{\partial \sqrt{g_\beta}}{\partial \alpha} \sigma_{\alpha\beta} + \frac{\partial}{\partial z} (\sqrt{g_\alpha g_\beta} \sigma_{\beta z}) + \frac{B \sqrt{g_\alpha}}{R_\beta} \sigma_{\beta z} + \sqrt{g_\alpha g_\beta} q_\beta^* = 0 \quad (1.117b)$$

$$-\frac{A \sqrt{g_\beta}}{R_\alpha} \sigma_\alpha - \frac{B \sqrt{g_\alpha}}{R_\beta} \sigma_\beta + \frac{\partial}{\partial \alpha} (\sqrt{g_\beta} \sigma_{\alpha z}) + \frac{\partial}{\partial \beta} (\sqrt{g_\alpha} \sigma_{\beta z}) + \frac{\partial}{\partial z} (\sqrt{g_\alpha g_\beta} \sigma_z) + \sqrt{g_\alpha g_\beta} q_n^* = 0 \quad (1.117c)$$

where the symmetry of the stress tensor has been assumed and where the term $\sqrt{g_\alpha g_\beta} q_\alpha^*$ is, for example, a combined body and surface force intensity in the direction \hat{i}_α .

Upon multiplying equations (1.117) through by dz , integrating over the thickness, and making use of the generalized Mainardi-Codazzi equations (1.30) and the definitions of the force resultants given by equations (1.72) and (1.73), one obtains the force equilibrium equations (1.112), with the following definitions for q_α , q_β and q_n :

$$\left. \begin{aligned} q_\alpha &= \frac{1}{AB} [\sqrt{g_\alpha g_\beta} \sigma_{\alpha z}]_{-h/2}^{h/2} + \frac{1}{AB} \int_{-h/2}^{h/2} \sqrt{g_\alpha g_\beta} q_\alpha^* dz \\ q_\beta &= \frac{1}{AB} [\sqrt{g_\alpha g_\beta} \sigma_{\beta z}]_{-h/2}^{h/2} + \frac{1}{AB} \int_{-h/2}^{h/2} \sqrt{g_\alpha g_\beta} q_\beta^* dz \\ q_n &= \frac{1}{AB} [\sqrt{g_\alpha g_\beta} \sigma_z]_{-h/2}^{h/2} + \frac{1}{AB} \int_{-h/2}^{h/2} \sqrt{g_\alpha g_\beta} q_n^* dz \end{aligned} \right\} \quad (1.118)$$

Upon multiplying equations (1.117) through by $z dz$, integrating over the thickness, and making use of equations (1.30) and the definitions of the force and moment resultants given by equations (1.72), (1.73) and (1.74), one obtains the first two moment equilibrium equations (1.115a) and (1.115b). However, equation (1.117c) does not give equation (1.115c); rather, it gives a relationship between M_α , M_β and certain higher order stress resultants not used in classical shell theory.

1.6.3 Equations of Donnell and Mushtari

The equations of Donnell and Mushtari are arrived at by neglecting the terms containing Q_α and Q_β in the two tangential force equilibrium equations (1.112a, b). The remaining force equilibrium equation (1.112c) and the moment equilibrium equations (1.115) remain unchanged.

1.6.4 Equations of Sanders

In section 1.4.5 the strain-displacement equations of Sanders' theory were derived from the principle of virtual work. The "generally accepted" equilibrium equations (1.112) and (1.115) were accepted as basic axioms for which a consistent set of strain-displacements were deduced. However, the process of reducing the number of independent force and moment results (not including Q_α and Q_β) from eight to six requires derivation of a new, consistent set of equilibrium equations by another application of the principle of virtual work.

Beginning with the virtual change in strain energy due to the internal force and moment resultants as given by the area integral in equation (1.61), reintroducing the transverse force resultants Q_α and Q_β , and integrating by parts gives

$$\left. \begin{aligned} & \int_{\alpha} \int_{\beta} (N_{\alpha} \delta \epsilon_{\alpha} + S \delta \epsilon_{\alpha\beta} + N_{\beta} \delta \epsilon_{\beta} + M_{\alpha} \delta \kappa_{\alpha} + H \delta \tau + M_{\beta} \delta \kappa_{\beta} + Q_{\alpha} \delta \gamma_{\alpha z} + Q_{\beta} \delta \gamma_{\beta z}) AB d\alpha d\beta \\ & = \oint_c \left[\left\{ N_{\alpha} \delta u + S \delta v + Q_{\alpha} \delta w + M_{\alpha} \delta \theta_{\alpha} + H \delta \left[\theta_{\beta} + \frac{1}{2} \left(\frac{1}{R_{\beta}} - \frac{1}{R_{\alpha}} \right) v \right] \right\} B \delta \beta \right. \\ & \quad \left. - \left\{ N_{\beta} \delta v + S \delta u + Q_{\beta} \delta w + M_{\beta} \delta \theta_{\beta} + H \delta \left[\theta_{\alpha} + \frac{1}{2} \left(\frac{1}{R_{\alpha}} - \frac{1}{R_{\beta}} \right) u \right] \right\} A \delta \alpha \right] \\ & \quad \left. - \int_{\alpha} \int_{\beta} (F_1 \delta u + F_2 \delta v + F_3 \delta w + F_4 \delta \theta_{\alpha} + F_5 \delta \theta_{\beta}) d\alpha d\beta \right\} \quad (1.119) \end{aligned}$$

where the functionals F_1, \dots, F_5 are defined by

$$\left. \begin{aligned} F_1 &= \frac{\partial}{\partial \alpha} (BN_{\alpha}) + \frac{\partial}{\partial \beta} (AS) + S \frac{\partial A}{\partial \beta} - N_{\beta} \frac{\partial B}{\partial \alpha} + \frac{A}{2} \frac{\partial}{\partial \beta} \left[\left(\frac{1}{R_{\alpha}} - \frac{1}{R_{\beta}} \right) H \right] + \frac{AB}{R_{\alpha}} Q_{\alpha} \\ F_2 &= \frac{\partial}{\partial \beta} (AN_{\beta}) + \frac{\partial}{\partial \alpha} (BS) + S \frac{\partial B}{\partial \alpha} - N_{\alpha} \frac{\partial A}{\partial \beta} + \frac{B}{2} \frac{\partial}{\partial \alpha} \left[\left(\frac{1}{R_{\beta}} - \frac{1}{R_{\alpha}} \right) H \right] + \frac{AB}{R_{\beta}} Q_{\beta} \\ F_3 &= -\frac{AB}{R_{\alpha}} N_{\alpha} - \frac{AB}{R_{\beta}} N_{\beta} + \frac{\partial}{\partial \alpha} (BQ_{\alpha}) + \frac{\partial}{\partial \beta} (AQ_{\beta}) \\ F_4 &= \frac{\partial}{\partial \alpha} (BM_{\alpha}) + \frac{\partial}{\partial \beta} (AH) + H \frac{\partial A}{\partial \beta} - M_{\beta} \frac{\partial B}{\partial \alpha} - ABQ_{\alpha} \\ F_5 &= \frac{\partial}{\partial \beta} (AM_{\beta}) + \frac{\partial}{\partial \alpha} (BH) + H \frac{\partial B}{\partial \alpha} - M_{\alpha} \frac{\partial A}{\partial \beta} - ABQ_{\beta} \end{aligned} \right\} \quad (1.120)$$

For the shell to be in equilibrium, the principle of virtual work requires that the left-hand side of equation (1.119) must equal the line integral on the right-hand side, in which case the area integral on the right-hand side must vanish. Because the virtual displacements $\delta u, \dots, \delta \theta_{\beta}$ are independent and arbitrary, each term of the area integral must vanish independently. Thus, setting

$$F_1 = F_2 = F_3 = F_4 = F_5 = 0 \quad (1.121)$$

in equations (1.120) equal to zero gives the modified equations of equilibrium for the internal forces according to Sanders' theory. Adding suitable inertia terms to them gives corresponding equations of motion.

1.6.5 Remarks on the Equations of Motion

There is widespread agreement on what constitutes the equations of motion. Equations (1.112) and (1.115) were directly arrived at either by summing force and moment resultants acting upon a shell element, or by integrating the three-dimensional equilibrium equations of elasticity. Kraus (ref. 1.42) obtained the same equations by means of variational calculus and Hamilton's principle. Sanders' equations (1.120) and (1.121) were seen to be different. This difference resulted from his initial assumption that the rotation about the normal θ_n , is a basic entity to be included in the virtual work principle and then later redefining θ_n to be dependent upon u and v (cf., eq. (1.54)). As a result of this redefinition, a second application of the principle of virtual work resulted in additional terms appearing in the force equilibrium equations taken in the α and β directions (that is, corresponding to u and v).

If the sixth equilibrium equation (1.115c) is rewritten in terms of the force and moment resultants (eqs. (1.72), (1.73), and (1.74)) then it becomes

$$\int_{-h/2}^{h/2} (\sigma_{\alpha\beta} - \sigma_{\beta\alpha}) \left(1 + \frac{z}{R_\alpha}\right) \left(1 + \frac{z}{R_\beta}\right) dz = 0 \quad (1.122)$$

which is identically satisfied if the symmetry of the stress tensor is assumed. This symmetry was assumed *a priori* in the alternative derivation given in section 1.6.2.

1.7 SYNTHESIS OF EQUATIONS

At this point the equations governing the motion of each point within a shell are now complete for each theory considered except for the boundary conditions (initial conditions are not needed for the problem of determining free vibration frequencies and mode shapes for a given configuration). Because of the relatively large numbers of equations and unknowns which were necessarily introduced in the preceding sections, it is now desirable to delineate the necessary and sufficient sets of equations which define the motion and lay out the procedure which is customarily followed in combining them to reduce their number. A summary of the sets

of equations and the independent and dependent variables is now given.

Strain-displacement equations. Six strain-displacement equations are summarized for each theory by equations (1.41) and tables 1.2 and 1.3. Substituting for the rotations θ_α and θ_β from equations (1.39), there remain six generalized components of strain ϵ_α , ϵ_β , $\epsilon_{\alpha\beta}$, κ_α , κ_β , and τ which are given explicitly in terms of the three displacement components u , v , and w .

Force and moment resultants. Eight equations summarized by tables 1.4 and 1.5 express the eight force and moment resultants N_α , N_β , $N_{\alpha\beta}$, $N_{\beta\alpha}$, M_α , M_β , $M_{\alpha\beta}$, and $M_{\beta\alpha}$ as explicit functions of the six strain components ϵ_α , ϵ_β , $\epsilon_{\alpha\beta}$, κ_α , κ_β , and τ .

Equations of motion. Five equations of motion must be satisfied. These are given by equations (1.112) and (1.115a and b) (or by equations (1.120) and (1.121) in the case of the Sanders theory). Equation (1.115c) is satisfied identically. The five equations are implicit relations among the ten force and moment resultants N_α , N_β , $N_{\alpha\beta}$, $N_{\beta\alpha}$, Q_α , Q_β , M_α , M_β , $M_{\alpha\beta}$, and $M_{\beta\alpha}$.

Thus, in general, there are 19 equations relating 19 unknowns— u , v , w ; ϵ_α , ϵ_β , $\epsilon_{\alpha\beta}$, κ_α , κ_β , τ ; N_α , N_β , $N_{\alpha\beta}$, $N_{\beta\alpha}$, Q_α , Q_β , M_α , M_β , $M_{\alpha\beta}$, $M_{\beta\alpha}$. For some theories (e.g., Love, Timoshenko, Reissner), $N_{\alpha\beta} = N_{\beta\alpha}$ and $M_{\alpha\beta} = M_{\beta\alpha}$, thereby reducing the number of equations and unknowns to 17.

The usual procedure followed to reduce the number of equations and unknowns to a more manageable number is to begin by eliminating Q_α and Q_β from the five equations of motion, which reduces their number to three. This is done, for example, by solving equations (1.115a and b) for Q_α and Q_β and substituting into equations (1.112). The force and moment resultant expressions are then substituted into the equations of motion, giving them in terms of the generalized strains. Finally, the strain-displacement equations are substituted, yielding three differential equations of motion having u , v , and w as dependent variables and α , β , and t (time) as independent variables. The set of differential equations is of the eighth order.

Time enters the equations of motion through inertial terms. For the free vibration problem the body force intensities q_α , q_β , and q_n will be

replaced by their translatory inertia equivalents given by

$$\left. \begin{aligned} q_\alpha &= -\rho h \frac{\partial^2 u}{\partial t^2} \\ q_\beta &= -\rho h \frac{\partial^2 v}{\partial t^2} \\ q_n &= -\rho h \frac{\partial^2 w}{\partial t^2} \end{aligned} \right\} \quad (1.123)$$

where ρ is mass density per unit volume and t is time. Rotary inertia can be included by suitably replacing m_α , and m_β in equations (1.115a and b), but this effect is generally negligible unless the shells become relatively thick (say, $h/R > 1/10$, where R is the *least* radius of curvature of the shell). However, in this case it becomes equally important to include the effects of shear deformation, which requires a complete reformulation of the shell theory and leads to a tenth order set of differential equations of motion. Thus, the effects of shear deformation and rotary inertia will be considered as a separate subject in later chapters.

Following the systematic procedure outlined in the paragraph before the last, it would be possible to display general equations of motion in terms of u , v , and w for shells having *arbitrary* curvature properties. However, the equations would be extremely unwieldy, especially when the radii of curvature R_α and R_β (and, consequently, the Lamé parameters A and B) are not constant, but depend upon α and β . Thus, the procedure will be followed only for specific curvatures (cylindrical, spherical, conical, etc.) and the resulting equations of motion will be presented where relevant in the subsequent chapters.

If the equations of motion are solved to find u , v , and w (in the case of free vibration the mode shape is determined), then the resulting stresses σ_α , σ_β and $\sigma_{\alpha\beta}$ can be found in the following manner:

(1) Substitute u , v , and w into the strain-displacement equations.

(2) Determine the strains at points throughout the shell thickness (particularly at $z = \pm h/2$) by using the expressions given in table 1.1.

(3) Find the stress components at any point by means of the stress-strain equations (1.71).

1.8 BOUNDARY CONDITIONS

Assume that the boundaries lie along coordinate curves. The work done by the reactions at the boundaries is zero; i.e.,

$$W_1 = \int_{\beta_1}^{\beta_2} (\vec{F}_\alpha \cdot \vec{u} + \vec{\mathcal{M}}_\alpha \cdot \vec{\Omega}) \Big|_{\alpha=\alpha_2} B d\beta = 0 \quad (1.124)$$

along the boundary $\alpha = \alpha_2$ and

$$W_2 = \int_{\alpha_1}^{\alpha_2} (\vec{F}_\beta \cdot \vec{u} + \vec{\mathcal{M}}_\beta \cdot \vec{\Omega}) \Big|_{\beta=\beta_2} A d\alpha = 0 \quad (1.125)$$

along the boundary $\beta = \beta_2$. The vectors \vec{F}_α , \vec{F}_β , $\vec{\mathcal{M}}_\alpha$ and $\vec{\mathcal{M}}_\beta$ are given by equations (1.110a and b) and (1.113a and b), respectively, and

$$\vec{u} = u\hat{i}_\alpha + v\hat{i}_\beta + w\hat{i}_n \quad (1.126)$$

$$\vec{\Omega} = -\theta_\beta\hat{i}_\alpha + \theta_\alpha\hat{i}_\beta \quad (1.127)$$

By substituting equations (1.110), (1.113), (1.126), (1.127), and (1.39) into equations (1.124) and (1.125), one obtains

$$\left. \begin{aligned} W_1 &= \int_{\beta_1}^{\beta_2} \left[N_\alpha u + N_{\alpha\beta} v + Q_\alpha w + M_{\alpha\beta} \left(\frac{v}{R_\beta} - \frac{1}{B} \frac{\partial w}{\partial \beta} \right) + M_\alpha \theta_\alpha \right]_{\alpha=\alpha_2} B d\beta = 0 \\ W_2 &= \int_{\alpha_1}^{\alpha_2} \left[N_{\beta\alpha} u + N_\beta v + Q_\beta w + M_{\beta\alpha} \theta_\beta + M_{\beta\alpha} \left(\frac{u}{R_\alpha} - \frac{1}{A} \frac{\partial w}{\partial \alpha} \right) \right]_{\beta=\beta_2} A d\alpha = 0 \end{aligned} \right\} \quad (1.128)$$

but, integrating by parts

$$\left. \begin{aligned} \int_{\beta_1}^{\beta_2} M_{\alpha\beta} \frac{\partial w}{\partial \beta} d\beta &= M_{\alpha\beta} w \Big|_{\beta_1}^{\beta_2} - \int_{\beta_1}^{\beta_2} \frac{\partial}{\partial \beta} (M_{\alpha\beta}) w d\beta \\ \int_{\alpha_1}^{\alpha_2} M_{\beta\alpha} \frac{\partial w}{\partial \alpha} d\alpha &= M_{\beta\alpha} w \Big|_{\alpha_1}^{\alpha_2} - \int_{\alpha_1}^{\alpha_2} \frac{\partial}{\partial \alpha} (M_{\beta\alpha}) w d\alpha \end{aligned} \right\} \quad (1.129)$$

By substituting equations (1.129) into equations (1.128) and collecting terms, one obtains

$$W_1 = \int_{\beta_1}^{\beta_2} \left[N_\alpha u + \left(N_{\alpha\beta} + \frac{M_{\alpha\beta}}{R_\beta} \right) v + \left(Q_\alpha + \frac{1}{B} \frac{\partial M_{\alpha\beta}}{\partial \beta} \right) w + M_\alpha \theta_\alpha \right]_{\alpha=\alpha_2}^{\alpha=\alpha_1} B d\beta - M_{\alpha\beta} w \Big|_{\beta_1}^{\beta_2} = 0 \quad (1.130a)$$

$$W_2 = \int_{\alpha_1}^{\alpha_2} \left[\left(N_{\beta\alpha} + \frac{M_{\beta\alpha}}{R_\alpha} \right) u + N_\beta v + \left(Q_\beta + \frac{1}{A} \frac{\partial M_{\beta\alpha}}{\partial \alpha} \right) w + M_\beta \theta_\beta \right]_{\beta=\beta_2}^{\beta=\beta_1} A d\alpha - M_{\beta\alpha} w \Big|_{\alpha_1}^{\alpha_2} = 0 \quad (1.130b)$$

Equations (1.130) are satisfied if the integrand and the second parts of the equations are set equal to zero. Thus the boundary conditions, on an edge where $\alpha = \text{constant}$, are

$$N_\alpha \quad \text{or} \quad u = 0 \quad (1.131a)$$

$$\left(N_{\alpha\beta} + \frac{M_{\alpha\beta}}{R_\beta} \right) \quad \text{or} \quad v = 0 \quad (1.131b)$$

$$\left(Q_\alpha + \frac{1}{B} \frac{\partial M_{\alpha\beta}}{\partial \beta} \right) \quad \text{or} \quad w = 0 \quad (1.131c)$$

$$M_\alpha \quad \text{or} \quad \theta_\alpha = 0 \quad (1.131d)$$

$$M_{\alpha\beta} w \Big|_{\beta_1}^{\beta_2} = 0 \quad (1.131e)$$

and on an edge where $\beta = \text{constant}$

$$\left(N_{\beta\alpha} + \frac{M_{\beta\alpha}}{R_\alpha} \right) \quad \text{or} \quad u = 0 \quad (1.132a)$$

$$N_\beta \quad \text{or} \quad v = 0 \quad (1.132b)$$

$$\left(Q_\beta + \frac{1}{A} \frac{\partial M_{\beta\alpha}}{\partial \alpha} \right) \quad \text{or} \quad w = 0 \quad (1.132c)$$

$$M_\beta \quad \text{or} \quad \theta_\beta = 0 \quad (1.132d)$$

$$M_{\beta\alpha} w \Big|_{\alpha_1}^{\alpha_2} = 0 \quad (1.132e)$$

If the β curve is a closed curve, then equation (1.131e) is identically satisfied. Similarly, if the α curve is a closed curve, equation (1.132e) is identically satisfied. Equations (1.131) and (1.132) are the boundary conditions associated with the equations of equilibrium given in equations (1.112) and (1.115).

The boundary conditions associated with Sanders' equations of equilibrium are obtained by setting the virtual work of the forces acting on the boundaries of the shell equal to zero. Thus from equation (1.119) one obtains

$$N_\alpha \quad \text{or} \quad u = 0 \quad (1.133a)$$

$$\left[S + \left(\frac{3}{2R_\beta} - \frac{1}{2R_\alpha} \right) H \right] \quad \text{or} \quad v = 0 \quad (1.133b)$$

$$\left(Q_\alpha + \frac{1}{B} \frac{\partial H}{\partial \beta} \right) \quad \text{or} \quad w = 0 \quad (1.133c)$$

$$M_\alpha \quad \text{or} \quad \theta_\alpha = 0 \quad (1.133d)$$

$$Hw \Big|_{\beta_1}^{\beta_2} = 0 \quad (1.133e)$$

on an edge where $\alpha = \text{constant}$ and

$$\left[S + \left(\frac{3}{2R_\alpha} - \frac{1}{2R_\beta} \right) \right] \quad \text{or} \quad u = 0 \quad (1.134a)$$

$$N_\beta \quad \text{or} \quad v = 0 \quad (1.134b)$$

$$\left(Q_\alpha + \frac{1}{A} \frac{\partial H}{\partial \alpha} \right) \quad \text{or} \quad w = 0 \quad (1.134c)$$

$$M_\beta \quad \text{or} \quad \theta_\beta = 0 \quad (1.134d)$$

$$Hw \Big|_{\alpha_1}^{\alpha_2} = 0 \quad (1.134e)$$

on an edge where $\beta = \text{constant}$.

1.9 SHALLOW SHELL THEORY

A shallow shell may be regarded as a slightly curved plate. A shell whose smallest radius of curvature at every point is large compared with the greatest lengths measured along the middle surface of the shell is one definition of a shallow shell. Vlasov (ref. 1.19) describes a shallow shell as follows:

Consider a shell outlined in part by some surface and which is a thin-walled spatial structure with a comparatively small rise above the plane covered by this structure. We call such shells shallow. If, for example, a building which has a rectangular floor plan is covered by a shell with a rise of not more than 1/5 of the smallest side of the rectangle lying in the plane of the supporting points of the structure, then we class such a spatial structure in the category of shallow shells.

The development of the shallow shell theory is principally credited to Marguerre (ref. 1.53),

Reissner (refs. 1.54 and 1.55), and Vlasov (ref. 1.19). An extensive bibliography on shallow shells is given by Leissa and Kadi (ref. 1.56).

No attempt to present a rigorous derivation of shallow shell theory will be made in this section. For rigorous derivations the reader is referred particularly to references 1.19, 1.54, 1.55, and 1.56. The primary purpose of this section is simply to present the shallow shell equations for shells having arbitrary curvatures for reference in subsequent chapters.

The terms containing Q_α and Q_β in the first two equilibrium equations (1.112a) and (1.112b) are neglected as in the Donnell-Mushtari theory (sec. 1.6.3). Further, the tangential loads q_α and q_β (which are tangential inertia terms in the free vibration problem) are neglected. With these two assumptions equations (1.112a) and (1.112b) are identically satisfied by the introduction of an Airy type of stress function φ defined by

$$\left. \begin{aligned} N_\alpha &= \frac{1}{B} \frac{\partial}{\partial \beta} \left(\frac{1}{B} \frac{\partial \varphi}{\partial \beta} \right) + \frac{1}{A^2 B} \frac{\partial B}{\partial \alpha} \frac{\partial \varphi}{\partial \alpha} \\ N_\beta &= \frac{1}{A} \frac{\partial}{\partial \alpha} \left(\frac{1}{A} \frac{\partial \varphi}{\partial \alpha} \right) + \frac{1}{A B^2} \frac{\partial A}{\partial \beta} \frac{\partial \varphi}{\partial \beta} \\ N_{\alpha\beta} &= N_{\beta\alpha} = - \frac{1}{AB} \left(\frac{\partial^2 \varphi}{\partial \alpha \partial \beta} - \frac{1}{A} \frac{\partial A}{\partial \beta} \frac{\partial \varphi}{\partial \alpha} - \frac{1}{B} \frac{\partial B}{\partial \alpha} \frac{\partial \varphi}{\partial \beta} \right) \end{aligned} \right\} \quad (1.135)$$

The expressions for changes of curvature are taken as in the Donnell-Mushtari theory (eqs. 1.63) and the compatibility condition for displacements of the middle surface are approximated (in particular, the Gaussian curvature, $1/R_\alpha R_\beta$, is assumed negligibly small). The resulting equations of equilibrium and compatibility which govern the deflected region of a shallow shell then become, respectively (ref. 1.19)

$$\left. \begin{aligned} D \nabla^4 w + \nabla_R^2 \varphi &= q_n \\ \nabla^4 \varphi - E h \nabla_R^2 w &= 0 \end{aligned} \right\} \quad (1.136)$$

where $\nabla^4 = \nabla^2 \nabla^2$ and

$$D = \frac{E h^3}{12(1-\nu^2)} \quad (1.137)$$

$$\left. \begin{aligned} \nabla^2 &= \frac{1}{AB} \left[\frac{\partial}{\partial \alpha} \left(\frac{B}{A} \frac{\partial}{\partial \alpha} \right) + \frac{\partial}{\partial \beta} \left(\frac{A}{B} \frac{\partial}{\partial \beta} \right) \right] \\ \nabla_R^2 &= \frac{1}{AB} \left[\frac{\partial}{\partial \alpha} \left(\frac{1}{R_2} \frac{B}{A} \frac{\partial}{\partial \alpha} \right) + \frac{\partial}{\partial \beta} \left(\frac{1}{R_1} \frac{A}{B} \frac{\partial}{\partial \beta} \right) \right] \end{aligned} \right\} \quad (1.138)$$

Further, according to the shallow shell theory

$$\left. \begin{aligned} M_\alpha &= -D(\kappa_\alpha + \nu \kappa_\beta) \\ M_\beta &= -D(\kappa_\beta + \nu \kappa_\alpha) \\ M_{\alpha\beta} &= M_{\beta\alpha} = -\frac{D}{2} \tau \end{aligned} \right\} \quad (1.139)$$

and

$$\left. \begin{aligned} Q_\alpha &= \frac{D}{A} \frac{\partial}{\partial \alpha} (\kappa_1 + \kappa_2) \\ Q_\beta &= \frac{D}{B} \frac{\partial}{\partial \beta} (\kappa_1 + \kappa_2) \end{aligned} \right\} \quad (1.140)$$

with the expressions for κ_1 , κ_2 , and τ given by equations (1.63). The governing eighth order set of equations (1.136) is then solved in terms of the two dependent variables w and φ , with physical quantities being determined from equations (1.135), (1.139), and (1.140).

REFERENCES

1. KOITER, W. T.: A Consistent First Approximation in the General Theory of Thin Elastic Shells. Proc. Symp. on Theory of Thin Elastic Shells, I.U.T.A.M. (Delft), 24-28 Aug. 1959, North Holland Pub. Co. (Amsterdam), 1960, pp. 12-33.
2. JOHN, F.: Estimates for the Derivatives of the Stress in Thin Shells and Interior Shell Equations. Comm. Pure and Appl. Math., vol. 18, no. 12, 1965.
3. BUDIANSKY, B.; AND SANDERS, J. L.: On the 'Best' First Order Linear Shell Theory. Prog. Appl. Mech., The Prager Anniversary Volume, Mac-Millan (New York), 1963, pp. 129-140.
4. GOLDENVEIZER, A. L.: Method for Justifying and Refining the Theory of Shells (Survey of Recent Results). Appl. Math. Mech. (transl. of Prikl. Mat. Mekh.), vol. 32, no. 4, Mar. 1968, pp. 704-718.
5. NOVOZHILOV, V. V.; AND FINKELSHTEIN, R. O.: On the Error in Kirchhoff's Hypothesis in the Theory of Shells. Prikl. Mat. Mekh., vol. 7, no. 5, 1943.
6. HOUGHTON, D. S.; AND JOHNS, D. J.: A Comparison of the Characteristic Equations in the Theory of Circular Cylindrical Shells. Aeronaut. Quart., Aug. 1961, pp. 228-236.

- 1.7. KLOSNER, J. M.; AND LEVINE, H. S.: Further Comparison of Elasticity and Shell Theory Solutions. *AIAA J.*, vol. 4, no. 3, Mar. 1966, pp. 467-480.
- 1.8. NIGUL, U. K.: Linear Equations for the Dynamics of a Circular Cylindrical Shell, Free of Assumptions. *Trud. Tallin. politech. inst-ta*, no. 176, 1960. (In Russian.)
- 1.9. DONNELL, L. H.: Stability of Thin Walled Tubes Under Torsion. *NACA Rept. No. 479*, 1933.
- 1.10. DONNELL, L. H.: A Discussion of Thin Shell Theory. *Proc. Fifth Intern. Congr. Appl. Mech.*, 1938.
- 1.11. MUSHTARI, KH. M.: On the Stability of Cylindrical Shells Subjected to Torsion. *Trudy Kaz. avais, in-ta*, 2, 1938. (In Russian.)
- 1.12. MUSHTARI, KH. M.: Certain Generalizations of the Theory of Thin Shells. *Izv. Fiz. Mat. ob-va. pri Kaz. un-te*, vol. 11, no. 8, 1938. (In Russian.)
- 1.13. LOVE, A. E. H.: A Treatise on the Mathematical Theory of Elasticity. First ed., Cambridge Univ. Press, 1892; fourth ed., Dover Pub., Inc. (New York), 1944.
- 1.14. LOVE, A. E. H.: The Small Free Vibrations and Deformations of a Thin Elastic Shell. *Phil. Trans. Roy. Soc. (London)*, ser. A, 179, 1888, pp. 491-549.
- 1.15. TIMOSHENKO, S.: *Theory of Plates and Shells*. McGraw-Hill (New York), 1959.
- 1.16. REISSNER, E.: A New Derivation of the Equations of the Deformation of Elastic Shells. *Amer. J. Math.*, vol. 63, no. 1, Jan. 1941, pp. 177-184.
- 1.17. NAGHDI, P. M.; AND BERRY, J. G.: On the Equations of Motion of Cylindrical Shells. *J. Appl. Mech.*, vol. 21, no. 2, June 1964, pp. 160-166.
- 1.18. VLASOV, V. Z.: *Osnovnye Differentsialnye Uravnenia Obshche Teorii Uprugikh Obolochek*. Prikl. Mat. Mekh., vol. 8, 1944. (English transl.: *NACA TM 1241*, Basic Differential Equations in the General Theory of Elastic Shells, Feb. 1951.)
- 1.19. VLASOV, V. Z.: *Obshchaya teoriya obolochek; yeye prilozheniya v tekhnike*. Gos. Izd. Tekh.-Teor. Lit., Moscow-Leningrad, 1949. (English transl.: *NASA TT F-99*, General Theory of Shells and Its Applications in Engineering, Apr. 1964.)
- 1.20. SANDERS, J. L., JR.: An Improved First Approximation Theory for Thin Shells. *NASA TR-R24*, 1959.
- 1.21. BYRNE, R.: Theory of Small Deformations of a Thin Elastic Shell. *Seminar Reports in Math.*, Univ. of Calif. Pub. in Math., N.S. vol. 2, no. 1, 1944, pp. 103-152.
- 1.22. FLÜGGE, W.: *Statik und Dynamik der Schalen*. Julius Springer (Berlin), 1934. (Reprinted by Edwards Brothers Inc., Ann Arbor, Mich., 1943.)
- 1.23. FLÜGGE, W.: *Stresses in Shells*. Springer-Verlag (Berlin), 1962.
- 1.24. GOLDENVEIZER, A. L.: *Theory of Thin Shells*. Pergamon Press (New York), 1961.
- 1.25. LUR'YE, A. I.: General Theory of Elastic Shells. *Prikl. Mat. Mekh.*, vol. 4, no. 1, 1940, pp. 7-34. (In Russian.)
- 1.26. NOVOZHILOV, V. V.: *The Theory of Thin Elastic Shells*. P. Noordhoff Lts (Groningen, The Netherlands), 1964.
- 1.27. ARON, H.: Das Gleichgewicht und die Bewegung einer unendlich dünnen, beliebig gekrümmten elastischen Schale. *J. für Math.*, vol. 78, 1874, pp. 136-174.
- 1.28. BASSET, A. B.: On the Extension and Flexure of Cylindrical and Spherical Thin Shells. *Phil. Trans. Roy. Soc. (London)*, ser. A, vol. 181, no. 6, 1890, pp. 433-480.
- 1.29. EPSTEIN, P. S.: On the Theory of Elastic Vibrations in Plates and Shells. *J. Math. Phys.*, vol. 21, 1942, pp. 198-209.
- 1.30. TREFFTZ, E.: Ableitung der Schalenbiegungsgleichungen mit dem Castiglianoschen Prinzip. *ZAMM*, Bd. 15, 1935, pp. 101-108.
- 1.31. SYNGE, J. L.; AND CHIEN, W. Z.: The Intrinsic Theory of Elastic Shells and Plates. *Applied Mechanics. Theodore von Kármán Anniversary Volume*, 1941, pp. 103-120.
- 1.32. CHIEN, W. Z.: The Intrinsic Theory of Thin Shells and Plates. Part I.—General Theory. *Quart. Appl. Math.*, vol. I, no. 4, Jan. 1944, pp. 297-327; Part III.—Application to Thin Shells, vol. II, no. 2, July 1944, pp. 120-135.
- 1.33. LAMB, H.: On the Deformation of an Elastic Shell. *Proc. Lond. Math. Soc.*, vol. 21, 1891, pp. 119-146.
- 1.34. OSGOOD, W. A.; AND JOSEPH, J. A.: On the Strain Energy of Shells. *J. Appl. Mech.*, vol. 17, no. 4, Dec. 1950, pp. 397-398.
- 1.35. HAYWOOD, J. H.; AND WILSON, L. B.: The Strain-Energy Expression for Thin Elastic Shells. *J. Appl. Mech.*, vol. 25, no. 4, Dec. 1958, pp. 546-552.
- 1.36. KOITER, W. T.: The Stability of Elastic Equilibrium. Chapter 5: Shell Theory for Finite Deflections. *Dissertation, Technische Hooze School, Delft*, 1945. (In Dutch.) (English Transl.: *Tech. Rept. AFFDL-TR-70-25*, Air Force Flight Dynamics Lab., Air Force Systems Command, Wright-Patterson AFB, Feb. 1970.)
- 1.37. COHEN, J. W.: On Stress Calculations in Helicoidal Shells and Propeller Blades. *Dissertation, Technische Hooze School, Delft*, 1955.
- 1.38. COHEN, J. W.: The Inadequacy of the Classical Stress-Strain Relations for the Right Helicoidal Shell. *Proc. Symp. on Theory of Thin Shells, I.U.T.A.M. (Delft)*, Aug. 24-28, 1959, North-Holland Publishing Co. (Amsterdam), 1960, pp. 415-433.
- 1.39. KNOWLES, J. K.; AND REISSNER, E.: A Derivation of the Equations of Shell Theory for General Orthogonal Coordinates. *J. Math. Phys.*, vol. 35, no. 4, 1957, pp. 351-358.
- 1.40. KNOWLES, J. K.; AND REISSNER, E.: Notes on the Stress-Strain Relations for Thin Elastic Shells. *J. Math. Phys.*, vol. 37, no. 3, Oct. 1958, pp. 269-282.
- 1.41. HILDEBRAND, F. B.; REISSNER, E.; AND THOMAS, G. B.: Notes on the Foundation of the Theory of

- Small Displacements of Orthotropic Shells. NACA TN 1833, Mar. 1949, pp. 1-59.
- 1.42. KRAUS, H.: Thin Elastic Shells. John Wiley and Sons, Inc. (New York), 1967.
- 1.43. NAGHDI, P. M.: A Survey of Recent Progress in the Theory of Elastic Shells. Appl. Mech. Reviews, vol. 9, no. 9, Sept. 1956, pp. 365-367.
- 1.44. KADI, A. S.: A Study and Comparison of the Equations of Thin Shell Theories. Dissertation, Ohio State University, June 1970.
- 1.45. HU, W. C. L.: A Rigorous Derivation of Second-Approximation Theory of Elastic Shells. Tech. Rept. No. 5, Contract NASr-94(06), SwRI Proj. 02-1504, Southwest Research Institute, Nov. 10, 1965.
- 1.46. KALNINS, A.: Dynamic Problems of Elastic Shells. Appl. Mech. Reviews, vol. 18, no. 11, Nov. 1965, pp. 867-872.
- 1.47. SIMMONDS, J. G.: A Set of Simple, Accurate Equations for Circular Cylindrical Elastic Shells. Report SM-4 (NASA N66-15403), Div. of Eng. and Appl. Phys., Harvard Univ., 1966.
- 1.48. KREYSZIG, E.: Advanced Engineering Mathematics. John Wiley and Sons, Inc. (New York), 1966.
- 1.49. WEATHERBURN, C. E.: Differential Geometry. Cambridge Press, 1927.
- 1.50. SOKOLNIKOFF, I. S.: Mathematical Theory of Elasticity. McGraw-Hill (New York), 1956.
- 1.51. PHILLIPS, H. B.: Vector Analysis. John Wiley and Sons, Inc. (New York), 1933.
- 1.52. BALABUKH, L. I.: Bending and Torsion of Conical Shells. Trud. Tsentr. aero-gl'dr. inst., no. 577, 1946.
- 1.53. MARGUERRE, K.: Zur Theorie der gekrümmten Platte grosser Formänderung. Proc. Fifth Intern. Congr. Appl. Mech., 1938, pp. 93-101.
- 1.54. REISSNER, E.: Stress and Displacements of Shallow Spherical Shells. J. Math. Phys., pt. I, vol. 25, 1946, pp. 80-85; pt. II, vol. 26, 1947, pp. 279-300.
- 1.55. REISSNER, E.: On the Determination of Stresses and Displacements for Unsymmetrical Deformations of Shallow Spherical Shells. J. Math. Phys., vol. 38, 1959, pp. 16-35.
- 1.56. LEISSA, A. W.; AND KADI, A. S.: Analysis of Shallow Shells by the Method of Point Matching. Tech. Rept. AFFDL-TR-69-71, Air Force Flight Dynamics Lab., Air Force Systems Command, Wright-Patterson AFB, Aug. 1969.

Thin Circular Cylindrical Shells

This chapter will be limited to the study of thin circular cylindrical shells, *not* including the effects of initial stress, anisotropy, variable thickness, shear deformation, rotary inertia, large deflections, nonhomogeneity, or surrounding media. These complicating effects will be studied (as they pertain to circular cylindrical shells) in chapter 3.

Nevertheless, there is a great deal of complexity in the organization of the remaining material. The standard or classical theories of thin shells are governed by eighth order systems of differential equations which, as was seen in chapter 1, take many forms, depending upon the assumptions made. For some problems, simplifying assumptions leading to the fourth order inextensional or extensional theories can be justified. Cylindrical shells can be opened or closed, and edge restraint conditions can take many forms. Several physical parameters can be varied, including

- (1) Number of circumferential waves
- (2) Thickness/radius ratio
- (3) Length/radius ratio
- (4) Poisson's ratio.

The governing differential equations of motion are sometimes simplified by neglecting tangential inertia, or by neglecting other terms in the equations for various justifying reasons. Solution of the governing equations is often accomplished by one of several approximate methods. Finally, experimental, as well as theoretical, results are frequently available for comparison.

In the first section of this chapter the shell equations derived in chapter 1 will be expressed in terms of circular cylindrical shell parameters and the corresponding equations of motion will be synthesized. The remainder of the chapter is devoted to reporting vibration results. The case

of the shell of infinite length is discussed first because of its relative mathematical simplicity.

Results are subsequently presented both for closed and open thin circular cylindrical shells of finite length. By far, most of the results available are for closed shells, although in some cases the results for closed shells can also be interpreted in terms of open shells. Open shells can be either shallow or deep. Although there are 136 combinations of "simple" boundary conditions possible for a closed circular cylindrical shell, most of the results are available for a single one of these cases—when both ends are supported by shear diaphragms. Two types of boundary conditions not axisymmetric but of practical value have no reported results. These are

- (1) Point supports.
- (2) Boundary conditions that are discontinuous along a single edge; for example, one portion of a boundary may be clamped and the remainder free.

Furthermore, little has been done with circular cylindrical shells when the natural cylindrical coordinates of the problem are incompatible with the boundaries, as in the case of closed shells having noncircular edges or cutouts.

2.1 EQUATIONS OF MOTION

The shell coordinates to be used are x and θ as shown in figure 2.1. Further, the length coordinate x is replaced by a nondimensional length s defined by

$$s = x/R \quad (2.1)$$

where R is the cylindrical radius. Following the procedure outlined in section 1.7 the equations of motion are synthesized for the case of a circular cylindrical shell by using the following parameters in tables 1.1 through 1.5:

$$\left. \begin{aligned} \alpha = s, & \quad \beta = \theta \\ A = R, & \quad B = R \\ R_\alpha = \infty, & \quad R_\beta = R \end{aligned} \right\} \quad (2.2)$$

The equations of motion for thin circular cylindrical shells can be written in matrix form as

$$[\mathcal{L}]\{u_i\} = \{0\} \quad (2.3)$$

where $\{u_i\}$ is the displacement vector

$$\{u_i\} \equiv \begin{bmatrix} u \\ v \\ w \end{bmatrix} \quad (2.4)$$

u , v , and w are the orthogonal components of displacement in the x , θ , and radial directions, respectively, and $[\mathcal{L}]$ is a matrix differential operator.

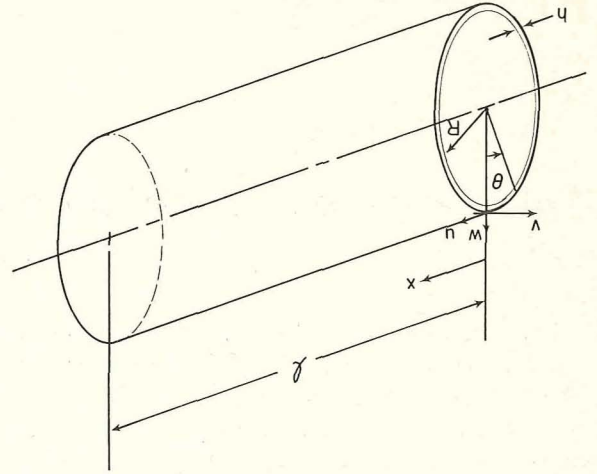


FIGURE 2.1.—Closed circular cylindrical shell and coordinate system.

2.1.1 Eighth Order Equations

Different eighth order systems of equations are commonly used to model the vibrational behavior of circular cylindrical shells. In this case the $[\mathcal{L}]$ operator in equation (2.3) can be treated as the sum of two operators; i.e.,

$$[\mathcal{L}] = [\mathcal{L}_{D-M}] + k[\mathcal{L}_{MOD}] \quad (2.5)$$

where $[\mathcal{L}_{D-M}]$ is the differential operator according to the Donnell-Mushtari theory, $[\mathcal{L}_{MOD}]$ is a "modifying" operator which alters the Donnell-Mushtari operator to yield another shell theory, and k is the nondimensional thickness parameter defined by

$$k \equiv h^2/12R^2 \quad (2.6)$$

Thus, each eighth order shell theory for circular cylindrical shells differs from the Donnell-Mushtari theory by an operator $[\mathcal{L}_{MOD}]$ which is multiplied by the constant k , which is very small for small h/R ratios.

The Donnell-Mushtari operator is found to take the form

$$[\mathcal{L}_{D-M}] = \begin{bmatrix} \left[\frac{\partial^2}{\partial s^2} + \frac{(1-\nu)}{2} \frac{\partial^2}{\partial \theta^2} - \rho \frac{(1-\nu^2)R^2}{E} \frac{\partial^2}{\partial t^2} \right] & \frac{(1+\nu)}{2} \frac{\partial^2}{\partial s \partial \theta} & \nu \frac{\partial}{\partial s} \\ \frac{(1+\nu)}{2} \frac{\partial^2}{\partial s \partial \theta} & \left[\frac{(1-\nu)}{2} \frac{\partial^2}{\partial s^2} + \frac{\partial^2}{\partial \theta^2} - \rho \frac{(1-\nu^2)R^2}{E} \frac{\partial^2}{\partial t^2} \right] & \frac{\partial}{\partial \theta} \\ \nu \frac{\partial}{\partial s} & \frac{\partial}{\partial \theta} & 1 + k\nabla^4 + \rho \frac{(1-\nu^2)R^2}{E} \frac{\partial^2}{\partial t^2} \end{bmatrix} \quad (2.7)$$

where $\nabla^4 = \nabla^2 \nabla^2$ and

$$\nabla^2 \equiv \frac{\partial^2}{\partial s^2} + \frac{\partial^2}{\partial \theta^2} \quad (2.8)$$

Similarly, the modifying operators for various circular cylindrical shell theories take the forms shown below.

Love-Timoshenko:

$$[\mathcal{L}_{MOD}] = \begin{bmatrix} 0 & 0 & 0 \\ 0 & (1-\nu)\frac{\partial^2}{\partial s^2} + \frac{\partial^2}{\partial \theta^2} & -\frac{\partial^3}{\partial s^2 \partial \theta} - \frac{\partial^3}{\partial \theta^3} \\ 0 & -(2-\nu)\frac{\partial^3}{\partial s^2 \partial \theta} - \frac{\partial^3}{\partial \theta^3} & 0 \end{bmatrix} \quad (2.9a)$$

Goldenveizer-Novozhilov (also Arnold-Warburton):

$$[\mathcal{L}_{MOD}] = \begin{bmatrix} 0 & 0 & 0 \\ 0 & 2(1-\nu)\frac{\partial^2}{\partial s^2} + \frac{\partial^2}{\partial \theta^2} & -(2-\nu)\frac{\partial^3}{\partial s^2 \partial \theta} - \frac{\partial^3}{\partial \theta^3} \\ 0 & -(2-\nu)\frac{\partial^3}{\partial s^2 \partial \theta} - \frac{\partial^3}{\partial \theta^3} & 0 \end{bmatrix} \quad (2.9b)$$

Houghton-Johns (simplified Goldenveizer-Novozhilov):

$$[\mathcal{L}_{MOD}] = \begin{bmatrix} 0 & 0 & 0 \\ 0 & 0 & -(2-\nu)\frac{\partial^3}{\partial s^2 \partial \theta} - \frac{\partial^3}{\partial \theta^3} \\ 0 & -(2-\nu)\frac{\partial^3}{\partial s^2 \partial \theta} - \frac{\partial^3}{\partial \theta^3} & 0 \end{bmatrix} \quad (2.9c)$$

Flügge-Byrne-Lur'ye (also Biezeno-Grammel):

$$[\mathcal{L}_{MOD}] = \begin{bmatrix} \frac{(1-\nu)}{2} \frac{\partial^2}{\partial \theta^2} & 0 & -\frac{\partial^3}{\partial s^3} + \frac{(1-\nu)}{2} \frac{\partial^3}{\partial s \partial \theta^2} \\ 0 & \frac{3(1-\nu)}{2} \frac{\partial^2}{\partial s^2} & -\frac{(3-\nu)}{2} \frac{\partial^3}{\partial s^2 \partial \theta} \\ -\frac{\partial^3}{\partial s^3} + \frac{(1-\nu)}{2} \frac{\partial^3}{\partial s \partial \theta^2} & -\frac{(3-\nu)}{2} \frac{\partial^3}{\partial s^2 \partial \theta} & 1 + 2\frac{\partial^2}{\partial \theta^2} \end{bmatrix} \quad (2.9d)$$

Reissner-Naghdi-Berry:

$$[\mathcal{L}_{MOD}] = \begin{bmatrix} 0 & 0 & 0 \\ 0 & \frac{(1-\nu)}{2} \frac{\partial^2}{\partial s^2} + \frac{\partial^2}{\partial \theta^2} & -\frac{\partial^3}{\partial s^2 \partial \theta} - \frac{\partial^3}{\partial \theta^3} \\ 0 & -\frac{\partial^3}{\partial s^2 \partial \theta} - \frac{\partial^3}{\partial \theta^3} & 0 \end{bmatrix} \quad (2.9e)$$

Sanders:

$$[\mathcal{L}_{MOD}] = \begin{bmatrix} \frac{(1-\nu)}{8} \frac{\partial^2}{\partial \theta^2} & -\frac{3(1-\nu)}{8} \frac{\partial^2}{\partial s \partial \theta} & \frac{(1-\nu)}{2} \frac{\partial^3}{\partial s \partial \theta^2} \\ -\frac{3(1-\nu)}{8} \frac{\partial^2}{\partial s \partial \theta} & \frac{9(1-\nu)}{8} \frac{\partial^2}{\partial s^2} + \frac{\partial^2}{\partial \theta^2} & -\frac{(3-\nu)}{2} \frac{\partial^3}{\partial s^2 \partial \theta} - \frac{\partial^3}{\partial \theta^3} \\ \frac{(1-\nu)}{2} \frac{\partial^3}{\partial s \partial \theta^2} & -\frac{(3-\nu)}{2} \frac{\partial^3}{\partial s^2 \partial \theta} - \frac{\partial^3}{\partial \theta^3} & 0 \end{bmatrix} \quad (2.9f)$$

Vlasov:

$$[\mathcal{L}_{MOD}] = \begin{bmatrix} 0 & 0 & -\frac{\partial^3}{\partial s^3} + \frac{(1-\nu)}{2} \frac{\partial^3}{\partial s \partial \theta^2} \\ 0 & 0 & -\frac{(3-\nu)}{2} \frac{\partial^3}{\partial s^2 \partial \theta} \\ -\frac{\partial^3}{\partial s^3} + \frac{(1-\nu)}{2} \frac{\partial^3}{\partial s \partial \theta^2} & -\frac{(3-\nu)}{2} \frac{\partial^3}{\partial s^2 \partial \theta} & 1 + 2 \frac{\partial^2}{\partial \theta^2} \end{bmatrix} \quad (2.9g)$$

Epstein-Kennard:

$$[\mathcal{L}_{MOD}] = \begin{bmatrix} \left[-\nu \frac{(2-9\nu+6\nu^2)}{2(1-\nu)^2} \frac{\partial^2}{\partial s^2} + \frac{(1-\nu)}{2} \frac{\partial^2}{\partial \theta^2} + \frac{\nu^2}{(1-\nu)^2} \frac{\partial^4}{\partial s^4} + \frac{\nu^2}{(1-\nu)^2} \frac{\partial^4}{\partial s^2 \partial \theta^2} \right] & \left[-\frac{(2-7\nu+5\nu^2-\nu^3)}{2(1-\nu)^2} \frac{\partial^2}{\partial s \partial \theta} + \frac{\nu^2}{(1-\nu)^2} \frac{\partial^4}{\partial s^3 \partial \theta} + \frac{\nu^2}{(1-\nu)^2} \frac{\partial^4}{\partial s \partial \theta^3} \right] & \left[-\frac{(2-9\nu+6\nu^2)}{2(1-\nu)^2} \frac{\partial}{\partial s} - \frac{(2-5\nu+\nu^2)}{2(1-\nu)^2} \frac{\partial^3}{\partial s^3} + \frac{(1-\nu+4\nu^2-2\nu^3)}{2(1-\nu)^2} \frac{\partial^3}{\partial s \partial \theta^2} \right] \\ \left[-\frac{(3+\nu-17\nu^2+12\nu^3)}{2(1-\nu)^2} \frac{\partial^2}{\partial s \partial \theta} + \frac{\nu^2}{(1-\nu)^2} \frac{\partial^4}{\partial s^3 \partial \theta} + \frac{\nu^2}{(1-\nu)^2} \frac{\partial^4}{\partial s \partial \theta^3} \right] & \left[-\frac{(10-23\nu+12\nu^2)}{2(1-\nu)^2} \frac{\partial^2}{\partial \theta^2} + \frac{\nu^2}{(1-\nu)^2} \frac{\partial^4}{\partial s^2 \partial \theta^2} + \frac{\nu^2}{(1-\nu)^2} \frac{\partial^4}{\partial \theta^4} \right] & \left[-\frac{(10-26\nu+15\nu^2)}{2(1-\nu)^2} \frac{\partial}{\partial \theta} + \frac{\nu(3-\nu)}{2(1-\nu)^2} \frac{\partial^3}{\partial \theta^3} - \frac{(3-9\nu+6\nu^2-2\nu^3)}{2(1-\nu)^2} \frac{\partial^3}{\partial s^2 \partial \theta} \right] \\ \left[\frac{\nu(1+3\nu)}{(1-\nu)} \frac{\partial}{\partial s} + \frac{3\nu^2}{2(1-\nu)^2} \frac{\partial^3}{\partial s^3} + \frac{(4-5\nu+\nu^2+3\nu^3)}{2(1-\nu)^2} \frac{\partial^3}{\partial s \partial \theta^2} \right] & \left[\frac{5\nu}{2(1-\nu)} \frac{\partial}{\partial \theta} + \frac{(2-7\nu+11\nu^2-3\nu^3)}{2(1-\nu)^2} \frac{\partial^3}{\partial s^2 \partial \theta} + \frac{3(2-4\nu+3\nu^2)}{2(1-\nu)^2} \frac{\partial^3}{\partial \theta^3} \right] & \left[\frac{(1+3\nu)}{(1-\nu)} + \frac{(2-2\nu+\nu^2+2\nu^3)}{2(1-\nu)^2} \frac{\partial^2}{\partial s^2} + \frac{(10-17\nu+10\nu^2)}{2(1-\nu)^2} \frac{\partial^2}{\partial \theta^2} \right] \end{bmatrix} \quad (2.9h)$$

Kennard simplified:

$$[\mathcal{L}_{MOD}] = \begin{bmatrix} 0 & 0 & 0 \\ 0 & 0 & \frac{3\nu}{2(1-\nu)} \frac{\partial}{\partial \theta} + \frac{3\nu}{2(1-\nu)} \frac{\partial^3}{\partial \theta^3} \\ 0 & 0 & \frac{(2+\nu)}{2(1-\nu)} + \frac{(4-\nu)}{2(1-\nu)} \frac{\partial^2}{\partial \theta^2} \end{bmatrix} \quad (2.9i)$$

For the various shell theories the modifying operators are simple in some cases and complicated in others. Furthermore, several of them are seen to be nonsymmetric, which has resulted in much criticism in the literature of shell theory (cf., refs. 2.1 and 2.2). Nonsymmetric equations of motion can yield imaginary vibration frequencies.

The shell theories described by the differential operators in some cases are specializations of the theories derived in chapter 1 for arbitrary shells and, in other cases, were developed specially for circular cylindrical shells. The theories of Donnell-Mushtari, Love-Timoshenko, Goldenveizer-Novozhilov, Flügge-Lur'ye-Byrne, Reissner-Naghdi-Berry, Sanders, and Vlasov were derived in chapter 1.

Arnold and Warburton (refs. 2.3 and 2.4) derived their widely used equations of motion of circular cylindrical shells by using Lagrange equations with suitable strain energy and kinetic energy expressions. Although they began with Timoshenko strain-displacement equations, particular assumptions made when integrating over the thickness yielded the equations of Goldenveizer and Novozhilov. This equivalence has apparently been pointed out in the literature.

Houghton and Johns (ref. 2.5) suggested a set of simplified equations of equilibrium for static problems of circular cylindrical shells which are obtained by neglecting k with respect to unity in the Goldenveizer-Novozhilov equations. This procedure was also carried out by Bijlaard (ref. 2.6) on the Timoshenko-Love equations. Epstein (ref. 2.7) derived a general set of equations of shell theory from the three-dimensional theory of elasticity by means of expansion of stresses and displacements with respect to the thickness coordinate, z . These equations were subsequently rederived and specialized to circular cylindrical shells by Kennard (refs. 2.8 through 2.11).

As indicated in chapter 1, in addition to the theories derived there, there exist many other distinct theories for thin shells having arbitrary curvature. In addition there are theories derived specially for circular cylindrical shells which will not be accounted for in this chapter, for example, those of Coupry (refs. 2.12 and 2.13), Morley (ref. 2.14), Herrmann and Armenakas (refs. 2.15 and 2.16), Yu (ref. 2.17), Galerkin (ref. 2.18 and

ref. 2.19, p. 295), Miller (ref. 2.20), Simmonds (ref. 2.21), and Mugnier and Schroeter (ref. 2.22).

The strain energy of a circular cylindrical shell is obtained by substituting the appropriate strain-displacement equations into equation (1.84) and integrating over the thickness. The total strain energy can be written as

$$V = \frac{Eh}{2(1-\nu^2)} \int_0^{2\pi} \int_0^1 (I_{D-M} + kI_{MOD}) ds d\theta \quad (2.10)$$

where I_{D-M} is the integrand of the strain energy of the shell according to the Donnell-Mushtari theory and is given by

$$\begin{aligned} I_{D-M} = & \left(\frac{\partial u}{\partial s} + \frac{\partial v}{\partial \theta} + w \right)^2 \\ & - 2(1-\nu) \left[\frac{\partial u}{\partial s} w - \frac{1}{4} \left(\frac{\partial v}{\partial s} - \frac{\partial u}{\partial \theta} \right)^2 \right] \\ & + k \left\{ (\nabla^2 w)^2 - 2(1-\nu) \left[\frac{\partial^2 w}{\partial s^2} \frac{\partial^2 w}{\partial \theta^2} \right. \right. \\ & \left. \left. - \left(\frac{\partial^2 w}{\partial s \partial \theta} \right)^2 \right] \right\} \end{aligned} \quad (2.11)$$

and I_{MOD} is the "modifying integrand" which differs depending upon the shell theory being used. Some examples of modifying integrands which are appropriate to the shell theories being considered here are given below.

Goldenveizer-Novozhilov:

$$\begin{aligned} I_{MOD} = & -2 \frac{\partial v}{\partial \theta} \nabla^2 w + \left(\frac{\partial v}{\partial \theta} \right)^2 \\ & - 2(1-\nu) \left[-\frac{\partial v}{\partial \theta} \frac{\partial^2 w}{\partial s^2} + 2 \frac{\partial v}{\partial s} \frac{\partial^2 w}{\partial s \partial \theta} - \left(\frac{\partial v}{\partial s} \right)^2 \right] \end{aligned} \quad (2.12a)$$

Houghton-Johns:

$$I_{MOD} = -2 \frac{\partial v}{\partial \theta} \frac{\partial^2 w}{\partial \theta^2} - 2\nu \frac{\partial v}{\partial \theta} \frac{\partial^2 w}{\partial s^2} - 4(1-\nu) \frac{\partial v}{\partial s} \frac{\partial^2 w}{\partial s \partial \theta} \quad (2.12b)$$

Flügge-Lur'ye-Byrne:

$$\begin{aligned} I_{MOD} = & \frac{(1-\nu)}{2} \left(\frac{\partial u}{\partial \theta} \right)^2 + (1-\nu) \frac{\partial u}{\partial \theta} \frac{\partial^2 w}{\partial s \partial \theta} - 2 \frac{\partial u}{\partial s} \frac{\partial^2 w}{\partial s^2} \\ & + 3 \frac{(1-\nu)}{2} \left(\frac{\partial v}{\partial s} \right)^2 - 3(1-\nu) \frac{\partial v}{\partial s} \frac{\partial^2 w}{\partial s \partial \theta} \\ & - 2\nu \frac{\partial v}{\partial \theta} \frac{\partial^2 w}{\partial s^2} + w^2 + 2w \frac{\partial^2 w}{\partial \theta^2} \end{aligned} \quad (2.12c)$$

Reissner-Naghdi-Berry:

$$I_{MOD} = -2 \frac{\partial v}{\partial \theta} \nabla^2 w + \left(\frac{\partial v}{\partial \theta} \right)^2 - 2(1-\nu) \left[-\frac{\partial v}{\partial \theta} \frac{\partial^2 w}{\partial s^2} + \frac{\partial v}{\partial s} \frac{\partial^2 w}{\partial s \partial \theta} - \frac{1}{4} \left(\frac{\partial v}{\partial s} \right)^2 \right] \quad (2.12d)$$

Sanders:

$$I_{MOD} = \frac{(1-\nu)}{8} \left(\frac{\partial u}{\partial \theta} \right)^2 - 3 \frac{(1-\nu)}{4} \frac{\partial v}{\partial s} \frac{\partial u}{\partial \theta} + (1-\nu) \frac{\partial u}{\partial \theta} \frac{\partial^2 w}{\partial s \partial \theta} + 9 \frac{(1-\nu)}{8} \left(\frac{\partial v}{\partial s} \right)^2 + \left(\frac{\partial v}{\partial \theta} \right)^2 - 2\nu \frac{\partial v}{\partial \theta} \frac{\partial^2 w}{\partial s^2} - 3(1-\nu) \frac{\partial v}{\partial s} \frac{\partial^2 w}{\partial s \partial \theta} - 2 \frac{\partial v}{\partial \theta} \frac{\partial^2 w}{\partial \theta^2} \quad (2.12e)$$

Vlasov:

$$I_{MOD} = (1-\nu) \frac{\partial u}{\partial \theta} \frac{\partial^2 w}{\partial s \partial \theta} - 2 \frac{\partial u}{\partial s} \frac{\partial^2 w}{\partial s^2} - 3(1-\nu) \frac{\partial v}{\partial s} \frac{\partial^2 w}{\partial s \partial \theta} - 2\nu \frac{\partial v}{\partial \theta} \frac{\partial^2 w}{\partial s^2} + w^2 + 2w \frac{\partial^2 w}{\partial \theta^2} \quad (2.12f)$$

It is further noted that the strain energy integrands given by equations (2.11) and (2.12) are consistent with the equations of motion given earlier in this section for these theories. Consistency requires that the equations of motion are derivable from an energy principle by means of a variational procedure.

For example, one variational principle which may be invoked is Hamilton's principle, which may be written as

$$\delta \int_{t_0}^{t_1} (T - V) dt = 0 \quad (2.13)$$

That is, the variation of the time integral between given time limits of the difference between the kinetic and potential energies must vanish. The kinetic energy of the shell is

$$T = \frac{1}{2} \rho h \int_0^{2\pi} \int_0^1 \left[\left(\frac{\partial u}{\partial t} \right)^2 + \left(\frac{\partial v}{\partial t} \right)^2 + \left(\frac{\partial w}{\partial t} \right)^2 \right] R^2 ds d\theta \quad (2.14)$$

Substituting equations (2.10), (2.11), (2.12), and (2.14), it can be seen that equation (2.13) can be written in the form

$$\delta \int_{t_0}^{t_1} \int_0^{2\pi} \int_0^1 \mathcal{F} \left(u, v, w, \frac{\partial u}{\partial s}, \frac{\partial u}{\partial \theta}, \frac{\partial u}{\partial t}, \frac{\partial v}{\partial s}, \frac{\partial v}{\partial \theta}, \frac{\partial v}{\partial t}, \frac{\partial w}{\partial s}, \frac{\partial w}{\partial \theta}, \frac{\partial w}{\partial t}, \frac{\partial^2 w}{\partial s^2}, \frac{\partial^2 w}{\partial s \partial \theta}, \frac{\partial^2 w}{\partial \theta^2} \right) ds d\theta dt = 0 \quad (2.15)$$

and the functions $u, \dots, \partial^2 w / \partial \theta^2$ are functions of s, θ , and t . From the calculus of variations, the conditions that equation (2.15) be satisfied are the Euler-Lagrange equations, given by

$$\left. \begin{aligned} \frac{\partial \mathcal{F}}{\partial u} - \frac{\partial}{\partial s} \left(\frac{\partial \mathcal{F}}{\partial u_s} \right) - \frac{\partial}{\partial \theta} \left(\frac{\partial \mathcal{F}}{\partial u_\theta} \right) - \frac{\partial}{\partial t} \left(\frac{\partial \mathcal{F}}{\partial u_t} \right) &= 0 \\ \frac{\partial \mathcal{F}}{\partial v} - \frac{\partial}{\partial s} \left(\frac{\partial \mathcal{F}}{\partial v_s} \right) - \frac{\partial}{\partial \theta} \left(\frac{\partial \mathcal{F}}{\partial v_\theta} \right) - \frac{\partial}{\partial t} \left(\frac{\partial \mathcal{F}}{\partial v_t} \right) &= 0 \\ \frac{\partial \mathcal{F}}{\partial w} - \frac{\partial}{\partial s} \left(\frac{\partial \mathcal{F}}{\partial w_s} \right) - \frac{\partial}{\partial \theta} \left(\frac{\partial \mathcal{F}}{\partial w_\theta} \right) - \frac{\partial}{\partial t} \left(\frac{\partial \mathcal{F}}{\partial w_t} \right) \\ &+ \frac{\partial^2}{\partial s^2} \left(\frac{\partial \mathcal{F}}{\partial w_{ss}} \right) + \frac{\partial^2}{\partial s \partial \theta} \left(\frac{\partial \mathcal{F}}{\partial w_{s\theta}} \right) \\ &+ \frac{\partial^2}{\partial \theta^2} \left(\frac{\partial \mathcal{F}}{\partial w_{\theta\theta}} \right) = 0 \end{aligned} \right\} \quad (2.16)$$

where, for example, $\partial \mathcal{F} / \partial u_s$ indicates the partial derivative of the functional \mathcal{F} with respect to the function $\partial u / \partial s$.

Using the various strain energy functionals given by equations (2.11) and (2.12) in conjunction with equations (2.16), the equations of motion determined by equations (2.7) and (2.9) will result.

Strain energy integrands which are consistent with the other theories included in equations (2.9) cannot be found because the equations of motion are not symmetric.

The total strain energy integrand given in equation (2.10) can be written as the sum of two parts—one part due to stretching (membrane) and one part due to the addition of bending stiffness; i.e.,

$$I_{\text{total}} = I_{\text{membrane}} + I_{\text{bending}} \quad (2.17)$$

where

$$I_{\text{membrane}} = \left(\frac{\partial u}{\partial s} + \frac{\partial v}{\partial \theta} + w \right)^2 - 2(1-\nu) \left[\frac{\partial u}{\partial s} w - \frac{1}{4} \left(\frac{\partial v}{\partial s} - \frac{\partial u}{\partial \theta} \right)^2 \right] \quad (2.18)$$

and I_{bending} is the sum of those terms of the integrand of equation (2.10) which contain k , taken both from equations (2.11) and (2.12).

2.1.2 Extensional (Membrane) Equations

The extensional or membrane theory for circular cylindrical shells has an extensive history, including the early works of Rayleigh (refs. 2.23 and 2.24) and Love (refs. 2.25 and 2.26). In using this theory it is assumed that the bending rigidity of the shell is negligible at every point. Thus, the extensional equations of motion can be arrived at by setting $k=0$ in equations (2.5) and (2.7), yielding

$$\left. \begin{aligned} \frac{\partial^2 u}{\partial s^2} + \frac{(1-\nu)}{2} \frac{\partial^2 u}{\partial \theta^2} + \frac{(1+\nu)}{2} \frac{\partial^2 v}{\partial s \partial \theta} + \nu \frac{\partial w}{\partial s} \\ = \frac{\rho(1-\nu^2)R^2}{E} \frac{\partial^2 u}{\partial t^2} \\ \frac{(1+\nu)}{2} \frac{\partial^2 u}{\partial s \partial \theta} + \frac{(1-\nu)}{2} \frac{\partial^2 v}{\partial s^2} + \frac{\partial^2 v}{\partial \theta^2} + \frac{\partial w}{\partial \theta} \\ = \frac{\rho(1-\nu^2)R^2}{E} \frac{\partial^2 v}{\partial t^2} \\ \nu \frac{\partial u}{\partial s} + \frac{\partial v}{\partial \theta} + w = -\frac{\rho(1-\nu^2)R^2}{E} \frac{\partial^2 w}{\partial t^2} \end{aligned} \right\} \quad (2.19)$$

This system of differential equations is of the fourth order in s and θ . The strain energy integrand given in equation (2.18) is consistent with these equations.

2.2 SHELLS OF INFINITE LENGTH

Consider first the closed circular cylindrical shell of infinite length having displacements of the form

$$\left. \begin{aligned} u &= A \cos \lambda s \cos n\theta \cos \omega t \\ v &= B \sin \lambda s \sin n\theta \cos \omega t \\ w &= C \sin \lambda s \cos n\theta \cos \omega t \end{aligned} \right\} \quad (2.20)$$

where A , B , C , and λ are undetermined constants, n is an integer for closed shells, and ω is the frequency of free vibration in radians per second (if the mass density ρ is expressed in units involving seconds). The cyclic frequency (cps) is obtained by dividing ω by 2π . The form of solution taken in equations (2.20) assumes that the time and spatial variables are separable, giving rise to normal modes executing simple harmonic motion, the period and phase of the motion being the same for all points on the shell. The periodic functions of θ used in equations (2.20) guarantee that the displacements are periodic (e.g., $w(s, \theta) = w(s, \theta + 2\pi)$) and continuous (e.g., $w(s, \pi) = w(s, -\pi)$).

Substituting equations (2.20) into equations (2.1) and (2.3), using any form of the eighth order shell theories given by equations (2.7) and (2.9), it can easily be seen that the number of differentiations in each term of the equation of motion are such that each equation of motion permits factorization of terms containing s , θ , and t out of each equation. The equations of motion must be satisfied for all values of s , θ , and t allowed to vary independently. This leads to a set of homogeneous equations which, for the Donnell-Mushtari theory, for example, can be written in matrix form as in equation (2.21). For a nontrivial solution, the determinant of the coefficient matrix in equation (2.21) is set equal to zero, which yields either of the following two eigenvalue problems:

(1) For a given λ , there exists one or more proper values of the frequency parameter $\rho(1-\nu^2)R^2\omega^2/E$ such that the determinant vanishes, or

$$\left[\begin{array}{ccc} \left[-\lambda^2 - \frac{(1-\nu)}{2}n^2 + \frac{\rho(1-\nu^2)R^2\omega^2}{E} \right] & \frac{(1+\nu)}{2}\lambda n & \nu\lambda \\ \frac{(1+\nu)}{2}\lambda n & \left[-\frac{(1-\nu)}{2}\lambda^2 - n^2 + \frac{\rho(1-\nu^2)R^2\omega^2}{E} \right] & -n \\ -\nu\lambda & n & \left[1 + k(\lambda^2 + n^2)^2 - \frac{\rho(1-\nu^2)R^2\omega^2}{E} \right] \end{array} \right] \begin{bmatrix} A \\ B \\ C \end{bmatrix} = \begin{bmatrix} 0 \\ 0 \\ 0 \end{bmatrix} \quad (2.21)$$

(2) For a given frequency ω , there exists one or more proper values of λ such that the determinant vanishes.

Of course, since $s = x/R$, then the half-wavelength of the displacement functions in the x direction is l if λ is chosen to be $\pi R/l$, and the frequencies of free vibration can be found which correspond to the given wavelength.

As will be seen in section 2.3 the displacement functions chosen as in equation (2.20) also exactly satisfy the freely-supported or shear diaphragm end conditions of *finite* length shells. Thus, a circular cylindrical shell of infinite length vibrating in a mode, so that the half-wavelength in the x -direction is l , corresponds to a finite shell of length l having a particular set of end conditions.

One simple mathematical model of a cylindrical shell of infinite length is obtained by using the concept of *plane strain*. The necessary assumptions are that there is no motion in the direction of the length of the shell and that the physical quantities (displacements, membrane forces, bending moments, etc.) do not depend upon location along the length. Thus, the case of plane strain requires

$$u = 0, \quad v = v(\theta), \quad w = w(\theta) \quad (2.22)$$

which changes the character of the shell motion from two-dimensional to one-dimensional (variation only with θ) and simplifies the analysis considerably. For example, under the assumption of equations (2.22) the Flügge equations of motion given by equations (2.1), (2.3), (2.7), and (2.9d) reduce to (refs. 2.27 through 2.29)

$$\left. \begin{aligned} \frac{\partial^2 v}{\partial \theta^2} + \frac{\partial w}{\partial \theta} &= \frac{\rho(1-\nu^2)R^2}{E} \frac{\partial^2 v}{\partial t^2} \\ \frac{\partial v}{\partial \theta} + \left[1 + k \left(1 + \frac{\partial^2}{\partial \theta^2} \right)^2 \right] w &= - \frac{\rho(1-\nu^2)R^2}{E} \frac{\partial^2 w}{\partial t^2} \end{aligned} \right\} \quad (2.23)$$

Equations (2.23) may be solved by assuming

$$\left. \begin{aligned} v &= B \sin n\theta \cos \omega t \\ w &= C \cos n\theta \cos \omega t \end{aligned} \right\} \quad (2.24)$$

Substituting equations (2.24) into (2.23) yields

$$\begin{bmatrix} n^2 - \Omega^2 & n \\ n & 1 + k(1 - n^2)^2 - \Omega^2 \end{bmatrix} \begin{bmatrix} B \\ C \end{bmatrix} = \begin{bmatrix} 0 \\ 0 \end{bmatrix} \quad (2.25)$$

where

$$\Omega^2 \equiv \frac{\rho(1-\nu^2)R^2\omega^2}{E} \quad (2.26)$$

For a nontrivial solution, setting the determinant of the coefficient matrix in equation (2.25) equal to zero gives the roots

$$\left. \begin{aligned} \Omega^2 &= 0, 1+k & (n=0) \\ \Omega^2 &= \frac{1}{2} \left[1+n^2+k(n^2-1)^2 \right. \\ &\quad \left. \mp \sqrt{[1+n^2+k(n^2-1)^2]^2 - 4kn^2(n-1)^2} \right] & (n \neq 0) \end{aligned} \right\} \quad (2.27)$$

as was shown by Reismann (refs. 2.27 and 2.28). The root $\Omega^2 = 0$ for $n=0$ corresponds to rigid body torsional rotation of the shell.

Now consider the solution functions given in equations (2.20) for the case when the wavelength in the x (and s) direction becomes infinitely long. The solution functions can then be represented as

$$\left. \begin{aligned} u &= A \cos n\theta \cos \omega t \\ v &= B \sin n\theta \cos \omega t \\ w &= C \cos n\theta \cos \omega t \end{aligned} \right\} \quad (2.28)$$

Taking, for example, the Donnell-Mushtari theory and substituting equations (2.28) into the equations of motion yields a set of homogeneous equations which can also be arrived at by taking the limit as $l \rightarrow \infty$ (i.e., $\lambda \rightarrow 0$) in equations (2.21); that is,

$$\begin{bmatrix} \frac{(1-\nu)}{2}n^2 - \Omega^2 & 0 & 0 \\ 0 & n^2 - \Omega^2 & n \\ 0 & n & (1+kn^4) - \Omega^2 \end{bmatrix} \begin{bmatrix} A \\ B \\ C \end{bmatrix} = \begin{bmatrix} 0 \\ 0 \\ 0 \end{bmatrix} \quad (2.29)$$

It is seen that from equations (2.29) the motion uncouples, giving a purely axial (or longitudinal) motion characterized by the frequency parameter

$$\Omega^2 = \frac{(1-\nu)}{2}n^2 \quad (2.30)$$

and, because the v and w displacements are now uncoupled from u , the other two modes for a given n are the same as the plane strain modes discussed earlier in this section. In the case of the Donnell-Mushtari theory, finding the roots of the uncoupled second order determinant arising from equations (2.29) gives

$$\left. \begin{aligned} \Omega^2 = 0, 1 \quad (n=0) \\ \Omega^2 = \frac{1}{2} \left[(1+n^2+kn^4) \right. \\ \left. \pm \sqrt{(1+n^2+kn^4)^2 - 4kn^6} \right] (n \neq 0) \end{aligned} \right\} \quad (2.31)$$

which can be compared with the corresponding plane strain frequencies from the Flügge equations of motion given in equations (2.27).

The off-diagonal terms \mathfrak{L}_{12} , \mathfrak{L}_{21} , \mathfrak{L}_{13} , and \mathfrak{L}_{31} in the matrix operators in the equations of motion for the remaining theories (equations (2.9)) are also either zero or contain derivatives with respect to s (giving λ) in each term, so the same uncoupling for a circular cylindrical shell of infinite length occurs for each theory. The resulting frequency formulas for the three roots Ω^2 for each theory are listed in table 2.1. In deriving the frequency formulas for table 2.1 terms containing k^2 were neglected.

TABLE 2.1.—Frequency Parameter Formulas for Circular Cylindrical Shells of Infinite Length According to Various Theories

Shell theory	Ω^2 (Axial mode)	Ω^2 (Radial and circumferential modes)
Donnell-Mushtari	$\frac{1}{2}(1-\nu)n^2$	$\frac{1}{2}\{(1+n^2+kn^4) \mp [(1+n^2)^2 + 2kn^4(1-n^2)]^{1/2}\}$
Love-Timoshenko	Same as Donnell-Mushtari	$\frac{1}{2}\{(1+n^2)(1+kn^2) \mp [(1+n^2)^2 - 2kn^2(1-6n^2+n^4)]^{1/2}\}$
Goldenveizer-Novozhilov (also Arnold-Warburton)	Same as Donnell-Mushtari	Same as Love-Timoshenko
Houghton-Johns (Simplified Goldenveizer- Novozhilov)	Same as Donnell-Mushtari	$\frac{1}{2}\{(1+n^2+kn^4) \mp [(1+n^2)^2 + 2kn^4(5-n^2)]^{1/2}\}$
Biezeno-Grammel	$\frac{1}{2}(1+k)(1-\nu)n^2$	$\frac{1}{2}\{[1+n^2+k(1-n^2)^2] \mp [(1+n^2)^2 + 2k(1-n^2)^3]^{1/2}\}$
Flügge	Same as Donnell-Mushtari	$\frac{1}{2}\{[1+n^2+kn^4] \mp [(1+n^2)^2 - 2kn^6]^{1/2}\}$
Sanders	$\frac{1}{2}\left(1+\frac{k}{4}\right)(1-\nu)n^2$	Same as Love-Timoshenko
Reissner-Naghdi-Berry	Same as Donnell-Mushtari	Same as Love-Timoshenko
Vlasov	Same as Donnell-Mushtari	Same as Biezeno-Grammel
Epstein-Kennard	$\frac{1}{2}(1+k)(1-\nu)n^2$	$\frac{1}{2}\left\{1 + \frac{1+3\nu}{1-\nu}k + n^2 - \left(\frac{10-20\nu+11\nu^2}{(1-\nu)^2}\right)kn^2 + \frac{1-2\nu}{(1-\nu)^2}kn^4\right\} \\ \mp \left[(1+n^2)^2 + 2\frac{1+3\nu}{1-\nu}k - \frac{22-52\nu+32\nu^2}{(1-\nu)^2}kn^2 - \frac{10-20\nu+14\nu^2}{(1-\nu)^2}kn^4 - \frac{2-4\nu+4\nu^2}{(1-\nu)^2}kn^6 \right]^{1/2} \Bigg\}$
Kennard Simplified	Same as Donnell-Mushtari	$\frac{1}{2}\left\{1 + \frac{2+\nu}{2(1-\nu)}k + n^2 - \frac{4-\nu}{2(1-\nu)}kn^2 + kn^4\right\} \\ \mp \left[1 + \frac{2+\nu}{1-\nu}k + 2(1-3k)n^2 + n^4 + \frac{3(2-3\nu)}{1-\nu}kn^4 - 2kn^6 \right]^{1/2} \Bigg\}$
Membrane	Same as Donnell-Mushtari	$0, 1+n^2$

In table 2.1 the "Biezeno and Grammel shell theory" is listed separately. It is actually the same as that of Flügge, but a subtle difference exists between their frequency equations (ref. 2.30) and those of Flügge (ref. 2.31). In their work only the terms containing k^2 are discarded when expanding the frequency determinant, whereas Flügge also neglected k with respect to unity, thereby discarding additional terms.

It is interesting to note that the membrane, Biezeno-Grammel and Vlasov formulas are the only ones in table 2.1 that yield the correct zero frequency (corresponding to rigid body translation in the transverse direction) for the lowest radial-circumferential vibration mode in the case $n=1$. On the other hand the Vlasov, Epstein-Kennard, and Kennard Simplified formulas do not yield zero frequencies for the torsional mode for $n=0$ as they should.

In tables 2.2 and 2.3 frequency parameters are given for infinite shells and $\nu=0.3$ according to the various theories for $R/h=20$ and 500, respectively, and for $n=0, 1, 2, 3, 4$. The formulas of table 2.1 are the basis for tables 2.2 and 2.3. Only the Epstein-Kennard and Kennard Simplified formulas for the radial and circumferential frequency parameter Ω^2 depend upon ν . Significant differences among the shell theories exist only for certain of the radial-circumferential modes, usually those modes which are primarily radial

in nature, and these differences decrease as R/h is increased.

Considering table 2.2, which shows up the largest differences among the theories, one observes that:

(1) For $n=0$, the agreement among all theories is excellent for the one nontrivial frequency which exists.

(2) For $n=1$, the differences among the theories for the rigid body "beam bending" mode are clearly seen. The Houghton-Johns equations yield an imaginary frequency.

(3) For $n=1$, considering the highest frequency, the theories fall into two groups having frequencies differing by approximately eight percent.

(4) For $n \geq 2$, all theories are in close agreement except for those of Donnell-Mushtari, Flügge, Houghton-Johns, and the membrane theory for the lowest frequency.

The significant difference arising out of the Flügge theory for infinite circular cylindrical shells by neglecting k with respect to unity in the characteristic equation apparently has not been pointed out previously in the literature.

Considering table 2.3 for thinner shells ($R/h=500$) it is seen that the Donnell-Mushtari, Flügge, Houghton-Johns, and membrane equations again give results which differ considerably

TABLE 2.2.—Frequency Parameters for Circular Cylindrical Shells of Infinite Length According to Various Theories; $\nu=0.3$, $R/h=20$

Shell theory	n	Axial modes	Ω	
			Radial-circumferential modes	
			Lowest	Highest
Donnell-Mushtari	0	0 ↓	0	1
Love-Timoshenko			0	1
Goldenveizer-Novozhilov			0	1
Houghton-Johns			0	1
Flügge			0	1
Biezeno-Grammel			1.03441×10^{-4}	1.00010
Reissner-Naghdi-Berry			0	1
Sanders			0	1
Vlasov			1.03441×10^{-4}	1
Epstein-Kennard			0	1.00028
Kennard Simplified			1.71796×10^{-4}	1.00013
Membrane			0	1

TABLE 2.2.—Frequency Parameters for Circular Cylindrical Shells of Infinite Length According to Various Theories; $\nu=0.3$, $R/h=20$ —Concluded

Shell theory	n	Axial modes	Ω	
			Radial-circumferential modes	
			Lowest	Highest
Donnell-Mushtari	1	0.591608	1.02062×10^{-2}	1.41425
Love-Timoshenko		.591608	1.47648×10^{-4}	1.30676
Goldenveizer-Novozhilov		.591608	1.47648×10^{-4}	1.30676
Houghton-Johns		.591608	1.02052×10^{-2}	1.30672
Flügge		.591608	1.25000×10^{-2}	1.30657
Biezeno-Grammel		.591670	0	1.41416
Reissner-Naghdi-Berry		.591608	1.47648×10^{-4}	1.30676
Sanders		.591623	1.47648×10^{-4}	1.30676
Vlasov		.591608	0	1.41416
Epstein-Kennard		.591676	0	1.41372
Kennard Simplified		.591608	0	1.41420
Membrane		.591608	0	1.41416
Donnell-Mushtari	2	1.18322	5.16417×10^{-2}	2.23622
Love-Timoshenko		1.18322	3.87307×10^{-2}	2.23666
Goldenveizer-Novozhilov		1.18322	3.87307×10^{-2}	2.23666
Houghton-Johns		1.18322	3.65151×10^{-2}	2.23652
Flügge		1.18322	5.47755×10^{-2}	2.23614
Biezeno-Grammel		1.18334	3.87306×10^{-2}	2.23615
Reissner-Naghdi-Berry		1.18322	3.87307×10^{-2}	2.23666
Sanders		1.18325	3.87307×10^{-2}	2.23666
Vlasov		1.18322	3.87307×10^{-2}	2.23615
Epstein-Kennard		1.18334	3.87307×10^{-2}	2.23457
Kennard Simplified		1.18322	3.87313×10^{-2}	2.23606
Membrane		1.18322	0	2.23607
Donnell-Mushtari	3	1.77482	.123256	3.16254
Love-Timoshenko		1.77482	.109548	3.16334
Goldenveizer-Novozhilov		1.77482	.109548	3.16334
Houghton-Johns		1.77482	.108691	3.16308
Flügge		1.77482	.126637	3.16301
Biezeno-Grammel		1.77501	.109557	3.16249
Reissner-Naghdi-Berry		1.77482	.109548	3.16334
Sanders		1.77487	.109548	3.16334
Vlasov		1.77482	.109557	3.16249
Epstein-Kennard		1.77501	.109638	3.15962
Kennard Simplified		1.77482	.109560	3.16232
Membrane		1.77482	0	3.16228
Donnell-Mushtari	4	2.36643	.224118	4.12348
Love-Timoshenko		2.36643	.210077	4.12463
Goldenveizer-Novozhilov		2.36643	.210077	4.12463
Houghton-Johns		2.36643	.209617	4.12424
Flügge		2.36643	.227600	4.12482
Biezeno-Grammel		2.36668	.210102	4.12344
Reissner-Naghdi-Berry		2.36643	.210077	4.12463
Sanders		2.36650	.210077	4.12463
Vlasov		2.36643	.210102	4.12344
Epstein-Kennard		2.36668	.210267	4.11897
Kennard Simplified		2.36643	.210108	4.12319
Membrane		2.36643	0	4.12311

TABLE 2.3.—*Frequency Parameters for Circular Cylindrical Shells of Infinite Length According to Various Theories; $\nu=0.3$, $R/h=500$*

Shell theory	n	Axial modes	Ω	
			Radial-circumferential modes	
			Lowest	Highest
Donnell-Mushtari	0	0 ↓	0	1 ↓
Love-Timoshenko			0	
Goldenveizer-Novozhilov			0	
Houghton-Johns			0	
Flügge			0	
Biezeno-Grammel			1.00000×10^{-5}	
Reissner-Naghdi-Berry			0	
Sanders			0	
Vlasov			1.00000×10^{-5}	
Epstein-Kennard			0	
Kennard Simplified			3.69865×10^{-4}	
Membrane			0	
Donnell-Mushtari	1	0.59161 ↓	4.08166×10^{-4}	1.41421 ↓
Love-Timoshenko			.541195	
Goldenveizer-Novozhilov			.541195	
Houghton-Johns			.540924	
Flügge			.541196	
Biezeno-Grammel			0	
Reissner-Naghdi-Berry			.541195	
Sanders			.541195	
Vlasov			0	
Epstein-Kennard			6.90534×10^{-4}	
Kennard Simplified			2.61725×10^{-4}	
Membrane			0	
Donnell-Mushtari	2	1.18322 ↓	2.06553×10^{-2}	2.23607 ↓
Love-Timoshenko			1.54919×10^{-3}	
Goldenveizer-Novozhilov			1.54919×10^{-3}	
Houghton-Johns			1.46045×10^{-3}	
Flügge			2.19075×10^{-3}	
Biezeno-Grammel			1.54916×10^{-3}	
Reissner-Naghdi-Berry			1.54919×10^{-3}	
Sanders			1.54919×10^{-3}	
Vlasov			1.54916×10^{-3}	
Epstein-Kennard			1.69146×10^{-3}	
Kennard Simplified			1.55785×10^{-3}	
Membrane			0	
Donnell-Mushtari	3	1.77482 ↓	4.92926×10^{-3}	3.16228 ↓
Love-Timoshenko			4.38155×10^{-3}	
Goldenveizer-Novozhilov			4.38155×10^{-3}	
Houghton-Johns			4.34721×10^{-3}	
Flügge			4.42416×10^{-3}	
Biezeno-Grammel			4.38156×10^{-3}	
Reissner-Naghdi-Berry			4.38155×10^{-3}	
Sanders			4.38155×10^{-3}	
Vlasov			4.38156×10^{-3}	
Epstein-Kennard			4.36732×10^{-3}	
Kennard Simplified			4.38316×10^{-3}	
Membrane			0	

TABLE 2.3.—Frequency Parameters for Circular Cylindrical Shells of Infinite Length According to Various Theories; $\nu=0.3$, $R/h=500$ —Concluded

Shell theory	n	Axial modes	Ω	
			Radial-circumferential modes	
			Lowest	Highest
Donnell-Mushtari	4	2.36643 ↓	8.96144×10^{-3}	4.12311
Love-Timoshenko			8.40119×10^{-3}	4.12311
Goldenveizer-Novozhilov			8.40119×10^{-3}	4.12311
Houghton-Johns			8.38257×10^{-3}	4.12311
Flügge			7.92069×10^{-3}	4.12311
Biezeno-Grammel			8.40126×10^{-3}	4.12311
Reissner-Naghdi-Berry			8.40119×10^{-3}	4.12311
Sanders			8.40119×10^{-3}	4.12311
Vlasov			8.40126×10^{-3}	4.12311
Epstein-Kennard			8.28641×10^{-3}	4.12310
Kennard Simplified			8.40174×10^{-3}	4.12311
Membrane			0	4.12311

for those of the other theories for the lowest frequency for $n \geq 2$. The Epstein-Kennard theory now also differs considerably.

The amplitude ratios B/C for the coupled radial-circumferential modes are determined by substituting the corresponding frequency into either of the homogeneous equations governing these modes (e.g., either of the last two of eqs. (2.29)). Thus, for example, from equation (2.29) for the Donnell-Mushtari theory the amplitude ratio B/C is given by

$$\frac{B}{C} = \frac{n^2}{n^2 - \Omega^2} \quad (2.32)$$

where Ω^2 is given by equations (2.31). For a discussion of the ordering of the frequencies and the corresponding mode shapes for various n , see section 2.3.2 in the case of long shells (small λ) of finite length.

2.3 CLOSED SHELLS—SHEAR DIAPHRAGMS AT BOTH ENDS

Consider the closed circular cylindrical shell of finite length l which satisfies the boundary conditions

$$w = M_x = N_x = v = 0 \quad \text{at} \quad x = 0, l \quad (2.33)$$

These conditions can be closely approximated in physical application simply by means of rigidly

attaching a thin, flat, circular cover plate at each end. The plates would have considerable stiffnesses in their own planes, thereby restraining the v and w components of shell displacement at their mutual boundaries. However, the plates, by virtue of their thinness, would have very little stiffness in the x direction transverse to their planes; consequently, they would generate negligible bending moment M_x and longitudinal membrane force N_x in the shell as the shell deforms. Because of the capability of the plates to supply shearing forces $N_{x\theta}$ to the shell, the type of boundary conditions satisfied by equations (2.33) will be called *shear diaphragm* in this work. Other terminologies frequently found in the literature to describe the edge conditions given by equations (2.33) are "simply supported" and "freely supported." The phrase "simply supported" is a carryover from linear beam and plate theory where it is thought of as a flat edge either supported by knife edges or hinged. In the case of a beam or plate, hinged ends are usually found in practical application as *fixed* hinges; that is, fixed with respect to their longitudinal or inplane directions as well as the transverse direction. For small deflections yielding the classical linear theory, this fixity has no effect on the transverse deflections. Of course, in the case of a shell the degree of tangential fixity at the edges has a major effect on transverse deflections and vibra-

tion frequencies. The phrase "freely supported" is also misleading for it may connote no tangential fixity (i.e., $N_{xy}=0$ at $x=0, l$) at first encounter with the reader, although it has also been used by some authors to identify boundary conditions of the type $u=v=w=M_x=0$ (cf., refs. 2.32 through 2.34).

The circular cylindrical shell supported at both ends by shear diaphragms (referred to later in this monograph as SD-SD) has received by far the most attention in the literature. This is due to the fact that one simple form of the solutions to the eighth order differential equations of motion is also capable of satisfying the SD-SD boundary conditions exactly. This solution has already been presented as equations (2.20). Choosing

$$\lambda = m\pi R/l \quad (m=1, 2, \dots) \quad (2.34)$$

the boundary condition equations (2.33) are satisfied exactly. Further substitution of equations (2.20) into equations (2.1), (2.3), (2.7), and (2.9) yields the *characteristic* (or *frequency*) *determinant*. The characteristic determinant according to the Donnell-Mushtari theory has already been indicated as the determinant of the coefficient matrix of equation (2.21). The determinant may be expanded to yield a *characteristic equation*, the roots of which are the nondimensional frequency parameter eigenvalues.

2.3.1 Comparison of Theories

The solution procedure described above has been carried out for each of the shell theories given in section 2.1.1. The resulting characteristic equations can be written as

$$\Omega^6 - (K_2 + k \Delta K_2) \Omega^4 + (K_1 + k \Delta K_1) \Omega^2 - (K_0 + k \Delta K_0) = 0 \quad (2.35)$$

where Ω is the nondimensional frequency parameter given previously in equation (2.26); k is the nondimensional thickness parameter given in equation (2.6); K_0, K_1, K_2 are constants arising from the Donnell-Mushtari theory; and $\Delta K_1, \Delta K_2, \Delta K_3$ are modifying constants depending upon the shell theory being used.

When the characteristic equations are written in the form of equation (2.35), the differences among the shell theories insofar as they affect the computed free vibration frequencies can be seen

more clearly. That is, each coefficient of the cubic equation in Ω^2 differs from the Donnell-Mushtari theory (and each other) by a term multiplied by k , which is a small number for thin shells. The Donnell-Mushtari constants are

$$\left. \begin{aligned} K_2 &= 1 + \frac{1}{2}(3-\nu)(n^2 + \lambda^2) + k(n^2 + \lambda^2)^2 \\ K_1 &= \frac{1}{2}(1-\nu) \left[(3+2\nu)\lambda^2 + n^2 + (n^2 + \lambda^2)^2 \right. \\ &\quad \left. + \frac{(3-\nu)}{(1-\nu)} k(n^2 + \lambda^2)^3 \right] \\ K_0 &= \frac{1}{2}(1-\nu)[(1-\nu^2)\lambda^4 + k(n^2 + \lambda^2)^4] \end{aligned} \right\} \quad (2.36)$$

The modifying constants for each shell theory are given in table 2.4. For simplicity the modifying constants given in table 2.4 have been linearized with respect to k . That is, terms containing k^3 and k^2 which arise in the expansion of the characteristic determinants have been neglected with respect to those containing only k . A further simplification which can be made at this point is to neglect k with respect to unity in the coefficients $K_0 + \Delta K_0$, etc. of equation (2.35). This is precisely the difference between the Biezeno and Grammel modifying constants and those of Flügge. Flügge (ref. 2.31) made this further simplification, while Biezeno and Grammel (ref. 2.30), using the same characteristic determinant, did not. The two types of simplification described above are examples of why it is often difficult to compare equations used in different references on shell vibrations.

The characteristic equation for the membrane theory is obtained from that of the Donnell-Mushtari theory by simply setting $k=0$.

The cubic equation (2.35) in the nondimensional frequency parameter Ω^2 will have three roots for fixed values of n and λ ($=m\pi R/l$) (cf., the discussion in ref. 2.3). Thus a shell of a given length may vibrate in any of three distinct modes, each having the same number of circumferential and longitudinal waves, and each having its own distinct frequency. The modes associated with each frequency can be classified as primarily radial (or flexural), longitudinal (or axial), or circumferential (or torsional). The lowest frequency is usually associated with a motion that is primarily radial.

TABLE 2.4—*Modifying Constants for the Characteristic Equation (2.35)*

Shell theory	ΔK_2	ΔK_1	ΔK_0
Donnell-Mushtari	0	0	0
Love-Timoshenko	$(1-\nu)\lambda^2+n^2$	$(1-\nu)\lambda^2+n^2+(1-\nu)\lambda^4$ $-\frac{1}{2}(3-\nu^2)\lambda^2n^2-\frac{1}{2}(3+\nu)n^4$	$\frac{1}{2}(1-\nu)[2(1-\nu^2)\lambda^4+(3+\nu)\lambda^2n^2+n^4]$ $-(2+\nu)(3-\nu)\lambda^4n^2-(7+\nu)\lambda^2n^4-2n^6]$
Goldenveizer-Novozhilov (also Arnold-Warburton)	$2(1-\nu)\lambda^2+n^2$	$2(1-\nu)\lambda^2+n^2+2(1-\nu)\lambda^4$ $-(2-\nu)\lambda^2n^2-\frac{1}{2}(3+\nu)n^4$	$\frac{1}{2}(1-\nu)[4(1-\nu^2)\lambda^4+4\lambda^2n^2+n^4]$ $-2(2-\nu)(2+\nu)\lambda^4n^2-8\lambda^2n^4-2n^6]$
Houghton-Johns (Simplified Goldenveizer-Novozhilov)	0	$2(2-\nu)\lambda^2n^2-2n^4$	$\frac{1}{2}(1-\nu)[-2(2-\nu)(2+\nu)\lambda^4n^2-8\lambda^2n^4-2n^6]$
Biezeno-Grammel ^a	$1-\frac{1}{2}(3+\nu)n^2+\frac{3}{2}(1-\nu)\lambda^2$	$-(3-2\nu)\lambda^2+(2-\nu)n^2+\frac{1}{2}(3-7\nu)\lambda^4$ $-(5-\nu)\lambda^2n^2-\frac{1}{2}(5-\nu)n^4$	$\frac{1}{2}(1-\nu)[(4-3\nu^2)\lambda^4+2(2-\nu)\lambda^2n^2+n^4]$ $-2\nu\lambda^6-6\lambda^4n^2-2(4-\nu)\lambda^2n^4-2n^6]$
Flügge ^b	0	0	$\frac{1}{2}(1-\nu)[2(2-\nu)\lambda^2n^2+n^4-2\nu\lambda^6]$ $-6\lambda^4n^2-2(4-\nu)\lambda^2n^4-2n^6]$
Reissner-Naghdi-Berry	$\frac{1}{2}(1-\nu)\lambda^2+n^2$	$\frac{1}{2}(1-\nu)\lambda^2+n^2+\frac{1}{2}(1-\nu)\lambda^4$ $-\frac{1}{4}(1+\nu)(3-\nu)\lambda^2n^2-\frac{1}{2}(3+\nu)n^4$	$\frac{1}{2}(1-\nu)\left[\frac{1}{2}(5+3\nu)\lambda^2n^2+n^4-2(2+\nu)\lambda^4n^2\right]$ $-2(3+\nu)\lambda^2n^4-2n^6]$
Sanders	$\frac{9}{8}(1-\nu)\lambda^2+\frac{1}{8}(9-\nu)n^2$	$\frac{9}{8}(1-\nu)\lambda^2+\frac{1}{8}(9-\nu)n^2+\frac{9}{8}(1-\nu)\lambda^4$ $-\frac{1}{4}(4-3\nu+3\nu^2)\lambda^2n^2-\frac{1}{8}(11+5\nu)n^4$	$\frac{1}{2}(1-\nu)\left[\frac{9}{4}(1-\nu^2)\lambda^4+4\lambda^2n^2+n^4\right]$ $-6\lambda^4n^2-8\lambda^2n^4-2n^6]$

^a Obtained from equation (2.9d) by keeping *all* linear terms in *k* in the expanded determinant.^b Obtained from Biezeno and Grammel frequency equation by neglecting *k* with respect to unity.

TABLE 2.4—*Modifying Constants for the Characteristic Equation (2.35)—Concluded*

Shell theory	ΔK_2	ΔK_1	ΔK_0
Vlasov	$1 - 2n^2$	$\frac{1}{2}(3 - \nu)(n^2 + \lambda^2) - 2\nu\lambda^4$ $-(6 - 3\nu + \nu^2)\lambda^2 n^2 - (3 - \nu)n^4$	$\frac{1}{2}(1 - \nu)[(n^2 + \lambda^2)^2 + 2\nu\lambda^6 - 6\lambda^4 n^2]$ $- 2(4 - \nu)\lambda^2 n^4 - 2n^6]$
Epstein-Kennard	$\frac{(1+3\nu)}{(1-\nu)} - \frac{(2-8\nu^2+3\nu^3)\lambda^2}{2(1-\nu)^2}$ $-\frac{(19-37\nu+19\nu^2+\nu^3)}{2(1-\nu)^2} - \frac{\nu^2(n^2+\lambda^2)}{(1-\nu)^2}$	$\frac{(3+8\nu-5\nu^2-\nu^3)\lambda^2}{2(1-\nu)} + \frac{(2+\nu)n^2}{2}$ $-\frac{(6+4\nu-8\nu^2+3\nu^3)\lambda^4}{4(1-\nu)} - \frac{\nu^2(n^2+\lambda^2)^3}{2(1-\nu)}$ $-\frac{(26-60\nu+40\nu^2-3\nu^3-8\nu^4)\lambda^2 n^2}{2(1-\nu)}$ $-\frac{(13-22\nu+10\nu^2)n^4}{2(1-\nu)}$	$\frac{1}{2}(1 - \nu) \left[\frac{(2+6\nu-2\nu^2-3\nu^3)\lambda^4}{2(1-\nu)} + 4\lambda^2 n^2 \right.$ $\left. + n^4 - \frac{(1+\nu)}{(1-\nu)}\lambda^6 - \frac{(7-5\nu)}{(1-\nu)}\lambda^4 n^2 \right.$ $\left. - 8\lambda^2 n^4 - 2n^6 \right]$
Kennard Simplified	$\frac{(2+\nu)}{2(1-\nu)} - \frac{(4-\nu)n^2}{2(1-\nu)}$	$\frac{(2+\nu)(3-\nu)\lambda^2}{4(1-\nu)} + \frac{(6+\nu)n^2}{4}$ $-\frac{(4-\nu)(3-\nu)\lambda^2 n^2}{4(1-\nu)} - \frac{(12-17\nu+\nu^2)n^4}{4(1-\nu)}$	$\frac{1}{2}(1 - \nu) \left[\frac{(2+\nu)\lambda^4}{2(1-\nu)} + \frac{(2+\nu)(2-3\nu)\lambda^2 n^2}{2(1-\nu)} + n^4 \right.$ $\left. - \frac{(4-\nu)\lambda^4 n^2}{2(1-\nu)} - \frac{(8-8\nu-3\nu^2)\lambda^2 n^4}{2(1-\nu)} - 2n^6 \right]$
Membrane	$-(n^2 + \lambda^2)$	$-\frac{1}{2}(3 - \nu)(n^2 + \lambda^2)^3$	$-\frac{1}{2}(1 - \nu)(n^2 + \lambda^2)^4$

^a Obtained from equation (2.9d) by keeping *all* linear terms in *k* in the expanded determinant.^b Obtained from Biezeno and Grammel frequency equation by neglecting *k* with respect to unity.

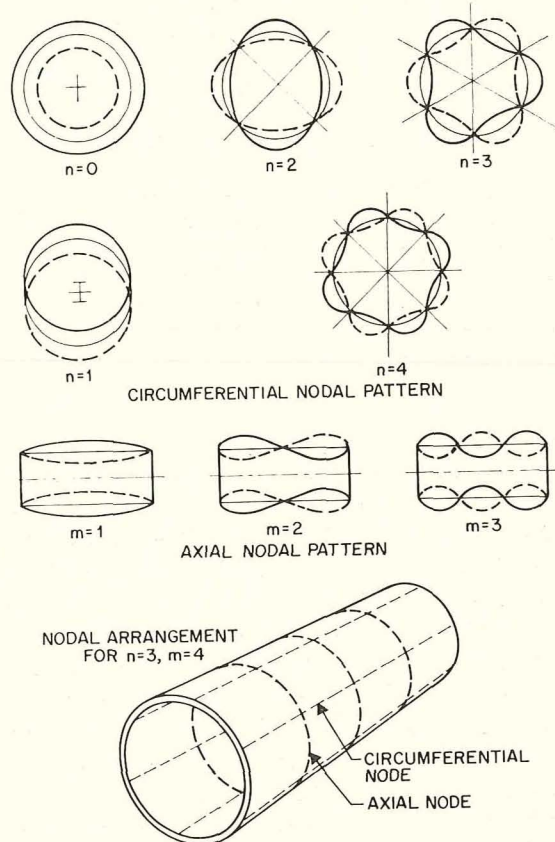
The mode shapes (or eigenfunctions) of free vibration are found by returning to the homogeneous set of equations which yielded the characteristic equation. In the case of the Donnell-Mushtari theory, this set is given by equation (2.21). Any two of the equations are chosen and the third is discarded. The two remaining equations can be solved for the ratios of amplitudes, the most convenient ratios to choose being A/C and B/C . For example, using the first two of equations (2.21), it is clear that they can be rewritten as

$$\begin{bmatrix} -\lambda^2 - \frac{(1-\nu)}{2}n^2 + \Omega^2 & \frac{(1+\nu)}{2}\lambda n \\ \frac{(1+\nu)}{2}\lambda n & -\frac{(1-\nu)}{2}\lambda^2 - n^2 + \Omega^2 \end{bmatrix} \begin{bmatrix} A/C \\ B/C \end{bmatrix} = \begin{bmatrix} -\nu\lambda \\ n \end{bmatrix} \quad (2.37)$$

which can be inverted to find A/C and B/C corresponding to each of the three frequency parameters Ω which exist for fixed values of n and λ . The resulting mode shapes will not have true nodal lines; that is, there will be no lines on the surface of the shell for which u , v , and w will all be zero.* As can be seen from equations (2.20) nodal lines will occur so that two of the displacement components will be zero and the other will be a maximum. As indicated above, the lowest of the three frequencies for each n and λ will usually yield A/C and B/C ratios less than unity, indicating that the motion is primarily radial. Typical radial nodal patterns for circular cylindrical shells supported by shear diaphragms are shown in figure 2.2 (taken from ref. 2.35).

Because exact solutions of equation (2.35) can readily be found, this permits comparison of differences in frequencies according to the various theories for the particular shell curvature and boundary conditions being used here. Numerous references are available which take this approach to obtain exact solutions; these references, and the shell theories which they use are summarized in table 2.5. In addition to the references in table 2.5, there are others following the same exact solution procedure, but using a theory other than those included in table 2.5; this group includes references 2.50 and 2.93 through 2.97. Other works, including references 2.98 through 2.107 deal with an energy formulation of the problem. Other analytical methods such as Galerkin, finite

differences, and finite element techniques are used in references 2.12, 2.13, 2.16, 2.36, 2.79, 2.84, and 2.108 through 2.114. In many of these cases the approximate method was used to solve a more complicated problem (cf., chapter 3) and



* In the case of axisymmetric modes ($n=0$), the radial, longitudinal, and circumferential motions do completely uncouple, giving distinct nodal lines.

FIGURE 2.2.—Nodal patterns for circular cylindrical shells supported at both ends by shear diaphragms. (After ref. 2.35)

TABLE 2.5.—References Using the Exact Solution Equations (2.9)

Shell theory	References
Donnell-Mushtari	2.32 through 2.53, 2.115
Love-Timoshenko	2.32, 2.37, 2.47, 2.54 through 2.59, 2.130
Goldenveizer-Novozhilov (also Arnold & Warburton)	2.3, 2.4, 2.32, 2.42, 2.48, 2.54, 2.60 through 2.67
Houghton and Johns (Simplified Goldenveizer-Novozhilov)	2.68
Flügge	2.20, 2.27, 2.28, 2.31, 2.35, 2.47, 2.48, 2.49, 2.50, 2.54, 2.59, 2.62, 2.66, 2.69 through 2.82
Reissner-Naghdi-Berry	2.83
Sanders	2.84, 2.85
Vlasov	2.47, 2.86, 2.87
Epstein and Kennard	2.54, 2.66, 2.88, 2.89, 2.90
Kennard Simplified	2.91, 2.92
Coupry	2.12, 2.13, 2.62
Yu	2.227

results for the more simple problem discussed in this section were included as a special case. Literature sources for experimental results include references 2.3, 2.4, 2.12, 2.29, 2.33, 2.36, 2.37, 2.39, 2.45, 2.62, 2.64, 2.70, 2.74, 2.83, 2.85, 2.87, 2.88, 2.90, 2.98, 2.99, 2.101, 2.102, 2.103, 2.106, 2.107, 2.116, and 2.117.

To allow for a meaningful comparison between the various theories on the circular cylindrical shell supported at both ends by shear diaphragms it was necessary to perform an independent set of calculations for the roots of the cubic equation (2.35) in Ω^2 . This procedure was necessary because of the different thickness/radius and length/radius ratios used by the various references listed above and because of the paucity of numerical results which are available in the

literature for some theories. Furthermore, to allow an accurate comparison of theories, tabular results must be available.

Numerical results for fundamental frequencies arising from the solution of equation (2.35) by digital computer are given in table 2.6 for the shell theories shown, for five circumferential wave numbers ($n=0, 1, 2, 3, 4$), for six values of length/radius ratio ($l/mR=0.1, 0.25, 1, 4, 20, 100$), for $R/h=20$, and for $\nu=0.3$. The quotient l/m indicates that a shell having twice the length and twice the number of axial half-waves as another will vibrate at the same frequency as the latter, because node lines duplicate shear diaphragm edge conditions. For simplicity, m is considered to be unity in the discussion of the tables below. In table 2.7 corresponding results are given for $R/h=500$.

To emphasize the differences in free vibration frequencies which can result from the various theories, tables 2.6 and 2.7 list the percent by which the shell frequency parameters differ from those found by an exact three-dimensional elasticity solution. Values of the frequency parameter Ω arising from the elasticity solution are given in table 2.8. The elasticity solution is explained in appendix A. In reference 2.118 comparisons of the results of eighth order shell theories with the exact three-dimensional elasticity solutions are also made.

For the case of the very thin shell ($R/h=500$) for $l/mR=0.1$ and 0.25, the numerical procedure was not able to find the roots of the characteristic determinant of the elasticity solution even though 30 significant figures were carried during all phases of the calculations (expansion of the series for Bessel functions, set-up of the frequency determinant, evaluating the determinant, etc.). Consequently, the corresponding ten values listed in table 2.8 are from the widely-used Flügge theory instead.

Tables 2.6 and 2.7 also divide the shell theories into four categories: (1) the Donnell-Mushtari theory, (2) other general first approximation shell theories, (3) two "simplified" shell theories obtained from other theories by neglecting k with respect to unity in the equations of motion (see sec. 2.1.1), and (4) the membrane theory.

From tables 2.6 and 2.7 the following general conclusions are evident:

(1) The theories *within each group* show close agreement with each other over essentially the entire range of length parameter l/mR and for both thickness ratios. Significant differences exist only between one group and another.

(2) All theories show close agreement for shells of moderate length ($l/mR = 1, 4$) and small numbers of circumferential waves ($n = 0, 1, 2$).

(3) For very thin shells ($R/h = 500$) the theories are in closer agreement than for thicker ones ($R/h = 20$).

(4) For very short shells ($l/mR = 0.1, 0.25$) none of the shell theories compare favorably with elasticity theory (due to end effects), although they compare well with each other. The membrane theory is inadequate in this region.

(5) For very long shells, and $n = 0$ ($l/mR = 20, 100$) the theories are in essentially exact agreement (the mode shape is pure torsional for the fundamental frequency).

(6) For very long shells the membrane theory is grossly inadequate except for $n = 0, 1$.

(7) For very long shells and $n = 1$, most of the "simplified" theories are completely inadequate, yielding frequencies which are imaginary (negative values of the roots for Ω^2). These theories behave acceptably, however, for all other n . This same type of behavior was found for corresponding "simplified" versions of the Love-Timoshenko, Reissner-Naghdi-Berry, and Sanders theories, although the simplified Kennard theory behaved acceptably.

(8) For very long shells and $n = 1, 2$ the Donnell theory is in substantial error, although the error decreases if n continues to increase ($n = 3, 4, \dots$).

These qualitative conclusions are more readily apparent from figures 2.3 through 2.10 (from ref. 2.119) wherein Ω is plotted versus l/mR for the thicker shell ($R/h = 20$). The numbers used on these graphs identify the groups of shell theories as in tables 2.6 and 2.7. The number "5" indicates the exact, three-dimensional elasticity solution.

As indicated previously, for each n three roots of the frequency equation exist. Tables 2.6 and 2.7 give the percent by which the lowest non-trivial frequency for each n deviates from the corresponding three-dimensional elasticity solu-

tion. The agreement is generally much better for the higher two modes than the lowest. It was found that the higher frequencies agreed within 0.01 percent for all theories, all n , and all l/mR when R/h was 500. The percentages by which the higher two frequencies differ from those of the Flügge theory are listed in table 2.9 for $R/h = 20$. Again it is seen that the agreement among the theories is excellent, with only the Epstein-Kennard theory showing significant deviation for very short shells. The frequency parameters according to the Flügge theory which are the basis for the comparisons made in table 2.9 are given in table 2.10.

The amplitude ratios A/C and B/C according to the Flügge theory for the lowest frequencies are presented in table 2.11 for $n = 0, 1, 2, 3, 4$ and $l/mR = 0.25, 1, 4, 20$. The percentages by which the amplitude ratios differ from these values according to the other shell theories are given in table 2.12 for $R/h = 20$. These ratios and the corresponding mode shapes agree very closely for all the theories except for very short shells ($l/mR = 0.25$). The Biezeno-Grammel, Vlasov, and Flügge equations agree closely on amplitude ratios even for short shells. For $R/h = 500$, the agreement among the theories for the amplitude ratios was even better. For $l/mR = 1, 4, 20$ the values of A/C and B/C differed from the Flügge theory by less than 0.01 percent for all theories, as well as for the B/C ratio for $l/mR = 0.25$. The A/C ratio for $l/mR = 0.25$ differed among the theories by 0.02 percent or less for all theories except for $n = 1$ where the Flügge, Biezeno-Grammel, Vlasov, and Epstein-Kennard results agreed to within 0.01 percent, but the others all differed from Flügge by approximately 4 percent.

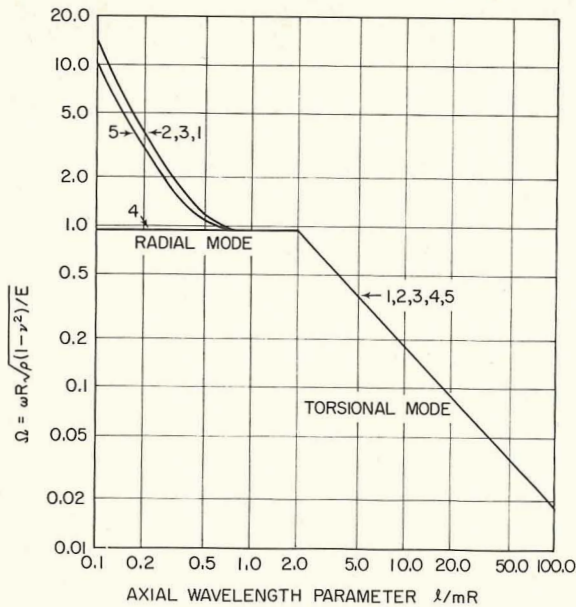


FIGURE 2.3.—Variation of the fundamental frequency parameter Ω with l/mR ; $\nu=0.3$, $R/h=20$, $n=0$. (Nos. 1, 2, 3, 4 refer to the groups listed in tables 2.6 and 2.7. No. 5 indicates the three-dimensional elasticity solution.) (After ref. 2.119)

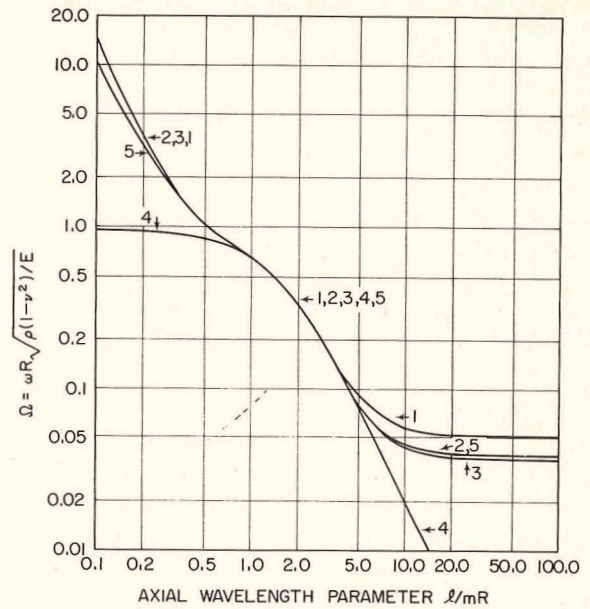


FIGURE 2.5.—Variation of the fundamental frequency parameter Ω with l/mR ; $\nu=0.3$, $R/h=20$, $n=2$. (Nos. 1, 2, 3, 4 refer to the groups listed in tables 2.6 and 2.7. No. 5 indicates the three-dimensional elasticity solution.) (After ref. 2.119)

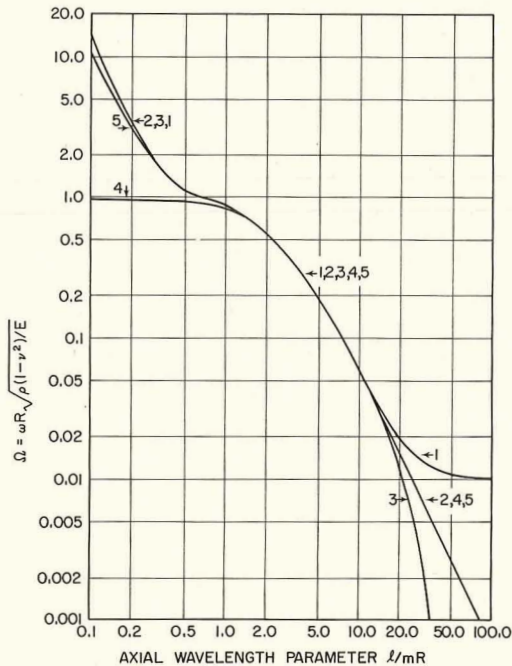


FIGURE 2.4.—Variation of the fundamental frequency parameter Ω with l/mR ; $\nu=0.3$, $R/h=20$, $n=1$. (Nos. 1, 2, 3, 4 refer to the groups listed in tables 2.6 and 2.7. No. 5 indicates the three-dimensional elasticity solution.) (After ref. 2.119)

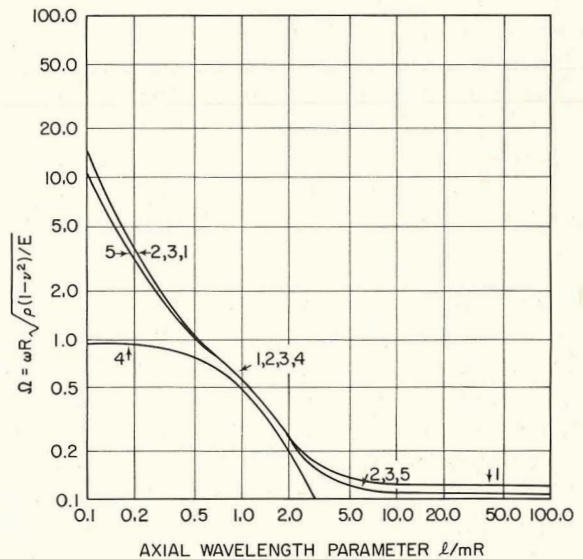


FIGURE 2.6.—Variation of the fundamental frequency parameter Ω with l/mR ; $\nu=0.3$, $R/h=20$, $n=3$. (Nos. 1, 2, 3, 4 refer to the groups listed in tables 2.6 and 2.7. No. 5 indicates the three-dimensional elasticity solution.) (After ref. 2.119)

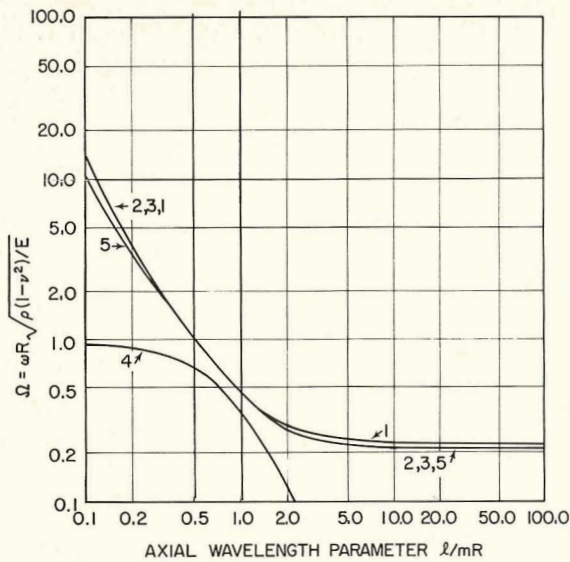


FIGURE 2.7.—Variation of the fundamental frequency parameter Ω with l/mR ; $\nu=0.3$, $R/h=20$, $n=4$. (Nos. 1, 2, 3, 4 refer to the groups listed in tables 2.6 and 2.7. No. 5 indicates the three-dimensional elasticity solution.) (After ref. 2.119)

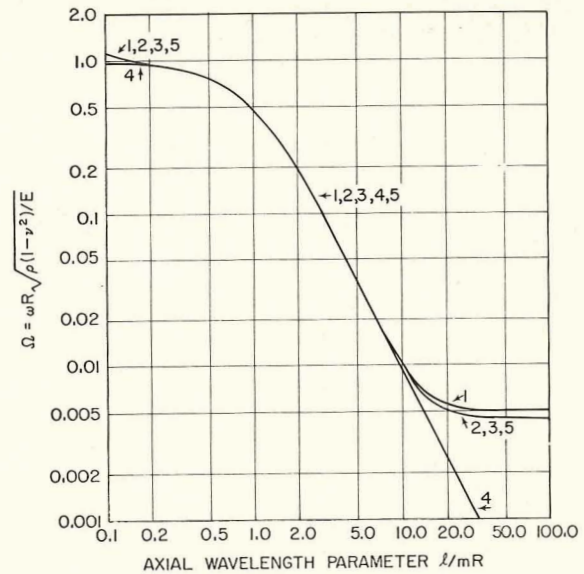


FIGURE 2.9.—Variation of the fundamental frequency parameter Ω with l/mR ; $\nu=0.3$, $R/h=500$, $n=3$. (Nos. 1, 2, 3, 4 refer to the groups listed in tables 2.6 and 2.7. No. 5 indicates the three-dimensional elasticity solution.) (After ref. 2.119)

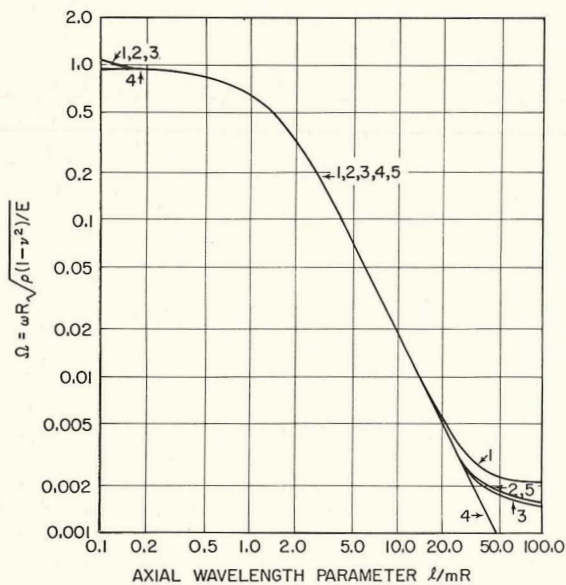


FIGURE 2.8.—Variation of the fundamental frequency parameter Ω with l/mR ; $\nu=0.3$, $R/h=500$, $n=2$. (Nos. 1, 2, 3, 4 refer to the groups listed in tables 2.6 and 2.7. No. 5 indicates the three-dimensional elasticity solution.) (After ref. 2.119)

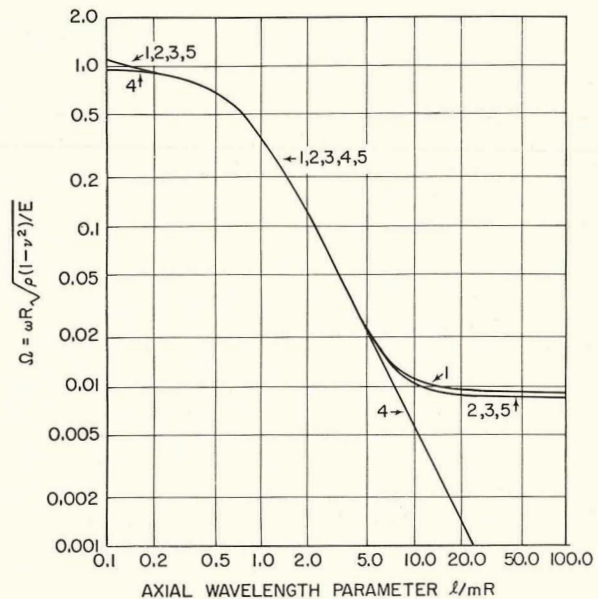


FIGURE 2.10.—Variation of the fundamental frequency parameter Ω with l/mR ; $\nu=0.3$, $R/h=500$, $n=4$. (Nos. 1, 2, 3, 4 refer to the groups listed in tables 2.6 and 2.7. No. 5 indicates the three-dimensional elasticity solution.) (After ref. 2.119)

TABLE 2.6.—*Percent Differences in Lowest Frequency Parameters Between Shell Theories and Three-Dimensional Elasticity Theory; SD-SD Supports; $\nu=0.3$; $R/h=20$*

Shell theory		n	l/mR					
Group	Name		0.1	0.25	1	4	20	100
1	Donnell-Mushtari	0	36.51	8.10	0.17	(a)	(a)	(a)
2	Love-Timoshenko		36.44	8.08	.17	(a)	0.02	0.02
	Goldenveizer-Novozhilov		36.37	8.06	.17	0.03	.04	.04
	Biezeno-Grammel		36.35	7.89	.11	.03	.03	.03
	Flügge		36.38	7.90	.07	−.01	(a)	(a)
	Reissner-Naghdi-Berry		36.47	8.09	.15	−.01	−.01	−.01
	Sanders		36.43	8.08	.17	.02	.02	.02
	Vlasov		36.45	7.92	.11	(a)	(a)	(a)
	Epstein-Kennard		39.78	7.90	(a)	−.09	−.07	−.05
3	Houghton-Johns Kennard Simplified		36.51	8.10	.17	(a)	(a)	(a)
			36.51	8.10	.19	(a)	(a)	(a)
4	Membrane		−90.88	−58.27	−.93	(a)	(a)	(a)
1	Donnell-Mushtari	1	36.53	8.16	.25	.15	18.89	1683.80
2	Love-Timoshenko		36.46	8.12	.16	−.02	−.02	−.06
	Goldenveizer-Novozhilov		36.39	8.10	.14	−.02	−.02	−.06
	Biezeno-Grammel		36.38	7.94	.12	.01	(a)	−.05
	Flügge		36.41	7.94	.07	−.05	−.05	−.11
	Reissner-Naghdi-Berry		36.50	8.14	.17	−.02	.14	3.90
	Sanders		36.45	8.12	.16	−.02	−.02	−.08
	Vlasov		36.48	7.97	.11	−.05	−.67	−17.92
	Epstein-Kennard		39.81	7.95	(a)	−.01	.02	−.02
3	Houghton-Johns Kennard Simplified		36.53	8.14	.13	−.16	−23.45	1432.23i
			36.53	8.16	.24	.68	.94	20.97
4	Membrane		−90.90	−58.69	−1.34	−.05	−.03	−.03
1	Donnell-Mushtari	2	36.62	8.33	.62	4.85	32.97	33.21
2	Love-Timoshenko		36.55	8.26	.21	.15	.17	−.11
	Goldenveizer-Novozhilov		36.48	8.23	.13	−.04	.10	−.12
	Biezeno-Grammel		36.47	8.09	.19	.17	.17	−.10
	Flügge		36.49	8.09	.10	.08	.12	−.14
	Reissner-Naghdi-Berry		36.59	8.28	.28	.35	.25	−.10
	Sanders		36.54	8.26	.20	.02	.09	−.11
	Vlasov		36.57	8.12	.17	.06	.13	−.09
	Epstein-Kennard		39.92	8.13	.02	.03	.19	−.02
3	Houghton-Johns Kennard Simplified		36.62	8.27	.01	−.74	−5.52	−5.82
			36.62	8.32	.46	1.11	.60	−.07
4	Membrane		−90.94	−59.93	−3.46	−7.07	−86.68	−99.45

^a Differences of less than 0.01 percent.

TABLE 2.6.—*Percent Differences in Lowest Frequency Parameters Between Shell Theories and Three-Dimensional Elasticity Theory; SD-SD Supports; $\nu=0.3$; $R/h=20$ —Concluded*

Shell theory		n	l/mR					
Group	Name		0.1	0.25	1	4	20	100
1	Donnell-Mushtari	3	36.77	8.62	1.57	10.35	12.87	12.87
2	Love-Timoshenko		36.69	8.50	.39	.46	.32	.31
	Goldenveizer-Novozhilov		36.62	8.45	.21	.25	.31	.30
	Biezeno-Grammel		36.61	8.35	.39	.46	.33	.32
	Flügge		36.63	8.35	.31	.40	.28	.26
	Reissner-Naghdi-Berry		36.72	8.53	.56	.69	.33	.31
	Sanders		36.68	8.50	.35	.28	.30	.30
	Vlasov		36.71	8.38	.36	.04	.34	.33
	Epstein-Kennard		40.09	8.42	.15	.35	.42	.42
3	Houghton-Johns	4	36.75	8.50	.16	-.37	-.47	-.47
	Kennard Simplified		36.76	8.59	.98	1.54	.40	.33
4	Membrane		-91.03	-61.89	-10.82	-55.48	-97.74	-99.93
1	Donnell-Mushtari		36.97	9.01	2.94	7.18	7.34	7.34
2	Love-Timoshenko		36.88	8.83	.78	.70	.61	.61
	Goldenveizer-Novozhilov		36.81	8.77	.53	.61	.61	.61
	Biezeno-Grammel		36.81	8.70	.79	.71	.63	.63
	Flügge		36.83	8.70	.71	.64	.57	.56
	Reissner-Naghdi-Berry		36.92	8.87	1.03	.78	.62	.61
	Sanders		36.88	8.83	.69	.62	.61	.60
	Vlasov		36.91	8.73	.77	.71	.64	.64
	Epstein-Kennard		40.33	8.82	.55	.74	.74	.74
3	Houghton-Johns		36.95	8.81	.47	.41	.39	.39
	Kennard Simplified		36.97	8.95	1.68	1.13	.65	.63
4	Membrane		-91.14	-64.44	-28.13	-84.34	-99.32	-99.52

TABLE 2.7.—Percent Differences in Lowest Frequency Parameters Between Shell Theories and Three-Dimensional Elasticity Theory; SD-SD Supports; $\nu=0.3$; $R/h=500$

Shell theory		n	l/mR					
Group	Name		^a 0.1	^a 0.25	1	4	20	100
1	Donnell-Mushtari	0	(b)	(b)	(b)	(b)	(b)	(b)
2	Love-Timoshenko		(b)	(b)	(b)	(b)	(b)	(b)
	Goldenveizer-Novozhilov		(b)	(b)	(b)	(b)	(b)	(b)
	Biezeno-Grammel		(b)	(b)	(b)	(b)	(b)	(b)
	Flügge		(b)	(b)	(b)	(b)	(b)	(b)
	Reissner-Naghdi-Berry		(b)	(b)	(b)	(b)	(b)	(b)
	Sanders		(b)	(b)	(b)	(b)	(b)	(b)
	Vlasov		(b)	(b)	(b)	(b)	(b)	(b)
	Epstein-Kennard		-0.01	(b)	(b)	(b)	(b)	(b)
3	Houghton-Johns		(b)	(b)	(b)	(b)	(b)	(b)
	Kennard Simplified		(b)	(b)	(b)	(b)	(b)	(b)
4	Membrane		-14.14	-0.45	(b)	(b)	(b)	(b)
1	Donnell-Mushtari	1	(b)	(b)	(b)	(b)	0.03	17.37
2	Love-Timoshenko		(b)	(b)	(b)	(b)	(b)	(b)
	Goldenveizer-Novozhilov		(b)	(b)	(b)	(b)	(b)	(b)
	Biezeno-Grammel		(b)	(b)	(b)	(b)	(b)	(b)
	Flügge		(b)	(b)	(b)	(b)	(b)	(b)
	Reissner-Naghdi-Berry		(b)	(b)	(b)	(b)	(b)	0.01
	Sanders		(b)	(b)	(b)	(b)	(b)	(b)
	Vlasov		(b)	(b)	(b)	(b)	(b)	-0.03
	Epstein-Kennard		-.01	(b)	(b)	(b)	(b)	(b)
3	Houghton-Johns		(b)	(b)	(b)	(b)	(b)	-21.10
	Kennard Simplified		(b)	(b)	(b)	(b)	(b)	.04
4	Membrane		-14.19	-.46	(b)	(b)	(b)	(b)
1	Donnell-Mushtari	2	(b)	(b)	(b)	0.01	.02	32.92
2	Love-Timoshenko		(b)	(b)	(b)	(b)	.02	.09
	Goldenveizer-Novozhilov		(b)	(b)	(b)	(b)	.01	.09
	Biezeno-Grammel		(b)	(b)	(b)	(b)	.02	.09
	Flügge		(b)	(b)	(b)	(b)	.02	.09
	Reissner-Naghdi-Berry		(b)	(b)	(b)	(b)	.02	.10
	Sanders		(b)	(b)	(b)	(b)	.01	.09
	Vlasov		(b)	(b)	(b)	(b)	.01	.09
	Epstein-Kennard		-.01	(b)	(b)	(b)	.01	.09
3	Houghton-Johns		(b)	(b)	(b)	(b)	-.44	-5.53
	Kennard Simplified		(b)	(b)	(b)	(b)	.05	.11
4	Membrane		-14.32	-.50	-0.01	-.01	-4.16	-86.53

^a Comparisons for $l/mR=0.1, 0.25$ are made with the Flügge theory, rather than with the three-dimensional elasticity theory.

^b Differences of less than 0.01 percent.

TABLE 2.7.—Percent Differences in Lowest Frequency Parameters Between Shell Theories and Three-Dimensional Elasticity Theory; SD-SD Supports; $\nu=0.3$; $R/h=500$ —Concluded

Shell theory		n	l/mR					
Group	Name		^a 0.1	^a 0.25	1	4	20	100
1	Donnell-Mushtari	3	(b)	(b)	(b)	0.09	9.71	12.42
2	Love-Timoshenko		(b)	(b)	(b)	(b)	.09	-.07
	Goldenveizer-Novozhilov		(b)	(b)	(b)	(b)	.09	-.07
	Biezeno-Grammel		(b)	(b)	(b)	(b)	.09	-.07
	Flügge		(b)	(b)	(b)	(b)	.09	-.07
	Reissner-Naghdi-Berry		(b)	(b)	(b)	(b)	.10	-.07
	Sanders		(b)	(b)	(b)	(b)	.08	-.07
	Vlasov		(b)	(b)	(b)	(b)	.09	-.07
	Epstein-Kennard		-.01	(b)	(b)	(b)	.08	-.07
3	Houghton-Johns		(b)	(b)	(b)	-.01	-.51	-.85
	Kennard Simplified		(b)	(b)	(b)	.01	.14	-.06
4	Membrane		-14.56	-.56	(b)	-.33	-50.89	-97.74
1	Donnell-Mushtari	4	(b)	(b)	.01	-.15	6.48	6.66
2	Love-Timoshenko		(b)	(b)	(b)	.01	(b)	-.01
	Goldenveizer-Novozhilov		(b)	(b)	(b)	(b)	(b)	-.01
	Biezeno-Grammel		(b)	(b)	(b)	.01	(b)	-.01
	Flügge		(b)	(b)	(b)	(b)	(b)	-.01
	Reissner-Naghdi-Berry		(b)	(b)	(b)	.01	(b)	-.01
	Sanders		(b)	(b)	(b)	(b)	(b)	-.01
	Vlasov		(b)	(b)	(b)	(b)	(b)	-.01
	Epstein-Kennard		-.01	(b)	(b)	(b)	(b)	-.01
3	Houghton-Johns		(b)	(b)	(b)	-.01	-.22	-.20
	Kennard Simplified		(b)	(b)	(b)	.03	.02	-.01
4	Membrane		-14.88	-.66	(b)	-3.08	-83.30	-99.32

^a Comparisons for $l/mR=0.1, 0.25$ are made with the Flügge theory, rather than with the three-dimensional elasticity theory.

^b Differences of less than 0.01 percent.

TABLE 2.8.—Lowest Frequency Parameters According to Three-Dimensional Theory; SD-SD Supports; $\nu=0.3$

R/h	n	l/mR					
		0.1	0.25	1	4	20	100
20	0	10.4586	2.28505	0.958083	0.464648	0.0929296	0.0185859
	1	10.4670	2.29380	.856414	.257011	.0161063	.000665031
	2	10.4914	2.32041	.675486	.121249	.0392332	.0347711
	3	10.5326	2.36597	.539294	.129881	.109477	.109186
	4	10.5898	2.43231	.492343	.219098	.209008	.208711
500	0	(1.11103)	(.957994)	.949203	.464648	.0929296	.0185859
	1	(1.11049)	(.951993)	.844952	.256883	.0161011	.002664824
	2	(1.10890)	(.934462)	.652148	.112689	.00545243	.00156235
	3	(1.10630)	(.906734)	.481028	.0580087	.00503724	.00438626
	4	(1.10276)	(.870765)	.354118	.0353927	.00853409	.00840299

Note: Values in parentheses are from the Flügge shell theory.

TABLE 2.9.—Percent Differences in Higher Frequency Parameters Between Shell Theories and Flügge Theory; SD-SD Supports; $\nu=0.3$; $R/h=20$

Shell theory		n	l/mR					
Group	Name		0.1	0.25	1	4	20	100
1	Donnell-Mushtari	0	−0.07 (a)	−0.03 (a)	−0.04 (a)	(a) (a)	(a) (a)	(a) (a)
	Love-Timoshenko		−.02 (a)	(a) (a)	−.02 (a)	(a) (a)	(a) (a)	(a) (a)
2	Goldenveizer-Novozhilov		.03 (a)	.02 (a)	(a) (a)	(a) (a)	(a) (a)	(a) (a)
	Biezeno-Grammel		(a) .01	(a) (a)	(a) .01	(a) 0.01	(a) 0.01	(a) 0.01
	Reissner-Naghdi-Berry		−.04 (a)	−.02 (a)	−.02 (a)	(a) (a)	(a) (a)	(a) (a)
	Sanders		(a) (a)	(a) (a)	−.01 (a)	(a) (a)	(a) (a)	(a) .01
	Vlasov		−.07 .01	−.03 (a)	−.04 .01	(a) .01	(a) 0.01	(a) .01
	Epstein-Kennard		−.07 −2.43	−.03 −.31	−.02 −.03	.29 −.19	.17 −.08	.17 −.07
3	Houghton-Johns	1	−.07 (a)	−.03 (a)	−.04 (a)	(a) (a)	(a) (a)	(a) (a)
	Kennard Simplified		−.07 (a)	−.03 (a)	−.04 (a)	(a) .01	(a) .02	(a) .02
4	Membrane		−.07 (a)	−.03 (a)	−.04 (a)	(a) (a)	(a) (a)	(a) (a)
1	Donnell-Mushtari	1	−.07 (a)	−.03 (a)	−.05 (a)	−.02 (a)	−.02 (a)	−.02 (a)
	Love-Timoshenko		−.02 (a)	(a) (a)	−.02 (a)	−.02 .01	−.02 (a)	−.02 (a)
	Goldenveizer-Novozhilov		.03 (a)	.01 (a)	(a) (a)	−.02 .01	−.02 (a)	−.02 (a)
	Biezeno-Grammel		(a) .01	(a) .01	−.03 .02	−.04 .02	−.02 (a)	−.02 (a)
	Reissner-Naghdi-Berry		−.04 (a)	−.02 (a)	−.02 (a)	−.02 .01	−.02 (a)	−.02 (a)
	Sanders		−.01 (a)	(a) (a)	−.01 (a)	−.02 .01	−.02 (a)	−.02 (a)
	Vlasov		−.07 .01	−.03 .01	−.05 .01	−.03 (a)	−.02 (a)	−.02 (a)
	Epstein-Kennard		−.07 −2.43	−.03 −.31	−.04 −.02	−.01 −.03	−.03 −.03	−.03 −.03

^a Difference <0.01 percent.

TABLE 2.9.—Percent Differences in Higher Frequency Parameters Between Shell Theories and Flügge Theory; SD-SD Supports; $\nu=0.3$; $R/h=20$ —Continued

Shell theory		n	l/mR					
Group	Name		0.1	0.25	1	4	20	100
3	Houghton-Johns	1	−0.07 (a)	−0.03 (a)	−0.03 (a)	−0.02 .01	−0.02 (a)	−0.02 (a)
	Kennard Simplified		−.07 (a)	−.03 (a)	−.05 (a)	−.02 (a)	−.01 (a)	−.01 (a)
4	Membrane		−.07 (a)	−.03 (a)	−.06 (a)	−.03 (a)	−.02 (a)	−.02 (a)
1	Donnell-Mushtari		−.07 (a)	−.04 (a)	−.07 (a)	−.06 (a)	−.06 (a)	−.06 (a)
	Love-Timoshenko		−.02 (a)	(a) (a)	−.03 .01	−.05 .03	−.06 .02	−.06 .02
	Goldenveizer-Novozhilov		.03 (a)	.01 (a)	−.01 .02	−.05 .03	−.06 .02	−.06 .02
	Biezeno-Grammel		(a) .01	(a) .01	−.06 .03	−.07 .03	−.07 .02	−.07 .02
2	Reissner-Naghdi-Berry	2	−.04 (a)	−.02 (a)	−.03 .01	−.05 .02	−.06 .02	−.06 .02
	Sanders		−.01 (a)	(a) (a)	−.02 .02	−.05 .02	−.05 .02	−.06 .02
	Vlasov		−.07 .01	−.03 .01	−.06 .02	−.06 (a)	−.06 (a)	−.06 (a)
	Epstein-Kennard		−.07 −2.44	−.04 −.31	−.09 (b)	−.13 .02	−.14 .02	−.14 .02
3	Houghton-Johns		−.07 (a)	−.03 (a)	−.03 .01	−.05 .02	−.06 .02	−.06 .02
	Kennard Simplified		−.07 (a)	−.04 (a)	−.07 (a)	−.05 (a)	−.04 (a)	−.04 (a)
4	Membrane		−.07 (a)	−.04 (a)	−.09 (a)	−.07 (a)	−.06 (a)	−.06 (a)
1	Donnell-Mushtari		−.07 (a)	−.04 (a)	−.08 .01	−.08 (a)	−.07 −.07	−.07 (a)
	Love-Timoshenko		−.02 (a)	−.01 (a)	−.04 .02	−.07 .03	−.07 .03	−.07 .03
	Goldenveizer-Novozhilov	3	.03 (a)	.01 (a)	−.03 .03	−.07 .03	−.07 .03	−.07 .03
	Biezeno Grammel		(a) .01	−.01 .01	−.08 .03	−.09 .03	−.09 .06	−.09 .03
2	Reissner-Naghdi-Berry		−.04 (a)	−.02 (a)	−.05 .02	−.07 .03	−.07 .03	−.07 .03

^a Difference <0.01 percent.

TABLE 2.9.—*Percent Differences in Higher Frequency Parameters Between Shell Theories and Flügge Theory; SD-SD Supports; $\nu=0.3$; $R/h=20$ —Concluded*

Shell theory		n	l/mR					
Group	Name		0.1	0.25	1	4	20	100
2	Sanders	3	−0.01 (a)	(a) (a)	−0.03 .02	−0.07 .03	−0.07 .03	−0.07 .03
	Vlasov		−.07 .01	−.04 .01	−.08 .02	−.08 (a)	−.07 .04	−.07 (a)
	Epstein-Kennard		−.07 −2.46	−.05 −.32	−.13 (a)	−.18 .03	−.19 .04	−.19 .04
3	Houghton-Johns	3	−.07 (a)	−.03 (a)	−.05 .02	−.07 .02	−.07 .02	−.07 .02
	Kennard Simplified		−.07 (a)	−.04 (a)	−.08 (a)	−.06 (a)	−.06 (a)	−.06 (a)
4	Membrane		−.07 (a)	−.05 (a)	−.11 (a)	−.08 (a)	−.07 (a)	−.07 (a)
1	Donnell-Mushtari		−.08 (a)	−.05 (a)	−.09 .01	−.08 (a)	−.08 (a)	−.08 (a)
	Love-Timoshenko		−.02 (a)	−.01 (a)	−.05 .03	−.08 .04	−.08 .04	−.08 .04
2	Goldenveizer-Novozhilov	4	.03 (a)	(a) (a)	−.05 .03	−.08 .04	−.08 .04	−.08 .04
	Biezeno-Grammel		(a) .01	−.02 .02	−.09 .04	−.10 .03	−.10 .03	−.10 .03
	Reissner-Naghdi-Berry		−.04 (a)	−.03 (a)	−.06 .03	−.08 .04	−.08 .07	−.08 .04
	Sanders		−.01 (a)	(a) (a)	−.04 .03	−.07 .04	−.08 .10	−.08 .04
	Vlasov		−.07 .01	−.05 .01	−.08 .02	−.08 (a)	−.08 (a)	−.08 (a)
	Epstein-Kennard		−.08 −2.48	−.06 −.33	−.16 (a)	−.20 .03	−.21 .04	−.21 .04
	Houghton-Johns		−.07 (a)	−.03 (a)	−.06 .02	−.08 .03	−.08 .03	−.08 .03
	Kennard Simplified		−.08 (a)	−.05 (a)	−.09 (a)	−.07 (a)	−.06 .02	−.06 (a)
4	Membrane		−.08 (a)	−.06 (a)	−.12 (a)	−.09 (a)	−.08 (a)	−.08 (a)

^a Difference <0.01 percent.

TABLE 2.10.—*Higher Frequency Parameters According to Flügge Theory; SD-SD Supports; $\nu=0.3$*

R/h	n	l/mR					
		0.1	0.25	1	4	20	100
20	0	18.5983	7.43666	1.85928	0.710511	0.149675	0.029968
		31.4164	12.5696	3.15724	1.05458	1.00113	1.00004
	1	18.6079	7.46093	1.98755	.888499	.609951	.592466
		31.4323	12.6095	3.31870	1.52574	1.41818	1.41440
	2	18.6368	7.53317	2.27370	1.32106	1.19015	1.18415
		31.4800	12.7281	3.75991	2.34035	2.24024	2.23628
	3	18.6847	7.65176	2.63998	1.85602	1.77950	1.77627
		31.5593	12.9235	4.39158	3.24657	3.16569	3.16245
	4	18.7516	7.81423	3.06600	2.42323	2.37061	2.36845
		31.6699	13.1921	5.13976	4.19160	4.12587	4.12323
500	0	18.5859	7.43437	1.85859	.710460	.149674	.029968
		31.4173	12.5700	3.15731	1.05456	1.00113	1.00004
	1	18.5954	7.45847	1.98631	.888232	.609841	.592359
		31.4332	12.6098	3.31882	1.52571	1.41815	1.41437
	2	18.6237	7.53021	2.27160	1.32017	1.18946	1.18347
		31.4809	12.7285	3.76012	2.34034	2.24019	2.23623
	3	18.6708	7.64802	2.63711	1.85451	1.77817	1.77496
		31.5603	12.9239	4.39184	3.24657	3.16566	3.16241
	4	18.7366	7.80949	3.06248	2.42114	2.36867	2.36652
		31.6710	13.1927	5.14004	4.19162	4.12585	4.12321

TABLE 2.11.—*Amplitude Ratios for the Lowest Frequencies According to the Flügge Theory; SD-SD Supports; $\nu=0.3$*

R/h	n	Mode No.	l/mR							
			0.25		1		4		20	
			A/C	B/C	A/C	B/C	A/C	B/C	A/C	B/C
20	0	1	0.027453	0	0.105051	0	0.560678	0	2.80248	0
	1	1	.028648	.023467	.175923	.358264	.993739	1.30367	.407336	1.03268
	2	1	.032050	.045471	.248136	.427311	.410777	.575505	.105419	.504356
	3	1	.037160	.064801	.253258	.372694	.209999	.360895	.047283	.334954
	4	1	.043299	.080678	.224076	.302545	.125034	.263035	.026765	.251122
500	0	1	.024004	0	.104146	0	.560487	0	2.80243	0
	1	1	.025077	.021729	.174560	.356523	.994089	1.30423	.407511	1.03293
	2	1	.028120	.042056	.246201	.425264	.410458	.575377	.105361	.504293
	3	1	.032664	.059825	.250773	.370494	.209260	.360420	.047129	.334617
	4	1	.038064	.074290	.221055	.300182	.124085	.262315	.026570	.250544

TABLE 2.12.—Percent Differences in Amplitude Ratios Between Shell Theories and Flugge Theory; SD-SD Supports; Lowest Frequency $\nu=0.3$, $R/h=20$

Shell theory		n	l/mR							
			0.25		1		4		20	
Group	Name		A/C	B/C	A/C	B/C	A/C	B/C	A/C	B/C
1	Donnell-Mushtari	0	-9.87	(a)	-0.66	(a)	-0.03	(a)	(a)	(a)
2	Love-Timoshenko		-9.87	(a)	-.66	(a)	-.01	(a)	0.02	(a)
	Goldenveizer-Novozhilov		-9.87	(a)	-.66	(a)	(a)	(a)	.04	(a)
	Biezeno-Grammel		(a)	(a)	(a)	(a)	.04	(a)	.03	(a)
	Reissner-Naghdi-Berry		-9.87	(a)	-.67	(a)	-.05	(a)	(a)	(a)
	Sanders		-9.87	(a)	-.66	(a)	-.01	(a)	.02	(a)
	Vlasov		(a)	(a)	(a)	(a)	(a)	(a)	(a)	(a)
	Epstein-Kennard		-3.32	(a)	-.24	(a)	-.08	(a)	-.06	(a)
3	Houghton-Johns	1	-9.87	(a)	-.66	(a)	-.03	(a)	(a)	(a)
	Kennard Simplified		-9.87	(a)	-.66	(a)	-.03	(a)	(a)	(a)
4	Membrane		-12.58	(a)	-.86	(a)	-.03	(a)	(a)	(a)
1	Donnell-Mushtari		-9.33	1.94	-.25	0.21	.09	0.08	.08	0.04
2	Love-Timoshenko		-9.46	-.92	-.39	-.07	(a)	-.02	.01	-.02
	Goldenveizer-Novozhilov		-9.55	-2.92	-.46	-.24	-.02	-.03	.01	-.02
	Biezeno-Grammel		(a)	(a)	.02	.02	.02	.01	(a)	(a)
	Reissner-Naghdi-Berry		-9.46	-.89	-.38	-.05	(a)	(a)	.01	-.02
	Sanders		-9.52	-1.91	-.44	-.14	-.03	-.03	(a)	-.02
	Vlasov		(a)	(a)	.02	.03	.03	.03	.03	.02
	Epstein-Kennard		-3.19	.79	-.13	.10	.12	.19	.12	.20
3	Houghton-Johns	2	-9.54	-2.82	-.43	-.15	-.02	-.02	(a)	(a)
	Kennard Simplified		-9.33	1.94	-.26	.20	.07	.07	.05	.02
4	Membrane		-12.48	-7.42	-.78	-.49	.04	.04	.04	.02
1	Donnell-Mushtari		-8.01	1.98	(a)	.26	.16	.09	.16	.05
2	Love-Timoshenko		-8.46	-.95	-.27	-.11	-.02	-.07	(a)	-.08
	Goldenveizer-Novozhilov		-8.76	-2.96	-.38	-.27	-.03	-.08	(a)	-.08
	Biezeno-Grammel		(a)	(a)	.01	.01	(a)	(a)	(a)	(a)
	Reissner-Naghdi-Berry		-8.45	-.92	-.24	-.08	-.01	-.07	(a)	-.08
	Sanders		-8.68	-1.95	-.36	-.19	-.07	-.08	-.05	-.08
	Vlasov		(a)	(a)	.02	.03	.03	.03	.04	.02
	Epstein-Kennard		-2.88	.83	-.06	.18	.10	.25	.11	.27
3	Houghton-Johns	2	-8.74	-2.86	-.34	-.21	-.02	-.06	(a)	-.06
	Kennard Simplified		-8.01	2.01	(a)	.26	.11	.09	.10	.06
4	Membrane		-12.28	-7.52	-.78	-.48	-.08	-.02	-.05	-.01

^a Difference <0.01 percent.

TABLE 2.12.—*Percent Differences in Amplitude Ratios Between Shell Theories and Flügge Theory; SD-SD Supports; Lowest Frequency $\nu=0.3$, $R/h=20$ —Concluded*

Shell theory		n	l/mR							
Group	Name		0.25		1		4		20	
			A/C	B/C	A/C	B/C	A/C	B/C	A/C	B/C
1	Donnell-Mushtari	3	-6.45	2.03	0.13	0.30	0.22	0.09	0.22	0.06
2	Love-Timoshenko		-7.30	-1.00	-.25	-.17	-.05	-.17	-.04	-.19
	Goldenveizer-Novozhilov		-7.85	-3.01	-.36	-.32	-.06	-.18	-.04	-.19
	Biezeno-Grammel		(a)	(a)	(a)	(a)	(a)	(a)	(a)	(a)
	Reissner-Naghdi-Berry		-7.29	-.98	-.22	-.15	-.05	-.17	-.04	-.19
	Sanders		-7.72	-2.03	-.39	-.27	-.14	-.18	-.12	-.19
	Vlasov		(a)	.01	.03	.03	.04	.02	.04	.02
	Epstein-Kennard		-2.52	.89	-.04	.28	.08	.35	.09	.38
3	Houghton-Johns	4	-7.82	-2.92	-.33	-.27	-.05	-.16	-.03	-.17
	Kennard Simplified		-6.43	2.11	.14	.35	.19	.16	.18	.13
4	Membrane		-12.12	-7.69	-.98	-.59	-.35	-.13	-.33	-.10
1	Donnell-Mushtari		-5.02	2.10	.23	.33	.28	.09	.28	.06
2	Love-Timoshenko		-6.27	-1.08	-.27	-.27	-.09	-.31	-.08	-.33
	Goldenveizer-Novozhilov		-7.05	-3.10	-.38	-.42	-.10	-.32	-.08	-.33
	Biezeno-Grammel		(a)	(a)	(a)	(a)	(a)	(a)	(a)	(a)
	Reissner-Naghdi-Berry		-6.25	-1.05	-.25	-.25	-.09	-.31	-.08	-.33
	Sanders		-6.90	-2.14	-.47	-.39	-.23	-.33	-.22	-.33
	Vlasov		(a)	.01	.03	.03	.04	.02	.04	.02
	Epstein-Kennard		-2.19	-.98	-.05	.41	.05	.50	.06	.52
3	Houghton-Johns	-7.02	-3.00	-.35	-.38	-.09	-.30	-.07	-.31	
	Kennard Simplified	-4.97	2.26	.29	.46	.30	.25	.30	.22	
4	Membrane	-12.11	-7.93	-1.35	-.78	-.76	-.27	-.73	-.23	

^a Difference <0.01 percent.

2.3.2 Additional Results for Frequencies and Mode Shapes

In the previous subsection the accuracy of the shell theories was compared for $n=0, 1, 2, 3, 4$ circumferential waves. The lowest of three frequencies for each n was determined. However, no attempt was made to determine the "fundamental frequency" (i.e., the lowest frequency for all n) for any shell. Some fundamental frequencies may have occurred in the tables for particular values of l/mR , but others will require larger values of n .

Thus, the complexity of the frequency spectrum for the shell is apparent. There appears to be no simple rule for determining the spacing of the frequencies as the wave numbers m and n are varied. This condition is in contrast with other, more simple, physical systems. For example, in the case of the transversely vibrating prestretched string, the successive natural frequencies are spaced according to the longitudinal wave number n (an integer), while for a simply supported beam they are spaced by $1/n^2$. Considering two dimensional problems, for an initially taut rectangular membrane the frequencies depend upon $\sqrt{(m/a)^2 + (n/b)^2}$, where m and n are integers and a and b are the membrane length and width, and for a simply supported rectangular plate they vary according to $(m/a)^2 + (n/b)^2$. Such simple behavior is not the case for the circular cylindrical shell supported by shear diaphragms (which is the generalization of the simple support conditions used in the other problems described above). To determine the response of a structure excited in a very complex or random manner it is important to know the relative spacing of the frequencies. This spacing can be expressed in terms of the "modal density" concept. Studies of the modal density of circular cylindrical shells supported by shear diaphragms were made in references 2.88, 2.90, 2.120, and 2.195.

A comprehensive study of the circular cylindrical shell supported at both ends by shear diaphragms was made by Forsberg (refs. 2.35, 2.72, and 2.73) using the Donnell and Flügge theories. In figure 2.11 (taken from ref. 2.35) the frequency parameter $\Omega = \omega R \sqrt{\rho(1-\nu^2)/E}$ is plotted as a function of the length/radius ratio

l/mR for numbers of circumferential waves n varying between 0 and 28 for a relatively thin shell ($R/h=500$) according to the Flügge theory. It is obvious from figure 2.11 that, for a fixed number of circumferential waves, the frequency increases with an increased number of longitudinal half-waves m , and that the fundamental (lowest) frequency always occurs for $m=1$, but for varying n depending strongly upon the length/radius ratio of the shell. For example, for a shell having $R/h=500$ and $l/R=2$, the fundamental frequency occurs for $m=1, n=8$. However, there are over 90 modes with values of m up to 6 and n up to 24 having natural frequencies which are less than that for the simple mode shape $m=1, n=2$ (ref. 2.35)! The fundamental frequencies, which are given by the envelope of figure 2.11 when $m=1$, are shown in figure 2.12 for various R/h ratios (ref. 2.35). Results from both the Flügge and Donnell-Mushtari theories are given. Further comparisons of frequencies obtained from the Donnell-Mushtari and Flügge theories can be made in figures 2.13 where n is taken to be 2.

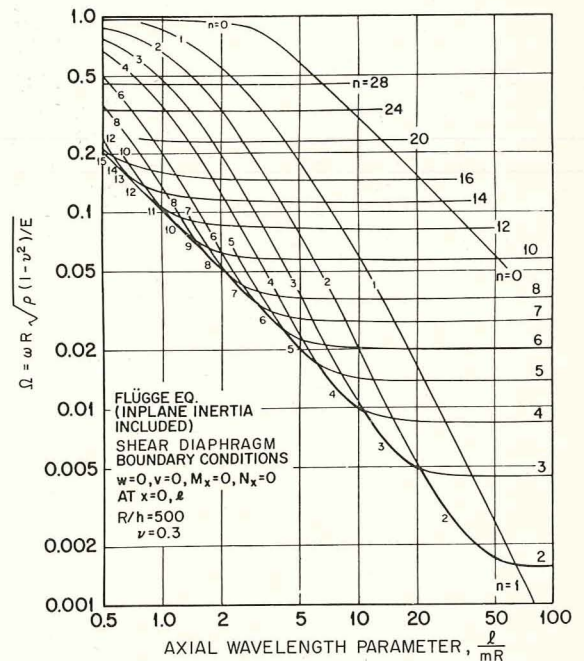


FIGURE 2.11.—Variation of the frequency parameter Ω according to the Flügge theory ($R/h=500$). (After ref. 2.35)

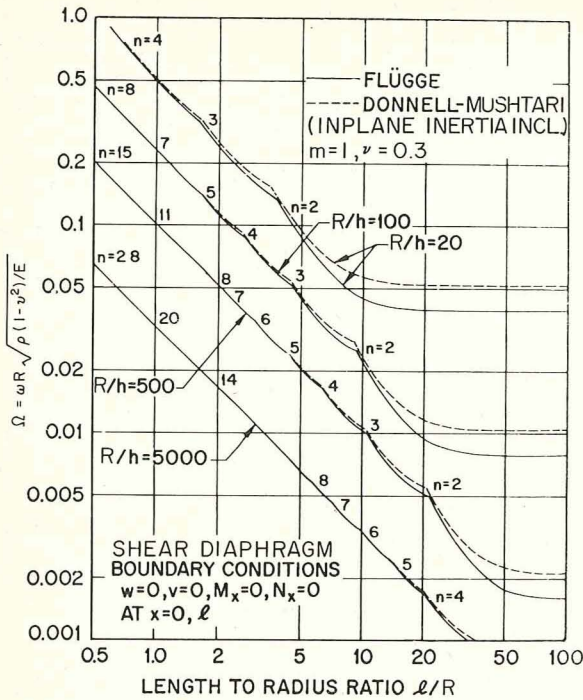


FIGURE 2.12.—Fundamental frequency parameters Ω for various l/R and R/h ratios. (After ref. 2.35)

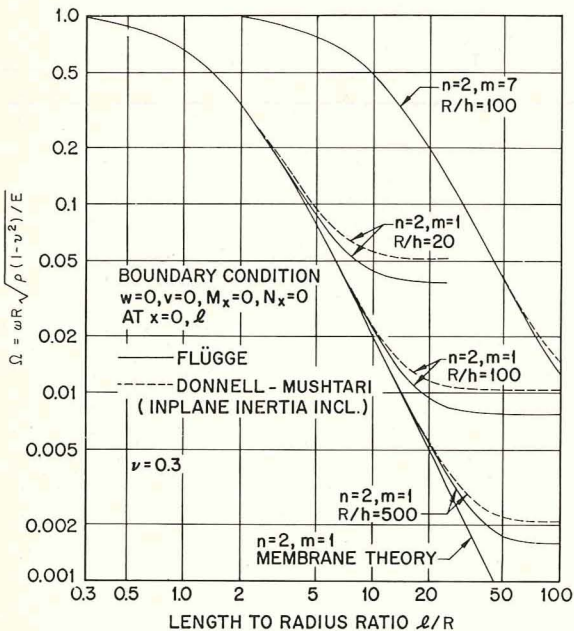


FIGURE 2.13.—Comparison of Flügge and Donnell frequency spectra for $n=2$. (After ref. 2.35)

As found in section 2.3.1, figures 2.12 and 2.13 show that the Flügge and Donnell theories agree closely for short shells, but that the frequencies differ increasingly as the length (l/R) and thickness (h/R) ratios increase.

A similar numerical study was made by Bozich (ref. 2.69), also using the Flügge theory and (apparently) $\nu=0.3$. Figures 2.14 through 2.17 show lowest values of Ω plotted versus l/mR for $R/h=20, 50, 100$, and 2000, respectively. In these figures the solid lines correspond to motions which are primarily radial ($A < C, B < C$). However, it is also seen that for the axisymmetric ($n=0$) and beam bending ($n=1$) modes, as l/mR is increased, the motions become axial and mixed, respectively, as shown by the dashed lines. More precisely, Bozich showed that for $n=0$ the motion associated with $l/mR < 2$ in these figures is primarily radial, and for $l/mR > 2$ it is torsional. Furthermore, for $l/mR > \pi$, radial motion corresponds to the largest of the three eigenvalues. For $n=1$ the amplitude of the radial and circumferential displacements corresponding to the lowest eigenvalue are approximately equal and greater than the axial (or longitudinal) displacement for $l/mR > 3.5$, and the resulting deflection is similar to beam bending with little deviation in circular cross section.

In figure 2.14 the envelope of the frequency curves establishes the fundamental frequency for the R/h ratio of 20. It is interesting to note that for shells having an l/R ratio in the vicinity of unity, the fundamental frequency is associated with four circumferential waves ($n=4$), whereas for both larger and smaller l/R ratios the fundamental frequency occurs for smaller n . For very short shells ($l/R < 0.3$) it is seen that the fundamental mode is axisymmetric.

Figures 2.18 and 2.19 (taken from ref. 2.69) show the frequency spectra of the second and third eigenvalues for given n and λ . A single figure covers the range of R/h from 20 to 5000 for modes corresponding to the second and third eigenvalues. For small values of l/mR and n the second eigenvalue yields amplitude ratios such that $B > A, C$ (torsional modes) while modes having larger l/mR and n have amplitude ratios such that $A > B, C$ (axial modes). The converse of this is found for the third eigenvalues. In figures 2.20, 2.21, and 2.22 the

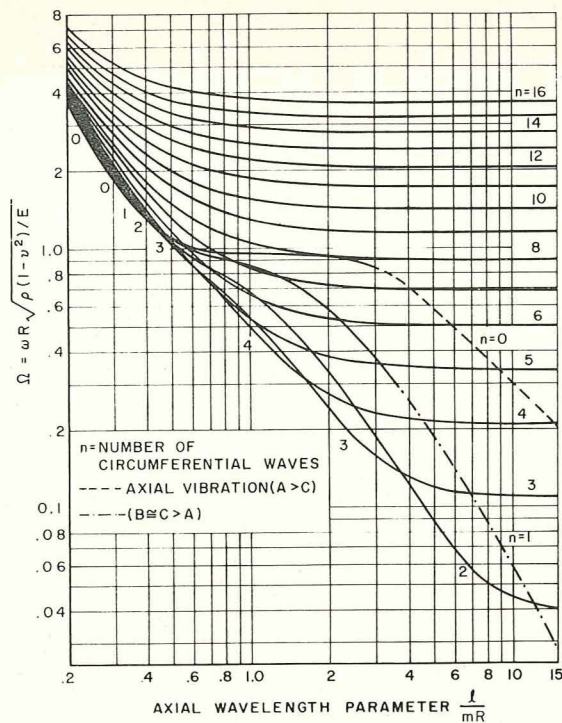


FIGURE 2.14.—Variation of the fundamental frequency parameter Ω with l/mR according to the Flügge theory; $\nu = 0.3$, $R/h = 20$. (After ref. 2.69)

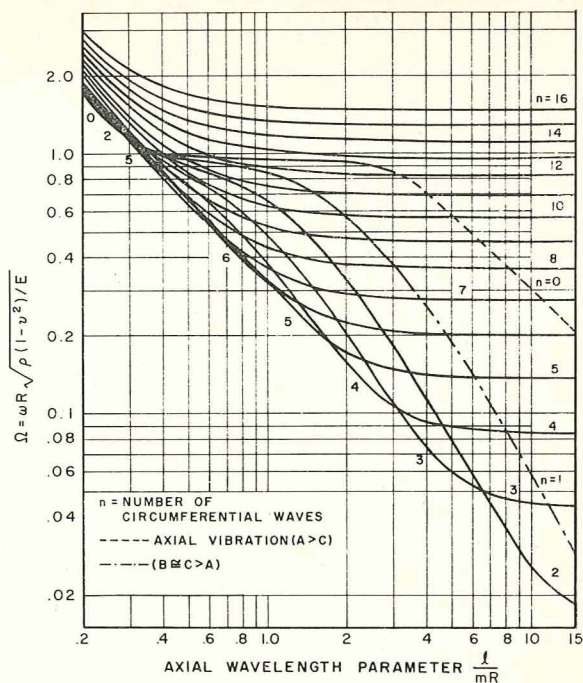


FIGURE 2.15.—Variation of the fundamental frequency parameter Ω with l/mR according to the Flügge theory; $\nu = 0.3$, $R/h = 50$. (After ref. 2.69)

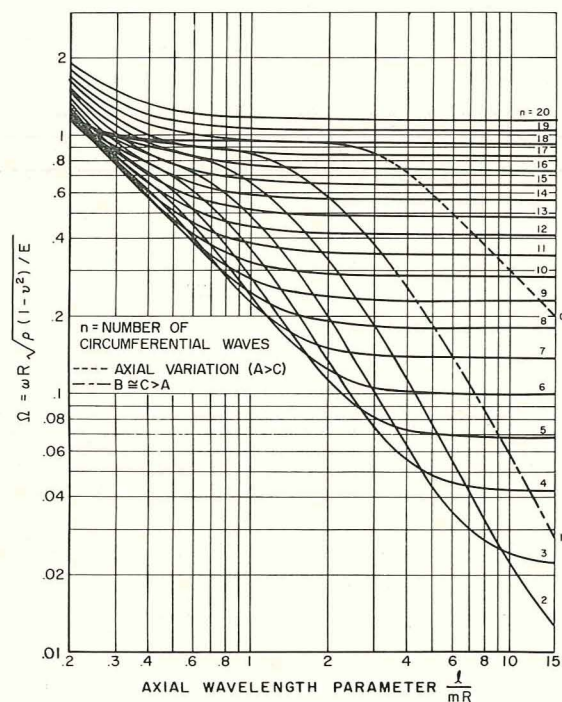


FIGURE 2.16.—Variation of the fundamental frequency parameter Ω with l/mR according to the Flügge theory; $\nu = 0.3$, $R/h = 100$. (After ref. 2.69)

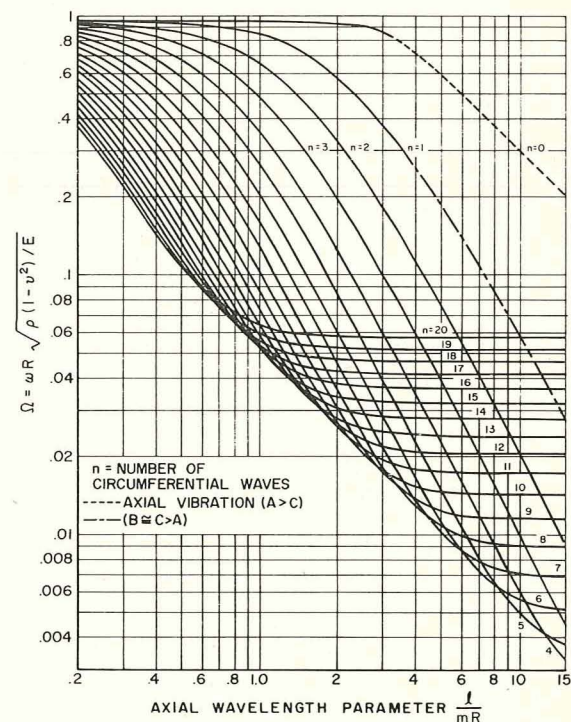


FIGURE 2.17.—Variation of the fundamental frequency parameter Ω with l/mR according to the Flügge theory; $\nu = 0.3$, $R/h = 2000$. (After ref. 2.69)

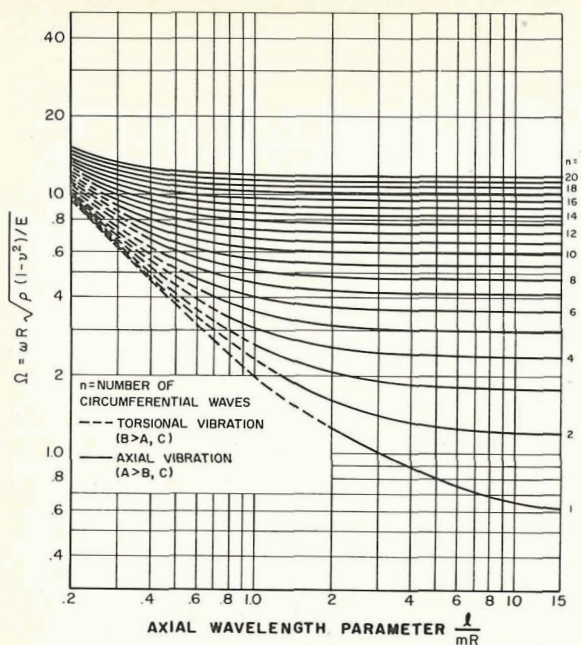


FIGURE 2.18.—Second vibration frequencies; Flügge theory, $\nu=0.3$, $R/h=20$ to 5000. (After ref. 2.69)

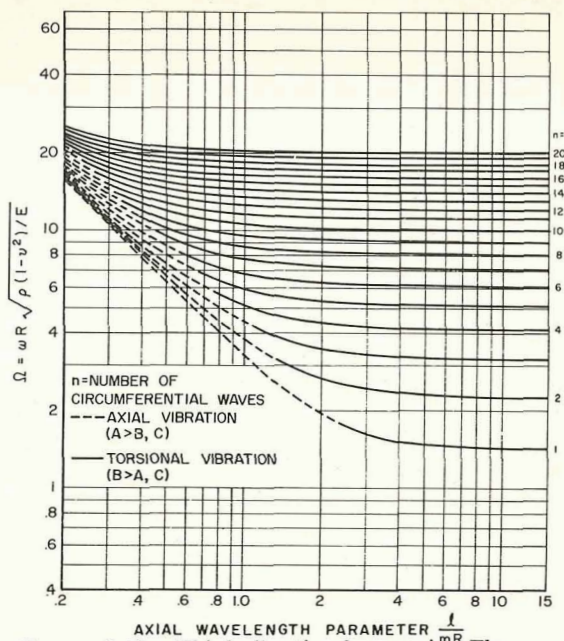


FIGURE 2.19.—Third vibration frequencies; Flügge theory, $\nu=0.3$, $R/h=20$ to 5000. (After ref. 2.69)

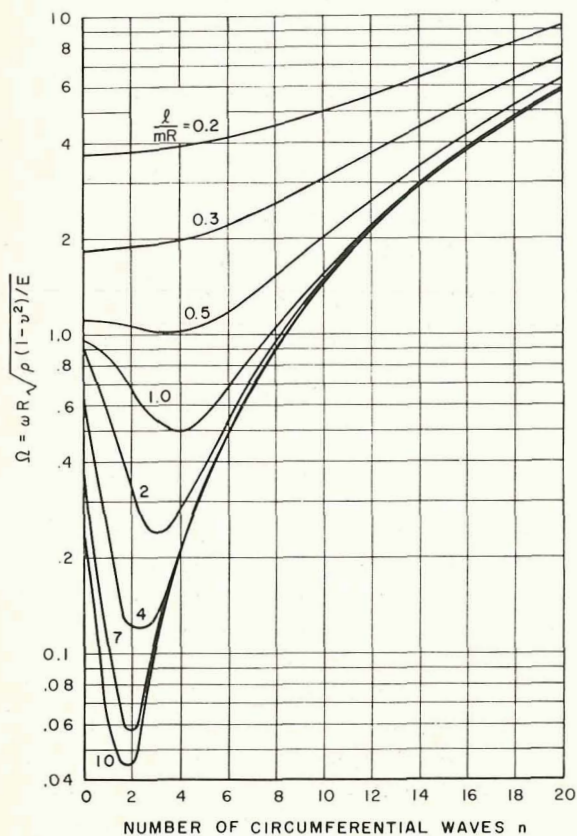


FIGURE 2.20.—Variation of the fundamental frequency parameter Ω with n ; Flügge theory, $\nu=0.3$, $R/h=20$. (After ref. 2.69)

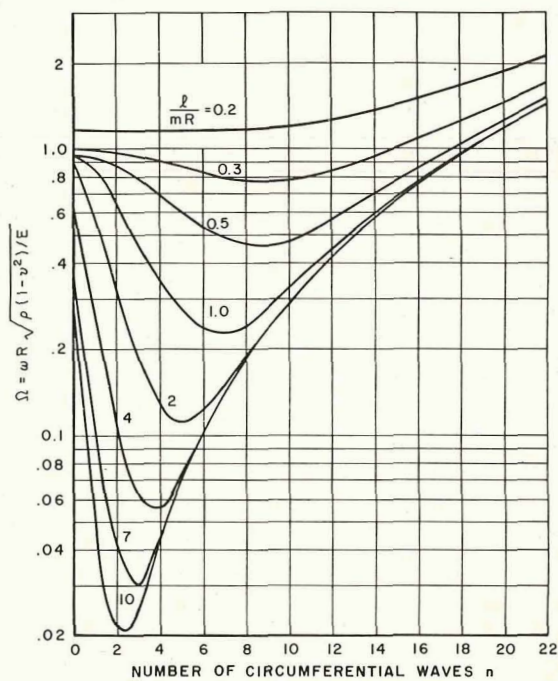


FIGURE 2.21.—Variation of the fundamental frequency parameter Ω with n ; Flügge theory, $\nu=0.3$, $R/h=100$. (After ref. 2.69)

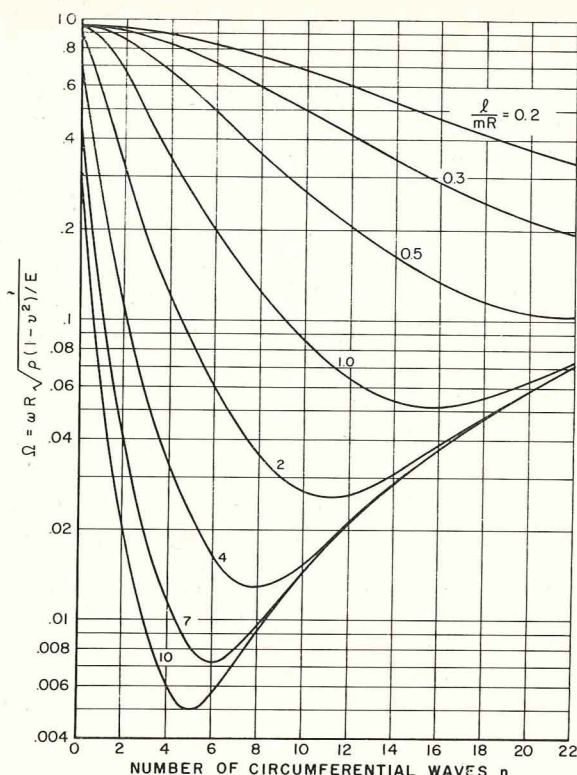


FIGURE 2.22.—Variation of the fundamental frequency parameter Ω with n ; Flügge theory, $\nu = 0.3$, $R/h = 2000$. (After ref. 2.69)

lowest frequency parameter is plotted versus n for $R/h = 20, 100$, and 2000 , respectively (in ref. 2.69 similar plots are also given for $R/h = 50, 500, 1000$, and 5000). This last set of figures serves to emphasize clearly that the minimum frequency for a thin circular cylindrical shell of given length and supported by shear diaphragms occurs for $n=2$ or greater, unless $l/R > 10$. On the other for very long shells, the minimum frequency always occurs for $n=1$, that is in the beam bending mode.

Axisymmetric motion ($n=0$) in the case of shear diaphragm supports leads to more simple solutions than for $n \neq 0$. Looking at the matrix differential operators for the various theories, equations (2.7) and (2.9), it is seen that substitution of the shear diaphragm displacement functions given by equations (2.20) results in the vanishing of the terms arising from the off-diagonal elements \mathcal{L}_{12} , \mathcal{L}_{21} , \mathcal{L}_{23} , and \mathcal{L}_{32} of the matrix in the case of $n=0$ for every theory. This

can be seen explicitly in equation (2.21) for the Donnell-Mushtari theory. Thus, the second of the three equations of motion becomes uncoupled and yields a purely torsional mode shape. From equation (2.21) the frequency parameter for this torsional mode according to the Donnell-Mushtari theory is found to be

$$\Omega^2 = \frac{(1-\nu)}{2} \lambda^2 = \frac{(1-\nu)}{2} \left(\frac{m\pi R}{l} \right)^2 \quad (2.38)$$

Furthermore, the other theories lead to varying results for the simple formula given in equation (2.38). Corresponding formulas arising from the various theories are given in table 2.13. It is important to note that in every case the formulas differ from each other by a term which is multiplied by $k = h^2/12R^2$, which is small for thin shells. Thus, for practical purposes the theories all agree for axisymmetric torsion.

Returning to the equations of motion in the axisymmetric case, the two remaining equations are uncoupled from the torsional mode, but do yield a coupling of radial and axial displacements. These equations can be written as

$$\begin{bmatrix} a - \Omega^2 & b \\ b & c - \Omega^2 \end{bmatrix} \begin{bmatrix} A \\ C \end{bmatrix} = \begin{bmatrix} 0 \\ 0 \end{bmatrix} \quad (2.39)$$

where, for example, in the case of the Donnell-Mushtari theory

$$a = \lambda^2, \quad b = -\nu\lambda, \quad c = 1 + k\lambda^4 \quad (2.40)$$

as seen from equations (2.21). The roots of the characteristic determinant can be determined from the quadratic formula to be

$$\Omega^2 = \frac{1}{2} [(a+c) \pm \sqrt{(a-c)^2 + 4b^2}] \quad (2.41)$$

Equation (2.41) has two real, positive roots for Ω^2 provided that $ac > b^2$. Substituting from equation (2.40), it is seen that this inequality is always satisfied for the Donnell-Mushtari theory. Frequency parameters for the axial-radial modes are given in table 2.13 for each of the theories considered here. A plot of all three frequency parameters Ω^2 arising in the axisymmetric case is shown in figure 2.23 for the Flügge theory (from ref. 2.69). The lowest frequency in the axisymmetric case can correspond to either a radial or torsional mode, depending upon l/mR , but is never an axial mode.

TABLE 2.13.—*Axisymmetric ($n=0$) Frequency Formulas According to the Various Shell Theories*

Shell theory	Ω^2	
	Torsional mode	Coupled axial-radial modes
Donnell-Mushtari	$\frac{1}{2}(1-\nu)\lambda^2$	$\frac{1}{2}\{(1+\lambda^2+k\lambda^4) \mp [(1-\lambda^2)^2+2\lambda^2(2\nu^2+k\lambda^2-k\lambda^4)]^{1/2}\}$
Love-Timoshenko	$\frac{1}{2}(1-\nu)(1+2k)\lambda^2$	Same as Donnell-Mushtari
Goldenveizer-Novozhilov (also Arnold-Warburton)	$\frac{1}{2}(1-\nu)(1+4k)\lambda^2$	Same as Donnell-Mushtari
Houghton-Johns (Simplified Goldenveizer-Novozhilov)	Same as Donnell-Mushtari	Same as Donnell-Mushtari
Biezeno-Grammel	$\frac{1}{2}(1-\nu)(1+3k)\lambda^2$	$\frac{1}{2}\{(1+k+\lambda^2+k\lambda^4) \mp [(1-\lambda^2)^2+2k+2(2\nu^2-k)\lambda^2+2(1-4\nu)k\lambda^4-2k\lambda^6]^{1/2}\}$
Flügge	Same as Donnell-Mushtari	$\frac{1}{2}\{(1+\lambda^2+k\lambda^4) \mp [(1-\lambda^2)^2+4\nu^2\lambda^2-2k\lambda^6]^{1/2}\}$
Reissner-Naghdi-Berry	$\frac{1}{2}(1-\nu)(1+k)\lambda^2$	Same as Donnell-Mushtari
Sanders	$\frac{1}{2}(1-\nu)\left(1+\frac{9}{4}k\right)\lambda^2$	Same as Donnell-Mushtari
Vlasov	Same as Donnell-Mushtari	Same as Biezeno-Grammel
Epstein-Kennard	Same as Donnell-Mushtari	$\frac{1}{2}\left\{\left(1+\frac{1+3\nu}{1-\nu}k+\lambda^2-\frac{1-4\nu^2+4\nu^3}{(1-\nu)^2}k\lambda^2+k\lambda^4\right) \mp \left[(1-\lambda^2)^2+\frac{2(1+3\nu)}{1-\nu}k+4\nu^2\lambda^2-\frac{4+3\nu-18\nu^2+12\nu^4}{(1-\nu)^2}k\lambda^2+\frac{4(1-\nu-2\nu^2-2\nu^3)}{(1-\nu)^2}k\lambda^4-2k\lambda^6\right]^{1/2}\right\}$
Kennard Simplified	Same as Donnell-Mushtari	$\frac{1}{2}\left\{\left(1+\frac{2+\nu}{2(1-\nu)}k+\lambda^2+k\lambda^4\right) \mp \left[(1-\lambda^2)^2+\frac{2+\nu}{1-\nu}k+4\nu^2\lambda^2-\frac{2+\nu}{1-\nu}k\lambda^2+4\nu^2\lambda^2+2k\lambda^4-4k\lambda^6\right]^{1/2}\right\}$
Membrane	Same as Donnell-Mushtari	$\frac{1}{2}\{(1+\lambda^2) \mp [(1-\lambda^2)^2+4\nu^2\lambda^2]^{1/2}\}$

Another interesting set of frequency spectra is shown in figures 2.24 through 2.27. In these figures the frequency Ω is plotted versus λ giving rise to a family of curves for different thickness ratios in the range $0.002 < h/R < 0.100$. Looking at these curves, it is obvious that the frequency increases as the length of the shell decreases and as h/R increases; but, in addition, as one moves from figure 2.24 to figure 2.27 it is apparent that the family of curves spreads apart, indicating greater frequency differences with increasing h/R for larger values of n . These curves were presented by Arnold and Warburton (ref. 2.4) using their

own theory (which is the same as the Goldenveizer-Novozhilov theory).

Behavior of the amplitude ratios for $n=1$ and $n=2$ is shown pictorially in figures 2.28 and 2.29 (from ref. 2.50, where the Flügge theory was used). The ratios A/C and B/C are shown for $h/R=0.01$ and 0.1 for the three possible modes which can occur for a fixed value of n and mR/l . The change in character of the vibration modes with changing mR/l (as was discussed in conjunction with figures 2.14 through 2.19) is clearly seen from these curves.

It should be mentioned that another extensive

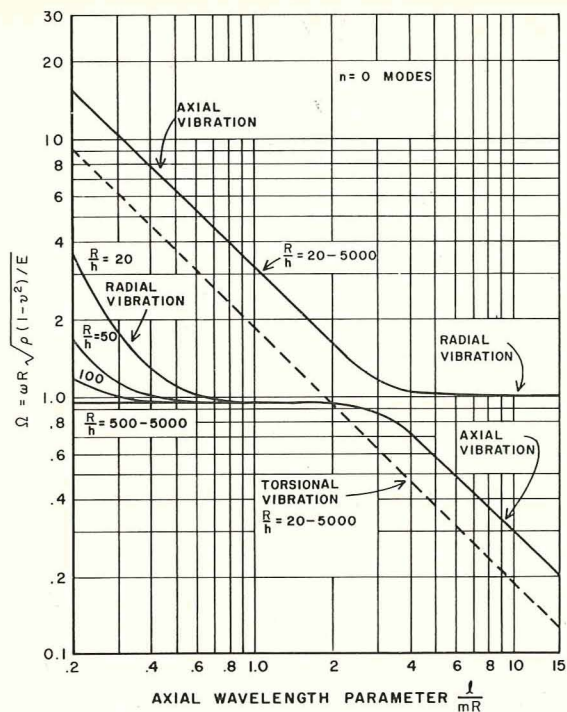


FIGURE 2.23.—Axisymmetric ($n=0$) frequency parameters; Flugge theory, $\nu=0.3$. (After ref. 2.69)

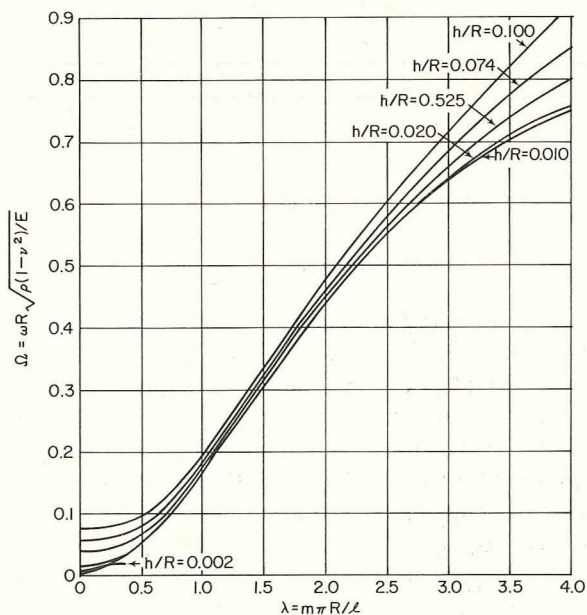


FIGURE 2.24.—Variation of the fundamental Ω with λ and h/R ; Arnold and Warburton theory, $n=2$. (After ref. 2.4)

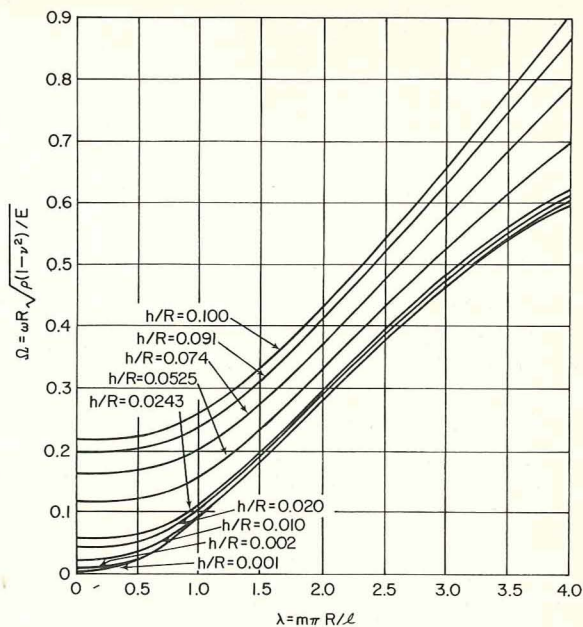


FIGURE 2.25.—Variation of the fundamental Ω with λ and h/R ; Arnold and Warburton theory, $n=3$. (After ref. 2.4)

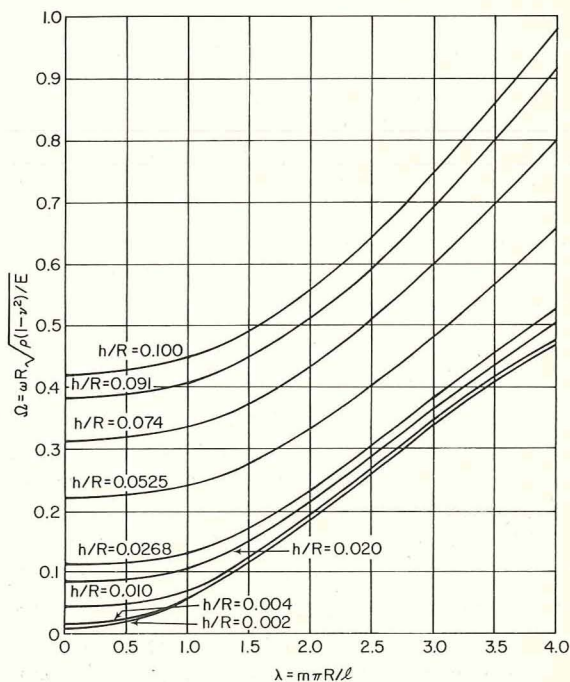


FIGURE 2.26.—Variation of the fundamental Ω with λ and h/R ; Arnold and Warburton theory, $n=4$. (After ref. 2.4)

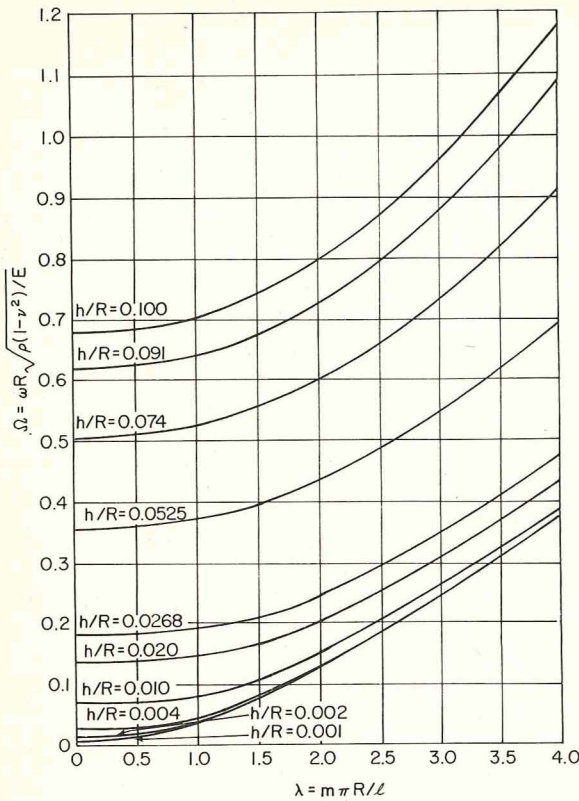


FIGURE 2.27.—Variation of the fundamental Ω with λ and h/R ; Arnold and Warburton theory, $n=5$. (After ref. 2.4)

set of results is available in the paper by Baron and Bleich (ref. 2.121), where the three frequencies and their corresponding amplitude ratios for fixed n and λ are given for $n=0$ through 6, $\nu=0.3$, and over a range of λ . The procedure followed by them is particularly interesting because of the saving in numerical computation time. First, they obtained the frequencies and corresponding amplitude ratios according to membrane theory (see sec. 2.3.1). Then they substituted the mode shapes determined from membrane theory into a strain energy integral including bending effects which was derived in ref. 2.122 using the Flügge theory. Finally, adding the kinetic energy, they computed corrected frequencies by the simple Rayleigh method. This procedure is particularly useful because it not only avoids finding roots of the cubic equation in Ω^2 , equation (2.35), but at the same time it includes tangential inertia effects, although the

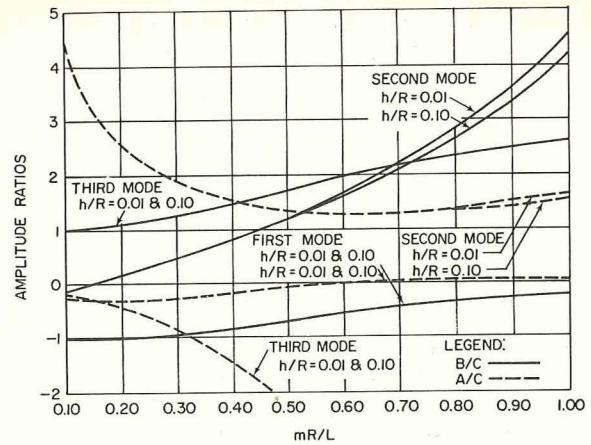


FIGURE 2.28.—Amplitude ratios for $n=1$; Flügge theory. (After ref. 2.50)

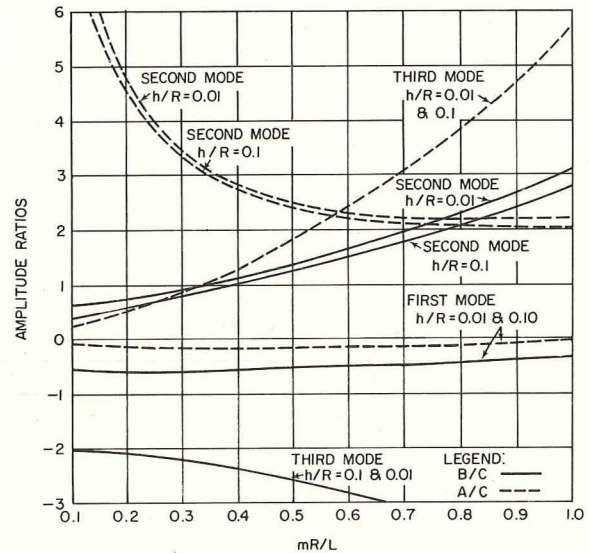


FIGURE 2.29.—Amplitude ratios for $n=2$; Flügge theory. (After ref. 2.50)

tangential displacement amplitudes are only approximated in the final results.

No information is available in the literature which shows the variation of the frequency parameter as a function of Poisson's ratio. To gain insight into this question a separate set of calculations were made for this monograph using the Flügge theory. The results are shown in tables 2.14 and 2.15 for $R/h=20$ and 500, respectively. Data are given for shells of short, medium, and

TABLE 2.14.—*Variation of Ω with Poisson's Ratio; Flügge Theory, $R/h=20$*

n	l/mR	ν			n	l/mR	ν		
		0	0.25	0.49			0	0.25	0.49
0	0.25	2.48900 8.88576 12.5664	2.47205 7.69720 12.5685	2.43032 6.34969 12.5758	4	20	0.210224 2.83314 4.12548	0.210197 2.45374 4.12582	0.210146 2.02382 4.12606
		1.00063 1.11072 1.57079	.944513 .967521 1.60179	.788615 .823925 1.67245			2.76785 9.57999 13.5242	2.75579 8.29843 13.5284	2.72697 6.84604 13.5360
		.111072 .157080 1.00000	.0961909 .151972 1.00079	.0793209 .136518 1.00302			.383129 3.63215 5.31967	.382416 3.23062 5.32368	.380482 2.66477 5.32757
	2	2.49923 8.91476 12.6060	2.48252 7.72232 12.6083	2.44144 6.37042 12.6157	5	2	.339780 3.54024 5.10085	.339735 3.06614 5.10124	.339648 2.52894 5.10152
		.617720 1.49179 1.89647	.584886 1.29248 1.93845	.513257 1.06622 1.98842			2.90202 9.86783 13.9251	2.89148 8.54771 13.9299	2.86658 7.05182 13.9374
		.0169336 .727043 1.41716	.0163488 .631095 1.41796	.0146782 .521410 1.41919			.535651 4.40258 6.27214	.535328 3.81310 6.27492	.534499 3.14516 6.27751
1	0.25	2.53045 9.00109 12.7243	2.51444 7.79708 12.7270	2.47525 6.43216 12.7343	6	20	.498294 4.24760 6.08415	.498225 3.67878 6.08463	.498094 3.03425 6.08494
		.353470 1.91566 2.62966	.339731 1.65992 2.65154	.304552 1.36949 2.67526			3.26240 10.5619 14.8974	3.25461 9.14881 14.9029	3.23667 7.54803 14.9101
		.0393118 1.42214 2.23972	.0392916 1.23187 2.24015	.0392237 1.01610 2.24061			.936933 5.77598 8.20864	.936740 5.00253 8.21038	.936327 4.12622 8.21185
	2	2.58419 9.14283 12.9192	2.56927 7.91982 12.9223	2.53297 6.53349 12.9297	8	2	.901993 5.66266 8.06298	.901862 4.90435 8.06362	.901608 4.04516 8.06404
		.248049 2.45960 2.49463	.242124 2.13089 3.49223	.225888 1.75794 3.50394			3.74921 11.3884 16.0616	3.74347 9.86473 16.0675	3.73060 8.13902 16.0741
		.109795 2.12666 3.16533	.109782 1.84190 3.16563	.109753 1.51918 3.16591			1.45587 7.16734 10.1685	1.45562 6.20758 10.1699	1.45513 5.12024 10.1710
2	0.25	2.66257 9.33700 13.1872	2.64901 8.08798 13.1909	2.61629 6.67232 13.1984	10	20	1.42114 7.07796 10.0501	1.42092 6.13015 10.0509	1.42049 5.05630 10.0514
		.274969 3.07645 4.38543	.272912 2.66482 4.39181	.267254 2.19817 4.39820					
	2								

TABLE 2.15.—*Variation of Ω with Poisson's Ratio; Flügge Theory, $R/h = 500$*

n	l/mR	ν			n	l/mR	ν		
		0	0.25	0.49			0	0.25	0.49
0	0.25	1.00415	0.972321	0.875778	4	20	0.00854580	0.00853766	0.00851444
		8.88576	7.69530	6.34571			2.83109	2.45181	2.02182
		12.5664	12.5689	12.5760			4.12576	4.12585	4.12592
	2	1.00000	.949456	.793191		0.25	.868558	.841133	.758256
		1.11072	.961939	.818764			9.57575	8.29285	6.83847
		1.57079	1.60184	1.67244			13.5252	13.5292	13.5362
1	20	1.11072	.0961911	.0793213	5	2	.0892546	.0864402	.0780402
		1.57080	.151972	.136518			3.72665	3.22755	2.66160
		1.00000	1.00079	1.00302			5.32028	5.32385	5.32744
	0.25	.997853	.966227	.870312		20	.0136348	.0136326	.0136266
		8.91456	7.72024	6.36628			3.53754	3.06360	2.52632
		12.6061	12.6087	12.6158			5.10125	5.10130	5.10134
2	2	.616967	.584281	.512748	6	0.25	.820611	.794789	.716833
		1.49094	1.29165	1.06532			9.86211	8.54085	7.04298
		1.89672	1.93854	1.98841			13.9265	13.9308	13.9376
	20	.0169361	.0163518	.0146818		2	.0667205	.0647987	.0590512
		.726941	.630987	.521288			4.39870	3.80948	3.14142
		1.41714	1.41792	1.41916			6.27284	6.27509	6.27734
3	0.25	.979464	.948425	.854349	8	20	.0199572	.0199565	.0199545
		9.00031	7.79450	6.42752			4.24425	3.67564	3.03101
		12.7245	12.7274	12.7345			6.08468	6.08471	6.08473
	2	.346579	.332670	.296780		0.25	.721495	.699090	.631558
		1.91416	1.65854	1.36807			10.5532	9.13931	7.53648
		2.63002	2.65165	2.67524			14.8996	14.9041	14.9104
4	20	.00569731	.00552868	.00502229	10	2	.0525428	.0517266	.0493413
		1.42144	1.23118	1.01536			5.77090	4.99777	4.12129
		2.23975	2.24011	2.24053			8.20954	8.21058	8.21161
	0.25	.950371	.920267	.829109		20	.0361080	.0361078	.0361075
		9.14111	7.91644	6.52808			5.65801	4.89999	4.04063
		12.9196	12.9228	12.9299			8.06375	8.06375	8.06376
5	2	.204007	.196852	.176627	10	0.25	.628660	.609649	.552444
		2.45747	2.12892	1.75591			11.3769	9.85264	8.12471
		3.48142	3.49238	3.50388			16.0644	16.0688	16.0744
	20	.00510157	.00506018	.00494075		2	.0630049	.0627190	.0619007
		2.12528	1.84058	1.51780			7.16100	6.20162	5.11400
		3.16547	3.16563	3.16579			10.1696	10.1702	10.1707
6	0.25	.912612	.883735	.796384	10	20	.0568884	.0568884	.0568883
		9.33410	8.08358	6.66591			7.07198	6.12452	5.05041
		13.1879	13.1915	13.1986			10.0511	10.0511	10.0511
	2	.129782	.125497	.112898					
		3.07373	2.66228	2.19557					
		4.38594	4.39195	4.39811					

long length (i.e., $l/mR = 0.25, 2, 20$) and over a range of circumferential wave numbers $0 \leq n \leq 10$. Poisson's ratio is allowed to vary over its limiting range for isotropic materials, $0 \leq \nu \leq 0.5$, although the value 0.49 was taken to avoid difficulties associated with dividing by zero at certain places in the computer routine. In addition to the lowest frequency for each n , the higher two frequencies are also given.

As shown in table 2.14 the frequencies corresponding to modes which are predominantly transverse are affected only slightly by changing Poisson's ratio (see earlier discussion in this section to associate frequencies with modes), that the effect is most important for shells of moderate length ($l/mR = 2$), and that the effect is reduced as the number of circumferential waves increases. Further, comparing tables 2.14 and 2.15 it is seen that the frequency parameter Ω is more significantly affected by ν for thinner shells. Finally, it must be remembered that the frequency parameter Ω contains ν (i.e., $\Omega = \omega R \sqrt{\rho(1-\nu^2)/E}$). Thus, although Ω may decrease with increasing ν , the actual free vibration frequency ω will increase with increasing ν , as expected.

From tables 2.14 and 2.15 it can be seen that the two largest frequencies for given values of n and l/mR essentially do not depend upon R/h .

Forsberg (ref. 2.35) used the exact solution obtained from the Flügge theory (including tangential inertia) for the SD-SD shell as a basis for comparison of approximate solutions obtained by the finite difference method. Sinusoidal variation of u , v , and w with respect to θ and t was assumed, as in equations (2.20), and the resulting set of ordinary differential equations of motion were replaced by their finite difference equivalents. Convergence of the finite difference technique was then studied, using 10, 20, 50, and 100 equally spaced points along the length of the shell. Results for the frequency parameters and modal characteristics exhibited by the various solutions are displayed in figure 2.30 for a shell having $R/h = 500$, $l/R = 10$, $n = 4$, $m = 1$, and $\nu = 0.3$. It is interesting to note that although the eigenfunctions (mode shapes) are represented very accurately with as little as 10 points, the eigenvalues (frequency parameters) converge much more slowly. This is due to significant differences between the higher derivatives of the

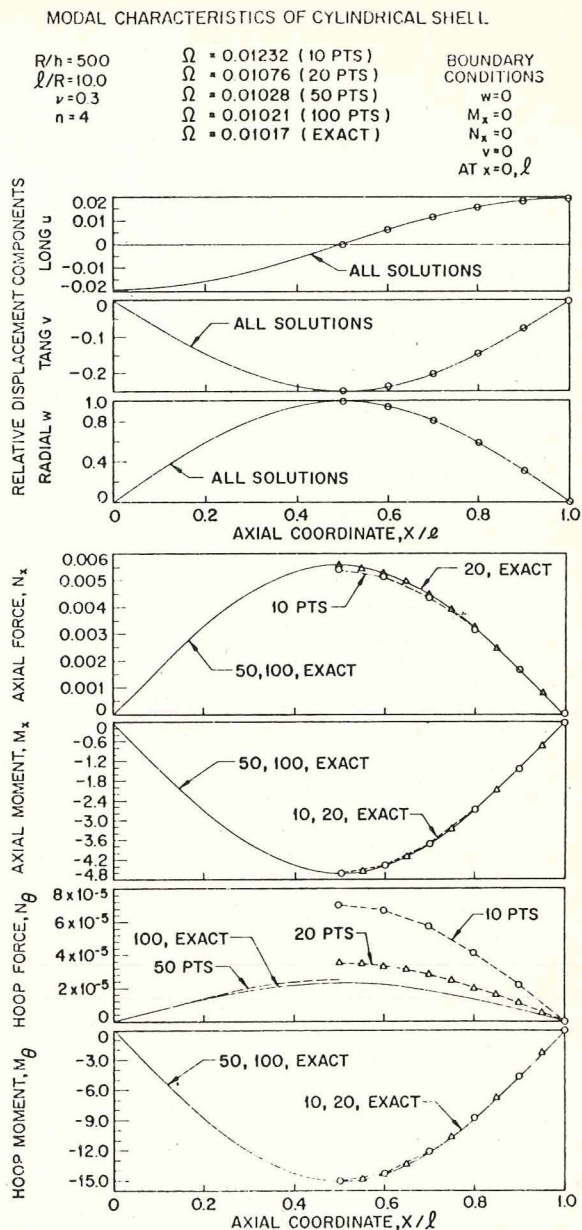


FIGURE 2.30.—Comparison of finite difference and exact (Flügge) solutions for an SD-SD shell; $R/h = 500$, $l/R = 10$, $n = 4$, $m = 1$. (After ref. 2.35)

eigenfunctions, as shown by the plots of the force and moment resultants in figure 2.30, particularly for the circumferential (hoop) force resultant N_θ . Further results showing the convergence of eigenvalues obtained from finite difference solutions are shown in table 2.16. In reference 2.35 the

TABLE 2.16.—Comparison of Frequencies Obtained from Finite Difference and Exact (Flügge) Solutions for a SD-SD Shell; $\nu=0.3$

n	l/mR	R/h	Number of grid points				
			10	20	50	100	Exact
2	2	100	0.3277	0.3275	0.3275	0.3274	0.3274
		500	.3274	.3272	.3272	.3272	.3272
		5000	.3274	.3272	.3272	.3272	.3271
	10	100	.02520	.02282	.02210	.02200	.02195
		500	.02397	.02146	.02069	.02058	.02053
		5000	.02392	.02140	.02063	.02052	.02047
4	2	500	.1264	.1243	.1237	.1237	.1236
	10	500	.01232	.01076	.01028	.01021	.01017

following was generally found for frequency parameters:

(1) Finite difference solutions will give better results for a short (small l/mR), thick (small R/h) shell than for a long, thin one.

(2) The accuracies of the finite difference results slowly decrease as R/h or n increases.

(3) The accuracies of the finite difference results rapidly decrease as l/mR is increased.

These statements are substantiated by table 2.16.

Further comparisons of the results obtained using various shell theories and various solution techniques were made in an excellent survey paper by Warburton (ref. 2.123).

2.3.3 Strain Energy Distribution

It is interesting to observe how the total strain energy which occurs at any instant in the shell (being a maximum, of course, when $\cos \omega t = 1$ in eqs. (2.20); i.e., at maximum amplitude) is apportioned between bending and stretching (see eqs. (2.17) and (2.18)). Arnold and Warburton (ref. 2.3) plotted curves (figs. 2.31 and 2.32) showing this apportionment for a circular cylindrical shell having $h/R = 0.0525$ and $n = 2$ and 4. In figure 2.31 for $n = 2$ the strain energy is extremely small for values of λ up to 0.5, resulting almost entirely from bending. At higher values of λ , however, the stretching energy increases rapidly and becomes predominant, as may be seen from the shaded

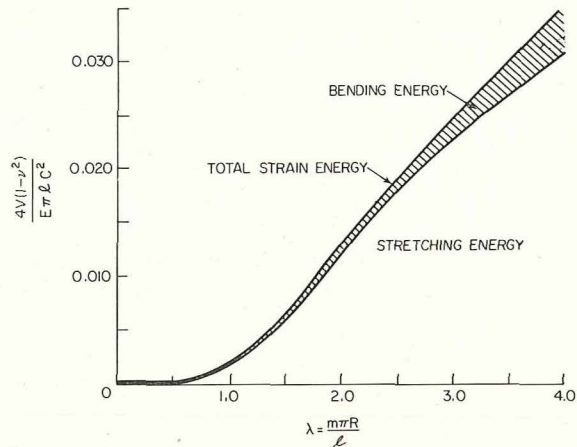


FIGURE 2.31.—Nondimensional strain energy due to bending and stretching; $h/R = 0.0525$, $n = 2$. (After ref. 2.3)

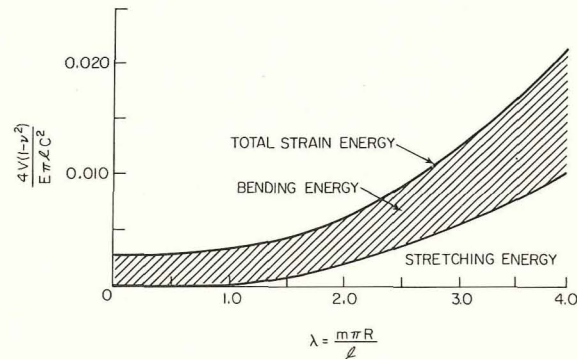


FIGURE 2.32.—Nondimensional strain energy due to bending and stretching; $h/R = 0.0525$, $n = 4$. (After ref. 2.3)

area representing the bending contribution. For $n=4$, however, the bending effect is predominant throughout the range $0 < \lambda < 4$, always contributing over 1/2 of the total strain energy. Comparing the two figures for $\lambda=1.2$, it is seen that although the total strain energy is approximately the same for either $n=2$ or $n=4$, the portions due to bending in the two cases are altogether different. Looking at figure 2.14 (where $h/R=0.0500$ and the Flügge theory was used) it is evident that the frequency parameter curves for $n=2$ and $n=4$ cross at the corresponding value of $l/mR=\pi/\lambda=2.6$. Another plot of the strain energy as a function of the circumferential wave number n is shown in figure 2.33 (from ref. 2.3) for a thinner shell ($R/h=100$) and for $\lambda=3.82$. One observes that the stretching energy decreases rapidly as n increases, whereas the bending energy increases. This results in a curve for total strain energy which has a minimum at $n=7$. As seen in figure 2.21, the corresponding minimum in frequency parameter occurs also in the vicinity of $n=7$ for

$$l/mR=\pi/3.82=0.82$$

Strain energy apportionment between bending and stretching for circular cylindrical shells supported by shear diaphragms was also discussed in references 2.35 and 2.61.

Figure 2.33 helps to demonstrate the rationale

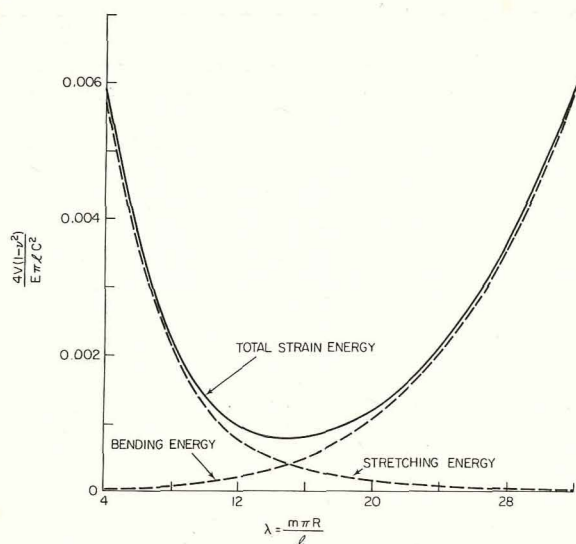


FIGURE 2.33.—Nondimensional strain energy due to bending and stretching; $h/R=0.01$, $\lambda=3.82$. (After ref. 2.3)

for using the membrane theory for small n and a theory which considers bending only for large n . This latter theory (called an "inextensional theory") was proposed by Rayleigh (ref. 2.124) in 1881 and will be discussed in connection with free-free shells (see sec. 2.4.5).

2.3.4 Neglect of Tangential Inertia

As seen earlier in this section, for wide ranges of h/R , λ , and n (but not for all values) the fundamental frequency corresponds to a mode shape which is primarily radial, and the tangential displacements are then relatively small. Consequently, one important simplification which is frequently made in the equations of motion is to neglect the tangential (axial and circumferential) inertia terms.

Neglect of tangential inertia terms in the equations of motion eliminates two of the terms containing Ω^2 in the characteristic determinant (cf., eq. (2.21)) and reduces the characteristic equation (2.35) to a linear equation in Ω^2 . The resulting simple formulas for the frequency parameter can be written as

$$\Omega^2 = \frac{K_0 + k \Delta K_0}{\bar{K}_1 + k \Delta \bar{K}_1} \quad (2.42)$$

where K_0 and $\Delta \bar{K}_0$ are as given previously in equation (2.36) and table 2.4, respectively,

$$\bar{K}_1 = \frac{(1-\nu)}{2} (\lambda^2 + n^2)^2 \quad (2.43)$$

and values of ΔK_1 , according to the various theories, are given in table 2.17. The single frequency in every case, of course, describes a radial mode of vibration.

The effects of neglecting tangential inertia in the various theories can be seen in tables 2.18 and 2.19. In these tables the percent change in the frequency parameter Ω when tangential inertia is neglected is given relative to the value of Ω obtained from each shell theory when tangential inertia is included.

The following general conclusions are apparent:

- (1) Neglecting tangential inertia causes all frequencies associated with radial modes to increase, with the exception of the axisymmetric ($n=0$) case.
- (2) For $R/h=20$ and any given n and l/mR ,

the frequency changes are approximately the same for all theories. The approximation becomes practically exact for $R/h=500$.

(3) The frequency changes are essentially independent of R/h ratio.

(4) The differences are generally more significant for long shells than for short ones.

(5) Large differences occur for small n ($n=0, 1, 2$) and decrease as n increases. Neglecting tangential inertia is completely unacceptable for long shells in their beam bending ($n=1$) modes.

It must be remembered that tables 2.18 and 2.19 only indicate the *changes* in frequencies due to neglecting tangential inertia, and that considerable differences can exist among the frequencies generated by the various theories, as was discussed earlier in section 2.3.1.

It was pointed out by Forsberg (ref. 2.35) that neglect of tangential inertia in the beam bending ($n=1$) mode effectively results in leaving half of the shell inertia out of the calculations. Because the frequency depends upon the square root of the mass, having half as much mass yields a frequency which is $\sqrt{2}$ greater when tangential inertia is omitted for long shells and $n=1$. This was also observed in tables 2.18 and 2.19.

The change in frequency spectrum in the case of axisymmetric ($n=0$) motion is clearly shown in figure 2.34 (from ref. 2.35). The three distinct modes are replaced by a single mode which is primarily radial when tangential inertia is neglected. This causes the significant negative difference where the transition zone between longitudinal and radial modes normally occur (i.e., $2 < l/mR < 5$).

A comparison of the effects of neglecting tangential inertia for other numbers of circumferential waves can also be seen in figure 2.35 (from ref. 2.35), where the lowest Ω is plotted versus l/R for various R/h ratios. Results from the Flügge theory, with and without tangential inertia, and the Donnell theory without tangential inertia are shown in this figure. For very thin shells ($R/h=5000$) the effect of neglecting tangential inertia is essentially negligible, but the frequency is increased considerably for large h/R and l/R ratios. Again it is seen that the differences between the Donnell-Mushtari and Flügge theories (this time neglecting tangential inertia) increase as h/R and l/R increase.

TABLE 2.17.—Parameters $\Delta\bar{K}_1$ for the Direct Calculation of Frequency Parameters (by eq. (2.42)) when Tangential Inertia Is Neglected

Shell theory	$\Delta\bar{K}_1$
Donnell-Mushtari	0
Love-Timoshenko	$(1-\nu)\lambda^4 + (3-2\nu+\nu^2)\frac{\lambda^2 n^2}{2} + (1-\nu)\frac{n^4}{2}$
Goldenveizer-Novozhilov (also Arnold-Warburton)	$2(1-\nu)\lambda^4 + (2-2\nu+\nu^2)\lambda^2 n^2 + (1-\nu)\frac{n^4}{2}$
Biezeno-Grammel	$3(1-\nu)\frac{\lambda^4}{2} + (1-\nu)^2 \lambda^2 n^2 + (1-\nu)\frac{n^4}{2}$
Flügge	0
Reissner-Naghdi-Berry	$(1-\nu)\frac{\lambda^4}{2} + (5-2\nu+\nu^2)\frac{\lambda^2 n^2}{2} + (1-\nu)\frac{n^4}{2}$
Sanders	$9(1-\nu)\frac{\lambda^4}{8} + (8-5\nu+\nu^2)\frac{\lambda^2 n^2}{4} + 5(1-\nu)\frac{n^4}{2}$
Vlasov	0
Epstein-Kennard	$\frac{\nu(2-9\nu+6\nu^2)}{4(1-\nu)}\lambda^4 - \frac{14-23\nu+7\nu^2}{4(1-\nu)}\lambda^2 n^2 - \frac{8-17\nu+10\nu^2}{4(1-\nu)}n^4 - \frac{\nu^2}{2(1-\nu)}(\lambda^2+n^2)^3$
Houghton-Johns (Simplified Golden.-Novo.)	0
Kennard Simplified	0
Membrane	0

TABLE 2.18.—Percent Change in Transverse Mode Frequency Parameter by Neglecting Tangential Inertia Terms; SD-SD Supports, $\nu=0.3$, $R/h=20$

Shell theory		n	l/mR					
Group	Name		0.1	0.25	1	4	20	100
1	Donnell-Mushtari	0	0.01	0.03	0.50	-9.54	-4.71	-4.61
2	Love-Timoshenko		.04	.03	.50	-9.54	-4.71	-4.61
	Goldenveizer-Novozhilov		.06	.03	.50	-9.54	-4.71	-4.61
	Biezeno-Grammel		.05	.04	.51	-9.54	-4.71	-4.61
	Flügge		.07	.06	.54	-9.54	-4.71	-4.61
	Reissner-Naghdi-Berry		.02	.03	.51	-9.55	-4.72	-4.62
	Sanders		-2.80	.03	.50	-9.54	-4.71	-4.61
	Vlasov		.01	.04	.51	-9.54	-4.71	-4.61
	Epstein-Kennard		-.53	.02	.51	-9.35	-4.61	-4.51
3	Houghton-Johns		.01	.03	.50	-9.54	-4.71	-4.61
	Kennard Simplified		.01	.03	.50	-9.63	-4.70	-4.61
4	Membrane		(a)	.03	.50	-9.54	-4.71	-4.61
1	Donnell-Mushtari	1	.01	.04	2.53	41.69	42.67	41.48
2	Love-Timoshenko		.04	.04	2.54	41.69	42.67	41.48
	Goldenveizer-Novozhilov		.07	.05	2.55	41.68	42.67	41.48
	Biezeno-Grammel		.06	.05	2.54	41.68	42.67	41.48
	Flügge		.07	.07	2.57	41.72	42.69	41.51
	Reissner-Naghdi-Berry		.02	.04	2.54	41.68	42.67	41.48
	Sanders		.04	.04	2.54	41.69	42.67	41.48
	Vlasov		.14	.05	2.54	41.69	42.67	41.48
	Epstein-Kennard		-.53	.03	2.54	41.70	42.67	41.48
3	Houghton-Johns		.01	.04	2.55	42.09	42.68	41.49 ^b
	Kennard Simplified		.01	.04	2.53	41.69	42.67	41.49
4	Membrane		(a)	.04	2.51	41.68	42.67	41.48
1	Donnell-Mushtari	2	.01	.07	4.13	13.13	11.92	11.82
2	Love-Timoshenko		.04	.07	4.16	13.15	11.93	11.83
	Goldenveizer-Novozhilov		.07	.08	4.16	13.15	11.93	11.83
	Biezeno-Grammel		.06	.08	4.14	13.13	11.92	11.81
	Flügge		.07	.10	4.21	13.19	11.98	11.88
	Reissner-Naghdi-Berry		.02	.07	4.14	13.14	11.93	11.83
	Sanders		.04	.07	4.16	13.15	11.93	11.83
	Vlasov		.02	.07	4.14	13.13	11.92	11.81
	Epstein-Kennard		-.53	.06	4.14	13.12	11.89	11.79
3	Houghton-Johns		.01	.07	4.17	13.16	11.93	11.83
	Kennard Simplified		.01	.07	4.12	13.13	11.92	11.82
4	Membrane		.01	.06	4.10	13.12	11.91	11.81

^a Frequency changes less than 0.01 percent.^b Imaginary frequencies.

TABLE 2.18.—*Percent Change in Transverse Mode Frequency Parameter by Neglecting Tangential Inertia Terms; SD-SD Supports, $\nu=0.3$, $R/h=20$ —Concluded*

Shell theory		n	l/mR					
Group	Name		0.1	0.25	1	4	20	100
1	Donnell-Mushtari	3	0.01	0.10	3.78	5.84	5.44	5.42
2	Love-Timoshenko		.04	.12	3.82	5.86	5.46	5.44
	Goldenveizer-Novozhilov		.07	.12	3.82	5.86	5.46	5.44
	Biezeno-Grammel		.06	.12	3.79	5.84	5.44	5.42
	Flügge		.08	.14	3.85	5.91	5.51	5.49
	Reissner-Naghdi-Berry		.03	.11	3.80	5.84	5.46	5.44
	Sanders		.05	.12	3.82	5.86	5.46	5.44
	Vlasov		.02	.11	3.79	5.84	5.44	5.42
	Epstein-Kennard		-.54	.01	3.79	5.82	5.41	5.39
3	Houghton-Johns		.01	.12	3.83	5.86	5.46	5.44
	Kennard Simplified		.01	.10	3.78	5.84	5.45	5.42
4	Membrane		.01	.10	3.75	5.82	5.43	5.41
1	Donnell-Mushtari	4	.01	.15	2.89	3.25	3.10	3.09
2	Love-Timoshenko		.05	.17	2.92	3.27	3.11	3.11
	Goldenveizer-Novozhilov		.08	.17	2.93	3.27	3.11	3.11
	Biezeno-Grammel		.07	.16	2.90	3.25	3.09	3.08
	Flügge		.08	.19	2.97	3.22	3.17	3.16
	Reissner-Naghdi-Berry		.03	.16	2.91	3.27	3.11	3.11
	Sanders		.05	.17	2.93	3.27	3.11	3.11
	Vlasov		.02	.16	2.90	3.25	3.09	3.09
	Epstein-Kennard		-.54	.14	2.89	3.22	3.06	3.06
3	Houghton-Johns		.02	.17	2.93	3.27	3.11	3.11
	Kennard Simplified		.01	.15	2.88	3.25	3.10	3.09
4	Membrane		.01	.14	2.85	3.23	3.09	3.08

TABLE 2.19.—Percent Change in Transverse Mode Frequency Parameter by Neglecting Tangential Inertia Terms; SD-SD Supports; $\nu = 0.3$, $R/h = 500$

Shell theory		n	l/mR					
Group	Name		0.1	0.25	1	4	20	100
1	Donnell-Mushtari	0	(a)	0.03	0.50	-9.54	-4.71	-4.61
2	Love-Timoshenko		(a)	.03	.50	-9.54	-4.71	-4.61
	Goldenveizer-Novozhilov		(a)	.03	.50	-9.54	-4.71	-4.61
	Biezeno-Grammel		(a)	.03	.50	-9.54	-4.71	-4.61
	Flügge		(a)	.03	.50	-9.54	-4.71	-4.61
	Reissner-Naghdi-Berry		(a)	.03	.50	-9.54	-4.71	-4.61
	Sanders		(a)	.03	.50	-9.54	-4.71	-4.61
	Vlasov		(a)	.03	.50	-9.54	-4.71	-4.61
	Epstein-Kennard		(a)	.03	.50	-9.54	-4.71	-4.61
3	Houghton-Johns		(a)	.03	.50	-9.54	-4.71	-4.61
	Kennard Simplified		(a)	.03	.50	-9.54	-4.71	-4.61
4	Membrane		(a)	.03	.50	-9.54	-4.71	-4.61
1	Donnell-Mushtari	1	(a)	.04	2.51	41.68	42.67	41.48
2	Love-Timoshenko		(a)	.04	2.51	41.68	42.67	41.48
	Goldenveizer-Novozhilov		(a)	.04	2.51	41.68	42.67	41.48
	Biezeno-Grammel		(a)	.04	2.51	41.68	42.67	41.48
	Flügge		(a)	.04	2.51	41.68	42.67	41.48
	Reissner-Naghdi-Berry		(a)	.04	2.51	41.68	42.67	41.48
	Sanders		(a)	.04	2.51	41.68	42.67	41.48
	Vlasov		(a)	.04	2.51	41.68	42.67	41.48
	Epstein-Kennard		(a)	.04	2.51	41.68	42.67	41.48
3	Houghton-Johns		(a)	.04	2.51	41.68	42.67	41.48
	Kennard Simplified		(a)	.04	2.51	41.68	42.67	41.48
4	Membrane		(a)	.04	2.51	41.68	42.67	41.48
1	Donnell-Mushtari	2	.01	.06	4.10	13.12	11.91	11.81
2	Love-Timoshenko		.01	.06	4.10	13.12	11.91	11.81
	Goldenveizer-Novozhilov		.01	.06	4.10	13.12	11.91	11.81
	Biezeno-Grammel		.01	.06	4.10	13.12	11.91	11.81
	Flügge		.01	.06	4.10	13.12	11.91	11.81
	Reissner-Naghdi-Berry		.01	.06	4.10	13.12	11.91	11.81
	Sanders		.01	.06	4.10	13.12	11.91	11.81
	Vlasov		.01	.06	4.10	13.12	11.91	11.81
	Epstein-Kennard		.01	.06	4.10	13.12	11.91	11.81
3	Houghton-Johns		.01	.06	4.10	13.12	11.91	11.81
	Kennard Simplified		.01	.06	4.10	13.12	11.91	11.81
4	Membrane		.01	.06	4.10	13.12	11.91	11.81

* Frequency changes less than 0.01 percent.

TABLE 2.19.—*Percent Change in Transverse Mode Frequency Parameter by Neglecting Tangential Inertia Terms; SD-SD Supports; $\nu=0.3$, $R/h=500$ —Concluded*

Shell theory		n	l/mR					
Group	Name		0.1	0.25	1	4	20	100
1	Donnell-Mushtari	3	0.01	0.10	3.75	5.83	5.43	5.41
2	Love-Timoshenko		.01	.10	3.75	5.83	5.43	5.41
	Goldenveizer-Novozhilov		.01	.10	3.75	5.82	5.42	5.41
	Biezeno-Grammel		.01	.10	3.75	5.82	5.43	5.41
	Flügge		.01	.10	3.75	5.83	5.43	5.41
	Reissner-Naghdi-Berry		.01	.10	3.75	5.83	5.43	5.41
	Sanders		.01	.10	3.75	5.82	5.43	5.41
	Vlasov		.01	.10	3.75	5.82	5.43	5.41
	Epstein-Kennard		.01	.10	3.75	5.82	5.43	5.41
3	Houghton-Johns		.01	.10	3.75	5.83	5.43	5.41
	Kennard Simplified		.01	.10	3.75	5.82	5.43	5.41
4	Membrane		.01	.10	3.73	5.83	5.43	5.41
1	Donnell-Mushtari	4	.01	.14	2.85	3.23	3.09	3.08
2	Love-Timoshenko		.01	.14	2.85	3.23	3.09	3.08
	Goldenveizer-Novozhilov		.01	.14	2.85	3.23	3.09	3.08
	Biezeno-Grammel		.01	.14	2.85	3.23	3.09	3.08
	Flügge		.01	.14	2.85	3.23	3.09	3.08
	Reissner-Naghdi-Berry		.01	.14	2.85	3.23	3.09	3.08
	Sanders		.01	.14	2.85	3.23	3.09	3.08
	Vlasov		.01	.14	2.85	3.23	3.09	3.08
	Epstein-Kennard		.01	.14	2.85	3.23	3.09	3.08
3	Houghton-Johns		.01	.13	2.85	3.23	3.09	3.08
	Kennard Simplified		.01	.14	2.85	3.23	3.09	3.08
4	Membrane		.01	.14	2.77	3.23	3.09	3.08

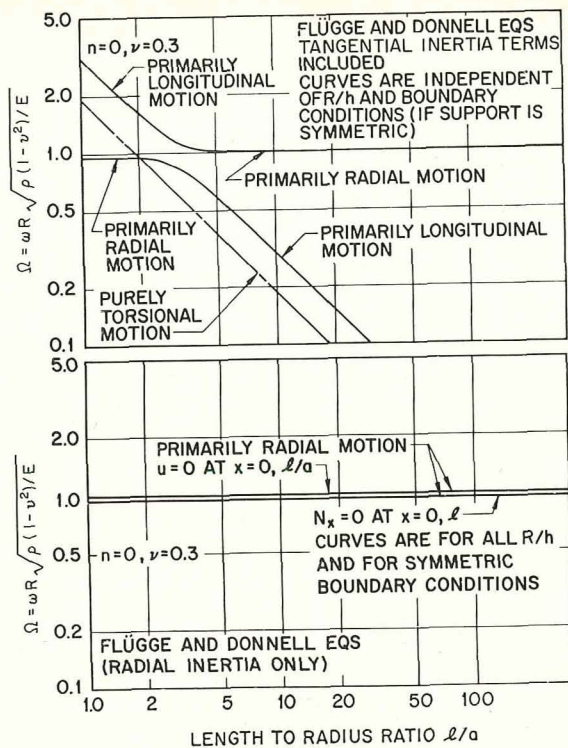


FIGURE 2.34.—Effect of tangential inertia terms on axisymmetric ($n=0$) mode. (After ref. 2.35)

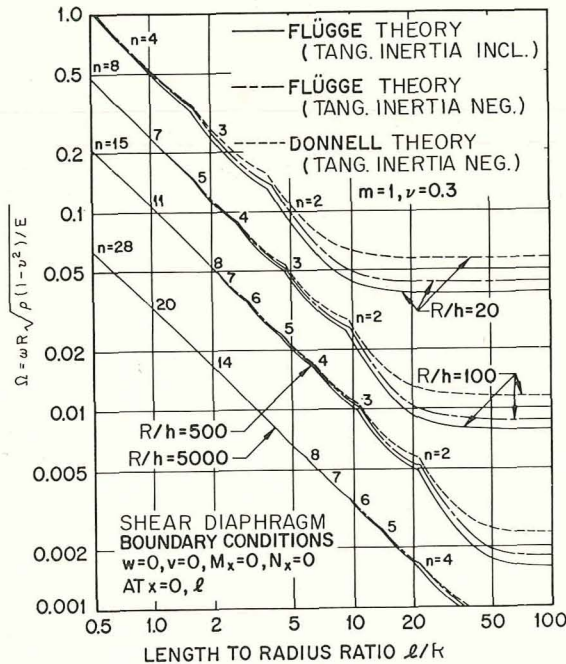


FIGURE 2.35.—Effect upon Ω of neglecting tangential inertia. (After ref. 2.35)

Neglecting tangential inertia also allows some simplification of the equations of motion (ref. 2.125) and permits uncoupling of them. Considering, for example, the Donnell-Mushtari equations (2.1) and (2.7), if the inertia terms are dropped from the first two of the three detailed scalar equations, it is easily found that the resulting equations can be manipulated to give

$$k\nabla^8 w + (1-\nu^2)\frac{\partial^4 w}{\partial s^4} + \frac{\rho(1-\nu^2)R^2}{E}\nabla^4\frac{\partial^2 w}{\partial t^2} = 0 \quad (2.44)$$

and two other fourth order equations in terms of u and w , and v and w containing the tangential displacements which are

$$\left. \begin{aligned} \nabla^4 u &= \nu \frac{\partial^2 w}{\partial s^3} - \frac{\partial^3 w}{\partial s \partial \theta^2} \\ \nabla^4 v &= -(2+\nu) \frac{\partial^3 w}{\partial s^2 \partial \theta} - \frac{\partial^3 w}{\partial s^3} \end{aligned} \right\} \quad (2.45)$$

This uncoupling permits the calculation of the eigenvalues directing from the single equation (2.44), whereas amplitude ratios are obtained by substituting the resulting solutions for w into equations (2.45). Further, whereas the type of uncoupling shown above in equations (2.44) and (2.45) can be accomplished for each of the theories when tangential inertia is neglected, the Donnell-Mushtari equations can also be uncoupled *without* neglecting tangential inertia. The resulting Donnell-type equations, which are more complicated than equations (2.44) and (2.45) are given by Yu (ref. 2.32).

2.3.5 Further Simplifications

Another type of simplification in the shell equations can be made when the circumferential wave length is small relative to the axial wave length, i.e.,

$$\lambda^2 \ll n^2 \quad (2.46)$$

This simplification was proposed by Yu (ref. 2.32) and seems particularly reasonable for a Donnell-Mushtari (or shallow shell) type of theory because, as seen earlier in this chapter, the Donnell-Mushtari theory is less applicable for small n . Thus, as in reference 2.32, under the assumption of equation (2.46) the Donnell-Mushtari coefficients of the characteristic equa-

tion (2.35) simplify from those of equations (2.36) to give

$$\left. \begin{aligned} K_2 &= 1 + \frac{1}{2}(3-\nu)n^2 + kn^4 \\ K_1 &= \frac{1}{2}[(1-\nu)n^2(n^2+1) + (3-\nu)kn^6] \\ K_0 &= \frac{1}{2}(1-\nu)[(1-\nu^2)\lambda^4 + kn^8] \end{aligned} \right\} \quad (2.47)$$

The modifying constants for equation (2.35) given in table 2.4 for other shell theories can similarly be simplified by the assumption of equation (2.46). For example, the modifying constants for the Flügge characteristic equation become (ref. 2.32)

$$\left. \begin{aligned} \Delta K_2 &= 0 \\ \Delta K_1 &= 0 \\ \Delta K_0 &= \frac{(1-\nu)}{2}n^4(1-2n^2) \end{aligned} \right\} \quad (2.48)$$

No extensive calculations are available in the literature which show the effect of Yu's simplification on the results obtained, although some discussion of loss of accuracy is given in references 2.32 and 2.48. Armenakas (ref. 2.50) examined the effect of the Yu simplification when tangential inertia was *also* neglected. He showed that for this extensive simplification the frequency parameter reduces to

$$\Omega^2 = \frac{(1-\nu^2)\lambda^4}{(n^2-\lambda^2)^2} + k(n^2-\lambda^2)^2 \quad (2.49)$$

for both the Flügge and Donnell-Mushtari theories. This formula was also obtained by Reissner (ref. 2.125) by making the same assumptions in shallow shell theory. In figures 2.36 and 2.37 (from ref. 2.50) the percent change in Ω resulting from neglecting tangential inertia alone (in the Flügge theory) and from Yu's simplification in addition (i.e., using eq. (2.49)) is shown for $R/h=100$ and 10, respectively.

Another simplification of equation (2.35) can be made when it is known that one of the three roots is much smaller than the others (cf., refs. 2.33, 2.62 and 2.69), as in the case of large values of R/h and l/mR (however, often the lowest two roots are of the *same* order of magnitude, despite

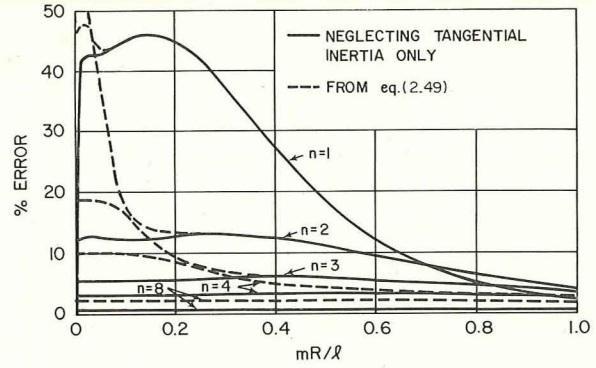


FIGURE 2.36.—Percent error in frequency parameter by neglecting tangential inertia and assuming $\lambda^2 \ll n^2$ in the Flügge theory; $R/h=100$. (After ref. 2.50)

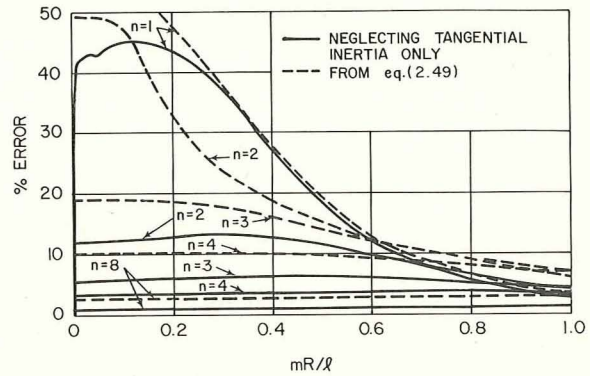


FIGURE 2.37.—Percent error in frequency parameter by neglecting tangential inertia and assuming $\lambda^2 \ll n^2$ in the Flügge theory; $R/h=10$. (After ref. 2.50)

frequent statements to the contrary which appear in the literature). In such cases the cubic and second degree terms in Ω^2 can be dropped from equation (2.35), leaving a linear equation for the fundamental frequency. The frequency parameter thus obtained is given by

$$\Omega^2 = -\frac{K_0 + k \Delta K_0}{K_1 + k \Delta K_1} \quad (2.50)$$

where K_0 and K_1 are as given previously in equations (2.36) and ΔK_0 and ΔK_1 as given in table 2.4. The single frequency thus obtained is *not* the same, however, as that when tangential inertia is ignored.

In reference 2.50 the errors introduced by using either equation (2.49) or equation (2.50) (for the Flügge theory) are compared.

(2) Neglecting tangential inertia in equations of motion.

(3) Neglecting terms containing k^2 and k^3 in characteristic equation.

(4) Neglecting k with respect to unity in characteristic equation.

(5) Neglecting Ω^6 and Ω^4 terms in characteristic equation (linearization).

(6) Neglecting Ω^6 terms in characteristic equation.

(7) Modified quadratic form of characteristic equation, $\Omega^2 = (K_0/K_1) + (K_0/K_1)^2(K_2/K_1)$.

(8) Yu's assumption, $\lambda^2 \ll n^2$.

Most of these assumptions are capable of causing very large changes in the calculated values of Ω over some ranges of the shell parameters.

Finally, an interesting simplification of an altogether different type was suggested by Simmonds (ref. 2.128) to account for the "beam-like" ($n=1$) vibrations of thin shells and was demonstrated for the case of shear diaphragm end supports. The shell was represented in turn by a set of Timoshenko beam equations (i.e., including shear deformation), a set of modified Euler-Bernoulli beam equations, and a set of modified Timoshenko equations derived so as to include Poisson ratio and normal pressure effects in the computation of overall stress-displacement relations for the beam. A cubic frequency equation in Ω^3 which is identical to that of membrane shell theory (see sec. 2.3.1) evolved from the modified Timoshenko equations. Of course, as seen in section 2.3.2, membrane theory is very accurate to describe the beam-like mode

providing the shell is not exceptionally short. Results for natural frequencies of a thin shell according to the three beam theories used in reference 2.128 are given in figure 2.38. Kornecki (ref. 2.129) showed that the "beam-like" ($n=1$) modes of long ($l/R \gg 1$), circular cylindrical shells can be represented by the elementary beam theory, including rotary inertia, but neglecting shear deformation.

2.4 OTHER SIMPLE EDGE CONDITIONS

We now turn to the remaining 135 cases of closed circular cylindrical shells of finite length having "simple" boundary conditions of the type given in section 1.8 at each end. By assuming solution functions which are generalizations of equations (2.20) it is possible to obtain exact solutions for the frequencies and mode shapes of free vibration for each of the 135 cases, although the amount of computational work required is relatively great. The procedure which will be followed was suggested by Flügge (ref. 2.31) in 1934, although he did not solve any specific problem using it. Subsequently, several other researchers (cf., refs. 2.17, 2.32, 2.34, 2.35, 2.40, 2.72, 2.73, 2.78) have carried the method through to its fruition.

Suppose that the Donnell-Mushtari thin shell theory is to be used. The equations of motion are then determined by the matrix operator (eq. (2.7)). Periodic behavior with respect to time and the circumferential angle θ is preserved in the solution functions for u , v , and w , but the periodic variation with respect to s in equations (2.20) is generalized to an exponential one; i.e.,

$$\left. \begin{aligned} u &= Ae^{\lambda s} \cos n\theta \cos \omega t \\ v &= Be^{\lambda s} \sin n\theta \cos \omega t \\ w &= Ce^{\lambda s} \cos n\theta \cos \omega t \end{aligned} \right\} \quad (2.53)$$

where $s = x/R$; A , B , C , and λ are undetermined constants; n determines the number of circumferential waves; and ω is the frequency, all as before. Substituting equations (2.53) into the equations of motion (eq. 2.3) leads to the same set of equations given in matrix form by equation (2.21) except that λ^2 is replaced by $-\lambda^2$ in the diagonal elements, and λ is replaced by $-\lambda$ in the first column of the coefficient matrix.

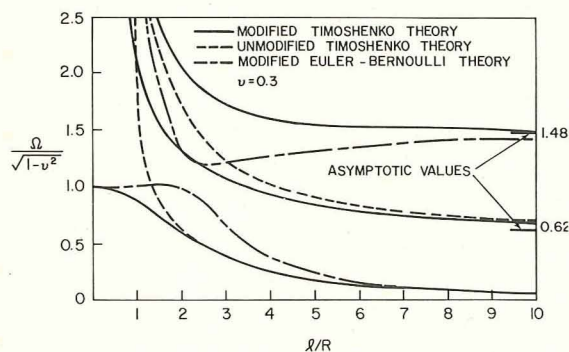


FIGURE 2.38.—Frequency parameters of an SD-SD shell as predicted by various beam theories. (After ref. 2.128)

For a nontrivial solution, the determinant of the coefficient matrix is set equal to zero, which yields an algebraic equation of the fourth degree in λ^2 :

$$\lambda^8 + g_6 \lambda^6 + g_4 \lambda^4 + g_2 \lambda^2 + g_0 = 0 \quad (2.54)$$

where (ref. 2.40)

$$\left. \begin{aligned} g_6 &= \left(\frac{3-\nu}{1-\nu} \right) \Omega^2 - 4n^2 \\ g_4 &= 6n^4 - \frac{3(3-\nu)}{1-\nu} n^2 \Omega^2 \\ &\quad + \frac{2}{1-\nu} \Omega^4 + \frac{1}{k} (1-\nu^2 - \Omega^2) \\ g_2 &= \frac{n^2 \Omega^2}{1-\nu^2} [3(3-\nu)n^2 - 4\Omega^2] \\ &\quad - 4n^6 + \frac{\Omega^2}{k} \left[3 + 2\nu + 2n^2 - \frac{3-\nu}{1-\nu} \Omega^2 \right] \\ g_0 &= \frac{1}{k(1-\nu)} [(1-\nu)n^2 - 2\Omega^2] \\ &\quad [kn^6 - \Omega^2(1+kn^4+n^2-\Omega^2)] \end{aligned} \right\} \quad (2.55)$$

and Ω^2 is the nondimensional frequency parameter given by equation (2.26).

The characteristic equation (2.54) is also obtainable from equation (2.35) by substituting $-\lambda^2$ for λ^2 (in this case, of course, λ is *not* given by eq. (2.34)) into the terms of equations (2.36) and collecting terms having like powers of λ^2 instead of ω^2 . In this manner characteristic equations corresponding to equation (2.35) can be obtained for the other shell theories by substituting $-\lambda^2$ for λ^2 in table 2.4.

For the usual range of parameters and $n \geq 1$, the roots of equation (2.54) were found by Hu and Wah (ref. 2.40) to have the form

$$\lambda = \pm \lambda_1, \pm i\lambda_2, \pm (\lambda_3 \pm i\lambda_4) \quad (2.56)$$

where $\lambda_1, \lambda_2, \lambda_3$, and λ_4 are real, positive numbers. Similar roots were found by Forsberg (ref. 2.72) for the more complicated characteristic equation arising from the Flügge theory. For a finite shell there will always be at least two roots of the form $\pm i\lambda_2$. For each root the ratios A/C and B/C can be found by returning to the original matrix equation in A, B , and C . The general solutions for u, v , and w are then expressible in terms of eight independent, real constants $A_1, A_2, A_3, \dots, A_8$ as follows (ref. 2.40):

$$\left. \begin{aligned} u &= \{ A_1 \eta_1 e^{\lambda_1 s} - A_2 \eta_1 e^{-\lambda_1 s} - A_3 \eta_2 \sin \lambda_2 s \\ &\quad + A_4 \eta_2 \cos \lambda_2 s + A_5 e^{\lambda_3 s} (\eta_3 \cos \lambda_4 s \\ &\quad - \eta_4 \sin \lambda_4 s) + A_6 e^{\lambda_3 s} (\eta_4 \cos \lambda_4 s \\ &\quad + \eta_3 \sin \lambda_4 s) - A_7 e^{-\lambda_3 s} (\eta_3 \cos \lambda_4 s \\ &\quad + \eta_4 \sin \lambda_4 s) + A_8 e^{-\lambda_3 s} (\eta_4 \cos \lambda_4 s \\ &\quad - \eta_3 \sin \lambda_4 s) \} \cos n\theta \cos \omega t \\ v &= \{ A_1 \xi_1 e^{\lambda_1 s} + A_2 \xi_1 e^{-\lambda_1 s} + A_3 \xi_2 \cos \lambda_2 s \\ &\quad + A_4 \xi_2 \sin \lambda_2 s + A_5 e^{\lambda_3 s} (\xi_3 \cos \lambda_4 s \\ &\quad - \xi_4 \sin \lambda_4 s) + A_6 e^{\lambda_3 s} (\xi_4 \cos \lambda_4 s \\ &\quad + \xi_3 \sin \lambda_4 s) + A_7 e^{-\lambda_3 s} (\xi_3 \cos \lambda_4 s \\ &\quad + \xi_4 \sin \lambda_4 s) - A_8 e^{-\lambda_3 s} (\xi_4 \cos \lambda_4 s \\ &\quad - \xi_3 \sin \lambda_4 s) \} \sin n\theta \cos \omega t \\ w &= \{ A_1 e^{\lambda_1 s} + A_2 e^{-\lambda_1 s} + A_3 \cos \lambda_2 s \\ &\quad + A_4 \sin \lambda_2 s + A_5 e^{\lambda_3 s} \cos \lambda_4 s \\ &\quad + A_6 e^{\lambda_3 s} \sin \lambda_4 s + A_7 e^{-\lambda_3 s} \cos \lambda_4 s \\ &\quad + A_8 e^{-\lambda_3 s} \sin \lambda_4 s \} \cos n\theta \cos \omega t \end{aligned} \right\} \quad (2.57)$$

where

$$\begin{aligned} \xi_1 &= G_1/D_1, \quad \xi_2 = G_2/D_2, \quad \eta_1 = H_1/D_1, \quad \eta_2 = H_2/D_2, \\ \xi_3 &= \frac{R_1 Q_1 + R_2 Q_2}{Q_1^2 + Q_2^2}, \quad \eta_3 = \frac{S_1 Q_1 + S_2 Q_2}{Q_1^2 + Q_2^2}, \\ \xi_4 &= \frac{R_2 Q_1 - R_1 Q_2}{Q_1^2 + Q_2^2}, \quad \eta_4 = \frac{S_2 Q_1 - S_1 Q_2}{Q_1^2 + Q_2^2}; \end{aligned} \quad (2.58)$$

with

$$\begin{aligned} D_1 &= (1-\nu)\lambda_1^4 + \lambda_1^2 [2n^2(\nu-1) + (3-\nu)\Omega^2] \\ &\quad + (n^2 - \Omega^2) [(1-\nu)n^2 - 2\Omega^2] \\ G_1 &= n[\lambda_1^2(\nu^2 + \nu - 2) + (1-\nu)n^2 - 2\Omega^2] \\ H_1 &= -\lambda_1[\lambda_1^2 \nu(1-\nu) + 2\nu(\Omega^2 - n^2) + n^2(1+\nu)] \\ D_2 &= (1-\nu)\lambda_2^4 - \lambda_2^2 [2n^2(\nu-1) + (3-\nu)\Omega^2] \\ &\quad + (n^2 - \Omega^2) [(1-\nu)n^2 - 2\Omega^2] \\ G_2 &= n[-\lambda_2^2(\nu^2 + \nu - 2) + (1-\nu)n^2 - 2\Omega^2] \\ H_2 &= \lambda_2[\lambda_2^2 \nu(1-\nu) - 2\nu(\Omega^2 - n^2) - n^2(1+\nu)] \\ Q_1 &= (1-\nu) \{ (\lambda_3^2 - \lambda_4^2)^2 - 4\lambda_3^2 \lambda_4^2 \} \\ &\quad + (\lambda_3^2 - \lambda_4^2) \{ 2n^2(\nu-1) + (3-\nu)\Omega^2 \} \\ &\quad + (n^2 - \Omega^2) \{ (1-\nu)n^2 - 2\Omega^2 \} \\ Q_2 &= 4\lambda_3 \lambda_4 (\lambda_3^2 - \lambda_4^2) (1-\nu) \\ &\quad + 2\lambda_3 \lambda_4 \{ 2n^2(\nu-1) + (3-\nu)\Omega^2 \} \\ R_1 &= n \{ (\lambda_3^2 - \lambda_4^2)(\nu^2 + \nu - 2) + (1-\nu)n^2 - 2\Omega^2 \} \\ R_2 &= 2n\lambda_3 \lambda_4 (\nu^2 + \nu - 2) \\ S_1 &= -\lambda_3 \{ \nu(1-\nu)(\lambda_3^2 - 3\lambda_4^2) \\ &\quad + 2\nu(\Omega^2 - n^2) + n^2(1+\nu) \} \\ S_2 &= -\lambda_4 \{ \nu(1-\nu)(3\lambda_3^2 - \lambda_4^2) \\ &\quad + 2\nu(\Omega^2 - n^2) + n^2(1+\nu) \} \end{aligned} \quad (2.59)$$

Note that the procedure followed above is the same as would be used to determine the deflected mode shapes of *statically* loaded circular cylindrical shells having arbitrary end conditions. The corresponding characteristic equation is obtained in this case simply by setting $\Omega=0$ in equation (2.35), with K_0 and ΔK_0 defined as before by equations (2.36) and table 2.4. However, for the static problem it is found that all of the roots of λ are complex (ref. 2.131, p. 228), in contrast with those (eqs. (2.56)) of the free vibration problem.

To complete the solution of the free vibration problem, four boundary conditions must next be applied at each end of the shell, $s=0$ and $s=l/R$. Because the boundary conditions must be satisfied for all values of θ and t allowed to vary independently this yields a set of eight homogeneous, simultaneous, linear, algebraic equations in terms of the eight unknown constants A_1, \dots, A_8 . For a nontrivial solution the determinant of the coefficient matrix of these equations is set equal to zero, which yields the frequency parameters Ω^2 . These are the roots of the characteristic determinant for each particular value of n . If the boundary conditions at the two ends are identical, the eighth order determinant can be replaced by two determinants of the fourth order by taking the origin of the x coordinate at the middle section of the cylinder and considering separately modes which are symmetric and antisymmetric with respect to the middle section.

Another procedure for the numerical evaluation of the frequency determinant was suggested by Flügge (ref. 2.131). Briefly, the procedure consists of selecting the circumferential wave number n and the frequency parameter Ω in advance and finding the proper length of the shell to give the chosen frequency.

Vronay and Smith (ref. 2.80) discussed a method of applying exact solutions whereby the arbitrary constants are *not* redefined as real constants, but are left complex, thereby eliminating the need to monitor the form of the roots of the characteristic equation (2.54) during its solution.

Yu (ref. 2.32) showed that the characteristic equation (2.54) is considerably simplified if one can assume

$$|\lambda^2| \ll n^2 \quad (2.60)$$

This assumption restricts one to longitudinal wave lengths which are large in comparison

to the circumferential wave lengths. The characteristic equation then simplifies to

$$(1-\nu)(1-\nu^2)\lambda^4 = 2\Omega^3 - \Omega^2[2 + (3-\nu)n^2 + 2kn^4] + \Omega[(1-\nu)n^2(n^2+1) + (3-\nu)kn^6] - (1-\nu)kn^8 \quad (2.61)$$

having four roots of the type

$$\lambda = K, -K, iK, -iK \quad (2.62)$$

where K is a real number. The ratios A/C and B/C in equation (2.53) are then

$$\left. \begin{aligned} \frac{A}{C} &= \frac{\lambda[2\nu\Omega + (1-\nu)n^2]}{2\Omega^2 - (3-\nu)n^2\Omega + (1-\nu)n^4} \\ \frac{B}{C} &= \frac{-2n\Omega + (1-\nu)n^3}{2\Omega^2 - (3-\nu)n^2\Omega + (1-\nu)n^4} \end{aligned} \right\} \quad (2.63)$$

Reismann (ref. 2.75) showed that the modes of vibration of circular cylindrical shells of finite length, for any of the 136 possible sets of simple boundary conditions, are related by the orthogonality condition

$$\int_0^l (U_{in}U_{jn} + V_{in}V_{jn} + W_{in}W_{jn}) dx = 0 \quad (2.64)$$

provided that $\Omega_{in} \neq \Omega_{jn}$, where i, j identify separate modes for a given value of n and U, V, W are the mode shapes such that

$$\left. \begin{aligned} u(x, \theta, t) &= U_n(x) \cos n\theta \cos \omega t \\ v(x, \theta, t) &= V_n(x) \sin n\theta \cos \omega t \\ w(x, \theta, t) &= W_n(x) \cos n\theta \cos \omega t \end{aligned} \right\} \quad (2.65)$$

Gontkevich (refs. 2.126 and 2.127) used the Rayleigh-Ritz method with beam functions (see sec. 2.4.1 for discussion of this solution method) to obtain characteristic equations for the six problems having clamped, shear diaphragm, or free end conditions at either or both ends of a circular cylindrical shell. The mode shapes used are

$$\left. \begin{aligned} u &= A_m X_m'(x) \cos n\theta \cos \omega t \\ v &= B_m X_m(x) \sin n\theta \cos \omega t \\ w &= C_m X_m(x) \cos n\theta \cos \omega t \end{aligned} \right\} \quad (2.66)$$

where A_m, B_m, C_m are amplitude coefficients; primes are used to indicate differentiation with respect to the independent variable x ; and $X_m(x)$ is a beam function which is the m th eigenfunction of free vibration of a beam having the

desired boundary conditions. After employing the Rayleigh-Ritz procedure, a cubic characteristic equation in Ω^2 was obtained as follows:

$$\Omega^6 - K_2\Omega^4 + K_1\Omega^2 - K_0 = 0 \quad (2.67)$$

where

$$K_2 = \frac{\mu_m^2}{\delta_m} + \frac{1}{2}(3-\nu)n^2 + 1 + \frac{1}{2}(1-\nu)\delta_m\mu_m^2 + k[n^2 + 2(1-\nu)\delta_m\mu_m^2 + \mu_m^4 - 2n^2\mu_m^2\gamma_m + n^4 + 2n^2\mu_m^2(1-\nu)(\delta_m + \gamma_m)] \quad (2.68a)$$

$$\begin{aligned} \delta_m K_1 = & \left[\mu_m^2 + \frac{1}{2}(1-\nu)\delta_m n^2 \right] \left[n^2 + \frac{1}{2}(1-\nu)\delta_m\mu_m^2 + 1 \right] + \frac{1}{2}(1-\nu)\delta_m^2\mu_m^2 - \nu^2\gamma_m^2\mu_m^2 - n^2\mu_m^2 \left[-\frac{\delta_m}{2} \right. \\ & + \nu \left(\gamma_m + \frac{1}{2}\delta_m \right) \left. \right]^2 + k \left\{ \left[\mu_m^2 + \frac{1}{2}(3-\nu)n^2\delta_m + \frac{1}{2}(1-\nu)\delta_m^2\mu_m^2 \right] \left[\mu_m^4 - 2n^2\mu_m^2\gamma_m^2 + n^4 \right. \right. \\ & + 2n^2\mu_m^2(1-\nu)(\delta_m + \gamma_m) \left. \right] + \left[n^2 + 2(1-\nu)\delta_m\mu_m^2 \right] \left[\mu_m^2 + \frac{1}{2}(1-\nu)\delta_m n^2 + \delta_m \right] \\ & \left. - 2n^2\delta_m \left(n^2 + \mu_m^2[2(1-\nu)\delta_m - \gamma_m\nu] \right) \right\} \quad (2.68b) \end{aligned}$$

$$\begin{aligned} \delta_m K_0 = & \frac{1}{2}(1-\nu)\delta_m\mu_m^4(1-\gamma_m^2\nu^2) + k \left\{ \left[\frac{1}{2}(1-\nu)\delta_m n^2 + \mu_m^2(1-\gamma_m^2\nu^2) \right] \left[n^2 + 2(1-\nu)\delta_m\mu_m^2 \right] \right. \\ & + \left[\left(\mu_m^2 + \frac{1}{2}(1-\nu)\delta_m n^2 \right) \left(n^2 + \frac{1}{2}(1-\nu)\delta_m\mu_m^2 \right) - n^2\mu_m^2 \left[-\frac{1}{2}\delta_m + \nu \left(\gamma_m + \frac{1}{2}\delta_m \right) \right]^2 \right] \left[\mu_m^4 \right. \\ & - 2n^2\mu_m^2\gamma_m + n^4 + 2n^2\mu_m^2(1-\nu)(\delta_m + \gamma_m) \left. \right] - n^2 \left[\mu_m^2\delta_m\gamma_m(1-\nu)\nu - 2\nu^2\mu_m^2\gamma_m^2 + 2 \left(\mu_m^2 \right. \right. \\ & \left. \left. + \frac{1}{2}(1-\nu)\delta_m n^2 \right) \right] \left[n^2 + \mu_m^2(2\delta_m(1-\nu) - \gamma_m\nu) \right] \left. \right\} \quad (2.68c) \end{aligned}$$

where $k = h^2/12R^2$, as before, and

where

$$\left. \begin{aligned} \mu_m &= \epsilon_m R/l \\ \delta_m &= \frac{l}{\alpha_m^2} \int_0^l (X_m')^2 dx \\ \gamma_m &= \frac{l}{\alpha_m^2} \int_0^l X_m'' X_m dx \end{aligned} \right\} \quad (2.69)$$

$$\left. \begin{aligned} l_1 &= \int_0^l \psi_m^{iv} \psi_m dx \\ l_2 &= \int_0^l \psi_m'' \psi_m dx \\ l_3 &= \int_0^l \psi_m'' X_m dx \\ l_4 &= \int_0^l X_m^{iv} X_m dx \\ l_5 &= \int_0^l X_m^2 dx \end{aligned} \right\} \quad (2.71)$$

and the values of ϵ_m , δ_m , γ_m are listed in table 2.21 (ref. 2.127) for the six types of boundary conditions.

Ivanyuta and Finkelshteyn (ref. 2.110) used the Donnell-Mushtari shell equations and the Bubnov-Galerkin approximate procedure with beam functions to arrive at the following general formula for frequency parameters for the *axisymmetric* modes of shells having arbitrary boundary conditions:

$$\Omega = k \frac{l_4}{l_5} + (1-\nu^2) \frac{l_2 l_3}{l_1 l_5} \quad (2.70)$$

where $\psi_m = \psi_m(x)$, $X_m = X_m(x)$ are beam functions separately chosen so that

$$\left. \begin{aligned} \varphi_m(x) &= A_m \psi_m(x) \\ w_m(x) &= B_m X_m(x) \end{aligned} \right\} \quad (2.72)$$

satisfy all of the boundary conditions at the ends.

TABLE 2.21.—*Constants for the Characteristic Equation (2.67)*

m	Item	SD-SD	Clamped-clamped	Clamped-free	Free-free	Clamped-SD	SD-free
0		—	—	1.321886	—	—	—
1		1.0	0.549880	1.471208	2.211601	0.723422	1.742905
2		1.0	.746684	1.252875	1.766169	.856926	1.422809
3		1.0	.818051	1.181963	1.545592	.902022	1.293787
4	δ_m	1.0	.858553	1.141465	1.424419	.925136	1.224722
5		1.0	.884249	1.115749	1.347244	.939525	1.181899
>5		1.0	$1 - \frac{2}{\left(m + \frac{1}{2}\right)\pi}$	$1 + \frac{2}{\left(m + \frac{1}{2}\right)\pi}$	$1 + \frac{6}{\left(m + \frac{1}{2}\right)\pi}$	$1 - \frac{1}{\left(m + \frac{1}{4}\right)\pi}$	$1 + \frac{3}{\left(m + \frac{1}{4}\right)\pi}$
0		—	—	0.244094	—	—	—
1		—	—	-.603337	-0.549879	—	-0.723422
2		—	—	-.744024	-.744024	—	-.902022
3		—	—	-.818169	-.818051	—	-.902022
4	γ_m	$-\delta_m$	$-\delta_m$	-.858524	-.858533	$-\delta_m$	-.925136
5		—	—	-.869100	-.884249	—	-.939525
>5		—	—	$-1 + \frac{2}{\left(m + \frac{1}{2}\right)\pi}$	$-1 + \frac{2}{\left(m + \frac{1}{2}\right)\pi}$	—	$-1 + \frac{1}{\left(m + \frac{1}{4}\right)\pi}$
0		—	—	1.875104	—	—	—
1		π	4.73004	4.69409	4.73004	3.92660	3.92660
2		2π	7.853204	7.854757	7.853204	7.06858	7.06858
3		3π	10.995608	10.995541	10.995608	10.2102	10.2102
4	ϵ_m	4π	14.137166	14.137168	14.137166	13.3518	13.3518
5		5π	17.27876	17.27880	17.27876	16.4934	16.4934
>5		$m\pi$	$\frac{(2m+1)}{2}\pi$	$\frac{(2m+1)}{2}\pi$	$\frac{(2m+1)}{2}\pi$	$\frac{(4m+1)}{4}\pi$	$\frac{(4m+1)}{4}\pi$

The function φ is an Airy stress function related to the stress resultants by

$$\left. \begin{aligned} N_x &= \frac{1}{R^2} \frac{\partial^2 \varphi}{\partial \theta^2} \\ N_\theta &= \frac{\partial^2 \varphi}{\partial x^2} \\ N_{x\theta} &= -\frac{1}{R} \frac{\partial^2 \varphi}{\partial x \partial \theta} \end{aligned} \right\} \quad (2.73)$$

It is clear that because of the independence of the beam function ψ and X that this procedure allows for more general boundary conditions than using equations (2.66).

2.4.1 Clamped-Clamped

The boundary conditions for the circular cylindrical shell which is completely clamped (the terms "fixed" or "fully fixed" are sometimes used

in the literature) at both ends are

$$u = v = w = \frac{\partial w}{\partial x} = 0 \quad \text{at} \quad x = 0, l \quad (2.74)$$

For this problem many authors have used the exact method for obtaining frequencies and mode shapes which was outlined in section 2.4 (cf., refs. 2.32, 2.33, 2.34, 2.35, 2.41, 2.44, 2.45, 2.72, 2.73, and 2.132 through 2.136). However, partly because of the complexity of the exact procedure, even more have used the Rayleigh-Ritz method or an equivalent (cf., refs. 2.4, 2.16, 2.33, 2.34, 2.42, 2.49, 2.65, 2.78, 2.85, 2.103, 2.107, 2.110, 2.114, 2.126, 2.127, and 2.137 through 2.140). The Ritz method depends upon selection of a set of trial functions and determination of the relative amplitudes of the trial functions by minimization of a suitable energy functional (refs. 2.141 and 2.142). The trial functions need only satisfy the "essential" or "geometric" boundary conditions

(these dealing with generalized displacements) of the problem. The additional boundary conditions (sometimes called "natural" or "generalized force" boundary conditions) are then approached in the limit as long as the set of trial functions has sufficient completeness. The Rayleigh procedure assumes a single trial function (or set of trial functions in u , v , w in this case) and a frequency is found by substituting this trial function into Rayleigh's Quotient (ref. 2.24) involving the maximum potential and kinetic energies of the system. One procedure equivalent to the Rayleigh-Ritz method for this problem uses Lagrange's equations and the assumed displacement components to obtain a characteristic determinant for the frequencies. Another equivalent procedure in this case for a given set of trial functions is that of Bubnov-Galerkin (cf., refs. 2.143, 2.144, 2.145, 2.146, and 2.196). All these procedures give *upper bounds* on the frequency parameters. Beam functions (see discussion later in this section) are usually used with the Rayleigh-Ritz methods.

The series method was used in reference 2.147; the Southwell method, giving lower bounds on frequency parameters, in reference 2.148; Bolotin's (ref. 2.149) "dynamic edge effect" method in reference 2.150; the method of "parallel springs" in reference 2.111; finite differences in references 2.35 and 2.151; and finite elements in reference 2.132. Experimental results were reported in references 2.4, 2.33, 2.34, 2.44, 2.45, 2.85, 2.103, 2.107, 2.117, 2.137, 2.139, 2.140, 2.152, and 2.153. The vibration of a clamped-clamped circular cylindrical shell was also discussed in references 2.68, 2.154, 2.155, and 2.156.

Warburton (ref. 2.78) used the exact procedure and gave the characteristic equations for *symmetric* modes which arises from applying the boundary conditions (for the Flügge theory):

$$\begin{aligned} & b_1 (\tanh \theta_3 \cos^2 \theta_4 + \coth \theta_3 \sin^2 \theta_4) \cos \theta_2 \\ & + b_2 (\tanh \theta_3 \tanh \theta_1 \\ & - \coth \theta_3 \coth \theta_1) \sin \theta_4 \cos \theta_4 \cos \theta_2 \\ & + b_3 \tanh \theta_1 \cos \theta_2 \\ & + b_4 (\coth \theta_3 - \tanh \theta_3) \sin \theta_4 \cos \theta_4 \sin \theta_2 \\ & + b_5 \sin \theta_2 \\ & + b_6 (\tanh \theta_3 \sin^2 \theta_4 + \coth \theta_3 \cos^2 \theta_4) \tanh \theta_1 \sin \theta_2 \\ & + b_7 (\coth \theta_3 - \tanh \theta_3) \tanh \theta_1 \sin \theta_4 \cos \theta_4 \cos \theta_2 \\ & = 0 \end{aligned} \quad (2.75)$$

where

$$\theta_1 = \lambda_1 l / 2R$$

$$\theta_2 = \lambda_2 l / 2R$$

$$\theta_3 = \lambda_3 l / 2R$$

$$\theta_4 = \frac{\lambda_4 l}{2R}$$

and the λ_i are the roots identified in equation (2.56). The corresponding equation for the *anti-symmetric* modes is obtained from equation (2.75) by making the following interchanges:

$$\left. \begin{aligned} \tanh \theta_1 &\leftrightarrow \coth \theta_1 \\ \sin \theta_2 &\rightarrow -\cos \theta_2 \\ \cos \theta_2 &\rightarrow \sin \theta_2 \\ \tanh \theta_3 &\leftrightarrow \coth \theta_3 \end{aligned} \right\} \quad (2.76)$$

The coefficients b_i which appear in equation (2.75) are given by

$$\left. \begin{aligned} b_1 &= (k_3 - k_1)(k_7 \lambda_4 - k_8 \lambda_3) \\ b_2 &= (k_7 \lambda_1 - k_2 \lambda_3)(k_5 - k_3) \\ &\quad + k_6(k_8 \lambda_1 - k_2 \lambda_4) \\ b_3 &= (k_7 \lambda_1 - k_2 \lambda_3)k_6 \\ &\quad - (k_5 - k_3)(k_8 \lambda_1 - k_2 \lambda_4) \\ b_4 &= (k_5 - k_1)(k_4 \lambda_3 - k_7 \lambda_2) \\ &\quad + k_6(k_4 \lambda_4 - k_8 \lambda_2) \\ b_5 &= -k_6(k_4 \lambda_3 - k_7 \lambda_2) \\ &\quad + (k_5 - k_1)(k_4 \lambda_4 - k_8 \lambda_2) \\ b_6 &= k_6(k_4 \lambda_1 - k_2 \lambda_2) \\ b_7 &= 0 \end{aligned} \right\} \quad (2.77)$$

with the constants k_i related to the amplitude ratios by

$$\left. \begin{aligned} k_1 &= B/C, & \text{with } \lambda_r &= \lambda_1 \\ k_2 &= A/C, & \text{with } \lambda_r &= \lambda_1 \\ k_3 &= B/C, & \text{with } \lambda_r &= \lambda_2 \\ k_4 &= A/C, & \text{with } \lambda_r &= \lambda_2 \\ k_5 + ik_6 &= B/C, & \text{with } \lambda_r &= \lambda_3 + i\lambda_4 \\ k_7 + ik_8 &= A/C, & \text{with } \lambda_r &= \lambda_3 + i\lambda_4 \end{aligned} \right\} \quad (2.78)$$

and, for $\nu = 0.3$,

$$\left. \begin{aligned} A/C &= \lambda_r \{ 0.35 - 0.65\Omega^2 + k[0.65(\lambda_r^2 - n^2)^2 + 1.405\lambda_r^2 - 0.95n^2 + 0.65] \} \div \{ 0.35n^2 - 0.805\lambda_r^2 - \Omega^2 + k[-0.7\lambda_r^2 n^2 + 0.7\lambda_r^4 + 0.35n^2 + 1.35\lambda_r^2 \Omega^2] \} \\ B/C &= n \{ 0.35 - 0.65\Omega^2 + k[0.65(\lambda_r^2 - n^2)^2 + 1.405\lambda_r^2 - 0.95n^2 + 0.65] \} \div \{ 0.35n^2 + 0.105\lambda_r^2 + 0.3\Omega^2 + k[-0.35\lambda_r^4 + 0.35n^4 - \lambda_r^2 \Omega^2 - 0.35n^2 \Omega^2 + 0.315\lambda_r^2] \} \end{aligned} \right\} \quad (2.79)$$

Approximate solutions (to provide initial values for iterative solutions) can be found by setting the hyperbolic functions in equations (2.75) equal to unity, giving

$$(b_1 + b_3) \cos \theta_2 + (b_5 + b_6) \sin \theta_2 = 0 \quad (2.80)$$

for symmetric modes. Similarly, for antisymmetric modes

$$(b_1 + b_3) \sin \theta_2 - (b_5 + b_6) \cos \theta_2 = 0 \quad (2.81)$$

Successive roots taken alternatively from equations (2.80) and (2.81) have increments θ_2 of $\pi/2$. The solutions of equations (2.75) and (2.76) depend only slightly upon the θ_1 and θ_3 terms.

Forsberg (ref. 2.35) used the exact procedure and obtained results using the Flügge and Donnell-Mushtari theories, with and without tangential inertia. It was found that for the axisymmetric ($n=0$) mode the frequencies are essentially the same as for the SD-SD boundary conditions (see sec. 2.3) when the tangential inertia is considered, and that the frequency differs slightly when it is neglected, as shown in figure 2.34. For the beam-type ($n=1$) modes, however, there is considerable difference between the results obtained from the two types of boundary conditions, as shown in figure 2.39. It is clear from figure 2.39 that the frequency increase for clamped ends is almost entirely due to the added stiffness resulting from restraining the axial displacement u at the ends, rather than from restraining the end rotations $\partial w/\partial x$. For large values of l/R the effect of end fixity disappears in this mode. The effects of neglecting tangential inertia in the two theories for the clamped boundaries is seen in figure 2.40. Envelopes of lowest frequencies according to the Flügge and Donnell-Mushtari theories, with and without tangential inertia, for all n are shown

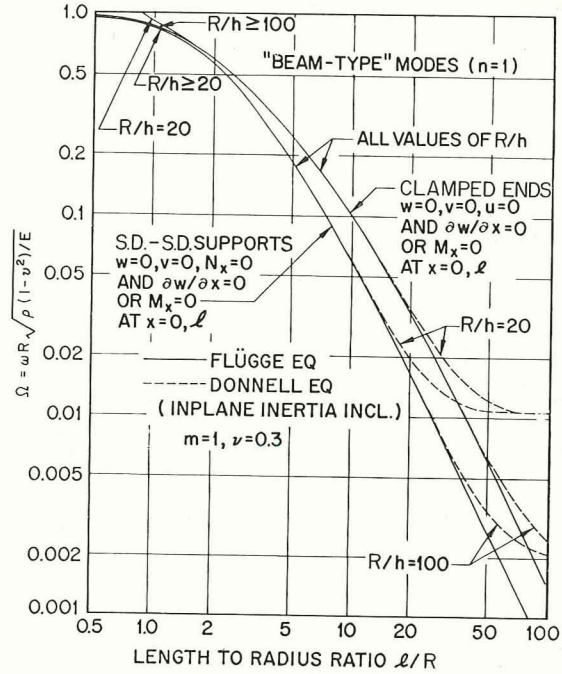


FIGURE 2.39.—Effects of SD-SD and clamped-clamped ends upon the frequency parameter; beam bending mode ($n < 1$). (After ref. 2.35)

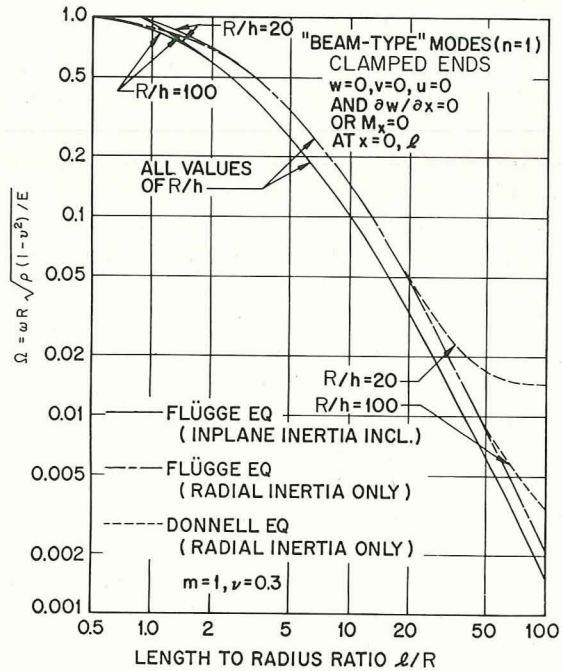


FIGURE 2.40.—Effects of neglecting tangential inertia on the frequency parameter for clamped-clamped circular cylindrical shells; beam bending mode ($n = 1$). (After ref. 2.35)

in figure 2.41. As for the SD-SD supports, increasing the number of longitudinal half-waves m always increases the associated vibration frequency, as shown in figure 2.42 for $n=2$, $R/h=100$.

Forsberg (ref. 2.72) made some further comparisons between the circular cylindrical shell having both ends fixed and one having shear diaphragm supports at both ends (see sec. 2.3). Exact solutions according to the Flügge theory were used in both cases. These comparisons are shown in figures 2.43, 2.44, and 2.45. In each case as the number of axial half-waves m is increased the frequency becomes less dependent upon the type of boundary conditions. This statement is, of course, qualitatively extendable to changing the shell length rather than m . However, for $m=1$, figure 2.43 shows that the clamped-clamped frequency is almost 100 percent higher than the SD-SD frequency in the range $5 < l/R < 15$. In this range the difference in *minimum* frequencies is about 50 percent.

An interesting three-dimensional plot showing the variation of the frequency parameter as a function of the parameters n and l/R is depicted in figure 2.46 (ref. 2.72) for $R/h=100$, $\nu=0.3$, and $m=1$. Two surfaces are shown on the same figure—one for the clamped-clamped shell, the other for the SD-SD shell. The difference between the surfaces, for $l/R < 1$, is primarily due to the effect of moment restraint; for $l/R > 1$, the difference is primarily due to the effect of axial restraint. The curves for $m=1$ given previously in figures 2.43 through 2.45 are cross sections of figure 2.46. Although figure 2.46 is only for one longitudinal half-wave $m=1$, for $l/R=1$ there are nine values of n which have frequencies less than the minimum value for $m=2$, and for $l/R=10$ there are three values, as can be seen in figure 2.44.

Yu (ref. 2.32) showed that a considerable simplification of the procedure for finding the eigenvalues results if one uses the Donnell equations and the assumption that the number of circumferential waves is large relative to the number of axial waves (in particular, if $|\lambda|^2 \ll n^2$). In this case the characteristic equation determining the frequency parameter Ω for clamped-clamped circular cylindrical shells reduces to

$$\cos \epsilon \cosh \epsilon - 1 = 0 \quad (2.82)$$

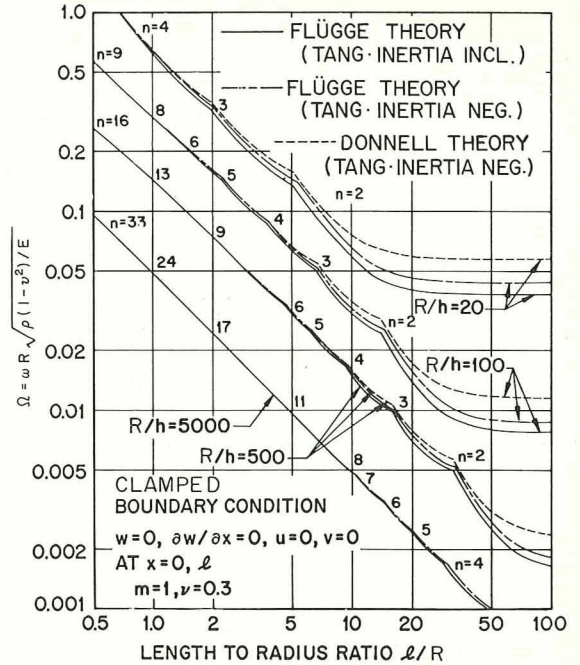


FIGURE 2.41.—Effects of lowest frequencies for clamped-clamped circular cylindrical shells (n =number of circumferential waves). (After ref. 2.35)

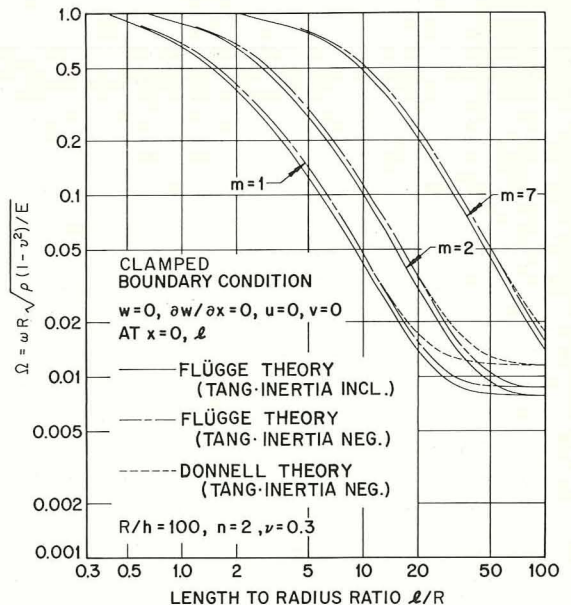


FIGURE 2.42.—Variation of frequency parameter with number of longitudinal half-waves (m); clamped-clamped circular cylindrical shell. (After ref. 2.35)

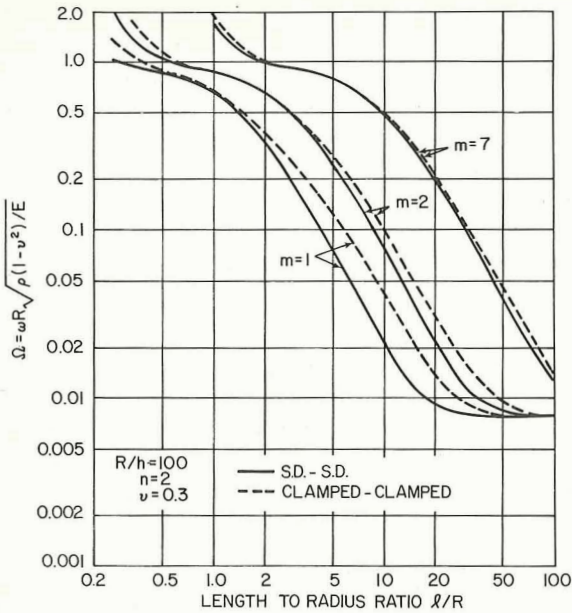


FIGURE 2.43.—Comparison of frequency parameters between shells having clamped and shear diaphragm supports at both ends; $n=2$, $m \geq 1$. (After ref. 2.72)

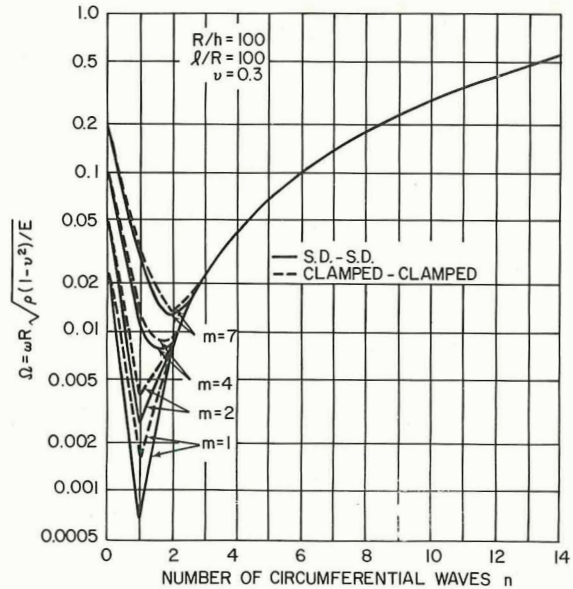


FIGURE 2.45.—Comparison of frequency parameters between shells having clamped and shear diaphragm supports at both ends, $l/R=100$; $m \geq 1$. (After ref. 2.72)

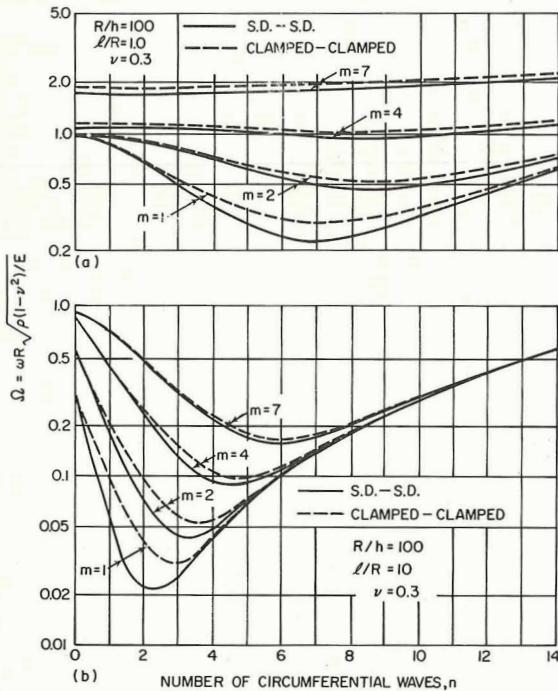


FIGURE 2.44.—Comparison of frequency parameters between shells having clamped and shear diaphragm supports at both ends; $l/R=1, 10$; $m \geq 1$. (After ref. 2.72)

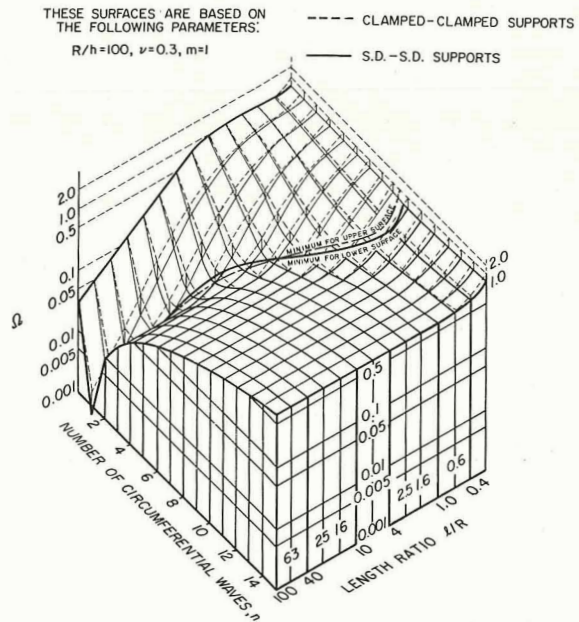


FIGURE 2.46.—Frequency parameter surfaces for clamped-clamped and SD-SD shells; $R/h=100$, $\nu=0.3$, $m=1$. (After ref. 2.72)

where

$$\epsilon = \lambda \left(\frac{l}{R} \right) \quad (2.83)$$

and where λ is related to the frequency parameter by

$$(1-\nu)(1-\nu^2)\lambda^4 = 2\Omega^6 - \Omega^4[2 + (3-\nu)n^2 + kn^4] + \Omega^2[(1-\nu)n^2(n^2+1) + (3-\nu)kn^6] - (1-\nu)kn^8 \quad (2.84)$$

(Yu actually gave $2kn^4$ for the term kn^4 in eq. (2.84), but it was corrected by Koval (ref. 2.33), and the correct form can also be seen from eq. (2.36) by neglecting λ^2 with respect to n^2 .) Equation (2.82) is recognized to take the same form as the characteristic equation of free vibration for a clamped-clamped beam. Successive roots of equation (2.82) are

$$\epsilon = 1.506\pi, 2.500\pi, 3.500\pi, 4.500\pi, \dots \quad (2.85)$$

Substituting these roots into equation (2.84) permits solution for the corresponding Ω . The mode shapes are given by

$$\left. \begin{aligned} w &= 2C \left[\sinh \epsilon - \sin \epsilon - \frac{1}{\cosh \epsilon - \cos \epsilon} \right] \\ &\quad \left[(\sinh \epsilon - \sin \epsilon)(\cosh \lambda s - \cos \lambda s) \right. \\ &\quad \left. - (\cosh \epsilon - \cos \epsilon)(\sinh \lambda s - \sin \lambda s) \right] \\ &\quad \cos n\theta \cos \omega t \\ u &= \frac{2\nu\Omega^2 + (1-\nu)n^2}{2\Omega^4 - (3-\nu)n^2\Omega^2 + (1-\nu)n^4} \frac{\partial w}{\partial s} \\ v &= \frac{2n\Omega^2 - (1-\nu)n^3}{2\Omega^4 - (3-\nu)n^2\Omega^2 + (1-\nu)n^4} \left(\frac{1}{n} \right) \frac{\partial w}{\partial \theta} \end{aligned} \right\} \quad (2.86)$$

Koval and Cranch (refs. 2.33 and 2.34) used equation (2.84) to obtain frequencies of clamped, steel shells and compared results with experiment. Calculations were further simplified by neglecting the terms containing Ω^6 and Ω^4 in equation (2.84) (see the relevant discussion in sec. 2.3.5). The resulting frequency formula is

$$\Omega^2 = \frac{kn^8 + (1-\nu^2)\lambda^4}{n^2(n^2+1) + \frac{3-\nu}{1-\nu}kn^6} \quad (2.87)$$

Numerical results are shown in table 2.22 for steel shells 6 in. in diameter, 12 in. long, and 0.010 in. thick. Theoretical results were calculated from equation (2.87). In table 2.22 the

parameter $|\lambda/n|^2$ is also given, which was assumed to be much less than unity in the theory used. The percent difference between the theoretical and experimental frequencies increases as $|\lambda/n|^2$ increases.

Nodal patterns were determined experimentally by sprinkling a mixture of tiny polyvinylchloride (PVC) pellets and magnesium stearate (in a fine powder form) in a ratio of 10 parts PVC to one part magnesium stearate. The stearate coated the PVC pellets so that they tended to stick to a curved surface and gather at the nodes. In this way it was possible to count the number of axial and circumferential waves over the top 180 degrees of the cylinder. One of the nodal patterns obtained with this technique is shown in figure 2.47. Nodal lines over the bottom half of the cylinder were detected either by use of a medical stethoscope or by lightly running a finger over the shell surface.

In reference 2.33 a comparison was also made between the Donnell equations and the Morley (ref. 2.14) modification of the Donnell equations. When tangential inertia is neglected and Yu's assumption (see sec. 2.3.5) is made the Donnell frequency formula becomes

$$\Omega^2 = kn^4 + (1-\nu)^2 \left(\frac{\lambda}{n} \right)^4 \quad (2.88)$$

whereas Morley's modification gives

$$\Omega^2 = k(n^2-1)^2 + (1-\nu^2) \left(\frac{\lambda}{n} \right)^4 \quad (2.89)$$

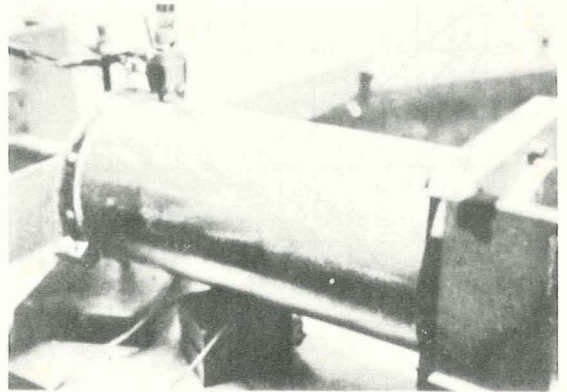


FIGURE 2.47.—Experimentally observed nodal pattern for a clamped-clamped circular cylindrical shell; $m=5$, $n=11$. (After refs. 2.33 and 2.34)

TABLE 2.22.—*Experimental and Theoretical Frequencies (cps) for a Steel Shell; $l/R=4$, $R/h=300$, $h=0.010$ in.*

Number of axial half-waves, m	Source	Number of circumferential waves, n											
		3	4	5	6	7	8	9	10	11	12	13	14
1	Experiment	1025	700	522 ^a	525	592 ^a	720	885	1095	1310	1560	1850	2140
	Equation (2.87)	1587	926	646	563	606	727	891	1088	1311	1554	1827	2118
	Equation (2.88)	1671	951	655	564	603	721	855	1082	1305	1552	1821	2113
	Equation (2.89)	1673	955	659	573	614	733	899	1097	1316	1563	1833	2124
	Equation (2.90)	1431	872	629	565	617	739	905	1101	1323	1569	1837	2127
	Equation (2.98)	1176	783	597	552	611	736	902	1100	1321	1568	1837	2128
	$ \lambda/n ^2$	0.155	0.087	0.056	0.039	0.028	0.022	0.017	0.013	0.012	0.010	0.008	0.007
2	Experiment	—	1620	1210	980	856 ^a	900	995	1140 ^a	1365	1578 ^a	1865	2160
	Equation (2.87)	4365	2515	1645	1197	987	940	1009	1153	1349	1577	1841	2128
	Equation (2.88)	—	2592	1676	1211	992	940	1006	1149	1343	1575	1835	2113
	Equation (2.89)	—	2593	1678	1214	998	948	1015	1160	1356	1586	1847	2134
	Equation (2.90)	—	2084	1460	1118	964	949	1034	1186	1384	1616	1877	2162
	Equation (2.98)	—	—	—	—	—	—	—	—	—	—	—	—
	$ \lambda/n ^2$	0.428	0.241	0.154	0.107	0.079	0.060	0.048	0.039	0.032	0.027	0.023	0.020
3	Experiment	—	—	—	1650	1395	1350	1278 ^a	1325	1465	1690 ^a	1915 ^a	2210
	Equation (2.87)	8551	4921	3193	2256	1721	1434	1323	1346	1466	1650	1886	2156
	Equation (2.88)	—	5072	3253	2284	1735	1439	1324	1344	1462	1647	1881	2151
	Equation (2.89)	—	5073	3255	2287	1739	1445	1331	1353	1472	1658	1892	2163
	Equation (2.90)	—	3434	2503	1911	1551	1366	1319	1380	1520	1717	1955	2228
	Equation (2.98)	4350	3139	2342	1823	1503	1338	1302	1369	1512	1710	1950	2224
	$ \lambda/n ^2$	0.840	0.472	0.302	0.210	0.154	0.118	0.093	0.076	0.062	0.052	0.045	0.039
4	Experiment	—	—	—	—	1960	1765	—	1690	1730	1830	2020	2260
	Equation (2.87)	14135	8133	5267	3695	2759	2190	1862	1715	1709	1806	1989	2224
	Equation (2.88)	—	—	5370	3744	2786	2203	1868	1715	1707	1807	1985	2219
	Equation (2.89)	—	—	5370	3745	2787	2207	1874	1724	1716	1816	1995	2230
	Equation (2.90)	—	—	—	2800	2268	1928	1746	1695	1751	1888	2088	2335
	Equation (2.98)	—	—	—	—	—	—	—	—	—	—	—	—
	$ \lambda/n ^2$	1.388	0.781	0.500	0.347	0.255	0.195	0.154	0.125	0.103	0.087	0.074	0.064
5	Experiment	—	—	—	—	—	—	2300	2100	2080	2190	2200	2330
	Equation (2.87)	21116	12147	7860	5502	4080	3181	2606	2265	2102	2077	2174	2349
	Equation (2.88)	—	—	—	—	—	—	—	—	—	—	—	—
	Equation (2.89)	—	—	—	—	—	—	—	—	—	—	—	—
	Equation (2.90)	—	—	—	—	—	—	—	—	—	—	—	—
	Equation (2.98)	—	—	—	—	—	—	—	—	—	—	—	—
	$ \lambda/n ^2$	2.073	1.166	0.746	0.518	0.381	0.292	0.230	0.187	0.154	0.124	0.110	0.095

^a Experimental data obtained from the average of two values.

with values of λ determined by equations (2.83) and (2.85). The differences between results predicted by these theories can be seen in table 2.22. It is seen that the frequencies differ little from each other. However, when compared with the results from equation (2.87) in table 2.22, one observes that neglecting tangential inertia for the clamped-clamped shell (as was seen for the SD-SD case in sec. 2.3.4) can cause considerable difference, particularly for small n .

Weingarten (refs. 2.64 and 2.197) also used the Donnell equations and neglected tangential inertia to obtain the following frequency formula:

$$\Omega^2 = k(\lambda^2 + n^2)^2 + \frac{(1 - \nu^2)\lambda^4}{(\lambda^2 + n^2)^2} \quad (2.90)$$

It is clear that if Yu's assumption ($\lambda^2 \ll n^2$) is made, then equation (2.88) results. He used this formula to compare frequencies with the experimental results of Koval and Cranch. These numerical results are also included in table 2.22.

Consider now approximate solutions of the clamped-clamped circular cylindrical shell problem by use of the Rayleigh-Ritz technique or equivalent methods. Displacement functions of the following form may be assumed:

$$\left. \begin{aligned} u &= \sum_m A_m X_m'(x) \cos n\theta \cos \omega t \\ v &= \sum_m B_m X_m(x) \sin n\theta \cos \omega t \\ w &= \sum_m C_m X_m(x) \cos n\theta \cos \omega t \end{aligned} \right\} \quad (2.91)$$

where A_m , B_m , C_m are amplitude coefficients, primes are used to indicate differentiation, and $X_m(x)$ is a clamped-clamped "beam function"; i.e., it represents the m th mode shape of free vibration of a clamped-clamped beam according to the classical Euler-Bernoulli theory. Obviously, equations (2.91) will satisfy the boundary condition equations (2.74) exactly.

Beam functions are widely used also in the solution of plate vibration problems (ref. 2.157). The clamped-clamped beam function is

$$\begin{aligned} X_m(x) &= \cosh \lambda_m s - \cos \lambda_m s \\ &\quad - \alpha_m (\sinh \lambda_m s - \sin \lambda_m s) \end{aligned} \quad (2.92)$$

with $s = x/R$ and $\lambda_m = R\epsilon_m/l$ as before, ϵ_m are the roots of the equation

$$\cosh \epsilon_m \cos \epsilon_m = 1 \quad (2.93)$$

and

$$\alpha_m = \frac{\cosh \epsilon_m - \cos \epsilon_m}{\sinh \epsilon_m - \sin \epsilon_m} \quad (2.94)$$

Accurate values of ϵ_m and α_m are given in table 2.23. A comparison of the clamped-clamped mode shape with that of the SD-SD case can be seen in figure 2.48 for $m = 1$.

Two of the advantages of the beam functions have already been suggested above: (1) the equation of motion and (2) the boundary con-

TABLE 2.23.—Eigenfunction Parameters for a Clamped-Clamped Beam

m	α_m	ϵ_m
1	0.98250222	4.7300408
2	1.00077731	7.8532046
3	.99996645	10.9956078
4	1.00000145	14.1371655
5	.99999994	17.2787596
6	1.00000000	20.4203522
$m > 6$	1.0	$(2m+1)\pi/2$

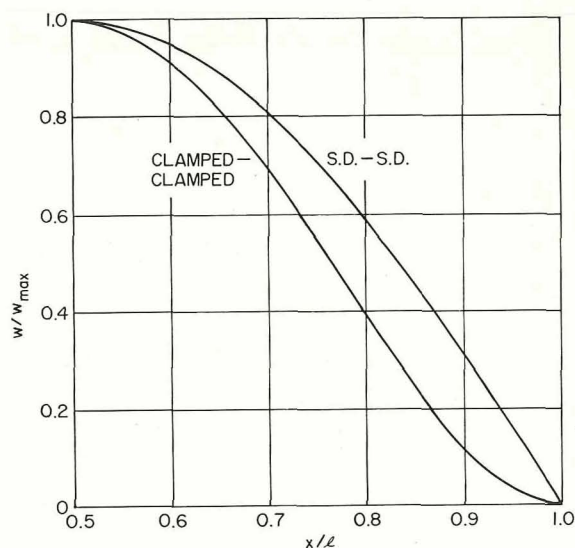


FIGURE 2.48.—Comparison of mode shapes between shells having clamped and shear diaphragm supports at $x = 0, l$. (After ref. 2.78)

ditions of the *beam* are exactly satisfied. Because the behavior of a longitudinal strip of shell between its ends is similar to that of a beam, quite often the beam functions can adequately represent the shell displacements by single terms of equations (2.91), rather than requiring a series of terms. There is one contradiction in using the clamped-clamped beam functions as in equations (2.91) to represent the shell boundary conditions, namely, not only is $\nu=0$, but also $N_{x\theta}=0$. Another advantage of the beam functions is the orthogonality of the integrals of their products and of products of certain of their derivatives over the interval of interest ($0 \leq s \leq 1$). Those integrals which do not vanish due to the orthogonality of the beam functions have been tabulated in a number of places (cf., refs. 2.127, 2.139, 2.158, 2.159, and 2.160).

Arnold and Warburton (ref. 2.4), using their theory (see sec. 2.1.1) and only a single term of each summation in equation (2.91) arrived at the following frequency equation for the clamped-clamped shell:

$$\Omega^6 - K_2 \Omega^4 + K_1 \Omega^2 - K_2 = 0 \quad (2.95)$$

where

$$\begin{aligned} K_2 = & \left[\zeta_1 + \frac{1}{2}(1-\nu)\zeta_2 \right] \lambda^2 + \frac{1}{2}(3-\nu)n^2 + 1 \\ & + k[\lambda^4 + 2\zeta_2 \lambda^2 n^2 + n^4 \\ & + 2(1-\nu)\zeta_2 \lambda^2 + n^2] \\ K_1 = & \frac{1}{2}(1-\nu)(\lambda^4 + n^4) \\ & + (\zeta_1 - \nu\zeta_2)\lambda^2 n^2 + \frac{1}{2}(1-\nu)n^2 \\ & + \left[\frac{1}{2}(1-\nu-2\nu^2)\zeta_2 + \zeta_1 \right] \lambda^2 \\ & + k \left\{ \left[\frac{1}{2}(1-\nu)\zeta_2 + \zeta_1 \right] \lambda^6 \right. \\ & + \left[\frac{1}{2}(7-\nu) + (1-\nu)\zeta_2^2 \right] \lambda^4 n^2 \\ & + \left[\frac{1}{2}(7-3\nu)\zeta_2 + \zeta_1 \right] \lambda^2 n^4 \\ & + \frac{1}{2}(3-\nu)n^6 + 2(1-\nu)\lambda^4 \\ & - [(3-\nu^2)\zeta_2 - \zeta_1]\lambda^2 n^2 \\ & \left. - \frac{1}{2}(3+\nu)n^4 + 2(1-\nu)\zeta_2 \lambda^2 + n^2 \right\} \quad (2.96) \end{aligned}$$

$$\begin{aligned} K_0 = & \frac{1}{2}(1-\nu)(1-\nu^2\zeta_2^2)\lambda^4 \\ & + k \left\{ \frac{1}{2}(1-\nu)(\lambda^8 + n^8) \right. \\ & + [(1-2\nu)\zeta_2 + \zeta_1][\lambda^6 n^2 + \mu^2 n^6] \\ & + [3-\nu-2\nu\zeta_2^2]\lambda^4 n^4 \\ & - (2-\nu)[2-(1+\nu)\nu\zeta_2^2]\lambda^2 n^2 \\ & - [2\zeta_1 + 2(1-2\nu)\zeta_2]\lambda^2 n^4 - (1-\nu)n^6 \\ & + [2(1-\nu)-2\nu^2(1-\nu)\zeta_2^2]\lambda^4 \\ & \left. + [(1-2\nu)\zeta_2 + \zeta_1]\lambda^2 n^2 + \frac{1}{2}(1-\nu)n^4 \right\} \end{aligned}$$

and where

$$\zeta_1 = \frac{1 + (-1)^{m+1}\alpha_m^2}{1 + (-1)^{m+1}\left(\frac{2}{\epsilon_m} \sin \epsilon_m - \alpha_m^2\right)} = \frac{1}{\zeta_2} \quad (2.97)$$

and $\nu, k, n, \Omega, \lambda, \epsilon$, and α are as used consistently elsewhere in this chapter.

The corresponding characteristic equation (2.95) for the Donnell theory using the clamped-clamped beam functions was shown by Kraus (ref. 2.138) to be determined by the coefficients

$$\begin{aligned} K_2 = & \left[\zeta_1 + \frac{1}{2}(1-\nu)\zeta_2 \right] \lambda^2 + \frac{1}{2}(3-\nu)n^2 \\ & + 1 + k(\lambda^4 + 2\zeta_2 \lambda^2 n^2 + n^4) \\ K_1 = & \frac{1}{2}(1-\nu)(\lambda^4 + n^4) + (\zeta_1 - \nu\zeta_2)\lambda^2 n^2 \\ & + \frac{1}{2}(1-\nu)n^2 + \left[\frac{1}{2}(1-\nu-2\nu^2)\zeta_2 + \zeta_1 \right] \lambda^2 \\ & + k \left[\frac{1}{2}(1-\nu)(n^2 + \lambda^2 \zeta_2) + n^2 + \lambda^2 \zeta_1 \right] \\ & [\lambda^4 + n^4 + 2\lambda^2 n^2 \zeta_2] \quad (2.98) \end{aligned}$$

$$\begin{aligned} K_0 = & \frac{1}{2}(1-\nu)(1-\nu\zeta_2^2)\lambda^4 \\ & + k \left\{ \lambda^2 n^2 \left[\frac{1}{2}(1+\nu)\zeta_2 - \zeta_1 - \frac{1}{4}(1-\nu)^2 \zeta_2^2 \right] \right. \\ & \left. - \frac{1}{2}(1-\nu)(\lambda^4 + n^4) \right\} [\lambda^4 + n^4 + 2\lambda^2 n^2 \zeta_2] \end{aligned}$$

with ζ_1, ζ_2 , and λ given in equations (2.97) as before. Equations (2.96) and (2.98) should agree with each other for terms not multiplied by k . However, the first term in K_0 for one has $1-\nu^2\zeta_2^2$, whereas the other has $1-\nu\zeta_2^2$. Un-

TABLE 2.24.—Length Ratios (l/R) of Clamped-Clamped Shells for a Given Ω^2 from Equation (2.75) and Some Comparisons; $\nu=0.3$

n	R/h	Ω^2	Item	m		
				1	3	5
4	500	8×10^{-5}	l/R	20.5	48.1	75.7
			e	.45	.19	.13
			\mathfrak{R}	.953	.974	.982
		1×10^{-4}	l/R	15.4	35.9	56.5
			e	.89	.52	.34
			\mathfrak{R}	.876	.932	.954
		4×10^{-4}	l/R	8.20	19.3	30.4
			e	3.9	1.9	1.2
			\mathfrak{R}	.597	.800	.869
		0.003	l/R	4.49	10.8	17.1
			e	5.9	3.5	2.3
			\mathfrak{R}	.524	.784	.861
		0.03	l/R	2.10	5.35	8.62
			e	8.6	6.5	4.3
			\mathfrak{R}	.654	.866	.916
		0.15	l/R	1.03	2.88	4.73
			e	9.6	6.7	4.5
			\mathfrak{R}	.878	.963	.978
4	100	0.0018	l/R	15.9	38.8	61.6
			e	.06	.02	.01
			\mathfrak{R}	.994	.997	.998
		0.0021	l/R	8.45	20.1	31.7
			e	.58	.31	.20
			\mathfrak{R}	.940	.969	.979
		0.003	l/R	5.87	14.0	22.1
			e	1.8	1.1	.71
			\mathfrak{R}	.835	.916	.944
		0.01	l/R	3.35	8.14	13.0
			e	4.4	3.5	2.4
			\mathfrak{R}	.654	.846	.901
		0.04	l/R	1.98	4.98	8.04
			e	5.1	5.9	4.0
			\mathfrak{R}	.673	.881	.926
		0.17	l/R	1.03	2.78	4.57
			e	5.4	5.7	3.8
			\mathfrak{R}	.843	.959	.975

Notes:

(1) e = Percent error in Rayleigh-Ritz frequency.

(2) \mathfrak{R} = Ratio of frequency of SD-SD shell to clamped-clamped shell.

TABLE 2.24.—Length Ratios (l/R) of Clamped-Clamped Shells for a Given Ω^2 from Equation (2.75) and Some Comparisons; $\nu=0.3$ —Concluded

n	R/h	Ω^2	Item	m		
				1	3	5
4	20	0.0445	l/R	13.2	36.8	60.4
			e	.04	.02	.01
			\mathfrak{R}	.999	1.000	1.000
		0.045	l/R	9.41	25.5	41.6
			e	.08	.04	.03
			\mathfrak{R}	.997	.999	.999
		0.047	l/R	5.98	15.6	25.3
			e	.25	.13	.08
			\mathfrak{R}	.988	.995	.997
		0.06	l/R	3.24	8.25	13.3
			e	1.1	.80	.52
			\mathfrak{R}	.931	.970	.980
16	500	0.021591	l/R	68.4	204	340
			e			
			\mathfrak{R}			
		0.021595	l/R	2.11	62.3	103
			e			
			\mathfrak{R}			
	100	0.02161	l/R	10.5	30.5	50.5
			e			
			\mathfrak{R}			
		0.02166	l/R	5.50	15.4	25.3
			e			
			\mathfrak{R}			
		0.02210	l/R	2.45	6.42	10.4
			e			
			\mathfrak{R}			
	100	0.53977	l/R	48.7	146	243
			e			
			\mathfrak{R}			
		0.53986	l/R	19.8	59.3	98.7
			e			
	100	0.5402	l/R	10.0	29.8	49.5
			e			
			\mathfrak{R}			
	100	0.5415	l/R	5.07	15.0	24.9
			e			
	100	0.5505	l/R	2.10	6.06	10.0
			e			

Notes:

- (1) e = Percent error in Rayleigh-Ritz frequency.
- (2) \mathfrak{R} = Ratio of frequency of SD-SD shell to clamped-clamped shell.

fortunately, the writer has no knowledge of another reference source to adjudicate this disagreement.

Numerical results for frequency parameters using equations (2.95) and (2.98) were also given in reference 2.138 for the shell used by Koval and Cranch (as discussed earlier). These results are presented for comparison in table 2.22. Although all the theoretical results given in table 2.22 are based upon some form of the Donnell-Mushtari shell theory, they differ widely particularly for low values of n .

Warburton (ref. 2.78) compared numerical results obtained by using the approximate method of reference 2.4 outlined above and the exact solution determined by the characteristic equation (2.75). These results are listed in table 2.24 wherein selected values of the square of the frequency parameter Ω are prescribed and the l/R ratios corresponding to given values of m are determined (i.e., the numerical procedure suggested by Flügge (ref. 2.31)) from equation (2.75). The percentage by which the approximate Rayleigh-Ritz frequency exceeds the exact frequency is also listed in each instance. The ratio Ω of the frequency of the SD-SD shell to

that of the clamped-clamped shell is also given. Poisson's ratio is 0.3. Table 2.24 shows that the greatest error for the approximate method occurs for relatively thin (large R/h) and short (small l/R) shells. This implies a considerable difference between the behavior of a thin shell and a beam in the vicinity of the fixed edges. As the number of axial half-waves m increases, the edge effects become less important, the behavior for any support conditions approaches that of a SD-SD shell, and the Arnold-Warburton approximate method becomes better. Correspondingly, as m increases the importance of the hyperbolic functions in equation (2.92) decreases, and the behavior is governed by the sinusoidal terms which correspond to SD-SD supports. The error also decreases with increasing n ; for $l/mR > 10$ and $n = 16$, $e \leq 0.01$ percent (ref. 2.78).

The approximate solution of Arnold and Warburton (ref. 2.4) using beam functions was also compared with the exact solution from the Flügge theory by Forsberg (ref. 2.35). The results are shown in figures 2.49 and 2.50. Here too the differences are small, being maxima for small m , n , and l/R . Unlike the Donnell equa-

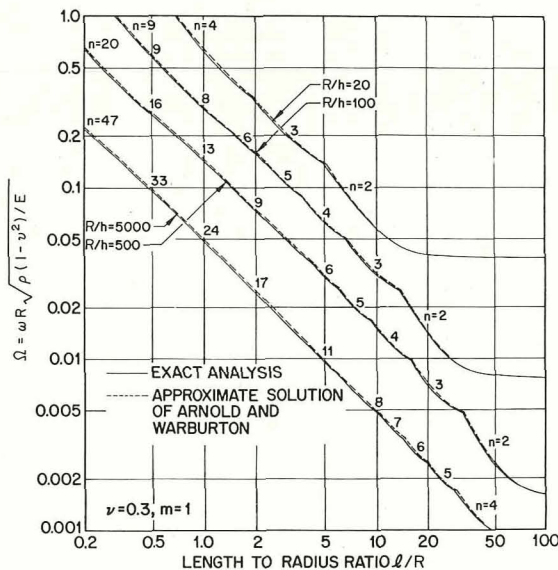


FIGURE 2.49.—Comparison of frequency parameters between the approximate Arnold-Warburton method and the exact method using the Flügge theory. (After ref. 2.35)

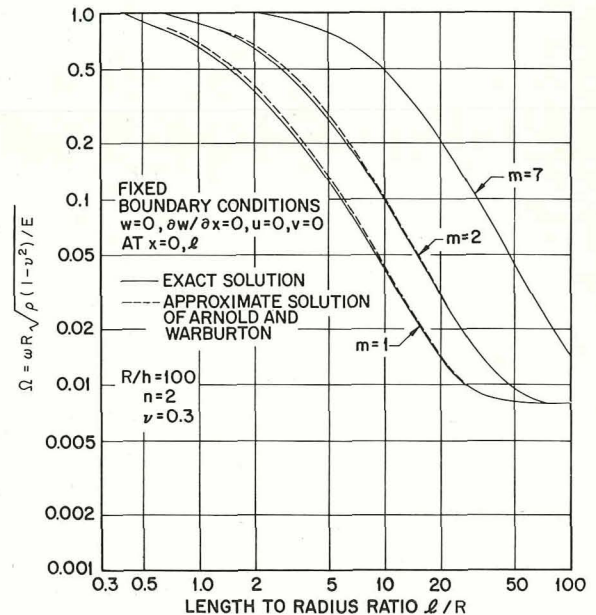


FIGURE 2.50.—Comparison of frequency parameters between the approximate Arnold-Warburton method and the exact method using the Flügge theory; $n = 2$. (After ref. 2.35)

tions, the Arnold and Warburton results represent the asymptotic behavior accurately as $l/mR \rightarrow \infty$, but are in error for small values of l/mR where the membrane behavior is predominant.

Arnold and Warburton (ref. 2.4) proposed the formula

$$\lambda_e = \frac{m\pi R}{l - l_0} \quad (2.99)$$

to give an "equivalent wavelength" for clamped-clamped shells to replace the expression given in equation (2.34) for SD-SD shells. The quantity λ_e would, of course, be greater than the λ for the corresponding SD-SD shell and would give larger frequencies when used with the frequency curves for SD-SD shells. On the basis of comparing theoretical results obtained from the approximate solution using beam functions described earlier in this section and equation (2.99) applied to theoretical SD-SD results, they determined the length l_0 to be

$$l_0 = l \left(\frac{0.3}{m + 0.3} \right) \quad (2.100)$$

where m is the axial half-wave length number (the number of circumferential nodal circles plus one).

Additional results for lowest frequency parameters were given by Gontkevich (refs. 2.126 and 2.127) as shown in figures 2.51 through 2.55. The Rayleigh-Ritz method using beam functions is the basis for the results. For the general for-

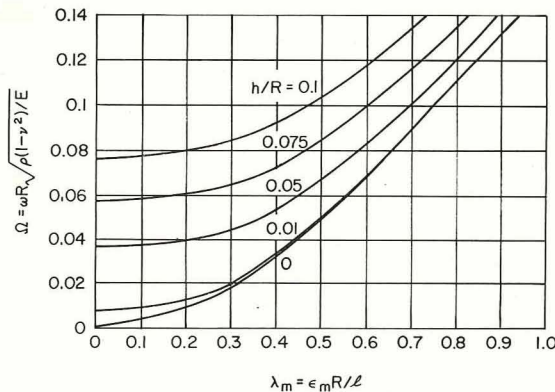


FIGURE 2.51.—Lowest frequency parameters for clamped-clamped shells (see table 2.21 for admissible ϵ_m); $n=2$, $0 < \alpha_m R/l < 1.0$. (After ref. 2.127)

mula yielding these curves, see equations (2.67) and (2.68) in section 2.4. The curves of figures 2.51 through 2.55 have the axial wave length parameter $\lambda_m = \epsilon_m R/l$ as abscissas, where the ϵ_m corresponding to each m are given in table 2.23. Of course, ϵ_m is approximated very closely by $(2m+1)\pi/2$, where m is the axial wave number. Poisson's ratio is not known, but is *probably* 0.3.

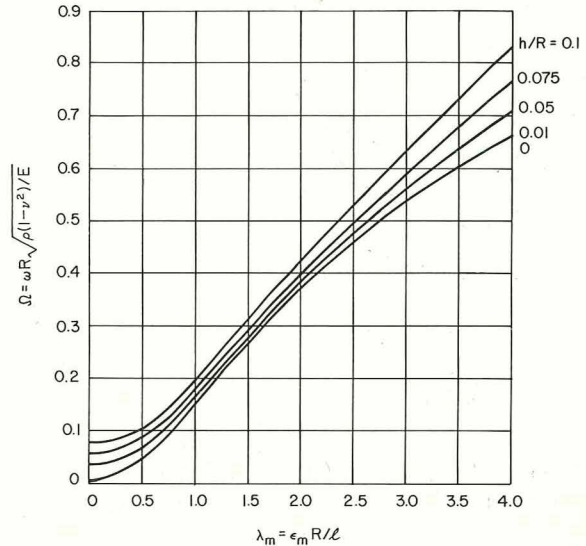


FIGURE 2.52.—Lowest frequency parameters for clamped-clamped shells; $n=2$, $0 < \lambda_m < 4.0$. (After ref. 2.127)

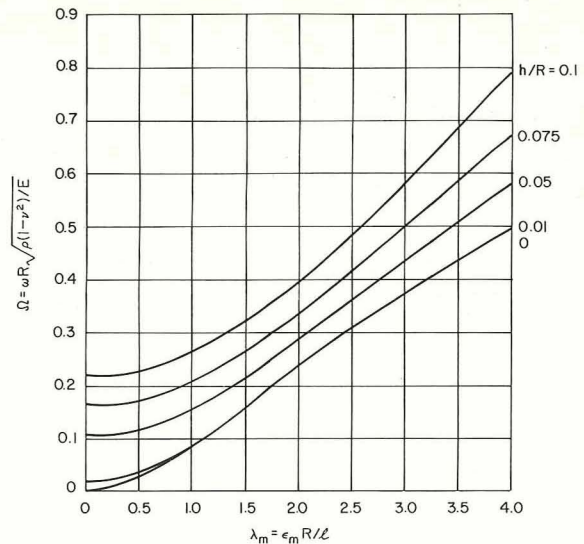


FIGURE 2.53.—Lowest frequency parameters for clamped-clamped shells; $n=3$, $0 < \lambda_m < 4.0$. (After ref. 2.127)

Sewall and Naumann (ref. 2.107) also used the Rayleigh-Ritz technique with beam functions and a strain energy functional equivalent to that of Arnold and Warburton to obtain lowest frequency parameters for clamped-clamped

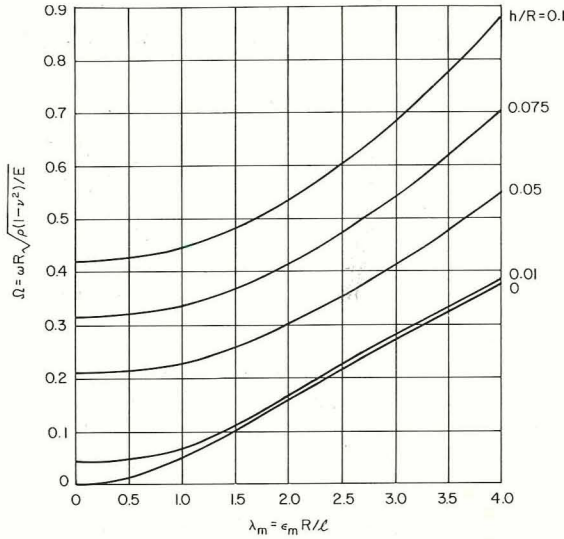


FIGURE 2.54.—Lowest frequency parameters for clamped-clamped shells; $n=4$, $0 < \lambda_m < 4.0$. (After ref. 2.127)

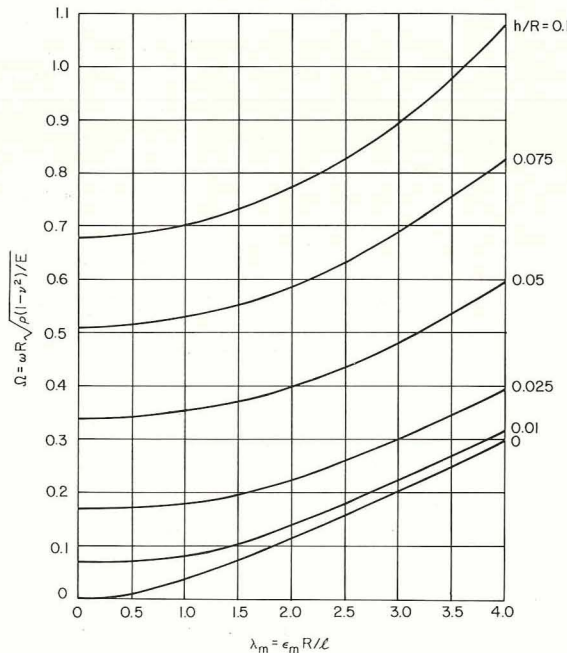


FIGURE 2.55.—Lowest frequency parameters for clamped-clamped shells; $n=5$, $0 < \lambda_m < 4.0$. (After ref. 2.127)

shells and compared them with experimental results. However, they employed eight terms in each of the series of the assumed mode shapes appearing in equations (2.91) to obtain convergence of the Ritz procedure. The results are shown in figure 2.56 for a 6061-T6 aluminum alloy shell having $h=0.0255$ in., $R=9.538$ in., and $l=24.00$ in.

Lyons, Russell, and Herrmann (ref. 2.16) used the Galerkin procedure to obtain closed form approximate frequency formulas for clamped-clamped shells. The shell equations used are those of Herrmann and Armenakas (ref. 2.15) neglecting shear deformation and rotary inertia which are defined for circular cylindrical shells by the the modifying operator (see sec. (2.1.1))

$$[\mathcal{L}_{MOD}] = \begin{bmatrix} 0 & 0 & 0 \\ 0 & 0 & 0 \\ 0 & 0 & 1 + 2\partial^2/\partial\theta^2 \end{bmatrix} \quad (2.101)$$

Approximate mode shapes of the form

$$\left. \begin{aligned} u &= A \sin \frac{2\pi x}{l} \cos n\theta \cos \omega t \\ v &= B \left(\cos \frac{2\pi x}{l} - 1 \right) \sin n\theta \cos \omega t \\ w &= C \left(\cos \frac{2\pi x}{l} - 1 \right) \cos n\theta \cos \omega t \end{aligned} \right\} \quad (2.102)$$

(which ref. 2.157 shows to be less accurate than beam functions in representing *plate* vibration modes) were taken. The resulting frequency formula is

$$\Omega^2 = \frac{(3-\nu^2)(1-\nu)\lambda_2^4}{9(1-\nu)n^4 + 6(3-\nu)\lambda_2^2 n^2 + 3(1-\nu)\lambda_2^4} + \frac{1}{36} \left(\frac{h}{R} \right)^2 [(\lambda_2^2 + n^2)^2 + 2n^4 - 6n^2 + 3] \quad (2.103)$$

where $\lambda_2 = 2\pi R/l$.

Ivanyuta and Finkelshtein (ref. 2.114) used the Galerkin method with the Donnell-Mushtari shell equations and a single set of beam functions to arrive at the following frequency formula:

$$\Omega^2 = \frac{(1-\nu^2)\lambda_m^4}{\lambda_m^4 + n^4 + 1.110n^2\lambda_m^2} + \frac{1}{12} \left(\frac{h}{R} \right)^2 (\lambda_m^4 + n^4 + 1.110n^2\lambda_m^2) \quad (2.104)$$

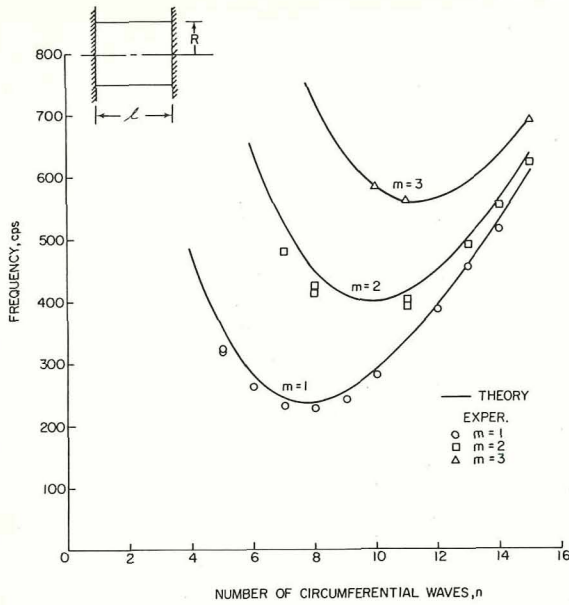


FIGURE 2.56.—Theoretical and experimental frequencies for a clamped-clamped aluminum shell; $R/h=374$, $l/R=2.52$, $h=0.0255$ in. (After ref. 2.107)

where, in this case,

$$\lambda_m = \frac{(2m+1)\pi R}{2l}; \quad m=1, 2, \dots \quad (2.105)$$

Other simplified formulas can be obtained by making simplifications in the characteristic equation of the type described in section 2.3.5.

Kondrashov (ref. 2.148) used the Southwell method (cf., refs. 2.161 and 2.162) to obtain *lower bounds* for the frequency parameter Ω . This method depends upon finding the frequencies from two separate problems, one where the bending stiffness is neglected (giving ω_1), and another where membrane effects are neglected (giving ω_2). The frequency ω for the combined problem is then related to ω_1 and ω_2 by

$$\omega^2 \geq \omega_1^2 + \omega_2^2 \quad (2.106)$$

In reference 2.148 the Donnell-Mushtari theory was used to derive the following formula for computing the lower bounds on Ω^2 :

$$\Omega^2 = (1-\nu^2)C_1 + kn^4C_2^2 \quad (2.107)$$

where $k=h^2/12R^2$, ν is Poisson's ratio, and n =number of circumferential waves, as before,

and the coefficients C_1 and C_2 for clamped-clamped shells are the roots of the equations

$$\frac{(1+\sqrt{C_1})^3 - (1-\sqrt{C_1})^3}{2(1-C_1)\sqrt{1-C_1}} \sin z_1 \xi_0 \sinh z_2 \xi_0 - \cos z_1 \xi_0 \cosh z_2 \xi_0 + 1 = 0 \quad (2.108)$$

$$\cos k_1 \xi_0 \cosh k_2 \xi_0 - \frac{1}{\sqrt{C_2^2 - 1}} \sin k_1 \xi_0 \sinh k_2 \xi_0 = 1 \quad (2.109)$$

with $\xi_0 = nl/R$ and

$$\left. \begin{aligned} z_1 &= \sqrt{\frac{C_1 + \sqrt{C_1}}{1 - C_1}}, & z_2 &= \sqrt{\frac{\sqrt{C_1} - C_1}{1 - C_1}} \\ k_1 &= \sqrt{C_2 - 1}, & k_2 &= \sqrt{C_2 + 1} \end{aligned} \right\} \quad (2.110)$$

Some useful values of C_1 and C_2 are presented in tables 2.25 and 2.26, respectively. In using the tables it is generally necessary to interpolate between values shown for nl/R . The value of Poisson's ratio for which the tables apply is not given in reference 2.148, but appears to be 0.3. The frequency according to the membrane theory is obtained from equation (2.107) by setting $k=0$.

As a check on the accuracy of the lower bound formula given in equation (2.107), Kondrashov (ref. 2.148) also computed upper bounds for the clamped-clamped shell by the Galerkin method and the Donnell-Mushtari theory. The same trigonometric trial functions given by equation (2.102) were used, yielding the following formula for frequency parameters for $m=1$:

$$\Omega^2 = \frac{(1.066)(1-\nu^2)\lambda_2^4}{\lambda_2^4 + 7.60\lambda_2^2 n^2 + 3n^4} + \frac{1}{36} \left(\frac{h}{R} \right)^2 [(\lambda_2^2 + n^2)^2 + 2n^4] \quad (2.111)$$

where $\lambda_2 = 2\pi R/l$, as before. Some sample frequency parameters computed by means of equations (2.107) and (2.111) are given in table 2.27 (from ref. 2.148).

It is interesting to compare equation (2.108) with equation (2.103), which was arrived at from a different shell theory, and with equation (2.104) which was obtained from the same shell theory by using beam functions. In table 2.27 one column lists values of Ω computed using beam functions.

TABLE 2.25.—*Values of the Coefficient C_1 in Equation (2.107) for Frequency Parameters of Clamped-Clamped Shells*

$\frac{l}{R}$	Number of axial half-waves— m				
	1	2	3	4	5
2	0.5431	0.8250	0.9160	0.9511	0.9683
3	.3354	.6670	.8253	.8951	.9310
4	.210	.5168	.7205	.8249	.8821
5	.1372	.3932	.6141	.7465	.8249
6	.9230 $\times 10^{-1}$.2983	.5149	.6656	.7625
7	.6393 $\times 10^{-1}$.2274	.4275	.5866	.6977
8	.4541 $\times 10^{-1}$.1750	.3533	.5125	.6330
9	.3297 $\times 10^{-1}$.1360	.2916	.4452	.5705
10	.2439 $\times 10^{-1}$.1068	.2410	.3852	.5114
12	.1405 $\times 10^{-1}$.6784 $\times 10^{-1}$.1663	.2872	.4065
14	.8563 $\times 10^{-2}$.4464 $\times 10^{-1}$.1168	.2145	.3207
16	.5470 $\times 10^{-2}$.3030 $\times 10^{-1}$.8357 $\times 10^{-1}$.1614	.2527
18	.3636 $\times 10^{-2}$.2115 $\times 10^{-1}$.6091 $\times 10^{-1}$.1226	.1995
20	.2493 $\times 10^{-2}$.1513 $\times 10^{-1}$.4518 $\times 10^{-1}$.9049 $\times 10^{-1}$.1583
22	.1768 $\times 10^{-2}$.1105 $\times 10^{-1}$.3402 $\times 10^{-1}$.7303 $\times 10^{-1}$.1264
24	.1286 $\times 10^{-2}$.8240 $\times 10^{-2}$.2602 $\times 10^{-1}$.5729 $\times 10^{-1}$.1017
26	.9539 $\times 10^{-3}$.6246 $\times 10^{-2}$.2018 $\times 10^{-1}$.4540 $\times 10^{-1}$.8228 $\times 10^{-1}$
28	.7435 $\times 10^{-3}$.4790 $\times 10^{-2}$.1610 $\times 10^{-1}$.3680 $\times 10^{-1}$.6650 $\times 10^{-1}$
30	.5564 $\times 10^{-3}$.3762 $\times 10^{-2}$.1258 $\times 10^{-1}$.2935 $\times 10^{-1}$.5510 $\times 10^{-1}$
32	.4350 $\times 10^{-3}$.2980 $\times 10^{-2}$.1010 $\times 10^{-1}$.2390 $\times 10^{-1}$.4556 $\times 10^{-1}$
36	.2768 $\times 10^{-3}$.1934 $\times 10^{-2}$.6706 $\times 10^{-2}$.1626 $\times 10^{-1}$.3175 $\times 10^{-1}$
40	.1840 $\times 10^{-3}$.1306 $\times 10^{-2}$.4607 $\times 10^{-2}$.1138 $\times 10^{-1}$.2266 $\times 10^{-1}$
42	.1523 $\times 10^{-3}$.1070 $\times 10^{-2}$.3830 $\times 10^{-2}$.9500 $\times 10^{-2}$.1950 $\times 10^{-1}$
44	.1269 $\times 10^{-3}$.9109 $\times 10^{-3}$.3257 $\times 10^{-2}$.8167 $\times 10^{-2}$.1653 $\times 10^{-1}$
48	.9040 $\times 10^{-4}$.6541 $\times 10^{-3}$.2364 $\times 10^{-2}$.5997 $\times 10^{-2}$.1229 $\times 10^{-1}$
50	.770 $\times 10^{-4}$.599 $\times 10^{-3}$.203 $\times 10^{-2}$.518 $\times 10^{-2}$.1067 $\times 10^{-1}$

TABLE 2.27.—*Comparison of Frequency Parameters Obtained from Equations (2.107) and (2.108), and by Using Beam Functions; $R/h=200$*

$\frac{l}{R}$	n	Ω_{LB} from eq. (2.107)	Ω_T from eq. (2.111)	Percent difference between Ω_{LB} and Ω_T	Ω_{BF} using beam functions	Percent difference between Ω_{BF} and Ω_{LB}
4.0	2	0.2132	0.2175	2	0.2395	11
	3	.1192	.1228	3	.1415	16
	4	.0782	.0807	4	.0950	18
	5	.0630	.0652	4	.0748	16
	6	.0660	.0672	2	.0726	10
	7	.0790	.0805	2	.0835	5
	8	.0994	.1002	1	.1016	2
	9	.1245	.1250	1	.1253	1
	10	.1530	.1533	1	.1535	1
1.0	2	.7370	.7590	3	.8710	15
	3	.5790	.5970	3	.6510	11
	4	.4610	.4845	5	.5070	9
	5	.3740	.3950	5	.4110	9
	6	.3120	.3300	6	.3440	9
	7	.2265	.2845	6	.2980	11
	8	.2382	.2540	6	.2685	11
	9	.2250	.2395	6	.2525	11
	10	.2245	.2394	6	.2505	11

TABLE 2.26.—*Values of the Coefficient C_2 in Equation (2.107) for Frequency Parameters of Clamped-Clamped Shells*

$n \frac{l}{R}$	Number of axial half-waves — m				
	1	2	3	4	5
2	6.205	16.180	31.050	50.800	75.550
3	3.145	7.630	14.250	23.050	34.050
4	2.110	4.640	8.390	13.350	19.540
5	1.661	3.275	5.680	8.860	12.830
6	1.431	2.504	4.212	6.470	9.910
7	1.301	2.105	3.332	4.960	6.990
8	1.220	1.826	2.765	4.010	5.562
9	1.176	1.668	2.435	3.410	4.475
10	1.132	1.508	2.105	2.900	3.891
12	1.086	1.340	1.748	2.300	2.995
14	1.061	1.243	1.538	2.005	2.451
16	1.046	1.182	1.406	1.716	2.100
18	1.034	1.142	1.317	1.557	1.861
20	1.028	1.113	1.253	1.447	1.694
22	1.023	1.092	1.207	1.367	1.568
24	1.019	1.078	1.172	1.305	1.475
26	1.016	1.065	1.146	1.258	1.402
28	1.014	1.056	1.125	1.221	1.344
30	1.012	1.048	1.108	1.192	1.298
32	1.010	1.042	1.094	1.166	1.261
36	1.008	1.033	1.078	1.131	1.204
40	1.007	1.027	1.060	1.106	1.165
42	1.006	1.024	1.054	1.096	1.148
44	1.005	1.021	1.048	1.086	1.136
48	1.004	1.018	1.041	1.073	1.113
50	1.003	1.017	1.038	1.068	1.104

TABLE 2.28.—*Experimentally Determined Frequencies for a Clamped-Clamped Steel Shell; $R/h=19.1$, $l/R=8.13$, $h=0.101$ in.*

m	n					
	2	3	4	5	6	7
1	1,240	2,150	3,970	6,320	9,230	12,600
2	2,440	2,560	4,160	6,475	9,380	12,750
3	3,380	4,540	6,720	9,540	12,900
4	4,480	5,130	7,100	9,890	13,220
5	8,020	5,740	5,910	7,710	10,310	13,570
6	9,440	7,010	6,840	8,350	10,820	14,020
7	10,775	8,320	7,900	9,130	11,480	14,600
8	11,950	9,490	8,990	10,000	12,220
9	12,980	10,640	10,140	10,965	13,070
10	13,900	11,270	12,010	13,980
11	12,410

The single term trigonometric functions used to obtain equation (2.108) apparently give closer upper bounds than the beam functions.

Experimental results for a clamped-clamped steel shell having $l=15.65$ in., $R=1.924$ in., and $h=0.101$ in. were given in reference 2.4 and are repeated in table 2.28.

The lowest root of a cubic characteristic equation in Ω^2 for clamped-clamped shells (cf., eqs. (2.84) and (2.95)) is usually much smaller than the two larger roots. This was also seen in the case of SD-SD shells (sec. 2.3). The relative spacing of the roots is clearly seen in table 2.29 (from ref. 2.138) for a particular steel shell (that used by Koval and Cranch and discussed earlier in this section) having $R=3$ in., $h=0.01$ in., $l=12$ in., using the coefficients given by equations (2.98) in equation (2.95). Table 2.29 begins with $n=3$. It is clear from observing the trends in the table, as well as the results for SD-SD shells, that for $n=0, 1, 2$ the three roots can be much closer to each other. As for SD-SD shells, it is also seen that the higher frequencies (at least, beginning with $n=3$) increase monotonically with an increase either in m or n , whereas the lowest frequency find a minimum for some particular value of n . In table 2.29 the minimum occurs at $n=6$ for $m=1$, and $n=9$ for $m=3$. As for SD-SD shells this anomaly can be explained by consideration of the strain energies

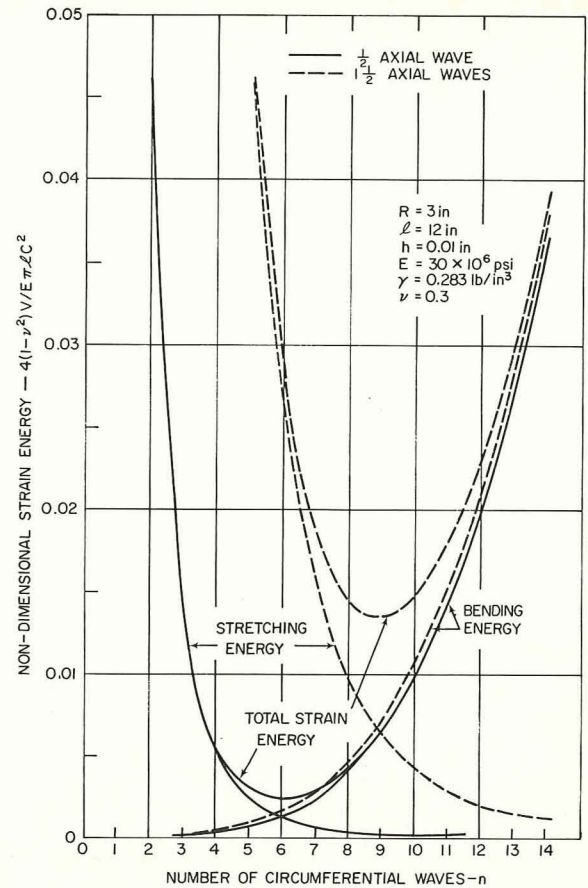


FIGURE 2.57.—Distribution of strain energy for a freely-vibrating clamped-clamped shell. (After ref. 2.138)

TABLE 2.29.—Comparison of the Three Roots (Cyclic Frequencies, in cps) of the Frequency Equation (Eqs. (2.95) and (2.98)) for a Clamped-Clamped Steel Shell; $R/h=300$, $l/R=4$, $h=0.01$ in.

n	1/2 Axial wave ($m=1$)			1-1/2 Axial waves ($m=3$)		
	f_1	f_2	f_3	f_1	f_2	f_3
3	1,176	27,071	36,866	4,350	30,578	46,524
4	783	32,418	47,318	3,139	36,021	54,848
5	597	38,118	58,107	2,342	41,551	64,210
6	552	44,071	69,055	1,823	47,242	74,170
7	611	50,194	80,092	1,503	53,096	84,489
8	736	56,436	91,184	1,338	59,088	95,038
9	902	62,763	102,313	1,302	65,192	105,742
10	1,100	69,151	113,467	1,369	71,386	116,555
11	1,321	75,586	124,639	1,512	77,651	127,449
12	1,568	82,056	135,825	1,710	83,973	138,402
13	1,837	88,554	147,022	1,950	90,340	149,401
14	2,128	95,074	158,228	2,224	96,746	160,437

associated with bending and stretching of the shell (see sec. 2.3.3), as shown in figure 2.57. Figure 2.57 also shows that the stretching energy is greatly affected by the number of axial half-waves m , whereas the bending energy is only slightly changed.

The behavior of the three modes associated with the three roots of the characteristic equation for given m and n can also be seen in table 2.30 (from ref. 2.138). Here amplitude ratios A/C and B/C (in terms of the displacement amplitudes A , B , and C , as used in eqs. (2.91)) are given for the same shell described by table 2.29 and figure 2.57. Ratios are shown for a fixed n ($n=6$, the minimum frequency for $m=1$) and various numbers of axial half-waves m . From table 2.30 it is clear that the motion for the lowest frequency is predominantly radial for $n=6$. For low m , the second frequency is primarily axial, but as m is increased, it becomes circumferential.

Kraus (ref. 2.138) also presented an interesting plot which compares frequencies obtained by four analytical methods and by experiment. This plot is shown as figure 2.58. The same shell used previously in figure 2.57 and tables 2.29 and 2.30 is the basis for the figure. The four curves derived by analytical methods are

TABLE 2.30.—Amplitude Ratios of the Three Modes Associated with Each m and n for a Clamped-Clamped Steel Shell; $R/h=300$, $l/R=4$, $h=0.01$ in.

m	Amplitude ratio	Associated frequency		
		f_1	f_2	f_3
1	A/C	0.003	37.455	1.296
	B/C	.016	3.379	6.072
3	A/C	.004	9.818	3.376
	B/C	.016	3.864	6.694
5	A/C	.004	6.801	6.290
	B/C	.016	4.756	7.740
7	A/C	.003	5.944	10.053
	B/C	.014	5.964	9.000
9	A/C	.002	5.797	14.515
	B/C	.012	7.532	10.292

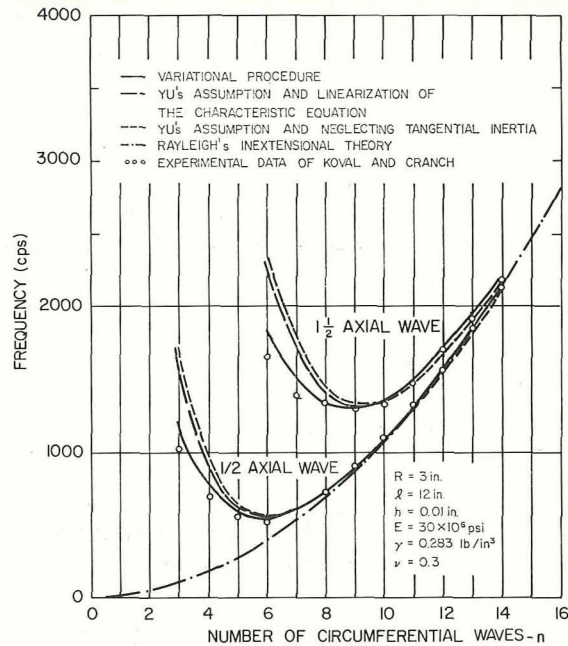


FIGURE 2.58.—Comparison of frequencies obtained from various analytical methods and experiment for a clamped-clamped shell. (After ref. 2.138)

(1) The Rayleigh-Ritz type variational procedure using the Donnell theory and beam functions, which resulted in equations (2.98) for the coefficients of the characteristic equation (2.95).

(2) Yu's assumption ($\lambda^2 \ll n^2$) using the Donnell theory, with linearization of the characteristic equation, which resulted in equation (2.87).

(3) Yu's assumption using the Donnell theory, with neglect of tangential inertia, which resulted in equation (2.88).

(4) The "inextensional" frequency parameter given by (see sec. 2.4.5).

$$\Omega^2 = k \frac{n^2(n^2 - 1)^2}{n^2 + 1} \quad (2.112)$$

The experimental data of Koval and Cranch reported earlier in this section are used in figure 2.58. In figure 2.58 after the minimum point is passed for each m , all of the analytical solutions agree very closely with each other and the experimental data. Before the minimum is reached, the variational procedure (which gives theoretical upper bounds on the frequencies) gives the closest agreement with the experimental data, whereas the other solutions become totally in-

adequate as n is decreased sufficiently. The effect of neglecting λ^2 with respect to n^2 causes large errors for the lesser values of n . The effect of neglecting tangential inertia is small for this problem.

The modal characteristics of clamped-clamped cylindrical shells are shown in figures 2.59, 2.60, and 2.61 (taken from ref. 2.35). In figure 2.59 results for the Flügge and Donnell theories are compared for a thin shell ($R/h=500$) having

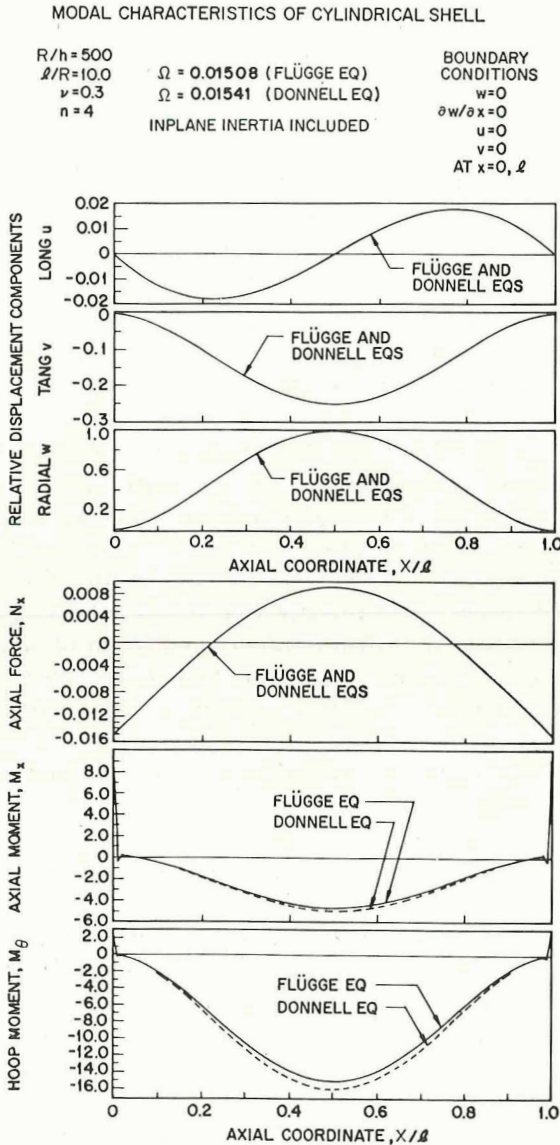


FIGURE 2.59.—Modal characteristics for a clamped-clamped shell; $R/h=500$, $l/R=10$, $m=1$, $n=4$. (After ref. 2.35)

$l/R=10$, $m=1$, and $n=4$. No difference can be seen in the mode shapes, although some differences occur for the bending moments, particularly M_θ . In figures 2.60 and 2.61 a thicker shell

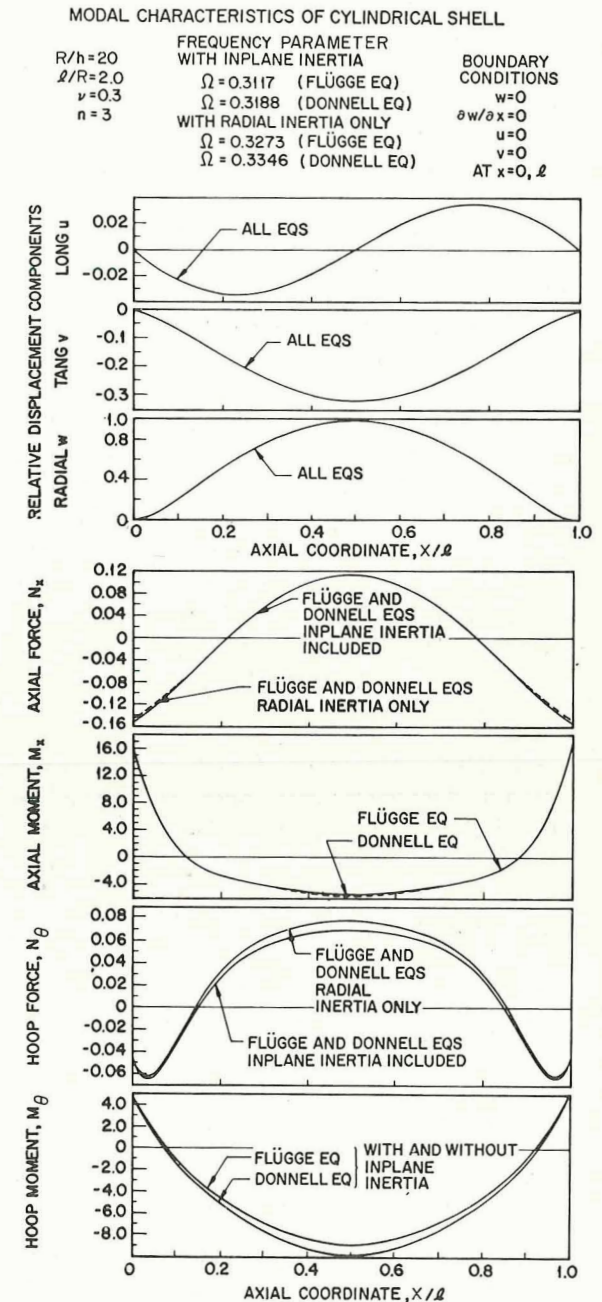


FIGURE 2.60.—Modal characteristics for a clamped-clamped shell; $R/h=20$, $l/R=2$, $m=1$, $n=3$. (After ref. 2.35)

($R/h=20$) is being considered and tangential inertia is both retained and omitted. In figure 2.60 a shell of moderate length is taken ($l/R=20$) and $n=3$. There is essentially no difference in

the mode shapes among the four types of theories (equations) used. Slight differences result among the axial forces N_x and bending moments M_x generated during vibration; however, significant differences arise in the circumferential (hoop) forces and moments. The forces and moments

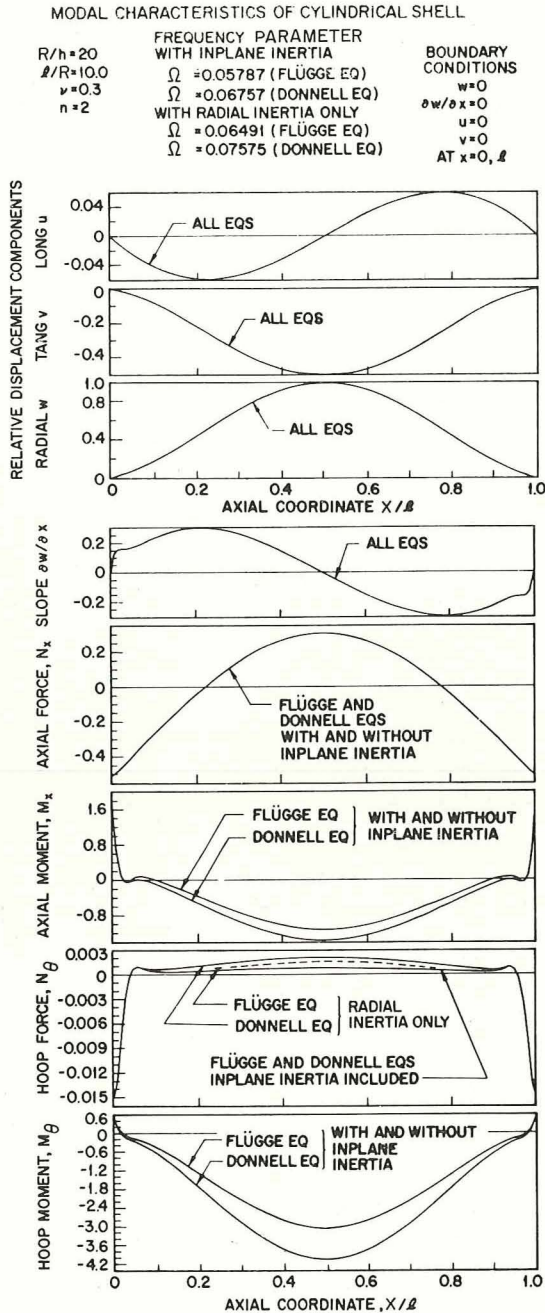


FIGURE 2.61.—Modal characteristics for a clamped-clamped shell; $R/h=20$, $l/R=10$, $m=1$, $n=2$. (After ref. 2.35)

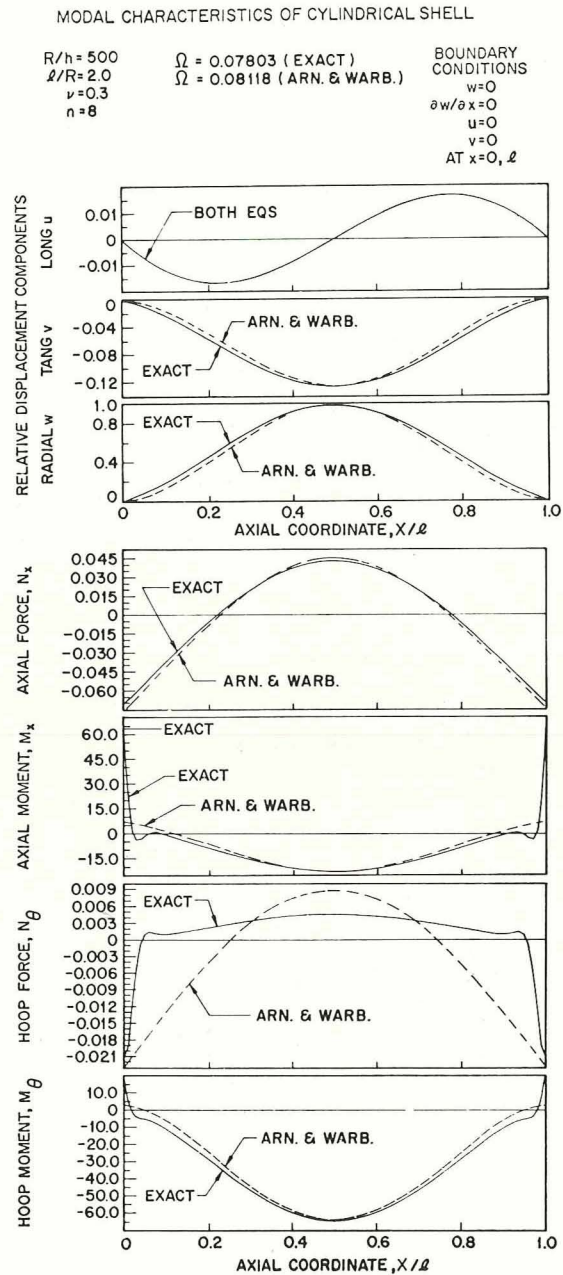


FIGURE 2.62.—Comparison of modal characteristics for a clamped-clamped shell; $R/h=500$, $l/R=2$, $m=1$, $n=8$. (After ref. 2.35)

are normalized with respect to a unit amplitude of deflection. In figure 2.61 (for $n=2$) the differences in forces and moments are even more pronounced. The differences in modal characteristics arising from the Flügge and Donnell

theories, with and without tangential inertia, are elaborated further in table 2.31.

The modal characteristics of the approximate solution of Arnold and Warburton (ref. 2.4) using the equivalent of the Rayleigh-Ritz method

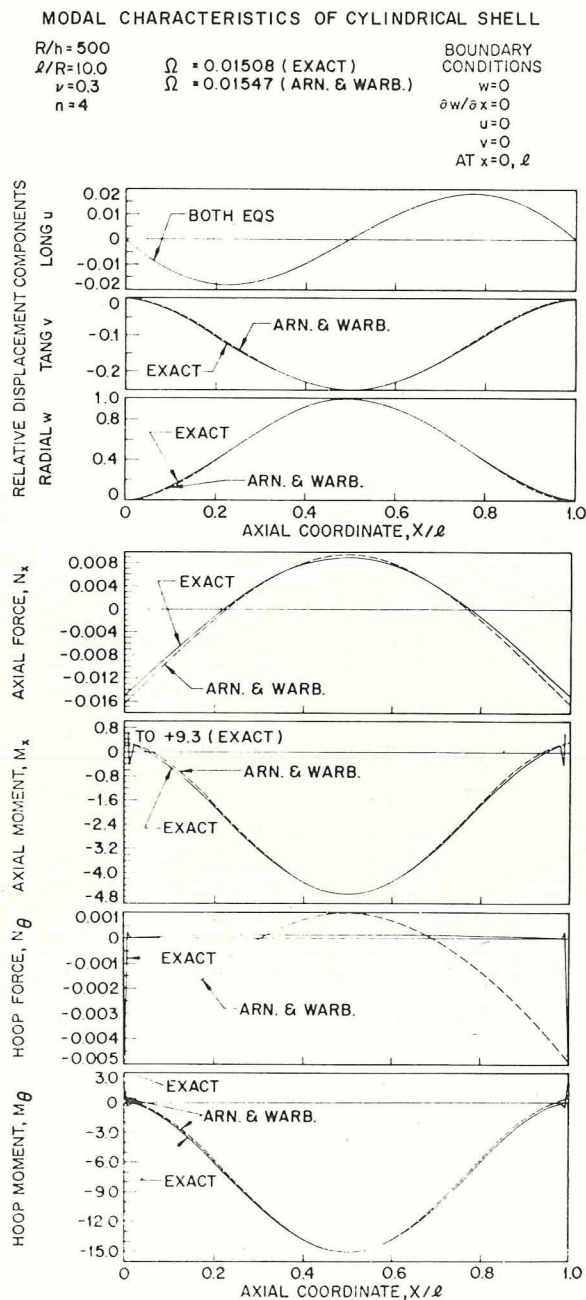


FIGURE 2.63.—Comparison of modal characteristics for a clamped-clamped shell; $R/h=500$, $l/R=10$, $m=1$, $n=4$. (After ref. 2.35)

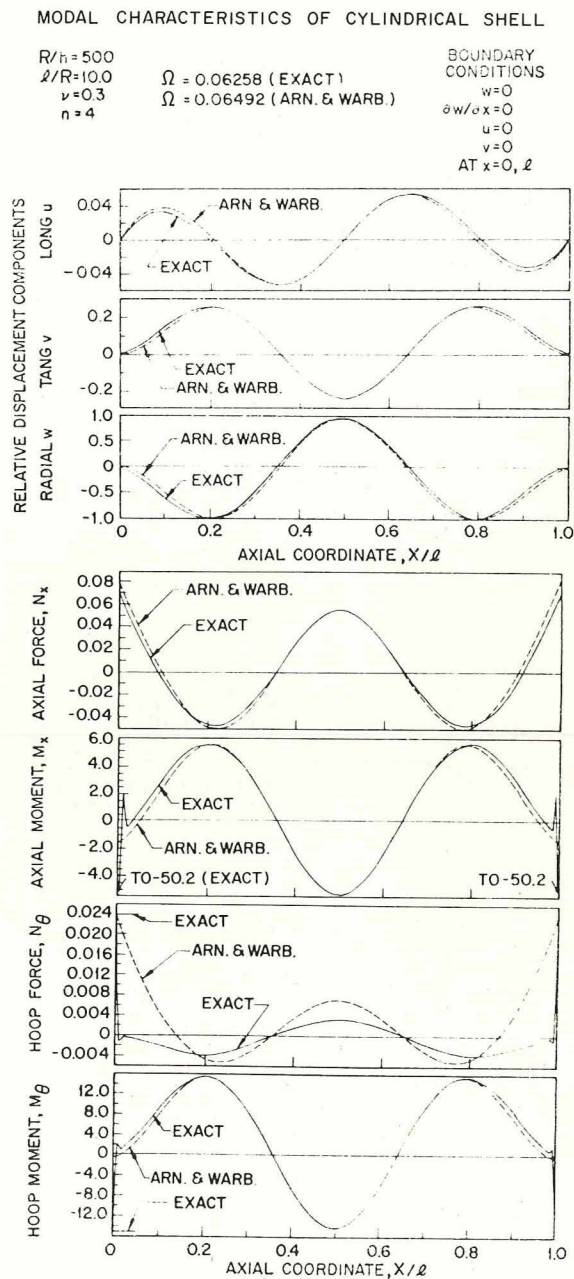


FIGURE 2.64.—Comparison of modal characteristics for a clamped-clamped shell; $R/h=500$, $l/R=10$, $m=3$, $n=4$. (After ref. 2.35)

with beam functions are compared with those of the exact (Flügge) solution in figures 2.62, 2.63, and 2.64. As expected, the Arnold-Warburton solution gives a better estimate for the eigenvalues Ω than for the mode shapes and modal forces. The Arnold-Warburton solution represents reasonably well the forces in the interior of the shell, but the sharp changes at the boundaries are not even approximated. For $R/h=500$, $l/R=2$, $m=1$ (fig. 2.62), the error in Ω is about 4 percent, while the error in the mode shape is 8 percent (comparing the maximum deviation of any point to the maximum amplitude of the function) and is clearly visible. The error lies in the shape of the modes themselves, rather than in the amplitude ratios A/C and B/C . This was observed for all values of R/h and l/R in reference 2.35. In figure 2.62 it is seen that

the circumferential (hoop) stress resultant N_θ is grossly in error. Fortunately, it is relatively small over most of the interval $0 \leq x \leq l$ in comparison with N_x , thereby decreasing its effect. In figure 2.63 the shell is relatively longer ($l/R=10$) and the errors due to the edge effects are greatly reduced (except for the hoop forces, N_θ). In figure 2.64 the same shell is taken as in figure 2.63, but now $m=3$. This has the effect of increasing the errors in the modal characteristics, but most of the error in the mode shapes and generalized forces are confined to the half wave nearest the boundary. The sharp changes in M_x and M_θ are still not predicted, but N_θ is approximated more closely than was done for the lower mode (fig. 2.63). Thus, the Arnold-Warburton approach using a Rayleigh-Ritz type of method gives good results for the frequencies and mode shapes, but

TABLE 2.31.—Comparison of Modal Characteristics for Clamped-Clamped Shells
Obtained by Various Analytical Methods

Case	Item	Exact solutions				Approximate solutions		
		With tangential inertia		No tangential inertia		Finite differences		Arnold-Warburton
		Flügge	Donnell	Flügge	Donnell	20 points	50 points	
1 ^a	Ω	0.01508	0.01541	0.01555	0.01589	0.01689	0.01540	0.01548
	u max	$\pm .01799$	$\pm .01799$	$\pm .01799$	$\pm .01799$	$\pm .01749$	$\pm .01794$	$\pm .01803$
	v max	-.2507	-.2507	-.2507	-.2507	-.2507	-.2507	-.2505
	w max	1	1	1	1	1	1	1
	N_x max	.009127	.009126	.009130	.009129	.008903	.009101	.009424
	N_x min	-.01504	-.01504	-.01504	-.01505	-.01398	-.01510	-.01649
	N_θ max	.000162	.000162	.000162	.000165	.000204	.000156	.001000
	N_θ min	-.004511	-.004512	-.004512	-.004513	-.004193	-.004530	-.004945
	M_x max	9.291	9.278	9.293	9.281	.378	.691	.302
	M_x min	-4.676	-4.966	-4.676	-4.966	-4.674	-4.675	-4.681
	M_θ max	2.783	2.784	2.784	2.784	.109	.203	.0961
	M_θ min	-15.05	-16.05	-15.05	-16.05	-15.05	-15.05	-15.05
2 ^b	Ω	0.3117	0.3188	0.3273	0.3345	0.3105	0.3117	0.3256
	u max	$\pm .03482$	$\pm .03494$	$\pm .03374$	$\pm .03381$	$\pm .03447$	$\pm .03477$	$\pm .03689$
	v max	-.3195	-.3195	-.3159	-.3158	-.3196	-.3195	-.3161
	w max	1	1	1	1	1	1	1
	N_x max	.1131	.1126	.1131	.1127	.1107	.1127	.1190
	N_x min	-.1545	-.1541	-.1506	-.1500	-.1362	-.1460	-.1702
	N_θ max	.06971	.07144	.07956	.08174	.06899	.06963	.08088
	N_θ min	-.06447	-.06513	-.06309	-.06368	-.03991	-.04279	-.05065
	M_x max	16.63	16.58	16.57	16.53	15.14	16.37	7.219
	M_x min	-5.471	-5.652	-5.468	-5.648	-5.438	-5.466	-6.803
	M_θ max	4.943	4.974	4.928	4.958	4.502	4.868	2.121
	M_θ min	-8.888	-9.886	-8.887	-9.885	-8.878	-8.886	-9.286

^a Case 1: $R/h=500$, $l/R=10$, $n=4$, $m=1$, $\nu=0.3$

^b Case 2: $R/h=20$, $l/R=2$, $n=3$, $m=1$, $\nu=0.3$

is unable to predict internal forces and moments, at least with a single beam function as used in equations (2.91) and (2.92). If equations (2.91) were generalized to be a finite series of beam functions, there would still remain the difficulty of representing the sharply changing moment resultants M_x and M_θ near the boundaries. Further comparisons among the modal characteristics obtained by the Arnold-Warburton and exact approaches can be seen in table 2.31.

The clamped-clamped circular cylindrical shell was also used as the basis for a finite difference convergence study in reference 2.35. The Flügge equations of motion, including tangential inertia, assumed the same sinusoidal variation with respect to θ and t as in equations (2.91). The resulting set of ordinary differential equations in the independent variable s ($s=x/l$) were then cast into finite difference form and applied at a set of equally spaced stations (or grid points) in the axial direction. Four steps were taken in the convergence study—10, 20, 50, and 100 equally spaced grid points—yielding eigenvalue determinants of the 30th, 60th, 150th, and 300th orders. Results for frequency parameters and modal characteristics are given in figures 2.65 through 2.67. In figures 2.65 through 2.67 the word "exact" identifies the exact solution of the Flügge equations by the method described at the beginning of this chapter.

In figure 2.65 the shell is relatively thick ($R/h=20$) and long ($l/mR=10$); consequently, the solution is very well behaved. With only ten grid points, Ω is less than 8 percent above the exact value. With twenty points it is within 2 percent. Not only the mode shapes, but the internal force and moment resultants are also determined accurately. Only the rapid changes in M_x and M_θ near the boundaries are difficult to approximate. The peak stresses at the boundary were not adequately determined; even when 100 grid points were used, the boundary moment resultants are less than 90 percent of their exact values.

However, for a shorter shell ($l/mR=2$) the finite difference scheme is much better at representing the edge effects, as can be seen in table 2.31. With a 50-point grid the boundary value of M_x is within 98 percent of the exact value. Here also the frequency for a 20-point grid is

only 0.4 percent below the exact eigenvalue. In this case the shell is short and thick enough so that edge effects propagate throughout the shell instead of being localized.

MODAL CHARACTERISTICS OF CYLINDRICAL SHELL

$R/h=20$	$\Omega = 0.05787$ (EXACT)	BOUNDARY
$l/R=10.0$	$\Omega = 0.06228$ (10 POINTS)	CONDITIONS
$\nu=0.3$	$\Omega = 0.05905$ (20 POINTS)	$w=0$
$n=2$	$\Omega = 0.05805$ (50 POINTS)	$\partial w/\partial x=0$
	$\Omega = 0.05794$ (100 POINTS)	$u=0$
		$v=0$
		AT $x=0, l$

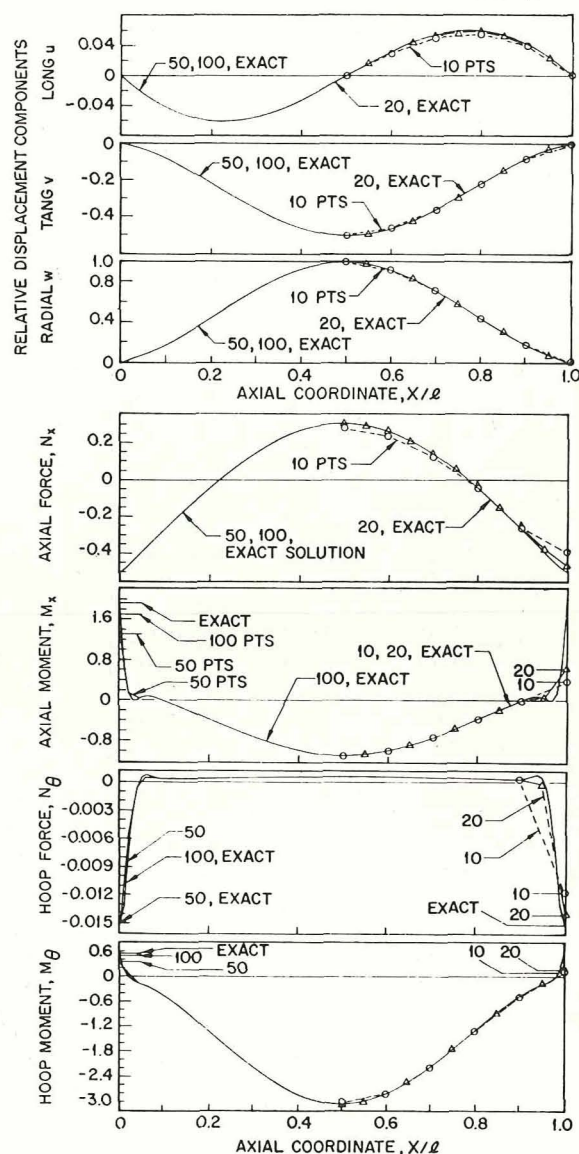


FIGURE 2.65.—Comparison of finite difference solution with exact (Flügge) solution for a clamped-clamped shell; $R/h=20$, $l/R=10$, $n=2$, $m=1$. (After ref. 2.35)

A much thinner shell ($R/h=500$) is the basis for figure 2.66. The length parameter l/mR is kept at 10, although the value of n was changed to $n=4$ to have the mode of minimum frequency (see fig. 2.41). In this case the effect of axial

restraint on N_θ and the effects of clamping on M_x and M_θ are highly localized at the boundary and causes a 40 percent error in the frequency when 10 points are used, and an 11 percent error for 20 points. What is particularly striking here in comparison with figure 2.65 is that the eigen-

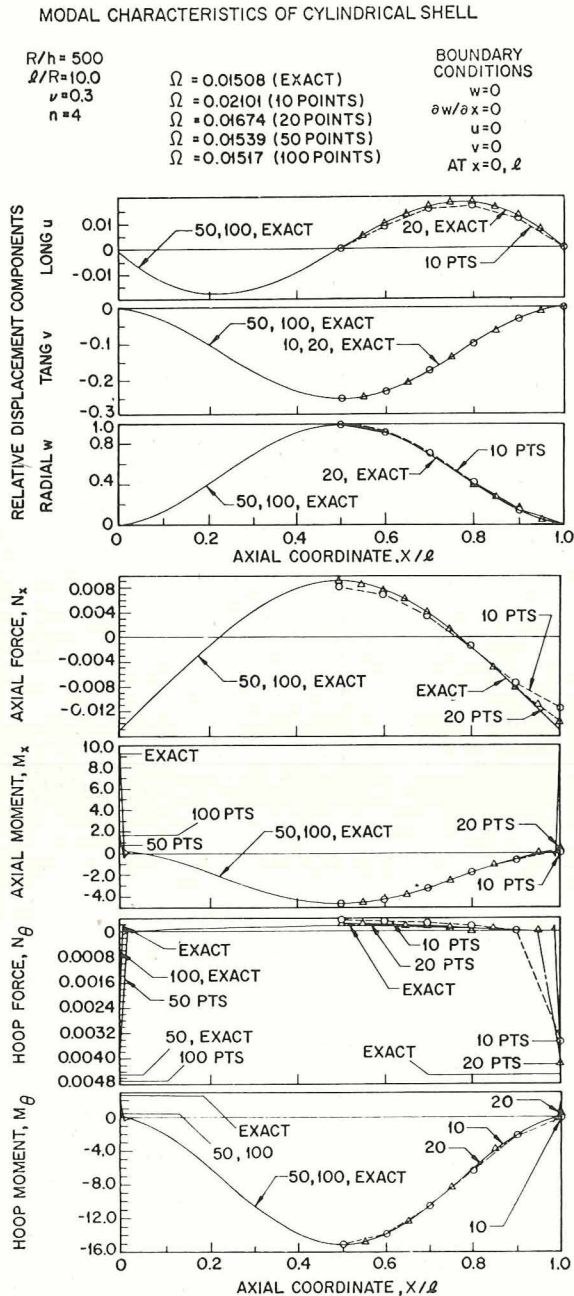


FIGURE 2.66.—Comparison of finite difference solution with exact (Flügge) solution for a clamped-clamped shell; $R/h=500$, $l/R=10$, $n=4$, $m=1$. (After ref. 2.35)

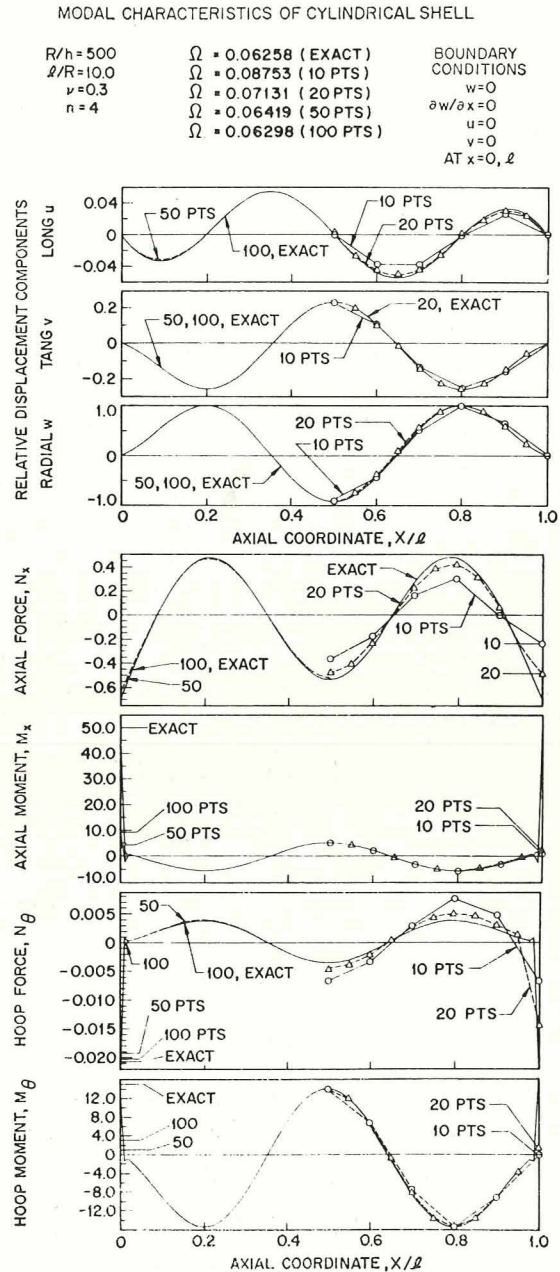


FIGURE 2.67.—Comparison of finite difference solution with exact (Flügge) solution for a clamped-clamped shell; $R/h=500$, $l/R=10$, $n=4$, $m=3$. (After ref. 2.35)

functions appear to be equally well represented in the two cases (the eigenfunctions converged to within 3 percent of the exact value in u and within 0.1 percent in v with 20 points used). One normally expects better agreement between the eigenvalues (frequency parameters) than the eigenfunctions (mode shapes); here the error is caused by large differences in the higher derivatives of the eigenfunctions in the vicinity of the boundaries.

In figure 2.67 a higher axial mode ($m=3$) was taken for comparison with figure 2.66. It is seen that the representation of the mode shapes and force and resultants with the 10 and 20 point solutions is not as good for the higher mode as it was for the lowest one; yet the error in the eigenvalue has not changed significantly. The reasons behind the slow convergence of the eigenvalues in figure 2.67 are discussed in detail in reference 2.35.

Adelman, Catherines, and Walton (ref. 2.132) used the clamped-clamped circular cylindrical shell to determine the accuracy of a finite element computational procedure. The structural elements used to represent the shell were themselves segments of the shell, and each element was assumed to follow the Goldenveizer-Novozhilov shell theory. Within each shell element it was assumed that each displacement function u , v , w could be expressed as a finite polynomial in the axial coordinate, x . That is,

$$\left. \begin{aligned} w &= \sum_{j=0}^{j=N_w} a_j x^j \\ u &= \sum_{i=0}^{i=N_u} b_i x^i \\ v &= \sum_{i=0}^{i=N_v} c_i x^i \end{aligned} \right\} \quad (2.113)$$

Three types of polynomial expansions were considered, the upper limits of the summations being

- (1) $(N_w, N_u, N_v) = (3, 1, 1)$
- (2) $(N_w, N_u, N_v) = (3, 3, 3)$
- (3) $(N_w, N_u, N_v) = (5, 3, 3)$

Three types of element layouts were used as shown in figure 2.68. The first had 10 equally

spaced elements. The second and third took cognizance of the rapidly changing higher derivatives of the displacements in the vicinity of the boundaries and used smaller widths of shell elements there, as shown in figure 2.68(b) and (c). A specific shell having the following geometrical and material parameters was used as an example:

$$\rho = 7.33 \times 10^{-4}$$

Results for the minimum frequencies obtained from the various finite element solutions, compared with the exact solution procedure (see sec. 2.4) using the Goldenveizer-Novozhilov theory, for three circumferential waves ($n=3$) are given in table 2.32. The modal characteristics of the three finite element solutions using ten *equally spaced* elements are compared with the exact solution in figures 2.69 through 2.72.

Koval (ref. 2.137) discussed the effects of asymmetry due to longitudinal seams and deviations from a circular cross section in the experimental results obtained for clamped-clamped shells.

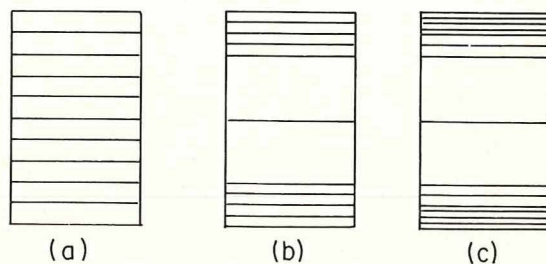


FIGURE 2.68.—Finite element layouts. (After ref. 2.132)

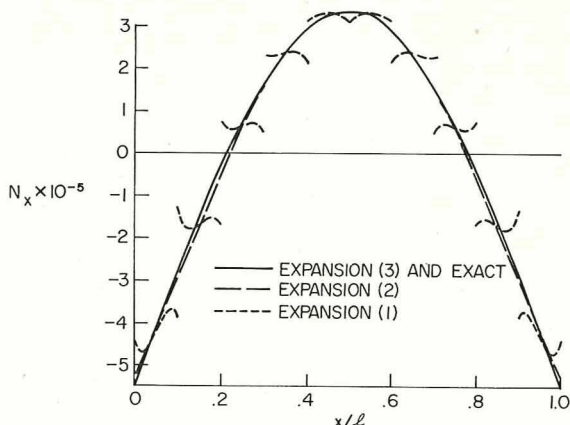


FIGURE 2.69.—Comparison of axial force resultants arising from finite element solutions. (After ref. 2.132)

TABLE 2.32.—Comparison of Finite Element and Exact Lowest Frequencies for a Clamped-Clamped Steel Shell; $R/h=300$, $l/R=4$, $h=0.01$, $m=1$, $n=3$

Type of polynomial expansion, eq. (2.110)	Element layout, fig. 2.68	Approx. ω^2 Exact ω^2
1	(a)	1.083
2	(a)	1.015
3	(a)	1.002
3	(b)	1.0001
3	(c)	1.0001

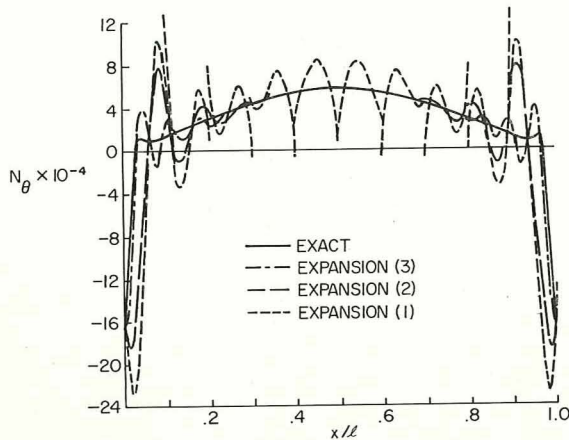


FIGURE 2.70.—Comparison of circumferential force resultants arising from finite element solutions. (After ref. 2.132)

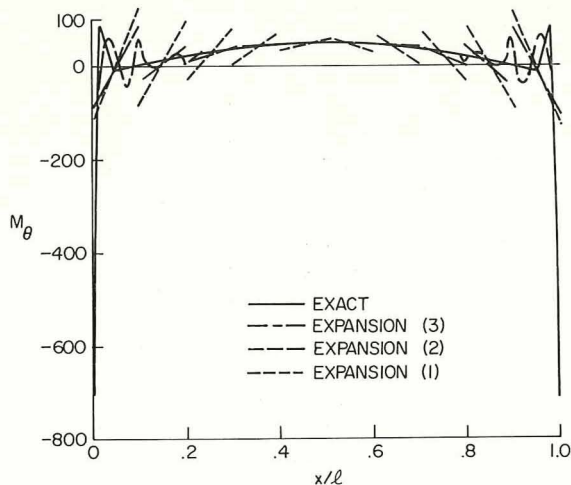


FIGURE 2.71.—Comparison of circumferential moment resultants arising from finite element solutions. (After ref. 2.132)

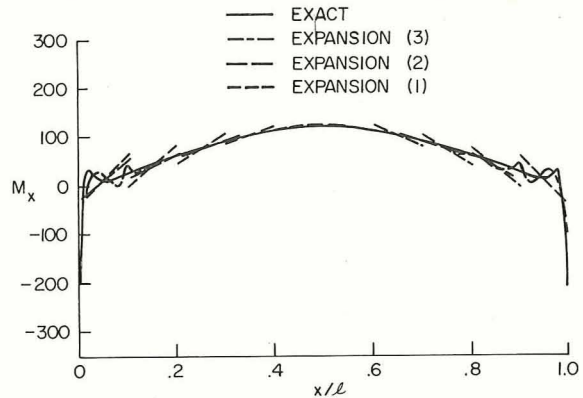


FIGURE 2.72.—Comparison of axial moment resultants arising from finite element solutions. (After ref. 2.132)

Clamped-clamped circular cylindrical shells are also discussed in references 2.59, 2.80, and 2.163.

2.4.2 Clamped-Shear Diaphragm

The boundary conditions for the circular cylindrical shell which is clamped at one end and supported by shear diaphragms at the other are

$$\left. \begin{aligned} u=v=w=\frac{\partial w}{\partial x}=0 & \quad \text{at} \quad x=0 \\ N_x=V=w=M_x=0 & \quad \text{at} \quad x=l \end{aligned} \right\} \quad (2.115)$$

Much information is available for this problem by considering the longitudinally antisymmetric modes of a clamped-clamped shell discussed previously in section 2.4.1. That is, for $m=2, 4, 6, \dots$, the shear diaphragm boundary conditions are duplicated at the center ($x=l/2$) of a clamped-clamped shell. In particular, $m=2$ for the clamped-clamped shell corresponds to the fundamental mode of the clamped-SD shell, while $m=4$ corresponds to a higher mode having one circumferential "node line" located at some intermediate value of x (not $x=l/4$, however). For example, fundamental frequency information can be obtained from the curves for $m=2$ in figures 2.42 and 2.50, as well as table 2.22 simply by considering the l/R ratio of the clamped-SD shell to be one-half of the corresponding clamped-clamped shell.

Kondrashov (ref. 2.148) used the Donnell-Mushtari theory and the Southwell method to

obtain lower bounds for Ω . The frequency parameters can be calculated from equation (2.107), with C_1 and C_2 for clamped-SD shells being the roots of the equations

$$\left[\frac{1+\sqrt{C_1}}{1-\sqrt{C_1}} \right]^{3/2} \sin z_1 \xi_0 \cosh z_2 \xi_0 - \cos z_1 \xi_0 \sinh z_2 \xi_0 = 0 \quad (2.116)$$

$$\left[\frac{C_2-1}{C_2+1} \right]^{1/2} \cos k_1 \xi_0 \sinh k_2 \xi_0 - \sin k_1 \xi_0 \cosh k_2 \xi_0 = 0 \quad (2.117)$$

with $\xi_0 = nl/R$, and z_1, z_2, k_1 , and k_2 are given in equations (2.110). Some useful values of C_1 and C_2 are given in tables 2.33 and 2.34. In using the tables it is generally necessary to interpolate between values shown for nl/R . The frequency parameter according to the membrane theory is

$$\Omega^2 = (1-\nu^2)C_1 \quad (2.118)$$

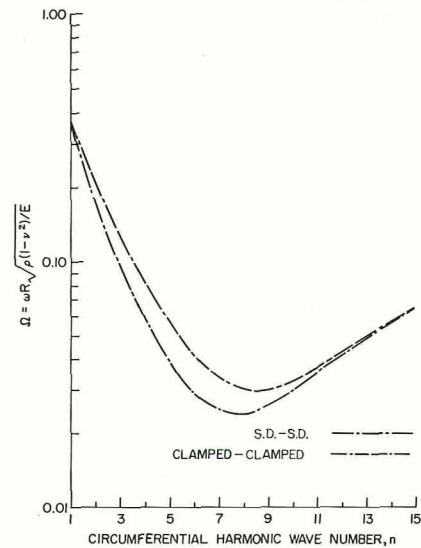


FIGURE 2.73.—Comparison of lowest frequency parameters between clamped-SD and SD-SD shells; $R/h = 1000$, $l/R = 3$, $\nu = 0.3$, $m = 1$. (After ref. 2.84)

TABLE 2.33.—Values of the Coefficient C_1 in Equation (2.107) for Frequency Parameters of Clamped-SD Shells

$\frac{l}{nR}$	Number of circumferential nodal circles — m				
	0	1	2	3	4
2	0.5169	0.8250	0.9156	0.9514	0.9681
3	.2982	.6656	.8248	.8951	.9307
4	.1750	.5124	.7192	.8246	.8819
5	.1068	.3853	.6113	.7459	.8245
6	.6783 $\times 10^{-1}$.2872	.5105	.6647	.7622
7	.4466 $\times 10^{-1}$.2145	.4215	.5847	.6966
8	.3029 $\times 10^{-1}$.1613	.3457	.5094	.6319
9	.2115 $\times 10^{-1}$.1226	.2828	.4412	.5689
10	.1512 $\times 10^{-1}$.9408 $\times 10^{-1}$.2315	.3803	.5088
12	.8238 $\times 10^{-2}$.5729 $\times 10^{-1}$.1563	.2807	.4027
14	.4815 $\times 10^{-2}$.3634 $\times 10^{-1}$.1073	.2070	.3156
16	.2980 $\times 10^{-2}$.2391 $\times 10^{-1}$.751 $\times 10^{-1}$.1537	.2468
18	.1934 $\times 10^{-2}$.1626 $\times 10^{-1}$.5366 $\times 10^{-1}$.1152	.1933
20	.1305 $\times 10^{-2}$.1138 $\times 10^{-1}$.3907 $\times 10^{-1}$.8721 $\times 10^{-1}$.1521
22	.9110 $\times 10^{-3}$.8168 $\times 10^{-2}$.2897 $\times 10^{-1}$.6686 $\times 10^{-1}$.1204
24	.6537 $\times 10^{-3}$.5996 $\times 10^{-2}$.2184 $\times 10^{-1}$.5182 $\times 10^{-1}$.9586 $\times 10^{-1}$
26	.4810 $\times 10^{-3}$.4491 $\times 10^{-2}$.1671 $\times 10^{-1}$.4063 $\times 10^{-1}$.7697 $\times 10^{-1}$
28	.3613 $\times 10^{-3}$.3426 $\times 10^{-2}$.1299 $\times 10^{-1}$.3217 $\times 10^{-1}$.6223 $\times 10^{-1}$
30	.2766 $\times 10^{-3}$.2653 $\times 10^{-2}$.1022 $\times 10^{-1}$.2577 $\times 10^{-1}$.5073 $\times 10^{-1}$
32	.2151 $\times 10^{-3}$.2086 $\times 10^{-2}$.8138 $\times 10^{-2}$.2082 $\times 10^{-1}$.4162 $\times 10^{-1}$
36	.1357 $\times 10^{-3}$.1337 $\times 10^{-2}$.5329 $\times 10^{-2}$.1396 $\times 10^{-1}$.2863 $\times 10^{-1}$
40	.8970 $\times 10^{-4}$.8945 $\times 10^{-2}$.3619 $\times 10^{-2}$.9661 $\times 10^{-2}$.2021 $\times 10^{-1}$
42	.7400 $\times 10^{-4}$.7417 $\times 10^{-3}$.3020 $\times 10^{-2}$.8123 $\times 10^{-2}$.1713 $\times 10^{-1}$
44	.6160 $\times 10^{-4}$.6199 $\times 10^{-3}$.2539 $\times 10^{-2}$.6870 $\times 10^{-2}$.1461 $\times 10^{-1}$
48	.4370 $\times 10^{-4}$.4425 $\times 10^{-3}$.1829 $\times 10^{-2}$.5009 $\times 10^{-2}$.1078 $\times 10^{-1}$
50	.3720 $\times 10^{-4}$.3777 $\times 10^{-3}$.1567 $\times 10^{-2}$.4311 $\times 10^{-2}$.9335 $\times 10^{-2}$

Cooper (ref. 2.84) used the clamped-SD shell as a specific example for demonstrating a computational procedure for general shells of revolution. Linearized equations of reference 2.164 were used in finite difference form. Numerical results are shown in figure 2.73, where the lowest value of the frequency parameter is plotted for each circumferential wave number n for both the clamped-SD and the SD-SD shells. The following parameters complete the specification of figure 2.73: $R/h = 1000$, $l/R = 3$, $\nu = 0.3$, $m = 1$. The clamped-SD shell of figure 2.73 has a minimum frequency which is 26 percent greater than that of the SD-SD shell.

Ivanyuta and Finkelshtein (ref. 2.114) used the Galerkin method with the Donnell-Mushtari shell equations and a single set of beam functions to arrive at the following frequency formula:

$$\Omega = \frac{(1-\nu^2)\lambda_m^4}{\lambda_m^2 + n^2 + 1.748n^2\lambda_m^2} + \frac{1}{12}\left(\frac{h}{R}\right)^2(\lambda_m^4 + n^4 + 1.748m^2\lambda_m^2) \quad (2.119)$$

where

$$\lambda_m = \frac{(4m+1)\pi R}{4l}, \quad m = 1, 2, \dots$$

The modal characteristics of a clamped-SD shell are shown in figures 2.74 and 2.75 for $R/h = 20$, $l/R = 10$, $n = 2$, $m = 1$, $\nu = 0.3$ (from ref. 2.72).

Other sources containing limited information about the free vibrations of clamped-SD circular cylindrical shells include references 2.32, 2.33, 2.34, 2.42, 2.44, 2.73, 2.139, and 2.165.

TABLE 2.34.—Values of the Coefficient C_2 in Equation (2.107) for Frequency Parameters of Clamped-SD Shells

$n \frac{l}{R}$	Number of circumferential nodal circles — m				
	0	1	2	3	4
2	4.640	13.330	26.950	45.450	68.900
3	2.580	6.430	12.480	21.400	31.150
4	1.828	4.002	7.425	12.067	17.950
5	1.510	2.900	5.090	8.060	11.820
6	1.341	2.322	3.822	5.881	8.133
7	1.243	1.850	3.060	4.595	6.500
8	1.182	1.714	2.563	3.731	5.200
9	1.142	1.558	2.228	3.145	4.309
10	1.112	1.444	1.988	2.732	3.675
12	1.077	1.303	1.678	2.192	2.847
14	1.055	1.222	1.495	1.868	2.351
16	1.041	1.167	1.373	1.665	2.028
18	1.032	1.071	1.291	1.519	1.687
20	1.025	1.106	1.237	1.424	1.664
22	1.021	1.086	1.195	1.345	1.538
24	1.017	1.072	1.164	1.289	1.450
26	1.014	1.063	1.139	1.243	1.382
28	1.013	1.052	1.118	1.211	1.328
30	1.010	1.044	1.103	1.181	1.286
32	1.008	1.039	1.092	1.161	1.249
36	1.006	1.030	1.071	1.126	1.197
40	1.004	1.025	1.057	1.101	1.158
42	1.003	1.023	1.051	1.093	1.144
44	1.002	1.019	1.047	1.078	1.120
48	1.000	1.017	1.039	1.070	1.111
50	1.000	1.015	1.036	1.063	1.100

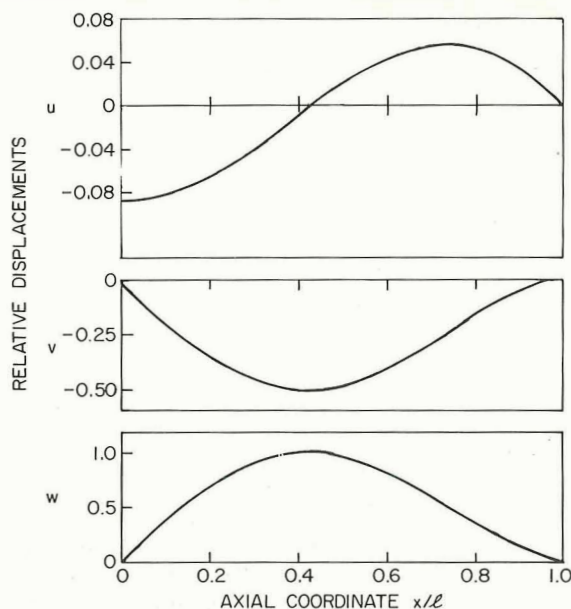


FIGURE 2.74.—Amplitude ratios for a clamped-SD shell; $R/h=20$, $l/R=10$, $n=2$, $\nu=0.3$. (After ref. 2.72)

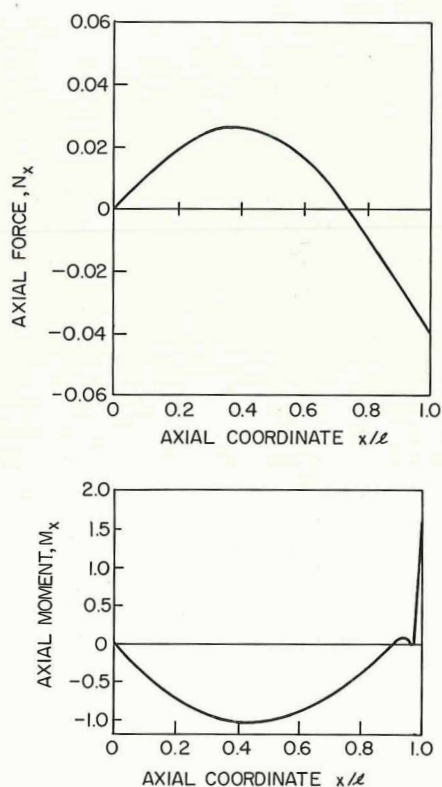


FIGURE 2.75.—Axial force and moment resultants for a clamped-SD shell; $R/h=20$, $l/R=10$, $n=2$, $\nu=0.3$. (After ref. 2.72)

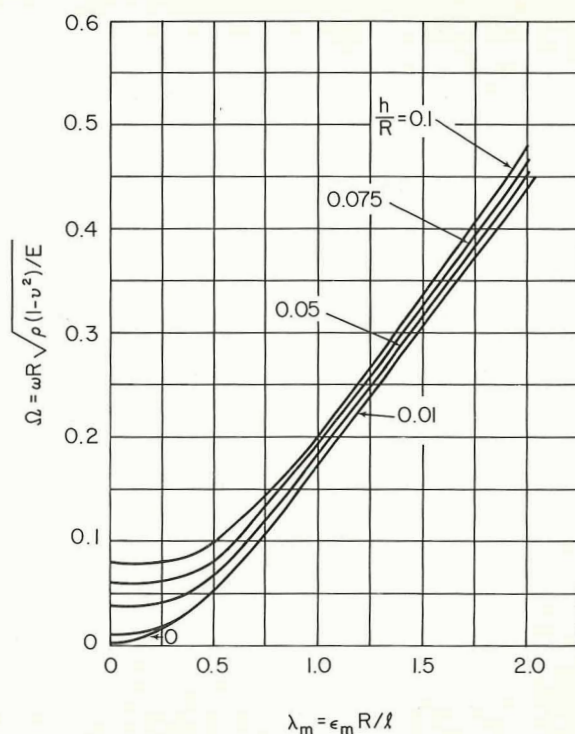


FIGURE 2.76.—Lowest frequency parameters for clamped-free shells (see table 2.21 for admissible ϵ_m); $n=2$. (After ref. 2.127)

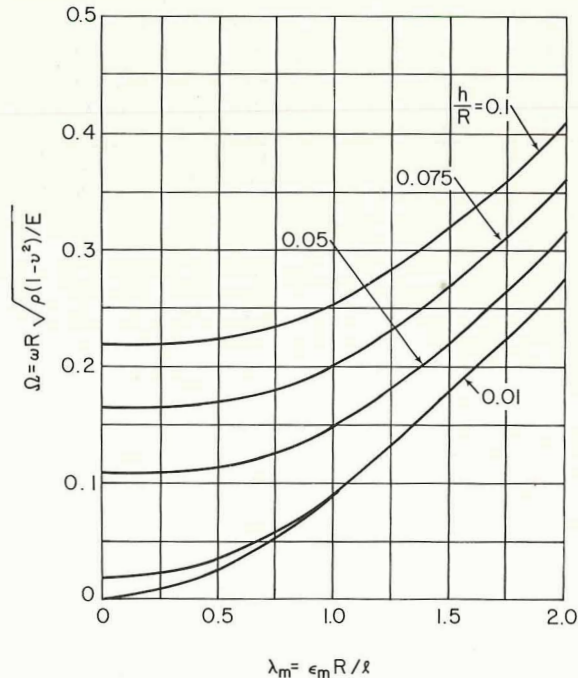


FIGURE 2.77.—Lowest frequency parameters for clamped-free shells (see table 2.21 for admissible ϵ_m); $n=3$. (After ref. 2.127)

2.4.3 Clamped-Free

The boundary conditions for the circular cylindrical shell which is clamped at one end and free at the other are (see sec. 1.8)

$$\left. \begin{aligned} u=v=w=\frac{\partial w}{\partial x}=0 & \quad \text{at} \quad x=0 \\ N_x=N_{x\theta}+\frac{M_{x\theta}}{R}=Q_x+\frac{1}{R}\frac{\partial M_{x\theta}}{\partial \theta}=M_x=0 & \quad \text{at} \quad x=l \end{aligned} \right\} \quad (2.120)$$

Lowest frequency parameters were given by Gontkevich (refs. 2.126 and 2.127) as shown in figures 2.76 through 2.79. The Rayleigh-Ritz method using beam functions and the Donnell-Mushtari shell theory is the basis for the results. For the general formula yielding these curves, see equations (2.67) and (2.68) in section 2.4. Admissible values of ϵ_m for the abscissas of figures 2.76 through 2.79 are available in table

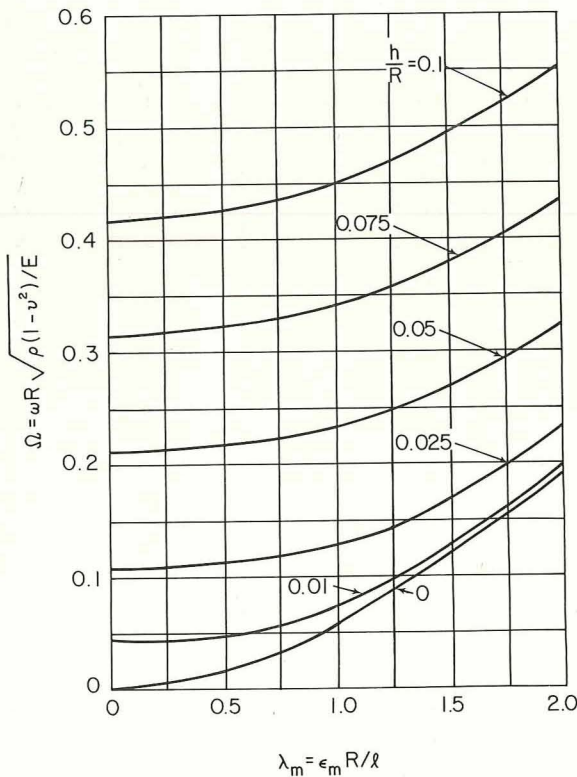


FIGURE 2.78.—Lowest frequency parameters for clamped-free shells (see table 2.21 for admissible ϵ_m); $n=4$. (After ref. 2.127)

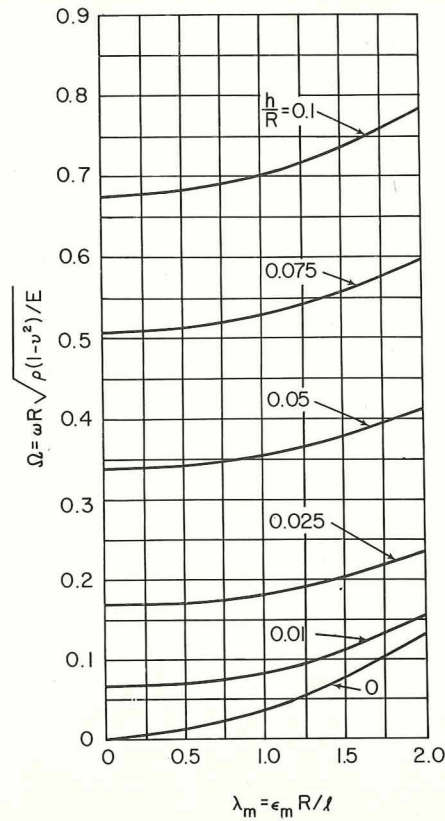


FIGURE 2.79.—Lowest frequency parameters for clamped-free shells (see table 2.21 for admissible ϵ_m); $n=5$. (After ref. 2.127)

2.21. It should be noted that the beam functions satisfy the free edge boundary conditions of the shell in only an approximate manner.

Sewall and Naumann (ref. 2.107) also used the Rayleigh-Ritz technique with beam functions and the Goldenveizer-Novozhilov shell theory to obtain lowest frequency parameters for clamped-free shells and compared them with experimental results. They used seven terms in each of the series of the assumed mode shapes (i.e., clamped-free beam functions) in equations (2.91) to obtain convergence of the Ritz procedure. The results are shown in figure 2.80 for a 6061-T6 aluminum alloy shell having $h=0.0255$ in., $R=9.538$ in., and $l=24.625$ in. Mode shapes of the lowest frequencies for $m=1$ and $m=2$ are depicted in figure 2.81.

Numerical results were also obtained by Resnick and Dugundji (ref. 2.85) using an energy method equivalent to Rayleigh-Ritz, beam func-

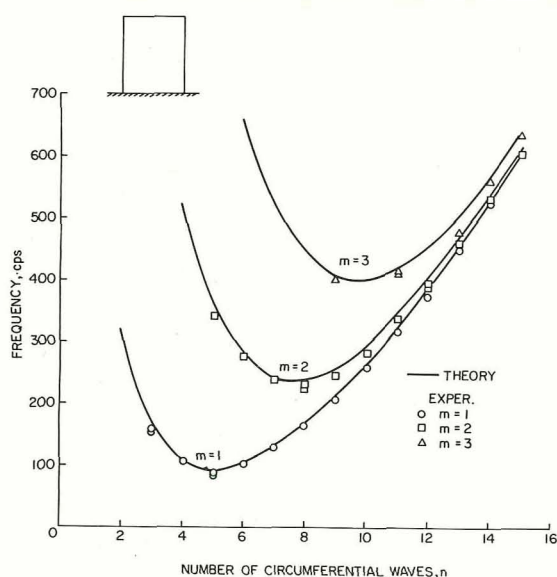


FIGURE 2.80.—Theoretical and experimental frequencies for a clamped-free aluminum shell; $R/h=374$, $l/R=2.58$, $h=0.0255$ in. (After ref. 2.107)

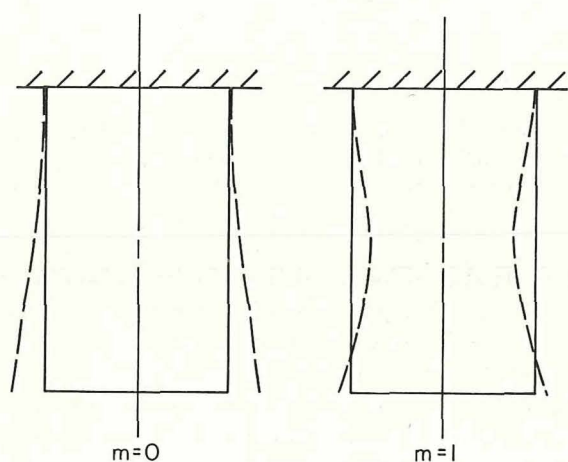


FIGURE 2.81.—Mode shape for a clamped-free shell.

tions, and the Sanders shell theory. These are shown in table 2.35 and figure 2.82 for a 6061 aluminum shell ($E=9.9 \times 10^6$ psi., $\rho=0.254 \times 10^{-3}$ lb-sec²/in⁴, $\nu=0.3$) having $R=2.91$ in., $l=12.02$ in., and $h=0.0070$ in. Good agreement between theory and experiment was found for $n \geq 5$ for $m=1$. Below $n=5$, the experimental results tended towards the SD-free results. Larger disagreement between the theoretical clamped-free values and those of the experiment also is ap-

parent as m is increased. These disagreements were regarded as resulting from insufficient axial constraint at the boundaries during the experiments. In figure 2.83 (from ref. 2.85) the effect of a small change in thickness is seen, particularly for large n . Theoretical frequencies are also compared between the clamped-free and clamped-clamped shells.

Weingarten (refs. 2.64, 2.140, and 2.197) obtained theoretical and experimental frequencies for clamped-free shells. Theoretical results were based upon the Donnell theory and used Yu's assumption ($\lambda^2 \ll n^2$) (see sec. 2.3.5). Numerical

TABLE 2.35.—Theoretical and Experimental Frequencies (cps) for an Aluminum Shell; $l/R=4.13$, $R/h=415$, $h=0.0070$ in.

m	n	Experimental	Theoretical	
			Clamped-free	SD-free
0	2	149	489	21
	3	165	246	60
	4	158	181	115
	5	200	207	186
	6	276	280	272
	7	374	378	375
	8	490	494	493
	9	626	627	626
	10	776	775
	11	941	940
1	2	2512	1913
	3	984	1353	987
	4	675	827	596
	5	505	576	429
	6	436	476	389
	7	454	479	432
	8	531	549	525
	9	642	661	647
	10	783	799	791
	11	959	953
2	2	4968	4544
	3	3081	2694
	4	2013	1712
	5	1223	1401	1175
	6	954	1047	881
	7	803	857	739
	8	745	787	708
	9	773	807	757
	10	873	892	861
	11	1021	1002

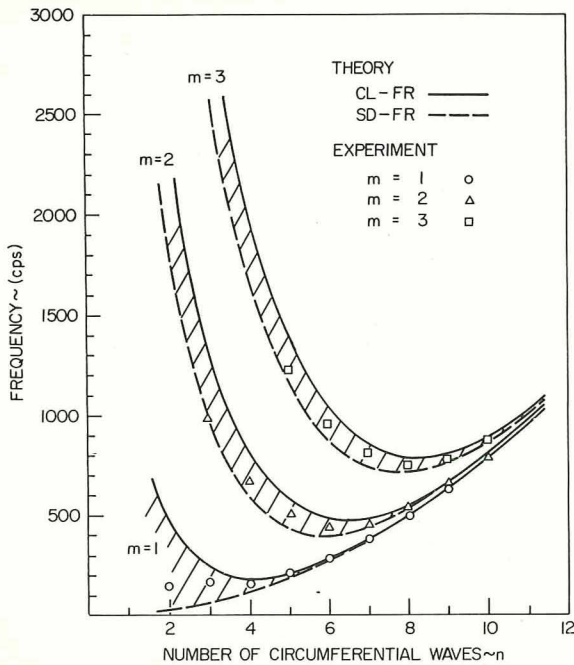


FIGURE 2.82.—Theoretical and experimental frequencies (cps) for an aluminum shell; $R/h=415$, $l/R=4.13$, $h=0.0070$ in. (After ref. 2.85)

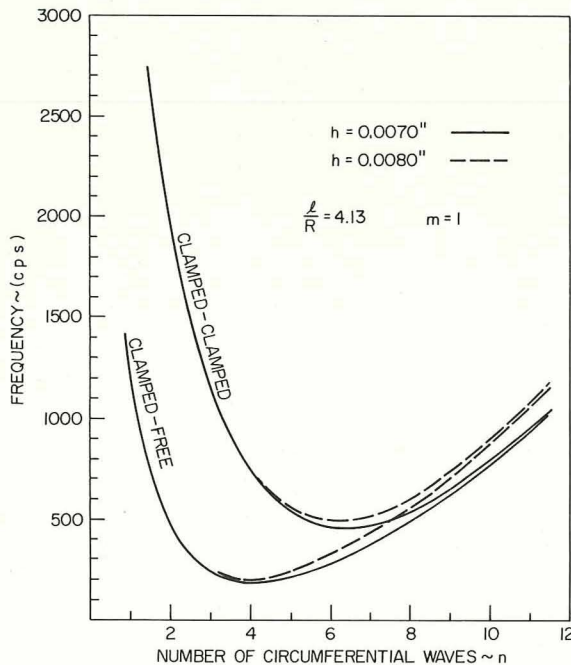


FIGURE 2.83.—Theoretical frequencies for an aluminum shell; $l=12.02$ in. $R=2.91$ in. (After ref. 2.85)

results are available from figures 2.84 and 2.85 for a shell made of 1020 steel and having $R/h=400$, $l/R=2.23$, and $h=0.010$ in. Additional results for a similar shell having $R/h=100$ and $h=0.040$ in. can be seen in figures 2.86 and 2.87. The effects of imperfect clamping in the experimental models are again seen in these figures. Overall structural clamping coefficients were also obtained experimentally for the models in references 2.140 and 2.197.

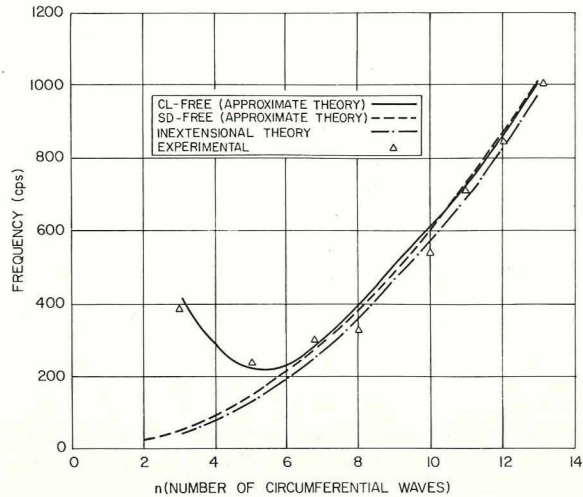


FIGURE 2.84.—Theoretical and experimental frequencies (cps) for a steel shell; $R/h=400$, $l/R=2.23$, $h=0.010$ in., $m=0$. (After ref. 2.64)

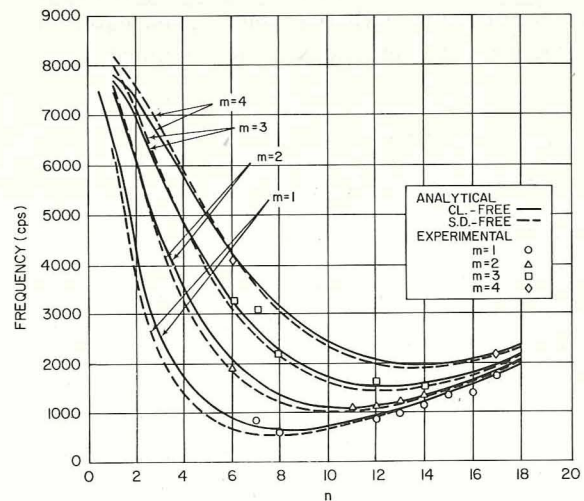


FIGURE 2.85.—Theoretical and experimental frequencies (cps) for a steel shell, $R/h=400$, $l/R=2.23$, $h=0.010$ in., $m>0$. (After ref. 2.64)

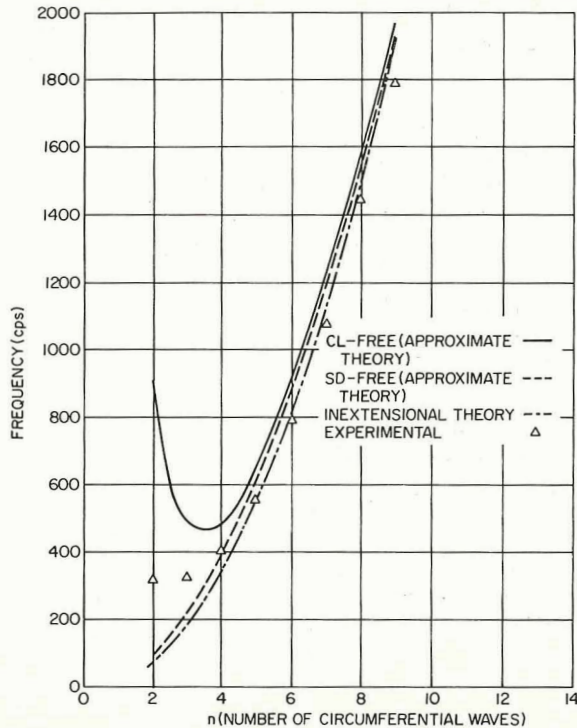


FIGURE 2.86.—Theoretical and experimental frequencies (cps) for a steel shell; $R/h=100$, $l/R=2.23$, $h=0.040$ in., $m=0$. (After ref. 2.64)

Extensive numerical results for clamped-free shells were obtained by Sharma and Johns (refs. 2.166, 2.167, and 2.168) using the Ritz method in conjunction with the Flügge shell equations. Displacement functions were assumed in the form

$$\left. \begin{aligned} u &= [A_1\varphi'(x) + A_2\psi'(x)] \cos n\theta \cos \omega t \\ v &= [B_1\varphi(x) + B_2\psi(x)] \sin n\theta \cos \omega t \\ w &= [C_1\varphi(x) + C_2\psi(x)] \cos n\theta \cos \omega t \end{aligned} \right\} \quad (2.121)$$

where $\varphi(x)$ and $\psi(x)$ are the clamped-free and clamped-SD beam functions, respectively. Taking equations (2.121) as they are written leads to a sixth degree characteristic determinant; setting $A_2=B_2=C_2=0$ reduces the determinant to the third degree. Finally, imposing the conditions zero hoop (circumferential) and shear strain in the median plane leads to the relationships

$$\frac{\partial v}{\partial \theta} + w = 0, \quad \frac{\partial v}{\partial s} + \frac{\partial u}{\partial \theta} = 0 \quad (2.122)$$

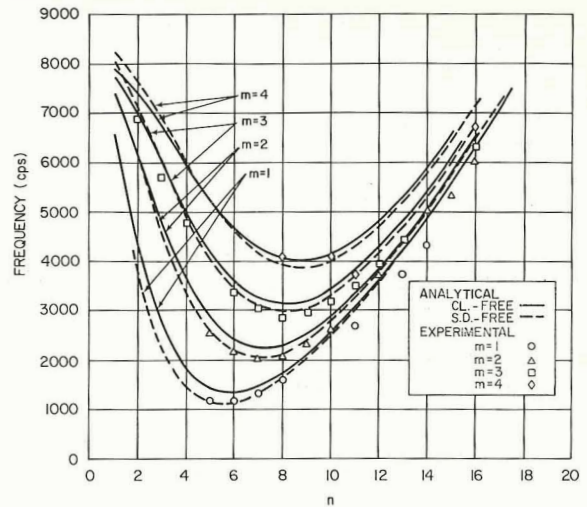


FIGURE 2.87.—Theoretical and experimental frequencies (cps) for a steel shell, $R/h=100$, $l/R=2.23$, $h=0.040$ in., $m>0$. (After ref. 2.64)

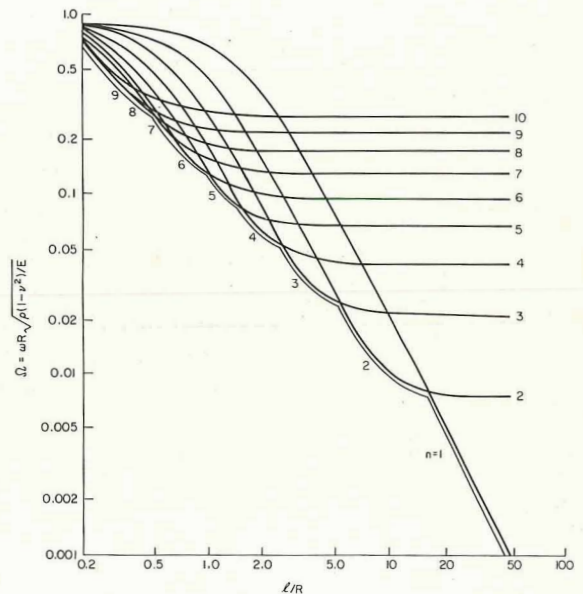


FIGURE 2.88.—Frequency parameters for clamped-free shells; $m=1$, $\nu=0.3$, $R/h=100$. (After ref. 2.166)

respectively, and reduces the sixth degree determinant to one of the second degree. Frequency curves obtained using the third degree determinant are shown in figure 2.88 for $m=1$, $\nu=0.3$, and $R/h=100$. Envelopes for various R/h ratios are depicted in figure 2.89. Numerical results obtained using the sixth degree (sextic),

third degree (cubic), and second degree (quadratic) frequency equations described above are listed in table 2.36 for the swaying ($n=1$) and ovaling ($n=2$) modes of long shells (such as smokestacks). Another study was made in reference 2.169 using the Love-Timoshenko theory which yielded only small differences from the above results.

Kondrashov (ref. 2.148) used the Donnell-Mushtari theory and the Southwell method to obtain lower bounds for Ω . The frequency parameters can be calculated from equation (2.107), with C_1 and C_2 for clamped-free shells being the roots of the equations

$$\sqrt{\frac{C_1}{1-C_1}} \sin z_1 \xi_0 \sinh z_2 \xi_0 - \frac{1+C_1}{1-C_1} \cos z_1 \xi_0 \cosh z_2 \xi_0 = 1 \quad (2.123)$$

$$\left(A - \frac{1}{A}\right) \sin k_1 \xi_0 \sinh k_2 \xi_0 - \left(B + \frac{1}{B}\right) \cos k_1 \xi_0 \cosh k_2 \xi_0 = 2 \quad (2.124)$$

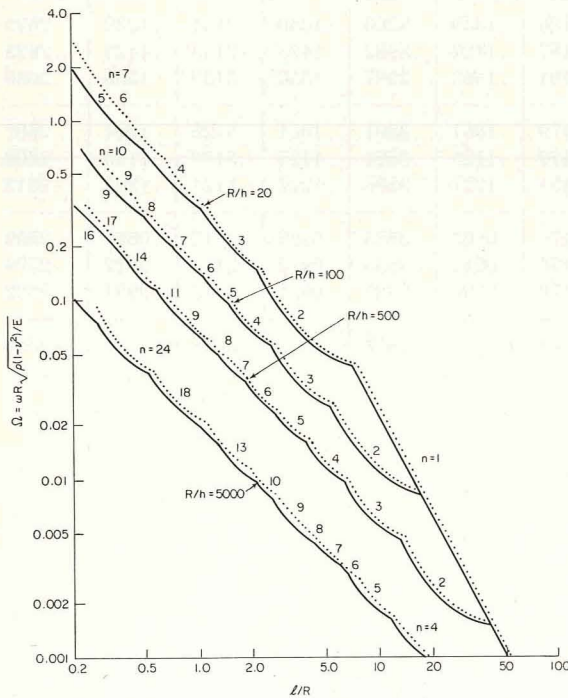


FIGURE 2.89.—Frequency envelopes for clamped-free shells; $m=1$, $\nu=0.3$. (After ref. 2.166)

$$A = \left[\frac{C_2+1}{C_2-1} \right]^{1/2} \left[\frac{C_2-(1-\nu)}{C_2+(1-\nu)} \right] \quad (2.125)$$

$$B = \frac{C_2-(1-\nu)}{C_2+(1-\nu)} \quad (2.126)$$

with $\xi_0 = nl/R$, and z_1 , z_2 , k_1 , and k_2 are given in equations (2.110). Some useful values of C_1 and C_2 are given in tables 2.37 and 2.38. In using the tables it is generally necessary to interpolate between values shown for nl/R . The frequency parameter according to the membrane theory is

$$\Omega^2 = (1-\nu^2)C_1 \quad (2.118)$$

Other sources containing limited information about the free vibrations of clamped-free circular cylindrical shells include references 2.25, 2.44, 2.64, 2.103, 2.156, 2.170, 2.171, 2.172, 2.173, 2.174, and 2.175.

Chapter 5 contains additional information for a clamped-free conical shell having a zero apex angle.

2.4.4 Shear Diaphragm-Free

The boundary conditions for the circular cylindrical shell which is supported by a shear diaphragm at one end and is free at the other are

$$\left. \begin{aligned} N_x = v = w = M_x = 0 & \quad \text{at} \quad x = 0 \\ N_x = N_{x\theta} + \frac{M_{x\theta}}{R} = Q_x \\ + \frac{1}{R} \frac{\partial M_{x\theta}}{\partial \theta} = M_x = 0 & \quad \text{at} \quad x = l \end{aligned} \right\} \quad (2.127)$$

Much information is available for this problem by considering the longitudinally antisymmetric modes of a free-free shell, which is discussed in section 2.4.5. That is, for $m=2, 4, 6, \dots$, the shear diaphragm boundary conditions are duplicated at the center ($x=l/2$) of a free-free shell. In particular, $m=2$ for the free-free shell corresponds to the fundamental mode of the SD-free shell, while $m=4$ corresponds to a higher mode having one circumferential "node line."

Numerical results were obtained for this problem by Resnick and Dugundi (ref. 2.85) and are shown in table 2.35 and figure 2.82. For additional discussion of this figure and table see section 2.4.3.

TABLE 2.36.—Frequency Parameters $\omega R \sqrt{\rho(1-\nu^2)/E} \times 10^2$ for a Clamped-Free Shell; $m=1$, $\nu=0.3$

$\frac{L}{R}$	Degree of char. eq.	R/h											
		50		100		150		200		250		300	
		$n=1$	$n=2$	$n=1$	$n=2$	$n=1$	$n=2$	$n=1$	$n=2$	$n=1$	$n=2$	$n=1$	$n=2$
10	S	2.0835	1.7081	2.0834	1.0351	2.0834	0.8540	2.0834	0.7808	2.0834	0.7445	2.0834	0.7240
	C	2.2042	1.7226	2.2041	1.0619	2.2041	.8871	2.2040	.8171	2.2040	.7826	2.2040	.7632
	Q	2.4579	1.7528	2.4578	1.1094	2.4578	.9432	2.4578	.8776	2.4578	.8455	2.4578	.8276
15	S	.9406	1.5867	.9405	.8351	.9405	.6001	.9405	.4921	.9405	.4331	.9405	.3973
	C	.9984	1.5892	.9983	.8415	.9983	.6096	.9983	.5038	.9983	.4464	.9983	.4119
	Q	1.0994	1.5958	1.0993	.8533	1.0993	.6256	1.0993	.5230	1.0993	.4679	1.0993	.4351
20	S	.5320	1.5632	.5320	.7953	.5320	.5450	.5320	.4238	.5320	.3539	.5320	.3095
	C	.5655	1.5638	.5654	.7973	.5654	.5482	.5654	.4281	.5654	.3591	.5624	.3154
	Q	.6198	1.5660	.6198	.8013	.6198	.5539	.6198	.4353	.6198	.3677	.6198	.3251
25	S	.3414	1.5560	.3414	.7838	.3414	.5288	.3414	.4030	.3414	.3290	.3414	.2807
	C	.3631	1.5561	.3630	.7845	.3630	.5300	.3630	.4048	.3630	.3311	.3630	.2832
	Q	.3971	1.5570	.3971	.7861	.3971	.5324	.3971	.4079	.3971	.3349	.3971	.2876
30	S	.2374	1.5531	.2374	.7794	.2374	.5227	.2374	.3952	.2374	.3194	.2374	.2695
	C	.2526	1.5531	.2326	.7797	.2526	.5232	.2526	.3960	.2526	.3204	.2526	.2706
	Q	.2759	1.5535	.2759	.7805	.2759	.5244	.2759	.3975	.2759	.3223	.2759	.2729
35	S	.1746	1.5517	.1746	.7774	.1746	.5200	.1746	.3918	.1746	.3152	.1746	.2645
	C	.1858	1.5517	.1858	.7775	.1858	.5202	.1858	.3921	.1858	.3156	.1858	.2650
	Q	.2028	1.5519	.2028	.7780	.2028	.5209	.2028	.3929	.2028	.3167	.2028	.2663
40	S	.1339	1.5509	.1339	.7764	.1339	.5186	.1339	.3900	.1339	.3131	.1339	.2620
	C	.1423	1.5509	.1423	.7764	.1423	.5187	.1423	.3902	.1423	.3133	.1423	.2623
	Q	.1553	1.5510	.1553	.7767	.1553	.5191	.1553	.3907	.1553	.3139	.1553	.2630
45	S	.1061	1.5504	.1061	.7758	.1061	.5179	.1061	.3891	.1061	.3120	.1061	.2607
	C	.1125	1.5504	.1125	.7758	.1125	.5179	.1125	.3891	.1125	.3120	.1125	.2608
	Q	.1227	1.5505	.1227	.7760	.1227	.5181	.1227	.3895	.1227	.3124	.1227	.2612
50	S	.0863	1.5501	.0862	.7755	.0862	.5174	.0862	.3885	.0862	.3113	.0862	.2599
	C	.0912	1.5501	.0912	.7755	.0912	.5174	.0912	.3885	.0912	.3113	.0912	.2599
	Q	.0994	1.5501	.0994	.7756	.0994	.5176	.0994	.3887	.0994	.3116	.0994	.2602
∞	S,C,Q	0	1.5492	0	.7746	0	.5164	0	.3873	0	.3098	0	.2582

Notes:

- (1) S=sextic.
 (2) C=cubic.
 (3) Q=quadratic.

TABLE 2.37.—*Values of the Coefficient C_1 in Equation (2.107) for Frequency Parameters of Clamped-Free Shells*

$n \frac{l}{R}$	Number of circumferential nodal circles — m				
	0	1	2	3	4
2	0.1830	0.6854	0.8786	0.9355	0.9607
3	.6857 $\times 10^{-1}$.4512	.7512	.8621	.9578
4	.2934 $\times 10^{-1}$.2851	.6129	.7714	.8541
5	.1414 $\times 10^{-1}$.1821	.4839	.6739	.7845
6	.7501 $\times 10^{-2}$.1194	.3747	.5778	.7100
7	.4300 $\times 10^{-2}$.8049 $\times 10^{-1}$.2880	.4883	.6349
8	.2626 $\times 10^{-2}$.5566 $\times 10^{-1}$.2212	.4088	.5617
9	.1686 $\times 10^{-2}$.3946 $\times 10^{-1}$.1708	.3404	.4928
10	.1129 $\times 10^{-2}$.2858 $\times 10^{-1}$.1327	.2827	.4302
12	.5594 $\times 10^{-3}$.1586 $\times 10^{-1}$.8626 $\times 10^{-1}$.1951	.3242
14	.3071 $\times 10^{-3}$.9394 $\times 10^{-2}$.5285 $\times 10^{-1}$.1360	.2430
16	.1819 $\times 10^{-3}$.5871 $\times 10^{-2}$.3509 $\times 10^{-1}$.9629 $\times 10^{-1}$.1826
18	.1144 $\times 10^{-3}$.3837 $\times 10^{-2}$.2402 $\times 10^{-1}$.6934 $\times 10^{-1}$.1381
20	.7540 $\times 10^{-4}$.2602 $\times 10^{-2}$.1689 $\times 10^{-1}$.5080 $\times 10^{-1}$.1054
22	.5170 $\times 10^{-4}$.1823 $\times 10^{-2}$.1218 $\times 10^{-1}$.3786 $\times 10^{-1}$.8122 $\times 10^{-1}$
24	.3660 $\times 10^{-4}$.1313 $\times 10^{-2}$.8970 $\times 10^{-2}$.2866 $\times 10^{-1}$.6323 $\times 10^{-1}$
26	.2660 $\times 10^{-4}$.9685 $\times 10^{-3}$.6734 $\times 10^{-2}$.2202 $\times 10^{-1}$.4977 $\times 10^{-1}$
28	.1980 $\times 10^{-4}$.7287 $\times 10^{-3}$.5147 $\times 10^{-2}$.1715 $\times 10^{-1}$.3956 $\times 10^{-1}$
30	.1500 $\times 10^{-4}$.5585 $\times 10^{-3}$.3996 $\times 10^{-2}$.1352 $\times 10^{-1}$.3175 $\times 10^{-1}$
32	.1160 $\times 10^{-4}$.4353 $\times 10^{-3}$.3144 $\times 10^{-2}$.1078 $\times 10^{-1}$.2571 $\times 10^{-1}$
36	.7200 $\times 10^{-5}$.2750 $\times 10^{-3}$.2020 $\times 10^{-2}$.7080 $\times 10^{-2}$.1730 $\times 10^{-1}$
40	.4700 $\times 10^{-5}$.1822 $\times 10^{-3}$.1354 $\times 10^{-2}$.4821 $\times 10^{-2}$.1200 $\times 10^{-1}$
42	.3900 $\times 10^{-5}$.1503 $\times 10^{-3}$.1124 $\times 10^{-2}$.4027 $\times 10^{-2}$.1010 $\times 10^{-1}$
44	.3200 $\times 10^{-5}$.1253 $\times 10^{-3}$.9395 $\times 10^{-3}$.3387 $\times 10^{-2}$.8550 $\times 10^{-2}$
48	.2200 $\times 10^{-5}$.8890 $\times 10^{-4}$.6717 $\times 10^{-3}$.2444 $\times 10^{-2}$.6243 $\times 10^{-2}$
50	.1900 $\times 10^{-5}$.7560 $\times 10^{-4}$.5734 $\times 10^{-3}$.2095 $\times 10^{-2}$.5375 $\times 10^{-2}$

TABLE 2.38.—*Values of the Coefficient C_2 in Equation (2.107) for Frequency Parameters of Clamped-Free Shells*

$\frac{l}{nR}$	Number of circumferential nodal circles— m				
	0	1	2	3	4
2	1.473	5.578	14.70	28.76	47.77
3	1.208	3.082	7.117	13.36	21.80
4	1.116	2.200	4.463	7.966	12.710
5	1.073	1.781	3.232	5.471	8.505
6	1.049	1.556	2.562	4.115	6.220
7	1.035	1.408	2.156	3.297	4.842
8	1.025	1.314	1.891	2.766	3.948
9	1.019	1.249	1.706	2.400	3.300
10	1.015	1.203	1.576	2.138	2.895
12	1.009	1.141	1.403	1.795	2.322
14	1.006	1.103	1.230	1.587	1.975
16	1.003	1.079	1.228	1.451	1.749
18	1.002	1.062	1.180	1.357	1.594
20	1.001	1.050	1.146	1.290	1.482
22	1.0	1.041	1.121	1.240	1.399
24	1.0	1.034	1.101	1.202	1.335
26	1.0	1.029	1.086	1.172	1.286
28	1.0	1.025	1.074	1.148	1.247
30	1.0	1.022	1.065	1.129	1.215
32	1.0	1.019	1.057	1.113	1.189
36	1.0	1.015	1.045	1.090	1.150
40	1.0	1.012	1.036	1.073	1.121
42	1.0	1.010	1.033	1.066	1.110
44	1.0	1.009	1.030	1.060	1.100
48	1.0	1.008	1.025	1.050	1.084
50	1.0	1.007	1.023	1.046	1.077

Additional results were obtained by Weingarten (refs. 2.64 and 2.140) and are shown in figures 2.84 through 2.87. For additional discussion of these figures see section 2.4.3.

The free vibration problem for SD-free shells is also discussed in references 2.44 and 2.62.

2.4.5 Free-Free

The boundary conditions for the completely free circular cylindrical shell are

$$N_x = N_{x\theta} + \frac{M_{x\theta}}{R} = Q_x$$

$$+ \frac{1}{R} \frac{\partial M_{x\theta}}{\partial \theta} = M_x = 0 \quad \text{at} \quad x=0, l \quad (2.128)$$

where, of course, expressions for the generalized forces N_x , $N_{x\theta}$, M_x , $M_{x\theta}$, and Q_x must be taken according to the shell theory being used (see sec. 1.5).

The free-free circular cylindrical shell is an appropriate place to discuss the classical and well-known inextensional theory of shells. The kinematics of deformation of this theory require that the middle surface of the shell deforms without stretching. For a circular cylindrical shell this in turn requires that the generators of the cylinder remain straight during vibration.

The inextensional theory was used in an early study by Rayleigh (ref. 2.124) in 1881 to describe the deformation and vibration of thin shells of revolution. Rayleigh claimed that, if the shell were sufficiently thin and vibrating in one of its lower modes, the middle surface behaves as if it is inextensible. This hypothesis was subsequently criticized by Love (ref. 2.25) because of its failure to satisfy the equations of motion and the necessary boundary conditions. Rayleigh, undaunted, continued by applying the theory to the circular cylindrical shell (refs. 2.24 and 2.176).

The theory consists of two sets of vibration modes for circular cylindrical shells. The first set is due to Rayleigh and is characterized by the displacements

$$\left. \begin{aligned} u &= 0 \\ v &= C \sin n\theta \cos \omega t \\ w &= C \cos n\theta \cos \omega t \end{aligned} \right\} \quad (2.129)$$

and was assumed to be applicable for long shells. Setting the maximum strain energy stored in the shell during vibration equal to the maximum kinetic energy, Rayleigh obtained

$$\Omega^2 = k \frac{n^2(n^2-1)^2}{n^2+1} \quad (2.130)$$

The second set, more applicable to shells of arbitrary length, assumes displacements of the form

$$\left. \begin{aligned} u &= \frac{R}{n} C \cos n\varphi \cos \omega t \\ v &= \bar{x} C \sin n\varphi \cos \omega t \\ w &= n\bar{x} C \cos n\varphi \cos \omega t \end{aligned} \right\} \quad (2.131)$$

where \bar{x} is the length coordinate measured from the center section of the shell ($x=l/2$). Using this set of mode shapes, Love (ref. 2.26) obtained the following formula for frequency parameters:

$$\Omega^2 = k \frac{n^2(n^2-1)}{n^2+1} \frac{1 + \frac{24(1-\nu)R^2}{n^2l^2}}{1 + \frac{12R^2}{n^2(n^2+1)l^2}} \quad (2.132)$$

which gives equation (2.130) as a special case as $l/R \rightarrow \infty$.

References 2.3, 2.62, 2.78, 2.138, 2.173, 2.177, 2.178, 2.179, and 2.180 also contain discussions of the inextensional vibrations of circular cylindrical shells.

Beam functions for use with equations (2.91) the Rayleigh-Ritz or an equivalent technique are given by

$$\left. \begin{aligned} X_R(x) &= 1 \\ X_L(x) &= \frac{x}{l} - \frac{1}{2} \\ X_m(x) &= \cosh \lambda_m s + \cos \lambda_m s \\ &\quad - \alpha_m (\sinh \lambda_m s + \sin \lambda_m s), \\ &\quad m=1, 2, \dots \end{aligned} \right\} \quad (2.133)$$

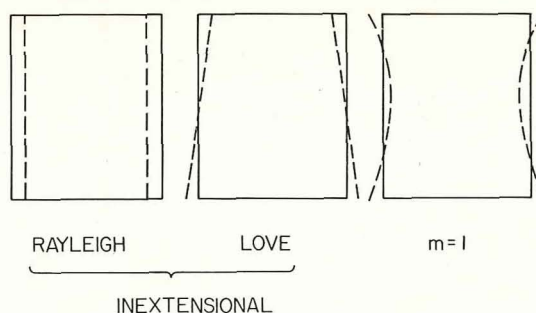


FIGURE 2.90.—Mode shapes of a free-free circular cylindrical shell. (After ref. 2.107)

with $s=x/R$ and $\lambda_m = R\epsilon_m/l$ as before, ϵ_m are the roots of equation (2.93), α_m is given by equation (2.94) and values of ϵ_m and α_m are given in table 2.23. The first two mode shapes in equation (2.133), denoted as $X_R(x)$ and $X_L(x)$, are the rigid body translation and rotation modes, respectively, of a free-free beam. In the beam vibration problem they are trivial modes having zero frequencies. However, for the circular cylindrical shell they yield the Rayleigh and Love inextensional modes, respectively, as discussed earlier in this section. The mode shapes of a free-free shell in the Rayleigh, Love, and $m=1$ modes are shown in figure 2.90.

Warburton (ref. 2.78) followed the procedure outlined in section 2.4 to obtain an exact solution to the Flügge equations of motion in the form of equations (2.53) and satisfied the free-free boundary conditions exactly. However, instead of using the second of the conditions given by equation (2.128), which is necessary to be consistent in the calculus of variations, the conditions $N_{x\theta}=0$ was used. After substituting into the boundary conditions, the resulting frequency equation for the symmetric modes is the one given previously as equation (2.75), where $\theta_1 = \lambda_1 l/2R$, etc., as before, and where equations (2.76) are still used to obtain the antisymmetric frequency equation. However, the coefficients b_i which appear in equation (2.75) are now given by

$$\left. \begin{aligned} b_1 &= (l_1 l_6 - l_2 l_5)(l_{11} l_{16} - l_{12} l_{15}) \\ b_2 &= 0 \\ b_3 &= (l_{12} l_{13} - l_9 l_{16})(l_3 l_6 - l_2 l_8) \\ &\quad + (l_9 l_{15} - l_{11} l_{13})(l_4 l_6 - l_2 l_7) \end{aligned} \right\} \quad (2.134)$$

$$\left. \begin{aligned}
 b_4 &= (l_1 l_8 - l_3 l_5)(l_{11} l_{14} - l_{10} l_{15}) \\
 &\quad + (l_1 l_7 - l_4 l_5)(l_{12} l_{14} - l_{10} l_{16}) \\
 b_5 &= (l_1 l_8 - l_3 l_5)(l_{12} l_{14} - l_{10} l_{16}) \\
 &\quad - (l_1 l_7 - l_4 l_5)(l_{11} l_{14} - l_{10} l_{15}) \\
 b_6 &= (l_{10} l_{13} - l_9 l_{14})(l_4 l_8 - l_3 l_7) \\
 b_7 &= -(l_9 l_{15} - l_{11} l_{13})(l_3 l_6 - l_2 l_8) \\
 &\quad + (l_{12} l_{13} - l_9 l_{16})(l_4 l_6 - l_2 l_7)
 \end{aligned} \right\} \quad (2.134)$$

where

$$\left. \begin{aligned}
 l_1 &= k_2 \alpha_1 + \nu n k_1 - \nu + \beta \alpha_1^2 \\
 l_2 &= -k_4 \gamma_2 + \nu n k_3 - \nu - \beta \gamma_2^2 \\
 l_3 &= -k_7 q - k_8 p - \nu n k_6 - 2\beta p q \\
 l_4 &= k_7 p - k_8 q + \nu n k_5 - \nu + \beta(p^2 - q^2) \\
 l_5 &= \alpha_1^2 - \nu n^2 + \nu n k_1 + \alpha_1 k_2 \\
 l_6 &= -\gamma_2^2 - \nu n^2 + \nu n k_3 - \gamma_2 k_4 \\
 l_7 &= p^2 - q^2 - \nu n^2 + k_7 p - k_8 q + \nu n k_5 \\
 l_8 &= -2p q - k_7 q - k_8 p - \nu n k_6 \\
 l_9 &= -n k_2 + (1 + \beta) k_1 \alpha_1 - \beta n \alpha_1 \\
 l_{10} &= n k_4 - (1 + \beta) k_3 \gamma_2 + \beta n \gamma_2 \\
 l_{11} &= n k_8 - (1 + \beta)(k_5 q + k_6 p) + \beta n q \\
 l_{12} &= -n k_7 + (1 + \beta)(k_5 p - k_6 q) - \beta n p \\
 l_{13} &= \alpha_1^3 - (2 - \nu) n^2 \alpha_1 + k_2 \alpha_1^2 \\
 &\quad + \frac{1}{2}(1 - \nu) n^2 k_2 + \frac{1}{2}(3 - \nu) n k_1 \alpha_1 \\
 l_{14} &= \gamma_2^3 + (2 - \nu) n^2 \gamma_2 + k_4 \gamma_2^2 \\
 &\quad - \frac{1}{2}(1 - \nu) n^2 k_4 - \frac{1}{2}(3 - \nu) n k_3 \gamma_2 \\
 l_{15} &= -q(3p^2 - q^2) + (2 - \nu) n^2 q \\
 &\quad - 2p q k_7 - k_8(p^2 - q^2) \\
 &\quad - \frac{1}{2}(3 - \nu) n(k_5 q + k_6 p) \\
 &\quad - \frac{1}{2}(1 - \nu) n^2 k_8 \\
 l_{16} &= p(p^2 - 3q^2) - (2 - \nu) n^2 p \\
 &\quad + k_7(p^2 - q^2) - 2p q k_8 \\
 &\quad + \frac{1}{2}(1 - \nu) n^2 k_7 \\
 &\quad + \frac{1}{2}(3 - \nu) n(k_5 p - k_6 q)
 \end{aligned} \right\} \quad (2.135)$$

with the constants k_i related to the amplitude ratios by equations (2.78), and with the amplitude ratios determined by equations (2.79) for $\nu = 0.3$.

In reference 2.78, Warburton compared frequency parameters for free-free shells obtained by using two procedures:

(1) The exact procedure, using Flügge's equations, as described previously in this section.

(2) The Rayleigh-Ritz procedure, using a single set of free-free beam functions and the Flügge strain energy integrand.

Numerical results are listed in table 2.39 wherein selected values of the square of the frequency parameter Ω are prescribed and the l/R ratios corresponding to given values of m are determined from equation (2.75). The percentage by which the Rayleigh-Ritz frequency exceeds the exact frequency is also listed in each instance. The ratio of the transverse deflection at one end of the shell ($x=l$) to that at the center section ($x=l/2$) in the corresponding vibration mode is also given for the exact solution. It is seen that typically the percentage error in Ω increases as l/R decreases. However, for $n=2$ the frequency increases to a maximum and then decreases as l/R increases further; this is shown in table 2.39 for $R/h=500$, but was found typical for $n=2$ with three other values of R/h in reference 2.78. For the range of parameters considered in the investigation, the maximum error found was approximately 10 percent and occurred for $m=2$, $n=2$, and $l/R \approx 4$. The error tends to decrease with increasing n , although for large n (≥ 12), it is essentially independent of n , as shown in the table for $n=16$. It is interesting to note that the maximum error in the frequency determined by the approximate Rayleigh-Ritz procedure is of the same order, and occurs for the same parameters, as was found in a similar approximate analysis for clamped-clamped shells (see table 2.24), even though the clamped-clamped beam functions satisfy the clamped shell boundary conditions exactly, while the free-free beam functions only approximate the free boundary conditions for a shell. This is in contrast to what is found in the vibration of rectangular plates (ref. 2.157) where the effect of free edges is to increase the error in the approximate frequencies obtained

TABLE 2.39.—Length Ratios (l/R) of Free-Free Shells for a Given Ω^2 from Equation (2.75) and Some Comparisons; $\nu=0.3$

n	R/h	Ω^2	Item	m		
				1	3	5
2	500	4×10^{-6}	l/R	61.5	143	224
			e	1.4	.66	.43
			Z	-1.64	1.41	-1.41
		1×10^{-4}	l/R	21.9	50.8	79.8
			e	3.9	1.8	1.2
			Z	-1.64	1.40	-1.41
		0.001	l/R	12.1	28.0	44.0
			e	3.7	2.3	1.7
			Z	-1.62	1.38	-1.39
		0.2	l/R	2.57	5.59	8.67
			e	6.7	8.5	6.4
			Z	-1.40	1.11	-1.15
		0.5	l/R	1.58	3.27	5.01
			e	6.6	6.9	5.2
			Z	-1.24	1.02	-1.08
6	500	4×10^{-4}	l/R	22.3	50.7	79.1
			e	.05	.03	.02
			Z	-1.40	1.34	-1.34
		4.8×10^{-4}	l/R	8.30	19.1	30.0
			e	.62	.32	.22
			Z	-1.61	1.41	-1.42
		8×10^{-4}	l/R	5.46	12.6	19.8
			e	1.8	1.0	.70
			Z	-1.62	1.40	-1.41
		0.01	l/R	2.37	5.44	8.52
			e	4.1	3.4	2.5
			Z	-1.58	1.34	-1.35
		0.06	l/R	1.41	3.17	4.94
			e	5.4	5.8	4.5
			Z	-1.49	1.25	-1.27
	100	0.01	l/R	15.7	34.7	53.7
			e	.11	.06	.04
			Z	-1.11	1.11	-1.11
		0.0105	l/R	6.77	14.9	23.0
			e	.29	.17	.11
			Z	-1.38	1.35	-1.35
		0.015	l/R	3.19	7.18	11.2
			e	1.1	.81	.59
			Z	-1.52	1.39	-1.39
		0.08	l/R	1.41	3.15	4.90
			e	4.2	4.6	3.6
			Z	-1.48	1.27	-1.28

Notes:

- (1) e = Percent error in Rayleigh-Ritz frequency.
 (2) $Z = w(l)/w(l/2)$.

TABLE 2.39.—Length Ratios (l/R) of Free-Free Shells for a Given Ω^2 from Equation (2.75) and Some Comparisons; $\nu=0.3$ —Concluded

n	R/h	Ω^2	Item	m		
				1	3	5
6	20	0.249	l/R	19.6	45.7	71.9
			e	.12	.06	.04
			Z	— .83	.83	— .83
		.255	l/R	7.96	17.0	26.0
			e	.31	.19	.12
			Z	—1.13	1.13	—1.13
		.27	l/R	4.71	9.90	15.1
			e	.47	.34	.24
			Z	—1.21	1.21	—1.21
		.5	l/R	1.60	3.41	5.23
			e	1.1	1.2	.95
			Z	—1.33	1.29	—1.29
16	500	.021591	l/R	71.6	207	343
			e	0	0	0
			Z	— .10	.10	— .10
		.021595	l/R	24.3	65.4	107
			e	.02	.01	0
			Z	— .33	.33	— .33
		.02161	l/R	13.4	33.4	53.4
			e	.04	.02	.01
			Z	— .61	.61	— .61
		.02166	l/R	7.66	17.6	27.5
			e	.10	.05	.03
			Z	— .91	.91	— .91
	100	.02210	l/R	3.40	7.37	11.3
			e	.24	.14	.09
			Z	—1.21	1.21	—1.21
		.53977	l/R	51.4	149	246
			e	0	0	0
			Z	— .11	.11	— .11
		.53986	l/R	22.6	62.1	102
			e	.02	.01	0
			Z	— .27	.27	— .27
		.5402	l/R	12.6	32.4	52.2
			e	.05	.02	.01
			Z	— .50	.50	— .50
		.5415	l/R	7.29	17.2	27.1
			e	.12	.05	.03
			Z	— .80	.80	— .80
		.5505	l/R	3.41	7.37	11.3
			e	.29	.16	.11
			Z	—1.08	1.08	—1.08

Notes:

- (1) e = Percent error in Rayleigh-Ritz frequency.
 (2) $Z = w(l)/w(l/2)$.

by the Rayleigh-Ritz method using beam functions. In reference 2.78 it was also reported that the frequencies obtained by the Rayleigh-Ritz method were in good agreement with experimental values obtained from a series of experiments with free-ended shells having $R/h = 19.1$ and different lengths, giving a difference in frequency in excess of 5 percent for only six modes out of a total of 66.

In addition to the mode shape deflection ratios $w(l)/w(l/2)$ given in table 2.39, some examples of mode shapes for $m = 1$ are given in figure 2.91 (from ref. 2.78). For $n = 2$ and l/R large, the mode shape is given by curve I, which is coincident with the free-free beam mode shape (values of $w(l)/w(l/2)$ for the free-free beam are -1.645 , 1.405 , and -1.414 for $m = 1, 3, 5$, respectively). As l/R decreases the mode shape diverges from curve I and tends towards curve II, which corresponds to $l/R = 1.59$, $100 \leq R/h \leq 500$. For intermediate values of l/R the mode shape lies between curves I and II and essentially passes through the intersection point of curves I and II. For large values of n and l/R a curve such as V is typical of the mode shape; as l/R decreases the shape progressively changes, passing approxi-

mately through curves IV and III. Specifically, curve V corresponds to $n = 16$, $R/h = 100$, and $l/R = 22.6$. If l/R is reduced to approximately 10 or 3 and other parameters are left unchanged, then the mode shapes correspond to curves IV and III, respectively. For $l/R = \text{constant}$ and n increasing, the curves tend further away from curve I. For intermediate values of n , such as $n = 6$, curve III also corresponds to a mode shape for $l/R = 15.7$ and $R/h = 100$. As l/R is reduced the mode shape approaches curve I and then, for very low values of l/R , tends to cross curve I and give a curve similar to curve II. For n and l/R large, the axial nodal circle moves towards the end of the shell. The mode shapes of the axial and circumferential displacements u and v were not investigated in detail in reference 2.78, but it was found that when both n and l/R are small, $v(l/2)/w(l/2)$ decreases slightly as l/R increases and tends to $1/n$ as $l/R \rightarrow \infty$; $v(l)/w(l)$ is slightly less than $1/n$; $u(l)/w(l)$ is small and decreases with increasing l/R or n .

Lowest frequency parameters were given by Gontkevich (refs. 2.126 and 2.127) as shown in figures 2.92 through 2.96. The Rayleigh-Ritz method using beam functions and the Donnell-Mushtari shell theory is the basis for the results. For the general formula yielding these curves, see equations (2.67) and (2.68) in section 2.4. Admissible values of ϵ_m for the abscissas of figures 2.92 through 2.96 are available in table 2.21.

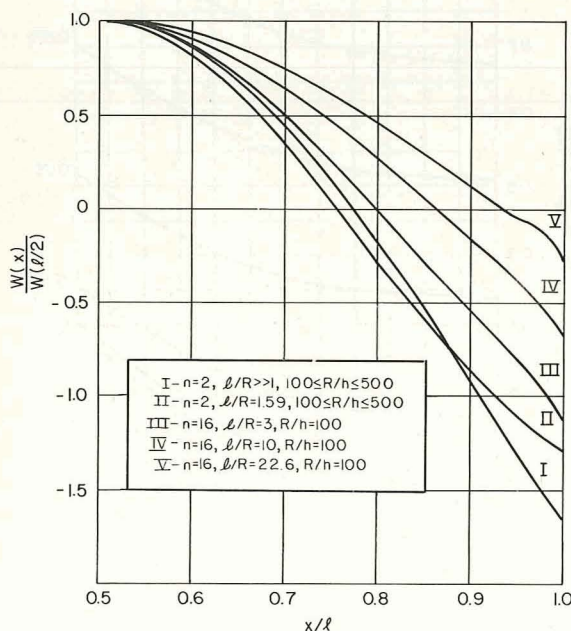


FIGURE 2.91.—Mode shapes (radial components) for free-free shells; $m = 1$. (After ref. 2.78)

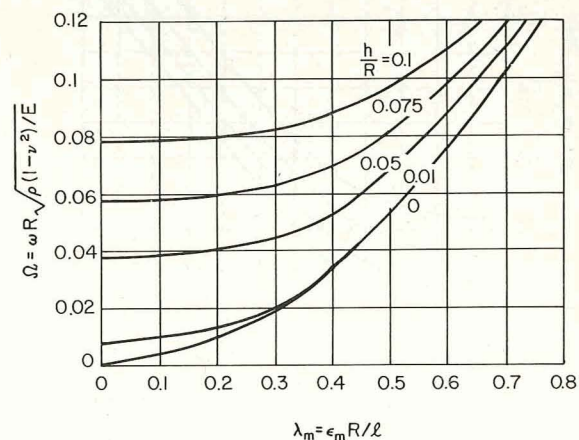


FIGURE 2.92.—Lowest frequency parameters for free-free shells (see table 2.21 for admissible ϵ_m); $n = 2$, $0 \leq \lambda_m \leq 0.8$. (After ref. 2.127)

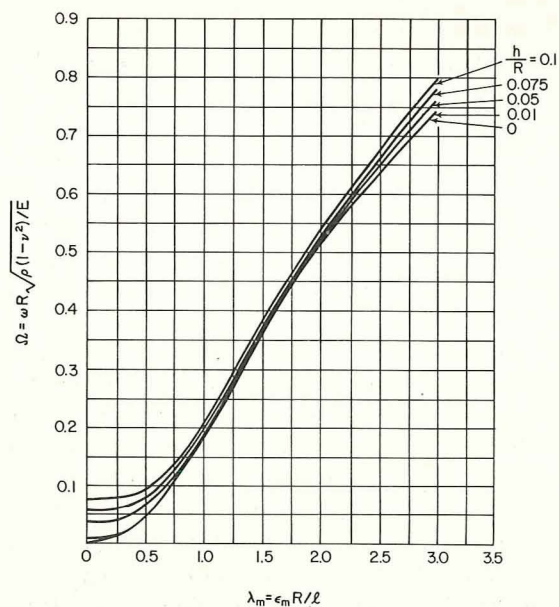


FIGURE 2.93.—Lowest frequency parameters for free-free shells (see table 2.21 for admissible ϵ_m); $n=2$, $0 \leq \lambda_m \leq 3.5$. (After ref. 2.127)

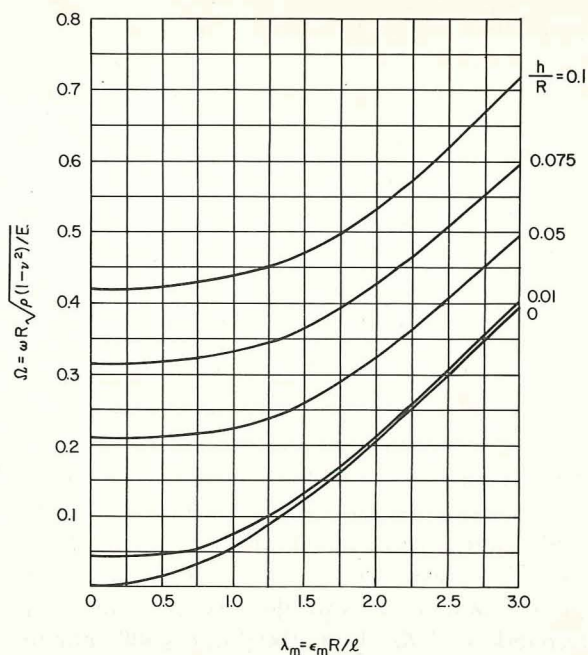


FIGURE 2.95.—Lowest frequency parameters for free-free shells (see table 2.21 for admissible ϵ_m); $n=4$, $0 \leq \lambda_m \leq 3.0$. (After ref. 2.127)

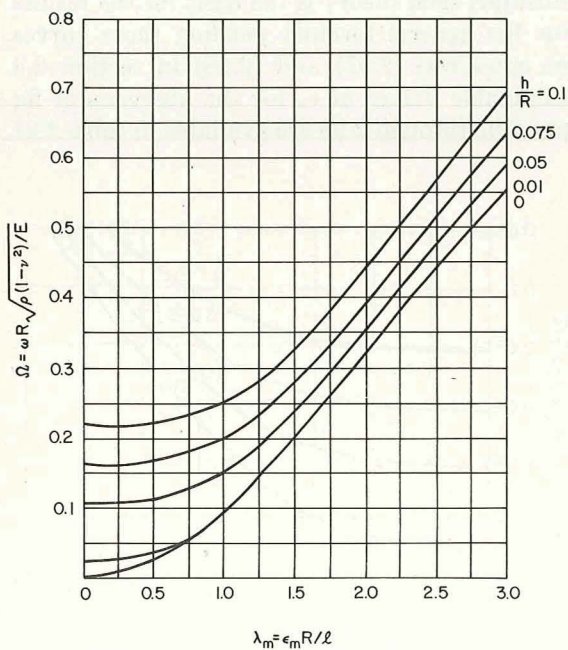


FIGURE 2.94.—Lowest frequency parameters for free-free shells (see table 2.21 for admissible ϵ_m), $n=3$, $0 \leq \lambda_m \leq 3.0$. (After ref. 2.127)

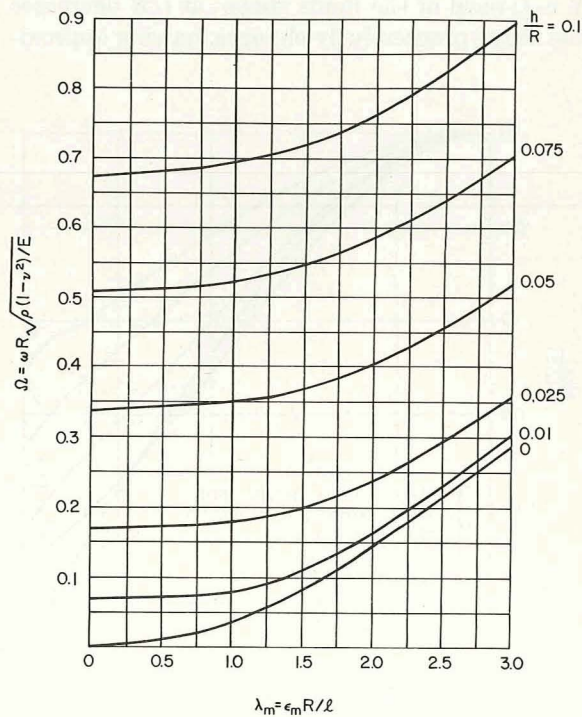


FIGURE 2.96.—Lowest frequency parameters for free-free shells (see table 2.21 for admissible ϵ_m), $n=5$, $0 \leq \lambda_m \leq 3.0$. (After ref. 2.127)

Sewall and Naumann (ref. 2.107) also used the Rayleigh-Ritz technique with beam functions and the Goldenveizer-Novozhilov shell theory to obtain lowest frequency parameters for free-free shells and compared them with experimental results. However, they employed nine terms in each of the series of the assumed mode shapes appearing in equations (2.91) to obtain convergence of the Ritz procedure, except for the modes which are similar to Rayleigh and Love inextensional modes. For the latter modes, only a single term of the series was required for convergence over most of the range of n values, with the exception of the range $10 \leq n \leq 15$ for the Love-type mode. This rapid convergence of the method for the Rayleigh and Love-type modes to modes which are, for all practical purposes, the Rayleigh and Love modes themselves (as given by equations (2.129) and (2.131)), is a strong indication of the accuracy of these approximations. The results are shown in figure 2.97 for a 6061-T6 aluminum alloy shell having $h=0.0255$ in., $R=9.538$ in., and $l=25.125$ in. In this figure it is seen that the Rayleigh and Love modes have very nearly the same frequencies. For figure 2.97 the measured frequencies for the two inextensional modes were obtained with an air shaker; experimental frequencies for

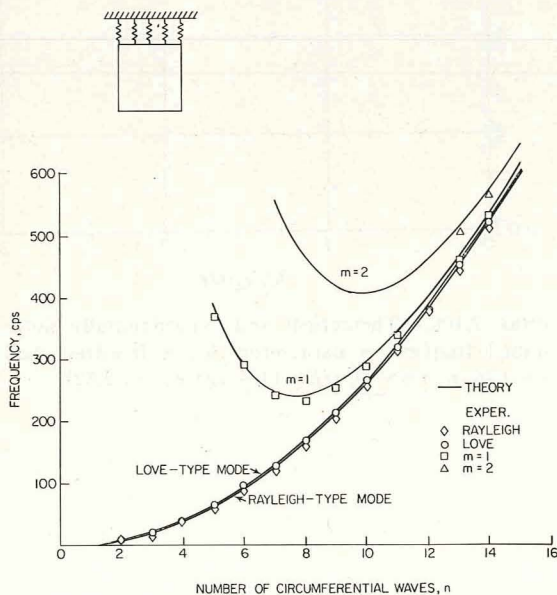


FIGURE 2.97.—Theoretical and experimental frequencies for a free-free aluminum shell; $R/h=374$, $l/R=2.63$, $h=0.0255$ in., (After ref. 2.107)

the higher modes ($m=1, 2$) were obtained with an electrodynamic shaker.

Grützacher, Kallenbach, and Nellesen (ref. 2.62) proposed an interesting method of obtaining frequencies for circular cylindrical shells having *arbitrary* boundary conditions. The procedure consists of using the characteristic equations for an SD-SD shell (as given for the various theories by eqs. (2.35) and (2.36) and table 2.4) and use the appropriate values of λ arising in the beam functions for the desired boundary conditions instead of the λ for an SD-SD shell. They demonstrated this procedure for a free-free shell and compared the frequencies obtained with experimentally measured ones. The Flügge characteristic equation (see table 2.4) is taken in its linearized form (neglecting Ω^6 and Ω^4 terms). In addition the theory of Coupry (refs. 2.12 and 2.13) is used (a theory which arrives at a *symmetric* form of Love's equations of motion in an

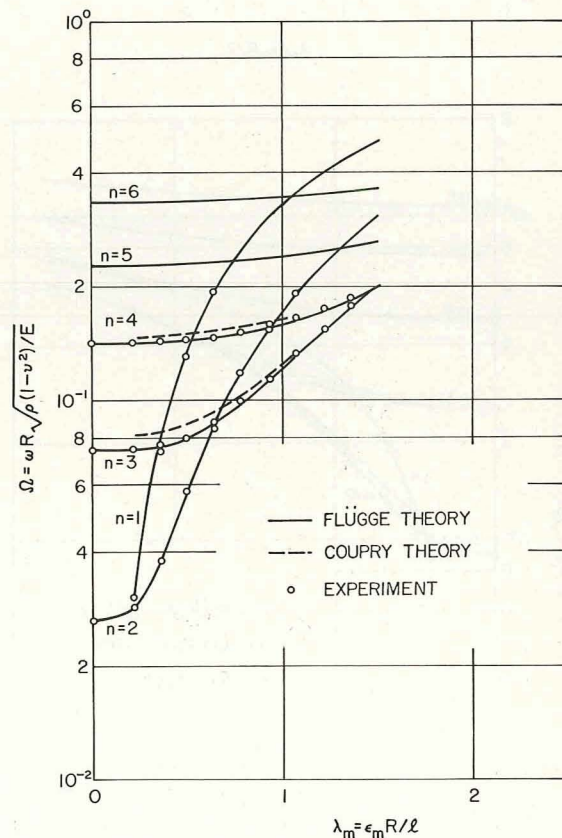


FIGURE 2.98.—Theoretical and experimentally determined frequencies parameters for a free-free shell; $\nu=0.35$, $R/h=2.94$, $l/R=2.17$. (After ref. 2.62)

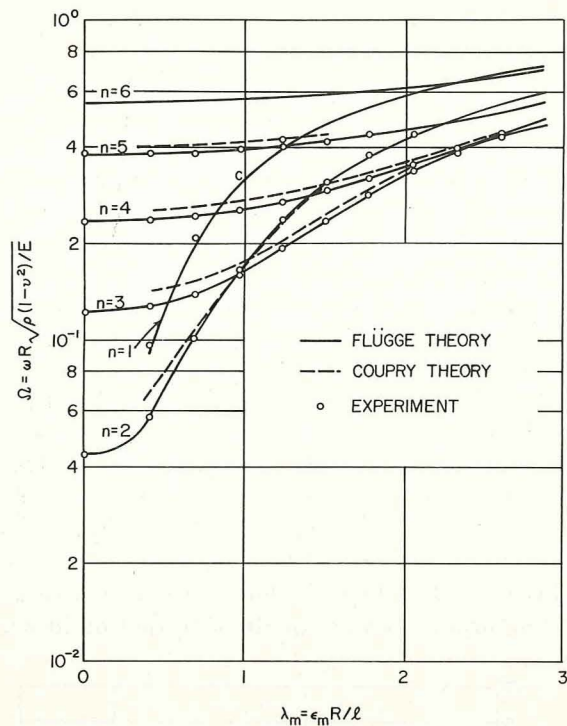


FIGURE 2.99.—Theoretical and experimentally determined frequencies parameters for a free-free shell; $\nu=0.35$, $R/h=17.6$, $l/R=11.42$. (After ref. 2.62)

←

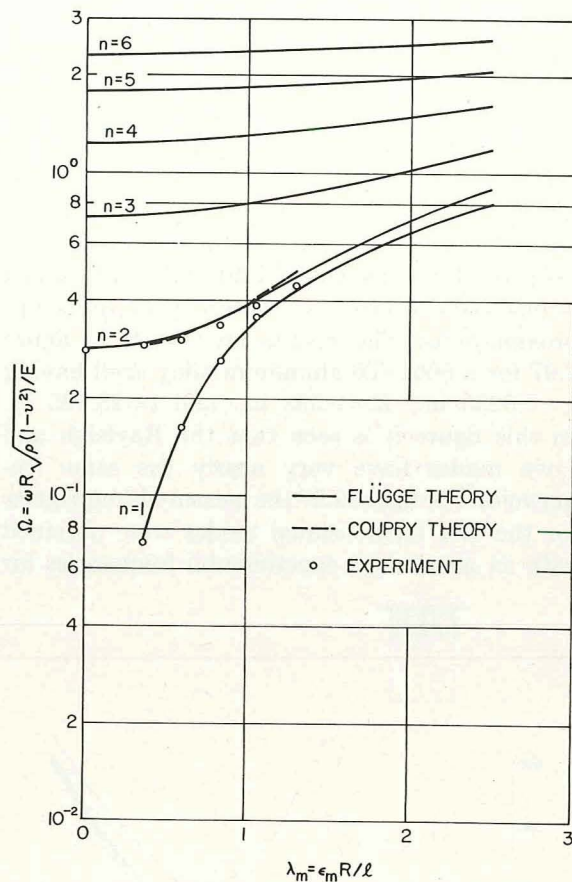
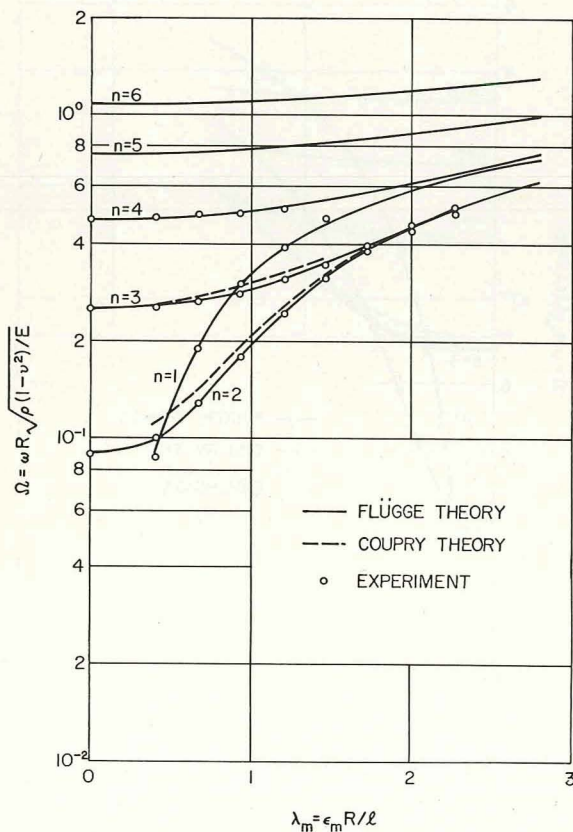


FIGURE 2.100.—Theoretical and experimentally determined frequencies parameters for a free-free shell; $\nu=0.35$, $R/h=8.48$, $l/R=11.8$. (After ref. 2.62)

←

FIGURE 2.101.—Theoretical and experimentally determined frequencies parameters for a free-free shell; $\nu=0.35$, $R/h=2.5$, $l/R=13.3$ (After ref. 2.62)

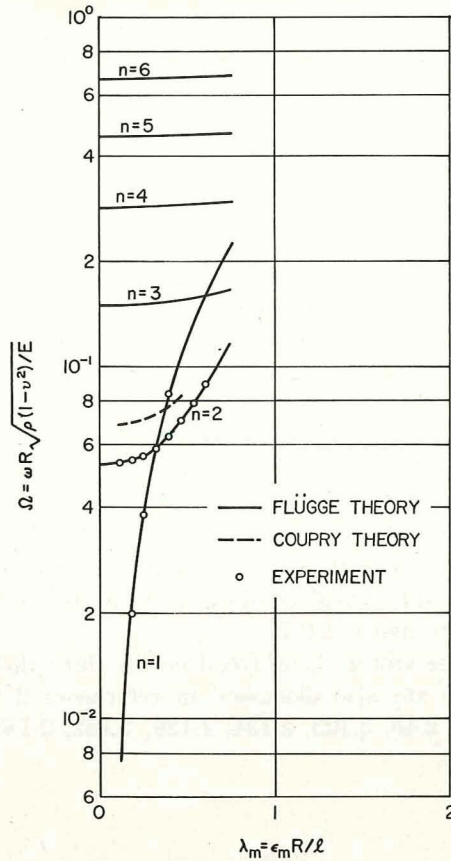


FIGURE 2.102.—Theoretical and experimentally determined frequencies parameters for a free-free shell; $\nu=0.35$, $R/h=14.5$, $l/R=43.5$. (After ref. 2.62)

unclear manner). Theoretical and experimental results obtained for various shells are shown in figures 2.98 through 2.103 for $\nu=0.35$. Admissible values of ϵ_m for the figures are available in table 2.21. The usefulness of the theoretical results in figure 2.101 is questionable because it applies to shells having a thickness ratio ($R/h=2.5$) beyond acceptable limits for eighth order shell theory. Figure 2.103 used measured frequencies for eight shells having

$$2.5 \leq R/h \leq 44.5$$

and

$$10.2 \leq l/R \leq 143$$

Kondrashov (ref. 2.148) used the Donnell-Mushtari theory and the Southwell method to obtain lower bounds for Ω . The frequency param-

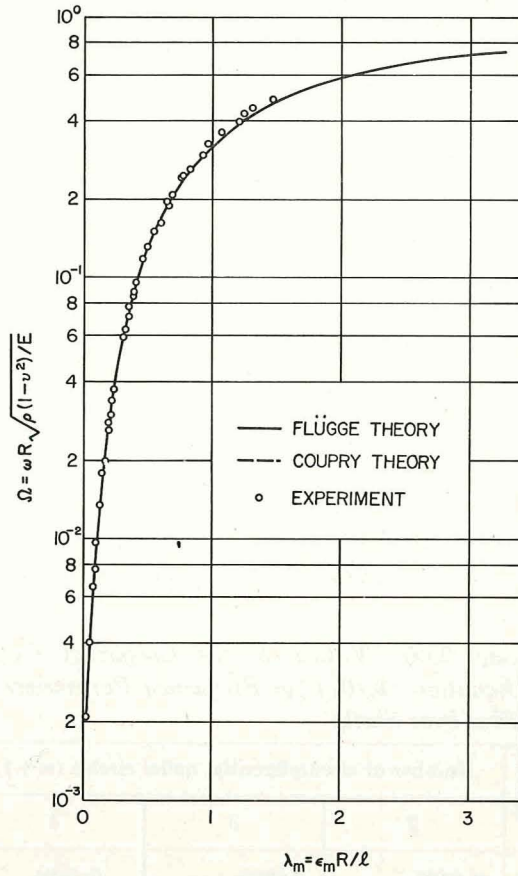


FIGURE 2.103.—Theoretical and experimentally determined frequencies parameters for a free-free shell; $n=1$; $\nu=0.35$; experimental values are from eight shells. (After ref. 2.62)

eters can be calculated from equation (2.107), with C_1 and C_2 for free-free shells being the roots of the equations

$$\cos z_1 \xi_0 \cosh z_2 \xi_0 + \sqrt{C_1/(1-C_1)} \sin z_1 \xi_0 \sinh z_2 \xi_0 = 1 \quad (2.136)$$

$$\cos k_1 \xi_0 \cosh k_2 \xi_0 - \frac{1}{2} \left(C - \frac{1}{C} \right) \sin k_1 \xi_0 \sinh k_2 \xi_0 = 0 \quad (2.137)$$

$$C = \left[\frac{C_2 + 1}{C_2 - 1} \right]^{1/2} \left[\frac{C_2 - (1-\nu)}{C_2 + (1-\nu)} \right]^2 \quad (2.138)$$

with $\xi_0 = nl/R$, and z_1 , z_2 , k_1 , and k_2 are as given in equations (2.110). Some useful values of C_1 and C_2 are listed in tables 2.40 and 2.41. In using these tables it is generally necessary to interpo-

late between values shown for nl/R . The frequency parameter according to the membrane theory is

$$\Omega^2 = (1 - \nu^2)C_1 \quad (2.139)$$

Experimentally determined frequencies obtained by Grinsted (ref. 2.181) for $R/h=78.2$, $l/R=2.4$, and $h=0.064$ in. (the material is not known, but presumably is steel) are shown in figure 2.104.

The modal characteristics of a particular free-free shell having $R/h=20$, $l/R=8.1$, $\nu=0.3$, $m=1$, and $n=0$ (axisymmetric) are shown in figure 2.105 (from ref. 2.73). The value of Ω associated with these curves is 0.3671 and was obtained from the Flügge theory by the exact method. It is interesting to compare the various generalized displacements and forces shown in the plots with the corresponding plots for an SD-SD shell,

TABLE 2.40.—Values of the Coefficient C_1 in Equation (2.107) for Frequency Parameters of Free-Free Shells

$\frac{n}{R}$	Number of circumferential nodal circles ($m+1$)		
	2	3	4
2	0.8107	0.9065	0.9501
3	.6199	.8042	.8909
4	.4327	.6840	.8146
5	.2863	.5619	.7277
6	.1860	.4493	.6375
7	.1216	.3529	.5494
8	.8096 $\times 10^{-1}$.2742	.4672
9	.5522 $\times 10^{-1}$.2124	.3937
10	.3859 $\times 10^{-1}$.1646	.3295
12	.2020 $\times 10^{-1}$.1004	.2291
14	.1144 $\times 10^{-1}$.6298 $\times 10^{-1}$.1592
16	.6918 $\times 10^{-2}$.4087 $\times 10^{-1}$.1117
18	.4412 $\times 10^{-2}$.2741 $\times 10^{-1}$.7957 $\times 10^{-1}$
20	.2938 $\times 10^{-2}$.1894 $\times 10^{-1}$.5759 $\times 10^{-1}$
22	.2029 $\times 10^{-2}$.1345 $\times 10^{-1}$.4240 $\times 10^{-1}$
24	.1445 $\times 10^{-2}$.9782 $\times 10^{-2}$.3174 $\times 10^{-1}$
26	.1056 $\times 10^{-2}$.7272 $\times 10^{-2}$.2414 $\times 10^{-1}$
28	.7888 $\times 10^{-3}$.5506 $\times 10^{-2}$.1864 $\times 10^{-1}$
30	.6012 $\times 10^{-3}$.4242 $\times 10^{-2}$.1458 $\times 10^{-1}$
32	.4659 $\times 10^{-3}$.3317 $\times 10^{-2}$.1154 $\times 10^{-1}$
36	.2923 $\times 10^{-3}$.2109 $\times 10^{-2}$.7494 $\times 10^{-2}$
40	.1924 $\times 10^{-3}$.1403 $\times 10^{-2}$.5054 $\times 10^{-2}$
42	.1585 $\times 10^{-3}$.1160 $\times 10^{-2}$.4206 $\times 10^{-2}$
44	.1318 $\times 10^{-3}$.9677 $\times 10^{-3}$.3526 $\times 10^{-2}$
48	.9320 $\times 10^{-4}$.6885 $\times 10^{-3}$.2529 $\times 10^{-2}$
50	.7920 $\times 10^{-4}$.5866 $\times 10^{-3}$.2162 $\times 10^{-2}$

where a radial constraint ($w=0$) would be applied at the ends. The SD-SD shell gives sinusoidal variations in all quantities plotted (see secs. 2.3 and 2.3.2). The only noticeable deviation from sinusoidal patterns in figure 2.105 is seen in the force distributions. The moment resultants M_x and M_θ show very slight distortions at the boundary. The circumferential (hoop) force resultant N_θ is not zero at the boundary, but is very small. The largest distortion from sinusoidal behavior is in the shearing force Q_x , which would yield a cosine curve for the SD-SD shell.

For $n=1$ (beam bending mode) the modal characteristics of a free-free shell are shown in figures 2.106 and 2.107 for $l/R=5$, $\nu=0.3$, $m=1$, $n=1$. The curves fit both $R/h=20$ and 500, and $\Omega=0.3583$ for both thickness ratios, showing the importance of overall beam bending behavior compared with localized bending through the shell wall. Local bending near the free edges is seen in figure 2.107.

Free vibrations of free-free circular cylindrical shells are also discussed in references 2.3, 2.7, 2.44, 2.45, 2.103, 2.134, 2.139, 2.182, 2.183, and 2.184.

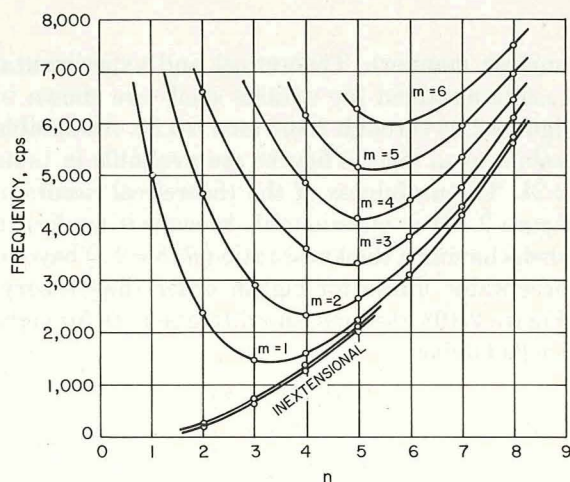


FIGURE 2.104.—Experimentally observed frequencies for a free-free shell; $R/h=78.2$, $l/R=2.4$, $h=0.064$ in. (After ref. 2.181)

TABLE 2.41.—Values of the Coefficient C_2 in Equation (2.107) for Frequency Parameters of Free-Free Shells

$\frac{l}{nR}$	Number of circumferential nodal circles ($m+1$)				
	0	1	2	3	4
2	2.263	7.170	16.840	32.550	51.200
3	1.682	3.950	8.230	14.730	23.450
4	1.423	2.770	5.195	8.830	13.710
5	1.282	2.191	3.765	6.100	9.210
6	1.200	1.860	2.975	4.595	6.760
7	1.148	1.650	2.485	3.685	5.280
8	1.113	1.507	2.160	3.080	4.300
9	1.088	1.408	1.932	2.670	3.635
10	1.071	1.342	1.764	2.365	3.155
12	1.047	1.236	1.541	1.967	2.521
14	1.032	1.173	1.404	1.724	2.130
16	1.021	1.132	1.308	1.557	1.874
18	1.016	1.103	1.245	1.446	1.698
20	1.014	1.087	1.202	1.365	1.568
22	1.011	1.073	1.167	1.302	1.474
24	1.009	1.061	1.142	1.255	1.400
26	1.007	1.051	1.122	1.217	1.343
28	1.006	1.042	1.104	1.187	1.294
30	1.004	1.037	1.091	1.164	1.257
32	1.002	1.032	1.078	1.143	1.226
36	1.001	1.024	1.061	1.112	1.179
40	1.0	1.020	1.050	1.092	1.146
42	1.0	1.018	1.043	1.081	1.131
44	1.0	1.015	1.041	1.076	1.120
48	1.0	1.012	1.034	1.062	1.100
50	1.0	1.010	1.030	1.058	1.092

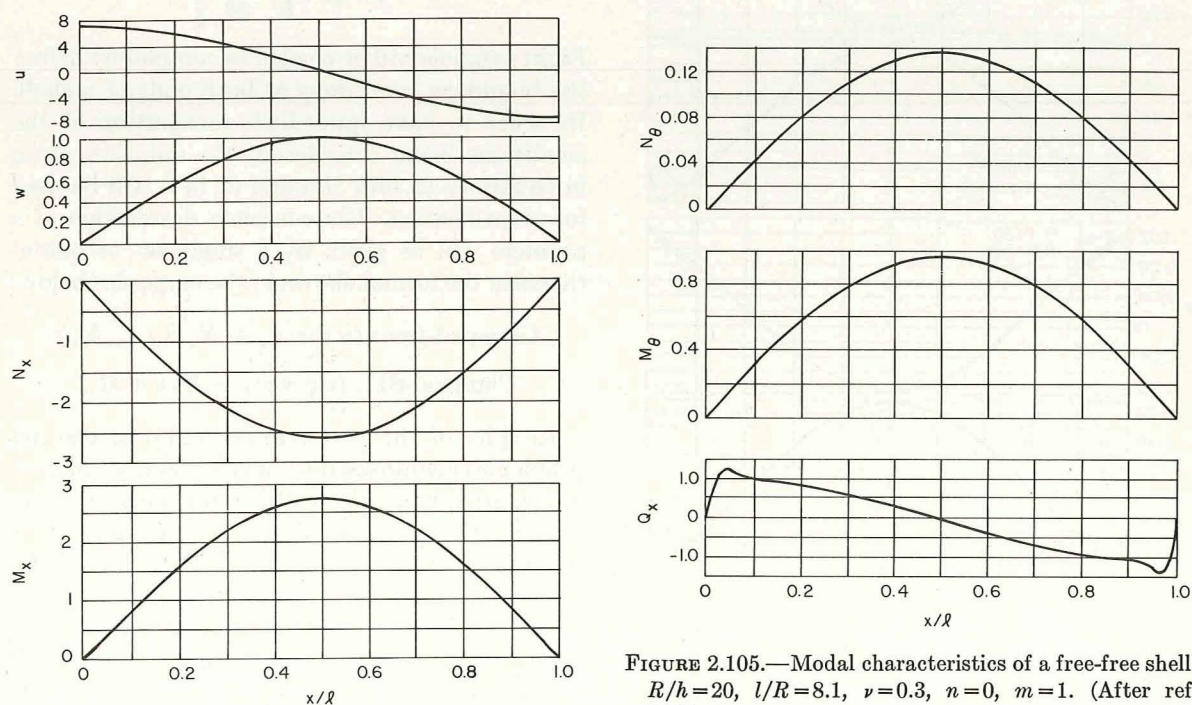


FIGURE 2.105.—Modal characteristics of a free-free shell; $R/h=20$, $l/R=8.1$, $\nu=0.3$, $n=0$, $m=1$. (After ref. 2.73)

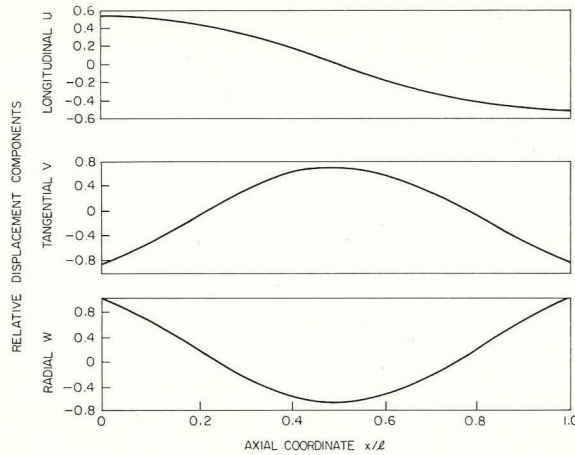


FIGURE 2.106.—Mode shape for a free-free shell; $R/h=20$ and 500; $l/R=5$, $\nu=0.3$, $m=1$, $n=1$. (After ref. 2.73)

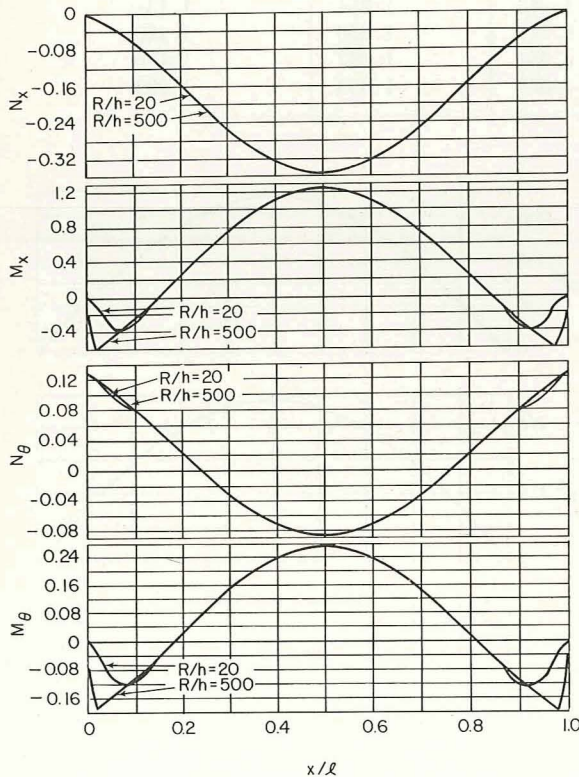


FIGURE 2.107.—Force and moment resultants for the mode shape of figure 2.106. (After ref. 2.73)

2.4.6 Edges Not Necessarily Clamped, SD, or Free

Thus far only six cases of circular cylindrical shells of finite length having some combination of clamped, shear diaphragm, or free edges have been considered. The remaining 130 possible combinations of simple boundary conditions will now be taken up. Remembering the possible conditions

$$(a) u=0 \quad \text{or} \quad (b) N_x=0 \quad (2.140)$$

$$(a) v=0 \quad \text{or} \quad (b) N_{x\theta} + \frac{M_{x\theta}}{R} = 0 \quad (2.141)$$

$$(a) w=0 \quad \text{or} \quad (b) Q_x + \frac{1}{R} \frac{\partial M_{x\theta}}{\partial \theta} = 0 \quad (2.142)$$

$$(a) \frac{\partial w}{\partial x} = 0 \quad \text{or} \quad (b) M_x = 0 \quad (2.143)$$

A somewhat more compact notation will now be used to aid in labeling future problems:

$$\left. \begin{aligned} w_x &\equiv \frac{\partial w}{\partial x} \\ S_{x\theta} &\equiv N_{x\theta} + \frac{M_{x\theta}}{R} \\ V_x &\equiv Q_x + \frac{1}{R} \frac{\partial M_{x\theta}}{\partial \theta} \end{aligned} \right\} \quad (2.144)$$

Eight symbols will be needed to completely define the boundary conditions at both ends of a shell. In order to have immediate recognition of the conditions being considered, the notation given in equations (2.140) through (2.144) will be used for identification. The complete description of a problem will be given by a single set of parentheses in the format shown in the examples below:

Clamped-free: $(u v w w_x - N_x S_{x\theta} V_x M_x)$

Clamped-SD: $(u v v w_x - N_x v w M_x)$

In spite of the vast number (130) of distinct problems encompassed by this section, significant information is available below for most of them.

$(u S_{x\theta} V_x w_x - u S_{x\theta} V_x w_x)$ shells have the same frequencies as $(N_x v w M_x - N_x v w M_x)$ shells (i.e., SD-SD). The displacement functions given by equations (2.20) with $\lambda = m\pi R/l$ are simply shifted by $\pi/2$ with respect to the longitudinal coordinate s , giving

$$\left. \begin{aligned} u &= A \sin \lambda s \cos n\theta \cos \omega t \\ v &= B \cos \lambda s \sin n\theta \cos \omega t \\ w &= C \cos \lambda s \cos n\theta \cos \omega t \end{aligned} \right\} \quad (2.145)$$

which satisfy the $(u S_{x\theta} V_x w_{,x} - u S_{x\theta} V_x w_{,x})$ boundary conditions exactly. Physically stated, the boundary conditions for this shell are met at the antinodal section (e.g., $x=l/2$ for $m=1$) of an SD-SD shell. All modal characteristics of $(u S_{x\theta} V_x w_{,x} - u S_{x\theta} V_x w_{,x})$ shells are similarly shifted by $\pi/2$.

Because in most cases the modes having the lowest frequencies are predominantly radial in nature ($A/C, B/C \ll 1$), lines where $w=0$ are usually called "nodal circles." In the case of *antisymmetric* modes ($m=2, 4, \dots$) of a circular cylindrical shell having symmetric boundary conditions, the nodal circle occurring at $x=l/2$ also has $v=0$, and the shear diaphragm boundary conditions are exactly reproduced at that section. Similarly, in the case of *symmetric* modes ($m=1, 3, \dots$) for *symmetric* boundary conditions, the complementary $(u S_{x\theta} V_x w_{,x})$ boundary conditions are exactly reproduced at $x=l/2$. This leads to the following two useful statements which can be applied to obtain further information from the problems having symmetric (with respect to $x=l/2$) boundary conditions:

(1) Frequencies and modal characteristics of a circular cylindrical shell having shear diaphragm ($N_x v w M_x$) boundary conditions at one end and any of the 16 possible sets of boundary conditions at the other end can be obtained directly from the *antisymmetric* modes of the problem having the same boundary conditions at both ends.

(2) Frequencies and modal characteristics of a circular cylindrical shell having complementary $(u S_{x\theta} V_x w_{,x})$ boundary conditions at one end and any of the 16 possible sets of boundary conditions at the other end can be obtained directly from the *symmetric* modes of the problem having the same boundary conditions at both ends.

Thus, for example, the results for the symmetric modes of a $(u v w w_{,x} - u v w w_{,x})$ shell can be applied to the problem of a $(u v w w_{,x} - u S_{x\theta} V_x w_{,x})$ shell.

Kondrashov (ref. 2.148) used the Donnell-

Mushtari theory and the Southwell method (cf., refs. 2.161 and 2.162) to obtain *lower bounds* for the frequency parameter Ω . This method depends upon finding the frequencies from two separate problems, one where the bending stiffness is neglected, and another where membrane effects are neglected. The sums of the squares of the two frequencies is then known to be less than or equal to the square of the actual frequency. The following formula was derived for computing lower bounds on Ω^2 :

$$\Omega^2 = (1 - \nu^2) C_1 + k n^4 C_2^2 \quad (2.146)$$

where $k = h^2/12R^2$, ν is Poisson's ratio, n = number of circumferential waves, and C_1 and C_2 are coefficients depending upon the particular boundary conditions of the shell. The coefficient C_1 arises from the membrane solution and depends only upon the membrane constraints ($u, v, N_x, S_{x\theta}$). Similarly, C_2 is found from the bending solution and depends only upon the boundary conditions involving $w, w_{,x}, V_x$, and M_x . There are 10 distinct membrane problems possible using all combinations of boundary conditions. Similarly, there are 10 distinct bending problems. When put together, these yield the 136 possible, distinct shell problems. Although Kondrashov gave extensive results, he only considered four sets of membrane conditions and six sets of bending conditions. Each set of conditions leads to a characteristic equation for the determination of either C_1 or C_2 . Four membrane and four bending characteristic equations have already been given for the clamped-clamped, clamped-SD clamped-free, and free-free problems. The remaining two bending equations include one for $(w M_x - w M_x)$ boundary conditions given by

$$\sin k_1 \xi_0 = 0 \quad (2.147)$$

and one for $(w M_x - V_x M_x)$ boundary conditions given by

$$\left[\frac{C_2 + 1}{C_2 - 1} \right]^{1/2} \left[\frac{C_2 - (1 - \nu)}{C_2 + (1 - \nu)} \right]^2 \sin k_1 \xi_0 \cosh k_2 \xi_0 - \cos k_1 \xi_0 \sinh k_2 \xi_0 = 0 \quad (2.148)$$

with $\xi_0 = nl/R$ and k_1 and k_2 given in equations (2.110). Roots of equation (2.147) are $k_1 \xi_0 = \pi, 2\pi, 3\pi, \dots$. Roots of equation (2.148) are given in table 2.42. The types of membrane and bending boundary conditions which can be accommo-

TABLE 2.42.—Values of the Coefficient C_2 in Equation (2.107) for $(w M_x - V_x M_x)$ Boundary Conditions

$n \frac{l}{R}$	Number of axial half-waves — m				
	0	1	2	3	4
2	1.416	5.190	13.720	27.410	47.700
3	1.201	2.970	6.760	12.730	20.900
4	1.114	2.158	4.305	7.665	11.226
5	1.070	1.764	3.155	5.300	8.250
6	1.047	1.542	2.521	4.022	6.030
7	1.033	1.402	2.132	3.238	4.640
8	1.025	1.312	1.877	2.775	3.878
9	1.019	1.247	1.698	2.375	3.285
10	1.015	1.201	1.570	2.120	2.864
12	1.007	1.140	1.400	1.787	2.305
14	1.005	1.102	1.296	1.584	1.965
16	1.000	1.077	1.227	1.447	1.744
18	1.000	1.061	1.178	1.355	1.590
20	1.0	1.048	1.147	1.288	1.480
22	1.0	1.041	1.121	1.240	1.398
24	1.0	1.033	1.102	1.202	1.334
26	1.0	1.029	1.086	1.172	1.288
28	1.0	1.025	1.073	1.148	1.247
30	1.0	1.021	1.064	1.128	1.214
32	1.0	1.017	1.056	1.112	1.188
36	1.0	1.014	1.042	1.086	1.141
40	1.0	1.012	1.038	1.072	1.122
42	1.0	1.009	1.032	1.061	1.103
44	1.0	1.008	1.030	1.059	1.100
48	1.0	1.007	1.022	1.046	1.083
50	1.0	1.006	1.018	1.044	1.078

dated by Kondrashov's results are summarized in table 2.43.

For example, one can find frequency parameters for $(uvw M_x - N_x v w w_x)$ shells by using values of C_1 and C_2 from tables 2.33 and 2.34, respectively, in equation (2.146). Thus the lower bounds predicted by this method are exactly the same as for the clamped-SD case. Both cases have the same separate membrane and bending problems. In using the tables care must be exercised in using numbers of axial half-waves which are compatible with the combined boundary conditions for the shell problem. Of course, the membrane and bending solutions are not entirely compatible in axial wave length to begin with; the accuracy of the bounds will be limited particularly in those modes where the bending and stretching strain energies are of comparable magnitude and coupling is significant.

Forsberg (ref. 272) wrote an excellent paper

TABLE 2.43.—Sources of Characteristic Equations and Their Roots for Use in Equation (2.146)

Boundary conditions	Characteristic equation	Roots
$uv - uv$	eq. (2.108)	table 2.25
$uv - N_x v$	eq. (2.116)	table 2.33
$uv - N_x N_{x\theta}$	e.q (2.123)	table 2.37
$N_x S_{x\theta} - N_x S_{x\theta}$	eq. (2.136)	table 2.40
$w w_x - w w_x$	eq. (2.109)	table 2.26
$w w_x - w M_x$	eq. (2.117)	table 2.34
$w w_x - V_x M_x$	eq. (2.124)	table 2.38
$V_x M_x - V_x M_x$	eq. (2.137)	table 2.41
$w M_x - w M_x$	eq. (2.147)	$\pi, 2\pi, 3\pi \dots$
$w M_x - V_x M_x$	eq. (2.148)	table 2.42

comparing the significance of types of boundary conditions upon free vibration frequencies and modal characteristics. The following 10 problems were considered in detail.

- Case:
1. $N_x v w M_x - N_x v w M_x$ (SD-SD)
 2. $N_x v w M_x - u v w M_x$
 3. $u v w M_x - u v w M_x$
 4. $N_x S_{x\theta} w M_x - N_x S_{x\theta} w M_x$
 5. $u S_{x\theta} w M_x - u S_{x\theta} w M_x$
 6. $N_x v w w_{,x} - N_x v w w_{,x}$
 7. $u v w_{,x} - u v w w_{,x}$
(clamped-clamped)
 8. $N_x S_{x\theta} w w_{,x} - N_x S_{x\theta} w w_{,x}$
 9. $u S_{x\theta} w w_{,x} - u S_{x\theta} w w_{,x}$
 10. $N_x v w M_x - u v w w_{,x}$ (SD-clamped)

Results were obtained by the exact procedure using the Flügge equations of motion. Tangential inertia terms were retained.

The effect of edge moment restraint ($w_{,x}=0$) is illustrated in figure 2.108. In this figure frequency envelopes (lowest frequencies) are plotted for various R/h ratios for cases 1 and 6. It is seen that the effect of fixing the slope at the boundary rapidly diminishes as l/R increases and is more important for thicker (small R/h) shells. The effect of moment restraint is also seen in figures 2.39 and 2.40, where, for the beam bending mode ($n=1$), relaxation of the $w_{,x}$ condition for the clamped-clamped shell (case 7) causes changes in Ω which are too small to plot.

The effect of axial constraint at the edge ($u=0$) is illustrated in figure 2.109. Here the frequency parameter envelope for an SD-SD shell without axial constraint is compared with that of one having axial constraint at one or both ends. In direct contrast to the previous case, the effect of axial constraint is significant even for very long shells and all values of R/h . The minimum frequency for case 3 is about 40 to 60 percent higher than that of case 1 throughout most of the region of interest.

The physical reason for the difference in the influence of $u=0$ as compared with $w_{,x}$ can be understood by examining the modal characteristics. From the modal characteristics of clamped-clamped shells (cf., figs. 2.59 through 2.72) it is seen that the influence of the condition $w_{,x}=0$ is localized to the boundary region (unless the shell is relatively short and thick), whereas the membrane forces caused by $u=0$ perpetuate throughout the length of the shell.

Consider next the relation of the circumferential restraint $v=0$. The effects of this con-

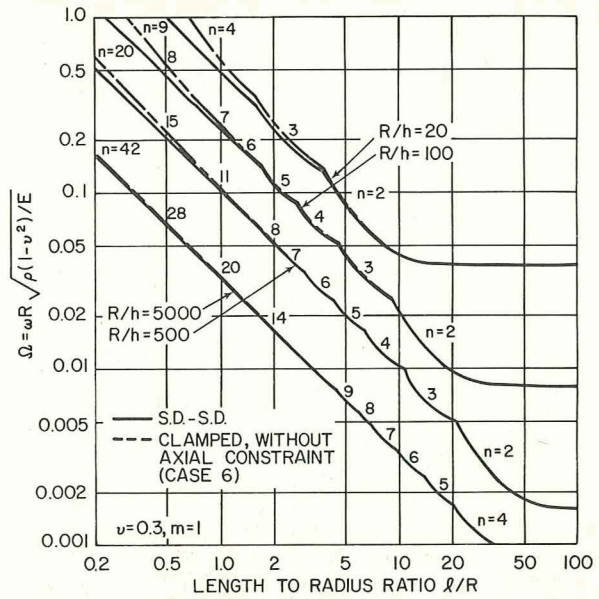


FIGURE 2.108.—Effect of slope restraint ($w_{,x}=0$) upon envelopes for Ω . (After ref. 2.72)

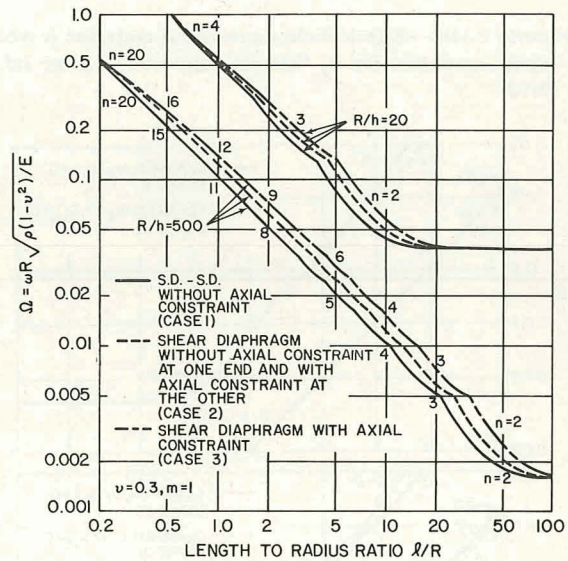


FIGURE 2.109.—Effect of axial restraint ($u=0$) upon envelopes for Ω . (After ref. 2.72)

straint can be observed in figures 2.110 and 2.111. In figure 2.110 various types of "simple support" conditions are used (i.e., all have $w=M_x=0$ at both ends). In figure 2.111 all have "clamped" types (i.e., $w=w_{,x}=0$ at both ends) of boundary conditions. It is clear from these figures that the effects of $v=0$ are more

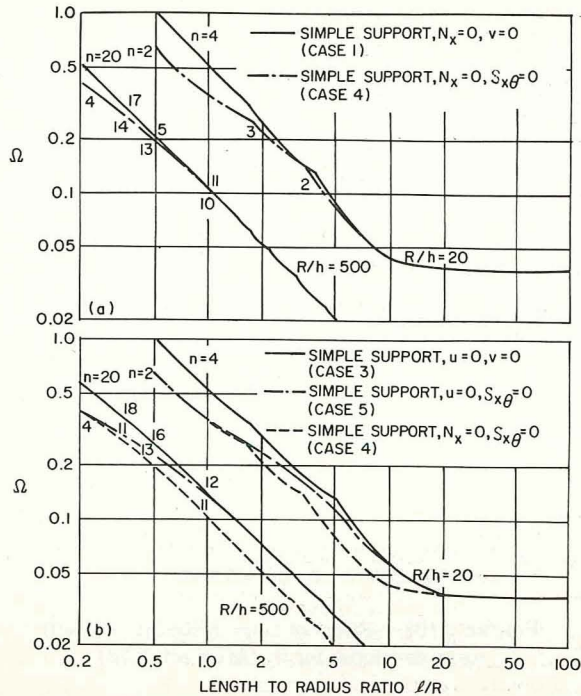


FIGURE 2.110.—Effect of circumferential restraint ($v=0$) upon envelopes for Ω ; “simple supports.” (After ref. 2.72)

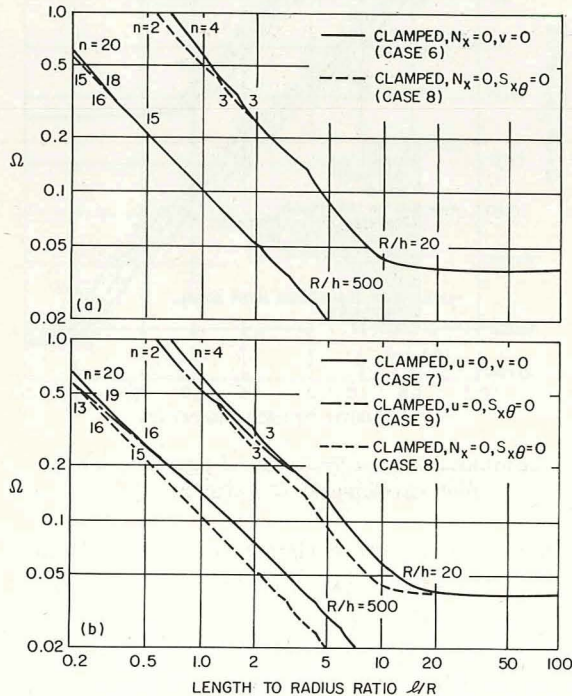


FIGURE 2.111.—Effect of circumferential restraint upon envelopes for Ω ; “clamped” ends. (After ref. 2.72)

important for short and thick shells and become less important than the effects of $u=0$ for long shells. As pointed out in reference 2.72 the greatest change in frequency due to relaxing the condition $v=0$ occurs for $n=1$.

In another very useful paper (ref. 2.73) Forsberg investigated the accuracy of representing a shell by a rod for the axisymmetric ($n=0$) mode and by a beam for the overall bending ($n=1$) mode. Solutions using these beam and rod models were compared with the exact solutions from Flügge's theory. For the $n=0$ and $n=1$ modes, the response of the shell is governed almost entirely by the membrane behavior. This means that the modal characteristics are essentially independent of the bending stiffness (i.e., independent of R/h) and those boundary conditions involving the tangential displacements (u , v) or the force resultant (N_x , $S_{x\theta}$) are the ones of prime significance. In general the boundary restraints placed upon w , v_x , M_x , and V_x have no significant influence on the frequencies; their effects on the moment resultants are localized to a small zone near the boundary. This permits the beam and rod representations of shell problems to be suitable over wide ranges of interest. However, if one is interested in modes having short axial wave lengths ($l/mR < 1$) the beam and rod models may be inadequate. These statements are elaborated upon below.

For $n=0$ the equations of motion uncouple, regardless of the boundary conditions (cf., eqs. 2.21), yielding a second-order differential equation involving v only and a sixth-order set involving u and w . The torsional frequency is the same if $v=0$ at $x=0$, l or if $S_{x\theta}=0$ at $x=0$, l . Having both ends fixed results (from symmetry) in having the middle section ($x=l/2$) free, and vice versa. If $v=0$ at $x=0$ and $S_{x\theta}=0$ at $x=l$, then the effective length of the mode shape is twice as long and the frequency is half as great. These frequencies are shown in figure 2.112.

Considering the radial and longitudinal modes for $n=0$, figure 2.112 shows that for small axial wave lengths the bending stiffness does make a difference in Ω ; however, for $l/mR > 1$ the frequency varies by less than one-half of 1 percent (ref. 2.73). The boundary conditions on u do have significant influence on Ω , even for those modes which are predominantly radial. If the

shell is axially restrained at one end ($u=0$) and is axially free at the other ($N_x=0$) and if $l/mR > 3$, the minimum frequency is one-half that obtained when $u=0$ at both ends (see fig. 2.112). The restraints placed on w cause less than 0.5 percent change in Ω . In the transition region $1 < l/mR < 5$ the amplitudes of the radial and longitudinal displacement components are nearly equal. This coupling is due entirely to the Poisson effect—bending effects are negligible. If $\nu=0$, the equations of motion would effectively (depending to a small extent upon the shell theory used) reduce to three uncoupled equations of motion representing torsional, radial, and longitudinal behavior independently. The effects of neglecting tangential inertia terms were already seen in figure 2.34. Reference 2.73 shows that one could make reasonable estimates of natural frequencies in the axisymmetric mode by considering the shell to be a bar for longitudinal motions and to be a ring in plane stress for small l/mR , or plain strain for large l/mR , and that these approximations break down in the transition region $1 < l/mR < 5$.

Generally speaking, regardless of the boundary conditions, the lowest of the three frequencies arising for $n=1$ corresponds to motion which is

beam-like (ref. 2.73). For very long shells, v and w are essentially equally large, and the motion consists of rigid body translations of cross sections. As the shell becomes shorter, the circumferential displacement v becomes gradually larger than w up to an l/mR ratio of about 5; for still shorter shells v decreases until, for very short shells ($l/R \approx 0.1$), v is nearly zero and the motion is almost entirely radial. As in the case for $n=0$, the behavior is governed primarily by the membrane stiffness of the shell and the tangential boundary conditions. For $n=1$, v is not uncoupled, and its presence in the boundary conditions is very significant.

If $v=0$ at both ends of the shell, then Ω is essentially independent of the bending stiffness of the shell unless the axial half-wave length becomes small enough (e.g., $l/mR < 1$ for $R/h=20$, $l/mR < 0.1$ for $R/h=500$) (ref. 2.73). The frequency spectrum for beam-type of behavior is shown in figure 2.113. Three cases are included for which the shell acts as (1) a free-free beam, (2) a simply-supported beam, and (3) a clamped beam. The transverse conditions involving w , w_x , V_x , M_x have no measurable influence on the

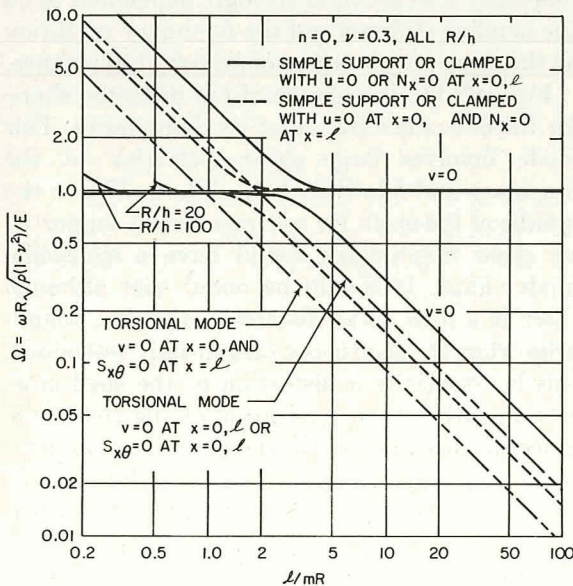


FIGURE 2.112.—Axisymmetric ($n=0$) frequency parameters for arbitrary boundary condition; $m=1$. (After ref. 2.73)

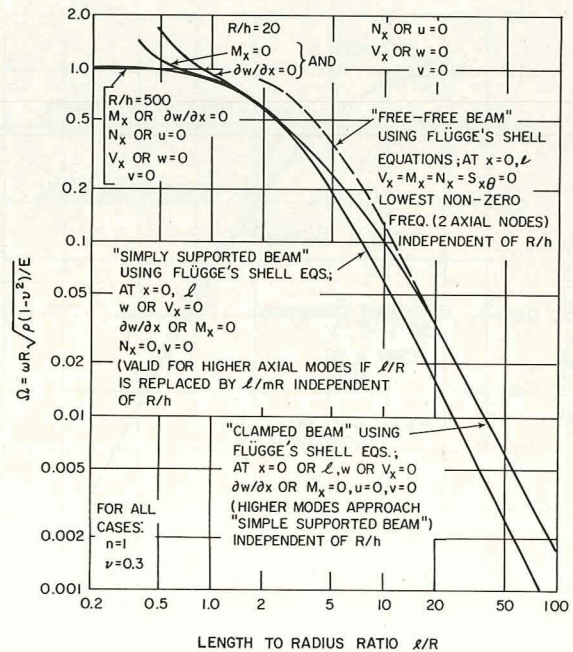


FIGURE 2.113.—Frequency spectrum for beam-like ($n=1$) modes of circular cylindrical shells; $m=1$. (After ref. 2.73)

frequency spectrum (ref. 2.73). The shell is forced to behave as a clamped beam by requiring $u=0$ at the boundaries.

Comparison of the shell frequencies with beam frequencies is made in figure 2.114 (ref. 2.73) for the "simply supported" beam. The simple (Euler-Bernoulli beam theory) approximation gives good results only for long shells ($l/mR > 20$). This is consistent with the usual assumptions of simple beam theory regarding limits of the length/depth ratio. Inclusion of shear deformation and rotary inertia effects (Timoshenko beam theory) greatly improves the accuracy of the beam approximation and makes it acceptable as low as $l/mR = 7$. It is important to note that the shell equations automatically include the shear deformation and rotary inertia effects of the overall cross sections, even though the local effects through the shell thickness are neglected in the eighth order shell theory. Similar comparisons were made in reference 2.73 for the clamped-clamped beam, and behavior essentially the same as figure 2.114 was found. For an even more sophisticated beam model to represent the beam-like modes of a shell, see the discussion of the work by Simmonds (ref. 2.128) in section 2.3.5.

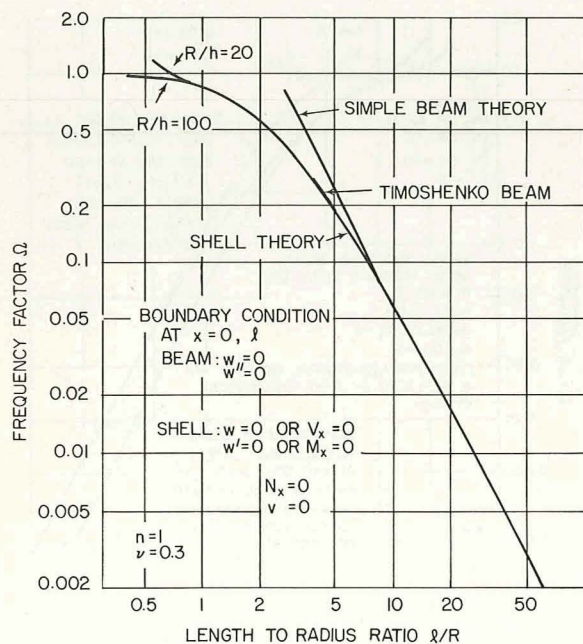


FIGURE 2.114.—Comparison of shell frequencies ($n=1$) with those of a simple-supported beam; $m=1$. (After ref. 2.73)

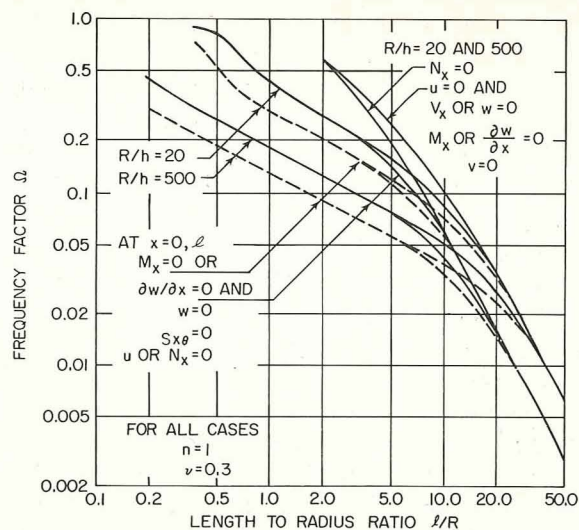
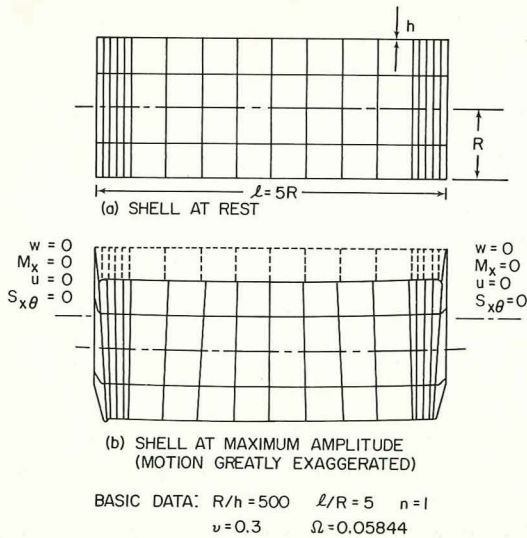


FIGURE 2.115.—Effect of the boundary condition $v=0$ upon the frequencies; $m=1$, $n=1$. (After ref. 2.73)

The importance of the circumferential displacement v in the $n=1$ mode is shown in figure 2.115 (from ref. 2.73). Two sets of curves are depicted. One set has $v=0$ as a boundary condition at both ends of the shell; the other set has $S_{x\theta}=0$, and gives a considerable drop in frequencies except for long ($l/R > 20$) shells where beam theory becomes applicable. When $S_{x\theta}=0$ on the ends the frequency also becomes strongly dependent upon the bending stiffness and the boundary condition on the slope ($w_{,x}$) becomes of primary importance.

Figure 2.116 is a sketch of the deflected shape for the case when $S_{x\theta}=0$ at the boundaries. This mode involves large shear distortion at the boundary and relatively little deformation in the middle of the shell. By contrast a shell supported by shear diaphragms would have a sinusoidal mode shape. It should be noted that although there is a high shear distortion near the boundaries when the shell is not tangentially restrained, this is essentially a distortion of the shell cross section rather than a shearing of the shell wall. Since the distortion of the shell cross section takes place in a region about 75 times as long as the shell wall thickness, it is certain that the shear effects on the shell wall can be neglected. One should also note that the slope $w_{,x}$ near the boundary is very large compared to the slope computed for other mode shapes which have one axial half-wave and a unit radial deflection. The amplitude



THE DEFORMATION OF THE SHELL HAS BEEN GREATLY EXAGGERATED IN ORDER TO ILLUSTRATE THE GENERAL CHARACTER OF THE MOTION. THE LONGITUDINAL MOTION HAS BEEN MAGNIFIED BY A FACTOR OF 20 COMPARED WITH THE RELATIVE RADIAL DISPLACEMENT.

FIGURE 2.116.—Sketch of deformed shell when $S_{x\theta}=0$ at boundaries; $m=1$, $n=1$. (After ref. 2.73)

of vibration can always be kept small enough so that the resulting motion is linear; however, it is evident that nonlinear behavior will occur for smaller amplitudes for this mode shape than for the more usual case.

To better understand the dynamic behavior of a cylindrical shell in the beam-type mode, it is necessary to examine the modal displacements and modal forces that correspond to the minimum frequency. In figures 2.117 and 2.118 (from ref. 2.73) results are presented for a shell having an R/h ratio of 20 and l/R ratios of 5 and 10. Two sets of boundary conditions are considered, SD-SD and $(N_x \nu V_x M_x)$. There is no noticeable difference in the mode shapes and force distribution, although the amplitude ratio A/C is different, and the frequency is extremely close for these two sets of boundary conditions. This again emphasizes that the behavior when $\nu=0$ at the boundaries is essentially extensional in character. The maximum bending stress is less than 7 percent of the maximum membrane stress. For the shell which is not radially restrained, there is a slight distortion in the moment diagram which is barely noticeable in figure 2.118. As in the axi-

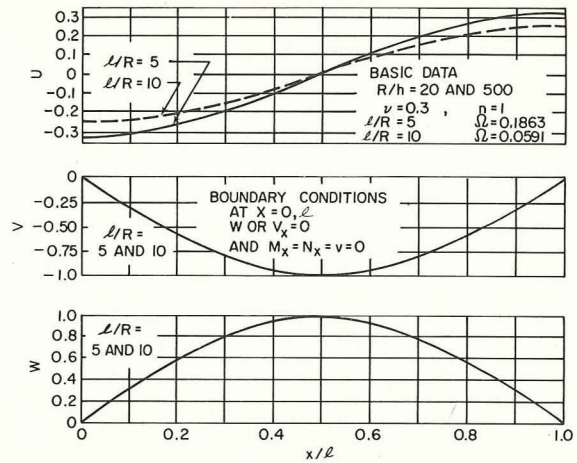


FIGURE 2.117.—Mode shapes for SD-SD and $(N_x \nu V_x M_x - N_x \nu V_x M_x)$ shells; $R/h=20$ and 500 , $\nu=0.3$, $m=1$, $n=1$. (After ref. 2.73)

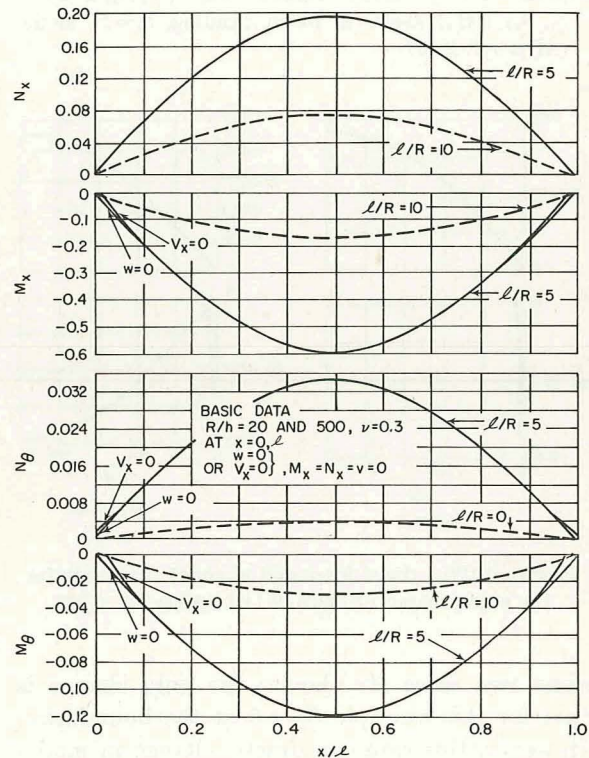


FIGURE 2.118.—Force and moment resultants for the mode shapes of figure 2.117. (After ref. 2.73)

symmetric case the noticeable change in force distribution occurs for the shear force V_x and again as in the above case, this change is entirely local in character. In figures 2.119 and 2.120 the

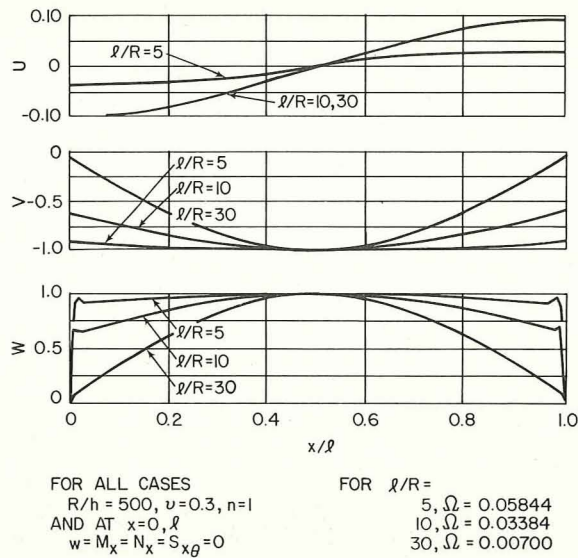


FIGURE 2.119.—Mode shapes for $(N_x S_{x\theta} w M_x - N_x S_{x\theta} w M_x)$ shells in beam bending ($n=1$) mode. (After ref. 2.73)

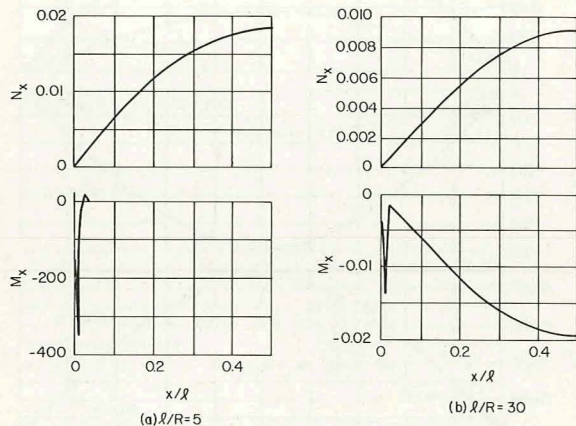


FIGURE 2.120.—Axial force and moment resultants for the mode shapes of figure 2.119. (After ref. 2.73)

same two cases are shown; the only change is that for this example $S_{x\theta} = 0$ at the boundaries. However, this causes a drastic change in modal character. As the l/R ratio is reduced, the effects of the radial restraint at the boundaries becomes more and more localized and, as it becomes small, this mode becomes a simple lateral rigid body translation with end effects. This mode represents essentially a lateral translation of a beam on soft shear springs at the boundary. This

characteristic is reflected not only in the mode shape but also in the internal force distribution.

The higher modes of this shell when $S_{x\theta} = 0$ at the boundaries again represent essentially the behavior of a free-free beam on shear springs. The second mode represents a rigid body rotation of a beam about its center with weak shear springs at the boundary as can be seen in figure 2.121. The third mode ($m=3$) introduces appreciable flexible deformation of the shell as a beam, but is similar to the lowest non-zero mode for a free-free shell shown previously in figure 2.106. It is clear then that the dependence of the frequency and force distribution on the bending stiffness when $S_{x\theta} = 0$ arises only from the high shear distortion which occurs near the boundary, which can be represented as a very weak shear spring.

One of the important quantities used in determining forced response by modal analysis is the generalized mass. The generalized mass is defined as

$$\mu = \int_{\text{vol.}} (u^2 + v^2 + w^2) dm$$

where the dependence of time has been removed and μ obviously depends upon n .

For a simply supported beam having a unit transverse displacement, one can easily show

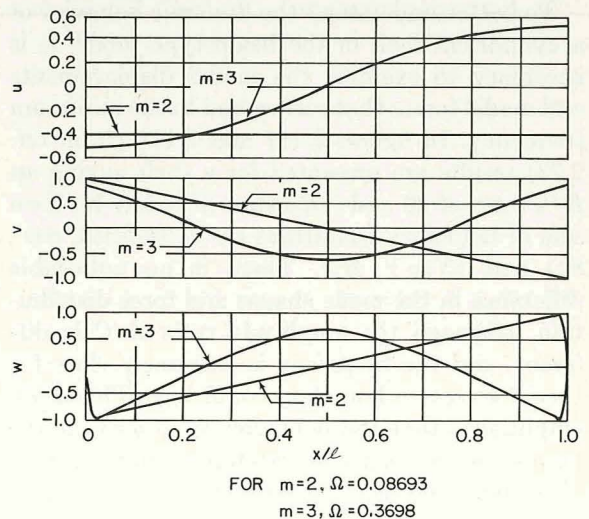


FIGURE 2.121.—Higher beam bending ($n=1$) mode shapes ($n=2, 3$) for a $(N_x S_{x\theta} w M_x - N_x S_{x\theta} w M_x)$ shell; $R/h=500$, $l/R=5$, $\nu=0.3$. (After ref. 2.73)

that the generalized mass for all the modes is equal to one-half and is independent of the l/R ratio of the beam. For a clamped beam having a unit transverse displacement, the integration is more complicated, but the formula is relatively simple and one finds that for the lowest mode the beam equations yield a value of $\mu = 0.39$. These values are plotted in figure 2.122 (from ref. 2.73). Use of Timoshenko beam theory when rotary inertia is included leads to a generalized mass which varies with l/R for the beam; the generalized mass increases as the length decreases, as indicated in figure 2.122. From shell theory it is found that the generalized mass approaches beam theory results asymptotically for a long shell. As the shell becomes shorter the behavior is adequately represented by the Timoshenko beam theory for shell with a l/R ratio greater than about 7. For shorter shells the deviation between shell theory and beam theory becomes significant. The behavior outlined above holds exactly for higher modes of a freely supported beam (use l/mR in fig. 2.122), and is essentially the same for a clamped beam. The significance of the deviation between shell theory and beam theory and its importance in determining forced response quantities has not been entirely established.

The $(u v w M_x - u v w M_x)$ shell has received a small amount of attention in the literature. In addition to the analysis by Forsberg (refs. 2.72 and 2.73) described earlier in this section, the small effect of relaxing the clamping restraint

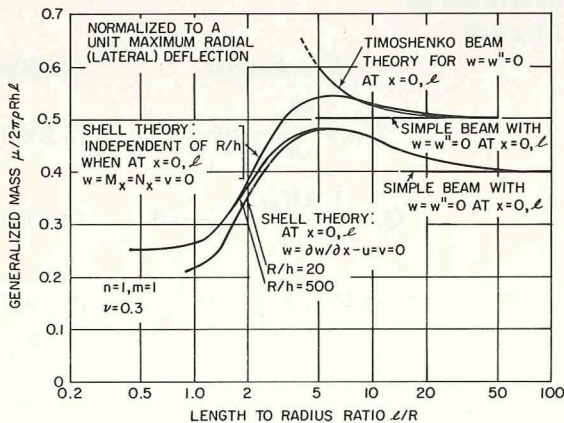


FIGURE 2.122.—Comparison of generalized mass as predicted by beam and shell theory. (After ref. 2.73)

(w_x) at the boundary was also shown in figures 2.39 and 2.40 of section 2.4.1. Ivanyuta and Finkelshtein (ref. 2.114) used the Donnell-Mushtari shell equations and the Galerkin approximate procedure with a single set of beam functions to arrive at the following equation for frequency parameters:

$$\Omega^2 = \frac{(1-\nu^2)\lambda_m^2(m\pi R/l)^2}{2.29(\lambda_m^4 + n^4 + 1.110n^2\lambda_m^2)} + \frac{1}{12}\left(\frac{h}{R}\right)^2(\lambda_m^2 + n^2)^2 \quad (2.149)$$

where λ_m is given by equation (2.105). Lower bounds for this problem can also be computed by using equation (2.146). These are also the "freely supported" boundary conditions posed in references 2.32, 2.33, and 2.34, although the condition $u=0$ was not enforced, and the SD-SD problem was eventually solved along with the statement that the condition " $u=0$ is the least essential one." As we have seen elsewhere in this section, the condition $u=0$ is indeed a very important one.

The axisymmetric modal characteristics for the lowest frequency of a $(u w M_x - u w M_x)$ shell are depicted in figure 2.123 (from ref. 2.73) in comparison with those of the SD-SD shell. It is interesting to note that

(1) The fundamental mode in this case has a nodal circle at $x=l/2$.

(2) The curves for u and N_x are essentially the same as those for the SD-SD shell, except shifted by $\pi/2$.

(3) The curve for w is also shifted by $\pi/2$ but, in addition, has boundary zones where w must rapidly change to zero to meet the boundary conditions.

(4) The rapid change in w near the boundary causes large curvature changes and, consequently, large M_x near the boundary, although the maximum bending stress is still less than 21 percent of the maximum direct stress (ref. 2.73).

(5) In spite of the large differences in w and M_x from those of the SD-SD shell, the axial effects predominate, and the frequencies only differ by 0.5 percent.

The axisymmetric modal characteristics for the lowest frequency of a $(N_x w w_x - u w M_x)$ shell (remembering that the circumferential displace-

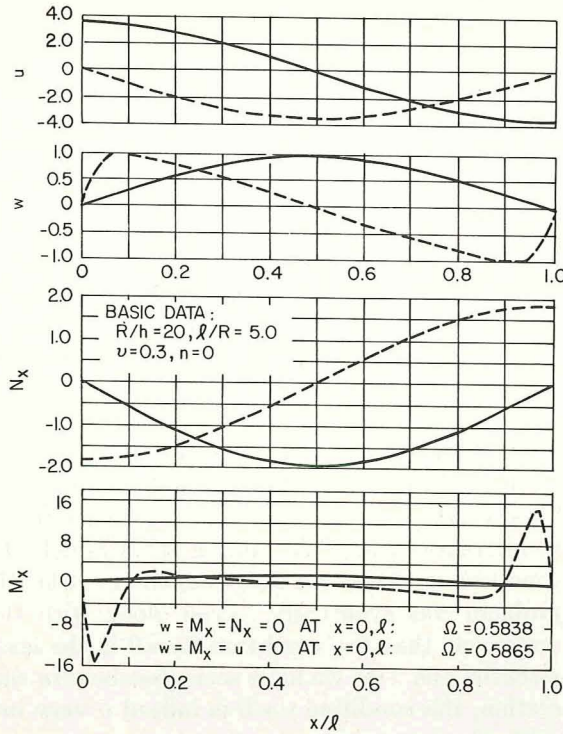


FIGURE 2.123.—Axisymmetric ($n=0$) modal characteristics of a ($u w M_x - u w M_x$) shell compared with an SD-SD shell. (After ref. 2.73)

ment v is uncoupled for $n=0$) are displayed in figure 2.124 (from ref. 2.73). Here the edge effects are much more localized than those of figure 2.123 because the shell is much thinner ($R/h=20$, in comparison with $R/h=500$). The small, but abrupt change in M_x near $x=0$ is due to the condition $w_{,x}=0$. The larger change near $x=l$ arises from requiring both u and w to be zero at $x=l$.

The ($N_x v w w_{,x} - N_x v w w_{,x}$) case was used by Filippov (ref. 2.97) to demonstrate the solution of free vibration problems for circular cylindrical shells by the series method. A set of equations of motion for the shell attributed to Galerkin was used. For $R/h=83.3$, $l/R=2$, $\nu=1/6$, $m=1$, $n=4$, a frequency increase of 2.0 percent from the SD-SD frequency was calculated.

The ($u v w M_x - N_x S_{x\theta} V_x M_x$) shell was used to model a storage tank in references 2.185 and 2.186. Methods for computing frequencies and mode shapes were developed according to the membrane theory, and procedures for including the bending strain energy were subsequently added. No specific numerical results were given.

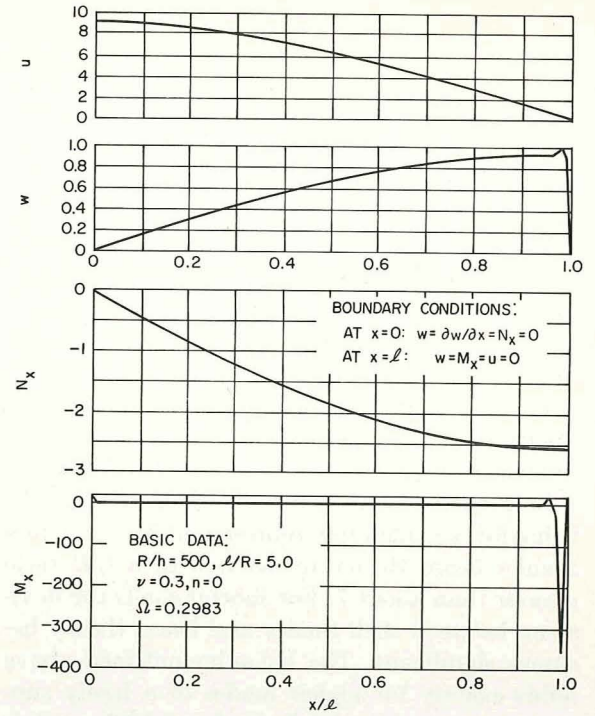


FIGURE 2.124.—Axisymmetric ($n=0$) modal characteristics of a ($N_x w w_{,x} - u w M_x$) shell. (After ref. 2.73)

2.5 ELASTIC SUPPORTS

Boundary conditions of elastic supports at the ends of a circular cylindrical shell are generalizations of the simple boundary conditions discussed in the previous sections of this chapter. In complete generality, the boundary conditions for this case (neglecting damping effects, of course) can be written as

At $x=0$:

$$N_x - k_1 u = 0 \quad (2.150a)$$

$$N_{x\theta} + \frac{M_{x\theta}}{R} - k_2 v = 0 \quad (2.150b)$$

$$Q_x + \frac{1}{R} \frac{\partial M_{x\theta}}{\partial \theta} - k_3 w = 0 \quad (2.150c)$$

$$M_x + k_4 \frac{\partial w}{\partial x} = 0 \quad (2.150d)$$

At $x=l$:

$$N_x + k_5 u = 0 \quad (2.150e)$$

$$N_{x\theta} + \frac{M_{x\theta}}{R} + k_6 v = 0 \quad (2.150f)$$

$$Q_x + \frac{1}{R} \frac{\partial M_{x\theta}}{\partial \theta} + k_7 w = 0 \quad (2.150g)$$

$$M_x - k_8 \frac{\partial w}{\partial x} = 0 \quad (2.150h)$$

where k_1, \dots, k_8 are the distributed stiffness coefficients associated with the elastic supporting structure. It is assumed that the supporting structure has axisymmetric stiffness with respect to the axis of the shell; otherwise k_1, \dots, k_8 would not be constants, but functions of θ . Careful attention must be given to the signs of the terms containing the spring constants in equations (2.150) if meaningful results are to be obtained. All of the 136 sets of boundary conditions discussed previously in this chapter can be obtained as special cases of equations (2.150) by simply setting the appropriate constants k_i equal to either zero or infinity.

The distinction is carefully made here that the stiffness of the support structure must be capable of being represented by the distributed spring constants k_1, \dots, k_8 . Consider a circular cylindrical shell with a stiffening ring at the end. If it is necessary to consider the equations of motion of the ring simultaneously with the equations of motion of shell, with conditions of continuity of generalized forces and displacements enforced at the junction, the ring-shell combination is considered herein to be a structure. Vibrations of structures containing shells as structural elements are purposely omitted from this work because of the obvious geometrical complexities and limitless combinations which can arise.

The problem of the circular cylindrical shell supported elastically is possible of being solved exactly in all its generality by the procedure outlined in section 2.4. That is, once the λ_i are determined as the roots of equation (2.54), thereby satisfying the equations of motion, the boundary condition equations (2.150) can then be written, yielding an eighth order determinant, the roots of which are the frequency parameters. However, in the general determinant arising from equations (2.150) there would be no simplification and its expanded form would be extremely lengthy. Britvec (ref. 2.187) followed this procedure for the special case when all the k_i are zero except k_4 and k_8 , and also admitted damping terms into the moment boundary conditions. In reference 2.187

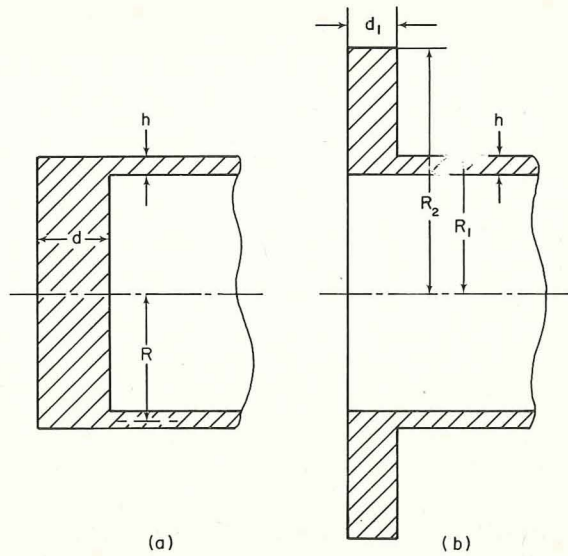


FIGURE 2.125.—Solid (a) and flanged (b) elastic end constraints. (After ref. 2.4)

the resulting eighth order determinant is given in detail, but will not be repeated here. No numerical results were given.

Arnold and Warburton (ref. 2.4) studied circular cylindrical shells having elastic end restraints of the two types depicted in figure 2.125. Figure 2.125(a) shows a cylinder with a solid end, (b) a flanged end. The inertias of these types of ends can, of course, be neglected because the motions at the ends are negligible. Using the "equivalent wave length" concept Arnold and Warburton wrote equation (2.99) as

$$\lambda_e = (m+c) \frac{\pi R}{l} \quad (2.151)$$

where, of course, $c = ml_0/l - l_0$ to be consistent with equation (2.99). For the cylinder with solid ends they proposed

$$c = 0.3e^{-qh/d} \quad (2.152)$$

as an empirical relationship for c , with d as shown in figure 2.125 and q a constant to be determined. To study the effect of changing d , and to determine c , experiments were conducted on a shell having $R = 1.924$ in., $h = 0.101$ in., $l = 7.81$ in. by changing d on one end such that the ratio h/d took on the values 0.050, 0.101, 0.202, 0.376, 0.595, and 1.000. On the other end, SD-SD boundary conditions were duplicated. The results

of these experiments are shown by the dashed curves in figure 2.126. In figure 2.126 the percentage difference in frequency from that of the SD-SD shell is plotted versus end thickness d . The solid curves are obtained by taking $q=2$ in equation (2.152), and using 0.15 instead of 0.3 because the SD boundary condition is the same as a nodal circle for the $m=2$ mode of a shell of twice the length having solid ends at $x=0$ and l , giving

$$\lambda_e = (m + 0.15e^{-2h/d}) \frac{\pi R}{l} \quad (2.153)$$

as the basis for the curves. Of course, $d/h \rightarrow 0$ is equivalent to an SD support at the solid end. For two cases, $n=4, m=2$ and $n=4, m=3$, the experimental and theoretical curves are essentially coincident, and have been shown by a single solid curve in figure 2.126.

Miserentino and Vosteen (ref. 2.188) used Arnold and Warburton's "effective wave length" concept to compare extensive results obtained for clamped-clamped shells with theoretical results for SD-SD shells using the Donnell-Mushtari theory.

In reference 2.4 flanged ends (fig. 2.125) were accommodated by a formula giving an equivalent thickness for solid ends as follows:

$$d = \left[\frac{\eta^2 - 1}{\left(\frac{1+\nu}{1-\nu} \right) \eta^2 + 1} \right]^{1/3} d_1 \quad (2.154)$$

where $\eta = R_2/R_1$ and d_1, R_1, R_2 are shown in figure 2.125. The formula is based upon treating

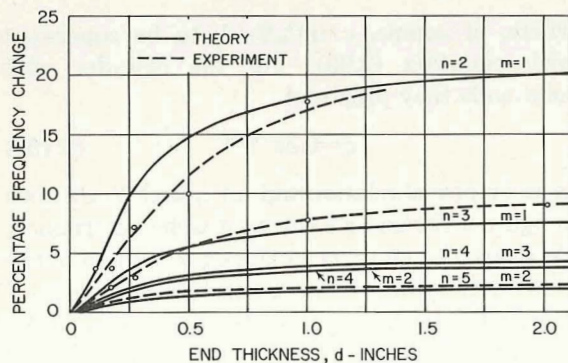


FIGURE 2.126.—Effect of end thickness on frequency; $R/h=19.1, l/R=4.05, h=0.101$ in. (After ref. 2.4)

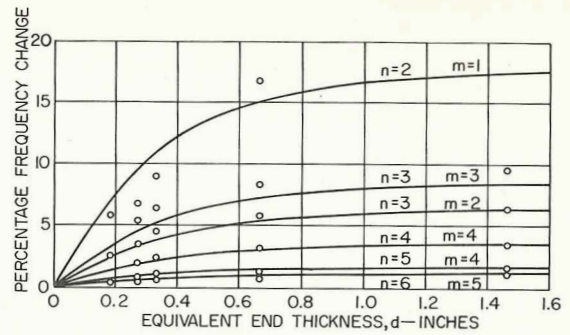


FIGURE 2.127.—Effect of flange dimensions on frequency; $R/h=19.1, l/R=8.13, h=0.101$ in. (After ref. 2.4)

the flange as a circular plate in bending. As $d_1 \rightarrow 0, d \rightarrow 0$ as for an SD support. And as $\eta \rightarrow \infty, d \rightarrow 0.82 d_1$; thus, using equation (2.154) a flange, however large, can never give the same degree of end restraint as a solid end having the same thickness. Experiments were conducted on a steel shell having $R=1.924$ in., $h=0.101$ in., and $l=15.65$ in. having flanges at both ends, and the results are shown by the points in figure 2.127. The solid curves are based on theoretical results using equation 2.154.

In reference 2.151 an attempt was made to simulate an aluminum shell having clamped ends by machining integral rings at each end of an aluminum shell. The shell dimensions were $l=6.00$ in., $R=4.69$ in., $h=0.026$ in. and the rings were each 1 inch long and 1/2 inch thick. However, these rings were insufficiently rigid and were actually elastic constraints giving the frequencies shown in figure 2.128.

Considering the beam bending mode ($n=1$) of a circular cylindrical shell, it was pointed out in reference 2.73 that the vibration frequencies and modal characteristics are strongly influenced by the degree of circumferential restraint (i.e., the magnitudes of k_2 and k_6) at the boundaries (cf. sec. 2.4.6). In reference 2.73 a ring of square cross section having a side equal to 8 times the shell thickness is necessary to provide enough circumferential stiffness to simulate the simple boundary condition $v=0$. Quantitative results are shown in figure 2.129 where a stiffening ring of square cross section is added to each end of a shell. The width and depth of the ring are denoted by H . The other boundary conditions at $x=0$ and $x=l$ are $w=M_x=u=0$. The mass of the ring is

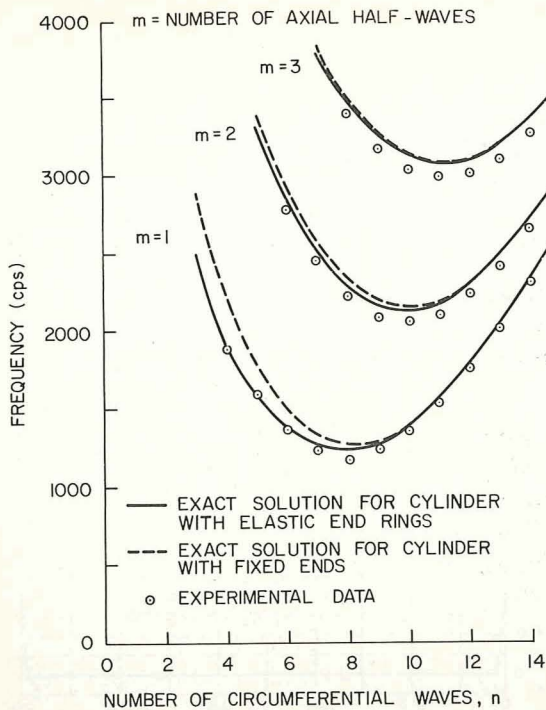


FIGURE 2.128.—Comparison of theoretical and experimental frequencies for clamped-clamped and elastically supported cylinders; $R/h=180$, $l/R=1.27$, $E=10^7$ psi. (After ref. 2.151)

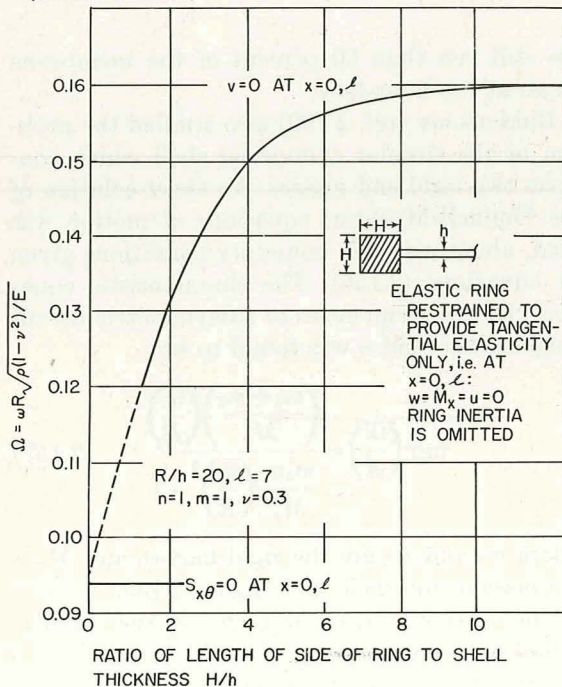


FIGURE 2.129.—Effect of circumferential stiffening upon frequencies; $R/h=20$, $l/R=7$, $m=1$, $n=1$, $\nu=0.3$. (After ref. 2.73)

neglected. The frequency parameter Ω is plotted versus H/h between the limiting boundary conditions $S_{x\theta}=0$ and $\nu=0$.

Circular cylindrical shells with elastic end supports are also briefly discussed in references 2.49, 2.98, and 2.189.

2.6 ADDED MASS

In this section the effects of adding lumped mass to a shell will be considered. Information for at least the following two types of problems is available:

- (1) The rigid ring mass attached to either one or both ends of the shell. In this case the mass enters through the shell boundary conditions.
- (2) An internal point mass. This is accommodated in the equations of motion by a double Fourier series solution.

An internal rigid ring mass usually implies separating the shell into two portions and combining them by means of equations of continuity. Such a configuration is considered herein as a structure and will not be discussed.

Consider the axisymmetric longitudinal motion of circular cylindrical shells. The primary effect of stiffening rings in these modes is to add additional mass to the system, thereby reducing the overall frequency. The magnitude of the frequency reduction depends upon the location of the ring; a ring placed at either a longitudinal or circumferential displacement nodal circle will add no significant mass to the system for that mode.

Forsberg (ref. 2.73) considered the case where ring masses m_1 and m_2 which are large compared to the total mass of the shell M_s are attached at the ends of the shell as shown in figure 2.130. If half of the mass of the shell is lumped at each end as shown, then the frequency parameter for the spring-mass system shown can then be obtained from

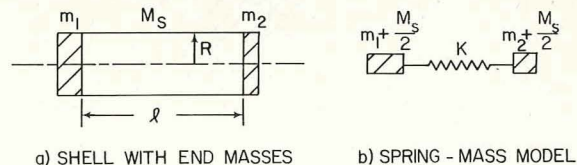


FIGURE 2.130.—Modeling of a shell having large end masses. (After ref. 2.73)

$$\Omega^2 = (1 - \nu^2) \frac{(m_1 + m_2 + M_s) M_s}{\left(m_1 + \frac{M_s}{2}\right) \left(m_2 + \frac{M_s}{2}\right)} \left(\frac{R}{l}\right)^2 \quad (2.155)$$

The variation of Ω with l/R according to equation (2.155) is plotted by dashed lines in figure 2.131 for several values of the total mass $m_T = m_1 + m_2 + M_s$, for $m_1 = 2m_2$ and $\nu = 0.3$. The solid curves represent the lowest frequencies arising from solution of the shell vibration problem having the boundary conditions

$$w = \frac{\partial w}{\partial x} = N_x + m_i \frac{\partial^2 u}{\partial t^2} = 0 \quad (2.156)$$

where $m_i = -m_1$ at $x=0$ and $+m_2$ at $x=l$ and $R/h=500$. In figure 2.131 the accurate frequencies for $m_T/M_s = 10$ are slightly greater than those predicted by equation (2.155) for large l/R ratios.

The modal characteristics obtained from the shell equations for the above problem are shown in figure 2.132. As the ratio of the total mass to the shell mass (m_T/M_s) increases, the node for the longitudinal displacement gradually approaches the one-third point of the shell length. The radial displacement gradually increases until it is almost uniform along the length of the shell, except for sharp changes near the boundaries. As m_T/M_s increases, N_x changes from a sinusoidal variation to be nearly uniform along the length, and M_x becomes more localized and sharply changing at the boundaries. However, the bending stresses

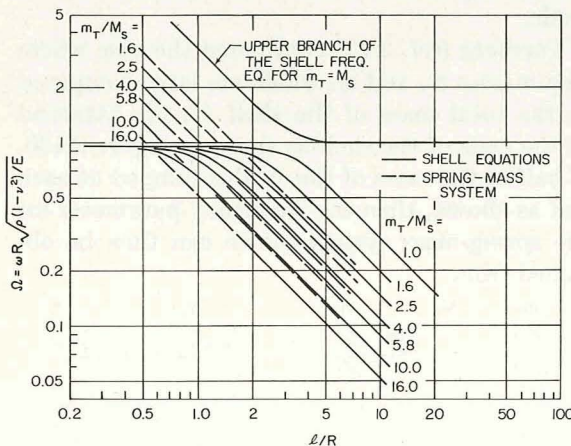


FIGURE 2.131.—Frequency parameters for a shell with unequal end masses. (After ref. 2.73)

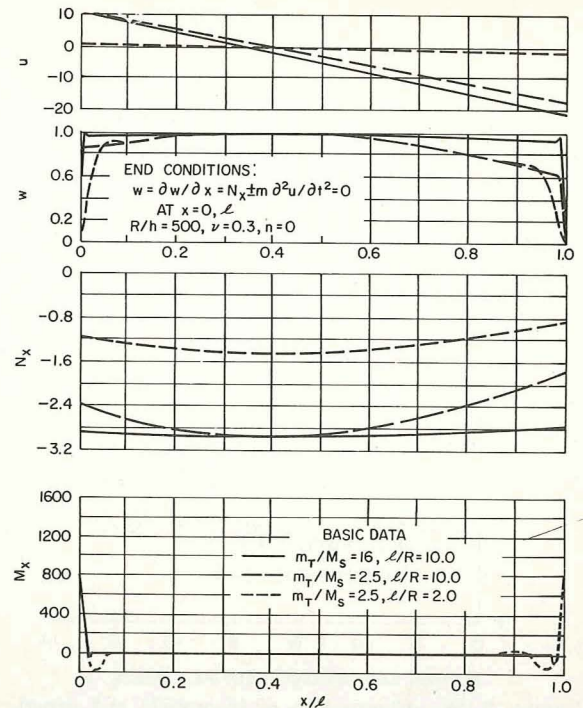


FIGURE 2.132.—Modal characteristics for a shell having large end masses. (After ref. 2.73)

are still less than 60 percent of the membrane stress at the boundary.

Bukharinov (ref. 2.190) also studied the problem of the circular cylindrical shell which connects two rigid end masses. An exact solution of the Donnell-Mushtari equations of motion was used, along with the boundary conditions given by equations (2.156). The characteristic equation yielding frequencies of axisymmetric ($n=0$) longitudinal modes was found to be

$$\tan\left(\frac{\Omega l}{R}\right) = \frac{\left(\frac{m_1 + m_2}{M_s}\right) \left(\frac{\Omega l}{R}\right)}{\frac{m_1 m_2}{M_s^2} \left(\frac{\Omega l}{R}\right)^2 - 1} \quad (2.157)$$

where m_1 and m_2 are the rigid masses and M_s is the mass of the shell, as in figure 2.130.

The free vibration problem of the circular cylindrical shell having end masses was also briefly discussed in references 2.191. The problem for the shell having one end free and the other end attached to a rigid mass was formulated in reference 2.192, but no results were obtained.

The SD-SD shell with a concentrated mass was considered in reference 2.193. A number of papers and reports exist which deal with stiffened circular cylindrical shells, where the stiffness have both flexibility and mass. However, such configurations are considered to be structures and will not be included here.

Some interesting results were given in reference 2.166 for the case of the clamped-free shell having a single stiffening ring at the free end. The stiffening ring was of the same material as the shell, thereby being elastic as well as having mass. The increased rigidity of the system, even for the elastic ring, usually more than compensated for the added mass of the ring and increased the frequencies in the swaying ($n=1$) and ovaling ($n=2$) modes. This problem was also studied in references 2.167, 2.168, and 2.169.

Closed circular cylindrical shells are frequently fabricated by the simple procedure of curling a flat sheet about a cylindrical radius. The shells are then closed by means of a butt or lap joint which lies in the axial direction. This type of fabrication can result in significant asymmetry in mass or stiffness or both, which causes experimental results to deviate from expected theoretical values. This problem is frequently discussed in the literature of cylindrical shell vibrations, for example, in references 2.29, 2.33, 2.34, 2.37, and 2.194.

2.7 NONCIRCULAR BOUNDARIES AND CUTOUTS

Consider first the case where a closed circular cylindrical shell of finite length is cut by two surfaces *other than* planes perpendicular to its generators. No results are known to exist for such a problem.

Brogan, Forsberg, and Smith (ref. 2.151) analyzed the interesting problem of the circular cylindrical shell having a rectangular cutout defined by the boundaries $x=l_1$, $x=l_2$, $\theta = \pm \phi$ as shown in figure 2.133. Because the cutout destroys the axisymmetry of the shell geometry, an analytical solution would require all the Fourier components in θ , and the problem would require using both space variables x and θ in uncoupled form. Therefore, finite difference solutions were employed. An energy approach was used, rather

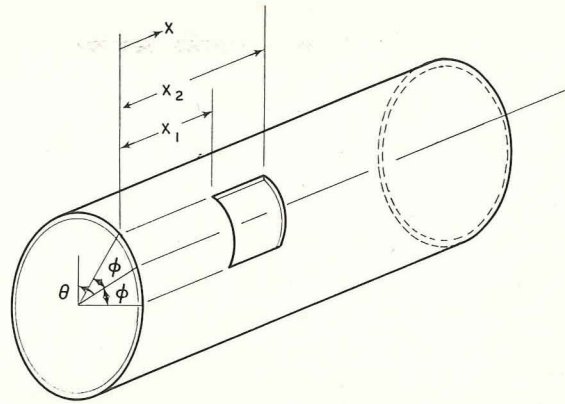


FIGURE 2.133.—Circular cylindrical shell having a rectangular cutout.

than taking the equations of motion, giving the following advantages:

- (1) Only first and second order finite difference approximations are required.
- (2) Boundary conditions are simplified; in particular, stress-free edges are natural boundary conditions.
- (3) A symmetric matrix system is guaranteed.

Finite difference meshes using as many as 4209 degrees of freedom were used, although most of the idealizations used 2196 unknowns. The shells were intended to be clamped-clamped, but actually were supported elastically at both ends as discussed previously in section 2.5 (see fig. 2.128).

A study was made of six different shell configurations with cutouts ranging from a 10° arc to a 120° arc and having a length of one-tenth of the length of the shell. These cutouts were centered at the mid-span. The results of the experimentally determined frequency spectra are given in table 2.44 and are displayed graphically in figure 2.134. The results for the zero degree cutout (the complete shell) are a repeat of the data contained in figure 2.128. In figure 2.134 the frequencies have simply been arranged in ascending numerical order with the appropriate mode shape noted at the right-hand side of the figure.

For the complete shell, the motion is sinusoidal in the circumferential direction and there is no difficulty in identifying the mode shapes. For the shell with the cutout it was somewhat surprising to find that many of the modes were still reasonably distinct and had a sinusoidal appearance.

TABLE 2.44.—*Experimentally Determined Frequency Spectra for a Shell*
($a/h=180$, $l/a=1.27$, $E=10^7$ psi) with Different Size Cutouts^a

No hole	$0.1l \times 10^\circ$	$0.1l \times 22.5^\circ$	$0.1l \times 30^\circ$	$0.1l \times 60^\circ$	$0.1l \times 90^\circ$	$0.1l \times 120^\circ$	$0.3l \times 120^\circ$
1182(8,1)	1180(8,1)	1168(S)	1179(S)	1163(8,1)	1150(8,1)	1132(8,1)	1104(8,1)
1225(7,1)	1222(7,1)	1214(7,1)	1216(7,1)	1208(S)	1201(7,1)	1198(7,1)	1199(7,1)
1230(9,1)	1228(9,1)	1224(S)	1224(S)		1215(9,1)	1210(9,1)	1210(9,1)
1349(10,1)	1345(10,1)	1343(10,1)	1342(10,1)	1338(10,1)	1335(10,1)	1332(S)	1280(S)
1362(6,1)	1359(6,1)	1352(S)	1355(S)	1355(S)			
1528(11,1)	1523(11,1)	1521(11,1)	1521(S)	1518(S)	1512(11,1)	1510(11,1)	1449(11,1)
1594(5,1)	1598(5,1)	1589(5,1)	1590(S)	1592(S)	1568(5,1)	1541(5,1)	1533(5,1)
1750(12,1)	1740(12,1)	1741(12,1)	1742(12,1)	1740(S)	1735(12,1)	1734(12,1)	1719(12,1)
1882(4,1)	1919(4,1)	1922(S)					
2011(13,1)	2003(13,1)	1996(13,1)	2005(S)	2007(S)	2001(13,1)	2000(13,1)	2030(13,1)
2056(10,2)	2049(10,2)	2065(AS)		2072(AS)			
2090(9,2)	2086(9,2)	2074(AS)					
2102(11,2)	2098(11,2)	2100(AS)	2070(AS)		2068(11,2)	2062(11,2)	2066(11,2)
2218(8,2)	2214(8,2)						2184(8,2)
2230(12,2)	2229(12,2)	2185(AS)	2172(AS)	2190(AS)	2172(12,2)	2135(12,2)	2127(AS)
2302(14,1)	2295(14,1)	2288(14,1)	2295(S)	2293(14,1)	2290(14,1)	2282(14,1)	
2412(13,2)	2409(13,2)	2382(AS)	2368(AS)	2375(AS)	2342(13,2)	2311(13,2)	2305(13,2)
2452(7,2)	2445(7,2)	2430(AS)	2480(AS)		2460(AS)	2460(AS)	2395(AS)
2621(15,1)	2613(15,1)	2610(AS)	2610(S)		2600(15,1)	2605(S)	2570(S)
2649(14,2)	2645(14,2)	2632(14,2)	2630(AS)	2604(14,2)		2550(AS)	2460(AS)
2785(6,2)	2773(6,2)	2750(AS)					
2930(15,2)	2927(15,2)	2925(AS)	2920(AS)	2870(AS)	2860(AS)	2840(AS)	2840(AS)
2965(16,1)	2958(16,1)	2948(16,1)	2940(S)	2930(AS)	2936(16,1)	2940(S)	
2992(11,3)	2984(S)	2960(S)	2975(S)	2980(S)			2970(S)
3004(12,3)	2989(12,3)	2990(S)	2990(S)	3000(S)	2991(12,3)	2990(S)	2990(AS)
3031(10,3)	3025(10,3)	3025(S)	3020(S)	3020(S)	3015(S)	3020(S)	3010(S)
3101(13,3)	3094(13,3)	3085(13,3)	3085(S)	3090(S)	3095(13,3)	3100(S)	3100(S)
3175(9,3)	3170(9,3)	3170(S)	3155(S)	3160(S)	3155(9,3)	3150(S)	3200(S)

^a For the $0.3l$ cutout, the hole centerline is located at $x=0.6l$; for all other cases the hole centerline is located at $x=0.5l$.

Notes:

- (1) Data are given in cycles per second.
- (2) The dominant wave form in the mode shape is identified wherever possible by the notation (n, m) after the value for the frequency; when no particular wave form could be distinguished, the axial variation is noted by (S) for a symmetric mode and (AS) for an antisymmetric mode.

There were, however, a number of modes which were either badly distorted or were too irregular to be identified in reference 2.151 as any specific wave form. Such irregular wave forms have been denoted in table 2.44 as simply symmetric or antisymmetric modes (with respect to the axial behavior).

In some cases, for certain size cutouts, mode shapes became irregular while, for larger cutouts, the wave form again assumed a distinct "sinusoidal" pattern. Other modes having a specific dominant wave form could be traced throughout the series of cutouts and a very gradual decrease in frequency was noted in these cases. Based on these results and based on the gradual shift

downward in the overall frequency spectrum, it was assumed that the unidentified modes would follow this same pattern of a gentle, rather than a drastic, shift in frequency. Hence, the data points plotted in figure 2.134 were connected together by straight lines to indicate the effect of the increase in cutout angle on the frequency for a given mode. For those cases in which the mode shape could not be identified with a given wave form (which occurred in about 20 percent of the cases plotted in figure 2.134) the adjacent frequencies were selected on the assumption that the change would be gradual with increasing angle of cutout.

It is interesting to note the very gradual de-

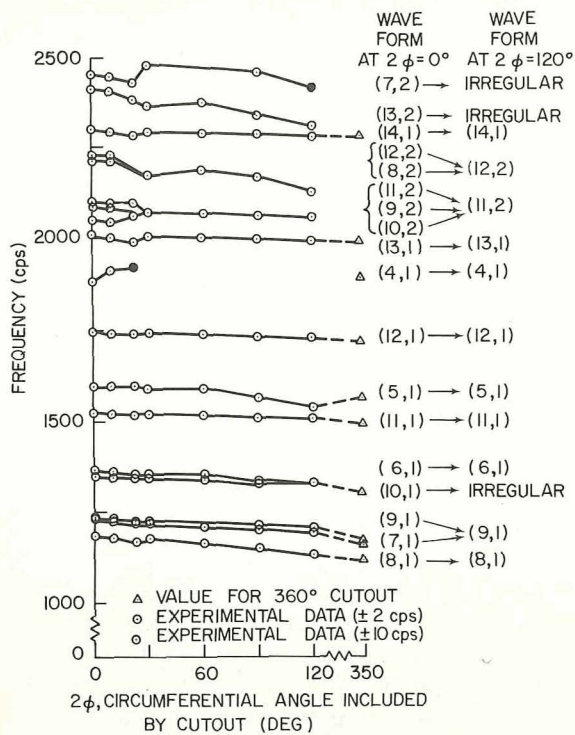


FIGURE 2.134.—Experimentally determined frequencies for symmetrically located rectangular cutouts. (After ref. 2.151)

crease in the natural frequency with the increase in cutout angle even though the shell is relatively short ($l/R=1.27$). As an example, for the 120° hole the minimum natural frequency decreased only 4 percent from the value for the complete shell. However, the asymptotic value for a 360°

degree cutout (i.e., a shell with a ring support at one end and free at the other, having a length, $l=2.7$ in.) is relatively close to that for the complete shell. For certain modes this asymptote has been plotted in figure 2.134 (denoted by a triangle).

One would expect the greatest effect of the cutout to occur for the axisymmetric ($n=0$) or beam type ($n=1$) modes. However, for this shell, these modes were of a sufficiently high frequency that they could not be experimentally observed in reference 2.151. Indeed, a long shell would have to be studied to determine the effect of cutouts on these modes. Such modes are of considerable practical interest, and, although not included in the work of reference 2.151, deserve further investigation.

Excellent agreement was obtained in reference 2.151 in the comparison of the finite difference results and the experimental data. The finite difference results were obtained using a grid having 11 equally spaced grid points in the axial direction and 60 equally spaced intervals in the θ direction (2196 degrees of freedom), covering the one-quarter of the shell surface bounded by $0 \leq x \leq 0.5l$, $0 \leq \theta \leq \pi$. Results are shown in table 2.45 and in figure 2.135 where six modes have been selected for comparison. As seen in figure 2.135 the analytical and experimental results have a maximum discrepancy for $n=5$ and $n=13$. The discrepancy noted in figure 2.135 is a result of inability to represent the experimental boundary conditions exactly. The boundary conditions have maximum effect for low values of n for the

TABLE 2.45.—Comparison of Analytical (Finite Difference) and Experimental Frequencies for Shells Having Symmetrically Located Rectangular Cutouts

Dominant mode shape		Angle of cutout, 2ϕ , degrees									
		0		30		60		90		120	
n	m	Exper.	Anal.	Exper.	Anal.	Exper.	Anal.	Exper.	Anal.	Exper.	Anal.
8	1	1182	1195	^a 1179	1183	1163	1171	1150	1162	1132	1145
10	1	1349	1346	1342	1341	1338	1338	1335	1335	^a 1332	1330
11	1	1528	1513	^a 1521	1507	^a 1518	1504	1512	1500	1510	1497
5	1	1594	1646	^a 1590	1639	^a 1592	1639	1568	1632	1541	1621
12	2	2230	2197	^a 2172	2191	^a 2190	2155	2172	...	2135	2122
13	2	2412	2365	^a 2368	2371 2327	^a 2375	2326	2342	2295	2311	2275

^a Experimentally determined mode shape was highly irregular.

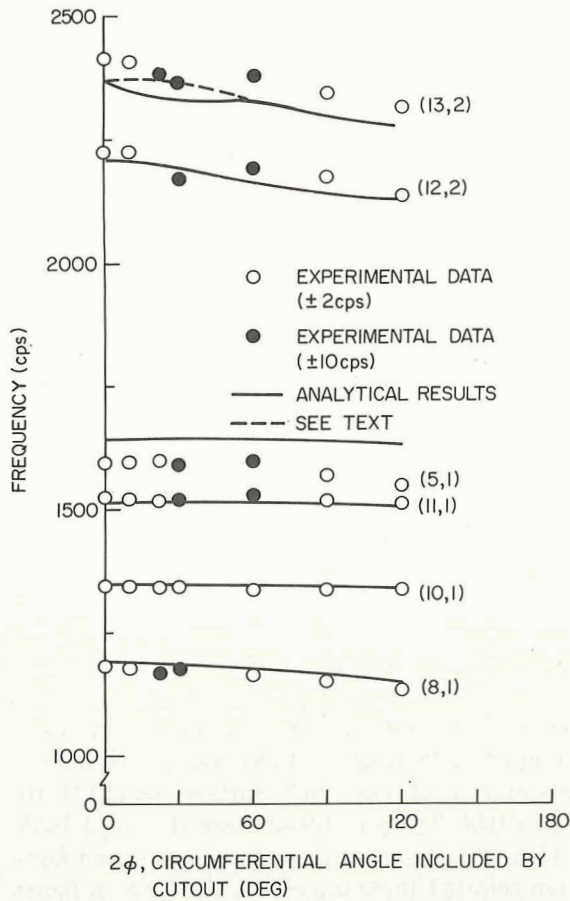


FIGURE 2.135.—Comparison of analytical (finite difference) and experimental frequencies for symmetrically located rectangular cutouts. (After ref. 2.151)

present geometry. The discrepancy for $n=13$ is caused by having only five finite difference stations in a circumferential half wave. For a fixed grid size, the error will always increase for higher n for this reason.

Contrary to the experimental data, no increase in the frequency for a given dominant wave form was noted analytically for any of the modes studied. However, both experimentally and analytically some of the modes were shown to be insensitive to the existence of a cutout, particularly ($n=5, m=1$), ($n=10, m=1$), and ($n=11, m=1$). The modes having antisymmetric behavior in the axial direction ($m=2$) appear to be the ones most affected by the cutout, as can be seen in figure 2.135.

As has been noted above, certain modes become difficult to identify for certain sizes of cut-

out. This occurred, in one instance, for the mode (13,2) and thus prevented the construction of a unique curve for the variation of frequency versus arc width of cutout (shown by the dashed line in figure 2.135). For very small cutout angles (less than 10°) the wave form for the mode $n=13, m=2$ is quite distinct. For very large cutouts (for instance, 90°) the wave form for this mode is also reasonably clear although it is no longer a sinusoidal variation.

Comparisons between experimental and theoretical results were made in reference 2.151 for certain of the mode shapes. All results are based on a normalization to a maximum radial deflection of unity. Figure 2.136 shows the modal characteristics for $n=8, m=1$ for the 120 degree by 0.11 cutout. This mode has the minimum natural frequency for this shell. This is the only mode showing this particular behavior, which looks like a damped sinusoidal motion along the circle at $x=2.7$ in. This general trend was noted for all of the (8, 1) modes for cutout angles in excess of 10° . It is interesting to note the nearly linear

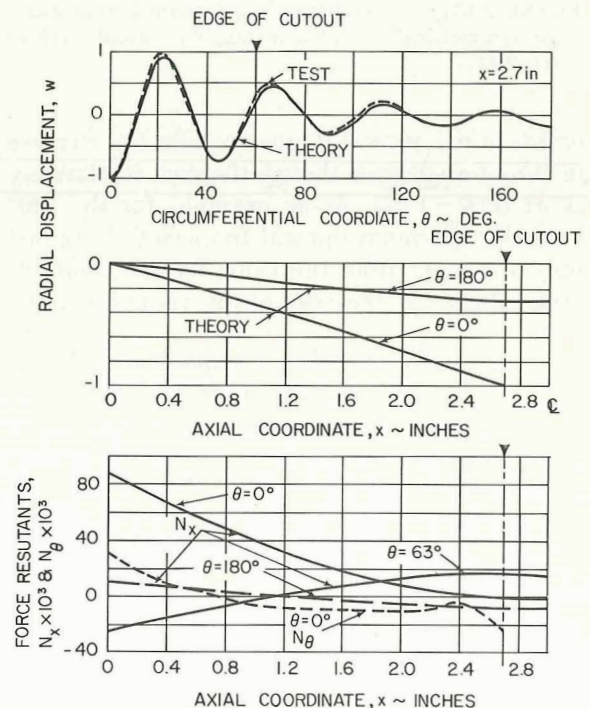


FIGURE 2.136.—Modal characteristics for the mode ($n=8, m=1$) on a shell having a 120° cutout. (After ref. 2.151)

axial variation of w for $\theta = 0$. The correspondence between the analytical and experimental results in predicting the radial component of the mode shape is excellent. The membrane stress resultants are also shown for several points in the shell. Although not shown, the bending stress resultants have a similar smooth behavior. No stress concentrations were found for this configuration. The stresses at the edge of the hole ($\theta = 60^\circ$) were much lower than those shown for a point 0.25 inch from the edge ($\theta = 63^\circ$).

Figure 2.137 shows a comparison between experimentally and analytically determined mode shapes for $n = 11$, $m = 1$ for the 90 degree cutout. This mode is typical of many in which the overall wave form is quite distinct and only slightly modified by the presence of the hole. The usual effect is that the amplitude is slightly larger in those regions directly above or below the hole and diminishes as one moves away circumferentially from the hole although the opposite behavior was observed in some cases. The axial variation is more strongly affected, in that it remains essentially linear in the region over the hole while

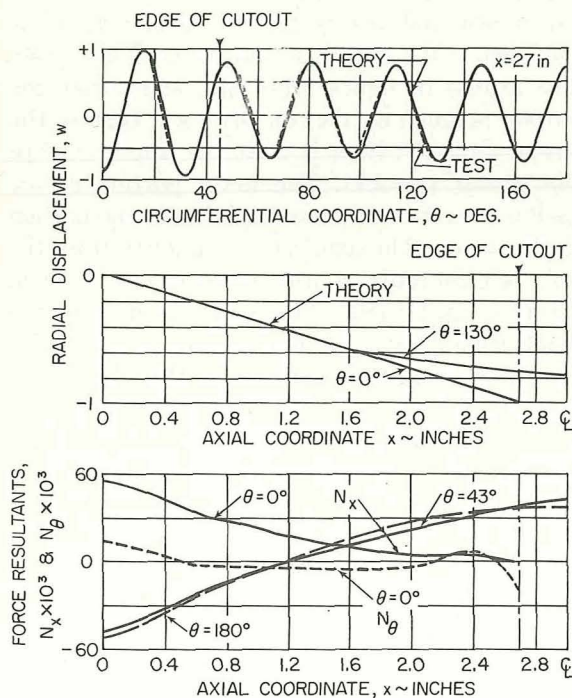


FIGURE 2.137.—Modal characteristics for the mode ($n = 11$, $m = 1$) on a shell having a 90° cutout. (After ref. 2.151)

becoming sinusoidal in the region away from the hole. As in the previous case the stress resultants are well behaved throughout the shell.

Figure 2.138 shows the results for $n = 13$, $m = 2$ for the 90 degree cutout. Here the strongest influence is on the axial mode shape. The axial variation is approximately linear for $\theta < 45^\circ$ with the maximum value reached at the middle of the shell. Away from the hole the axial variation is essentially sinusoidal with a node point at the middle of the shell as expected for the asymmetric mode. For the $n = 13$, $m = 1$ mode the hole has a very small influence on the natural frequency. For the $m = 2$ mode however, the size of the hole has a much stronger effect on the natural frequency. The significant change in the axial wave shape is the probable explanation for this. The circumferential wave form is also quite distorted for this mode shape and is one identified as irregular on figure 2.134. There is a good agreement between the analytical and experimental results in this case.

Most of the modes observed in the analytical and experimental studies had the maximum amplitudes in the portions of the shell directly

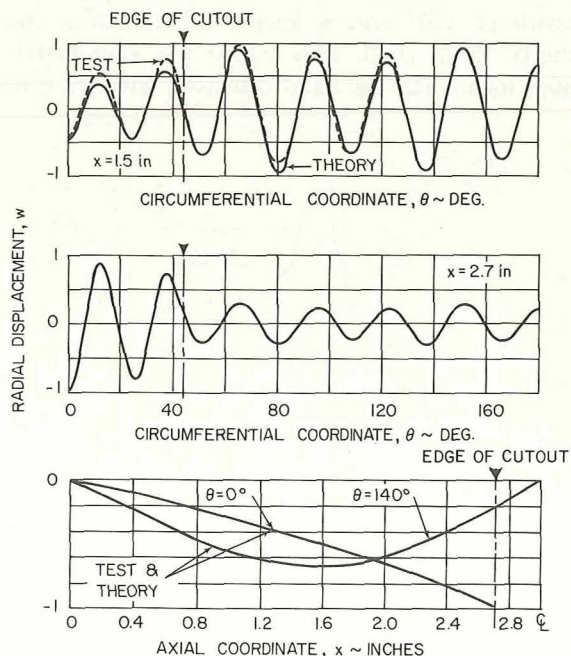


FIGURE 2.138.—Mode shapes for the mode ($n = 13$, $m = 2$) on a shell having a 90° cutout. (After ref. 2.151)

above or below the cutout. However, several modes were noted in which the motion was very small in regions near the hole, the maximum amplitude being reached on the back side of the shell away from the cutout. Such a mode is shown in figure 2.139. This mode has no strong wave form and is one which in the experimental program was termed irregular, but based on the frequency and on its dominant wave form it appears to be associated with the mode which the complete shell would be ($n=8, m=2$). In figure 2.139 the radial displacement is shown for two different values of the axial displacement ($x=1.5$ which is at the point of maximum amplitude for the axial variation and at point $x=2.7$ which is the upper boundary of the cutout). In addition, the radial displacement is shown for two different cutout angles: 30° and 120° . The axial variation in both cases is essentially a sine wave with a node at the midpoint of the shell except over the region of the cutout where the radial displacement varies linearly from zero at the edge of the shell to a maximum at the cutout. This is the same behavior which has been observed for other modes.

The final configuration examined in reference 2.151 was a shell with a cutout having an arc width of 120° and a length of 0.3 times the length of the shell. This cutout was asymmetrically located in the axial direction with its cen-

ter at $x=0.6l$. The experimentally determined frequency spectrum for this configuration is also given in table 2.44. The trend is that the frequency for most of the modes either remains the same or drops slightly compared to the value for a 120° by $0.1l$ cutout. However, in several instances the frequency did increase.

The analytical studies of this configuration were limited because of the increased computer run time required to generate the eigenvalues and eigenvectors. The run time is approximately five times that for the symmetrically located cutout. However, two modes, ($n=8, m=1$) and ($n=7, m=1$), were examined in detail, and the results are summarized here. For the (8, 1) mode the analysis predicted a frequency of 1128 cps compared to an experimentally determined value of 1104 cps and for the (7, 1) mode the analytically determined frequency is 1230 cps compared with the experimental value of 1199 cps, the difference being about 2 percent.

The comparison of the mode shapes produced analytically and experimentally for the (8, 1) mode showed excellent agreement for the radial component of the displacement. The comparison between test and theory for the displacement at the edge of the cutout is shown in figure 2.140. The results in figure 2.140 also show that the motion is much smaller on the lower edge of the cutout ($x=4.5$) than it is at the upper edge of the cutout ($x=2.7$). The lower portion of the shell is in fact barely participating in the motion in this mode. The axial variation away from the hole is essentially sinusoidal as can be seen in the plot for $\theta=180^\circ$. The axial variation of the displacement over the hole $\theta \leq 60^\circ$ is essentially linear, reaching its maximum at the edge of the hole. The behavior for this configuration is essentially identical to that for the (8, 1) mode shown in figure 2.136. The nonsymmetric axial variation is the major difference between these two cases. The variation of the stresses for this case showed no particular stress concentration arising from the hole or any other unusual behavior caused by the cutout. It should be noted that a high stress concentration is to be expected very locally in the corner of any of the cutouts studied here and such effects would be noticed if the finite difference grid were continually refined to predict the stress distribution in the immediate

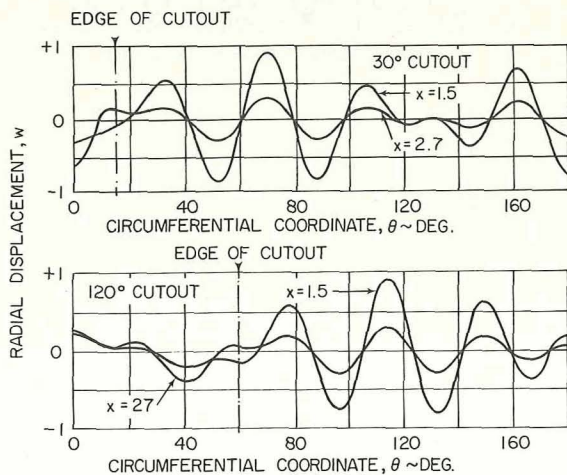


FIGURE 2.139.—Analytically determined mode shapes for the mode ($n=8, m=2$) for two different cutout sizes ($2\phi=30^\circ, 120^\circ$). (After ref. 2.151)

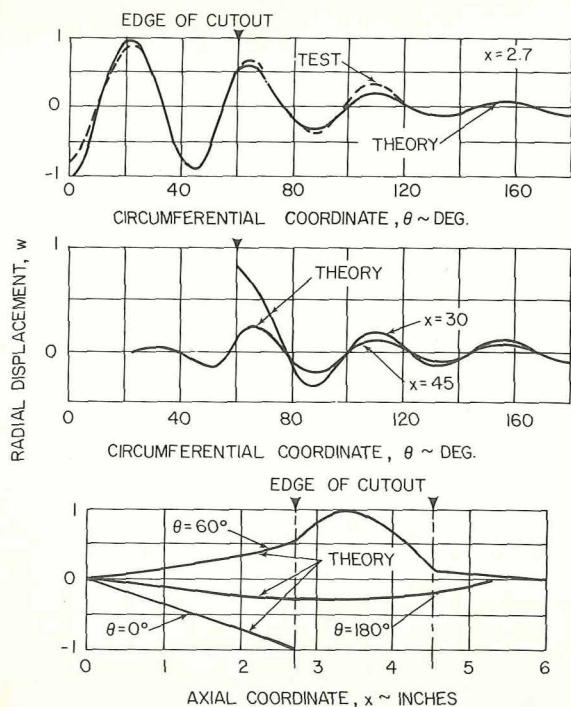


FIGURE 2.140.—Mode shapes for the mode ($n=8$, $m=1$) on a shell having a 120° asymmetrically located cutout. (After ref. 2.151)

vicinity of this sharp corner. The stresses generated by this concentration evidently decay very rapidly as one moves away from the vicinity of the corner.

No other work is known which studies the effects of cutouts upon the free vibration frequencies and mode shapes of circular cylindrical shells.

2.8 OPEN CIRCULAR CYLINDRICAL SHELLS

An open circular cylindrical shell of length l and included angle θ_0 is shown in figure 2.141. The shell boundaries shown in figure 2.141 are a special case where the lateral edges are generators of the shell and the ends are circle arcs which are the intersections of the shell surface with planes which are perpendicular to the shell axis. Thus, if one were to view the shell from a point in its symmetry plane, $\theta = \theta_0/2$, the boundaries would appear as a rectangle. The special configuration of figure 2.141 is chosen, of course, because virtually all of the results reported in the litera-

ture are for such boundaries. One exception to this (the case where the lateral edges are taken to be helices) will be discussed later in this section.

The equations of motion given previously by equations (2.1) through (2.9) apply to open circular cylindrical shells as well as to closed shells. The general boundary conditions given by equations (2.140) through (2.144) are applicable to the ends $x=0$ and $x=s$. Along the lateral edges $\theta=0$ and $\theta=\theta_0$ the following possible simple boundary conditions may arise (see sec. 1.8):

$$(a) u=0 \quad \text{or} \quad (b) N_{\theta x}=0 \quad (2.158)$$

$$(a) v=0 \quad \text{or} \quad (b) N_{\theta}=0 \quad (2.159)$$

$$(a) w=0 \quad \text{or} \quad (b) Q_{\theta} + \frac{\partial M_{\theta x}}{\partial x} = 0 \quad (2.160)$$

$$(a) \frac{\partial w}{\partial \theta} = 0 \quad \text{or} \quad (b) M_{\theta} = 0 \quad (2.161)$$

In addition, at the corners resulting from the intersection of the edges, the following equation must be satisfied:

$$M_{x\theta}w = M_{\theta x}w = 0 \quad (2.162)$$

which has significance if $w \neq 0$ on any two intersecting edges (e.g., a free corner).

As noted earlier in this chapter there were 136 possible combinations of the simple boundary conditions in equations (2.140) through (2.144) yielding distinct problems for closed shells. For open shells there exist 136 combinations for *each combination* of equations (2.158) through (2.162), thereby yielding $(136)^2$ or 18 496 distinct possible problems! Nevertheless, it will be seen later in this section that the majority of the references deal solely with one of these 18 496 sets of

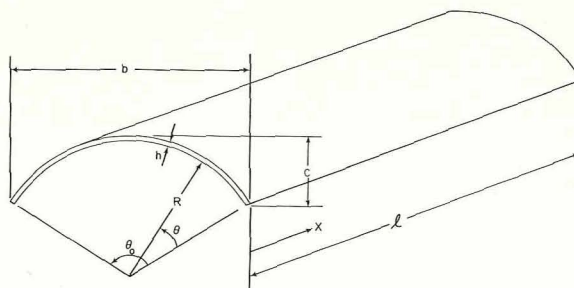


FIGURE 2.141.—Open circular cylindrical shell.

boundary conditions—that is, when all four edges are supported by shear diaphragms.

When the angle θ_0 becomes relatively small in comparison with 2π , then the shell is considered to be *shallow*. Otherwise, it is open and *deep*. The phrase “curved plate” frequently found in the literature usually identifies a shallow shell. For shallow shells the assumption is made that the terms containing the transverse shearing force resultants are negligibly small compared with the other terms in the first two equations of motion, equations (1.112a) and (1.112b). Because this corresponds to the case when the bending moments (from equations (1.115a) and (1.115b)) have negligibly small influence upon these tangential equations of motion, the resulting theory is sometimes called the “momentless theory” or “technical theory” of thin shells (cf., ref. 2.19). However, this assumption was also used to derive the Donnell-Mushtari equations of motion (sec. 1.6.3). Thus, the Donnell-Mushtari and shallow shell equations are equivalent for circular cylindrical shells.

2.8.1 All Edges Supported by Shear Diaphragms

From section 1.8 the boundary conditions for this case are seen to be

$$N_x = v = w = M_x = 0 \quad \text{along} \quad x = 0, l \quad (2.163a)$$

$$N_\theta = u = v = M_\theta = 0 \quad \text{along} \quad \theta = 0, \theta_0 \quad (2.163b)$$

These boundary conditions are satisfied exactly by choosing displacement functions of the form

$$\left. \begin{aligned} u &= A \cos \lambda s \sin n\theta \cos \omega t \\ v &= B \sin \lambda s \cos n\theta \cos \omega t \\ w &= C \sin \lambda s \sin n\theta \cos \omega t \end{aligned} \right\} \quad (2.164)$$

where $s = x/R$, as before, $\lambda = m\pi R/l$ ($m = 1, 2, \dots$), and n is not an integer, in general, but is given by

$$n = \frac{k\pi}{\theta_0} \quad (k = 1, 2, \dots) \quad (2.165)$$

In equation (2.165) k is one more than the number of longitudinal node lines along the shell.

Substituting equations (2.164) into the equations of motion (2.3) for a particular shell theory yields the same sets of homogeneous equations given in section 2.2 such as equations (2.21) for

the Donnell-Mushtari theory, and the same characteristic equations as given by equations (2.35) and (2.36) and table 2.4.

In the special case where θ_0 is π divided by an integer, then the frequencies and mode shapes determined by solution function equations (2.164) and (2.165) is the same as those for the closed shell solution equations (2.20), except for the reference plane from which θ is measured. Thus, the results given in section 2.3 for closed shells having shear diaphragm supports at both ends for $n = 1, 2, 3, \dots$ are applicable to open shells having $\theta_0 = \pi, \pi/2, \pi/3, \dots$, respectively. In addition, numerical results for values of n which are not integers can be obtained from those figures of section 2.3 having n as a continuously varying parameter (e.g., figs. 2.20, 2.21, and 2.22). Similarly, results for closed shells of infinite length given previously in section 2.2 are directly applicable to open shells having $\theta_0 = \pi, \pi/2, \pi/4, \dots$. Frequency formulas such as those given by table 2.1 for infinite shells and by equations (2.42), (2.49), (2.50), and (2.51) and tables 2.13 and 2.17 are directly applicable for arbitrary angle θ_0 by using n as it is defined in equation (2.165).

The Donnell-Mushtari or shallow shell theory is most frequently used to analyze circular cylindrical shell panels. It was seen previously in section 2.3 that this theory is inaccurate for small nonzero n ($n = 1, 2, 3$), particularly for long shells ($l/R > 2$). For open shells n can take on even smaller non-zero values. For example, from equation (2.165) the lowest value (no longitudinal node lines) of n for $\theta_0 = 3\pi/2$ is $2/3$. For $\theta_0 = 2\pi$ ($n = 1/2$) the shell is not closed; i.e., there is no continuity of the quantities $v, N_{x\theta}, Q_\theta$ and $\partial w / \partial \theta$ across the longitudinal edges. Furthermore, it is possible to have $\theta_0 > 2\pi$ without significantly changing the cylindrical curvature, provided $h/R \ll 1$.

No published results are available for $0 < n < 1$ even though the same characteristic equations and computer programs used for SD-SD closed shells can be used straightforwardly. In section 2.3.1 frequencies obtained from the various theories were compared for several integral values of n . The same computer programs were subsequently used to determine lowest frequency parameters for $n = 1/3, 1/2$, and $2/3$. These

results are shown in tables 2.46 and 2.47, where the effects of tangential inertia are included. Data are given for three of the most widely used shell theories: Donnell-Mushtari, Flügge, and membrane. Thickness ratios (R/h) of 20 and 500, $\nu=0.3$, and $l/mR=0.1, 0.25, 1, 4, 20$, and 100 are chosen to allow direct comparison with $n=2, 3, \dots$ by means of tables 2.6, 2.7, and 2.8.

Tables 2.6 and 2.7 showed that for shells having

moderate length/radius ratios ($l/mR=1, 4$) the three theories agreed closely with each other and with results from the three-dimensional elasticity theory for both values of R/h and for all n . In tables 2.46 and 2.47 the agreement among the theories for the nonintegral values of n are also apparent for $l/mR=1, 4$. For these values of l/mR the monotonic behavior of the function Ω over the closed interval $0 \leq n \leq 1$ for all three

TABLE 2.46.—Lowest Frequency Parameters $\Omega = \omega R \sqrt{\rho(1-\nu^2)/E}$ for Deep, Open Shells Supported on All Edges by Shear Diaphragms; Tangential Inertia Included; $R/h=20$, $\nu=0.3$

n	Theory	l/mR					
		0.1	0.25	1	4	20	100
$\frac{1}{3}$	Donnell-Mushtari	14.2782	2.47132	0.946544	0.422183	0.0514333	0.00268829
	Flügge	14.2649	2.46663	.945521	.422137	.0515972	.00483989
	Membrane	.953802	.952985	.935728	.422169	.0514301	.00263976
$\frac{1}{2}$	Donnell-Mushtari	14.2802	2.47281	.930899	.381416	.0368447	.00232640
	Flügge	14.2669	2.46809	.929793	.381341	.0371231	.00512219
	Membrane	.953668	.952137	.919689	.381375	.0368056	.00167343
$\frac{2}{3}$	Donnell-Mushtari	14.2830	2.47491	.910330	.337827	.0274266	.00374949
	Flügge	14.2697	2.47014	.909109	.337681	.0275360	.00459872
	Membrane	.953479	.950952	.898540	.337723	.0271806	.00117104

TABLE 2.47.—Lowest Frequency Parameters $\Omega = \omega R \sqrt{\rho(1-\nu^2)/E}$ for Deep, Open Shells Supported on All Edges by Shear Diaphragms; Tangential Inertia Included; $R/h=500$, $\nu=0.3$

n	Theory	l/mR					
		0.1	0.25	1	4	20	100
$\frac{1}{3}$	Donnell-Mushtari	1.11106	0.957341	0.935745	0.422169	0.0514301	0.00263984
	Flügge	1.11097	.957324	.935744	.422168	.0514304	.00264474
	Membrane	.953788	.952986	.935728	.422169	.0514301	.00263976
$\frac{1}{2}$	Donnell-Mushtari	1.11098	.956504	.919707	.381375	.0368056	.00167468
	Flügge	1.11089	.956487	.919705	.381374	.0368061	.00168460
	Membrane	.953653	.952137	.919689	.381375	.0368056	.00167343
$\frac{2}{3}$	Donnell-Mushtari	1.11088	.955334	.898560	.337723	.0271810	.00117967
	Flügge	1.11079	.955317	.898558	.337723	.0271812	.00118447
	Membrane	.953466	.950952	.898541	.337723	.0271806	.00117103

theories is also notable. The large errors in the membrane theory for low values of n are reproduced, as well as the large errors in the membrane and Donnell-Mushtari theories for $R/h=20$ and large l/mR (100). For l/mR , Ω is seen to be non-monotonic over $0 \leq n \leq 1$ for the theories.

The effects of neglecting tangential inertia for the same shells are shown in tables 2.48 and 2.49. For closed shells it was seen in tables 2.18 and 2.19 that neglecting tangential inertia caused a

maximum change of -9.5 percent in Ω for $n=0$ ($l/mR=4$) and $+42.7$ percent for $n=1$ ($l/mR=20$). Comparing tables 2.48 and 2.46 ($R/h=20$), for example, it is interesting to note that neglecting tangential inertia causes only positive changes in Ω for nonintegral values, and that these changes are considerably greater (for example, 222 percent increase for $n=1/3$, $l/mR=100$, according to the Flügge theory).

Sewall (ref. 2.198) used the solution functions

TABLE 2.48.—Lowest Frequency Parameters $\Omega = \omega R \sqrt{\rho(1-\nu^2)}/E$ for Deep, Open Shells Supported on All Edges by Shear Diaphragms; Tangential Inertia Neglected; $R/h=20$, $\nu=0.3$

n	Theory	l/mR					
		0.1	0.25	1	4	20	100
$\frac{1}{3}$	Donnell-Mushtari	14.2790	2.47208	0.954256	0.808405	0.173355	0.0085533
	Flügge	14.2747	2.46806	.953555	.808354	.173884	.0153958
	Membrane	.953845	.953267	.943319	.808336	.173344	.00839890
$\frac{1}{2}$	Donnell-Mushtari	14.2810	2.47361	.941768	.678938	.0857841	.00521490
	Flügge	14.2767	2.46956	.940991	.678848	.0864238	.0114806
	Membrane	.953711	.952430	.930372	.678822	.0856925	.00375119
$\frac{2}{3}$	Donnell-Mushtari	14.2838	2.47575	.924892	.554664	.0506287	.00676778
	Flügge	14.2795	2.47167	.924007	.554480	.0508296	.00830042
	Membrane	.953524	.951261	.912833	.554453	.0501739	.00211369

TABLE 2.49.—Lowest Frequency Parameters $\Omega = \omega R \sqrt{\rho(1-\nu^2)}/E$ for Deep, Open Shells Supported on All Edges by Shear Diaphragms; Tangential Inertia Neglected; $R/h=500$, $\nu=0.3$

n	Theory	l/mR					
		0.1	0.25	1	4	20	100
$\frac{1}{3}$	Donnell-Mushtari	1.11111	0.957625	0.943337	0.808337	0.173344	0.00839915
	Flügge	1.11102	.957608	.943336	.808336	.173345	.00841474
	Membrane	.953832	.953268	.943319	.808336	.173344	.00839890
$\frac{1}{2}$	Donnell-Mushtari	1.11104	.956799	.930391	.678823	.0856926	.00375399
	Flügge	1.11109	.956782	.930389	.678822	.0856936	.00377621
	Membrane	.953697	.952431	.930372	.678822	.0856925	.00375119
$\frac{2}{3}$	Donnell-Mushtari	1.11093	.955645	.912852	.554453	.0501746	.00212927
	Flügge	1.11084	.955628	.912851	.554453	.0501749	.00213793
	Membrane	.953510	.951262	.912833	.554453	.0501739	.00211368

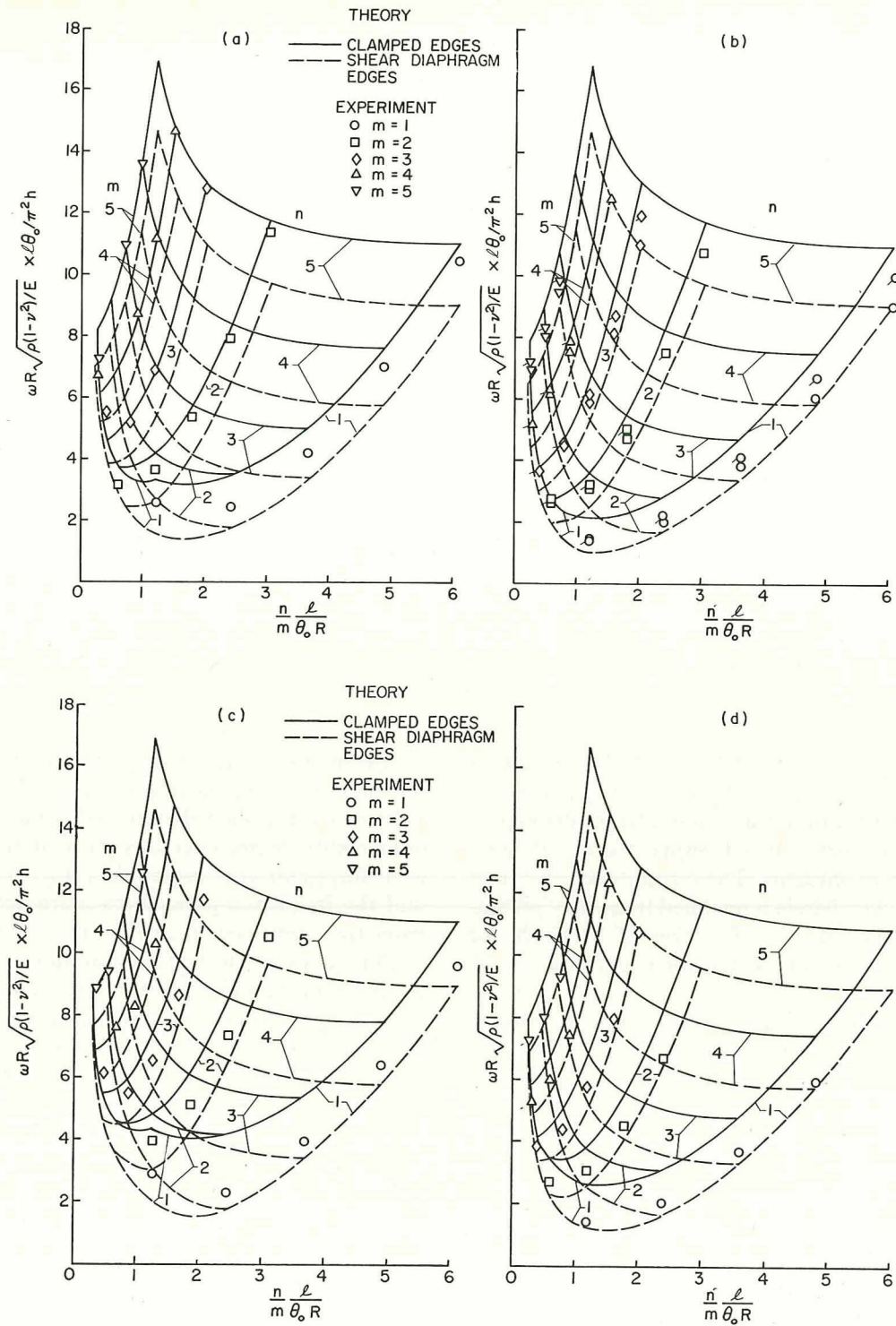


FIGURE 2.142.—Nondimensional frequency parameters for aluminum cylindrical panels supported by shear diaphragms on all edges; $l/\theta_0 R = 1.22$. (After ref. 2.198) (a) $\theta_0 = 5.4^\circ$, $R/h = 3430$. (b) $\theta_0 = 5.4^\circ$, $R/h = 2000$. (c) $\theta_0 = 7.2^\circ$, $R/h = 2570$. (d) $\theta_0 = 7.2^\circ$, $R/h = 1500$. (e) $\theta_0 = 10.7^\circ$, $R/h = 1715$. (f) $\theta_0 = 10.7^\circ$, $R/h = 1000$.

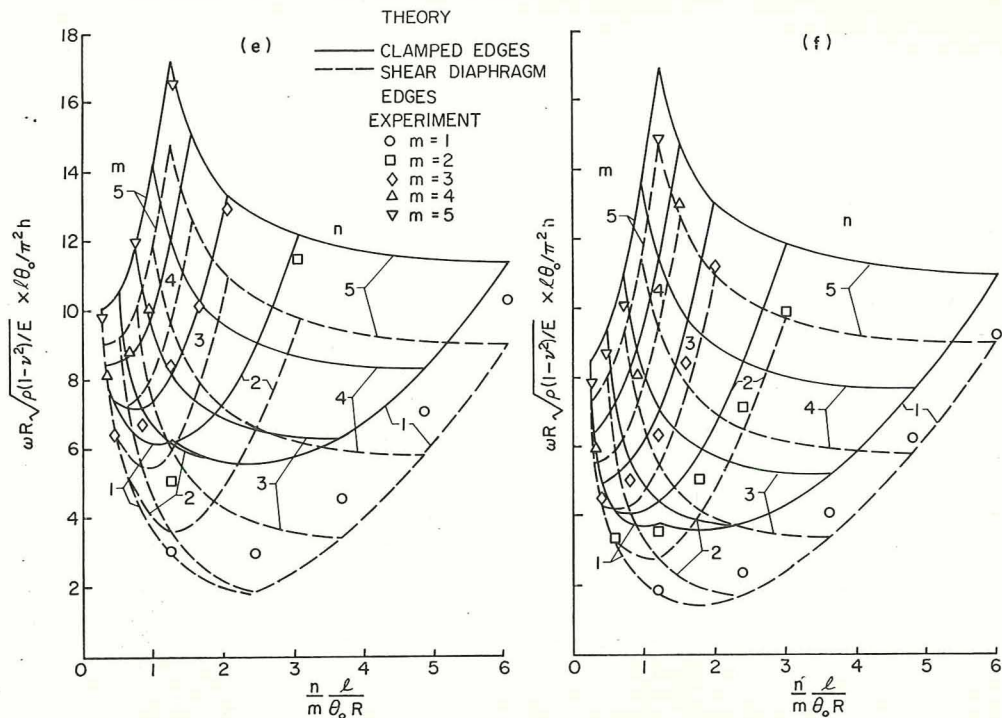


FIGURE 2.142.—Concluded

given by equations (2.164) and (2.165) along with the Donnell-Mushtari theory and neglected tangential inertia to obtain numerical results explicitly for cylindrical panels supported on all edges by shear diaphragms. These results are shown in figure 2.142 wherein a modified frequency parameter is plotted as a function of $nl/m\theta_0 R$ for shallow shells having included angles $\theta_0 = 5.4^\circ$, 7.2° , and 10.7° .

The free vibrations of open circular cylindrical shells are also discussed in references 2.19, 2.38, 2.66, and 2.199 through 2.212.

2.8.2 Lateral Edges Having SD Supports

Consider next the generalization where an open circular cylindrical shell has shear diaphragm supports at the sides $\theta=0$, θ_0 (see fig. 2.141) as defined by boundary condition equations (2.163b), but has arbitrary edge conditions along $x=0, l$. The exact solution procedure outlined in section 2.4 for closed shells having arbitrary edge conditions is also applicable for this case. That is, solution functions in the form of equations (2.53) can be taken, (interchanging

$\sin n\theta$ for $\cos n\theta$) with n not generally an integer, but determined by equation (2.165). The proper values of λ are then determined from the roots of an eighth degree characteristic equation (2.54) as before, and the amplitude ratios A/C , B/C and the frequency parameters Ω are determined from the equations of motion, as in sec. 2.4.

Thus a great deal of information is already available in the subsequent subsections of section 2.4 for open shells having $n=1, 2, 3, \dots$ (i.e., $\theta_0 = \pi, \pi/2, \pi/3, \dots$) because the longitudinal node lines generated are equivalent to shear diaphragm supports along these lines. For example, the abundant data available for clamped-clamped shells in the figures and tables found in section 2.4.1 can also be used for cylindrical shell panels having clamped ends and lateral edges supported by shear diaphragms. Moreover, simplified frequency formulas such as equations (2.87), (2.88), (2.89), and (2.90) can be applied for values of n which are not integers.

2.8.3 Ends Having SD Supports

An exact solution of the free vibration problem

is also possible for a circular cylindrical shell having its curved edges $x=0, l$ (see fig. 2.141) supported by shear diaphragms and arbitrary fixity conditions along the longitudinal edges. Thus the boundary conditions along $x=0, l$ are given by equations (2.163a). These conditions are satisfied exactly by choosing

$$u = A \cos \lambda s e^{n\theta} \cos \omega t \quad v = B \sin \lambda s e^{n\theta} \cos \omega t \quad w = C \sin \lambda s e^{n\theta} \cos \omega t \quad (2.166)$$

with $s = x/R$ and $\lambda = m\pi R/l$ ($m=1, 2, \dots$). Substituting equations (2.166) into the equations of motion gives, for example, for the Donnell-Mushtari theory (cf., eqs. (2.7))

$$\begin{bmatrix} -\lambda^2 + \frac{(1-\nu)}{2} n^2 + \Omega^2 & \frac{(1+\nu)}{2} \lambda n & \nu \lambda \\ -\frac{(1+\nu)}{2} \lambda n & -\frac{(1-\nu)}{2} \lambda^2 + n^2 + \Omega^2 & n \\ -\nu \lambda & n & 1 + k(-\lambda^2 + n^2)^2 - \Omega^2 \end{bmatrix} \begin{bmatrix} A \\ B \\ C \end{bmatrix} = \begin{bmatrix} 0 \\ 0 \\ 0 \end{bmatrix} \quad (2.167)$$

The coefficient matrix in equation (2.167) can easily be put into symmetric form simply by multiplying the last two equations through by negative one. For a nontrivial solution the determinant of the coefficient matrix in equation (2.167) is set equal to zero, thereby yielding an eighth degree characteristic equation for the proper values of n . The vibration frequencies and amplitude ratios A/C and B/C are then determined by applying the four boundary conditions which exist at each of the sides $\theta=0$ and $\theta=\theta_0$.

In spite of the straightforwardness of the approach outlined above and its obvious parallelism to the solution procedure outlined in section 2.4, the only work using it known to the writer is that by Heki (ref. 2.172). In that work the solution is derived in detail for the Donnell-Mushtari the-

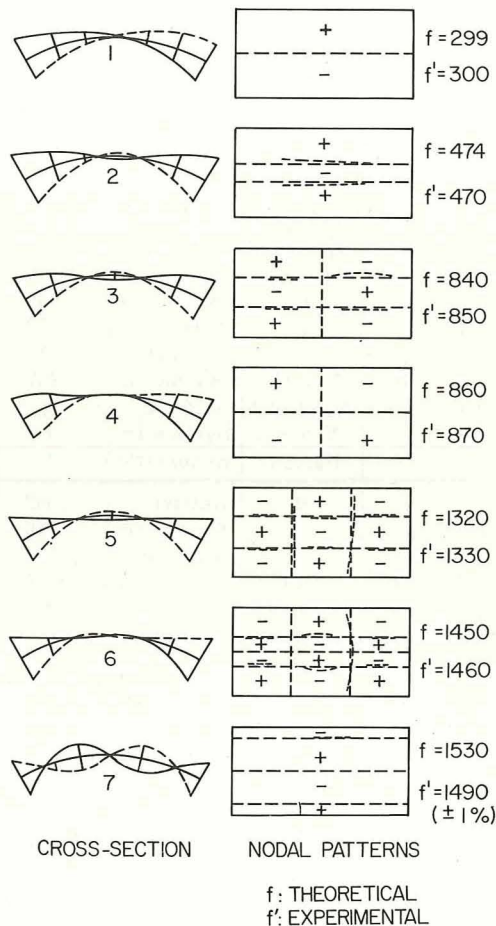


TABLE 2.50.—Frequency Parameters for a Cylindrical Shell Panel Having Its Straight Edges Free and the Others Supported by Shear Diaphragms

Number of longitudinal half-waves, m	Type of mode	$\frac{\omega^2 \rho R l^2 \sqrt{3(1-\nu^2)}}{m^2 \pi^2 E h}$
1	Antisym.	0.088
1	Symmetric	.220
1	Antisym.	2.28
2	Symmetric	.172
2	Antisym.	.182
3	Symmetric	.190
3	Antisym.	.228

FIGURE 2.143.—Mode shapes, nodal patterns, and cyclic frequencies (theoretical- f , experimental- f') for a cylindrical shell panel having its straight edges free and the others supported by shear diaphragms. (After ref. 2.172)

TABLE 2.51.—*Modal Characteristics for a Cylindrical Shell Panel Having Its Straight Edges Free and the Others Supported by Shear Diaphragms*

m	f , cps	Function	Symmetry of function	Amplitudes of function $\theta =$						
				0°, edge	5°	10°	15°	20°	25°	30°, center
1	299	u	Antisym.	0.035	0.002	-0.014	-0.020	-0.017	-0.010	0
		v	Symmetric	-.311	-.179	-.079	-.007	.044	.072	0.081
		w	Antisym.	1.559	1.273	.979	.740	.483	.237	0
		$N_x \times 10^{-3}$	Antisym.	-.542	-.033	.226	.314	.273	.156	0
		$N_{x\theta} \times 10^{-3}$	Symmetric	0	-.050	-.037	-.013	.025	.054	.063
		$N_\theta \times 10^{-3}$	Antisym.	0	.004	.012	.015	.014	.008	0
		$M_\theta \times 10^{-6}$	Antisym.	0	-.03	.08	.07	.09	.07	0
	474	u	Symmetric	.041	.012	-.002	-.007	-.008	-.006	-.006
		v	Antisym.	-.276	-.156	-.072	-.022	.003	.007	0
		w	Symmetric	1.576	1.169	.798	.440	.158	-.035	-.092
		$N_x \times 10^{-3}$	Symmetric	-.638	-.195	.034	.122	.129	.104	.105
		$N_{x\theta} \times 10^{-3}$	Antisym.	0	-.054	-.064	-.049	-.031	-.012	0
		$N_\theta \times 10^{-3}$	Symmetric	0	.004	.013	.020	.026	.029	.030
		$M_\theta \times 10^{-6}$	Symmetric	0	.043	.366	.778	1.185	1.469	1.570
	1530	u	Antisym.	.030	.016	-.003	-.019	-.023	-.015	0
		v	Symmetric	.179	.187	.154	.071	-.032	-.116	-.150
		w	Antisym.	1.63	.52	-.28	-.98	-1.13	-.72	0
		$N_x \times 10^{-3}$	Antisym.	-.46	-.25	-.04	.30	.37	.25	0
		$N_{x\theta} \times 10^{-3}$	Symmetric	0	.04	.05	.02	-.03	-.07	-.09
		$N_\theta \times 10^{-3}$	Antisym.	0	-.07	-.01	-.02	-.02	-.01	0
		$M_\theta \times 10^{-6}$	Antisym.	0	1.2	4.1	6.0	6.2	3.9	0
2	840	u	Symmetric	.039	.000	-.012	-.009	-.002	.006	.008
		v	Antisym.	-.209	-.094	-.018	.022	.032	.021	0
		w	Symmetric	1.555	1.105	.671	.281	-.026	-.219	-.286
		$N_x \times 10^{-3}$	Symmetric	-1.207	0.004	.379	.302	.058	-.165	-.247
		$N_{x\theta} \times 10^{-3}$	Antisym.	0	-.183	-.133	-.027	.036	.041	0
		$N_\theta \times 10^{-3}$	Symmetric	0	.028	.058	.064	.048	.027	.019
		$M_\theta \times 10^{-6}$	Symmetric	0	.02	.49	1.04	1.45	1.66	1.72
	860	u	Antisym.	.052	.005	-.013	-.016	-.012	-.006	0
		v	Symmetric	-.239	-.122	-.043	.004	.027	.036	.038
		w	Antisym.	1.543	1.125	.735	.406	.184	.060	0
		$N_x \times 10^{-3}$	Antisym.	-1.615	-.149	.437	.549	.420	.219	0
		$N_{x\theta} \times 10^{-3}$	Symmetric	0	-.217	-.159	-.041	.114	.203	.236
		$N_\theta \times 10^{-3}$	Antisym.	0	.038	.093	.121	.107	.061	0
		$M_\theta \times 10^{-6}$	Antisym.	0	.08	.59	1.12	1.20	.77	0
3	1320	u	Symmetric	.048	-.004	-.015	-.010	.000	.008	.011
		v	Antisym.	-.200	-.077	-.004	.029	.033	.023	0
		w	Symmetric	1.64	1.11	.62	.22	-.06	-.21	-.26
		$N_x \times 10^{-3}$	Symmetric	-2.244	.188	.735	.470	-.001	-.352	-.494
		$N_{x\theta} \times 10^{-3}$	Antisym.	0	-.33	-.10	.17	.27	.21	0
		$N_\theta \times 10^{-3}$	Symmetric	0	.11	.21	.19	.09	.00	-0.05
		$M_\theta \times 10^{-6}$	Symmetric	0	-.27	.66	1.39	1.56	1.46	1.41
	1450	u	Antisym.	.061	-.003	-.013	-.008	-.002	.001	0
		v	Symmetric	-.200	-.079	-.010	.018	.021	.014	.010
		w	Antisym.	1.606	1.070	.576	.188	-.024	-.065	0
		$N_x \times 10^{-3}$	Antisym.	-2.38	.07	.66	.50	.21	.04	0
		$N_{x\theta} \times 10^{-3}$	Symmetric	0	-.38	-.19	.07	.21	.25	.26
		$N_\theta \times 10^{-3}$	Antisym.	0	.11	.24	.26	.20	.11	0
		$M_\theta \times 10^{-6}$	Antisym.	0	-.26	.98	2.02	2.15	1.33	0

ory neglecting tangential inertia and is illustrated by the problem where the two longitudinal edges $\theta=0$, θ_0 are completely free. Numerical results were obtained for a steel shell having the following physical parameters (expressed in the c.g.s. system): $\rho=7.8$, $R=10.0$, $\nu=0.3$, $E=2.1 \times 10^{12}$, $l=20.0$, $h=0.100$, $\theta_0=60^\circ$. Nondimensional frequency parameters are given in table 2.50. Modes are labeled either symmetric or antisymmetric with respect to the line $\theta=\theta_0/2$. In figure 2.143 the mode shapes are shown, along with theoretical and experimentally measured cyclic frequencies for the physical parameters given above. Modal characteristics associated with each of these frequencies are listed in table 2.51.

2.8.4 Other Boundary Conditions

Problems involving open circular cylindrical shells not having two opposite sides supported by shear diaphragms (or the boundary conditions complementary to SD supports as discussed in sec. 2.4.6) are not capable of exact solution by analytical methods, and approximate techniques must be used. For this purpose the Ritz method using beam vibration eigenfunctions is frequently employed.

Gontkevich (refs. 2.127 and 2.202) developed a method of analysis for open circular cylindrical shells which need not be shallow. The Rayleigh-Ritz method was used along with displacement components in the form

$$\left. \begin{aligned} u &= A_{mn} X_m'(x) \Theta_n(\theta) \cos \omega t \\ v &= B_{mn} X_m(x) \Theta_n'(\theta) \cos \omega t \\ w &= C_{mn} X_m(x) \Theta_n(\theta) \cos \omega t \end{aligned} \right\} \quad (2.168)$$

where the $X_m(x)$ are conventional beam functions and $\Theta_n(\theta)$ are the eigenfunctions of free vibration of *circular* beams determined for the appropriate boundary conditions at $\theta=0$, θ_0 . In references 2.127 and 2.202 a characteristic determinant is given in a general form for arbitrary boundary conditions. The characteristic determinant is

$$\begin{vmatrix} a_{11} & a_{12} & a_{13} \\ a_{12} & a_{22} & a_{23} \\ a_{13} & a_{23} & a_{33} \end{vmatrix} = 0 \quad (2.169)$$

where, after sorting through several misprints in reference 2.127, it appears that

$$\left. \begin{aligned} a_{11} &= \mu_m^2 \theta_n + \frac{1-\nu}{2} \delta_m \mu_n^2 \delta_n - \delta_m \theta_n \Omega^2 \\ a_{12} &= \mu_m \mu_n \left(\frac{1-\nu}{2} \delta_m \delta_n + \nu \gamma_m \gamma_n \right) \\ a_{13} &= -\nu \mu_m \gamma_m \theta_n \\ a_{22} &= \mu_n^2 \eta_n + \frac{1-\nu}{2} \mu_m^2 \delta_m \delta_n \\ &\quad + k [\mu_n^2 \eta_n + 2(1-\nu) \mu_m^2 \delta_m \delta_n] - \delta_n \Omega^2 \\ a_{23} &= \mu_n \{ -\gamma_n + k [\mu_n^2 \eta_n \\ &\quad + 2(1-\nu) \mu_m^2 \delta_m \delta_n + \nu \mu_m^2 \gamma_m \gamma_n] \} \\ a_{33} &= \theta_n + k [\mu_m^4 \theta_n + 2\nu \mu_m^2 \gamma_m + \mu_n^2 \gamma_n \\ &\quad + \mu_n^4 \eta_n + 2(1-\nu) \mu_m^2 \delta_m \mu_n^2 \delta_n] \\ &\quad - \theta_n \Omega^2 \end{aligned} \right\} \quad (2.170)$$

and $k=h^2/12R^2$ as before. The straight beam eigenfunction constants δ_m , γ_m , and $\mu_m=\alpha_m R/l$ to be used in equations (2.170) were given previously in table 2.21. The curved beam constants μ_n , δ_n , γ_n , η_n , and θ_n are defined by

$$\begin{aligned} \mu_n &= \frac{\alpha_n}{\theta_0} \\ \delta_n &= \frac{l}{\alpha_n^2} \int_0^{R\theta_0} (\Theta_n')^2 R d\theta \\ \gamma_n &= \frac{l}{\alpha_n^2} \int_0^{R\theta_0} \Theta_n'' \Theta_n R d\theta \\ \eta_n &= \frac{l^3}{\alpha_n^4} \int_0^{R\theta_0} (\Theta_n'')^2 R d\theta \\ \theta_n &= \frac{1}{l} \int_0^{R\theta_0} \Theta_n^2 R d\theta \end{aligned} \quad (2.171)$$

Values of α_n for circular curved beams are presented in figure 2.144. A double subscript is used, the first subscript indicating the mode number and the second is an edge fixity identifier having the following key:

1. clamped-clamped
2. free-free
3. clamped-free

Thus, for example, α_{23} is identified with the second mode of a clamped-free circular beam. The clamped-SD and free-SD modes are included

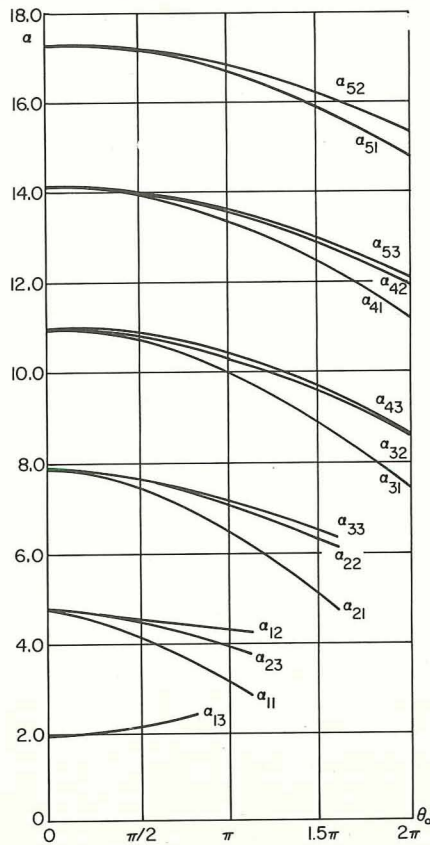


FIGURE 2.144.—Eigenfunction constants for curved circular beams. (After refs. 2.127 and 2.202)

within the antisymmetric clamped-clamped and free-free modes, respectively. The values of α_n for SD-SD supports are π , 2π , 3π , The values of α_n in figure 2.144 approach those of table 2.21 for straight beams as the included angle θ_0 approaches zero. The constants δ_n , γ_n , η_n , and θ_n for the curved beam functions are available for free-free, clamped-free, and clamped-clamped beams in figures 2.145, 2.146, and 2.147, respectively. Upon substituting the appropriate constants from these figures and table 2.21 into the terms of the characteristic determinant (2.169), the frequency parameters $\Omega^2 = \omega^2 R^2 \rho (1 - \nu^2) / E$ may then be evaluated directly as the three roots of the determinant. The expanded determinant is, of course, a cubic characteristic equation in Ω^2 which takes the form of equation (2.35). Usually, one of the three roots of the cubic equation (the root associated with

a transverse bending mode) is much smaller than the other two. In such cases some of the approximate frequency formulas such as equations (2.50) and (2.51) can be employed.

The modal density (number of natural frequencies per unit frequency interval) for shallow shells having arbitrary edge conditions is discussed by Bolotin in references 2.149 and 2.195.

In reference 2.213 the frequencies of completely clamped shallow shells made of aluminum and having dimensions $l = 11.5/8$ in., $R\theta_0 = 9.5/8$ in., and $h = 0.032$ in. were calculated using the Ritz method and straight beam functions. These results are exhibited in table 2.52 for two types of analysis. The first used the Donnell-Mushtari shell equations with only a single product of beam functions and neglected tangential inertia; the second used the Sanders equations with three beam function products and included tangential inertia. For shells having this extent of shallowness the two approaches give only slightly differing results. A similar comparison is made in table 2.53 for a set of shallow shells having *square* planforms (from ref. 2.214). Experiments were also conducted on these shells and the results are shown in tables 2.54 and 2.55. Difficulty was encountered in obtaining rigid clamping in the test set-ups, which caused a significant decrease in the frequencies from the theoretical values for clamped shells, particularly for the lowest modes. For $R = 96$ in. and $m = n = 1$ in table 2.54 the clamping was very ineffective in restraining the tangential displacements at the boundary and the measured frequency (150 cps) is essentially the

TABLE 2.52.—Frequencies of Completely Clamped Aluminum Shell Panels ($l = 11.5/8$ in., $R\theta_0 = 9.5/8$ in., $h = 0.032$ in.); $m = 1$

Number of circumferential half-waves, n	Frequencies, cps, for—			
	$R = 96.0$ in.		$R = 48.0$ in.	
	Donnell-Mushtari	Sanders	Donnell-Mushtari	Sanders
1	314.4	314.0	602.7	601.9
2	334.1	333.15	531.0	529.8
3	479.2	477.7	595.05	593.5
4	722.5	720.5	784.7	782.8
5	1045		1078	

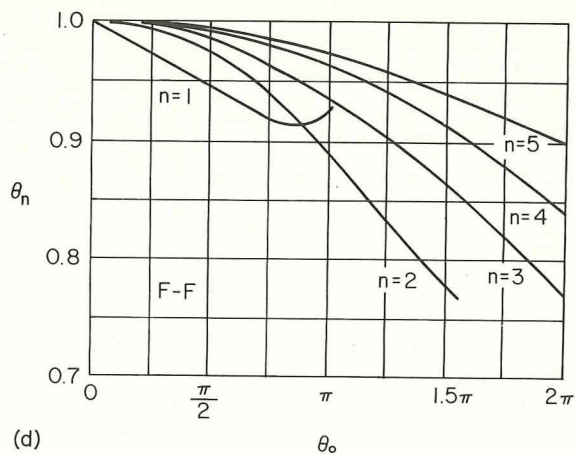
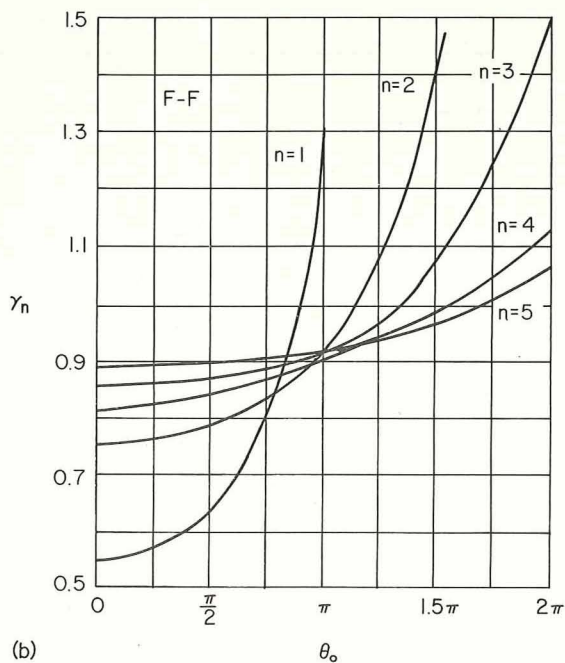
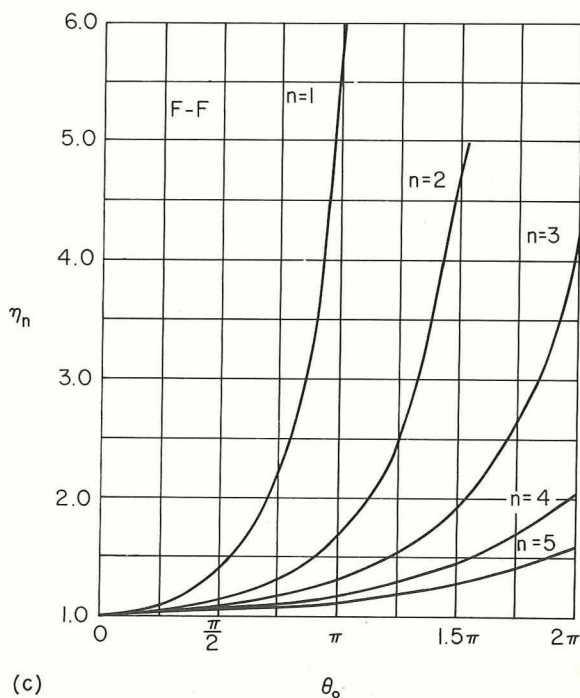
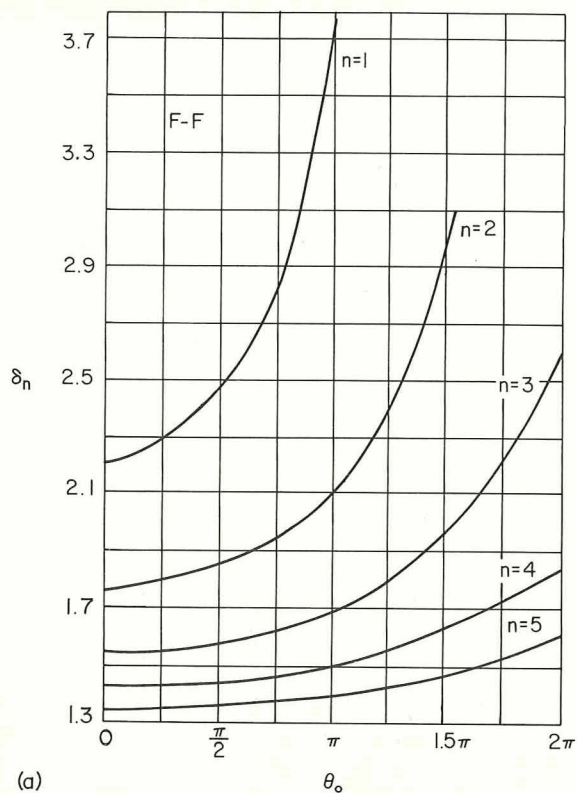


FIGURE 2.145—Constants for free-free curved beam functions. (After refs. 2.127 and 2.202) (a) δ_n . (b) $+\gamma_n$. (c) η_n . (d) θ_n .

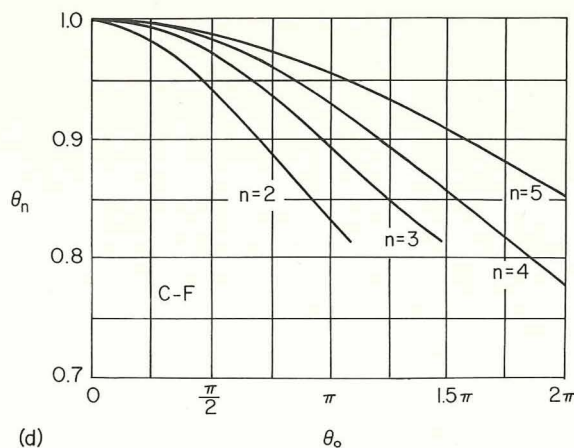
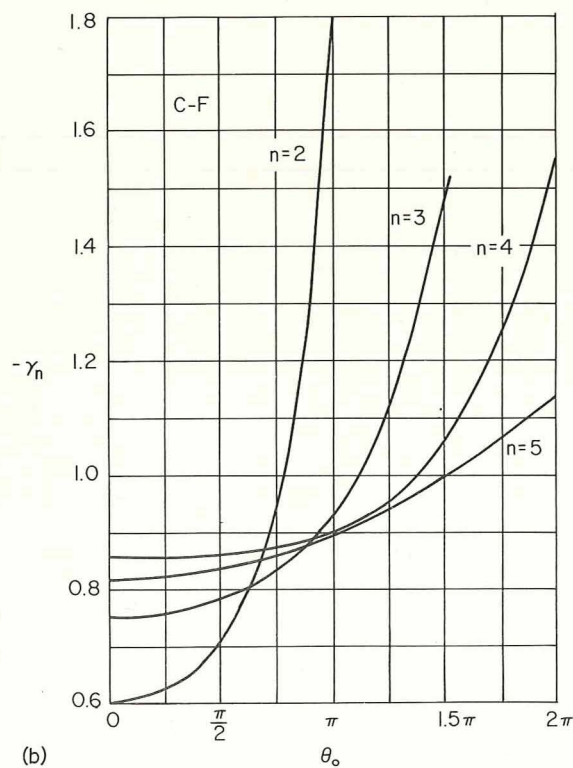
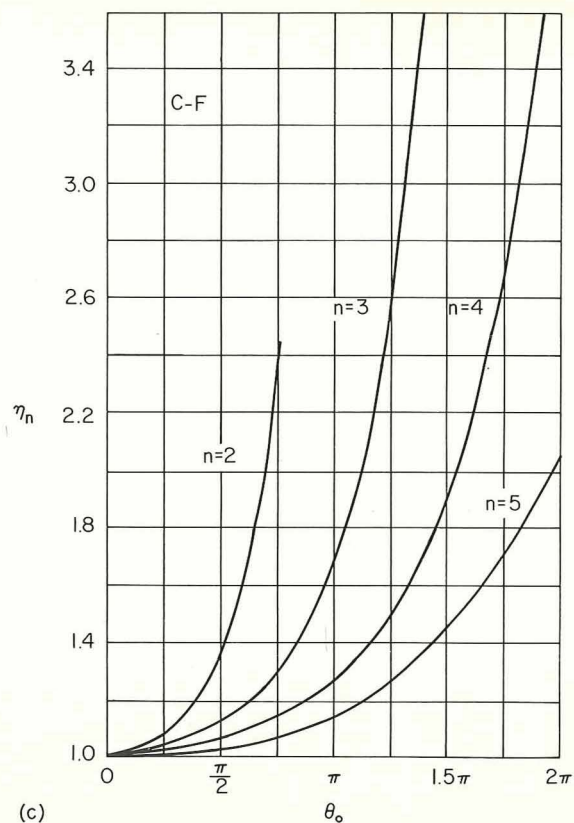
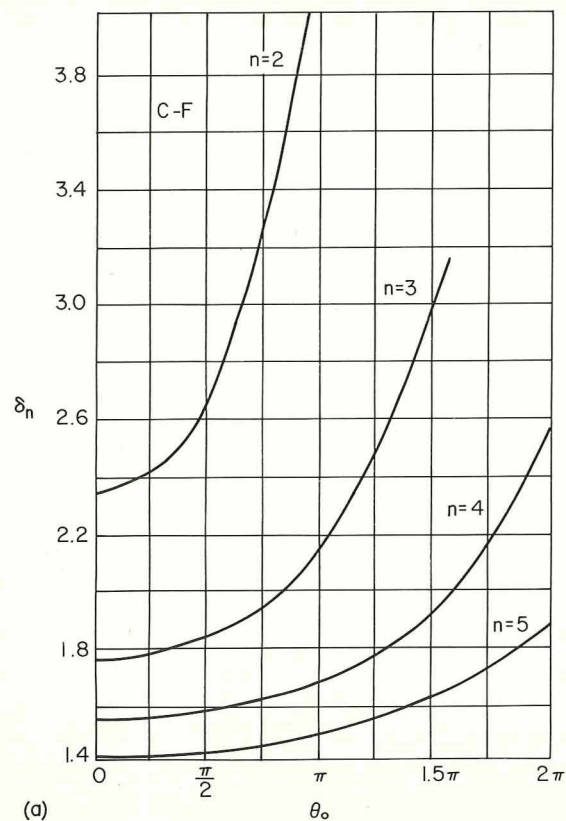


FIGURE 2.146—Constants for clamped-free curved beam functions. (After refs. 2.127 and 2.202) (a) δ_n . (b) $-\gamma_n$. (c) η_n . (d) θ_n .

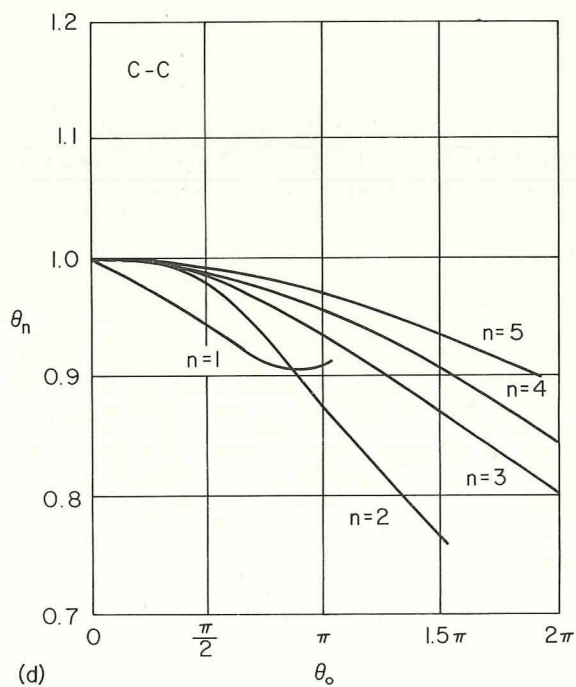
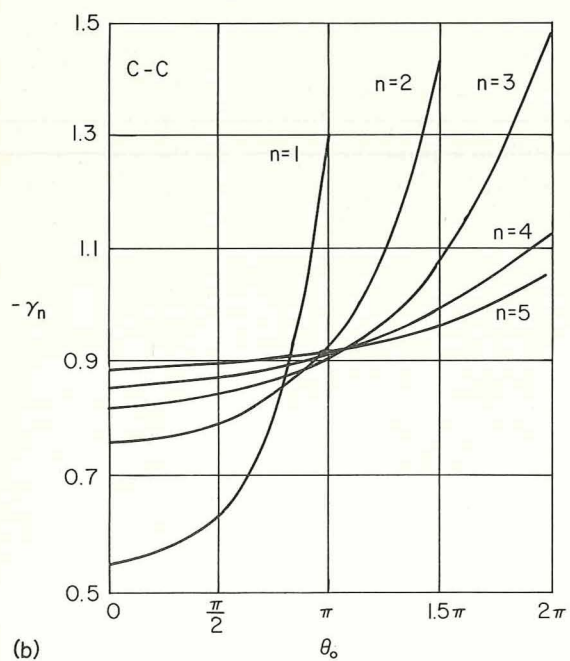
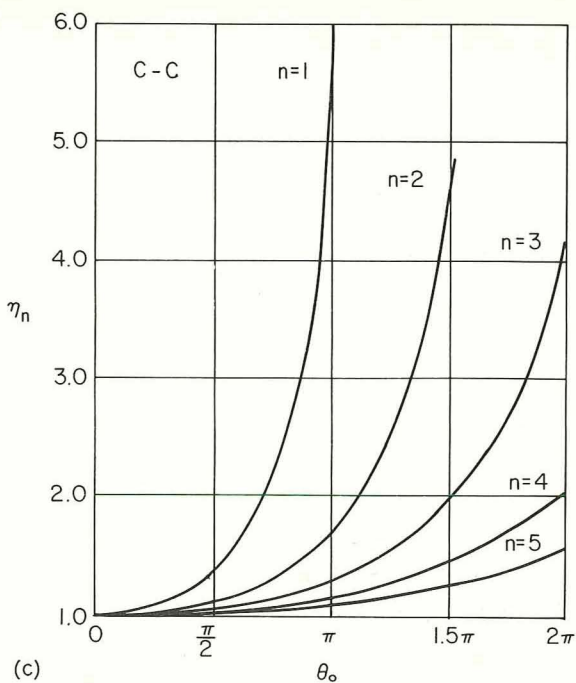
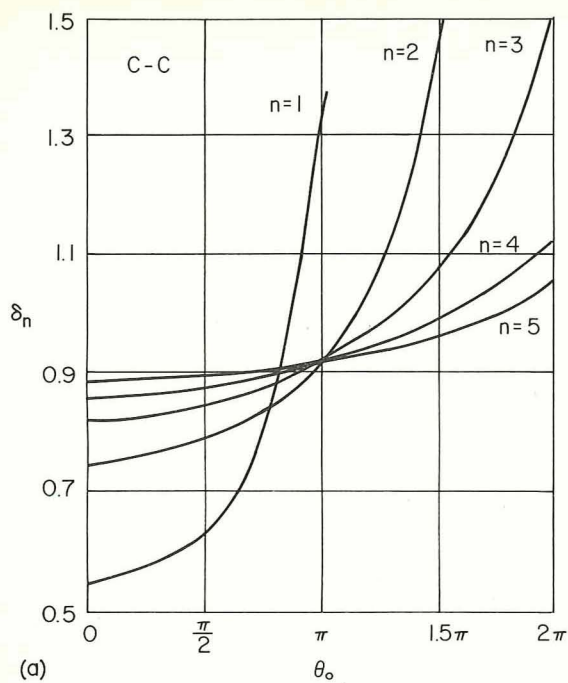


FIGURE 2.147—Constants for clamped-clamped curved beam functions. (After refs. 2.127 and 2.202)

(a) δ_n . (b) $-\gamma_n$. (c) η_n . (d) θ_n .

TABLE 2.53.—Comparison of Calculated and Measured Frequencies ($l=11\text{-}5/8$ in., $R\theta_0=9\text{-}5/8$ in., $h=0.032$ in.), cps

R , in.	m	n	Theory		Experiment
			Shear diaphragm supports	Clamped	
96	1	1	146.7	314.4	150
	1	2	163.2	334.1	250
	1	3	322.8	479.2	440
	1	4	554.8	722.5	725
	1	5	853.9	1045	
	2	1	274.3	356.6	
	3	1	373.1	446.4	345
	4	1	501.6	593.0	540
	5	1	680.1	769.2	800
48	1	1	277.5	602.7	350
	1	2	183.2	531.0	270
	1	3	323.4	595.05	445
	1	4	551.9	784.7	760
	1	5	848.7	1078	
	2	1	505.1	635.9	
	3	1	622.1	699.9	560
	4	1	729.7	808.2	770
	5	1	872.3	971.4	935

same as the theoretical result for shear diaphragm supports all around. The method of clamping consisted of a simple lap attachment at the boundaries using closely spaced bolts (1/8 in. in diameter and spaced 1-1/16 in. on centers in ref. 2.213; 3/16 in. in diameter and spaced 1-1/2 in. on centers in ref. 2.214).

Theoretical results obtained in a similar manner for shells having $l=11.0$ in., $R\theta_0=9.0$ in., and $h=0.028$ in. were compared in reference 2.198 with experimental results presented in reference 2.215. Graphs of these results have been exhibited earlier as figures 2.142. In these figures the effects of adding an additional clamping strip over the tops of the lap attachments is shown by squares having additional flags. Sewall (ref. 2.198) also gave the following formula for the frequencies of completely clamped shallow cylindrical shells (using the Donnell-Mushtari theory and neglecting tangential inertia) when only a single term in the products of beam functions is used:

$$\begin{aligned}\Omega^2 &= \rho \omega^2 R^2 (1 - \nu^2) / E \\ &= \frac{h^2 R^2}{12} \left(N_m^4 + 2 \frac{\bar{N}_m \bar{N}_n}{R \theta_0 l} + N_n^4 \right) \\ &+ \left\{ (N_m N_n)^4 \left[1 - \left(\frac{\bar{N}_n}{N_n} \right)^2 \left(\frac{1}{N_n R \theta_0} \right)^2 \right. \right. \\ &\quad \left. \left. - \left(\frac{\bar{N}_m}{N_m} \right)^2 \left(\frac{\nu}{N_m l} \right)^2 \right] \right. \\ &+ \frac{1 - \nu}{2} \frac{\bar{N}_m \bar{N}_n}{R \theta_0 l} \left[N_m^2 \left(N_m^2 - \frac{\nu^2 \bar{N}_m^2}{N_m^2 l^2} \right) \right. \\ &\quad \left. + N_n^2 \left(N_n^2 - \frac{\bar{N}_n^2}{N_n^2 R^2 \theta_0^2} \right) \right] \\ &+ \nu^2 \left(\frac{\bar{N}_m \bar{N}_n}{R \theta_0 l} \right)^2 \left. \right\} \div \left\{ (N_m N_n)^4 \right. \\ &+ \frac{1 - \nu}{2} \frac{\bar{N}_m \bar{N}_n}{R \theta_0 l} (N_m^4 + N_n^4) \\ &\quad \left. - \nu \left(\frac{\bar{N}_m \bar{N}_n}{R \theta_0 l} \right)^2 \right\} \quad (2.172)\end{aligned}$$

where

$$N_m = \epsilon_m / l, \quad N_n = \epsilon_n / R \theta_0, \quad \bar{N}_m = \alpha_m N_m (\alpha_m N_m l - 2) \\ \bar{N}_n = \alpha_n N_n (\alpha_n N_n R \theta_0 - 2), \quad \text{and } \alpha_m, \epsilon_m, \epsilon_n$$

are the eigenfunction constants for clamped-clamped beams as defined by equations (2.93) and (2.94) and are listed in table 2.23.

Webster (ref. 2.199) obtained theoretical results for completely clamped shallow shells by using Flügge's shell equations and a variational approach. The procedure consisted of applying Hamilton's principle subject to the constraints supplied by the geometric boundary conditions, which are enforced by means of Lagrange multipliers in the variational problem. The displacement functions are taken in the form of polynomials; i.e.,

$$\left. \begin{aligned}u &= \sum_{m=0}^{M-1} \sum_{n=0}^{N-1} A_{mn} (x/l)^m (\theta/\theta_0)^n \\ v &= \sum_{m=0}^{M-1} \sum_{n=0}^{N-1} B_{mn} (x/l)^m (\theta/\theta_0)^n \\ w &= \sum_{m=0}^{M-1} \sum_{n=0}^{N-1} C_{mn} (x/l)^m (\theta/\theta_0)^n\end{aligned} \right\} \quad (2.173)$$

where A_{mn} , B_{mn} , and C_{mn} are undetermined coefficients. The order of the resultant character-

TABLE 2.54.—Frequencies of Completely Clamped Square Aluminum Shell
Panels ($l = R\theta_0 = 17.0$ in.); $m = 1$

h , in.	Number of circumferential half-waves, n	Frequencies, cps, for —			
		$R = 96.0$ in.		$R = 48.0$ in.	
		Donnell- Mushtari	Sanders	Donnell- Mushtari	Sanders
0.020	1	299.5	299.0	597.3	596.3
	2	245.9	245.2	484.1	482.55
	3	225.55	225.0	423.7	422.6
	4	232.3	231.8	393.7	393.0
	5	267.1	266.5	392.9	393.0
	6	326.9	326.2	421.1	420.45
	7	407.7	407.0	476.9	476.2
0.032	1	301.0	300.5	598.1	597.0
	2	253.6	252.9	488.0	486.6
	3	251.6	250.9	438.1	437.0
	4	292.6	291.8	432.0	431.05
	5	373.4	372.4	471.6	470.6
	6	486.7	485.6	554.3	553.3
	7	627.4	626.3	674.4	673.2
0.040	1	302.4	301.9	598.8	597.75
	2	260.5	259.8	491.65	490.25
	3	273.4	272.6	451.0	449.8
	4	338.8	337.8	464.5	463.4
	5	449.7	448.5	534.0	532.85
	6	597.4	596.1	653.6	652.3
	7	776.9	775.5	815.2	813.8

istic determinant to be evaluated by this procedure is $3MN$ plus the number of boundary constraint equations. In figures 2.148 through 2.152 the parameter $\rho\omega^2(1-\nu^2)l^2R^2\theta_0^2/Eh^2$ for fundamental frequencies obtained by the above procedure is plotted against the geometric parameter $\theta_0 l/h$ for five aspect ratios $R\theta_0/l$. Terms of degree up to $x^5\theta^8$ and $x^7\theta^7$ were taken to ensure convergence. Data resulting from Sewall's equation (2.172) are also depicted on these graphs. The notation (m,n) used in figures 2.148 through 2.152 indicates that the normal displacement w , in the modes corresponding to these frequencies, has m and n half-waves in the x and θ directions, respectively.

When Sewall's formula (2.172) is converted to the frequency parameter $\rho\omega^2(1-\nu^2)l^2R^2\theta_0^2/Eh^2$ used in figures 2.148 through 2.152, it is found to be independent of θ_0 for a given $R\theta_0/l$ and

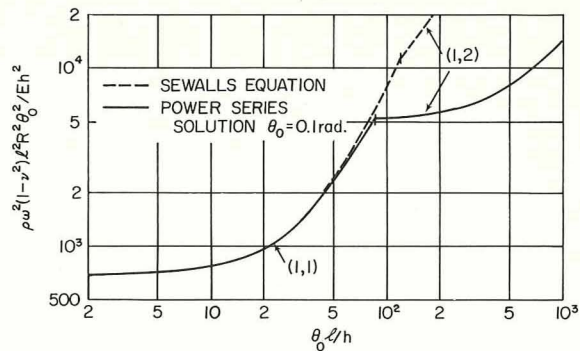


FIGURE 2.148.—Fundamental frequency parameter for completely clamped shallow shells; $R\theta_0/l = 0.25$. (After ref. 2.199)

TABLE 2.55.—Comparison of Calculated and Measured Frequencies
 ($l=17.0$ in., $R\theta_0=17.0$ in.), cps; $m=1$

h , in.	n	$R=96.0$ in.			$R=48.0$ in.		
		Theory		Experiment	Theory		Experiment
		SD	Clamped		SD	Clamped	
0.020	1	167.3	299.5	240	332.7	597.3	310
	2	74.6	245.9		137.4	484.1	
	3	74.4	225.55	85	94.1	423.7	86
	4	114.7	232.3	129	119.55	393.7	148
	5	173.3	267.1	190	174.7	392.9	241
	6	246.2	326.9	345	246.6	421.1	387
	7	332.5	407.7		332.6	476.9	
0.032	1	168.1	301.0	117	333.1	598.1	102
	2	85.3	253.6		143.5	488.0	
	3	111.5	251.6	125	125.4	438.1	144
	4	181.9	292.6	229	184.9	432.0	270
	5	276.9	373.4	295	277.6	471.6	294
	6	393.7	486.7		393.9	554.3	
	7	532.0	627.4		532.0	674.4	613
0.040	1	168.9	302.4	123	333.5	598.8	169
	2	94.2	260.5		148.9	491.65	
	3	137.1	273.4	197	148.6	451.0	180
	4	226.9	338.8	278	229.2	464.5	289
	5	346.0	449.7	388	346.5	534.0	398
	6	492.1	597.4	727	492.2	653.6	735
	7	665.0	776.9		664.9	815.2	

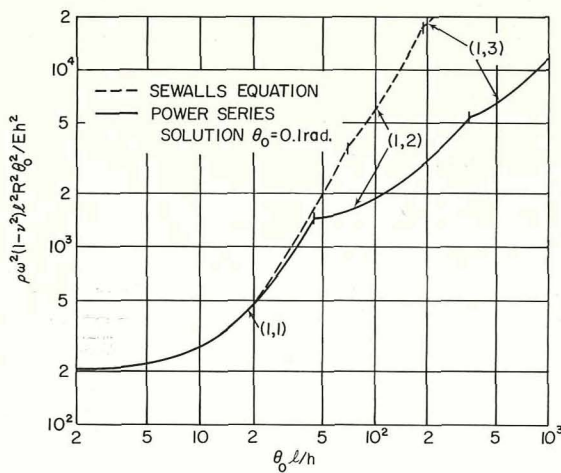


FIGURE 2.149.—Fundamental frequency parameter for completely clamped shallow shells; $R\theta_0/l=0.5$. (After ref. 2.199)

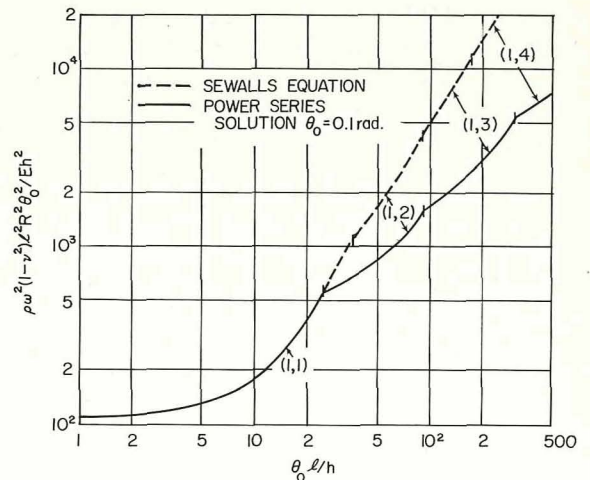


FIGURE 2.150.—Fundamental frequency parameter for completely clamped shallow shells; $R\theta_0/l=1.0$. (After ref. 2.199)

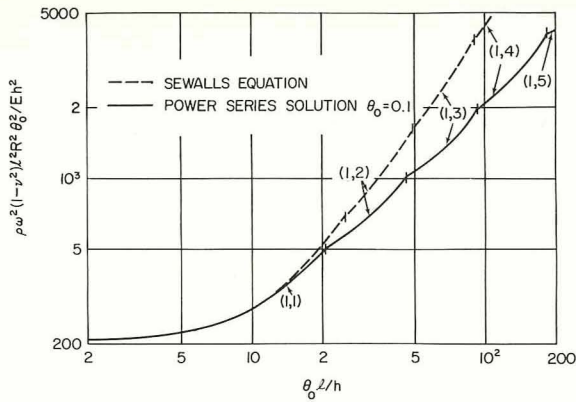


FIGURE 2.151.—Fundamental frequency parameter for completely clamped shallow shells; $R\theta_0/l = 2.0$. (After ref. 2.199)

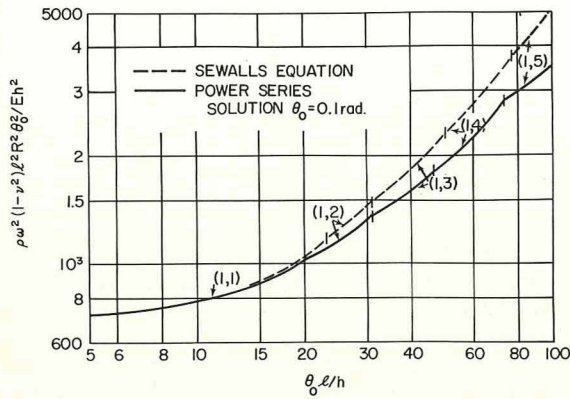


FIGURE 2.152.—Fundamental frequency parameter for completely clamped shallow shells; $R\theta_0/l = 4.0$. (After ref. 2.199)

$\theta_0 l/h$, but the solution using the power series given by equations (2.173) is not. The results shown in the figures 2.148 through 2.152 are for $\theta_0 = 0.1$ rad (5.73°), but as pointed out in reference 2.199 they may be used for shallow shells, in general, with little error. At $\theta_0 = 1.0$ rad. (57.3°) the results would be approximately 2 to 3 percent less than those for $\theta_0 = 0.1$ rad.

Figures 2.148 through 2.152 also show that Sewall's equation gives accurate results for small values of $\theta_0 l/h$ but becomes inaccurate as $\theta_0 l/h$ increases because the beam functions do not represent the true displacements very accurately in this range (ref. 2.199). In particular, the representation of the v displacement is poor for modes having more than one half-wave in the θ direc-

tion. For thick panels having large curvatures, these errors have a small effect upon the frequencies because the stretching strain energy is small compared to the bending strain energy. For thinner, less shallow panels the stretching energy becomes more significant.

If one considers the nodal patterns of a clamped square plate (cf., ref. 2.157), it is found that some of them have node lines which are not at all parallel to the sides of the plate (see ref. 2.157). These modes are identified as $(m,n) \pm (n,m)$ modes because they may be approximated by combinations of two assumed modes (m,n) and (n,m) , which do have nodal lines parallel to the edges. The patterns of these modes are sensitive to asymmetry which is introduced by making the aspect ratio slightly different from unity. A similar effect occurs in shallow shells when asymmetry is introduced by virtue of having curvature in only one direction. Figure 2.153 (from ref. 2.199) shows the transformation of the nodal patterns of the $(3,1) \pm (1,3)$ modes of a square flat plate to $(1,3)$ and $(3,1)$ modes by the introduction of curvature in one direction. For $\theta_0 l/h = 8$ the rise of the square curved panel is approximately equal to the thickness. It is seen that curvatures of this order change the nodal patterns considerably.

Rectangular curved panels, like flat plates, will have two modes with equal frequencies. However, for this to occur the two modes must have different symmetries with respect to the x and θ axes, or both. If the two modes have the same type of symmetry (or antisymmetry) then two modes having *nearly* the same frequency can occur. The nodal patterns of these two modes can be quite complex (cf., ref. 2.157). In figures 2.148

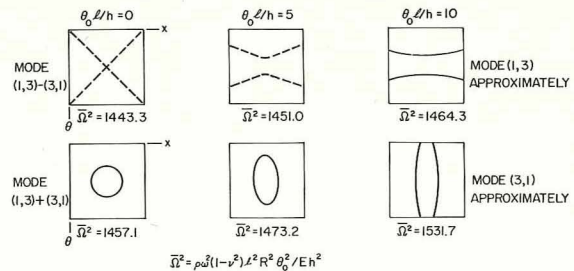


FIGURE 2.153.—Effect of curvature upon the nodal patterns of clamped square curved panels; $R\theta_0/h = 100$. (After ref. 2.199)

through 2.152 the mode changes do all occur with changes of symmetry, giving actual crossings of frequency curves.

Lisowski (refs. 2.216 and 2.217) computed the first eight frequencies of a completely clamped shallow shell of celluloid having dimensions in centimeters as shown in figure 2.154. A flexibility matrix expressed in terms of the eight interior points shown in figure 2.154 was obtained by experimental measurement with point loads. Frequencies were then calculated by treating the problem as one having eight transverse degrees of freedom associated with the eight mesh points. Frequencies in cycles per second and corresponding mode shapes are shown in figure 2.155.

The Rayleigh method using the Love-Timoshenko shell equations neglecting tangential inertia and a simple mode shape of the form

$$w = x^2 \theta^2 (x-l)^2 (\theta - \theta_0)^2 \quad (2.174)$$

was used by Palmer (ref. 2.211) for the completely clamped shallow shell. Results for aluminum plates are shown in figure 2.156, where f is the cyclic frequency.

In reference 2.221 the finite element technique

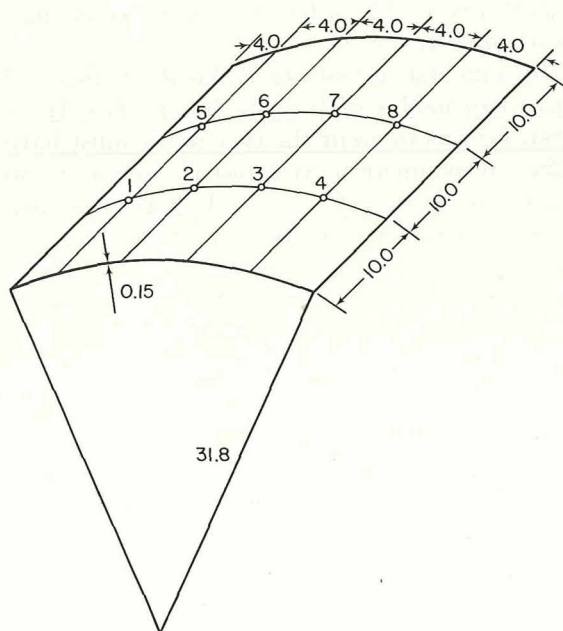


FIGURE 2.154.—Dimensions (in centimeters) of a completely clamped shallow shell of celluloid used for the results of figure 2.155. (After refs. 2.216 and 2.217)

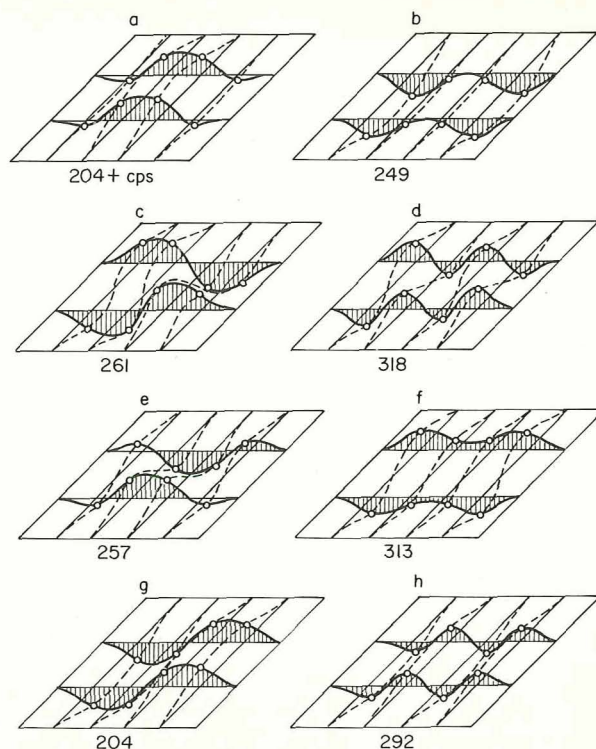


FIGURE 2.155.—Frequencies (cps) and mode shapes of a completely clamped shallow shell. (After refs. 2.216 and 2.217)

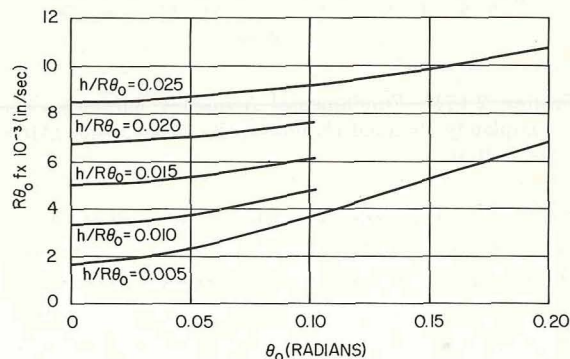


FIGURE 2.156.—Frequencies of a completely clamped aluminum shallow shell (f in cps). (After ref. 2.211)

is used to calculate the natural frequencies of an arch dam of particular dimensions. The structure can also be regarded as a clamped-free-clamped-free circular cylindrical shell.

Experimental results for curved cylindrical panels were presented in reference 2.213. The panels were made of 0.032 in. thick 2024-T3

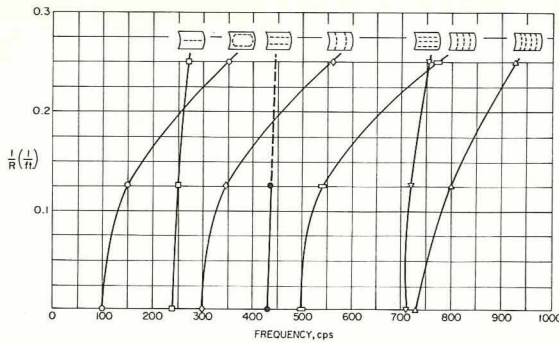


FIGURE 2.157.—Experimentally determined frequencies for panels having riveted edges. (After ref. 2.213)

aluminum alloy. The planform dimensions were $b = 11$ in. and $l = 13$ in. (see fig. 2.141). The panels were riveted to rigid supporting frames having unsupported internal dimensions of $9\frac{5}{8}$ in. by $11\frac{5}{8}$ in. Results are shown in figures 2.157 for $R = 48$ in., 96 in., and ∞ where it is demonstrated that there is little difference in the natural frequencies between flat and curved panels when the node lines are parallel to the longitudinal (x) direction.

2.8.5 Added Concentrated Mass

Chen (refs. 2.201 and 2.225) analyzed the problem of a circular cylindrical shell panel having a concentrated mass M attached at its center ($\bar{x} = l/2$, $\theta = \theta_0/2$ in terms of figure 2.141). All four edges of the panel were supported by shear diaphragms. The Donnell-Mushtari shell equations were used. The procedure consisted of using an infinite set of solution functions in the form of equations (2.164) and (2.165) which satisfy the boundary conditions exactly, expanding the concentrated inertia load in terms of the same functions, and substituting into the equations of motion. This procedure yields a characteristic determinant of infinite order which can be solved to any desired degree of accuracy by successive truncation. Detailed numerical results showing the rate of convergence of this method are seen in table 2.56 for the fundamental frequencies of panels having $\theta_0 = \pi/6$, $\nu = 0.3$, and a ratio of concentrated mass to shell mass ($M/\rho h l R \theta_0$) of $1/4$. Similar results for higher frequencies of a particular panel having $\theta_0 = \pi/6$, $l/R\theta_0 = 1$, and $R/h = 100$ are given in table 2.57. Figure 2.158

TABLE 2.56.—Convergence of the Fundamental Frequency Parameter $\omega l \sqrt{\rho(1-\nu^2)/\pi^2 E}$ (Breathing Mode) of a Cylindrical Panel Carrying a Concentrated Mass

Number of terms in series	Upper limit on—		$\omega l \sqrt{\rho(1-\nu^2)/\pi^2 E}$	
	m	n	$l/R\theta_0 = 1$ $R/h = 100$	$l/R\theta_0 = 2$ $R/h = 1000$
1	1	1	0.06101	0.04473
2	1	3	.05888	.02252
3	3	1	.05767	.02245
4	3	3	.05710	.02181
5	1	5	.05682	.02137
6	3	5	.05665	.02137
7	5	1	.05644	
8	5	3	.05624	
9	5	5	.05616	
10	1	7	.05608	
11	3	7	.05600	
12	5	7	.05600	

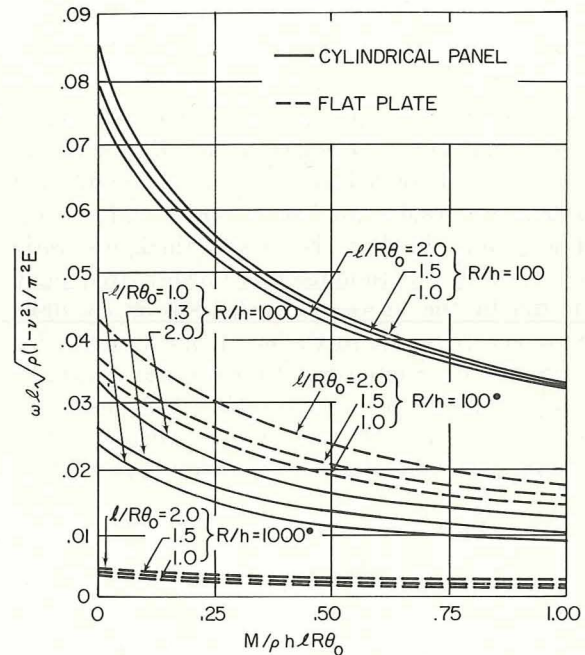


FIGURE 2.158.—Variation of the fundamental frequency parameters with mass ratio for cylindrical panels having a concentrated mass. (After ref. 2.201)

shows the variation of $\omega l \sqrt{\rho(1-\nu^2)/\pi^2 E}$ with the mass ratio for the fundamental frequency. The results shown in the figure are obtained by using

TABLE 2.57.—Higher Frequency Parameters $\omega l \sqrt{\rho(1-\nu^2)/\pi^2 E}$ for a Cylindrical Panel Carrying a Concentrated Mass

Number of terms	Mode	Number of axial and longitudinal half waves — m, n					
		1,1	1,3	3,1	3,3	1,5	3,5
1	Breathing, w	0.0610					
2		.0589	0.1467				
3		.0577	.1408	0.2067			
4		.0571	.1386	.2051	0.2973		
5		.0568	.1376	.2044	.2945	0.4211	
6		.0567	.1370	.2040	.2932	.4171	0.5576
1	Extensional, u	0.8396					
2		.8405	1.8715				
3		.8411	1.8715	2.8976			
4		.8414	1.8715	2.8976	2.5118		
5		.8416	1.8715	2.8976	2.5118	3.0165	
6		.8418	1.8715	2.8976	2.5118	3.0165	3.4509
1	Torsional, v	1.4145					
2		1.4170	3.1648				
3		1.4174	3.1654	1.8718			
4		1.4176	3.1656	1.8718	4.2436		
5		1.4177	3.1656	1.8718	4.2436	5.1011	
6		1.4178	3.1656	1.8718	4.2436	5.1011	5.8321

six term series of approximations for u , v , and w . Results are given for aspect ratios $l/R\theta_0=1.0, 1.5$, and 2.0 and for thickness ratios $R/h=100$ and 1000 . All results are for $\theta_0=\pi/6$ and $\nu=0.3$. For panels having the lower thickness ratio ($R/h=100$), the fundamental (lowest) frequency occurs in the $m=n=1$ mode. For $R/h=1000$, however, it occurs in the $m=1, n=3$ mode. For purposes of comparison to show the effects of shallow shell curvature, figure 2.158 also gives the results for the case of a rectangular plate having the same dimensions and edge supports.

2.8.6 Other Boundary Shapes

Wieckowski (ref. 2.226) presented a procedure for the solution of the free vibration of a shell having circular cylindrical curvature bounded by the edges $x=0, l$ and two helices. The edge $x=0$ is clamped and all other edges are free, which is intended to simulate a stream turbine blade. The Donnell-Mushtari shell equations are used and are transformed into skew coordinates which are compatible with the edges of the shell. The procedure outlined is tedious and leads to an infinite sequence of ordinary differential equations having

constant coefficients. No numerical results are given.

REFERENCES

- 2.1. NAGHDI, P. M.: A Survey of Recent Progress in the Theory of Elastic Shells. *Appl. Mech. Rev.*, vol. 9, no. 9, Sept. 1956, pp. 365-368.
- 2.2. MIRSKY, I.; AND HERRMANN, G.: Nonaxially Symmetric Motions of Cylindrical Shells. *J. Acoust. Soc. Amer.*, vol. 29, no. 10, Oct. 1957, pp. 1116-1123.
- 2.3. ARNOLD, R. N.; AND WARBURTON, G. B.: Flexural Vibrations of the Walls of Thin Cylindrical Shells Having Freely Supported Ends. *Proc. Roy. Soc. (London)*, ser. A, 197, June 1949, pp. 238-256.
- 2.4. ARNOLD, R. N.; AND WARBURTON, G. B.: The Flexural Vibrations of Thin Cylinders. *Inst. Mech. Engineers (ser. A)*, Proc. 167, 1953, pp. 62-80.
- 2.5. HOUGHTON, D. S.; AND JOHNS, D. J.: A Comparison of the Characteristic Equations in the Theory of Circular Cylindrical Shells. *Aeronaut. Quart.*, Aug. 1961, pp. 228-236.
- 2.6. BIJLAARD, P. P.: Stresses from Local Loadings in Cylindrical Pressure Vessels. *Trans. ASME*, vol. 77, no. 6, Aug. 1955, pp. 805-816.
- 2.7. EPSTEIN, P. S.: On the Theory of Elastic Vibrations in Plates and Shells. *J. Math. Phys.*, vol. 21, 1942, pp. 198-209.

- 2.8. KENNARD, E. H.: The New Approach to Shell Theory: Circular Cylinders. *J. Appl. Mech.*, vol. 20, no. 1, Mar. 1953, pp. 33-40.
- 2.9. KENNARD, E. H.: Cylindrical Shells: Energy, Equilibrium Addenda and Erratum. *J. Appl. Mech.*, vol. 22, no. 1, Mar. 1955, pp. 111-116.
- 2.10. KENNARD, E. H.: Approximate Energy and Equilibrium Equations for Cylindrical Shells. *J. Appl. Mech.*, vol. 23, no. 4, Dec. 1956, pp. 645-646.
- 2.11. KENNARD, E. H.: A Fresh Test of the Epstein Equations for Cylinders. *J. Appl. Mech.*, vol. 25, no. 4, Dec. 1958, pp. 553-555.
- 2.12. COUPRY, G.: Breathing Vibrations in Homogeneous or Non-Homogeneous Thin Cylindrical Shells. *La Recherche Aéronautique*, no. 91, Nov.-Dec. 1962, pp. 59-65. (In French.)
- 2.13. COUPRY, G.: On the Breathing (Flexural) Vibrations of Thin Shells, Application to Solid Rockets. Office National d'Etudes et de Recherches Aérospatiales, Pub. No. 110, 1964. (In French.)
- 2.14. MORLEY, L. S. D.: An Improvement on Donnell's Approximation for Thin-Walled Circular Cylinders. *Quart. J. Mech. Appl. Math.*, vol. 12, Feb. 1952, pp. 89-99.
- 2.15. HERRMANN, G.; AND ARMENAKAS, A. E.: Dynamic Behavior of Cylindrical Shells Under Initial Stress. Tech. Note 60-425, Air Force Office of Sci. Res., Apr. 1960.
- 2.16. LYONS, W. C.; RUSSELL, J. E.; AND HERRMANN, G.: Dynamics of Submerged Reinforced Cylindrical Shells. *J. Engng. Mech. Div., Proc. Amer. Soc. Civil Engrs. EM*, vol. 94, EM2, Apr. 1968, pp. 397-420.
- 2.17. YU, Y. Y.: Application of Donnell-Type Dynamic Equations Including and Excluding the Effects of Transverse Shear and Rotational Inertia to Vibrations of Infinitely Long Cylindrical Shells. AD 132 465, July 1957.
- 2.18. GALERKIN, B. G.: *Ravnesoye uprugoy tsilindricheskoy obolochki*. (The Equilibrium of an Elastic Cylindrical Shell.) Trudy Leningradskogo Instituta Sooruzheniy, 1935.
- 2.19. VLASOV, V. Z.: *Obschaya teoriya obolochek i yeye prilozheniya v tekhnike*. Gos. Izd. Tekh.-Teor. Lit., Moscow-Leningrad, 1949. (English transl.: NASA TT F-99, General Theory of Shells and Its Application in Engineering, Apr. 1964.)
- 2.20. MILLER, P. R.: Free Vibrations of a Stiffened Cylindrical Shell. Aero. Res. Coun. Lond. Rpt. Mem. 3154, 1960.
- 2.21. SIMMONDS, J. G.: A Set of Simple, Accurate Equations for Circular Cylindrical Elastic Shells. Report SM-4 (NASA N66-15403), Div. of Eng. and Appl. Phys., Harvard Univ., 1966.
- 2.22. MUGNIER D.; AND SCHROETER, D.: Vibrations of a Homogeneous Circular Cylindrical Tank, Empty or Filled With Liquid, About a Prestablished Static Stress State—Case of the Inhomogeneous Cylinder—Comparison With Experiment. *J. de Mécanique*, vol. 6, Sept. 1967, pp. 417-441. (In French.)
- 2.23. RAYLEIGH, LORD: Note on the Free Vibrations of an Infinitely Long Shell. *Proc. Roy Soc.*, vol. 45, 1889, p. 443.
- 2.24. RAYLEIGH, LORD: *Theory of Sound*. Vol. 1, second ed., MacMillan Co., 1894; also Dover Publications, 1945.
- 2.25. LOVE, A. E. H.: On the Small Free Vibrations and Deformations of a Thin Elastic Shell. *Phil. Trans. Roy. Soc. (London)*, ser. A, vol. 179, 1888, pp. 491-546.
- 2.26. LOVE, A. E. H.: *A Treatise on the Mathematical Theory of Elasticity*. Fourth ed., Dover Pub., Inc. (New York), 1944.
- 2.27. REISMANN, H.; AND PAWLIK, P. S.: On the Plane Strain Dynamic Response of a Cylindrical Shell Under Lateral Loads. Rept. No. 22, ARO-D Proj. No.: 5637-E*, Div. of Interdisciplinary Studies and Research, School of Engineering, State Univ. of N.Y. at Buffalo, Apr. 1967.
- 2.28. REISMANN, H.; AND PAWLIK, P. S.: Plane-Strain Dynamic Response of a Cylindrical Shell: A Comparison Study of Three Different Shell Theories. *J. Appl. Mech.*, vol. 35, no. 2, June 1968, pp. 297-305.
- 2.29. GOODIER, J. N.; AND McIVOR, I. K.: The Elastic Cylindrical Shell Under Nearly Uniform Radial Impulse. *J. Appl. Mech.*, vol. 31, no. 2, June 1964, pp. 259-266.
- 2.30. BIEZENO, C. B.; AND GRAMMEL, R.: *Engineering Dynamics*. Vol. II. Blackie and Son, Ltd., 1956.
- 2.31. FLÜGGE, W.: *Statik und Dynamik der Schalen*. Springer-Verlag, 1962.
- 2.32. YU, Y. Y.: Free Vibrations of Thin Cylindrical Shells Having Finite Lengths with Freely Supported and Clamped Edges. *J. Appl. Mech.*, vol. 22, no. 4, Dec. 1955, pp. 547-552.
- 2.33. KOVAL, L. R.: On the Free Vibrations of a Thin-Walled Circular Cylindrical Shell Subjected to an Initial Static Torque. Ph.D. Thesis, Cornell Univ., Sept. 1961.
- 2.34. KOVAL, L. R.; AND CRANCH, E. T.: On the Free Vibrations of Thin Cylindrical Shells Subjected to an Initial Static Torque. *Proc. 4th U.S. Nat'l. Congr. Appl. Mech.*, June 18-21, 1962, vol. 1, pp. 107-117.
- 2.35. FORSBERG, K.: A Review of Analytical Methods Used to Determine the Modal Characteristics of Cylindrical Shells. NASA CR-613, Sept. 1966.
- 2.36. CHU, W. H.: Breathing Vibrations of a Partially Filled Cylindrical Tank—Linear Theory. *J. Appl. Mech.*, vol. 30, no. 4, Dec. 1963, pp. 523-536.
- 2.37. FUNG, Y. C.; SECHLER, E. E.; AND KAPLAN, A.: On the Vibration of Thin Cylindrical Shells Under Internal Pressure. *J. Aeronaut. Sci.*, vol. 24, no. 9, Sept. 1957, pp. 650-661.
- 2.38. MALKINA, R. L.: *Vynuzhdennye Kolebaniia Tsilindricheskikh obolochek*. *Aviatsionnaya Tekhnika*, vol. 3, no. 4, 1960, pp. 51-60.

- 2.39. HU, W. C. L.; GORMLEY, J. F.; AND LINDHOLM, U. S.: An Analytical and Experimental Study of Vibrations of Ring-Stiffened Cylindrical Shells. Tech. Rept. No. 9, Contract NASr-94(06), SWRI Proj. 02-1504, Southwest Research Institute, June 1967.
- 2.40. HU, W. C. L.; AND WAH, T.: Vibrations of Ring-Stiffened Cylindrical Shells—An "Exact" Method. Tech. Rept. No. 7, Contract NASr-94(06), SWRI Proj. 02-1504, Southwest Research Institute, Oct. 1966.
- 2.41. BRUSILOVSKII, A. D.; MEL'NIKOVA, L. M.; AND SHVEIKO, I. U.: Vibrations and Stability of a Cylindrical Shell in a Gas Flow. *Inzh. Zh., Mekh. Tverdogo Tela*, vol. 6, no. 1, Jan.-Feb. 1966, pp. 67-73. (English trans.: Lockheed Missiles & Space Co.)
- 2.42. IVANYUTA, E. I.; AND FINKEL'SHTEYN, R. M.: Investigation of Axially Symmetric Vibrations of Cylindrical Shells. AD-630 414. (English transl.: FTD-MT-64-450, Foreign Technology Div., Wright-Patterson Air Force Base, 1966, pp. 112-128.)
- 2.43. IVANYUTA, E. I.; AND FINKEL'SHTEYN, R. M.: On the Influence of Tangential Forces of Inertia on Magnitude of Frequency of Free Vibrations of a Thin Cylindrical Shell. *Invest. of Elasticity and Plasticity*, Jan. 1966, pp. 255-259.
- 2.44. RAPOPORT, L. D.: The Calculation of Free Vibrations of Circular Cylindrical Shells not Previously Loaded. *Aviatsionnaya Tekhnika*, vol. 3, no. 3, 1960, pp. 43-50. (In Russian.)
- 2.45. PALLADINO, J. L.; AND NEUBERT, V. H.: Mobility of a Long Cylindrical Shell. *J. Acoust. Soc. Amer.*, vol. 42, no. 8, Aug. 1967, pp. 403-411.
- 2.46. SHENG, J.: The Response of a Thin Cylindrical Shell to Transient Surface Loading. *AIAA J.*, vol. 3, no. 4, 1965, pp. 701-709.
- 2.47. SHULMAN, Y.: Vibration and Flutter of Cylindrical and Conical Shells. Tech. Rept. No. ASRL 74-2 (AFOSR 59-776, ASTIA AD-226 444), Aeroelastic and Structures Res. Lab., Mass. Inst. of Tech., June 1959.
- 2.48. WARBURTON, G. B.: Free Vibrations of Thin Cylindrical Shells Having Finite Lengths with Freely Supported and Clamped Edges. *J. Appl. Mech.*, vol. 23, no. 3, Sept. 1956, pp. 484-487.
- 2.49. YU, Y. Y.: Dynamic Equations of Donnell Type for Cylindrical Shells with Application to Vibration Problems. Ninth Congres. Intern. Mecan. Appl., Univ. Bruxelles, 1957; vol. 7, pp. 261-278.
- 2.50. ARMENAKAS, A. E.: On the Accuracy of Some Dynamic Shell Theories. *J. Engng. Mech. Div., Proc. Amer. Soc. Civil Engrs. EM*, vol. 93, EM 5, Oct. 1967, pp. 95-109.
- 2.51. IL'INA, A. M.; AND KORBUT, B. A.: Vibrations of a Cylindrical Shell Containing an Elastic Filler. *Inzh. Zh.—Mekh. Tverdogo Tela*, July-Aug. 1968, pp. 183-186. (In Russian.)
- 2.52. SHASHKOV, I. E.: Elastic Vibrations of a Cylindrical Shell Filled with Liquid. *Inzhenernyi Zhurnal*, vol. 5, no. 3, 1965, pp. 575-579.
- 2.53. DIGIOVANNI, P. R.; AND DUGUNDJI, J.: Vibrations of Freely-Supported Orthotropic Cylindrical Shells Under Internal Pressure. AFOSR Sci. Rept. No. AFOSR 65-0640, ASRL TR 112-4, Feb. 1965.
- 2.54. GREENSPON, J. E.: Vibrations of a Thick-Walled Cylindrical Shell—Comparison of the Exact Theory with Approximate Theories. *J. Acoust. Soc. Amer.*, vol. 32, no. 5, May 1960, pp. 571-578.
- 2.55. REISMANN, H.; AND PADLOG, J.: Forced Axisymmetric Motions of Cylindrical Shells. *J. Franklin Inst.*, vol. 284, no. 5, Nov. 1967, pp. 308-319.
- 2.56. TANG, S.-c.: Response of a Finite Tube to Moving Pressure. *J. Engng. Mech. Div., Proc. Amer. Soc. Civil Engrs. EM*, vol. 93, EM 3, June 1967, pp. 239-256.
- 2.57. FUNG, Y. C.: On the Vibration of Thin Cylindrical Shells Under Internal Pressure. Rept. No. AM 5-8, The Ramo-Wooldridge Corp., Guided Missile Research Div., Oct. 1955.
- 2.58. HU, W. C. L.: Comments on Axisymmetric Vibrations of Thin Elastic Shells. *J. Acoust. Soc. Amer.*, vol. 38, no. 2, Aug. 1965, pp. 365-366.
- 2.59. WARBURTON, G. B.: Comments on "Natural Frequencies of Clamped Cylindrical Shells." *AIAA J.*, vol. 7, no. 2, Feb. 1969, pp. 382-383.
- 2.60. GALLETTY, G. D.: On the In-Vacuo Vibrations of Simply Supported, Ring Stiffened Cylindrical Shells. *Proc. 2nd U.S. Natl. Cong. Appl. Mech.*, June 1954; *ASME*, 1955, pp. 225-231.
- 2.61. GEERS, T. L.: An Approximate Method for Analyzing the Vibrations of Stiffened Plates and Shells. AD 646 353, Nov. 1966.
- 2.62. GRÜTZMACHER, M.; KALLENBACH, W.; AND NELLESSEN, E.: Comparison Between Resonance Frequencies of Circular Cylindrical Shells Calculated According to Different Methods and Measured Values. *Acustica*, vol. 17, no. 2, 1966, pp. 79-89. (In German.)
- 2.63. PETROV, V. I.; AND FINKEL'SHTEYN, R. M.: Free Vibration of Cylindrical Shells. *Issledovaniya Po Uprugosti i Plastichnosti*, no. 5, 1966, pp. 170-187. (In Russian.)
- 2.64. WEINGARTEN, V. I.: On the Free Vibration of Thin Cylindrical Shells. Contract No. AF04(695)-169 (AD405 117), Rept. No. TDR-169(3560-30)TN-3, Aerospace Corp., Dec. 20, 1962.
- 2.65. WEINGARTEN, V. I.: Free Vibrations of Multilayered Cylindrical Shells. *Exptl. Mech.*, vol. 4, July 1964, pp. 200-205.
- 2.66. WARBURTON, G. B.: Tables for Frequencies and Modes of Free Vibrations of Infinitely Long Thin Cylindrical Shells—Discussion. *J. Appl. Mech.*, vol. 22, no. 1, Mar. 1955, pp. 135-136.
- 2.67. VOSS, H. M.: The Effect of an External Supersonic Flow on the Vibration Characteristics of Thin Cylindrical Shells. *J. Aerospace Sci.*, vol. 28, Dec. 1961, pp. 945-956.

- 2.68. KIRIN, E. IA.: Oscillations of a Cylindrical Shell. Issledovaniia Po Uprugosti i Plastichnosti. Sbornik 3., 1964, pp. 265-270. (In Russian.)
- 2.69. BOZICH, W. F.: The Vibration and Buckling Characteristics of Cylindrical Shells Under Axial Load and External Pressure. AFFDL-TR-67-28, May 1967.
- 2.70. BRESLAVSKII, V. E.: On the Vibrations of Cylindrical Shells. Inzhen. Sbornik, Akad. Nauk SSSR, vol. 16, 1953, pp. 109-118. (In Russian.)
- 2.71. FEDERHOFER, K.: Über die Eigenschwingungen der Kreiszyinderschale mit veränderlicher Wandstärke. Öster. Akad. der Wiss., Mat.-Nat. Klasse, Abt. IIa, 161 Bd., June 1952, pp. 89-105.
- 2.72. FORSBERG, K.: Influence of Boundary Conditions on the Modal Characteristics of Thin Cylindrical Shells. AIAA J., vol. 2, no. 12, Dec. 1964, pp. 2150-2157.
- 2.73. FORSBERG, K.: Axisymmetric and Beam-Type Vibrations of Thin Cylindrical Shells. Paper 66-447, AIAA, 4th Aerospace Sci. Mtg. (Los Angeles, Calif.), June 27-29, 1966.
- 2.74. HERRMANN, G.; AND SHAW, J.: Vibration of Thin Shells Under Initial Stress. J. Engng. Mech. Div., Proc. Amer. Soc. Civil Engrs. EM, vol. 91, EM 5, Oct. 1965, pp. 37-59.
- 2.75. REISMANN, H.: Forced Motion of Cylindrical Shells. Rept. no. 9, School of Engineering, New York State Univ. at Buffalo, Dec. 1965.
- 2.76. REISMANN, H.; AND MEDIGE, J.: Forced Motion of Cylindrical Shells. J. Engng. Mech. Div., Proc. Amer. Soc. Civil Engrs. EM, vol. 94, EM 5, Oct. 1968, pp. 1167-1182.
- 2.77. REISMANN, H.: Response of a Cylindrical Shell to an Inclined, Moving Pressure Discontinuity (Shock Wave). J. Sound Vib., vol. 8, Sept. 1968, pp. 240-255.
- 2.78. WARBURTON, G. B.: Vibration of Thin Cylindrical Shells. J. Mech. Engng. Sci., vol. 7, Dec. 1965, pp. 399-407.
- 2.79. WEBSTER, J. J.: Free Vibrations of Shells of Revolution Using Ring Finite Elements. Intern. J. Mech. Sci., vol. 9, no. 8, Aug. 1967, pp. 559-570.
- 2.80. VRONAY, D. F.; AND SMITH, B. L.: Free Vibration of Circular Cylindrical Shells of Finite Length. AIAA J., vol. 8, no. 3, March 1970, pp. 601-603.
- 2.81. FLÜGGE, W.: Schwingungen zylindrischer Schalen. ZAMM, Bd. 13, 1933, p. 425.
- 2.82. WARBURTON, G. B.: Comments on "Vibration Studies of a Ring-Stiffened Circular Cylindrical Shell." J. Sound Vib. vol. 9, no. 2, 1969, pp. 349-353.
- 2.83. LINDHOLM, U. S.; KANA, D. D.; AND ABRAMSON, H. N.: Breathing Vibrations of a Circular Cylindrical Shell with an Internal Liquid. J. Aerospace Sci., vol. 29, no. 9, Sept. 1962, pp. 1052-1059.
- 2.84. COOPER, P. A.: Vibration and Buckling of Prestressed Shells of Revolution. NASA TN D-3831, Mar. 1967.
- 2.85. RESNICK, B. S.; AND DUGUNDJI, J.: Effects of Orthotropicity, Boundary Conditions, and Eccentricity on the Vibrations of Cylindrical Shells. AFOSR Sci. Rept. AFOSF 66-2821, ASRL TR 134-2 (AD648 077), Nov. 1966.
- 2.86. LIVANOV, K. K.: Axisymmetric Vibrations of Simply Supported Cylindrical Shells. J. Appl. Math. Mech. (Prikl. Mat. Mekh.), vol. 25, no. 4, 1961, pp. 1095-1101.
- 2.87. MEN'SHOV, A. I.: The Effect of Rigid Elements on Free Oscillation Frequencies of Circular, Cylindrical Shells. Inzhen. zh., vol. 4, no. 4, 1964, pp. 773-781. (In Russian.) (Also Eng. J., vol. 26, Apr. 1965, pp. 184-197.)
- 2.88. HECKL, M.: Vibrations of Point-Driven Cylindrical Shells. J. Acoust. Soc. Amer., vol. 34, no. 10, Oct. 1962, pp. 1553-1557.
- 2.89. JUNGER, M. C.; AND ROSATO, F. J.: The Propagation of Elastic Waves in Thin-Walled Cylindrical Shells. J. Acoust. Soc. Amer., vol. 26, no. 5, Sept. 1954, pp. 709-713.
- 2.90. MILLER, D. K.; AND HART, F. D.: Modal Density of Thin Circular Cylinders. NASA CR-897, Dec. 1967.
- 2.91. SMITH, P. W., JR.: Phase Velocities and Displacement Characteristics of Free Waves in a Thin Cylindrical Shell. J. Acoust. Soc. Amer., vol. 27, no. 6, Nov. 1955, pp. 1065-1072.
- 2.92. SMITH, P. W., JR.: Minimum Axial Phase Velocity in Shells. J. Acoust. Soc. Amer., vol. 30, no. 2, Feb. 1958, pp. 140-141.
- 2.93. ISHIZAKI, H.: On the Vibration of Circular Cylindrical Shells. Research Rept. of the Architectural Inst. of Japan, Nos. 27 and 29, 1954. (In Japanese.)
- 2.94. MIZOGUCHI, K.: On Fundamental Differential Equations of Vibrations of Cylindrical Shells. Bull. Japan Soc. Mech. Engrs. vol. 5, no. 17, Feb. 1962, pp. 43-49.
- 2.95. TOLOK, V. A.: Contribution to the Investigation of Free Oscillations of a Thin Cylindrical Shell. Akad. Nauk Uzbekskoi SSR, Izv. Ser. Tekh. Nauk, vol. 8, no. 5, 1964, pp. 25-28. (In Russian.)
- 2.96. YAMANE, J. R.: Natural Frequency Curves of Simply Supported Cylindrical Shells. AIAA J., vol. 3, no. 1, Jan. 1965, pp. 180-181.
- 2.97. FILIPPOV, A. P.: Oscillations of Cylindrical Shells. Prikl. Mat. Mekh., vol. 1, no. 2., 1937, pp. 177-186. (In Russian.)
- 2.98. BLEICH, H. H.: Approximate Determination of the Frequencies of Ring Stiffened Cylindrical Shells. Oest. Ingen.-Arch. 15, 1961, pp. 6-25.
- 2.99. EGGLE, D.M.; AND SEWALL, J. L.: An Analysis of Free Vibration of Orthogonally Stiffened Cylindrical Shells with Stiffeners Treated as Discrete Elements. AIAA J., vol. 6, no. 3, Mar. 1968, pp. 518-526.
- 2.100. GARNET, H.; AND GOLDBERG, M. A.: Free Vibrations of Ring Stiffened Shells. Contract Nonr-3465(00)FBM, Proj. NR 064-463, Tech. Rept. No. 2, Mar. 1962.

- 2.101. HOPPMANN, W. H., II.: Some Characteristics of the Flexural Vibrations of Orthogonally Stiffened Cylindrical Shells. *J. Acoust. Soc. Amer.*, vol. 30, no. 1, Jan. 1958, pp. 77-82.
- 2.102. HOPPMANN, W. H., II.: Flexural Vibrations of Orthogonally Stiffened Cylindrical Shells. 9th *Conféres Intern. Mecan. Appl.*, Univ. Bruxelles, 1957, pp. 225-237.
- 2.103. MEYEROVICH, I. I.: Approximate Method for the Determination of the Natural Oscillation Frequencies of Cylindrical, Conic, and Toroidal Shells. NASA TTF-10,377 (N67-17389), Nov. 1966.
- 2.104. MICHALOPOULOS, C. D.: The In-Vacuo Vibrations of a Simply Supported, Ring Stiffened, Mass-Loaded Cylindrical Shell. AD 633 676, June 1966.
- 2.105. MICHALOPOULOS, C. D.; AND MUSTER, D.: The Effect of Plane-Symmetric Mass Loading on the Response of Ring-Stiffened Cylindrical Shells. NR 185 602, Tech. Rept. No. 4 (AD 636 630), Office of Naval Res., Aug. 1966.
- 2.106. MIXSON, J. S.: An Investigation of the Vibration Characteristics of Pressurized Thin-Walled Circular Cylinders Partially Filled With Liquid. Thesis, Univ. of Virginia, Mar. 1962.
- 2.107. SEWALL, J. L.; AND NAUMANN, E. C.: An Experimental and Analytical Vibration Study of Thin Cylindrical Shells With and Without Longitudinal Stiffeners. NASA TN D-4705, Sept. 1968.
- 2.108. AGAMIROV, V. L.; AND VOLMIR, A. S.: Behavior of Cylindrical Shells Under Dynamic Loading of All-Sided Pressure or Axial Compression. *Izv. Akad. Nauk SSSR, Otd. Tekh. Nauk* no. 3, May-June 1959, pp. 78-83.
- 2.109. BUBLIK, B. N.: Vibrations and Stability of a Ribbed Cylindrical Shell in a Flow of Compressible Liquid. *Dop. Akad. Nauk Ukr. SSR*, no. 2, 1963, pp. 178-183. (In Ukrainian.)
- 2.110. IVANYUTA, E. I.; AND FINKEL'SHTEYN, R. M.: Determination of Frequencies of Free Vibrations of Cylindrical Shells. *Invest. Elasticity and Plasticity*, Jan. 1966, pp. 101-111.
- 2.111. TANG, C. T.: The Vibration Modes and Eigenfrequencies of Circular Conical (and Cylindrical) Shells. *Scientia Sinica*, vol. 13, no. 8, Aug. 1964, pp. 1189-1210.
- 2.112. YOUNG, R.; AND MCCALLUM, H.: The Determination of Frequencies and Modes of Undamped Structures Using Finite-Element Stiffness and Consistent-Mass Matrices. ASRL TR 121-8, June 1965.
- 2.113. ADELMAN, H. M.; CATHERINES, D. S.; AND WALTON, W. C., JR.: A Method for Computation of Vibration Modes and Frequencies of Orthotropic Thin Shells of Revolution Having General Meridional Curvature. NASA TN D-4972, Jan. 1969.
- 2.114. IVANYUTA, E. I.; AND FINKEL'SHTEYN, R. M.: On a Variational Method for the Solution of Certain Dynamic Problems of the Theory of Shells. *Prikl. Mekh.*, vol. 9, no. 1, 1963, pp. 42-51. (In Ukrainian.)
- 2.115. ILGAMOV, M. A.; AND KAMALOV, A. Z.: Free and Parametric Oscillations of a Cylindrical Shell of Infinite Length in an Acoustic Medium. *Aviatsionnaia Tekhnika*, vol. 9, no. 4, 1966, pp. 41-50. (In Russian.)
- 2.116. LISOWSKI, A.: Measurement of the Vibrations of Shell Models and Three Dimensional Models of Bar Systems by Means of an Electronic Apparatus. *Studii si Cercetari de Mecanica Aplicata*, vol. 12, no. 2, 1961, pp. 433-440. (In Rumanian.)
- 2.117. WATTS, G. A.: Vibration and Damping of Thin-Walled Cylinders. Thesis, Calif. Inst. Tech., 1962.
- 2.118. GREENSPON, J. E.: Flexural Vibrations of a Thick-Walled Circular Cylinder. *Proc. 3rd U.S. Nat. Congr. of Appl. Mech.*, Providence, R.I., 1958, pp. 163-173.
- 2.119. KADI, A. S.: A Study and Comparison of the Equations of Thin Shell Theories. Ph.D. Dissertation, Ohio State Univ., 1970.
- 2.120. BOLOTIN, V. V.: On the Density of the Distribution of Natural Frequencies of Thin Elastic Shells. *Prikl. Mat. Mekh.*, vol. 27, no. 2, 1963, pp. 363-364. (In Russian.)
- 2.121. BARON, M. L.; AND BLEICH, H. H.: Tables for Frequencies and Modes of Free Vibration of Infinitely Long Thin Cylindrical Shells. *J. Appl. Mech.* vol. 21, no. 2, 1954, pp. 178-188.
- 2.122. BLEICH, H. H.; AND DIMAGGIO, F.: A Strain-Energy Expression for Thin Cylindrical Shells. *Trans. ASME (J. Appl. Mech.)*, vol. 20, no. 3, 1953, pp. 448-449.
- 2.123. WARBURTON, G. B.: Dynamics of Shells. *Proc. of Symp. on Struct. Dyn.*, Mar. 23-27, 1970.
- 2.124. RAYLEIGH, LORD: On the Infinitesimal Bending of Surfaces of Revolution. *London Math. Soc. Proc.*, vol. 13, Nov. 1881, p. 4.
- 2.125. REISSNER, E.: Non-Linear Effect in Vibrations of Cylindrical Shells. Rept. No. AM 5-6, Guided Missile Research Div., The Ramo-Wooldridge Corp., Sept. 1955.
- 2.126. GONTKEVICH, V. S.: Natural Oscillations of Closed Cylindrical Shells With Various Boundary Conditions. *Prikl. Mekh.*, vol. 9, no. 2, 1963, pp. 216-220. (In Ukrainian.)
- 2.127. GONTKEVICH, V. S.: Natural Vibrations of Plates and Shells. A. P. Filipov, ed., *Nauk Dumka* (Kiev), 1964. (Transl. by Lockheed Missiles and Space Co.)
- 2.128. SIMMONDS, J. G.: Modifications of the Timoshenko Beam Equations Necessary for Thin-Walled Circular Tubes. *Int. J. Mech. Sci.*, vol. 9, 1967, pp. 237-244.
- 2.129. KORNECKI, A.: A Note on Beam-Type Vibrations of Circular Cylindrical Shells. *J. Sound Vib.*, vol. 14, no. 1, 1971, pp. 1-6.
- 2.130. FRANKEN, P. A.: Input Impedances of Simple Cylindrical Structures. *J. Acoust. Soc. Amer.*, vol. 32, no. 4, Apr. 1960, pp. 473-477.

- 2.131. FLÜGGE, W.: Stresses in Shells. Springer-Verlag, 1960.
- 2.132. ADELMAN, H. M.; CATHERINES, D. S.; AND WALTON, W., JR.: A Geometrically Exact Finite Element for Thin Shells of Revolution. AIAA 7th Aerospace Sci. Meeting (New York), Jan. 1969.
- 2.133. BERGLUND, J. W.; AND KLOSNER, J. M.: Interaction of a Ring-Reinforced Shell and a Fluid Medium. *J. Appl. Mech.*, vol. 35, no. 1, Mar. 1968, pp. 139-147.
- 2.134. DESILVA, C. N.; AND TERSTEEG, C. E.: Axisymmetric Vibrations of Thin Elastic Shells. *J. Acoust. Soc. Amer.*, vol. 36, no. 4, Apr. 1964, pp. 666-672.
- 2.135. SMITH, B. L.; AND HAFT, E. E.: Natural Frequencies of Clamped Cylindrical Shells. *AIAA J.*, vol. 6, no. 4, Apr. 1968, pp. 720-721.
- 2.136. WANG, J. T-S; STADLER, W.; AND LIN, C-W.: The Axisymmetric Response of Cylindrical and Hemispherical Shells to Time-Dependant Loading. NASA CR-572, Sept. 1966.
- 2.137. KOVAL, L. R.: A Simplified Frequency Equation for a Clamped Cylindrical Shell and its Application to Initially Stressed Cylinders. Rept. No. EM 12-9, Space Technology Laboratories, Feb. 1962.
- 2.138. KRAUS, H.: Thin Elastic Shells. John Wiley and Sons, Inc. (New York), 1967.
- 2.139. SEWALL, J. L.; CLARY, R. R.; AND LEADBETTER, S. A.: An Experimental and Analytical Vibration Study of a Ring-Stiffened Cylindrical Shell Structure with Various Support Conditions. NASA TN D-2398, Aug. 1964.
- 2.140. WEINGARTEN, V. I.: Investigation of the Free Vibrations of Multi-Layered Cylindrical Shells. Rept. No. TDR-69(2240-65)TR-2, Air Force Systems Command, Sept. 1962.
- 2.141. RITZ, W.: Über eine neue Methode zur Lösung gewisser variations-probleme der mathematischen Physik. *J. für Reine und Angew. Math.*, vol. 135, 1908.
- 2.142. RITZ, W.: Theorie der Transversalschwingungen einer quadratischen Platte mit freien Rändern. *Ann. Phys.*, vol. 28, 1909, pp. 737-786.
- 2.143. HOPPER, A. T.; LEISSA, A. W.; HULBERT, L. E.; AND CLAUSEN, W. E.: Numerical Analysis of Equilibrium and Eigenvalue Problems. AFFDL-TR-67-121, U.S. Air Force, Nov. 1967.
- 2.144. LEISSA, A. W.; CLAUSEN, W. E.; HULBERT, L. E.; AND HOPPER, A. T.: A Comparison of Approximate Methods for the Solution of Plate Bending Problems. *AIAA J.*, vol. 7, no. 5, May 1969, pp. 920-928.
- 2.145. KANTOROVICH, L. V.; AND KRYLOV, V. I.: Approximate Methods of Higher Analysis. Interscience Publishers, Inc. (New York), 1964.
- 2.146. BUBNOV, I. G.: Report on the Works of Prof. Timoshenko Which were Awarded the Zhuranskii Prize. *Sborn. Inta. Inzh. Putei Soobshch.*, no. 81, All Union Special Planning Office (SPB), 1913.
- 2.147. LIN, C. W.; AND BELL, F. L.: On the Nonsymmetric Vibrations of Thin Cylindrical Shells with Clamped-Clamped Edges. *Nuclear Eng. and Design*, vol. 7, no. 3, Mar. 1968, pp. 194-200.
- 2.148. KONDRASHOV, N. S.: Lower Bounds of the Natural Frequencies of Circular Cylindrical Shells. *Izdatel'stvo Mashinostr.*, 1966, pp. 54-76. (In Russian.)
- 2.149. BOLOTIN, V. V.: Edge Effects in the Vibration of Elastic Shells. *Prikl. Mat. Mekh.*, vol. 24, no. 5, 1960, pp. 831-843. (In Russian.)
- 2.150. GAVRILOV, YU. V.: Determination of the Frequency of Natural Vibrations of Closed Circular Cylindrical Shells. *Izv. Akad. Nauk SSSR, Mekh. i Mashinostr.* no. 6, Nov./Dec. 1963, pp. 144-146. (In Russian.)
- 2.151. BROGAN, F.; FORSBERG, K.; AND SMITH, S.: Experimental and Analytical Investigation of the Dynamic Behavior of a Cylinder With a Cutout. Paper No. 68-318, AIAA/ASME 9th Structures, Structural Dynamics and Materials Conference (Palm Springs, Calif.), Apr. 1-3, 1968.
- 2.152. KOVAL, L. R.: Note on the Effect of Dynamic Asymmetry on the Vibration of Cylindrical Shells. *J. Acoust. Soc. Amer.*, vol. 35, no. 2, Feb. 1963, pp. 252-253.
- 2.153. KOVAL, L. R.: Vibration Analysis of Thin-Walled Cylindrical Shells. *Vibration Notebook*, vol. 8, no. 1, Jan. 1962.
- 2.154. FEDERHOFER, K.: Über die Eigenschwingungen der zylinder-, kegel- und kugelschalen. *Proc. 5th Internat. Cong. Appl. Mech.*, 1938, pp. 719-723.
- 2.155. WANG, J. T. S.; LIN, C. W.; AND STADLER, W.: Axisymmetric Dynamic Response of Spherical and Cylindrical Shells. *Am. Astronautical Soc., Southeastern Symposium on Missiles and Aerospace Vehicles Sciences*, (Huntsville, Ala.), Dec. 5-7, 1966.
- 2.156. GONTKEVICH, V. S.: Natural Vibrations of Spherical Shells. *Issled. po Teorii Sooruzh.*, no. 13, 1964, pp. 77-83. (English transl.: Lockheed Missiles & Space Co.)
- 2.157. LEISSA, A. W.: Vibration of Plates. U.S. Government Printing Office, 1969.
- 2.158. FELGAR, R.: Formulas for Integrals Containing Characteristic Functions of a Vibrating Beam. Circular No. 14, Univ. of Texas, 1950.
- 2.159. YOUNG, D.; AND FELGAR, R.: Tables of Characteristic Functions Representing Normal Modes of Vibration of a Beam. Bull. No. 4913, Univ. of Texas, 1949.
- 2.160. ELSBERND, G. F.: The Free Vibrations of a Rectangular Plate Clamped on Three Edges, Free on the Fourth Edge by the Ritz Method. M. Sci. Thesis, Ohio State Univ., 1966.
- 2.161. SOUTHWELL, R. V.: On the Free Vibrations of a Uniform Circular Disc Clamped at Its Centre and on the Effect of Rotation. *Proc. Roy. Soc. of London (series A)*, 1922, vol. 101, p. 133.
- 2.162. SOUTHWELL, R. V.: Some Extensions of Rayleigh

- Principle. Quart. J. Mech. Appl. Math., vol. 6, 1953, p. 257.
- 2.163. ABDULLA, K. M.; AND GALLETTY, G. D.: Free Vibration of Cones, Cylinders, and Cone-Cylinder Combinations. Proc. of Symp. on Struct. Dyn., Mar. 23-27, 1970.
 - 2.164. SANDERS, J. L., JR.: Nonlinear Theories for Thin Shells. Quart. Appl. Math., vol. 21, no. 1, Apr. 1963, pp. 21-36.
 - 2.165. BLUM, R. E.; AND FULTON, R. E.: A Modification of Potters' Method for Solving Eigenvalue Problems Involving Tridiagonal Matrices. AIAA J., vol. 4, no. 12, Dec. 1966, pp. 2231-2232.
 - 2.166. SHARMA, C. B.; AND JOHNS, D. J.: Vibration Characteristics of a Clamped-Free and Clamped-Ring-Stiffened Circular Cylindrical Shell. J. Sound Vib., vol. 14, no. 4, 1971, pp. 459-474.
 - 2.167. SHARMA, C. B.; AND JOHNS, D. J.: Vibration Characteristics of a Clamped-Free and Clamped Ring Stiffened Cylindrical Shell. Technol. Rept. TT7001, Loughborough Univ., 1970.
 - 2.168. JOHNS, D. J.; AND SHARMA, C. B.: The Structural Design of Self Supporting Steel Chimneys: Deduced from B. S. 4076: 1966. Technol. Rept. TT6915, Loughborough Univ., 1969.
 - 2.169. JOHNS, D. J.; AND ALLWOOD, R. J.: Vibration Studies of a Ring Stiffened Circular Cylindrical Shell. J. Sound Vib., vol. 8, no. 1, July 1968, pp. 147-155.
 - 2.170. ANON.: Study on Bell-Mode Vibrations of Conical Nozzles. Final Rept., Contract No. NASr-111, Rept. No. 2581, Aerojet-General Corp., May 1963.
 - 2.171. FREESE, C. E.: Vibration of Vertical Pressure Vessels. ASME Trans. 81B (J. Engng. Indus.), no. 1, Feb. 1959, pp. 77-91.
 - 2.172. HEKI, K.: Vibration of Cylindrical Shells. J. of the Inst. of Polytechniques, Osaka City Univ., vol. 1, no. 1, 1957.
 - 2.173. PLATUS, D. H.: Conical Shell Vibrations. NASA-TN-2767.
 - 2.174. Warburton, G. B.; AND HIGGS, J.: Natural Frequencies of Thin Cantilever Cylindrical Shells. J. Sound Vib., vol. 11, no. 3, 1970, pp. 335-338.
 - 2.175. SHKENEV, YU. S.: Dynamics of Elastic and Elastic-Viscous Shells Filled With an Ideal Liquid. Theory of Shells and Plates, 1966, pp. 925-935.
 - 2.176. RAYLEIGH, LORD: On the Bending and Vibration of Thin Elastic Shells, Especially of Cylindrical Form. Proc. Roy. Soc. London, vol. 45, 1888, pp. 105-123.
 - 2.177. OGIBALOV, P. M.: Voprosy Dinamiki I Ustoichivosti Obolochek. Izdatel'stvo Moskovskogo Universiteta, Moscow, 1963, pp. 1-419. (English transl.: FTD-MT-64-351, Problems in Dynamics and Stability of Shells, Transl. Div., Foreign Tech. Div., Wright Patterson Air Force Base.)
 - 2.178. STERN, M.: Breathing Vibrations of a Cylindrical Membrane under Internal Pressure. Convair Memo. DC-7-057, Convair, 1954.
 - 2.179. SERBIN, H.: Breathing Vibrations of a Pressurized Cylindrical Shell. Rept. No. A-Atlas-152, Convair, Jan. 1955.
 - 2.180. HU, W. C. L.: A Survey of The Literature on the Vibrations of Thin Shells. Proj. No. 02-1504, Southwest Research Institute, June 1964.
 - 2.181. GRINSTED, B.: Nodal Pattern Analysis. Proc. Inst. Mech. Eng. (ser. A), vol. 166, 1952, p. 313.
 - 2.182. GOTTENBERG, W. G.: Experimental Study of the Vibrations of a Circular Cylindrical Shell. J. Acoust. Soc. Amer., vol. 32, no. 8, Aug. 1960, pp. 1002-1006.
 - 2.183. GRINSTED, B.: Communications on the Flexural Vibration of Thin Cylinders (to paper by Arnold, R. N.; and Warburton, G. B.). Proc. Inst. Mech. Eng. (ser. A), vol. 167, no. 1, 1953, pp. 75-77.
 - 2.184. WATKINS, J. D.; AND CLARY, R. R.: Vibrational Characteristics of Some Thin-Walled Cylindrical and Conical Frustum Shells. NASA TN D-2729.
 - 2.185. DiMaggio, F. L.: Dynamic Response of Cylindrical Tanks. Armed Forces Special Weapons Project, Contract DA-29-004-X2-54. AFSWP No. 1075, May 1958.
 - 2.186. BARON, M. L.; AND BLEICH, H. H.: The Dynamic Analysis of Empty and Partially Full Cylindrical Tanks. Final Rept., DASA No. 1123A, Defense Atomic Support Agency, May 1959.
 - 2.187. BRITVEC, S. J.: Sur Les Vibrations Des Coques Cylindriques Minces Soumises A Un Amortissement Visqueux. Tech. Note 101 (N67-23076), Office National D'études et de Recherches Aéropatiales, 1966.
 - 2.188. MISERENTINO, R.; AND VOSTEEN, L. F.: Vibration Tests of Pressurized Thin-Walled Cylindrical Shells. NASA TN D-3066.
 - 2.189. STEARMAN, R. O.; LOCK, M. H.; AND FUNG, Y. C.: Ames Tests on the Flutter of Cylindrical Shells. Aeroelasticity and Structural Dynamics SM 62-37, Calif. Inst. of Tech., Dec. 1962.
 - 2.190. BUKHARINOV, G. N.: Oscillations of Two Bodies Joined by a Circular Cylindrical Shell. Issled. po Uprugosti i Plastichnosti, Leningrad, Leningr. Un-ta, no. 2, 1963, pp. 74-80. (In Russian.)
 - 2.191. KANA, D. D.; AND HU, W. C. L.: Transmission Characteristics of Conical and Cylindrical Shells Under Lateral Excitation. J. Acoust. Soc. Amer., vol. 44, no. 6, Dec. 1968, pp. 1647-1657.
 - 2.192. SMIRNOV, M. M.: Oscillation of a System of Masses Connected to a Cylindrical Shell. Investigations of Elasticity and Plasticity. (Issledovaniia po Uprugosti i Plastichnosti), Izdatel'stvo Leningradskogo Universiteta, 1964, pp. 114-123. (In Russian.)
 - 2.193. DAREVSKII, V. M.; AND SHARINOV, I. L.: Free Oscillations of a Cylindrical Shell With Concentrated Mass. Transactions of All-Union Conference on the Theory of Shells and Plates, 6th, Baku, Azerbaidzhan SSR, Sept. 15-20, 1966, pp. 350-354. (In Russian.)
 - 2.194. TOBIAS, S. A.: A Theory of Imperfection for the

- Vibration of Elastic Bodies of Revolution. Engineering, vol. 172, 1951, p. 409.
- 2.195. BOLOTIN, V. V.: The Density of Eigenvalues in Vibration Problems of Elastic Plates and Shells. Proc. Vibration Problems (Polska Akad. Nauk, Inst. Podstawowych,¹ Problemow Tech.), vol. 6, no. 4, 1965, pp. 341-351.
 - 2.196. GALERKIN, B. G.: Rods and Plates. Series Occurring in Various Questions Concerning the Elastic Equilibrium of Rods and Plates. Vestnik Inzhenerov, vol. 19, 1915, pp. 897-908. (In Russian.)
 - 2.197. WEINGARTEN, V. I.: Free Vibration of Thin Cylindrical Shells. AIAA J., vol. 2, no. 4, Apr. 1964, pp. 717-722.
 - 2.198. SEWALL, J. L.: Vibration Analysis of Cylindrically Curved Panels With Simply Supported or Clamped Edges and Comparison With Some Experiments. NASA TN D-3791, Jan. 1967.
 - 2.199. WEBSTER, J. J.: Free Vibration of Rectangular Curved Panels. Intern. J. Mech. Sci., vol. 10, no. 7, July 1968, pp. 571-582.
 - 2.200. STADLER, W.; AND WANG, J. T. S.: Dynamic Response of a Cylindrical Shell Segment Subjected to an Arbitrary Load. Proc. 9th Midwestern Mechanics Conf., Aug. 1965, pp. 189-201.
 - 2.201. CHEN, R.: Vibrations of Cylindrical Panels and Rectangular Plates Carrying a Concentrated Mass. Paper No. 3702, Douglas Missile & Space System Div., Nov. 1965.
 - 2.202. GONTKEVICH, V. S.: Natural Vibrations of Rising Cylindrical Shells. Trans. Akad. Nauk URSS, Kiev, Laboratoriya Hidraulichnykh Mashyn. Sbornik Trudov, No. 10, 1962, pp. 27-37.
 - 2.203. GRIGOLYUK, E. I.: On the Oscillations of Shallow Circular Cylindrical Panels Experiencing Finite Deflections. Prikl. Mat. Mekh., vol. 19, no. 3, 1955, pp. 376-382, (In Russian.)
 - 2.204. KISLEVSKAYA, L. M.: On the Calculation of the Frequencies of Vibration of a Shell Reinforced by Stiffening Ribs. Prikl. Mekh., vol. 17, no. 4, 1961, pp. 377-387. (In Russian.)
 - 2.205. KISLEVSKAYA, L. M.: Free Oscillations of a Shell Reinforced with Stiffening Ribs. Dop. Akad. Nauk Ukrain. SSR, 1959, pp. 730-735. (In Ukrainian.)
 - 2.206. KISLEVSKAYA, L. M.: Effect of Stiffening Ribs on the Frequency of the Natural Oscillations of a Shallow Cylindrical Shell. Theor. Plas. i Obolochek, Kiev, Akad. Nauk USSR, 1962, pp. 289-294. (In Russian.)
 - 2.207. MAURO, A.: Una Soluzione Completa Del Problema Delle Vibrazioni Libere Di Volte Sottili Ribassate Su Pianta Rettangolare. Technica Italiana, vol. 32, no. 3, Mar. 1967, pp. 145-161.
 - 2.208. NEMAT-NASSER, S.: On the Response of Shallow Thin Shells to Random Excitations. AIAA J., vol. 6, no. 7, July 1968, pp. 1327-1331.
 - 2.209. NOWACKI, W.: Dynamics of Elastic Systems. John Wiley & Sons, Inc. (New York), 1963.
 - 2.210. ONIASHVILI, O. D.: Some Dynamical Problems in the Theory of Shells. Akad. Nauk SSSR, Moscow, 1957. (In Russian.) (Transl. and pub. by M. D. Friedmann, Inc.)
 - 2.211. PALMER, P. J.: The Natural Frequency Vibration of Curved Rectangular Plates. Aeronaut. Quart., vol. V, pt. 2, July 1954, pp. 101-110.
 - 2.212. WIECKOWSKI, J.: Dynamic Properties of Thin, Semiinfinite Cylindrical Shells Exposed to Stationary Vibration. Prace Inst. Maszyn Przeplywowych (Polska Akad. Nauk), vol. 20, 1964, pp. 23-48. (In Polish).
 - 2.213. HESS, R. W.; HERR, R. W.; AND MAYES, W. H.: A Study of the Acoustic Fatigue Characteristics of Some Flat and Curved Aluminum Panels Exposed to Random and Discrete Noise. NASA TN D-1, Aug. 1959.
 - 2.214. RUCKER, C. E.: Some Experimental Effects of Curvature on Response of Simple Panels to Intense Noise. Paper presented at 67th Meeting of the Acoust. Soc. Amer. (New York), May 1964.
 - 2.215. BALLENTINE, J. R.; PLUMBLEE, H. E.; AND SCHNEIDER, C. W.: Sonic Fatigue in Combined Environment. AFFDL-TR-66-7, U.S. Air Force, May 1966.
 - 2.216. LISOWSKI, A.: Investigation of Shell Vibration and Stability by Means of Model Tests. Rozprawy Inz. vol. 6, no. 1, 1958. (In Polish).
 - 2.217. LISOWSKI, A.: Buckling and Vibration of Shells in the Light of Model Tests. Bauingenieur, vol. 35, no. 3, Mar. 1960, pp. 86-89. (In German.)
 - 2.218. KURT, C. E.; AND BOYD, D. E.: Free Vibrations of Noncircular Cylindrical Shell Segments. AIAA J., vol. 9, no. 2, Feb. 1971, pp. 239-244.
 - 2.219. TOTTENHAM, H.; TAHBILDAR, U.; AND BREBBIA, C.: Finite Element Analyses of Shell Response for Arbitrary Excitations. Proc. of Symp. on Struct. Dyn., Mar. 23-27, 1970.
 - 2.220. PETYT, M.: Vibration of Curved Plates. Proc. Conf. on Current Developments in Sonic Fatigue (Southampton Univ.), July 1970.
 - 2.221. DUNGAR, R.; SEVERN, R. T.; AND TAYLOR, P. R.: Vibration of Plate and Shell Structures Using Triangular Finite Elements. J. Strain Analysis, vol. 2, no. 1, Jan. 1967, pp. 73-83.
 - 2.222. DEB NATH, J. M.; AND PETYT, M.: Free Vibrations of Doubly Curved Rectangular Plates Including the Presence of Membrane Stresses With Special Reference to the Finite Element Technique. Tech. Rept. 22, Inst. of Sound and Vibr. Research (Southampton), 1969.
 - 2.223. DEB NATH, J. M.: Dynamics of Rectangular Curved Plates. Ph.D. Thesis, Univ. of Southampton, 1969.
 - 2.224. DEB NATH, J. M.; AND PETYT, M.: Application of the Method of Kantorovich to the Solution of Problems of Free Vibration of Singly Curved Rectangular Plates Including the Presence of Membrane Stresses. Tech. Rept. 19, Inst. of Sound and Vib. Research (Southampton), 1969.

- 2.225. CHEN, R.: Vibration of Cylindrical Panels Carrying a Concentrated Mass. *J. Appl. Mech.*, vol. 37, no. 3, Sept. 1970, pp. 874-875.
- 2.226. WIECKOWSKI, J.: Free Vibration Equations of a Thin Elastic Shell as a Simplified Model of a Long Cantilever Steam Turbine Blade. *Prace Inst. Maszyn Przeplywowych (Polska Akad. Nauk)*, vol. 17, 1963, pp. 3-38. (In Polish.)
- 2.227. WAH, T.; AND HU, W. C. L.: Vibration Analysis of Stiffened Cylinders Including Inter-Ring Motion. *J. Acoust. Soc. Amer.*, vol. 43, no. 5, May 1968, pp. 1005-1016.

Complicating Effects in Circular Cylindrical Shells

In the previous chapter the equations of motion for circular cylindrical shells were restricted to their most simple forms as derived in chapter 1. This permitted the study of the effects of different types of edge constraints, added mass, cutouts, and varying geometric and material parameters upon natural frequencies and mode shapes. In this chapter the complicating effects of anisotropy, initial stress, variable thickness, large deflections, shear deformation and rotary inertia, nonhomogeneity, and surrounding media will each be considered. Each effect causes complications of one or more of the following types in the differential equations of motion:

- (1) Adding simple terms, thereby somewhat changing the forms of analytical solutions and increasing their complexity.
- (2) Changing constant coefficients to variable coefficients, thereby reducing the possibility of solution in terms of simple functions.
- (3) Adding *nonlinear* terms which completely change the character of the solutions.
- (4) Increasing the *order* of the equations.

In some instances the boundary conditions are also changed. In each instance the type of shell considered in chapter 2 is a special case of the more generalized analysis which includes a given complicating effect.

A separate section in this chapter will be devoted to each of the complicating effects listed above. From a logical standpoint it is possible to organize each section in the same manner as chapter 2. That is, for example, the section *titles* for sections 2.1, 2.2, . . . , 2.8 could also be used for subsections 3.1.1, 3.1.2, . . . , 3.1.8 of section 3.1 dealing with the effects of anisotropy, and similarly for each other section of this chapter. However, of course, the added complexities have

greatly reduced the number of solved problems, and for many of the subsection titles there are no results in the literature to report. Nevertheless, the organization described above will be followed in each section of this chapter insofar as it is appropriate.

The coordinate notation of chapter 2 as shown in figure 2.1 will apply throughout this chapter.

3.1 ANISOTROPY

For a general elastic solid (neglecting couple stresses) there are 21 independent elastic constants relating stresses and strains. In the case of a thin plate or shell, only the stresses σ_α , σ_β , and $\tau_{\alpha\beta}$ (in the notation of chapter 1) and their corresponding strains are involved, and the number of independent elastic constants is thereby reduced to six (cf., the appendix of ref. 3.1).

However, particularly because of the complexity arising from having six independent constants, no numerical results have been found in the literature for the vibrations of circular cylindrical shells having general anisotropy. Rather, all results given are for the special case of orthotropy. Equations of motion for a number of theories in the case of general anisotropy will be given in section 3.1.1.

For an orthotropic shell the stress-strain equations (1.70) are

$$\left. \begin{aligned} e_\alpha &= \frac{1}{E_\alpha}(\sigma_\alpha - \nu_{\alpha\beta}\sigma_\beta) \\ e_\beta &= \frac{1}{E_\beta}(\sigma_\beta - \nu_{\beta\alpha}\sigma_\alpha) \\ \sigma_{\alpha\beta} &= \frac{\tau_{\alpha\beta}}{G} \end{aligned} \right\} \quad (3.1)$$

which, when inverted, become

$$\left. \begin{aligned} \sigma_\alpha &= \frac{1}{1 - \nu_\alpha \nu_\beta} (E_\alpha e_\alpha + \nu_\alpha E_\beta e_\beta) \\ \sigma_\beta &= \frac{1}{1 - \nu_\alpha \nu_\beta} (E_\beta e_\beta + \nu_\beta E_\alpha e_\alpha) \\ \tau_{\alpha\beta} &= G \gamma_{\alpha\beta} \end{aligned} \right\} \quad (3.2)$$

However, the five elastic constants E_α , E_β , ν_α , ν_β , and G are not all independent; symmetry considerations require that

$$\nu_\alpha E_\beta = \nu_\beta E_\alpha \quad (3.3)$$

thereby reducing the number of independent elastic constants to four.

Equations (3.2) and (3.3) are written in terms of the principal coordinates of the middle surface of the shell, but they need not be. Indeed, it would be physically realistic to have a circular cylindrical shell wherein the axes of orthotropy are not coincident with the x and θ directions. Such a situation could arise, for example, in the case of a filament-wound shell. Nevertheless, no results have been found in the literature except when the two sets of axes are coincident (in ref. 3.2 the procedure for transforming the shell equations from rotated coordinate axes to the shell coordinates is discussed, but no problems are solved).

One of the most important uses of orthotropic circular cylindrical shell equations is in the representation of a shell which is stiffened by longitudinal beam-like elements (stringers) and/or circumferential rings. An example of this type of construction is shown in figure 3.1 (from ref. 3.3). This representation can be accurately made for the purpose of determining free vibration frequencies and mode shapes (but not stress resultants) if the stiffening elements are relatively closely spaced. When the distance of separation is too large, or if the wave length of the vibration is too short relative to the stiffener spacing, then the structure must be represented as a combination of shell elements and stiffener elements each having its own equations of motion and coupled to each other by equations of continuity. For the sake of consistency with the rest of this monograph, such structures will not be considered. However, when the rings and/or stringers can be "smeared out" along the shell to yield a single equivalent orthotropic shell (by methods that

will be discussed in the next section), the problem will be included here. In order to establish the validity of the equivalent orthotropic analysis a few comparisons will be included, where available, which include both the orthotropic analysis and the more accurate, complex structural analysis. These comparisons will help in establishing the limits of applicability of the equivalent orthotropic shell representation.

No results are available for orthotropic shells of infinite length. It would be interesting to determine the differences arising from various shell theories in the manner of section 2.2 in cases of severe orthotropy (e.g., $E_x \gg E_\theta$) for the analytically simple case of plane strain. Similarly, no results exist for elastic edge supports, added mass, noncircular boundaries and cutouts, and very little for open shells (except the special case where all four sides are supported by shear diaphragms, which is included among the vibration modes of a closed shell supported by shear diaphragms).

3.1.1 Equations of Motion

Substituting equations (3.2) into the generalized force resultant integrals of the shell theories of, for example, Love-Timoshenko, Reissner, Naghdi, Berry, Mushtari, and Donnell as given by equations (1.72) through (1.74) (neglecting z/R_α and z/R_β with respect to unity) yields

$$\left. \begin{aligned} N_\alpha &= C_{11}\epsilon_\alpha + C_{12}\epsilon_\beta \\ N_\beta &= C_{12}\epsilon_\alpha + C_{22}\epsilon_\beta \\ N_{\alpha\beta} &= N_{\beta\alpha} = C_{66}\epsilon_{\alpha\beta} \end{aligned} \right\} \quad (3.4)$$

$$\left. \begin{aligned} M_\alpha &= D_{11}\kappa_\alpha + D_{12}\kappa_\beta \\ M_\beta &= D_{12}\kappa_\alpha + D_{22}\kappa_\beta \\ M_{\alpha\beta} &= M_{\beta\alpha} = D_{66}\tau \end{aligned} \right\} \quad (3.5)$$

where C_{11} , C_{12} , C_{22} , and C_{66} are the extensional stiffness constants defined by

$$\left. \begin{aligned} C_{11} &= \frac{E_\alpha h}{1 - \nu_\alpha \nu_\beta}, & C_{22} &= \frac{E_\beta h}{1 - \nu_\alpha \nu_\beta} \\ C_{12} &= \frac{\nu_\alpha E_\beta h}{1 - \nu_\alpha \nu_\beta} = \frac{\nu_\beta E_\alpha h}{1 - \nu_\alpha \nu_\beta} \\ C_{66} &= Gh \end{aligned} \right\} \quad (3.6)$$

and D_{11} , D_{12} , D_{22} , and D_{66} are the flexural stiffness constants defined by

$$\left. \begin{aligned} D_{11} &= \frac{E_\alpha h^3}{12(1-\nu_\alpha\nu_\beta)}, & D_{22} &= \frac{E_\alpha h^3}{12(1-\nu_\alpha\nu_\beta)} \\ D_{12} &= \frac{\nu_\alpha E_\beta h^3}{12(1-\nu_\alpha\nu_\beta)} = \frac{\nu_\beta E_\alpha h^3}{12(1-\nu_\alpha\nu_\beta)} \\ D_{66} &= \frac{Gh^3}{12} \end{aligned} \right\} \quad (3.7)$$

Substituting the generalized stress-strain equations (3.4) and (3.5) into the equations of motion from chapter 1 and using the proper generalized strain-displacement equations ultimately gives equations of motion in terms of displacements which are in the form of equation (2.3). For the Donnell-Mushtari theory these equations are for circular cylindrical shells:

$$\frac{\partial^2 u}{\partial s^2} + \frac{G(1-\nu_\alpha\nu_\beta)}{E_x} \frac{\partial^2 u}{\partial \theta^2} + \frac{\nu_x E_\theta + G(1-\nu_x\nu_\theta)}{E_x} \frac{\partial^2 v}{\partial s \partial \theta} + \frac{\nu_x E_\theta}{E_x} \frac{\partial w}{\partial s} = \frac{\rho R^2(1-\nu_x\nu_\theta)}{E_x} \frac{\partial^2 u}{\partial t^2} \quad (3.8a)$$

$$\frac{\nu_x E_\theta + G(1-\nu_x\nu_\theta)}{E_x} \frac{\partial^2 u}{\partial s \partial \theta} + \frac{G(1-\nu_\alpha\nu_\beta)}{E_x} \frac{\partial^2 v}{\partial s^2} + \frac{E_\theta}{E_x} \frac{\partial^2 v}{\partial \theta^2} + \frac{E_\theta}{E_x} \frac{\partial w}{\partial \theta} = \frac{\rho R^2(1-\nu_x\nu_\theta)}{E_x} \frac{\partial^2 v}{\partial t^2} \quad (3.8b)$$

$$\begin{aligned} \frac{\nu_x E_\theta}{E_x} \frac{\partial u}{\partial s} + \frac{E_\theta}{E_x} \frac{\partial v}{\partial \theta} + \frac{E_\theta}{E_x} w^{(-)} \left[\frac{\partial^4 w}{\partial s^4} \right. \\ \left. + 2 \frac{\nu_x E_\theta + 2G(1-\nu_x\nu_\theta)}{E_x} \frac{\partial^4 w}{\partial s^2 \partial \theta^2} + \frac{E_\theta}{E_x} \frac{\partial^4 w}{\partial \theta^4} \right] \\ = - \frac{\rho R^2(1-\nu_x\nu_\theta)}{E_x} \frac{\partial^2 w}{\partial t^2} \end{aligned} \quad (3.8c)$$

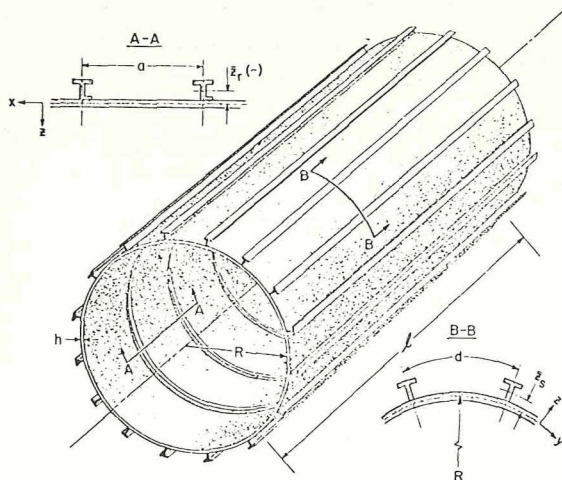


FIGURE 3.1.—Typical stiffened circular cylindrical shell. (After ref. 3.3)

where $s = x/R$ and $k = h^2/12R^2$ as used in chapter 2 and α and β in the stiffness constants given by equations (3.6) and (3.7) are replaced by x and θ , consistent with circular cylindrical shell coordinates. It is clear that the isotropic form of equations (3.8) is obtained simply by substituting E for E_x and E_θ , ν for ν_x and ν_θ , and $E/2(1+\nu)$ for G , which then agrees with equation (2.7).

Nelson, Zapotowski, and Bernstein (ref. 3.4) used the Love-Timoshenko strain-displacement equations to arrive at a set of equations of motion which can be written as

$$\frac{\partial^2 u}{\partial s^2} + \frac{C_{66}}{C_{11}} \frac{\partial^2 u}{\partial \theta^2} + \frac{C_{12} + C_{22}}{C_{11}} \frac{\partial^2 v}{\partial s \partial \theta} + \frac{C_{12}}{C_{11}} \frac{\partial w}{\partial s} = \frac{\rho h R^2}{C_{11}} \frac{\partial^2 u}{\partial t^2} \quad (3.9a)$$

$$\begin{aligned} \frac{C_{12} + C_{22}}{C_{11}} \frac{\partial^2 u}{\partial s \partial \theta} + \frac{C_{66} + D_{66}}{C_{11}} \frac{\partial^2 v}{\partial s^2} + \frac{C_{12} + C_{22}}{C_{11}} \frac{\partial^2 v}{\partial \theta^2} \\ + \frac{C_{22}}{C_{11}} \frac{\partial w}{\partial \theta} - \frac{D_{22}}{C_{11}} \frac{\partial^3 w}{\partial \theta^3} - \frac{D_{12} + D_{66}}{C_{11}} \frac{\partial^3 w}{\partial s \partial \theta^2} \\ = \frac{\rho h R^2}{C_{11}} \frac{\partial^2 v}{\partial t^2} \end{aligned} \quad (3.9b)$$

$$\begin{aligned} \frac{C_{12}}{C_{11}} \frac{\partial u}{\partial s} + \frac{C_{22}}{C_{11}} \frac{\partial v}{\partial \theta} - \frac{D_{22}}{C_{11}} \frac{\partial^3 v}{\partial \theta^3} - \frac{D_{12} + D_{66}}{C_{11}} \frac{\partial^3 v}{\partial s^2 \partial \theta} + \frac{C_{22}}{C_{11}} w \\ + \frac{D_{11}}{C_{11}} \frac{\partial^4 w}{\partial s^4} + \frac{D_{22}}{C_{11}} \frac{\partial^4 w}{\partial \theta^4} + \frac{2D_{12} + D_{66}}{C_{11}} \frac{\partial^4 w}{\partial s^2 \partial \theta^2} \\ = - \frac{\rho h R^2}{C_{11}} \frac{\partial^2 w}{\partial t^2} \end{aligned} \quad (3.9c)$$

where, as before, the subscripts 1 and 2 correspond to the x and θ directions, respectively. Using equations (3.6) and (3.7) it is seen that the above equations are of the same form as equations (3.8) except for the addition of terms having D_{ij} 's in the numerators. The added terms are modifying terms of the same form as found in isotropic shell equations. Indeed, if in equation (3.9c) the numerator $2D_{12} + D_{66}$ in one term were replaced by $2(D_{12} + 2D_{66})$, then the Reissner-Naghdi-Berry equations (2.9c) would follow for the isotropic case. Equations (3.9) are also of a more general form than equations (3.8) because they permit separate stretching and bending thicknesses h_s and h_b in the equations (3.6) and (3.7) which then do not, in general, cancel out in terms of the type D_{22}/C_{11} . In the case of stiffened shell simulation this distinction is necessary.

For general anisotropy, equations (3.4) and (3.5) are generalized to

$$\left. \begin{aligned} N_x &= C_{11}\epsilon_x + C_{12}\epsilon_\theta + C_{16}\gamma_{x\theta} \\ N_\theta &= C_{12}\epsilon_x + C_{22}\epsilon_\theta + C_{26}\gamma_{x\theta} \\ N_{x\theta} &= C_{16}\epsilon_x + C_{26}\epsilon_\theta + C_{66}\gamma_{x\theta} \end{aligned} \right\} \quad (3.10)$$

$$\left. \begin{aligned} M_x &= D_{11}\kappa_x + D_{12}\kappa_\theta + D_{16}\tau \\ M_\theta &= D_{12}\kappa_x + D_{22}\kappa_\theta + D_{26}\tau \\ M_{x\theta} &= D_{16}\kappa_x + D_{26}\kappa_\theta + D_{66}\tau \end{aligned} \right\} \quad (3.11)$$

where the C_{ij} and D_{ij} are generalized extensional and flexural stiffness coefficients arising from the three-dimensional form of Hooke's law and the force and moment resultant integrals taken over the thickness of the shell, and where it is now assumed that the coordinate axes used to define the elastic constants are parallel to the x and θ shell coordinates.

DiGiovanni and Dugundji (ref. 3.2) performed a notable service by deriving the general anisotropic forms of equations of motion according to a number of shell theories. These, as for isotropic shells (see sec. 2.1.1), can be written in terms of a Donnell-Mushtari matrix operator $[\mathcal{L}_{D-M}]$ and a modifying operator $[\mathcal{L}_{MOD}]$ as given by eqs. (2.3) and (2.5), where the anisotropic form of $[\mathcal{L}_{D-M}]$ is

$$[\mathcal{L}_{D-M}] = \begin{bmatrix} a_{11} & a_{12} & a_{13} \\ a_{21} & a_{22} & a_{23} \\ a_{31} & a_{32} & a_{33} \end{bmatrix} \quad (3.12)$$

where

$$\begin{aligned} a_{11} &= \frac{C_{11}}{C_{22}} \frac{\partial^2}{\partial s^2} + 2 \frac{C_{16}}{C_{22}} \frac{\partial^2}{\partial s \partial \theta} + \frac{C_{66}}{C_{22}} \frac{\partial^2}{\partial \theta^2} - \frac{\rho h R^2}{C_{22}} \frac{\partial^2}{\partial t^2} \\ a_{22} &= \frac{C_{66}}{C_{22}} \frac{\partial^2}{\partial s^2} + 2 \frac{C_{26}}{C_{22}} \frac{\partial^2}{\partial s \partial \theta} + \frac{\partial^2}{\partial \theta^2} - \frac{\rho h R^2}{C_{22}} \frac{\partial^2}{\partial t^2} \\ a_{33} &= 1 + k \left[\frac{D_{11}}{D_{22}} \frac{\partial^4}{\partial s^4} + 2 \left(\frac{D_{12} + 2D_{66}}{D_{22}} \right) \frac{\partial^4}{\partial s^2 \partial \theta^2} + \frac{\partial^4}{\partial \theta^4} \right] + \frac{\rho h R^2}{C_{22}} \frac{\partial^2}{\partial t^2} \\ a_{12} &= a_{21} = \frac{C_{16}}{C_{22}} \frac{\partial^2}{\partial s^2} + \left(\frac{C_{12} + C_{66}}{C_{22}} \right) \frac{\partial^2}{\partial s \partial \theta} + \frac{C_{26}}{C_{22}} \frac{\partial^2}{\partial \theta^2} \\ a_{13} &= a_{31} = \frac{C_{12}}{C_{22}} \frac{\partial}{\partial s} + \frac{C_{26}}{C_{22}} \frac{\partial}{\partial \theta} \\ a_{23} &= a_{32} = \frac{C_{26}}{C_{22}} \frac{\partial}{\partial s} + \frac{\partial}{\partial \theta} \end{aligned} \quad (3.13)$$

and the modifying operators are written as

$$[\mathcal{L}_{MOD}] = \begin{bmatrix} b_{11} & b_{12} & b_{13} \\ b_{21} & b_{22} & b_{23} \\ b_{31} & b_{32} & b_{33} \end{bmatrix} \quad (3.14)$$

The coefficients b_{ij} for use in equation (3.14) are given below (ref. 3.2).

Love-Timoshenko:

$$\begin{aligned} b_{11} &= b_{12} = b_{13} = b_{31} = 0 \\ b_{22} &= 2 \frac{D_{66}}{D_{22}} \frac{\partial^2}{\partial s^2} + 3 \frac{D_{26}}{D_{22}} \frac{\partial^2}{\partial s \partial \theta} + \frac{\partial^2}{\partial \theta^2} \\ b_{33} &= 4 \frac{D_{16}}{D_{22}} \frac{\partial^4}{\partial s^3 \partial \theta} + 4 \frac{D_{26}}{D_{22}} \frac{\partial^4}{\partial s \partial \theta^3} \\ b_{23} &= -\frac{D_{16}}{D_{22}} \frac{\partial^3}{\partial s^3} - \left(\frac{D_{12} + 2D_{66}}{D_{22}} \right) \frac{\partial^3}{\partial s^2 \partial \theta} - 3 \frac{D_{26}}{D_{22}} \frac{\partial^3}{\partial s \partial \theta^2} - \frac{\partial^3}{\partial \theta^3} \\ b_{32} &= -2 \frac{D_{16}}{D_{22}} \frac{\partial^3}{\partial s^3} - \left(\frac{D_{12} + 4D_{66}}{D_{22}} \right) \frac{\partial^3}{\partial s^2 \partial \theta} - 4 \frac{D_{26}}{D_{22}} \frac{\partial^3}{\partial s \partial \theta^2} - \frac{\partial^3}{\partial \theta^3} \end{aligned} \quad (3.15a)$$

Goldenveizer-Novozhilov:

$$\begin{aligned} b_{11} &= b_{12} = b_{13} = b_{31} = 0 \\ b_{22} &= 4 \frac{D_{66}}{D_{22}} \frac{\partial^2}{\partial s^2} + 4 \frac{D_{26}}{D_{22}} \frac{\partial^2}{\partial s \partial \theta} + \frac{\partial^2}{\partial \theta^2} \\ b_{33} &= 4 \frac{D_{16}}{D_{22}} \frac{\partial^4}{\partial s^3 \partial \theta} + 4 \frac{D_{26}}{D_{22}} \frac{\partial^4}{\partial s \partial \theta^3} \\ b_{23} &= b_{32} = -2 \frac{D_{16}}{D_{22}} \frac{\partial^3}{\partial s^3} - \left(\frac{D_{12} + 4D_{66}}{D_{22}} \right) \frac{\partial^3}{\partial s^2 \partial \theta} - 4 \frac{D_{26}}{D_{22}} \frac{\partial^3}{\partial s \partial \theta^2} - \frac{\partial^3}{\partial \theta^3} \end{aligned} \quad (3.15b)$$

Flügge-Byrne-Lur'ye

(also Herrmann and Armenakias):

$$\begin{aligned} b_{11} &= \frac{D_{66}}{D_{22}} \frac{\partial^2}{\partial \theta^2} \\ b_{22} &= 3 \frac{D_{66}}{D_{22}} \frac{\partial^2}{\partial s^2} + 2 \frac{D_{26}}{D_{22}} \frac{\partial^2}{\partial s \partial \theta} \\ b_{33} &= 4 \frac{D_{16}}{D_{22}} \frac{\partial^4}{\partial s^3 \partial \theta} + 4 \frac{D_{26}}{D_{22}} \frac{\partial^4}{\partial s \partial \theta^3} + 2 \frac{D_{26}}{D_{22}} \frac{\partial^2}{\partial s \partial \theta} + 2 \frac{\partial^2}{\partial \theta^2} + 1 \end{aligned}$$

$$b_{12}=b_{21}=\frac{D_{16}}{D_{22}}\frac{\partial^2}{\partial s^2}$$

$$b_{13}=-\frac{D_{11}}{D_{22}}\frac{\partial^3}{\partial s^3}-\frac{D_{16}}{D_{22}}\frac{\partial^3}{\partial s^2\partial\theta}+\frac{D_{66}}{D_{22}}\frac{\partial^3}{\partial s\partial\theta^2}+\frac{D_{26}}{D_{22}}\frac{\partial^3}{\partial\theta^3}+\frac{D_{26}}{D_{22}}\frac{\partial}{\partial\theta}$$

$$b_{23}=b_{32}=-2\frac{D_{16}}{D_{22}}\frac{\partial^3}{\partial s^3}-\left(\frac{D_{12}+3D_{66}}{D_{22}}\right)\frac{\partial^3}{\partial s^2\partial\theta}-2\frac{D_{26}}{D_{22}}\frac{\partial^3}{\partial s\partial\theta^2}$$

$$b_{31}=-\frac{D_{11}}{D_{22}}\frac{\partial^3}{\partial s^3}-\frac{D_{16}}{D_{22}}\frac{\partial^3}{\partial s^2\partial\theta}+\frac{D_{66}}{D_{22}}\frac{\partial^3}{\partial s\partial\theta^2}+\frac{D_{26}}{D_{22}}\frac{\partial}{\partial\theta} \quad (\text{see comment below}) \quad (3.15c)$$

Sanders:

$$b_{11}=\frac{1}{4}\frac{D_{66}}{D_{22}}\frac{\partial^2}{\partial\theta^2}$$

$$b_{22}=\frac{9}{4}\frac{D_{66}}{D_{22}}\frac{\partial^2}{\partial s^2}+3\frac{D_{26}}{D_{22}}+\frac{\partial^2}{\partial\theta^2}$$

$$b_{33}=4\frac{D_{16}}{D_{22}}\frac{\partial^4}{\partial s^3\partial\theta}+4\frac{D_{26}}{D_{22}}\frac{\partial^4}{\partial s\partial\theta^3}$$

$$b_{12}=b_{21}=-\frac{3}{4}\frac{D_{66}}{D_{22}}\frac{\partial^2}{\partial s\partial\theta}-\frac{1}{2}\frac{D_{26}}{D_{22}}\frac{\partial^2}{\partial\theta^2}$$

$$b_{13}=b_{31}=\frac{1}{2}\frac{D_{16}}{D_{22}}\frac{\partial^3}{\partial s^2\partial\theta}+\frac{D_{66}}{D_{22}}\frac{\partial^3}{\partial s\partial\theta^2}+\frac{1}{2}\frac{D_{26}}{D_{22}}\frac{\partial^3}{\partial\theta^3}$$

$$b_{23}=b_{32}=-\frac{3}{2}\frac{D_{16}}{D_{22}}\frac{\partial^3}{\partial s^3}-\left(\frac{D_{12}+3D_{66}}{D_{22}}\right)\frac{\partial^3}{\partial s^2\partial\theta}-\frac{7}{2}\frac{D_{26}}{D_{22}}\frac{\partial^3}{\partial s\partial\theta^2}-\frac{\partial^3}{\partial\theta^3} \quad (3.15d)$$

Note in equations (3.15c) that $b_{13} \neq b_{31}$ as taken from reference 3.2. Inasmuch as the Flügge-Byrne-Lur'ye theory has a symmetric set of equations of motion for *isotropic* materials, it is recommended that the reader verify the b_{13} and b_{31} coefficients of equations (3.15d) before attempting to use them.

Methods of representing stiffened shells by orthotropic analyses will now be briefly considered. In order to do this the stretching and bending stiffnesses of the stiffening elements must be properly treated. Consider first the isotropic shell which is reinforced by longitudinal

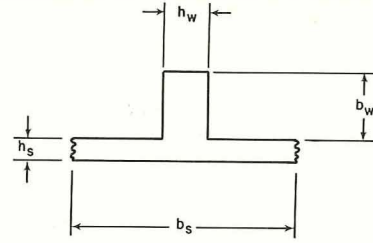


FIGURE 3.2.—Shell with integral stiffener.

stiffeners which are integral with the skin as shown in figure 3.2. The stiffener has thickness h_w and depth b_w and the repeating section is of length b_s as shown. The following formulas were given in reference 3.2 for the calculation of equivalent orthotropic stretching constants (assuming no stress lag):

$$\left. \begin{aligned} C_{11} &= \frac{Eh_s}{1-\nu^2}(1+k_1)\left[\frac{1+(1-\nu^2)k_1k_2}{1+k_1k_2}\right] \\ C_{12} &= \frac{\nu Eh_s}{1-\nu^2}\left(\frac{1+k_1}{1+k_1k_2}\right) \\ C_{22} &= \frac{Eh_s}{1-\nu^2}\left(\frac{1+k_1}{1+k_1k_2}\right) \\ C_{66} &= \frac{Eh_s}{2(1+\nu)}\left(\frac{1+k_1}{1+k_1k_2}\right) \end{aligned} \right\} \quad (3.16)$$

where $k_1 = h_w b_w / b_s h_s$, $k_2 = (1 - h_w / b_s) / (1 + h_s / h_w)$, and ν and E are the elastic properties of the skin and stiffener, which are assumed to be of the same material. The bending constants are

$$\left. \begin{aligned} D_{11} &= \frac{D_s}{(1+k_1)^2} \left\{ 1 + 4k_1 \left(\frac{b_w}{h_s}\right)^2 (1-\nu^2) \right. \\ &\quad + k_1^2 \left(\frac{b_w}{h_s}\right)^2 [2(1-\nu^2) + 3] \\ &\quad + k_1^3 \left(\frac{b_w}{h_s}\right)^2 (1-\nu^2) \\ &\quad + 6k_1 \left(\frac{b_w}{h_s}\right) (1-\nu^2 + k_1) \\ &\quad \left. + 4k_1^2 + k_1[3(1-\nu^2) + 2] \right\} \\ D_{12} &= \nu D_s \\ D_{22} &= \frac{D_s}{1 - \frac{h_w}{b_s} \left[1 - \frac{1}{(1 + b_w/h_s)^3} \right]} \end{aligned} \right\} \quad (3.17)$$

$$\left. \begin{aligned} D_{66} &= \frac{Gh_s^3}{12} + \frac{C}{2b_s} \\ &= \frac{D_s(1-\nu)}{2} \left[1 + 6\frac{b_w}{b_s} \left(\frac{h_w}{h_s} \right)^3 \beta \right] \end{aligned} \right\} \quad (3.17)$$

where C is the torsional rigidity of the web, β is a constant depending upon b_w and h_w which varies from 0.333 to 0.141 and D_s is the bending stiffness of the unstiffened skin; i.e., $D_s = Eh_s^3/12(1-\nu^2)$. For the case of circumferential stiffeners, where figure 3.2 still represents a typical repeating section, C_{11} , C_{22} , D_{11} , D_{22} are calculated by the formulas given above for C_{22} , C_{11} , D_{22} , D_{11} , respectively, and the remaining constants are calculated as above.

In reference 3.5 the orthotropic stiffness constants for the skin-stiffener repeating section (shown in figure 3.2) were given as

$$\left. \begin{aligned} C_{11} &= \frac{Eh_s}{1-\nu^2} (1+k_1) \left[\frac{1 + \frac{b_w}{h_s} + (1-\nu^2)k_1 \left(\frac{b_w}{h_s} \right) \left(1 - \frac{h_w}{b_s} \right)}{1 + \frac{b_w}{h_s} + k_1 \left(\frac{b_w}{h_s} \right) \left(1 - \frac{h_w}{b_s} \right)} \right] \\ C_{12} &= \frac{\nu Eh_s}{1-\nu^2} \left(\frac{1 + \frac{b_w}{h_s}}{1 - \frac{b_w}{h_s} - k_1} \right) \\ C_{22} &= \frac{Eh_s}{1-\nu^2} \left(\frac{1 + \frac{b_w}{h_s}}{1 - \frac{b_w}{h_s} - k_1} \right) \\ C_{66} &= \frac{Eh_s}{2(1+\nu)} \left(\frac{1 + \frac{b_w}{h_s}}{1 - \frac{b_w}{h_s} - k_1} \right) \\ D_{11} &= D_s \left[1 + 3(1-\nu^2)k_1 + 6(1-\nu^2)k_1 \left(\frac{b_w}{h_s} \right) + 4(1-\nu^2)k_1 \left(\frac{b_w}{h_s} \right)^2 \right] \\ D_{12} &= \nu D_s \end{aligned} \right\} \quad (3.18)$$

$$\left. \begin{aligned} D_{11} &= D_s \left[1 + 3(1-\nu^2)k_1 + 6(1-\nu^2)k_1 \left(\frac{b_w}{h_s} \right) + 4(1-\nu^2)k_1 \left(\frac{b_w}{h_s} \right)^2 \right] \\ D_{12} &= \nu D_s \end{aligned} \right\} \quad (3.19)$$

$$\left. \begin{aligned} D_{22} &= \frac{D_s}{1 - \frac{h_w}{b_s} \left[1 - \frac{1}{(1+b_w/h_s)^3} \right]} \\ D_{66} &= \frac{D_s(1-\nu)}{2} \left[1 + 3\frac{b_w}{b_s} \left(\frac{h_w}{h_s} \right)^3 k_w \right] \end{aligned} \right\} \quad (3.19)$$

where k_w is a torsional constant which takes on values 0, 0.14, 0.23, 0.33 as b_w/h_w is 0, 1, 2, ∞ . It appears that the sets of equations (3.16) and (3.17) differ considerably from equations (3.18) and (3.19).

Nelson, Zapatowski, and Bernstein (ref. 3.4) gave the following formulas for the calculation of the equivalent orthotropic stiffness constants for a shell stiffened by stringers having the same modulus of elasticity as the shell, and rings which have a modulus which may be different:

$$\left. \begin{aligned} C_{11} &= \frac{E_{LS}}{L_{R\theta}} [A_L + A_{Sx}/(1-\nu^2)] \\ C_{12} &= \nu C_{11} \\ C_{22} &= \frac{1}{L_{Rx}} [E_F A_F + E_{LS} A_{S\theta}/(1-\nu^2)] \\ C_{66} &= (1-\nu) C_{11}/2 \end{aligned} \right\} \quad (3.20a)$$

$$\left. \begin{aligned} D_{11} &= \frac{E_{LS}}{L_{R\theta}} [I_{Lx} + I_{Sx}(1-\nu^2)] \\ D_{12} &= \nu D_{11} \\ D_{22} &= \frac{1}{L_{Rx}} [E_F I_{F\theta} + E_{LS} I_{SS}/(1-\nu^2)] \\ D_{66} &= 2(1-\nu) D_{11} \end{aligned} \right\} \quad (3.20b)$$

where

$$\left. \begin{aligned} A_{Sx} &= h L_{R\theta} \\ A_{S\theta} &= h L_{Rx} \\ I_{F\theta} &= I_F + A_F (y_F + h - r_\theta)^2 \\ I_{Lx} &= I_L + A_L (y_L + h - r_x)^2 \\ I_{SS} &= \bar{L}_{Rx} h^3/12 + \beta \bar{L}_{Rx} h (r_\theta - h/2)^2 \\ I_{Sx} &= L_{R\theta} h^3/12 + L_{R\theta} h (r_x - h/2)^2 \\ r_\theta &= \frac{A_F (y_F + h) + \beta \bar{L}_{Rx} h^2/2}{A_F + \beta \bar{L}_{Rx} h} \\ r_x &= \frac{A_L (y_L + h) + L_{R\theta} h^2/2}{A_L + L_{R\theta} h} \end{aligned} \right\} \quad (3.21)$$

and A_F and A_L are the cross-sectional areas of rings (frames) and stringers (longerons), respectively; I_F and I_L are the area moments of inertia of frames and longerons about their own centroidal axes; I_{Lx} and I_{sx} are the area moments of inertia of the longerons and skins, respectively, about the centroidal axis of the skin-longeron cross section; I_{FS} and I_{SS} are the area moments of inertia of the frames and skins, respectively, about the centroidal axis of the skin-frame cross section; h = skin (shell) thickness; y_F and y_L are the distances from the centroidal axes of frames and longerons to the underside of the skin; E_F and E_{LS} are the moduli of elasticity of the frames and longerons (and skins), respectively; L_{Rx} and $L_{R\theta}$ are the lengths of repeating section in the axial and circumferential directions, respectively; \bar{L}_{Rx} is the effective length of repeating section in the axial direction (taken as $0.75L_{Rx}$ in ref. 3.4); $\beta = 0$ if the skin is attached to the longerons but not to the frames, and $\beta = 1$ if it is attached to both.

Mikulas and McElman (ref. 3.3) wrote the potential energy for a shell stiffened by ribs and stringers as shown in figure 3.1. A minimum of the total potential was found by allowing the variations of the three displacements δu , δv , and δw to be arbitrary, which yielded the following equations of motion:

$$\left[1 + \frac{E_s A_s (1 - \nu^2)}{E h d} \right] \frac{\partial^2 u}{\partial s^2} + \frac{(1 - \nu)}{2} \frac{\partial^2 u}{\partial \theta^2} + \frac{(1 + \nu)}{2} \frac{\partial^2 v}{\partial s \partial \theta} + \nu \frac{\partial w}{\partial s} - \frac{\bar{z}_s E_s A_s (1 - \nu^2)}{E h d R} \frac{\partial^3 w}{\partial s^3} = 0 \quad (3.22a)$$

$$\left[1 + \frac{E_r A_r (1 - \nu^2)}{E h a} \right] \frac{\partial^2 v}{\partial \theta^2} + \frac{(1 - \nu)}{2} \frac{\partial^2 v}{\partial s^2} + \frac{(1 + \nu)}{2} \frac{\partial^2 u}{\partial s \partial \theta} + \left[1 + \frac{E_r A_r (1 - \nu^2)}{E h a} \right] \frac{\partial w}{\partial \theta} - \frac{\bar{z}_r E_r A_r (1 - \nu^2)}{E h a R} \frac{\partial^3 w}{\partial \theta^3} = 0 \quad (3.22b)$$

$$\begin{aligned} & \frac{E h}{(1 - \nu^2)} \left(\nu \frac{\partial u}{\partial s} + \frac{\partial v}{\partial \theta} + w + k \nabla^4 w \right) - \frac{\bar{z}_s E_s A_s}{d R} \frac{\partial^3 u}{\partial s^3} \\ & + \frac{E_s (I_s + \bar{z}_s^2 A_s)}{d R^2} \frac{\partial^4 w}{\partial s^4} + \frac{E_r A_r}{a} w + \frac{E_r (I_r + \bar{z}_r^2 A_r)}{a R^2} \frac{\partial^4 w}{\partial \theta^4} \\ & + \frac{E_r A_r}{a} \frac{\partial v}{\partial \theta} - \frac{\bar{z}_r E_r A_r}{a R} \frac{\partial^3 v}{\partial \theta^3} - 2 \frac{\bar{z}_r E_r A_r}{a R} \frac{\partial^2 w}{\partial \theta^2} \\ & + \frac{1}{R^2} \left(\frac{G_s J_s}{d} + \frac{G_r J_r}{a} \right) \frac{\partial^4 w}{\partial s^2 \partial \theta^2} = M R^2 \frac{\partial^2 w}{\partial t^2} \end{aligned} \quad (3.22c)$$

where E and ν are the modulus of elasticity and Poisson's ratio, respectively, for the shell; E_s , A_s , I_s , \bar{z}_s , and $G_s J_s$ are the modulus of elasticity, cross-sectional area, moment of inertia about the centroid, distance to the centroid from the shell middle surface, and torsional stiffness, respectively, of a stringer; E_r , A_r , I_r , \bar{z}_r , and $G_r J_r$ are corresponding constants for a ring; R , d , a , and h are dimensions shown in figure 3.1; $k = h^2/12R^2$, as before; and M is the average smeared-out mass per unit area of the stiffened cylinder. It is easy to see that equations (3.22) are the Donnell-Mushtari equations of motion neglecting tangential inertia with added terms to account for the stringers and rings. In this case the variational procedure smears the stringer and ring stiffnesses into the shell orthotropy in contrast with structural representation methods depending upon physical behavior of the stiffened shell.

3.1.2 Shear Diaphragm End Conditions

The closed circular cylindrical shell of orthotropic material having axes of orthotropy coincident with the shell coordinates has the same relatively simple, exact, closed form solution for the displacements as in section 2.3 for isotropic shells. That is, taking

$$\left. \begin{aligned} u &= A \cos \lambda s \cos n\theta \cos \omega t \\ v &= B \sin \lambda s \sin n\theta \cos \omega t \\ w &= C \sin \lambda s \cos n\theta \cos \omega t \end{aligned} \right\} \quad (3.23)$$

where $\lambda = m\pi R/l$, satisfies the boundary condition equations (2.33) exactly as before, and substituting equations (3.23) into the equations of motion (e.g., eqs. (3.8)) yields a third order characteristic equation for the frequencies as in the case of isotropic shells. A small amount of added complexity then occurs in the coefficients of the characteristic equation for the orthotropic case. However, probably the greatest added complication to the problem is that instead of having one independent ratio of elastic constants (say, ν) to vary as a parameter, there are three in the orthotropic case (say, E_x/E_θ , ν_x , G/E_θ).

Das (ref. 3.6) used the Donnell-Mushtari theory neglecting tangential inertia and the exact solution functions given in equations (3.23). Correcting a misprint in reference 3.6, one arrives at the following frequency formula:

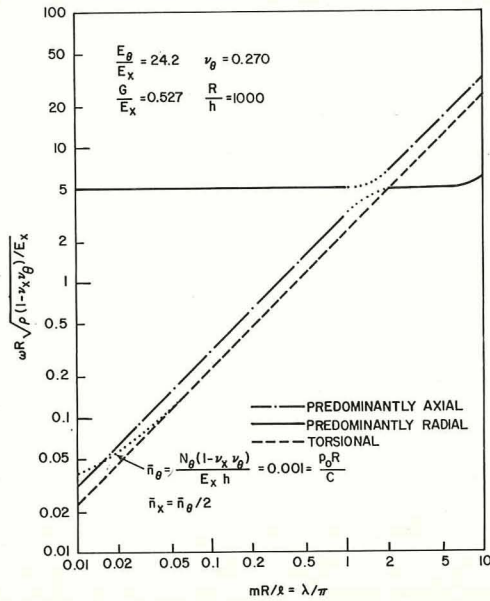


FIGURE 3.3.—Variation of frequency parameter with mR/l for an orthotropic shell; SD-SD supports; $R/h = 1000$, $n = 0$, $E_\theta/E_x = 24.2$, $\nu_\theta = 0.270$, $G/E_x = 0.527$. (After ref. 3.2)

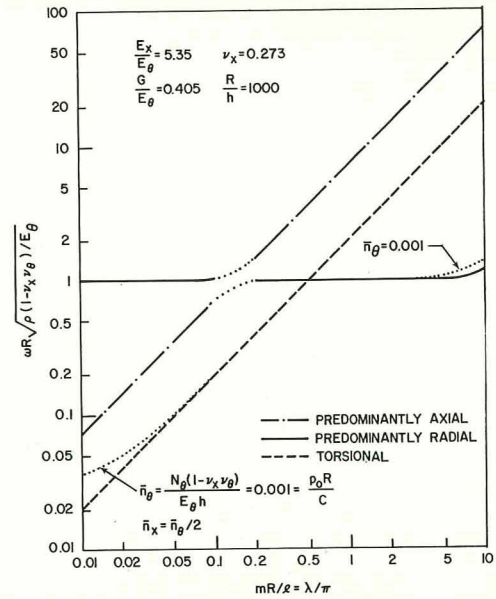


FIGURE 3.5.—Variation of frequency parameter with mR/l for an orthotropic shell; SD-SD supports; $R/h = 1000$, $n = 0$, $E_x/E_\theta = 5.35$, $\nu_x = 0.273$, $G/E_\theta = 0.405$. (After ref. 3.2)

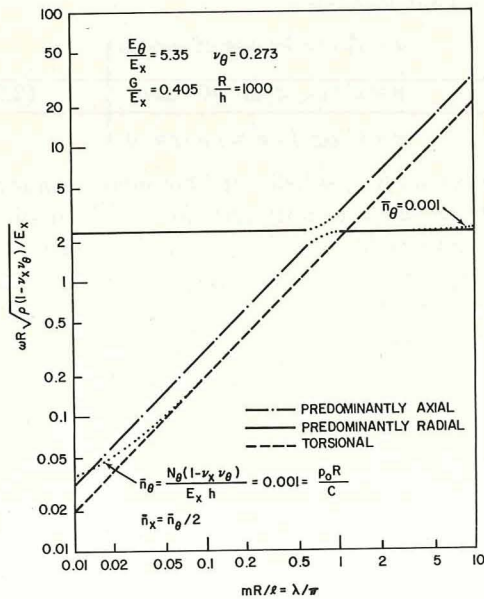


FIGURE 3.4.—Variation of frequency parameter with mR/l for an orthotropic shell; SD-SD supports; $R/h = 1000$, $n = 0$, $E_\theta/E_x = 5.35$, $\nu_\theta = 0.273$, $G/E_x = 0.405$. (After ref. 3.2)

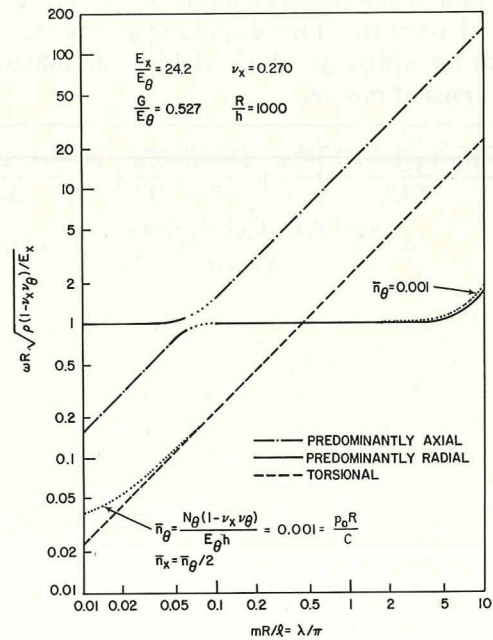


FIGURE 3.6.—Variation of frequency parameter with mR/l for an orthotropic shell; SD-SD supports; $R/h = 1000$, $n = 0$, $E_x/E_\theta = 24.2$, $\nu_x = 0.270$, $G/E_\theta = 0.527$. (After ref. 3.2)

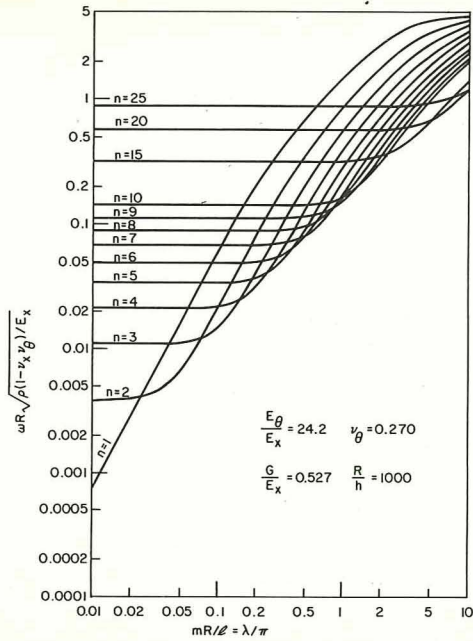


FIGURE 3.7.—Variation of lowest frequency parameters with mR/l for an orthotropic shell; SD-SD supports; $R/h=1000$, $n \geq 1$, $E_\theta/E_x=24.2$, $\nu_\theta=0.270$, $G/E_x=0.527$. (After ref. 3.2)

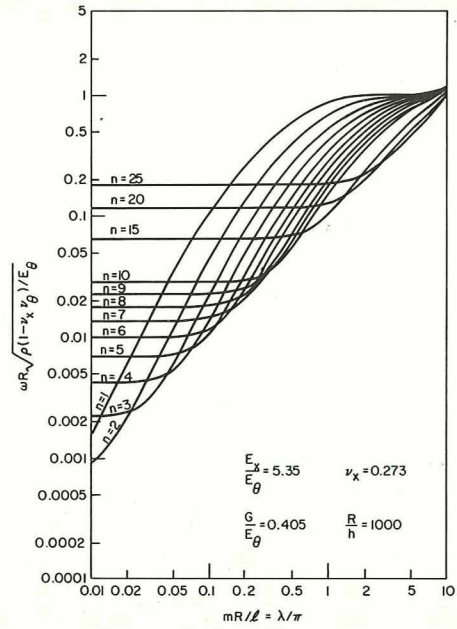


FIGURE 3.9.—Variation of lowest frequency parameter with mR/l for an orthotropic shell; SD-SD supports; $R/h=1000$, $n \geq 1$, $E_x/E_\theta=5.35$, $\nu_x=0.273$, $G/E_\theta=0.405$. (After ref. 3.2)

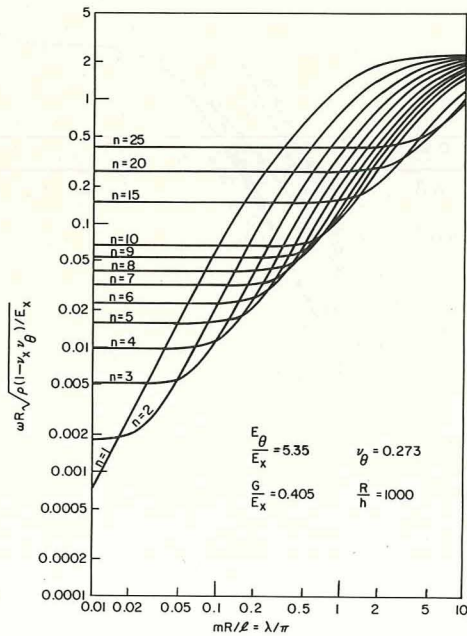


FIGURE 3.8.—Variation of lowest frequency parameter with mR/l for an orthotropic shell; SD-SD supports; $R/h=1000$, $n \geq 1$, $E_\theta/E_x=24.2$, $\nu_\theta=0.273$, $G/E_x=0.405$. (After ref. 3.2)

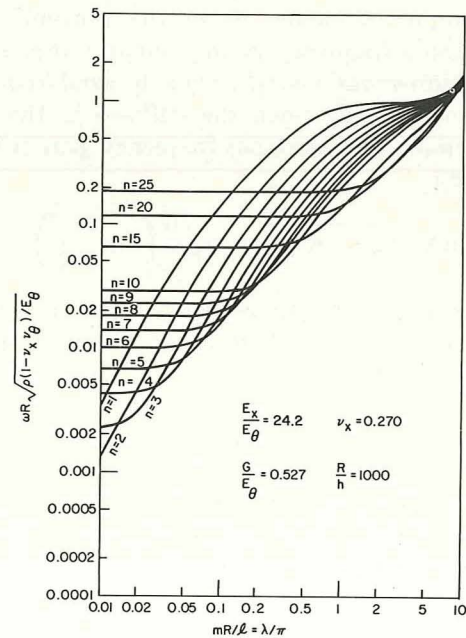


FIGURE 3.10.—Variation of lowest frequency parameter with mR/l for an orthotropic shell; SD-SD supports; $R/h=1000$, $n \geq 1$, $E_x/E_\theta=24.2$, $\nu_x=0.270$, $G/E_\theta=0.527$. (After ref. 3.2)

$$\frac{\omega^2 R^2 \rho (1 - \nu_x \nu_\theta)}{E_x} = \frac{1}{k K_1} \left[K_0 K_1 + k \lambda^4 \frac{C_{11} C_{22} - C_{12}^2}{C_{11}^2} \right] \quad (3.24)$$

where the coefficients K_0 and K_1 are given by

$$\left. \begin{aligned} K_0 &= \lambda^4 + \frac{2(C_{12} + 2C_{66})}{C_{11}} \lambda^2 n^2 + \frac{C_{22}}{C_{11}} n^4 \\ K_1 &= \lambda^4 + \frac{C_{11} C_{22} - C_{12}^2 - 2C_{12} C_{66}}{C_{11} C_{66}} \lambda^2 n^2 + \frac{C_{22}}{C_{11}} n^4 \end{aligned} \right\} \quad (3.25)$$

DiGiovanni and Dugundji (ref. 3.2) used the Goldenveizer-Novozhilov theory with exact mode shapes in the form of equations (3.23) to analyze a set of orthotropic shells having $R/h = 1000$ and various ratios of orthotropic elastic constants. Numerical results for $n=0$ are shown in figures 3.3 through 3.6, and for $n \geq 1$ in figures 3.7 through 3.10. In figures 3.3 through 3.6 all three frequency parameters arising from the solution of the characteristic equation in ω^2 are shown. The torsional mode for an orthotropic circular cylindrical shell uncouples from the other two axisymmetric modes as in the isotropic case. Torsional frequency is only slightly affected by the stiffness ratio E_θ/E_x , while the axial frequency depends mainly upon the stiffness in the axial direction. The torsional frequency parameter is simply

$$\omega R \sqrt{\rho(1 - \nu_x \nu_\theta)/E_x} = \lambda \sqrt{\frac{G}{E_x} \left(1 + \frac{1}{3} \frac{h^2}{R^2} \right)} \quad (3.26)$$

while the torsional frequency of a thin-walled circular bar according to St. Venant torsion theory is

$$\omega R \sqrt{\rho(1 - \nu_x \nu_\theta)/E_x} = \lambda \sqrt{\frac{G}{E_x}} \quad (3.27)$$

The other two frequencies shown in figures 3.3 through 3.6 have as asymptotes the frequency of axial vibrations of a bar,

$$\omega R \sqrt{\rho(1 - \nu_x \nu_\theta)/E_x} = \lambda \sqrt{1 - \nu_x \nu_\theta} \quad (3.28)$$

the frequency of radial vibrations of a ring in plane strain for long axial wave lengths (small λ)

$$\omega R \sqrt{\rho(1 - \nu_x \nu_\theta)/E_x} = \sqrt{E_\theta/E_x} \quad (3.29)$$

and a ring in plane stress for short axial wave lengths (large λ)

$$\omega R \sqrt{\rho(1 - \nu_x \nu_\theta)/E_x} = \sqrt{\frac{E_\theta}{E_x}} (1 - \nu_x \nu_\theta) \quad (3.30)$$

The quantity $p_0 R/C$ shown in figures 3.3 through 3.6 is an internal pressure parameter which will be discussed in section 3.4.4.

In figures 3.7 through 3.10 the lowest of the three frequencies is shown for each value of n . For $n=1$ (beam bending mode) and long axial wave lengths the frequency parameters are asymptotic to those of beams according to the Euler-Bernoulli theory; i.e.,

$$\omega R \sqrt{\rho(1 - \nu_x \nu_\theta)/E_x} = \lambda^2 \sqrt{\frac{1}{2}} (1 - \nu_x \nu_\theta) \quad (3.31)$$

This asymptotic behavior is shown in figure 3.11 for cases when $E_x/E_\theta > 1$ and $E_\theta/E_x > 1$. These figures show that for long axial wave lengths the circumferential stiffening has negligible effect on

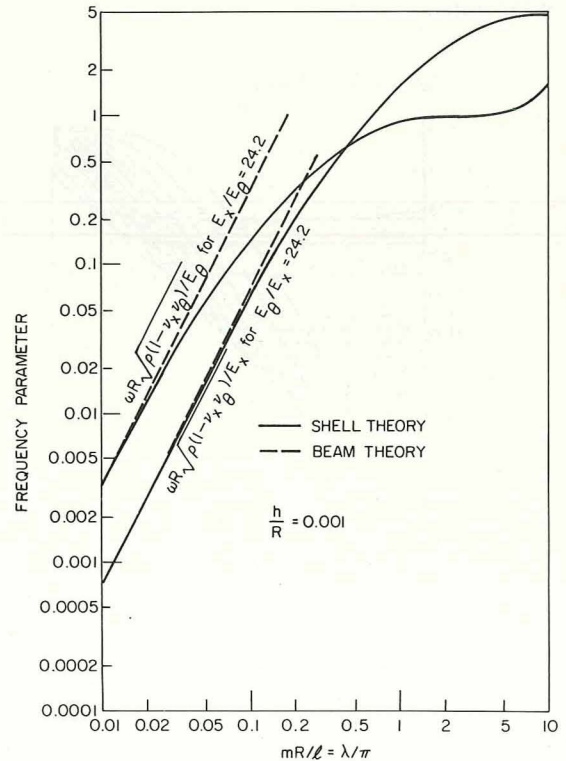


FIGURE 3.11.—Frequency parameters for the beam-type modes ($n=1$) of orthotropic shells. (After ref. 3.2)

the beam-type frequencies; however, for short axial wave lengths circumferential stiffening produces a major effect, whereas axial stiffening has only a slight effect.

For $n \geq 2$ the asymptotic values of the three frequencies for long axial wave lengths are those of the inextensional mode of a ring,

$$\omega R \sqrt{\rho(1 - \nu_x \nu_\theta) / E_x} = \frac{1}{2} \left(\frac{h}{R} \right) \sqrt{\frac{1}{3} \frac{E_\theta}{E_x} (1 - \nu_x \nu_\theta) \frac{n^2(n^2 - 1)^2}{n^2 + 1}} \quad (3.32)$$

the axial shear mode,

$$\omega R \sqrt{\rho(1 - \nu_x \nu_\theta) / E_x} = n \sqrt{G / E_x} \quad (3.33)$$

and the extensional mode of a ring,

$$\omega R \sqrt{\rho(1 - \nu_x \nu_\theta) / E_x} = \sqrt{\frac{E_\theta}{E_x} (1 - \nu_x \nu_\theta) (n^2 + 1)} \quad (3.34)$$

Figures 3.7 through 3.10 show that the stiffness ratio E_x/E_θ has little effect on the lowest frequency, which is for a predominantly radial mode, for long and intermediate wave lengths for $E_x > E_\theta$. However, for $E_\theta > E_x$ the frequency shows a marked increase with increasing E_θ/E_x (circumferential stiffening). As for the isotropic case, in all orthotropic cases for $n \geq 2$, the value of n for which the fundamental (minimum) frequency occurs increases with increasing λ .

Calculations were also made in reference 3.2 for circular cylindrical shells having integral stiffeners of the type shown in figure 3.2. The equivalent "smeared out" orthotropic stretching and bending constants were calculated according to equations (3.16) and (3.17). In one case integral ring stiffeners were used; in the second case the stiffeners were longitudinal stringers. For both cases R/h was taken at 1000, and the repeating section dimensions are determined by the ratios $b_w/h_s = 4$, $h_w/b_s = 0.10$, and $h_w/h_s = 0.40$ ($\beta = 0.280$). It is important to note that in these two cases of integrally stiffened shells the ratios of stretching stiffnesses to each other are, in general, different than the ratios of the bending stiffnesses, unlike the unstiffened orthotropic shells described in figures 3.3 through 3.11. The two cases were chosen, however, so that the ratios of bending stiffness D_{11}/D_{22} and D_{22}/D_{11} were both 24.2 as for two of the unstiffened orthotropic

shells. Axisymmetric ($n=0$) frequency parameters for the ring-stiffened and stringer-stiffened shells are shown in figures 3.12 and 3.13, respectively. Frequency parameters for the $n \geq 1$ modes are depicted in figures 3.14 and 3.15. In these figures ρ^* is an average mass density constant taking into account both the shell and the stiffeners.

From figures 3.7 and 3.14 it is evident, when comparing the two types of circumferential stiffening, that the frequency of the predominantly radial frequency is approximately the same as that of the uniform thickness orthotropic cylinder when $mR/l < 0.5$ and $n \geq 2$. For greater values of mR/l , the frequency of the stiffened cylinder decreases below that of the uniform cylinder for all values of $n \geq 2$. However, this decrease diminishes with increasing n , so that for very large n , the frequencies for both these cylinders (uniform and stiffened) again become approximately the same. This is because for large values of n and mR/l the influence of bending is predominant. Looking at the cases of axial stiffening (cf., figs. 3.10 and 3.15), one observes that for $n \geq 4$ frequencies for both types of cylindrical shells are nearly the same for long axial wave lengths; for intermediate axial wave lengths the differences in the frequencies between the two types become appreciable; while for short axial wave lengths the differences again become small. For $n=2$ and 3, the frequency of the shell having stringers is less than that of the corresponding uniform shell for all but large λ .

An interesting study of the effects of changing C_{22}/C_{11} and C_{66}/C_{11} ratios upon the frequencies of uniform orthotropic shells was made by Dong (ref. 3.7) using the Donnell-Mushtari theory and the exact displacement functions of equations (3.23). Numerical results are seen in figures 3.16 and 3.17 for shells having $R=40$ in., $h=0.4$ in., and $C_{12}/h=0.1 \times 10^6$ psi. In figure 3.16 C_{22}/h and C_{66}/h are taken to be 33.0×10^6 psi. and 14.5×10^6 psi., respectively. A family of frequency envelopes is shown for various C_{22}/C_{11} ratios, plotted over a range of l/R . In figure 3.17 C_{11}/h is 33.0×10^6 psi. and C_{22}/h is 330×10^6 psi. It is apparent in this latter figure that as l/R is increased the curves approach each other, indicating small dependence of ω upon the shear modulus for large l/R . This is because the vi-

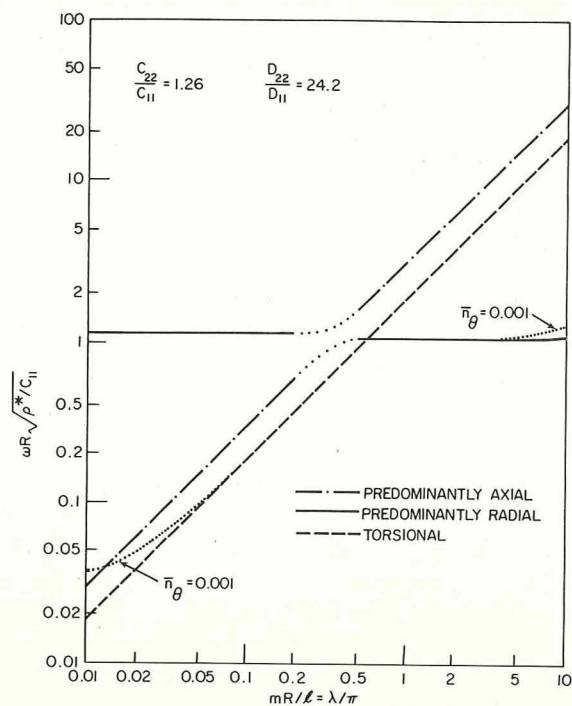


FIGURE 3.12.—Frequency parameters for a ring-stiffened cylindrical shell; SD-SD supports, $n=0$. (After ref. 3.2)

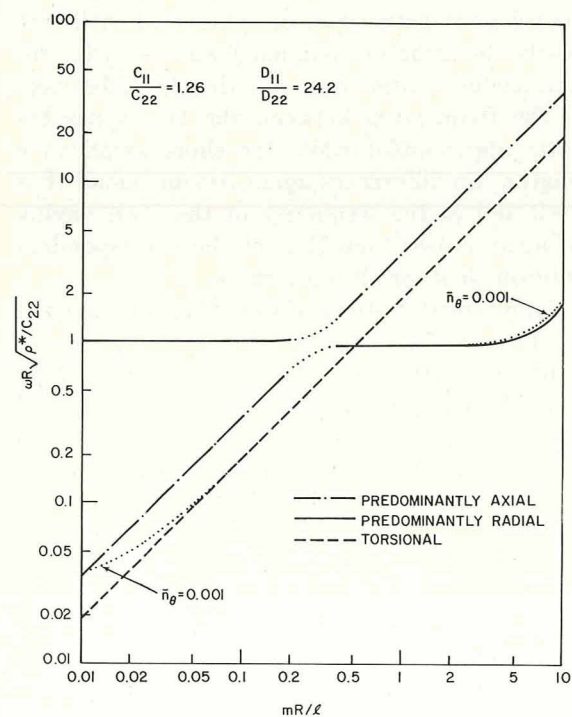


FIGURE 3.13.—Frequency parameter for a stringer-stiffened cylindrical shell; SD-SD supports, $n=0$. (After ref. 3.2)

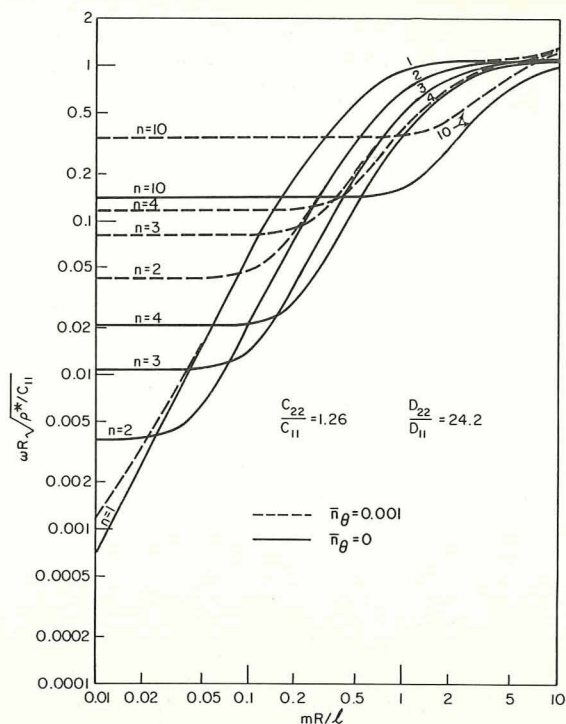


FIGURE 3.14.—Frequency parameter for a ring-stiffened cylindrical shell; SD-SD supports, $n=0$. (After ref. 3.2)

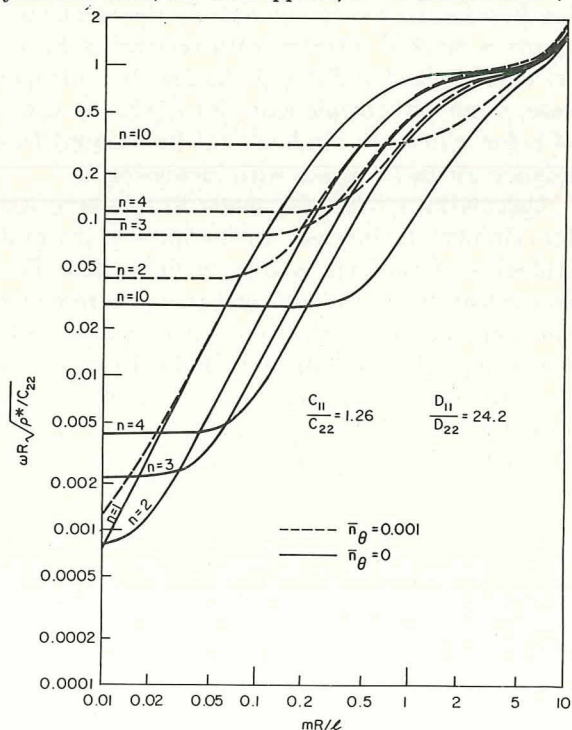


FIGURE 3.15.—Frequency parameter for a stringer-stiffened cylindrical shell; SD-SD supports, $n \geq 1$. (After ref. 3.2)

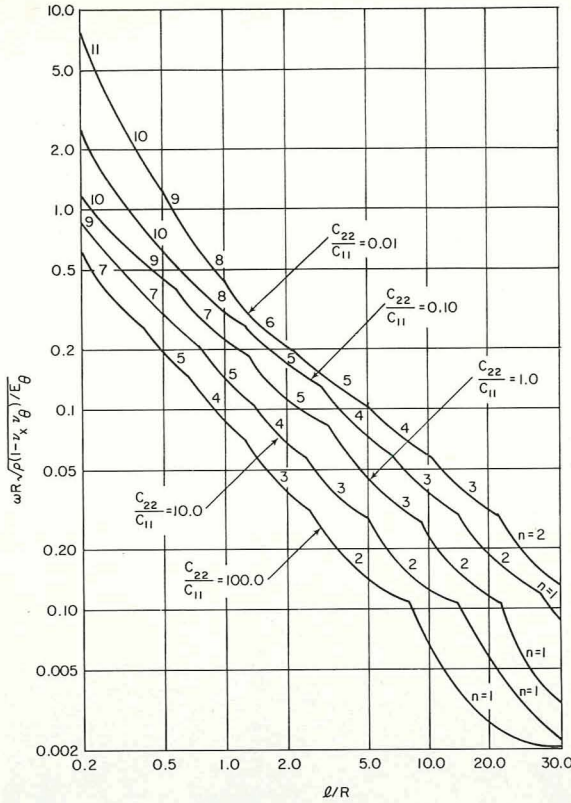


FIGURE 3.16.—Frequency envelopes for an orthotropic shell; SD-SD supports; $R/h=100$, $C_{22}/C_{11}=330$, $C_{66}/C_{22}=0.440$. (After ref. 3.7)

bration modes are predominantly radial for large l/R . For small values of l/R and large C_{66} , however, the lowest frequency can correspond to a mode which is predominantly circumferential. This is shown by the dotted line in figure 3.17 for $C_{66}/C_{11}=100$. For this mode, $n=1$.

Hoppmann (refs. 3.8 and 3.9) proposed determining the stretching and bending stiffness coefficients C_{ij} and D_{ij} of integrally stiffened shells from static deflection tests on flat plates, and then solving the cylindrical shell free vibration problem using these coefficients as input data. He used Love's strain-displacement equations and the exact solution equations (3.23) to arrive at a characteristic equation

$$\begin{vmatrix} \lambda_{11} - \Delta & \lambda_{12} & \lambda_{13} \\ \lambda_{12} & \lambda_{22} - \Delta & \lambda_{23} \\ \lambda_{13} & \lambda_{23} & \lambda_{33} - \Delta \end{vmatrix} = 0 \quad (3.35)$$

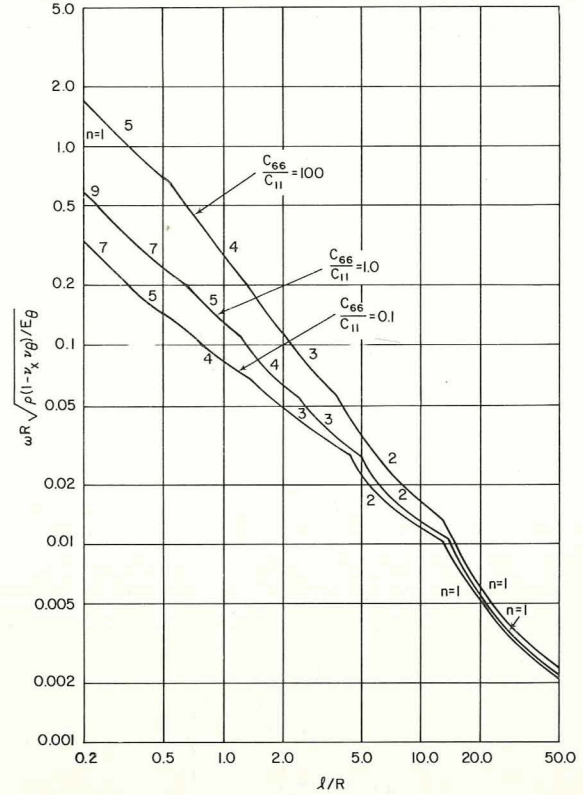


FIGURE 3.17.—Frequency envelopes for an orthotropic shell; SD-SD supports, $R/h=100$, $C_{22}/C_{11}=10$, $C_{22}/C_{12}=3300$. (After ref. 3.7)

where

$$\left. \begin{aligned} \lambda_{11} &= n^2 C_{66} + \lambda^2 C_{11} \\ \lambda_{22} &= n^2 C_{22} + kn^2 D_{22} + \lambda^2 C_{66} + 4k\lambda^2 C_{66} \\ \lambda_{33} &= C_{22} + k\lambda^4 D_{11} + kn^4 D_{22} + 2k\lambda^2 n^2 D_{12} \\ &\quad + 4kn^2 \lambda^2 D_{66} \\ \lambda_{12} &= -\lambda n C_{12} - \lambda n C_{66} \\ \lambda_{13} &= \lambda C_{12} \\ \lambda_{23} &= -nC_{22} - kn^3 D_{22} - kn\lambda^2 D_{12} \\ &\quad - 4kn\lambda^2 D_{66} \end{aligned} \right\} \quad (3.36)$$

A cursory comparison with equations (2.5), (2.7), and (2.9a) show that equations (3.36) do not agree with the Love-Timoshenko equations in the isotropic case, nor with any of the other shell theories included within equations (2.9). Results were obtained for aluminum shells having an internal diameter of 3.85 in. and a length of

15.53 in. The shell thickness was 0.065 in. and the stiffeners had a width of 0.125 in., a depth of 0.210 in., and spacing of 0.75 in. (see figure 3.18). The elastic constants as determined by static tests were

$$\left. \begin{aligned} c_{11}/h_s &= 1.4 \times 10^{-6} \\ c_{12}/h_s &= -0.21 \times 10^{-6} \\ c_{22}/h_s &= 0.83 \times 10^{-6} \\ c_{66}/h_s &= 2.11 \times 10^{-6} \end{aligned} \right\} \quad (3.37a)$$

$$\left. \begin{aligned} d_{11}/h_b^3 &= 306 \times 10^{-6} \\ d_{12}/h_b^3 &= -8.3 \times 10^{-6} \\ d_{22}/h_b^3 &= 13 \times 10^{-6} \\ d_{66}/h_b^3 &= 370 \times 10^{-6} \end{aligned} \right\} \quad (3.37b)$$

in units of inches and pounds, where h_s and h_b are the stretching and bending thicknesses, respectively, where in this case the elastic constants arise from the stress-strain relations for stretching

$$\left. \begin{aligned} \epsilon_{x_s} &= c_{11}\sigma_{x_s} + c_{12}\sigma_{\theta_s} \\ \epsilon_{\theta_s} &= c_{12}\sigma_{x_s} + c_{22}\sigma_{\theta_s} \\ \epsilon_{x\theta_s} &= c_{66}\tau_{x\theta_s} \end{aligned} \right\} \quad (3.38a)$$

and bending

$$\left. \begin{aligned} \epsilon_{x_b} &= d_{11}\sigma_{x_b} + d_{12}\sigma_{\theta_b} \\ \epsilon_{\theta_b} &= d_{12}\sigma_{x_b} + d_{22}\sigma_{\theta_b} \\ \epsilon_{x\theta_b} &= d_{66}\tau_{x\theta_b} \end{aligned} \right\} \quad (3.38b)$$

Theoretical frequencies from equation (3.35) and experimentally measured frequencies are given in table 3.1 for shells having circumferential stiffeners and in table 3.2 for shells having longitudinal stiffeners.

In table 3.1 theoretical results taken from reference 3.4 are also given for Hoppmann's ring-stiffened shells. These values were obtained using the Love-Timoshenko equations of motion given in equations (3.9) and the method of calculating equivalent orthotropic constants given in equations (3.20) and (3.21). Hu and Wah (refs. 3.10 and 3.11) also gave theoretical results for this problem as shown in table 3.1. They treated the shell segments and rings as discrete elements by means of stiffness matrices. Two factors contributed to error in the latter calculation: (1) Neglect of ring eccentricity and (2) the use of a slightly greater length of shell (15.0 in., rather than

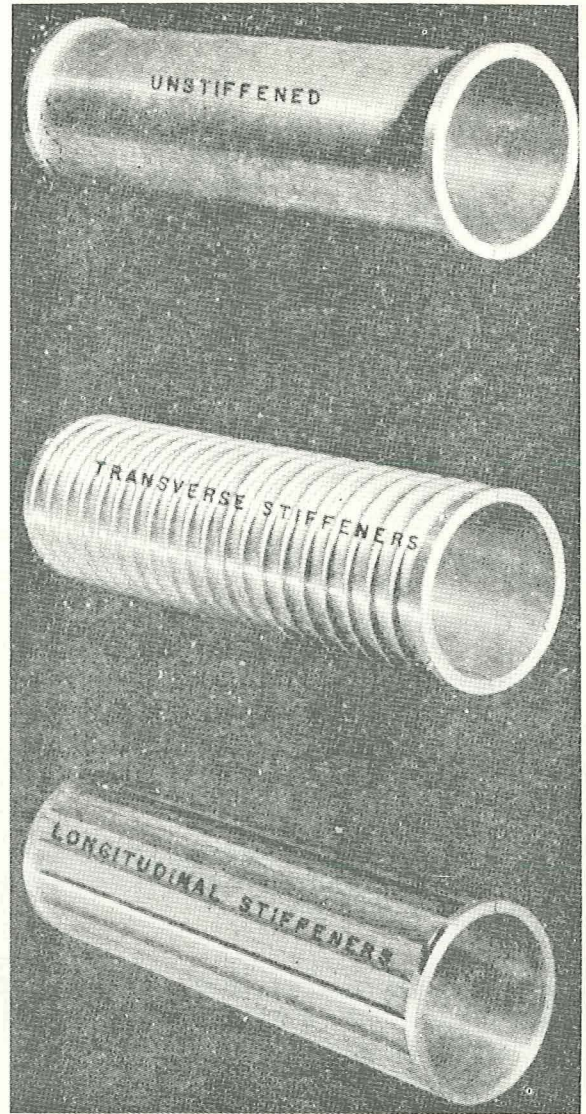


FIGURE 3.18.—Test models of stiffened shells.
(After ref. 3.8)

15.53 in.). Finally, results are shown in table 3.1 taken from reference 3.12 wherein stiffeners were smeared out by means of an "effective width" and the Arnold-Warburton strain-displacement equations were used.

Sewall and Naumann (ref. 3.13) accomplished the smearing out of rings and stringers into the shell by means of a Ritz procedure using beam functions which included the strain energies of the rings and stringers and assumed vibration modes (eqs. (3.23) in the case of SD-SD supports) and used their method to compare results

TABLE 3.1.—*Lowest Frequencies (cps) for a Ring-Stiffened Shell Supported by Shear Diaphragms*

n	Reference	m				
		1	2	3	4	5
2	3.8 (exper.)	1530	2040	3200	4440	6200
	3.8 (theor.)	1530	2100	3330	4860	6480
	3.4	1529	2112	3266	4608	5932
	3.10	1413	2447	4031	5668	7188
	3.12	1660	2270	3500	4960	6420
3	3.8 (exper.)	4080	4090	4520	5000	5700
	3.8 (theor.)	4230	4320	4500	5040	5760
	3.4	4171	4234	4472	4933	5576
	3.10	3537	3731	4261	5094	6090
	3.12	4500	4590	4850	5360	6070
4	3.8 (exper.)	7520	7800	7920
	3.8 (theor.)	8100	8100	8190	8280
	3.4	7994	8000	8055	8179	8395
	3.10	6700	6772	6957	7296	7787
	3.12	8520	8680	8950
5	3.8 (exper.)	11,400
	3.8 (theor.)	13,050	13,100	13,140	13,230
	3.4	12,928	12,930	19,946	12,990	(a)
	3.10	10,730	10,783	10,892	11,079	11,357
	3.12

^a Meaningless value given in reference 3.4.

for Hoppmann's ring-stiffened shell. The comparison is shown in figure 3.19. Donnell-type strain-displacement relationships were used for the shell.

In table 3.2 numerical results are also available from references 3.14 and 3.15 for Hoppmann's stringer-stiffened shell. Adelman, Catherines, and Walton (ref. 3.14) used a finite element approach to compare with Hoppmann's exact solution and to obtain better accuracy for comparison with their method they programmed the accurate solution of Hoppmann's exact characteristic equation (Hoppmann's theoretical results given in tables 3.1 and 3.2 carry no more than three significant figures and may have been calculated by slide rule). The agreement between the exact and finite element solutions is clearly outstanding,

FIGURE 3.19.—Frequencies of a cylindrical shell having 19 integral stiffening rings and shear diaphragm supports. (After ref. 3.13)

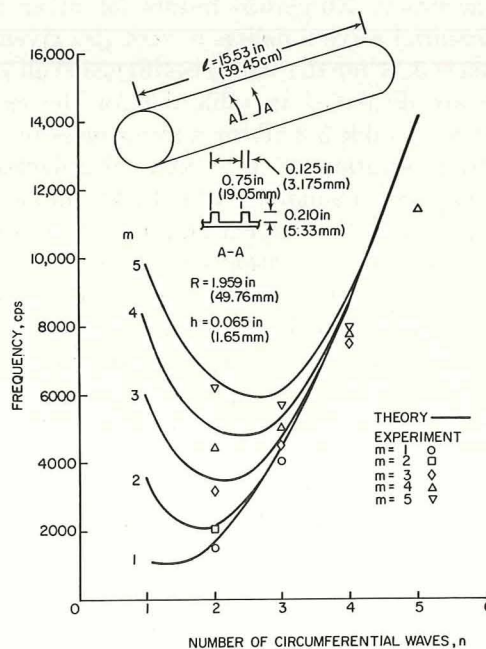


TABLE 3.2.—*Lowest Frequencies (cps) for a Stringer-Stiffened Shell Supported by Shear Diaphragms*

n	Reference	m				
		1	2	3	4	5
2	3.8 (exper.)	700
	3.8 (theor.)	750	2300	4200	6100	7900
	3.14 (exact)	739	2229	4234	6299	8206
	3.14 (fin.el.)	739	2229	4234	6300	8210
	3.15	836	2698	6267
3	3.8 (exper.)	1270	1830	2640	5490	6100
	3.8 (theor.)	1150	1700	2870	4360	5900
	3.14 (exact)	1184	1719	2840	4318	5962
	3.14 (fin.el.)	1184	1719	2840	4319	5968
	3.15	1276	1750	3059	5178
4	3.8 (exper.)	2200	2600	3360	4100	5200
	3.8 (theor.)	2100	2350	2970	3960	5100
	3.14 (exact)	2167	2414	3002	3966	5234
	3.14 (fin.el.)	2167	2414	3002	3967	5240
	3.15	2255	2358	2762	3636	5016
5	3.8 (exper.)	3460	4080	4120	5130	6100
	3.8 (theor.)	3340	3510	3900	4620	5600
	3.14 (exact)	3468	3650	4040	4706	5669
	3.14 (fin.el.)	3468	3650	4040	4707	5675
	3.15	3552	3580	3699	4002	4577

especially for the lower values of m . Only 10 elements in the axial direction were needed for this accuracy. Numerical results for other circumferential wave numbers n were also given in reference 3.14 for the stringer-stiffened shell and these are displayed in table 3.3 for the exact solution. In table 3.3 all three frequencies resulting from solution of the cubic characteristic equation are tabulated. Note that, unlike for isotropic shells, the frequencies for $n=0$ and $n=1$ do not increase monotonically with the value of m . A plot of the minimum ω^2 versus n taken from these data is shown in figure 3.20. Figure 3.21 shows the three frequencies arising for $n=2$ and $1 \leq m \leq 5$.

The results of Penzes (ref. 3.15) shown in table 3.2 were obtained by using Hoppmann's elastic constants, the Donnell-Mushtari shell theory with Yu's simplifying assumption (see sec. 2.3.5),

FIGURE 3.20.—Minimum circular frequencies for a stringer-stiffened shell supported by shear diaphragms. (After ref. 3.14)

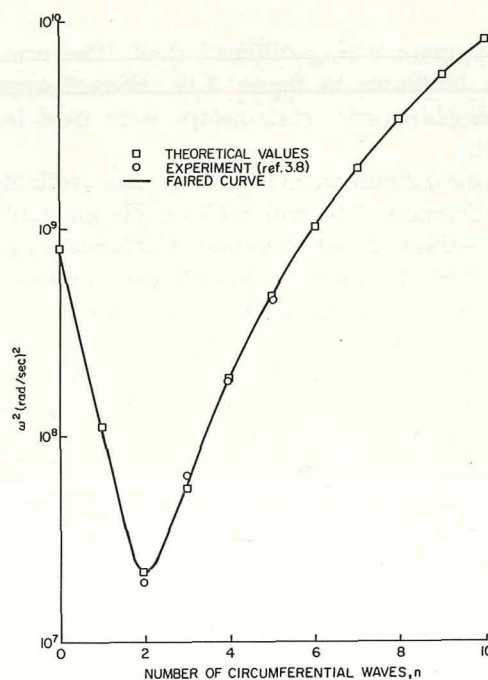


TABLE 3.3.—*Frequency Sets (cps) for a Stringer-Stiffened Shell Supported by Shear Diaphragms*

<i>n</i>	<i>m</i>				
	1	2	3	4	5
0	1.457×10 ⁴ 7.135×10 ³ 1.425×10 ⁴	1.307×10 ⁴ 1.592×10 ⁴ 9.010×10 ³	1.404×10 ⁴ 2.227×10 ⁴ 1.352×10 ⁴	1.422×10 ⁴ 2.946×10 ⁴ 1.802×10 ⁴	1.440×10 ⁴ 3.673×10 ⁴ 2.252×10 ⁴
1	1.666×10 ³ 1.331×10 ⁴ 2.114×10 ⁴	4.863×10 ³ 1.634×10 ⁴ 2.363×10 ⁴	7.920×10 ³ 2.824×10 ⁴ 1.894×10 ⁴	1.025×10 ⁴ 3.410×10 ⁴ 2.169×10 ⁴	1.183×10 ⁴ 4.052×10 ⁴ 2.502×10 ⁴
2	7.390×10 ² 2.354×10 ⁴ 3.320×10 ⁴	2.229×10 ³ 2.462×10 ⁴ 3.561×10 ⁴	4.234×10 ³ 2.617×10 ⁴ 3.933×10 ⁴	6.299×10 ³ 4.401×10 ⁴ 2.816×10 ⁴	8.206×10 ³ 4.933×10 ⁴ 3.064×10 ⁴
3	1.184×10 ³ 3.477×10 ⁴ 4.653×10 ⁴	1.719×10 ³ 3.508×10 ⁴ 4.862×10 ⁴	2.840×10 ³ 3.576×10 ⁴ 5.178×10 ⁴	4.318×10 ³ 3.690×10 ⁴ 5.575×10 ⁴	5.962×10 ³ 6.032×10 ⁴ 3.853×10 ⁴
4	2.167×10 ³ 4.624×10 ⁴ 6.033×10 ⁴	2.414×10 ³ 4.625×10 ⁴ 6.213×10 ⁵	3.002×10 ³ 4.647×10 ⁴ 6.487×10 ⁴	3.966×10 ³ 4.703×10 ⁴ 6.833×10 ⁴	5.234×10 ³ 4.800×10 ⁴ 7.236×10 ⁴
5	3.468×10 ³ 5.777×10 ⁴ 7.437×10 ⁴	3.650×10 ³ 5.766×10 ⁴ 7.593×10 ⁴	4.040×10 ³ 5.765×10 ⁴ 7.833×10 ⁴	4.706×10 ³ 5.787×10 ⁴ 8.140×10 ⁴	5.669×10 ³ 5.839×10 ⁴ 8.502×10 ⁴
6	5.064×10 ³ 6.933×10 ⁴ 8.854×10 ⁴	5.227×10 ³ 6.917×10 ⁴ 8.990×10 ⁴	5.549×10 ³ 6.905×10 ⁴ 9.203×10 ⁴	6.079×10 ³ 6.906×10 ⁴ 9.479×10 ⁴	6.858×10 ³ 6.929×10 ⁴ 9.806×10 ⁴
7	6.951×10 ³ 8.089×10 ⁴ 1.028×10 ⁵	7.108×10 ³ 7.914×10 ⁴ 1.040×10 ⁵	7.401×10 ³ 8.054×10 ⁴ 1.059×10 ⁵	7.867×10 ³ 8.043×10 ⁴ 1.084×10 ⁵	8.543×10 ³ 8.047×10 ⁴ 1.114×10 ⁵
8	9.129×10 ³ 9.246×10 ⁴ 1.171×10 ⁵	9.284×10 ³ 9.229×10 ⁴ 1.182×10 ⁵	9.563×10 ³ 9.208×10 ⁴ 1.199×10 ⁵	9.995×10 ³ 9.190×10 ⁴ 1.222×10 ⁵	1.061×10 ⁴ 9.182×10 ⁴ 1.249×10 ⁵
9	1.160×10 ⁴ 1.040×10 ⁵ 1.314×10 ⁵	1.175×10 ⁴ 1.039×10 ⁵ 1.324×10 ⁵	1.202×10 ⁴ 1.036×10 ⁵ 1.340×10 ⁵	1.243×10 ⁴ 1.034×10 ⁵ 1.361×10 ⁵	1.301×10 ⁴ 1.033×10 ⁵ 1.386×10 ⁵
10	1.436×10 ⁴ 1.156×10 ⁵ 1.458×10 ⁵	1.451×10 ⁴ 1.154×10 ⁵ 1.467×10 ⁵	1.478×10 ⁴ 1.152×10 ⁵ 1.481×10 ⁵	1.518×10 ⁴ 1.150×10 ⁵ 1.500×10 ⁵	1.573×10 ⁴ 1.148×10 ⁵ 1.524×10 ⁵

and exact solution functions in the form of equations (3.23).

Using the exact solution functions given by equations (3.23) and substituting into the equations (3.22) of motion, Mikulas and McElman (ref. 3.3) derived the following frequency formula to take into account the "smeared out" orthotropy of stiffening rings and stringers:

$$\frac{\omega^2 M l^4}{\pi^4 D} = m^4 (1 + \delta^2)^2 + m^4 \left[\frac{E_s I_s}{D d} + \delta^2 \left(\frac{G_s J_s}{D d} + \frac{G_r J_r}{D a} \right) + \delta^4 \frac{E_r I_r}{D a} \right] + \frac{12 l^4 (1 - \nu^2)}{h^2 R^2} \left[\frac{1 + \bar{S} \Lambda_s + \bar{R} \Lambda_r + \bar{S} \bar{R} \Lambda_{rs}}{\Lambda} \right] \quad (3.39)$$

where

$$\left. \begin{aligned} \Lambda_s &= 1 + 2\lambda^2 (\bar{z}_s/R) (\delta^2 - \nu) + \lambda^4 (\bar{z}_s/R)^2 (1 + \delta^2)^2 \\ \Lambda_r &= 1 + 2n^2 (\bar{z}_r/R) (1 - \nu \delta^2) + n^4 (\bar{z}_r/R)^2 (1 + \delta^2)^2 \\ \Lambda_{rs} &= n^2 \lambda^2 [\delta^2 (1 - \nu^2) + 2(1 + \nu)] (\bar{z}_s/R)^2 + n^4 [1 - \nu^2 + 2\delta^2 (1 + \nu)] (\bar{z}_r/R)^2 + 2n^2 (1 - \nu^2) (\bar{z}_s/R) (\bar{z}_r/R) + 2n^4 (1 + \nu)^2 (\bar{z}_r/R) (\bar{z}_s/R) + 1 - \nu^2 \\ \Lambda &= (1 + \delta^2)^2 + 2\delta^2 (1 + \nu) (\bar{R} + \bar{S}) + (1 - \nu^2) [\bar{S} + \delta^4 \bar{R} + 2\delta^2 \bar{R} \bar{S} (1 + \nu)] \end{aligned} \right\} \quad (3.40)$$

where $\lambda = m\pi R/l$, as before,

$$\left. \begin{aligned} \bar{S} &= \frac{E_s A_s}{E h d}, & \bar{R} &= \frac{E_r A_r}{E h a} \\ \delta &= \frac{n l}{m \pi R} \end{aligned} \right\} \quad (3.41)$$

and other notation is as used previously in equations (3.22).

Frequencies determined in reference 3.3 for two stringer-stiffened shells are shown in figures 3.22 and 3.23. Dimensions of the stringers used in each case are shown on the figures. The eccentricity of the stiffeners causes considerable difference in the rigidity of the cylinders; for both cases the lowest frequency for external stiffening was 35 percent greater than for internal stiffening. However, for the second case the curves for external and

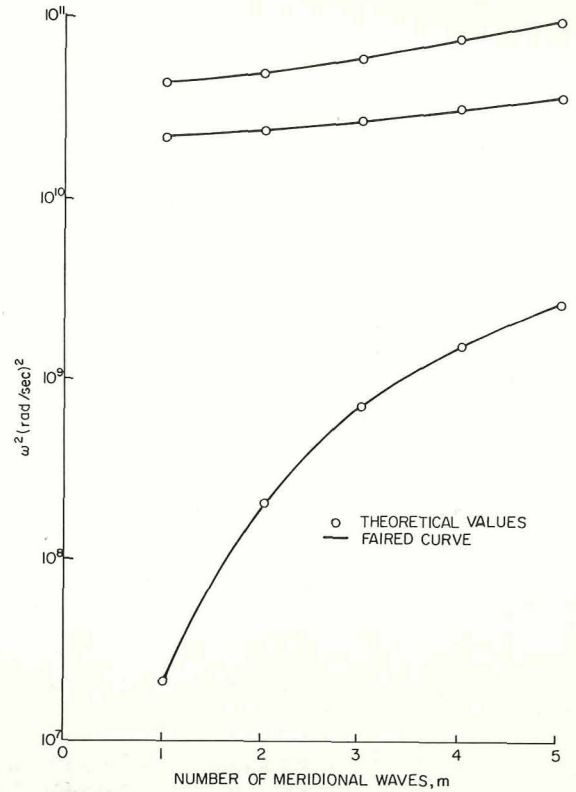


FIGURE 3.21.—Frequencies (rad/sec)² of a stringer-stiffened shell supported by shear diaphragms. (After ref. 3.14)

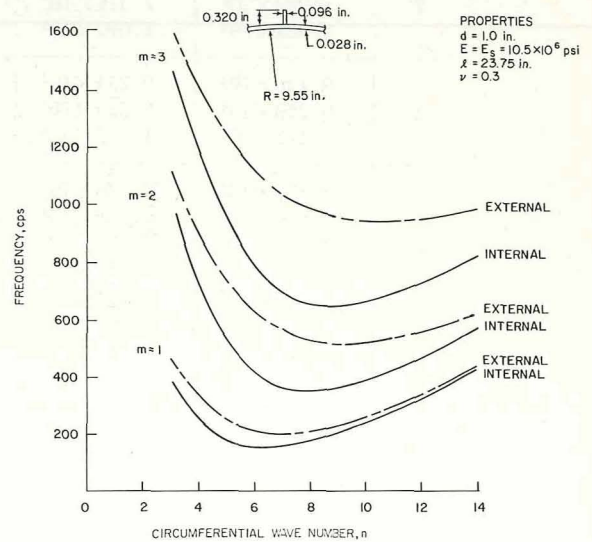


FIGURE 3.22.—Frequencies of a stringer-stiffened shell supported by shear diaphragms. (After ref. 3.3)

internal stiffeners cross for $m=2$. It was also found in reference 3.3 that a stringer-stiffened shell having the same dimensions as in figure 3.22, except increased stringer depth (0.302 in. becomes 0.500 in.), the lowest frequency for external stiffening was 64 percent greater than for internal stiffening.

In reference 3.13 the effect of additional *circumferential* stiffening due to the presence of stringers is quantitatively compared with the results of figure 3.22. This effect is significant for both small and large n , but not in the vicinity of the lowest frequency. The decrease in frequencies due to the rotary inertia of a stiffener is also evaluated. This effect is significant for large n .

In figure 3.24 (from refs. 3.3 and 3.16) frequencies are given for a ring-stiffened shell. This configuration was obtained by replacing the stringers of figure 3.22 with rings having the same cross section and spacing. Comparing figures 3.22 and 3.24 it is seen that the rings give considerably larger values of fundamental frequency than do the stringers; hence, they provide more effective stiffening. For this ring-stiffened shell the lowest frequencies occur for *internal* stiffeners. However, the effects of eccentricity are not as important, giving a lowest frequency which is only 6 percent higher for internal rings than for

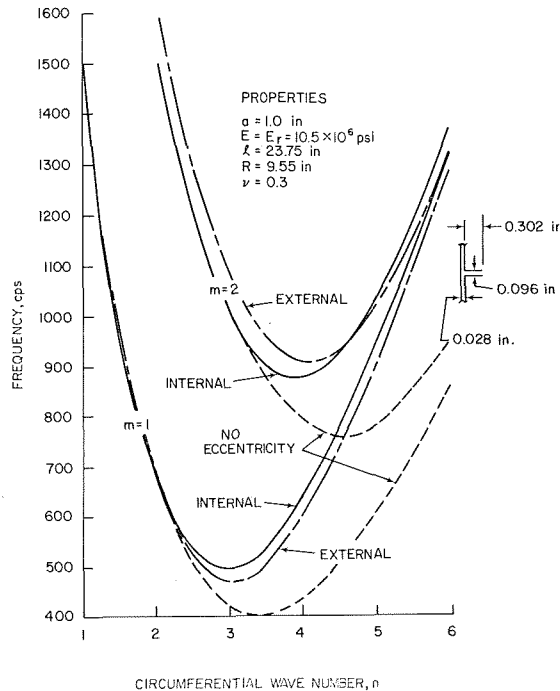


FIGURE 3.24.—Frequencies of a ring-stiffened shell supported by shear diaphragms. (After refs. 3.3 and 3.10)

external ones. For $m=2$, however, external rings give a higher frequency at the lower portions of the curves than internal rings.

Hu and Wah (refs. 3.10 and 3.11) also obtained results for the ring-stiffened shell of figure 3.24 in the case where the rings are assumed symmetric with respect to the shell thickness (i.e., no eccentricity). Shell segments and rings were taken as separate finite elements in their analysis. It is seen in figure 3.24 that eccentricity is not important for small values of n where membrane stresses play a primary role, but it is important for large n where bending strain energy predominates.

Hu, Gormley, and Lindholm (ref. 3.17) extended the discrete method of references 3.10 and 3.11 to include the effects of ring eccentricity. Numerical results were obtained by this procedure and compared with those of the "smeared out" method of Mikulas and McElman (ref. 3.3) for the ring-stiffened shells shown in figure 3.25. Each shell has 12 bays. It is interesting to note the marked difference between the two methods concerning the importance of ring eccentricity. The method of reference 3.3 shows the effect of

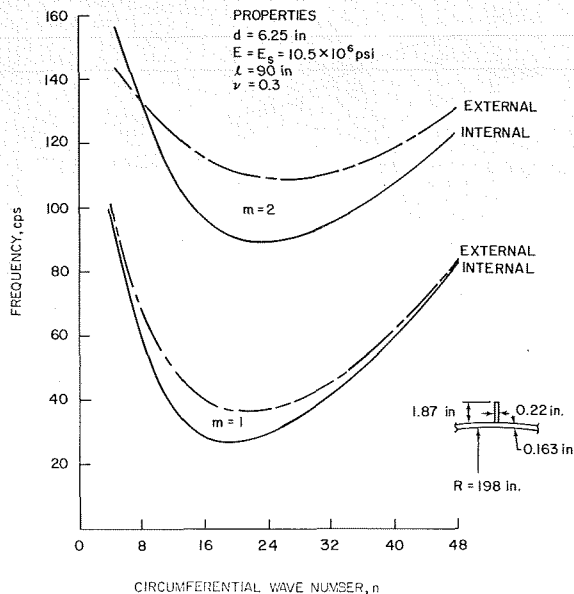


FIGURE 3.23.—Frequencies of another stringer-stiffened shell supported by shear diaphragms. (After ref. 3.3)

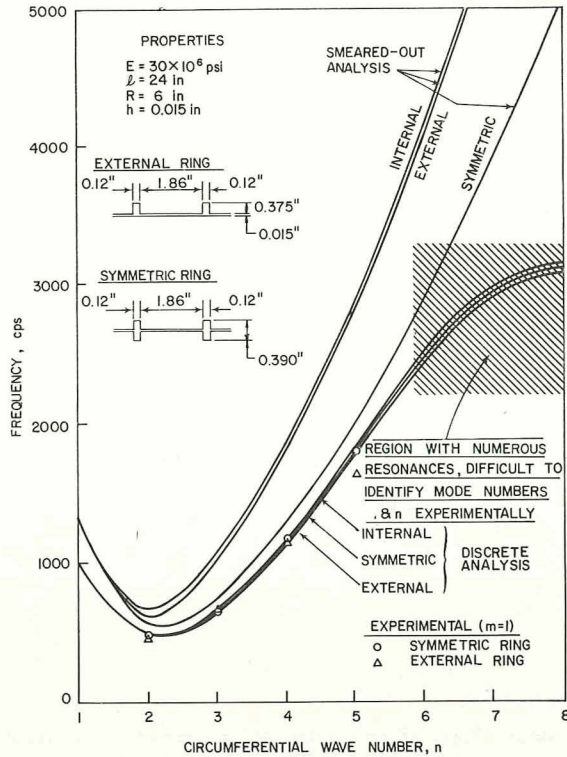


FIGURE 3.25.—Comparison of discrete and smeared-out analyses for ring-stiffened SD-SD shells. (After ref. 3.17)

eccentricity to be very important, whereas the method of reference 3.17 shows little effect at all. The experimental results tend to support the latter analysis. Furthermore, for circumferential wave numbers $n \geq 6$ the latter analysis, unlike the former, shows a flattening of the frequency curve.

Figure 3.26 shows some interesting relationships between the frequencies of the ring-stiffened shell of figure 3.25 and certain reference frequencies such as those of the unstiffened shell (no ring), those of the short cylindrical shell segment between two adjacent rings (assuming SD-SD supports), and those of the free ring separated from its two adjacent shell elements. The frequencies of the three types of stiffened shells (internal, external, and symmetric) obtained from the discrete analysis of reference 3.17 are too close to be shown distinctly on the scale of figure 3.26; therefore, only the frequency curve for the symmetric case is shown. The frequency

curve for the stiffened shell is divided into three regions according to abscissa values of the intersection points of: (1) the two frequency curves for the unstiffened shell and for the free ring, and (2) the two frequency curves for the free ring and for the uncoupled short cylindrical shell segment. These three regions, shown in figure 3.26, are characterized as

Region I: The rings contribute more inertia effect than stiffness effect, so that the frequency of the stiffened shell is lower than that of the unstiffened one.

Region II: The rings contribute the dominant stiffness, so that the frequency is higher than that of the unstiffened shell, but lower than the ring frequency.

Region III: The ring motion becomes so small compared to the shell panel motion between rings that the frequency asymptotically approaches

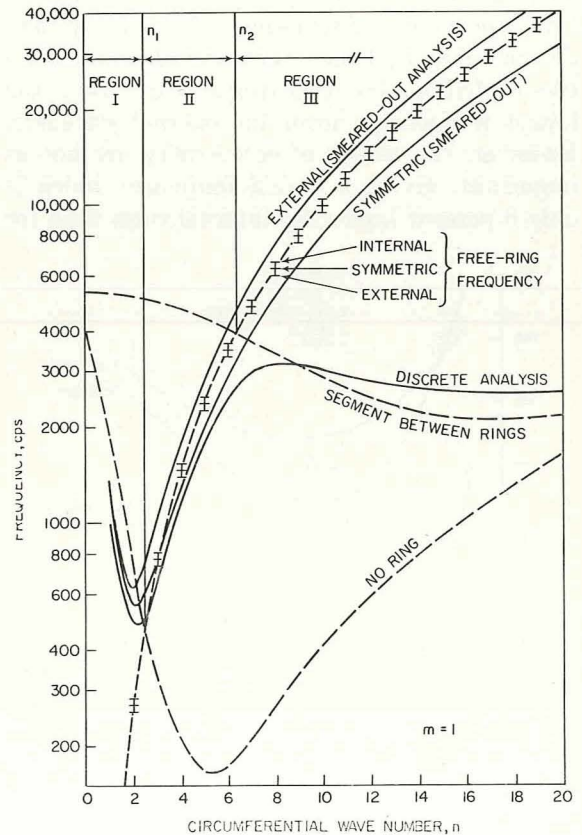


FIGURE 3.26.—Comparison of ring-stiffened SD-SD shell frequencies (cps) with other reference frequencies. (After ref. 3.17)

that of the clamped-clamped shell segment (the curve shown in figure 3.26 is for a SD-SD shell segment).

In the last region it is clear that equivalent orthotropic analyses are not applicable. It should be emphasized that the frequencies for $m=1$ are plotted in figure 3.26, and this is not the lowest frequency mode for all n . Reference 3.17 shows that in region III the lowest frequencies will occur for m equal to the number of bays between rings, in this case 12.

Similar parametric studies are shown in figures 3.27 and 3.28 wherein the number of stiffening rings is varied for the same length of shell and the depth of the ring stiffeners is varied. Changing the number of rings has a significant effect only in region III. Decreasing the ring depth lowers the minimum frequency only slightly and increases the value of n at which the minimum occurs (the shell of fig. 3.28 has 12 bays).

Schnell and Heinrichsbauer (refs. 3.18 and

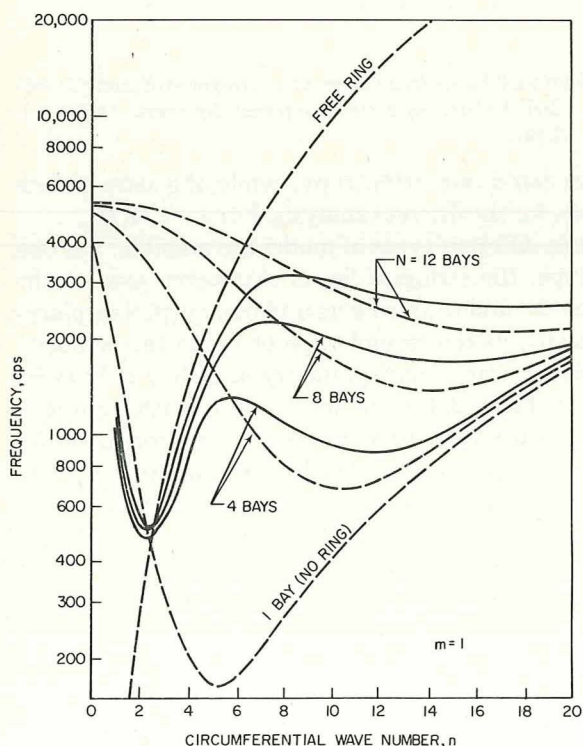


FIGURE 3.27.—Influence of number of rings upon the frequencies of a ring-stiffened SD-SD shell. (After ref. 3.17)

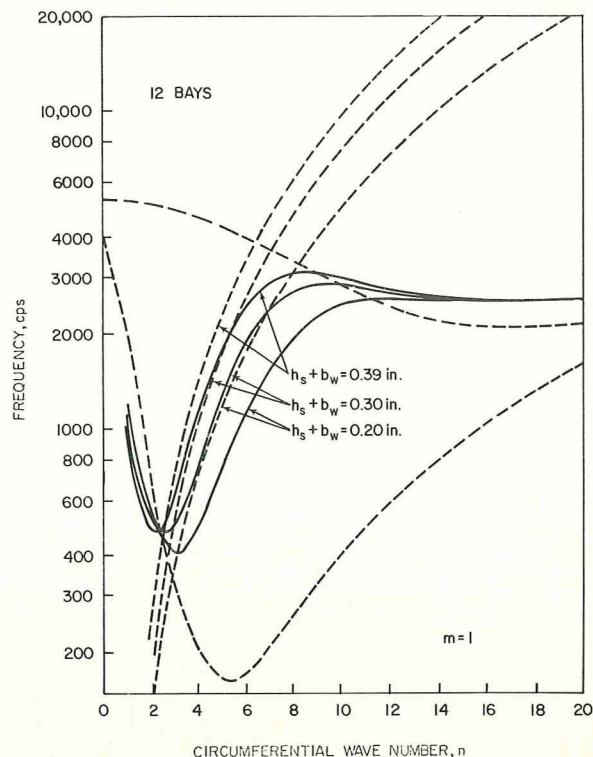


FIGURE 3.28.—Influence of ring depth upon the frequencies of a ring-stiffened SD-SD shell. (After ref. 3.17)

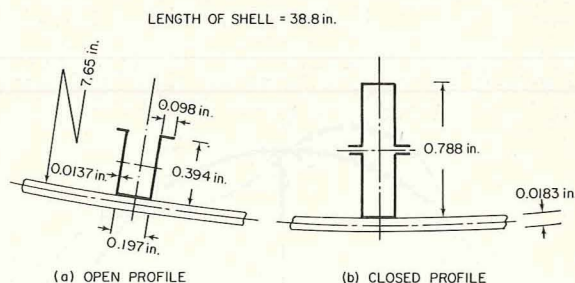


FIGURE 3.29.—Details of stringer cross sections. (After ref. 3.19)

3.19) analyzed the effects of internal stiffening by means of stringers having a "hat shape" as shown in figure 3.29(a). Two theoretical approaches were followed. One smeared the stringers out into orthotropic elastic constants of an equivalent circular cylindrical shell; the other represented the stringers and shell segments as separate, discrete elements. In figure 3.30 frequencies are given for the shell having four equally spaced stringers. The dashed curves are for the calculations using

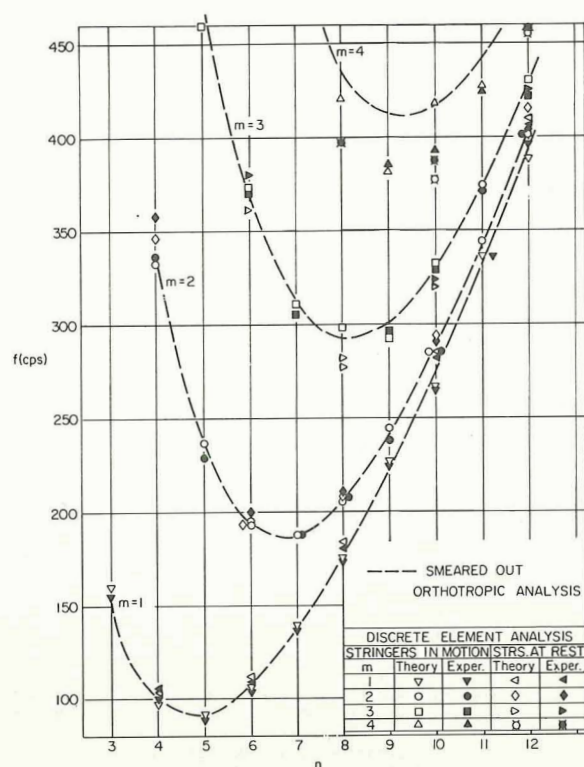


FIGURE 3.30.—Frequencies of a stringer-stiffened SD-SD shell having *four single* internal stringers. (After ref. 3.19)

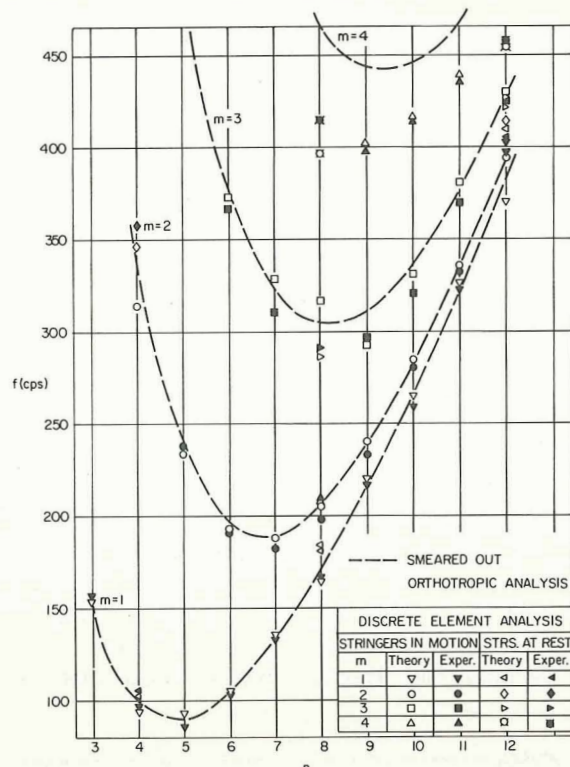


FIGURE 3.32.—Frequencies of a stringer-stiffened SD-SD shell having *eight single* internal stringers. (After ref. 3.19)

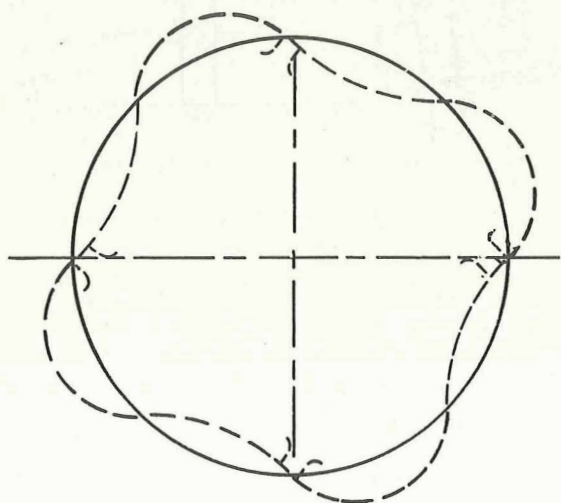


FIGURE 3.31.—Mode shape where stringers only twist (stringers "at rest"). (After ref. 3.19)

smeared out orthotropy, while the data points are for the discrete analysis. For $n = 2, 4, 6, \dots$, two different types of modes are possible. For one type, the stringers lie on symmetry axes of the mode, and the stringers undergo normal displacement; in the second type of mode the stringers lie on axes of antisymmetry and they only twist (see figure 3.31) and are "at rest" with respect to displacement. Similar results are presented for eight equally spaced stringers in figure 3.32. Figures 3.33 and 3.34 show frequencies when doubled stringers are used (see figure 3.29(b)). The simple sine function assumed in the θ direction for an exact solution of the "smeared out" equivalent orthotropic shell problem only approximates the true behavior of the shell as can be seen in figure 3.35. Here the mode shapes for the shell having four single stringers are given from discrete element and experimental studies for $m=2, n=4$ and $m=1, n=10$, where n now identifies the number of circumferential *approximate* half-sine waves.

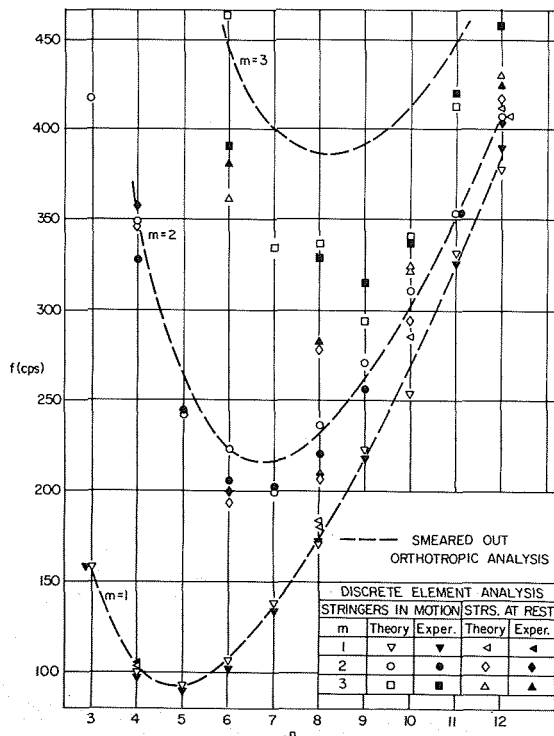


FIGURE 3.33.—Frequencies of a stringer-stiffened SD-SD shell having four double internal stringers. (After ref. 3.19)

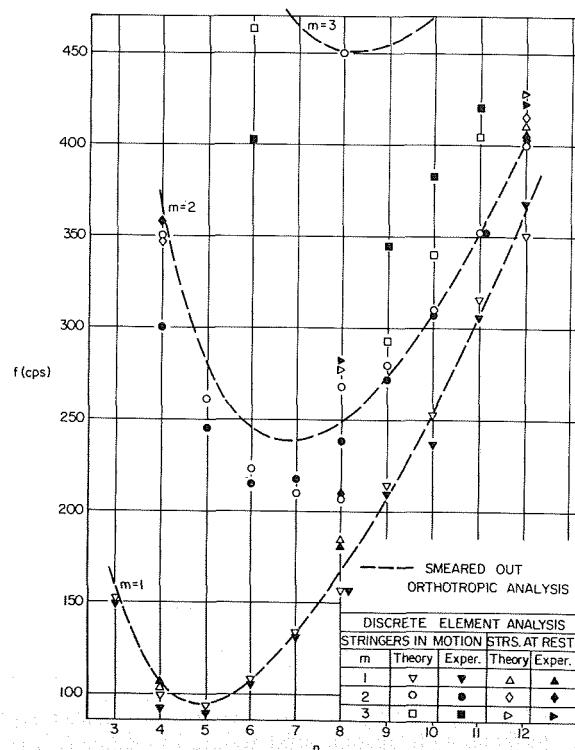


FIGURE 3.34.—Frequencies of a stringer-stiffened SD-SD shell having eight double internal stringers. (After ref. 3.19)

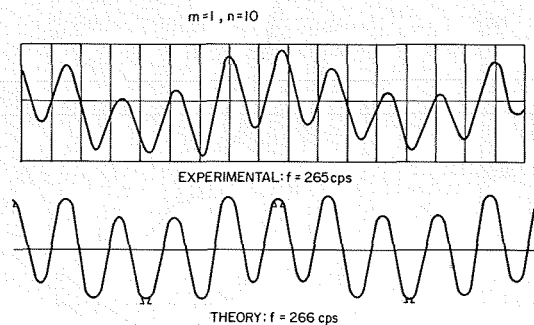
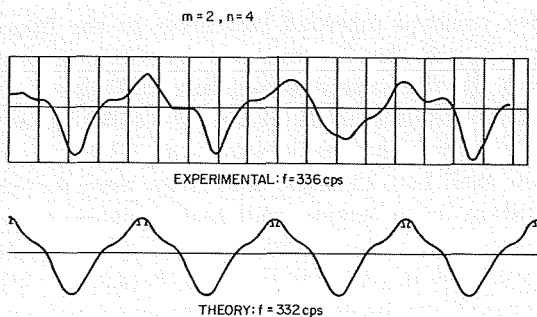


FIGURE 3.35.—Theoretical (discrete element) and experimental mode shapes in the circumferential direction for an SD-SD shell having four equally spaced stringers. (After ref. 3.19)

Another comparison with the results shown in figures 3.30 and 3.32 was made by Egle and Sewall (ref. 3.20) using a "smeared out" orthotropic approach wherein *more than* a single trigonometric term is used to represent the circumferential variation in the mode shapes. The problem is then eventually solved by the Ritz method. Results using twenty terms are shown in figures 3.36 and 3.37; twenty terms were necessary to

obtain good numerical convergence. Typical mode shapes encountered for w are shown in figures 3.38 and 3.39. Comparisons with figure 3.32 were also made in reference 3.13 for a smeared-out, Ritz type of analysis using a single trigonometric term to represent the circumferential variation. The results were very close to the smeared-out results shown in figure 3.32.

Another set of stiffened shell problems which

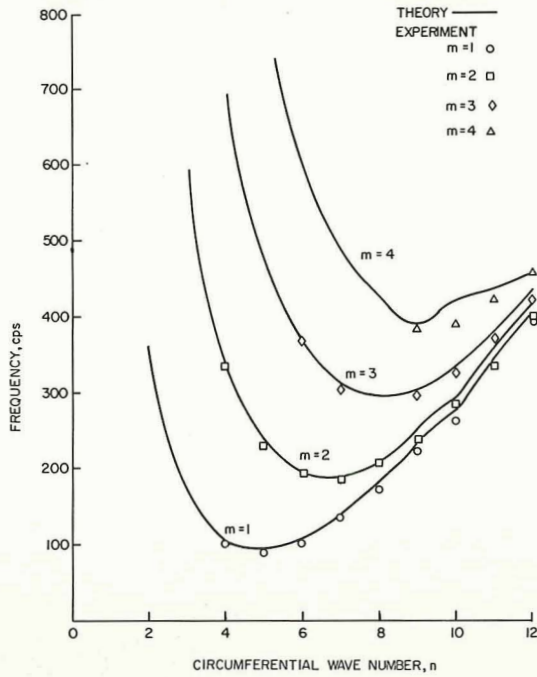


FIGURE 3.36.—Comparison of theoretical "smeared out" analysis with experimental results of reference 3.18; four stringers. (After ref. 3.20)

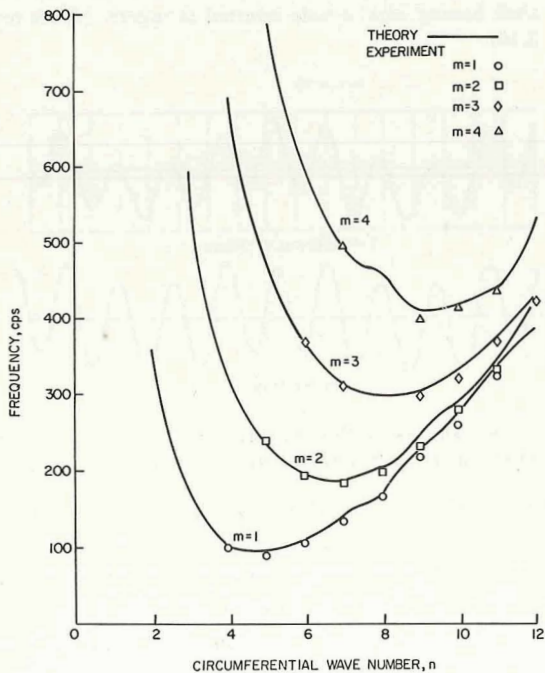


FIGURE 3.37.—Comparison of theoretical "smeared out" analysis with experimental results of reference 3.18; eight stringers. (After ref. 3.20)

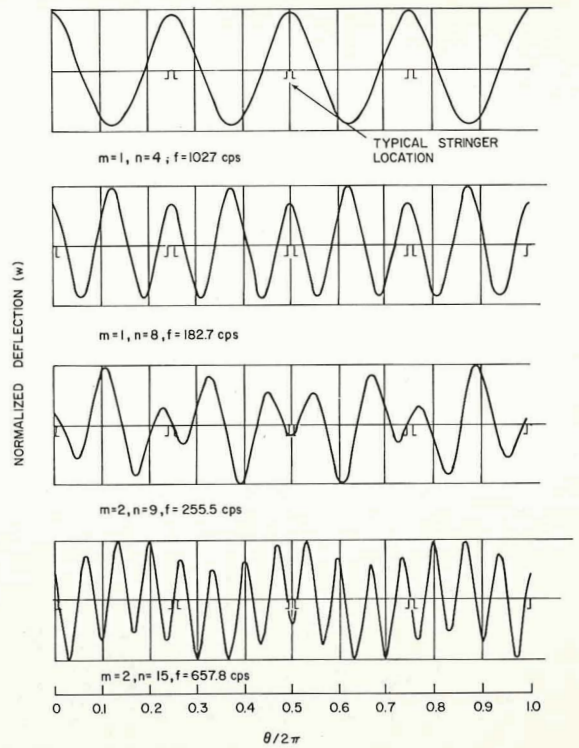


FIGURE 3.38.—Theoretical circumferential variation in mode shapes for a stringer-stiffened SD-SD shell; four stringers (After ref. 3.20)

have received repeated treatment in the literature was originally proposed by Galletly (ref. 3.21). In this case external ring stiffeners were added to a steel shell having $R=4.082$ in. and $h=0.047$ in. The ring spacing was 1.236 in. and each shell had 15 bays. The rings were rectangular in cross section and had dimensions (in terms of fig. 3.2) of width, $h_w=0.086$ in.; depth, $b_w=0.1145$ in., 0.2290 in., and 0.3435 in. His approach was based upon energy using assumed displacement functions which allowed an additional term to account for inter-ring warping. Comparisons were subsequently made by Geers (ref. 3.12) using a continuum approach and by Wah and Hu (refs. 3.10 and 3.11) using a discrete element approach. Results obtained from these various methods are summarized in table 3.4. The frequencies from references 3.10 and 3.11 are considerably less than those of the three other methods, undoubtedly, because of neglect of eccentricity of the externally mounted rings. The effect of inter-ring displacements deviating

TABLE 3.4.—Comparison of Frequencies (cps) for Three Ring-Stiffened Shells Supported by Shear Diaphragms

Ring depth, b_w	n	Reference			
		Galletly (ref. 3.21)		Geers (ref. 3.12)	Wah and Hu (refs. 3.10 and 3.11)
		Inter-ring warping included	Inter-ring warping neglected		
0.1145 in.	2	708	713	719	687
	3	570	582	597	505
	4	903	948	932	727
	5	1430	1514	1457	1124
0.2290 in.	2	704	709	730	675
	3	1008	994	735
	4	1879	1774	1271
	5	3030	2780	2020
0.3435 in.	2	756	774	806	697
	3	1367	1512	1495	1060
	4	2595	2870	2652	1937
	5	3770	4070	4102	3060

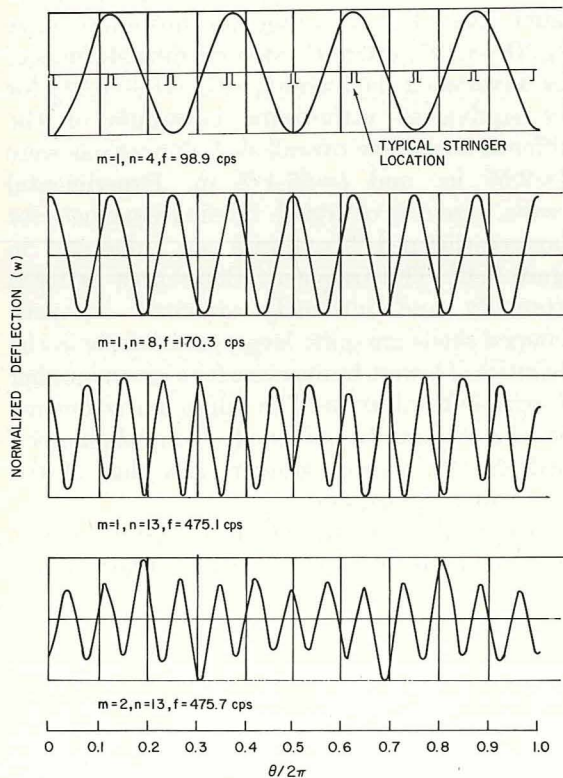


FIGURE 3.39.—Theoretical circumferential variation in mode shapes for a stringer-stiffened SD-SD shell; eight stringers. (After ref. 3.20)

from the overall sine curve with increasing values of n is clearly seen in figure 3.40 for the case of the deepest ring ($b_w=0.3435$ in.).

A number of other authors have contributed to the literature of vibrations of orthotropic circular cylindrical shells supported at both ends by shear diaphragms, particularly in the case of representing stiffened shells by "smeared out" orthotropy. In references 3.22 and 3.23 methods based upon using the total energy of the stiffened shell are presented, but no numerical results are given. Other relevant works include references 3.24 through 3.40.

3.1.3 Other Simple End Conditions

Relatively few results are available for the 135 problems of free vibration of orthotropic closed circular cylindrical shells having one of the possible sets of simple boundary conditions other than shear diaphragm supports at both ends. The exact procedure outlined in section 2.4 for solving such problems for isotropic shells is also straightforwardly applicable to the orthotropic case when the axes of material orthotropy are parallel to the shell axes. However, it was seen in section 2.4 that the exact procedure is quite complicated even for isotropic shells, re-

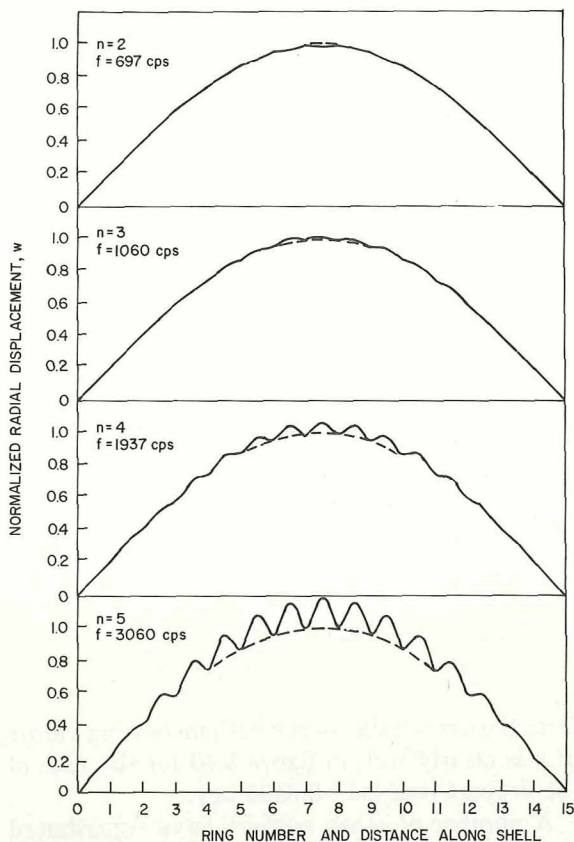


FIGURE 3.40.—Mode shapes of a ring-stiffened circular cylindrical shell supported by shear diaphragms. (After refs. 3.11 and 3.10)

quiring the solution of an eighth order determinant to determine the forms of the solution functions for u , v , w to satisfy the boundary conditions, and the solution of a subsequent sixth order characteristic determinant arising from the equations of motion to determine the eigenfrequencies. The added algebraic complexity arising in the orthotropic case apparently has deterred anyone from extending the exact solution procedure with this added generality.

The Raleigh-Ritz method is particularly well-suited to yield approximate solutions for the problem of the orthotropic shell having arbitrary edge conditions in the same manner as for the isotropic shell. That is, solutions are taken in the form of equations (2.66) involving beam functions in the axial direction. Gontkevich (ref. 3.41) showed that this procedure leads to a cubic characteristic equation in the form of equation

(2.67) where the coefficients are given by equations (3.42), and where $k = h^2/12R^2$ as before, values of δ_m , γ_m and $\mu_m = \alpha_m R/l$ are given by table 2.22 for the various types of beam functions and, in this case, the orthotropic frequency parameter Ω_s replacing Ω in equation (2.67) is given by

$$\Omega_s = \omega R \sqrt{\rho(1 - \nu_{x\theta})/E_\theta} \quad (3.43)$$

The stiffness constants C_{11}, \dots, C_{66} ; D_{11}, \dots, D_{66} are defined in equations (3.6) and (3.7) as before. For the clamped-clamped and clamped-SD shells equations (3.42) can be simplified because $\delta_m = -\gamma_m$. For SD-SD shells the equations are exact and further simplified ($\gamma_m = -\gamma_m = 1$). The cubic characteristic equation can be approximated still further by one of the simplifying techniques suggested in section 2.3.5.

Sewall and Naumann (ref. 3.13) used a smeared-out orthotropic representation (see sec. 3.1.2) for aluminum shells having external and internal longitudinal stiffeners as shown in figure 3.41. The smearing out procedure gave $D_{22}/D = 1.197$, where D is the bending stiffness of the unstiffened shell, and $\nu_y = D_{12}/D_{11} = 0.346$ for the equivalent orthotropic constants of the stiffened shell. The overall shell dimensions were $R = 9.55$ in. and $l = 25-1/8$ in. Experimental results were also obtained. Cyclic frequencies for clamped-clamped boundaries are presented in figure 3.42. The frequency differences between externally and internally stiffened clamped-clamped shells are quite large, particularly in the vicinities of lowest frequencies for a given number of axial half-waves m . The minimum frequency for the externally stiffened clamped-clamped shell was 39 percent greater than that of the internally-stiffened one.

Analytical and experimental results for a clamped-clamped shell stiffened by a large num-

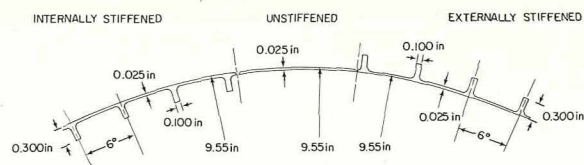


FIGURE 3.41.—Structural details of stringer-stiffened shells. (After ref. 3.13)

$$K_2 = \frac{\mu_m^2}{\delta_m} + n^2 \left(\frac{C_{66} + C_{22}}{C_{11}} \right) + \frac{C_{66}}{C_{11}} \delta_m \mu_m^2 + \frac{C_{22}}{C_{11}} + k \left(n^2 \frac{D_{22}}{D_{11}} + 4 \frac{D_{66}}{D_{11}} \delta_m \mu_m^2 + \mu_m^4 - 2n^2 \mu_m^2 \frac{D_{12}}{D_{11}} + n^4 \frac{D_{22}}{D_{11}} + 4 \frac{D_{66}}{D_{11}} n^2 \mu_m^2 \delta_m \right) \quad (3.42a)$$

$$\begin{aligned} \delta_m K_1 = & \left(\mu_m^2 + \delta_m n^2 \frac{C_{66}}{C_{11}} \right) \left[\delta_m \mu_m^2 \frac{C_{66}}{C_{11}} + (n^2 + 1) \frac{C_{22}}{C_{11}} \right] + \left[\frac{C_{22}}{C_{11}} \left(1 - \frac{C_{22}}{C_{11}} \right) n^2 + \frac{C_{66}}{C_{11}} \delta_m \mu_m^2 \right] \delta_m \\ & - \mu_m^2 \gamma_m^2 \left(\frac{D_{12}}{D_{11}} \right)^2 - n^2 \mu_m^2 \left(\delta_m \frac{C_{66}}{C_{11}} - \frac{C_{12}}{C_{11}} \gamma_m \right)^2 + k \left\{ \left[\mu_m^2 + \delta_m n^2 \left(\frac{C_{66} + C_{22}}{C_{11}} \right) + \delta_m^2 \mu_m^2 \frac{C_{66}}{C_{11}} \right] \right. \\ & \left[\mu_m^4 - 2n^2 \mu_m^2 \gamma_m \frac{D_{12}}{D_{11}} + n^4 \frac{D_{22}}{D_{11}} + 4 \frac{D_{66}}{D_{11}} n^2 \mu_m^2 \delta_m \right] + \left(\mu_m^2 + \delta_m n^2 \frac{C_{66}}{C_{11}} + \delta_m \right) \left(n^2 \frac{D_{22}}{D_{11}} + 4 \frac{D_{66}}{D_{11}} \delta_m \mu_m^2 \right) \\ & \left. - 2n^2 \delta_m \frac{C_{22}}{C_{11}} \left(n^2 \frac{D_{22}}{D_{11}} + 4 \frac{D_{66}}{D_{11}} \delta_m \mu_m^2 - \mu_m^2 \gamma_m \frac{D_{12}}{D_{11}} \right) \right\} \quad (3.42b) \end{aligned}$$

$$\begin{aligned} \delta_m K_0 = & \frac{C_{66}}{C_{11}} \delta_m \mu_m^4 \left[\frac{C_{22}}{C_{11}} - \gamma_m^2 \left(\frac{C_{12}}{C_{11}} \right)^2 \right] + k \left\{ \left[\frac{C_{66}}{C_{11}} \delta_m n^2 + \mu_m^2 \left(1 - \gamma_m^2 \left(\frac{C_{12}}{C_{11}} \right)^2 \right) \right] \left[\frac{D_{22}}{D_{11}} n^2 + 4 \frac{D_{66}}{D_{11}} \delta_m \mu_m^2 \right] \right. \\ & \left. + \left[\left(\delta_m n^2 \frac{C_{66}}{C_{11}} + \mu_m^2 \right) \left(\frac{C_{22}}{C_{11}} n^2 + \frac{C_{22}}{C_{11}} \delta_m \mu_m^2 \right) - n^2 \mu_m^2 \left(\delta_m \frac{C_{66}}{C_{11}} - \frac{C_{12}}{C_{11}} \gamma_m \right)^2 \right] \right. \\ & \left[\mu_m^4 - 2n^2 \mu_m^2 \gamma_m \frac{D_{12}}{D_{11}} + n^4 \frac{D_{22}}{D_{11}} + 4 \frac{D_{66}}{D_{11}} n^2 \mu_m^2 \delta_m \right] - n^2 \left[2 \left(\mu_m^2 + \delta_m n^2 \frac{C_{66}}{C_{11}} \right) \frac{C_{22}}{C_{11}} \right. \\ & \left. + 2 \left(\delta_m \frac{C_{66}}{C_{11}} - \gamma_m \frac{C_{12}}{C_{11}} \right) \mu_m^2 \gamma_m n \frac{C_{12}}{C_{11}} \right] \left[n^2 \frac{D_{22}}{D_{11}} + \left(4 \frac{D_{66}}{D_{11}} \delta_m - \gamma_m \frac{D_{12}}{D_{11}} \right) \mu_m^2 \right] \left. \right\} \quad (3.42c) \end{aligned}$$

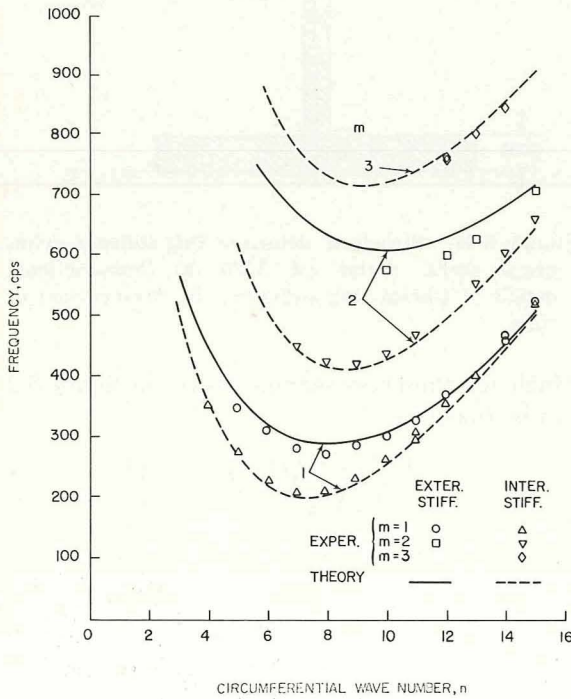


FIGURE 3.42.—Frequencies of stringer-stiffened, clamped-clamped shells. (After ref. 3.13)

ber (eleven) of integral rings are seen in figure 3.43 (from ref. 3.13). The experimental data shown in figure 3.43 are from reference 3.38. The difference between theoretical and experimental data becomes large for large n .

Sewall, Clary, and Leadbetter (ref. 3.35) used the smeared-out approach of reference 3.4 (see eqs. (3.19)) to analyze *clamped-clamped* shells having ring stiffeners in the form of I-beams as depicted in figure 3.44(a). The shell had dimensions $l = 29.42$ in., $h = 0.049$ in., and $R = 14.35$ in. The I-beam stiffener spacing is shown in figure 3.44(b). Shell and ring materials were both steel. The rings were spotwelded to the shell along their inside flanges. Figure 3.45 shows the mode shapes (in the axial direction) and the associated frequencies for $m = 1$ and $n = 3, 4, 5$ for clamped-clamped ends. Both analytical and experimental results are given. The effect of discrete ring stiffeners is considerable in this case.

Resnick and Dugundji (ref. 3.5) analyzed the free vibrations of clamped-clamped, stiffened shells by smearing out the stiffeners according to equations (3.18) and (3.19). The strain energy of the equivalent orthotropic shell was formulated

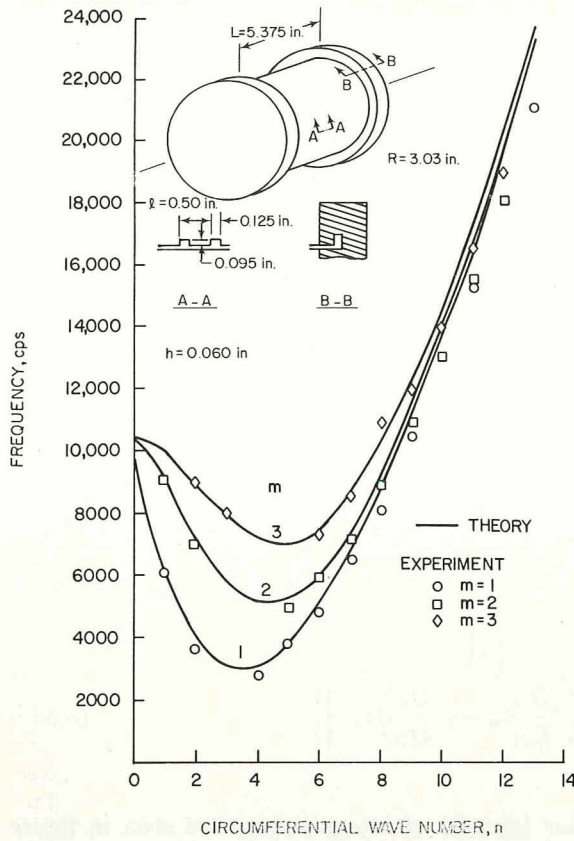


FIGURE 3.43.—Cyclic frequencies for ring-stiffened clamped-clamped shells. (After ref. 3.13)

using the Sanders shell theory, and beam functions were used for the displacements. Integral ring and stringer stiffeners of the type shown in the repeating section of figure 3.2 were used. Using the Sanders shell theory (see chapter 1), the generalized stress-strain equations (3.4) and (3.5) must be replaced by

$$\left. \begin{aligned} N_x &= C_{11}\epsilon_x + C_{12}\epsilon_\theta + H_{11}\kappa_x + H_{12}\kappa_\theta \\ N_\theta &= C_{12}\epsilon_x + C_{22}\epsilon_\theta + H_{12}\kappa_x + H_{22}\kappa_\theta \\ N_{x\theta} &= C_{66}\epsilon_{x\theta} + H_{66}\tau_{x\theta} \end{aligned} \right\} \quad (3.44)$$

$$\left. \begin{aligned} M_x &= D_{11}\kappa_x + D_{12}\kappa_\theta + H_{11}\epsilon_x + H_{12}\epsilon_\theta \\ M_\theta &= D_{12}\kappa_x + D_{22}\kappa_\theta + H_{12}\epsilon_x + H_{22}\epsilon_\theta \\ M_{x\theta} &= D_{66}\tau_{x\theta} + H_{66}\epsilon_{x\theta} \end{aligned} \right\} \quad (3.45)$$

where the coordinates x and θ for circular cylindrical shells have been used and where H_{11} , H_{12} , H_{22} , H_{66} are additional coupling coefficients

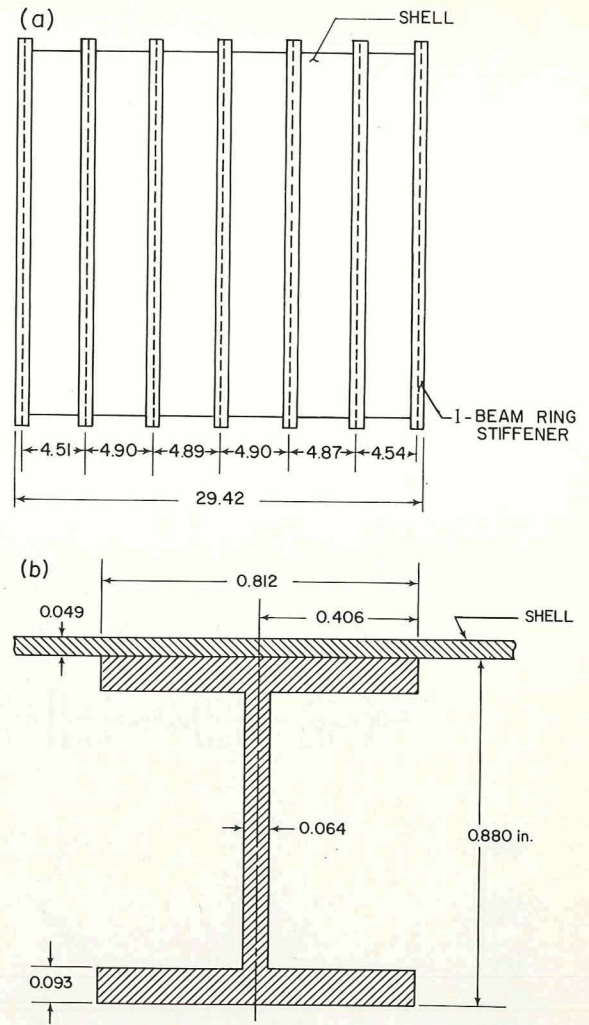


FIGURE 3.44.—Structural details of ring-stiffened cylindrical shells. (After ref. 3.35) (a) Cross-sectional details of I-beam ring stiffeners. (b) Arrangement of rings.

which for the cross section shown in figure 3.2 can be taken as

$$\left. \begin{aligned} H_{11} &= \frac{Eh_s^2}{2} \left(\frac{h_w}{b_s} \right) \left(\frac{b_w}{h_s} \right) \left(1 + \frac{b_w}{h_s} \right) \\ H_{12} &= H_{22} = H_{66} = 0 \end{aligned} \right\} \quad (3.46)$$

in the case of longitudinal stiffeners, for example. Numerical results were obtained for aluminum shells having dimensions and material properties as given in table 3.5. The resulting smeared out ratios of equivalent orthotropic stiffness coefficients are also listed in table 3.6. Theoretical and

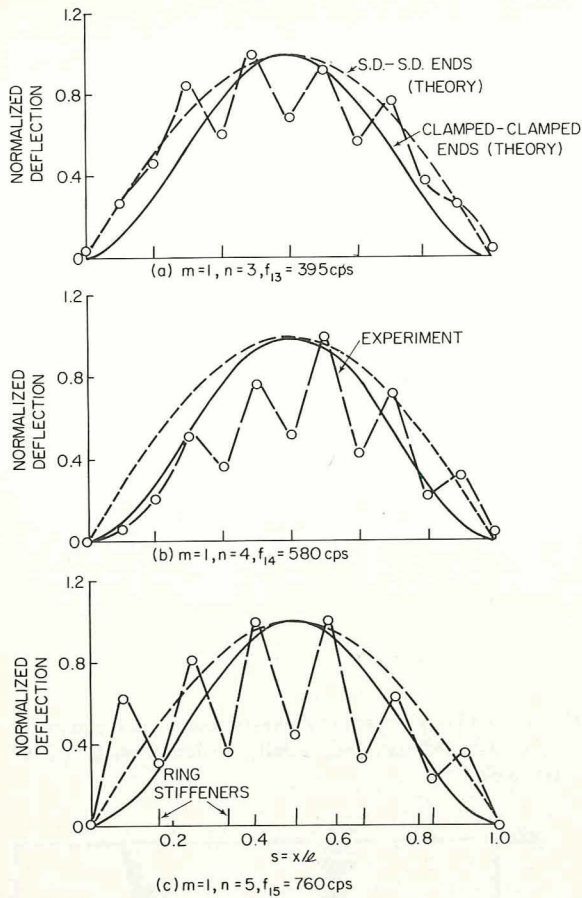


FIGURE 3.45.—Comparison of measured and calculated longitudinal mode shapes for a ring-stiffened, clamped-clamped shell. (After ref. 3.35)

experimental frequencies for *clamped-clamped* ends are shown in figures 3.46 and 3.47 corresponding to axial and circumferential *external* stiffening, respectively. In these figures results for shells supported at both ends by shear diaphragms are also presented. The difficulty of obtaining adequate clamping in the experimental models is seen in these figures.

It was found in reference 3.5 that the addition of axial stiffeners had only a small effect on the

TABLE 3.5.—Dimensions and Material Properties of Integrally Stiffened Shells

Dimension	Type of stiffening	
	Axial	Circumferential
R	2.91 in.	2.92 in.
l	12.22	12.05
h_s	0.0075	0.0080
b_s	0.120	0.120
h_w/b_s	0.23	0.10
b_w/h_s	5.33	3.63
E	9.9×10^6 psi	9.9×10^6 psi
ρ	0.254 $\times 10^{-3}$ lb-sec ² /in. ⁴	0.254 $\times 10^{-3}$ lb-sec ² /in. ⁴
ν	0.3	0.3
Stretching stiffness	$C_{22} = 101,200$ lb/in.	$C_{11} = 94,400$ lb/in.
Bending stiffness	$D_{22} = 0.496$ lb-in.	$D_{11} = 0.514$ lb-in.

TABLE 3.6.—Calculated Ratios of Stiffness Coefficients for Integrally Stiffened Shells

Ratio of stiffness coefficients	Type of eccentricity					
	External		None		Internal	
	Axial stiffeners	Circum. stiffeners	Axial stiffeners	Circum. stiffeners	Axial stiffeners	Circum. stiffeners
C_{22}/C_{11}	0.578	1.24	0.578	1.24	0.578	1.24
C_{12}/C_{11}	.174	.30	.174	.30	.174	.30
C_{66}/C_{11}	.202	.35	.202	.35	.202	.35
D_{22}/D_{11}	.00775	23.9	.01374	19.1	.00775	23.9
D_{12}/D_{11}	.00178	.27	.00316	.27	.00178	.27
D_{66}/D_{11}	.0198	.48	.035	.48	.0198	.48
H_{22}/RC_{11}	.00423	.00193	0	0	-.00423	-.00193
H_{12}/RC_{11}	0	0	0	0	0	0
H_{66}/RC_{11}	0	0	0	0	0	0

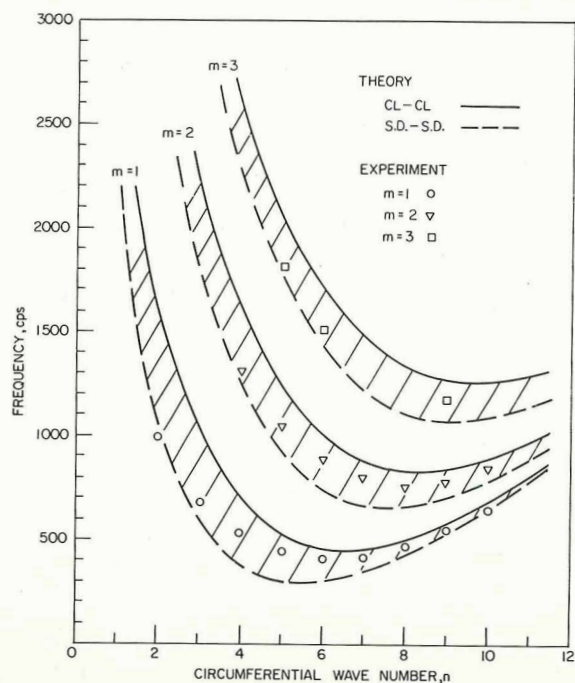


FIGURE 3.46.—Comparison of the effects of clamped-clamped and SD-SD boundaries upon the frequencies of an axially stiffened shell. (After ref. 3.5)

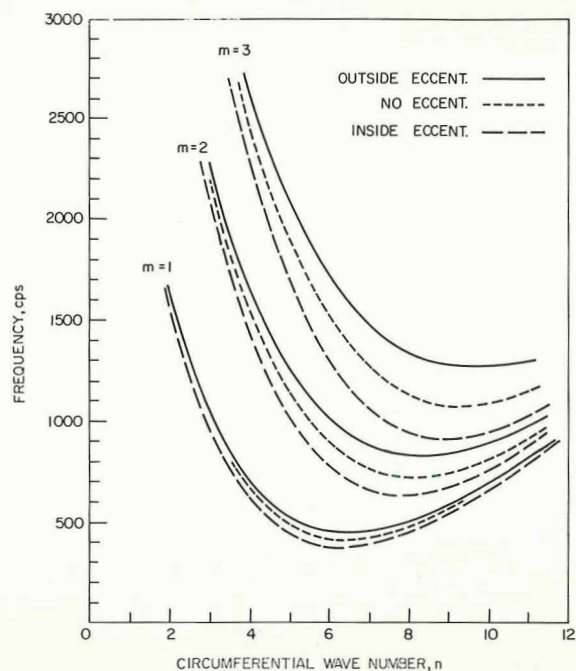


FIGURE 3.48.—Eccentricity effects upon the frequencies of a clamped-clamped, axially stiffened shell. (After ref. 3.5)

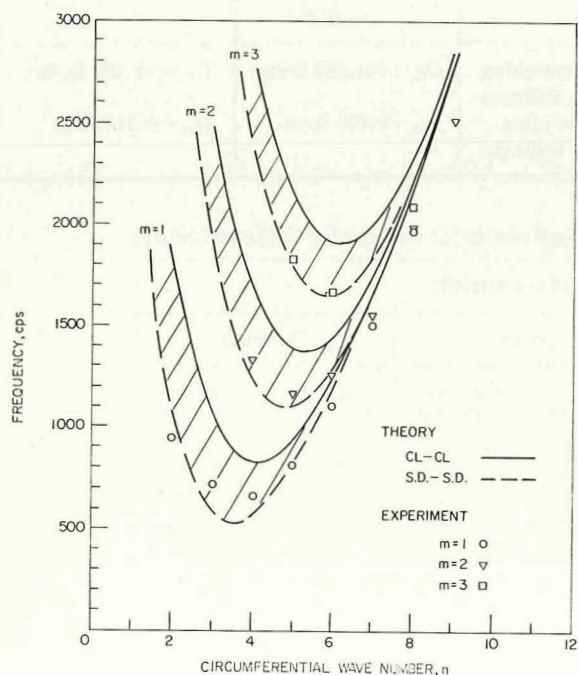


FIGURE 3.47.—Comparison of the effects of clamped-clamped and SD-SD boundaries upon the frequencies of a circumferentially stiffened shell. (After ref. 3.5)

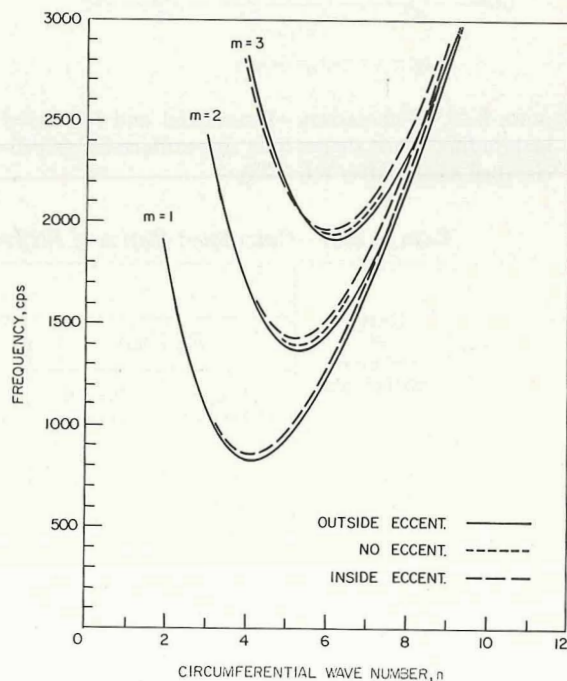


FIGURE 3.49.—Eccentricity effects upon the frequencies of a clamped-clamped, circumferentially stiffened shell. (After ref. 3.5)

frequency distribution for the shell. That is, for $m=1$ the minimum frequencies are about the same and occur at the same value of n , while for larger n the axially stiffened shell has somewhat lower frequencies than for the isotropic case. This occurs because the vibration modes for large n involve D_{22} , which is about the same in both cases, but the stiffened shell has about twice as much effective mass. For $m=3$, the axially stiffened shell has somewhat higher frequencies than the unstiffened one because of the importance of D_{11} .

The addition of circumferential stiffeners increased most frequencies of the shell. For all m the minimum frequencies were significantly higher and sharper and occurred at lower values of n . For $m=1$ and higher values of n , the increase in frequency is even greater. However, for small n the circumferentially stiffened cylinder has somewhat lower frequencies than the unstiffened shell. This is due to the important role of stretching stiffness C_{11} which is the same in this case for both shells. Thus, the circumferential stiffeners were of much smaller size than the axial ones, but had a much greater effect in raising the frequencies.

The effects of stiffener eccentricity for the clamped-clamped shells of reference 3.5 are described by figures 3.48 and 3.49. All results

shown are theoretical. The external axial stiffeners generally cause higher frequencies than internal axial stiffeners. This effect is more pronounced for higher values of m . Conversely, external circumferential stiffeners generally yield lower frequencies than internal ones. Again, the effect is more pronounced for higher n . For very low values of n , external stiffeners may cause *slightly* higher frequencies for a small region of n .

Theoretical results for Hoppmann's longitudinally stiffened shell were also computed by Penzes (ref. 3.15) for clamped-clamped and clamped-SD boundary conditions (see earlier discussion of analytical method and test model in sec. 3.1.2). Numerical data are compared with the SD-SD case in table 3.7.

In reference 3.42 the free vibrations of orthotropic shells of semi-infinite length and having a free end are examined. The application of transfer matrices to orthotropic shell vibration problem is discussed.

Theoretical and experimental frequencies for *clamped-free*, stringer-stiffened shells are shown in figure 3.50 (from ref. 3.13) (see fig. 3.41 and earlier discussion in this section for additional details).

In reference 3.5 frequencies for axially and circumferentially stiffened shells were also found for the cases of clamped-free and SD-free bound-

TABLE 3.7.—*Frequencies (cps) of Longitudinally Stiffened Shells Having Various Edge Conditions*

m	Edge conditions	n				
		1	2	3	4	5
2	Clamped-clamped	1579	4233	9171
	Clamped-SD	1149	3412	7557
	SD-SD	836	2698	6267
3	Clamped-clamped	1422	2298	4019	6552
	Clamped-SD	1328	1997	3514	5838
	SD-SD	1276	1750	3059	5178
4	Clamped-clamped	2284	2509	3135	4264	5891
	Clamped-SD	2265	2422	2932	3934	5439
	SD-SD	2255	2358	2762	3636	5016
5	Clamped-clamped	3560	3623	3821	4251	4984
	Clamped-SD	3555	3598	3754	4117	4770
	SD-SD	3552	3580	3699	4002	4577

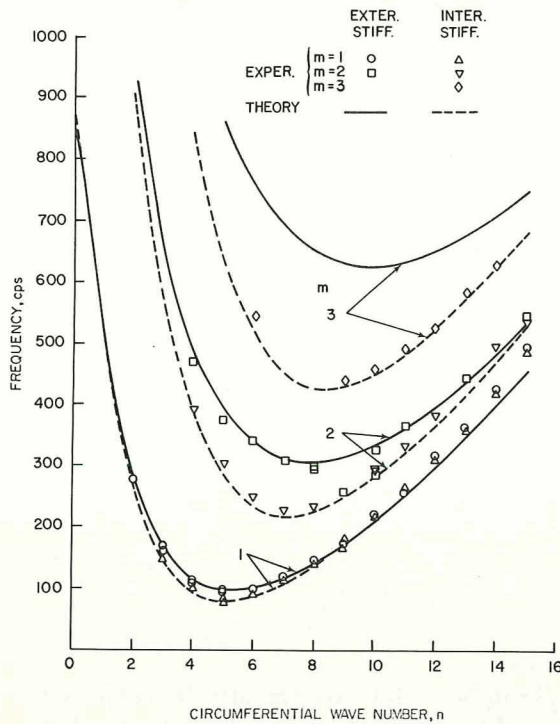


FIGURE 3.50.—Cyclic frequencies for stringer-stiffened, clamped-free shells. (After ref. 3.13)

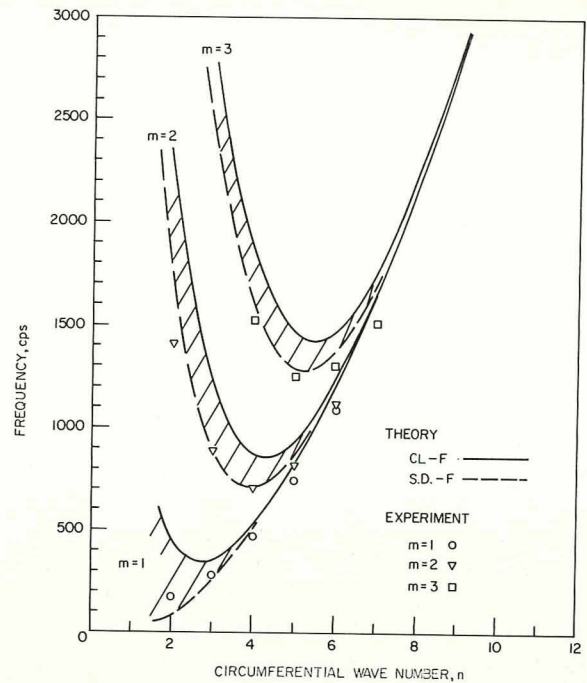


FIGURE 3.52.—Comparison of the effects of clamped-free and SD-free boundaries upon the frequencies of a circumferentially stiffened shell. (After ref. 3.5)

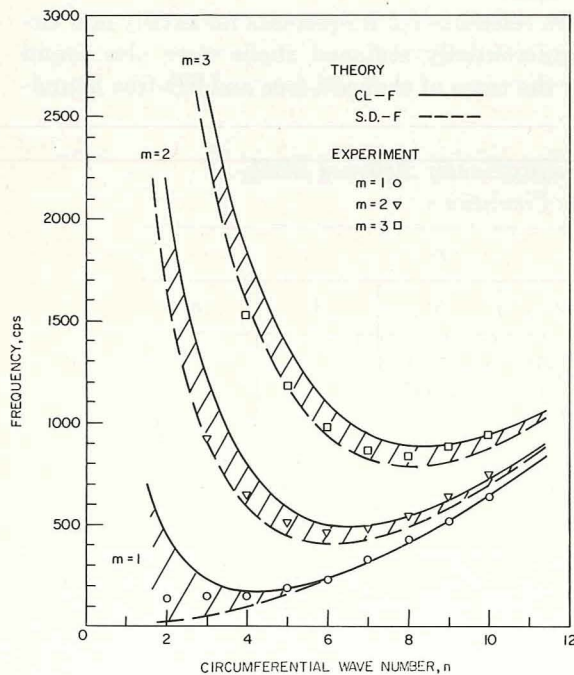


FIGURE 3.51.—Comparison of the effects of clamped-free and SD-free boundaries upon the frequencies of an axially stiffened shell. (After ref. 3.5)

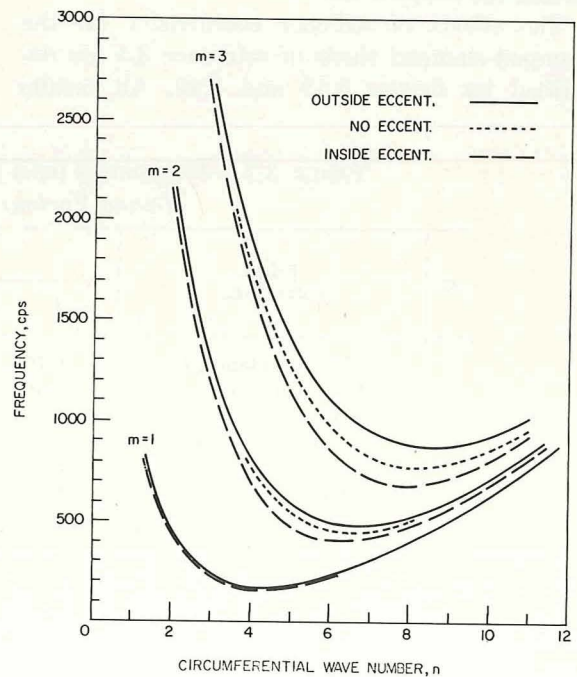


FIGURE 3.53.—Eccentricity effects upon the frequencies of a clamped-free, axially stiffened shell. (After ref. 3.5)

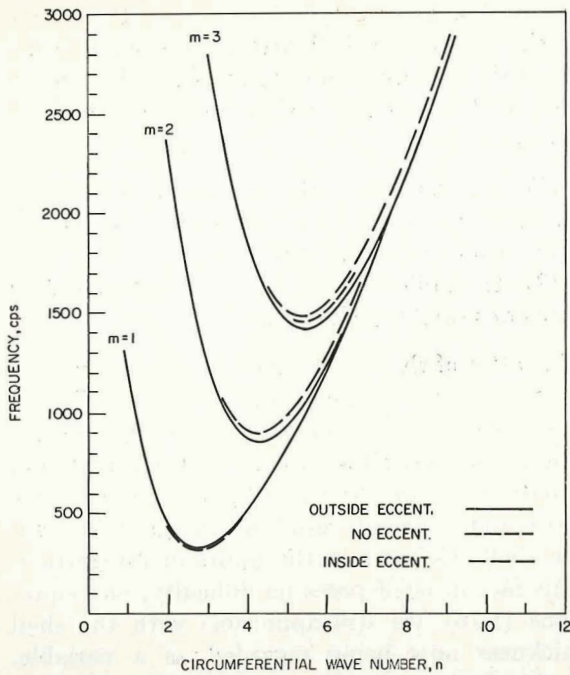


FIGURE 3.54.—Eccentricity effects upon the frequencies of a clamped-free, circumferentially stiffened shell. (After ref. 3.5)

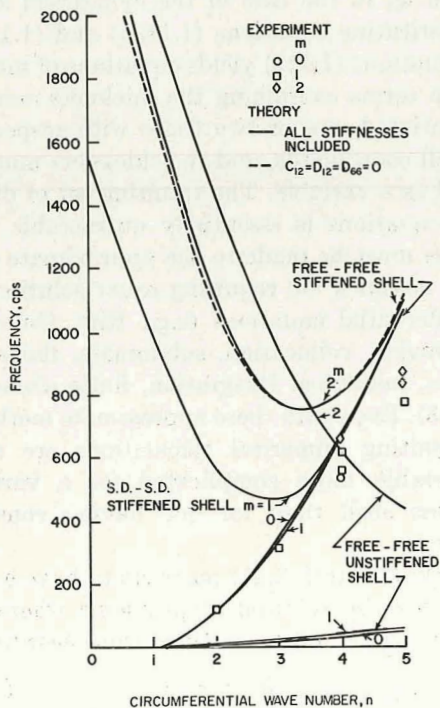


FIGURE 3.55.—Frequencies (cps) of a free-free, ring-stiffened cylindrical shell. (After ref. 3.35)

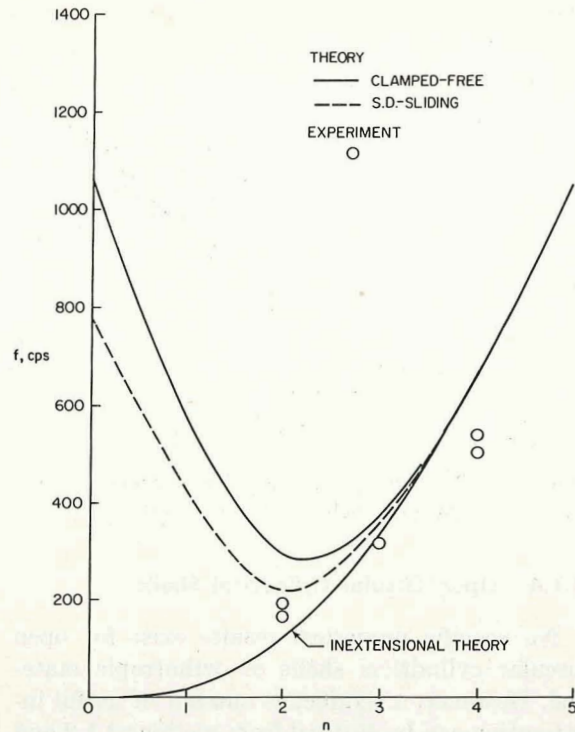


FIGURE 3.56.—Frequencies (cps) of clamped-free and SD-sliding support, ring-stiffened shells. (After ref. 3.35)

aries (see discussion of clamped-clamped case earlier in this section). Frequency distributions are depicted in figures 3.51 and 3.52. The effects of eccentricity for clamped-free ends are shown in figures 3.53 and 3.54. To observe the effects of stiffening in comparison with the unstiffened shell, the reader is referred to figure 2.82.

Theoretical and experimental frequencies for the shell of reference 3.35 (see earlier discussion in this section) having free-free ends are shown in figure 3.55. The discrepancy between theory and experiment clearly increases as n increases. The results of two analyses are shown, one including all stiffnesses, and the other neglecting C_{12} , D_{12} , and D_{66} . Results for two other types of end conditions are shown in figure 3.56: (1) clamped-free and (2) shear diaphragm-sliding.

Theoretical and experimental frequencies for free-free, stringer-stiffened shells are shown in figure 3.57 (from ref. 3.13) (see fig. 3.41 and earlier discussion in this section for additional details).

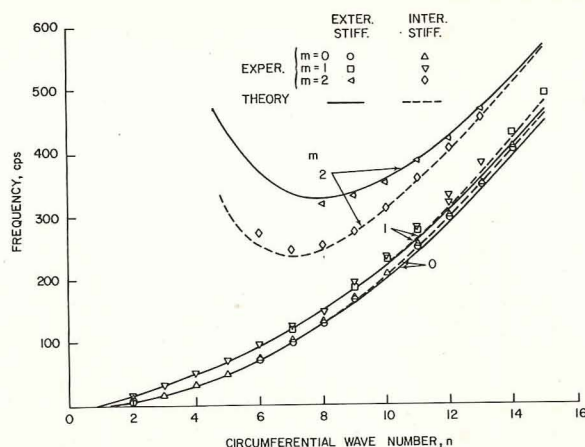


FIGURE 3.57.—Cyclic frequencies for stringer-stiffened, free-free shells. (After ref. 3.13)

3.1.4 Open Circular Cylindrical Shells

No specific numerical results exist for open circular cylindrical shells of orthotropic material. However, a significant amount of useful information can be gleaned from sections 3.1.2 and 3.1.3 for those cases where the two lateral edges are supported by shear diaphragms, because the displacements and force and moment resultants which exist at "node lines" ($w=0$) are precisely those required for shear diaphragm boundary conditions. Thus, as discussed previously for the isotropic case (see sec. 2.8.1) considerable information can be inferred for open orthotropic shells supported on all four edges by shear diaphragms from the results given in section 3.1.2. Similarly, for open orthotropic shells having their lateral edges supported by shear diaphragms and arbitrary edge conditions along the curved edges, useful results can be obtained from section 3.1.3 (similarly discussed for isotropic shells in sec. 2.8.2).

3.2 VARIABLE THICKNESS

Variable thickness in circular cylindrical shells often takes the form of a step discontinuity in thickness at some point along the length. The analysis of such shells requires piecing together of shell segments by means of continuity equations across the common boundary. These shells are considered to be structures and will not be treated here.

Few references exist which deal with the vibrations of circular cylindrical shells having continuously variable wall thickness. This lack of treatment is no doubt the result of two types of difficulties:

- (1) Mathematical difficulties associated with the solution of systems of eighth order partial differential equations, and
- (2) The difficulties inherent in manufacturing shells of variable thickness.

The latter of these two difficulties is obvious and needs no further discussion. The first difficulty has its source in the force and moment resultant equations. Returning to chapter 1 and scanning equations (1.75), for example, it is seen that the force and moment resultant integrals contain the shell thickness in the limits of integration. This fact in itself poses no difficulty, and equations (1.76) are still applicable with the shell thickness now being regarded as a variable, $h=h(x,\theta)$, instead of a constant. The difficulty arises when equations (1.76) are substituted into the equations of motion (e.g., eqs. (1.112) and (1.115)). The process of eliminating Q_α and Q_β (Q_x and Q_θ in the case of the cylindrical shell) by substituting equations (1.115a) and (1.115b) into equations (1.112) yields equations of motion wherein terms containing the thickness must be differentiated one or two times with respect to the shell coordinates, and the thickness must be treated as a variable. The resulting set of differential equations is essentially untractable, and recourse must be made to the approximate analytical methods *not* requiring exact solutions of the differential equations (e.g., Ritz, Galerkin, Kantorovich, collocation, subdomain, finite differences, numerical integration, finite elements, ref. 3.43). Even with these approximate methods, the resulting numerical calculations are often considerably more complicated for a variable thickness shell than for one having constant thickness.

Gontkevich (ref. 3.41) purports to have a procedure for the solution of problems where the thickness varies in the axial direction according to

$$h = h_0 x^i \quad (3.47)$$

where h_0 and i are constants. According to reference 3.41, the equations of motion for the axi-

symmetric problem are solvable in terms of Bessel functions of nonintegral order for some values of i . A method is then proposed for the solution of problems for arbitrary numbers n of circumferential waves where the mode shapes are either the eigenfunctions of the axisymmetric problem or beam functions. A characteristic determinant is then obtained containing terms which are complicated integrals having the products of x^i and the beam (or axisymmetric Bessel) functions as integrands. The same procedure is also proposed in reference 3.41 for shallow shells.

Oniashvili (ref. 3.44) made extensive calculations for shallow shells using the Galerkin method and the products of beam functions. The procedure was demonstrated on a shell panel supported by shear diaphragms on all edges and having a thickness variation in the circumferential direction determined by

$$h = h_0(1 + 2k\theta/\theta_0) \quad (3.48)$$

where θ is measured from the symmetry axis, θ_0 is the total circumferential angle included between the edges of the shell ($R\theta_0$ is the arc length between edges), h_0 is the thickness at the symmetry axis, and k is a constant determining the degree of thickness variability. Numerical results were obtained for concrete shells having $k=0.5$, $l=98.3$ in., $h_0=0.394$ in., $E=2.84 \times 10^6$ lb/in², $\rho g=0.0867$ lb/ft³, $\nu=0.12$, and various radii (R) and width/rise (b/c in fig. 2.141) ratios given in table 3.8. For comparison, frequencies are also given in table 3.8 for the constant thickness shell ($k=0$). Table 3.8 clearly shows that for relatively deep shells (small b/c) the effect of variable thickness is negligible; however, for very shallow shells (large b/c), the added stiffness near the lateral

boundaries due to increasing thickness more than offsets the added mass and the frequency is significantly increased.

Vibrations of circular cylindrical shells of variable thickness were also discussed by Federhofer (ref. 3.45).

3.3 LARGE (NONLINEAR) DISPLACEMENTS

In the case of plates transverse deflections which are on the order of the shell thickness or greater cause additional stiffening of the plate and result in equations of motion which are nonlinear. Because of the nonlinearity, approximate solution techniques such as the Galerkin method must be employed to obtain numerical results. However, in spite of slight disagreements among various writers concerning which nonlinear terms are essential in the theory, as well as the approximate character of solutions, it is universally agreed among writers (see ref. 3.1) that large displacements cause positive stiffening of the plate and a resulting *increase* in natural frequencies (i.e., "hard spring" behavior), regardless of the shape of plate or the boundary conditions.

Such is not the case, however, for circular cylindrical shells. Widespread disagreement exists as to whether the shell behaves as a hard spring or a soft spring, and whether the *type* of behavior depends upon the boundary conditions and/or the shell being open or closed.

The first investigation of nonlinear vibrations of cylindrical shells was reported by Reissner (ref. 3.46) in 1955. The shallow shell (Donnell-Mushtari) theory served as a basis for the work and mode shapes having sinusoidal variation in the axial and circumferential directions were taken, although the time response was *not* assumed to be sinusoidal. This led to results which indicated that the nonlinearity could be either of the hardening or softening type, depending upon the number of circumferential waves. Chu (ref. 3.47) subsequently made a similar analysis which gave results indicating that the nonlinearity was of the hardening type.

Evenson (ref. 3.48) attempted to obtain experimental verification for closed shells of the theoretical conclusions obtained previously. Instead, he found that (1) the nonlinearity was always of the softening type and (2) the nonlinearity effects were small. From this he concluded that

TABLE 3.8.—Frequencies (cps) for Shallow Circular Cylindrical Shells of Variable Thickness Having Shear Diaphragm Supports on All Edges

R , in.	Shallowness ratio, b/c	Variable thickness, $k=0.5$	Constant thickness, $k=0$
12.5	4	6.36	6.36
20	8	3.98	3.9
40	16	2.00	1.94
80	32	1.03	.98
160	64	.6	.49
320	128	.421	.246

the assumed modes used in the previous theoretical analyses gave rise to circumferential displacements v which were not single-valued and continuous, and that this caused serious error in the analyses. Nowinski (refs. 3.49 and 3.50) generalized the solution function to permit satisfaction of the continuity condition, but this resulted in different boundary conditions satisfied at the ends of the shell ($v=0$ rather than $w=0$). This led to hard spring behavior. Cummings (ref. 3.51) also obtained frequency which increases with amplitude.

Subsequently, Olson (ref. 3.52) observed softening nonlinearity in a series of experiments. Then, in a later work, Evensen and Fulton (ref. 3.53) found the nonlinearity to be either hardening or softening, depending upon the ratio of the number of axial waves to the number of circumferential waves, although the shear diaphragm boundary conditions were not exactly satisfied at the shell ends in their analysis. In reference 3.53 some results were also obtained where for large deflections the shell behaves as a soft spring, but as the amplitude is increased further, the nonlinearity becomes hard. This phenomenon was also seen in a recent paper by Leissa and Kadi (ref. 3.54). Mayers and Wrenn (refs. 3.55 and 3.56) used the more complicated shell theory of Sanders to arrive at the conclusion that free vibration is nonperiodic and of the hardening type.

This confusing state of affairs will be elaborated upon in the following subsections.

3.3.1 Nonlinear Equations of Motion

The *detailed* derivations of nonlinear equations of motion will not be given here. Only the important differences with linear theory and the final forms of the equations of motion will be summarized. For additional information it is suggested that the reader consult references 3.44, 3.46, 3.47, 3.49, 3.50, 3.55, and 3.56. A comprehensive treatise on nonlinear shell theory also exists in the monograph by Mushtari and Galimov (ref. 3.57).

The middle surface strains of linear shell theory given earlier by equations (1.41) are specialized to the case of circular cylindrical curvature and generalized to include the nonlinear stretching terms arising from relatively large slopes, giving

$$\left. \begin{aligned} \epsilon_x &= \frac{\partial u}{\partial x} + \frac{1}{2} \left(\frac{\partial w}{\partial x} \right)^2 \\ \epsilon_y &= \frac{\partial v}{\partial y} + \frac{w}{R} + \frac{1}{2} \left(\frac{\partial w}{\partial y} \right)^2 \\ \epsilon_{xy} &= \frac{\partial u}{\partial y} + \frac{\partial v}{\partial x} + \frac{\partial w}{\partial x} \frac{\partial w}{\partial y} \end{aligned} \right\} \quad (3.49)$$

where, for convenience, the shallow shell notation is used; i.e., $\partial/\partial y = (1/R)\partial/\partial\theta$. Adding the bending strains to equations (3.49) according to the Donnell-Mushtari theory, inverting the isotropic stress-strain equations, and integrating over the thickness gives the following expressions for the force resultants (cf., ref. 3.47):

$$N_x = C \left\{ \left[\frac{\partial u}{\partial x} + \frac{1}{2} \left(\frac{\partial w}{\partial x} \right)^2 \right] + \nu \left[\frac{\partial v}{\partial y} + \frac{w}{R} + \frac{1}{2} \left(\frac{\partial w}{\partial y} \right)^2 \right] \right\} \quad (3.50a)$$

$$N_y = C \left\{ \left[\frac{\partial v}{\partial y} + \frac{w}{R} + \frac{1}{2} \left(\frac{\partial w}{\partial y} \right)^2 \right] + \nu \left[\frac{\partial u}{\partial x} + \frac{1}{2} \left(\frac{\partial w}{\partial x} \right)^2 \right] \right\} \quad (3.50b)$$

$$N_{xy} = Gh \left(\frac{\partial u}{\partial y} + \frac{\partial v}{\partial x} + \frac{\partial w}{\partial x} \frac{\partial w}{\partial y} \right) \quad (3.50c)$$

$$M_x = -D \left(\frac{\partial^2 w}{\partial x^2} + \nu \frac{\partial^2 w}{\partial y^2} \right) \quad (3.50d)$$

$$M_y = -D \left(\frac{\partial^2 w}{\partial y^2} + \nu \frac{\partial^2 w}{\partial x^2} \right) \quad (3.50e)$$

where $C = Eh/(1-\nu^2)$ and $D = Eh^3/12(1-\nu^2)$, as before.

Using the Donnell-Mushtari equations of motion of section 1.6 along with equations (3.50) gives (neglecting tangential inertia)

$$D \nabla^4 w + \rho h \frac{\partial^2 w}{\partial t^2} = h \left(\frac{\partial^2 w}{\partial x^2} \frac{\partial^2 \varphi}{\partial y^2} + \frac{\partial^2 w}{\partial y^2} \frac{\partial^2 \varphi}{\partial x^2} - 2 \frac{\partial^2 w}{\partial x \partial y} \frac{\partial^2 \varphi}{\partial x \partial y} - \frac{1}{R} \frac{\partial^2 \varphi}{\partial x^2} \right) \quad (3.51)$$

where φ is an Airy stress function defined by

$$\left. \begin{aligned} \frac{N_x}{h} &= \frac{\partial^2 \varphi}{\partial y^2} & \frac{N_y}{h} &= \frac{\partial^2 \varphi}{\partial x^2} \\ \frac{N_{xy}}{h} &= -\frac{\partial^2 \varphi}{\partial x \partial y} \end{aligned} \right\} \quad (3.52)$$

Another equation is obtained from the equation of compatibility of strains for the middle surface. From equations (3.49) it is seen to be

$$\frac{\partial^2 \epsilon_x}{\partial y^2} + \frac{\partial^2 \epsilon_y}{\partial x^2} - \frac{\partial^2 \epsilon_{xy}}{\partial x \partial y} = \left(\frac{\partial^2 w}{\partial x \partial y} \right)^2 - \frac{\partial^2 w}{\partial x^2} \frac{\partial^2 w}{\partial y^2} + \frac{1}{R} \frac{\partial^2 w}{\partial x^2} \quad (3.53)$$

Using equations (3.52) and the stress-strain equations for an isotropic material, equation (3.53) becomes

$$\nabla^4 \varphi = E \left[\left(\frac{\partial^2 w}{\partial x \partial y} \right)^2 - \frac{\partial^2 w}{\partial x^2} \frac{\partial^2 w}{\partial y^2} + \frac{1}{R} \frac{\partial^2 w}{\partial x^2} \right] \quad (3.54)$$

Thus, the governing nonlinear equations for a circular cylindrical shell according to the Donnell-Mushtari (or shallow shell) theory are given by equations (3.51) and (3.54). In the case where $R = \infty$ the equations properly reduce to the corresponding ones for a flat plate. In the case of an orthotropic shell having axes of orthotropy coincident with the shell coordinates ($\alpha \sim x$, $\beta \sim y$), the equations are generalized to (cf., refs. 3.49 and 3.50)

$$D_{11} \frac{\partial^4 w}{\partial x^4} + 2(\nu_y D_{11} + D_{66}) \frac{\partial^4 w}{\partial x^2 \partial y^2} + D_{22} \frac{\partial^4 w}{\partial y^4} + \rho h \frac{\partial^2 w}{\partial t^2} = h \left(\frac{\partial^2 w}{\partial x^2} \frac{\partial^2 \varphi}{\partial y^2} + \frac{\partial^2 w}{\partial y^2} \frac{\partial^2 \varphi}{\partial x^2} - 2 \frac{\partial^2 w}{\partial x \partial y} \frac{\partial^2 \varphi}{\partial x \partial y} - \frac{1}{R} \frac{\partial^2 \varphi}{\partial x^2} \right) \quad (3.55a)$$

$$\frac{\partial^4 \varphi}{\partial x^4} + \left(\frac{E_x}{G} - 2\nu_x \right) \frac{\partial^4 \varphi}{\partial x^2 \partial y^2} + \frac{E_x}{E_y} \frac{\partial^4 \varphi}{\partial y^4} = E_x \left[\left(\frac{\partial^2 w}{\partial x \partial y} \right)^2 - \frac{\partial^2 w}{\partial x^2} \frac{\partial^2 w}{\partial y^2} + \frac{1}{R} \frac{\partial^2 w}{\partial x^2} \right] \quad (3.55b)$$

The nonlinear, middle surface strain-displacement relationships of the Sanders theory were found to be (see refs. 3.56 and 3.58):

$$\left. \begin{aligned} \epsilon_x &= \frac{\partial u}{\partial x} + \frac{1}{2} \left(\frac{\partial w}{\partial x} \right)^2 \\ \epsilon_y &= \frac{\partial v}{\partial y} + \frac{w}{R} + \frac{1}{2} \left(\frac{\partial w}{\partial y} \right)^2 - \frac{v}{R} \frac{\partial w}{\partial y} \\ \epsilon_{xy} &= \frac{\partial u}{\partial y} + \frac{\partial v}{\partial x} + \frac{\partial w}{\partial x} \frac{\partial w}{\partial y} - \frac{v}{R} \frac{\partial w}{\partial x} \end{aligned} \right\} \quad (3.56)$$

In reference 3.56 equations (3.56), along with the other corresponding equations of the Sanders

theory (see chapter 1) are used to derive a set of nonlinear equations of motion in terms of the displacements u , v , and w . The resulting equations are quite lengthy and will not be repeated here; they are displayed as equations (21), (22), and (23) in reference 3.56.

The nonlinear form of the Morley equations of motion for circular cylindrical shells are exhibited in reference 3.51.

3.3.2 Infinitely Long Shells

Evensen (ref. 3.59) showed that in the case of plane strain for an infinitely long circular cylindrical shell, the equations of motion reduce to

$$\frac{\partial N_y}{\partial y} = 0 \quad (3.57a)$$

$$D \frac{\partial^4 w}{\partial y^4} + \rho h \frac{\partial^2 w}{\partial t^2} - \frac{N_y}{R} - N_y \frac{\partial^2 w}{\partial y^2} = 0 \quad (3.57b)$$

The radial displacement was assumed to take the form

$$w(y, t) = A_n(t) \cos \frac{ny}{R} + A_0(t) \quad (3.58)$$

Equation (3.57a) and the continuity condition

$$v(y + 2\pi R, t) = v(y, t) \quad (3.59)$$

were exactly satisfied, and equation (3.57b) was approximately satisfied by the Galerkin procedure.

If the amplitude $A_0(t)$ of the axisymmetric mode is taken to be zero, the resulting modal equation is

$$\frac{d^2 a_n}{d\tau^2} + a_n + 3a_n^3 = 0 \quad (3.60)$$

where a_n is the nondimensional amplitude, A_n/h , and τ is nondimensional time, $\omega_n t$, with

$$\omega_n^2 = \frac{E h^2 n^4}{12(1 - \nu^2) \rho R^4} \quad (3.61)$$

Equation (3.60) exhibits a hard spring behavior and results from considerable stretching of the middle surface of the shell. Its solution is, of course, expressible exactly in terms of elliptic integrals, but an approximate solution can be written as

$$a_n(\tau) = \bar{a} \cos \omega^* \tau \quad (3.62)$$

where

$$\omega^{*2} = \frac{\omega^2}{\omega_n^2} = 1 + \frac{9}{4}\bar{a}^2 \quad (3.63)$$

The nonlinearity is independent of the circumferential wave number n as well as the thickness ratio, h/R . It was pointed out in reference 3.59 that the corresponding modal equations of references 3.47 and 3.49 yield

$$\frac{d^2 a_n}{d\tau^2} + a_n + \frac{3}{4}(1 - \nu^2)a_n^3 = 0 \quad (3.64)$$

instead of equation (3.60). Clearly while equation (3.64) also characterizes a hard spring, it is much less strongly nonlinear than equation (3.60).

For the case of inextensional vibrations (no stretching of the middle surface of the shell), $A_0(t)$ is related to $A_n(t)$ by

$$A_0(t) = -\frac{n^2 A_n^2(t)}{4R} \quad (3.65)$$

yielding the modal equation

$$\frac{d^2 a_n}{d\tau^2} + \frac{1}{2}\epsilon a_n \left[a_n \frac{d^2 a_n}{d\tau^2} + \left(\frac{da_n}{d\tau} \right)^2 \right] + a_n = 0 \quad (3.66)$$

where

$$\epsilon = \left(\frac{n^2 h}{R} \right)^2 \quad (3.67)$$

Taking an approximate solution to equation (3.66) in the form of equation (3.62) yields

$$\begin{aligned} \left(\frac{\omega}{\omega_n} \right)^2 &= \frac{1}{1 + (\epsilon \bar{a}^2/4)} \\ &= 1 - \epsilon \frac{\bar{a}^2}{4} + 0(\epsilon^2) \end{aligned} \quad (3.68)$$

For small n and small h/R , terms of order ϵ^2 and greater in equation (3.68) can be neglected, and a soft spring response is indicated. When the length of the shell is taken to approach infinity, the analysis of reference 3.60 yields an equation identical to equation (3.66) except that the coefficient $1/2$ in the second term is replaced by $3/8$.

Finally, consider the case when $A_n(t)$ and $A_0(t)$ in equation (3.58) are permitted to be independent modes. This yields the two coupled modal equations

$$\left. \begin{aligned} \frac{d^2 a_n}{d\tau^2} + a_n + 12a_n \left(r + \frac{a_n^2}{4} \right) &= 0 \\ \epsilon \frac{d^2 r}{d\tau^2} + 12 \left(r + \frac{a_n^2}{4} \right) &= 0 \end{aligned} \right\} \quad (3.69)$$

where $A_0/h = n(h/R)r$, and ϵ , a_n , and τ as defined previously. An approximate solution to equations (3.69) as found in reference 3.59 is

$$\left. \begin{aligned} a_n(\tau) &= \bar{a} \cos \omega^* \tau \\ r(\tau) &= \bar{r}_0 + \bar{r}_2 \cos 2\omega^* \tau \end{aligned} \right\} \quad (3.70)$$

where

$$\left. \begin{aligned} \bar{r}_0 &= -\bar{a}^2/8 \\ \bar{r}_2 &= -\bar{a}^2/8[1 - \omega^{*2}/3] \end{aligned} \right\} \quad (3.71)$$

and

$$1 - \omega^{*2} - \frac{\epsilon \bar{a}^2}{4} \left[1 - \frac{\epsilon \omega^{*2}}{3} \right]^{-1} = 0 \quad (3.72)$$

Expanding equation (3.72) gives

$$\frac{\omega^2}{\omega_n^2} = 1 - \epsilon \frac{\bar{a}^2}{4} + 0(\epsilon^2) \quad (3.73)$$

which is the same as equation (3.68) for terms up to order ϵ .

The conclusions reached in reference 3.59 for the infinitely long shell as a result of the foregoing analysis are

(1) The shell vibrates in such a manner that the midsurface remains practically inextensible.

(2) The frequency-amplitude relation is of the softening type and depends upon $\epsilon = (n^2 h/R)^2$.

(3) A radial contraction involving double-frequency ($\cos 2\omega^* \tau$) motions is indicated and has been observed experimentally by Olson (ref. 3.52).

(4) Vibration modes that do not permit an axisymmetric radial contraction, in addition to the primary vibration shape, appear to place an unrealistic constraint on the shell.

Dowell and Ventres (ref. 3.61) used the Donnell-type shell equations (3.51) and (3.53) and a radial displacement function of the form

$$\begin{aligned} w(x, y, t) &= A_{mn}(t) \sin \frac{m\pi x}{l} \cos \frac{ny}{R} \\ &+ B_{mn}(t) \sin \frac{m\pi x}{l} \sin \frac{ny}{R} \\ &+ A_{m0}(t) \sin \frac{m\pi x}{l} \end{aligned} \quad (3.74)$$

A corresponding φ was obtained by integrating the compatibility equation (3.54). The equation of motion was approximated by the Galerkin procedure, yielding three complicated, coupled, nonlinear equations involving the amplitudes A_{mn} , B_{mn} , and A_{m0} and their time derivatives. These equations were investigated in the limit as $l/R \rightarrow \infty$ and found to yield a nonlinearity of the hardening type (at least for m even).

3.3.3 Large Deflections of Closed Shells Having "Shear Diaphragm" End Conditions

The term "shear diaphragm" is used with quotation marks because in the numerous analyses which are described below most of them attempt to satisfy shear diaphragm boundary conditions (eqs. (2.33)), but end up only by approximating them.

Evensen and Fulton (ref. 3.53 and 3.60) used the Donnell theory (eqs. (3.51) and (3.54)) and the following two-mode approximation for the radial displacement:

$$w(x, y, t) = \left\{ A_{mn}(t) \cos \frac{ny}{R} + B_{mn}(t) \sin \frac{ny}{R} \right\} \sin \frac{m\pi x}{l} + \frac{n^2}{4R} [A_{mn}^2(t) + B_{mn}^2(t)] \sin^2 \frac{m\pi x}{l} \quad (3.75)$$

where the bracketed term involving A_{mn}^2 and B_{mn}^2 is added to satisfy the continuity condition on v . Substituting equation (3.75) into the compatibility equation (3.54) and integrating gives the stress function φ as follows:

$$\begin{aligned} \varphi(x, y, t) = & a_1(A_{mn} \cos \beta y + B_{mn} \sin \beta y) \sin \alpha x \\ & - a_2(A_{mn}^2 - B_{mn}^2) \cos 2\beta y \\ & - a_3 A_{mn} B_{mn} \sin 2\beta y \\ & + a_4(A_{mn}^2 + B_{mn}^2)(A_{mn} \cos \beta y \\ & + B_{mn} \sin \beta y) \sin 3\alpha x \end{aligned} \quad (3.76)$$

where $\alpha = m\pi/l$, $\beta = n/R$ and

$$\begin{aligned} a_1 &= \frac{\alpha^2 E h}{R(\alpha^2 + \beta^2)^2} \\ a_2 &= \frac{\alpha^2 E h}{32\beta^2} \\ a_3 &= \frac{\alpha^2 E h}{16\beta^2} \\ a_4 &= \frac{\alpha^2 \beta^2 R E h}{4} \left[\frac{1}{(9\alpha^2 + \beta^2)^2} - \frac{1}{(\alpha^2 + \beta^2)^2} \right] \end{aligned}$$

Although equation (3.75) exactly satisfies the shear diaphragm boundary condition $w=0$ at the ends $x=0$ and $x=l$, it will be found upon integration of the strain-displacement equations (3.49) that v will not be zero at the ends. Similarly, using equations (3.50) it is found that N_x and M_x are not identically zero at the ends. For these quantities the coefficients of the linear terms in A_n and B_n do vanish at $x=0, l$, but the terms involving A_n^2 , $A_n B_n$, and B_n^2 do not vanish there. Thus, the shear diaphragm boundary conditions are only approximated. However, the continuity condition (3.59) is exactly satisfied.

Finally, the equation of motion (3.51) is satisfied approximately by the Galerkin procedure, giving rise to the two following coupled, nonlinear, nondimensionalized equations:

$$\begin{aligned} \frac{d^2 \zeta_c}{d\tau^2} + \zeta_c + \frac{3}{8} \epsilon \zeta_c \left[\zeta_c \frac{d^2 \zeta_c}{d\tau^2} + \left(\frac{d\zeta_c}{d\tau} \right)^2 + \zeta_s \frac{d^2 \zeta_s}{d\tau^2} + \left(\frac{d\zeta_s}{d\tau} \right)^2 \right] - \epsilon \gamma \zeta_c (\zeta_c^2 + \zeta_s^2) \\ + \epsilon^2 \delta \zeta_c (\zeta_c^2 + \zeta_s^2)^2 = 0 \end{aligned} \quad (3.77a)$$

$$\begin{aligned} \frac{d^2 \zeta_s}{d\tau^2} + \zeta_s + \frac{3}{8} \epsilon \zeta_s \left[\zeta_s \frac{d^2 \zeta_s}{d\tau^2} + \left(\frac{d\zeta_s}{d\tau} \right)^2 + \zeta_c \frac{d^2 \zeta_c}{d\tau^2} + \left(\frac{d\zeta_c}{d\tau} \right)^2 \right] - \epsilon \gamma \zeta_s (\zeta_s^2 + \zeta_c^2) \\ + \epsilon^2 \delta \zeta_s (\zeta_s^2 + \zeta_c^2)^2 = 0 \end{aligned} \quad (3.77b)$$

where $\zeta_c = A_{mn}/h$, $\zeta_s = B_{mn}/h$, $\tau = \omega_{mn} t$, ω_{mn} is the linear free vibration frequency, $\epsilon = (n^2 h/R)^2$ as before, and γ and δ are defined by

$$\gamma = \frac{\xi^4 \left[\frac{1}{(\xi^2 + 1)^2} - \frac{1}{16} - \frac{\epsilon}{12(1 - \nu^2)} \right]}{\left[\frac{\xi^4}{(\xi^2 + 1)^2} + \frac{\epsilon(\xi^2 + 1)^2}{12(1 - \nu^2)} \right]} \quad (3.78a)$$

$$\delta = \frac{\frac{3}{16} \xi^4 \left[\frac{1}{(\xi^2 + 1)^2} + \frac{1}{(9\xi^2 + 1)^2} \right]}{\left[\frac{\xi^4}{(\xi^2 + 1)^2} + \frac{\epsilon(\xi^2 + 1)^2}{12(1 - \nu^2)} \right]} \quad (3.78b)$$

where ξ is the aspect ratio of the particular mode, given by $\xi = m\pi R/nl$. It is interesting to note that the nonlinearity of the problem depends upon the parameter ϵ ; that is, as ϵ approaches zero, the problem becomes linear.

Consider first the solution of equations (3.77) for the case when only a single mode is retained

in the solution function (equation (3.75)); i.e., $A_{mn} \neq 0$, $B_{mn} = 0$. The method of averaging was used in references 3.53 and 3.60 to obtain the following approximate solution:

$$\left. \begin{aligned} \zeta_c(\tau) &= \bar{A} \cos \omega^* \tau \\ \zeta_s(\tau) &= 0 \end{aligned} \right\} \quad (3.79)$$

with the frequency-amplitude relationship given by

$$\omega^{*2} = \left(\frac{\omega}{\omega_{mn}} \right)^2 = \frac{1 - \frac{3}{4} \epsilon \gamma \bar{A}^2 + \frac{5}{8} \epsilon^2 \delta \bar{A}^4}{1 + \frac{3}{16} \epsilon \bar{A}^2} \quad (3.80)$$

Numerical results for five values of ϵ ranging from 0 to 1.0 are shown in figure 3.58. The solid and dashed lines were calculated for values of γ and δ corresponding to aspect ratios of $\xi = 1/2$ and 2, respectively. Poisson's ratio was taken as $\nu = 0.3$.

Both sets of curves in figure 3.58 demonstrate that the strength of the nonlinearity is highly dependent upon $\epsilon = (n^2 h / R)^2$. The nonlinearity is small for vibrations involving very thin cylinders and/or small values of n , and conversely.

The character of the nonlinearity (i.e., whether it is hardening or softening) depends strongly

upon the aspect ratio ξ . This result is apparent from equations (3.77), which show that ϵ is a multiplying factor in every nonlinear term. The effect is illustrated in figure 3.59, which shows frequency-amplitude response curves computed from equation (3.80) for values of ξ ranging from 0.1 to 4.0. The solid lines are the results of Evensen and Fulton (refs. 3.53 and 3.60) and are calculated for $\epsilon = 1.0$ and $\nu = 0.3$. For comparison purposes, Chu's results (ref. 3.47) (discussed later in this section) are shown as dashed curves in figure 3.59. The results of references 3.53 and 3.60 are of the softening type for $\xi < 1$ and of the hardening type for larger values of ξ , whereas Chu's results are all of the hardening type.

Another fundamental difference between the results of Evensen and Fulton and those of Chu are that the latter's results possess a symmetric dependence on the aspect ratio parameter ξ ; i.e., Chu's curves for $\xi = 1/2, 1/4, 1/8, \dots$ coincide with those for $\xi = 2, 4, 8, \dots$, respectively. Such a symmetric dependence on ξ seems to conflict with the basic geometric nonsymmetry of the shell; i.e., the shell has curvature in the circumferential direction, but not in the axial

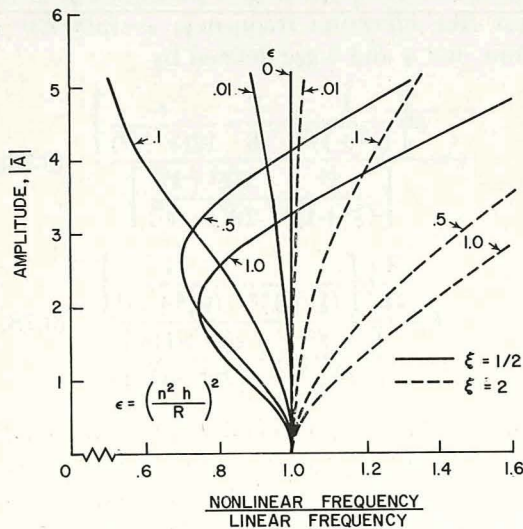


FIGURE 3.58.—Frequency ratio versus amplitude for large deflections of a cylindrical shell; $\nu = 0.3$. (After refs. 3.53 and 3.60)

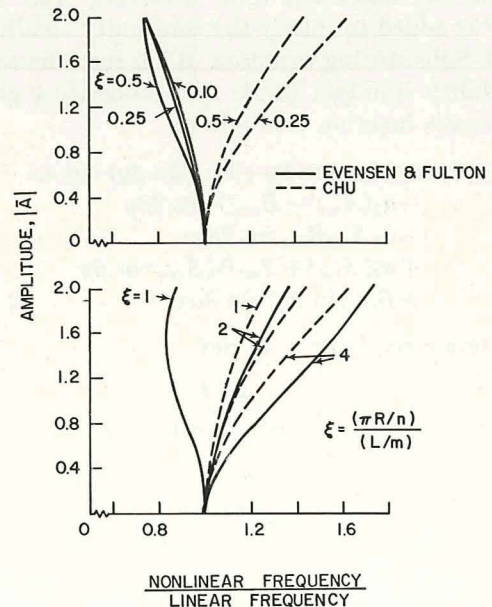


FIGURE 3.59.—Frequency ratios for large deflections of a cylindrical shell; $\nu = 0.3$. (After refs. 3.53 and 3.60)

direction. The results of Evensen and Fulton do not display this form of symmetric dependence.

Another effect which is apparent from the curves of figures 3.58 and 3.59 for some values of ϵ and ξ is that although the initial response may be of the softening type, as the amplitude continues to increase the \bar{A}^4 term in the numerator of equation (3.80) eventually dominates, resulting in hardening nonlinearity.

Results were also presented in references 3.53 and 3.60 for solutions using both the A_{mn} and B_{mn} terms in equation (3.75). These are shown in figure 3.60 for a forced motion where the applied normal loading $q(x,y,t)$ is chosen so that only one mode is directly excited (driven); i.e.,

$$q(x,y,t) = Q_{mn} \cos \frac{n\pi y}{R} \sin \frac{m\pi x}{l} \cos \omega t \quad (3.81)$$

The solid lines in figure 3.60 are the forced response curves of the driven mode and the companion mode for $\epsilon=0.01$, $\xi=0.1$, and $\nu=0.3$. The free vibration curves are shown dashed and exhibit the same initial soft spring response seen previously with a single mode. The corresponding curves for a single mode analysis are depicted in

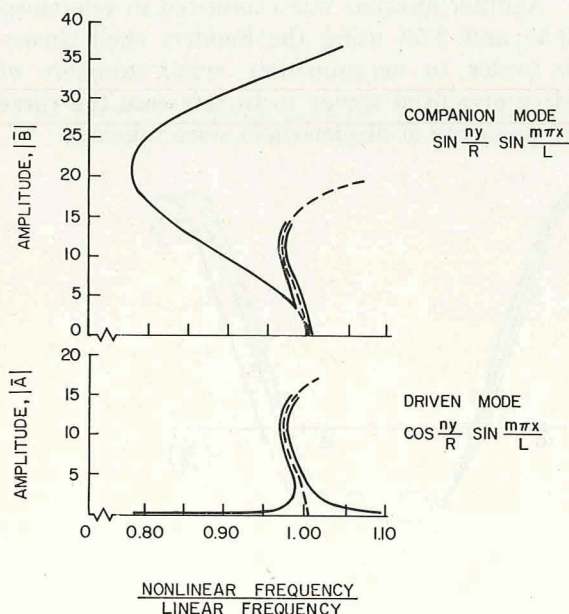


FIGURE 3.60.—Forced vibration frequency ratios for large deflections of a cylindrical shell; two mode analysis, $\xi=0.1$, $\epsilon=0.01$, $\nu=0.3$. (After refs. 3.53 and 3.60)

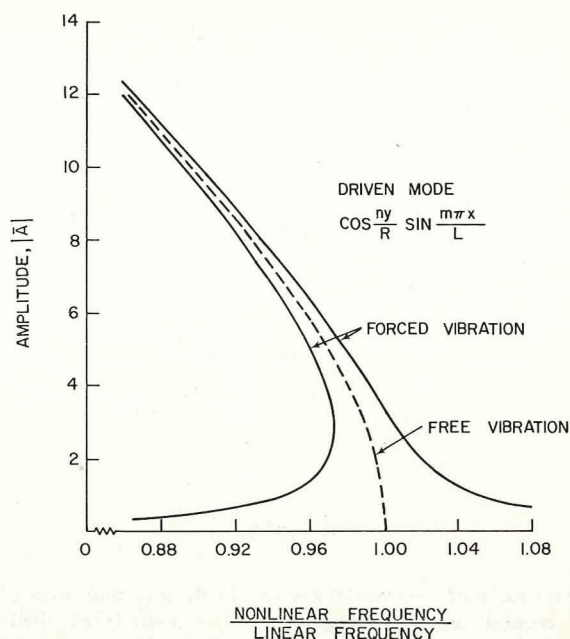


FIGURE 3.61.—Forced vibration frequency ratios for large deflections of a cylindrical shell; single mode analysis, $\xi=0.1$, $\epsilon=0.01$, $\nu=0.3$. (After refs. 3.53 and 3.60)

figure 3.61. For further discussion of the forced response curves, see references 3.53 and 3.60.

Experimental results for the nonlinear vibrations of cylindrical shells is scarce. Kana, Lindholm, and Abramson (ref. 3.62) obtained results for circular cylindrical shells which showed a very slight nonlinearity of the softening type. Quantitative results obtained by Olson (ref. 3.52) are shown by the circles and dashed lines in figure 3.62. The solid line shown is the free vibration curve calculated from equation (3.80) with the values of ϵ , γ , δ that correspond to Olson's experiment (copper shell, $h=0.0044$ in., $R=8.00$ in., and $l=15-3/8$ in., yielding $\epsilon=3.025 \times 10^{-3}$, $\xi=0.1635$, $\nu=0.365$). The experimental and theoretical results are nondimensionalized with respect to the experimental and theoretical linear frequencies, respectively. Again, the results show nonlinearity which, at least initially for moderate amplitudes, is of the softening type.

Mayers and Wrenn (refs. 3.55 and 3.56) used the Donnell equations and the single mode ($A_{mn} \neq 0$, $B_{mn} = 0$) special case of the deflection function given in equation (3.75) to duplicate the

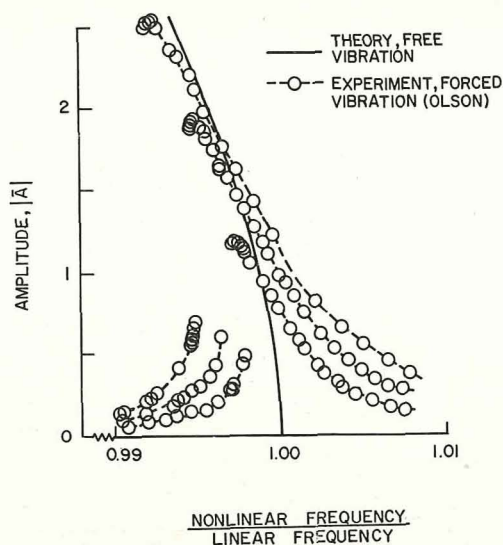


FIGURE 3.62.—Comparison of theoretical and experimental nonlinear responses for a cylindrical shell; $\epsilon = 3.025 \times 10^{-3}$, $\xi = 0.1635$, $\nu = 0.365$. (After refs. 3.53 and 3.60)

results of Evensen and Fulton (refs. 3.53 and 3.60) which were presented previously in figures 3.58 and 3.59. They found this motion to be *periodic* in time. A two-mode solution was also taken in the form

$$\frac{w}{h} = A_1(t) \cos \frac{m\pi x'}{l} \cos \frac{ny}{R} + \frac{n^2}{8} \left(\frac{h}{R} \right) A_1^2(t) + A_3(t) \cos \frac{2m\pi x'}{l} \quad (3.82)$$

where x' is measured from the longitudinal symmetry plane of the shell; i.e.; $x' = x - l/2$. Using this solution function the resulting motion was found to be *nonperiodic* in time, as shown in figure 3.63. In figure 3.63 the dashed curve represents the periodic solution obtained from the single mode solution. The deflection function for this mode in terms of the shifted coordinate x' is given by

$$\frac{w}{h} = A_1(t) \cos \frac{m\pi x'}{l} \cos \frac{ny}{R} + \frac{n^2}{8} \left(\frac{h}{R} \right) A_1^2(t) + \frac{n^2}{8} \left(\frac{h}{R} \right) A_1(t) \cos \frac{2m\pi x'}{l} \quad (3.83)$$

The solid line is the nonperiodic response arising from the two mode function used in equation (3.82). The interrupted line is the nonperiodic response arising from a two mode function of the form

$$\begin{aligned} \frac{w}{h} = & A_1(t) \cos \frac{m\pi x'}{l} \cos \frac{ny}{R} \\ & - \left[A_3(t) + \frac{n^2}{8} \left(\frac{h}{R} \right) A_1^2(t) \right] \cos \frac{4m\pi x'}{l} \\ & - A_3(t) \cos \frac{2m\pi x'}{l} + \frac{n^2}{8} \left(\frac{h}{R} \right) A_1^2(t) \quad (3.84) \end{aligned}$$

Another analysis was conducted in references 3.55 and 3.56 using the Sanders shell theory in order to accommodate small numbers of circumferential waves n . In this case the three components of displacement were taken as

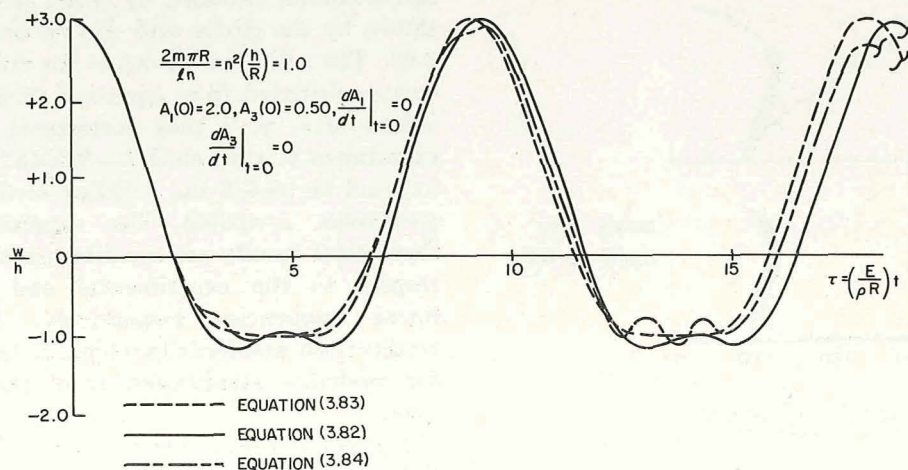


FIGURE 3.63.—Comparison of periodic and nonperiodic radial displacements as functions of time. (After refs. 3.55 and 3.56)

$$\left. \begin{aligned}
 \frac{w}{h} &= A_1(t) \cos \frac{m\pi x'}{l} \cos \frac{ny}{R} \\
 \frac{u}{h} &= A_3(t) \sin \frac{m\pi x'}{l} \cos \frac{ny}{R} \\
 &\quad + A_5(t) \sin \frac{2m\pi x'}{l} \cos \frac{2ny}{R} \\
 &\quad + A_7(t) \sin \frac{2m\pi x'}{l} \\
 \frac{v}{h} &= A_9(t) \cos \frac{m\pi x'}{l} \sin \frac{ny}{R} \\
 &\quad + A_{11}(t) \cos \frac{2m\pi x'}{l} \sin \frac{2ny}{R} \\
 &\quad + A_{13}(t) \sin \frac{2ny}{R}
 \end{aligned} \right\} \quad (3.85)$$

The results of this analysis yielded nonlinearity of the hardening type as depicted in figures 3.64 and 3.65 for $n=2$ and the aspect ratio

$$\frac{2m\pi R}{ln} = 1.0 \text{ and } 0.50$$

respectively.

Cummings (ref. 3.51) developed the nonlinear form of the Morley equations and applied the Galerkin procedure using a radial displacement function

$$w(x,y,t) = A(t) \sin \frac{\pi x}{l} \cos \frac{ny}{R} \quad (3.86)$$

to arrive at a nonlinear equation of the hard spring type (Duffing's equation):

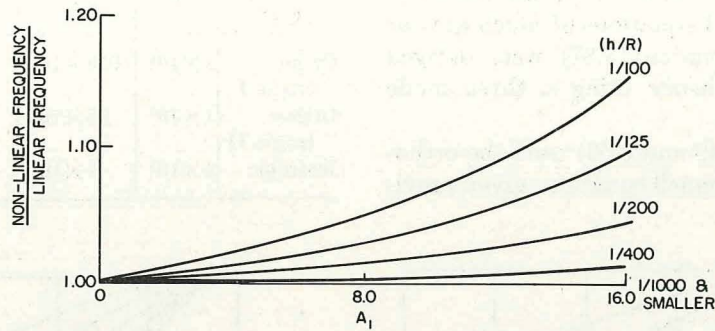


FIGURE 3.64.—Frequency ratios according to the Sanders theory; $n=2$, $2m\pi R/ln=1.0$. (After refs. 3.55 and 3.56)

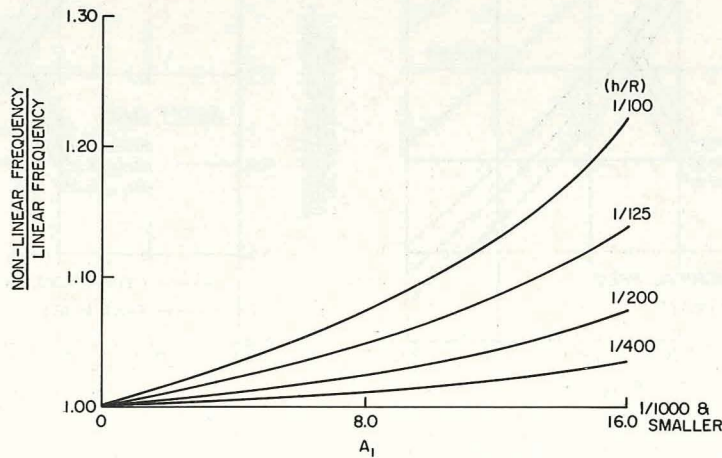


FIGURE 3.65.—Frequency ratios according to the Sanders theory; $n=2$, $2m\pi R/ln=0.50$. (After refs. 3.55 and 3.56)

$$\frac{d^2 A}{dt^2} + k_1 A + k_2 A^3 = 0 \quad (3.87)$$

i.e., where k_1 and k_2 are positive constants.

Chu (ref. 3.47) used the Donnell theory and equation (3.86) to arrive at an equation of the same form as equation (3.87) differing only by a factor of two in k_2 . Numerical results found in reference 3.47 for a shell having $R/h=100$ and $\nu=0.318$ are exhibited in figures 3.66 and 3.67 for $n=8$ and 10 (circumferential wave numbers), respectively. In these figures the nonlinear/linear frequency ratio is plotted versus the amplitude ratio A_{\max}/h for a series of aspect ratios, $\pi R/\ell n$. Results are also shown for the flat plate. According to this analysis, the nonlinearity is of the hardening type, as for flat plates, although the nonlinearity is not as strong.

As described in section 3.3.3, in reference 3.61 a set of three coupled equations of much greater complexity than equation (3.87) were derived from the Donnell theory using a three mode representation for w .

Nowinski (refs. 3.49 and 3.50) used the orthotropic form of the Donnell equations given previ-

ously as equations (3.55) with the displacement function

$$w(x,y,t) = A(t) \sin \frac{m\pi x}{l} \sin \frac{ny}{R} + \frac{n^2}{8R} A^2(t) \quad (3.88)$$

and the Galerkin procedure to obtain numerical results for shells having material types as shown in table 3.9 (correcting a misprint in ref. 3.49). Duffing's equation (3.87) was also obtained from this analysis. Frequency ratios versus amplitude ratios are shown in figure 3.68 for shells having the types of materials listed in table 3.9, $R/h=100$, and various values of n and $\lambda = m\pi R/l$.

TABLE 3.9.—Properties of Orthotropic and Isotropic Shells

Material type	E_x	E_y	G	ν_x	ν_y
Orthotropic I	1×10^5	0.5×10^5	0.1×10^5	0.05	0.025
Orthotropic II	1×10^5	$.05 \times 10^5$	$.05 \times 10^5$.20	.01
Isotropic	1×10^5	1×10^5	$.384 \times 10^5$.30	.30

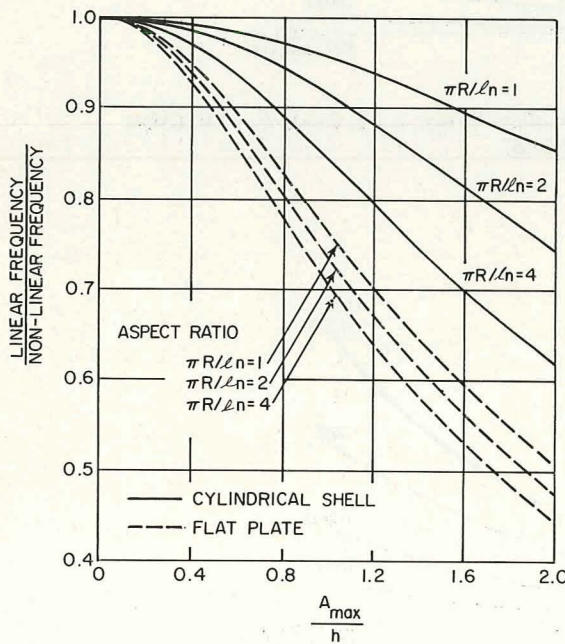


FIGURE 3.66.—Comparison of nonlinear response of a circular cylindrical shell with a flat plate; $n=8$. (After ref. 3.47)

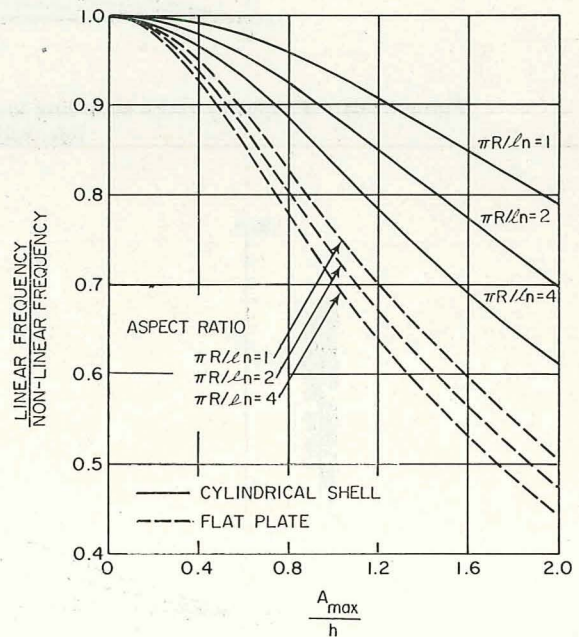


FIGURE 3.67.—Comparison of nonlinear response of a circular cylindrical shell with a flat plate; $n=10$. (After ref. 3.47)

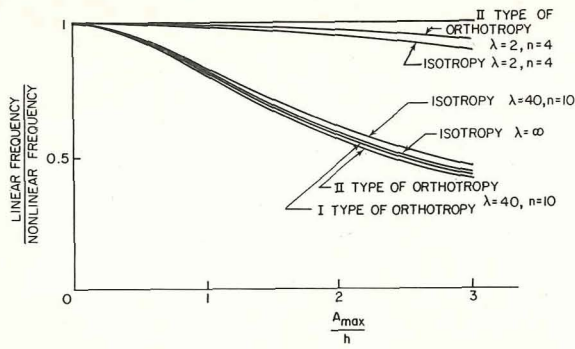


FIGURE 3.68.—Frequency ratio versus amplitude ratio for SD cylindrical shells; $R/h = 100$, $\lambda = m\pi R/l$. (After ref. 3.49)

Large amplitude vibrations of closed circular cylindrical shells ostensibly having shear diaphragm end conditions are also discussed in references 3.46 and 3.63 through 3.65.

3.3.4 Other End Conditions

Sun and Lu (ref. 3.65) is the only reference in the literature purporting to deal with closed circular cylindrical shells having end conditions other than shear diaphragms. Reference 3.65 briefly considers (as a special case of a conical shell) the instance when the constraint $u=0$ is added to the SD end conditions giving

$$u=v=w=M_n=0$$

at both ends. Shallow shell theory was employed, and Hamilton's principle was applied to obtain the nonlinear equations of motion. The only result obtained in reference 3.65 which has any relevance at all to this monograph is the *post-buckling* amplitude frequency relationship of the hardening nonlinearity type derived for the case of thermal loading.

3.3.5 Large Deflections of Open Cylindrical Shells

The only results available in the literature for the nonlinear motions of cylindrically curved shell panels are for the case when the edges are all nominally supported by shear diaphragms (i.e., the SD boundary conditions are exactly satisfied if the nonlinear terms in the functions for v , N_x , and M_x are neglected in the statement of the boundary conditions).

The earliest results were obtained by Reissner (ref. 3.46) using the shallow shell theory (i.e., eqs. (3.51) and (3.54)). Solution functions of the form

$$\begin{aligned} w(x,y,t) &= A(t) \sin \frac{\pi x}{l} \cos \frac{ny}{R} \\ \varphi(x,y,t) &= B(t) \sin \frac{\pi x}{l} \cos \frac{ny}{R} \end{aligned} \quad (3.89)$$

were assumed, and a variational procedure was followed to arrive at the following equation of motion:

$$\frac{d^2 A}{dt^2} + \omega_0^2 A + \omega_{0m}^2 \left(\frac{16n^2}{\pi^2 R} \right) \left[A^2 + \frac{2}{9} \left(\frac{16n^2}{\pi^2 R} \right) A^3 \right] = 0 \quad (3.90)$$

A perturbation technique was used to solve equation (3.90), yielding the following relationship for where ω_0 is the frequency according to linear bending theory; i.e.,

$$\rho h \omega_0^2 = D \left[\left(\frac{n}{R} \right)^2 + \left(\frac{\pi}{l} \right)^2 \right]^2 + \frac{Eh}{R^2} \frac{(\pi/l)^4}{[(n/R)^2 + (\pi/l)^2]^2} \quad (3.91)$$

and ω_{0m} is the frequency according to linear membrane theory; i.e.,

$$\rho h \omega_{0m}^2 = \frac{Eh}{R^2} \frac{(\pi/l)^4}{[(n/R)^2 + (\pi/l)^2]} \quad (3.92)$$

A perturbation technique was followed to arrive at the relationship between nonlinear frequency ω and amplitude A_{\max} as follows:

$$\left(\frac{\omega}{\omega_0} \right)^2 = 1 + \frac{1}{6} \frac{\omega_{0m}^2}{\omega_0^2} \left(1 - 5 \frac{\omega_{0m}^2}{\omega_0^2} \right) \left(\frac{16n^2}{\pi^2} \right) \left(\frac{h}{R} \right)^2 \left(\frac{A_{\max}}{h} \right)^2 \quad (3.93)$$

From equation (3.93) it is seen that the nonlinearity increases or decreases the frequency depending upon whether ω_{0m}/ω_0 is less than or greater than $1/\sqrt{5}$, or 0.45. Also, the nonlinear correction effect is strongly dependent upon the value of the circumferential wave number n .

Looking at the amplitude $A(t)$ in equation (3.89), it was shown in reference 3.46 to take the form (retaining only first order correction terms)

$$A(t) = A_0 \left\{ \cos \omega t - \frac{16n^2}{\pi^2} \left(\frac{h}{R} \right) \left(\frac{A_0}{h} \right) \left(\frac{\omega_{0m}^2}{\omega^2} \right) \left[\frac{1}{2} - \frac{1}{3} \cos \omega t - \frac{1}{6} \cos 2\omega t \right] \right\} \quad (3.94)$$

which takes the shape shown in figure 3.69, along with its components. This graph shows that the shell does not spend equal time intervals deflected outwards and deflected inwards. Rather, more than half of the cycle is spent during the inward deflection. Also, the inward deflection is larger than the outward deflection, the ratio of amplitudes being given by

$$\frac{A_{\text{inward}}}{A_{\text{outward}}} = 1 + \frac{32n^2}{3\pi^2} \left(\frac{h}{R} \right) \left(\frac{A_0}{h} \right) \left(\frac{\omega_{0m}^2}{\omega^2} \right) \quad (3.95)$$

Equation (3.90) was also obtained by Cummings (ref. 3.51) using the shallow shell equations and the Galerkin procedure. Integrating it gives

$$\left(\frac{d\psi}{dt} \right)^2 + \omega_0^2 \left[\psi^2 + \epsilon \left(\frac{2}{3} \psi^3 + \frac{1}{9} \psi^4 \right) \right] \quad (3.96)$$

where $\psi(t) = (16n^2/\pi^2 R) A(t)$ and $\epsilon = \omega_{0m}^2/\omega_0^2$. Equation (3.96) yields phase-plane diagrams as depicted in figure 3.70.

In reference 3.51 another approach was also taken wherein only the displacement function for w as given in the first of equations (3.89) is assumed, and the compatibility equation (3.54) is integrated to yield

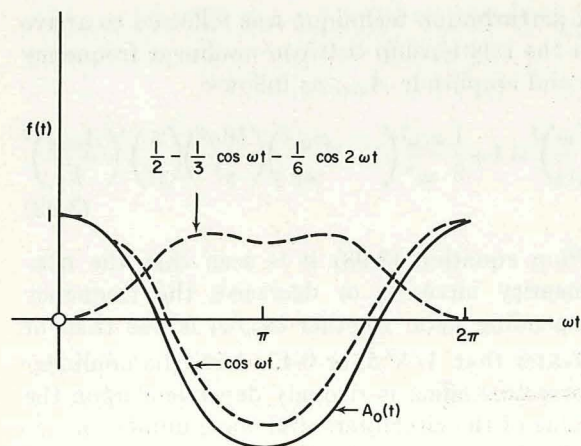


FIGURE 3.69.—Amplitude and its component parts as functions of time during nonlinear vibration. (After ref. 3.46)

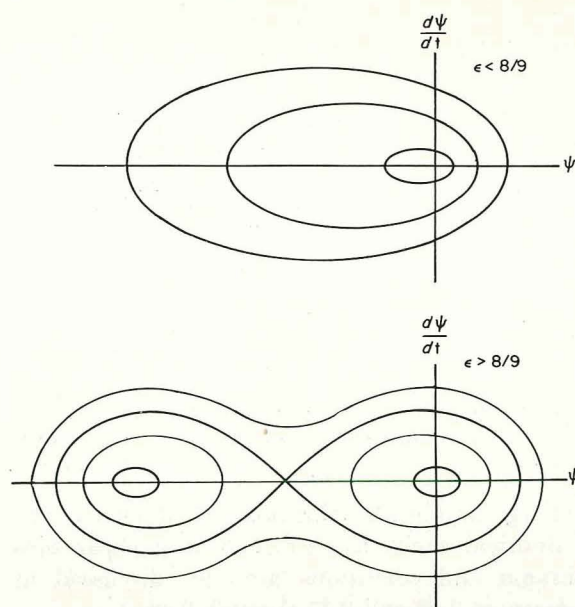


FIGURE 3.70.—Phase plane trajectories for nonlinear vibrations of a cylindrical shell according to Reissner's equation. (After ref. 3.51)

$$\varphi = E h A(t) \left\{ -\frac{1}{R} \left(\frac{\pi}{l} \right)^2 \left[\left(\frac{\pi}{l} \right)^2 + \left(\frac{h}{R} \right)^2 \right] \sin \frac{\pi x}{l} \cos \frac{ny}{R} + \frac{A(t)}{32} \left[\left(\frac{nl}{\pi R} \right)^2 \cos \frac{2\pi x}{l} - \left(\frac{\pi R}{nl} \right)^2 \cos \frac{2ny}{R} \right] \right\} \quad (3.97)$$

Applying the Galerkin procedure then gives the equation of motion

$$\frac{d^2\psi}{dt^2} + \omega_0^2 \left\{ \psi + \frac{7}{9} \epsilon \left[\psi^2 + \frac{9}{28} \left(\frac{\pi}{4} \right)^4 \mathcal{R}^{-4} (1 + \mathcal{R}^2)^2 (1 - \mathcal{R}^4) \psi^3 \right] \right\} = 0 \quad (3.98)$$

where ψ and ϵ are as defined in the preceding paragraph, and $\mathcal{R} = nl/\pi R$ is an "aspect ratio" for the panel. Depending upon \mathcal{R} , equation (3.98) can yield either hard spring or soft spring nonlinear response. The corresponding phase plane trajectories are displayed in figure 3.71. Figure 3.71 shows that the oscillations for a very long panel become less stable as the length of the panel increases. Comparisons of the assumptions made in the derivations of equations (3.90) and (3.98), the Galerkin and perturbation methods

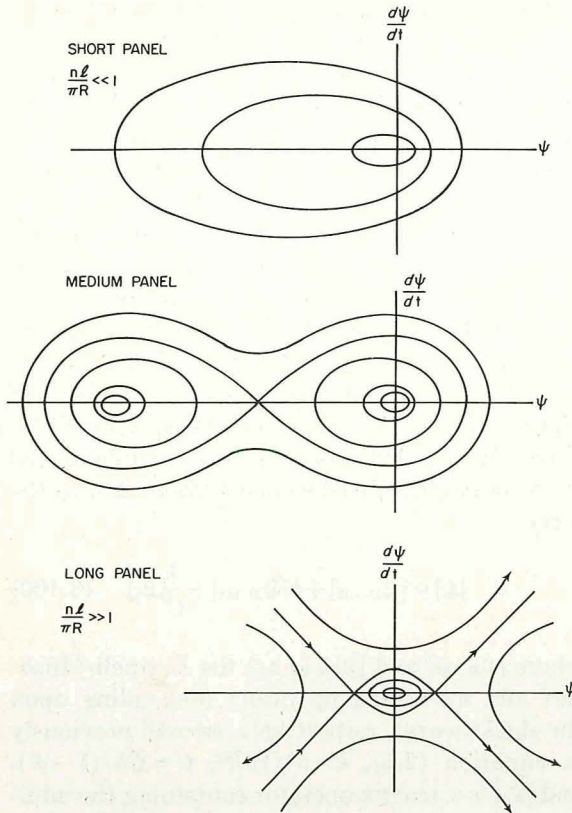


FIGURE 3.71.—Phase plane trajectories according to Cumming's equation. (After ref. 3.51)

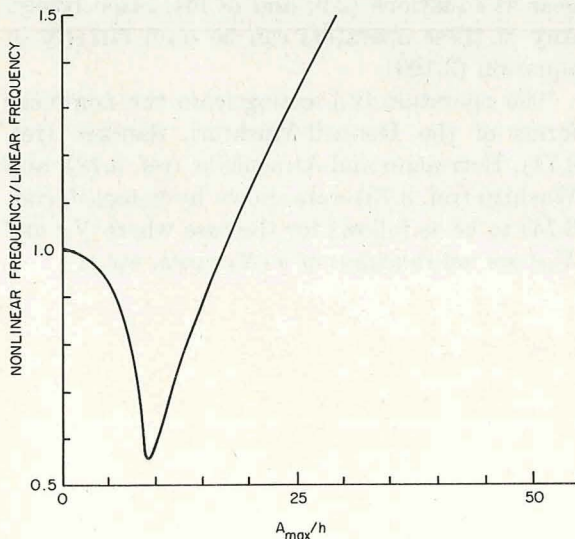


FIGURE 3.72.—Frequency ratio versus amplitude ratio; $l/R\theta_0=1$, $R/h=1000$, $\theta_0=22.9^\circ$, $\nu=0.3$. (After ref. 3.54)

for their solution, and the stability of the solutions are investigated further in reference 3.66.

Leissa and Kadi (ref. 3.54) obtained an equation similar to equation (3.98) for shallow shells having arbitrary, constant radii of curvature (see chapter 10 for further discussion) and obtained the amplitude-frequency curve shown in figure 3.72 for a cylindrical panel having $l/R\theta_0=1$ (square planform, with θ_0 as depicted in figure 2.141), $R/h=1000$, $\theta_0=0.4$ radians (22.9°), $\nu=0.3$, and $m=n=1$. The shell behaves initially as a soft spring but, as the amplitude is increased, a region of hard spring behavior is eventually reached.

The nonlinear vibrations of circular cylindrical shell panels are also discussed to a limited extent in references 3.67 through 3.70.

3.4 INITIAL STRESS

The voluminous results of chapter 2, as well as the preceding sections of this chapter, dealt with circular cylindrical shells under the assumption that the only stresses present in the shells are those arising from the vibratory motions themselves. In many (if not most) practical applications, shells are subjected to static loadings causing internal stress fields. The presence of such stresses affects the vibrational characteristics of the shells significantly.

There is, of course, no limit to the number of possible types of initial stress fields which may be encountered in practice. However, some of the most important ones are those in which the stresses are uniform (not varying with the spatial coordinates, x and θ). These loadings can occur, for example, for shells acting as axial or torsional load transmitting structures, for pressurized (internal or external) cylinders, or for shells spinning about their longitudinal axes. For this reason, as well as because of the relative mathematical simplicity, uniform initial stresses (or prestresses) have received much attention in the published literature.

Incorporating initial stress effects requires a generalization of the equations of motion. These changes will be discussed in section 3.4.1. Subsequent sections give extensive numerical results for various types of loadings, particularly those yielding uniform prestresses. It will be seen that, as usual, because of the relative mathematical

simplicity, the vast majority of references deal with shells having their boundaries supported by shear diaphragms. Straightforward methods for handling other edge conditions (including an exact procedure) are available but, as will be subsequently indicated, have been sparingly applied because of the great deal of effort required.

In the cases involving pressurization, except where otherwise indicated, it is assumed that the pressure is "constant directional"; i.e., the direction of the pressure does not change as the shell deforms during vibration, but remains in its initial direction.

3.4.1 Equations for Circular Cylindrical Shells

Consider a circular cylindrical shell acted upon by a static initial stress or prestress field σ_x^i , σ_θ^i , and $\sigma_{x\theta}^i$ which is in equilibrium. The initial stresses within the shell result from the solution of a static problem having prescribed loading and/or end conditions. In general the initial stress field is not uniform; i.e., $\sigma_x^i = \sigma_x^i(x, \theta)$, etc. During vibration the internal stresses in the shell consist of the initial stresses and the additional vibratory stresses σ_x , σ_θ , and $\sigma_{x\theta}$. The bending stresses in the initial loading state are usually neglected, and the displacements due to the membrane stresses are also usually neglected. These assumptions result in uncoupling of the initial and vibratory stresses; that is, there is no interaction between the prestress displacements and the vibratory stresses. Because the initial stress state is in equilibrium, the potential energy of the system in this state is taken as the reference level. Thus, the internal strain energy of the shell can be written as (cf., eq. (1.84))

$$U = \frac{1}{2} \int_V (\sigma_x e_x + \sigma_\theta e_\theta + \sigma_{x\theta} \gamma_{x\theta}) dV + \int_V (\sigma_x^i e_x + \sigma_\theta^i e_\theta + \sigma_{x\theta}^i \gamma_{x\theta}) dV \quad (3.99)$$

The vibratory stresses σ_x , σ_θ , $\sigma_{x\theta}$ are related to the vibratory strains by Hooke's law as indicated by equations (1.70). Next the strain-displacement relationships of a given shell theory (see sec. 1.4) must be substituted into equation (3.99). However, because the initial stresses may be large it is necessary to use the second-order, nonlinear strain-displacement equations (cf., section 3.3)

in the second integral of equation (3.99) while using only the linear relationships in the first integral. This maintains the proper homogeneity in the orders of magnitude of the terms in the integrands. Because the initial stresses are assumed to be membrane in nature (uniform through the thickness), it is sufficient to retain only the linear terms in the equations relating curvature changes to displacements. Applying Hamilton's principle (cf., eq. (2.13)) and taking the necessary variations with respect to the displacement components u , v , and w then straightforwardly leads to the desired equations of motion, which is the linear form of equation (2.3). However, in this case the matrix differential operator is generalized from equation (2.5) to the form

$$[\mathcal{L}] = [\mathcal{L}_{D-M}] + k[\mathcal{L}_{MOD}] + \frac{1}{C}[\mathcal{L}_i] \quad (3.100)$$

where $[\mathcal{L}_{D-M}]$ and $[\mathcal{L}_{MOD}]$ are the Donnell-Mushtari and modifying operators (depending upon the shell theory), respectively, as used previously in equation (2.5), $k = h^2/12R^2$, $C = Eh/(1-\nu^2)$, and $[\mathcal{L}_i]$ is a matrix operator containing the additional terms which account for the initial stresses. The $[\mathcal{L}_{D-M}]$ operator for isotropic and anisotropic materials is given by equations (2.7) and (3.12), respectively. Corresponding $[\mathcal{L}_{MOD}]$ operators appear as equations (2.9) and (3.14), respectively. Any of these operators can be used directly in equation (3.100).

The operators $[\mathcal{L}_i]$ arising from the nonlinear forms of the Donnell-Mushtari, Sanders (ref. 3.71), Herrmann and Armenakias (ref. 3.72), and Washizu (ref. 3.73) were shown by Sampath (ref. 3.74) to be as follows for the case where N_θ^i and $N_{x\theta}^i$ are not functions of θ ($N_\theta = \sigma_\theta^i h$, etc.):

Donnell-Mushtari:

$$[\mathcal{L}_i] = \begin{bmatrix} 0 & 0 & 0 \\ 0 & 0 & 0 \\ 0 & 0 & \begin{bmatrix} -\frac{\partial}{\partial s} \left(N_x^i \frac{\partial}{\partial s} \right) - N_\theta^i \frac{\partial^2}{\partial \theta^2} \\ -\frac{\partial}{\partial s} \left(N_{x\theta}^i \frac{\partial}{\partial \theta} \right) - N_{x\theta}^i \frac{\partial^2}{\partial s \partial \theta} \end{bmatrix} \end{bmatrix} \quad (3.101a)$$

Sanders:

$$[\mathcal{L}_i] = \begin{bmatrix} \frac{\partial}{\partial \theta} \left(\frac{N_x^i}{4} \frac{\partial}{\partial \theta} \right) + \frac{N_\theta^i}{4} \frac{\partial^2}{\partial \theta^2} & -\frac{\partial}{\partial \theta} \left(\frac{N_x^i}{4} \frac{\partial}{\partial s} \right) - \frac{N_\theta^i}{4} \frac{\partial^2}{\partial s \partial \theta} & 0 \\ -\frac{\partial}{\partial s} \left[\frac{1}{4} (N_x^i + N_\theta^i) \frac{\partial}{\partial \theta} \right] & \frac{\partial}{\partial s} \left[\frac{1}{4} (N_x^i + N_\theta^i) \frac{\partial}{\partial s} \right] - N_\theta^i & N_\theta^i \frac{\partial}{\partial \theta} + N_{x\theta}^i \frac{\partial}{\partial s} \\ 0 & N_\theta^i \frac{\partial}{\partial \theta} + 2N_{x\theta}^i \frac{\partial}{\partial s} + \frac{\partial N_{x\theta}^i}{\partial s} & \begin{bmatrix} -\frac{\partial}{\partial s} \left(N_x^i \frac{\partial}{\partial s} \right) - N_\theta^i \frac{\partial^2}{\partial \theta^2} \\ -\frac{\partial}{\partial s} \left(N_{x\theta}^i \frac{\partial}{\partial \theta} \right) - N_{x\theta}^i \frac{\partial^2}{\partial s \partial \theta} \end{bmatrix} \end{bmatrix} \quad (3.101b)$$

Herrmann-Armendak and Washizu:

$$[\mathcal{L}_i] = \begin{bmatrix} \Delta & 0 & 0 \\ 0 & \Delta - N_\theta^i & 2N_\theta^i \frac{\partial}{\partial \theta} + 2N_{x\theta}^i \frac{\partial}{\partial s} + \frac{\partial N_{x\theta}^i}{\partial s} \\ 0 & 2N_\theta^i \frac{\partial}{\partial \theta} + 2N_{x\theta}^i \frac{\partial}{\partial s} + \frac{\partial N_{x\theta}^i}{\partial s} & -(\Delta - N_\theta^i) \end{bmatrix} \quad (3.101c)$$

where

$$\Delta = \frac{\partial}{\partial s} \left(N_x^i \frac{\partial}{\partial s} \right) + N_\theta^i \frac{\partial^2}{\partial \theta^2} + N_{x\theta}^i \frac{\partial^2}{\partial s \partial \theta} + \frac{\partial}{\partial s} \left(N_{x\theta}^i \frac{\partial}{\partial \theta} \right)$$

and where $s = x/R$, as before. The $[\mathcal{L}_{MOD}]$ operator for the Herrmann-Armendak theory is the same as that of the Flügge theory. The $[\mathcal{L}_{MOD}]$ operator for the Washizu theory is the same as for the Goldenveizer-Novozhilov theory (ref. 3.74).

The initial stress matrix operator for the Flügge theory in the case of uniform N_x^i , N_θ^i , and $N_{x\theta}^i$ is (ref. 3.75)

$$[\mathcal{L}_i] = \begin{bmatrix} N_\theta^i \frac{\partial^2}{\partial \theta^2} + N_x^i \frac{\partial^2}{\partial s^2} + 2N_{x\theta}^i \frac{\partial^2}{\partial s \partial \theta} & 0 & -N_\theta^i \frac{\partial}{\partial s} \\ 0 & N_\theta^i \frac{\partial^2}{\partial \theta^2} + N_x^i \frac{\partial^2}{\partial s^2} + 2N_{x\theta}^i \frac{\partial^2}{\partial s \partial \theta} & N_\theta^i \frac{\partial}{\partial \theta} + 2N_{x\theta}^i \frac{\partial}{\partial s} \\ -N_\theta^i \frac{\partial}{\partial s} & N_\theta^i \frac{\partial}{\partial \theta} + 2N_{x\theta}^i \frac{\partial}{\partial s} & -N_\theta^i \frac{\partial^2}{\partial \theta^2} - N_x^i \frac{\partial^2}{\partial s^2} - 2N_{x\theta}^i \frac{\partial^2}{\partial s \partial \theta} \end{bmatrix} \quad (3.102)$$

The symmetry of the operator in equation (3.102) as well as the repetition of terms along the principal diagonal is striking in comparison with those given in equations (3.101).

In the case of *uniform* initial stresses the single nonvanishing term of the Donnell-Mushtari operator (eq. (3.101a)) simplifies to

$$-\left(N_x^i \frac{\partial^2}{\partial s^2} + 2N_{x\theta}^i \frac{\partial^2}{\partial s \partial \theta} + N_\theta^i \frac{\partial^2}{\partial \theta^2}\right) \quad (3.103)$$

which is the same as the terms on the diagonal of the Flügge operator (eq. (3.102)).

The initial stress operator for use with equation (2.9a) in equation (3.100) according to the Timoshenko theory (ref. 3.76) is

$$[\mathcal{L}_i] = \begin{bmatrix} 0 & -N_\theta^i \frac{\partial^2}{\partial s \partial \theta} & -N_\theta^i \frac{\partial}{\partial s} \\ 0 & N_x^i \frac{\partial^2}{\partial s^2} & 0 \\ 0 & 0 & -N_x^i \frac{\partial^2}{\partial s^2} \\ & & -N_\theta^i \left(1 + \frac{\partial^2}{\partial \theta^2}\right) \end{bmatrix} \quad (3.104)$$

for the case of uniform N_x^i and N_θ^i .

Voss (ref. 3.77) derived a form of the equations of motion according to the *Goldenveizer-Novozhilov* theory. In this case, for uniform N_x^i and N_θ^i and for $N_{x\theta}^i = 0$ the initial stress operator becomes

$$[\mathcal{L}_i] = \begin{bmatrix} 0 & -N_\theta^i \frac{\partial^2}{\partial s \partial \theta} & -N_\theta^i \frac{\partial}{\partial s} \\ 0 & N_x^i \frac{\partial^2}{\partial s^2} & 0 \\ 0 & N_\theta^i \frac{\partial}{\partial \theta} & -N_x^i \frac{\partial^2}{\partial s^2} \\ & & -N_\theta^i \frac{\partial^2}{\partial \theta^2} \end{bmatrix} \quad (3.105)$$

It is disturbing to note that this operator is unsymmetric, even though the modifying operator (2.9b) is symmetric. However, the Washizu equations (3.101c), which also use the $[\mathcal{L}_{MOD}]$ of the Goldenveizer-Novozhilov theory, are symmetric. As further examples of the great variety of shell theories employed in the literature, Fung,

Sechler, and Kaplan (refs. 3.78 and 3.79) used a set of equations of motion consisting of the $[\mathcal{L}_{MOD}]$ operator of Timoshenko theory, eq. (2.9a), and the same $[\mathcal{L}_i]$ operator used by Voss, eq. (3.105). Mugnier and Schroeter (ref. 3.80) followed a derivation similar to that of the Flügge theory, but arrived at a set of equations of motion for which both the $[\mathcal{L}_{MOD}]$ and $[\mathcal{L}_i]$ operators are different from any of those given previously in section 2.1.1 or in this section, respectively.

Reissner (ref. 3.81) derived the equations of motion for initially stressed (uniform N_x^i and N_θ^i only) circular cylindrical shells for the *membrane* theory. These are obtained by taking $k=0$ in equation (3.100) (including where it appears in $[\mathcal{L}_{D-M}]$ and using for $[\mathcal{L}_i]$:

$$[\mathcal{L}_i] = \begin{bmatrix} 0 & 0 & 0 \\ 0 & 0 & 0 \\ 0 & 0 & -N_x^i \frac{\partial^2}{\partial s^2} - N_\theta^i \left(1 + \frac{\partial^2}{\partial \theta^2}\right) \end{bmatrix} \quad (3.106)$$

3.4.2 Uniform Axial Prestress

A closed circular cylindrical shell having a uniform axial initial stress field is obtained by simply loading the ends of the shell with a uniform axial stress resultant as shown in figure 3.73. The

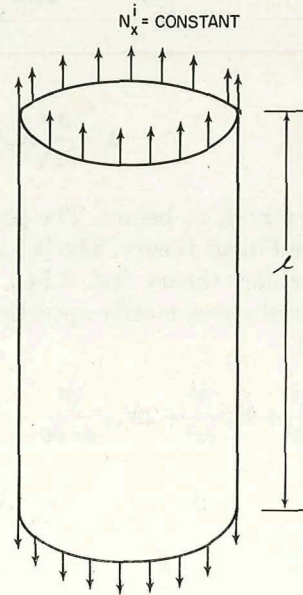


FIGURE 3.73.—Circular cylindrical shell subjected to uniform axial prestress.

resulting internal stress field is then simply given by $N_x^i = \text{constant}$, $N_\theta^i = N_{x\theta}^i = 0$, where N_x^i is positive in tension as indicated in the figure.

Consider first a shell supported at both ends by shear diaphragms. The boundary conditions for the vibratory force and moment resultants and displacement components are given by equations (2.33). As in the case of an unloaded shell, displacement functions taken in the form of equations (2.20) satisfy the boundary conditions exactly, provided λ is taken as $\lambda = m\pi R/l$. For the Donnell-Mushtari theory the operator $[\mathcal{L}_{MOD}]$ is null. Substituting the operators from equations (2.7) and (3.101a) and the displacement equations (2.20) into equation (3.100) yields a set of equations for the eigenfrequencies ω which is the same as equation (2.21) except that the element in the third row and third column is now changed to

$$1 + k(\lambda^2 + n^2) + N_x^i \frac{\lambda^2}{C} - \Omega^2 \quad (3.107)$$

where $\Omega^2 = \omega^2 R^2 \rho(1 - \nu^2)/E$. Further, let the tangential inertia be neglected, an assumption which is often justifiable, especially when the Donnell-Mushtari theory is used (see sec. 2.3.4). Then Ω^2 disappears from the coefficient matrix of equation (2.21), except for the term given by equation (3.107), and an explicit equation for the frequency parameters can be written as

$$\Omega^2 - N_x^i \frac{\lambda^2}{C} = \frac{K_0 + k \Delta K_0}{\bar{K}_1} \quad (3.108)$$

where K_0 , ΔK_0 , and \bar{K}_1 are given in equation (2.36), table 2.1, and equation (2.43), respectively. The significance of equation (3.108) is that, if tangential inertia is neglected, the numerical results for the frequency parameters of circular cylindrical shells supported by shear diaphragms obtained using the Donnell-Mushtari theory are directly applicable to the case where uniform axial prestress is present; one simply replaces Ω^2 by $\Omega^2 - N_x^i \lambda^2/C$ ($C = Eh/(1 - \nu^2)$, $\lambda = m\pi R/l$).

The above statement is even capable of further generalization. Consider, for example, the case when the shell is orthotropic. Then the Donnell-Mushtari equations of motion are given by equations (3.8). Again, if tangential inertia is neglected, then it is clear that numerical results for orthotropic shells supported by shear

diaphragms can be used simply by replacing $\omega^2 R^2 \rho(1 - \nu_x \nu_y)/E_x$ by $\omega^2 R^2 \rho(1 - \nu_x \nu_y)E_x - N_x^i \lambda^2/C$.

Clearly, if tangential inertia is neglected the same useful simplification can be made for the membrane theory in the case of initial axial stress. From equation (3.106) it is seen that equation (3.108) also applies to membrane theory by taking $k = 0$.

It is interesting to note that the Flugge equations permit a similar manipulation in the case where the tangential inertia terms are retained. Looking at the Flugge initial stress operator given by equation (3.102) it is seen that in the case where $N_\theta^i = N_{x\theta}^i = 0$ that identical terms $N_x^i \partial^2/\partial s^2$ in each element of the principal diagonal are all that remain. Thus, in formulating the characteristic determinant for the case of the shell supported by shear diaphragms by means of equations (3.100), (2.7), (2.9d), and (2.20) it is found that the same determinant arises except that Ω^2 is replaced by $\Omega^2 - N_x^i \lambda^2/C$. This fortunate circumstance was pointed out by Bozich (ref. 3.82) and permits the direct utilization of the extensive data presented earlier in those tables and figures of section 2.3 which result from the Flugge theory. One simply replaces Ω^2 by $\Omega^2 - N_x^i \lambda^2/C$ wherever it appears.

Because of the identical mode shapes of free vibration and classical, linear buckling for the case of shear diaphragm end supports, it is easy to show that the frequency ω can be expressed as

$$\omega^2 = \omega_0^2 \left[1 + \frac{N_x^i}{(N_x^i)_{cr}} \right] \quad (3.109)$$

where ω_0 is frequency in the absence of initial stress and $(N_x^i)_{cr}$ is the critical value of N_x^i which causes buckling. If one were to plot ω/ω_0 versus $N_x^i/(N_x^i)_{cr}$, according to equation (3.109) it is clear that the curve would be a parabola having its vertex at $N_x^i/(N_x^i)_{cr} = -1$ as shown in figure 3.74. A positive (tensile) N_x^i stress resultant field increases the natural frequency without limit, whereas negative (compressive) values of N_x^i decrease the frequency until, at $\omega = 0$, buckling ensues.

Nikulin (ref. 3.83) used the Donnell-Mushtari equations including tangential inertia and the exact displacement functions (2.20) to obtain a characteristic equation for the shell supported

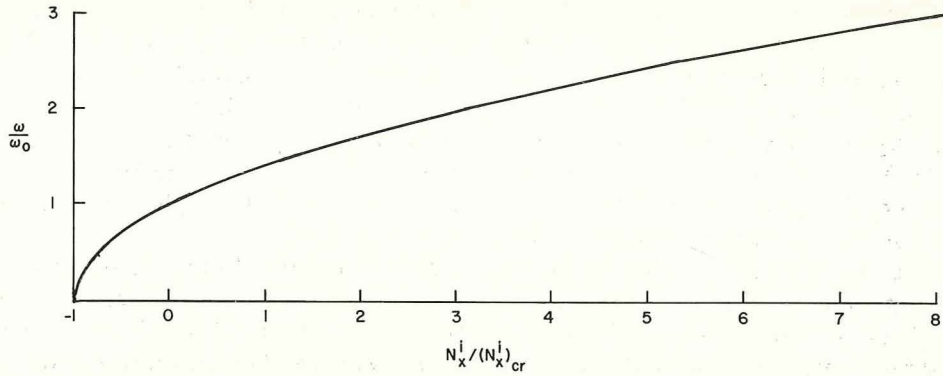


FIGURE 3.74.—Frequency ratio versus axial initial stress ratio; shear diaphragm end conditions.

by shear diaphragms at both ends. The characteristic equation is

$$\Omega^6 - \left[K_2 + \frac{\lambda^2}{C} N_x^i \right] \Omega^4 + \left[K_1 + \left(\frac{3-\nu}{2} \right) (\lambda^2 + n^2) \frac{\lambda^2}{C} N_x^i \right] \Omega^2 - \left[K_0 - \left(\frac{1-\nu}{2} \right) (\lambda^2 + n^2) \frac{\lambda^2}{C} N_x^i \right] = 0 \quad (3.110)$$

where K_0 , K_1 , and K_2 are the Donnell-Mushtari coefficients in the absence of initial stress, given in equations (2.36). The solution of equation (3.110) for its lowest root Ω^2 was accomplished in references 3.83 and 3.84 by the commonly used device of neglecting the terms containing Ω^6 and Ω^4 (see sec. 2.3.5) and by neglecting $k(\lambda^2 + n^2)^2$ and $\lambda^2 N_x^i / C$ with respect to unity to give

$$\Omega^2 = \frac{(1-\nu^2)\lambda^4 + k(\lambda^2 + n^2)^4 + \frac{\lambda^2}{C} N_x^i (\lambda^2 + n^2)^2}{(\lambda^2 + n^2)^2 + n^2 + (3+2\nu)\lambda^2} \quad (3.111)$$

$$= \Omega_0^2 \left(1 + \beta_1 \frac{N_x^i}{Eh} \right) \quad (3.112)$$

where Ω_0^2 is the frequency parameter in the absence of initial stress and β_1 is defined by

$$\beta_1 = \frac{(\lambda^2 + n^2)^2 / \lambda^2}{1 + \frac{k}{(1-\nu^2)} \frac{(\lambda^2 + n^2)^2}{\lambda^2}} \quad (3.113)$$

It is interesting to note that Nikulin in reference 3.84 arrived at equations (3.111) and (3.112) by

using an altogether different shell theory (see the discussion in sec. 3.4.3).

Variation of the parameter β_1 with R/h and n is shown in figure 3.75 for $l/R=2$ and $\nu=0.3$. Numerical results showing the behavior of the frequency (cps) with the initial stress and n were also given in references 3.83 and 3.84 for shells having $R/h=500$, $h=0.1$ cm., $E=2 \times 10^6$ dyne/cm², $\nu=0.3$, $m=1$, and $\rho=8 \times 10^{-6}$ dyne-sec²/cm⁴ and are presented in figures 3.76 through 3.80 for $l/R=1/2, 1, 2$, and 6.

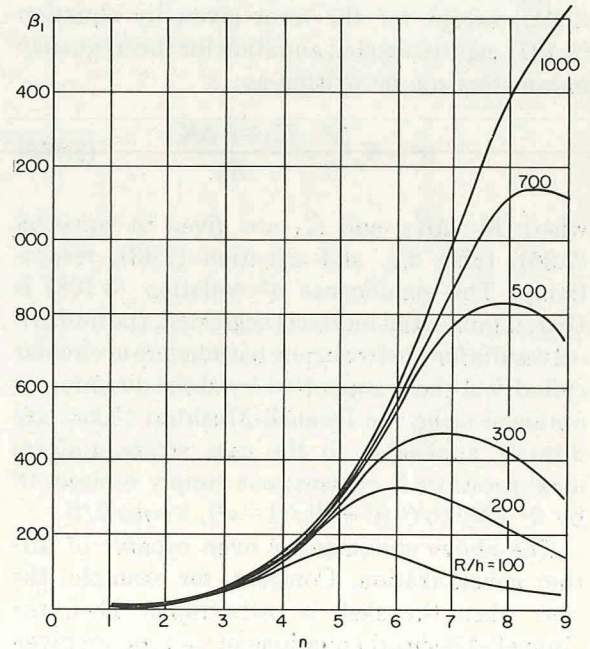


FIGURE 3.75.—Variation of the parameter β_1 used in equation (3.112) with R/h and n for $l/R=2$. (After refs. 3.83 and 3.84)

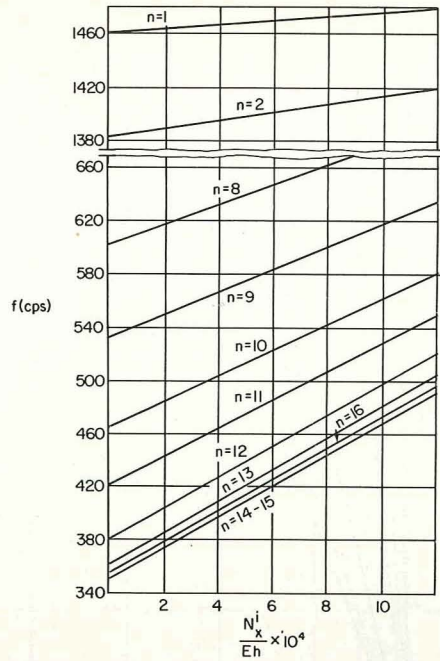


FIGURE 3.76.—Frequencies (cps) of axially prestressed SD-SD shells for $l/R=1/2$; other dimensions in text. (After refs. 3.83 and 3.84)

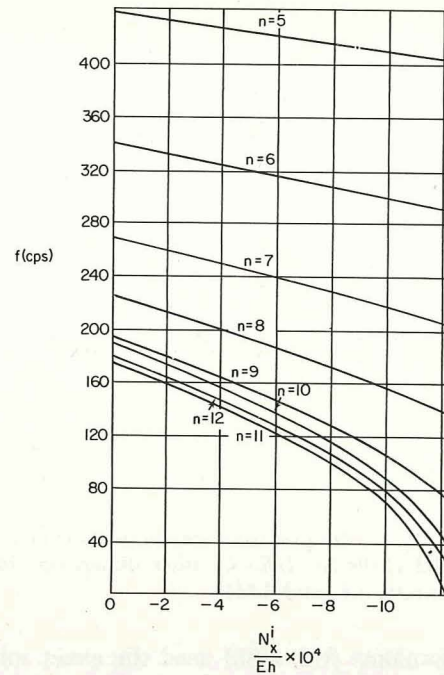


FIGURE 3.78.—Frequencies (cps) of axially prestressed SD-SD shells for $l/R=1$ (compressive stress); other dimensions in text. (After refs. 3.83 and 3.84)

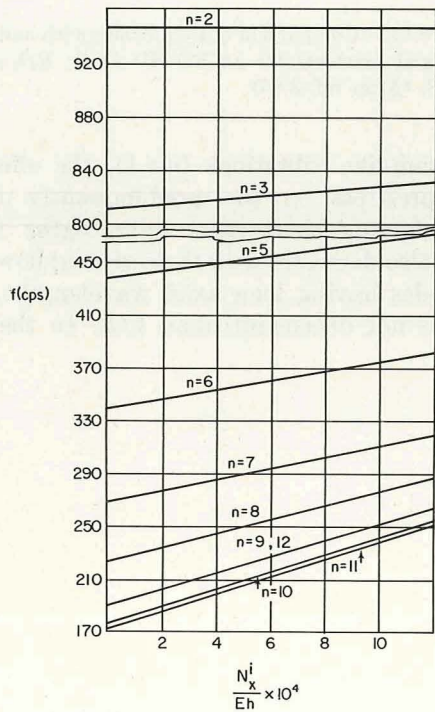


FIGURE 3.77.—Frequencies (cps) of axially prestressed SD-SD shells for $l/R=1$ (tensile stress); other dimensions in text. (After refs. 3.83 and 3.84)

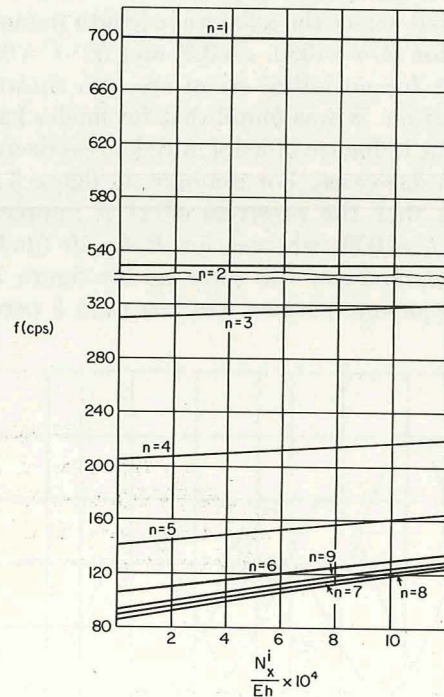


FIGURE 3.79.—Frequencies (cps) of axially prestressed SD-SD shells for $l/R=2$; other dimensions in text. (After refs. 3.83 and 3.84)

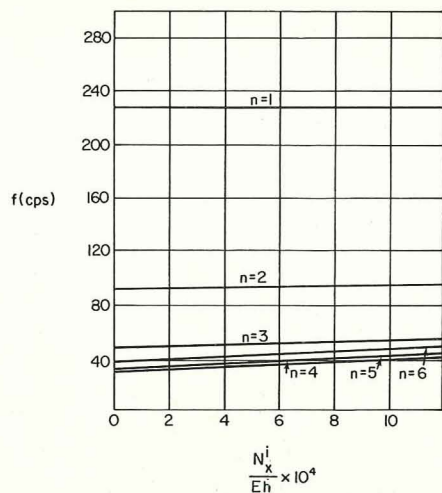


FIGURE 3.80.—Frequencies (cps) of axially prestressed SD-SD shells for $l/R=6$; other dimensions in text. (After refs. 3.83 and 3.84)

Armenakias (ref. 3.85) used the exact solution (2.20) in the Herrmann-Armenakias equations to obtain numerical results for axially prestressed SD-SD shells. These are shown in figure 3.81, where the frequency parameter $\omega h \sqrt{2\rho(1+\nu)/E}$ is plotted versus the axial wave length parameter mR/l for $R/h=1000$, $\nu=0.3$, and $N_x^i/C=0.001$. Results for no initial stress are also shown for comparison. It was found that for modes having $n \neq 1$ the influence of axial initial stress decreases as R/h decreases. For example, in figure 3.82 it is seen that the prestress effect is appreciable for $R/h=1000$, whereas for $R/h=20$ (and the other parameters the same as for figure 3.82) the frequency increase was less than 5 percent.

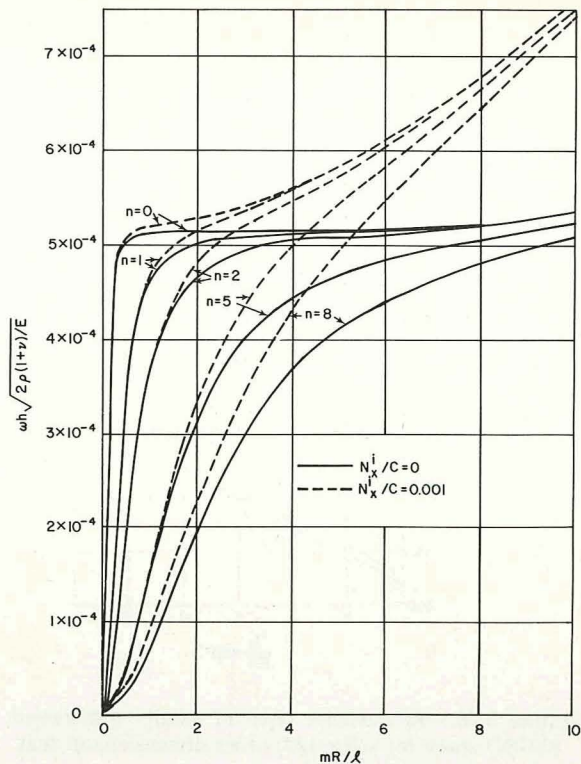


FIGURE 3.81.—Comparison of frequencies with and without axial prestress for an SD-SD shell; $R/h=1000$, $\nu=0.3$. (After ref. 3.85)

For beam-like vibrations ($n=1$), the effect of axial prestress on the predominantly radial modes having short axial wavelengths (large mR/l) also decreases as R/h decreases; however, for modes having long axial wavelengths, this effect is not dependent upon h/R . In the case

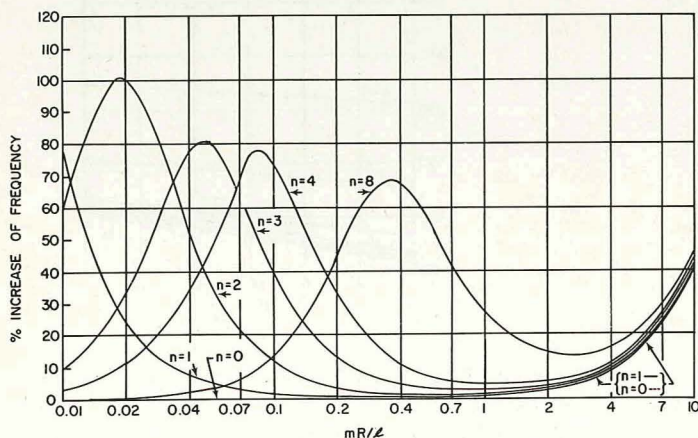


FIGURE 3.82.—Relative effect of axial prestress ($N_x^i/C = 0.001$) on the frequency of an SD-SD shell; $R/h = 1000$, $\nu = 0.3$. (After ref. 3.85)

of thin shells ($R/h=1000$) vibrating in modes having short axial wave lengths, the relative effect of initial stress on the frequency is not dependent upon n inasmuch as in these modes the effect of the axial wavelength on ω is of greater significance than that of the circumferential wavelength. As seen in figure 3.82, in the other frequency spectrum range, the relative effect of axial prestress is negligible for axisymmetric ($n=0$) modes, but can become large for flexural modes. The value of mR/l at which this relative effect is a maximum increases as n increases.

Experimental results for a shell subjected to compressive axial initial stress were obtained by Herrmann and Shaw (ref. 3.86) for a stainless steel SD-SD shell having $R=1.50$ in, $h=0.010$ in, and $l=29$ in. These are shown in figure 3.83 for a compressive axial force of 2000 lb. Analytical results calculated from equation (3.156) of section 3.4.4 are also given. To show the change in frequencies due to the initial stress, figure 3.84 is also given for the case of no initial stress.

Very little has been reported in the literature for axially loaded shells having boundary conditions other than shear diaphragms, although the same exact, straightforward procedure could be followed as for unloaded shells (see sec. 2.4).

Ivanyuta and Finkelshteyn (ref. 3.87) used the Donnell-Mushtari shell equations and the Bubnov-Galerkin approximate procedure with beam functions (cf., secs. 2.4 and 2.4.1) to arrive at the following general formula for the frequency parameters $\Omega = \omega R \sqrt{\rho(1-\nu^2)/E}$ of axisymmetric modes:

$$\Omega = k \frac{l_4}{l_5} + (1-\nu^2) \frac{l_2 l_3}{l_1 l_5} + \frac{N_x^i}{Eh} (1-\nu^2) \frac{l_6}{l_5} \quad (3.114)$$

where l_1, \dots, l_5 are the integrals of beam functions as defined by equations (2.71) and

$$l_6 = \int_0^l X_m'' X_m dx \quad (3.115)$$

(see the discussion in sec. 2.4). Equation (3.114) permits the evaluation of frequencies for shells having arbitrary edge conditions and axial initial stress.

Nikulin (ref. 3.84) obtained results for a circular cylindrical shell clamped at both ends and subjected to an initial axial load. The shell di-

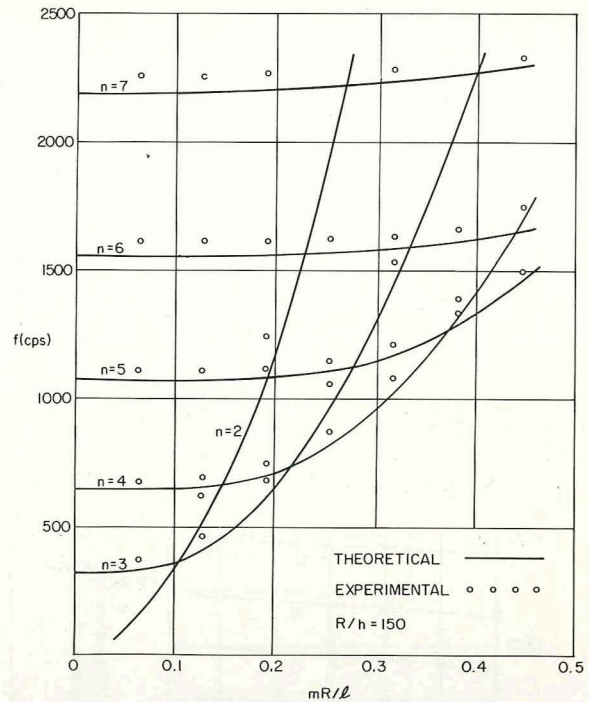


FIGURE 3.83.—Theoretical and experimental frequencies for an SD-SD shell (dimensions given in text) subjected to a compressive initial axial force. (After ref. 3.86)

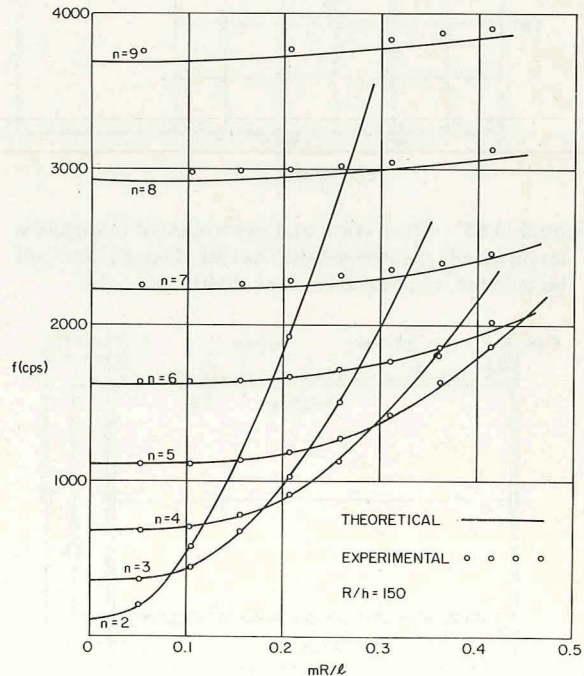


FIGURE 3.84.—Frequencies for the shell of figure 3.83 without initial stress. (After ref. 3.86)

mensions used were $h=0.5$ mm., $l=238$ mm., $R=118$ mm. and the material properties were given by

$$E=2 \times 10^6 \text{ dyne/cm}^2, \nu=0.3$$

$$\rho=8 \times 10^{-6} \text{ dyne-sec}^2/\text{cm}^4$$

Theoretical and experimental results for frequencies (cps) versus axial initial stress are compared in figure 3.85 for various circumferential wave numbers n . Similar results were obtained for a shell having structural orthotropy (integral ring stiffeners) as shown in figure 3.86 for $H=2.5$ mm. These results are given in figure 3.87.

Miserentino and Vosteen (ref. 3.88) presented

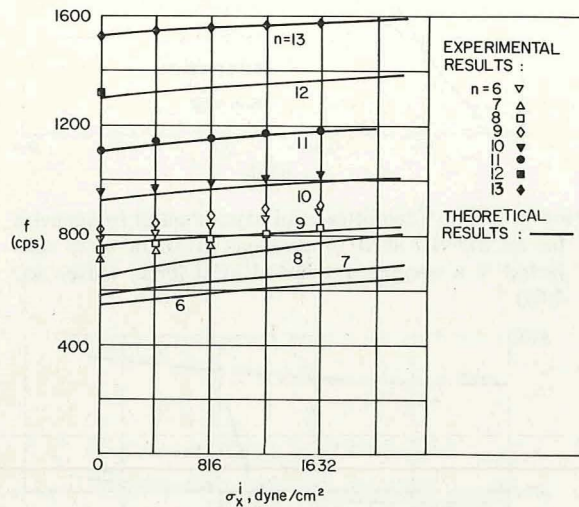


FIGURE 3.85.—Theoretical and experimental frequencies for an axially prestressed shell having clamped-clamped boundaries; dimensions in text. (After ref. 3.84)

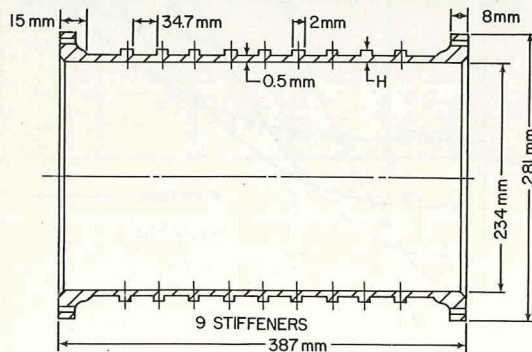


FIGURE 3.86.—Dimensions of shell having structural orthotropy. (After ref. 3.84)

experimental results for a clamped-clamped shell. Model 324 described by the physical properties listed in table 3.12 (see section 3.4.4) was tested.

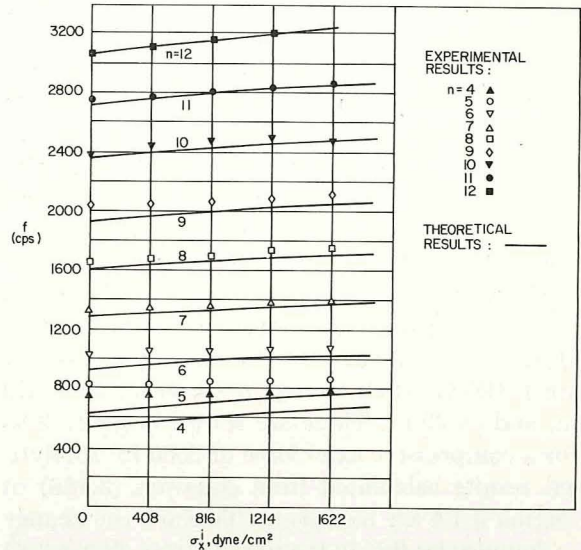


FIGURE 3.87.—Theoretical and experimental frequencies for the orthotropic shell of figure 3.86 subjected to axial initial stress. (After ref. 3.84)

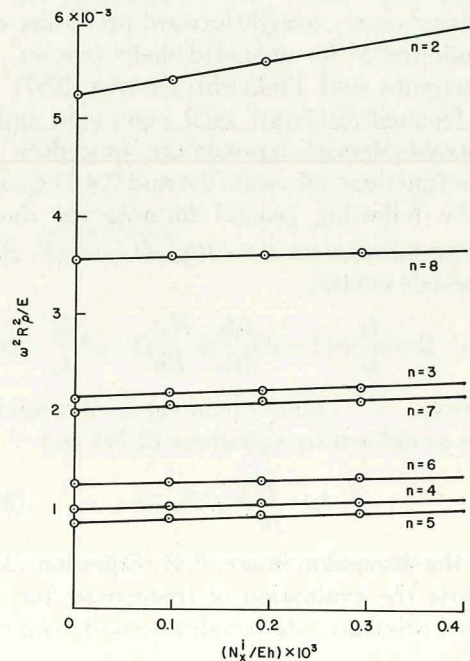


FIGURE 3.88.—Experimentally determined frequency parameters for an axially prestressed, clamped-clamped shell. (After ref. 3.88)

The frequency parameter $\omega^2 R^2 \rho / E$ is plotted versus the axial tension parameter N_z^i / Eh in figure 3.88 for $m=1$ and various values of n .

Free vibrations of axially prestressed circular cylindrical shells are also discussed in references 3.89 through 3.93.

3.4.3 Uniform Circumferential Prestress

Uniform circumferential initial stresses can arise from either of the following causes:

- (1) Internal or external pressure
- (2) Constant velocity rotation about the axis of the cylindrical shell.

In the former case an internal pressure p_0 causes a stress resultant $N_\theta^i = p_0 R$, whereas an external pressure p_0 causes $N_\theta^i = -p_0 R$, where p_0 is a positive number. In the case of rotation it is assumed that the spin frequency ω_s is small compared with the vibration frequency, so that Coriolis and gyroscopic effects can be ignored. Then $N_\theta^i = \rho h \omega_s^2 R^2$. Both cases are only truly valid for the infinite shell, for the effect of edge conditions on a finite length shell would alter the uniformity of the static initial stress field. However, for thin shells (large R/h) and certain types of edge constraints, the nonuniformity in membrane initial stress are localized to the vicinity of the edges, and the gross vibrational characteristics of the shell (particularly, frequency) are not greatly affected and the results contained in this section can be meaningfully applied.

The same logic which led to the simple formula (3.108) in the preceding section dealing with axial prestress can also be applied to circumferential prestress. That is: (1) taking the case of the circular cylindrical shell supported at both ends by shear diaphragms, (2) employing the Donnell-Mushtari shell theory (see section 2.3.1 for information concerning its range of applicability); and (3) neglecting tangential inertia leads to the simple formula

$$\Omega^2 - N_\theta^i \frac{n^2}{C} = \frac{K_0 + k \Delta K_0}{\bar{K}_1} \quad (3.116)$$

which is of the same form as equation (3.108). The statements made in the preceding section dealing with the usefulness of equation (3.108) apply here to equation (3.116) as well. That is, a

great deal of the numerical results available in chapter 2 and elsewhere can be used directly as the right-hand side of equation (3.116). Furthermore, from equation (3.116) it is clear that the effect of positive (tensile) circumferential initial stress is to increase the frequency, that negative (compressive) N_θ^i decreases the frequency and can lead to zero frequency (buckling), and that the effects of initial stress become more pronounced with increasing circumferential wave number n .

Another characteristic behavior for circumferentially prestressed shells can be seen from equation (3.116). As seen in chapter 2, unloaded shells *usually* (depending upon h/R , l/R , etc.) have fundamental (lowest) frequencies occurring at values of n greater than unity (cf., figs. 2.19 through 2.22). Equation (3.116) shows that the effect of tensile N_θ^i is to decrease the value of n at which the fundamental frequency of the loaded shell occurs, whereas compressive N_θ^i increases the circumferential wave number of the fundamental frequency.

It would appear from equation (3.116) that circumferential prestress has no effect upon the axisymmetric ($n=0$) modes. However, it must be remembered that the Donnell-Mushtari theory is generally not considered applicable for small values of n (see sec. 2.3.1) even though acceptable results for vibration frequencies of unloaded shells having small l/R ratios are seemingly given. Further, looking at the matrix operators for initial stresses according to the other theories (eqs. 3.101 and 3.102) it is seen in each of them that there are terms containing N_θ^i which are *not* multiplied by a derivative with respect to θ . Thus, the effect of N_θ^i does not vanish in the other theories for $n=0$.

From equation (3.106) it is seen that for the *membrane* theory equation (3.116) is replaced by

$$\Omega^2 - N_\theta^i \frac{(n^2 - 1)}{C} = \frac{K_0}{\bar{K}_1} \quad (3.117)$$

Section 3.4.2 shows that the Flügge theory *including* tangential inertia permits the direct application of results for unloaded shells to problems of axially loaded, SD-SD shells. Because of the appearance of off-diagonal terms involving N_θ^i in equation (3.102) there is no equivalent simple replacement for the case of circumferential initial stress.

Nikulin (ref. 3.84) analyzed SD-SD shells subjected to circumferential prestress. A shell theory was used which resembles the Love-Timoshenko theory except that $(1-\nu)\partial^2/\partial s^2 + \partial^2/\partial \theta^2$ is replaced by ∇^2 (i.e., ν is neglected relative to unity in the first term) in the element of the second row and second column of the modifying differential operator given by equation (2.9a). The initial stress matrix operator $[\mathcal{L}_i]$ (see eq. (3.100)) corresponding to this theory was found in reference 3.84 to be (for uniform initial stresses)

$$[\mathcal{L}_i] = \begin{bmatrix} N_{x\theta}^i \frac{\partial^2}{\partial s \partial \theta} & (N_x^i - N_\theta^i) \frac{\partial^2}{\partial s \partial \theta} - N_{x\theta}^i \frac{\partial^2}{\partial s^2} & (N_x^i - N_\theta^i) \frac{\partial}{\partial s} \\ N_\theta^i \frac{\partial^2}{\partial s \partial \theta} & N_x^i \frac{\partial^2}{\partial s^2} + 2N_{x\theta}^i \frac{\partial^2}{\partial s \partial \theta} & 2N_{x\theta}^i \frac{\partial}{\partial s} \\ 0 & 2N_{x\theta}^i \frac{\partial}{\partial s} & -N_x^i \frac{\partial^2}{\partial s^2} - N_\theta^i \left(1 + \frac{\partial^2}{\partial \theta^2}\right) - 2N_{x\theta}^i \frac{\partial^2}{\partial s \partial \theta} \end{bmatrix} \quad (3.118)$$

Tangential inertia was retained. Using the exact displacement functions (eq. (2.20)) led to the following formula for frequency parameters of SD-SD shells:

$$\Omega^2 = \frac{(1-\nu^2)\lambda^4 + k(\lambda^2 + n^2)^4 + \frac{(n^2-1)}{C} N_\theta^i (\lambda^2 + n^2)^2}{(\lambda^2 + n^2)^2 + n^2 + (3+2\nu)\lambda^2} \quad (3.119)$$

Equation (3.119) is comparable to equation (3.111) for axially loaded shells and can be rewritten as

$$\Omega^2 = \Omega_0^2 \left(1 + \beta_2 \frac{N_\theta^i}{Eh}\right) \quad (3.120)$$

where

$$\beta_2 = \frac{(n^2-1)(\lambda^2 + n^2)^2}{\lambda^4 + k(\lambda^2 + n^2)^4} \quad (3.121)$$

comparable to equation (3.113). Variation of the parameter β_2 with R/h and n is shown in figure 3.89 for $l/R=2$ and $\nu=0.3$. Again, from equations (3.119) and (3.120) it is clear that positive values of N_θ^i increase the free vibration frequencies, whereas negative values decrease them. It is interesting to note that in this case (*including* tangential inertia) the theory used gives the result that circumferential initial stress has no effect on the vibration frequencies for $n=1$ modes (in contrast to $n=0$ modes when the Donnell-Mushtari theory is used and tangential inertia is neglected, as seen earlier in this section).

The frequency parameter can also be expressed as

$$\Omega^2 = \Omega_0^2 [1 + N_\theta^i / (N_\theta^i)_{cr}] \quad (3.122)$$

where $(N_\theta^i)_{cr}$ is the critical value of circumferential initial stress which causes buckling. In figure 3.90 a plot of the frequency ratio ω/ω_0 versus $N_\theta^i / (N_\theta^i)_{cr}$ is given for various circumferential wave numbers n . The particular shell upon which figure 3.90 is based has the following dimensions and physical properties: $R/h=500$, $l/R=2$, $h=0.1$ cm, $E=2 \times 10^6$ dyne/cm², $\nu=0.3$, and $\rho=8 \times 10^{-6}$ dyne-sec²/cm⁴. In this case the critical buckling load, as can be seen in the figure, occurs for $n=9$ and has the value

$$(N_\theta^i)_{cr} = \frac{0.92}{(1-\nu^2)^{3/4}} \left(\frac{h}{l}\right) Eh \sqrt{\frac{h}{R}} \quad (3.123)$$

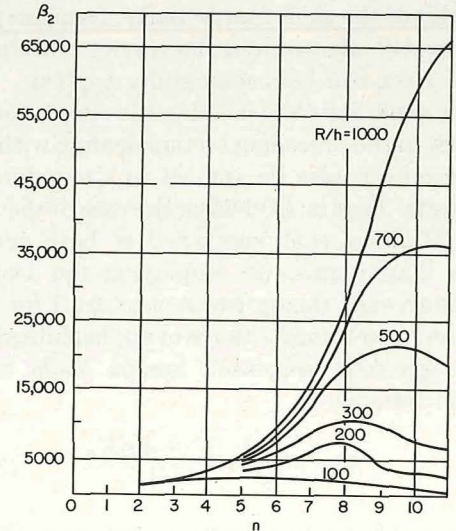


FIGURE 3.89.—Variation of the parameter β_2 used in equation (3.120) with R/h and n for $l/R=2$. (After ref. 3.84)

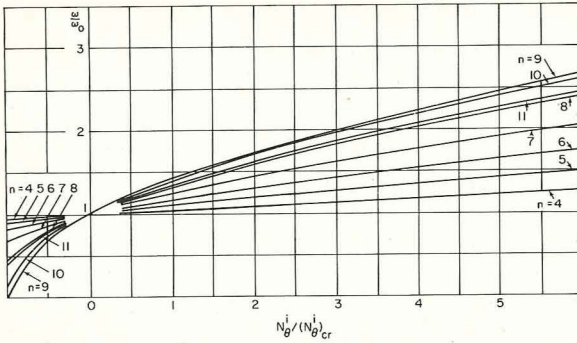


FIGURE 3.90.—Frequency ratio versus circumferential initial stress ratio for an SD-SD shell; dimensions in text. (After ref. 3.84)

Bleich and Baron (ref. 3.94) used an energy method to arrive at the following formula for frequencies of circumferentially prestressed SD-SD shells:

$$\omega^2 = \omega_0^2 + B \left(\frac{N_{\theta}^i}{\rho h R^2} \right) \quad (3.124)$$

The parameter B is a function of l/R and n and was tabulated in reference 3.94 over ranges of these ratios. This table is repeated as table 3.10. It is interesting to note that these results include negative values of B in most cases for $n=1$, indi-

TABLE 3.10.—Values of B for Equation (3.124) for Circumferentially Prestressed SD-SD Shells

$\frac{l}{R}$	n			
	1	2	3	4
1.00	0.282	2.604	7.108	13.86
1.25	.111	2.362	6.956	13.81
1.50	-.0427	2.222	6.906	13.82
1.75	-.0457	2.152	6.903	13.85
2.00	-.212	2.126	6.922	13.89
2.25	-.240	2.123	6.947	13.92
2.50	-.248	2.132	6.973	13.95
2.75	-.245	2.147	6.997	13.97
3.00	-.236	2.165	7.019	13.99
3.50	-.211	2.200	7.056	14.02
4.00	-.185	2.231	7.083	14.04
5.00	-.140	2.278	7.120	14.07
6.00	-.107	2.310	7.143	14.08
7.00	-.0842	2.330	7.157	14.09
8.00	-.0672	2.345	7.166	14.10
9.00	-.0547	2.356	7.173	14.10
10.00	-.0452	2.364	7.178	14.10

cating that positive N_{θ}^i cause decreases in the frequencies in these cases, and vice versa.

Armenàkas (ref. 3.85) used the exact solution (2.20) in the Herrmann-Armenàkas equations to obtain numerical results for SD-SD shells circumferentially prestressed due to prestress. Particular attention was paid to comparing the differences arising between considering the pressure to be either constant directional or normal to the surface (hydrostatic). The corresponding initial stress terms and characteristic equations are given in a more generalized form (including axial prestress as well) in section 3.4.4. According to this theory, circumferential initial stress does not influence the axisymmetric ($n=0$) modes of free vibration. Figure 3.91 depicts results for the frequency parameter $\omega h \sqrt{2\rho(1+\nu)/E}$ versus the axial wavelength parameter mR/l for the beam-like ($n=1$) modes of shells having $N_{\theta}^i/C=0.001$, $R/h=100$, 200, and 1000 and $\nu=0.3$. Hydrostatic and constant directional frequencies are also

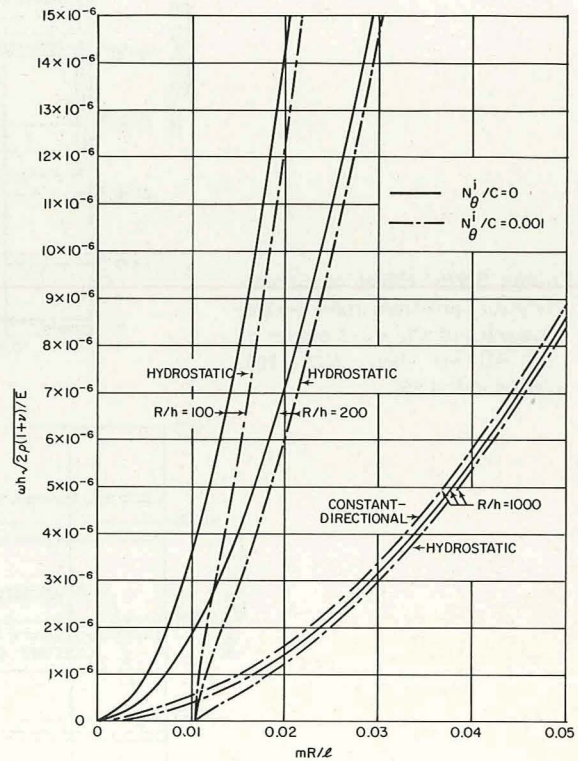


FIGURE 3.91.—Comparison of effects of hydrostatic, constant directional and no circumferential prestress upon the frequencies of the beam like ($n=1$) modes of an SD-SD shell. (After ref. 3.85)

compared with the case of no initial stress. According to this plot, internal pressure *decreases* the frequency of this mode, whereas constant directional internal pressure *increases* the frequency; this effect becomes negligible for large mR/l ($mR/l > 5$). However, the effect becomes very significant for small mR/l ; the frequency can be decreased to zero, indicating that the shell reaches a condition of instability due to *internal* pressure. The critical pressure is $E\pi^2Rh/l^2$, and is independent of the R/h ratio. The corresponding critical mR/l ratio for $N_\theta^i/C=0.001$ is 0.0102. It must be remembered that this phenomenon assumes the absence of axial initial stress.

The effect of the circumferential prestress upon the lobar-type flexural modes ($n=2,3,4$) can be seen in figures 3.92, 3.93, and 3.94. It is clear that internal pressure increases the frequency for these modes, regardless of whether the pressure is considered to be hydrostatic or constant directional. The effect is larger for large R/h and for small mR/l . For example, it was found in reference 3.85 that the frequency of a steel shell having $R/h=1000$ and $mR/l=0.03$ subjected to an internal hydrostatic pressure of 1 psi and vibrating in a mode with $n=2$ is approximately 420 times the frequency of the unloaded shell! This finding appears to be in contradiction with that of Fung, Sechler, and Kaplan (ref. 3.78), who indicated

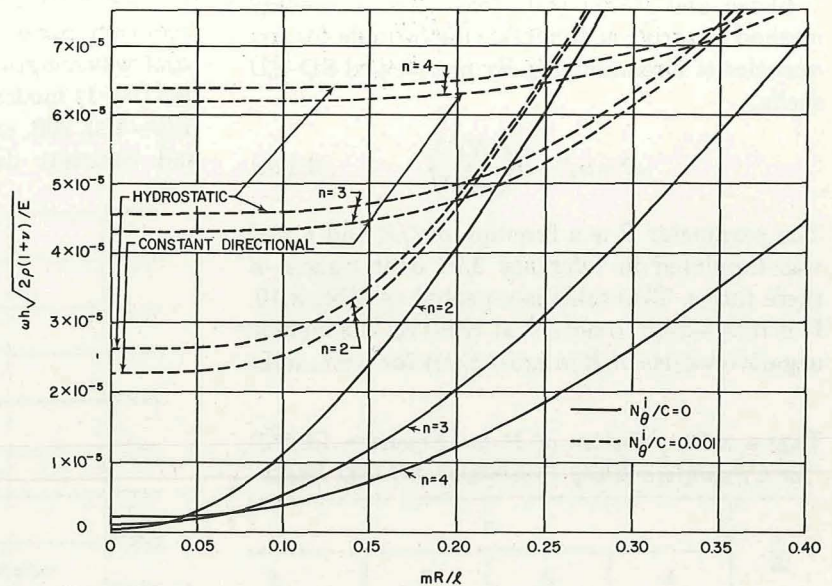


FIGURE 3.92.—Effect of circumferential prestress upon the frequencies of the $n \geq 2$ modes of an SD-SD shell; $R/h=100$. (After ref. 3.85)

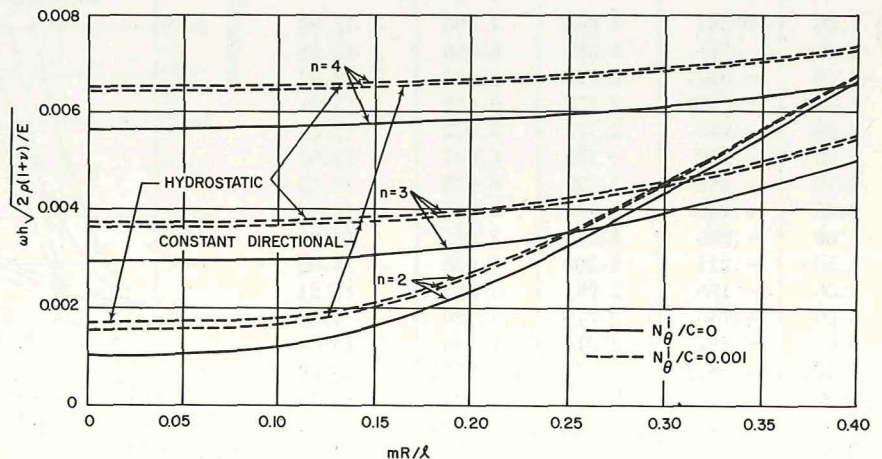


FIGURE 3.93.—Effect of circumferential prestress upon the frequencies of the $n \geq 2$ modes of an SD-SD shell; $R/h=20$. (After ref. 3.85)

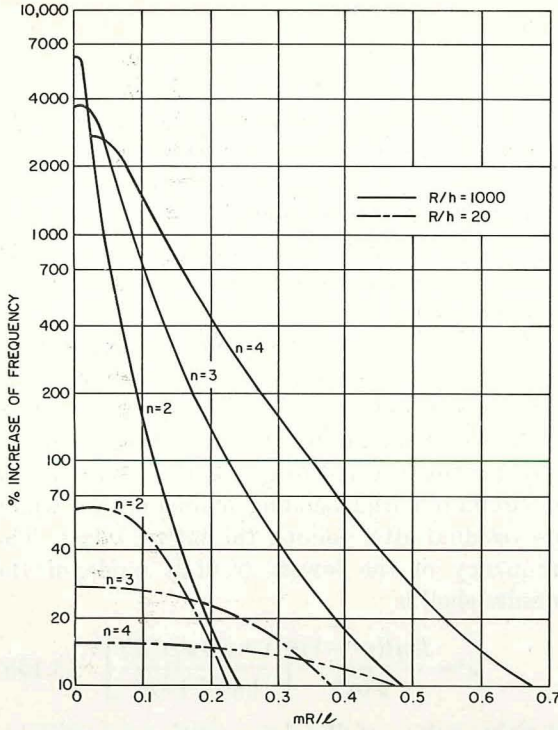


FIGURE 3.94.—Relative effect of internal hydrostatic pressure ($N_{\theta}^i/C=0.001$) upon the frequencies of an SD-SD shell. (After ref. 3.85)

that initial stresses have a significant effect on the frequency only for $n > 3$. This discrepancy may be because in reference 3.78 results were studied only for relatively large mR/l . From figure 3.94, for example, for $mR/l > 0.45$ the effect of circumferential prestress becomes negligible for $n < 4$ and $R/h < 1000$. Also from figure 3.94, the effect of circumferential prestress upon the frequency depends to a large extent upon n ; this effect is larger for modes having values of n close to that for which an SD-SD shell of length l/m will buckle.

Armenakos and Herrmann (ref. 3.95) analyzed the *infinitely long* shell subjected to circumferential initial stress. Three types of pressures were considered as being active during the vibratory displacements of the shell wall:

- (1) Constant directional
- (2) Hydrostatic
- (3) Centrally directed.

The first two types have been discussed above. In the third case, during deformation the magni-

tude per unit original area remains constant and the direction remains toward the center of the shell. In all three cases the system of applied loads is conservative. The equations of reference 3.72 are used with exact plane strain displacement functions (2.24) to arrive at the following characteristic equations for the cases of:

constant directional pressure

$$\omega^4 - \frac{\omega^2}{\rho h R^2} \left[C(1+n^2) + \frac{D}{R^2}(n^2-1)^2 + N_{\theta}^i(1+n^2) \left(2 \mp \frac{h}{2R} \right) \right] + \frac{N_{\theta}^i}{\rho^2 h^2 R^4} \left[C(n^2-1)^2 \left(1 \mp \frac{h}{2R} \right) + \frac{D}{R^2}(n^2-1)^2 \left(n^2 + 1 \mp \frac{h}{2R} \right) + N_{\theta}^i(n^2-1)^2 \left(1 \mp \frac{h}{2R} \right) \right] + \frac{CD}{\rho^2 h^2 R^6} n^2(n^2-1)^2 = 0 \quad (3.125)$$

hydrostatic pressure

$$\omega^4 - \frac{\omega^2}{\rho h R^2} \left\{ C(1+n^2) + \frac{D}{R^2}(n^2-1)^2 + N_{\theta}^i \left[2n^2 \mp \frac{h}{2R}(1-n^2) \right] \right\} + \frac{N_{\theta}^i}{\rho^2 h^2 R^4} \left[C(n^2-1)n^2 \left(1 \pm \frac{h}{2R} \right) + \frac{D}{R^2}n^2(n^2-1)^2 + N_{\theta}^i n^2(n^2-1) \left(1 \pm \frac{h}{2R} \right) \right] + \frac{CD}{\rho^2 h^2 R^6} n^2(n^2-1)^2 = 0 \quad (3.126)$$

centrally directed pressure

$$\omega^4 - \frac{\omega^2}{\rho h R^2} \left[C(n^2+1) + \frac{D}{R^2}(n^2-1)^2 + N_{\theta}^i \left(1 + 2n^2 \mp \frac{n^2 h}{2R} \right) \right] + \frac{N_{\theta}^i}{\rho^2 h^2 R^4} \left\{ (C + N_{\theta}^i) \left[n^2(n^2-2) \pm n^2(1-n^2) \frac{h}{2R} \right] + \frac{D}{R^2} n^2(n^2-1)^2 \right\} + \frac{CD}{\rho^2 h^2 R^6} n^2(n^2-1)^2 = 0 \quad (3.127)$$

where $C = Eh/(1-\nu^2)$ and $D = Eh^3/12(1-\nu^2)$, as before, and

$$N_{\theta}^i = \pm p_0 R \left(1 \mp \frac{h}{2R} \right) \quad (3.128)$$

the upper sign in all these equations applying to internal pressure, while the lower sign applies to external pressure.

The lowest roots of equations (3.125), (3.126), and (3.127) which correspond to the predominantly radial mode are (according to ref. 3.95)

constant directional pressure,

$$\omega^2 = K \left[1 + \frac{N_{\theta}^i R^2}{D n^2} \left(1 \mp \frac{h}{2R} + k n^2 \right) \right] \quad (3.129)$$

hydrostatic pressure,

$$\omega^2 = K \left[1 + \frac{N_{\theta}^i R^2}{D(n^2 - 1)} \left(1 \pm \frac{h}{2R} + k n^2 \right) \right] \quad (3.130)$$

centrally directed pressure,

$$\omega^2 = K \left\{ 1 + \frac{N_{\theta}^i R^2}{D(n^2 - 1)^2} \left[n^2 - 2 \mp \frac{h}{2R} (n^2 - 1) + k n^4 \right] \right\} \quad (3.131)$$

where

$$K = \frac{D n^2 (n^2 - 1)^2}{\rho h R^4 [1 + n^2 + (h^2 n^4 / 12 R^2)]} \quad (3.132)$$

$k = h^2 / 12 R^2$, as usual, and where terms of order of magnitude $(N_{\theta}^i / C)^2$ and $(h/R)^2$ have been neglected in comparison with unity.

In equations (3.129), (3.130), and (3.131) it may be observed that the frequency of the radial mode increases with initial internal pressure and

decreases with external pressure. The relative effect becomes very large for very large values of R/h , as illustrated in figure 3.95 for $n=2$. The slopes of the curves change at the origin as the pressure changes from external to internal; ω_0 is the frequency in the absence of initial stress. In figure 3.96 Ω is plotted versus R/h for $n=2, 3$ and $N_{\theta}^i / C = 0, 1/1200$. The differences among the types of pressure representations decreases as n increases; for $n=6$, it is negligible.

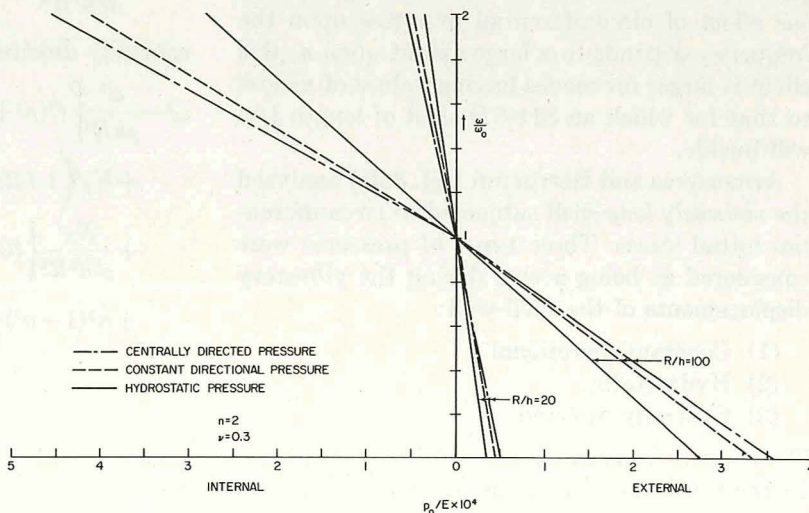
Two other interesting types of circumferential initial stress were considered by Armenak and Herrmann in reference 3.95. This first case arises when, for example, during fabrication a circular cylinder is generated from a flat plate by means of circumferential bending moments M_{θ}^i which are residual after joining the lateral edges. The frequency of the lowest (radial) mode of the infinite shell is

$$\omega^2 = \frac{D n^2 (n^2 - 1)^2}{\rho h R^4} \left[\frac{1 + (M_{\theta}^i / C R)}{1 + n^2 + k n^4} \right] \quad (3.133)$$

Positive values of M_{θ}^i (ones causing compressive stresses on the inner boundary of the shell) are seen to increase the frequency. However, the effect is generally small because, for most materials the yield stress is reached before M_{θ}^i becomes significant in equation (3.133).

The second type of circumferential initial stress alluded to above is when the internal and external boundaries of the infinite shell are subjected to oppositely directed uniform, circumferential, surface shearing forces f_{in} and f_{ex} , respectively, as

FIGURE 3.95.—Effects of various pressure representations upon the frequency ratios of circumferentially prestressed infinite shells: $n=2$, $\nu=0.3$. (After ref. 3.95)



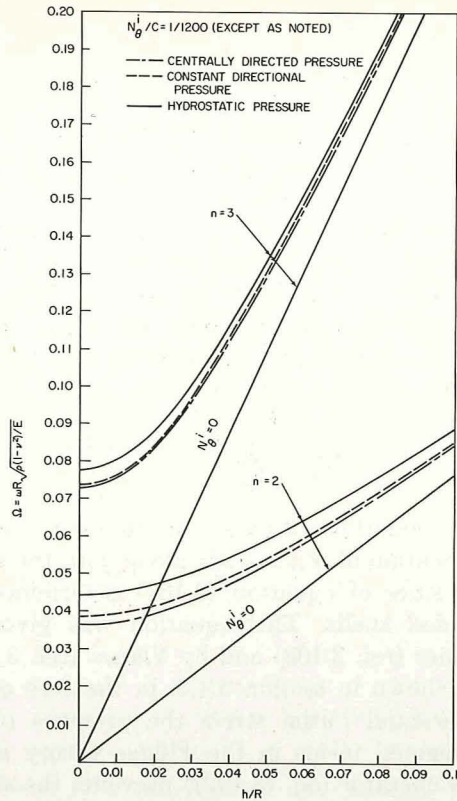


FIGURE 3.96.—Effects of various pressure representations upon the frequency ratios of circumferentially prestressed infinite shells; $n=2, 3$. (After ref. 3.95)

shown in figure 3.97, thereby generating a transverse shearing force resultant Q_θ^i . Neglecting circumferential inertia, reference 3.95 shows that the frequency becomes

$$\omega^2 = \frac{D(n^2-1)^2}{\rho h R^4} \left[1 - \frac{(Q_\theta^i)^2 R^2}{CDn^2} \right] \quad (3.134)$$

The effect of Q_θ^i can be very large for large values of R/h .

Experimental results for a shell subjected to circumferential initial stress due to *external* pressure were given in reference 3.86 for a stainless steel shell having $R=1.50$ in., $h=0.010$ in., and $l=29$ in. These are shown in figure 3.98 for an external pressure of 3.5 psi. Analytical results calculated from equation (3.156) of section 3.4.4 are also given. The change in frequencies due to the initial stress can be seen by comparing figure 3.98 with figure 3.84.

Koval (ref. 3.96) obtained simple frequency

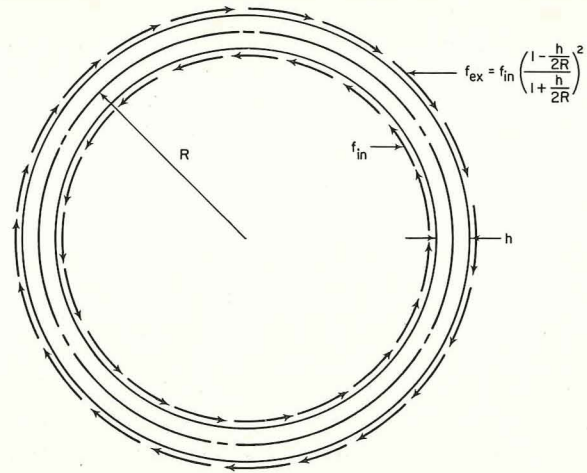


FIGURE 3.97.—Shell subjected to circumferential, surface shearing forces. (After ref. 3.95)

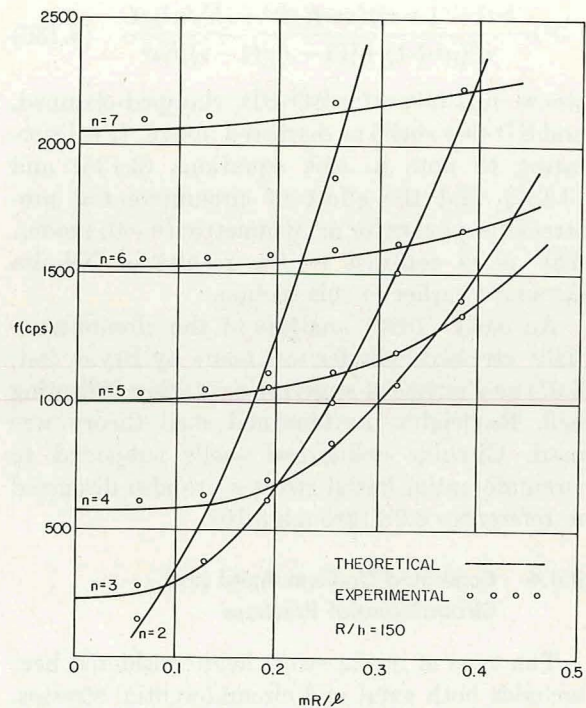


FIGURE 3.98.—Theoretical and experimental frequencies for an SD-SD shell (dimensions given in text) subjected to an initial *external* pressure. (After ref. 3.86)

formulas for shells subjected to circumferential initial stress and having various boundary conditions. The Donnell-Mushtari shell equations, neglecting tangential inertia, were used, as well

as Yu's assumption, $\lambda^2/n^2 \ll 1$ (see sec. 2.3.5 for further discussion). For shells supported at both ends by shear diaphragms (SD-SD shells) the resulting formula for the frequency parameter is

$$\Omega^2 = kn^4 + (1 - \nu^2)(m\pi R/nl)^4 + N_{\theta}^i \frac{n^2}{C} \quad (3.135)$$

where $m = 1, 2, \dots$. Using the same assumptions reference 3.96 shows that equation (3.135) can also be applied to clamped-clamped shells provided that the eigenvalues of the clamped-clamped beam are used; i.e., $m = 1.506, 2.500, 3.500, \dots$. Similarly, the SD-free shell is governed by the SD-free beam eigenvalues, giving $m = 1.250, 2.250, 3.250, \dots$ for use in equation (3.135). Reference 3.96 also shows that using the Donnell-Mushtari theory and *retaining* tangential inertia leads to the frequency formula

$$\Omega^2 = \frac{kn^8 + (1 - \nu^2)(m\pi R/l)^4 + (N_{\theta}^i n^2)/C}{n^2(n^2 + 1) + [(3 - \nu)/(1 - \nu)]kn^6} \quad (3.136)$$

where m is taken for SD-SD, clamped-clamped, and SD-free shells as discussed above. It is interesting to note in *both* equations (3.135) and (3.136) that the effect of circumferential prestress disappears for axisymmetric ($n = 0$) modes. This is in contrast to the results of Nikulin discussed earlier in this section.

An early (1890) analysis of the circumferentially stressed cylinder was made by Bryan (ref. 3.97) as a means of studying a rotating, vibrating bell. Rayleigh's inextensional shell theory was used. Circular cylindrical shells subjected to circumferential initial stresses are also discussed in references 3.98 through 3.101.

3.4.4 Combined Uniform Axial and Circumferential Prestress

The type of initial stress field considered here includes both axial and circumferential stresses. Thus, sections 3.4.2 and 3.4.3 can be considered as special cases of this section. One other important special case occurs in this section, namely, when $N_{\theta}^i = 2N_x^i$, and $N_{x\theta}^i = 0$. This case occurs when a completely enclosed cylindrical tank is subjected to uniform internal or external pressure. The axial prestress is caused by the pressure acting upon the ends of the tank. In the case of a tank having ends made of relatively thin, circular,

flat plates, the SD-SD boundary conditions are reasonably approximated.

Sections 3.4.2 and 3.4.3 show that in the case of the SD-SD shells, using the Donnell-Mushtari theory neglecting tangential inertia gave rise to simple formulas (3.108) and (3.116) which permit the vibration frequencies obtained for unloaded shells to be used directly to determine the frequencies for shells having either axial or circumferential uniform prestress. The extension to combined axial and circumferential uniform prestress is obvious, yielding

$$\Omega^2 - N_x^i \frac{\lambda^2}{C} - N_{\theta}^i \frac{n^2}{C} = \frac{K_0 + k \Delta K_0}{\bar{K}_1} \quad (3.137)$$

Thus, equation (3.137) can be used for any combination of N_x^i and N_{θ}^i along with the right-hand sides of equation (3.137) determined for unloaded shells. This equation was given by Reissner (ref. 3.102) and by Vlasov (ref. 3.103).

As shown in section 3.4.3, in the case of circumferential initial stress the presence of the off-diagonal terms in the Flügge theory initial stress operator (eq. (3.102)) prevents the simple solution form of equation (3.137) for this theory. However, Greenspon (refs. 3.24 and 3.25) and Bozich (ref. 3.82) pointed out that in many practical cases these terms are small in comparison with the terms arising from the other two operators required in equation (3.100). In such cases the off-diagonal initial stress operator terms can be neglected and, consequently, *retaining* tangential inertia terms in the Flügge theory, one can utilize the numerous results of section 2.3 simply by replacing Ω^2 by $\Omega^2 - N_x^i \lambda^2/C - N_{\theta}^i n^2/C$.

Reissner, along with his other numerous significant contributions in the field of shell vibrations, studied the effects of initial stress according to the *membrane* theory (ref. 3.102). The shear diaphragm (SD) boundary conditions were satisfied at both ends by using the exact displacement functions (2.20), with $\lambda = m\pi R/l$. The initial stresses were those due to internal pressure; i.e., $N_x^i = p_0 R/2$, $N_{\theta}^i = p_0 R$. Substituting equations (2.20) into the equations of motion determined by equations (3.100) and (3.106) gives the characteristic equation

$$\Omega^6 - K_2' \Omega^4 + K_1' \Omega^2 - K_0' = 0 \quad (3.138)$$

where

$$\left. \begin{aligned} K_2' &= \frac{1}{3} \left[4(\lambda^2 + n^2) + 3 \right. \\ &\quad \left. + \frac{8p_0 R}{3Eh} \left(n^2 - 1 + \frac{\lambda^2}{2} \right) \right] \\ K_1' &= \frac{1}{9} \left[3(\lambda^2 + n^2)^2 + 11\lambda^2 + 3n^2 \right. \\ &\quad \left. + \frac{32p_0 R}{3Eh} \left(n^2 - 1 + \frac{\lambda^2}{2} \right) (\lambda^2 + n^2) \right] \\ K_0' &= \frac{1}{27} \left[8\lambda^4 + 8 \frac{p_0 R}{Eh} \left(n^2 - 1 \right. \right. \\ &\quad \left. \left. + \frac{\lambda^2}{2} \right) (\lambda^2 + n^2)^2 \right] \end{aligned} \right\} \quad (3.139)$$

for $\nu = 1/3$. (When $p_0 = 0$, these coefficients are the same as equations (2.36) with $k=0$ and $\nu = 1/3$.) Extensive numerical results were given in reference 3.102 for $\lambda = 0, \pi/10, \pi/4, \pi/2, 3\pi/4, \pi, 3\pi/2, 2\pi$; $n = 1, 2, \dots, 6$; and $4p_0 R/3Eh = 0, 1/400, 1/200, 1/100$. These are listed in table 3.11. All three frequencies arising as roots of equation (3.138) are given in this table. The same behavior is also seen in figures 3.99, 3.100,

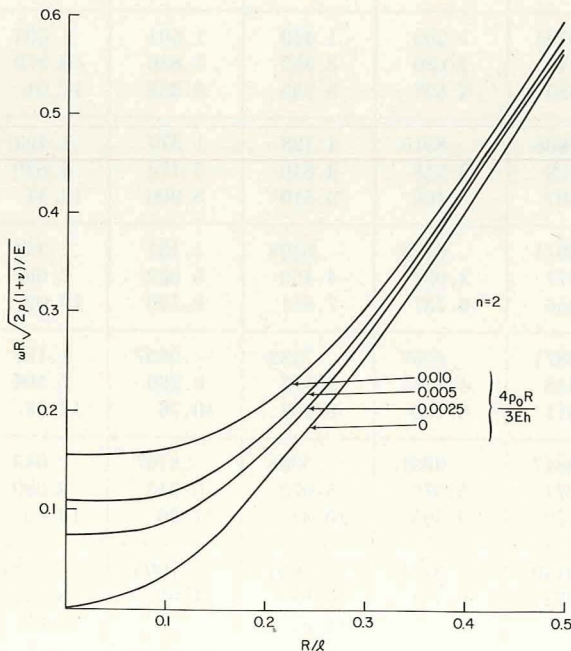


FIGURE 3.99.—Frequency parameters for SD-SD shells subjected to internal pressure p_0 (i.e., $N_{\theta}^i = 2N_x^i$); membrane theory, $\nu = 1/3$; $n = 2$. (After ref. 3.102)

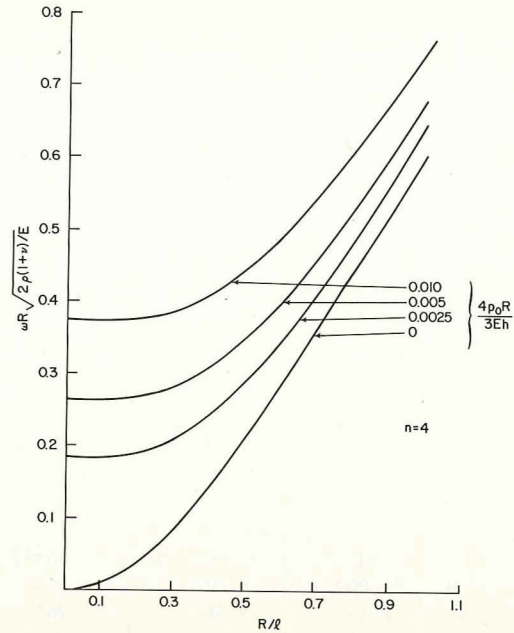


FIGURE 3.100.—Frequency parameters for SD-SD shells subjected to internal pressure p_0 (i.e., $N_{\theta}^i = 2N_x^i$); membrane theory $\nu = 1/3$; $n = 4$. (After ref. 3.102)

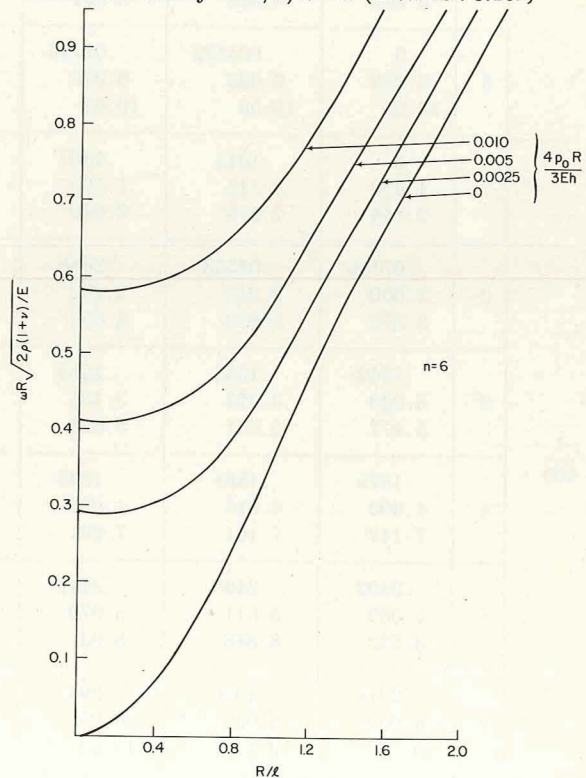


FIGURE 3.101.—Frequency parameters for SD-SD shells subjected to internal pressure p_0 (i.e., $N_{\theta}^i = 2N_x^i$); membrane theory $\nu = 1/3$; $n = 6$. (After ref. 3.102)

TABLE 3.11.—Frequency Parameters $\omega R \sqrt{2\rho(1+\nu)/E}$ for SD-SD Shells Subjected to an Internal Pressure p_0 (i.e., $N_{\theta}^i = \frac{1}{2}N_{\theta}^i$); Membrane Theory; $\nu = \frac{1}{3}$

$\frac{4p_0R}{3Eh}$	n	$\lambda = m\pi R/l$							
		0	$\pi/10$	$\pi/4$	$\pi/2$	$3\pi/4$	π	$3\pi/2$	2π
0	1	0 1.000 2.499	0.1011 1.115 2.4783	0.5383 1.503 2.649	0.9771 2.109 3.386	1.297 2.686 4.507	1.445 3.358 5.755	1.552 4.836 8.368	1.588 6.370 11.04
	2	0 2.000 3.873	.03505 2.042 3.902	.1927 2.232 4.056	.5593 2.709 4.606	.8845 3.248 5.466	1.115 3.840 6.519	1.364 5.173 8.900	1.474 6.620 11.44
	3	0 3.000 5.477	.0168 3.023 5.501	.09896 3.135 5.624	.3315 3.477 6.056	.5927 3.932 6.737	.8228 4.458 7.611	1.141 5.661 9.720	1.318 7.007 12.09
	4	0 4.000 7.141	.009729 4.015 7.161	.05872 4.092 7.261	.2109 4.348 7.611	.4071 4.721 8.170	.6055 5.177 8.906	.9325 6.260 10.76	1.150 7.504 12.93
	5	0 5.000 8.832	.006366 5.011 8.848	.03854 5.070 8.931	.1436 5.271 9.223	.2903 5.579 9.695	.4527 5.972 10.33	.7564 6.943 11.96	.9898 8.089 13.95
	6	0 6.000 10.54	.004632 6.009 10.55	.02716 6.056 10.62	.1032 6.221 10.87	.2149 6.481 11.28	.3461 6.821 11.82	.6151 7.691 13.28	.8461 8.745 15.09
$\frac{1}{400}$	1	0 1.000 2.449	.1013 1.115 2.478	.4387 1.503 2.649	.9781 2.110 3.386	1.299 2.686 4.507	1.449 3.358 5.755	1.561 4.836 8.368	1.604 6.370 11.04
	2	.07746 2.000 3.873	.08533 2.042 3.902	.2088 2.232 4.056	.5668 2.709 4.607	.8915 3.248 5.466	1.123 3.840 6.519	1.377 5.173 8.900	1.493 6.620 11.44
	3	.1342 3.000 5.477	.1355 3.023 5.501	.1683 3.135 5.624	.3611 3.477 6.056	.6129 3.933 6.737	.8408 4.458 7.611	1.161 5.662 9.720	1.344 7.007 12.09
	4	.1879 4.000 7.142	.1884 4.015 7.161	.1984 4.093 7.261	.2871 4.348 7.611	.4553 4.721 8.170	.7432 5.177 8.906	.9657 6.260 10.76	1.187 7.504 12.93
	5	.2402 5.000 8.832	.2405 5.011 8.848	.2446 5.070 8.931	.2847 5.271 9.223	.3851 5.579 9.695	.5238 5.972 10.33	.8107 6.943 11.96	1.043 8.089 13.95
	6	.2918 6.000 10.54	.2920 6.009 10.55	.2942 6.056 10.62	.3140 6.221 10.87	.3711 6.481 11.28	.4654 6.821 11.82	.7005 7.691 13.28	.9221 8.745 15.09

TABLE 3.11.—Frequency Parameters $\omega R \sqrt{2\rho(1+\nu)/E}$ for SD-SD Shells Subjected to an Internal Pressure p_0 (i.e., $N_z^i = \frac{1}{2}N_\theta^i$); Membrane Theory; $\nu = \frac{1}{3}$ —Concluded

$\frac{4p_0R}{3Eh}$	n	$\lambda = m\pi R/l$							
		0	$\pi/10$	$\pi/4$	$\pi/2$	$3\pi/4$	π	$3\pi/2$	2π
$\frac{1}{200}$	1	0 1.000 2.449	0.1016 1.115 2.478	0.4391 1.503 2.649	0.9791 2.110 3.386	1.302 2.686 4.507	1.453 3.358 5.755	1.569 4.836 8.368	1.619 6.370 11.04
	2	.1095 2.000 3.873	.1155 2.042 3.902	.2237 2.232 4.056	.5742 2.709 4.607	.8985 3.248 5.466	1.131 3.840 6.519	1.389 5.173 8.900	1.512 6.620 11.44
	3	.1897 3.000 5.478	.1909 3.023 5.501	.2165 3.135 5.624	.3885 3.477 6.056	.6324 3.933 6.737	.8584 4.458 7.611	1.181 5.662 9.720	1.369 7.007 12.09
	4	.2657 4.000 7.142	.2662 4.015 7.161	.2743 4.093 7.261	.3469 4.348 7.611	.4989 4.721 8.170	.6788 5.177 8.906	.9977 6.260 10.76	1.222 7.504 12.93
	5	.3397 5.000 8.832	.3400 5.011 8.848	.3438 5.070 8.931	.3761 5.271 9.224	.4609 5.579 9.695	.5863 5.972 10.33	.8615 6.943 11.96	1.093 8.089 13.95
	6	.4126 6.000 10.54	.4129 6.009 10.55	.4152 6.056 10.62	.4319 6.221 10.87	.4789 6.481 11.28	.5599 6.822 11.83	.7765 7.691 13.28	.9922 8.745 15.09
$\frac{1}{100}$	1	0 1.000 2.449	.1022 1.115 2.478	.4399 1.503 2.649	.9811 2.110 3.022	1.306 2.687 4.507	1.461 3.358 5.755	1.587 4.836 8.368	1.649 6.370 11.04
	2	.1549 2.000 3.874	.1595 2.042 3.903	.2509 2.232 4.056	.5888 2.710 4.607	.9122 3.249 5.466	1.147 3.840 6.519	1.414 5.173 8.900	1.548 6.620 11.44
	3	.2683 3.000 5.478	.2694 3.023 5.502	.2897 3.135 5.625	.4381 3.477 6.056	.6697 3.933 6.738	.8926 4.458 7.612	1.219 5.662 9.720	1.418 7.008 12.09
	4	.3757 4.000 7.142	.3763 4.015 7.161	.3835 4.093 7.261	.4429 4.348 7.611	.5763 4.721 8.171	.7448 5.177 8.906	1.059 6.261 10.76	1.290 7.504 12.93
	5	.4804 5.000 8.832	.4808 5.011 8.848	.4846 5.070 8.931	.5121 5.271 9.224	.5835 5.580 9.696	.6946 5.972 10.33	.9552 6.943 11.96	1.187 8.090 13.95
	6	.5835 6.000 10.54	.5839 6.009 10.55	.5865 6.056 10.62	.6020 6.221 10.87	.6422 6.481 11.28	7.121 6.822 11.83	.9097 7.691 13.28	1.119 8.746 15.09

and 3.101 where only the lowest of the three frequencies is plotted.

In reference 3.102 comparisons were also made with the results arising from simplifications of membrane theory. The first results from neglecting tangential inertia, and yields the formula

$$2\omega^2 R^2 \rho(1+\nu)/E = \frac{8}{3} \frac{\lambda^4}{(n^2 + \lambda^2)^2} + \frac{4}{3} \frac{p_0 R}{Eh} \left(n^2 + \frac{1}{2} \lambda^2 \right) \quad (3.140)$$

for $\nu = 1/3$. The second is from reference 3.104 and is based on the assumptions that N_θ and the shear stress deformability of the shell walls are negligible and that axial wave lengths are large compared with circumferential wave lengths. The second formula is

$$2\omega^2 R^2 \rho(1+\nu)/E = \frac{3\lambda^4}{(n^2 + 1)n^2} + \frac{4}{3} \frac{p_0 R}{Eh} \frac{(n^2 - 1)^2}{n^2 + 1} \quad (3.141)$$

for $\nu = 1/3$. Comparisons of results obtained from equations (3.138), (3.140), and (3.141) are made in figures 3.102 and 3.103.

DiGiovanni and Dugundji (ref. 3.2) analyzed pressurized ($N_\theta = 2N_x$) SD-SD shells by the exact method. The Washizu shell equations were used; i.e., operators (3.101c) and (2.9b). The effect of internal pressure upon the axisymmetric frequency parameters of isotropic shells is shown in figure 3.104, where the pressure parameter $p_0 R/C$ (with $C = Eh/(1-\nu^2)$) has a value of 0.001 and $R/h = 1000$. The pressure has a significant effect upon the frequency only for the predominantly radial mode for large mR/l and for the torsional mode for small mR/l , whereas the axial mode is unaffected.

To grasp the significance of the magnitude of the pressure parameter, consider a shell having the material properties: $E = 10^7$ and $\nu = 0.3$. Then the circumferential initial stress is

$$\sigma_\theta^i = 1.1 \times 10^7 p_0 R/C \text{ psi}$$

Figures 3.105, 3.106, and 3.107 show the variation of the lowest value of Ω with $p_0 R/C$ for $n \geq 1$ and for shells having three values of axial wave length $-mR/l = 0.06, 0.5$, and 3. Poisson's ratio was taken at 0.3. Comparison of the figures

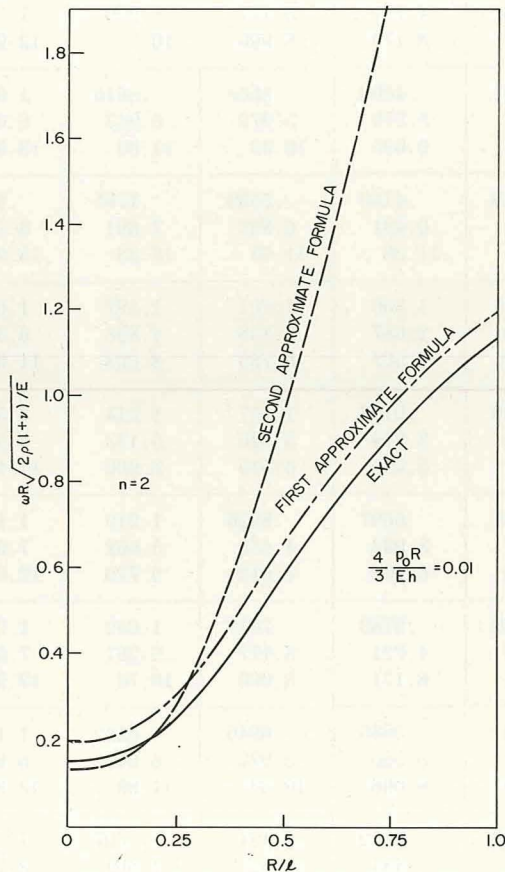


FIGURE 3.102.—Comparison of exact, first approximate, and second approximate formulas (eqs. (3.138), (3.140), and (3.141), respectively) for frequency parameters; $n=2$. (After ref. 3.102)

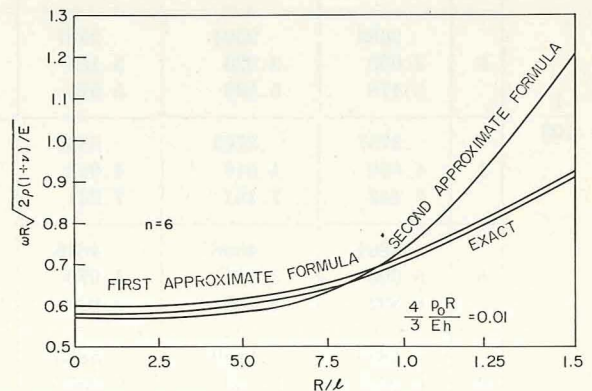


FIGURE 3.103.—Comparison of exact, first approximate, and second approximate formulas (eqs. (3.138), (3.140), and (3.141), respectively) for frequency parameters; $n=6$. (After ref. 3.102)

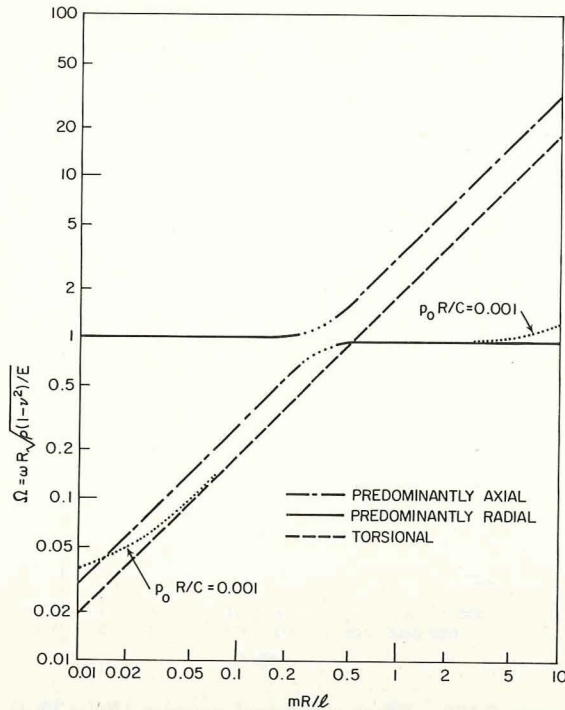


FIGURE 3.104.—Effect of internal pressure ($N_{\theta}^i = 2N_x^i$) upon the axisymmetric ($n=0$) frequency parameters of an SD-SD shell; $R/h=1000$. (After ref. 3.2)

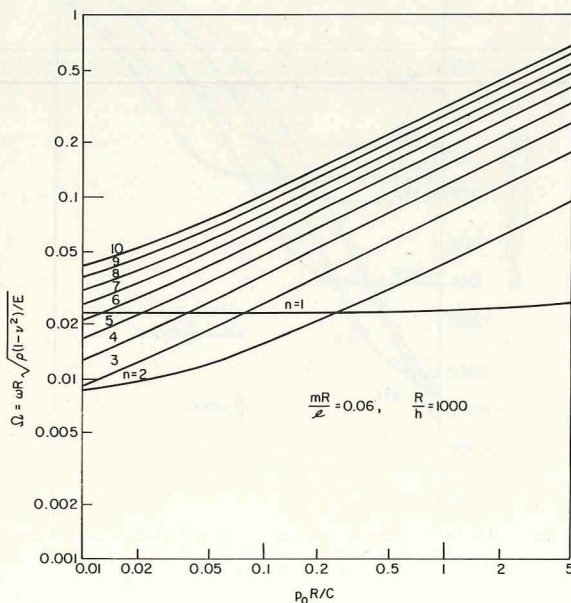


FIGURE 3.105.—Effect of internal pressure ($N_{\theta}^i = 2N_x^i$) upon the frequencies ($n \geq 1$) of an SD-SD shell; $mR/l=0.06$. (After ref. 3.2)

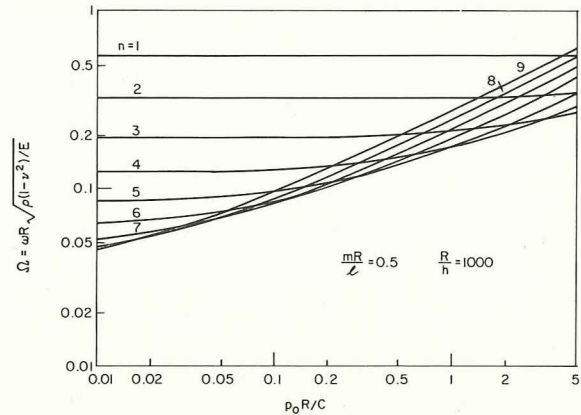


FIGURE 3.106.—Effect of internal pressure ($N_{\theta}^i = 2N_x^i$) upon the frequencies ($n \geq 1$) of an SD-SD shell; $mR/l=0.5$. (After ref. 3.2)

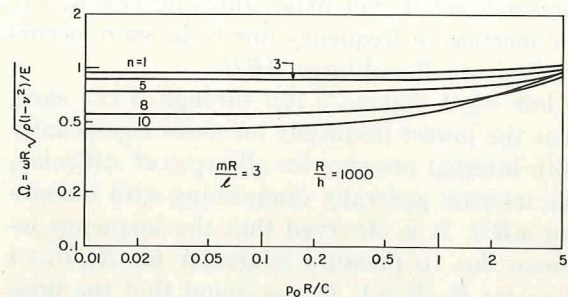


FIGURE 3.107.—Effect of internal pressure ($N_{\theta}^i = 2N_x^i$) upon the frequencies ($n \geq 1$) of an SD-SD shell; $mR/l=3$. (After ref. 3.2)

shows that the value of n for which the lowest frequency begins to vary significantly with the internal pressure depends upon the axial wave length mR/l . For long shells ($mR/l=0.06$) there is a significant increase of Ω with $p_0 R/C$ when $n \geq 2$, for $mR/l=0.5$ the increase becomes significant when $n \geq 5$, and for short shells ($mR/l=3$) when $n \geq 10$. For $n=1$ the frequency is virtually independent of pressure, especially for short shells. The two larger frequencies, which correspond to predominantly tangential motions, were little affected by internal pressure. The fact that the frequencies of the tangential modes are virtually unaffected by initial stresses has been pointed out in many references (cf., ref. 3.85).

In reference 3.2 pressurized orthotropic shells were also analyzed by the same method. Numerical results for the axisymmetric ($n=0$) modes

of a set of shells have already been included in figures 3.3 through 3.6 of section 3.1.2. In these figures it is seen that for both circumferential and axial stiffening, and all values of stiffness ratios, the frequency of the predominantly radial mode is slightly increased by the addition of internal pressure at large values of mR/l . The frequency of the torsional mode increases with pressure for small mR/l , whereas the pressure has a negligible effect on the frequency of the axial mode everywhere.

For the $n=1$ mode ("beam bending"), the effect of pressure on the lowest frequency is shown in figures 3.108 through 3.112. The direction and magnitude of the stiffness ratio E_x/E_θ varies from one figure to the next. For circumferential stiffening ($E_\theta/E_x > 1$) there is a significant increase in Ω for small mR/l . For axial stiffening ($E_x/E_\theta > 1$) the increase in frequency due to pressure occurs for both small and large mR/l .

For $n \geq 2$, figures 3.108 through 3.112 show that the lowest frequency increases significantly with internal pressure for all types of stiffening, the increase generally diminishing with increasing mR/l . It is observed that the frequency increase due to pressure is greater for $E_x/E_\theta > 1$ than for $E_\theta/E_x > 1$. It was found that the pressure had a negligible effect on the two higher frequencies over the entire range of parameters encompassed in these figures.

Fung, Sechler, and Kaplan (refs. 3.78 and 3.79) analyzed SD-SD shells by means of equations of motion (eq. (3.100)) which used equation (2.9a) for the $[\mathcal{L}_{MOD}]$ operator and equation (3.105) for the $[\mathcal{L}_i]$ operator. They found the resulting characteristic equation to be equation (3.138) where, in this case, the coefficients K_2' , K_1' , and K_0' are given by

$$\left. \begin{aligned} K_2' &= K_2 + k \Delta K_2 + 2\lambda^2 \bar{n}_x + n^2 \bar{n}_\theta \\ K_1' &= K_1 + k \Delta K_1 + b_1 \bar{n}_\theta + b_2 \bar{n}_x \\ &\quad + n^2 \lambda^2 \bar{n}_x \bar{n}_\theta + \lambda^4 \bar{n}_x^2 \\ K_0' &= K_0 + k \Delta K_0 + a_1 \bar{n}_\theta + a_2 \bar{n}_x + a_3 \bar{n}_x \bar{n}_\theta \\ &\quad + a_4 \bar{n}_x^2 + a_5 \bar{n}_\theta^2 \end{aligned} \right\} \quad (3.142)$$

where K_2 , K_1 , K_0 , ΔK_2 , ΔK_1 , and ΔK_0 are terms of the characteristic equation in the absence of initial stress as used previously in equation (2.35), $\bar{n}_x = N_x^i/Eh$, $\bar{n}_\theta = N_\theta^i/Eh$, and

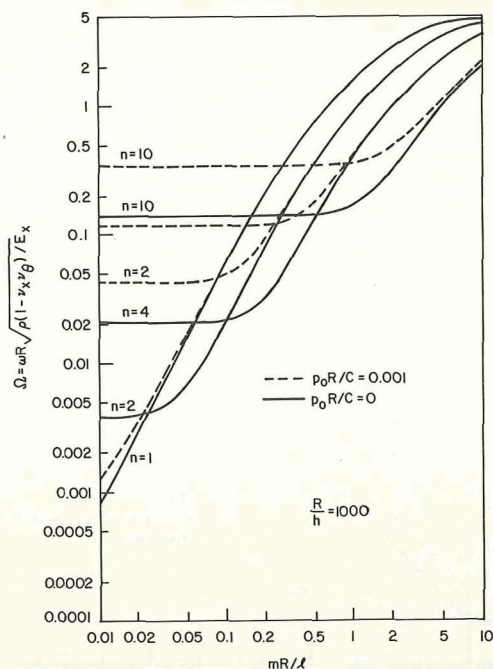


FIGURE 3.108.—Effect of internal pressure ($N_\theta^i = 2N_x^i$) upon the frequencies ($n \geq 1$) of an orthotropic, SD-SD shell; $E_\theta/E_x = 24.2$. (After ref. 3.2)

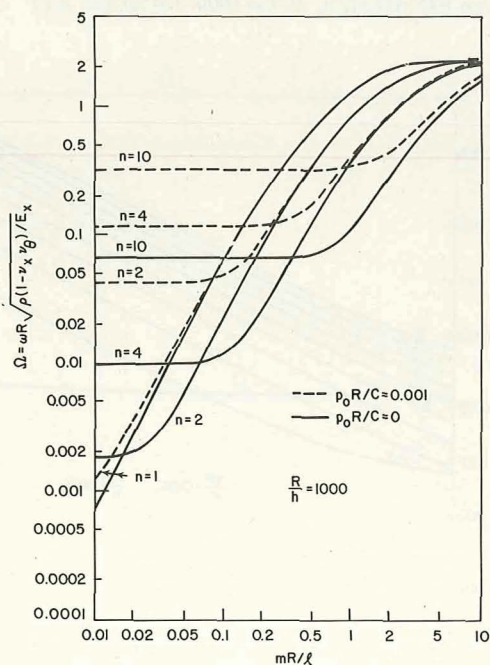


FIGURE 3.109.—Effect of internal pressure ($N_\theta^i = 2N_x^i$) upon the frequencies ($n \geq 1$) of an orthotropic, SD-SD shell; $E_\theta/E_x = 5.35$. (After ref. 3.2)

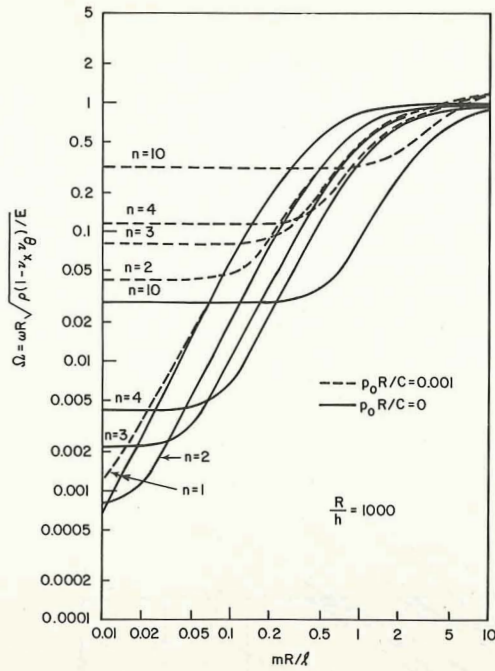


FIGURE 3.110.—Effect of internal pressure ($N_\theta^i = 2N_x^i$) upon the frequencies ($n \geq 1$) of an isotropic, SD-SD shell; $E_\theta/E_x = 1$. (After ref. 3.2)

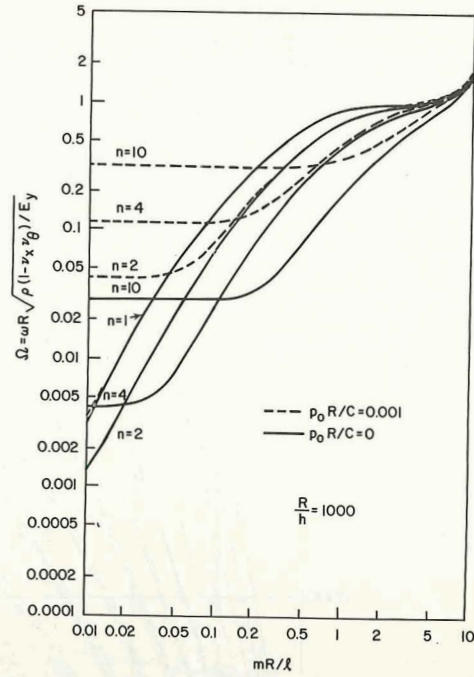


FIGURE 3.112.—Effect of internal pressure ($N_\theta^i = 2N_x^i$) upon the frequencies ($n \geq 1$) of an orthotropic, SD-SD shell; $E_x/E_\theta = 24.2$. (After ref. 3.2)

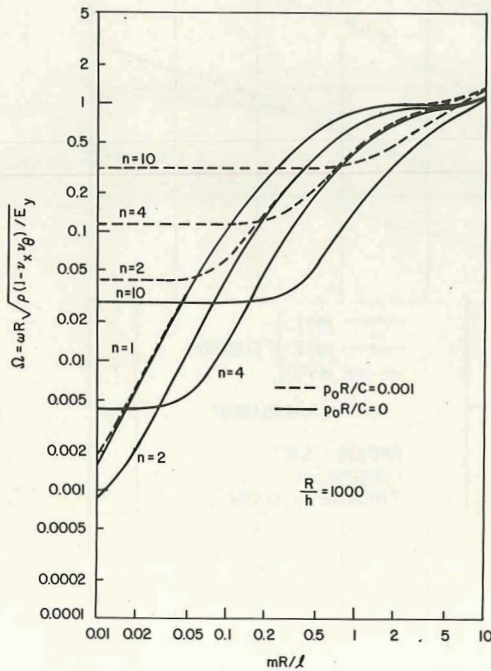


FIGURE 3.111.—Effect of internal pressure ($N_\theta^i = 2N_x^i$) upon the frequencies ($n \geq 1$) of an orthotropic, SD-SD shell; $E_x/E_\theta = 5.35$. (After ref. 3.2)

$$\left. \begin{aligned}
 a_1 &= \frac{1-\nu}{2} n^2 (n^2 - \lambda^2) - \frac{1-\nu}{2} n^4 \\
 &\quad + \frac{\nu(1-\nu)}{2} \lambda^4 - \frac{(2-\nu)(1-\nu)}{2} \lambda^2 n^2 \\
 &\quad - \nu \lambda n - k \left\{ (\lambda^2 + n^2) \left(n^2 \lambda^2 \right. \right. \\
 &\quad \left. \left. + \frac{1-\nu}{2} n^4 + \nu \lambda n \right) \right. \\
 &\quad \left. + \frac{1+\nu}{2} \lambda^2 n^2 [(2-\nu) \lambda^2 + n^2] \right. \\
 &\quad \left. - (\lambda^2 + n^2)^2 \right\} \\
 a_2 &= \lambda^2 \left\{ (1-\nu^2) \lambda^2 + \frac{1-\nu}{2} [n^2 + (n^2 - \lambda^2)^2] \right. \\
 &\quad \left. + k (\lambda^2 + n^2)^2 \left(\lambda^2 + \frac{1-\nu}{2} n^2 \right) \right\} \\
 a_3 &= \lambda^2 \left(\frac{3-\nu}{2} \lambda^4 n^2 + \frac{1-\nu}{2} n^4 + \nu \lambda^2 \right) \\
 a_4 &= \lambda^4 \left(\lambda^2 + \frac{1-\nu}{2} n^2 \right)
 \end{aligned} \right\} \quad (3.143)$$

$$\left. \begin{aligned}
 a_5 &= \frac{1+\nu}{2} \lambda^2 n^2 (n^2 - 1) \\
 b_1 &= \frac{3-\nu}{2} n^4 + 2\lambda^2 n^2 - n^2 + \nu \lambda^4 \\
 &\quad - kn^2(\lambda^2 + n^2) \\
 b_2 &= \frac{5-\nu}{2} \lambda^4 + \frac{5-2\nu}{2} \lambda^2 n^2 + \lambda^2 \\
 &\quad + k\lambda^2(\lambda^2 + n^2)^2
 \end{aligned} \right\} \quad (3.143)$$

Results obtained from equations (3.142) and

(3.143) were reported in references 3.78 and 3.79 and compared with the results obtained from the much more simple Donnell-Mushtari equation (3.137). It was found that equation (3.137) gives frequencies within 7 percent of the more exact values obtained from equation (3.142) for $0 < \lambda < \pi$ at $n=2$ over a wide range of pressures.

Experiments were also reported in references 3.79 and 3.105 for shells having ends which simulated SD-SD conditions. Tests were conducted

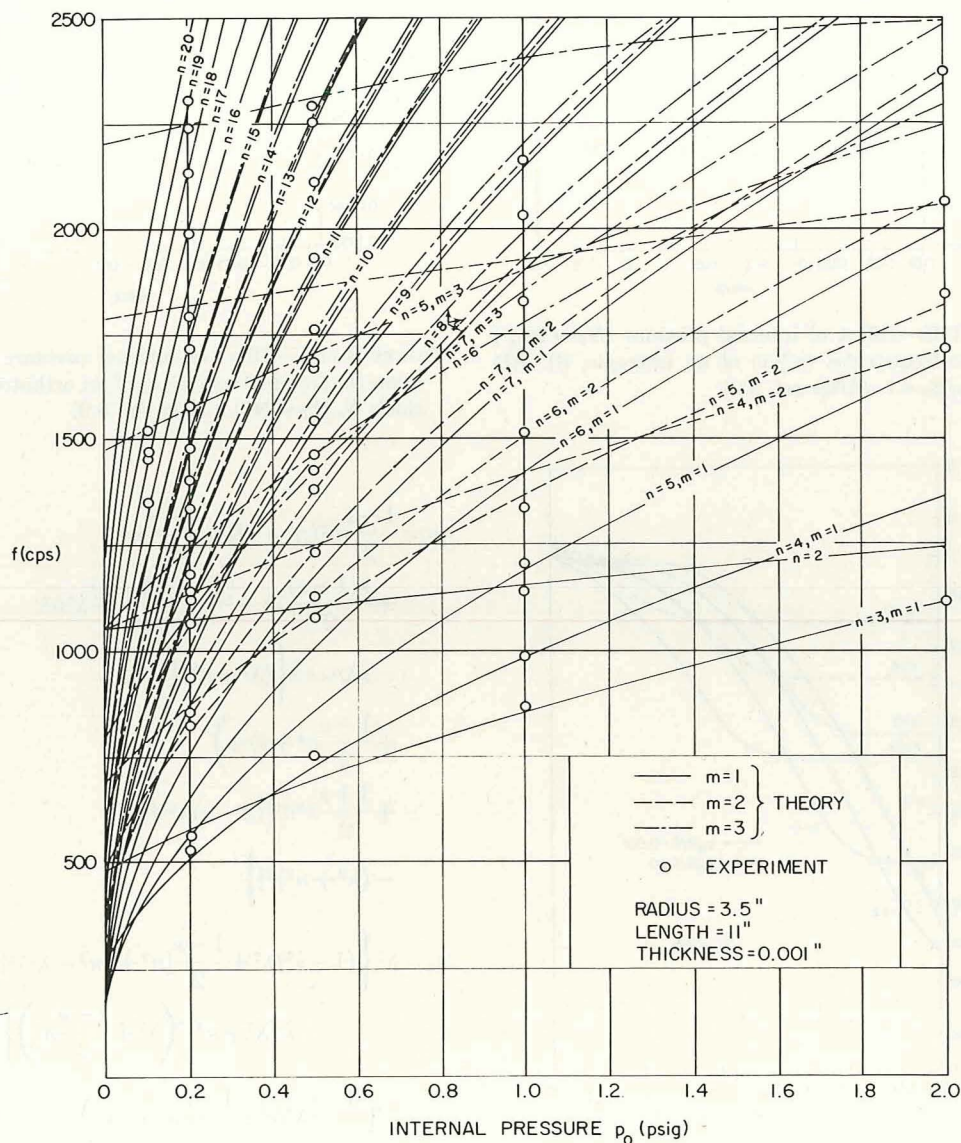


FIGURE 3.113—Theoretical and experimental frequencies (cps) for a pressurized ($N_\theta = 2N_x$) SD-SD aluminum shell. (After ref. 3.78)

on models made of 24S-H aluminum alloy having $R=3.5$ in.; $h=0.001$, 0.002 , and 0.003 in.; and three axial lengths —11, 7, and 3.5 in. Frequencies observed for the shell having $h=0.001$ in. and $l=11$ in. are plotted as small circles in figure 3.113. Theoretical results from equation (3.137) are plotted as lines. Figure 3.114 is a magnification of the lower left corner of figure 3.113. The

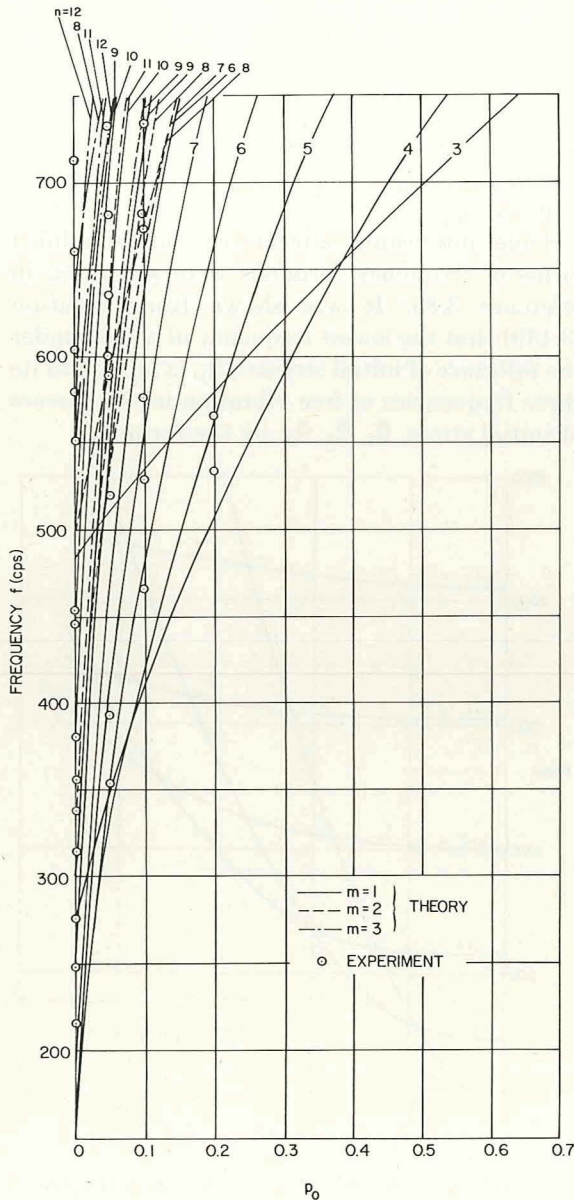


FIGURE 3.114.—Magnification of the lower left corner of figure 3.113. (After ref. 3.78)

overall bending modes ($n=1$) are omitted from these plots because the end masses used in the experiments affect the frequencies significantly. The density of frequencies occurring at any given pressure is readily apparent from these graphs. The actual experimental end conditions were somewhere between being shear diaphragm and clamped ends. Extensive tabular and graphical data are available in reference 3.105 for the other experimental shell models described above but, as in figures 3.113 and 3.114, no mode shapes are identified with the experimental frequency data, thus limiting its usefulness and excluding it from being reproduced here.

Herrmann and Armenàkas (ref. 3.72) derived a set of shell equations which take into account that, as the shell deforms, the direction of the internal or external pressure changes, always remaining normal to the shell. This is in contrast with the assumption that the direction of the pressure remains the same, (termed "constant directional pressure" by Herrmann and Armenàkas). The equations of motion (2.3) are generalized to (ref. 3.85):

$$[\mathcal{L}]\{u_i\} + \frac{R^2}{C}\{\Delta F_i\} + \frac{1}{C}\{\Delta M_i\} = \{0\} \quad (3.144)$$

where $[\mathcal{L}]$ and $\{u_i\}$ are as in equations (2.3) and (3.100); $\{\Delta F_i\} = \{\Delta F_x, \Delta F_\theta, \Delta q\}$; ΔF_x , ΔF_θ , and Δq are the axial, circumferential, and radial components, respectively, of the change of the initial shell surface tractions due to deformation, expressed per unit undeformed middle surface area; $C = Eh/(1-\nu^2)$; the vector $\{\Delta M_i\}$ has components

$$\left. \begin{aligned} \Delta M_1 &= 0 \\ \Delta M_2 &= -m_z v + m_z \frac{\partial w}{\partial \theta} + R \Delta m_\theta \\ \Delta M_3 &= m_z \frac{\partial v}{\partial \theta} - m_z w - R \frac{\partial \Delta m_x}{\partial s} - R \frac{\partial \Delta m_\theta}{\partial \theta} \end{aligned} \right\} \quad (3.145)$$

Δm_x , Δm_θ are the axial and circumferential components, respectively, of the change due to deformation of the moment induced by the surface tractions, expressed per unit undeformed middle surface area; and m_z is the sum of the products of the radial component of the initial

surface traction and the z -coordinate, evaluated at the two surfaces of the shell, expressed per unit undeformed middle surface area. The $[\mathcal{L}_{MOD}]$ operator used by Herrmann and Armenakias is the same as that of Flügge.

As shown in reference 3.72 for initial uniform lateral pressure p_0 ,

$$\left. \begin{aligned} N_{\theta}^i &= \pm p_0 R \left(1 \mp \frac{h}{2R} \right) \\ m_z &= -\frac{p_0 h}{2} \left(1 \mp \frac{h}{2R} \right) \end{aligned} \right\} \quad (3.146)$$

where the upper signs apply to internal pressure and the lower signs apply to external pressure. Correspondingly, it is found that

$$\left. \begin{aligned} \Delta F_x &= -\frac{N_{\theta}^i}{R^2} \frac{\partial w}{\partial s} \\ \Delta F_{\theta} &= \frac{N_{\theta}^i}{R^2} \left(v - \frac{\partial w}{\partial \theta} \right) \\ \Delta q &= \frac{N_{\theta}^i}{R^2} \left[\frac{\partial u}{\partial s} + \frac{\partial v}{\partial \theta} + w \right. \\ &\quad \left. \pm \frac{h}{2R} \left(w + \frac{\partial^2 w}{\partial s^2} + \frac{\partial^2 w}{\partial \theta^2} \right) \right] \\ \Delta m_x &= \pm \frac{h}{2} \frac{N_{\theta}^i}{R^2} \frac{\partial w}{\partial s} \\ \Delta m_{\theta} &= \mp \frac{h}{2} \frac{N_{\theta}^i}{R^2} \left(v - \frac{\partial w}{\partial \theta} \right) \end{aligned} \right\} \quad (3.147)$$

in the case where the pressure remains normal to the shell (hydrostatic pressure), and

$$\Delta F_x = \Delta F_{\theta} = \Delta m_{\theta} = \Delta q = 0 \quad (3.148)$$

in the case of constant directional pressure.

Using the exact solution function (2.20) for SD-SD ends, substituting into the equations of motion (3.144), and neglecting terms $(N_{\theta}^i/C)^2$ and $(h/R)^2$ with respect to unity yields the following generalization of the characteristic equation (2.35)

$$\Omega^6 - (K_2 + k \Delta K_2) \Omega^4 + (K_1 + k \Delta K_1) \Omega^2 - (K_0 + k \Delta K_0) + \frac{1}{C} (K_x N_x^i + K_{\theta} N_{\theta}^i) = 0 \quad (3.149)$$

where K_0 , K_1 , and K_2 are given by equations (2.36); ΔK_0 , ΔK_1 , and ΔK_2 are the Biezeno-Grammel coefficients of table 2.4; and

$$\left. \begin{aligned} K_x &= -\frac{(1-\nu)}{2} \lambda^2 [(\lambda^2 + n^2)^2 + 1 \\ &\quad + \lambda^2 (3 + 2\nu)] \\ K_{\theta h} &= -\frac{(1-\nu)}{2} \{ n^2 (\lambda^2 + n^2)^2 + n^2 (3\lambda^2 \\ &\quad + n^2) \mp k [(\lambda^2 + n^2)^3 - n^4 - 2\lambda^2 n^2] \} \\ K_{\theta c} &= -\frac{(1-\nu)}{2} \{ n^2 (\lambda^2 + n^2)^2 - n^2 + 2n^4 \\ &\quad + \lambda^2 [2(1+\nu) - n^2 (3+2\nu)] \\ &\quad \mp k [(\lambda^2 + n^2)^3 + n^2 - 2n^4 \\ &\quad + 2\lambda^2 (1+\nu - 2n^2 - 2\nu n^2)] \} \end{aligned} \right\} \quad (3.150)$$

where $K_{\theta h}$ and $K_{\theta c}$ refer to the cases wherein the circumferential prestress is induced by hydrostatic and constant directional pressure, respectively.

Some interesting alternative and simplified forms of frequency formulas were presented in reference 3.85. It was shown from equation (3.149) that the lowest frequency of a shell under the influence of initial stresses, Ω_1 , is related to its three frequencies of free vibration in the absence of initial stress, $\bar{\Omega}_1$, $\bar{\Omega}_2$, $\bar{\Omega}_3$, by the formula:

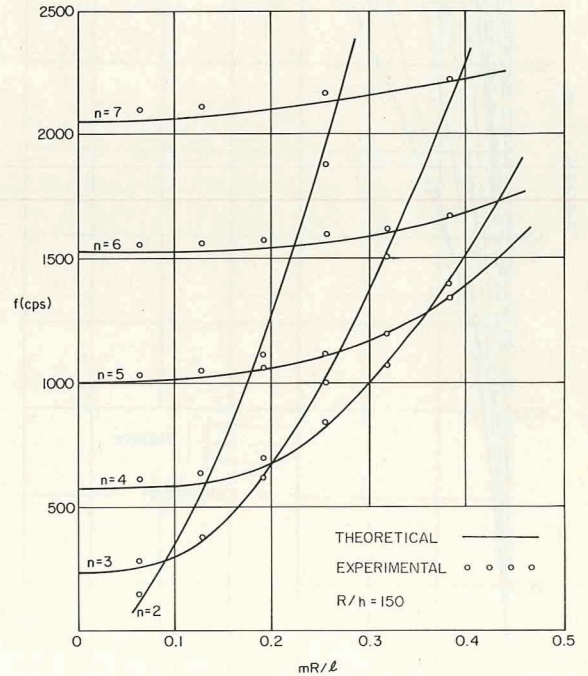


FIGURE 3.115.—Theoretical and experimental frequencies for an SD-SD shell (dimensions given in text) subjected to combined initial external pressure and axial compressive force. (After ref. 3.86)

$$\Omega_1^2 = \bar{\Omega}_1^2 - \frac{(K_x N_x^i + K_\theta N_\theta^i)}{C(\bar{\Omega}_2^2 \bar{\Omega}_3^2)} \quad (3.151)$$

In the case where tangential inertia is neglected it was shown that

$$\Omega^2 = \frac{K_0 + \Delta K_0 + \frac{1}{C}(K_x N_x^i + K_\theta N_\theta^i)}{\bar{K}_1} \quad (3.152)$$

where \bar{K}_1 was given previously in equation (2.43). For shells vibrating in modes having a large number of circumferential waves, $1/n^2$ can be disregarded in comparison with unity, giving

$$\Omega^2 = \frac{(1-\nu^2)\lambda^4}{(\lambda^2 + n^2)^2} + k(\lambda^2 + n^2) + \frac{1}{C}(\lambda^2 N_x^i + n^2 N_\theta^i) \quad (3.153)$$

Taking the linearized form of equation (3.149), that is, neglecting the Ω^6 and Ω^4 terms, which is a reasonable approximation if one frequency is much smaller than the other two, and neglecting λ^2/n^2 and kn^2 with respect to unity, gives for hydrostatic pressure,

$$\Omega^2 = \frac{(1-\nu^2)\lambda^4}{n^2(1+n^2)} + k \frac{n^2(n^2-1)^2}{(n^2+1)} + \lambda^2 \frac{N_x^i}{C} + \frac{n^2(n^2-1)}{n^2+1} \frac{N_\theta^i}{C} \quad (3.154)$$

and for constant directional pressure,

$$\Omega^2 = \frac{(1-\nu^2)\lambda^4}{n^2(1+n^2)} + \frac{kn^2(n^2-1)^2}{n^2+1} + \lambda^2 \frac{N_x^i}{C} + n^2 \frac{(n^2-1)^2}{n^2+1} \frac{N_\theta^i}{C} \quad (3.155)$$

Equations (3.154) and (3.155) are not valid for $n=0$ and $n=1$. In reference 3.86 the λ^2/n^2 terms were retained and λ^3/n^3 and kn^2 were discarded as compared to unity to arrive at a formula for the case of hydrostatic pressure which is more accurate than equation (3.154):

$$\Omega^2 = \{ (1-\nu^2)\lambda^4 + kn^2(n^2-1)^2(1+4\lambda^2) + n^2[n^2(n^2-1) + \lambda^2(2n^2-3)](N_\theta^i/C) + n^2\lambda^2(n^2+1)(N_x^i/C) \} \div \{ n^2(n^2+2\lambda^2) + (3+2\nu)\lambda^2 n^2 + n^2 \} \quad (3.156)$$

Experimental results for an SD-SD shell subjected to combined initial *external* pressure and *compressive* axial force were given in reference 3.86 for a stainless steel shell having $R=1.50$ in., $h=0.010$ in., and $l=29$ in. These are shown in

figure 3.115 for an external pressure of 2.0 psi and an axial compressive force of 1500 lb. Analytical results calculated from equation (3.156) are also given. The change in frequencies due to the combined initial stresses can be seen by comparing figure 3.115 with figure 3.84.

Values of the parameter B to be used in equation (3.124) for the case of pressurized ($N_\theta^i = 2N_x^i$) SD-SD shells were found by Bleich and Baron (ref. 3.94) by an energy approach. These values are exhibited in table 3.12 for $1 \leq l/R \leq 10$ and $n=1, 2, 3, 4$.

Experimental results were obtained by Gottenberg (ref. 3.106) for pressurized ($N_\theta^i = 2N_x^i$) stainless steel shells having

$$h=0.025 \text{ in.}, R=3.012 \text{ in.}, \text{ and } l/R=31.86$$

and simulated SD-SD end conditions. In figure 3.116 the variation of frequency (cps) with the number of axial nodal circles ($m-1$) and circumferential wave number (n) is depicted. The internal pressure used was 53 psig. Experimental data are compared with analytical results calculated from the formula (eq. (3.137)) of the Donnell-Mushtari theory neglecting tangential inertia. For $n=1$ the Donnell-Mushtari theory is grossly inaccurate and an additional curve (denoted by an asterisk) is plotted on the basis

TABLE 3.12.—Values of B for Equation (3.124) for Pressurized ($N_\theta^i = 2N_x^i$) SD-SD Shells

$\frac{l}{R}$	n			
	1	2	3	4
1.00	4.963	7.171	11.718	18.55
1.25	2.949	5.186	9.869	16.80
1.50	1.810	4.142	8.923	15.90
1.75	1.252	3.555	8.391	15.39
2.00	.763	3.207	8.071	15.07
2.25	.539	2.991	7.865	14.86
2.50	.405	2.851	7.726	14.72
2.75	.323	2.758	7.629	14.61
3.00	.273	2.693	7.559	14.53
3.50	.222	2.616	7.466	14.43
4.00	.202	2.574	7.410	14.36
5.00	.195	2.534	7.348	14.28
6.00	.201	2.518	7.316	14.24
7.00	.209	2.511	7.298	14.21
8.00	.215	2.507	7.286	14.20
9.00	.221	2.505	7.278	14.19
10.00	.225	2.503	7.273	14.18

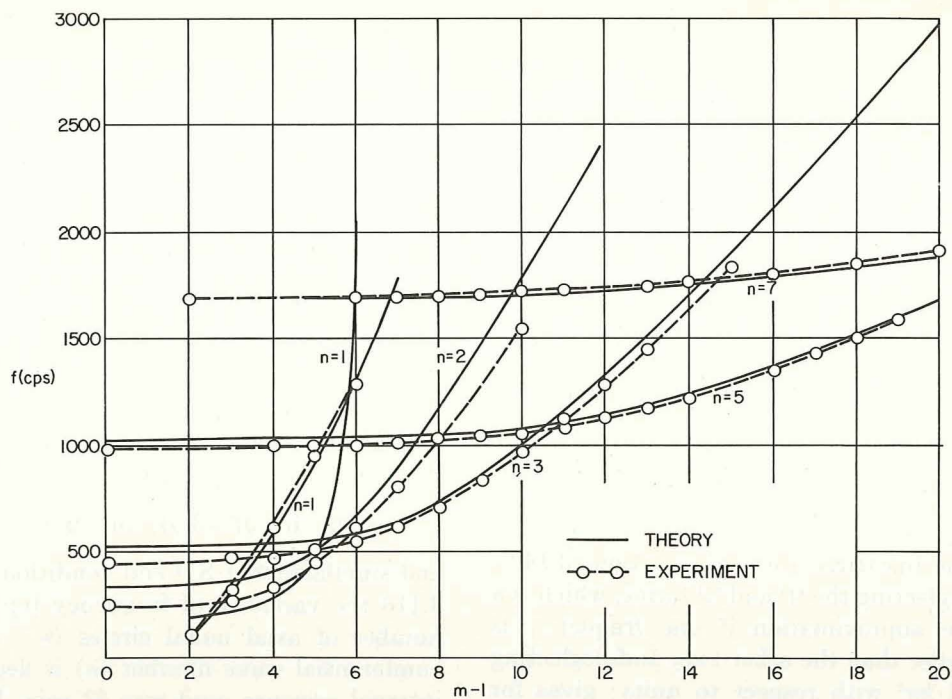


FIGURE 3.116.—Theoretical and experimental frequencies of an SD-SD shell (dimensions given in text) subjected to internal pressure ($N_{\theta}^i = 2N_x^i$). (After ref. 3.106)

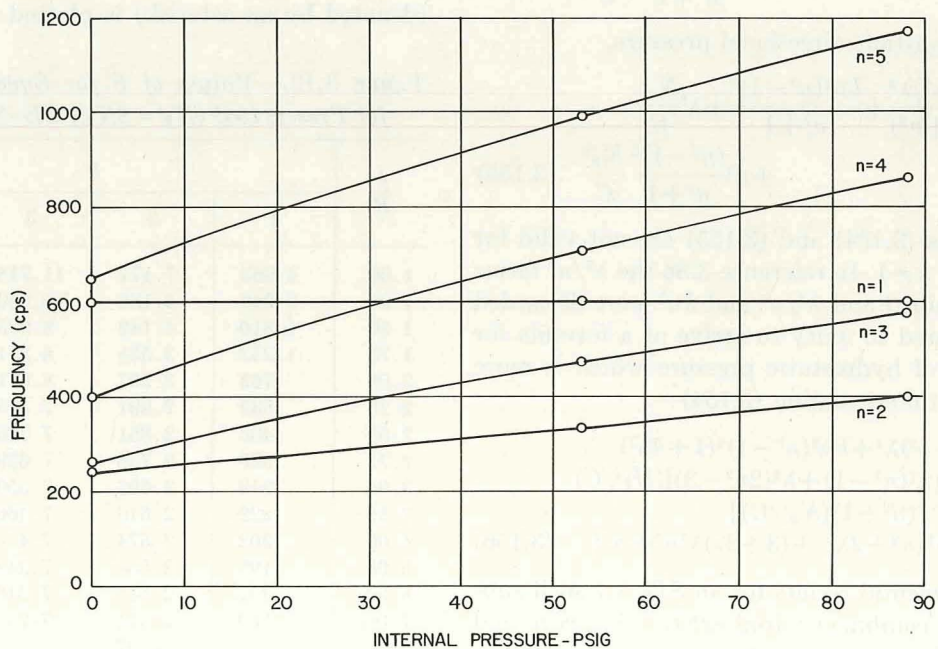


FIGURE 3.117.—Experimentally measured frequency variation with internal pressure ($N_{\theta}^i = 2N_x^i$) for an SD-SD shell (dimensions given in text). (After ref. 3.106)

of Timoshenko beam theory. Additional experimental data are shown in figure 3.117 where the frequency variation with internal pressure is shown for various n and for $m=4$. Free vibrations of circular cylindrical shells supported at both ends by shear diaphragms (SD-SD) and subjected to combined initial stress are also discussed to some extent in references 3.70, 3.77, 3.80, 3.84, 3.87, 3.91, 3.104, and 3.107 through 3.115. In most of these works the Donnell-Mushtari formula (3.137) neglecting tangential inertia is either derived or used.

The preceding results given in this section have all been for shells supported at both ends by shear diaphragms (SD-SD). In this case the equations of motion and the end conditions are exactly satisfied by the simple displacement solution function (eq. (2.20)). For other boundary conditions the problem is considerably more complicated and relatively few results are available.

The method of obtaining exact solutions for unloaded shells having *arbitrary* boundary conditions was discussed in section 2.4. This procedure can also be followed for shells having combined axial and circumferential uniform prestress, as pointed out by Seggelke (ref. 3.116). In reference 3.116 the procedure was used to obtain frequency parameters for *clamped-clamped* shells. Numerical results are indicated in figure 3.118. Equations for two theories (Donnell-Mushtari and Flügge) are developed in reference 3.116, but one cannot tell which theory was used. The shell length parameters used to obtain figure 3.118 are not defined. From other calculations in reference 3.116 it is inferred that $R/h=500$, $l/R=2$, and $\nu=0$.

The effects of replacing the boundary condition $u=0$ by $N_x=0$ (relaxing the constraint on the axial membrane force developed during vibration) are depicted in figures 3.119 and 3.120.

Note in figures 3.119 and 3.120 that the curves are straight lines, indicating a linear relationship between Ω^2 and N_x^i . This phenomenon was also observed in section 3.4.2 in the case of SD-SD end conditions when either the Donnell-Mushtari theory (neglecting tangential inertia) or the Flügge theory (including tangential inertia) are used. This is because terms containing N_x^i in the initial stress matrix operators (3.101a) and

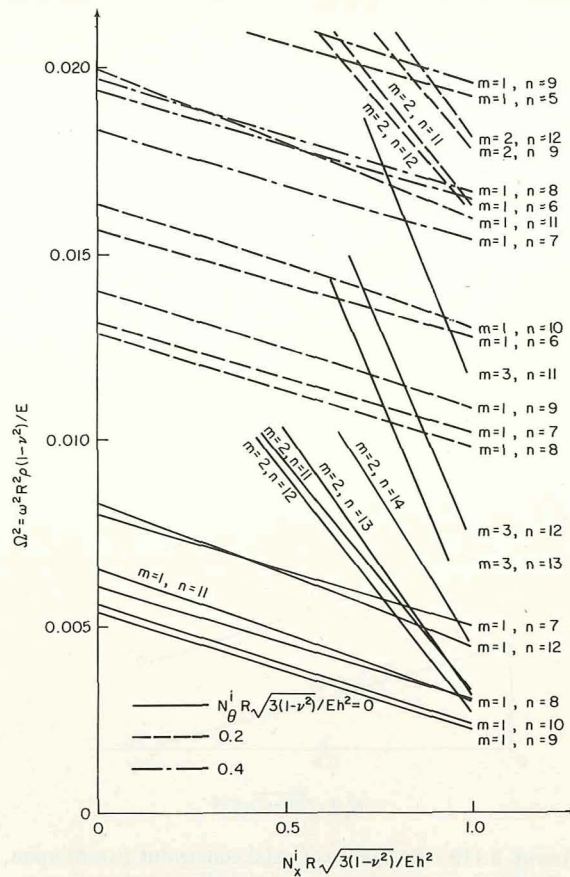


FIGURE 3.118.—Frequency parameters for a clamped-clamped shell subjected to combined uniform prestress. (After ref. 3.116)

(3.102) occur only along the principal diagonal and N_x^i enters each principal diagonal term in the same way. Thus, for *fixed* values of N_θ^i (as in figs. 3.119 and 3.120) the curves of Ω^2 versus N_x^i will be straight lines for *all* possible boundary conditions. Following the same reasoning, plots of Ω^2 versus N_θ^i for fixed values of N_x^i will be straight lines for the Donnell-Mushtari theory and curved lines for the Flügge theory.

Furthermore, it is important to note that if the mathematical statement of the boundary conditions is the same for prestressed and unstressed shells (as in the case of a clamped-clamped shell, where $u=v=w=\partial w/\partial x=0$), then the exact solution procedure described in section 2.4 will yield the same deflection functions (2.53) (i.e., the same values of λ) from satisfying the eight boundary conditions, independent of

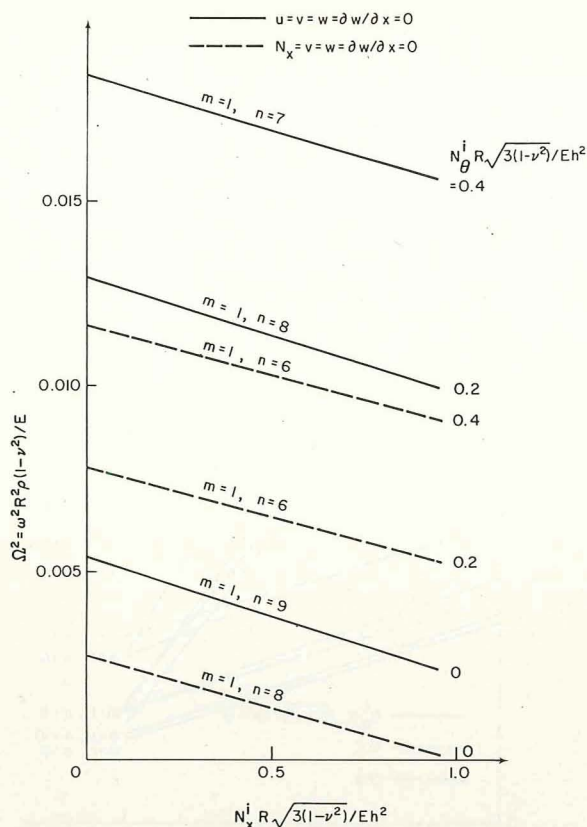


FIGURE 3.119.—Influence of axial constraint ($u=0$) upon the frequency parameters of a shell subjected to combined uniform prestress. (After ref. 3.116)

the prestress conditions. This permits one, for example, to use equation (3.137) for boundary conditions other than SD-SD provided the values of λ and the right-hand-sides (frequency parameters of unloaded shells) are known.

As discussed in section 2.4, the Ritz method or its equivalent for this class of problems, the Bubnov-Galerkin procedure, is a useful approximate technique for finding frequencies and mode shapes of circular cylindrical shells having *arbitrary* boundary conditions. Including the effects of initial stresses is a straightforward and simple extension to the procedure. Ivanyuta and Finkelshteyn (ref. 2.87) laid out the procedure in detail (see sec. 2.4 for details when prestress is not considered) and demonstrated it for the clamped-clamped shell subjected to internal pressure $p_0(N_\theta^i = 2N_x^i)$.

Koval (ref. 3.117) used the approximate deflection function

$$w = C(\cos \beta_{-1}s - \cos \beta_{+1}s) \cos n\theta \cos \omega t \quad (3.157)$$

where $\beta_{\pm 1} = (m \pm 1)\pi R/l$, to satisfy the boundary conditions for a *clamped-clamped* shell. The Donnell-Mushtari shell theory was used and Lagrange's equation was written in terms of the assumed mode. This yielded the following useful frequency formula:

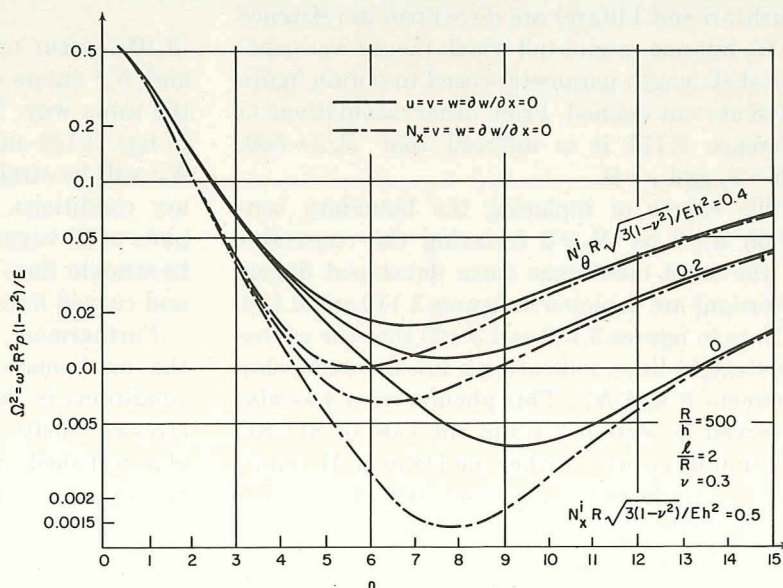


FIGURE 3.120.—Dependence of frequency parameter upon circumferential wave number (n) for partially and completely clamped shells subjected to combined uniform prestress. (After ref. 3.116)

$$\Omega^2 = \frac{(1-\nu^2)\beta_2^2}{3(\beta_2^2+n^2)^2} + \frac{k}{3}(\beta_2^4+2\beta_2^2n^2+3n^4) + \frac{1}{C}\left(\frac{4}{3}\beta_2^2N_{x^i}+n^2N_{\theta^i}\right), m=1 \quad (3.158a)$$

$$\Omega^2 = \frac{(1-\nu^2)}{2} \left[\frac{\beta_{-1}^4}{(\beta_{-1}^2+n^2)^2} + \frac{\beta_{+1}^4}{(\beta_{+1}^2+n^2)^2} \right] + \frac{k}{2}[(\beta_{-1}^2+n^2)^2 + (\beta_{+1}^2+n^2)^2] + \frac{1}{C} \left[\frac{1}{2}(\beta_{-1}^2+\beta_{+1}^2)N_{x^i} + n^2N_{\theta^i} \right], m=2, 3, \dots \quad (3.158b)$$

where

$$\beta_2 = 2\pi R/l, \quad k = h^2/12R^2, \quad \text{and} \quad C = Eh/(1-\nu^2)$$

as before.

Mixson and Heer (refs. 3.114 and 3.115) presented experimental results for two *clamped-clamped* circular cylindrical shells subjected to internal pressure ($N_{\theta^i} = 2N_{x^i}$). One shell was made of 2014-T6 aluminum and had the following

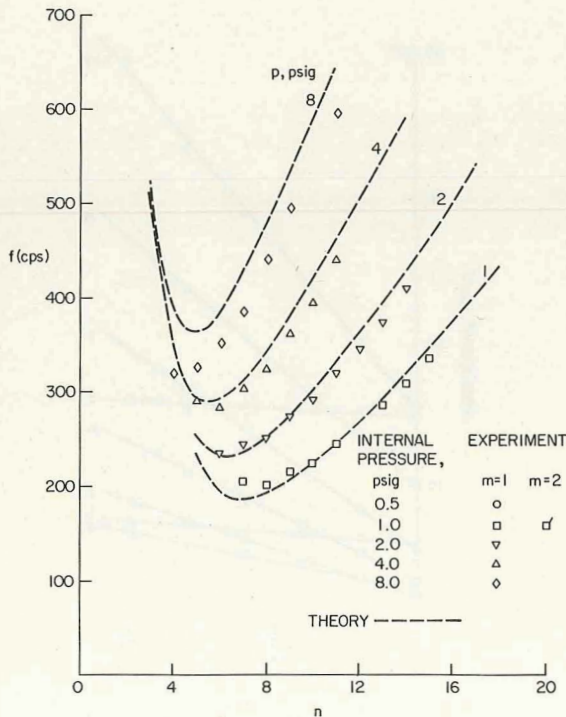


FIGURE 3.121.—Frequencies (cps) of a clamped-clamped, pressurized ($N_{\theta^i} = 2N_{x^i}$) aluminum shell (dimensions given in text). (After refs. 3.114 and 3.115)

dimensions: $l = 28.6$ in., $R = 15.0$ in., $h = 15.0$ in. Experimental data showing the variation of frequency with internal pressure p_0 and circumferential wave number n are exhibited in figure 3.121. A similar plot is made in figure 3.122 for a stainless steel shell having $l = 22.0$ in., $R = 12.0$ in., and $h = 0.004$ in. In both figures theoretical results are shown for SD-SD shells using the Donnell-Mushtari equation (3.137) neglecting tangential inertia. References 3.114 and 3.115 argue that the experimental data for clamped-clamped ends should compare reasonably well with the theoretical results for SD-SD ends because the end conditions have only a small effect upon the frequencies for values of n above the n for minimum frequency.

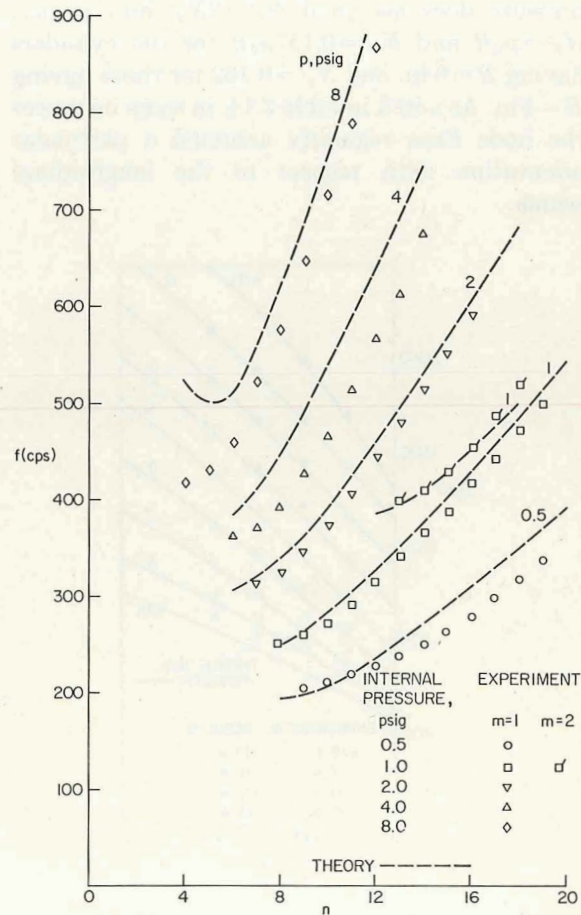


FIGURE 3.122.—Frequencies (cps) of a clamped-clamped, pressurized ($N_{\theta^i} = 2N_{x^i}$) steel shell (dimensions given in text). (After refs. 3.114 and 3.115)

Nikulin (ref. 3.84) obtained results for a circular cylindrical shell *clamped* at both ends and subjected to uniform combined initial stresses. The shell dimensions were $h=0.5$ mm., $l=357$ mm., $R=118$ mm., and the material properties were given by $E=2 \times 10^6$ dyne/cm², $\nu=0.3$, $\rho=8 \times 10^{-6}$ dyne-sec²/cm⁴. Theoretical and experimental frequencies (cps) are compared in figure 3.123 for $\sigma_x^i=1600$ dyne/cm² with varying σ_θ^i and n .

Miserentino and Vosteen (ref. 3.88) obtained extensive experimental data for *clamped-clamped* shells. Geometric and material properties of the models used are summarized in table 3.13. Experimental data for these shells are displayed in table 3.14 for various magnitudes of internal pressure loading. Because of the type of flange attachments used to clamp the ends the internal pressure does *not* yield $N_\theta^i=2N_x^i$ but, rather, $N_\theta^i=p_0R$ and $N_x^i=0.117p_0R$ for the cylinders having $R=6$ in. and $N_x^i=0.162$ for those having $R=4$ in. As noted in table 3.14, in some instances the node lines regularly assumed a particular orientation with respect to the longitudinal seams.

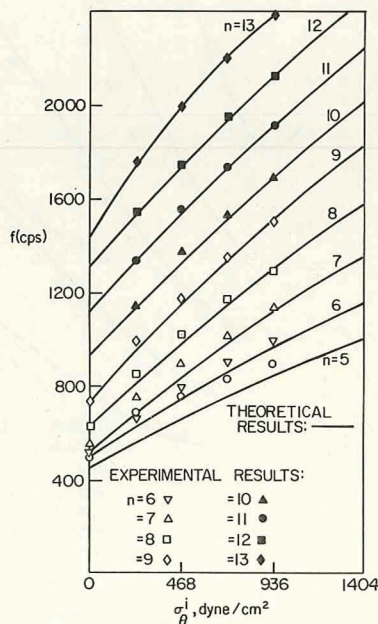


FIGURE 3.123.—Theoretical and experimental frequencies for a clamped-clamped shell (dimensions given in text) subjected to combined uniform initial stress. (After ref. 3.84)

The test results in table 3.14 for shell 324 (the one having the smallest R/h ratio) have also been plotted in figure 3.124. The square of the frequency is plotted as a function of internal pressure for modes having one-half wave length in the axial direction ($m=1$) and for a range of circumferential nodes ($n=2$ to 9). Solid straight lines representing a least squares fit through the data points are also shown. This straight line behavior is the type exemplified by the Donnell-Mushtari theoretical equation (3.137) for SD-SD shells.

In figure 3.125 the experimental results are compared directly with those from equation (3.137). The correction formula (2.151) suggested by Arnold and Warburton (ref. 2.3) to approximate clamped end conditions was used, with c taken as 0.3. The nondimensional frequency parameter $\omega^2 R^2 \rho / E$ is used as the ordinate in this plot. The correlation between theoretical and experimental results is reasonably good except for $n=2$. However, since the slopes of the two lines for $n=2$ are approximately the same, the error lies in the intercept with the ordinate axis,

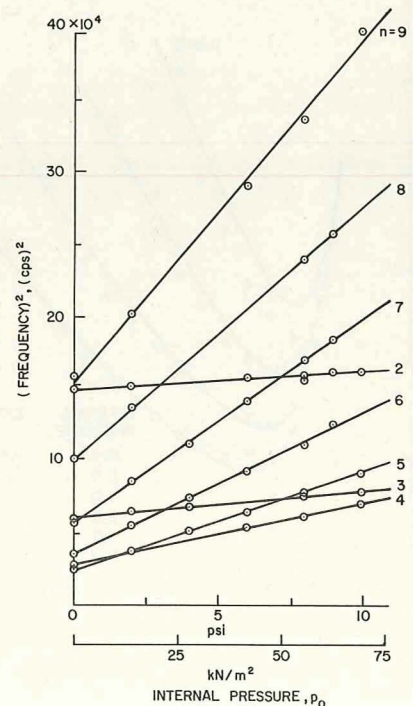


FIGURE 3.124.—Experimental results for pressurized shell 324, clamped-clamped. (After ref. 3.88)

TABLE 3.13.—Physical Properties of Circular Cylindrical Shells Referred to in Tables 3.14 and 3.15

R/h	R		l		h		Material	ρ		E		ν	Number of seam welds
	in.	cm	in.	cm	in.	mm		lb-s ² /in ⁴	kg/m ³	psi	GN/m ²		
324	6.01	15.27	36.00	91.44	0.0185	0.4699	17-7 PH stainless steel	0.7149×10^{-3}	7639	29.0×10^6	200	0.28	2
601	6.01	15.27	36.00	91.44	.0100	.2540	301 stainless steel	.7408	7916	29.0	200	.32	2
645	4.00	10.16	24.00	60.96	.0062	.1575	301 stainless steel	.7408	7916	29.0	200	.32	2
666	4.00	10.16	24.00	60.96	.0060	.1524	301 stainless steel	.7408	7916	29.0	200	.32	2
1001	6.01	15.27	36.00	91.44	.0060	.1524	2024 aluminum	.2524	2699	10.0	72.3	.32	4
1502	6.01	15.27	36.00	91.44	.0040	.1016	304 stainless steel	.7408	7916	29.0	200	.32	1
1624	6.01	15.27	38.20	97.03	.0037	.0940	301 stainless steel	.7408	7916	29.0	200	.32	2

that is to say, with the inaccuracy of the Donnell-Mushtari theory for $n=2$ for *unpressurized* shells (see sec. 2.3.1).

In reference 3.16 the effects of combined axial and circumferential prestress were included in the analysis of circular cylindrical shells having rings and stringers which are represented by "smeared-out" orthotropy. The resulting frequency formula for SD-SD end conditions is given by equation (3.39) where the term

$$-(N_x^i + N_{\theta}^i \delta^2) \frac{m^2 l^2}{\pi^2 D} \quad (3.159)$$

is added to the right-hand-side to account for the initial stresses. The vibration of prestressed structurally orthotropic shells is also discussed in reference 3.118.

The free vibration of orthotropic, circular cylindrical, *membrane* shells were studied by Dym (ref. 3.119).

Other references dealing with free vibrations of circular cylindrical shells subjected to uniform combined prestress include references 3.64, and 3.120 through 3.130.

3.4.5 Uniform Torsional Prestress

Applying a torque to each end of a circular cylindrical shell as in figure 3.126 yields a static initial stress throughout the interior of the shell which is essentially $N_{x\theta}^i = \text{constant}$ (that is, other membrane force resultants and bending moment resultants may be induced by the type of end constraints, but they are assumed to be negligibly small).

From an analytical viewpoint the case of uni-

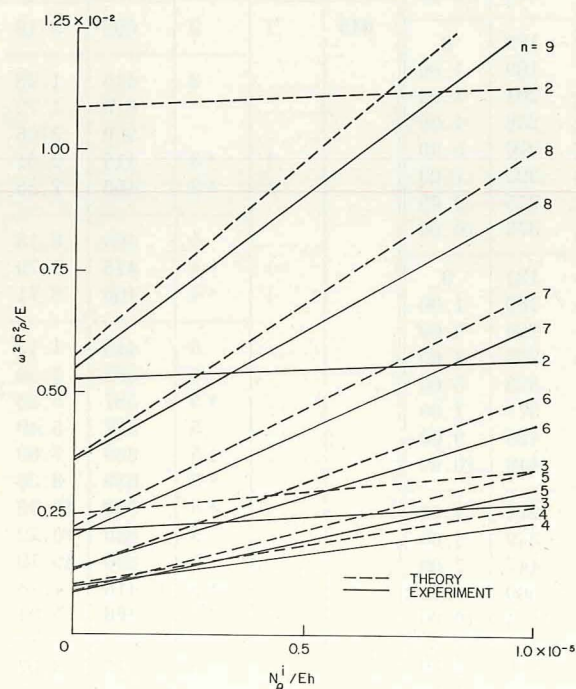


FIGURE 3.125.—Comparison of theoretical and experimental frequency parameters for pressurized shell 324, clamped-clamped. (After ref. 3.88)

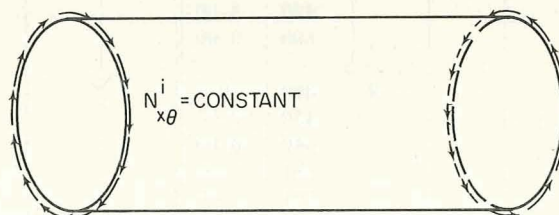


FIGURE 3.126.—Circular cylindrical shell subjected to uniform torsional initial stress.

TABLE 3.14.—*Experimentally Measured Frequencies (cps) for the Shells of Table 3.13 Having Clamped-Clamped Ends*

Shell	m	n	f, cps	p ₀ , psi	Shell	m	n	f, cps	p ₀ , psi	Shell	m	n	f, cps	p ₀ , psi
324	1	a 2	387	0	601	1	2	381	0	601	1	8	450	5.00
		a 2	391	2.00				392	1.00				519	7.00
		b 2	398	6.00				394	4.00				581	9.00
		b 2	400	8.00				395	5.00			9	222	0
		a 2	396	8.00				399	7.00				303	1.00
		b 2	403	9.00				397	9.00				365	2.00
		a 2	402	10.00				398	10.00				463	4.00
		3	245	0			3	252	0				502	5.00
			255	2.00				259	1.00				592	7.00
			262	4.00				269	2.00				662	9.00
			276	8.00				280	4.00				692	10.00
			281	10.00				297	7.00			10	420	2.00
		4	168	0				312	9.00				540	4.00
			193	2.00				313	10.00				585	5.00
			233	6.00			4	165	0				673	7.00
			249	8.00				190	1.00				744	9.00
			265	10.00				207	2.00				781	10.00
		5	160	0				241	4.00			11	338	0
			228	4.00				255	5.00			12	453	2.00
			256	6.00				283	7.00	645	1		2	698
			281	8.00				307	9.00		3	415	1.28	
			303	10.00				319	10.00			415	1.72	
		6	189	0			5	122	0			989	5.66	
			237	2.00				169	1.00		1	a 3	415	
			274	4.00				201	2.00		1	a 3	466	
			306	6.00				256	4.00		4	466	8.18	
			335	8.00				276	5.00			415	5.79	
		7	239	0				323	7.00		1	a 4	466	
			294	2.00				355	9.00			466	8.71	
			335	4.00				373	10.00		5	415	1.19	
			376	6.00			6	121	0			587	4.53	
			413	8.00				180	1.00		5	587	5.38	
		429	9.00	226				2.00	587			5.49		
		8	318	0				296	4.00		a 5	659	7.60	
			370	2.00				328	5.00			659	8.38	
			490	8.00				377	7.00		a 5	830	15.98	
			508	9.00				425	9.00			830	16.22	
			9	399			0	7	446		10.00	5	830	16.79
		450		2.00			270		2.00		a 5		415	
		540		6.00			349		4.00		a 5		466	
		581		8.00			447		7.00		a 6	415	3.07	
		631		10.00			500		9.00			523	5.28	
							524		10.00		8	315	2.00	
								410	4.00					

^a Nodes lines are on seam welds.^b Node lines are off seam welds.

TABLE 3.14.—Experimentally Measured Frequencies (cps) for the Shells of Table 3.13
Having Clamped-Clamped Ends—Continued

Shell	m	n	f, cps	p ₀ , psi	Shell	m	n	f, cps	p ₀ , psi	Shell	m	n	f, cps	p ₀ , psi		
645	1	a 6	587	6.84	645	1	b 9	740	4.30	645	2	8	740	5.51		
			659	8.78				784	4.94				784	6.31		
			698	10.00				830	5.66				830	7.28		
			830	14.31				988	8.44				988	10.79		
		b 6	415	3.21			a 9	415	.59			9	587	1.99		
			466	4.22				698	3.65				659	2.91		
			523	5.59				740	4.17				698	3.36		
			587	7.23				784	4.81				740	4.01		
			830	15.01				830	5.51				784	4.57		
		b 6	830	15.01			988	8.15	b 10			415	.37	10	587	1.32
							466	.75				659	1.99			
							659	2.30				698	2.40			
							784	3.69				740	2.85			
							932	5.53				988	6.06			
		b 6	988	8.15			988	6.34	a 10			466	.45	3	523	3.34
							587	1.45				587	5.00			
							659	2.11				659	6.84			
							698	2.56				698	8.09			
							740	2.98				740	9.31			
		a 7	784	9.01			988	6.19	11			587	.78		7	587
			830	10.20			698	1.58				659	5.35			
							784	2.42				698	6.24			
							988	4.77				740	7.16			
			b 8	329			.55	12	740			1.16	8	740	5.35	
				466			2.03		784			1.56		784	6.12	
				587			3.51		988			3.66		830	7.12	
				659			4.55		2			6		523	3.81	9
		698		5.16			587	5.49				698	3.26			
		740		5.91			659	7.38				10	698	2.31		
		784		6.78		830	12.85									
		830	7.73	7		415	1.46	666	1			b 2	659	0		
		988	11.20			659	5.60						671	4.05		
						698	6.54						669	6.20		
						740	7.50				671		6.60			
						784	8.61				672		6.90			
						830	9.86				673		8.00			
		a 8	466	1.76		8	587				3.08		675	8.10		
			587	3.32			698				4.71		677	8.30		
			784	6.57									675	8.70		
			830	7.46												
			988	11.08												
		b 9	329	.15												
			415	.67												
466	1.07															
587	2.29															
659	3.17															
698	3.74															

^a Node lines are on seam welds.^b Node lines are off seam welds.

TABLE 3.14.—*Experimentally Measured Frequencies (cps) for the Shells of Table 3.13 Having Clamped-Clamped Ends—Continued*

Shell	m	n	f, cps	p ₀ , psi	Shell	m	n	f, cps	p ₀ , psi	Shell	m	n	f, cps	p ₀ , psi
666	1	^b 2	674	8.90	666	1	5	418	4.75	666	1	6	635	8.78
			670	9.50				466	5.75				645	9.10
			672	10.00				492	6.80				675	10.00
			674	10.20				519	7.40				685	10.00
			679	11.10				508	7.40				703	10.90
			680	12.40				507	7.40				714	10.90
		3	415	2.00				513	7.60			7	579	4.00
			435	3.20				523	7.60				597	4.40
			439	3.30				524	7.95				639	5.30
			437	3.40				529	8.00				648	5.40
			447	4.30				529	8.10				656	5.60
			447	4.40				527	8.10				659	5.70
			448	4.50				536	8.10				677	5.95
			451	4.80				548	8.50				673	6.00
			458	5.10				544	8.70				690	6.35
			457	5.40				556	8.70				697	6.45
			462	6.00				549	9.00				701	6.60
			463	6.10				552	9.10				709	6.70
			473	6.55				578	9.50				713	6.80
			472	6.80				567	9.70				736	7.40
			472	6.90				590	10.10				761	8.00
			476	7.30				651	12.40				761	8.00
			479	7.60				651	12.75				766	8.20
			486	8.00			6	402	3.00				768	8.20
			484	8.10				412	3.20				794	8.70
			484	8.10				415	3.25				821	9.50
			491	8.30				437	3.60				818	9.50
			490	8.70				458	4.00				826	9.60
			490	8.78				471	4.30				820	9.60
			490	8.80				493	4.80				826	9.80
			492	8.90				498	5.00				850	10.40
			494	9.00				505	5.20			8	449	1.35
			494	9.00				515	5.30				568	2.90
			496	9.30				517	5.40				580	3.00
			500	9.60				531	5.70				631	3.90
			506	10.20				531	5.75				663	4.30
			513	11.10				548	6.20				684	4.80
			513	11.28				556	6.45				749	5.70
			522	12.40				573	6.70				755	6.00
		4	367	4.20				578	6.90				777	6.60
			373	4.30				580	7.10				781	6.60
			383	4.30				596	7.40				781	6.70
			394	4.79				600	7.60				850	7.95
			441	6.80				615	7.90				848	8.10
			446	7.65				620	8.00				883	8.70
			464	7.90				619	8.00				888	8.90
			485	8.10				621	8.10				884	9.00
			525	11.10				616	8.10				922	9.60
		5	402	4.30				631	8.30				915	9.60
			424	4.70				629	8.50				937	10.00
								639	8.70					

^b Node lines are off seam welds.

TABLE 3.14.—*Experimentally Measured Frequencies (cps) for the Shells of Table 3.13 Having Clamped-Clamped Ends—Continued*

Shell	<i>m</i>	<i>n</i>	<i>f</i> , cps	<i>p</i> ₀ , psi	Shell	<i>m</i>	<i>n</i>	<i>f</i> , cps	<i>p</i> ₀ , psi	Shell	<i>m</i>	<i>n</i>	<i>f</i> , cps	<i>p</i> ₀ , psi		
666	1	9	537	1.35	666	1	14	1077	2.25	666	2	5	537	3.30		
			648	2.90				1140	2.90				545	3.65		
			671	2.90				1253	4.10				556	3.90		
			719	3.60				1520	6.90				554	4.00		
			758	3.90									579	4.00		
			759	4.10			15	1029	.70				570	4.30		
			804	4.75				1628	6.00				581	4.80		
			902	6.40			16	1105	.70				579	4.80		
			927	7.00									585	5.00		
			1045	9.00			18	1425	.70				617	5.95		
													630	6.90		
		10	10	405			0	2	3				967	3.30	652	8.00
				543			1.00						964	3.40	645	8.10
				569			1.35						970	4.10	676	9.00
				591			1.35						970	4.75	678	9.25
				671			2.00						978	5.40	680	9.25
				731			2.90						978	5.80	684	9.50
				741			2.90						973	6.30	683	9.60
				800			3.35						982	6.35	684	9.60
				835			4.00						982	6.50	693	10.00
				890			4.75						980	6.60	696	10.20
				910			5.20						979	6.90	714	10.90
				910			5.20						982	7.00	723	11.10
				934			5.50						983	7.00		
				978			5.80					990	8.00	6	497	3.40
				1029			6.70					991	8.10		524	3.90
				1179			9.00					986	8.20		545	4.30
				1188			9.10					992	8.85		544	4.40
	11			11		149	0			991	8.90	591	5.25			
						598	1.00			990	9.00	607	5.70			
			622			1.00	997			9.60	609	6.00				
			751			2.00	997			9.60	624	6.20				
			798			2.25	995			9.80	630	6.45				
			800			2.27	993			9.90	646	6.90				
			850			3.25	1002			10.00						
			897			3.30	1054			11.11	1001	1	2	262	1.00	
			903			3.40								276	2.00	
			962			4.00								297	4.00	
	970		4.10	4		666	3.00			317			6.00			
	1120		6.45			670	3.40									
12	12		732			1.00	682			3.50			3	262	2.00	
			800			1.65	677			4.30				280	3.00	
			850			2.00	699			4.75				297	4.00	
			883			2.25	716			6.00				313	5.00	
			946			2.90	715			6.30						
			1054			4.10	723			6.42	4	212	1.00			
			1247			6.45	716			6.70		276	2.00			
							725			6.95		322	3.00			
							739			8.10		401	5.00			
							743			8.15		430	6.00			
		13	13			800	.65	758	9.33	5	225	1.00				
						814	.80	764	9.80		301	2.00				
						850	1.10	765	10.00		356	3.00				
						991	2.25	778	11.10							
1182	4.10				790	12.40										

TABLE 3.14.—*Experimentally Measured Frequencies (cps) for the Shells of Table 3.13 Having Clamped-Clamped Ends—Continued*

Shell	<i>m</i>	<i>n</i>	<i>f</i> , cps	<i>p</i> ₀ , psi	Shell	<i>m</i>	<i>n</i>	<i>f</i> , cps	<i>p</i> ₀ , psi	Shell	<i>m</i>	<i>n</i>	<i>f</i> , cps	<i>p</i> ₀ , psi
1001	1	5	413	4.00	1001	2	4	238	1.00	1502	1	10	595	2.00
			453	5.00				375	4.00				688	4.00
			494	6.00				423	5.00				551	2.00
		6	283	1.00			5	231	1.00			11	551	2.00
			365	2.00				315	2.00				653	2.00
			443	3.00				371	3.00			13	672	2.00
			507	4.00				426	4.00				494	5.00
			517	6.00				473	5.00			7	380	2.00
								514	6.00				495	4.00
	2	7	309	1.00			6	287	1.00				550	5.00
			421	2.00				520	4.00				506	2.00
			719	6.00				576	5.00					
		8	353	1.00			7	330	1.00			6	363	2.00
			480	2.00				432	2.00				410	3.00
			669	4.00				528	3.00				457	4.00
			748	5.00				613	4.00				494	5.00
			821	6.00				683	5.00					
		9	408	1.00			8	373	1.00			10	506	2.00
			729	4.00				608	3.00					
		10	474	1.00			9	764	5.00			12	424	1.00
			610	2.00									419	2.00
			816	4.00									416	3.00
	3	11	545	1.00	1502	1	2	451	2.00	1624	1	2	432	4.00
			717	2.00				452	3.00				420	4.00
			850	3.00				459	4.00				433	5.00
		12					3	283	2.00				426	5.00
			617	1.00				296	3.00				429	6.00
			784	2.00				314	4.00				448	6.90
			951	3.00				324	5.00				430	7.00
			1190	5.00									434	8.00
		13	657	1.00			4	240	2.00				432	9.00
			1303	5.00				296	4.00				432	10.00
													433	11.00
		14	699	1.00			5	257	2.00			3	444	11.00
			940	2.00				307	3.00				435	12.00
			1260	4.00				378	5.00				432	13.00
			1300	5.00									421	14.00
		15	798	1.00			6	298	2.00				279	1.00
			1019	2.00				404	4.00				285	2.00
			1568	5.00				441	5.00				290	2.00
	4	16	938	1.00			7	342	2.00			3	303	2.30
			1169	2.00				411	3.00				309	3.00
			1685	5.00				475	4.00				317	3.50
		17					8	392	2.00				344	4.00
								472	3.00				324	5.00
													334	6.00
													346	6.00
													352	6.90
													361	8.00
		18	276	2.00			9	445	2.00				371	8.00
			316	4.00				547	3.00				369	9.00
	5	3	336	5.00			10	616	4.00				380	9.00
			354	6.00				687	5.00					

TABLE 3.14.—*Experimentally Measured Frequencies (cps) for the Shells of Table 3.13 Having Clamped-Clamped Ends—Concluded*

Shell	<i>m</i>	<i>n</i>	<i>f</i> , cps	<i>p</i> ₀ , psi	Shell	<i>m</i>	<i>n</i>	<i>f</i> , cps	<i>p</i> ₀ , psi	Shell	<i>m</i>	<i>n</i>	<i>f</i> , cps	<i>p</i> ₀ , psi
1624	1	3	382	10.00	1624	1	6	113	0	1624	1	8	579	4.00
			389	10.00				156	1.00				633	5.00
			391	11.00				301	2.00				642	5.00
			402	11.00				321	2.00				671	5.46
			399	12.00				368	3.00				696	6.00
			414	12.00				379	3.00				709	6.10
			414	13.00				433	4.00				751	7.00
			418	13.00				482	5.00				807	8.00
			421	14.00				516	6.00				847	9.00
			437	14.00				525	6.00				892	10.00
		4	170	0				568	7.00				943	11.00
			203	1.00				596	8.00				1022	13.00
			249	2.00				628	9.00			9	261	.55
			279	3.00				641	9.00				344	1.00
			306	4.00				659	10.00				413	1.53
			327	5.00				706	11.00				472	2.03
			356	6.00				718	12.00				569	3.00
			380	7.00				745	13.00				682	4.40
			425	9.00				759	13.00				717	5.00
			446	10.00			7	199	.55				793	6.00
			466	11.00				256	1.00				813	6.30
			481	12.00				265	1.00				971	9.00
			494	13.00				316	1.46				1017	10.00
			514	14.00				364	2.00				1068	11.00
								382	2.2			10	237	.25
		5	126	0				441	3.00				294	.55
			203	1.00				479	3.5				389	1.00
			266	2.00				497	4.00				458	1.47
			281	2.30				524	4.4				530	2.00
			318	3.00				551	5.00				529	2.02
			323	3.00				558	5.00				569	2.38
			349	3.50				606	6.00				632	3.00
			370	4.00				617	6.00				631	3.00
			397	4.00				634	6.3				696	3.50
			405	5.00				652	7.00				772	4.44
			429	5.00				740	9.00			11	323	.55
			463	6.00				775	10.00				410	1.00
			472	6.00				814	11.00				763	3.50
			504	7.00				820	11.00				848	4.40
			521	7.00				881	13.00				1293	11.00
			505	8.00			8	231	0.55			12	208	0
			521	9.00				289	1.00				1004	6.20
			532	9.00				358	1.47				1077	7.00
			547	10.00				412	1.94				1223	9.00
			558	10.00				419	2.00				1350	11.00
			571	11.00				437	2.20			2	672	9.00
			586	11.00				468	2.56				473	11.00
			594	12.00				501	3.00				529	11.00
			609	12.00				502	3.00					
			613	13.00				510	3.00					
			627	13.00				539	3.50					
			665	14.00				564	4.00					
			639	14.00									1183	14.00

form torsional prestress is somewhat more complicated than the cases of uniform axial or circumferential stress because the initial stress matrix operators (see sec. 3.4.1) contain terms having mixed partial derivatives which are of odd order with respect to θ . Simple solutions using displacement functions of the forms given either by equations (2.20) or (2.53) require even numbers of derivatives with respect to θ in the equations of motion in order to be useful.

Koval and Cranch (refs. 3.131 and 3.132) generalized the solution procedure by choosing

$$\left. \begin{aligned} u &= A e^{\lambda s} e^{in\theta} \cos \omega t \\ v &= B e^{\lambda s} e^{in\theta} \cos \omega t \\ w &= C e^{\lambda s} e^{in\theta} \cos \omega t \end{aligned} \right\} \quad (3.160)$$

Substituting equations (3.160) into the equations of motion for the Donnell-Mushtari theory (see sec. 3.4.1) yields the characteristic equation:

$$\begin{aligned} 2\Omega^6 - \Omega^3 \{ 2 - (3 - \nu)n^2[(\lambda/n)^2 - 1] \\ + 2kn^4[(\lambda/n)^2 - 1] \} \\ + \Omega^2 \{ (3 - \nu)n^2[1 - (\lambda/n)^2] + 2n^2[\nu^2(\lambda/n)^2 - 1] \\ + (1 - \nu)n^4[(\lambda/n)^2 - 1]^2 \\ + (3 - \nu)kn^6[1 - (\lambda/n)^2]^3 \} \\ - (1 - \nu)kn^8[(\lambda/n)^2 - 1]^4 - (1 - \nu^2)(1 - \nu)\lambda^4 \\ + i(2N_{x\theta}i\lambda n/C) \{ -2\Omega^2 - n^2\Omega(3 - \nu)[(\lambda/n)^2 - 1] \\ - n^4(1 - \nu)[(\lambda/n)^2 - 1]^2 \} \end{aligned} \quad (3.161)$$

Upon examining equation (3.161) it is seen that it is of the same form as the characteristic equation (2.35) for unloaded shells for the Donnell-Mushtari theory (i.e., $\Delta K_2 = \Delta K_1 = \Delta K_0 = 0$) except that

(1) λ^2 is replaced by $-\lambda^2$ to account for the more general exponential variation in x used in equations (3.160) than in equations (2.20).

(2) An imaginary term is added which accounts for the torsional prestress. This imaginary term is a result of the odd derivative with respect to θ which occurs in the third equation of motion. The amplitude ratios were

$$\left. \begin{aligned} \frac{A}{C} &= \lambda \left\{ \nu\Omega^2 + \frac{1-\nu}{2}n^2[\nu(\lambda/n)^2 + 1] \right\} / \left\{ \Omega^4 + \frac{3-\nu}{2}n^2\Omega^2[(\lambda/n)^2 - 1] + \frac{1-\nu}{2}n^4[(\lambda/n)^2 - 1]^2 \right\} \\ \frac{B}{C} &= in \left\{ \Omega^2 + \frac{1-\nu}{2}n^2[(2+\nu)(\lambda/n)^2 - 1] \right\} / \left\{ \Omega^4 + \frac{3-\nu}{2}n^2\Omega^2[(\lambda/n)^2 - 1] + \frac{1-\nu}{2}n^4[(\lambda/n)^2 - 1]^2 \right\} \end{aligned} \right\} \quad (3.162)$$

where Ω is the usual nondimensional frequency parameter given by equation (2.26).

The standard procedure at this point is to determine the eight roots λ_j , of equation (3.161) and use these values to form the general solutions

$$\left. \begin{aligned} u &= \sum_{j=1}^8 A_j e^{\lambda_j s} e^{in\theta} \cos \omega t \\ v &= \sum_{j=1}^8 B_j e^{\lambda_j s} e^{in\theta} \cos \omega t \\ w &= \sum_{j=1}^8 C_j e^{\lambda_j s} e^{in\theta} \cos \omega t \end{aligned} \right\} \quad (3.163)$$

Substituting these solutions into the eight boundary conditions leads to a characteristic determinant, the three roots of which are the frequencies. This procedure parallels the one outlined in section 2.4 for unloaded shells.

In references 3.131 and 3.132 the algebra was somewhat simplified by making Yu's (see sec. 2.3.5) assumption, $|\lambda/n|^2 \ll 1$. Then equation (3.161) becomes

$$\lambda^4 - i(\alpha_1 N_{x\theta} i/C)\lambda - \alpha_2 = 0 \quad (3.164)$$

where

$$\left. \begin{aligned} (1 - \nu)(1 - \nu^2)\alpha_1 &= 2[2n\Omega^4 - n^3(3 - \nu)\Omega^2 \\ &\quad + (1 - \nu)n^5] \\ (1 - \nu)(1 - \nu^2)\alpha_2 &= 2\Omega^6 - \Omega^4[2 + (3 - \nu)n^2 \\ &\quad + kn^4] + \Omega^2[(1 - \nu) \\ &\quad (n^2 + n^4) + (3 - \nu)kn^6] \\ &\quad - (1 - \nu)kn^8 \end{aligned} \right\} \quad (3.165)$$

and the amplitude ratios reduce to

$$\left. \begin{aligned} \frac{A}{C} &= \lambda \frac{2\nu\Omega^2 + (1 - \nu)n^2}{2\Omega^4 - (3 - \nu)n^2\Omega^2 + (1 - \nu)n^4} \\ \frac{B}{C} &= in \frac{2\Omega^2 - (1 - \nu)n^2}{2\Omega^4 - (3 - \nu)n^2\Omega^2 + (1 - \nu)n^4} \end{aligned} \right\} \quad (3.166)$$

For a shell supported at both ends by shear diaphragms (boundary conditions given by eqs. (2.33)) references 3.131 and 3.132 show that the formal solution to the problem of finding the frequency parameters Ω is given implicitly by

$$-4\eta(\eta^2 + \xi^2) = \alpha_1 N_{x\theta}^i / C \quad (3.167a)$$

$$(\eta^2 - \xi^2)^2 - 4\eta^2(\eta^2 - \xi^2) = \alpha_2 \quad (3.167b)$$

where α_1 and α_2 are defined by equations (3.165) and, further,

$$\cos \frac{2\eta l}{R} - \cosh \frac{\xi l}{R} \cos \frac{\xi l}{R} = \frac{3\eta^4 + 2\eta^2\xi^2 + \xi^4}{2\xi\eta^2\sqrt{2\eta^2 + \xi^2}} \sinh \frac{\xi l}{R} \sin \frac{\xi l}{R} \quad (3.168)$$

where

$$\xi^2 = 2\eta^2 + \xi^2 \quad (3.169)$$

For large values of $\xi l/R$, equation (3.168) reduces to

$$\tan \frac{\xi l}{R} = -\frac{2\xi\eta^2\sqrt{2\eta^2 + \xi^2}}{3\eta^4 + 2\eta^2\xi^2 + \xi^4} \quad (3.170)$$

In reference 3.131 two approximate procedures were also used to obtain results for the SD-SD shell. The Donnell-Mushtari equations neglecting tangential inertia were used with the Galerkin procedure in one case. A deflection function

$$w = \cos n\theta \sum_{m=1}^{\infty} a_m \sin \lambda s + \sin n\theta \sum_{m=1}^{\infty} b_m \sin \lambda s \quad (3.171)$$

was used, where $\lambda = m\pi R/l$. A first approximation formula for frequency parameters is

$$\Omega^2 = \frac{M_1 + M_2}{2} - \sqrt{\left(\frac{M_1 - M_2}{2}\right)^2 + H_1 \frac{N_{x\theta}^i}{C}} \quad (3.172)$$

where

$$M_j = k \left(n^2 + \frac{j^2 \pi^2 R^2}{l^2} \right)^2 + \frac{(1-\nu^2)j^2 \pi^4 R^4}{l^4 \left(n^2 + \frac{j^2 \pi^2 R^2}{l^2} \right)^2} \quad j=1, 2, \dots \quad (3.173)$$

and

$$H_1 = \frac{4}{9} \left(\frac{8nR}{l} \right)^2 \quad (3.174)$$

A second and more accurate approximation for Ω^2 is the implicit formula

$$N_{x\theta}^i = \frac{Cl}{8nR} \left\{ [(M_1 - \Omega)(M_2 - \Omega)(M_3 - \Omega)] \div \left[\frac{4}{9}(M_3 - \Omega) + \frac{36}{25}(M_1 - \Omega) \right] \right\} \quad (3.175)$$

The second approximate procedure used in reference 3.131 was based upon assuming an approximate vibration mode shape, formulating the expressions for strain energy and kinetic energy, and applying Lagrange's equations to solve the problem. The assumed mode shapes are

$$\left. \begin{aligned} u &= A \frac{\partial}{\partial x} [\varphi(x) \cos(\beta x + n\theta)] \\ v &= B \varphi(x) \sin(\beta x + n\theta) \\ w &= C \varphi(x) \cos(\beta x + n\theta) \end{aligned} \right\} \quad (3.176)$$

where

$$\varphi(x) = \sin \lambda x \quad (3.177)$$

with $\lambda = m\pi R/l$ and β an undetermined parameter which varies with $N_{x\theta}^i$. These displacements yield $u=v=w=0$, $\partial^2 w / \partial x^2 \neq 0$ at the boundaries. Applying Lagrange's equations yields the characteristic equation

$$\bar{K}_3 \Omega^6 - \bar{K}_2 \Omega^4 + \bar{K}_1 \Omega^2 - \bar{K}_0 = 0 \quad (3.178)$$

where

$$\bar{K}_3 = \lambda^2 + \beta^2$$

$$\bar{K}_2 = A_1 + (\lambda^2 + \beta^2)(A_2 + A_3)$$

$$\bar{K}_1 = A_3[(\lambda^2 + \beta^2)A_2 + A_1] + A_1 A_2$$

$$\bar{K}_0 = A_1 A_2 A_3 + 2A_1 A_5 A_6 - A_2 A_6^2 - A_3 A_5^2 - A_1 A_4^2$$

$$A_1 = (\lambda^2 + \beta^2)^2 + 4\lambda^2 \beta^2 + \left(\frac{1-\nu}{2} \right) n^2 (\lambda^2 + \beta^2)$$

$$A_2 = n^2 + \left(\frac{1-\nu}{2} \right) (\lambda^2 + \beta^2) + k[n^2 + 2(1-\nu)(\lambda^2 + \beta^2)]$$

$$A_3 = 1 + k[(\lambda^2 + \beta^2)^2 + 4\lambda^2 \beta^2 + n^4 + 2n^2(\lambda^2 + \beta^2)] - 2\beta n N_{x\theta}^i / C$$

$$A_4 = n + k[n^2 + (2-\nu)n(\lambda^2 + \beta^2)]$$

$$A_5 = \left(\frac{1-\nu}{2} \right) n(\lambda^2 + \beta^2)$$

$$A_6 = \nu(\lambda^2 + \beta^2) \quad (3.179)$$

Assuming that the parameter β varies linearly with $N_{x\theta}^i$, taking on values $\beta=0$ when $N_{x\theta}^i=0$ and $\beta=\beta_{cr}$ for the limiting case of buckling ($\Omega^2=0$), the roots of equation (3.178) can be found. Numerical results for a shell having $R/h=300$, $l/R=4$, $\nu=0.3$, $E=30 \times 10^6$ psi., $m=1$ and $n=8$ are given in figure 3.127 for both the second approximation Galerkin procedure and the assumed mode energy procedure.

Nikulin (refs. 3.83 and 3.84) obtained the following formula for the frequency parameters of

SD-SD shells (see earlier references in this chapter) subjected to twisting moment:

$$\Omega^2 = \frac{(1-\nu^2)\lambda^4 + k(\lambda^2 + n^2)^4 - \frac{2N_{x\theta}^i}{C}\lambda n(\lambda^2 + n^2)^2}{(\lambda^2 + n^2)^2 + n^2 + (3+2\nu)\lambda^2} \quad (3.180)$$

where $\lambda = m\pi R/l$ and $k = h^2/12R^2$ as before. Curves showing the decrease in frequency ratio ω/ω_0 (ω_0 is the frequency in the absence of initial stress) are shown in figure 3.128 for a shell hav-

FIGURE 3.127.—Comparison of approximate solutions for a "freely supported" ($u=v=w=0$, $\partial^2 w/\partial^2 \neq 0$) shell. (After ref. 3.131)

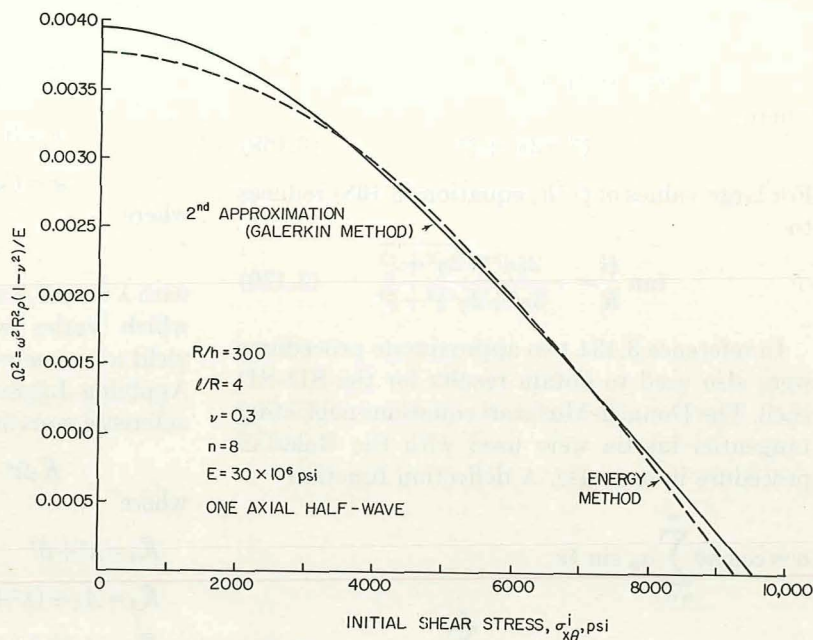
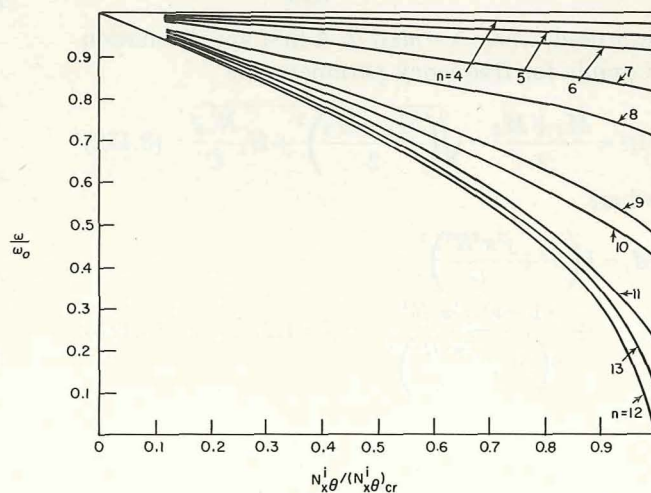


FIGURE 3.128.—Frequency ratio versus torsional stress ratio for an SD-SD shell; $R/h=500$, $l/R=2$, $m=1$. (After ref. 3.84)



ing $R/h=500$, $l/R=2$, and $m=1$. The quantity $(N_{x\theta})_{cr}$ used for the ratio of initial stresses is the least value of $N_{x\theta}^i$ at buckling (i.e., $\omega=0$, which occurs for $n=12$).

Koval and Cranch (refs. 3.131 and 3.132) also presented numerical results for clamped-clamped shells. Following the exact solution procedure outlined earlier in this section, it is found that the formal solution for frequency parameters is contained implicitly in equations (3.165), (3.167), and (3.169), and

$$\cos \frac{\xi l}{R} \cos \frac{\xi l}{R} - \cos \frac{2\eta l}{R} = \frac{3\eta^2}{\xi \zeta} \sinh \frac{\xi l}{R} \sin \frac{\xi l}{R} \quad (3.181)$$

In the case of long shells ($\xi l/R \gg 1$), equation (3.181) simplifies to

$$\eta = -\frac{0.6801\xi}{\tan(\xi l/R)} \quad (3.182)$$

The equations were further simplified by neglecting tangential inertia (see sec. 2.3.4), giving

$$(1-\nu^2)\alpha_1 = 2n^5 \quad (3.183a)$$

$$(1-\nu^2)\alpha_2 = \Omega^2 n^4 - kn^8 \quad (3.183b)$$

in place of equations (3.165). Then equations (3.167a), (3.182) and (3.183a) uniquely determine η and ξ for a given $N_{x\theta}^i$, and the frequency is determined from equations (3.167b) and (3.183b). A plot of the frequency parameter Ω^2 versus the torsional shear stress $\sigma_{r\theta}^i$ is shown in figure 3.129 for a shell having $R/h=300$, $l/R=4$, $\nu=0.3$, and $E=30 \times 10^6$ psi.

In reference 3.131 two approximate procedures

were also used to obtain results for the clamped-clamped shell. The Donnell-Mushtari equations neglecting tangential inertia were used with the Galerkin procedure to arrive at the following first approximation for a frequency parameter formula:

$$\Omega^2 = \frac{G+F}{2} - \sqrt{\left(\frac{G-F}{2}\right)^2 + H_2 \frac{N_{x\theta}^i}{C}} \quad (3.184)$$

where

$$\left. \begin{aligned} G &= (M_1 + M_3)/2 \\ F &= (2M_0 + M_2)/3 \\ H_2 &= (32)^3 n^2 R^2 / 675 l^2 \end{aligned} \right\} \quad (3.185)$$

and M_j is defined by equation (3.173). Furthermore, a second approximation was found from

$$\begin{aligned} N_{x\theta}^i &= \frac{Cl}{8nR} \left\{ (M_1 + M_3 - 2\Omega^2)(2M_0 + M_2 \right. \\ &\quad \left. - 3\Omega^2)(M_2 + M_4 - 2\Omega^2) - (M_2 - \Omega^2)^2 \right\} \\ &\quad \div \left\{ \left(\frac{32}{15}\right)^2 (M_2 + M_4 - 2\Omega^2) \right. \\ &\quad \left. - \left(\frac{64}{15}\right)\left(\frac{352}{105}\right)(M_2 - \Omega^2) \right. \\ &\quad \left. + \left(\frac{352}{105}\right)^2 (2M_0 + M_2 - 3\Omega^2) \right\}^{1/2} \quad (3.186) \end{aligned}$$

where it is computationally easier to substitute into equation (3.186) a value of Ω^2 lower than the load-free value and solve directly for the corresponding torsional stress. In figure 3.130 the first and second approximation Galerkin-type solutions are compared with the exact solution

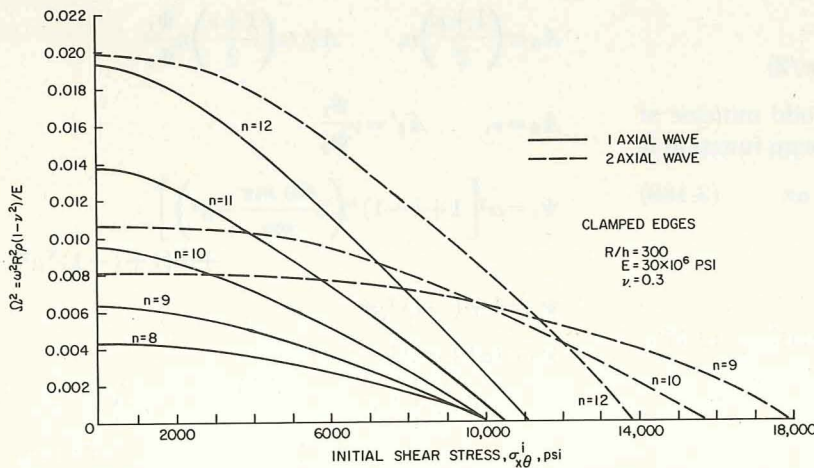


FIGURE 3.129.—Lowest frequency parameters for a clamped-clamped shell subjected to uniform torsional prestress. (After ref. 3.132)

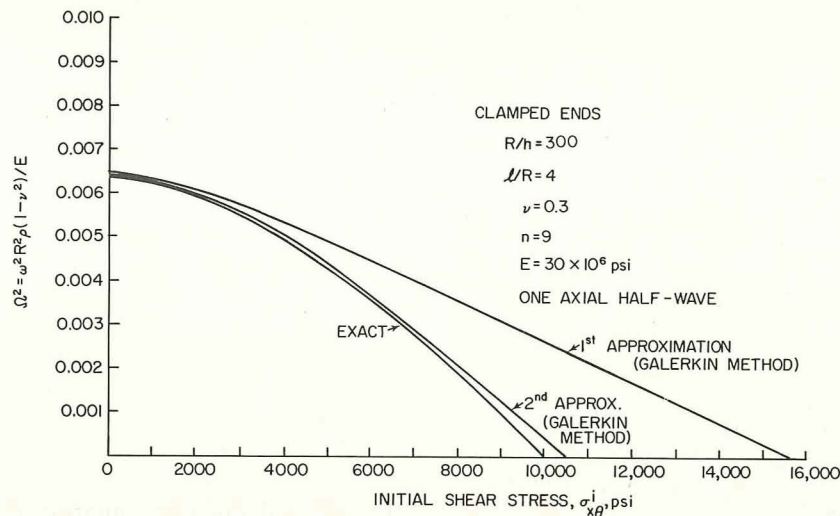


FIGURE 3.130.—Comparison of exact and approximate solutions for a clamped-clamped shell. (After ref. 3.131)

described earlier for the clamped-clamped shell having $R/h=300$, $l/R=4$, $\nu=0.3$, $E=30 \times 10^6$ psi., $m=1$ and $n=9$.

The assumed mode energy approach using Lagrange's equations described earlier was also used in references 3.131 and 3.132 to analyze the clamped-clamped shell. The function $\varphi(x)$ used in equations (3.176) is (in this case) the beam function for symmetric modes (odd numbers of axial half-waves)

$$\varphi(x) = \cos \alpha x + \mu \cosh \alpha x \quad (3.187)$$

in terms of a coordinate origin emanating from the middle of the shell, where

$$\alpha = m\pi R/l$$

$$m = 1.506, 3.500, 5.500, \dots$$

$$\mu = \sin(m\pi/2)/\sinh(m\pi/2)$$

For axially unsymmetric modes (odd number of nodal circles) the corresponding beam function is

$$\varphi(x) = \sin \alpha x - \mu \sinh \alpha x \quad (3.188)$$

where α and μ are as before, and

$$m = 2.500, 4.500, 6.500, \dots$$

The resulting characteristic equation (3.178) now has the coefficients

$$K_0 = 1$$

$$K_1 = A_1 + A_2 + A_3$$

$$K_2 = A_1 A_2 + A_1 A_3 + A_2 A_3 - A_6 A_6' - A_5 A_5' - A_4^2$$

$$K_3 = (A_1 A_2 - A_5 A_5') A_3 + A_4 (A_5' A_6 + A_5 A_6') - A_1 A_4^2 - A_2 A_6 A_6'$$

$$A_1 = \frac{\Psi_3}{\Psi_1} + \left(\frac{1-\nu}{2}\right) n^2$$

$$A_2 = n^2 + \left(\frac{1-\nu}{2}\right) \frac{\Psi_1}{\Psi_2} + k \left[n^2 + 2(1-\nu) \frac{\Psi_1}{\Psi_2} \right]$$

$$A_3 = 1 + k \left[\frac{\Psi_3}{\Psi_2} + n^4 + 2n^2 \frac{\Psi_1}{\Psi_2} \right] - 2n\beta \frac{N_{x\theta}^i}{C}$$

$$A_4 = n + k \left[n^3 + (2-\nu) n \frac{\Psi_1}{\Psi_2} \right]$$

$$A_5 = \left(\frac{1+\nu}{2}\right) n, \quad A_5' = \left(\frac{1+\nu}{2}\right) n \frac{\Psi_1}{\Psi_2}$$

$$A_6 = \nu, \quad A_6' = \nu \frac{\Psi_1}{\Psi_2}$$

$$\Psi_1 = \alpha^2 \left[1 + (-1)^N \left(2 \frac{\sin m\pi}{m\pi} - \mu^2 \right) \right] + \beta^2 [1 + (-1)^N \mu^2]$$

$$\Psi_2 = 1 + (-1)^N \mu^2$$

$$\Psi_3 = (\alpha^4 + \beta^4) [1 + (-1)^N \mu^2] + 6\alpha^2 \beta^2 \left[1 + (-1)^N \left(2 \frac{\sin m\pi}{m\pi} - \mu^2 \right) \right] \quad (3.189)$$

where N is the number of nodal circles (number of axial half-waves plus one).

In figure 3.131 comparisons of the lowest frequencies obtained by the two approximate methods are made with the "exact" values for the shell previously used ($R/h=300$, $l/R=4$, $\nu=0.3$, and $E=30 \times 10^6$ psi). The frequency for $\sigma_{x\theta}^i=0$ is lower from the energy method ($\Omega=0.00623$) than the corresponding values given by the "exact" solution ($\Omega=0.00635$) and by Galerkin method ($\Omega=0.00645$) because the energy solution includes tangential inertia, whereas the

others do not. It was found in reference 3.131 that the initial torsional stress has a negligible effect upon the two higher roots of the frequency equation (3.178).

Experimental data were also presented by Koval and Cranch (refs. 3.131 and 3.132) for clamped-clamped shells subjected to torsional prestress. The test specimens were made from steel shim stock 0.010 in. thick and had $R/h=300$ $l/R=4$ (the same as the shell parameters used in the previously discussed theoretical results). Numerical data are depicted in figure 3.132.

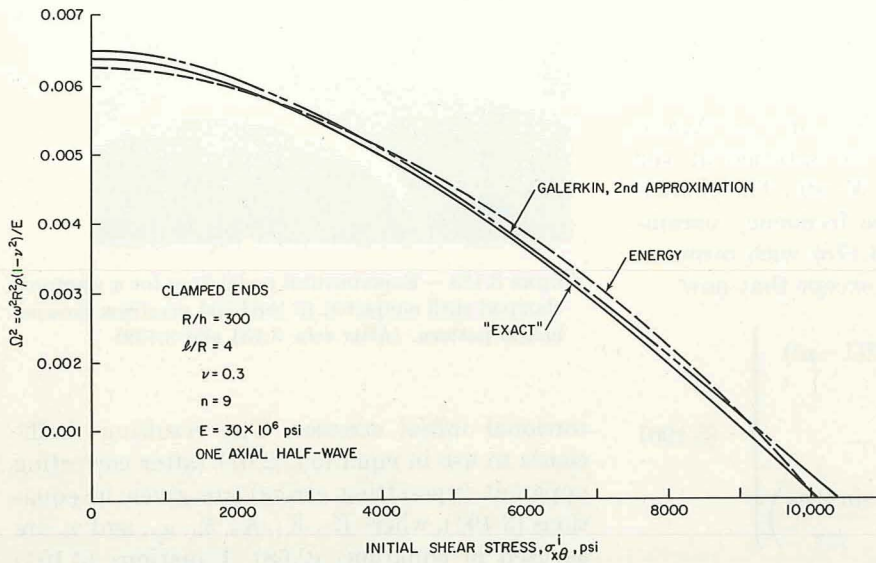


FIGURE 3.131.—Comparison of solutions from two approximate methods with an "exact" solution for a clamped-clamped shell; torsional prestress. (After ref. 3.132)

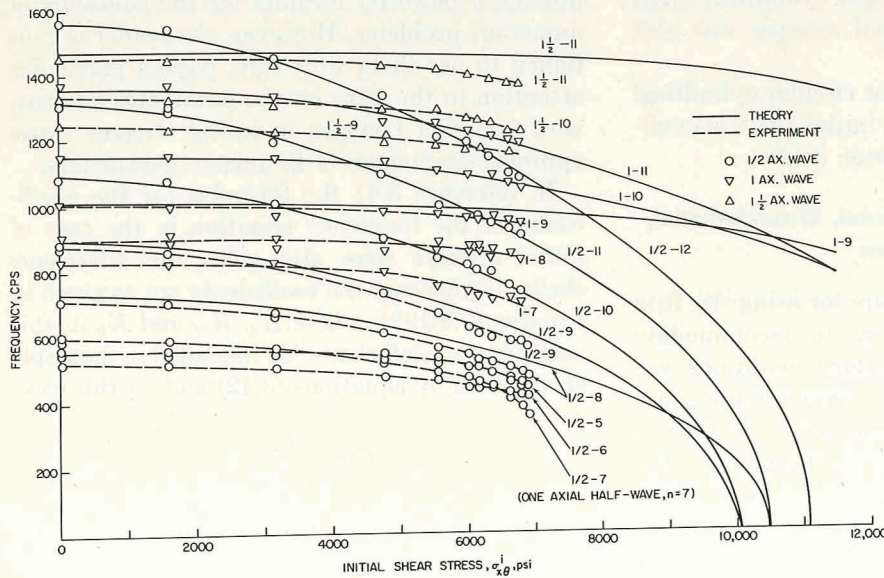


FIGURE 3.132.—Theoretical and experimental frequencies (cps) for a clamped-clamped shell (dimensions given in text) subjected to torsional prestress. (After refs. 3.131 and 3.132)

Theoretical values plotted are those of the previously described "exact" solution and are identified by number of axial half-waves and values of n . The experimental tests verified the theoretical implications that the axial nodal lines follow helices, the helix angle increasing as the torsional prestress is increased. This phenomenon is depicted in figure 3.133 wherein the mode having one axial half-wave and $n=10$ is excited under a prestress of $\sigma_{x\theta}^i=4200$ psi.

The assumed mode energy approach using Lagrange's equations described earlier was also used in references 3.131 and 3.132 to analyze the *clamped-freely supported* shell. The beam function $\varphi(x)$ used in equations (3.176) in this case is equation (3.188) where $\alpha=m\pi R/l$; $m=1.25, 2.25, 3.25, \dots$; and $\mu=\sin m\pi/\sinh m\pi$. Again, the conditions $u=v=w=0$ are satisfied at the "freely supported" end, and $M_x \neq 0$. The characteristic equation yielding the frequency parameters Ω^2 is again equation (3.178) with terms as defined in equation (3.189), except that now

$$\left. \begin{aligned} \Psi_1 &= \alpha^2 \left(1 + \mu^2 - \frac{\sin 2m\pi}{m\pi} \right) + \beta^2 (1 - \mu^2) \\ \Psi_2 &= 1 - \mu^2 \\ \Psi_3 &= (\alpha^4 + \beta^4) (1 - \mu^2) \\ &\quad + 6\alpha^2 \beta^2 \left(1 + \mu^2 - \frac{\sin 2m\pi}{m\pi} \right) \end{aligned} \right\} \quad (3.190)$$

The free vibration of circular cylindrical shells subjected to initial torsional stresses was also studied in reference 3.133.

Additional information for circular cylindrical shells subjected to torsional initial stress is available as a special case in section 3.4.6.

3.4.6 Combined Uniform Axial, Circumferential, and Torsional Prestress

In section 2.4 the procedure for using the Ritz method with beam functions to accommodate shells having arbitrary boundary conditions was laid out. The resulting cubic characteristic equation for the frequency parameter Ω^2 was given by equation (2.67), with the coefficients K_2 , K_1 , K_0 as defined by equations (2.68) and (2.69). Gontkevich (ref. 3.41) also gave the generalizations of these coefficients to account for the presence of uniform axial, circumferential, and

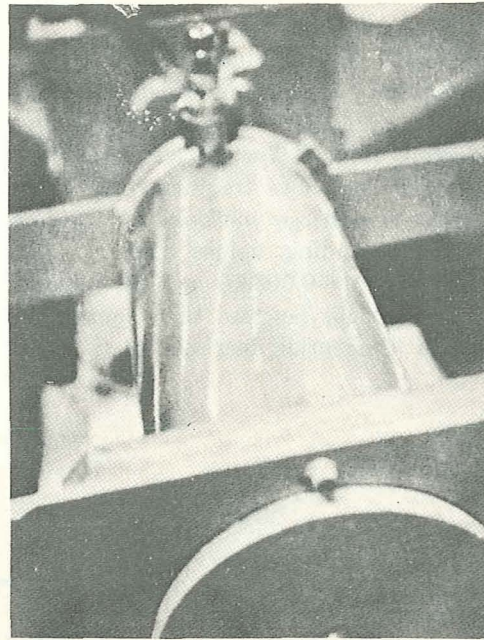


FIGURE 3.133.—Experimental nodal lines for a clamped-clamped shell subjected to torsional prestress showing helical pattern. (After refs. 3.131 and 3.132)

torsional initial stresses. The resulting coefficients to use in equation (2.67) (after correcting apparent typesetting errors) are given in equations (3.191), where K_2 , K_1 , K_0 , δ_m , μ_m , and γ_m are as used in equations (2.68). Equations (3.191) provide a powerful formula for the solutions of numerous problems. However, the reader is cautioned to use them with care, paying particular attention to the signs on the initial stress terms, verifying that changes in initial stresses cause appropriate changes in frequency parameters.

In reference 3.41 the formulas for the coefficients of the frequency equation in the case of initial stresses were also given for *orthotropic* shells. In this case the coefficients are as given in equations (3.192), where K_2 , K_1 , and K_0 in this case are the coefficients for unloaded orthotropic shells given by equations (3.42) and, in this case,

$$C = \frac{E_x h}{(1 - \nu_x \nu_\theta)}$$

The same caution must be applied for equations (3.192) as was mentioned in the previous paragraph.

$$\begin{aligned}
\bar{K}_2 &= K_2 + \frac{1}{C}(\mu_m^2 N_x^i + n^2 N_\theta^i - 2n\mu_m\gamma_m N_{x\theta}^i) \\
\bar{K}_1 &= K_1 + \frac{1}{C} \left\{ \left[\mu_m^2 + \frac{1}{2}(1-\nu)\delta_m n^2 \right] \left[n^2 + \frac{1}{2}(1-\nu)\delta_m \mu_m^2 \right] \delta_m + k[n^2 + 2(1-\nu)\delta_m \mu_m^2] \right\} (\mu_m^2 N_x^i + n^2 N_\theta^i - 2n\mu_m\gamma_m N_{x\theta}^i) \\
\bar{K}_0 &= K_0 + \frac{1}{C} \left\{ \left[\mu_m^2 + \frac{1}{2}(1-\nu)\delta_m n^2 \right] \left[n^2 + \frac{1}{2}(1-\nu)\delta_m \mu_m^2 \right] - \left[-\frac{\delta_m}{2} + \nu \left(\gamma_m + \frac{\delta_m}{2} \right) \right] \mu_m^2 n^2 + k \left[\mu_m^2 + \frac{1}{2}(1-\nu)\delta_m n^2 \right] \right\} (\mu_m^2 N_x^i + n^2 N_\theta^i - 2n\mu_m\gamma_m N_{x\theta}^i)
\end{aligned} \quad (3.191)$$

$$\begin{aligned}
\bar{K}_2 &= K_2 + \frac{1}{C}(\mu_m^2 N_x^i + n^2 N_\theta^i - 2n\mu_m\gamma_m N_{x\theta}^i) \\
\bar{K}_1 &= K_1 + \frac{1}{C} \left\{ \left[\mu_m^2 + \frac{C_{66}}{C_{11}}\delta_m n^2 \right] \left[\frac{C_{22}}{C_{11}}n^2 + \frac{C_{66}}{C_{11}}\delta_m \mu_m^2 \right] \delta_m + k \left[n^2 \frac{D_{22}}{D_{11}} + 4 \frac{D_{66}}{D_{11}}\delta_m \mu_m^2 \right] \right\} (\mu_m^2 N_x^i + n^2 N_\theta^i - 2n\mu_m\gamma_m N_{x\theta}^i) \\
\bar{K}_0 &= K_0 + \frac{1}{C} \left\{ \left[\mu_m^2 + \frac{C_{66}}{C_{11}}\delta_m n^2 \right] \left[\frac{C_{22}}{C_{11}}n^2 + \frac{C_{66}}{C_{11}}\mu_m^2 \delta_m \right] - \left[-\frac{C_{12}}{C_{11}}\gamma_m + \frac{C_{66}}{C_{11}} \right] \mu_m^2 n^2 + k \left(\mu_m^2 + \frac{C_{66}}{C_{11}}\delta_m n^2 \right) \left(\frac{C_{22}}{C_{11}}n^2 + \frac{C_{66}}{C_{11}}\mu_m^2 \delta_m \right) \right\} (\mu_m^2 N_x^i + n^2 N_\theta^i - 2n\mu_m\gamma_m N_{x\theta}^i)
\end{aligned} \quad (3.192)$$

Nikulin (refs. 3.83 and 3.84) analyzed SD-SD shells subjected to combined uniform axial, circumferential, and torsional prestresses (see discussion of method in sec. 3.4.3) and arrived at the following formula:

$$\begin{aligned}
\Omega^2 &= \left\{ (1-\nu^2)\lambda^4 + k(\lambda^2 + n^2)^4 + (\lambda^2 + n^2)^2 \frac{1}{C} [N_x^i \lambda^2 + N_\theta^i (n^2 - 1) - 2N_{x\theta}^i \lambda n] \right\} \div \{ (\lambda^2 + n^2)^2 + n^2 + (3+2\nu)\lambda^2 \}
\end{aligned} \quad (3.193)$$

This formula was also given by Prokopenko (ref. 3.134).

Results for a clamped-clamped shell having $h=0.5$ mm., $R=117$ mm., $l=357$ mm., and $m=1$ and having $E=2 \times 10^6$ dyne/cm², $\nu=0.3$, and $\rho=8 \times 10^{-6}$ dyne-sec²/cm⁴ are given in figure 3.134 (from ref. 3.84) for various combinations of initial stresses. Both experimental and theoretical data are shown.

3.4.7 Nonuniform Initial Stresses

Consider first the case of a circular cylindrical shell subjected to a gross bending moment M_b acting at its ends as shown in figure 3.135. Then the axial initial stress is given by

$$\sigma_x^i = \sigma_b \cos \theta \quad (3.194)$$

which is a case of the axial initial stress varying *circumferentially*. The gross bending moment is then determined by

$$M_b = \int_0^{2\pi} h \sigma_x^i R \cos \theta (R d\theta) = \pi R^2 h \sigma_b \quad (3.195)$$

Weingarten (ref. 3.135) analyzed the generalization of equation (3.194) which accounts for superimposed uniform axial and circumferential stresses as well; i.e.,

$$\left. \begin{aligned} \sigma_x^i &= \sigma_a + \sigma_b \cos \theta \\ \sigma_\theta^i &= pR/h \end{aligned} \right\} \quad (3.196)$$

where $\sigma_a = P/2\pi Rh$, P is axial end load (positive in tension), and p is internal pressure. The Donnell-Mushtari shell equations neglecting tangential inertia were used with the Galerkin method, with 18 terms of the deflection series

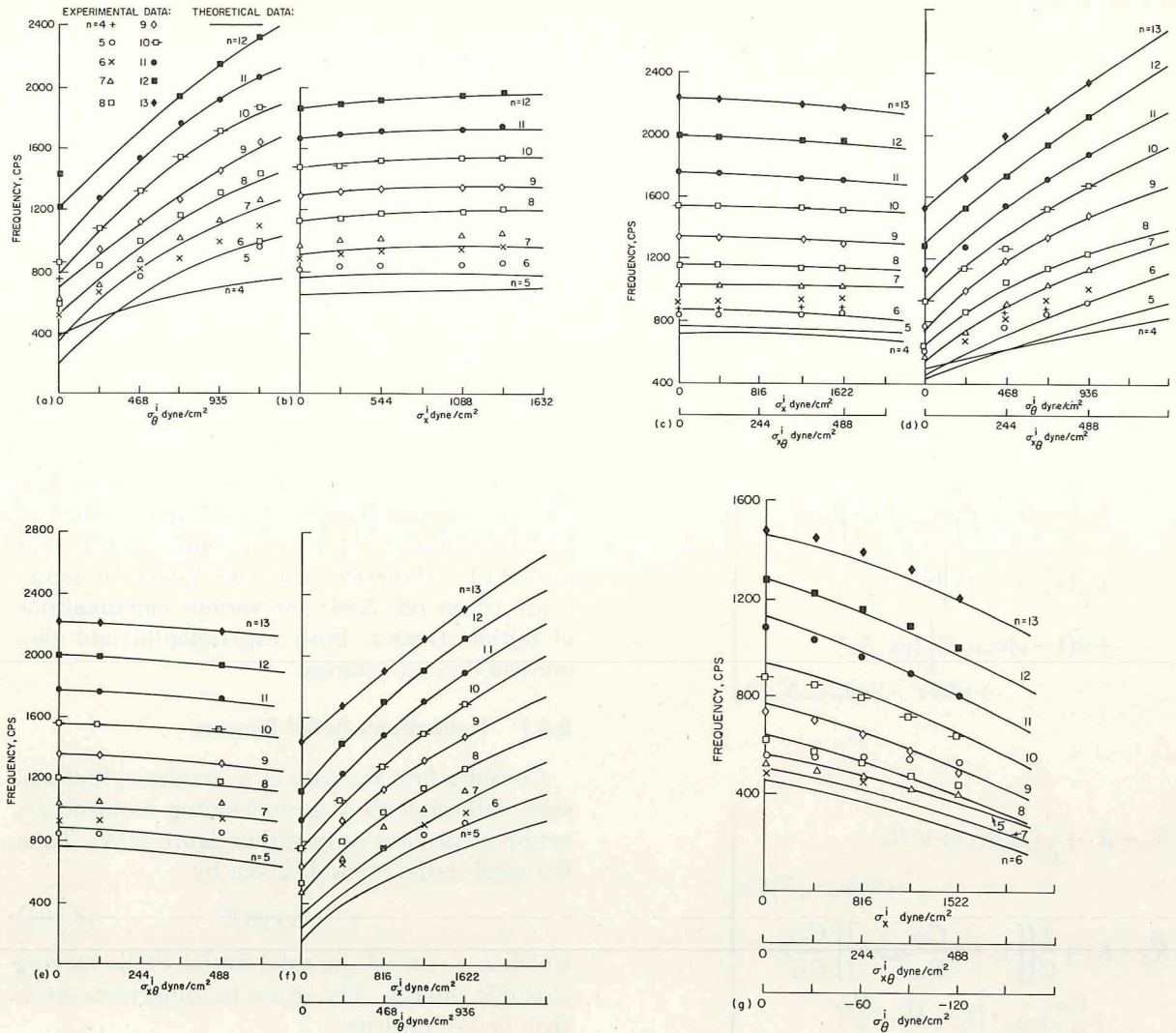


FIGURE 3.134—Frequencies (cps) of a clamped-clamped shell (dimensions given in text) subjected to combined uniform axial, circumferential, and torsional prestresses. (After ref. 3.84) (a) $\sigma_x^i = 1632$ dyne/cm², $\sigma_{x\theta}^i = 488$ dyne/cm². (b) $\sigma_\theta^i = 700$ dyne/cm², $\sigma_{x\theta}^i = 488$ dyne/cm². (c) $\sigma_\theta^i = 700$ dyne/cm². (d) $\sigma_x^i = 1632$ dyne/cm². (e) $\sigma_x^i = 1632$ dyne/cm², $\sigma_\theta^i = 700$ dyne/cm². (f) $\sigma_{x\theta}^i = 488$ dyne/cm². (g) All prestresses on abscissa.

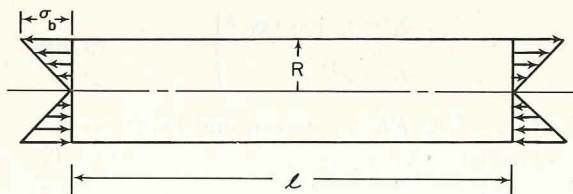


FIGURE 3.135.—Circular cylindrical shell subjected to gross bending moment.

$$w(x, \theta, t) = \sin \frac{n\pi x}{l} \cos \omega t \sum_{n=0}^N a_n \cos n\theta \quad (3.197)$$

to represent an SD-SD shell. Numerical results were obtained for an aluminum shell ($E = 10^6$ psi., $\rho g = 0.098$ lb/in.³, $\nu = 0.33$) having $R/h = 250$, $R = 4$ in., and $l/R = 1.91$. Computed frequencies for an external pressure of 2 psi and various values of gross bending moment are shown in table 3.15 and by the solid curves in figure 3.136.

TABLE 3.15.—*Theoretical Frequencies (cps) of an SD-SD Shell Subjected to Gross Bending Moment (Dimensions in Text)*

m	n	$\sigma_b/\bar{\sigma}_a$					
		0	0.2	0.4	0.6	0.8	1.0
1	0	8008	8008	8008	8008	8008	8008
	1	5849	5849	5849	5849	5849	5849
	2	3233	3233	3233	3233	3233	3233
	3	1849	1849	1849	1850	1851	1853
	4	1152	1152	1154	1158	1163	1169
	5	778	780	789	802	821	841
	6	583	601	624	630	466	(a)
	7	520	481	410	317	174	(a)
	8	565	564	542	509	(a)	413
	9	683	686	698	716	623	608
	10	846	847	851	858	868	883
	11	1040	1040	1042	1045	1050	1056
	12	1258	1258	1259	1261	1264	1267
	13	1498	1498	1499	1500	1501	1503
	14	1759	1759	1759	1760	1761	1762
2	0	8009	8009	8012	8014	8017
	1	7332	7332	7330	7328	7326
	2	5850	5850	5851	5851	5851
	3	4376	4376	4378	4379	4380
	4	3237	3237	3241	3244	3248
	5	2430	2431	2441	2449	2459
	6	1877	1880	1903	1924	1950
	7	1511	1519	1585	1632	1343
	8	1291	1330	797	581	190
	9	1194	1097	1239	1372	1665
	10	1203	1204	1048	938	805
	11	1296	1297	(a)	1183	1114
	12	1451	1458	(a)	1524	1755
	13	1652	1656	1685	1714	1524
	14	1889	1891	1907	1921	1939
3	0	8012	8015	8042	8062	8087
	1	7697	7694	7672	7657	7638
	2	6884	6884	6884	6883	6882
	3	5856	5856	5858	5859	5861
	4	4846	4847	4851	4855	4860
	5	3973	3974	3984	3992	4003
	6	3269	3271	3291	3308	3330
	7	2726	2731	2770	2850	2851
	8	2326	2337	2423	2466	1135
	9	2054	2084	1250	935	(a)
	10	1897	1936	2160	2140	(a)
	11	1845	1699	1792	2314	2312
	12	1884	1830	1551	1363	(a)
	13	1998	2028	2463	1677	1540
	14	2173	2186	1993	(a)	1849

^a Values did not converge.

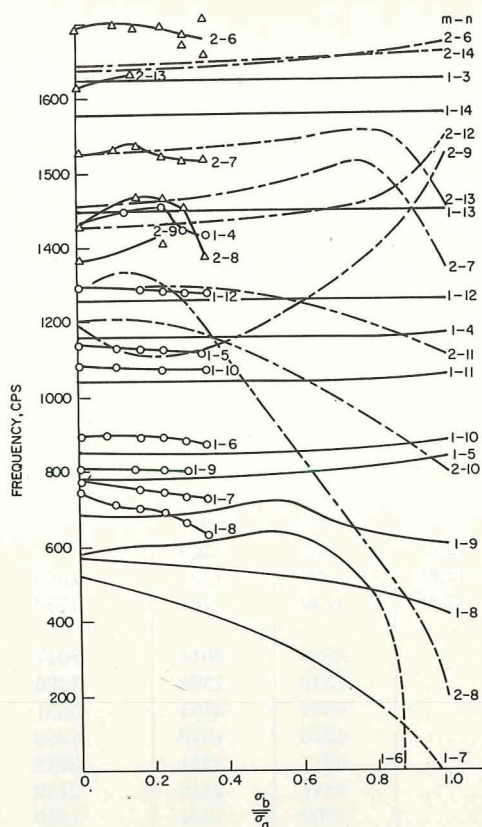


FIGURE 3.136.—Variation of frequency with gross initial bending moment; SD-SD (After ref. 3.135)

In the presentation of these results the bending moment is expressed nondimensionally as $\sigma_b/\bar{\sigma}_a$, where $\bar{\sigma}_a$ is the value of compressive axial stress which causes buckling in a long shell; i.e.,

$$\bar{\sigma}_a = \frac{Eh}{R\sqrt{3(1-\nu^2)}} \quad (3.198)$$

Identification of mode shapes for the shell loaded by end moments is difficult. As $\sigma_b/\bar{\sigma}_a$ increases the circumferential mode shapes become irregular and the value of n loses meaning. This behavior is shown in figure 3.137 for $m=1$ and $n=5$ and in figure 3.138 for $m=1$ and $n=6$. Because of symmetry about the vertical axis, only one-half of the mode shape is shown in figures 3.137 and 3.138. In plotting figure 3.136 it was found that by taking closely spaced values of $\sigma_b/\bar{\sigma}_a$ one could obtain smooth frequency curves for $0 \leq \sigma_b/\bar{\sigma}_a < 1$. The value of n for a given curve in figure 3.136 is that value when $\sigma_b/\bar{\sigma}_a = 0$. The results shown in figure 3.136 and table 3.15 indicate that as M_b increases some of the frequencies increase, whereas others decrease.

Experimental data were also presented in reference 3.135 for the same shell. These are listed in table 3.16 and are also shown by data points in figure 3.136. The experimental results in all cases fell above the analytical curves. The differ-

TABLE 3.16.—Experimental Frequencies (cps) of an SD-SD Shell Subjected to Gross Bending Moment (Dimensions Given in Text)

m	n	$\sigma_b/\bar{\sigma}_a$					
		0	0.106	0.168	0.232	0.293	0.355
1	4	1471	1509	1441	1435
	5	1134	1131	1127	1126	1112
	6	895	893	897	883	878
	7	782	761	752	748	734	730
	8	747	711	703	692	662	634
	9	805	803	807	800
	10	1081	1079	1076	1071
2	12	1292	1290	1286	1281	1277	1294
	6	1988	2009	1992	1977	1953	1926
	7	1655	1663	1675	1646	1631	2013
	8	1459	1447	1541	1525	1511	1637
	9	1361	1441	1415	1374
2	13	1833	1868

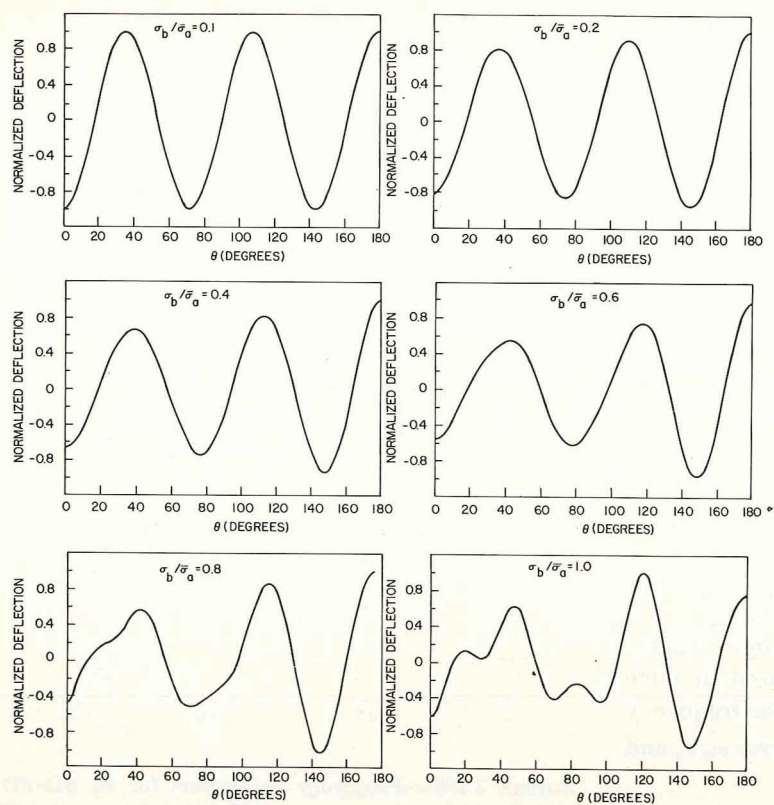


FIGURE 3.137.—Variation of circumferential mode shape with increasing bending moment; $m=1$, $n=5$. (After ref. 3.135)

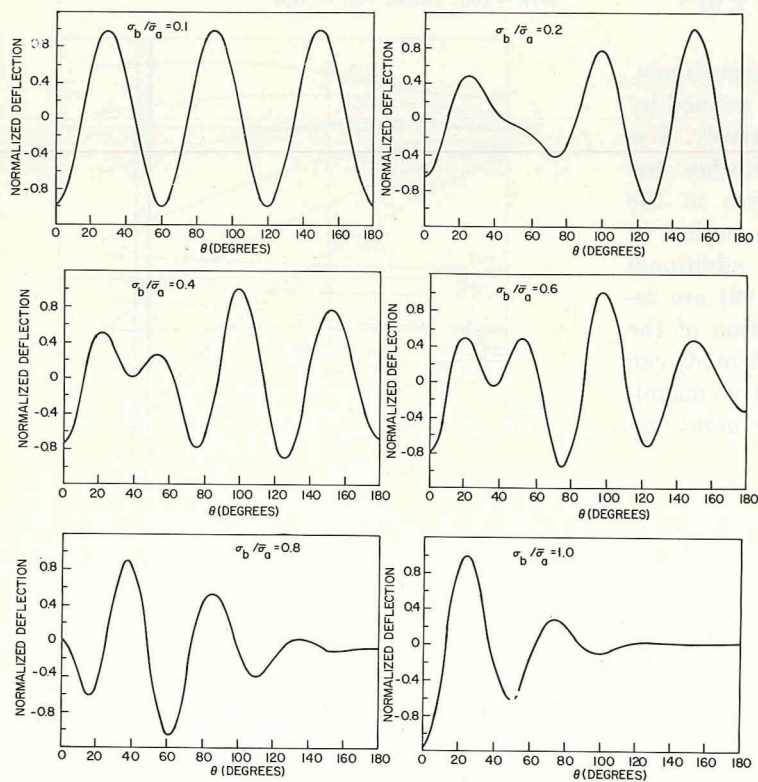


FIGURE 3.138.—Variation of circumferential mode shape with increasing bending moment; $m=1$, $n=6$. (After ref. 3.135)

ence was attributed to the difficulty in simulating SD-SD end conditions. No experimental results were obtained beyond $\sigma_b/\bar{\sigma}_a = 0.355$ since buckling occurred at $\sigma_b/\bar{\sigma}_a = 0.43$.

The problem of the circular cylindrical shell subjected to gross bending moments at its ends was also studied both theoretically and experimentally by Seggelke (ref. 3.136). The theoretical analysis was based upon the Donnell-Mushtari equations neglecting tangential inertia. The normal displacement for an SD-SD shell was taken as

$$w = \sin \frac{m\pi x}{l} \cos \omega t \sum_{n=0}^N (a_n \cos n\theta + b_n \sin n\theta) \quad (3.199)$$

along with a compatible Airy stress function. The a_n and b_n coefficients were used separately for symmetric and antisymmetric modes, respectively. The Galerkin method was used to solve the problem. Numerical results for the frequency parameters $\omega R \sqrt{\rho/E}$ are plotted versus $\sigma_b/\bar{\sigma}_a$ and σ_b/E in figures 3.139 and 3.140 for

$$\frac{h^2}{12}(1-\nu)^2 R^2 = 9.16 \times 10^{-6} \text{ and } 3.67 \times 10^{-7}$$

respectively (i.e., $R/h = 100$ and 500 , respectively, for $\nu = 0.3$). The stresses σ_b and $\bar{\sigma}_a$ are defined by equations (3.194) and (3.198), respectively. The circumferential wave number n identifies the number of circumferential sine waves in the unloaded ($\sigma_b = 0$) condition. As seen earlier in this section in Weingarten's work, additional Fourier components of equation (3.199) are required as σ_b increases. The contribution of the other Fourier components to the $n = 9$ mode can be seen in figure 3.141 where the relative magnitudes of the Fourier coefficients are indicated, subject to the normalizing condition

$$\sum_{n=0}^N a_n^2 = 1 \quad (3.200)$$

The necessity of using terms other than $n = 9$ clearly increases as σ_b increases as shown in figure 3.141. The appearances of the symmetric and antisymmetric modes for the lowest frequency ($n = 9$) for

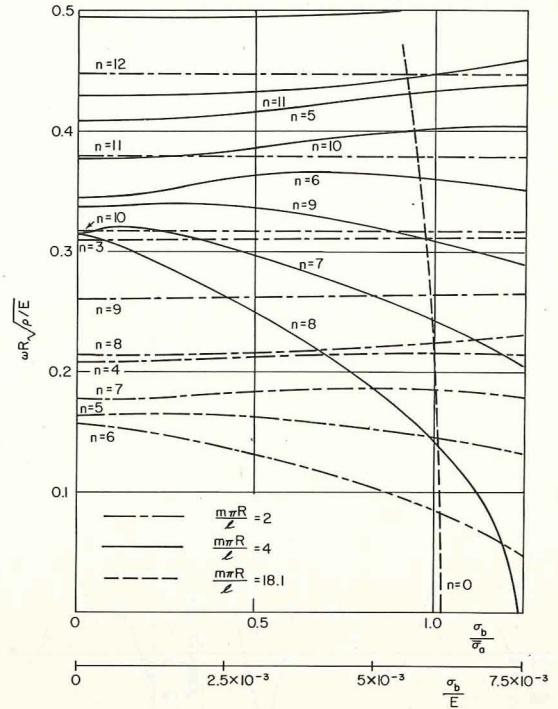


FIGURE 3.139.—Frequency parameters for an SD-SD shell subjected to gross initial bending moment; $R/h = 100$. (After ref. 3.136)

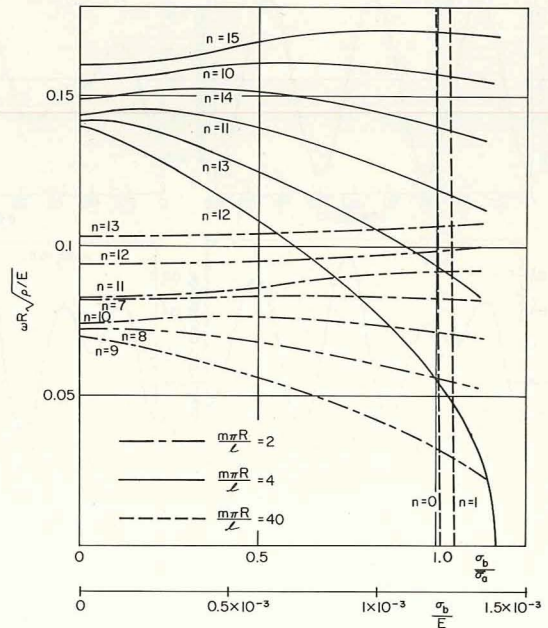


FIGURE 3.140.—Frequency parameters for an SD-SD shell subjected to gross initial bending moment; $R/h = 500$. (After ref. 3.136)

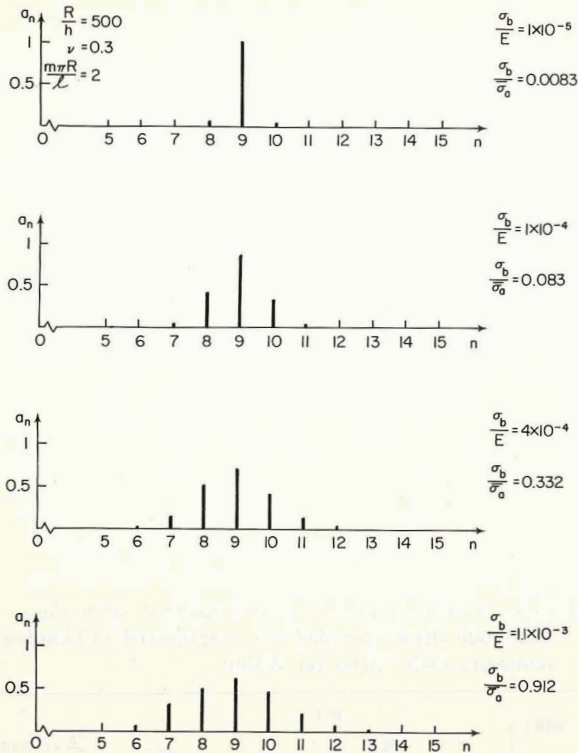


FIGURE 3.141.—Normalized Fourier coefficients a_n of the mode shapes of an SD-SD shell subjected to bending moment; $n=9$. (After ref. 3.136)

$$R/h = 500 \quad \sigma_b/E = 4 \times 10^{-4} \\ \lambda = m\pi R/l = 2$$

are depicted in figure 3.142.

Experimental results were also given by Seggelke (ref. 3.136). Figure 3.143 shows frequency (cps) versus bending moment $M_b(m \cdot kp)$ for two SD-SD shells having lengths of 48.5 mm. and 48 mm. Both shells had $R=25$ mm., $h=0.05$ mm., and were made of steel ($\rho=8 \times 10^{-6}$ $kp \cdot \text{sec}^2/\text{cm}^4$, $E=2.1 \times 10^6$ kp/cm^2). The bending moment was varied from 0 to 1.58 mkp ($\sigma_b/\sigma_a=0.63$). Figure 3.144 shows a similar plot for a third shell of the same material and having the same dimensions, except $l=75$ mm. In this figure the lowest frequencies for the first three axial wave numbers ($m=1,2,3$) are given. Examples of experimentally measured circumferential mode shapes for the second shell ($l=48$ mm.) are shown in figures 3.145, 3.146, and 3.147 for $n=9, 8$, and 11, respectively. Theoretical and experimental fre-

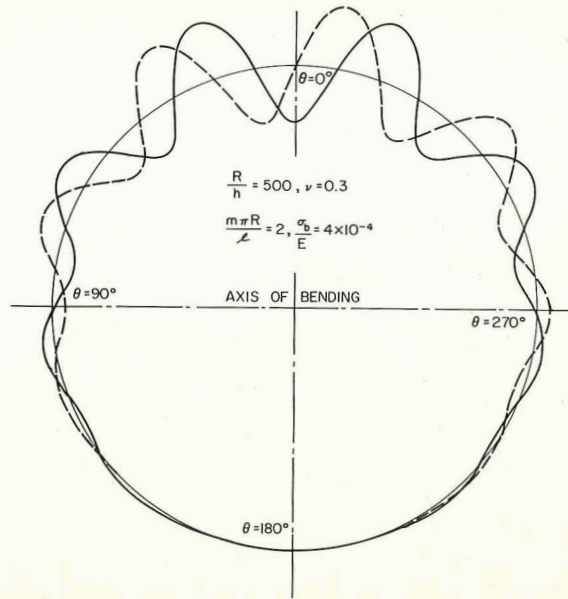


FIGURE 3.142.—Circumferential mode shapes of an SD-SD shell subjected to bending moment; $n=9$. (After ref. 3.136)

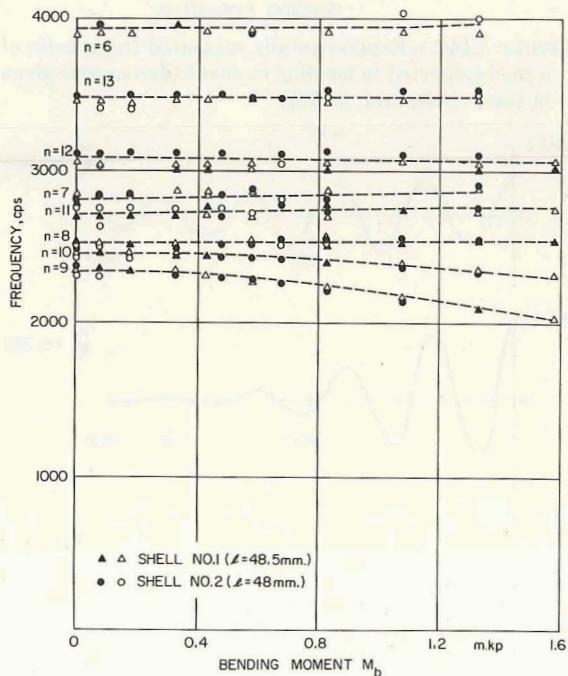


FIGURE 3.143.—Experimentally measured frequencies of shells subjected to gross initial bending moment (dimensions given in text). (After ref. 3.136)

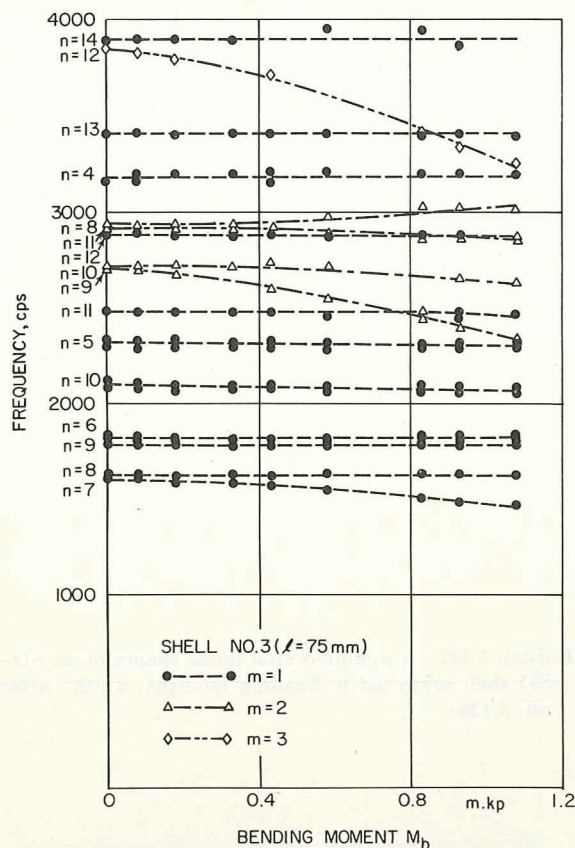


FIGURE 3.144.—Experimentally measured frequencies of a shell subjected to bending moment (dimensions given in text). (After ref. 3.136)

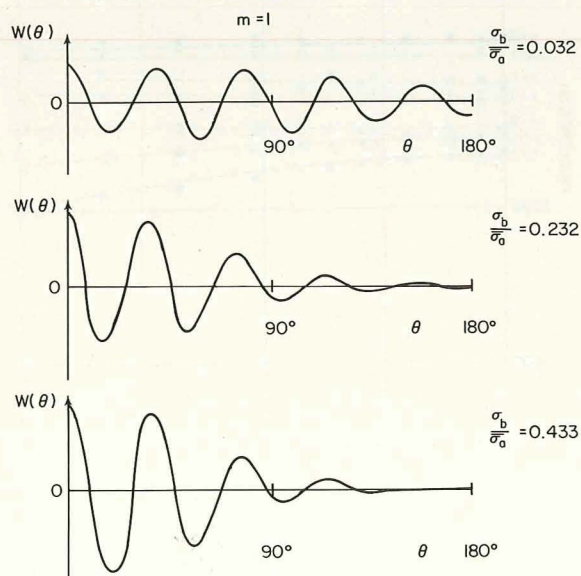


FIGURE 3.145.—Experimentally measured circumferential mode shapes for shell no. 2 subjected to bending moment; $n = 9$. (After ref. 3.136)

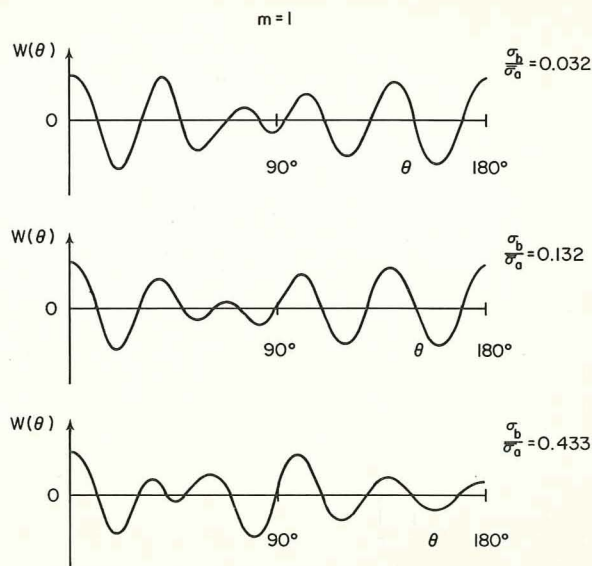


FIGURE 3.146.—Experimentally measured circumferential mode shapes for shell no. 2 subjected to bending moment; $n = 8$. (After ref. 3.136)

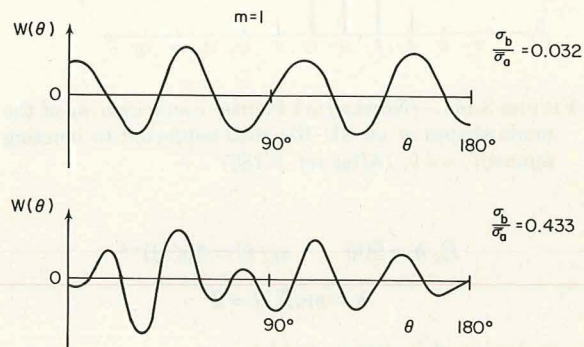


FIGURE 3.147.—Experimentally measured circumferential mode shapes for shell no. 2 subjected to bending moment; $n = 11$. (After ref. 3.136)

quencies for the first shell ($l = 48.5$ mm.) are compared in figure 3.148.

Sampath (ref. 3.74) also studied the problem of the SD-SD shell loaded by overall end moments. The Galerkin method was used with the Donnell-Mushtari equations, and the deflection function (eq. (3.199)) was assumed. Retaining 50 terms in the solution series, numerical results were obtained for a shell having $m = 1$, $l/R = 4$, $R/h = 1000$, and $\nu = 0.3$. Frequency parameters which have converged to five significant figures are listed in table 3.17 for various ratios of the loading parameter σ_b/σ_{cr} , where σ_b is the magni-

tude of the stress causing the gross bending moment, as in equation (3.196), $\sigma_a = 0$, and σ_{cr} is the lowest buckling stress in the case of uniform axial loading; i.e.,

$$\sigma_{cr} = 0.5606 \times 10^{-3} \frac{E}{(1-\nu^2)} \quad (3.201)$$

The ratio Ω^2/Ω_0^2 versus σ_b/σ_{cr} is plotted in figure 3.149, where Ω_0^2 is the square of the frequency parameter in the *unloaded* case for the same circumferential wave number, n .

In reference 3.74 an axial stress varying circumferentially according to

$$\sigma_x^i = \sigma_2 \cos 2n\theta \quad (3.202)$$

was also investigated. Again, using equation (3.197) and the Galerkin procedure yields table 3.18 and figure 3.150 as complements to table 3.17 and figure 3.149, respectively, for the same shell. Comparing tables 3.17 and 3.18 it is seen that the significant differences in frequencies occur for large loading parameters for $n > 3$.

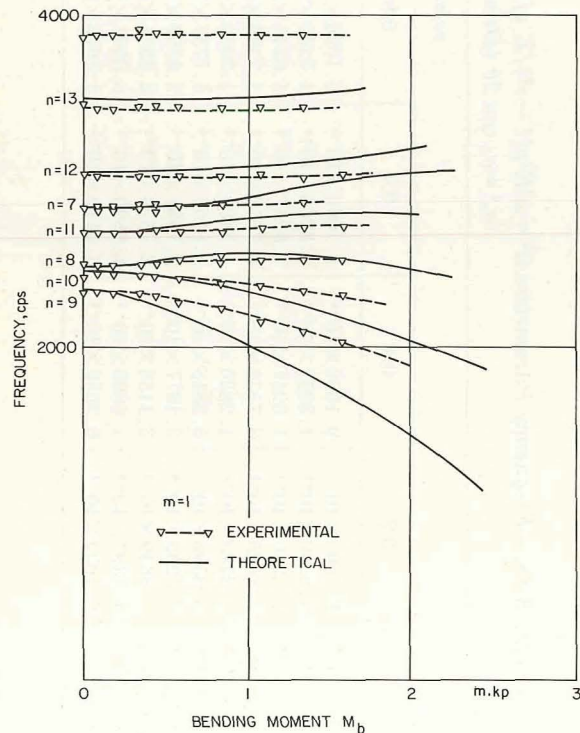


FIGURE 3.148.—Comparison of experimental and theoretical frequencies for shell no. 1 subjected to bending moment. (After ref. 3.136)

Two other problems having spatially-varying initial stresses were investigated in reference 3.74. The first of these is the shell subjected to axial stress which varies linearly in the axial direction; i.e.,

$$\sigma_x^i = k_0 + k_1 \frac{x}{l} \quad (3.203)$$

This is the situation which would arise if the shell were loaded axially by its own weight and supported at one or both of its ends. In the other problem the circumferential stress varies linearly in the axial direction.

A few other references deal with nonuniform initial stresses. Kessel and Schlack (ref. 3.137)

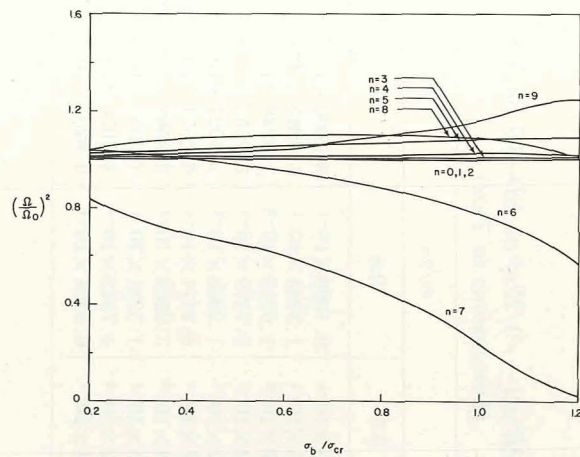


FIGURE 3.149.—Variation of the frequency ratio $(\Omega/\Omega_0)^2$ with loading ratio σ_b/σ_{cr} for an SD-SD shell subjected to gross bending (dimensions given in text). (After ref. 3.74)

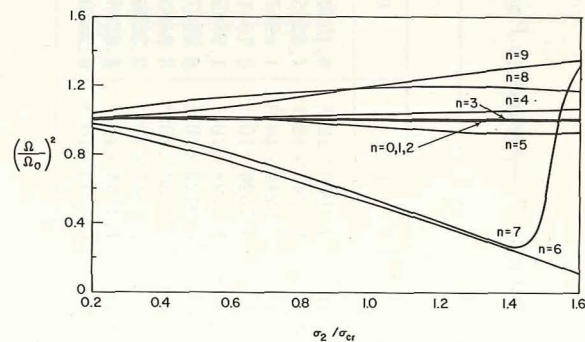


FIGURE 3.150.—Variation of the frequency ratio $(\Omega/\Omega_0)^2$ with loading ratio σ_2/σ_{cr} for an SD-SD shell subjected to an axial initial stress $\sigma_x^i = \sigma_2 \cos 2\theta$ (dimensions given in text). (After ref. 3.74)

TABLE 3.17.—Frequency Parameters $\Omega^2 = \omega^2 R^2 \rho (1 - \nu^2) / E$ of an SD-SD Shell Subjected to Gross Bending Moment
(Dimensions in Text)

n	σ_b / σ_{cr}								
	0	0.2	0.4	0.6	0.8	0.9	1	1.1	1.2
0	9.1000×10^{-1}	9.1000×10^{-1}	9.1000×10^{-1}	9.1000×10^{-1}	9.1000×10^{-1}	9.1000×10^{-1}	9.1000×10^{-1}	9.1000×10^{-1}	9.1000×10^{-1}
1	1.3245×10^{-1}	1.3245×10^{-1}	1.3245×10^{-1}	1.3245×10^{-1}	1.3245×10^{-1}	1.3245×10^{-1}	1.3245×10^{-1}	1.3245×10^{-1}	1.3245×10^{-1}
2	1.6246×10^{-2}	1.6246×10^{-2}	1.6247×10^{-2}	1.6247×10^{-2}	1.6248×10^{-2}	1.6248×10^{-2}	1.6248×10^{-2}	1.6249×10^{-2}	1.6250×10^{-2}
3	3.7517×10^{-3}	3.7526×10^{-3}	3.7541×10^{-3}	3.7552×10^{-3}	3.7579×10^{-3}	3.7595×10^{-3}	3.7614×10^{-3}	3.7656×10^{-3}	3.7706×10^{-3}
4	1.2770×10^{-3}	1.2798×10^{-3}	1.2848×10^{-3}	1.2882×10^{-3}	1.2968×10^{-3}	1.3021×10^{-3}	1.3079×10^{-3}	1.3100×10^{-3}	1.2951×10^{-3}
5	5.8234×10^{-4}	5.9122×10^{-4}	6.0607×10^{-4}	6.1367×10^{-4}	6.2471×10^{-4}	6.2871×10^{-4}	6.3193×10^{-4}	6.3601×10^{-4}	6.3686×10^{-4}
6	3.6998×10^{-4}	3.8136×10^{-4}	3.6485×10^{-4}	3.5243×10^{-4}	3.2263×10^{-4}	3.0592×10^{-4}	2.8827×10^{-4}	2.5072×10^{-4}	2.1077×10^{-4}
7	3.4580×10^{-4}	2.8847×10^{-4}	2.3606×10^{-4}	2.0865×10^{-4}	1.5231×10^{-4}	1.2357×10^{-4}	9.4533×10^{-5}	3.5726×10^{-5}	6.0170×10^{-6}
8	4.3087×10^{-4}	4.4868×10^{-4}	4.6698×10^{-4}	4.7222×10^{-4}	4.7372×10^{-4}	4.7076×10^{-4}	4.6600×10^{-4}	4.5175×10^{-4}	4.3318×10^{-4}
9	6.0709×10^{-4}	6.1253×10^{-4}	6.2370×10^{-4}	6.3374×10^{-4}	6.6404×10^{-4}	6.8207×10^{-4}	7.0081×10^{-4}	7.3821×10^{-4}	7.5605×10^{-4}

TABLE 3.18.—Frequency Parameters $\Omega^2 = \omega^2 R^2 \rho (1 - \nu^2) / E$ of an SD-SD Shell Subjected to an Axial Initial Stress
 $\sigma_x^i = \sigma_2 \cos 2\theta$ (Dimensions in Text)

n	σ_2 / σ_{cr}								
	0	0.2	0.4	0.6	0.8	1.0	1.2	1.4	1.6
0	9.1000×10^{-1}	9.1000×10^{-1}	9.1000×10^{-1}	9.1000×10^{-1}	9.1000×10^{-1}	9.1000×10^{-1}	9.1000×10^{-1}	9.1000×10^{-1}	9.1000×10^{-1}
1	1.3245×10^{-1}	1.3249×10^{-1}	1.3252×10^{-1}	1.3256×10^{-1}	1.3259×10^{-1}	1.3263×10^{-1}	1.3266×10^{-1}	1.3270×10^{-1}	1.3273×10^{-1}
2	1.6246×10^{-2}	1.6246×10^{-2}	1.6247×10^{-2}	1.6247×10^{-2}	1.6248×10^{-2}	1.6248×10^{-2}	1.6249×10^{-2}	1.6250×10^{-2}	1.6251×10^{-2}
3	3.7517×10^{-3}	3.7525×10^{-3}	3.7532×10^{-3}	3.7550×10^{-3}	3.7576×10^{-3}	3.7609×10^{-3}	3.7649×10^{-3}	3.7697×10^{-3}	3.7752×10^{-3}
4	1.2770×10^{-3}	1.2783×10^{-3}	1.2820×10^{-3}	1.2882×10^{-3}	1.2969×10^{-3}	1.3082×10^{-3}	1.3220×10^{-3}	1.3385×10^{-3}	1.3575×10^{-3}
5	5.8234×10^{-4}	5.8592×10^{-4}	5.8818×10^{-4}	5.8453×10^{-4}	5.7737×10^{-4}	5.6768×10^{-4}	5.5578×10^{-4}	5.4189×10^{-4}	5.2614×10^{-4}
6	3.6998×10^{-4}	3.5289×10^{-4}	3.1877×10^{-4}	2.7881×10^{-4}	2.3557×10^{-4}	1.9002×10^{-4}	1.4266×10^{-4}	9.3846×10^{-5}	4.3816×10^{-5}
7	3.4580×10^{-4}	3.3649×10^{-4}	3.1158×10^{-4}	2.7656×10^{-4}	2.3551×10^{-4}	1.9073×10^{-4}	1.4349×10^{-4}	9.4510×10^{-5}	4.4222×10^{-5}
8	4.3087×10^{-4}	4.4397×10^{-4}	4.6606×10^{-4}	4.8590×10^{-4}	5.0091×10^{-4}	5.1037×10^{-4}	5.1420×10^{-4}	5.1275×10^{-4}	5.0656×10^{-4}
9	6.0709×10^{-4}	6.1059×10^{-4}	6.2659×10^{-4}	6.5412×10^{-4}	6.8672×10^{-4}	7.2105×10^{-4}	7.5545×10^{-4}	7.8893×10^{-4}	8.2083×10^{-4}

considered gyroscopic forces induced by spin around the shell axis with simultaneous steady precession about a nutation axis. Bushnell (ref. 3.138) analyzed a shell subjected to constant axial stresses and an internal pressure which is proportional to the normal displacement w ; this situation arises, of course, when the shell contains an elastic core. Thermal initial stresses were considered by Buckens (ref. 3.139) and by Ong and Herrmann (refs. 3.81, 3.140, and 3.141).

3.4.8 Open Shells

The previous sections dealing with the effects of initial stresses upon vibration frequencies and mode shapes considered in great detail the closed circular cylindrical shell. As was found in chapter 2 in the case of unloaded shells, considerably less information is available for open shells, even though the number of possible types of boundary conditions is far greater.

Consider the open circular cylindrical panel depicted in figure 2.141. As in section 2.8 certain information is available for prestressed panels having their lateral edges $\theta=0$ and $\theta=\theta_0$ supported by shear diaphragms with various boundary conditions along the ends $x=0$ and $x=l$. This information comes from the modes of closed shells having one or more circumferential waves, the SD boundary conditions being duplicated at node lines of the closed shell. Section 2.8 may be reviewed for the technique of utilizing such results.

The case of an open shell supported on all four edges by shear diaphragms and subjected to uniform initial stresses is examined in references 3.44, 3.103, and 3.142. However, as indicated in the preceding paragraph, for these boundary conditions the same results can be obtained from closed shells. Procedures for analyzing open shallow shells subjected to initial stress and having arbitrary boundary conditions are laid out in references 3.46 and 3.143, but no numerical results are given.

Reissner (ref. 3.46) also included uniform initial stress terms in his nonlinear (large deflection) analysis of open circular cylindrical shells (see section 3.3.5 for further description of approach) supported on all edges by shear diaphragms. The ratio between nonlinear and linear frequencies is given by equation (3.93), where ω_0^2 is now given by

$$\rho h \omega_0^2 = D \left[\left(\frac{n}{R} \right)^2 + \left(\frac{\pi}{l} \right)^2 \right]^2 + \left[N_x \left(\frac{\pi}{l} \right)^2 + N_\theta \left(\frac{n}{R} \right)^2 \right] + \frac{Eh}{R^2} \frac{(\pi/l)^4}{[(n/R)^2 + (\pi/l)^2]^2} \quad (3.204)$$

3.5 OTHER COMPLICATING EFFECTS IN CIRCULAR CYLINDRICAL SHELLS

In this section three other types of complicating effects which affect the free vibrations of circular cylindrical shells will be reviewed briefly:

- (1) Effects of surrounding media
- (2) Shear deformation and rotary inertia
- (3) Nonhomogeneity.

A significant amount of literature deals with each of these, and a great deal of space could be devoted to each. However, each topic introduces considerable complexity into the picture, the intricate details of which are beyond the scope of this monograph.

The presence of a surrounding medium such as air or water introduces coupling of the shell equations with the governing field equations of the medium. As stated from the beginning of this work, coupling of shells with their environment (as in the case of structures) has generally been omitted. Nevertheless, some of the aspects of this topic which carry particular practical value will be examined briefly.

Introducing shear deformation into a shell theory results in a completely different theory. The order of the system of governing differential equations is raised from eight to ten, and the number of boundary conditions per edge which must be defined increases from four to five. Thus, the added complexity in this case is in the theory.

Nonhomogeneity introduces another set of independent physical parameters into the problem. For example, in chapter 2 the nondimensional frequency parameter Ω depends upon the l/R and R/h ratios, the wave numbers m and n , and Poisson's ratio. A nonhomogeneous (or heterogeneous) shell permits variation of the elastic constants E and ν (in the case of isotropy) in all three directions, x , θ , and z , which gives rise to a limitless number of material descriptions. In practical application, a great deal of current interest exists in layered (or laminated) shells—each layer is represented by an orthotropic ma-

terial. The numbers, thicknesses, and material properties of layers here again give rise to limitless configurations.

For the above reasons only a brief summary of some of the most important aspects of each of these topics appears herein. However, a substantial reference list will be provided for each topic to expedite further in-depth study.

3.5.1 Effects of Surrounding Media

The numerous theoretical results for the frequencies and mode shapes of free vibration of circular cylindrical shells which are given elsewhere in this chapter, as well as in chapter 2, apply when the shell is in a vacuum. Nevertheless, in virtually all practical applications, the shell is immersed in a surrounding medium, notably air or water, and/or contains a fluid. It is clear that vibration of the shell wall requires movement of the surrounding fluid, and this mass added to the system causes a reduction in the frequencies.

Thus, the shell is coupled with its surrounding medium by means of continuity conditions of displacement and velocity at the interface of the shell with the fluid. The shell must satisfy its equations of motion (see sec. 2.1) and boundary conditions. The fluid must satisfy (for example, in the commonly assumed case of a compressible, inviscid fluid) the wave equation for its velocity potential function and certain regularity conditions at the central axis of the shell ($r=0$) and/or at a large distance away from the shell ($r=\infty$). Consideration of the effect of the shell upon the fluid leads one into the field of acoustics. This work is only concerned with the effect of the fluid upon the shell.

However, before looking into the effects of surrounding fluids, consider first another significant type of surrounding medium—the elastic foundation. The elastic foundation receives a great deal of attention in the study of beams and plates; however, it is virtually ignored in the literature of shell vibrations, perhaps because it is less likely to be encountered in practical application.

The elastic foundation supplies components of restoring force which are proportional to the displacement components in magnitude and oppositely directed. Thus, in the matrix equation of motion (2.3) the force vector

$$\{F\} = - \begin{Bmatrix} K_u u \\ K_v v \\ K_w w \end{Bmatrix} \quad (3.205)$$

must be added to the right hand side, where K_u , K_v , and K_w are nondimensional spring constants associated with the u , v , and w displacements, respectively. In the case of sliding contact, $K_u = K_v = 0$. In general, the terms of equation (3.205) would be carried through the solution procedure in a straightforward manner. For example, the convenient solution form for infinite and SD-SD shells given by equations (2.20) could still be used; however, the resulting characteristic determinants (cf., eq. (2.21)) would have an added constant term in each of its diagonal elements. Furthermore, in three cases the added terms would cause no added algebraic complexity. These are

$$(a.) \quad K_u = K_v = 0$$

$$(b.) \quad K_u = K_v = K_w$$

In these cases the numerical results of chapter 2 (except those where tangential inertia is neglected) are directly applicable to the problem, except that the frequency parameter $\Omega^2 = \omega^2 R^2 \rho (1 - \nu^2) / E$ is replaced by

$$\bar{\Omega}^2 = \frac{\omega^2 R^2 \rho (1 - \nu^2)}{E} - K_w \quad (3.206)$$

Two of the earliest studies of the elastic shell of infinite length filled with, or surrounded by, a fluid were by Rayleigh (ref. 3.144) and Nikolai (ref. 3.145). In the first reference the shell enclosed a compressible fluid. In the second reference the fluid was assumed to be incompressible, but the shell could be either filled with or immersed in the liquid.

Gontkevich (ref. 3.146) shows how beam functions can be used to approximate the mode shapes of a shell having arbitrary end conditions. The surrounding compressible fluid medium, either inside or outside the shell, is represented by a potential function of a infinite field. Other works which study the effects of an infinite fluid field upon a circular cylindrical shell include references 3.24, 3.94, 3.99, 3.121, and 3.147 through 3.162.

Livanov (ref. 3.110) showed that if the total mass of the shell is much greater than that of an

enclosed compressible fluid (particularly in the case of a gas), then the coupled frequency equation of the shell and gas reduces approximately to the uncoupled frequency equations for the vibrations of a fluid in a rigid cylinder and the vibrations of a pressurized circular cylindrical shell.

Mnev (refs. 3.163 and 3.164) analyzed the problem of a thin, elastic circular cylindrical shell immersed in a compressible, inviscid fluid. However, the extent of the fluid is limited by a concentric rigid boundary either inside or outside of the shell as shown in figure 3.151. The fluid surrounding a shell of infinite length is considered by means of a suitable potential function.

The dynamic behavior of liquids in moving containers was the subject of a previous NASA monograph edited by Abramson (ref. 3.165). Chapter 9 of the monograph, by Kana, is devoted to the interaction of elastic shells with internal liquids and is a summary of relevant literature (see also ref. 3.166). References 3.46, 3.107, 3.113, 3.115, and 3.167 to 3.186 are summarized therein.

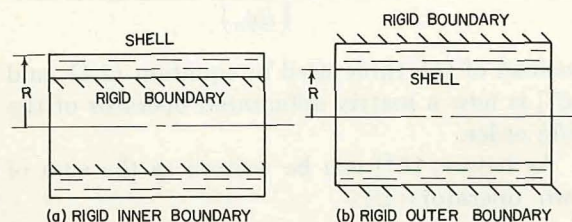


FIGURE 3.151.—Shell separated from a rigid boundary by a fluid.

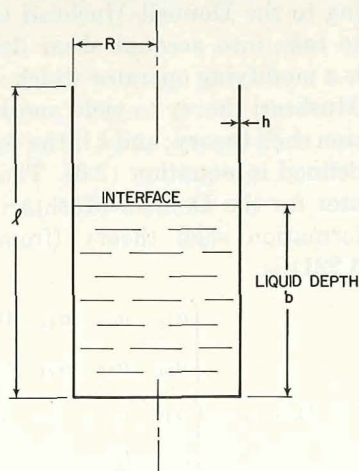


FIGURE 3.152.—Circular cylindrical shell partially filled with a liquid.

A comprehensive monograph dealing with the vibrations of an elastic shell partially filled with a liquid was written by Rapoport (ref. 3.187). The work is devoted to the formulation of the governing sets of equations and no numerical results are presented.

Abramson, Chu, Kana, and Lindholm (refs. 3.188 and 3.189) analyzed the bending ($n=1$) and breathing ($n \geq 2$) vibrations of full or partially full shells, where the surface of the liquid is perpendicular to the axis of the shell, as shown in figure 3.152. Reference 3.190 is an experimental study. An electromechanical analogue to the coupling which occurs between transverse shell wall vibrations and free surface oscillations of a liquid in a partially filled elastic shell is described in reference 3.191. Other works which pertain to flexible circular cylindrical shells containing liquids include references 3.64, 3.114, 3.184, and 3.192 through 3.210.

Note that although a number of the references listed in the preceding two paragraphs deal with circular cylindrical tanks which are partially filled with a liquid, none consider the case of the closed tank having a fluid surface which is *parallel* to the shell axis.

The nonhomogeneous shell filled with a liquid and subjected to internal pressure and axial initial compression was studied by Mugnier and Schroeter (ref. 3.80).

If a shell is surrounded by a *moving* fluid field, the problem becomes even more complicated leading to, for example, flutter analysis. Such problems will not be considered here.

Another type of surrounding medium which is considered completely beyond the scope of this work is the magnetic field. In general, the shell equations of motion are affected by nonlinear body force and body moment terms and the field is affected, in turn, by the motion of the shell.

Other investigations dealing with the free vibrations of circular cylindrical shells surrounded by a fluid medium include references 3.211 through 3.218.

3.5.2 Shear Deformation and Rotary Inertia

Consider the motion of the shell element depicted in figure 1.2. The drawing is misleading,

for the element has infinitesimal dimensions ds_α and ds_β parallel to the middle surface, whereas its dimension in the z -direction is finite, h . In a careful treatment of the six equations of motion, components of rotary inertia would be added to the three moment equations of motion, in addition to the translatory inertia terms which appear in the force equations of motion. Lord Rayleigh (ref. 3.219) showed, in the case of *beams*, that rotary inertia effects become significant as the length/depth ratio decreases. Subsequently, Timoshenko (ref. 3.220) established that, for beams having these depths, the effects of shear deformation are equally important. The incorporation of shear deformation and rotary inertia effects into plate vibration problems is summarized in reference 3.1.

To generalize the problem further to the shell, one can say that the effects of shear deformation and rotary inertia become increasingly significant as the thickness ratios R/h and l/h decrease. However, the effects can be significant for relatively thin (say $R/h > 20$) or long shells as well, as the numbers of circumferential and longitudinal waves increase. Thus, the effects become significant for short wave lengths, certainly for those of the same order as the thickness, or less.

Only a brief description of how shear deformation and rotary inertia enters into the derivation of shell theories will be given below. Shear deformation enters through the generalization of the strain-displacement equations. Rotary inertia enters in the fundamental forms of the equations of motion, as described above.

Not only are the resulting equations of motion greater in number (five, rather than three) and more complicated, but, as seen below, the numerical results are more difficult to interpret, for there exist five (rather than three) frequencies for each circumferential wave number n for closed, circularly symmetric cylindrical shells.

Equations (1.37) for the displacements U , V , and W become, for a circular cylindrical shell,

$$\left. \begin{aligned} U(x, y, z) &= u(x, \theta) + z\psi_x(x, \theta) \\ V(x, y, z) &= v(x, \theta) + z\psi_\theta(x, \theta) \\ W(x, y, z) &= w(x, \theta) \end{aligned} \right\} \quad (3.207)$$

where ψ_x and ψ_θ are now used to denote the

changes in the slope of the normal to the middle surface, in place of θ_α and θ_β . If shear deformation is to be permitted, then the first two of equations (1.34) stating the Kirchhoff hypothesis (normals remain normal) must be dropped as constraining equations. Then ψ_x and ψ_θ are no longer related to u , v , and w as in equations (1.39), but become additional variables in the problem.

The equations of motion can ultimately be written in the form

$$[\mathcal{L}^*]\{u_i\} = \{0\} \quad (3.208)$$

where now $\{u_i\}$ is the generalized displacement vector containing *five* components,

$$\{u_i\} = \begin{Bmatrix} u \\ v \\ w \\ R\psi_x \\ R\psi_\theta \end{Bmatrix} \quad (3.209)$$

instead of the three used in equation (2.4), and $[\mathcal{L}^*]$ is now a matrix differential operator of the *fifth* order.

As before, $[\mathcal{L}^*]$ can be written as the sum of two operators; i.e.,

$$[\mathcal{L}^*] = [\mathcal{L}_{D-M}^*] + k[\mathcal{L}_{MOD}^*] \quad (3.210)$$

where $[\mathcal{L}_{D-M}^*]$ is the differential operator according to the Donnell-Mushtari theory, generalized to take into account shear deformation; $[\mathcal{L}_{MOD}^*]$ is a modifying operator which alters the Donnell-Mushtari theory to yield another shear deformation shell theory; and k is the thickness parameter defined in equation (2.6). The differential operator for the Donnell-Mushtari type of shear deformation shell theory (from refs. 3.131 and 3.221) is

$$[\mathcal{L}_{D-M}^*] = \begin{Bmatrix} a_{11} & a_{12} & a_{13} & 0 & 0 \\ a_{21} & a_{22} & a_{23} & 0 & 0 \\ a_{31} & a_{32} & a_{33} & a_{34} & a_{35} \\ 0 & 0 & a_{43} & a_{44} & a_{45} \\ 0 & 0 & a_{53} & a_{54} & a_{55} \end{Bmatrix} \quad (3.211)$$

where

$$\begin{aligned}
a_{11} &= \frac{\partial^2}{\partial s^2} + \frac{(1-\nu)}{2} \frac{\partial^2}{\partial \theta^2} - \frac{\rho(1-\nu^2)R^2}{E} \frac{\partial^2}{\partial t^2} \\
a_{22} &= \frac{(1-\nu)}{2} \frac{\partial^2}{\partial s^2} + \frac{\partial^2}{\partial \theta^2} - \frac{\rho(1-\nu^2)R^2}{E} \frac{\partial^2}{\partial t^2} \\
a_{33} &= 1 - \kappa_1 \nabla^2 w + \frac{\rho(1-\nu^2)R^2}{E} \frac{\partial^2}{\partial t^2} \\
a_{44} &= k \left[\frac{\partial^2}{\partial s^2} + \frac{(1-\nu)}{2} \frac{\partial^2}{\partial \theta^2} \right] - \kappa_1 - \frac{k\rho(1-\nu^2)R^2}{E} \frac{\partial^2}{\partial t^2} \\
a_{55} &= k \left[\frac{(1-\nu)}{2} \frac{\partial^2}{\partial s^2} + \frac{\partial^2}{\partial \theta^2} \right] - \kappa_1 - \frac{k\rho(1-\nu^2)R^2}{E} \frac{\partial^2}{\partial t^2} \\
a_{12} &= a_{21} = \frac{(1+\nu)}{2} \frac{\partial^2}{\partial s \partial \theta} \\
a_{13} &= a_{31} = \nu \frac{\partial}{\partial s} \\
a_{34} &= a_{43} = -\kappa_1 \frac{\partial}{\partial s} \\
a_{35} &= a_{53} = -\kappa_1 \frac{\partial}{\partial \theta} \\
a_{45} &= a_{54} = \frac{k(1+\nu)}{2} \frac{\partial^2}{\partial s \partial \theta} \quad (3.212)
\end{aligned}$$

where $s = x/R$, as before,

$$\kappa_1 = \frac{1-\nu}{2} \kappa^2 \quad (3.213)$$

and κ^2 is a shear correction coefficient taken variously as $5/6$ (ref. 3.221), 0.86 (ref. 3.222), $8/9$ (ref. 3.223), and $\pi^2/12$ (ref. 3.224). The coefficients a_{11} , a_{22} , a_{12} , a_{21} , a_{13} , and a_{31} are the same as those of the eighth-order shell theory given in equation (2.7). The rotary inertia terms are clearly seen in the coefficients a_{44} and a_{55} .

An example of the modifying operator

$$[\mathcal{L}_{MOD}^*] = \begin{Bmatrix} b_{11} & b_{12} & b_{13} & b_{14} & b_{15} \\ b_{21} & b_{22} & b_{23} & b_{24} & b_{25} \\ b_{31} & b_{32} & b_{33} & b_{34} & b_{35} \\ b_{41} & b_{42} & b_{43} & b_{44} & b_{45} \\ b_{51} & b_{52} & b_{53} & b_{54} & b_{55} \end{Bmatrix} \quad (3.214)$$

is, for the theory of Naghdi and Cooper (ref. 3.221)

$$\begin{aligned}
b_{11} &= \frac{(1-\nu)}{2} \frac{\partial^2}{\partial \theta^2} \\
b_{22} &= -\frac{\kappa_1}{k} \\
b_{14} &= b_{41} = \frac{\partial^2}{\partial s^2} - \frac{(1-\nu)}{2} \frac{\partial^2}{\partial \theta^2} - \frac{\rho(1-\nu^2)R^2}{E} \frac{\partial^2}{\partial t^2} \\
b_{23} &= b_{32} = \frac{\kappa_1}{k} \frac{\partial}{\partial \theta} \\
b_{25} &= b_{52} = \frac{\kappa_1}{k} + \frac{(1-\nu)}{2} \frac{\partial^2}{\partial s^2} - \frac{\partial^2}{\partial \theta^2} - \frac{\rho(1-\nu^2)R^2}{E} \frac{\partial^2}{\partial t^2} \\
b_{35} &= b_{53} = -\frac{\partial}{\partial \theta} \\
b_{33} &= b_{44} = b_{55} = b_{12} = b_{21} = b_{13} = b_{31} = b_{15} = b_{51} \\
&= b_{24} = b_{42} = b_{34} = b_{43} = b_{45} = b_{54} = 0 \quad (3.215)
\end{aligned}$$

These equations reduce to equations (2.9e) if shear deformation and rotary inertia are neglected (ref. 3.221).

Similarly, the coefficients of the Herrmann-Armenakas (ref. 3.72) for use in equation (3.214) are (see also ref. 3.225)

$$\begin{aligned}
b_{11} &= \frac{(1-\nu)}{2} \frac{\partial^2}{\partial \theta^2} \\
b_{22} &= -\kappa_1 \left(\frac{1}{k} + 1 \right) + \frac{\partial^2}{\partial \theta^2} \\
b_{33} &= \left(\frac{1}{k} + 1 \right) \\
b_{55} &= -\kappa_1 \\
b_{14} &= b_{41} = \frac{\partial^2}{\partial s^2} - \frac{(1-\nu)}{2} \frac{\partial^2}{\partial \theta^2} - \frac{\rho(1-\nu^2)R^2}{E} \frac{\partial^2}{\partial t^2} \\
b_{23} &= b_{32} = (1+\kappa_1) \left(\frac{1}{k} + 1 \right) \frac{\partial}{\partial \theta} \\
b_{25} &= b_{52} = \kappa_1 \left(\frac{1}{k} + 1 \right) + \frac{(1-\nu)}{2} \frac{\partial^2}{\partial s^2} - \frac{\partial^2}{\partial \theta^2} \\
&\quad - \frac{\rho(1-\nu^2)R^2}{E} \frac{\partial^2}{\partial t^2} \\
b_{34} &= b_{43} = -\frac{\kappa_1}{k} \frac{\partial}{\partial s} \\
b_{35} &= b_{53} = -(1+\kappa_1) \frac{\partial}{\partial \theta} \quad (3.216)
\end{aligned}$$

The resulting equations of motion of this theory reduce to those of Flügge, Byrne, and Lur'ye (see eq. (2.9d)) if shear deformation and rotary inertia are neglected.

Other tenth order theories incorporating the effects of shear deformation and rotary inertia include those of Hildebrandt, Reissner, and Thomas (ref. 3.226); Vlasov (ref. 3.227); Herrmann and Mirsky (refs. 3.222, 3.224, and 3.228); Yu (ref. 3.229); Lin and Morgan (ref. 3.223); Chou (ref. 3.230); Mizoguchi (ref. 3.231); and Herrmann and Armenàkas (ref. 3.72) also included the effects of initial stress in their shear deformation theory. In addition, an orthotropic theory was developed by Mirsky (ref. 3.232) and a nonlinear (large deflection) theory by Yu (ref. 3.233).

Consider now the two closely related free vibration problems:

- (1) A shell of infinite length
- (2) A shell of finite length, l , supported at both ends by shear diaphragms.

As in the case of the eighth order theories (see secs. 2.2 and 2.3), both problems have the same exact solution functions for the generalized displacements in the form

$$\left. \begin{aligned} u &= A_{mn} \cos \lambda s \cos n\theta \cos \omega t \\ v &= B_{mn} \sin \lambda s \sin n\theta \cos \omega t \\ w &= C_{mn} \sin \lambda s \cos n\theta \cos \omega t \\ \psi_x &= D_{mn} \cos \lambda s \cos n\theta \cos \omega t \\ \psi_\theta &= E_{mn} \sin \lambda s \sin n\theta \cos \omega t \end{aligned} \right\} \quad (3.217)$$

In the case of the shell supported at both ends by shear diaphragms (SD-SD) the boundary conditions are given by

$$w = M_x = N_x = v = \psi_\theta = 0 \quad (3.218)$$

Equations (3.218) are exactly satisfied by equations (3.217) provided λ is taken as

$$\lambda = \frac{m\pi R}{l} \quad (m=1, 2, \dots) \quad (3.219)$$

In the case of the infinite shell, circumferential "node lines" ($v=w=0$, $u \neq 0$) will occur at intervals of l .

Substituting equations (3.217) into the tenth order set of equations of motion (3.208) yields,

for a nontrivial solution, a characteristic determinant of the fifth order. Expanding the determinant gives a fifth degree polynomial equation in the nondimensional frequency parameter $\Omega^2 = \omega^2 R^2 \rho (1 - \nu^2) / E$ of the type

$$\Omega^{10} - K_4 \Omega^8 + K_3 \Omega^6 - K_2 \Omega^4 + K_1 \Omega^2 - K_0 = 0 \quad (3.220)$$

This equation will have five real roots, and consequently five independent mode shapes, for each value of circumferential wave number n .

In the special case of axisymmetric modes ($n=0$), the five equations of motion become uncoupled into two sets (ref. 3.224). One set consisting of three equations, describes the flexural or radial modes in terms of u , w , and ψ_x . The other set corresponds to motions which are purely circumferential and involve v and ψ_θ . This yields a cubic characteristic equation for the first set and a quadratic equation for the second set.

Tang (ref. 3.234) used the shell theory of Herrmann and Mirsky (ref. 3.222) to analyze the axisymmetric motions (radial and flexural) of an SD-SD shell. Letting $n=0$, and substituting the solution functions for u , w , and ψ_x from equations (3.217) into the three uncoupled equations of motion yields the following characteristic equation for the frequency parameter Ω (ref. 3.234):

$$\begin{aligned} \Omega^6 - \Omega^4 \left[\lambda^2 (2 + \kappa_1) + \left(1 + \frac{\kappa_1}{k} \right) \right] \\ + \Omega^2 \left[\lambda^4 (1 + 2\kappa_1) + \lambda^2 \left(2 + \frac{\kappa_1}{k} - \nu^2 \right) \right. \\ \left. + \left(\frac{\kappa_1}{k} \right) \right] - \left[\lambda^6 \kappa_1 + \lambda^4 (1 - \nu^2) \right. \\ \left. + \lambda^2 (1 - \nu^2) \left(\frac{\kappa_1}{k} \right) \right] = 0 \end{aligned} \quad (3.221)$$

with κ_1 as defined previously in equation (3.213). Numerical results were obtained in reference 3.234 for one shell having $R/h=36$ and $l/R=4$ and another shell having $R/h=10$ and $l/R=8$. In both cases ν and κ^2 were taken as 0.25 and 0.86, respectively. The results are displayed in tables 3.19 and 3.20. In the tables the frequency parameters are also compared with those of eighth order theory (neglecting shear deformation and rotary inertia in the Herrmann-Mirsky theory). Significant differences exist between the theories for the lowest frequency (corresponding to a predominantly radial mode) as m increases,

TABLE 3.19.—Comparison of Frequency Parameters Ω for the Axisymmetric Modes of an SD-SD Shell; $R/h=36$, $l/R=4$ (from ref. 3.234)

m	Tenth order theory			Eighth order theory	
	Ω_1^*	Ω_2^*	Ω_3^*	Ω_1^*	Ω_2^*
1	0.7105	1.055	69.78	0.7105	1.055
2	.9285	1.614	69.80	.9285	1.614
3	.9458	2.379	69.83	.9460	2.379
4	.9523	3.158	69.88	.9525	3.158
5	.9585	3.940	69.93	.9590	3.940
6	.9675	4.723	69.98	.9685	4.723
7	.9818	5.505	70.00	.9828	5.505
8	1.002	6.290	70.15	1.004	6.290
9	1.031	7.075	70.25	1.034	7.075
10	1.070	7.860	70.35	1.074	7.860
11	1.121	8.645	70.48	1.126	8.645
12	1.183	9.430	70.60	1.190	9.430
13	1.258	10.22	70.58	1.268	10.22
14	1.346	11.00	70.90	1.360	11.00
15	1.448	11.79	71.05	1.465	11.79
16	1.562	12.57	71.23	1.585	12.57
17	1.688	13.36	71.43	1.718	13.36
18	1.827	14.14	71.60	1.865	14.14
19	1.977	14.93	71.83	2.024	14.93
20	2.138	15.71	72.03	2.196	15.71

TABLE 3.20.—Comparison of Frequency Parameters Ω for the Axisymmetric Modes of an SD-SD Shell: $R/h=10$, $l/R=8$ (from ref. 3.234)

m	Tenth order theory			Eighth order theory	
	Ω_1^*	Ω_2^*	Ω_3^*	Ω_1^*	Ω_2^*
1	0.3716	1.008	18.76	0.3716	1.008
2	.7105	1.055	19.40	.7105	1.055
3	.8895	1.264	19.43	.8900	1.264
4	.9299	1.614	19.46	.9308	1.614
5	.9446	1.993	19.51	.9461	1.994
6	.9558	2.379	19.56	.9580	2.379
7	.9686	2.768	19.64	.9720	2.768
8	.9858	3.158	19.71	.9906	3.158
9	1.009	3.548	19.80	1.016	3.549
10	1.040	3.939	19.89	1.049	3.939
11	1.079	4.331	20.00	1.093	4.331
12	1.128	4.723	20.13	1.147	4.723
13	1.186	5.114	20.24	1.213	5.115
14	1.255	5.506	20.36	1.291	5.506
15	1.334	5.899	20.50	1.381	5.899
16	1.424	6.290	20.65	1.485	6.291
17	1.521	6.683	20.80	1.600	6.683
18	1.629	7.075	20.96	1.728	7.075
19	1.745	7.468	21.14	1.868	7.468
20	1.870	7.860	21.31	2.019	7.860

particularly for the smaller R/h value. The second frequency corresponds to an axial mode and varies negligibly between the theories. The third frequency does not exist in the eighth order theory.

Herrmann (ref. 3.235) also obtained results for the axisymmetric modes of infinitely long shells. Comparisons were made between solutions obtained from eighth and tenth order shell theories and the three-dimensional elasticity theory. For the three-dimensional results, the approximate solutions of McFadden (ref. 3.236) were used. These are, for the radial (breathing or extensional) mode,

$$\frac{\omega}{\omega_c} = \frac{2\sqrt{1-2\nu}}{(1-\nu)\left(2-\frac{h}{R}\right)\left[1+\delta+\frac{1}{2}(\eta-1)\delta^2-\frac{1}{2}(\eta-1)\delta^3\right]} \quad (3.222)$$

where

$$\left. \begin{aligned} \omega_c^2 &= \frac{\lambda+2G}{\rho R^2} \\ \delta &= \frac{1}{2\frac{R}{h}-1} \\ \eta &= \frac{2(1-3\nu)}{3(1-\nu)} \end{aligned} \right\} \quad (3.223)$$

λ and G are the Lamé elastic constants,

$$\left. \begin{aligned} \lambda &= \frac{\nu E}{(1+\nu)(1-2\nu)} \\ G &= \frac{E}{2(1+\nu)} \end{aligned} \right\} \quad (3.224)$$

and for the thickness (or pinching) mode

$$\frac{\omega}{\omega_c} = \frac{\pi R}{h} \left[1 - \frac{\frac{4(1-2\nu)}{1-\nu} - \frac{1}{8}}{\pi^2 \left(4\frac{R^2}{h^2} - 1 \right)} \right]^{-1} \quad (3.225)$$

The shell theories used were taken from reference 3.228. Values of ω/ω_c are given in table 3.21 for $R/h=30$, 4, and 1.5. Note that the thin shell (i.e., eighth order) theory predicts the breathing mode frequencies quite well for R/h as large as four, whereas fairly large discrepancies exist between values for the thick shell (tenth order) and

elasticity theories for both the breathing and pinching modes. The thin shell theory does not recognize the pinching mode.

Reismann and Medige (ref. 3.237) obtained numerical results comparing frequency parameters with and without the inclusion of shear deformation and rotary inertia effects. The Herrmann-Armenakas theory (eqs. (3.216)) was used. Data were obtained using $\nu=0.3$, $\kappa^2=0.86$, $l/R=6$, and $R/h=5$. These results are exhibited in figures 3.153, 3.154, and 3.155 for $n=0$, 1, and 5, respectively, where the parameter Ω/λ is plotted versus the number of axial half-waves, m . The number of roots of the characteristic equations are seen by the separate curves in these plots for $n=0$ —three roots with shear deformation, two without; for $n>0$ —five roots with shear deformation, three without.

No numerical results are available in the literature which apply tenth order shell theories to boundary conditions *other than* SD-SD. However, an exact procedure similar to the one outlined in section 2.4 for eighth order theories

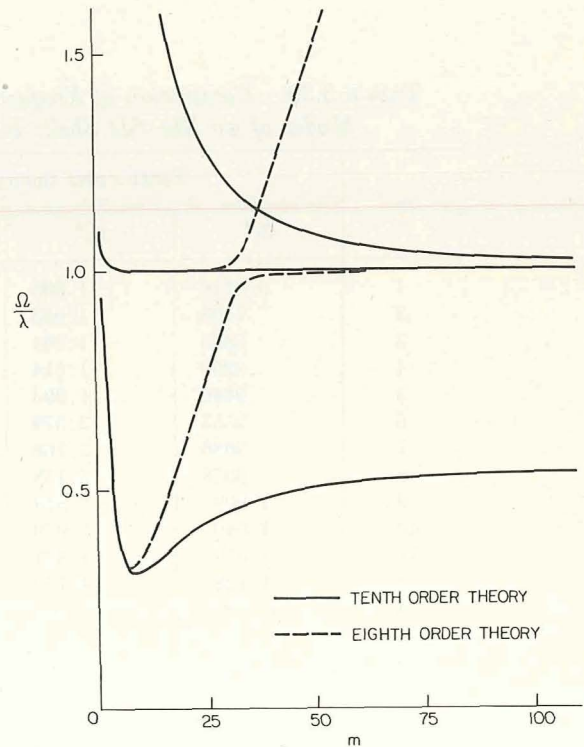
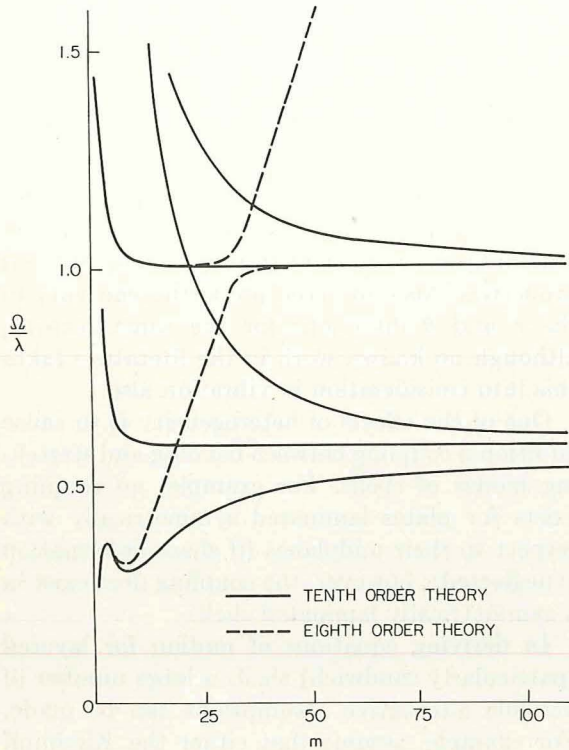
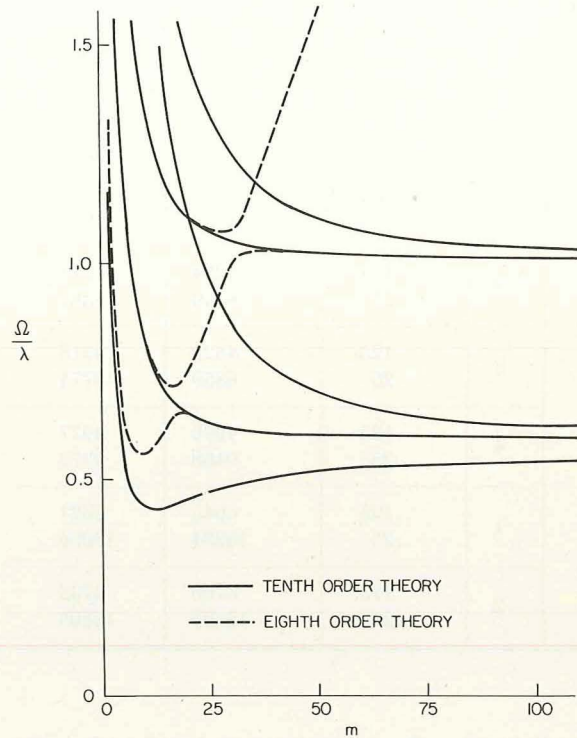


FIGURE 3.153.—Comparison of results for an SD-SD shell; $R/h=5$, $l/R=6$; $n=0$. (After ref. 3.237)

TABLE 3.21.—Comparison of Frequency Parameters ω/ω_c for an Infinite Shell According to Various Theories

$\frac{R}{h}$	Breathing mode			Pinching mode	
	Elasticity theory	Tenth order shell theory	Eighth order shell theory	Elasticity theory	Tenth order shell theory
30	0.906	0.990	0.904	94.3	104
4	.911	.985	.904	12.93	13.97
1.5	.939	.970	.904	6.07	5.42


 FIGURE 3.154.—Comparison of results for an SD-SD shell; $R/h=5$, $l/R=6$; $n=1$. (After ref. 3.237)

 FIGURE 3.155.—Comparison of results for an SD-SD shell; $R/h=5$, $l/R=6$; $n=5$. (After ref. 3.237)

could be followed. The solution equations (3.217) would then be generalized to

$$\left. \begin{aligned} u &= u_n(s) \cos n\theta \cos \omega t \\ v &= v_n(s) \sin n\theta \cos \omega t \\ w &= w_n(s) \cos n\theta \cos \omega t \\ \psi_x &= \psi_{xn}(s) \cos n\theta \cos \omega t \\ \psi_\theta &= \psi_{\theta n}(s) \sin n\theta \cos \omega t \end{aligned} \right\} \quad (3.226)$$

($s=x/R$) where the form of the functional variation in the longitudinal direction is yet to be

determined. Substituting equations (3.226) into equations (3.208) yields, for each n , a set of five (except three for $n=0$) simultaneous, linear, ordinary differential equations having constant coefficients. However, these equations may be solved and the boundary conditions may then be prescribed to determine the appropriate mode shapes in a manner analogous to that described in section 2.4.

The influence of rotary inertia alone (i.e., neglecting shear deformation) was studied by Warburton and Al-Najafi (ref. 3.238). An SD-SD

TABLE 3.22.—*Effect of Rotary Inertia Upon the Frequencies (cps) of SD-SD Shells ($R=2.073$ in., $l=17.56$ in.)*

n	m	h , in.	Rotary inertia	
			Neglected	Included
2	1	0.125	903	903
		.1875	1254	1253
		.25	1623	1620
3	1	.125	2174	2171
		.1875	3251	3242
		.25	4330	4308
	2	.1875	3492	3482
		.25	4595	4571
4	1	.125	4123	4113
		.25	8239	8165
	2	.125	4254	4244
		.25	8459	8381
	3	.125	4529	4518
		.25	8859	8774
	4	.125	4990	4977
		.25	9468	9372
5	1	.125	6645	6621
		.25	13284	13094
	2	.125	6760	6735
		.25	13500	13305

shell having $R=2.073$ in. and $l=17.56$ in. was analyzed using the Flügge eighth order theory. Numerical results are presented in table 3.22.

The effects of shear deformation and rotary inertia upon the free vibration frequencies and mode shapes of circular cylindrical shells are also referred to in references 3.239 through 3.254.

3.5.3 Nonhomogeneity

Nonhomogeneity (or heterogeneity) in materials can arise in many ways. One of the most frequent ways occurs in circular cylindrical shells when the shell is made of layers, each layer being homogeneous. The possible configurations of such combinations of layers is endless, although a great deal of attention has been paid to

(1) Two layered shells

(2) Sandwich (i.e., three-layered shells), where the middle layer (core) is considerably thicker and less rigid than its surrounding (face) layers

(3) Multilayered shells, as occur in laminated shells using composite materials.

The layers can be individually orthotropic, as well as isotropic. If the angles of material orthotropy are not parallel to the shell coordinates, the resulting shell equations appear, in general, to be anisotropic (more particularly, aelotropic) in form.

In addition to the stepwise heterogeneity discussed above, material properties can vary *continuously* through the thickness. Such a case arises, for example, when certain materials, such as styrofoam, are used or when severe thermal gradients exist, causing a degradation of material properties. Also, material properties can vary in the r and θ directions for the same reasons, although no known work in the literature takes this into consideration in vibration also.

One of the effects of heterogeneity is to cause additional coupling between bending and stretching modes of shells. For example, no coupling exists for plates laminated symmetrically with respect to their midplanes (if shear deformation is neglected); however, the coupling does exist in a symmetrically laminated shell.

In deriving equations of motion for layered (particularly sandwich) shells a large number of possible alternative assumptions can be made. For example, assume that either the Kirchhoff hypothesis or the linear displacements accounting for shear deformation remain valid over the entire thickness of the shell. Or it can be assumed that the linear variation exists for each layer, but changes from layer to layer. It may be assumed that the face layers carry no transverse shear strain, or that the core withstands no normal stresses, or that the flexural rigidity of the face layers about their own middle surfaces are negligible. Because of this complexity, no attempt will be made to sort out the numerous theories which exist for layered shells.

Consider now the development of a Donnell-type theory for a layered circular cylindrical shell. Assume that the shell consists of N layers, the k^{th} layer being typical and having a thickness

h_k bounded by the surfaces $z = z_k$ and $z = z_{k-1}$, where z is measured from a reference surface within the shell (see fig. 3.156). Assume further that each layer is homogeneous and orthotropic. Then, the stress-strain relations (3.2) can be written for the cylindrical shell coordinates as

$$\begin{bmatrix} \sigma_x^{(k)} \\ \sigma_\theta^{(k)} \\ \tau_{x\theta}^{(k)} \end{bmatrix} = \begin{bmatrix} A_{11}^{(k)} & A_{12}^{(k)} & 0 \\ A_{12}^{(k)} & A_{22}^{(k)} & 0 \\ 0 & 0 & A_{66}^{(k)} \end{bmatrix} \begin{bmatrix} e_x \\ e_\theta \\ \gamma_{x\theta} \end{bmatrix} \quad (3.227)$$

for the k^{th} layer, where

$$\left. \begin{aligned} A_{11} &= \frac{E_x}{1 - \nu_x \nu_\theta}, & A_{22} &= \frac{E_\theta}{1 - \nu_x \nu_\theta} \\ A_{12} &= \frac{\nu_x E_\theta}{1 - \nu_x \nu_\theta} = \frac{\nu_\theta E_x}{1 - \nu_x \nu_\theta}, & A_{66} &= G \end{aligned} \right\} \quad (3.228)$$

In evaluating the force and moment resultant integrals (eqs. (1.75)), the integrations must be carried out piecewise through the thickness. The resulting equations of motion can again be written as in equation (2.3), where the elements of the third order matrix differential operator are now given by (refs. 3.7, 3.255, and 3.256):

$$\begin{aligned} \mathcal{L}_{11} &= C_{11} \frac{\partial^2}{\partial s^2} + C_{66} \frac{\partial^2}{\partial \theta^2} - \rho h R^2 \frac{\partial^2}{\partial t^2} \\ \mathcal{L}_{22} &= C_{66} \frac{\partial^2}{\partial s^2} + C_{22} \frac{\partial^2}{\partial \theta^2} - \rho h R^2 \frac{\partial^2}{\partial t^2} \\ \mathcal{L}_{33} &= \frac{1}{R^2} \left[D_{11} \frac{\partial^4}{\partial s^4} + 2(D_{12} + 2D_{66}) \frac{\partial^4}{\partial s^2 \partial \theta^2} + D_{22} \frac{\partial^4}{\partial \theta^4} \right] \\ &\quad + \frac{2}{R} \left(D_{12}^* \frac{\partial^2}{\partial s^2} + D_{22}^* \frac{\partial^2}{\partial \theta^2} \right) + C_{22} + \rho h R^2 \frac{\partial^2}{\partial t^2} \\ \mathcal{L}_{12} = \mathcal{L}_{21} &= (C_{12} + C_{66}) \frac{\partial^2}{\partial s \partial \theta} \\ \mathcal{L}_{13} = \mathcal{L}_{31} &= C_{12} \frac{\partial}{\partial s} + \frac{D_{11}^*}{R} \frac{\partial^3}{\partial s^3} \\ &\quad + \frac{1}{R} (D_{12}^* + 2D_{66}^*) \frac{\partial^3}{\partial s \partial \theta^2} \\ \mathcal{L}_{23} = \mathcal{L}_{32} &= C_{22} \frac{\partial}{\partial \theta} + \frac{D_{22}^*}{R} \frac{\partial^3}{\partial \theta^3} \\ &\quad + \frac{1}{R} (D_{12}^* + 2D_{66}^*) \frac{\partial^3}{\partial s^2 \partial \theta} \end{aligned} \quad (3.229)$$

where

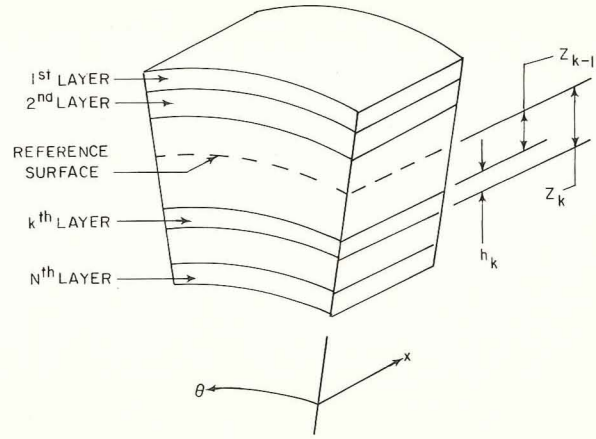


FIGURE 3.156.—Element of a layered shell.

$$\begin{aligned} \{C_{ij}, D_{ij}^*, D_{ij}\} &= \sum_{k=1}^N A_{ij}^{(k)} \left\{ (z_k - z_{k-1}), \frac{1}{2}(z_k^2 - z_{k-1}^2), \right. \\ &\quad \left. \frac{1}{3}(z_k^3 - z_{k-1}^3) \right\} \quad (3.230) \\ \rho &= \frac{1}{h} \sum_{k=1}^N \rho_k (z_k - z_{k-1}) \end{aligned}$$

and where h is the total thickness. The operators given by equations (3.229) are generalizations of those used in the *homogeneous*, orthotropic equations of motion (eq. (3.8)) and that additional cross-coupling terms containing D_{ij}^* coefficients are also present.

Other works which develop theories for shells having heterogeneous material properties with respect to the thickness direction include references 3.24, 3.91, 3.233 (nonlinear), 3.248, 3.257 through 3.274, and 3.275 (nonlinear).

Dong (ref. 3.7) analyzed the case of a two-layered, SD-SD shell having an isotropic inner layer and an orthotropic outer one, thereby simulating a layer overwrapped with filaments. The data for the layers are given in table 3.23, with the interface taken as the reference surface. The exact solution functions (eq. (2.20)) were used in equations (2.3) and (3.229), yielding a cubic characteristic equation in ω^2 . A plot of the frequency parameter $\omega R \sqrt{\rho h / C_{22}}$ versus the circumferential wave number is shown in figure 3.157 for a shell having $R/h = 25$, $l/R = 20$. In

TABLE 3.23.—Data for Two-layered Shell

Layer	A_{11} , psi	A_{12} , psi	A_{22} , psi	A_{66} , psi	h , in.	Density
1	6.70×10^6	2.11×10^6	12.0×10^6	2.51×10^6	0.20	$0.5\rho_0$
2	33.0×10^6	11.0×10^6	33.0×10^6	13.2×10^6	.20	$1.0\rho_0$

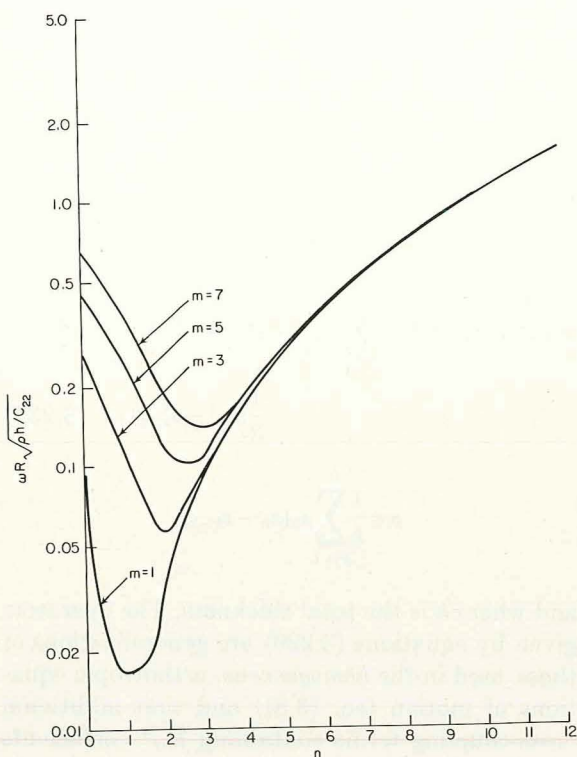


FIGURE 3.157.—Frequency spectrum for a two-layered, SD-SD shell. (After ref. 3.7)

figure 3.158 frequency envelopes (lowest frequencies) are shown for $m=1$ and for various R/h ratios, plotted versus the l/R ratio. Figure 3.158 can be compared with the frequency envelopes for homogeneous orthotropic shells given previously in figures 3.16 and 3.17.

In reference 3.7 it was found that neglecting tangential inertia terms in the equations of motion increased the frequencies in approximately the same ways as for homogeneous shells (see sec. 2.3.4), although tangential inertia was included in the subsequent calculations.

Other types of boundary conditions were also examined in reference 3.7 for two layered shells.

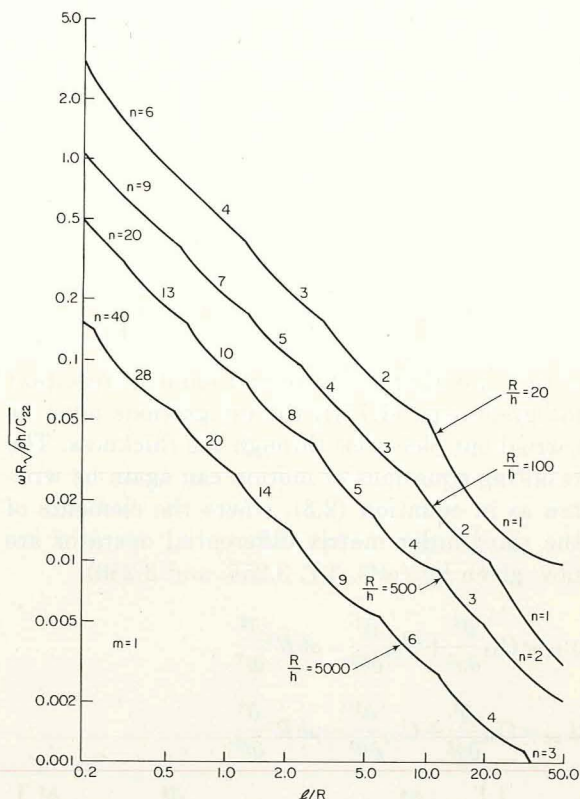


FIGURE 3.158.—Frequency envelopes for two-layered, SD-SD shells. (After ref. 3.7)

The exact solution procedure outlined in section 2.4 using equations (2.53) was followed. Numerical results were obtained for the shell described previously in table 3.23 for $R/h=100$ and $l/R=20$ for three sets of edge conditions:

- (1) Both ends supported by shear diaphragms (SD-SD)
- (2) Both ends clamped ($u=v=w=\partial w/\partial x=0$)
- (3) One end clamped and the other supported with axial restraint ($u=v=w=M_x=0$).

The frequency envelopes for these cases are exhibited in figure 3.159.

Jones and Whittier (refs. 3.270) made a study

of the axisymmetric motions of two-layered shells whose layers are connected by a thin, massless bond of arbitrary stiffness. Results were compared with those obtained from a theory derived by Payton (ref. 3.272), which assumes that the bond between the two layers is extremely flexible in shear. The behavior of the shell was shown to be highly dependent upon a bond stiffness parameter B defined as

$$B = \frac{Gh^2}{b(C_1 + C_2)} \quad (3.231)$$

where G and b are the shear moduli and thickness, respectively, of the bond material; $h = h_1 + h_2$, the sum of the thicknesses of the two layers; and C_1 and C_2 are the stretching stiffnesses of the two layers (i.e., $C_i = E_i h_i / (1 - \nu_i^2)$).

In reference 3.277 the two layered shell was analyzed by three approaches, one based upon the exact three-dimensional elasticity equations, and the others being modal and finite difference

solutions of a Flugge-type set of shell equations developed in reference 3.274.

Baker and Herrmann (ref. 3.257) analyzed three layered (sandwich) shells. It was assumed that the facing sheets of thickness t_1 and t_2 are very thin relative to the thickness h of the sandwich, that the elastic moduli of the facing sheets are much larger than the corresponding moduli of the core and, consequently, that the core material resists only transverse shear forces and the facing sheets do not resist transverse shear forces. Thus, the theory developed is of the tenth order, including the effects of shear deformation and rotary inertia. Initial stress terms were also included.

Numerical results and an excellent discussion were presented in reference 3.257 for SD-SD shells all having the following parameters:

$$\left. \begin{aligned} \frac{A_{12}}{A_{11}} &= 0.33, & \frac{A_{66}}{A_{11}} &= 0.376, & \frac{t_1}{t_2} &= 1 \\ \frac{\rho_1}{\rho_3} &= \frac{\rho_2}{\rho_3} = 50, & r_i &= \frac{t_1 + t_2}{h} = 0.1 \end{aligned} \right\} \quad (3.232)$$

where A_{11} , A_{12} , and A_{66} are the elastic constants of the identical facing sheets, as defined by equations (3.228); and ρ_1 and ρ_3 are the mass densities of the facing sheets and the core, respectively.

A typical example of the frequency as a function of $\lambda = m\pi R/l$ is given in figure 3.160 for $n=2$. The curves shown are for $R/h = 100$, $r_E = 1$, and $r_{\theta z} = r_{\theta \theta} = 1$, where

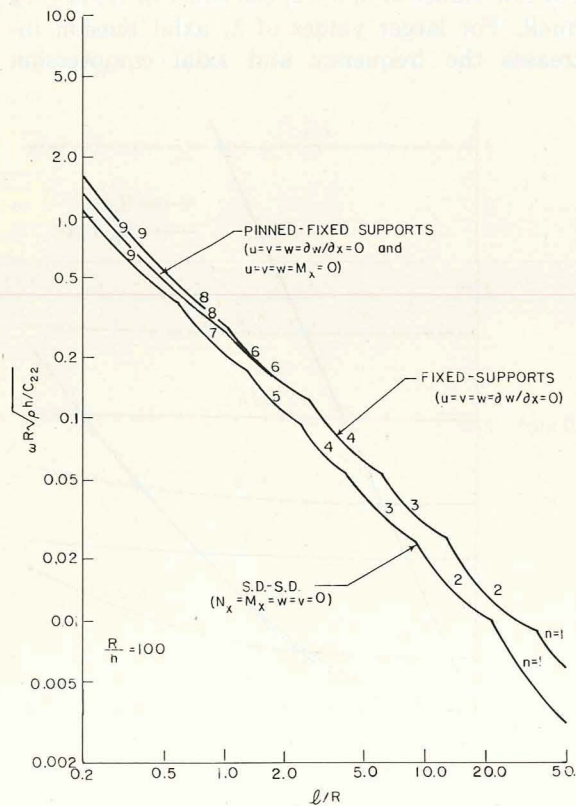


FIGURE 3.159.—Frequency envelopes for two-layered shells having various end conditions. (After ref. 3.7)

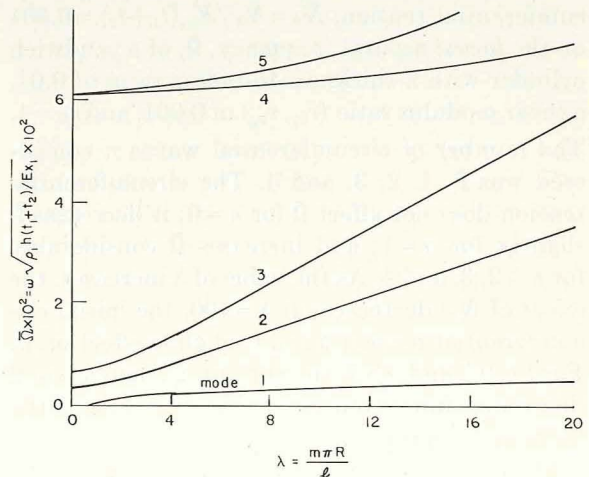


FIGURE 3.160.—Frequency parameters for a three-layered, SD-SD shell; dimensions given in text. (After ref. 3.257)

$$\left. \begin{aligned} r_E &= \frac{E_{\theta_1}}{E_{x_1}} \\ r_{\theta x} &= \frac{\kappa_x G_{x_3}}{E_{x_1}} \\ r_{\theta \theta} &= \frac{\kappa_\theta G_{\theta_3}}{E_{x_1}} \end{aligned} \right\} \quad (3.233)$$

E_{x_1} and E_{θ_1} are Young's moduli in the x -direction and θ -direction, respectively, for a facing sheet; G_{x_3} and G_{θ_3} are the transverse shear moduli of the core material, i.e.,

$$\left. \begin{aligned} \tau_{xz} &= G_{x_3} e_{xz} \\ \tau_{x\theta} &= G_{\theta_3} e_{x\theta} \end{aligned} \right\} \quad (3.234)$$

and κ_x and κ_θ are shear coefficients matching the cutoff frequency of the thickness-shear vibration from the shell theory to the frequency of the first antisymmetric thickness shear mode of the exact theory. For the sandwich shells considered here, the values of κ_x and κ_θ are close to unity. Because a tenth order shell theory was used, five values of the frequency parameter $\bar{\Omega} = \omega \sqrt{\rho_1 h(t_1 + t_2) / E_{x_1}}$ are shown in figure 3.160 for each value of λ . Although the modes are numbered in the proper order for small values of λ , this order is not necessarily preserved for larger λ ; for example, for $\lambda > 28$ the third mode has a higher frequency than the fourth mode. The value of $\bar{\Omega}$ for $\lambda = 0$ is 0.0035.

Figure 3.161 shows the effect of an initial circumferential tension, $\bar{N}_\theta = N_\theta^i / E_{x_1}(t_1 + t_2) = 0.001$ on the lowest natural frequency, $\bar{\Omega}$, of a sandwich cylinder with a thickness-to-radius ratio of 0.01, a shear modulus ratio ($r_{\theta x}, r_{\theta \theta}$) of 0.001, and $r_E = 1$. The number of circumferential waves n considered was 0, 1, 2, 3, and 4. The circumferential tension does not affect $\bar{\Omega}$ for $n = 0$; it decreases $\bar{\Omega}$ slightly for $n = 1$; and increases $\bar{\Omega}$ considerably for $n = 2, 3$, and 4. As the value of λ increases, the effect of N_θ^i decreases; at $\lambda = 100$, the initial circumferential tension has a negligible effect on $\bar{\Omega}$. For $\lambda < 0.2$ and $n > 1$, the percentage increase in $\bar{\Omega}$ due to the initial tension of N_θ^i decreases as the value of n increases.

If shear deformations are neglected, as in the case of monocoque cylinders under initial stress (see sec. 3.4), the effect of initial circumferential stress becomes negligible for very large values of

n . However, for sandwich cylinders this is not the case.

Also investigated in reference 3.257 was the effect of transverse shear modulus,

$$r_{\theta x} = r_{\theta \theta} = 0.001, 0.0001$$

and initial circumferential tension,

$$N_\theta^i / E_{x_1}(t_1 + t_2) = 0, 0.001$$

on $\bar{\Omega}$ for $\lambda < 0.4$, $n = 3, 4$. The remaining parameters were the same as those shown in figure 3.161. The increase in $\bar{\Omega}$ due to N_θ^i was approximately 8 percent greater if $r_{\theta \theta} = 0.0001$ rather than 0.001. The effect of initial circumferential stress on the four higher modes was negligible for every value of the parameters which was investigated.

The effect of axial initial stress, N_x^i , on the lowest natural frequency is shown in figure 3.162 for three values of transverse shear modulus, $r_{\theta x} = r_{\theta \theta} = 0.01, 0.001, 0.0001$. Curves are shown for $\bar{N}_x = N_x^i / E_{x_1}(t_1 + t_2) = 0, 0.005$, and -0.005 . For low values of λ , $\lambda < 2$, the effect of \bar{N}_x is very small. For larger values of λ , axial tension increases the frequency and axial compression

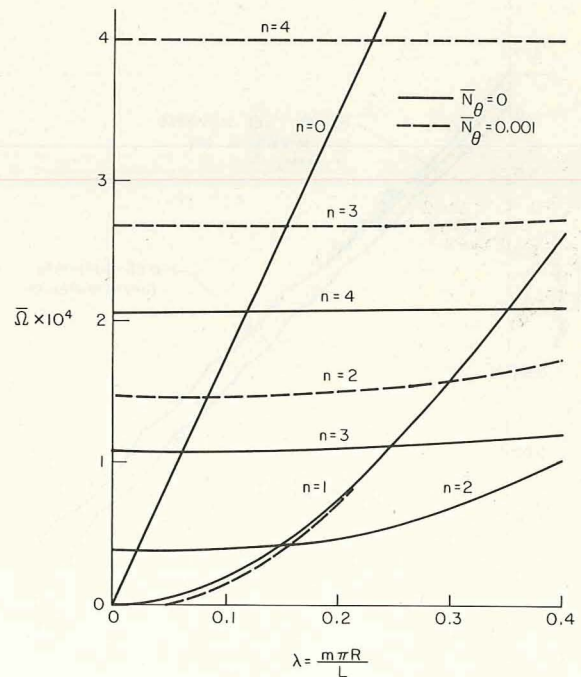


FIGURE 3.161.—The effect of circumferential prestress on the lowest natural frequency of an SD-SD, 3-layer shell; dimensions given in text. (After ref. 3.257)

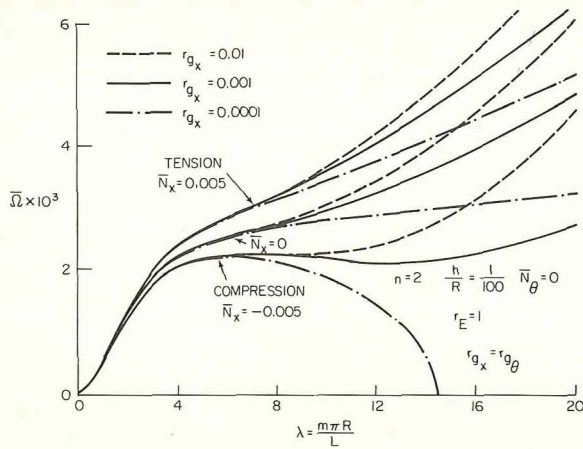


FIGURE 3.162.—The effect of longitudinal initial stress and the transverse shear modulus on the lowest natural frequency of an SD-SD, 3-layer shell. (After ref. 3.257)

decreases the frequency, as expected. When $\bar{N}_x = -0.005$ and $r_{g_x} = r_{g_\theta} = 0.0001$,

$$\bar{\Omega} = 0 \text{ at } \lambda = 14.5$$

indicating that the cylinder is statically unstable under a $\bar{N}_x = -0.005$. The critical buckling parameter \bar{N}_x for this case, therefore, is less than 0.005. As in the case of circumferential initial stress, as the transverse shear modulus decreases, $\bar{\Omega}$ decreases and the effect of initial axial stress increases. For this particular case, axial compression has a larger effect than axial tension of the same magnitude.

At large values of λ , the curves with initial stress become parallel to the corresponding curves without initial stress. If shear deflections had been neglected, the effect of initial axial stress would be negligible for very large values of λ . The value of n has very little effect on $\bar{\Omega}$ if λ is large; figure 3.162, therefore, would be very similar, except near the origin, for other values of n . The effect of initial axial stress on the four higher modes was found to be negligible in reference 3.257.

The effect of a positive initial moment on the natural frequency of an infinitely long cylinder ($\lambda = 0$) was investigated in reference 3.257 for $r_{g_\theta} = 0.001$ and $R/h = 30, 100, 1000$. Two values of n were included for each value of h/R ($n = 2$ and $n = \pi R/h$), and the stress due to initial moment was $\sigma_\theta^i/E_\theta = 6 \times 10^{-3}$. The maximum

effect of the initial moment was a decrease of the lowest natural frequency, $\bar{\Omega}$, by 0.5 percent.

If combined initial moment and hoop compression are considered, it was found that initial moments can have a large effect on $\bar{\Omega}$ at elastic stress levels if the compressive force is very near the critical buckling force. The compressive force, however, must be so near the critical buckling force (within 1 percent) that this case is of little practical interest.

A cylinder with $h/R = 1/30$ and $r_{g_\theta} = r_{g_x} = 0.0001$ was considered next by Baker and Herrmann (ref. 3.257). For very large positive initial moments in each direction ($\sigma_x^i/E_{x_1} = \sigma_\theta^i/E_{x_1} = 10^{-2}$) and for very short wavelengths ($n = 100, \lambda = 50$), the initial moment decreased $\bar{\Omega}$ by 6.5 percent. This example was given to show the very large values of σ/E , n , and λ which are necessary to cause a noticeable change of $\bar{\Omega}$ due to initial moment. Even though the effect of initial moment on the natural frequencies of sandwich cylinders appears negligibly small, the effect is much larger than for homogeneous isotropic cylinders. As in the previous cases of initial stresses, the effect of initial moments on the higher modes was negligible.

The effect of orthotropic facing sheets on the first three natural frequencies is shown in figure 3.163. Figure 3.164 shows only the first natural frequency for a wider range of λ . The ratios of moduli studied were $r_E = 0.5, 1$, and 2 ; whereas $h/R = 1/30$, $n = 2$, and $r_{g_x} = r_{g_\theta} = 0.001$. For simplicity, A_{12}/A_{11} and A_{66}/A_{11} were kept constant. As expected, values of r_E less than 1 decrease the natural frequencies, and values of r_E greater than one increase the natural frequencies. The largest effect of varying r_E on the third mode occurs at $\lambda = 0$ and might be expected because the mode shape associated with the third natural frequency at $\lambda = 0$ is mainly a circumferential displacement. The second mode is not affected at $\lambda = 0$ because the predominant motion is an axial displacement. Note that the second natural frequency decreases as λ increases for the case of $r_E = 0.5$. At $\lambda = 20$, the effect of varying r_E has very little effect on the second and third natural frequency. The first natural frequency is changed considerably by orthotropic facings at very low values of λ and at high values of λ . At $\lambda = 1$, $\bar{\Omega}$ is about the same for all three values of r_E . The orthotropic facings

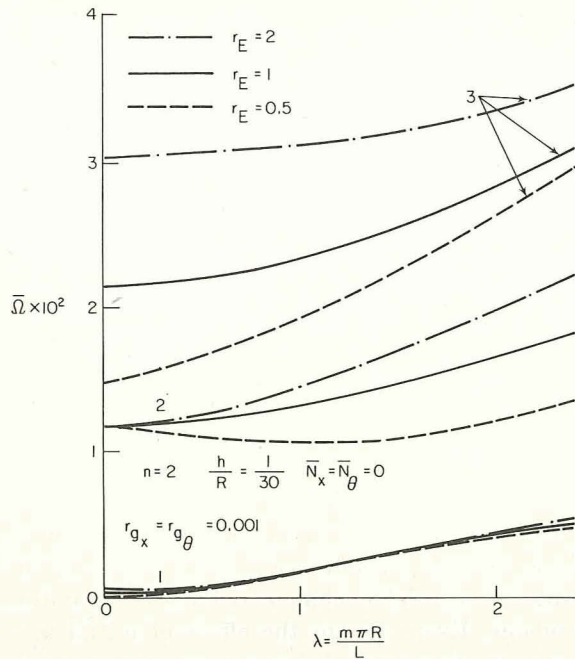


FIGURE 3.163.—Three lowest natural frequencies for SD-SD, three-layer shells with orthotropic facing sheets. (After ref. 3.257)

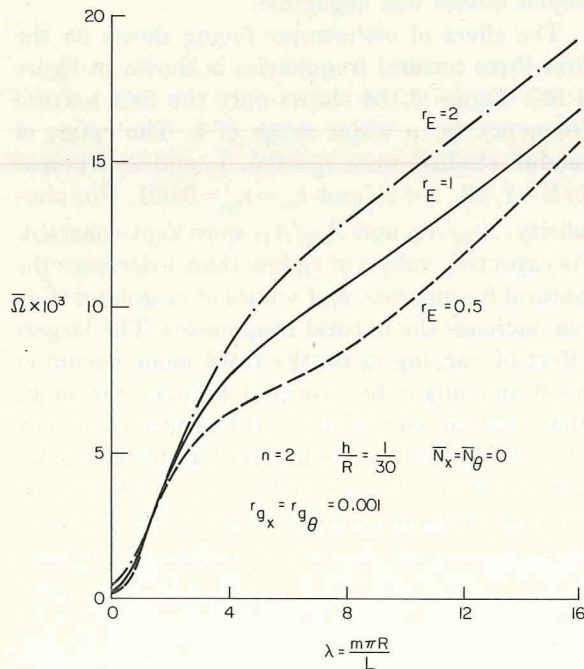


FIGURE 3.164.—Lowest natural frequency for SD-SD, three-layer shells with orthotropic facing sheets. (After ref. 3.257)

had very little effect on the fourth and fifth modes.

The lowest natural frequency for a sandwich cylinder with facing sheets of unequal thickness was investigated in reference 3.257 for

$$\left. \begin{aligned} n=2, \quad h/R &= \frac{1}{30}, \\ \bar{N}_x = \bar{N}_\theta &= 0, \quad r_{g_x} = r_{g_\theta} = 0.001, \\ r_E &= 1, \quad r_t = 0.1 \end{aligned} \right\} \quad (3.235)$$

The facing sheet ratios $r_h = t_1/t_2 = 1, 2, 3, 1/2, 1/3$ were investigated while the ratios h/R and t/h were kept constant. The total depth of the two facing sheets ($t = t_1 + t_2$), therefore, was a constant. If $\lambda < 0.2$, the value of $\bar{\Omega}$ for $r_h = 1/2$ or 2 was approximately 5 percent lower than that of $\bar{\Omega}$ for $r_h = 1$; whereas the value of $\bar{\Omega}$ for $r_h = 1/3$ or 3 was approximately 12 percent lower than that of $\bar{\Omega}$ for $r_h = 1$. This would be expected because the flexural rigidity of the sandwich is smaller if the total facing sheet thickness t is not divided equally between the two facing sheets.

As the value of λ increases, the effect of r_h decreased until at $\lambda = 20$ the values of $\bar{\Omega}$ for the five r_h ratios considered were within 2 percent of each other. The second and third modes are unaffected by r_h . The natural frequencies associated with the fourth and fifth modes ($\bar{\Omega}_4, \bar{\Omega}_5$) are increased if the facing sheets are unequal. This increase is due to the decrease in the rotary inertia of the sandwich. The percentage change in magnitude of $\bar{\Omega}_4$ and $\bar{\Omega}_5$, due to changing the value of r_h , is about the same as the percentage change in magnitude of Ω . At $\lambda = 20$, the effect of r_h on $\bar{\Omega}_4$ and $\bar{\Omega}_5$ is small. It can be shown that the thickness shear frequencies also increase if the facing sheets are unequal.

Kagawa (ref. 3.247) presented a set of equations for sandwich (three-layered) shells which are generalizations of Mirsky and Herrmann's ref. 3.224) formulation for homogeneous shells (i.e., including the shear deformation of the core). Exact solutions for SD-SD (or infinite) shells were obtained by using equations (3.217). Numerical results were given for sandwich shells where the isotropic core and face layers were assumed to be cellular cellulose acetate and aluminum, respectively, for which

$$\left. \begin{aligned} \frac{\rho_1}{\rho_2} &= 34.4, & \frac{E_1(1-\nu_2^2)}{E_2(1-\nu_1^2)} &= 2177, \\ \frac{E_1(1+\nu_2)}{E_2(1-\nu_1)} &= 1683, & \frac{\nu_1}{\nu_2} &= 3.27, \\ \nu_1 &= 0.091 \end{aligned} \right\} \quad (3.236)$$

where the subscripts 1 and 2 identify the (identi-

cal) face layers and core, respectively. Calculations were made for 0, 1, 2, and 6 circumferential waves n and $R/h=30$, 10, and 5, where h is the total shell thickness. The numerical results are depicted in figures 3.165 through 3.170 for $h_2/h_1=5$ (core thickness/thickness of each face).

Extensive numerical results for three-layered shells are also available in references 3.278, 3.279,

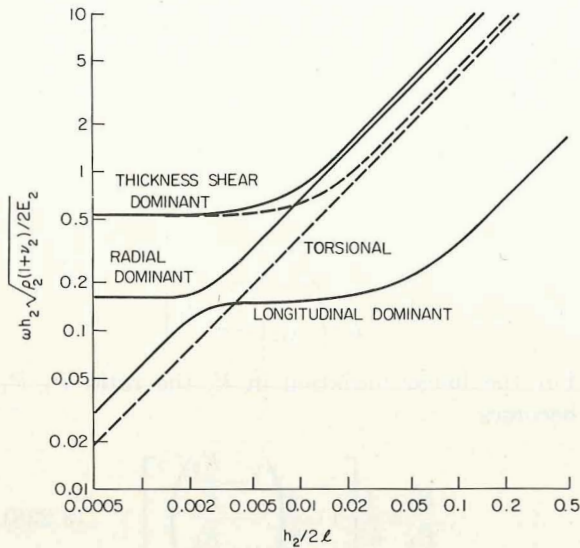


FIGURE 3.165.—Frequency parameters for SD-SD, three-layer shells; $n=0$, $R/h=30$. (After ref. 3.247)

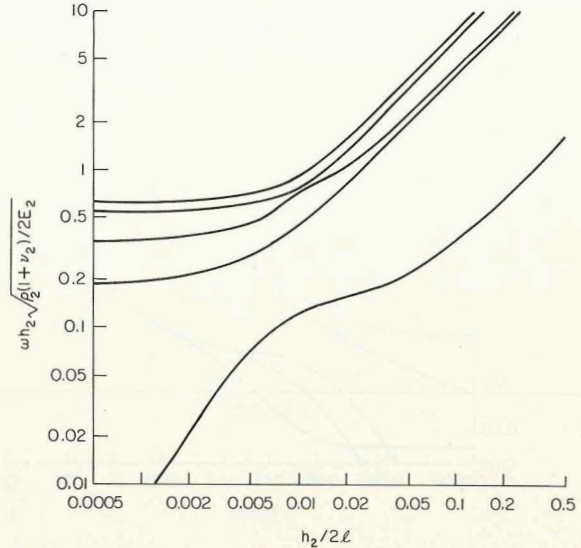


FIGURE 3.167.—Frequency parameters for SD-SD, three-layer shells; $n=2$, $R/h=30$. (After ref. 3.247)

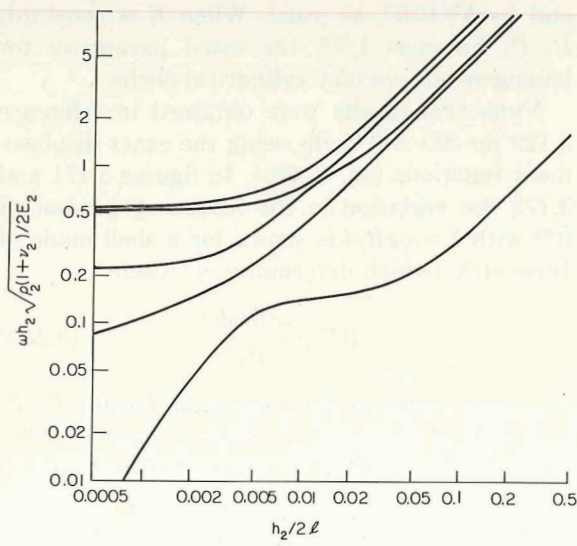


FIGURE 3.166.—Frequency parameters for SD-SD, three-layer shells; $n=1$, $R/h=30$. (After ref. 3.247)

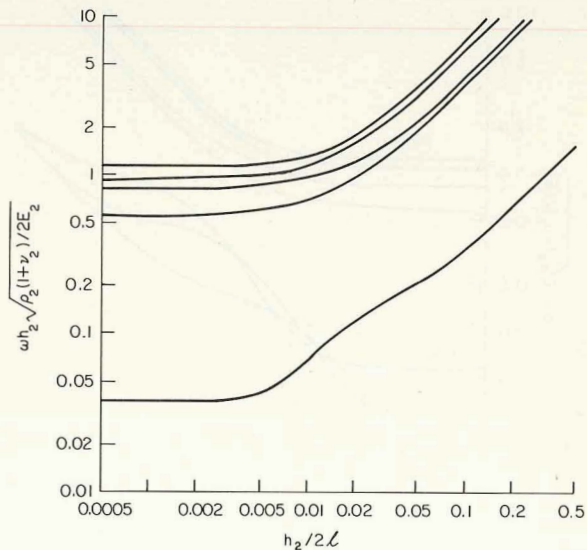


FIGURE 3.168.—Frequency parameters for SD-SD, three-layer shells; $n=6$, $R/h=30$. (After ref. 3.247)

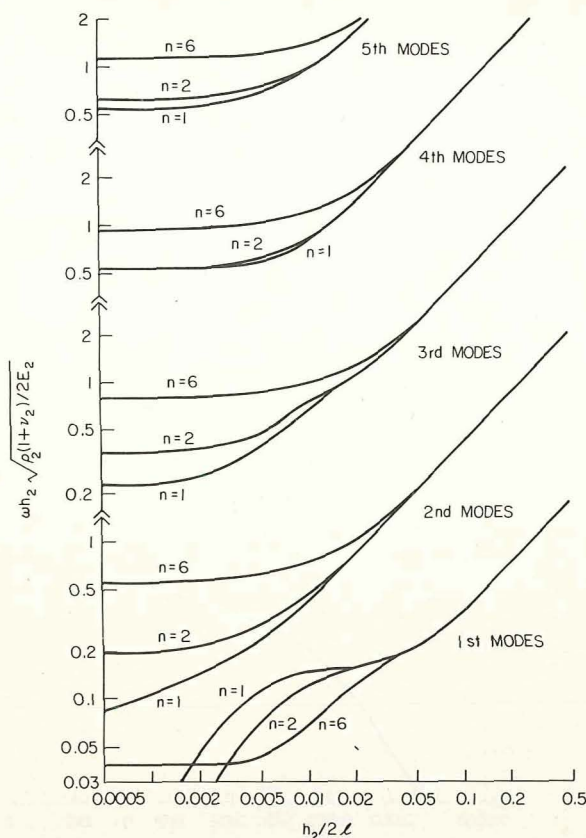


FIGURE 3.169.—Frequency parameters for SD-SD, three-layer shells; $n=1, 2, 6$; $R/h=30$. (After ref. 3.247)

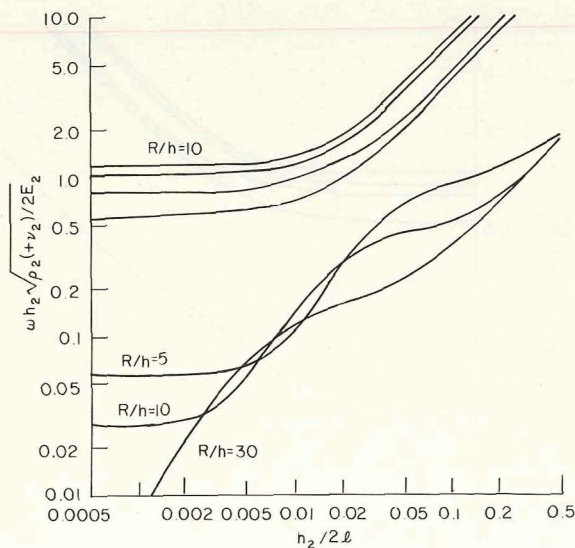


FIGURE 3.170.—Frequency parameters for SD-SD, three-layer shells; $n=2$; $R/h=5, 10, 30$. (After ref. 3.247)

and 3.280, including some results for clamped-clamped shells in reference 3.280.

Modi (refs. 3.129 and 3.281) considered isotropic circular cylindrical shells having *continuous* variation of the material properties through the thickness. Equations of motion were presented which accounted for arbitrary variations of E and ν with z . Particular attention was given to the case of thermal gradients through the thickness. Under this condition assume that the gradient is linear, causing a linear variation of E with z , and that ν is constant. It was found that the frequency parameters in this case do not depend explicitly upon the R/h ratio but, instead, upon the ratio P_5/P_1 , where

$$\left. \begin{aligned} P_1 &= \int_{-h/2}^{h/2} \frac{E}{1-\nu^2} dz \\ P_5 &= \frac{1}{R^2} \int_{-h/2}^{h/2} \frac{E z^2}{1-\nu^2} dz \end{aligned} \right\} \quad (3.237)$$

For the linear variation in E , the ratio P_5/P_1 becomes

$$\frac{P_5}{P_1} = \frac{1}{k^2} \left[1 - \frac{1}{3} \left(\frac{1 - \frac{E_0}{E_i}}{1 + \frac{E_0}{E_i}} \right)^2 \right] \quad (3.238)$$

where E_i and E_0 are the elastic moduli at the inner and outer radii of the shell, respectively, and $k = h^2/12R^2$, as usual. When E is constant, P_5/P_1 becomes $1/k^2$, the usual parameter for homogeneous circular cylindrical shells.

Numerical results were obtained in reference 3.129 for SD-SD shells using the exact displacement functions (eq. (2.20)). In figures 3.171 and 3.172 the variation in the frequency parameter Ω^{*2} with $\lambda = m\pi R/l$ is shown for a shell made of Inconel-X (which determines ν), where

$$\Omega^{*2} = \frac{\omega^2 R^2 \rho h}{P_1} \quad (3.239)$$

(Ω^* is the same as Ω for constant E), for $P_5/P_1 = 0.0258 \times 10^{-6}$. As seen from equation (3.238), there is no unique combination of k^2 or E_0/E_i for a particular value of P_5/P_1 ; however, P_5/P_1 can be obtained with an Inconel-X shell, for example, if $R/h = 1750$ with the outside maintained at room temperature and the inside heated to 1800° F.

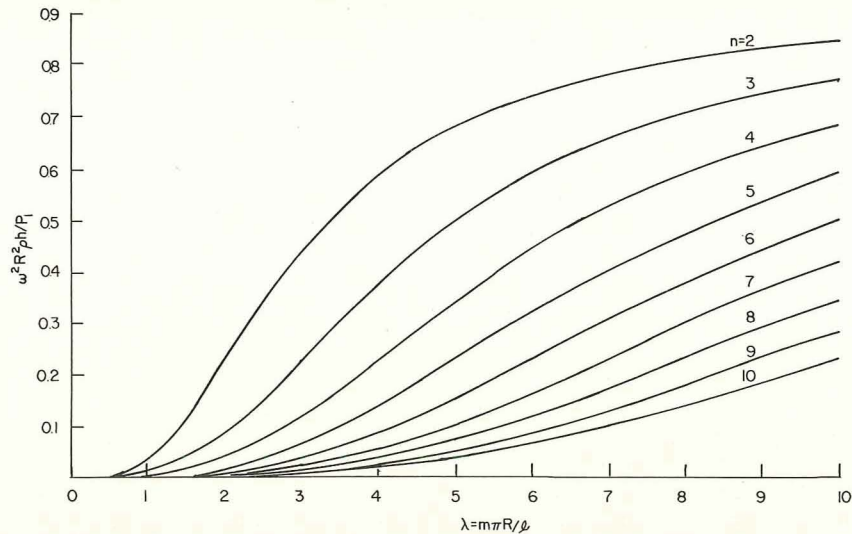


FIGURE 3.171.—Frequency spectrum for *large* values of λ for an SD-SD shell subjected to a radial thermal gradient. (After ref. 3.129)

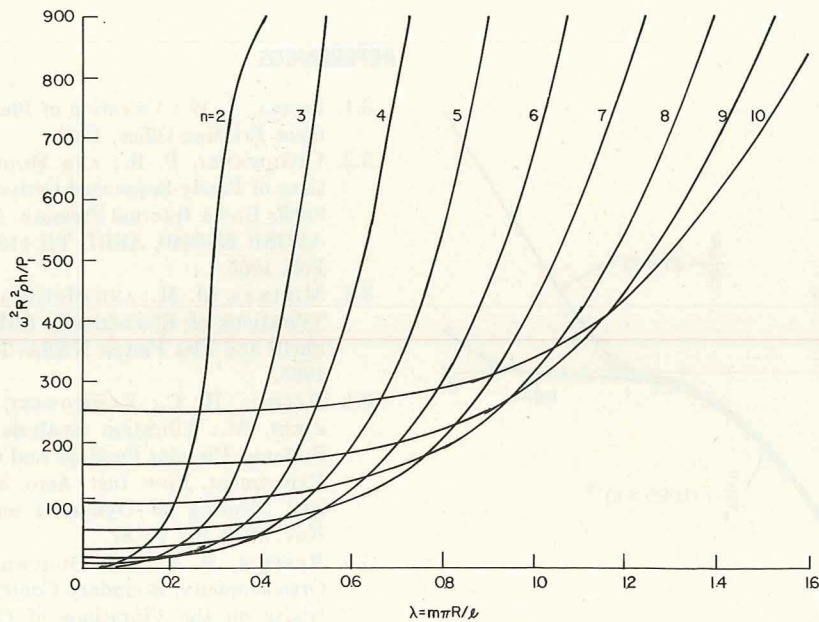


FIGURE 3.172.—Frequency spectrum for *small* values of λ for an SD-SD shell subjected to a radial thermal gradient. (After ref. 3.129)

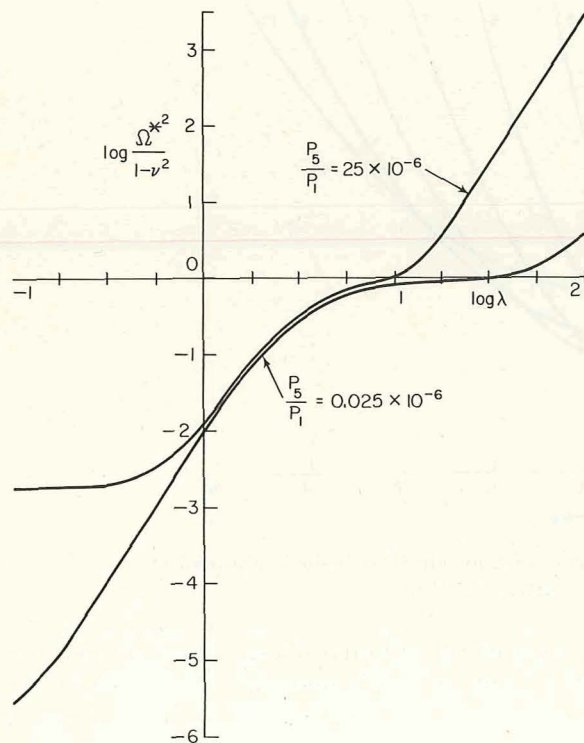
One of the effects of increased temperature is a reduction in the stiffness of the shell and, hence, in its frequencies. Percentage reduction in frequency for the case described above is given in table 3.24. Variation of the frequency parameter $\Omega^2/(1-\nu^2)$ with λ at two extreme values of P_5/P_1 is plotted in figure 3.173 for $n=3$.

The effects of initial stress (prestress) upon the free vibrations of nonhomogeneous shells are considered at least in part in references 3.7, 3.80, 3.129, 3.257, 3.278, 3.282, and 3.283.

Free vibrations of nonhomogeneous circular cylindrical shells are also discussed in references 3.3, 3.276, and 3.284 through 3.302.

TABLE 3.24.—Percentage Reduction in Frequency Due to Thermal Gradient in an SD-SD Shell

λ	n								
	2	3	4	5	6	7	8	9	10
0.0	10.96	20.53	2.61	5.56	8.2	7.99	9.41	8.97	8.90
.2	35.27	47.35	47.44	22.72	11.16	8.04	7.40	7.51	8.83
.4	8.48	14.35	10.11	8.73	9.33	8.23
.5	4.90
.640	9.00
.814	1.36	7.47	.55
1.0	11.20	11.19	4.05	6.57	7.16	7.51
2.0	6.52	8.92	5.27	14.26	5.08	1.87	5.0312
3.0	7.20	6.52	14.27	6.99	5.21	8.96	2.22	.78	.03
4.0	6.83	5.26	4.99	4.39	5.92	7.87	5.07	1.88	1.05
5.0	5.77	5.02	5.82	4.98	6.05	7.63	9.16	6.66	4.76
6.0	5.97	6.83	5.41	6.82	4.97	5.92	8.57	8.74	11.80
7.0	6.81	7.66	6.03	5.90	4.73	6.47	8.23	9.38	18.08
8.0	7.13	7.03	6.82	5.37	5.24	8.50	7.89	10.23	13.15
9.0	7.25	7.32	7.29	4.73	5.38	7.72	8.41	8.78	11.48
10.0	7.69	6.87	7.18	6.49	5.98	6.45	5.73	6.57	6.31

FIGURE 3.173.—Variation of frequency parameter $\Omega^2/(1-\nu^2)$ with λ for extreme values of P_5/P_1 . (After ref. 3.129)

REFERENCES

- 3.1. LEISSA, A. W.: *Vibration of Plates*. U.S. Government Printing Office, 1969.
- 3.2. DIGIOVANNI, P. R.; AND DUGUNDJI, J.: *Vibrations of Freely-Supported Orthotropic Cylindrical Shells Under Internal Pressure*. AFOSR Sci. Rept. AFOSR 65-0640, ASRL TR 112-4 (AD 617 269), Feb. 1965.
- 3.3. MIKULAS, M. M.; AND MCELMAN, J. A.: *On Free Vibrations of Eccentrically Stiffened Cylindrical Shells and Flat Plates*. NASA-TN-D-3010, Sept. 1965.
- 3.4. NELSON, H. C.; ZAPOTOWSKI, B.; AND BERNSTEIN, M.: *Vibration Analysis of Orthogonally Stiffened Circular Fuselage and Comparison With Experiment*. Proc. Inst. Aero. Sci. Natl. Specialists' Meeting on Dynamics and Aeroelasticity, Nov. 1958, pp. 77-87.
- 3.5. RESNICK, B. S.; AND DUGUNDJI, J.: *Effects of Orthotropy, Boundary Conditions, and Eccentricity on the Vibrations of Cylindrical Shells*. AFOSR Sci. Rept. AFOSR 66-2821, ASRL TR 134-2 (AD 648 077), Nov. 1966.
- 3.6. DAS, Y. C.: *Vibrations of Orthotropic Cylindrical Shells*. Appl. Sci. Res. ser. A, vol. 12, no. 4/5, 1964, pp. 317-326.
- 3.7. DONG, S. B.: *Free Vibration of Laminated Orthotropic Cylindrical Shells*. J. Acoust. Soc. Amer., vol. 44, no. 6, Dec. 1968, pp. 1628-1635.
- 3.8. HOPPMANN, W. H., II.: *Some Characteristics of the Flexural Vibrations of Orthogonally Stiffened Cylindrical Shells*. J. Acoust. Soc. Amer., vol. 30, no. 1, Jan. 1958, pp. 77-82.

- 3.9. HOPPMANN, W. H., II.: Flexural Vibrations of Orthogonally Stiffened Cylindrical Shells. 9th Congrès Intern. Mecan. Appl., Univ. Bruxelles, vol. 7, 1957, pp. 225-237.
- 3.10. HU, W. C. L.; AND WAH, T.: Vibrations of Ring-Stiffened Cylindrical Shells—An "Exact" Method. Tech. Rept. No. 7, Contract NASr-94(06). SwRI Project 02-1504, Southwest Res. Inst., Oct. 1966.
- 3.11. WAH, T.; AND HU, W. C. L.: Vibration Analysis of Stiffened Cylinders Including Inter-Ring Motion. J. Acoust. Soc. Amer., vol. 43, no. 5, May 1968, pp. 1005-1016.
- 3.12. GEERS, T. L.: An Approximate Method for Analyzing the Vibrations of Stiffened Plates and Shells. AD 646 353, Nov. 1966.
- 3.13. SEWALL, J. L.; AND NAUMANN, E. C.: An Experimental and Analytical Vibration Study of Thin Cylindrical Shells With and Without Longitudinal Stiffeners. NASA TN D-4705, Sept. 1968.
- 3.14. ADELMAN, H. M.; CATHERINES, D. S.; AND WALTON, W. C., JR.: A Method for Computation of Vibration Modes and Frequencies of Orthotropic Thin Shells of Revolution Having General Meridional Curvature. NASA TN D-4972, Jan. 1969.
- 3.15. PENZES, L. E.: Effect of Boundary Conditions on Flexural Vibrations of Thin Orthogonally Stiffened Cylindrical Shells. J. Acoust. Soc. Amer., vol. 42, no. 4, Oct. 1967, pp. 901-903.
- 3.16. McELMAN, J. A.; MIKULAS, M. M.; AND STEIN, M.: Static and Dynamic Effects of Eccentric Stiffening of Plates and Cylindrical Shells. Presented at the AIAA Annual Meeting and Technical Display (San Francisco, Calif.), July 26-29, 1965.
- 3.17. HU, W. C. L.; GORMLEY, J. F.; AND LINDHOLM, U. S.: An Analytical and Experimental Study of Vibrations of Ring-Stiffened Cylindrical Shells. Tech. Rept. No. 9, Contract NASr-94(06), SwRI Project 02-1504, Southwest Research Institute, June 1967.
- 3.18. SCHNEL, W.; AND HEINRICHSBAUER, F.: The Determination of Free Vibrations of Longitudinally-Stiffened, Thin-Walled, Circular Cylindrical Shells. Inst. of Strength of Materials of the German Aerospace Res. Inst. (DVL) Mülheim-Ruhr. Transl. by NASA, N66-29406, Apr. 1964.
- 3.19. HEINRICHSBAUER, F. J.: Beitrag zum Problem der Eigenschwingungen längsversteifter dünnwandiger Kreiszyllinderschalen von regelmä Bigem Aufbau. Doctoral dissertation, Rheinisch-Westfälischen Technischen Hochschule Aachen, June 1967.
- 3.20. EGGLE, D. M.; AND SEWALL, J. L.: An Analysis of Free Vibration of Orthogonally Stiffened Cylindrical Shells With Stiffeners Treated as Discrete Elements. AIAA Paper No. 67-71, Presented at AIAA 5th Aerospace Sci. Meeting (New York, N.Y.), Jan. 23-26, 1967.
- 3.21. GALLETLY, G. D.: On the In-Vacuo Vibrations of Simply Supported Ring-Stiffened Cylindrical Shells. Proc. U.S. Natl. Congr. Appl. Mech., 2nd (Ann Arbor, Mich.), 1954, pp. 225-231.
- 3.22. MILLER, P. R.: Free Vibrations of a Stiffened Cylindrical Shell. Aero. Res. Coun. (London), Rep. Mem. 3154, 1960.
- 3.23. BLEICH, H. H.: Approximate Determination of the Frequencies of Ring-Stiffened Cylindrical Shells. Contract No. Nonr 266(08), Tech. Rept. No. 14, Office of Naval Res., Columbia Univ., Mar. 1955.
- 3.24. GREENSPON, J. E.: Random Loading and Radiation from Stiffened and Sandwich Type Cylindrical Shell Structures. Part I: Basic Equations and Some Preliminary Results. Contract No. Nonr-2733(00) Tech. Rept. No. 7, J. G. Engineering Research Associates, Sept. 1962.
- 3.25. GREENSPON, J. E.: Effect of External or Internal Static Pressure on the Natural Frequencies of Unstiffened, Cross Stiffened, and Sandwich Cylindrical Shells. Contract No. Nonr-2733(00) (FBM), Proj. No. NR 185-300, Tech. Rept. No. 11, Office of Naval Research, Nov. 1964.
- 3.26. MOVISIAN, L. A.: On Nonstationary Forced Vibrations of Cylindrical Shells. Izv. AN ArmSSR, Ser. Fiz.-Mate. Nauka, vol. 16, no. 2, 1963, N67-18183.
- 3.27. VISARIAN, V.: Dynamic Calculation of Some Component Parts of Motorbus Bodies by Using Orthotropic Shells. Rev. Mecan. Appl., vol. 6, no. 1, 1961, pp. 119-142. (In Russian.)
- 3.28. YAO, J. C.: On the Response of Rocket Vehicle Structure to Certain Environmental Loads. 35th Symposium on Shock and Vibration (New Orleans, La.), Oct. 25-28, 1965.
- 3.29. DIET, W. K.: On the Formulation of Equations of Motion of an Eccentrically Stiffened Shallow Circular Cylindrical Shell. Rept. No. 1620. 1245-47, Syracuse Univ. Res. Inst., Feb. 1966.
- 3.30. PATEL, J. S.; AND NEUBERT, V. H.: Natural Frequencies and Strain Distribution in a Ring-Stiffened Thick Cylindrical Shell. J. Acoust. Soc. Amer., vol. 47, no. 1, pt 2, Jan. 1970, pp. 248-256.
- 3.31. PARTHAN, S.; AND JOHNS, D. J.: Effects of In-Plane and Rotary Inertia on the Frequencies of Eccentrically Stiffened Cylindrical Shells. AIAA J., vol 8, no. 3, Mar. 1970, pp. 592-594.
- 3.32. KAPLAN, I. I.: Beam-Type Oscillations of Cylindrical Shells With Allowance for Contour Deformation. Prikl. Mekh., vol. 4, Nov. 1968, pp. 57-64. (In Russian.)
- 3.33. KISLEVSKAYA, L. M.: On the Calculation of the Frequencies of Vibration of a Shell Reinforced by Stiffening Ribs. Prikl. Mekh., vol. 7, no. 4, 1961, pp. 377-387.
- 3.34. BLEICH, H. H.: Approximate Determination of the Frequencies of Ring-Stiffened Cylindrical Shells. Ost. Ing.- Arch., vol. 15, no. 1-4, 1961, pp. 6-25.
- 3.35. SEWALL, J. L.; CLARY, R. R.; AND LEADBETTER, S. A.: An Experimental and Analytical Vibration Study of a Ring-Stiffened Cylindrical Shell

- Structure With Various Support Conditions. NASA TN D-2398, Aug. 1968.
- 3.36. KOZAROV, M.: Investigations of the Oscillations of Orthotropic Shells. *Godishnik. Inzh.-stroit. in-t. Fak. stroit., arkhitekt., khidrotekhn.*, vol. 10, no. 1, 1958, pp. 69-93.
 - 3.37. SCHNELL, W.; AND HEINRICHSBAUER, F. J.: Zur Bestimmung der Eigenschwingungen längsversteifter, dünnwandiger Kreiszyinderschalen. *WGLR-Jahrbuch*, F. Vieweg and Sohn (Braunschweig), 1963, pp. 278-286.
 - 3.38. WEINGARTEN, V. I.: Free Vibrations of Ring-Stiffened Conical Shells. *AIAA J.*, vol. 3, no. 8, Aug. 1965, pp. 1475-1481.
 - 3.39. RESNICK, B. S.: The Influence of Orthotropicity and Boundary Conditions on the Frequency Response Characteristics of Cylindrical Shells. M.S. Thesis, Dept. of Aeronautics and Astronautics, MIT, Jan. 1966.
 - 3.40. HOPPMANN, W. H., II: Flexural Vibrations of Orthogonally Stiffened Cylindrical Shells. Tech. Rept. No. 11, Contract Nonr-248(12), Dept. Mech. Eng., The John Hopkins Univ., July 1956.
 - 3.41. GONTKEVICH, V. S.: Natural Vibrations of Plates and Shells. A. P. Filipov, Ed., *Nauk Dumka* (Kiev), 1964. (Transl. by Lockheed Missiles and Space Co.)
 - 3.42. TASI, J.: Reflection of Extensional Waves at the End of a Thin Cylindrical Shell. *J. Acoust. Soc. Amer.*, vol. 44, no. 1, July 1968, pp. 291-292.
 - 3.43. LEISSA, A. W.; CLAUSEN, W. E.; HULBERT, L. E.; AND HOPPER, A. T.: A Comparison of Approximate Methods for the Solution of Plate Bending Problems. *AIAA J.*, vol. 7, no. 5, May 1969, pp. 920-928.
 - 3.44. ONIASHVILI, O. D.: Some Dynamical Problems in the Theory of Shells. Moscow, Akad. Nauk SSR, 1957. (In Russian.) (Transl. and published by M. D. Friedmann, Inc.)
 - 3.45. FEDERHOFER, K.: Über die Eigenschwingungen der Kreiszyinderschale mit veränderlicher Wanderstärke. *Öster. Akad. der Wiss., Mat.-Nat. Klasse, Abt. IIa*, 161 Bd., June 1952, pp. 89-105.
 - 3.46. REISSNER, E.: Non-Linear Effect in Vibrations of Cylindrical Shells. Rept. AM 5-6, The Ramo-Wooldridge Corp., Sept. 1955.
 - 3.47. CHU, H. N.: Influence of Large Amplitudes on Flexural Vibrations of a Thin Circular Cylindrical Shell. *J. Aerospace Sci.*, vol. 28, Aug. 1961, pp. 602-609.
 - 3.48. EVENSEN, D. A.: Some Observations on the Nonlinear Vibration of Thin Cylindrical Shells. *AIAA J.*, vol. 1, no. 12, Dec. 1963, pp. 2857-2858.
 - 3.49. NOWINSKI, J. L.: Nonlinear Transverse Vibrations of Orthotropic Cylindrical Shells. *AIAA J.*, vol. 1, no. 3, Mar. 1963, pp. 617-620.
 - 3.50. NOWINSKI, J. L.: Response of a Cylindrical Shell to Transverse Nonlinear Oscillations. TR 9, Dept. Mech. Eng., Univ. Delaware, May 1962.
 - 3.51. CUMMINGS, B. E.: Some Nonlinear Vibration and Response Problems of Cylindrical Panels and Shells. AFOSR 3123, Graduate Aeronautical Labs, CIT, Aeroelasticity and Structural Dynamics SM 62-32, N62-16248, June 1962.
 - 3.52. OLSON, M. D.: Some Experimental Observations on the Nonlinear Vibration of Cylindrical Shells. *AIAA J.*, vol. 3, no. 9, Sept. 1965, pp. 1775-1777.
 - 3.53. EVENSEN, D. A.; AND FULTON, R. E.: Some Studies on the Nonlinear Dynamic Response of Shell-Type Structures. Rept. NASA TMX 56843, NASA Langley Research Center, Oct. 1965.
 - 3.54. LEISSA, A. W.; AND KADI, A. S.: Curvature Effects on Shallow Shell Vibrations. *J. Sound Vib.*, vol. 16, no. 2, May, 1971.
 - 3.55. MAYERS, J.; AND WRENN, B. G.: On the Nonlinear Free Vibrations of Thin Circular Cylindrical Shells. Proc. 10th Midwest Mech. Conf., Aug. 21-23, 1967, pp. 819-846.
 - 3.56. MAYERS, J.; AND WRENN, B. G.: On the Nonlinear Free Vibrations of Thin Circular Cylindrical Shells. SUDAAR No. 269 (AD 654 785), Stanford Dept. of Aero. and Astro., June 1966.
 - 3.57. MUSHTARI, KH. M.; AND GALIMOV, K. Z.: Nonlinear Theory of Thin Elastic Shells. *Tatnigoizdat, Kazan'*, 1957. NASA-TT-F62, 1961.
 - 3.58. MAYERS, J.; AND REHFELD, L.: Further Nonlinear Considerations in the Buckling of Axially Compressed Circular Cylindrical Shells. SUDAFR 197, Dept. Aero. and Astro., Stanford Univ., June 1964. (Also Proc. 9th Midwestern Mech. Conf., Univ. of Wisc., Madison, Wisc., Aug. 1965.)
 - 3.59. EVENSEN, D. A.: Nonlinear Vibrations of an Infinitely Long Cylindrical Shell. *AIAA J.*, vol. 6, no. 7, July 1968, pp. 1401-1403.
 - 3.60. EVENSEN, D. A.: Nonlinear Flexural Vibrations of Thin-Walled Circular Cylinders. NASA TN D-4090, (N67-33446), Aug. 1967.
 - 3.61. DOWELL, E. H.; AND VENTRES, C. S.: Modal Equations for the Nonlinear Flexural Vibrations of a Cylindrical Shell. *Internat. J. Solids Structures*, vol. 4, no. 10, Oct. 1968, pp. 975-991.
 - 3.62. KANA, D. D.; LINDHOLM, U. S.; AND ABRAMSON, H. N.: An Experimental Study of Liquid Instability in a Vibrating Elastic Tank. *J. Spacecraft Rockets*, vol. 3, no. 8, Aug. 1966, pp. 1183-1188.
 - 3.63. KALININ, V. S.: On the Calculation of Nonlinear Vibrations of Flexible Plates and Shallow Shells by the Small Parameter Method. *Theory of Shells and Plates*, 1966, pp. 435-443.
 - 3.64. SHKENEV, YU. S.: Dynamics of Elastic and Elastic-Viscous Shells Filled With an Ideal Liquid. *Theory of Shells and Plates*, N67 20142, 1966, pp. 925-935.
 - 3.65. SUN, C. L.; AND LU, S. Y.: Nonlinear Dynamic Behavior of Heated Conical and Cylindrical Shells. *Nuclear Engineering and Design*, vol. 7, no. 2, Feb. 1968, pp. 113-122.
 - 3.66. CUMMINGS, B. E.: Large Amplitude Vibration and Response of Curved Panels. Res. Paper P-13

- (AD 433 885), Inst. for Defense Analyses, Mar. 1963.
- 3.67. GRIGOLYUK, E. I.: On the Oscillations of Shallow Circular Cylindrical Panels Experiencing Finite Deflections. *Prikl. Mat. Mekh.*, vol. 19, 1955, pp. 376-382.
 - 3.68. GRIGOLYUK, E. I.: Nonlinear Vibrations and Stability of Rising Shells and Rods. *Izv. Otd. Tekh. Nauk, Akad. Nauk USSR*, no. 3, 1955, pp. 33-68. (In Russian.)
 - 3.69. MISHENKOV, G. V.: Forced Nonlinear Oscillations of Elastic Panels. *Akad. Nauk SSSR Izv. Otd. Tekh. Nauk Mekh. i Mash. no. 4*, July-Aug. 1961, pp. 97-103. (English transl.: FTD-MT-63-135 (AD 605 705), Foreign Technology Div., Air Force Systems Command, Wright Patterson AFB, pp. 25-35.)
 - 3.70. VOL'MIR, A. S.; AND KIL'DIBEKOV, I. G.: Nonlinear Acoustic Oscillations of a Cylindrical Shell. AD 640 259, Apr. 1966.
 - 3.71. SANDERS, J. L., JR.: Nonlinear Theories for Thin Shells. *Quart. Appl. Math.*, vol. 21, no. 1, Apr. 1963, pp. 21-36.
 - 3.72. HERRMANN, G.; AND ARMENAKAS, A. E.: Dynamic Behavior of Cylindrical Shells Under Initial Stress. *Proc. 4th U.S. Nat. Congr. Appl. Mech.*, The Univ. of Calif., Berkeley, June 18-21, 1962, pp. 203-213.
 - 3.73. WASHIZU, K.: *Variational Methods in Elasticity and Plasticity*. Pergamon Press, 1968.
 - 3.74. SAMPATH, S. G.: *Vibrations of Circular Cylindrical Shells Under Space-Varying Initial Stresses and Body Forces*. Ph.D. Dissertation, The Ohio State Univ., 1970.
 - 3.75. FLÜGGE, W.: *Stresses in Shells*. Springer-Verlag, 1960.
 - 3.76. TIMOSHENKO, S. P.; AND GERE, J. M.: *Theory of Elastic Stability*. Second ed., McGraw-Hill Book Co., 1961.
 - 3.77. VOSS, H. M.: The Effect of an External Supersonic Flow on the Vibration Characteristics of Thin Cylindrical Shells. *J. Aerospace Sci.*, vol. 28, Dec. 1961, pp. 945-956.
 - 3.78. FUNG, Y. C.; SECHLER, E. E.; AND KAPLAN, A.: On the Vibration of Thin Cylindrical Shells Under Internal Pressure. *J. Aeronaut. Sci.*, vol. 24, no. 9, Sept. 1957, pp. 650-661.
 - 3.79. FUNG, Y. C.: On the Vibration of Thin Cylindrical Shells Under Internal Pressure. Rept. AM 5-8 (AD 605 578), Guided Missile Res. Div., The Ramo-Wooldridge Corp., Oct. 14, 1955.
 - 3.80. MUGNIER, D.; AND SCHROETER, D.: Vibrations of a Homogeneous Circular Cylindrical Tank, Empty or Filled With Liquid, About a Preestablished Static Stress State—Case of the Inhomogeneous Cylinder—Comparison With Experiment. *Journal de Me'canique*, vol. 6, Sept. 1957, pp. 417-441. (In French.)
 - 3.81. REISSNER, E.: Stresses and Deformations of Thin, Pressurized Cylindrical Shells. Rept. AM 5-3, The Ramo-Wooldridge Corp., 1955.
 - 3.82. BOZICH, W. F.: The Vibration and Buckling Characteristics of Cylindrical Shells Under Axial Load and External Pressure. AFFDL-TR-67-28, May 1967.
 - 3.83. NIKULIN, M. V.: The Influence Exerted by Axial Forces on the Frequencies of Natural Oscillations of a Cylindrical Shell. *Strength of Cylindrical Shells*, Moskva, Oborongiz, 1959, pp. 131-145. (In Russian.)
 - 3.84. NIKULIN, M. V.: Natural Oscillations of Smooth and Structurally Anisotropic Cylindrical Shells in the Presence of Static Loads. *Strength and Dynamics of Aircraft Engines*. Moscow, Izdatel'stvo Mashinostroenie, 1965, pp. 52-128. (In Russian.)
 - 3.85. ARMENAKAS, A. E.: Influence of Initial Stress on the Vibrations of Simply Supported Circular Cylindrical Shells. *AIAA J.*, vol. 2, no. 9, Sept. 1964, pp. 1607-1612.
 - 3.86. HERRMANN, G.; AND SHAW, J.: Vibration of Thin Shells Under Initial Stress. *J. Eng. Mech. Div., Proc. ASCE*, vol. 91, EM 5, Oct. 1965, pp. 37-59.
 - 3.87. IVANYUTA, E. I.; AND FINKEL'SHLEYN: Determination of the Frequency of the Free Oscillations of Cylindrical Shells. *Issled. po uprugosti i plastichnosti*, no. 2, Leningrad, Leningr. Un-t, 1963, pp. 81-89. (In Russian.)
 - 3.88. MISERENTINO, R.; AND VOSTEEN, L. F.: Vibration Tests of Pressurized Thin-Walled Cylindrical Shells. NASA TN D 3066, Oct. 1965.
 - 3.89. BROGAN, W. L.: Radial Vibrations of a Thin Cylindrical Shell. *J. Acoust. Soc. Amer.*, vol. 33, no. 12, Dec. 1961, pp. 1778-1781.
 - 3.90. FEDERHOFER, K.: Über die Eigenschwingungen der Axial Gedruckten Kreiszylinderhale. *Sitzungsber. Akad. Wiss. Wien*, vol. 145, 1936, pp. 681-688.
 - 3.91. COUPRY, G.: On the Breathing (Flexural) Vibrations of Thin Shells, Application to Solid Rockets. Publication No. 110, Office National d'Etudes et de Recherches Aéropatiales, 1964. (In French.)
 - 3.92. NACHBAR, W.: Characteristic Roots for Donnell's Equations With Uniform Axial Prestress. *J. Appl. Mech.*, vol. 29, 1961, pp. 434-435.
 - 3.93. POPLAWSKI, B.: Elastic Vibrations of a Cylindrical Shell Filled With Liquid. Rept. 66-16 (ASTIA No. AD 635 777), Aerospace Technical Div., Library of Congress, Feb. 1966, p. 8.
 - 3.94. BLEICH, H. H.; AND BARON, M. L.: Free and Forced Vibrations of an Infinitely Long Cylindrical Shell in an Infinite Acoustic Medium. *J. Appl. Mech.*, vol. 21, no. 2, June 1954, pp. 167-177.
 - 3.95. ARMENAKAS, A. E.; AND HERRMANN, G.: Vibrations of Infinitely Long Cylindrical Shells Under Initial Stress. *AIAA J.*, vol. 1, no. 1, Jan. 1963, pp. 100-106.
 - 3.96. KOVAL, L. R.: On the Free Vibration of Thin Clamped Cylindrical Shells Subject to Radial Pressure. *J. Aerospace Sci.*, vol. 29, no. 5, May 1962, pp. 615-616.

- 3.97. BRYAN, G. H.: On a Revolving Cylinder or Bell. *Proc. Roy. Soc. London*, vol. 47, 1890, pp. 101-111.
- 3.98. KUKUDZHANOV, S. N.: Effect of Normal Pressure on the Natural Oscillation Frequencies of Cylindrical Shells. *Inzhenernyi Zhurnal—Mekhanika Tverdogo Tela*, May-June 1968, pp. 140-144. (In Russian.)
- 3.99. LYONS, W. C.; RUSSELL, J. E.; AND HERRMANN, G.: Dynamics of Submerged Reinforced Cylindrical Shells. *J. Engng. Mech. Div., Proc. Amer. Soc. Civil Engrs.*, vol. 94, EM2, Apr. 1968, pp. 397-420.
- 3.100. AGENOSOV, L. G.; AND SACHENKOV, A. V.: Stability and Free Oscillations of Thin Cylindrical and Conical Shells of a Circular Cross-Section With Various Boundary Conditions. Investigations on the Theory of Plates and Shells. *Sbornik II. Kazan', Izd-vo Kazan' Univ.*, 1964, pp. 111-126.
- 3.101. AGAMIROV, V. L.; AND VOL'MIR, A. S.: Behavior of Cylindrical Shells Under Dynamic Loading of All-Sided Pressure or Axial Compression. *Izv. Akad. Nauk SSSR, Otd. Tekh. Nauk* no. 3, May-June 1959, pp. 78-83. (In Russian.)
- 3.102. REISSNER, E.: Notes on Vibrations of Thin, Pressurized Cylindrical Shells. Rept. AM 5-4, The Ramo-Wooldridge Corp., Nov. 1955.
- 3.103. VLASOV, V. Z.: *Obshchaya teoriya obolochek i yeye prilozheniya v tekhnike*. Gos. Izd. Tekh.-Teor. Lit., Moscow-Leningrad, 1949. English transl.: NASA TT F-99, General Theory of Shells and Its Applications in Engineering. Apr. 1964.
- 3.104. SERBIN, H.: Breathing Vibrations of a Pressurized Cylindrical Shell. Rept. No. A-Atlas-152, Convair, Jan. 1955.
- 3.105. FUNG, Y. C.; KAPLAN, A.; AND SECHLER, E. E.: Experiments on the Vibration of Thin Cylindrical Shells Under Internal Pressure. Rept. AM 5-9 (AD 607 517), Guided Missile Res. Div., The Ramo-Wooldridge Corp., Dec. 15, 1955.
- 3.106. GOTTENBERG, W. G.: Experimental Study of the Vibrations of a Circular Cylindrical Shell. *J. Acoust. Soc. Amer.*, vol. 32, no. 8, Aug. 1960, pp. 1002-1006.
- 3.107. BERRY, J. G.; AND REISSNER, E.: The Effect of an Internal Compressible Fluid Column on the Breathing Vibrations of a Thin Pressurized Cylindrical Shell. *J. Aero. Sci.*, vol. 25, no. 5, May 1958, pp. 288-294.
- 3.108. CORTIS, M. G.: Green's-Function Technique in the Dynamics of a Finite Cylindrical Shell. *J. Acoust. Soc. Amer.*, vol. 37, no. 1, Jan. 1965, pp. 31-42.
- 3.109. LIPOVSKII, D. E.; AND TOKARENKO, V. M.: Effect of Initial Imperfections on Free Oscillation Frequencies of Cylindrical Shells. All-Union Conference on the Theory of Shells and Plates, 6th Baku, Azerbaidzhan SSR, Sept. 15-20, 1966, Transactions. Moscow, Izdatel'stvo Nauka, 1966, pp. 542-547. (In Russian.)
- 3.110. LIVANOV, K. K.: Vibrations of a Gas-Filled Cylindrical Shell. *Inzh. Zh. (USSR)*, vol. 5, no. 5, 1965, pp. 996-999. (Transl. by Lockheed Missiles and Space Co.)
- 3.111. OLSON, M. D.; AND FUNG, Y. C.: Comparing Theory and Experiment for the Supersonic Flutter of Circular Cylindrical Shells. *AIAA J.*, vol. 5, no. 10, Oct. 1967, pp. 1849-1856.
- 3.112. RAKHIMOV, I. S.: Effect of Axial Forces and Normal Pressure on Free Oscillations of Cylindrical Shells. Air Force FTD-TT-65-1035 (AD 640 475), Apr. 1966.
- 3.113. SALEME, E.; AND LIBER, T.: Breathing Vibrations of Pressurized Partially Filled Tanks. *AIAA J.*, vol. 3, no. 1, Jan. 1965, pp. 132-136.
- 3.114. MIXSON, J. S.: An Investigation of the Vibration Characteristics of Pressurized Thin-Walled Circular Cylinders Partially Filled With Liquid. Thesis, Univ. of Virginia, Mar. 1962.
- 3.115. MIXSON, J. S.; AND HERR, R. W.: An Investigation of the Vibration Characteristics of Pressurized Thin-Walled Circular Cylinders Partly Filled With Liquid. NASA TR R-145, 1962.
- 3.116. SEGGELE, P.: Vibration Behaviour of Axial-Symmetrically Loaded Thin-Walled Circular Cylinders Under Different Boundary Conditions. Rept. 64-43, Deutsche Luft-und Raumfahrt, 1964.
- 3.117. KOVAL, L. R.: A Simplified Frequency Equation for a Clamped Cylindrical Shell and Its Application to Initially Stressed Cylinders. Rept. No. EM 12-9, Space Technology Laboratories, Feb. 1962.
- 3.118. PROKÓPEV, V. I.: Free Axisymmetric Oscillations of Reinforced Cylindrical Shells. Strength and Dynamics of Aircraft Engines, Moscow, Izdatel'stvo Mashinostroenie, 1966, pp. 77-87. (In Russian.)
- 3.119. DYM, C. L.: Vibrations of Pressurized Orthotropic Cylindrical Membranes. *AIAA J.*, vol. 8, no. 4, Apr. 1970, pp. 693-699.
- 3.120. STERN, M.: Breathing Vibrations of a Cylindrical Membrane Under Internal Pressure. Convair Memo. DC-7-057, Convair, 1954.
- 3.121. GREENSPON, J. E.: Vibrations of Thick and Thin Cylindrical Shells Surrounded by Water. *J. Acoust. Soc. Amer.*, vol. 33, no. 10, Oct. 1961, pp. 1321-1328.
- 3.122. COOPER, P. A.: Vibration and Buckling of Prestressed Shells of Revolution. NASA TN D-3831, Mar. 1967.
- 3.123. BRESLAVSKII, V. E.: Natural Vibrations of a Circular Cylindrical Shell Under the Effect of Hydrostatic Pressure. *IAN SSSR, OTN*, no. 12, 1953. (In Russian.)
- 3.124. SZECHENYI, E.: Approximate Methods for the Determination of the Natural Frequencies of Stiffened and Curved Plates. Proc., Conf. on Current Developments in Sonic Fatigue, Southampton Univ., July 1970.
- 3.125. SZECHENYI, E.: An Approximate Solution for the

- Natural Frequencies of Cylindrically Curved Rectangular Shells With In-Plane Loads. Tech. Rept. 29, Inst. for Sound and Vib. Research, Southampton, Apr. 1970.
- 3.126. DEB NATH, J. M.; AND PETYT, M.: Application of the Method of Kantorovich to the Solution of Problems of Free Vibration of Singly Curved Rectangular Plates Including the Presence of Membrane Stresses. Tech. Rept. 19, Inst. for Sound and Vib. Research, Southampton, June 1969.
 - 3.127. DEB NATH, J. M.; AND PETYT, M.: Free Vibration of Doubly Curved Rectangular Plates Including the Presence of Membrane Stresses With Special Reference to the Finite Element Technique. Tech. Rept. 22, Inst. for Sound and Vib. Research, Southampton, July 1969.
 - 3.128. ÖRY, H.; HORNUNG, E.; AND FAHLBUSCH, G.: A Simplified Matrix Method for the Dynamic Examination of Different Shells of Revolution. AIAA Symposium on Structural Dynamics and Aeroelasticity (Boston, Mass.), Aug. 30–Sept. 1, 1965. Tech. Papers A65–35608 23–32, pp. 365–388.
 - 3.129. MODR, V. J.: Vibration of a Cylinder With Temperature Gradient Across the Thickness. Canadian Aeronautics and Space J., vol. 11, no. 7, Sept. 1965, pp. 227–233.
 - 3.130. WATTS, G. A.: Vibration and Damping of Thin-Walled Cylinders. Thesis, Calif. Inst. of Tech., 1962.
 - 3.131. KOVAL, L. R.: On the Free Vibrations of a Thin-Walled Circular Cylindrical Shell Subjected to an Initial Torque. Ph.D. Thesis, Cornell Univ., Sept. 1961.
 - 3.132. KOVAL, L. R.; AND CRANCH, E. T.: On the Free Vibrations of Thin Cylindrical Shells Subjected to an Initial Static Torque. Proc. 4th U.S. Nat. Congr. Appl. Mech., The Univ. of Calif., Berkeley, June 18–21, 1962, vol. 1, pp. 107–117.
 - 3.133. KUKUDZHANOV, S. N.: Vibrations of Long Cylindrical Shell Under the Effect of Torques. Trans. 6th All-Union Conf. on the Theory of Shells and Plates (Baku), Sept. 15–20, 1966, pp. 522–527.
 - 3.134. PROKOP'EV, V. I.: Relation Between Natural-Oscillation Frequencies and the Eigenvalues of the Stability Equations for Cylindrical Shells. Trans. 6th All-Union Conference on the Theory of Shells and Plates, (Baku, Azerbaidzhan SSR), Sept. 15–20, 1966, Transactions. pp. 636–640. (In Russian.)
 - 3.135. WEINGARTEN, V. I.: Free Vibrations of a Thin-Walled Cylindrical Shell Subjected to a Bending Moment. AIAA J., vol. 3, no. 1, Jan. 1965, pp. 40–44.
 - 3.136. SEGELKE, P.: The Oscillating Behavior of Transversely Loaded Circular Shells. Deutsche Forschungsanstalt für-und Raumfahrt. Burnswick (W. Germany) Inst. für Flugzeugbau. (DFL–231) DFL: DM 11.50, Dec. 1963. (In German.)
 - 3.137. KESSEL, P. G.; AND SCHLACK, A. L., JR.: Vibrations of Circular Cylindrical Shells Due to Gyroscopically Induced Inertia Loads. J. Acoust. Soc. Amer., vol. 45, no. 1, 1969, pp. 138–143.
 - 3.138. BUSHNELL, D.: Axisymmetric Dynamic Response of a Ring-Supported Cylinder to Time-Dependent Loads. J. Spacecraft and Rockets, vol. 3, no. 9, Sept. 1966, pp. 1369–1376.
 - 3.139. BUCKENS, F.: Dynamic Behavior of Shells Under Thermal Stress. AD 634 109, Dept. Appl. Mech., Univ. of Louvain, Belgium, 1965.
 - 3.140. ONG, C. C.; AND HERRMANN, G.: Vibrations of Thin Cylindrical Shells With Initial Stresses Due to Thermal Loadings. Paper 69–59, AIAA, Aerospace Sci. Meeting, 7th (New York, N.Y.), Jan. 20–22, 1969.
 - 3.141. ONG, C. C.; AND HERRMANN, G.: Vibrations of Thin Cylindrical Shells Under Axisymmetric Thermal Stresses. AIAA J., vol. 7, no. 1, Jan. 1969, pp. 27–34.
 - 3.142. NOWACKI, W.: Buckling and Free Vibrations of a Cylindrical Shell. Arch. Mech. Stos., vol. 7, no. 1, 1955, pp. 111–131. (In Polish).
 - 3.143. MAZURKIEWICZ, Z.; AND SUWALSKI, L.: Bending, Vibrations and Buckling of Shallow Cylindrical Shell With Variable Boundary Conditions. Bull. Acad. Polonaise Sci., Ser. Sci. Tech. (Polska Akad. Nauk), Warsaw 11, vol. 4, 1963, pp. 171–182.
 - 3.144. RAYLEIGH, LORD: On the Vibrations of a Cylindrical Vessel Containing Liquid. Philos. Mag., vol. 15, 1883, pp. 385–389.
 - 3.145. NIKOLAI, E. L.: On the Vibrations of a Thin-Walled Cylinder. Zhurnal Russkogo Fiziko-Khimicheskogo Obshchestva, vol. 11, sec. 1, 1909.
 - 3.146. GONTKEVICH, V. S.: Natural Vibrations of Shells in a Fluid. (English transl.: FTD-HT-23-1003-67, Foreign Tech. Div., Wright-Patterson AFB, Jan. 1968.)
 - 3.147. BUTLER, D. J.: Vibrations of an Infinitely Long Cylindrical Shell in a Semi-Infinite Acoustic Medium. J. Ship Research, vol. 3, no. 3, Dec. 1959, pp. 41–49.
 - 3.148. BUTLER, D. J.: Vibrations of an Infinitely Long Cylindrical Shell in a Semi-Infinite Acoustic Medium. Columbia Univ. Dissertation, May 1958. (Also Contract No. Nonr 266(08), Tech. Rept. No. 21, Office of Naval Research, Columbia Univ., May 1958.)
 - 3.149. JUNGER, M. C.: Vibrations of Elastic Shells in a Fluid Medium and the Associated Radiation of Sound. J. Appl. Mech., vol. 19, no. 4, Dec. 1952, pp. 439–445.
 - 3.150. JUNGER, M. C.: Radial Loading of Cylindrical and Spherical Surfaces, J. Acoust. Soc. Amer., vol. 24, no. 3, May 1952, pp. 288–289.
 - 3.151. JUNGER, M. C.: Sound Scattering by Thin Elastic Shells. J. Acoust. Soc. Amer., vol. 24, no. 4, July 1952, pp. 366–373.
 - 3.152. JUNGER, M. C.: The Physical Interpretation of the Expression for an Outgoing Wave in Cylindrical Coordinates. J. Acoust. Soc. Amer., vol. 25, no. 1, Jan. 1953, pp. 40–47.

- 3.153. JUNGER, M. C.: Dynamic Behavior of Reinforced Cylindrical Shells in a Vacuum and in a Fluid. *J. Appl. Mech.*, vol. 21, no. 1, 1954, p. 35.
- 3.154. GREENSPON, J. E.: Vibrations of Thick and Thin Cylindrical Shells Surrounded by Water. Proj. No. NR 385-412, Contract No. Nonr-2733(00), Tech. Rept. No. 4, Office of Naval Research, Sept. 1960.
- 3.155. GREENSPON, J. E.: Theoretical Calculations for Radiation From Lobar Modes of Cylindrical Shells Under Point Loading. Contract No. Nonr-2733(00), TR-9 (AD 601 182), Feb. 1964.
- 3.156. HAHNE, H. V.: Oscillations of a Gas in an Elastic Cylindrical Shell. *Proc. Third U.S. Natl. Congr. Appl. Mech.*, June 1958, pp. 753-760.
- 3.157. HUGHES, W. G.: Flexure of Thin-Walled Circular Cylindrical Shells. Tech. Note No. GW 525, JSRP Control No. 591377 (ASTIA AD 229 542), Roy. Aircraft Establishment (Great Britain), Sept. 1959.
- 3.158. KOLOLIKHINA, Z. V.: On the Vibration of a Cylindrical Shell in Water and the Complex Acoustical Spectrum of its Radiation. *Soviet Phys.-Acoustics*, vol. 4, no. 4, May 1959, pp. 344-351.
- 3.159. McCORMICK, J. M.; AND BARON, M. L.: Sound Radiation From Submerged Cylindrical Shells of Finite Length. Proj. NR 064-464, Contract No. Nonr-3454(00) FBM, Tech. Rept. No. 3 (AD 603 531), Office of Naval Research, June 1964.
- 3.160. MINDLIN, R. D.; AND BLEICH, H. H.: Response of an Elastic Cylindrical Shell to a Transverse, Step Shock Wave. *J. Appl. Mech.*, vol. 20, no. 2, June 1953, pp. 189-195.
- 3.161. FOXWELL, J. H.; AND FRANKLIN, R. E.: The Vibrations of a Thin-Walled Stiffened Cylinder in an Acoustic Field. *Aeronaut. Quart.*, vol. 10, 1959, p. 47.
- 3.162. WARBURTON, W. B.: Vibration of a Cylindrical Shell in an Acoustic Medium. *J. Mech. Engng. Sci.*, vol. 3, no. 1, Mar. 1961, pp. 69-79.
- 3.163. MNEV, E. N.: Small Vibrations of a Circular Cylindrical Shell Immersed in a Limited Space Filled With a Compressible Liquid. *Prikl. Mekh.*, URSSR, vol. 9, no. 2, 1963, pp. 133-142. (In Ukrainian.)
- 3.164. MNEV, YE. N.: Vibrations of a Circular Cylindrical Shell Submerged in a Closed Cavity Filled With an Ideal Compressible Liquid. Second All-Union Conf. on the Theory of Plates and Shells, Lvov, Sept. 15-21, 1961, Kiev, Izd-vo AN USSR, 1962, pp. 284-288.
- 3.165. ABRAMSON, H. N.: The Dynamic Behavior of Liquids in Moving Containers. U.S. Government Printing Office, NASA SP-106, 1966.
- 3.166. ABRAMSON, H. N.; AND KANA, D. D.: Some Recent Research on the Vibrations of Elastic Shells Containing Liquids. Symposium on Shell Theory, Univ. of Houston, April 4-6, 1966.
- 3.167. BARON, M. L.; AND BLEICH, H. H.: The Dynamic Analysis of Empty and Partially Full Cylindrical Tanks. Part I—Frequencies and Modes of Free Vibration and Transient Response by Mode Analysis. DASA No. 1123A, Defense Atomic Support Agency, May 1959.
- 3.168. BARON, M. L.; AND SKALAK, R.: Free Vibrations of Fluid-Filled Cylindrical Shells. *J. Engng. Mech. Div., Proc. Amer. Soc. Civil Engrs.*, EM 3, vol. 88, June 1962, pp. 17-43.
- 3.169. BEAL, T. R.; COALE, C. W.; AND NAGANO, M.: Influence of Shell Inertia and Bending Stiffness on the Axisymmetric Modes of a Partially-Filled Cylindrical Tank. Paper 65-412, AIAA 2nd Annual Meeting (San Francisco, Calif.), July 26-29, 1965.
- 3.170. CHU, W. H.; AND GONZALES, R.: Supplement to Breathing Vibrations of a Partially Filled Cylindrical Tank—Linear Theory. *Trans. ASME, J. Appl. Mech.*, Dec. 1964, pp. 722-723.
- 3.171. LINDHOLM, U. S.; KANA, D. D.; AND ABRAMSON, H. N.: Breathing Vibrations of a Circular Cylindrical Shell With an Internal Liquid. *J. Aerospace Sci.*, vol. 29, Sept. 1962, pp. 1052-1059.
- 3.172. LINDHOLM, U. S.; CHU, W. H.; KANA, D. D.; AND ABRAMSON, H. N.: Bending Vibrations of a Circular Cylindrical Shell With an Internal Liquid Having a Free Surface. *AIAA J.*, vol. 1, no. 9, Sept. 1963, pp. 2092-2099.
- 3.173. MILES, J. W.: On Sloshing of Liquid in a Flexible Tank. *J. Appl. Mech.*, vol. 25, no. 2, June 1958, pp. 277-283.
- 3.174. NATUSHKIN, V. F.; AND RAKHIMOV, I. S.: Vibrations of a Cylindrical Shell Partially Filled by Fluid. *News of Schools of Higher Education—Aeronautical Engineering* (AD 644 068), Sept. 1966, pp. 81-86.
- 3.175. RABINOVICH, B. I.: Equations of Transverse Vibrations of Fluid-Filled Shells. NASA TT F-216, July 1964.
- 3.176. CHU, W. H.: Breathing Vibrations of a Partially Filled Cylindrical Tank—Linear Theory. *J. Appl. Mech.*, vol. 30, no. 4, Dec. 1963, pp. 532-536.
- 3.177. SHMAKOV, V. P.: Equations of Axially Symmetric Vibrations of Liquid-Filled Cylindrical Shell. NASA TT F-219, July 1964.
- 3.178. LEROY, J.: On Breathing Vibrations of Thin Cylinders Partially Full of Liquid. *Comptes Rendus*, vol. 257, no. 18, Oct. 1963, pp. 2607-2609. (In French.)
- 3.179. BARON, M. L.; AND BLEICH, H. H.: The Dynamic Analysis of Empty and Partially Full Cylindrical Tanks. Part II—Analysis of Uplift and Structural Damage. DASA No. 1123B, Defense Atomic Support Agency, Sept. 1959.
- 3.180. BLEICH, H. H.: Longitudinal Forced Vibrations of Cylindrical Fuel Tanks. *Jet Propulsion*, vol. 26, no. 2, Feb. 1956, pp. 109-111.
- 3.181. PALMER, J. H.; AND ASHER, G. W.: Calculation of Axisymmetric Longitudinal Modes for Fluid-Elastic Tank-Ullage Gas System and Comparison With Model Test Results. *Proc. AIAA Symposium*

- Structural Dynamics and Aeroelasticity (Boston), 1965, pp. 189-193.
- 3.182. FONTENOT, L. L.; AND LIANIS, G.: The Free Vibrations of Thin Elastic Pressurized Cylindrical Shells Filled With a Perfect and Incompressible Liquid Having a Free Surface. International Symposium on Space Technology and Science (Tokyo, Japan), Sept. 1963.
 - 3.183. KANA, D. D.: Longitudinal Forced Vibrations of Partially Filled Tanks. Tech. Rept. No. 6, Contract No. NASw-146, Southwest Research Institute, Feb. 1963.
 - 3.184. CHU, W. H.; AND KANA, D. D.: A Theory for Nonlinear Transverse Vibrations of a Partially Filled Elastic Tank. Final Rept. Part I, Project 02-1748, Southwest Research Institute, Mar. 1966.
 - 3.185. BHUTA, P. G.; AND KOVAL, L. R.: Coupled Oscillations of a Liquid With a Free Surface in a Tank Having a Flexible Bottom. *J. Appl. Math. and Phys.*, vol. 15, no. 5, 1964.
 - 3.186. BHUTA, P. G.; AND KOVAL, L. R.: Hydroelastic Solution of the Sloshing of a Liquid in a Cylindrical Tank. *J. Acoust. Soc. Amer.*, vol. 36, no. 11, Nov. 1964, pp. 2071-2079.
 - 3.187. RAPOPORT, I. M.: Vibrations of an Elastic Shell Partially Filled With a Liquid. Moscow, Mashinostroyeniye, 1967.
 - 3.188. ABRAMSON, H. N.; CHU, W. H.; KANA, D. D.; AND LINDHOLM, U. S.: Bending Vibrations of a Circular Cylindrical Shell Containing an Internal Liquid With a Free Surface. Tech. Rept. No. 4, Contract No. NASw-146, SwRI Proj. No. 4-961-2, Southwest Research Institute, Mar. 31, 1962.
 - 3.189. ABRAMSON, H. N.; KANA, D. D.; AND LINDHOLM, U. S.: Breathing Vibrations of a Circular Cylindrical Shell Containing an Internal Liquid. Tech. Rept. No. 3, Contract NASw-146, SwRI Proj. No. 4-961-2, Southwest Research Institute, Feb. 1962.
 - 3.190. ABRAMSON, H. N.; KANA, D. D.; AND LINDHOLM, U. S.: An Experimental Study of Liquid Instability in a Vibrating Elastic Tank. AIAA Symposium on Structural Dynamics and Aeroelasticity (Boston, Mass.), Aug. 30-Sept. 1, 1965.
 - 3.191. KANA, D. D.: Parametric Coupling in a Nonlinear Electromechanical System. *J. Engng. Industry*, vol. 89, no. 4, Nov. 1967, pp. 839-847.
 - 3.192. REISSNER, E.: Notes on the Forced and Free Vibrations of Pressurized Cylindrical Shells Which Contain a Heavy Liquid With a Free Surface. AM No. 6-15, GMTR 87, Space Technology Lab., Inc., Nov. 1956.
 - 3.193. ANISIMOV, A. M.: Axisymmetrical Oscillations of a Fluid in a Cylindrical Shell. *Prochnost i Ustoichivost Elementov Tonkostennykh Konstruktsii Sbornik State No. 2*, Mashinostroyeniye, 1967, pp. 210-220. (In Russian.)
 - 3.194. BAGDASARIAN, G. E.; AND GNUNI, V. Ts.: Vibrations of a Cylindrical Shell Filled With a Liquid of Varying Depth. *Doklady Akademii Nauk Armianskoi SSR*, vol. 41, no. 4, 1965, pp. 199-203. (In Russian.)
 - 3.195. BEAM, R. M.; AND GUIST, L. R.: The Axially Symmetric Response of an Elastic Cylindrical Shell Partially Filled With Liquid. NASA TN-D-3877 (N67-18411), Feb. 1967.
 - 3.196. BRESLAVSKI, V. E.: Vibrations of Cylindrical Shells Filled With Liquid. *Izdatel'stvo Akademii Nauk Armianskoi SSR*, 1964, pp. 255-261. (In Russian.)
 - 3.197. COALE, C. W.; AND NAGANO, M.: Axisymmetric Modes of an Elastic Cylindrical-Hemispherical Tank Partially Filled With a Liquid. *Proc. of the AIAA Symposium on Structural Dynamics and Aeroelasticity* (Boston, Mass.), Aug. 1965, pp. 169-176.
 - 3.198. COALE, C. W.: Axisymmetric Vibrations of a Cylindrical-Hemispherical Tank Partially Filled With a Liquid. AIAA Paper No. 67-75, AIAA 5th Aerospace Sci. Meeting (New York, N.Y.), Jan. 23-26, 1967.
 - 3.199. GLASER, R. F.: Axisymmetric Vibrations of Partially Liquid-Filled Cylindrical Containers. NASA TN-D-4026 (N67-30124), July 1967.
 - 3.200. GOREE, J. G.; KAO, G. C.; LEE, T. N.; AND PEARSON, C. M.: Vibration of a Circular Cylindrical Elastic Tank, Partially Filled With an Incompressible Fluid, Undergoing an Axial Acceleration Composed of a Uniform and a Periodic Component. Tech. Memo. No. 102, Research and Analysis Sec., Northrop Space Lab., Sept. 1965.
 - 3.201. KANA, D. D.; AND CRAIG, R. R., JR.: Parametric Oscillations of a Longitudinally Excited Cylindrical Shell Containing Liquid. *J. Spacecraft*, vol. 5, no. 1, Jan. 1968, pp. 13-21.
 - 3.202. KANA, D. D.; GLASER, R. F.; EULITZ, W. R.; AND ABRAMSON, H. N.: Longitudinal Vibration of Spring-Supported Cylindrical Membrane Containing Liquid. *J. Spacecraft*, vol. 5, no. 2, Feb. 1968, pp. 189-196.
 - 3.203. KANA, D. D.; AND ABRAMSON, H. N.: Longitudinal Vibration of Ring Stiffened Cylindrical Shells Containing Liquids. N66-35018, CR 77396, Southwest Research Institute, June 1966.
 - 3.204. KANA, D. D.: Longitudinal Dynamics of Liquid Filled Elastic Shells. SwRI Proj. No. 02-1391, NASA CR-79725, Southwest Research Institute, Sept. 1966.
 - 3.205. KIL'CHEVSKYY, M. O.; PETRENKO, M. P.; BABICH, D. V.; AND BARSUK, R. P.: Approximate Calculation of Longitudinal-Radial Vibrations of a System of Cylindrical Shells, Partially Filled With Fluid. (English transl.: *Appl. Mech.* (selected articles), FTD-TT-65-975/1+2, Foreign Technology Div., Air Force Systems Command, Wright-Patterson AFB.)
 - 3.206. LEROY, J.: The Breathing-Vibrations of a Thin Cylinder Partially Filled With a Liquid. Office

- National d'Etudes et de Recherches Aerospatiales, Publ. No. 113, 1965. (In French.)
- 3.207. POZHALOSTIN, A. A.: Determination of the Parameters of a Mechanical Analog for Axisymmetric Vibrations of an Elastic Cylindrical Vessel With Fluid. *Mekh. Tverdogo Tela*, no. 5, 1966, pp. 157-159. AD 644 174. (Transl. by Lockheed Missile and Space Co.)
 - 3.208. REISSNER, E.: Complementary Energy Procedure for Vibrations of Liquid-Filled Circular Cylindrical Tanks. Rept. EM 7-9, The Ramo-Woolbridge Corp., June 1957.
 - 3.209. SHKLYARCHUK, F. N.: Axisymmetric Oscillations of a Fluid Inside an Elastic Cylindrical Shell With an Elastic Bottom. *Izv. Vush. Uch. Zav., Ser. Aviats. Tech.*, no. 4, 1965.
 - 3.210. SHKLYARCHUK, F. N.: Approximate Method of Solution of Axisymmetric Vibrations of Shells of Revolution Filled With a Liquid. *Izv. Akad. Nauk SSR, Me'h.* no. 6, 1965, pp. 123-129. (English transl.: FTD-HT-66-527, Foreign Tech. Div., Wright-Patterson AFB.)
 - 3.211. PASLAY, P. R.; WALSH, E. K.; AND MUSTER, D.: Field Equations for Underwater Sound Propagated by Ring-Stiffened Cylindrical Shells. Rept. No. 60GL51, (AD 239 339) General Engng. Lab., General Electric Co., Mar. 31, 1960.
 - 3.212. SHASHKOV, I. E.: Elastic Vibrations of a Cylindrical Shell Filled With Liquid. *Inzhen. Zh.*, vol. 5, no. 3, pp. 575-579, 1965.
 - 3.213. ZDEL', YU. U.; AND STEPANOV, A. P.: On the Influence of Water on the Frequency of Vibrations of Blades and Plates. *Gidroturbostroyeniye*, no. 4, Moscow, Mashgiz, 1957.
 - 3.214. TATGE, R. B.: Analysis of Measured Vibrational Modes of a Ring-Stiffened Cylindrical Shell. Rept. No. 61GL106, General Electric Co., May 15, 1961.
 - 3.215. TATGE, R. B.: Underwater Sound Propagation by Ring-Stiffened Cylindrical Shells. Rept. No. 62GL146, General Electric Co., Oct. 1962.
 - 3.216. PASLAY, P. R.; TATGE, R. B.; WERNICK, R. J.; WALSH, E. K.; AND MUSTER, D. F.: Vibration Characteristics of a Submerged Ring-Stiffened Cylindrical Shell of Finite Length. *J. Acoust. Soc. Amer.*, vol. 46, no. 3, pt. 2, Sept. 1969, pp. 701-710.
 - 3.217. SHUL'MAN, S. G.: Certain Cases of Free Vibrations of Plates and Cylindrical Shells in Contact With a Liquid. *Trans. of the All-Union Conf. on the Theory of Shells and Plates*, Baku, 1966, Moscow Nauk, 1966, pp. 853-858.
 - 3.218. WERNICK, R. J.; AND MUSTER, D.: Field Equations for Underwater Sound Propagated by Ring-Stiffened Cylindrical Shells. Rept. No. 60GL51-A, Addendum to Rept. No. 60GL51 (AD 239 339), General Electric Co., July 1960.
 - 3.219. RAYLEIGH, LORD: *Theory of Sound*. Vol. I and Vol. II. Dover Pub., 1945. (Originally published in 1877.)
 - 3.220. TIMOSHENKO, S.: On the Correction for Shear of the Differential Equations for Transverse Vibrations of Prismatic Bars. *Phil. Mag.*, ser. 6, vol. 41, 1921, p. 742.
 - 3.221. NAGHDİ, P. M.; AND COOPER, R. M.: Propagation of Elastic Waves in Cylindrical Shells, Including the Effects of Transverse Shear and Rotary Inertia. *J. Acoust. Soc. Amer.*, vol. 28, no. 1, Jan. 1956, pp. 56-63.
 - 3.222. HERRMANN, G.; AND MIRSKY, I.: Three-Dimensional and Shell Theory Analysis of Axially Symmetric Motions of Cylinders. *J. Appl. Mech.*, vol. 23, Dec. 1956, pp. 563-568.
 - 3.223. LIN, T. C.; AND MORGAN, G. W.: A Study of Axisymmetric Vibrations of Cylindrical Shells as Affected by Rotary Inertia and Transverse Shear. *J. Appl. Mech.*, vol. 23, no. 2, June 1956, pp. 255-261.
 - 3.224. MIRSKY, I.; AND HERRMANN, G.: Nonaxially Symmetric Motions of Cylindrical Shells. *J. Acoust. Soc. Amer.*, vol. 29, no. 10, Oct. 1957, pp. 1116-1123.
 - 3.225. REISMANN, H.; AND MEDIGE, J.: Dynamic Response of Cylindrical Shells (Part I). Rept. No. 13, School of Engineering, State Univ. of N.Y., Jan. 1966.
 - 3.226. HILDEBRAND, F. B.; REISSNER, E.; AND THOMAS, G. B.: Notes on the Foundations of the Theory of Small Displacements of Orthotropic Shells. NACA TN 1833, 1949.
 - 3.227. VLASOV, V. Z.: *Basic Differential Equations in General Theory of Elastic Shells*. NACA TM 1241 Translation, 1951.
 - 3.228. MIRSKY, I.; AND HERRMANN, G.: Axially Symmetric Motions of Thick Cylindrical Shells. *J. Appl. Mech.*, vol. 25, no. 1, Mar. 1958, pp. 97-103.
 - 3.229. YU, Y. Y.: Dynamic Equations of Donnell Type for Cylindrical Shells With Application to Vibration Problem. 9th Congres Intern. Mecan. Appl., Univ. Bruxelles, vol. 7, 1957, pp. 261-278.
 - 3.230. CHOU, P. C.: Analysis of Axisymmetrical Motions of Cylindrical Shells by the Method of Characteristics. *AIAA J.*, vol. 6, no. 8, Aug. 1968, pp. 1492-1497.
 - 3.231. MIZOGUCHI, K.: *Trans. Japan Soc. Mech. Engrs.*, vol. 20, no. 95, 1954, p. 483.
 - 3.232. MIRSKY, I.: Vibrations of Orthotropic, Thick, Cylindrical Shells. *J. Acoust. Soc. Amer.*, vol. 36, no. 1, Jan. 1964, pp. 41-51.
 - 3.233. YU, Y. Y.: Application of Variational Equation of Motion to the Nonlinear Analysis of Homogeneous and Layered Plates and Shells. *J. Appl. Mech.*, vol. 30, Mar. 1963, pp. 79-86.
 - 3.234. TANG, S. C.: Response of a Finite Tube to Moving Pressure. *J. Engng. Mech. Div., Proc. Amer. Soc. Civil Engrs.*, vol. 93, EM 3, June 1967, pp. 239-256.
 - 3.235. HERRMANN, G.: On the Dynamic Behavior of

- Shells. Proc. of the Ninth International Congress of Appl. Mech., vol. 7, 1957, pp. 293-299.
- 3.236. McFADDEN, J. A.: Radial Vibrations of Thick-Walled Hollow Cylinders. *J. Acoust. Soc. Amer.*, vol. 26, no. 5, 1954, pp. 714-715.
 - 3.237. REISMANN, H.; AND MEDIGE, J.: Forced Motion of Cylindrical Shells. Proc. of Amer. Soc. Civil Engrs., EM 5, Oct. 1968, pp. 1167-1182.
 - 3.238. WARBURTON, G. B.; AND AL-NAJAFI, A. M. J.: Free Vibration of Thin Cylindrical Shells With a Discontinuity in the Thickness. *J. Sound Vib.*, vol. 9, no. 3, 1969, pp. 373-382.
 - 3.239. GREENSPON, J. E.: Vibrations of a Thick-Walled Cylindrical Shell—Comparison of the Exact Theory With Approximate Theories. *J. Acoust. Soc. Amer.*, vol. 32, no. 5, May 1960, pp. 571-578.
 - 3.240. McIVOR, I. K.: Dynamic Stability and Non-Linear Oscillations of Cylindrical Shells (Plane Strain) Subjected to Impulse Pressure. Ph.D. Thesis, Stanford Univ., June 1962.
 - 3.241. MIRSKY, I.: Wave Propagation in Transversely Isotropic Circular Cylinders. Part II: Numerical Results. *J. Acoust. Soc. Amer.*, vol. 37, no. 6, June 1965, pp. 1022-1026.
 - 3.242. REISMANN, H.; AND PAWLIK, P. S.: On the Plane Strain Dynamic Response of a Cylindrical Shell Under Lateral Loads. Rept. No. 22, School of Engineering, State Univ. of N.Y., Apr. 1967.
 - 3.243. REISMANN, H.; AND PAWLIK, P. S.: Plane-Strain Dynamic Response of a Cylindrical Shell—A Comparison Study of Three Different Shell Theories. *J. Appl. Mech.*, vol. 35, no. 2, June 1968, pp. 297-305.
 - 3.244. REISMANN, H.; AND PADLOG, J.: Forced Axisymmetric Motions of Cylindrical Shells. *J. Franklin Inst.*, vol. 284, no. 5, Nov. 1967, pp. 308-319.
 - 3.245. WHITTIER, J. S.; AND JONES, J. P.: Axially Symmetric Wave Propagation in a Two-Layered Cylinder. *Internat. J. Solids and Structures*, vol. 3, no. 4, July 1967, pp. 657-675.
 - 3.246. MIZOGUCHI, K.: On Fundamental Differential Equations of Vibrations of Cylindrical Shells. *Bull. Japan Soc. Mech. Engrs.*, vol. 5, no. 17, Feb. 1962, pp. 43-49.
 - 3.247. KAGAWA, Y.: Non-Axially Symmetric Vibrations of Sandwich Cylindrical Shells. *J. Sound Vib.*, vol. 7, no. 1, Jan. 1968, pp. 39-48.
 - 3.248. GARNET, H.; CROUZET-PASCAL, J.; AND NOLAR, F.: The Free Vibrations of Thick, Composite, Orthotropic, Circular Cylindrical Shells. Contract No. Nonr-3465(00)FBM, Project NR 064-463, Tech. Rept. No. 3 (AD 416 167), Off. of Naval Research, Aug. 1963.
 - 3.249. HU, W. C. L.: A Survey of the Literature on the Vibrations of Thin Shells. Tech. Rept. No. 1, Contract No. NASr-94(06), SwRI Project 02-1504, Southwest Res. Inst., June 1964.
 - 3.250. MIRSKY, I.: Three-Dimensional and Shell-Theory Analysis for Axisymmetric Vibrations of Orthotropic Shells. *J. Acoust. Soc. Amer.*, vol. 39, no. 3, Mar. 1966, pp. 549-555.
 - 3.251. MIRSKY, I.: Three-Dimensional and Shell Theory Analysis for Axisymmetric Vibration of Orthotropic Cylinders. Durham Project No. DA-31-124-ARO-D-250 (AD 459 477), U. S. Army Research Office, March 1965.
 - 3.252. YU, Y. Y.: *J. Aeronaut. Space Sci.*, vol. 25, 1958, pp. 699-715.
 - 3.253. GREENSPON, J. E.: Vibrations of Thick Shells in a Vacuum and in an Acoustic Medium. Proj. No. NR385-412, Contract No. Nonr-2733(00) Tech. Rept. No. 1, Office of Naval Research, Feb. 1959.
 - 3.254. REISMANN, H.: Response of a Pre-Stressed Cylindrical Shell to Moving Pressure Load. Developments in Mech. Proc. Eighth Midwest Mech. Conf., Pergamon Press (Oxford), 1965, pp. 349-363.
 - 3.255. AMBARTSUMYAN, S. A.: Theory of Anisotropic Shells. State Publishing House for Phys. and Math. Literature, Moscow, 1961. (In Russian.) NASA TT F-118, May 1964.
 - 3.256. DONG, S. B.; PISTER, K. S.; AND TAYLOR, R. L.: On the Theory of Laminated Anisotropic Shells and Plates. *J. Aeron. Sci.*, vol. 29, 1962, pp. 969-975.
 - 3.257. BAKER, E. H.; AND HERRMANN, G.: Vibrations of Orthotropic Cylindrical Sandwich Shells Under Initial Stress. *AIAA J.*, vol. 4, no. 6, June 1966, pp. 1063-1070.
 - 3.258. CHU, H. N.: Vibrations of Honeycomb Sandwich Cylinders. *J. Aerospace Sci.*, vol. 28, no. 12, Dec. 1961, pp. 930-939.
 - 3.259. FREUDENTHAL, A. M.; AND BIENIEK, M. P.: Forced Vibrations of Sandwich Structures. Tech. Rept. 60-307 (AD 258 536), Wright Air Development Div., Wright-Patterson AFB, Jan. 1961.
 - 3.260. IL'GAMOV, M. I.: Equilibrium and Vibration Equations of Three-Layer Shells in the Asymmetric Form. *Aviatsionnaia Tekhnika*, no. 4, 1962, pp. 68-78. (In Russian.)
 - 3.261. KEEFFE, R. E.; AND WINDHOLZ, W. M.: Dynamic Analysis of a Multilayered Cylinder. AIAA Paper 68-350. AIAA and ASME, Structures, Structural Dynamics and Material Conferences, 9th (Palm Springs, Calif.), April 1-3, 1968.
 - 3.262. LIBRESCU, L.: Aeroelastic Vibrations and Stability of Nonhomogeneous Cylindrical Structures Placed in a Compressible Fluid Flow. *Rev. de Mécanique Appliquée*, vol. 8, no. 2, 1963, pp. 251-276. (In French.)
 - 3.263. MEAD, D. J.; AND PRETLOVE, A. J.: On the Vibrations of Cylindrically Curved Elastic Sandwich Plates. Part I—With the Solution for Flat Plates. Part II—The Solution for Cylindrical Plates. ARC-R & M-3363, Aeronautical Research Council (Great Britain), 1964.
 - 3.264. YU, Y. Y.: Vibrations of Elastic Sandwich Cylindrical Shells. Paper 60-WA-21, *J. Appl. Mech.*, vol. 27, no. 4, Dec. 1960, pp. 653-662.

- 3.265. BIENIEK, M. P.; AND FREUDENTHAL, A. M.: Forced Vibrations of Cylindrical Sandwich Shells. *J. Aerospace Sci.*, vol. 29, 1962, pp. 180-184.
- 3.266. CROUZET-PASCAL, J.; PIFKO, A.; MAHONEY, J. B.; AND SALERNO, V. L.: On the Deformation of Thick, Composite, Orthotropic, Circular Cylindrical Shells. Contract No. Nonr.-3465(00) FBM Tech. Rept. No. 1, Grumman Research Dept. Rept. RE-161, Office of Naval Research, Sept. 1962.
- 3.267. KURSHIN, L. M.: Equations of Sandwich Cylindrical Shells. *Bulletin of the Acad. of Sci. of the USSR, OTN (Dept. of Tech. Sci.)*, no. 3, 1958. (In Russian.)
- 3.268. MUSHTARI, KH. M.: Contribution to the General Theory of Slightly Curved Shells With a Core. *Bulletin of the Acad. of Sci. of the USSR, OTN*, no. 2, 1961. (In Russian.)
- 3.269. IL'GAMOV, M. I.: Contribution to the Theory of Sandwich Shells of Asymmetrical Form. *Proc. of the All-Union Conference on the Theory of Plates and Shells*, Lvov, 1961. (In Russian.)
- 3.270. JOHNS, J. P.; AND WHITTIER, J. S.: Axially Symmetric Motions of a Two-Layered Timoshenko-Type Cylindrical Shell. *J. Appl. Mech.*, vol. 33, Trans. ASME, Series E, 1966, pp. 838-844.
- 3.271. HSU, T. M.; AND WANG, J. T. S.: A Theory of Laminated Cylindrical Shells Consisting of Layers of Orthotropic Laminae. *AIAA J.*, vol. 8, no. 12, Dec. 1970, pp. 2141-2146.
- 3.272. PAYTON, R. G.: Bond Stress in Cylindrical Shells Subjected to an End Velocity Step. *J. Math. Phys.* vol. 43, no. 3, 1964.
- 3.273. GRIGOLYUK, E. I.: Equations of Three-Layered Shells, Simply Filled. *Izv. Akad. Nauk SSSR, Ser. Tech.*, no. 1, 1958.
- 3.274. BALL, R. E.; AND SCHJELDERUP, H. C.: A Feasibility Study of the Numerical Computation of the Inelastic Response of Impulsively Loaded Shells. Rept. P-443-2, National Engineering Science Co., June 1963.
- 3.275. GRIGOLYUK, E. I.; AND CHULKOV, P. P.: On the General Theory of Triple-Layer Shells Having Large Deflections. *Rept. of Acad. of Sci. SSSR*, vol. 150, no. 5, 1963. (In Russian.)
- 3.276. YU, Y. Y.; AND REN, N.: Damping Parameters of Layered Plates and Shells. *Acoustical Fatigue in Aerospace Structures*; *Proc. of the Second Intern. Conf. (Dayton, Ohio)*, Apr. 29-May 1, 1964. A66-10121 01-32, pp. 555-584.
- 3.277. KARLSSON, T.; AND BALL, R. E.: Exact Plane Strain Vibrations of Composite Hollow Cylinders—Comparison With Approximate Theories. *AIAA J.*, vol. 4, Jan. 1966, pp. 179-181.
- 3.278. SUVERNEV, V. G.: Small Natural Oscillations of Triple-Layer Shells of Revolution. *AN SSR. Sibirskoye Otd. Iav., Ser. Tekh. Nauk*, no. 2, 1964, pp. 93-98. FTD-TT-65-1874 (AD 639 556), June 1966, pp. 1-7.
- 3.279. SUVERNEV, V. G.: Natural Oscillations of Three-Layer Circular Cylindrical Shells With Freely Supported and Clamped Edges. *Rashchety Elementov Aviatsionnykh Konstruktsii*, no. 3, 1965, pp. 197-218. (In Russian.)
- 3.280. WEINGARTEN, V. I.: On the Free Vibration of Thin Cylindrical Shells. Contract No. AF04(695)-169 (AD 405 117), Rept. No. TDR-169(3560-30) TN-3, Aerospace Corp., Dec. 20, 1962.
- 3.281. MODI, V. J.: Similarity Relations for Vibrating Cylinder With Temperature Gradient Across the Thickness. *J. Roy. Aeronaut. Soc.*, vol. 69, June 1965, pp. 412-414.
- 3.282. DMITRIYEV, YU, V.: On the Free Vibration of Prestressed Cylindrical Sandwich Shells. *Izv. AN SSR, OTN, Mekh. i Mash.*, no. 6, 1962, pp. 155-158. (In Russian.)
- 3.283. KAN, S. N.: Stability and Free Oscillations of Triple Layer Cylindrical Shells. *Prikl. Mekh.*, Izdat. Akad. Nauk Ukr-SSR, vol. 8, no. 2, 1962, pp. 120-132.
- 3.284. BUSHNELL, D.: Dynamic Response of Two-Layered Cylindrical Shells to Time-Dependent Loads. *AIAA J.*, vol. 3, no. 9, 1965, pp. 1698-1703.
- 3.285. CHU, H. N.: On Simple Thickness Vibrations of Thin Sandwich Cylinders. *J. Appl. Mech.*, vol. 28, no. 1, Mar. 1961, pp. 145-146.
- 3.286. HABIP, L. M.: A Review of Recent Russian Work on Sandwich Structures. *Internat. J. Mech. Sci.*, vol. 6, Dec. 1964, pp. 483-487.
- 3.287. KABULOV, V. K.: Investigation of Oscillations of Three-Layer Shells With Rigid Filler. *Akademiia Nauk Uzbekshoi SSR, Izvestiia, Seriya Tekhnicheskikh Nauk*, vol. 8, no. 2, 1964, pp. 27-36. (In Russian.)
- 3.288. KHOLOD, A. I.: Nonlinear Transverse Oscillations of a Three-Layer Cylindrical Panel. *Prikl. Mekh.*, vol. 1, no. 6, 1965, pp. 123-126. (In Russian.)
- 3.289. KHOLOD, A. I.: Forced Oscillations of a Circular Cylindrical Shell With a Rigid Filler. *Soprotivl. Materialov i Teoriya Sooruzh.*, Kiev, Budivl'nyk. Part 2, 1965, pp. 44-51. (In Russian.)
- 3.290. KONDRASHOV, N. S.: Optimal Design for Three-Layer Cylindrical Shells Under Pulsed Pressure Loads. *Strength and Dynamics of Aircraft Engines*, Moscow, Izdatel'stvo Mashinostroenie, 1966, pp. 88-99. (In Russian.)
- 3.291. KUNUKKASSERIL, V. X.: Vibration of Multi-Layered Anisotropic Cylindrical Shells. *Tech. Rept. WVT-6717 (AD 649 662)*, Watervliet Arsenal Benet Labs., Feb. 1967.
- 3.292. LIBRESCU, L.: On the Elasto-Dynamic Problem of Nonhomogeneous Thin Shells. *Studii Si Cercetari Mecan. Apl., Inst. Mecan. Apl., Acad. Rep. Pop. Romine*, vol. 12, no. 4, 1961, pp. 861-876. (In Rumanian.)
- 3.293. LIBRESCU, L.: Vibrations of Elastic Structures of Circular Cylindrical Form Situated in a Supersonic Fluid Flow. *Studii Si Cercetari De Mecanica Aplicata (Rumanian)*, Nr. 1, 1961, pp. 139-156.

- (Transl.: FTD-TT-64-744/1+2+3+4, Foreign Tech. Div., Wright-Patterson AFB, Nov. 1963.)
- 3.294. PADOVAN, J.; AND KOPLIK, B.: Vibrations of Closed and Open Sandwich Cylindrical Shells Using Refined Theory. *J. Acoust. Soc. Amer.*, vol. 47, no. 3, pt. 2, Mar. 1970, pp. 862-869.
- 3.295. PRUSAKOV, A. P.: On One Form of the Equations of Bending and the Free Vibrations of Shallow Three-Layered Shells With a Rigid Filler. *Izv. AN SSSR, OTN (Mekh. i Mash.)*, no. 1, 1960. (In Russian.)
- 3.296. WHITE, J. C.: The Flexural Vibrations of Thin Laminated Cylinders. *Trans. ASME, J. Engng. Industr.*, vol. 83, no. 4, Nov. 1961, pp. 397-402.
- 3.297. WEINGARTEN, V. I.: Free Vibrations of Multilayered Cylindrical Shells. *Exptl. Mech.*, vol. 4, no. 7, July 1964, pp. 200-205.
- 3.298. BERT, C. W.; BAKER, J. L.; AND EGLE, D. M.: Free Vibrations of Multilayer Anisotropic Cylindrical Shells. *J. Composite Materials*, vol. 3, no. 3, July 1969, pp. 480-499.
- 3.299. PRUSAKOV, A. P.: Bending and Free Vibrations of Shallow Circular Cylindrical Shells With a Rigid Filler. *Izv. VUZ, Stroit. i Arkhit.*, no. 11-12, 1959, pp. 46-52. (In Russian.)
- 3.300. CHU, H. N.: Simple Thickness Vibrations of Cylindrical Sandwich Shells. *Informal Rept. MI-60-2, The Martin Co.*, Jan. 1960.
- 3.301. BERT, C. W.; AND EGLE, D. M.: Dynamics of Composite, Sandwich, and Stiffened Shell-Type Structures. *J. Spacecraft and Rockets*, vol. 6, no. 12, Dec. 1969, pp. 1345-1361.
- 3.302. YU, Y. Y.: Viscoelastic Damping of Vibrations of Sandwich Plates and Shells. *Proc. of the IASS Symposium on Non-Classical Shell Problems (Warsaw)*, Sept. 1963, pp. 551-571. North Holland Pub. Co. (Amsterdam), and Polish Sci. Pub. (Warsaw), 1964.

Page intentionally left blank

Noncircular Cylindrical Shells

A cylindrical surface is defined by a straight line (called the "generator") always moving parallel to itself. In the special case where the generator moves in a circular arc, it generates a circular cylindrical surface, for which both radii of curvature are both constant. In the general case, one of the radii of curvature is variable, thereby yielding equations of motion with variable coefficients. For this reason alone, relatively very few results are available in the literature for the free vibrations of noncircular cylindrical shells.

4.1 EQUATIONS OF MOTION

A noncircular cylindrical shell having thickness h and length l is shown in figure 4.1. The longitudinal coordinate is x (as in chapters 2 and 3), whereas the circumferential coordinate is defined either by θ or S , where S is the arc length such that

$$dS = r d\theta \quad (4.1)$$

and $r = r(\theta)$ is the radius of curvature.

To obtain the equations of motion (see sec. 1.7) the coordinates x and S are used in place of α and β in the general equations; correspondingly, $R_\alpha = \infty$, $R_\beta = r$, and $A = B = 1$. The Donnell-Mushtari equations (2.3) and (2.7), for example, are generalized to (cf., refs. 4.1 and 4.2)

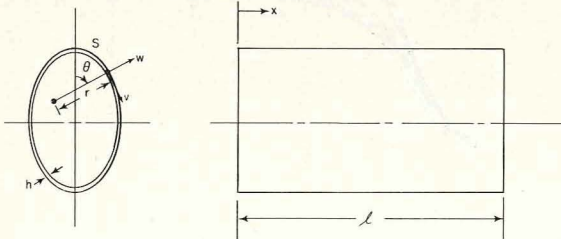


FIGURE 4.1.—Coordinates for a noncircular cylindrical shell.

$$\left. \begin{aligned} \frac{\partial^2 u}{\partial x^2} + \frac{1-\nu}{2} \frac{\partial^2 u}{\partial S^2} + \frac{1+\nu}{2} \frac{\partial^2 v}{\partial x \partial S} + \nu \frac{\partial}{\partial x} \left(\frac{w}{r} \right) \\ = \rho \frac{(1-\nu^2)}{E} \frac{\partial^2 u}{\partial t^2} \\ \frac{1+\nu}{2} \frac{\partial^2 u}{\partial x \partial S} + \frac{1-\nu}{2} \frac{\partial^2 v}{\partial x^2} + \frac{\partial^2 v}{\partial S^2} + \frac{\partial}{\partial S} \left(\frac{w}{r} \right) \\ = \rho \frac{(1-\nu^2)}{E} \frac{\partial^2 v}{\partial t^2} \\ \frac{\nu}{r} \frac{\partial u}{\partial x} + \frac{1}{r} \frac{\partial v}{\partial S} + \frac{w}{r^2} + \frac{h^2}{12} \nabla^4 w = -\rho \frac{(1-\nu^2)}{E} \frac{\partial^2 w}{\partial t^2} \end{aligned} \right\} \quad (4.2)$$

where $\nabla^4 = \nabla^2 \nabla^2$, and the ∇^2 operator is now given by

$$\nabla^2 \equiv \frac{\partial^2}{\partial x^2} + \frac{\partial^2}{\partial S^2} \quad (4.3)$$

The generalization of equations (4.2) corresponding to the Reissner-Naghdi-Berry theory of chapter 2 are obtained by adding the terms (cfs., refs. 4.3 and 4.4)

$$\frac{k^2}{r^2} \left[\frac{(1-\nu)}{2} \frac{\partial^2 v}{\partial x^2} + r \frac{\partial^2}{\partial S^2} \left(\frac{v}{r} \right) - r \frac{\partial^3 w}{\partial x^2 \partial S} - r \frac{\partial^3 w}{\partial S^3} \right] \quad (4.4a)$$

$$k^2 \left[-\frac{\partial^3}{\partial x^2 \partial S} \left(\frac{v}{r} \right) - \frac{\partial^3}{\partial S^3} \left(\frac{v}{r} \right) \right] \quad (4.4b)$$

to the left sides of the last two of equations (4.2), where the definition of k^2 is now generalized from that of equation (2.6) to

$$k \equiv \frac{h^2}{12r_0^2} \quad (4.5)$$

and r_0 is the average radius of the shell.

The generalization of equations (4.2) corresponding to the Donnell equations and the Flügge equations are given in reference 4.5 for an *orthotropic* material including nonlinear, large deflection terms. The orthotropic linear Donnell

equations are also given in references 4.6 and 4.7 for the case of added initial stress terms to account for external pressure.

The membrane theory results when h^2 is set equal to zero in equations (4.2).

4.2 ELLIPTICAL CYLINDRICAL

Consider first the elliptical cylindrical shell having a middle surface defined by

$$\frac{\xi^2}{a^2} + \frac{\eta^2}{b^2} = 1 \quad (4.6)$$

as shown in figure 4.2, where a and b are the semi-major and semi-minor axes, respectively.

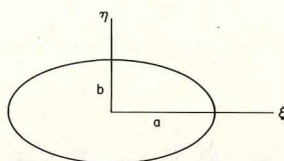


FIGURE 4.2.—Coordinates for an elliptic cross section.

Herrmann and Mirsky (ref. 4.8) analyzed the free vibration problem according to the *membrane* theory. Consider first the purely longitudinal motion ($v=w=0$). The motion is then governed by the first of equations (4.2) alone. The analysis for this case in reference 4.8 was limited to shells which are only slightly elliptical; i.e.,

$$\frac{b}{a} = 1 - \epsilon \quad (4.7)$$

where $\epsilon \ll 1$. Under this assumption the equation of motion can be transformed into a Mathieu equation which has an exact solution in terms of tabulated functions and that the resulting lowest frequency is given by

$$\frac{\omega^2 a^2 \rho}{G} = 1 + \epsilon \quad (4.8)$$

where $G = E/2(1+\nu)$. The corresponding frequency for a circular cylindrical shell is

$$\omega^2 a^2 \rho / G = 1 \quad (R=a)$$

Thus the square of the lowest longitudinal frequency of a slightly elliptic shell is the arithmetic mean of the frequencies of circular shells having radii a and b , respectively.

It was shown in reference 4.8 that in the case of torsional motion, $u=w=0$, and, if v is considered independent of S , the first and third of equations (4.2) are satisfied identically and the second reduced to

$$\frac{\partial^2 v}{\partial x^2} = \frac{\rho}{G} \frac{\partial^2 v}{\partial t^2} \quad (4.9)$$

Then the frequency of torsional motion is not influenced by the ellipticity of the cylinder.

Flexural motions of the elliptical cylindrical shell were studied in reference 4.8 for the case when the displacement components are independent of S . An energy method was used with displacements in the form

$$\left. \begin{aligned} u(x,t) &= A \sin \lambda x \cos \omega t \\ v(x,t) &= B \cos \lambda x \cos \omega t \\ w(x,t) &= C \cos \lambda x \cos \omega t \end{aligned} \right\} \quad (4.10)$$

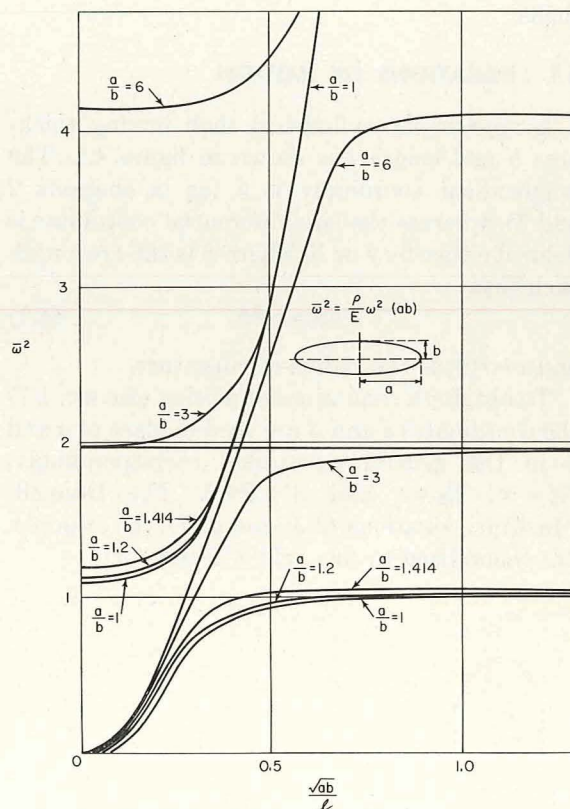


FIGURE 4.3.—Frequency parameters $\omega^2 ab \rho / E$ for the flexural modes of an elliptic, cylindrical, membrane shell. (After ref. 4.8)

where $\lambda = \pi/l$. Numerical results were obtained for $a/b = 1.2, \sqrt{2}, 3$, and 6. The frequency parameter $\omega^2 ab\rho/E$ is shown in figure 4.3 plotted versus the length ratio \sqrt{ab}/l . The frequency parameter thus implies a shell of a given cross-sectional area πab having a circumference which varies with a/b . The ratio \sqrt{ab}/l is a generalization of the R/l ratio of the circular cylindrical case. Because membrane theory is used, the results do not depend upon the thickness ratio, h/\sqrt{ab} .

For shells having the same cross-sectional area, the mass of the shell obviously increases with the ellipticity of the section. However, it is of interest to find the influence of ellipticity upon a shell which was originally circular, but was deformed into an ellipse without straining the middle surface; i.e., keeping the circumference constant. The circumference can be written as

$$C_e = \pi b \left(\frac{a}{b} + 1 \right) \kappa \quad (4.11)$$

where κ is a number greater than unity depending upon a/b . For example, for $a/b = 3$, $\kappa = 1.0635$. For $a/b = 19$, $\kappa = 1.216$. The ratios of the squares

of the frequencies of the two flexural modes to those of a circular cylindrical shell having the same circumference is shown in figure 4.4 for $a/b = 3$.

An experimental study of a clamped-free elliptical cylindrical shell was made by Park et al (ref. 4.9). The specifications of the model tested are shown in figure 4.5, as well as the transducer locations to measure amplitudes. Typical mode shapes are depicted in figure 4.6. The frequency spectrum is shown in figure 4.7. Resonant frequencies were found at 49.2, 65.5, 123.6, 126.7, 78.1, 98.5, 133.2, 149.0, 163.3, and 184.4 cps, although no well-defined mode shape could be determined for the 126.7 cps frequency. A comparison of the frequencies with those of a clamped-free *circular* cylindrical shell having the same specifications, except a radius of $R = 10$ in., is shown in figure 4.8. In making the comparison, note that the cross section of the elliptical shell is smaller than that of the circular shell.

Slepov (refs. 4.6 and 4.7) analyzed the problem of the elliptical cylindrical shell supported at both ends by shear diaphragms. The shell was considered to be orthotropic and loaded by an initial external pressure. The Donnell-Mushtari

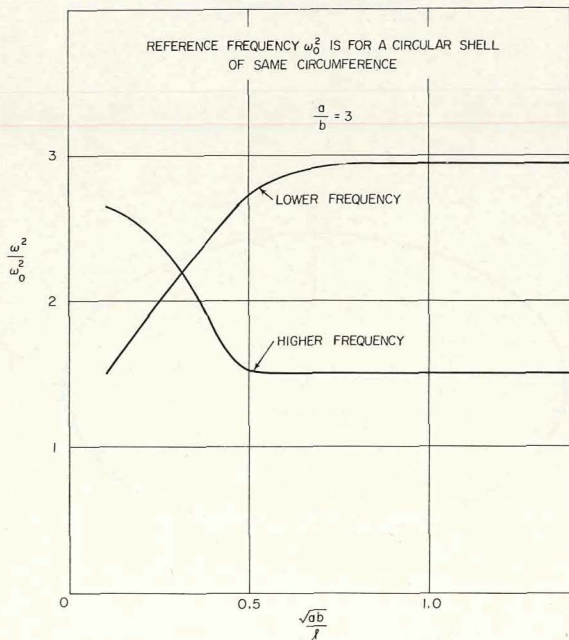


FIGURE 4.4.—Comparison of flexural mode frequencies for elliptic and circular cylindrical shells. (After ref. 4.8)

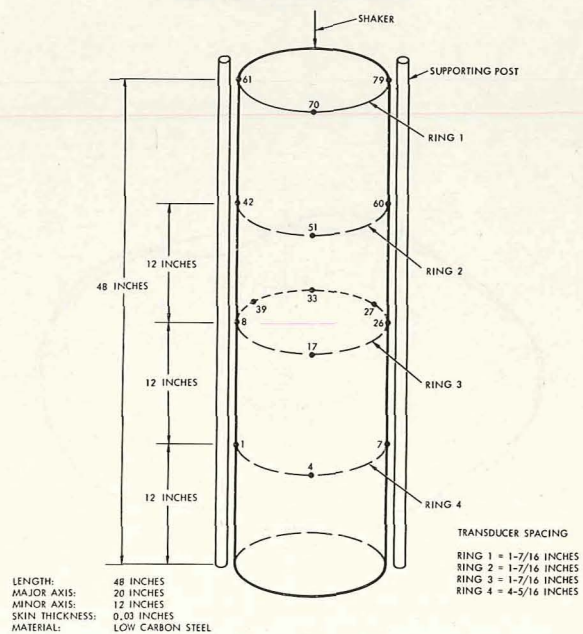


FIGURE 4.5.—Specifications of a clamped-free elliptical cylindrical shell. (After ref. 4.9)

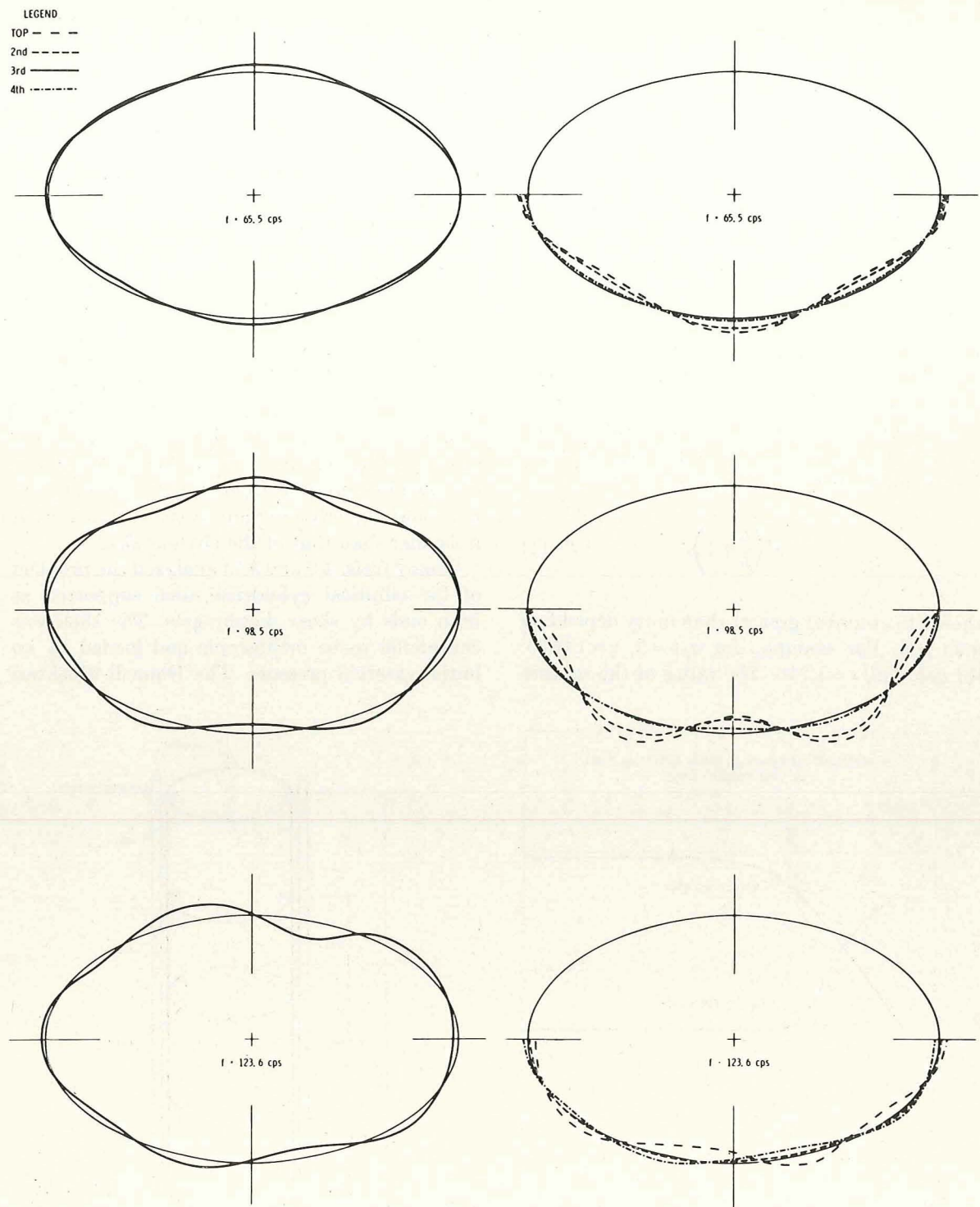


FIGURE 4.6.—Typical mode shapes of a clamped-free elliptical cylindrical shell. (After ref. 4.9)

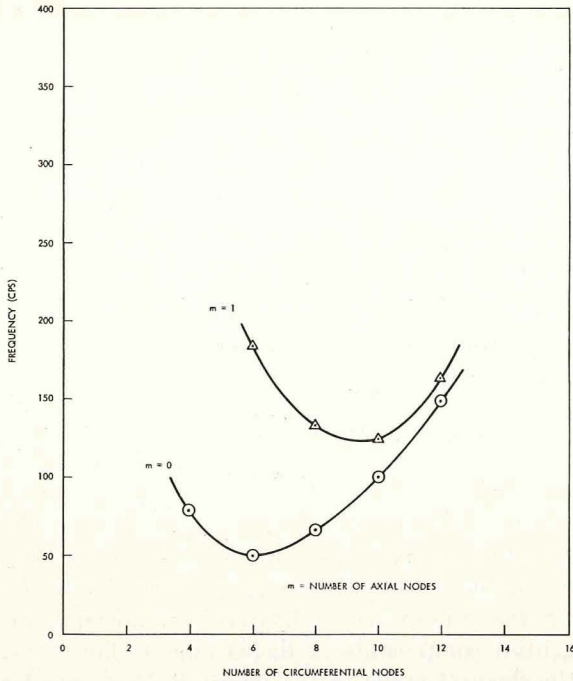


FIGURE 4.7.—Frequency plots for a clamped-free elliptical cylindrical shell. (After ref. 4.9)

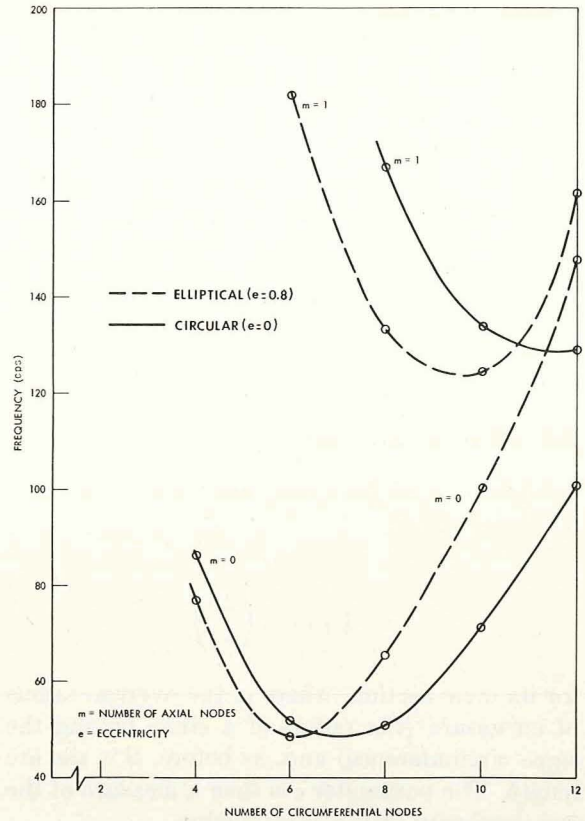


FIGURE 4.8.—Comparison of frequencies of clamped-free elliptical and circular shells. (After ref. 4.9)

form of the shell equations were used. The problem was solved by the Galerkin method using normal displacement functions in the form

$$w = \sin \lambda \xi \sum_n C_n \sin nk\eta \sin \omega t \quad (4.12)$$

where, in this case, $\lambda = \pi \bar{r}/l$, $\xi = x/\bar{r}$, $\eta = S/\bar{r}$, $k = 4\pi/\eta_0$, $\eta_0 = S_0/\bar{r}$, and \bar{r} is the maximum radius of curvature of the shell cross section. Assuming that the dimensionless radius of curvature $\rho_c = r/\bar{r}$ and its reciprocal are expanded in series as

$$\left. \begin{aligned} \rho_c &= \frac{1}{2}\rho_0 + \sum_{i=1} \rho_i \cos ik\eta \\ \frac{1}{\rho_c} &= \frac{1}{2}\left(\frac{1}{\rho}\right)_0 + \sum_{i=1} \left(\frac{1}{\rho}\right)_i \cos ik\eta \end{aligned} \right\} \quad (4.13)$$

It is shown in references 4.6 and 4.7 that the square of the frequency for the orthotropic shell is given by the formula

$$\begin{aligned} \omega^2 = \frac{D_x}{\rho h^* \rho_0} & \left\{ (E_x \lambda^4 + E_s n^4 k^4 + E_3 \lambda^2 n^2 k^2) \rho_0 \right. \\ & + \frac{4b_1^4 \lambda^4}{E_x \lambda^4 + E_s n^4 k^4 + E_3 \lambda^2 n^2 k^2} \left[\left(\frac{1}{\rho}\right)_0 - \left(\frac{1}{\rho}\right)_{2n} \right] \\ & - qk^2 \left[n^2 \left(\frac{1}{2} \rho_0^2 + \sum_{i=1,2} \rho_i^2 \right) \right. \\ & \left. \left. + \frac{1}{4} \left(\frac{\pi^2}{3} + 1 \right) \sum_{i=1,2} (i^2 \rho_i^2) + \frac{\pi ab \lambda^2}{S_0 \bar{r} k^2} \rho_0 \right] \right\} \quad (4.14) \end{aligned}$$

where $D_x = E_x h^3/12(1 - \nu_x \nu_s)$; ρ is the mass density, $h^* = h \bar{r}^4 E_x$; E_x and E_s are Young's moduli in the x and S directions, respectively;

$$E_3 \equiv \frac{2E_x(1 - \nu_x \nu_s)}{(1 + \nu_x)} + E_x \nu_s + E_s \nu_x \quad (4.15)$$

ν_x and ν_s are the orthotropic Poisson contraction coefficients (see sec. 3.1);

$$\left. \begin{aligned} b_1^4 &\equiv 3(1 - \nu_x \nu_s) E_x E_s \left(\frac{\bar{r}}{h} \right)^2 \\ q &\equiv 12p(1 - \nu_x \nu_s) \left(\frac{\bar{r}}{h} \right)^3 \end{aligned} \right\} \quad (4.16)$$

S_0 is the circumference of the shell; p is the uniformly distributed external pressure; and a , b are the semiaxes of the shell cross section. In the case of an isotropic shell, $E_x = E_s = E$ and $\nu_x = \nu_s = \nu$ in equation (4.14). For the unloaded shell, q is zero in equation (4.14). The sandwich elliptical shell was also analyzed in reference 4.7.

4.3 OVAL CYLINDRICAL

Consider next the oval cylindrical shell defined by the equation

$$r = \frac{r_0}{1 + \epsilon \cos \left(\frac{2S}{r_0} \right)} \quad (4.17)$$

for its cross section, where r_0 the average radius of curvature (the radius of a circle having the same circumference) and, as before, S is the arc length. The parameter ϵ is then a measure of the noncircularity of the cross section.

The free vibrations of oval shells defined by equation (4.17) were studied in a series of reports by Klosner and Pohle (refs. 4.4, 4.10, and 4.11). The generalization of the Reissner-Naghdi-Berry theory including bending terms was used (see sec. 4.1). The plane strain problem (u and all derivatives with respect to x are zero) was considered in reference 4.4. The non-zero displacements v and w were assumed as doubly infinite series in S as follows:

$$\left. \begin{aligned} v &= \sum_{n=0}^{\infty} B_n \sin \beta S \cos \omega t \\ w &= \sum_{n=0}^{\infty} C_n \cos \beta S \cos \omega t \end{aligned} \right\} \quad (4.18)$$

where $\beta = n/r_0$ and ω is a perturbed frequency which can be expressed as a power series in the parameter ϵ by

$$\omega^2 = \omega_0^2 + C_1 \epsilon + C_2 \epsilon^2 + \dots \quad (4.19)$$

where ω_0 is the frequency of a circular cylindrical

shell of radius r_0 . In reference 4.4 equations (4.18) were substituted into the equations of motion and terms multiplied by coefficients up to the order ϵ^2 were retained. Numerical results for the frequencies of the first five (primarily) extensional and flexural modes of an infinite shell having an axis ratio of $b/a = 1.1$ ($\epsilon = 0.1427$) and a thickness ratio of $r_0/h = 91.7$ are given in table 4.1. This table lists the percentages by which the frequencies of the circular cylindrical shell (having the same average radius r_0) are *increased*. Table 4.1 shows that the small noncircularity of the oval cross section causes only a small change in the frequencies. The effect of noncircularity on the primarily extensional modes is to stiffen the shell due to the increase in strain energy which results from coupling of the modes. For example, for $n=0$ the circular cylindrical shell has a purely radial ($v=0$) extensional motion, whereas the oval shell has both radial and tangential components of displacement. For $n=1$, the flexural mode of the infinitely long circular shell corresponds to rigid body translational motion having zero frequency, but not in the case of the oval shell. For $n > 2$ the frequencies of the flexural modes of the oval shell are less than those of the circular shell. Calculations for the plane strain case were subsequently carried out in reference 4.10 retaining terms up to the order ϵ^4 . The results obtained changed very little from those of table 4.1, thereby validating the rapidity of convergence of the perturbation approach.

In references 4.10 and 4.11 the analysis was

TABLE 4.1.—Percent Increase in Plane Strain Frequencies of an Oval Shell in Comparison with a Circular Shell ($b/a = 1.1$, $r_0/h = 91.7$)

n	Type of plane strain mode	
	Predominantly extensional, %	Predominantly flexural, %
0	0.255
1	.128
2	.136	0.924
3	.055	-.117
4	.032	-.096
5	.021	-.064

also extended to include the torsional and flexural modes having displacements of the form

$$\left. \begin{aligned} u &= A \sin \lambda x \cos \beta S \cos \omega t \\ v &= B \cos \lambda x \sin \beta S \cos \omega t \\ w &= C \cos \lambda x \cos \beta S \cos \omega t \end{aligned} \right\} \quad (4.20)$$

Numerical results for these modes for the shell described previously in table 4.1 are given in table 4.2 for various nondimensional half-lengths (l) of the longitudinal sine wave. Results are given for $b/a = 1.4$ ($\epsilon = 0.5$), as well as for $b/a = 1.1$ ($\epsilon = 0.1427$) and for $r_0/h = 91.7$. The frequencies of all modes in table 4.2 increase with noncircularity and with the wave length. The amplitudes of the lower flexural modes were found to vary

$$\begin{aligned} \text{from} \quad C/A &= -9.510 \text{ for } l=1 \\ \text{to} \quad C/A &= -0.1035 \text{ for } l=10 \end{aligned}$$

For the higher mode, C/A varied from 0.1052 for $l=1$ to 9.661 for $l=10$. For all flexural modes, $B/A = 0$. Thus for the lower modes the effect of noncircularity should be more significant for the

smaller wave lengths because the deformation is primarily dilatational rather than longitudinal extensional. The reverse is true for the higher modes since the displacements become primarily dilatational for the longer wave lengths.

Sathyamoorthy and Pandalai (ref. 4.5) investigated the nonlinear (large deflection) vibrations of orthotropic oval shells. The middle surface of the shell was defined as in equation (4.17). It was shown that the solutions for the plane strain modes of an infinitely long shell were the same as for oval rings, in both the isotropic and the orthotropic cases. Results for the plane strain modes were obtained according to the inextensional theory (i.e., the middle surface deforms without stretching; this theory is discussed for circular cylindrical shells in section 2.4.5). A mode shape for w was taken as

$$w(S, t) = A_0 + A_n \cos \beta S + B_n \sin \beta S \quad (4.21)$$

where, $\beta = n/r_0$, as before, $n \geq 2$, and the coefficients A_0 , A_n , and B_n are undetermined functions of time. The nonlinear differential equation is approximated by the Galerkin procedure.

Numerical results for the solution described above were presented in reference 4.5 for the infinitely long isotropic shell having $r_0/h = 100$ for three values of the noncircularity parameter: $\epsilon = 0, 1/2$, and 1. The circumferential wave number n was taken as 2 and 4 in equation (4.21). The nondimensionalized *average* amplitude \bar{A} (averaged over one cycle of vibration) is plotted versus the frequency parameter $\omega r_0^2 \sqrt{12\rho/Eh^3}$ for $n=2$ in figure 4.9, and for $n=4$ in figure 4.10. The nonlinearity is of the "softening type"; i.e., the frequency decreases with increasing amplitude. It was found that the effect of orthotropy is to increase the softening tendency of amplitude-frequency curves. For zero amplitude the motion corresponds to the linear, small displacement solution. Values of these linear frequencies are summarized in table 4.3. Note from figure 4.9 that, for $n=2$ and a given amplitude, an increase in the noncircularity parameter ϵ decreases the frequency for small amplitudes, whereas it increases the frequency for large amplitudes.

A study of oval shells of finite length having the boundary conditions

TABLE 4.2.—Percent Increase in Torsional and Flexural Frequencies of an Oval Shell in Comparison With a Circular Shell ($r_0/h = 91.7$)

l	b/a	Type of mode		
		Torsional, %	Lower flexural, %	Higher flexural, %
1.0	1.1	0	1.25	0.01
1.25		0	.81	.01
1.5		0	.58	.02
1.75		0	.45	.04
2		0	.36	.67
2.5		0	.27	-.03
3.5		0	.14	.04
5		0	.06	.14
10		0	.03	.20
1.0	1.4	0	14.47	.05
1.25		0	9.60	.10
1.5		0	6.93	.21
1.75		0	5.36	.58
2		0	4.38	7.86
2.5		0	3.26	-.51
3.5		0	1.68	.71
5		0	.72	1.74
10		0	.38	2.59

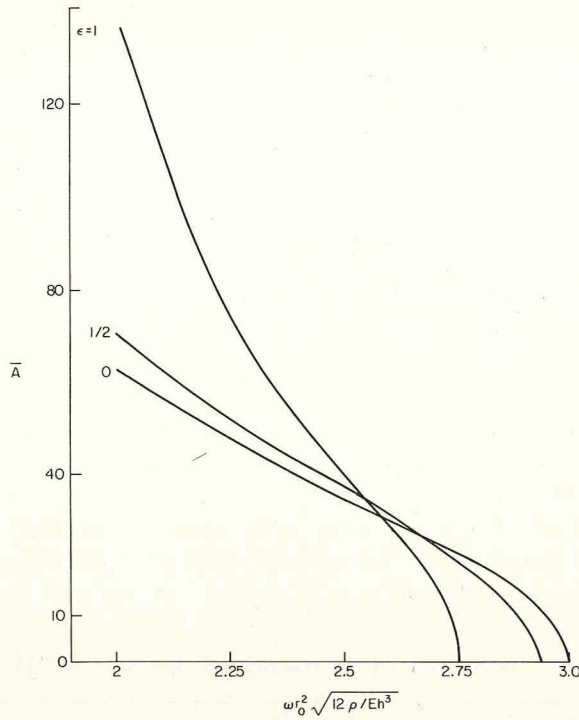


FIGURE 4.9.—Amplitude versus frequency for the large deflection plane strain vibrations of infinite oval shells; $r_0/h = 100$, $n = 2$. (After ref. 4.5)

TABLE 4.3.—Frequency Parameters $\omega r_0^2 \sqrt{12\rho/Eh^3}$ for the Linear (Small Deflection) Plane Strain Vibrations of Infinite Oval Shells; $r_0/h = 100$

n	ϵ		
	0	1/2	1
2	3	2.936	2.746
3	8	7.911	7.673
4	15	14.89	14.58
5	24	23.88	23.55
6	35	34.88	34.53

$$w = \frac{\partial^2 w}{\partial x^2} = u = N_{xs} = 0 \quad (4.22)$$

was also made in reference 4.5. For this case it was found that

- (1) The frequency increases with increasing noncircularity.
- (2) The amplitude-frequency curves are of the softening type.

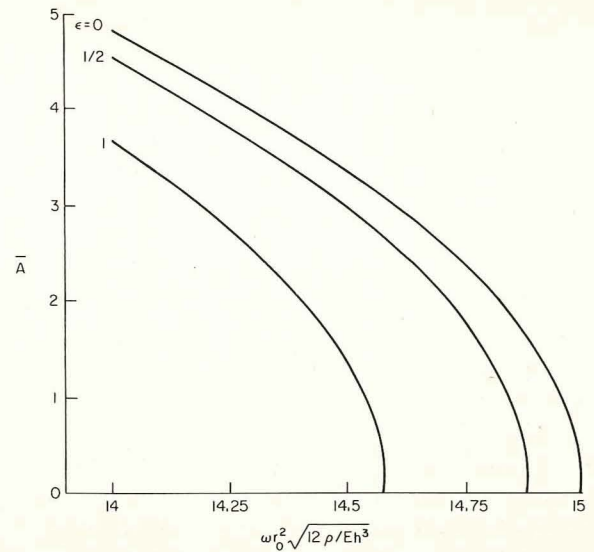


FIGURE 4.10.—Amplitude versus frequency for the large deflection plane strain vibrations of infinite oval shells; $r_0/h = 100$, $n = 4$. (After ref. 4.5)

The free vibration of oval cylindrical shells are also analyzed by a perturbation procedure in references 4.12, 4.13, and 4.14.

4.4 OPEN SHELLS

An open cylindrical shell was depicted by figure 2.141 in chapter 2. In that figure the radius of curvature is constant ($r = R$), the special case of the circular cylindrical shell.

A study of open noncircular cylindrical shells was made by Kurt and Boyd (ref. 4.2). The shells were assumed to be supported by shear diaphragms along their curved edges and to have arbitrary boundary conditions along the straight edges. The Donnell equations of motion (4.2) were used. Displacement functions were assumed to be mixed algebraic and trigonometric functions; i.e.,

$$\left. \begin{aligned} u &= \cos \lambda x \sum_{n=1}^{\infty} A_n \xi^{n-1} \cos \omega t \\ v &= \sin \lambda x \sum_{n=1}^{\infty} B_n \xi^{n-1} \cos \omega t \\ w &= \sin \lambda x \sum_{n=1}^{\infty} C_n \xi^{n-1} \cos \omega t \end{aligned} \right\} \quad (4.23)$$

where $\lambda = m\pi/l$, $\xi = S/l_s$, and l_s is the arc length of the cylinder in the S direction. It is clear that equations (4.23) satisfy the shear diaphragm boundary conditions exactly at $x=0$ and $x=l$. Substituting equations (4.23) into equations (4.2) yields a set of three simultaneous recursion relationships among the coefficients A_n , B_n , and C_n . If eight of the constants are found from the boundary conditions, the remainder are found from the recursion equations.

The procedure described above was applied to a class of noncircular cylindrical shell segments described by the equation

$$\frac{l_s}{r} = \frac{\pi}{4} + c\xi \quad (4.24)$$

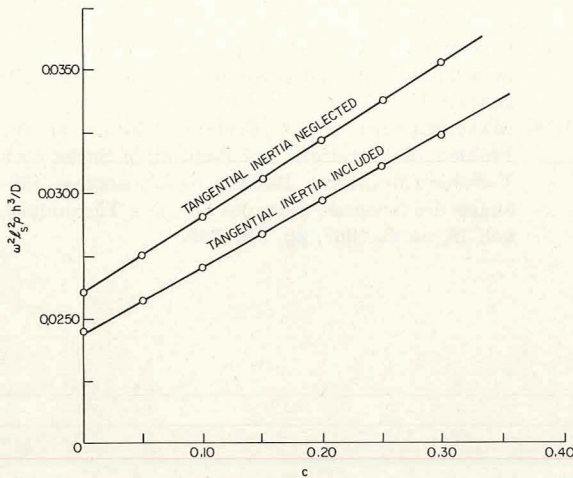


FIGURE 4.11.—Frequency parameters for a class of open, noncircular cylindrical shells. (After ref. 4.2)

TABLE 4.4.—Frequency Parameters $\omega^2 l_s^2 \rho h^3 / D$ for a Class of Open, Noncircular Cylindrical Shells

c	Tangential inertia	
	Included	Neglected
0	0.0245	0.0262
.05	.0257	.0276
.10	.0271	.0291
.15	.0284	.0306
.20	.0297	.0322
.25	.0311	.0338
.30	.0323	.0354

where c is an arbitrary constant. Boundary conditions along the straight edges were taken to be

$$u=v=w=M_\xi=0 \quad \text{at} \quad \xi=0,1 \quad (4.25)$$

Numerical results for frequency parameters $\omega^2 l_s^2 \rho h^3 / D$ (where $D = Eh^3/12(1-\nu^2)$) were obtained for $0 \leq c \leq 0.3$, $l/l_s = 4$, $l_s/h = 200$, $m = 1$, and $\nu = 0.3$ are shown in figure 4.11 and table 4.4. These results were obtained using 25 as the upper limit for n in the summations of equations (4.23). Note in figure 4.11 that the square of the frequency varies essentially linearly with c , with or without tangential inertia terms.

General methods were presented by Oniashvili (ref. 4.15) and Gontkevich (ref. 4.16) for the analysis of open noncircular cylindrical shells of arbitrary curvature and having arbitrary edge conditions. Both methods use the Galerkin procedure and beam functions as given previously in equations (2.168). However, Oniashvili suggests using *straight* beam functions to represent the variation in the θ (or S) direction, while Gontkevich recommends using the eigenfunctions of noncircular *curved* beams. Gontkevich (ref. 4.17) used his procedure to investigate the problem of the vibration of a *parabolic* cylindrical segment immersed in a fluid.

Mazurkiewicz (ref. 4.18) also developed a procedure for shell segments of varying curvature and having arbitrary edge conditions. A double Fourier series approach is used, leading to an infinite characteristic determinate, which must be solved by successive truncation to obtain convergent frequencies.

REFERENCES

- 4.1. KRAUS, H.: Thin Elastic Shells. John Wiley and Sons, Inc. (New York), 1967.
- 4.2. KURT, C. E.; AND BOYD, D. E.: Free Vibrations of Noncircular Cylindrical Shell Segments. AIAA J., vol. 9, no. 2, Feb. 1971, pp. 239-244.
- 4.3. KEMPNER, J.: Simplified Energy Expressions and Differential Equations for Stress and Displacement Analyses of Arbitrary Cylindrical Shells. PIBAL Rept. No. 372, Polytechnic Inst. of Brooklyn, 1958.
- 4.4. KLOSNER, J. M.; AND POHLE, F. V.: Natural Frequencies of an Infinitely Long Noncircular Cylindrical Shell. PIBAL Rept. No. 476, Polytechnic Inst. of Brooklyn, July 1958.
- 4.5. SATHYAMOORTHY, M.; AND PANDALAI, K. A. V.: Nonlinear Flexural Vibrations of Orthotropic Oval Cylindrical Shells. Studies in Structural Mechanics,

- Hoff's 65th Anniversary Volume, Indian Institute of Technology, Madras-36, 1970, pp. 47-74.
- 4.6. SLEPOV, B. I.: Vibrations and Stability of an Elliptical Shell. *Izv. Akad. Nauk USSR, Mekh. i Mashinostr.*, no. 3, 1964, pp. 144-146.
 - 4.7. SLEPOV, B. I.: Vibrations and Stability of Anisotropic and Sandwich Cylindrical Shells of Arbitrary Cross Section. *Theory of Shells and Plates*; Proc. IVth All-Union Conf. (Yerevan, Armenian SSR), Oct. 24-31, 1962, pp. 826-834.
 - 4.8. HERRMANN, G.; AND MIRSKY, I.: On Vibrations of Cylindrical Shells of Elliptic Cross-Section. Contract No. AF 18(600)-1247, Tech. Note No. 5, Columbia Univ., Dec. 1957.
 - 4.9. PARK, A. C.; ET AL.: Dynamics of Shell-Like Lifting Bodies. Part II—The Experimental Investigation. Tech. Rept. AFFDL-TR-65-17, pt. II, Air Force Flight Dynamics Lab., Research and Technology Div., Air Force Systems Command, Wright-Patterson AFB, June 1965.
 - 4.10. KLOSNER, J. M.: Frequencies of an Infinitely Long Noncircular Cylindrical Shell. Part II—Plane Strain, Torsional and Flexural Modes. PIBAL Rept. No. 552, Polytechnic Inst. of Brooklyn, Dec. 1959.
 - 4.11. KLOSNER, J. M.: Free and Forced Vibrations of a Long Noncircular Cylindrical Shell. PIBAL Rept. No. 561, Polytechnic Inst. of Brooklyn, Sept. 1960.
 - 4.12. MALKINA, R. L.: Vibrations of Noncircular Cylindrical Shells. *Izvestiia AN SSR, Mekhanika i Masinostroenie*, no. 1, 1960, pp. 172-175. (In Russian.)
 - 4.13. MALKINA, R. L.: Forced Oscillations of Cylindrical Shells. *Izvestiya Vysshikh Uchebnykh Zavedeniy, Aviatcionnaya Tekhnika*, Nr. 4, 1960. (English transl.: FTD-TT-63-742/1+2, Translation Div., Foreign Technology Div., Wright-Patterson AFB, Sept. 1963.)
 - 4.14. MALKINA, R. L.; AND GODZEVICH, V. G.: Free Oscillations of Shells with Zero Curvature. *Aviatcionnaia Tekhnika*, no. 1, 1963, pp. 48-57. (In Russian.)
 - 4.15. ONIASHVILI, O. D.: Certain Dynamic Problems of the Theory of Shells. Moscow, Akad. Nauk SSSR, 1957. (In Russian.) (Transl. and published by M. D. Friedmann, Inc.)
 - 4.16. GONTKEVICH, V. S.: Natural Vibrations of Plates and Shells. A. P. Filipov, Ed., *Nauk Dumka* (Kiev), 1964. (Transl. by Lockheed Missiles and Space Co.)
 - 4.17. GONTKEVICH, V. S.: Natural Vibrations of Shells in a Liquid. *Naukova Dumka*, Kiev, 1964. (In Russian.)
 - 4.18. MAZURKIEWICZ, Z.: A Certain Solution of the Problem of Vibrations and Bending of Shells with Variable Curvatures. *Bulletin de L'academie, Polonaise des Sciences, Série des Sciences Techniques*, vol. 15, no. 6, 1967, pp. 379-389.

Conical Shells

A conical shell has a middle surface which is generated by a straight line (called the "generator") which moves so that one point on the line (the vertex) is always fixed. For the practical purposes of this work, the shell will be limited to finite length; that is, the middle surface is generated by a line segment of length s_2 , having one end fixed, while the other end generates a curve in space (see fig. 5.1). If the generator rotates about a fixed axis, so that a constant angle α (vertex half-angle) is kept with respect to the fixed axis, then the resulting surface of revolution is a *circular* cone. If the generator of a circular cone retains constant length as it rotates about the axis, its end forms a circle arc, called the base or large end of the cone. The base can also be regarded as being the intersection of the conical surface with a plane. If the plane is perpendicular to the axis of the cone, the surface describes a *right* circular cone. Finally, if the cone is bounded by two planes ($s = s_1$ and $s = s_2$ in fig. 5.1), then

the surface is a *frustum* of a cone; otherwise, for a shell containing the vertex (i.e., having an *apex*) the term "complete conical shell" will be used here. This chapter is organizationally limited to shells having *circular* conical curvature. Furthermore, no results have been found in the literature for conical shells having noncircular boundaries; thus, the scope of the chapter is further limited.

The class of conical shells described above is a simple generalization of circular cylindrical shells. Put in another way, the cylindrical shells discussed in chapters 2 and 3 are the special case arising when the vertex half-angle α is zero. Thus, conical shells have all the classifying parameters of cylindrical shells described at the beginning of chapter 2 and in the separate sections of chapter 3, with α being an additional parameter. Thus, the primary organization of chapters 2 and 3 (i.e., boundary conditions and complicating effects) is repeated here, with α being treated as one more geometrical parameter to be considered in each problem discussed.

However, if the reader correlates the following sections of this chapter with those of chapters 2 and 3 the following will be readily noted:

- (1) No specific results exist in the literature for *open* conical shells (see sec. 5.4).
- (2) No information is available for conical shells of variable thickness.

One unfortunate (and unnecessary) complication which exists for conical shells is that there is no significant agreement among authors as to the proper nondimensional form for expression of the frequency parameter. This is due partly to disagreement on what constitutes the *fundamental* length parameters for a shell. That is, should one use $s_2 - s_1$ or l (see figs. 5.1 and 5.2)? Should one describe the radius by R_1 , R_2 , \bar{R} (the average

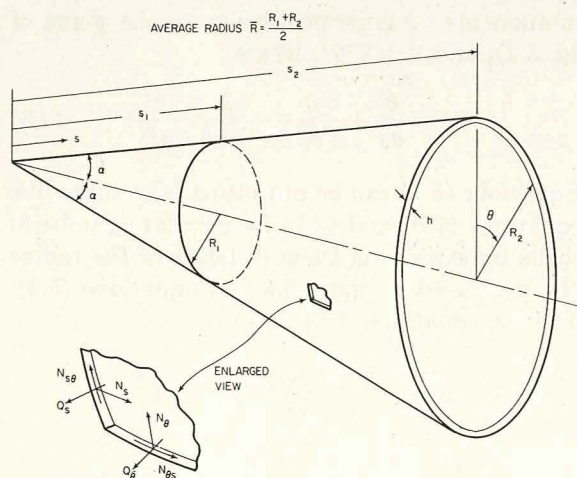


FIGURE 5.1.—Right circular conical shell, showing conventional force resultants.

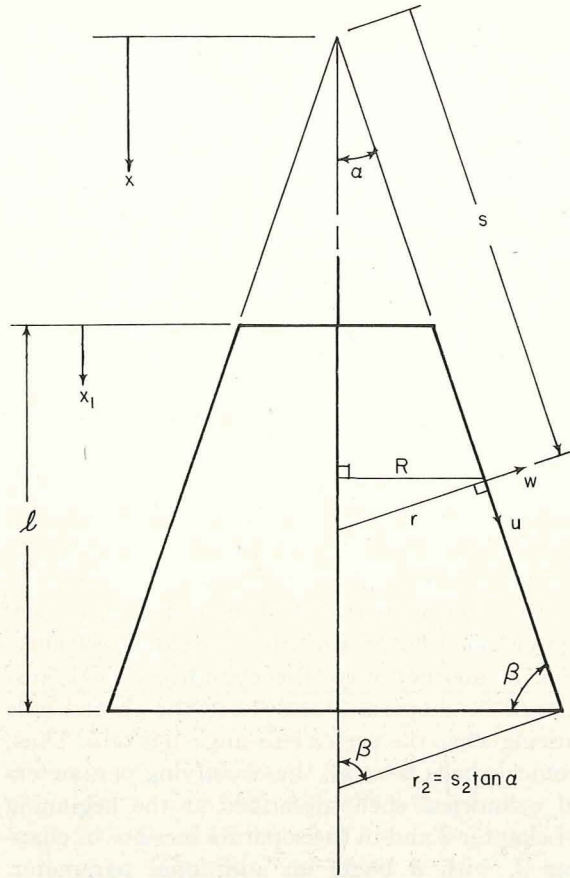


FIGURE 5.2.—Conical shell, side view.

radius, $(R_1 + R_2)/2$, r_1 , r_2 , or \bar{r} ($\bar{r} = (r_1 + r_2)/2$)? Additional choices for frequency parameters arise because of the choice of elastic constants. Thus, at least a dozen distinct forms of nondimensional frequency parameters have been found in the literature and are used in this chapter.

Finally, it should be mentioned that rudimentary surveys of the literature of free vibrations of conical shells are given in references 5.1, 5.2, and 5.3.

5.1 EQUATIONS OF MOTION

The shell coordinates to be used are s and θ as shown in figure 5.1. Following the procedure outlined in section 1.7 the equations of motion are synthesized for a conical shell by using the following parameters in tables 1.1 through 1.5 (see fig. 5.2):

$$\left. \begin{aligned} \alpha &= s, & \beta &= \theta \\ A &= 1, & B &= R = s \sin \alpha \\ R_\alpha &= \infty, & R_\beta &= r = s \tan \alpha \end{aligned} \right\} \quad (5.1)$$

In the case of the Donnell-Mushtari theory the equations of motion are found to be (cf., refs. 5.4 and 5.5)

$$\begin{aligned} & \left[\frac{\partial^2 u}{\partial s^2} + \frac{1}{s} \frac{\partial u}{\partial s} + \frac{(1-\nu)}{2} \frac{1}{s^2 \sin^2 \alpha} \frac{\partial^2 u}{\partial \theta^2} - \frac{u}{s^2} \right] \\ & + \left[\frac{(1+\nu)}{2} \frac{1}{s \sin \alpha} \frac{\partial^2 v}{\partial s \partial \theta} - \frac{(3-\nu)}{2} \frac{1}{s^2 \sin \alpha} \frac{\partial v}{\partial \theta} \right] \\ & + \frac{1}{\tan \alpha} \frac{1}{s^2} \left[\nu s \frac{\partial w}{\partial s} - w \right] = \frac{\rho(1-\nu^2)}{E} \frac{\partial^2 u}{\partial t^2} \quad (5.2a) \end{aligned}$$

$$\begin{aligned} & \left[\frac{(1+\nu)}{2} \frac{1}{s \sin \alpha} \frac{\partial^2 u}{\partial s \partial \theta} + \frac{(3-\nu)}{2} \frac{1}{s^2 \sin \alpha} \frac{\partial u}{\partial \theta} \right] \\ & + \left[\frac{(1-\nu)}{2} \frac{\partial^2 v}{\partial s^2} + \frac{1}{s^2 \sin^2 \alpha} \frac{\partial^2 v}{\partial \theta^2} \right] \\ & + \frac{(1-\nu)}{2} \frac{1}{s} \frac{\partial v}{\partial s} - \frac{(1-\nu)}{2} \frac{v}{s^2} \\ & + \left[\frac{\cos \alpha}{s^2 \sin^2 \alpha} \frac{\partial w}{\partial \theta} \right] = \frac{\rho(1-\nu^2)}{E} \frac{\partial^2 v}{\partial t^2} \quad (5.2b) \end{aligned}$$

$$\begin{aligned} & \frac{1}{\tan \alpha} \frac{1}{s^2} \left[\nu s \frac{\partial u}{\partial s} + u \right] + \left[\frac{\cos \alpha}{s^2 \sin^2 \alpha} \frac{\partial v}{\partial \theta} \right] \\ & + \left[\frac{w}{s^2 \tan^2 \alpha} + \frac{h^2}{12} \nabla^4 w \right] = -\frac{\rho(1-\nu^2)}{E} \frac{\partial^2 w}{\partial t^2} \quad (5.2c) \end{aligned}$$

where u , v , and w are the components of displacement in the s , θ , and z directions, respectively (see fig. 5.2 for true-length views of u and w components— v is perpendicular to the plane of fig. 5.2), and $\nabla^4 = \nabla^2 \nabla^2$, where

$$\nabla^2 \equiv \frac{\partial^2}{\partial s^2} + \frac{1}{s} \frac{\partial}{\partial s} + \frac{1}{s^2 \sin^2 \alpha} \frac{\partial^2}{\partial \theta^2} \quad (5.3)$$

Equations (5.2) can be put into a form more like equations (2.3) and (2.7) for circular cylindrical shells by expressing them in terms of the radius $R = R(s)$ used in figure 5.2 and equations (5.1). That is, equations (5.2) become

$$\begin{aligned} & \left[\frac{\partial^2 u}{\partial \bar{s}^2} + \sin \alpha \frac{\partial u}{\partial \bar{s}} + \frac{(1-\nu)}{2} \frac{\partial^2 u}{\partial \theta^2} - \sin^2 \alpha u \right] \\ & + \left[\frac{(1+\nu)}{2} \frac{\partial^2 v}{\partial \bar{s} \partial \theta} - \frac{(3-\nu)}{2} \sin \alpha \frac{\partial v}{\partial \theta} \right] \\ & + \cos \alpha \left[\nu \frac{\partial w}{\partial \bar{s}} - \sin \alpha w \right] = \frac{\rho(1-\nu^2) R^2}{E} \frac{\partial^2 u}{\partial t^2} \quad (5.4a) \end{aligned}$$

$$\left[\frac{(1+\nu)}{2} \frac{\partial^2 u}{\partial \bar{s} \partial \theta} + \frac{(3-\nu)}{2} \sin \alpha \frac{\partial u}{\partial \theta} \right] + \left[\frac{(1-\nu)}{2} \frac{\partial^2 v}{\partial \bar{s}^2} + \frac{\partial^2 v}{\partial \theta^2} + \frac{(1-\nu)}{2} \sin \alpha \frac{\partial v}{\partial \bar{s}} - \frac{(1-\nu)}{2} \sin^2 \alpha v \right] + \left[\cos \alpha \frac{\partial w}{\partial \theta} \right] = \frac{\rho(1-\nu^2)R^2}{E} \frac{\partial^2 v}{\partial t^2} \quad (5.4b)$$

$$\cos \alpha \left[\nu \frac{\partial u}{\partial \bar{s}} + \sin \alpha u \right] + \left[\cos \alpha \frac{\partial v}{\partial \theta} \right] + [\cos^2 \alpha w + k \bar{\nabla}^4 w] = -\frac{\rho(1-\nu^2)R^2}{E} \frac{\partial^2 w}{\partial t^2} \quad (5.4c)$$

where now

$$\bar{\nabla}^2 = \frac{\partial^2}{\partial \bar{s}^2} + \sin \alpha \frac{\partial}{\partial \bar{s}} + \frac{\partial^2}{\partial \theta^2} = \frac{1}{R^2} \nabla^2 \quad (5.5)$$

and where the nondimensional length, $\bar{s} = s/R$ has been introduced, and where $k = h^2/12R^2$. Letting $\alpha \rightarrow 0$ in equations (5.4) and (5.5), it is clearly seen that they take the forms for circular cylindrical shells, equations (2.7) and (2.8), respectively. Remember, however, that \bar{s} in equations (5.4) and (5.5) corresponds to s in equations (2.7) and (2.8).

The equations of motion of other shell theories (see chapter 1) are obtained by adding certain terms to the left-hand sides of equations (5.2) or (5.4). For example, the equations of the Novozhilov theory result when

$$0 \quad (5.6a)$$

$$\frac{h^2}{12} \left[-\frac{\cos \alpha}{s^3 \sin^3 \alpha} \frac{\partial^3 w}{\partial \theta^3} + (1-2\nu) \frac{\cos \alpha}{s^2 \sin \alpha} \frac{\partial^2 w}{\partial s \partial \theta} - (2-\nu) \frac{\cos \alpha}{s \sin \alpha} \frac{\partial^3 w}{\partial s^2 \partial \theta} \right] \quad (5.6b)$$

$$\frac{h^2}{12} \left[-\frac{\cos \alpha}{s^3 \sin^3 \alpha} \frac{\partial^3 v}{\partial \theta^3} + 3 \frac{\cos \alpha}{s^2 \sin \alpha} \frac{\partial^2 v}{\partial s \partial \theta} - (2-\nu) \frac{\cos \alpha}{s \sin \alpha} \frac{\partial^3 v}{\partial s^2 \partial \theta} \right] \quad (5.6c)$$

are added to equations (5.2a), (5.2b), and (5.2c), respectively (ref. 5.6, and after correcting some obvious errors, ref. 5.7).

The Flügge equations for a conical shell are given in reference 5.8, p. 399. A different set of equations was derived by Pflueger (ref. 5.9) and Federhofer (ref. 5.10) which also reduce to the circular cylindrical shell equations of Flügge (see eqs. (2.9d)) as $\alpha \rightarrow 0$.

Looking at the Donnell-Mushtari equations (5.2) and (5.4), note that they are not symmetric. That is, if they were written in matrix differential operator form as equation (2.7) for cylindrical shells, the matrix operator would be unsymmetric. The terms (5.6b) and (5.6c) added to yield the Novozhilov theory also add to the asymmetry of the equations. The Flügge-type equations given in references 5.8 and 5.10 also contain unsymmetric terms which are multiplied by $h^2/12$. Note that the equations of reference 5.10 were derived by a variational principle.

For the Donnell-Mushtari theory another formulation in terms of an Airy stress function (see sec. 1.9) is often used. Neglecting tangential inertias, the equations of motion and compatibility which must be satisfied are, respectively

$$\left. \begin{aligned} D \nabla^4 w + \nabla_R^2 \varphi &= -\rho h \frac{\partial^2 w}{\partial t^2} \\ \nabla^4 \varphi - E h \nabla_R^2 w &= 0 \end{aligned} \right\} \quad (5.7)$$

where $D = Eh^3/12(1-\nu^2)$, as before, $\nabla^4 = \nabla^2 \nabla^2$ for a conical shell is given by equation (5.3), ∇_R^2 is

$$\nabla_R^2 = \frac{1}{s \tan \alpha} \frac{\partial^2}{\partial s^2} \quad (5.8)$$

the membrane forces are related to the Airy stress function by (cf., refs. 5.11 and 5.12)

$$\left. \begin{aligned} N_s &= \frac{1}{s^2 \sin^2 \alpha} \frac{\partial^2 \varphi}{\partial \theta^2} + \frac{1}{s} \frac{\partial \varphi}{\partial s} \\ N_\theta &= \frac{\partial^2 \varphi}{\partial s^2} \\ N_{s\theta} = N_{\theta s} &= \frac{1}{s \sin \alpha} \left(\frac{1}{s} \frac{\partial \varphi}{\partial \theta} - \frac{\partial^2 \varphi}{\partial s \partial \theta} \right) \end{aligned} \right\} \quad (5.9)$$

the bending moments are related to w by

$$\left. \begin{aligned} M_s &= -D \left[\frac{\partial^2 w}{\partial s^2} + \nu \left(\frac{1}{s} \frac{\partial w}{\partial s} + \frac{1}{s^2 \sin^2 \alpha} \frac{\partial^2 w}{\partial \theta^2} \right) \right] \\ M_\theta &= -D \left[\nu \frac{\partial^2 w}{\partial s^2} + \frac{1}{s} \frac{\partial w}{\partial s} + \frac{1}{s^2 \sin^2 \alpha} \frac{\partial^2 w}{\partial \theta^2} \right] \\ M_{s\theta} = M_{\theta s} &= -\frac{D(1-\nu)}{s \sin \alpha} \left[\frac{\partial^2 w}{\partial s \partial \theta} - \frac{1}{s} \frac{\partial w}{\partial \theta} \right] \end{aligned} \right\} \quad (5.10)$$

and the transverse shearing forces are determined from

$$\left. \begin{aligned} Q_s &= -D \frac{\partial}{\partial s} (\nabla^2 w) \\ Q_\theta &= -\frac{D}{s \sin \alpha} \frac{\partial}{\partial \theta} (\nabla^2 w) \end{aligned} \right\} \quad (5.11)$$

5.2 COMPLETE CONE

The vast majority of numerical results for the free vibrations of conical shells deal with the frustrum of a cone; that is, the conical surface is cut by *two* planes located at distances s_1 and s_2 from the vertex as shown in figure 5.1. In the case of the *complete cone*, the shell includes the vertex and is bounded by a single plane located at $s = s_2$.

The complete cone can also be regarded as the limiting case of a cone frustrum as $s_1 \rightarrow 0$. However, two difficulties are encountered in taking this limit:

- (1) The solutions of the equations of motion contain singularities at $s = 0$.
- (2) Care must be exercised in using the proper boundary conditions at $s = s_1$ to obtain the correct convergence.

The first point will be elaborated upon later in this section where methods of solving the equations of motion are discussed. As an example of the second difficulty, consider the problem of obtaining a free vertex as a limiting case of a cone frustrum. If clamped conditions are applied at $s = s_1$, the vertex becomes fixed in the limit. If free boundary conditions are used, the vertex always has a small hole in it as $s_1 \rightarrow 0$. The correct boundary conditions for a free vertex are (see fig. 5.1 for force resultants)

$$\left. \begin{aligned} v = \frac{\partial w}{\partial s} &= 0 \\ u \sin \alpha - w \cos \alpha &= 0 \\ N_s \cos \alpha - Q_s \sin \alpha &= 0 \end{aligned} \right\} \quad (5.12)$$

whereas, for a completely fixed vertex

$$u = v = w = \frac{\partial w}{\partial s} = 0 \quad (5.13)$$

Other possible types of external *partial* constraint

can exist at a vertex, but these will not be elaborated upon here.

The equations of motion are solved by assuming displacement functions of the form

$$\left. \begin{aligned} u &= \sum_{n=0}^{\infty} u_n(s) \cos n\theta \cos \omega t \\ v &= \sum_{n=1}^{\infty} v_n(s) \sin n\theta \cos \omega t \\ w &= \sum_{n=0}^{\infty} w_n(s) \cos n\theta \cos \omega t \end{aligned} \right\} \quad (5.14)$$

where u_n , v_n , and w_n are yet undetermined functions of the meridional coordinate s . If the shell itself is axisymmetric (e.g., no cutouts) and has axisymmetric boundary conditions, then the vibration modes uncouple with respect to θ and the summations can be dropped in equations (5.14).

Substituting equations (5.14) into, for example, equations (5.2) yields an eighth order set of *ordinary* differential equations having variable coefficients which must be integrated in order to determine u_n , v_n , and w_n . However, equations (5.2) show that the variable coefficients which arise are all powers of s . This suggests a solution in terms of power series which, if convergent, will be exact.

Using the classical method of Frobenius, solutions for u_n , v_n , and w_n are assumed in the form

$$\left. \begin{aligned} u &= s^j \sum_{i=0}^{\infty} a_i s^i \\ v &= s^j \sum_{i=0}^{\infty} b_i s^i \\ w &= s^j \sum_{i=0}^{\infty} c_i s^i \end{aligned} \right\} \quad (5.15)$$

Dreher and Leissa (refs. 5.11 and 5.12) also added terms of the type $w = c/ns$ in order to improve convergence. Substituting equations (5.15) into the eighth order set of ordinary differential equations arising from equations (5.2) leads to a set of recursion equations among the coefficients a_i ,

b_i , and c_i and a characteristic equation yielding eight independent roots j . The ultimate result is eight independent constants a_i , b_i , and c_i (corresponding to the eight roots). In the case of a complete shell, four of the constants must be set equal to zero to satisfy regularity conditions at the apex. For a conical frustum, four boundary conditions are written at each edge, yielding an eighth order characteristic determinant for the eigenvalues (frequency parameters).

5.2.1 Clamped Base

The boundary conditions at the clamped base are (see figs. 5.1 and 5.2)

$$u = v = w = \frac{\partial w}{\partial s} = 0 \quad \text{at} \quad s = s_2 \quad (5.16)$$

Dreher and Leissa (refs. 5.11 and 5.12) used the exact solution procedure described in section 5.2 involving expansion of the displacements in

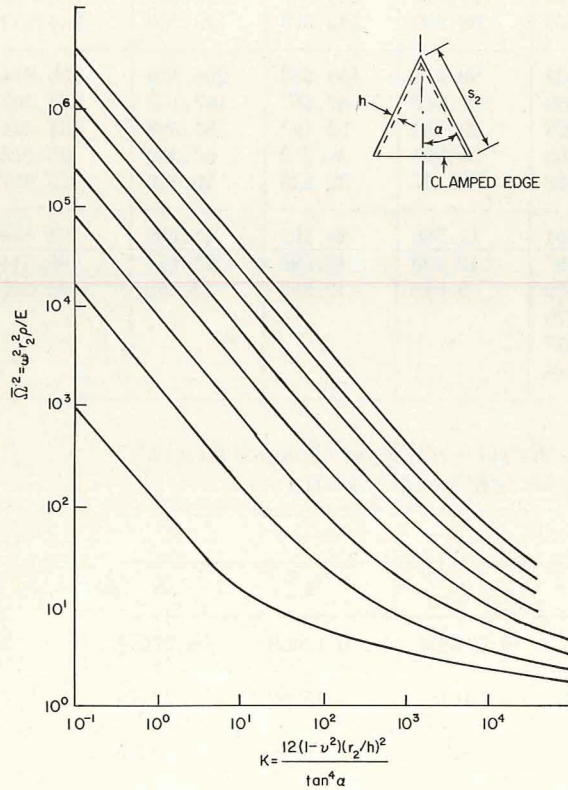


FIGURE 5.3.—Frequency parameter $\bar{\Omega}^2$ versus stiffness parameter K for the axisymmetric ($n=0$) modes of a clamped, complete conical shell. (After ref. 5.12)

terms of power series to study the *axisymmetric* $n=0$ free vibrations. The Donnell-Mushtari shell theory was used. Frequency parameters

$$\bar{\Omega}^2 = \frac{\omega^2 r_2^2 \rho}{E}$$

were obtained for the first eight axisymmetric modes for $\nu=0.3$ and over a wide range of the stiffness parameter $K=12(1-\nu^2)(r_2/h)^2/\tan^4 \alpha$. Numerical results are given in table 5.1 and figure 5.3 in the case where the vertex is free. A representative fundamental (i.e., lowest frequency) mode shape for $w_0(s)$ is shown in figure 5.4 for $K=1000$.

Note that if the parameters K and $\bar{\Omega}^2$ are used, there is no explicit dependence upon α . That is, the values in table 5.1 and figure 5.4 apply to all values of α .

The first solution of the free vibration of the clamped conical shell was presented by Federhofer (ref. 5.10) in 1934. In that paper the equations of motion of Pflueger (see sec. 5.1) were given and the difficulties of their solution in series were acknowledged. Thus, an approximate Ritz solution procedure was followed using the simple trial functions

$$\left. \begin{aligned} u &= A s^2 (s-s_2)^2 \cos n\theta \cos \omega t \\ v &= B s^2 (s-s_2)^2 \sin n\theta \cos \omega t \\ w &= C s^2 (s-s_2)^2 \cos n\theta \cos \omega t \end{aligned} \right\} \quad (5.17)$$

Although not mentioned in reference 5.10, equations (5.17) clearly satisfy equations (5.13) for a

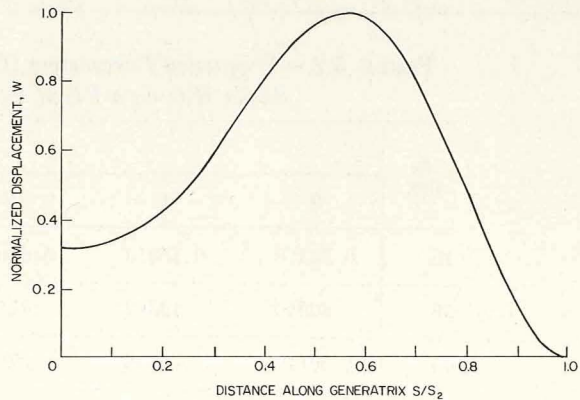


FIGURE 5.4.—Fundamental mode shape for a clamped, complete conical shell; $K=1000$, $\bar{\Omega}^2=3.574$, $\nu=0.3$. (After ref. 5.12)

TABLE 5.1.—Frequency Parameters $\bar{\Omega}^2 = \omega^2 r_2^2 \rho / E$ for the Axisymmetric ($n=0$) Modes of a Clamped, Complete Conical Shell Having a Free Vertex; $\nu=0.3$

$\frac{12(1-\nu^2)}{\tan^4 \alpha} \left(\frac{r_2}{h}\right)^2$	Mode number							
	1	2	3	4	5	6	7	8
0.1	1049.661	15826.797	79409.734	250241.404	610145.734			
.2	527.844	7918.076	39711.992	125130.175	305084.828	632176.406		
.4	266.933	3963.715	19863.121	62574.560	152554.375	316102.574	585364.445	998330.648
.6	179.961	2645.594	13246.830	41722.688	101710.891	210744.633	390254.223	665565.555
.8	136.474	1586.533	9938.685	31296.752	76289.147	158065.660	292699.094	499184.832
1	110.380	1591.096	7953.797	25041.191	61036.103	126458.276	234166.008	399354.262
2	58.184	800.221	3984.021	12530.067	30530.011	63243.509	117099.869	199696.465
4	32.065	404.779	1999.131	6274.503	15276.964	31636.125	58566.789	99867.565
6	23.341	272.961	1337.498	4189.313	10192.614	21100.329	39055.760	66591.354
8	18.966	207.048	1006.680	3146.717	7650.438	15832.430	29300.247	49953.068
10	16.330	167.498	808.187	2521.158	6125.132	12671.691	23446.939	39970.209
20	10.986	88.373	411.190	1270.032	3074.514	6350.207	11740.318	20004.372
40	8.154	48.740	212.654	644.445	1549.189	3189.454	5887.000	10021.464
60	7.095	35.457	146.435	435.891	1040.732	2135.858	3935.885	6693.822
80	6.498	28.757	113.291	331.592	786.489	1609.050	2960.321	5029.993
100	6.096	24.688	93.373	268.994	633.932	1292.957	2374.976	4031.699
200	5.082	16.215	53.268	143.621	328.704	660.693	1204.233	2035.051
400	4.317	11.373	32.522	80.395	175.715	344.299	618.675	1036.591
600	3.957	9.453	25.098	58.810	124.310	238.530	423.266	703.603
800	3.733	8.366	21.116	47.674	98.282	185.378	325.356	536.952
1000	3.574	7.648	18.575	40.764	82.415	153.263	266.425	436.814
2000	3.148	5.950	12.872	25.869	49.249	87.487	147.106	235.268
4000	2.800	4.805	9.353	17.208	30.785	52.127	84.598	131.544
6000	2.625	4.302	7.922	13.863	23.897	39.272	62.330	95.218
8000	2.511	4.000	7.102	12.008	20.167	32.428	50.619	76.297
10000	2.429	3.792	6.554	10.801	17.780	28.107	43.299	64.554
20000	2.200	3.256	5.229	7.997	12.400	18.596	27.471	39.514
40000	2.008	2.845	3.302	6.162	9.040	12.883	18.259	25.297
60000	1.911	2.646	3.883	5.379				
80000	1.848	2.521	3.627	4.917				
100000	1.802	2.431	3.449	4.604				

TABLE 5.2.—Frequency Parameters $\Omega^{*2} = \omega^2 R_2^2 \rho (1-\nu^2) / E$ for Clamped Conical Shells Having a Fixed Vertex; $h^2/12R_2^2 = 10^{-5}$, $\nu=0.3$

β , deg.	n					
	0	1	2	3	4	5
15	0.22318	0.15413	0.080113	0.071504	0.12968	0.27698
30	.80040	.49382	.21578	.13198	.15980	.29174
45	1.50149	.72558	.27640	.15463	.16841	.29213
60	1.76599	.54498	.19263	.11399	.14290	.27154
75	.73942	.15492	.059238	.051842	.10576	.24464

fixed vertex. Minimizing the functional with respect to A , B , and C the resulting characteristic determinant for the frequencies was in the form:

$$\begin{vmatrix} 2a_{11} & a_{12} & a_{13} \\ a_{12} & 2a_{22} & a_{23} \\ a_{13} & a_{23} & 2a_{33} \end{vmatrix} = 0 \quad (5.18)$$

where

$$\begin{aligned} a_{11} &= \left[\frac{11}{56} \tan^2 \alpha + \frac{3}{56} \left(\frac{1-\nu}{2} \right) \left(\frac{n}{\cos \alpha} \right)^2 \gamma_n \right] - \frac{1}{84} \Omega^2 \\ &\quad + k \left[\frac{1}{2} \tan^2 \alpha + \frac{1}{2} \left(\frac{1-\nu}{2} \right) \left(\frac{n}{\cos \alpha} \right)^2 \gamma_n \right] \\ a_{22} &= \left[\frac{11}{56} \left(\frac{1-\nu}{2} \right) \gamma_n \tan^2 \alpha + \frac{3}{56} \left(\frac{n}{\cos \alpha} \right)^2 \right] \\ &\quad - \frac{1}{84} \gamma_n \Omega^2 + k \left[\frac{3}{2} \left(\frac{1-\nu}{2} \right) \gamma_n \tan^2 \alpha \right] \\ a_{33} &= \frac{3}{56} - \frac{1}{84} \Omega^2 + k \left[7 \tan^4 \alpha + \tan^2 \alpha + \frac{1}{2} \right. \\ &\quad \left. - \left(\frac{n}{\cos \alpha} \right)^2 (1-\nu)(1-\gamma_n) \tan^2 \alpha \right. \\ &\quad \left. + \frac{1}{2} \left(\frac{n}{\cos \alpha} \right)^4 - \left(\frac{n}{\cos \alpha} \right)^2 \right] \\ a_{12} &= \frac{3}{28} \left(\frac{n}{\cos \alpha} \right) \tan \alpha \\ &\quad + \frac{3}{56} (1-\nu) \left(\frac{n}{\cos \alpha} \right) \gamma_n \tan \alpha \\ a_{13} &= -\frac{3}{28} \tan \alpha \\ &\quad + k \left[-\tan^3 \alpha + \left(\frac{n^2}{\cos^2 \alpha} - 1 \right) \tan \alpha \right] \\ a_{23} &= -\frac{3}{28} \left(\frac{n}{\cos \alpha} \right) - k \left[\nu \left(\frac{n}{\cos \alpha} \right) \tan^2 \alpha \right. \\ &\quad \left. + \frac{3}{2} (1-\nu) \left(\frac{n}{\cos \alpha} \right) \gamma_n \tan^2 \alpha \right] \end{aligned} \quad (5.19)$$

where

$$\begin{aligned} \gamma_n &= 0 & \text{for} & & n &= 0 \\ \gamma_n &= 1 & \text{for} & & n &\neq 0 \end{aligned}$$

and $\Omega^2 = \omega^2 r_2^2 \rho (1-\nu^2)/E$ and $k = h^2/12r_2^2$. Numerical results obtained in reference 5.10 for the lowest roots of equation (5.18) are presented in table 5.2 and figure 5.5 for shells having a thickness ratio of $h^2/12R_2^2 = k/\cos^2 \alpha = 10^{-5}$ and $\nu = 0.3$ and for $\beta = 15^\circ, 30^\circ, 45^\circ, 60^\circ, 75^\circ$ ($\beta = 90^\circ - \alpha$, as in figure 5.2). The frequency parameter used in

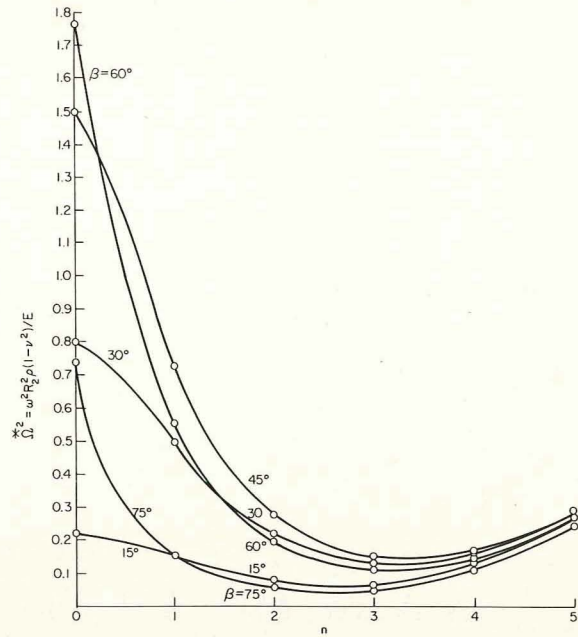


FIGURE 5.5.—Frequency parameters Ω^{*2} for clamped conical shells having a fixed vertex; $h^2/12R_2^2 = 10^{-5}$, $\nu = 0.3$. (After ref. 5.10)

table 5.2 and figure 5.5 is $\Omega^{*2} = \omega^2 R_2^2 \rho (1-\nu^2)/E$ (see fig. 5.1 for R_2). As for circular cylindrical shells, the fundamental frequency does not occur for $n=0$ but, for this value of k , at $n=3$ for all β . In figure 5.6 the frequency parameter is plotted versus β and $\tan \beta$. Amplitude ratios A/C and B/C corresponding to the roots Ω^{*2} for $n=0$ and $n=3$ are given in table 5.3. For $n=0$ the fundamental mode changes from predominantly transverse motion to predominantly meridional as β increases. Many of the previously given results are also discussed in reference 5.13.

TABLE 5.3.—Amplitude Ratios for Clamped Conical Shells Having a Fixed Vertex; $h^2/12R_2^2 = 10^{-5}$, $\nu = 0.3$

β , deg.	n		
	0	3	
	A/C	A/C	B/C
15	0.07416	-0.009611	0.07996
30	.1684	-.02094	.1584
45	.3334	-.03241	.2305
60	.8261	-.03703	.2876
75	3.075	-.02602	.3223

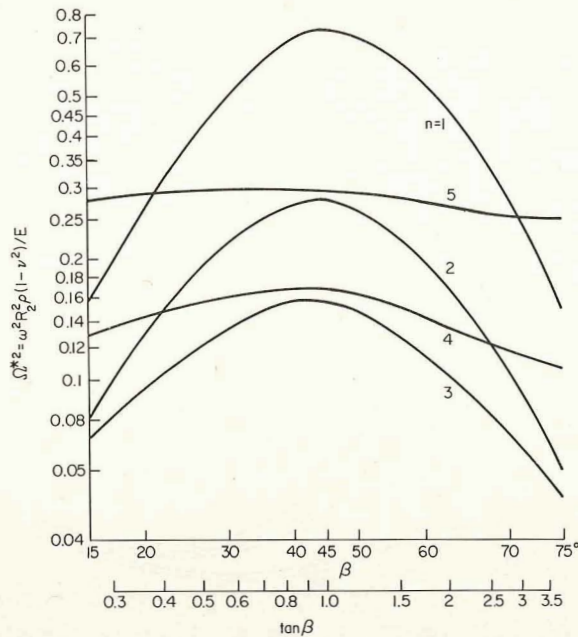


FIGURE 5.6.—Frequency parameter Ω^{*2} versus β for clamped conical shells having a fixed vertex; $h^2/12R_2^2 = 10^{-5}$, $\nu = 0.3$. (After ref. 5.10)

For purposes of comparison, frequency parameters for clamped conical shells were also presented in references 5.11 and 5.12 which were obtained using Kalnins' (ref. 5.14) numerical integration scheme for shells of revolution. The results are listed in table 5.4. It was necessary to use slightly different conditions at the apex ($N_s = Q_s = dw/ds = 0$, rather than eqs. (5.12)). Twenty equal segments were used, except for $\alpha = 35^\circ$, where fifty equal segments were used. Values obtained from numerical integration

TABLE 5.4.—Comparison of Frequency Parameters for the Complete Conical Shell Having a Clamped Base and a Free Vertex

α , deg.	$K = \frac{12(1-\nu^2)}{\tan^4 \alpha} \left(\frac{r_2}{h}\right)^2$	$\bar{\Omega}^2 = \omega^2 r_2^2 \rho / E$	
		Exact method	Numerical integration
75	10^3	3.574	3.538
65	10^3	3.574	3.471
45	10^4	2.429	2.384
35	10^4	2.429	2.431
15	10^5	1.802	1.898
10	10^5	1.802	1.736

should be less than the exact values because the conditions used at the apex are less rigid. For small vertex angle the exact solution results may be inaccurate because of limitations of the Donnell-Mushtari theory. The numerical inte-

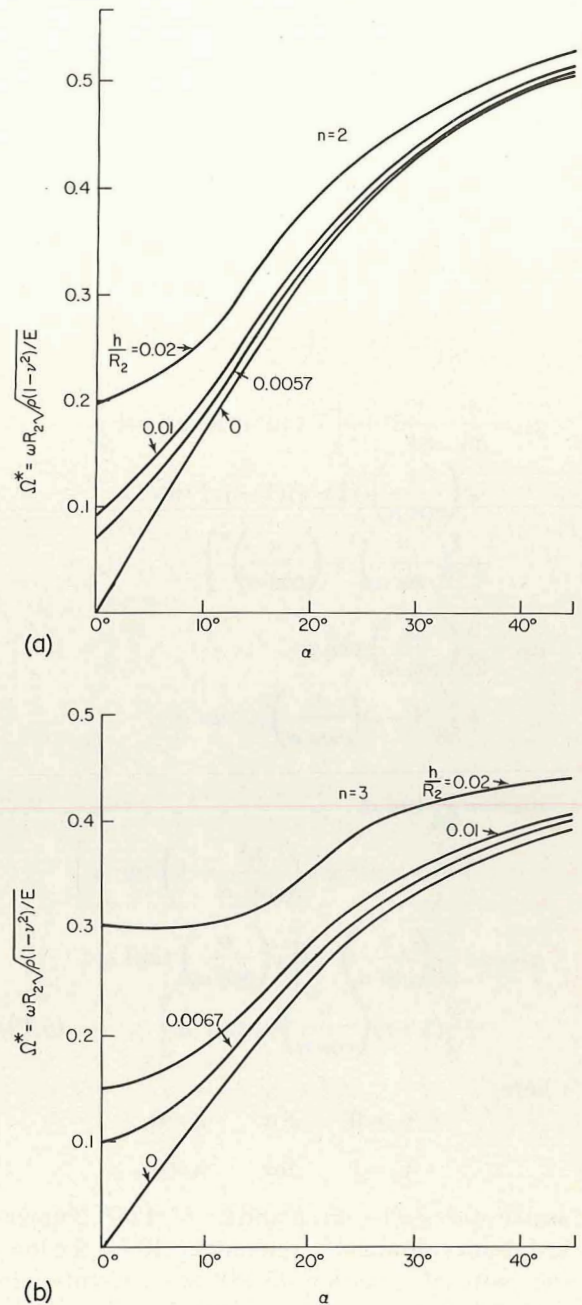


FIGURE 5.7.—Frequency parameter Ω^* for clamped conical shells (vertex conditions not known). (After ref. 5.3) (a) $n=2$. (b) $n=3$. (c) $n=4$. (d) $n=5$. (e) $n=6$.

gration method obviously yields frequency parameters which depend upon K and α explicitly.

The Ritz method was used by Gontkevich (ref. 5.3) to obtain extensive numerical results for clamped conical shells as shown in figures 5.7. The trial functions used were not given, nor was it stated whether the vertex was clamped or free, and Poisson's ratio is not known.

Kolman (ref. 5.7) used the Novozhilov theory and showed that the frequency parameters for the axisymmetric ($n=0$) *torsional* modes of a clamped shell having a fixed vertex are the roots of the equation

$$J_1(\tilde{\Omega}) = 0 \quad (5.20)$$

where $\tilde{\Omega} = \omega s_2 \sqrt{2\rho(1+\nu)/E}$, and J_1 is the Bessel function of the first kind. That is, $\tilde{\Omega}$ is independent of α .

In reference 5.5 the "method of parallel springs" (which is equivalent to the Southwell method) is demonstrated for a conical shell having a clamped base and vertex and having two particular sets of dimensions: $\alpha = 30^\circ$, $s_2 = 30$ cm., $h = 0.33$ mm. and 0.71 mm., $E = 2.05 \times 10^6$ kg/cm², $\rho = 7.95 \times 10^{-6}$ kg-sec²/cm⁴, and $\nu = 0.30$. Circular frequencies ω are shown for the two thicknesses in figure 5.8. Experimental data are also shown.

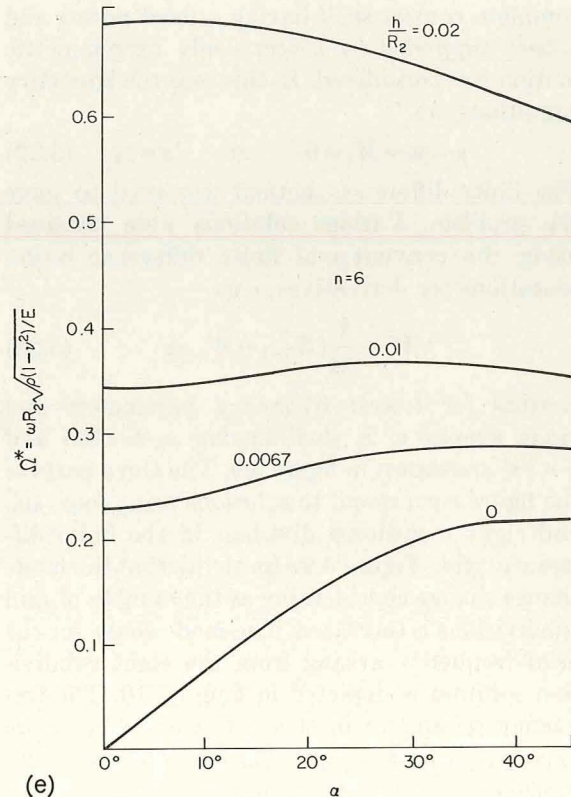
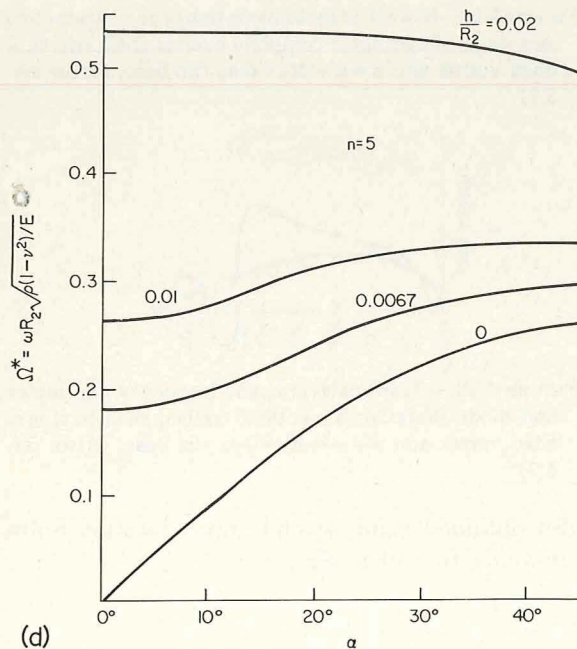
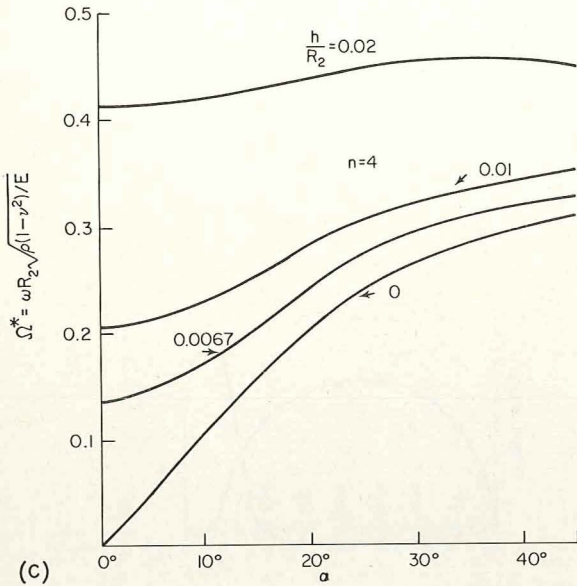


FIGURE 5.7.—Concluded.

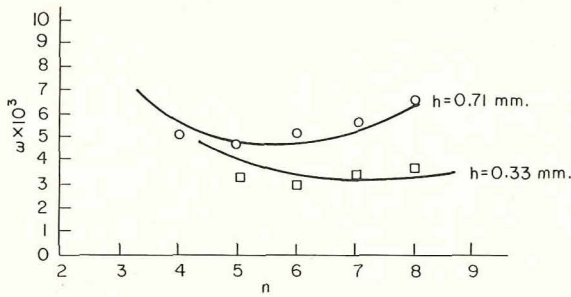


FIGURE 5.8.—Circular frequencies for a conical shell having a clamped base and vertex (dimensions given in text). (After ref. 5.5)

5.2.2 Base Supported by a Shear Diaphragm

The boundary conditions at the base of a conical shell supported by a shear diaphragm are (see figs. 5.1 and 5.2)

$$N_s = v = w = M_s = 0 \quad \text{at} \quad s = s_2 \quad (5.21)$$

where M_s is the meridional moment resultant. Strangely, this problem has no known solution in the literature of free vibrations.

Kolman (ref. 5.7) addressed the problem of the complete conical shell having a fixed vertex and a base supported by hinges. Only axisymmetric motion was considered. In this case the boundary conditions are

$$u = w = M_s = 0 \quad \text{at} \quad s = s_2 \quad (5.22)$$

The finite difference method was used to solve the problem. Various solutions were obtained using the conventional finite difference representations for derivatives; e.g.,

$$W' = \frac{1}{2\Delta} (W_{i+1} - W_{i-1}) \quad (5.23)$$

Results for lowest frequency parameters and mode shapes of a shell having $s_2/h = 400$ and $\alpha = 30^\circ$ are shown in figure 5.9. The three parts of the figure correspond to solutions using four, six, and eight meridional divisions in the finite difference grid. Figure 5.9 also shows that the mode shapes change considerably as the number of grid subdivisions is increased. The mode shape for the third frequency arising from the eight subdivision solution is depicted in figure 5.10. The frequency parameter in this case was found to be $\omega s_2 \sqrt{2\rho(1+\nu)/E} = 2.37$, whereas for four subdivisions the value found was 3.52.

In reference 5.7 improved accuracy results were

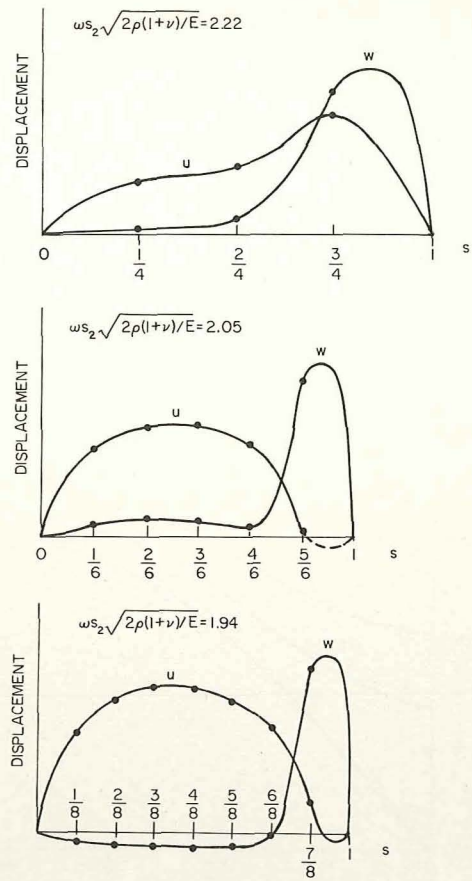


FIGURE 5.9.—Lowest axisymmetric frequency parameters and mode shapes for a complete conical shell having a fixed vertex and $u = w = M_s = 0$ at the base. (After ref. 5.7)

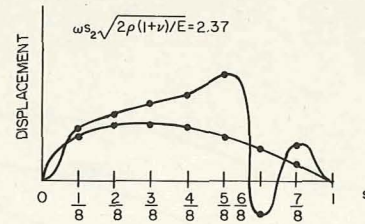


FIGURE 5.10.—Third axisymmetric frequency parameter and mode shape for a complete conical shell having a fixed vertex and $u = w = M_s = 0$ at the base. (After ref. 5.7)

also obtained using second approximation finite difference formulas; e.g.,

$$W' = \frac{1}{12\Delta} (-W_{i+2} + 8W_{i+1} - 8W_{i-1} + W_{i-2}) \quad (5.24)$$

A six subdivision solution for the problem described above was obtained using this approach. The resulting frequency parameter and mode shape is shown in figure 5.11, and can be

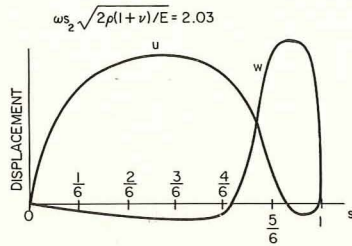


FIGURE 5.11.—Lowest frequency parameter and mode shape from a second approximation difference method. (After ref. 5.7)

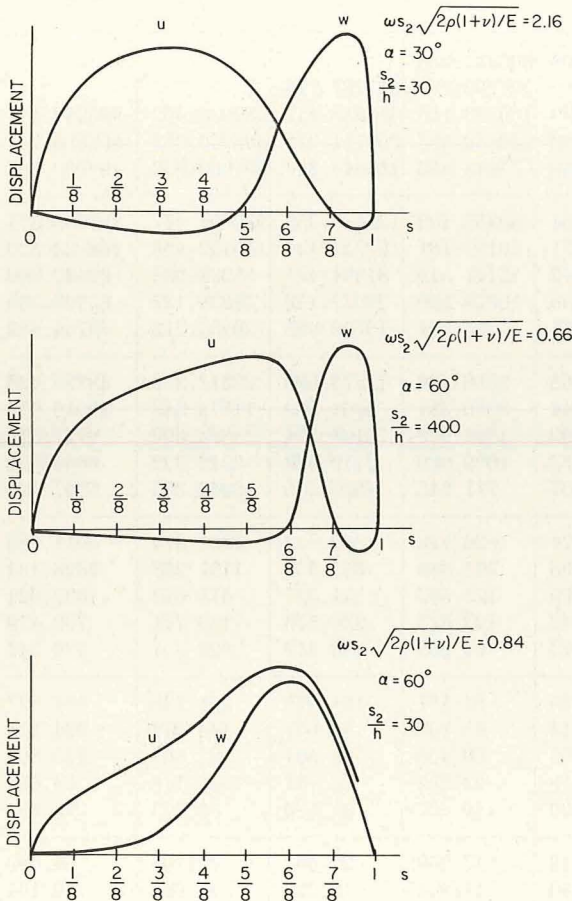


FIGURE 5.12.—Lowest axisymmetric frequency parameters and mode shapes for complete conical shells having fixed vertices and $u=w=M_s=0$ at the base. (After ref. 5.7)

compared with figure 5.9. Some results obtained by this improved method for shells having other s_2/h ratios and semivertex angles α are displayed in figure 5.12. As pointed out in reference 5.7 the free vibration mode shapes differ sharply from the deflection curves of the same shells loaded by uniform static pressure, and that the frequency parameters approach the true values from either above or below as more subdivisions are used, depending upon s_2/h and α .

Miller and Hart (ref. 5.15) obtained results for a particular conical shell having $\alpha = 15^\circ 40'$, $h = 0.0983$ in., and $s_2 = 36.4$ in. as a limiting case of their studies of eigenvalue densities for SD-SD truncated conical shells. Constant values of the frequency parameter $\Omega_4 = \omega s_2 \sqrt{\rho/E}$ are plotted in figure 5.13, where $m\pi s_2/(s_2 - s_1)$ and $n/\sin \alpha$ are the nondimensional meridional and circumferential wave numbers used as coordinates. For further discussion of the basis for this figure see section 5.3.3. In particular note that the displace-

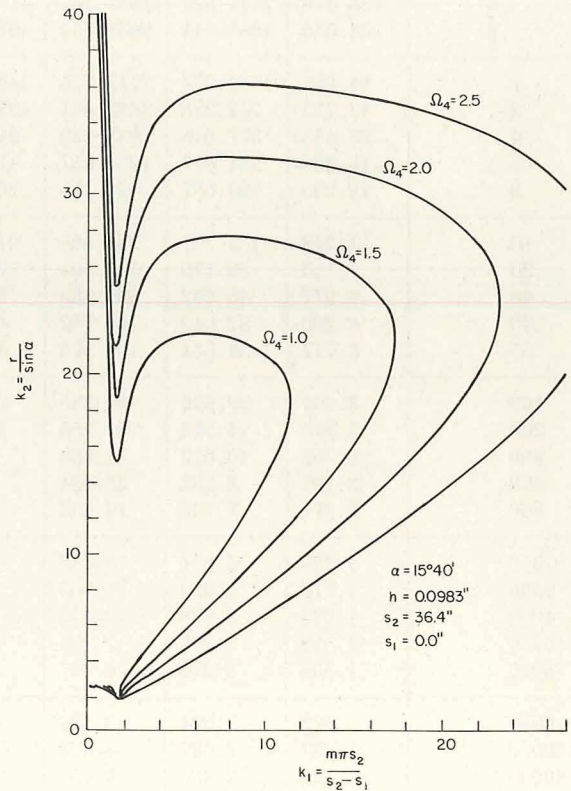


FIGURE 5.13.—Frequency parameter curves in k -space for a complete conical shell supported at its base by a shear diaphragm. (After ref. 5.15)

ment functions used in reference 5.15 satisfy SD conditions at the vertex and only approximate the free vertex conditions (5.12).

5.2.3 Free Base

The boundary conditions for a complete conical shell having a free base are (see figs. 5.1 and 5.2)

$$N_s = S_{s\theta} = V_s = M_s = 0 \quad \text{at} \quad s = s_2 \quad (5.25)$$

where V_s is the Kelvin-Kirchhoff shear defined by

$$V_s = Q_s + \frac{1}{s \sin \alpha} \frac{\partial M_{s\theta}}{\partial \theta} \quad (5.26)$$

and $S_{s\theta}$ is the shear resultant given by

$$S_{s\theta} = N_{s\theta} + \frac{M_{s\theta}}{s \tan \alpha} \quad (5.27)$$

(see sec. 1.8).

Dreher and Leissa (refs. 5.11 and 5.12) used the exact solution procedure described in section 5.2 involving expansion of the displacements in

TABLE 5.5.—Frequency Parameters $\bar{\Omega}^2 = \omega^2 r_2^2 \rho / E$ for the Axisymmetric ($n=0$) Modes of a Completely Free Conical Shell; $\nu=0.3$

$\frac{12(1-\nu^2)}{\tan^4 \alpha} \left(\frac{r^2}{h}\right)^2$	Mode number							
	1	2	3	4	5	6	7	8
0.1	813.785	14787.194	77014.656	245938.408	603381.938			
.2	408.501	7397.796	38514.141	122978.496	301702.750	627287.719		
.4	205.859	3703.096	19263.882	61498.539	150863.156	313658.117	582028.453	993962.414
.6	138.310	2471.529	12847.129	41005.220	100583.293	209114.918	388030.082	662656.211
.8	104.535	1855.744	9638.752	30758.560	75443.360	156843.316	291030.922	497000.527
1	84.269	1486.273	7713.725	24610.564	60359.400	125480.355	232831.467	397608.574
2	43.733	747.328	3863.671	12314.571	30191.481	62754.434	116432.463	198823.529
4	23.453	377.846	1938.639	6166.572	15107.519	31391.471	58232.963	99430.900
6	16.682	254.677	1298.957	4117.236	10079.530	20937.150	38833.127	65300.108
8	13.290	193.087	976.113	2093.566	7565.534	15709.988	29133.212	49734.642
10	11.248	156.127	783.604	2477.763	6056.136	12573.690	23313.259	39795.429
20	7.125	82.170	398.565	1248.144	3040.331	6301.089	11673.353	19916.909
40	4.977	45.092	205.989	633.302	1531.908	3164.774	5853.390	9977.646
60	4.200	32.642	141.742	428.323	1029.080	2119.322	3913.392	6664.550
80	3.777	26.351	109.574	325.807	777.649	1596.585	2943.385	5007.999
100	3.501	22.526	90.235	264.274	626.776	1282.932	2361.374	4014.063
200	2.845	14.548	51.256	141.008	324.899	655.539	1197.288	2026.134
400	2.392	10.012	31.053	78.799	173.552	341.557	615.042	1032.024
600	2.191	8.232	23.824	57.542	122.677	236.576	420.724	700.479
800	2.071	7.230	19.953	46.573	96.908	183.812	323.351	534.541
1000	1.989	6.571	13.487	39.769	81.197	151.925	264.738	434.827
2000	1.779	5.022	11.965	25.113	48.362	86.607	146.044	234.113
4000	1.623	3.988	8.570	16.603	30.100	51.501	83.863	130.802
6000	1.550	3.541	7.193	13.319	23.292	38.741	61.718	94.626
8000	1.505	3.276	6.407	11.500	19.607	31.950	50.073	75.781
10000	1.472	3.094	5.883	10.316	17.250	27.663	42.795	64.090
20000	1.387	2.637	4.623	7.569	11.941	18.229	27.062	39.161
40000	1.320	2.300	3.752	5.776	8.631	12.567	17.907	
60000	1.287	2.143	3.366	5.013				
80000	1.266	2.046	3.134	4.565				
100000	1.251	1.977	2.973	4.260				

terms of power series to study the *axisymmetric* ($n=0$) free vibrations. The Donnell-Mushtari shell theory was used. Frequency parameters $\bar{\Omega}^2 = \omega^2 r_2^2 \rho / E$ were obtained for the first eight axisymmetric modes for $\nu=0.3$ and over a wide range of the stiffness parameter

$$K = 12(1-\nu^2)(r_2/h)^2/\tan^4 \alpha$$

Numerical results are given in table 5.5 and figure 5.14 in the case where the vertex is free.

Bordoni (ref. 5.16) made experimental measurement of vibration frequencies on conical shells made of *paper*, as in the case of loudspeaker diaphragms. The shells were made with various types of seams, as shown in figure 5.15, in order to consider the asymmetry of the vibration modes due to the lap joint seams. One set of experiments was conducted to determine the effect of apex angle α upon the frequencies, keeping the shell thickness h and base radius R_2 constant. The results are summarized by figure 5.16; i.e., it was found that the frequencies did not vary with the

apex angle. The implication of this statement is that the complete conical shell having a fixed vertex and a free base undergoes purely inextensional motion and behaves essentially like a free circular plate. This is contrary to the experience of McLachlan (ref. 5.17) who found the frequency of a certain cone to be 5.1 times greater than that of a corresponding disk. Bordoni also found that the shell frequencies were proportional to the thickness h and the ratio $(E/\rho)^{1/2}$, and were

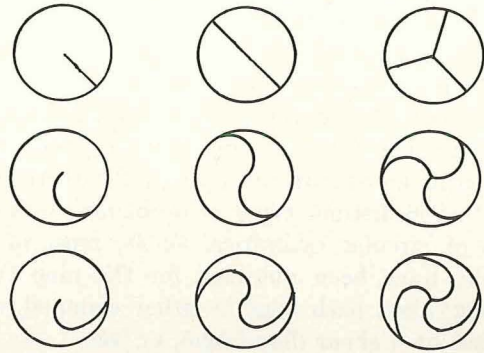


FIGURE 5.15.—Different types of seams. (After ref. 5.16)

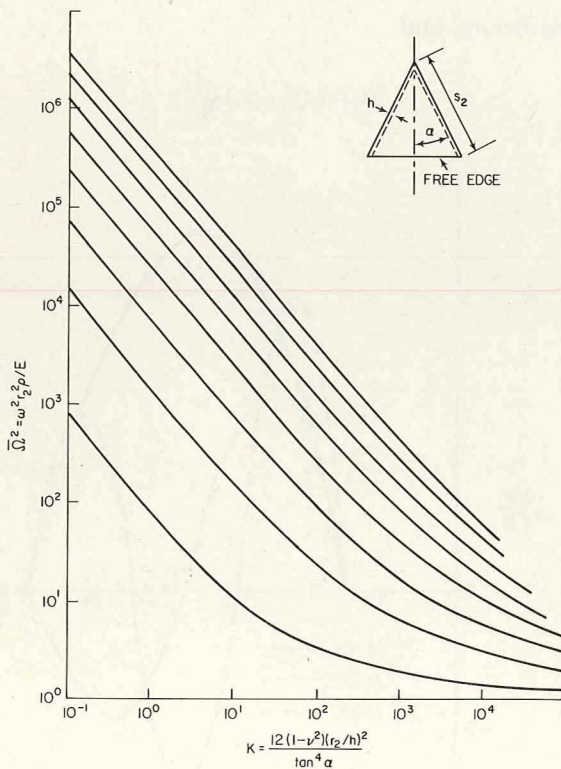


FIGURE 5.14.—Frequency parameter $\bar{\Omega}^2$ versus stiffness parameter K for the axisymmetric ($n=0$) modes of a completely free conical shell. (After ref. 5.12)

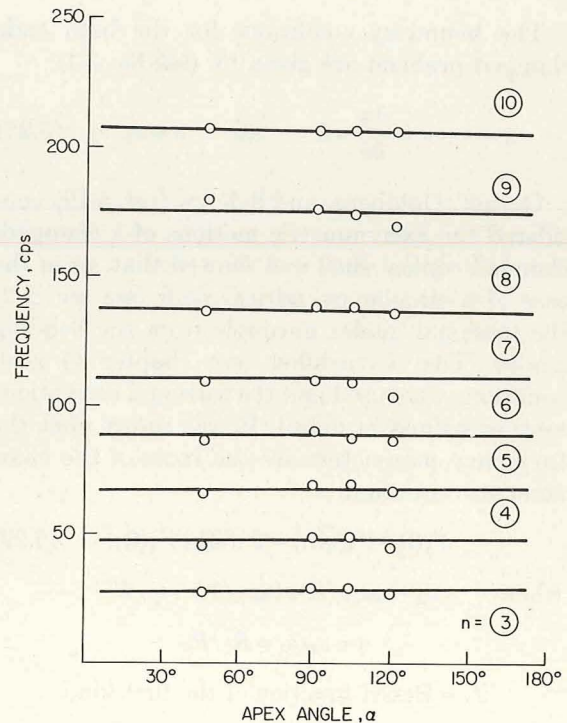


FIGURE 5.16.—Eigenfrequencies of paper cones of same radius and thickness, for different apex angles; n = number of nodal diameters. (After ref. 5.16)

inversely proportional to the square of the base radius.

The free vibration of a complete conical shell having a free base was also investigated in references 5.3 and 5.18.

5.3 FRUSTUM OF A CONE

Consider next the case where the conical shell has two boundaries located at $s = s_1$ and $s = s_2$, the associated radii of the bounding circles being R_1 and R_2 , respectively (see fig. 5.1). In the case of circular cylindrical shells (see sec. 2.4), 136 combinations of "simple" boundary conditions yielding distinct problems exist. However, because for conical shells there is symmetry with respect to the axial mid-plane ($s = (s_1 + s_2)/2$), there exist $(16)^2 = 256$ distinct types of problems. As in the case of circular cylindrical shells, most of the results have been obtained for the nine types arising when each edge is either clamped, supported by a shear diaphragm, or free.

5.3.1 Both Ends Clamped

The boundary conditions for the both ends clamped problem are given by (see fig. 5.1)

$$u = v = w = \frac{\partial w}{\partial s} = 0 \quad \text{at} \quad s = s_1, s_2 \quad (5.28)$$

Garnet, Goldberg, and Salerno (ref. 5.19) considered the axisymmetric motions of a clamped-clamped conical shell and showed that, as in the case of a circular cylindrical shell (see sec. 2.2) the torsional modes uncouple from the bending modes. The Novozhilov (see chapter 1) shell equations were used and the torsional oscillations were examined in detail. It was shown that the frequency parameters are the roots of the characteristic equation

$$J_1(\Omega_1) Y_1(\eta \Omega_1) = J_1(\eta \Omega_1) Y_1(\Omega_1) \quad (5.29)$$

$$\text{where} \quad \Omega_1 = \omega s_1 \rho / G = 2\omega s_1(1 + \nu)\rho / E$$

$$\eta = s_2/s_1 = R_2/R_1$$

J_1 = Bessel function of the first kind

Y_1 = Bessel function of the second kind

Note that Ω_1 does not depend upon the semivertex angle α . The first five roots of equation (5.29) are

reproduced in table 5.6 for values of η from 1 to 50. The mode shapes associated with the first three frequencies for the case $\eta = 10$ are shown in figure 5.17, where $v/\sin \alpha$ is plotted to show the variation of the displacement with s/s_2 . The torsional modes of a clamped-clamped conical shell were also studied in reference 5.20 where the effects of shear deformation and rotary inertia were included (see sec. 5.9.2).

The meridional axisymmetric modes of clamped-clamped conical shells were investigated by Keefe (ref. 5.21). It was assumed that during meridional motion the cross sections of the cone remain plane and that motion occurs *only* in the meridional direction s ; i.e., $w = 0$. This, of course, is an approximation. The actual motion would require coupling between u and w displacements. The following characteristic equation was derived:

$$J_0(\eta \Omega_2) Y_0(\Omega_2) = J_0(\Omega_2) Y_0(\eta \Omega_2) \quad (5.30)$$

where

$$\eta = s_2/s_1 = R_2/R_1$$

as before, and

$$\Omega_2 = \omega(s_2 - s_1) \sqrt{\frac{\rho}{E}}$$

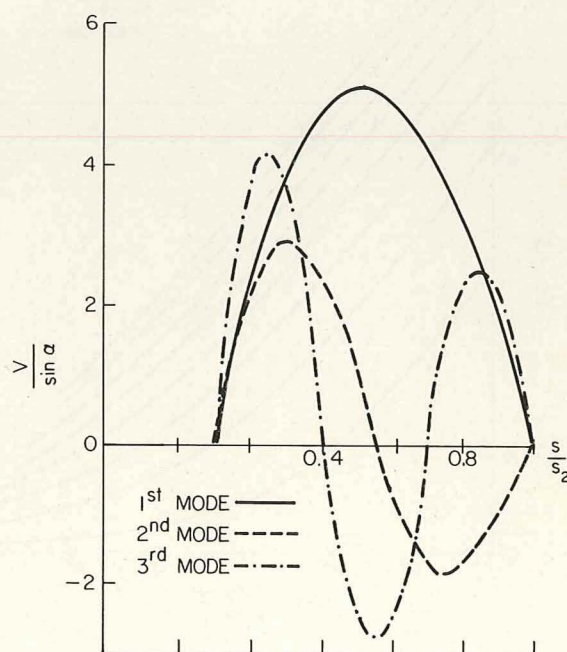


FIGURE 5.17.—Torsional mode shapes of a clamped-clamped conical shell. (After ref. 5.19)

TABLE 5.6.—*First Five Roots of Equation (5.29) for the Axisymmetric Torsional Vibrations of a Clamped-Clamped Conical Shell*

η	$(\eta-1)\Omega_1$				
	First root	Second root	Third root	Fourth root	Fifth root
1.0	3.1416	6.2832	9.4248	12.5664	15.7080
1.1	3.1427	6.2837	9.4251	12.5666	15.7082
1.2	3.1455	6.2852	9.4261	12.5674	15.7088
1.3	3.1498	6.2873	9.4275	12.5684	15.7096
1.4	3.1550	6.2900	9.4293	12.5698	15.7107
1.5	3.1609	6.2931	9.4314	12.5713	15.7119
1.6	3.1675	6.2965	9.4337	12.5731	15.7133
1.8	3.182	6.304	9.439	12.577	15.716
2.0	3.197	6.312	9.444	12.581	15.720
2.5	3.235	6.335	9.460	12.593	15.729
3.0	3.271	6.357	9.476	12.605	15.739
3.5	3.305	6.381	9.493	12.619	15.750
4.0	3.336	6.403	9.509	12.631	15.760
5	3.389	6.445	9.541	12.657	15.782
6	3.432	6.482	9.572	12.682	15.802
8	3.498	6.546	9.626	12.728	15.842
10	3.547	6.598	9.673	12.770	15.879
12	3.583	6.639	9.714	12.807	15.913
14	3.611	6.674	9.749	12.840	15.943
16	3.634	6.704	9.780	12.870	15.971
18	3.652	6.728	9.806	12.896	15.997
20	3.667	6.749	9.830	12.920	16.020
25	3.696	6.790	9.88	12.97	16.07
30	3.717	6.820	9.91	13.01	16.11
35	3.732	6.844	9.94	13.04	16.14
40	3.743	6.861	9.96	13.06	16.17
45	3.752	6.875	9.98	13.09	16.19
50	3.760	6.887	9.99	13.10	16.21

(see fig. 5.1). The first four roots of equation (5.30) are plotted versus the ratio R_1/R_2 in figure 5.18.

Wheeler and Shulman (ref. 5.22) used the Donnell-Mushtari theory along with the Galerkin procedure to obtain approximate solutions for the clamped-clamped conical shell. Vibrating beam functions (see sec. 2.4) were used as trial functions for the displacements. Numerical results were produced for a shell having the following parameters: $\alpha = 10^\circ$ and $\bar{R}/h = 30$, where \bar{R} is the average radius (i.e., $\bar{R} = (R_1 + R_2)/2$). These are shown in figure 5.19 for $n = 6$. In this

figure the frequency parameter $\omega \bar{R} \sqrt{\rho(1-\nu^2)/E}$ is plotted versus the length ratio l/\bar{R} .

The free vibrations of a clamped-clamped conical shell were also discussed in references 5.18, 5.23, 5.24, and 5.25.

5.3.2 Clamped-Shear Diaphragm

The boundary conditions for this problem are: at the clamped edge ($s = s_1$),

$$u = v = w = \frac{\partial w}{\partial s} = 0 \quad (5.31)$$

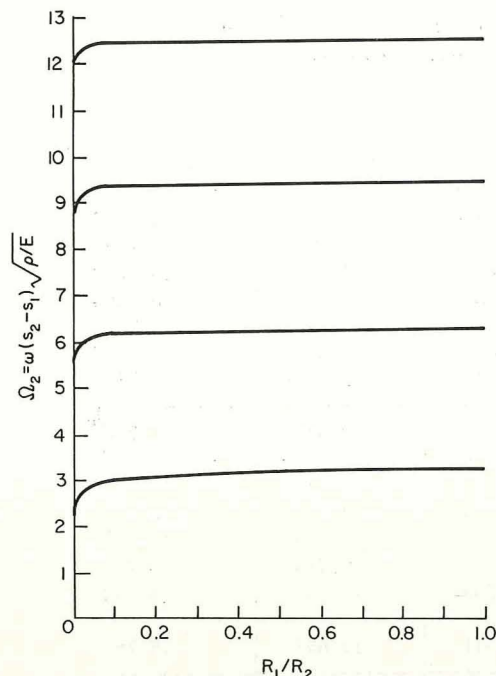


FIGURE 5.18.—Frequency parameters for the axisymmetric meridional motion of a clamped-clamped conical shell. (After ref. 5.21)

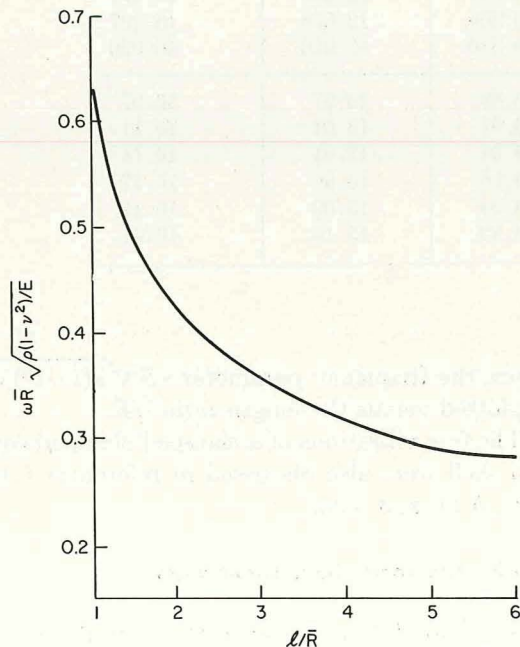


FIGURE 5.19.—Frequency parameters for clamped-clamped conical shells; $\alpha = 10^\circ$, $\bar{R}/h = 30$. (After ref. 5.22)

and at the edge supported by a shear diaphragm ($s = s_2$),

$$N_s = v = w = M_s = 0 \quad (5.32)$$

This assumes that the smaller radius is clamped and the larger one is supported by shear diaphragms. The opposite set of boundary conditions (i.e., SD-clamped) is a distinct class of problems.

The only known work dealing with this problem is that of Saunders, Wisniewski, and Paslay (ref. 5.26) which used Love's equations and the Ritz method to study the case when the smaller radius R_1 is clamped and the larger one R_2 is supported by a shear diaphragm. A solution function for w was chosen as

$$w = C_1[x^3 - (2x_1 + x_2)x^2 + x_1(x_1 + 2x_2)x - x_1^2x_2] \cos n\theta + C_2[x^4 - (3x_1^2 + 2x_1x_2 + x_2^2)x^2 + 2x_1(x_1 + x_2)^2x - x_1x_2^2(2x_1 + x_2)] \cos n\theta \quad (5.33)$$

where x is the axial coordinate, as shown in figure 5.2, and x_1 and x_2 are the boundary values of x at the radii $R = R_1$ and R_2 , respectively. This choice of w satisfies the *geometric* boundary conditions involving w in equations (5.31) and (5.32). The remaining displacements u and v are chosen so that the meridional and circumferential strains are zero. The resulting frequency equation is quite complicated (although reproduced in ref. 5.26). Numerical results were given for a shell having $\alpha = 14^\circ 33'$, $x_1 = 16.57$ in., $x_2 = 25.63$ in., $h = 0.50$ in., and the material properties of annealed copper. Frequencies (cps)

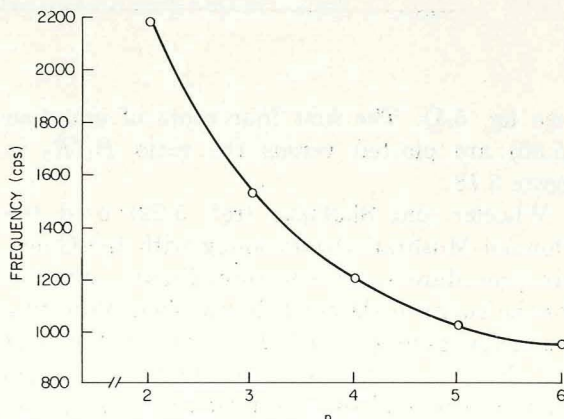


FIGURE 5.20.—Cyclic frequencies for a clamped-SD shell; dimensions in text. (After ref. 5.26)

are shown in figure 5.20 for various numbers of circumferential waves n .

Unlike the case of a clamped-SD circular cylindrical shell (see sec. 2.4.2), no information can be gleaned from the higher modes of a clamped-clamped shell. Nodal circles (i.e., circles having the conditions of equation (5.32)) do not exist for the conical shell because of the lack of symmetry with respect to the plane

$$x = \frac{x_1 + x_2}{2}$$

5.3.3 Both Ends Supported by Shear Diaphragms

The boundary conditions for this problem are

$$N_s = v = w = M_s = 0 \quad \text{at} \quad s = s_1, s_2 \quad (5.34)$$

Assuming solutions for the displacements in the form of equations (5.14), the boundary conditions can be satisfied by various choices of u_n , v_n , and w_n , while the equations of motion can be approximated by, for example, the Ritz or Galerkin procedures (both procedures are equivalent in this problem if the u_n , v_n , w_n satisfy all the boundary conditions). Numerous authors follow procedures of this type to obtain approximate solutions. In such cases, the frequency parameters obtained are upper bounds on the true frequency parameters.

Lindholm and Hu (refs. 5.27 and 5.28) did an extensive study of the problem. A set of shell equations derived by Hu (ref. 5.29) was used along with the Galerkin procedure. The shell equations included the effects of shear deformation and rotary inertia in the meridional direction, but neglected these effects in the circumferential direction. The resulting theory is supposed to be particularly applicable to short shells and small circumferential wave numbers (ref. 5.29) and has the interesting feature of requiring only an eighth order set of equations of motion, rather than a tenth order set as in conventional shear deformation theory. Although shear deformation and rotary inertia are *partially* accounted for, the numerical results obtained in references 5.27 and 5.28 will be discussed because: (1) the theory is of the eighth order, (2) the shells used as numerical examples are not particularly short, nor is the study limited to small n , and (3) this study serves as a basis for comparison with other authors later.

In references 5.27 and 5.28 the displacement components are assumed to take the form

$$u_n = \sum_{m=1}^{M_1} A_m \sin \frac{m\pi\bar{x}}{L} \quad (5.35a)$$

$$v_n = \sum_{m=1}^{M_2} B_m \sin \frac{m\pi\bar{x}}{L} \quad (5.35b)$$

$$w_n = \sum_{m=1}^{M_3} C_m \sin \frac{m\pi\bar{x}}{L} \quad (5.35c)$$

for use in equations (5.14), where \bar{x} and L are dimensionless lengths defined by

$$\left. \begin{aligned} \bar{x} &= \log \left(\frac{s_2}{s} \right) \\ L &= \log (s_2/s_1) \end{aligned} \right\} \quad (5.36)$$

In addition the rotation of the normal to the middle surface in the direction of s can be prescribed independently as

$$\beta_s = \sum_{n=1}^{\infty} \left[e^{v\bar{x}} \left(\frac{D_0}{2} + \sum_{m=1}^{M_4} D_m \cos \frac{m\pi\bar{x}}{L} \right) \right] \cos n\theta \cos \omega t \quad (5.37)$$

in the shell theory used.

Theoretical and experimental results were obtained in references 5.27 and 5.28 for four models made of steel shimstock and having the geometric parameters shown in table 5.7. Poisson's ratio was taken as 0.3. The upper limits of the summations used in equations (5.35) and

TABLE 5.7.—Geometric Parameters for Four Conical Shells

Model number	α , degrees	$\frac{s_2}{s_1}$	$\frac{h}{R_2}$	R_2 , in.
1	14.2	2.23	0.00166	6.07
2	30.2	2.27	.00127	7.95
3	45.1	2.25	.00112	8.96
4	60.5	2.25	.00101	10.00

(5.36) depend upon the accuracy required, but typically $M_1=4$, $M_2=4$, $M_3=5$, $M_4=6$, which yields a characteristic determinant of order 21. For large values of n (24 to 28), a determinant of order 28 was required.

Numerical results for the four shell models described in table 5.7 are depicted in figures 5.21 through 5.24. The divergence between experiment and theory is ascribed in references 5.27 and 5.28 to the difficulty in duplicating the theoretical boundary conditions and due to the finite trunca-

tions of the displacement function series. In figure 5.23 ($\alpha=45.1^\circ$) two theoretical curves are shown. The dashed curve is for a shell having added meridional constraint ($u=0$) at the boundaries. These figures show that for each axial wave number m the *minimum* frequency occurs for some relatively large value of n (>5). This was also seen previously in chapter 2 for circular cylindrical shells.

Mode shapes (w displacements) for the four shell models are depicted in figures 5.25 through

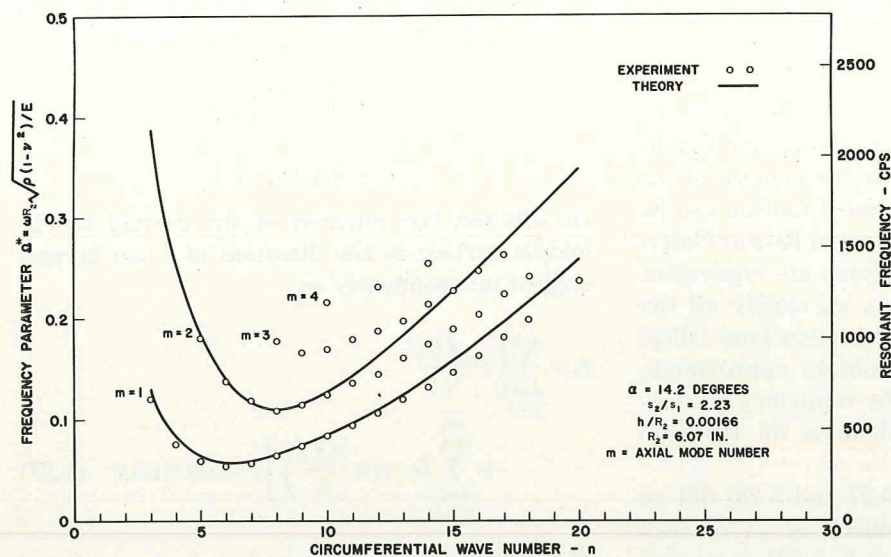


FIGURE 5.21.—Frequencies of an SD-SD conical shell; model 1. (After ref. 5.27)

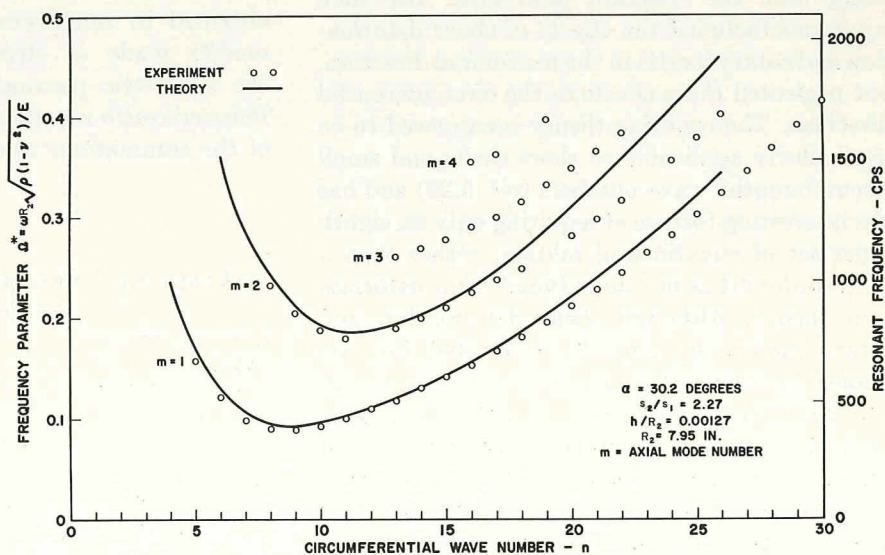


FIGURE 5.22.—Frequencies of an SD-SD conical shell; model 2. (After ref. 5.27)

FIGURE 5.23.—Frequencies of an SD-SD conical shell; model 3. (After ref. 5.27)

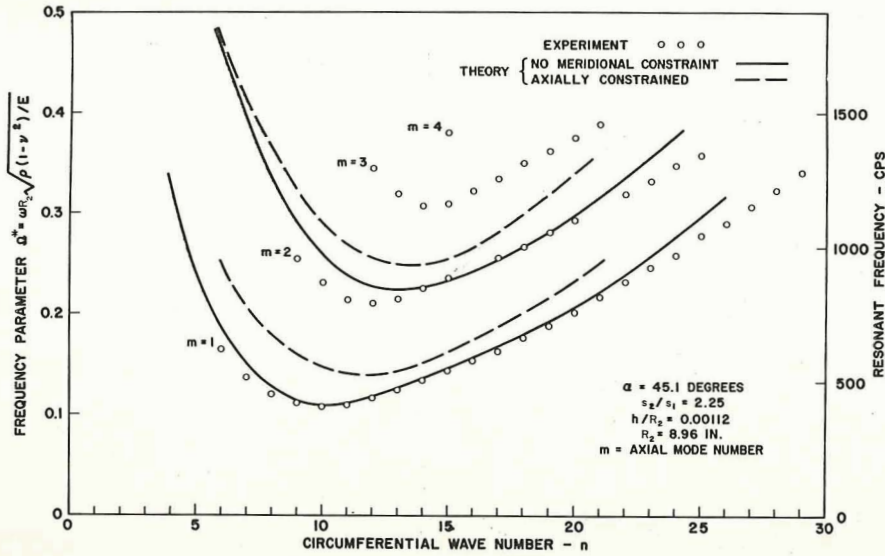
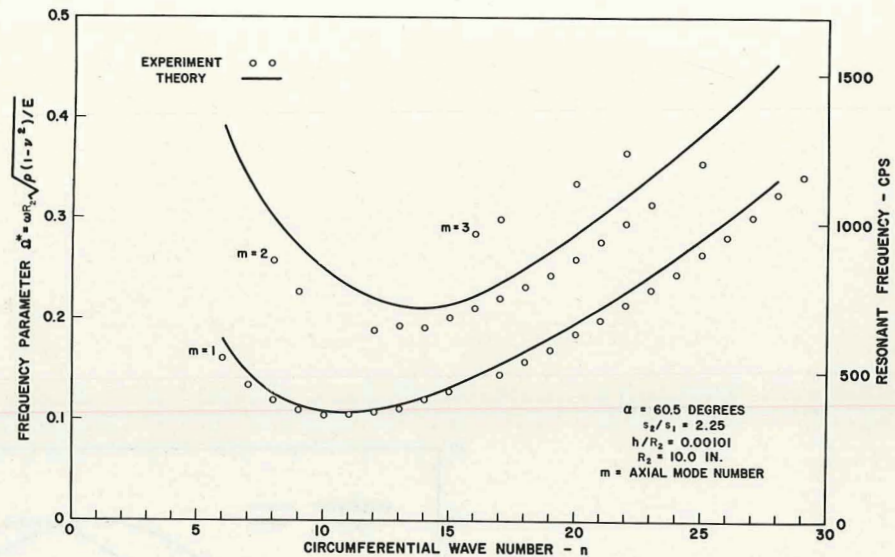


FIGURE 5.24.—Frequencies of an SD-SD conical shell; model 4. (After ref. 5.27)



5.28. The most striking feature of the axial mode shape is its strong dependence on the circumferential wave number n . This is seen in figures 5.26, 5.27(a), 5.27(b), and 5.28 for $m=1$, and figure 5.27(c) for $m=2$. In each case the position of maximum displacement (antinode) shifts towards the large end of the shell ($R=R_2$) as n increases. The suppression of normal displacement near the small end of the conical shell at large values of n is due to the short distance between nodal meridians in this region. The

curvatures and stresses in this region, however, are not necessarily small.

Observe that for a given mode ($n=8, m=1$) the maximum theoretical displacement moves in the direction of one end as α changes (as shown in figures 5.25, 5.26, 5.27(a), and 5.28). The negative deflections indicated for some of the theoretical curves of figures 5.25 through 5.28 are an indication of numerical inaccuracy due to a lack of terms in the series for w (eq. (5.35c)). Finally, note that the experimental mode shapes found in

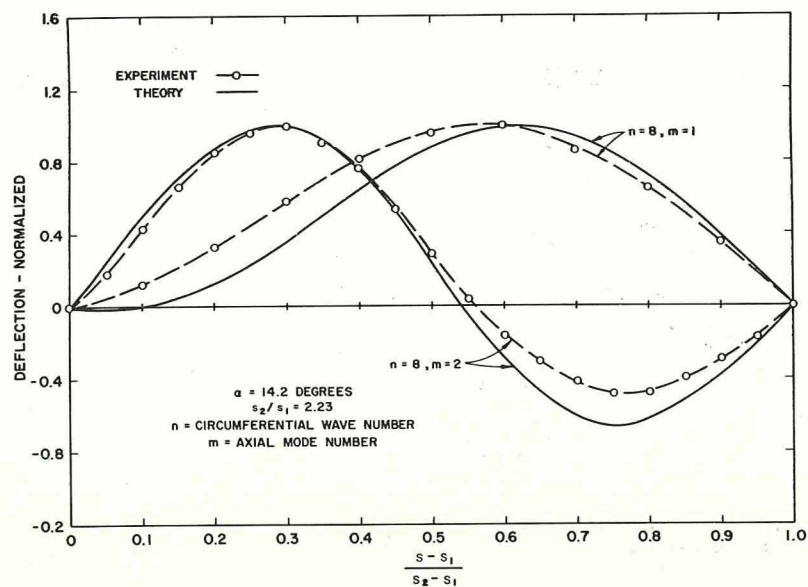


FIGURE 5.25.—Mode shapes for an SD-SD conical shell; model 1. (After ref. 5.27)

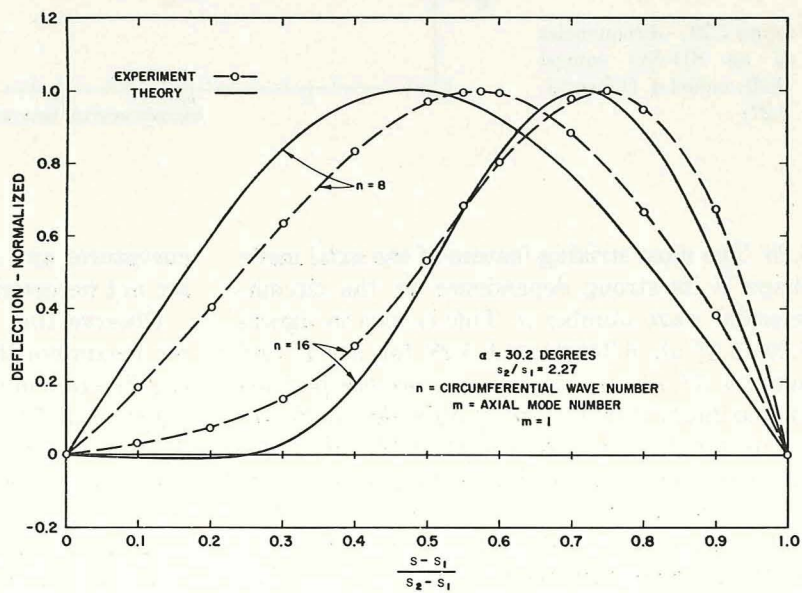


FIGURE 5.26.—Mode shapes for an SD-SD conical shell; model 2. (After ref. 5.27)

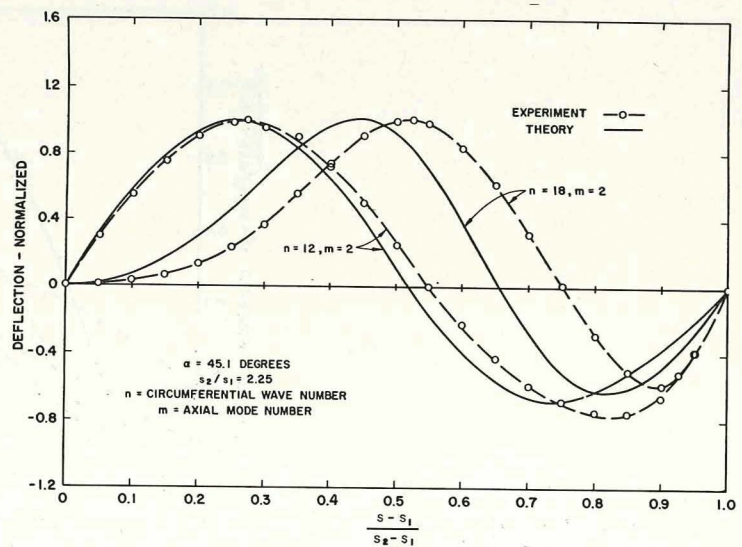
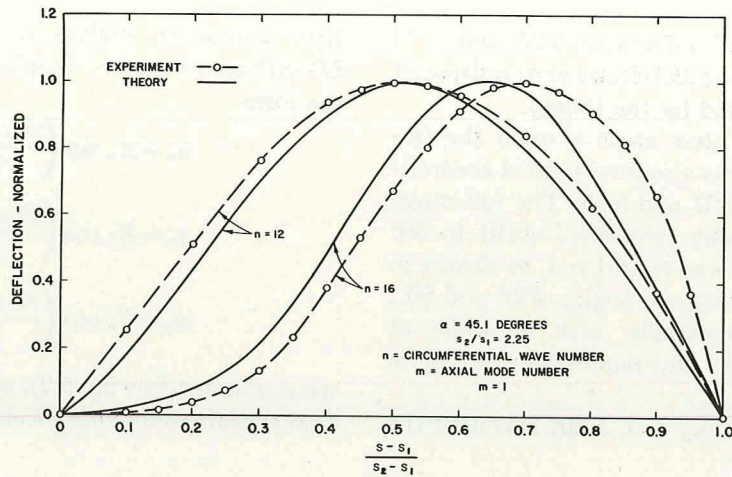
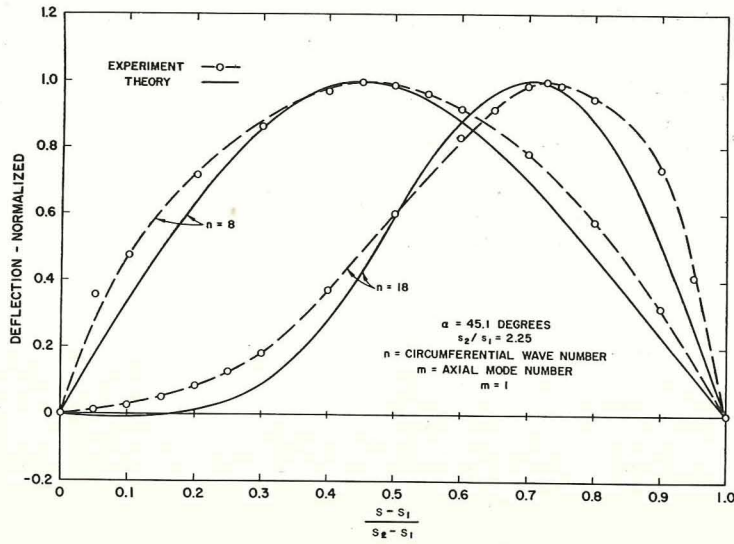


FIGURE 5.27.—Mode shapes for an SD-SD conical shell; model 3. (After ref. 5.27) (a) $n=8$, $n=18$; $m=1$. (b) $n=12$, $n=16$; $n=1$. (c) $n=12$, $n=18$; $m=2$.

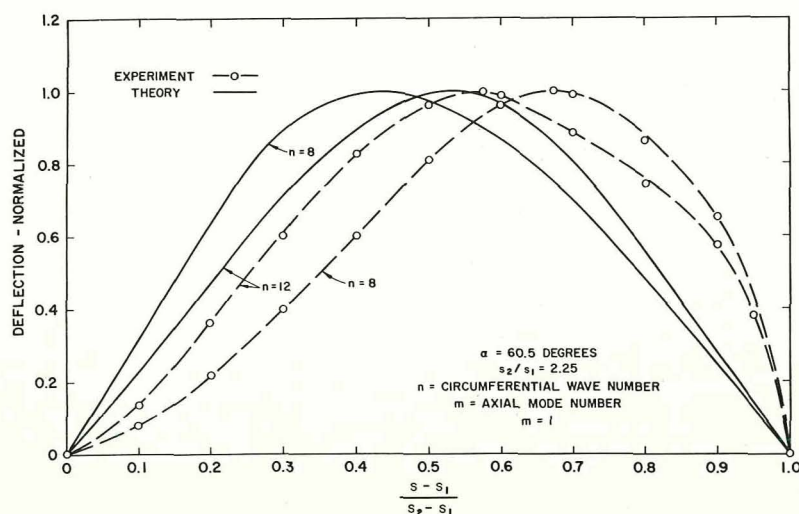


FIGURE 5.28.—Mode shapes for an SD-SD conical shell; model 4. (After ref. 5.27)

the investigations of references 5.27 and 5.28 *always* consisted of parallel circles and equispaced meridians as predicted by the theory.

The influence of apex angle α upon the frequency parameter was also investigated theoretically in references 5.27 and 5.28. The full range of α from 0° (circular cylindrical shell) to 90° (circular flat plate) was considered, as shown in figure 5.29. At the extreme angles of 0° and 90° , Ω^* increases monotonically with n , while at intermediate angles the relationship is more complicated.

Herrman and Mirsky (ref. 5.30) also used the

Ritz method to analyze the free vibrations of SD-SD conical shells. Displacement functions of the form

$$\left. \begin{aligned} u_n &= A_n \sin \left(\frac{\pi \bar{s} \cos \alpha}{l} \right) \\ v_n &= B_n \cos \left(\frac{\pi \bar{s} \cos \alpha}{l} \right) \\ w_n &= C_n \cos \left(\frac{\pi \bar{s} \cos \alpha}{l} \right) \end{aligned} \right\} \quad (5.38)$$

were assumed (see fig. 5.2), where \bar{s} is the meridional coordinate having its origin at $s = (s_1 + s_2)/2$

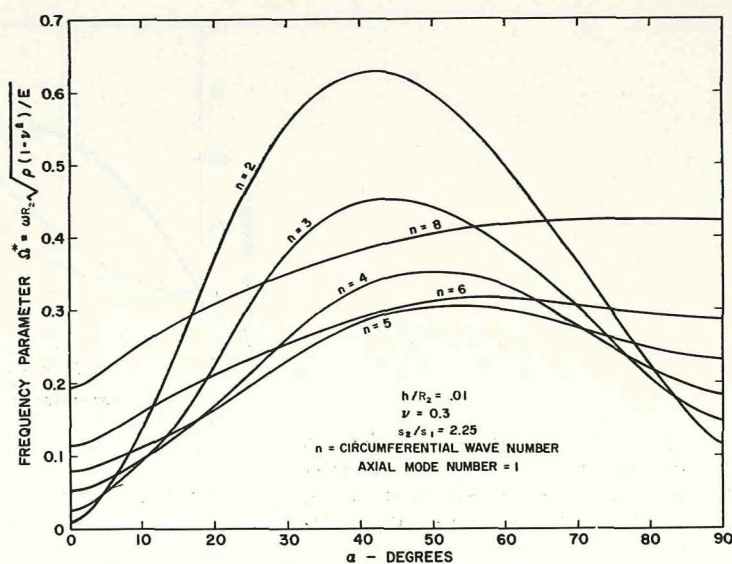


FIGURE 5.29.—Theoretical frequency parameter Ω^* versus α for an SD-SD conical shell. (After ref. 5.27)

(i.e., beginning at the midpoint of the generator). The resulting characteristic determinant for the frequency parameters is given in detail in reference 5.30, but it is too lengthy to bear repetition here.

Numerical results were obtained in reference 5.30 for three semivertex angles $\alpha = 5^\circ, 10^\circ$, and 15° . Two thickness to mean radius ratios ($2h/(R_1 + R_2)$) were considered: $1/30$ and $1/100$. Other parameters were varied over the intervals $0 \leq n \leq 6$ and $1 \leq 2l/(R_1 + R_2) \leq 10$. Frequency data were presented as the ratio of the frequency of a conical shell ω to that of the circular cylindrical shell ω_0 having the same length l , thickness h , and mean radius $\bar{R} = (R_1 + R_2)/2$. Frequency ratios for the three axisymmetric ($n=0$) modes

are depicted in figures 5.30 through 5.32. The frequencies are independent of h/\bar{R} . For short shells the frequency ratio is decreased to values less than unity as α increases, whereas unity is exceeded for long shells and is strongly dependent upon α . The same type of dependence is seen in the curves of figure 5.33, which is for the lowest frequency of the $n=1$ ("beam-like") modes.

For the lowest frequencies of the $n=2$ modes, ω/ω_0 becomes dependent upon the h/\bar{R} ratio, as seen in figure 5.34. A thinner shell is influenced more strongly by α than a thicker shell. Figure 3.35 illustrates the influence of n on ω/ω_0 as a function of α for the lowest mode. Here, $l/\bar{R} = 7$ and $h/\bar{R} = 1/100$. Finally, figure 5.36 shows the influence of α upon the three modes

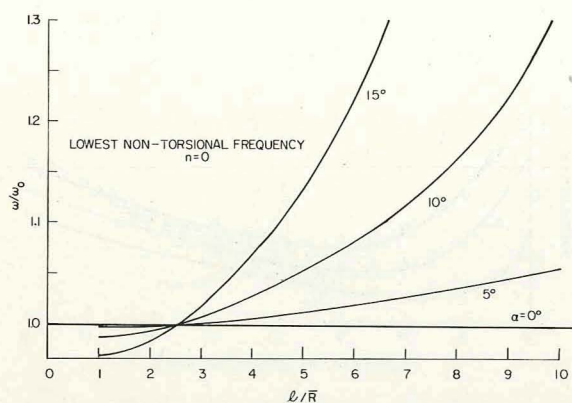


FIGURE 5.30.—Ratio of frequency of conical to cylindrical shell; clamped-clamped BC; $n=0$, lowest non-torsional frequency. (After ref. 5.30)

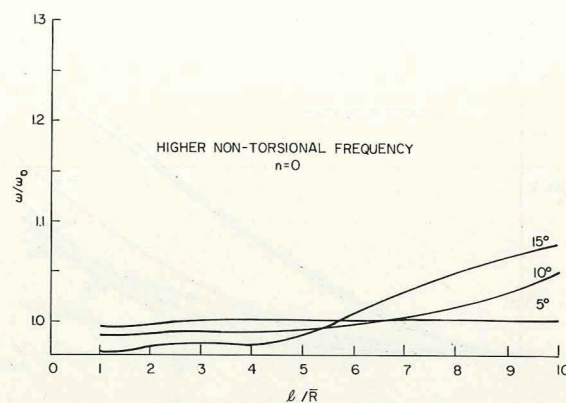


FIGURE 5.32.—Ratio of frequency of conical to cylindrical shell; clamped-clamped BC; $n=0$, higher non-torsional frequency. (After ref. 5.30)

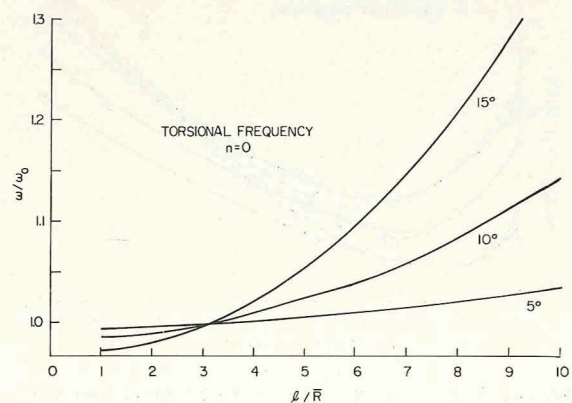


FIGURE 5.31.—Ratio of frequency of conical to cylindrical shell; clamped-clamped BC; $n=0$, torsional frequency. (After ref. 5.30)

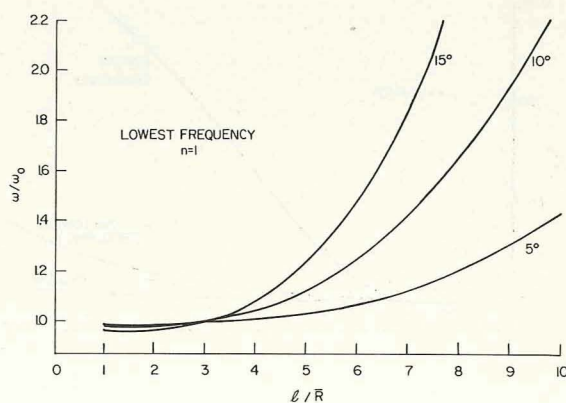


FIGURE 5.33.—Ratio of frequency of conical to cylindrical shell; clamped-clamped BC; $n=1$, lowest frequency. (After ref. 5.30)

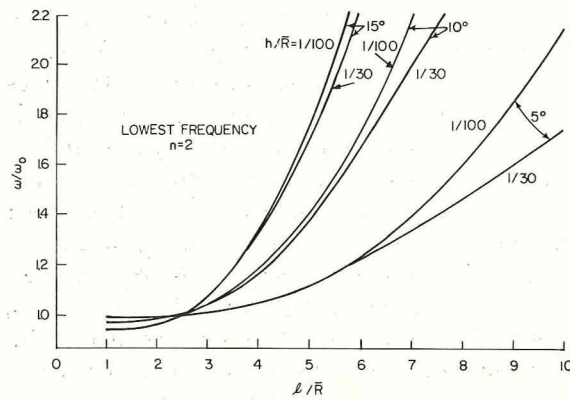


FIGURE 5.34.—Ratio of frequency of conical to cylindrical shell; clamped-clamped BC; $n=2$, lowest frequency. (After ref. 5.30)

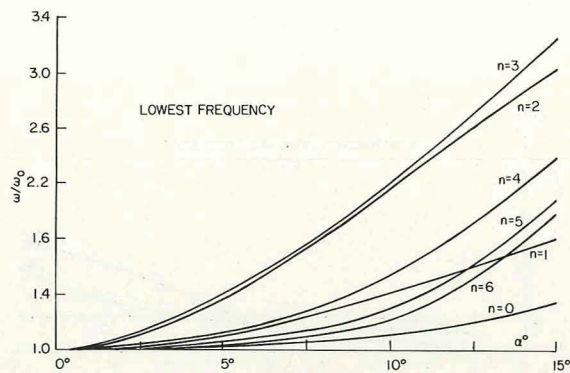


FIGURE 5.35.—Effect of α and n on frequency ratio; $l/R̄=7$, $h/R̄=1/100$. (After ref. 5.30)

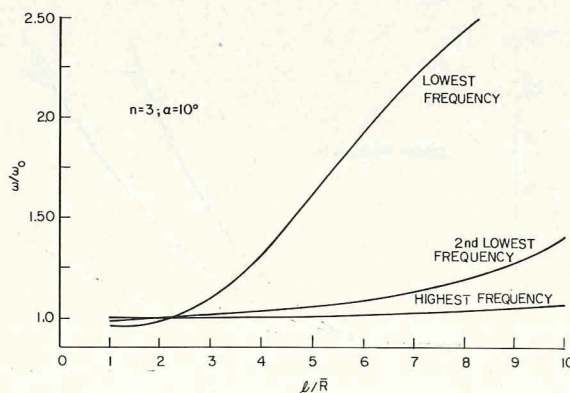


FIGURE 5.36.—Comparison of effects on frequency ratio for three modes; $n=3$, $\alpha=10^\circ$. (After ref. 5.30)

for representative values of $n=3$ and $\alpha=10^\circ$. The influence is much stronger for the lowest mode and weakest for the highest mode.

Weingarten (ref. 5.31) also used the Galerkin method with the Donnell-Mushtari shell equations and assumed displacement functions in the form of power series. Numerical results were evaluated and compared with experiment for two shells made of 1020 steel and having thicknesses of 0.020 in. and 0.040 in. The remaining dimensions were: $\alpha=20^\circ$, $R_1=2$ in., $s_2-s_1=8-3/8$ in. Theoretical and experimental frequencies for the two shell thicknesses and for 1, 2, and 3 axial half-waves m are exhibited in figures 5.37 and 5.38, respectively. In these figures theoretical results are also given for an "equivalent" circular

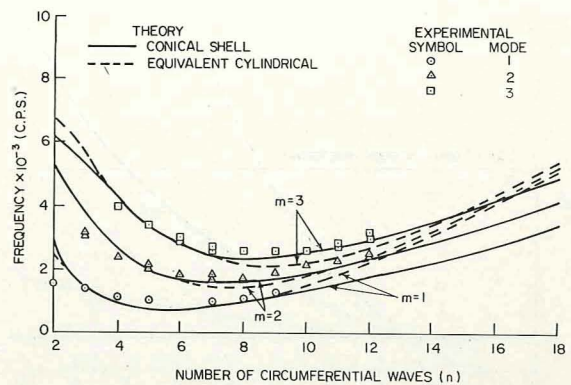


FIGURE 5.37.—Theoretical and experimental frequencies for an SD-SD conical shell; $h=0.020$ in. (After ref. 5.31)

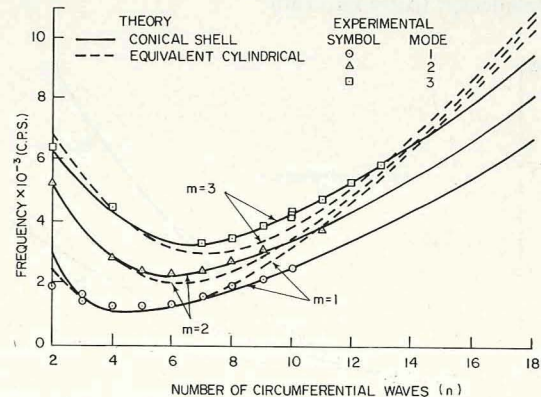


FIGURE 5.38.—Theoretical and experimental frequencies for an SD-SD conical shell; $h=0.040$ in. (After ref. 5.31)

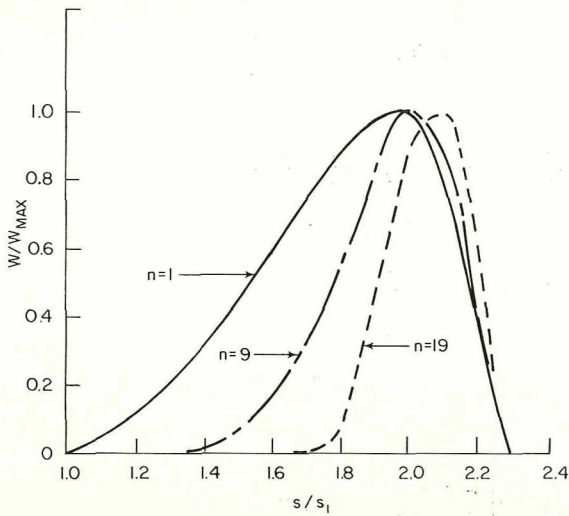


FIGURE 5.39.—Mode shapes of an SD-SD conical shell; $h = 0.040$ in. (After ref. 5.31)

cylindrical shell; these frequencies are considerably in error as n becomes large. Typical mode shapes for the normalized deflection w are shown in figure 5.39 for the thicker shell ($h = 0.020$ in.), where the shift of maximum amplitude towards the large end of the shell as n increases is clearly seen.

Grigolyuk (ref. 5.32) also used the Ritz method with displacement functions of the form

$$\left. \begin{aligned} u_n &= A_n R^2 \cos \frac{m\pi(s-s_1)}{s_2-s_1} \\ v_n &= B_n R^2 \sin \frac{m\pi(s-s_1)}{s_2-s_1} \\ w_n &= C_n R^2 \sin \frac{m\pi(s-s_1)}{s_2-s_1} \end{aligned} \right\} \quad (5.39)$$

(see figs. 5.1 and 5.2). The resulting frequency equation is given in detail in reference 5.32 but, because of its length it will not be repeated here. Frequency parameters

$$\Omega_3 = \omega(s_2-s_1) \sqrt{\frac{\rho(1-\nu^2)}{E}}$$

for the fundamental (lowest) modes of vibration are listed in table 5.8 for various values of α and h/R_2 . Table 5.9 lists the circumferential wave numbers n at which the minimum frequencies of table 5.8 occur. All results are for $m=1$ and

$\nu = 0.3$. Grigolyuk (ref. 5.32) also suggested that SD-SD shells having small conicity ($\alpha \leq 15^\circ$) can be adequately represented for purposes of calculation by circular cylindrical shells having radii equal to the *average* radius (i.e., $\bar{R} = (R_1 + R_2)/2$) of the conical shells. However, as was seen earlier (figs. 5.30 through 5.36), this is not necessarily the case.

Godzevich (ref. 5.33) used the Donnell-Mush-tari shell equations with the Galerkin method and displacement functions of the type given by equations (5.39) with R^2 replaced by unity. An explicit equation for frequency parameters of SD-SD conical shells was derived:

$$\frac{\omega^2 s_2^2 \rho}{E} = \frac{C_1}{C_2} \quad (5.40)$$

where

$$\begin{aligned} C_1 &= \frac{h^2}{12s_2^2(1-\nu_2^2)} \left\{ \frac{1}{10} a_m^4 (1-\beta_1^5) \right. \\ &\quad + a_m \left(1 + \frac{2n^2}{\sin^2 \alpha} \right) \left[\frac{1}{6} a_m (1-\beta_1^3) \right. \\ &\quad \left. \left. - \frac{1}{2a_m} (1-\beta_1) \right] \right. \\ &\quad + \frac{1}{2} (1-\beta_1) \left(\frac{n^4}{\sin^4 \alpha} - \frac{4n^2}{\sin^2 \alpha} \right) \left. \right\}^2 \\ &\quad + \frac{a_m^4}{\tan^4 \alpha} \left[\frac{1}{8} (1-\beta_1^4) \right. \\ &\quad \left. - \frac{3}{8a_m^2} (1-\beta_1^2) \right]^2 \end{aligned} \quad (5.41a)$$

$$\begin{aligned} C_2 &= \left\{ \frac{1}{10} a_m^4 (1-\beta_1^5) + a_m \left(1 + \frac{2n^2}{\sin^2 \alpha} \right) \right. \\ &\quad \left[\frac{1}{6} a_m (1-\beta_1^3) - \frac{1}{2a_m} (1-\beta_1) \right] \\ &\quad + \frac{1}{2} (1-\beta_1) \left(\frac{n^4}{\sin^4 \alpha} - \frac{4n^2}{\sin^2 \alpha} \right) \left. \right\} \\ &\quad \left[\frac{1}{10} (1-\beta_1^5) - \frac{1}{2a_m} (1-\beta_1^3) \right. \\ &\quad \left. + \frac{3}{8a_m^4} (1-\beta_1) \right] \end{aligned} \quad (5.41b)$$

and where $\beta_1 = s_1/s_2$ and $a_m = m\pi s_2/(s_2-s_1)$.

Miller and Hart (ref. 5.15) studied the density of eigenvalues of the SD-SD conical shell. Eigenvalue density is essentially the density of the frequencies with respect to frequency and is therefore an indication of the spacing of the frequencies in the frequency spectrum. Equations

TABLE 5.8.—Lowest Frequency Parameters $\omega(s_2-s_1)\sqrt{\rho(1-\nu^2)/E}$ for SD-SD Conical Shells; $m=1$, $\nu=0.3$

$\beta=90-\alpha$, degrees	h/R_2													
	0.03	0.02	0.015	0.01	0.009	0.008	0.007	0.006	0.005	0.004	0.003	0.002	0.001	0.0008
3	0.102	0.0931	0.0897	0.0769	0.0677	0.0580	0.0474	0.0340	0.0311
5	0.141	0.133	.126	.116	.106	.0967	.0877	.0748	.0623	.0448	.0408
10	0.281	0.242	.193	.184	.175	.162	.149	.138	.124	.108	.0895	.0656	.0590
15	0.419	.335	.288	.236	.223	.212	.201	.186	.169	.154	.134	.112	.0814	.0736
20	.479	.381	.355	.287	.267	.249	.231	.214	.199	.178	.157	.130	.0950	.0862
25	.519	.432	.369	.311	.293	.275	.258	.244	.223	.200	.177	.148	.107	.0968
30	.562	.467	.404	.337	.319	.302	.286	.271	.244	.222	.193	.161	.119	.107
35	.607	.499	.438	.362	.344	.328	.312	.288	.264	.242	.209	.174	.128	.116
40	.652	.529	.469	.386	.368	.351	.335	.307	.282	.259	.224	.187	.138	.125
45	.693	.559	.498	.408	.390	.372	.355	.326	.299	.274	.238	.198	.147	.133
50	.729	.586	.522	.430	.409	.390	.372	.345	.315	.288	.251	.210	.156	.141
55	.757	.614	.541	.452	.429	.406	.386	.366	.331	.299	.264	.223	.165	.149
60	.776	.644	.582	.479	.451	.424	.399	.376	.350	.312	.279	.231	.172	.157
65	.789	.688	.582	.493	.478	.450	.418	.388	.361	.331	.288	.243	.182	.166
70	.809	.695	.627	.504	.482	.462	.444	.414	.376	.341	.307	.256	.194	.176
75	.877	.701	.628	.548	.515	.483	.453	.425	.400	.367	.319	.276	.207	.190
80	.891	.810	.672	.553	.533	.514	.434	.480	.432	.387	.349	.298	.229	.211
85	.963	.779	.703	.643	.634	.625	.589	.537	.488	.445	.408	.358	.283	.256
87988	.818	.671	.645	.622	.600	.580	.564	.550	.472	.400	.322	.297

TABLE 5.9.—Circumferential Wave Numbers (n) at Which the Minimum Frequencies of Table 5.8 Occur

α , degrees	h/R_2													
	0.03	0.02	0.015	0.01	0.009	0.008	0.007	0.006	0.005	0.004	0.003	0.002	0.001	0.008
3	2	2	3	2	3	3	4	5	5
5	2	2	2	3	3	3	4	4	5	6	6
10	2	3	3	3	4	4	4	4	5	5	6	7	8
15	2	3	3	4	4	4	4	5	5	5	6	7	8	9
20	3	3	4	5	5	5	5	5	5	6	6	7	9	9
25	3	3	4	5	5	5	5	5	6	6	7	8	9	10
30	3	4	4	5	5	5	5	6	6	6	7	8	9	10
35	3	4	4	5	5	5	5	6	6	6	7	8	10	10
40	3	4	4	5	5	5	6	6	6	7	7	8	10	10
45	3	4	4	5	5	5	5	6	6	6	7	8	10	10
50	3	4	4	5	5	5	5	6	6	6	7	8	9	10
55	3	4	4	5	5	5	5	6	6	6	7	8	9	10
60	3	4	4	5	5	5	5	5	6	6	6	7	9	9
65	3	4	4	4	4	5	5	5	5	6	6	7	8	9
70	3	3	4	4	4	4	4	5	5	5	6	6	8	8
75	3	3	3	4	4	4	4	4	4	5	5	6	7	7
80	2	3	3	3	3	3	3	4	4	4	4	5	6	6
85	2	2	2	2	2	2	3	3	3	3	3	4	5	5
87	2	2	2	2	2	2	2	2	2	3	3	4	4

CONICAL SHELLS

(5.40) and (5.41) developed by Godzevich and discussed above served as one equation determining a " k -space" for the eigenvalues. The two coordinates chosen for the k -space were k_1 and k_2 , defined as

$$\left. \begin{aligned} k_1 &= a_n = \frac{m\pi s_2}{s_2 - s_1} \\ k_2 &= \frac{n}{\sin \alpha} \end{aligned} \right\} \quad (5.42)$$

That is, k_1 and k_2 are dimensionless wave numbers in the s and θ directions. By using the nondimensional frequency parameter

$$\Omega_4^2 = \frac{\omega^2 \rho s_2^2}{E} \quad (5.43)$$

equation (5.40) can be written in terms of the parameters k_1 , k_2 , and Ω_4 . Curves for constant values of Ω_4 in terms of the k_1 , k_2 coordinate

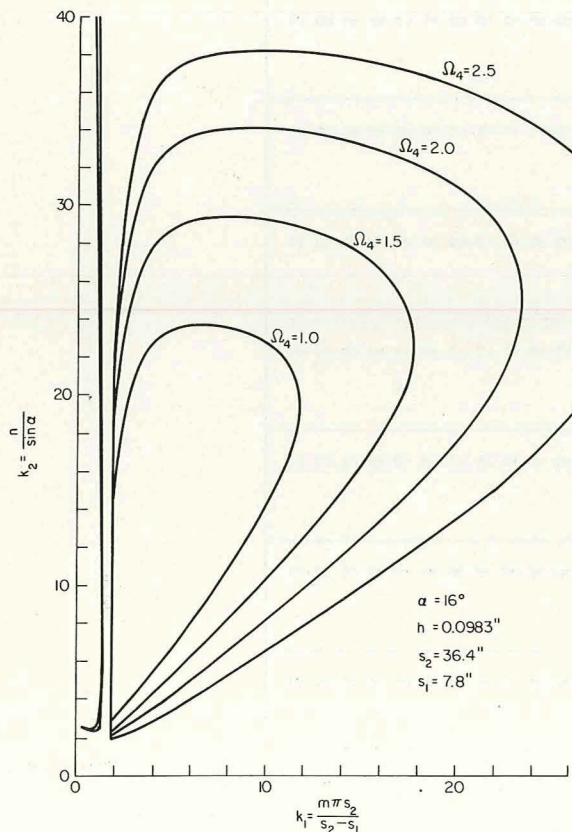


FIGURE 5.40.—Frequency parameter curves in k -space for an SD-SD conical shell. (After ref. 5.15)

system for $\alpha = 16^\circ$, $h = 0.0983$ in., $s_2 = 36.4$ in., and $s_1 = 7.8$ in. are shown in figure 5.40.

In reference 5.15 comparisons were also made between the theoretical frequencies arising from equations (5.40) and (5.41) and experimental frequencies given earlier in this section. Comparisons with Weingarten's (ref. 5.31) data are seen in figures 5.41 and 5.42. Comparisons with the results of Lindholm and Hu (refs. 5.27 and 5.28) are seen in figures 5.43 and 5.44. Note that $s_2 - s_1$ was taken as 8.00 in. for figures 5.41 and 5.42 in reference 5.15, whereas $s_2 - s_1$ was given as 8.375 in. in reference 5.31, as noted previously in this section.

Experimental results for SD-SD conical shells were also given in references 5.34 and 5.35.

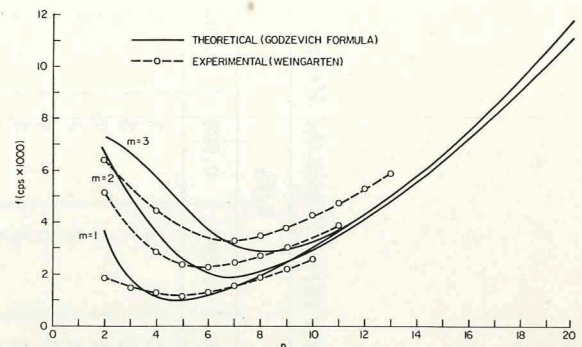


FIGURE 5.41.—Comparison of theoretical and experimental frequencies for an SD-SD conical shell; $\alpha = 20^\circ$, $s_2 = 14.14$ in., $s_1 = 6.14$ in., $h = 0.040$ in., 1020 steel. (After ref. 5.15)

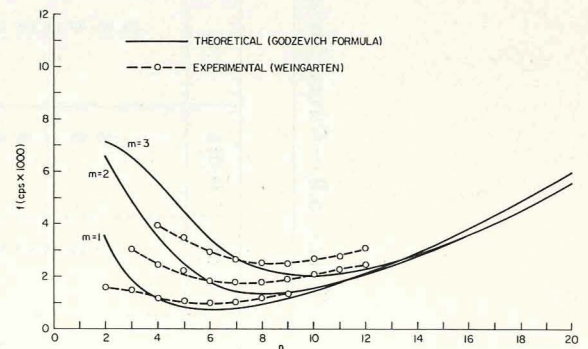


FIGURE 5.42.—Comparison of theoretical and experimental frequencies for an SD-SD conical shell; $\alpha = 20^\circ$, $s_2 = 14.14$ in., $s_1 = 6.14$ in., $h = 0.020$ in., 1020 steel. (After ref. 5.15)

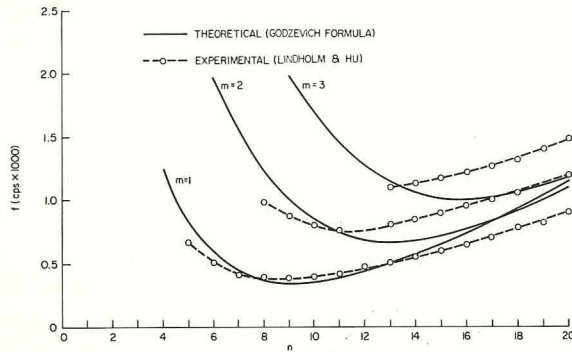


FIGURE 5.43.—Comparison of theoretical and experimental frequencies for an SD-SD conical shell; $\alpha = 30.2^\circ$, $s_2 = 15.7$ in., $s_1 = 6.94$ in., $h = 0.01$ in., steel shim stock. (After ref. 5.15)

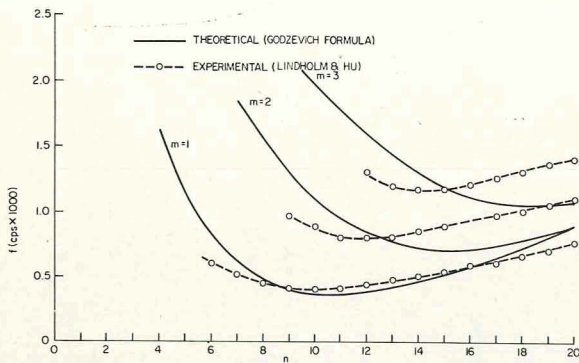


FIGURE 5.44.—Comparison of theoretical and experimental frequencies for an SD-SD conical shell; $\alpha = 45.1^\circ$, $s_2 = 12.7$ in., $s_1 = 5.61$ in., $h = 0.01$ in., steel shim stock. (After ref. 5.15)

Axisymmetric modes were investigated by Hartung and Loden (ref. 5.24) using a finite element representation. Extensive numerical values of frequency parameters were plotted for $\alpha = 5^\circ, 45^\circ, 60^\circ$, and 84° with $\bar{R}/h = 20$ and 500 ($\bar{R} = (R_1 + R_2)/2$).

Axisymmetric modes were also examined in references 5.6 and 5.36. Finite differences were used in reference 5.25. Considerable information on the free vibrations of SD-SD conical shells is available in reference 5.37. Other works dealing with this problem include references 5.3, 5.23, and 5.38 through 5.52.

5.3.4 Clamped-Free

The case of a conical shell clamped at one end

and free at the other has received much treatment in the literature because of its widespread use in such practical designs as loudspeaker cones (cf., ref. 5.17, 5.53, and 5.54). This practical application also accounts for the fact that the majority of the references deal with the instance where the small end is the clamped one and the large end is free. Assuming this case, the boundary conditions are

$$u = v = w = \frac{\partial w}{\partial s} = 0 \quad \text{at} \quad s = s_1 \quad (5.44a)$$

$$N_s = S_{s\theta} = V_s = M_s = 0 \quad \text{at} \quad s = s_2 \quad (5.44b)$$

(see sec. 5.2.3 for elaboration on free edge boundary conditions).

Dreher (ref. 5.11) used the exact solution procedure described in section 5.2 involving expansion of the displacements in terms of power series to study the *axisymmetric* ($n=0$) free vibrations. The Donnell-Mushtari shell theory was used. Frequency parameters $\bar{\Omega}^2 = \omega^2 r_2^2 \rho / E$ were obtained for the first four axisymmetric modes for $\nu = 0.3$ and over a wide range of the stiffness parameter $K = 12(1 - \nu^2)(r_2/h)^2 / \tan^2 \alpha$. Numerical results for $s_1/s_2 = 0.1, 0.2, 0.3, 0.4$, and 0.5 are given in figure 5.45 ($s = s_1$ is clamped, and $s = s_2$ is free). The lowest axisymmetric frequency is given in figure 5.46 for $0.1 \leq s_1/s_2 \leq 0.8$. Note that for the choice of stiffness parameter K , $\bar{\Omega}$ does not depend explicitly upon α . For comparison, results were also obtained in reference 5.11 using Kalnins' (ref. 5.14) numerical integration scheme for shells of revolution. Differences between the values of $\bar{\Omega}$ computed by the two methods were all found to be less than 1 percent.

The power series method was also used by Goldberg (ref. 5.55) for axisymmetric problems. Numerical results were found for a particular clamped-free shell having $\alpha = 60^\circ$, $h = 0.025$ in., $E = 150,000$ psi, $\nu = 0.25$, $\rho = 3 \times 10^{-5}$ in. sec²/in.⁴, $R_1 = 2$ in. (clamped), and $R_2 = 5$ in. (free). The first three frequencies and mode shapes obtained are exhibited in figure 5.47 where the amplitudes are normalized with respect to the free end *meridional* displacement of the shell. These data were also subsequently checked by a numerical integration method in references 5.56 and 5.57, yielding frequencies of 1072, 1315, and 1611 cps, compared with the frequencies of 1071, 1315, and

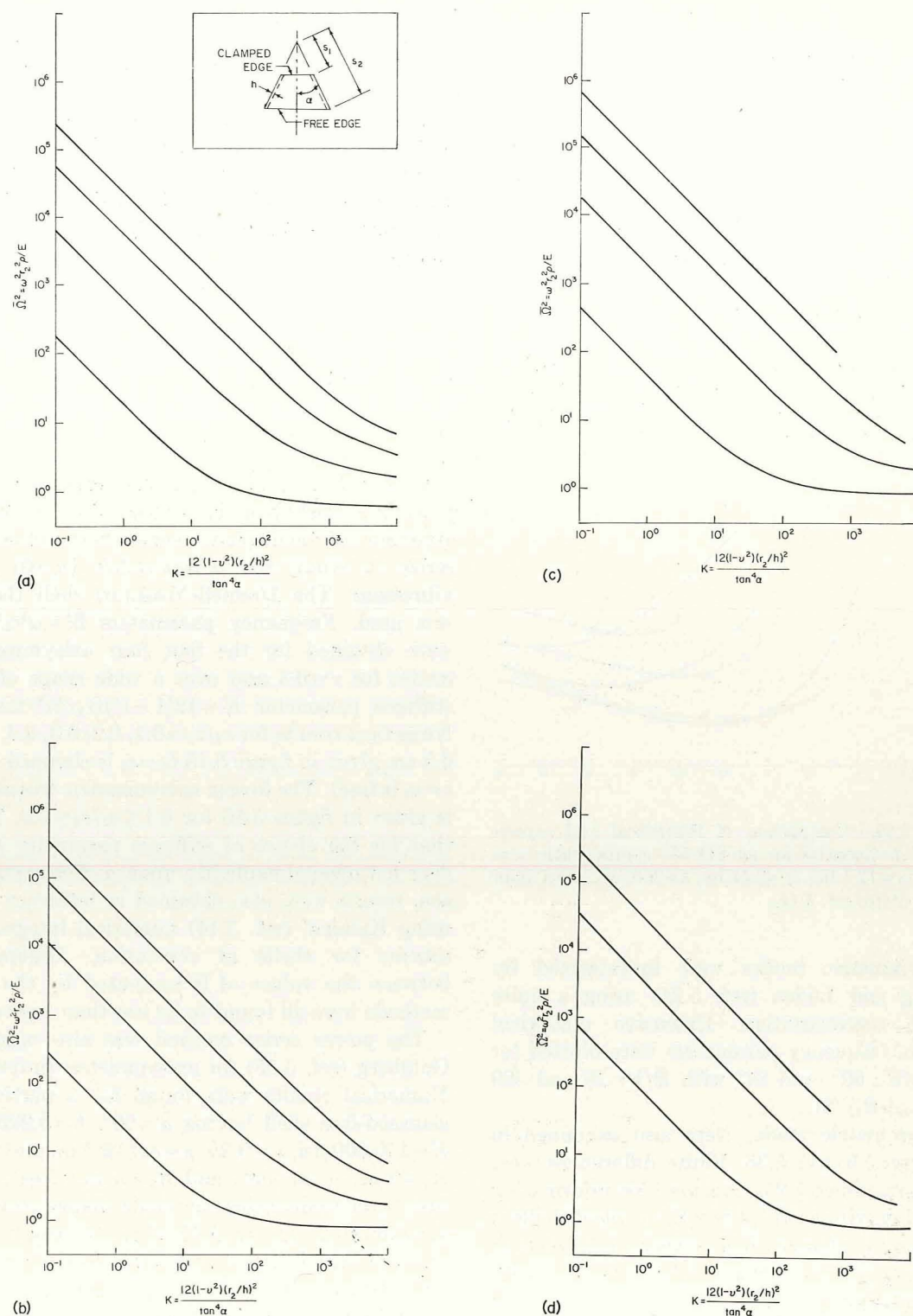


FIGURE 5.45.—Frequency parameter $\bar{\Omega}^2$ versus stiffness parameter K for the axisymmetric ($n=0$) modes of a clamped-free conical shell (After ref. 5.11). (a) $s_1/s_2=0.1$. (b) $s_1/s_2=0.2$. (c) $s_1/s_2=0.3$. (d) $s_1/s_2=0.4$. (e) $s_1/s_2=0.5$.

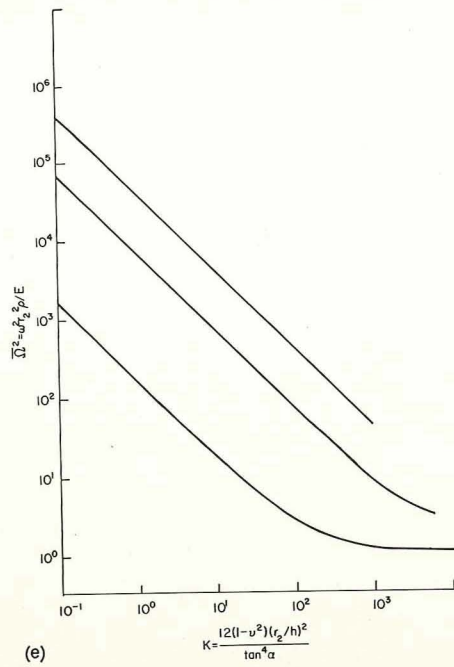
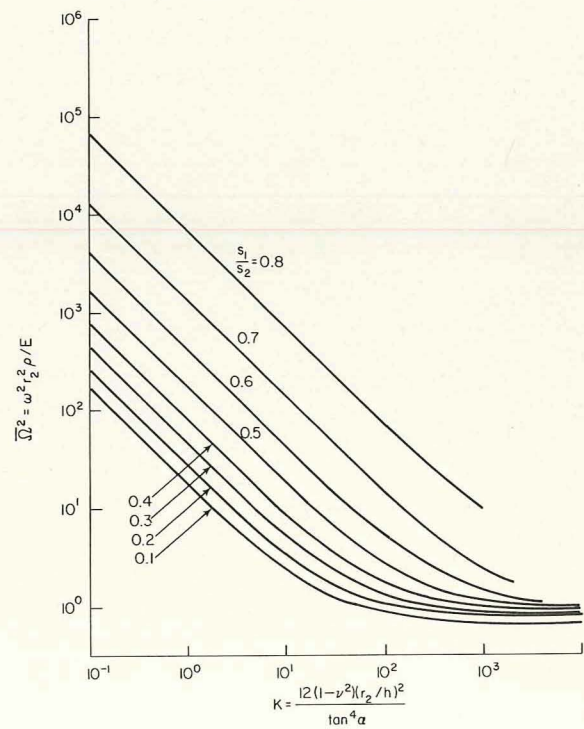


FIGURE 5.45.—Concluded.

FIGURE 5.46.—Axisymmetric frequency parameters of clamped-free conical shells for various s_1/s_2 ratios. (After ref. 5.11)

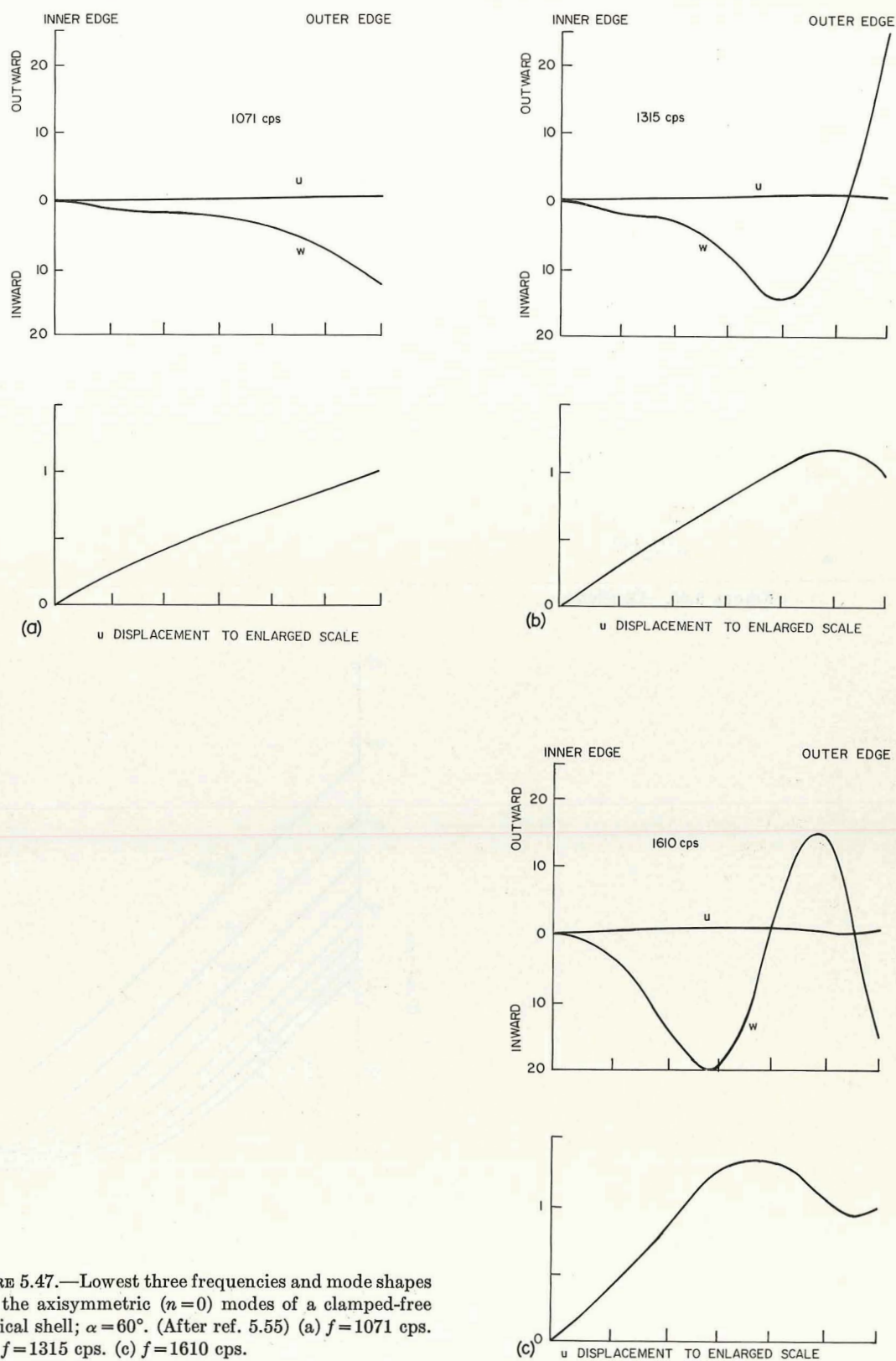


FIGURE 5.47.—Lowest three frequencies and mode shapes for the axisymmetric ($n=0$) modes of a clamped-free conical shell; $\alpha=60^\circ$. (After ref. 5.55) (a) $f=1071$ cps. (b) $f=1315$ cps. (c) $f=1610$ cps.

1610 cps given in figure 5.47. Kalnins (ref. 5.14) subsequently used his numerical integration method to duplicate these frequencies within 0.1 percent accuracy. He also duplicated the mode shapes for all practical purposes.

The meridional axisymmetric modes of clamped-free shells having either the small or large end clamped were investigated by Keefe (ref. 5.21), resulting in the following characteristic equation when the small end is fixed

$$J_0(\eta\Omega_2)Y_1(\Omega_2) = J_1(\Omega_2)Y_0(\eta\Omega_2) \quad (5.45a)$$

and when the small end is free

$$J_1(\eta\Omega_2)Y_0(\Omega_2) = J_0(\Omega_2)Y_1(\eta\Omega_2) \quad (5.45b)$$

(see discussion in sec. 5.3.1). The first four roots of equations (5.45a) and (5.45b) are plotted versus the ratio R_1/R_2 in figures 5.48 and 5.49, respectively.

The axisymmetric free vibrations of clamped-free conical shells were also analyzed in references 5.24, 5.54, 5.58, 5.59, and 5.60.

The general modes of clamped-free shells were investigated by Platus (refs. 5.61, 5.62, and 5.63). The procedure followed was similar to that of Saunders, Wisniewski, and Paslay (ref. 5.26), whereby the extensional (membrane) and in-

tensional frequency parameters are determined separately and are simply added to obtain an approximation for the true frequency parameters; i.e.,

$$\Omega_s^2 = (\Omega_s^2)_E + (\Omega_s^2)_I \quad (5.46)$$

where Ω_s is defined by

$$\Omega_s = \omega l \left(\frac{l}{R_1} \right) \sqrt{\frac{\rho(1-\nu^2)}{E}} \quad (5.47)$$

and $(\Omega_s)_E$ and $(\Omega_s)_I$ are the corresponding extensional and inextensional frequency parameters, respectively. This approximation is based upon the postulate that the kinetic energy is approximately the same for the extensional and inextensional cases (i.e., the mode shapes are approximately the same). Hence, because the total strain energy is the sum of the extensional and inextensional components, Rayleigh's Quotient yields equation (5.46).

The inextensional vibrations are characterized by the condition that the middle surface strains are zero; i.e.,

$$\epsilon_s = \epsilon_\theta = \epsilon_{s\theta} = \epsilon_{\theta s} = 0 \quad (5.48)$$

By choosing displacement functions u_n , v_n , and w_n for equations (5.14) in the form

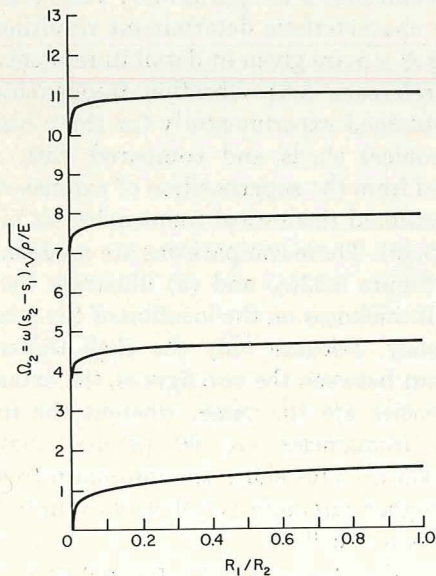


FIGURE 5.48.—Frequency parameters for the axisymmetric meridional motion of a clamped-free (*small end clamped*) conical shell. (After ref. 5.21)

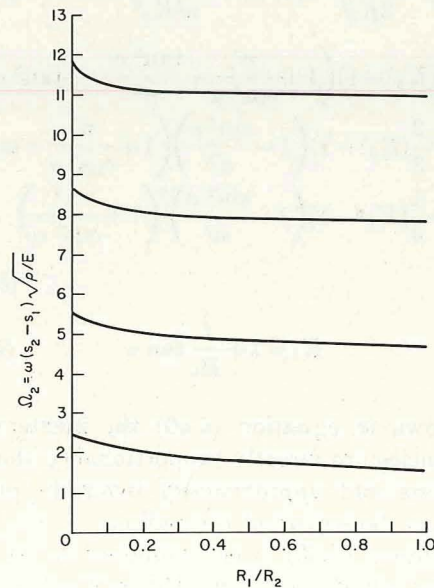


FIGURE 5.49.—Frequency parameters for the axisymmetric meridional motion of a clamped-free (*large end clamped*) conical shell. (After ref. 5.21)

$$\left. \begin{aligned} u_n &= \frac{R_1 \cos \alpha}{n \left(1 - \frac{\sin^2 \alpha}{n^2} \right)} \\ v_n &= x_1 - \frac{R_1 \sin \alpha \cos \alpha}{n^2 \left(1 - \frac{\sin^2 \alpha}{n^2} \right)} \\ w_n &= \left(\frac{n}{\cos \alpha} \right) x_1 \end{aligned} \right\} \quad (5.49)$$

where x_1 is measured from the smaller end of the shell as shown in figure 5.2, equations (5.48) are satisfied, in addition to the clamped edge condition, $w=0$ at $x_1=0$ (ref. 5.61). However, the other three boundary conditions of the clamped edge given in equations (5.44a) are not satisfied. Using equations (5.49), and equating the maximum potential and kinetic energies gives for the inextensional frequency (ref. 5.61)

$$\omega_I = \frac{n(n^2-1)h}{2R_1^2 \cos \alpha} \left[\frac{E}{3\rho(1-\nu^2)} \frac{K_1}{K_2} \right]^{1/2} \quad (5.50)$$

where

$$K_1 = \left(1 - \frac{\sin^2 \alpha}{n^2} \right)^2 \ln K_3 - \frac{2}{K_3} (K_3 - 1) \left(1 - \frac{\sin^2 \alpha}{n^2} \right) + \frac{(K_3^2 - 1)}{2K_3^2} + \frac{(1-\nu)K_3^2 - 1}{n^2 K_3^2} \sin^2 \alpha \quad (5.51a)$$

$$K_2 = \frac{1}{2} (K_3^2 - 1) \left(1 + \frac{n^2}{\cos^2 \alpha} + \frac{\tan^2 \alpha}{n^2} - 2 \tan^2 \alpha \right) - \frac{2}{3} (K_3^3 - 1) \left(1 - \frac{\sin^2 \alpha}{n^2} \right) \left(1 + \frac{n^2}{\cos^2 \alpha} - \tan^2 \alpha \right) + \frac{1}{4} (K_3^4 - 1) \left(1 - \frac{\sin^2 \alpha}{n^2} \right)^2 \left(1 + \frac{n^2}{\cos^2 \alpha} \right) \quad (5.51b)$$

$$K_3 = 1 + \frac{l}{R_1} \tan \alpha \quad (5.51c)$$

As shown in equation (5.50) the inextensional frequencies are directly proportional to the shell thickness and *approximately* inversely proportional to the square of the radius.

Equation (5.50) was evaluated in reference 5.61 for $\alpha=0^\circ$ (cylinder), 15° , and 30° and for $l/R_1=2, 4$, and 6 . The results are presented in figure 5.50 in terms of the nondimensional frequency parameter Ω_6^2 , where

$$\Omega_6 = \omega R_1 \left(\frac{R_1}{h} \right) \sqrt{\frac{\rho(1-\nu^2)}{E}} \quad (5.52)$$

The extensional (membrane) vibrations were analyzed in reference 5.61 by assuming polynomial forms for the displacements in terms of the coordinate x_1 ,

$$\left. \begin{aligned} u_n &= \frac{1}{n} \sum_{i=1}^{N+1} A_i x_i^i \\ v_n &= \sum_{i=1}^N B_i x_i^i \\ w_n &= n \sum_{i=2}^N C_i x_i^i \end{aligned} \right\} \quad (5.53)$$

to use in equations (5.14), where the A_i , B_i , and C_i are undetermined coefficients to be selected by the Ritz procedure. As shown in figure 5.51 all inertia terms were retained and results were obtained to complement the previously given inextensional results. The dependence of frequency upon the number of terms N retained in each of the polynomials (5.53) is exhibited in table 5.10. The value of N was taken at six for the results shown in figures 5.51. The coefficients of the characteristic determinant resulting from taking $N=6$ are given in detail in reference 5.63.

In reference 5.61 vibration frequencies were also obtained experimentally for three clamped-free conical shells and compared with results derived from the superposition of extensional and inextensional theoretical frequencies, as in equation (5.46). These comparisons are made in figure 5.52. Figure 5.52(a) and (b) illustrate the effect of shell thickness on the location of the minimum frequency. Because only the shell thickness is different between the two figures, the extensional frequencies are the same, whereas the inextensional frequencies are 60 percent lower for $h=0.006$ in. This shifts the minimum frequency to a higher circumferential wave number n for the thinner shell.

An earlier paper using a procedure similar to that of references 5.61, 5.62, and 5.63 was written by Saunders, Wisniewski, and Paslay (ref. 5.26). However, in the latter reference the assumed

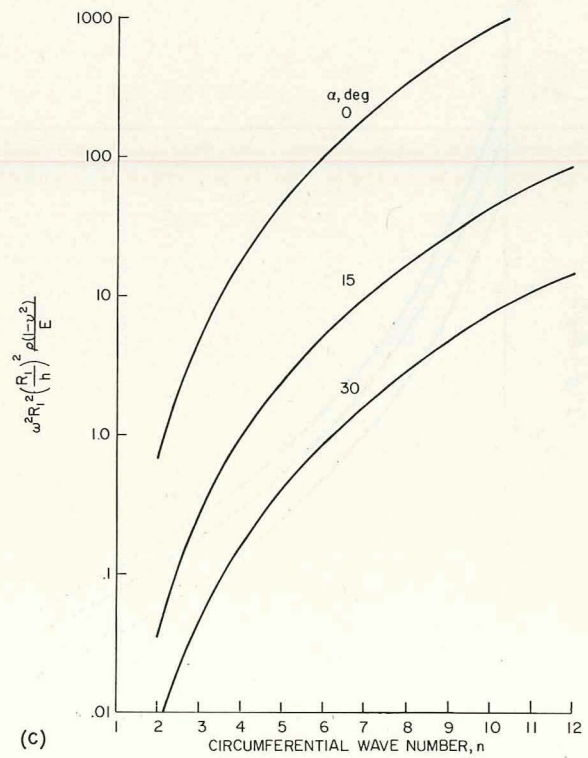
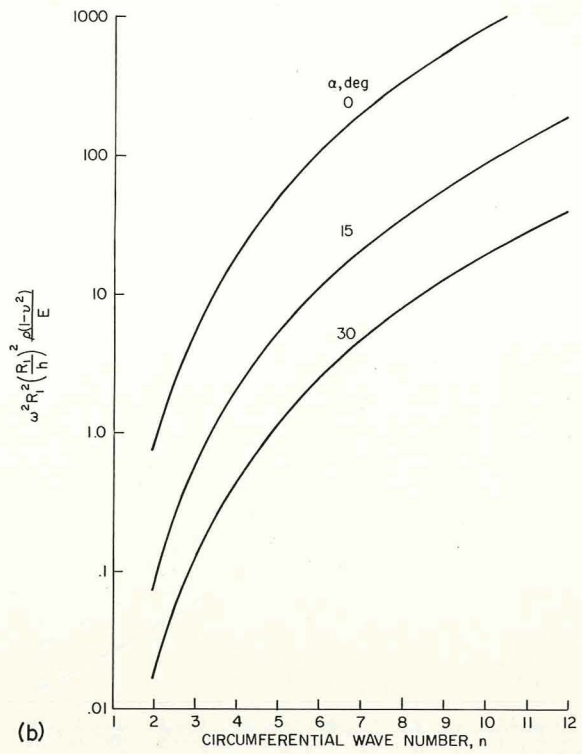
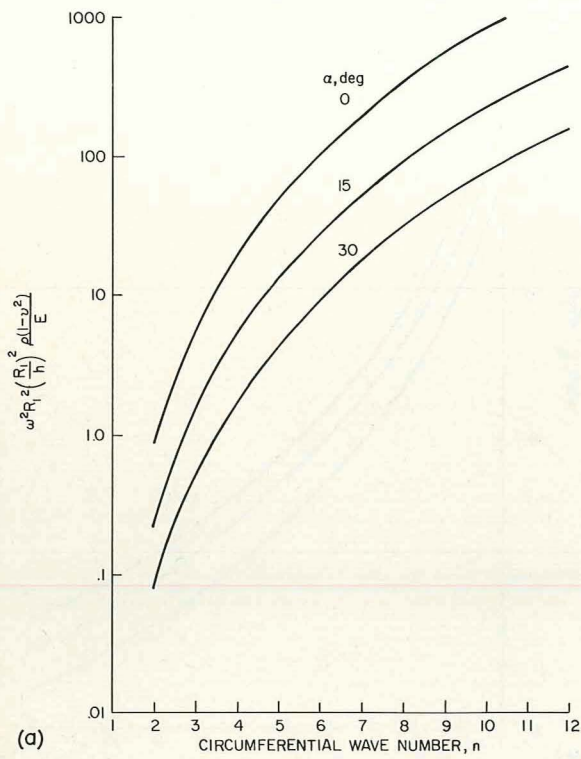


FIGURE 5.50.—Inextensional frequency parameters for clamped-free conical shells. (After ref. 5.61) (a) $l/R_1 = 2$. (b) $l/R_1 = 4$. (c) $l/R_1 = 6$.

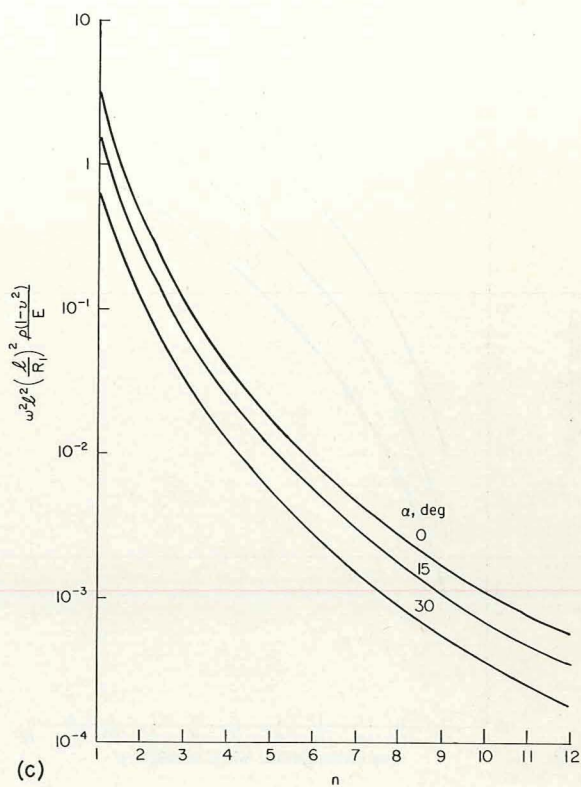
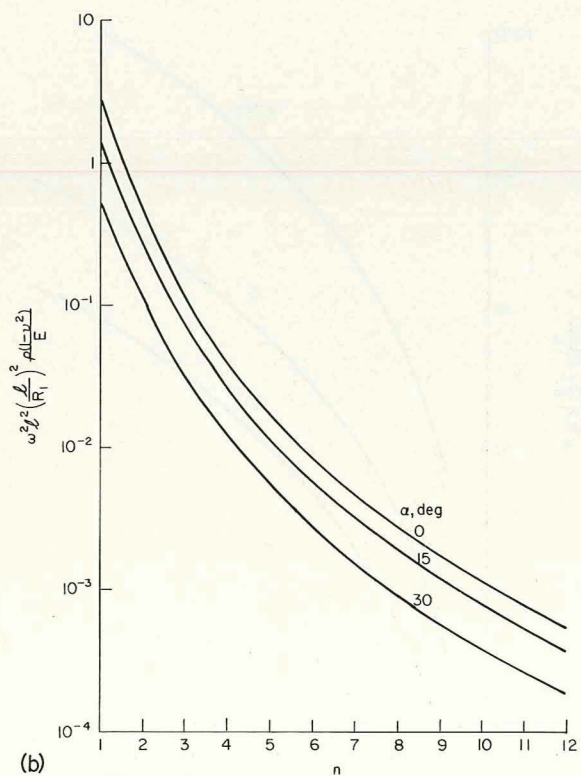
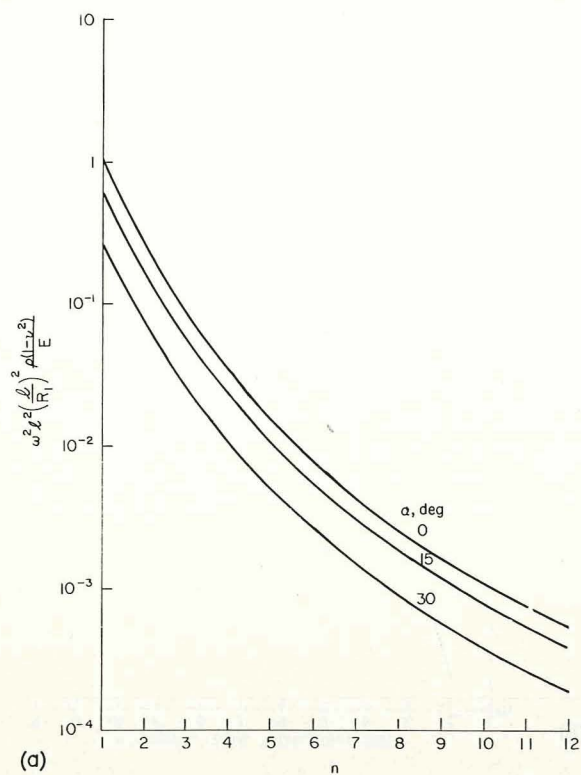


FIGURE 5.51.—Extensional (membrane) frequency parameters for clamped-free conical shells. (After ref. 5.61) (a) $l/R_1=2$. (b) $l/R_1=4$. (c) $l/R_2=6$.

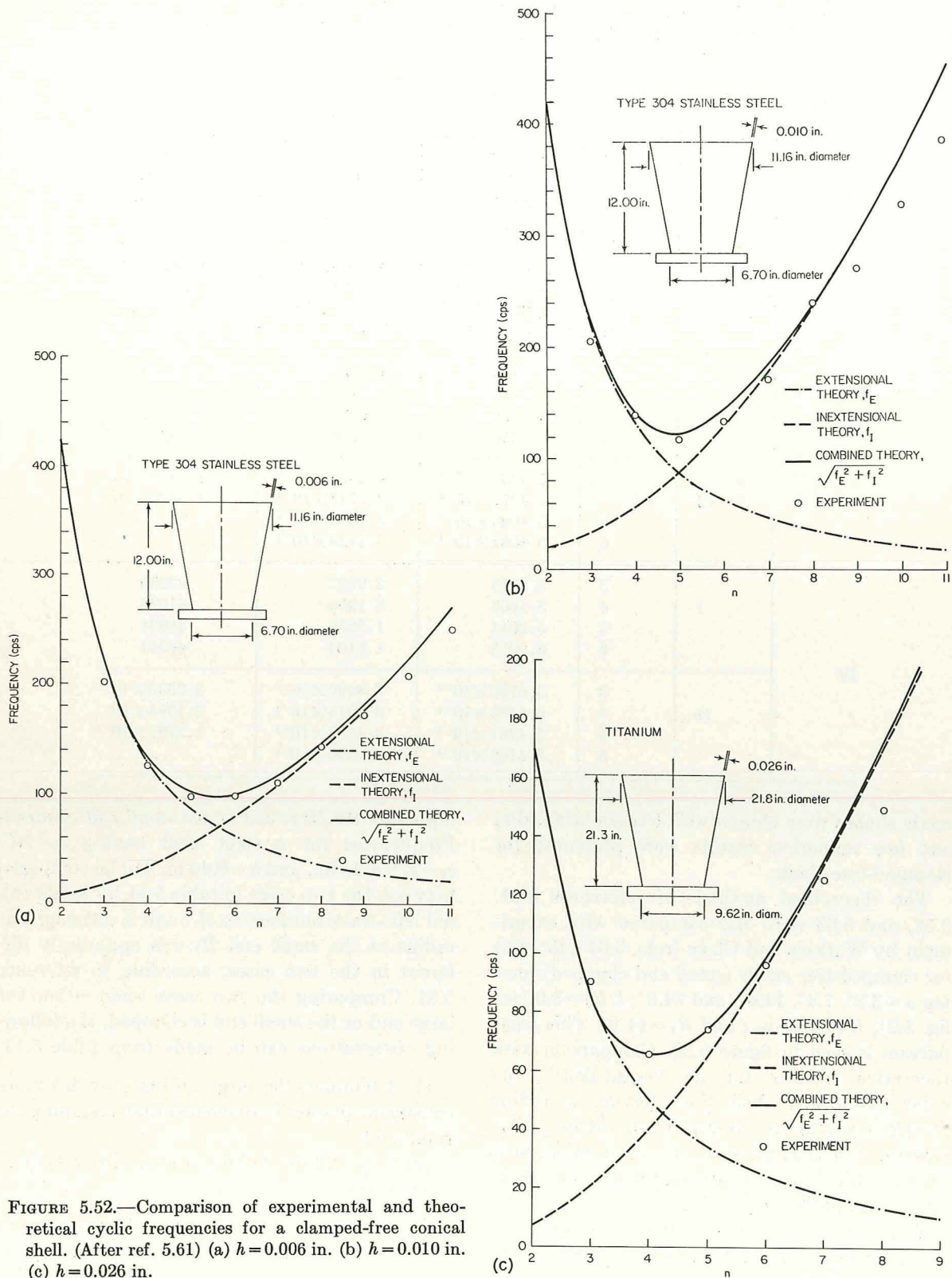


FIGURE 5.52.—Comparison of experimental and theoretical cyclic frequencies for a clamped-free conical shell. (After ref. 5.61) (a) $h = 0.006$ in. (b) $h = 0.010$ in. (c) $h = 0.026$ in.

TABLE 5.10.—*Dependence of Frequency Parameter $\omega^2 l^4 \rho (1 - \nu^2) / R_1^2 E$ Upon Number of Terms (N) Retained in Displacement Polynomials (5.53)*

$\frac{l}{R_1}$	n	N	α , degrees		
			0	20	40
1	1	3	0.31007	0.16353	0.054484
		4	.30740	.16202	.053756
		5	.30632	.16138	.053439
		6	.30576	.16105	.053361
	12	3	5.2357×10^{-4}	3.4466×10^{-4}	1.0327×10^{-4}
		4	5.1130×10^{-4}	3.2524×10^{-4}
		5	5.0854×10^{-4}	3.2150×10^{-4}
		6	5.0587×10^{-4}	3.1909×10^{-4}
4	1	3	3.2163	1.2158	.31436
		4	3.1004	1.1118	.27314
		5	3.0518	1.0721	.25627
		6	3.0245	1.0533	.24824
	12	3	5.4981×10^{-4}	4.2593×10^{-4}	1.9230×10^{-4}
		4	5.4271×10^{-4}	3.2717×10^{-4}	1.0826×10^{-4}
		5	5.4093×10^{-4}	3.1385×10^{-4}
		6	5.4001×10^{-4}	3.1129×10^{-4}
10	1	3	5.2343	2.9482	.92050
		4	5.1006	2.1900	.61074
		5	5.0611	1.9279	.48824
		6	5.0275	1.8105	.43014
	12	3	5.5106×10^{-4}	7.4946×10^{-4}	5.6632×10^{-4}
		4	5.4483×10^{-4}	3.9215×10^{-4}	2.1094×10^{-4}
		5	5.4261×10^{-4}	3.1483×10^{-4}	1.2701×10^{-4}
		6	5.4162×10^{-4}	2.9396×10^{-4}

mode shapes were chosen with less sophistication and few numerical results were presented for clamped-free shells.

The theoretical methods of references 5.61, 5.62, and 5.63 were also compared with experiment by Watkins and Clary (refs. 5.64 and 5.65) for clamped-free shells (small end clamped) having $\alpha = 3.2^\circ, 7.4^\circ, 14.0^\circ$, and 24.0° ; $l/R_1 = 3.0$ (see fig. 5.2); $h = 0.007$ in.; and $R_1 = 14$ in. This comparison is seen in figure 5.53. Comparison with theoretical results for an "equivalent" circular cylindrical shell (i.e., having a radius $\bar{R} = (R_1 + R_2)/2$) is available in figure 5.54. Observe here that the equivalent cylindrical shell model is highly inaccurate except for very small apex half-angles (i.e., $\alpha = 3.2^\circ$).

Weingarten (ref. 5.31) made experimental investigations of clamped-free conical shells hav-

ing either the large end or the small end clamped. Frequencies for a steel shell having $\alpha = 20^\circ$, $s_2 - s_1 = 8.25$ in., and $h = 0.40$ in. can be compared between the two cases in table 5.11 for longitudinal half-wave numbers m of 1 and 2, although the radius at the small end B_1 was apparently different in the two cases, according to reference 5.31. Comparing the two cases when either the large end or the small end is clamped, the following observations can be made from table 5.11:

(1) Clamping the large radius provides more constraint (higher frequencies) than clamping the small end.

(2) This difference becomes less important as m increases.

An extensive numerical study of the clamped-free (small end clamped) conical shell having an

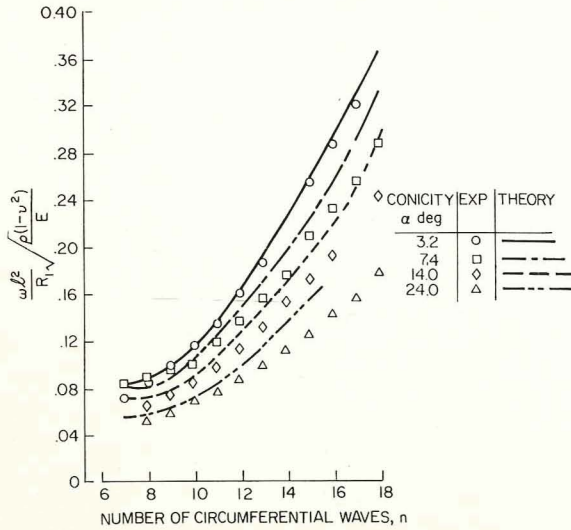


FIGURE 5.53.—Comparison of theoretical and experimental frequency parameters for a clamped-free conical shell. (After ref. 5.64)

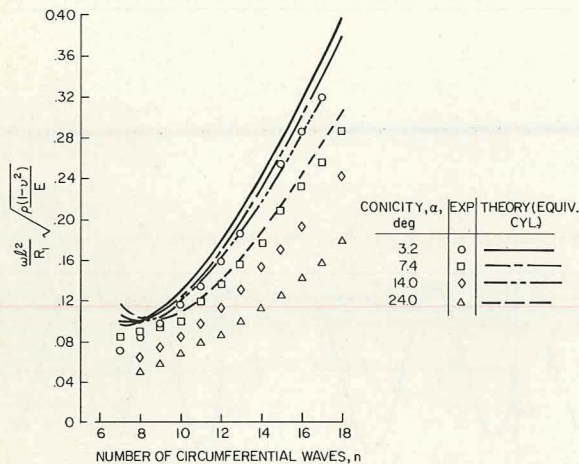


FIGURE 5.54.—Comparison of calculated "equivalent circular cylindrical shell" frequency parameters with experiment for a clamped-free conical shell. (After ref. 5.64)

apex half-angle of $\alpha=60^\circ$, $s_2-s_1=24.3$ in., $h=0.025$ in., $E=10 \times 10^6$ psi., $\nu=0.315$, and $\rho=2.54 \times 10^{-4}$ lb·sec²/in⁴ was made by Adelman, Catherines, and Walton (ref. 5.66) using the finite element method. The meridional length was divided into 10 finite shell elements. Mode shapes for each of the three frequencies arising for $n=2$ and $m=2, 3, 4, 5, 6$ are depicted in figures 5.55, 5.56, and 5.57, respectively, where

TABLE 5.11.—Experimental Frequencies for a Clamped-free Conical Shell (dimensions given in text)

n	$m=1$		$m=2$	
	Large radius clamped ^a	Small radius clamped ^b	Large radius clamped ^a	Small radius clamped ^b
2	421
3	^c 459–623	272	2078
4	878	342	1658	1328
5	1096	487	1814	1171
6	1287	667	2133
7	1530	873	2415	1533
8	1829	1106	2695	1841
9	2172	^c 1376–1379	3005	2192
10	2551	1681
11	3775

^a $R_1=2.0$ in.

^b $R_1=2.13$ in.

^c Two values listed in reference 5.31.

the abscissa is normalized to $(s-s_1)/(s_2-s_1)$ and the normalized amplitudes u/u_{\max} , v/v_{\max} , and w/w_{\max} are plotted.

The free vibrations of clamped-free conical shells were also analyzed by the finite element method in reference 5.67. The finite difference method was used in references 5.25 and 5.68.

Various types of boundary conditions representing clamped-free edges, but differing slightly from those of equations (5.44) are used in the free vibration problem in reference 5.69. This analysis will be discussed in section 5.3.7.

Other works dealing with the free vibrations of clamped-free conical shells include references 5.22, 5.23, 5.53, 5.70, 5.71, and 5.72.

5.3.5 Shear Diaphragm-Free

The boundary conditions for a conical shell supported by a shear diaphragm at the small end (for example) and free at the large end are

$$N_s = v = w = M_s = 0 \quad \text{at} \quad s = s_1 \quad (5.54a)$$

$$N_s = S_{s\theta} = V_s = M_s = 0 \quad \text{at} \quad s = s_2 \quad (5.54b)$$

Little data exist in the literature dealing with the free vibrations of SD-free conical shells.

This problem has received historical attention in the development and the application of the inextensional theory. Strutt (ref. 5.72) applied

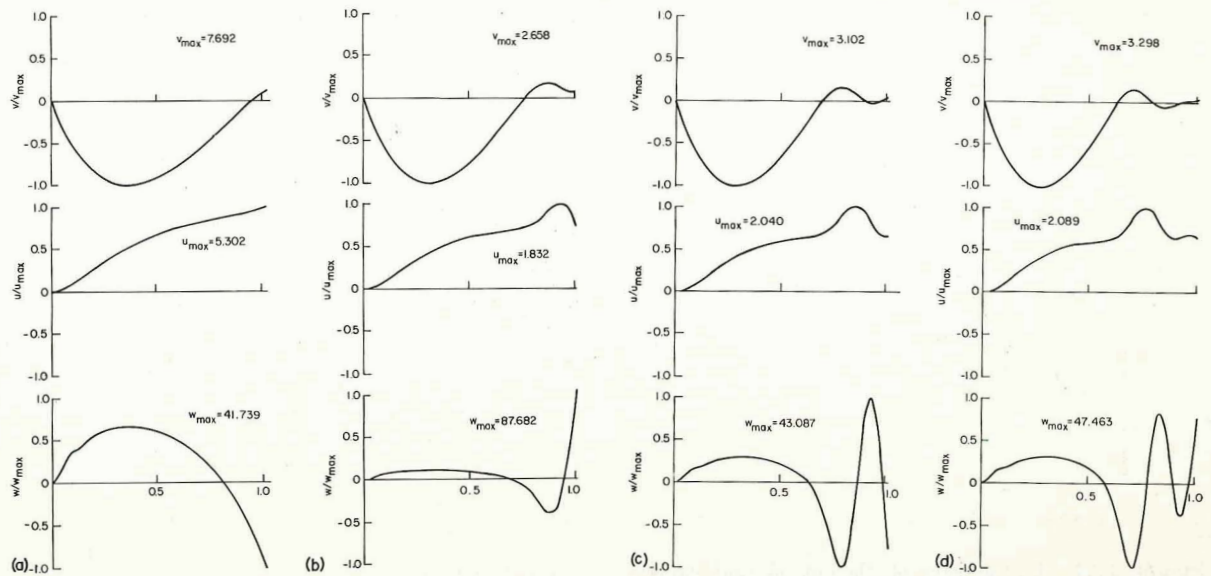


FIGURE 5.55.—Mode shapes for the *lowest* frequency of a clamped-free conical shell; $\alpha = 60^\circ$, $n = 2$. (After ref. 5.66) (a) $m = 2$. (b) $m = 3$. (c) $m = 4$. (d) $m = 5$. (e) $m = 6$.

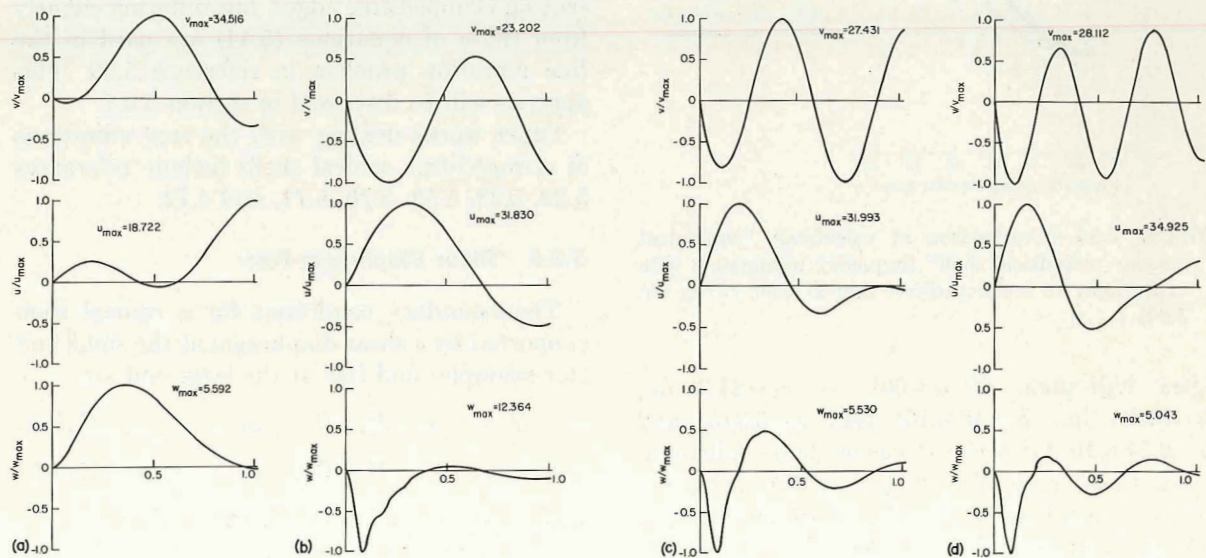


FIGURE 5.56.—Mode shapes for the *second* frequency of a clamped-free conical shell; $\alpha = 60^\circ$, $n = 2$. (After ref. 5.66) (a) $m = 2$. (b) $m = 3$. (c) $m = 4$. (d) $m = 5$. (e) $m = 6$.

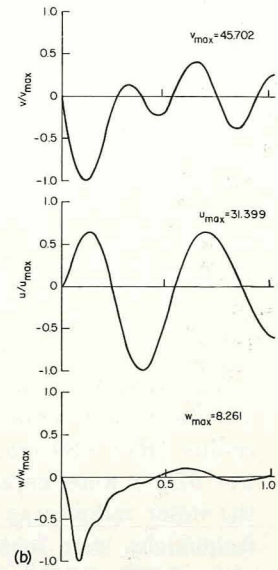
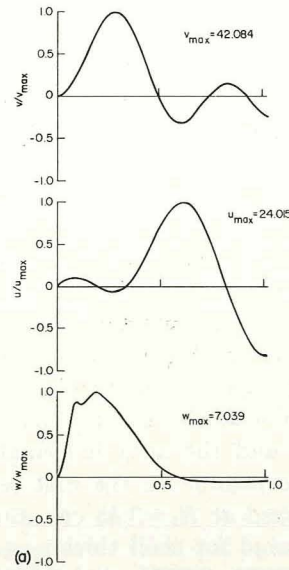
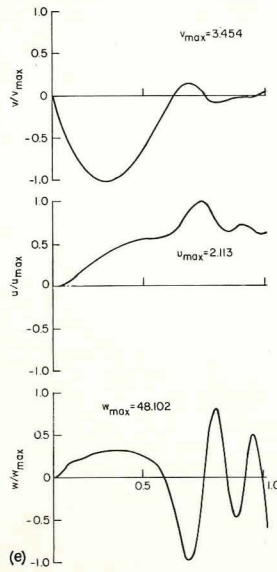
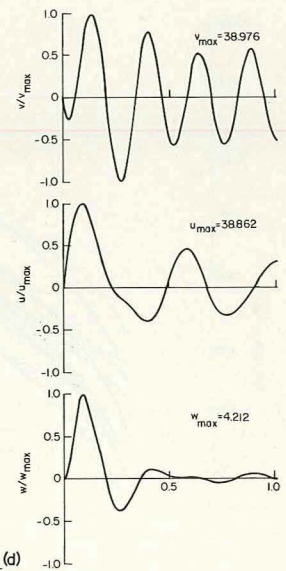
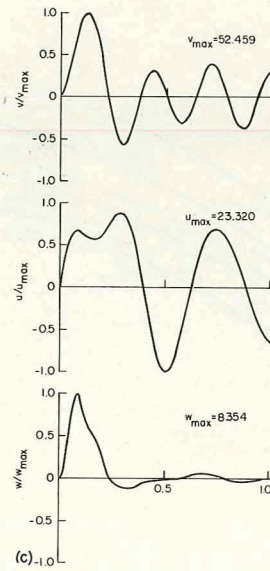
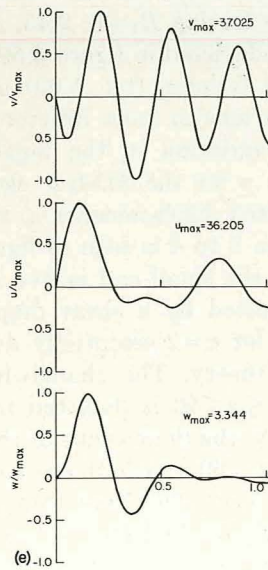


FIGURE 5.57.—Mode shapes for the *highest* frequency of a clamped-free conical shell; $\alpha = 60^\circ$, $n = 2$. (After ref. 5.66) (a) $m = 2$. (b) $m = 4$. (c) $m = 5$. (d) $m = 6$.



Rayleigh's (ref. 5.73) inextensional theory to obtain theoretical results. At the same time (1933), Van Urk and Hut (ref. 5.74) conducted experiments in a conical shell having the same boundary conditions. Federhofer (ref. 5.10) also analyzed the problem using the inextensional theory.

One of the principal difficulties with the inextensional theory is that of the two restraint conditions at the SD end, only $w=0$ is satisfied, whereas $v=0$ is not satisfied. This can cause considerable error in results, particularly for small circumferential wave numbers.

The use of inextensional theory for *part* of the analysis was demonstrated in section 5.3.4. Thus, equation (5.50) can be used directly for the SD-free shell, particularly for large values of n .

Van Urk and Hut (ref. 5.74) conducted two sets of experiments. For both sets the outer radius ($R_1=8.80$ cm.) and the apex half-angle ($\alpha=57.5^\circ$) were kept constant. In the first set the inner radius was fixed at $R_2=2.45$ cm. and frequencies were measured for shell thicknesses of $h=0.020$, 0.0114 , 0.0078 , 0.0064 , and 0.0042 cm. as shown by the dashed lines in figure 5.58.

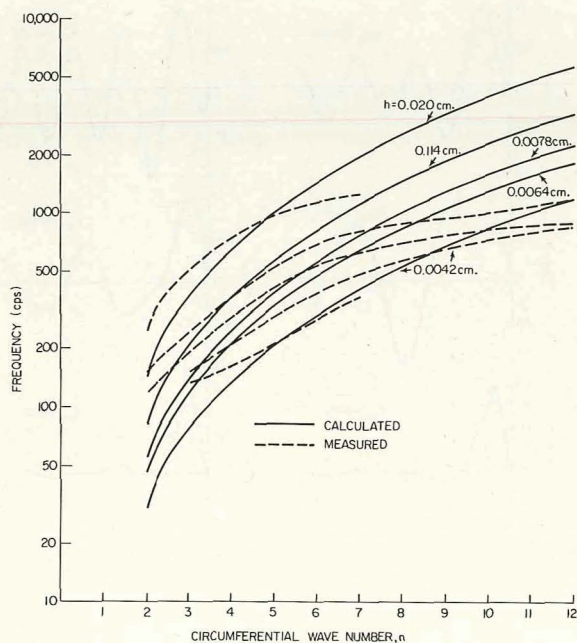


FIGURE 5.58.—Frequencies for SD-free conical shells (dimensions in text). (After ref. 5.74)

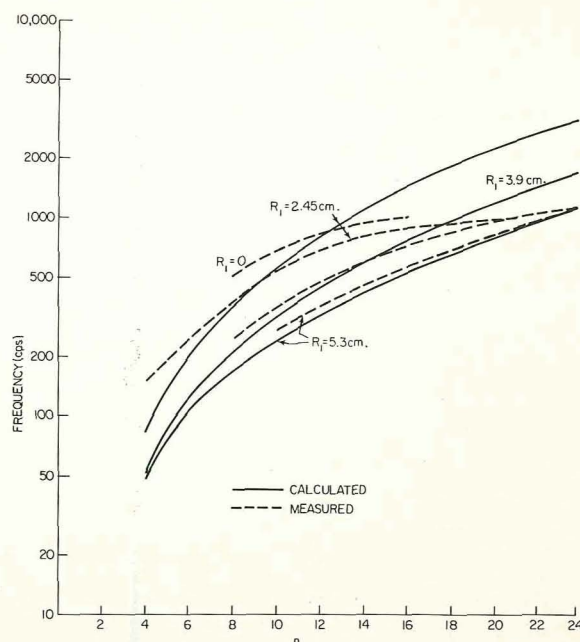


FIGURE 5.59.—Frequencies for SD-free conical shells (dimensions in text). (After ref. 5.74)

The solid lines in figure 5.58 show the calculated values of the frequency according to the inextensional theory. In the second set of experiments, h was kept at 0.0114 cm. and results were obtained for shells having $R_1=0$, 2.45 , 3.9 , and 5.3 cm. These are depicted in figure 5.59.

Weingarten and Gelman (ref. 5.69) used the Sanders shell equations in finite difference form and showed the variation in the longitudinal mode shapes with n for the SD-free shell. The change in normalized displacements u , v , and w as n increases from 2 to 4 is seen in figure 5.60 for the case when the small end is free and the large end is supported by a shear diaphragm. The mode shapes for $n=2$ essentially duplicate the inextensional theory. The change in mode shape for w for $1 \leq n \leq 10$ is depicted in figure 5.61. Unfortunately, the dimensions of the shells upon which figures 5.60 and 5.61 are based are not given in reference 5.69. Note that a mode shape is shown in figure 5.61 for $n=1$, and that it corresponds to $m=2$.

Free vibrations of SD-free conical shells are also discussed in reference 5.31.

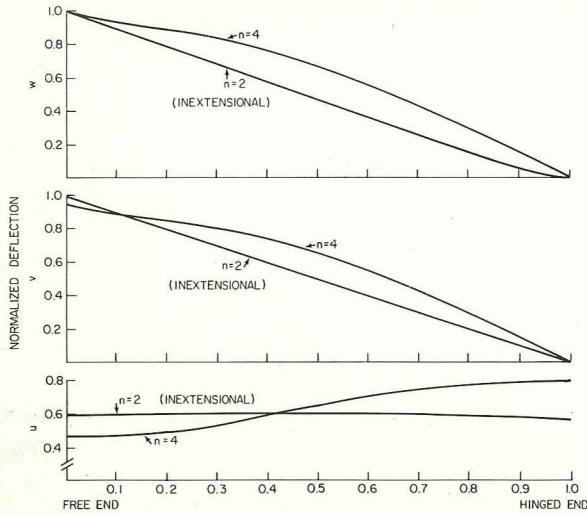


FIGURE 5.60.—Comparison of mode shapes for an SD-free conical shell. (After ref. 5.69)

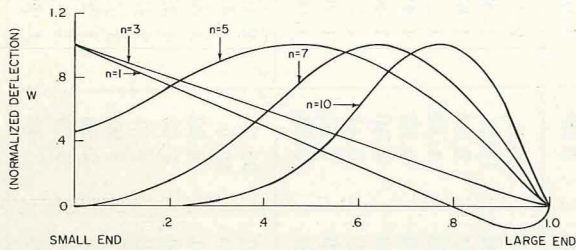


FIGURE 5.61.—Normal displacement mode shapes for an SD-free conical shell. (After ref. 5.69)

5.3.6 Free-Free

The boundary conditions for this case are

$$N_s = S_{s\theta} = V_s = M_s = 0 \quad \text{at} \quad s = s_1, s_2 \quad (5.55)$$

This problem has received long and careful attention in the literature of shell vibrations. Rayleigh (refs. 5.73 and 5.75) in 1881 demonstrated his inextensional shell theory on this example. Strutt (ref. 5.72) in 1933 and Federhofer (ref. 5.10) in 1938 also analyzed this case with the inextensional theory. Subsequent writers have used inextensional, membrane, and bending theories to analyze this problem, as will be seen below. The inextensional theory of shells is particularly applicable for this case because, as in the case of the cylindrical

shell, the middle surface of a conical shell having both ends free is mathematically capable of deforming inextensionally.

Hu, Gormley, and Lindholm (ref. 5.76) used the inextensional displacement functions

$$\left. \begin{aligned} u_n &= A \sin \alpha \cos \alpha \\ v_n &= \left(A + B \frac{s}{s_2} \right) n \cos \alpha \\ w_n &= \left[A (n^2 - \sin^2 \alpha) + B n^2 \frac{s}{s_2} \right] \end{aligned} \right\} \quad (5.56)$$

to define the longitudinal variation in equations (5.14). The Ritz method was used to arrive at the characteristic equation

$$(c_{11}c_{22} - c_{12}^2)\Omega_7^4 - (c_{11}d_{22} + c_{22}d_{11} - 2c_{12}d_{12})\Omega_7^2 + (d_{11}d_{22} - d_{12}^2) = 0 \quad (5.57)$$

where Ω_7^2 is the nondimensional frequency parameter defined by

$$\Omega_7^2 = \frac{\omega^2 R_2^2 \rho h}{D} \frac{(n^2 + \cos^2 \alpha)}{n^2(n^2 - 1)^2} \quad (5.58)$$

D is the flexural rigidity ($D = Eh^3/12(1 - \nu^2)$), and

$$\left. \begin{aligned} c_{11} &= \frac{1}{2} \left[1 - \frac{(2n^2 - 1) \sin^2 \alpha}{n^2(n^2 + \cos^2 \alpha)} \right] \left[1 - \left(\frac{s_1}{s_2} \right)^2 \right] \\ c_{12} &= \frac{1}{3} \left[1 - \frac{\sin^2 \alpha}{n^2 + \cos^2 \alpha} \right] \left[1 - \left(\frac{s_1}{s_2} \right)^3 \right] \\ c_{22} &= \frac{1}{4} \left[1 - \left(\frac{s_1}{s_2} \right)^4 \right] \\ d_{11} &= \frac{1}{2} \left[1 + \frac{2(1 - \nu) \sin^2 \alpha}{n^2} \right] \left[\left(\frac{s_1}{s_2} \right)^2 - 1 \right] \\ d_{12} &= \frac{s_2}{s_1} - 1 \\ d_{22} &= \log \frac{s_2}{s_1} \end{aligned} \right\} \quad (5.59)$$

(see figs. 5.1 and 5.2 for the dimensions used above).

Extensive tabular results were given in reference 5.76 for the two roots Ω_7^2 (which are both positive) arising from solving equation (5.57). The parameters Ω_7 are repeated in table 5.12. The frequency parameter Ω_7 depends mainly upon s_1/s_2 and becomes independent of α and n for large values of n . However, the inextensional

TABLE 5.12.—*Inextensional Frequency Parameters Ω_1 (Defined by Eq. (5.58)) for Free-Free Conical Shells*

n	$\frac{s_1}{s_2}$	α , degree											
		15		30		45		60		75		90	
2	0.1	2.14	14.6	2.22	26.1	2.29	28.9	2.35	33.3	2.38	38.9	2.39	42.1
	.2	1.79	10.5	1.88	11.5	1.95	13.2	2.00	15.6	2.01	18.7	2.02	20.5
	.3	1.60	6.25	1.71	7.09	1.77	8.37	1.80	10.2	1.80	12.6	1.80	14.1
	.4	1.49	4.30	1.59	5.11	1.64	6.24	1.65	7.85	1.64	10.1	1.64	11.5
	.5	1.41	3.26	1.50	4.10	1.52	5.16	1.52	6.68	1.50	8.96	1.50	10.6
	.6	1.36	2.69	1.41	3.59	1.41	4.60	1.39	6.07	1.37	8.64	1.37	11.0
	.7	1.29	2.45	1.31	3.37	1.29	4.28	1.27	5.75	1.25	8.82	1.24	12.6
	.8	1.20	2.51	1.20	3.29	1.17	4.06	1.15	5.50	1.13	9.25	1.13	17.0
	.9	1.10	2.73	1.09	3.18	1.06	3.81	1.04	5.19	1.02	9.46	1.02	31.5
3	.1	2.12	24.4	2.16	25.4	2.20	26.9	2.24	28.8	2.26	30.4	2.27	31.1
	.2	1.76	10.4	1.81	11.0	1.87	11.9	1.90	13.0	1.93	13.9	1.93	14.3
	.3	1.57	6.12	1.63	6.62	1.69	7.36	1.73	8.21	1.75	8.95	1.75	9.26
	.4	1.45	4.16	1.52	4.65	1.58	5.36	1.61	6.15	1.62	6.85	1.62	7.15
	.5	1.36	3.09	1.45	3.65	1.49	4.39	1.51	5.22	1.51	5.96	1.51	6.28
	.6	1.31	2.48	1.38	3.17	1.40	4.01	1.41	4.94	1.40	5.81	1.40	6.22
	.7	1.26	2.18	1.30	3.09	1.30	4.07	1.30	5.17	1.29	6.36	1.29	6.99
	.8	1.20	2.26	1.20	3.41	1.19	4.50	1.18	5.90	1.18	7.89	1.17	9.26
	.9	1.10	2.96	1.09	4.05	1.08	5.09	1.07	6.93	1.07	11.1	1.06	17.0
4	.1	2.11	24.3	2.13	24.9	2.16	25.8	2.19	26.8	2.21	27.6	2.21	27.9
	.2	1.76	10.3	1.79	10.7	1.82	11.2	1.85	11.8	1.87	12.3	1.87	12.4
	.3	1.56	6.05	1.60	6.36	1.64	6.80	1.67	7.27	1.69	7.64	1.70	7.78
	.4	1.43	4.09	1.48	4.39	1.53	4.82	1.57	5.27	1.58	5.63	1.59	5.77
	.5	1.34	3.01	1.41	3.35	1.46	3.83	1.48	4.32	1.49	4.70	1.50	4.85
	.6	1.28	2.36	1.35	2.82	1.39	3.40	1.40	3.98	1.40	4.44	1.40	4.62
	.7	1.24	2.01	1.29	2.68	1.30	3.44	1.30	4.18	1.30	4.79	1.30	5.04
	.8	1.19	1.98	1.20	3.02	1.20	4.05	1.20	5.10	1.19	6.09	1.19	6.56
	.9	1.10	2.72	1.10	4.22	1.09	5.55	1.09	7.32	1.08	9.97	1.08	11.9
5	.1	2.11	24.2	2.12	24.6	2.14	25.2	2.16	25.8	2.17	26.3	2.18	26.5
	.2	1.75	10.3	1.77	10.5	1.80	10.9	1.82	11.2	1.83	11.5	1.84	11.6
	.3	1.55	6.02	1.58	6.22	1.61	6.50	1.64	6.80	1.66	7.03	1.66	7.12
	.4	1.42	4.05	1.46	4.25	1.50	4.53	1.53	4.82	1.55	5.04	1.55	5.13
	.5	1.33	2.96	1.38	3.19	1.43	3.51	1.45	3.83	1.47	4.08	1.47	4.17
	.6	1.26	2.31	1.33	2.61	1.37	3.02	1.39	3.42	1.39	3.71	1.40	3.82
	.7	1.22	1.91	1.28	2.39	1.30	2.96	1.30	3.50	1.30	3.89	1.30	4.04
	.8	1.18	1.80	1.20	2.63	1.20	3.50	1.20	4.28	1.20	4.90	1.20	5.15
	.9	1.10	2.40	1.10	3.95	1.10	5.32	1.09	6.81	1.09	8.42	1.09	9.26

TABLE 5.12.—*Inextensional Frequency Parameters Ω_7 (Defined by Eq. (5.58)) for Free-Free Conical Shells—Concluded*

n	$\frac{s_1}{s_2}$	α , degree											
		15		30		45		60		75		90	
6	0.1	2.11	24.2	2.12	24.5	2.13	25.3	2.14	25.3	2.15	25.6	2.16	25.7
	.2	1.75	10.3	1.76	10.4	1.78	10.7	1.80	10.9	1.81	11.1	1.81	11.2
	.3	1.55	5.99	1.57	6.14	1.59	6.34	1.62	6.54	1.63	6.70	1.63	6.76
	.4	1.42	4.03	1.45	4.17	1.48	4.37	1.50	4.57	1.52	4.72	1.52	4.78
	.5	1.32	2.94	1.36	3.10	1.40	3.33	1.43	3.55	1.44	3.72	1.45	3.78
	.6	1.25	2.27	1.31	2.49	1.35	2.78	1.37	3.07	1.38	3.28	1.38	3.36
	.7	1.20	1.86	1.26	2.21	1.29	2.64	1.30	3.05	1.30	3.34	1.30	3.44
	.8	1.17	1.69	1.20	2.35	1.20	3.05	1.20	3.67	1.20	4.12	1.20	4.29
	.9	1.10	2.14	1.10	3.56	1.10	4.85	1.10	6.07	1.09	7.14	1.09	7.61
7	.1	2.11	24.2	2.11	24.4	2.12	24.7	2.13	25.0	2.14	25.2	2.14	25.3
	.2	1.75	10.3	1.76	10.4	1.77	10.6	1.78	10.7	1.79	10.9	1.80	10.9
	.3	1.55	5.98	1.56	6.09	1.58	6.24	1.60	6.39	1.61	6.50	1.61	6.54
	.4	1.42	4.01	1.44	4.12	1.46	4.27	1.48	4.41	1.50	4.52	1.50	4.57
	.5	1.32	2.92	1.35	3.04	1.38	3.21	1.41	3.38	1.42	3.50	1.43	3.55
	.6	1.24	2.25	1.29	2.41	1.33	2.63	1.35	2.85	1.36	3.01	1.37	3.07
	.7	1.19	1.83	1.25	2.09	1.28	2.43	1.29	2.74	1.30	2.97	1.30	3.05
	.8	1.16	1.61	1.19	2.14	1.20	2.72	1.20	3.23	1.20	3.58	1.20	3.71
	.9	1.10	1.94	1.10	3.19	1.10	4.35	1.10	5.38	1.10	6.17	1.10	6.49
8	.1	2.10	24.2	2.11	24.3	2.12	24.5	2.13	24.8	2.13	25.0	2.13	25.0
	.2	1.75	10.2	1.75	10.3	1.76	10.5	1.77	10.6	1.78	10.7	1.78	10.8
	.3	1.55	5.97	1.56	6.05	1.57	6.17	1.59	6.28	1.60	6.37	1.60	6.40
	.4	1.41	4.00	1.43	4.09	1.45	4.20	1.47	4.31	1.48	4.40	1.48	4.43
	.5	1.31	2.91	1.34	3.00	1.37	3.13	1.39	3.27	1.40	3.36	1.41	3.39
	.6	1.24	2.24	1.28	2.36	1.31	2.53	1.34	2.70	1.35	2.83	1.35	2.87
	.7	1.19	1.81	1.24	2.01	1.27	2.27	1.28	2.53	1.29	2.71	1.29	2.77
	.8	1.15	1.57	1.19	1.99	1.20	2.47	1.20	2.90	1.20	3.19	1.20	3.29
	.9	1.10	1.79	1.10	2.88	1.10	3.92	1.10	4.79	1.10	5.43	1.10	5.67

CONICAL SHELLS

theory becomes highly inaccurate for large n . The location of the nodal circle (i.e., where $w=0$) for a particular frequency parameter Ω_7 is given by (ref. 5.76)

$$s = s_2 \left(\frac{\sin^2 \alpha}{n^2} - 1 \right) \left(\frac{\Omega_7^2 c_{12} - d_{12}}{\Omega_7^2 c_{11} - d_{11}} \right) \quad (5.60)$$

Calculations for free-free shells were also made by Hu (ref. 5.29) by means of the membrane theory. The Galerkin procedure was used with solution functions in terms of trigonometric functions of s leading to an infinite determinant, the elements of which are given in detail in reference 5.29. Extensive results were obtained with truncated determinants retaining 11 terms. Figure 5.62 shows the dependency of the frequency parameter $\Omega^* = \omega R_2 \sqrt{\rho(1-\nu^2)/E}$ upon the semivertex angle α for axisymmetric modes ($n=0$) and for $s_2/s_1=2.0$. It was found that, for $\alpha > 15^\circ$ the frequencies appear as two groups, cor-

responding to longitudinal and transverse modes, with the frequencies of the longitudinal modes always being greater than those of the transverse modes. However, for $\alpha < 15^\circ$ the modes are coupled. Figure 5.63 describes similar results for $s_2/s_1=4.0$, for which strong coupling of modes occurs for $0 < \alpha < 45^\circ$.

Note in figures 5.62 and 5.63 that, while the frequency parameters of longitudinal modes extend to infinity, those of transverse modes are spaced in a finite interval shown by the shaded region. This result is the limiting case when the shell thickness tends to zero, as required for membrane theory. For real shells with finite bending rigidity, the frequencies of higher transverse modes are expected to be significantly increased. The curves labeled "R" in figures 5.62 and 5.63 are the so-called "ring modes." For this type of mode the entire shell vibrates without a nodal circle and uniform circumferential

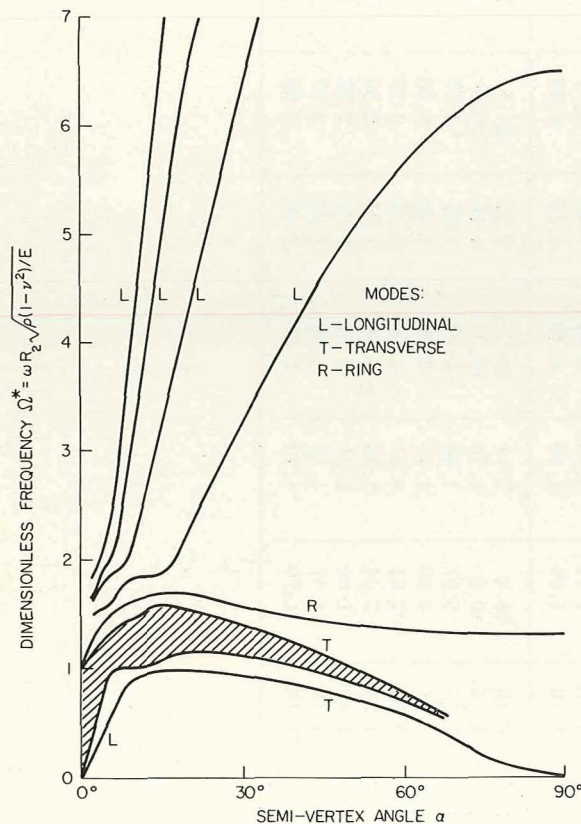


FIGURE 5.62.—Membrane frequency parameters for axisymmetric ($n=0$) modes of free-free conical shells; $s_2/s_1=2.0$. (After ref. 5.29)

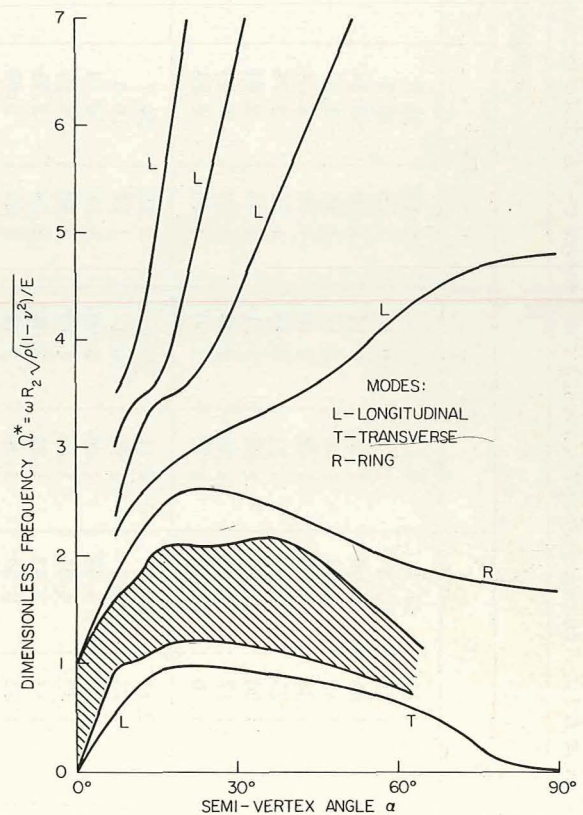


FIGURE 5.63.—Membrane frequency parameters for axisymmetric ($n=0$) modes of free-free conical shells; $s_2/s_1=4.0$. (After ref. 5.29)

(or "hoop") stress is the predominant type of membrane stress present.

Dependence of the frequency parameter upon the length ratio s_2/s_1 is shown in figure 5.64 for $\alpha = 15^\circ$. Extensive results are also available in reference 5.29 showing the variation of the membrane force resultants with s while executing free vibration modes.

Hu, Gormley, and Lindholm (refs. 5.76 and 5.77) also made experimental measurements of frequencies of free-free conical shells made of 0.010 in. steel shimstock. Data were taken on four experimental models as described by table 5.13. Variation of the frequency with the circum-

TABLE 5.13.—Dimensions of Four Shell Models

Model number	α , degrees	$\frac{s_1}{s_2}$	$\frac{h}{R_2}$	R_2 , in.
1	14.2	2.23	0.00166	6.07
2	30.2	2.27	.00127	7.95
3	45.1	2.25	.00112	8.96
4	60.5	2.25	.00101	10.00

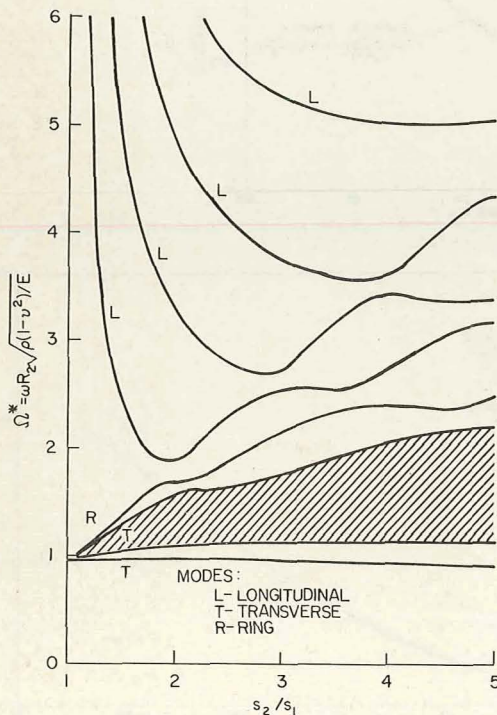


FIGURE 5.64.—Membrane frequency parameters for axi-symmetric ($n=0$) modes of free-free conical shells; $\alpha = 15^\circ$. (After ref. 5.29)

ferential wave number n is shown by the data points of figures 5.65 for the four models. For $m=1$ the experimental data points form a smooth curve which is essentially parabolic in shape. However, the curves for $m=2$ and $m=3$ are more complicated in shape.

In addition, the following semiempirical formula for frequency parameters was derived in reference 5.76 based upon inextensional deformation:

$$\Omega^* = \sqrt{k} \frac{n(n-1)}{\sqrt{n^2+1}} \left(n+1 - 4 \sin \frac{3\alpha}{2} \right) \quad (5.61)$$

where $k = h^2/12R_1^2$. Frequencies obtained from equation (5.61) are also plotted in figures 5.65 as solid curves, yielding excellent agreement with the experiment.

Experimental mode shapes for the four models of table 5.13 were also measured in references 5.76 and 5.77. Because the mode shapes for the four shells were similar, only the results for model 2 ($\alpha = 45.1^\circ$) were presented. Circumferential mode shapes were found to vary sinusoidally, as predicted by theory. Figure 5.66 and 5.67 show the normalized transverse mode shapes along a generator for $m=1$ and 2, respectively. In figure 5.66 the transverse displacement is essentially linear for $n=2$ to 10, as assumed by Rayleigh's inextensional theory. The nodal circle is near the small end of the conical shell for small values of n , but gradually shifts towards the middle as n increases. However, as n increases from 10 to 12, a drastic change in the mode shape occurs. The generator changes to a curved form with decreased motion near the smaller end of the shell.

In figure 5.67 a similar mapping of mode shapes is shown for $m=2$. Note that the number of nodal circles does not increase from one to two, as might be expected. Rather, the mode shapes resemble those of figure 5.66, except that the nodal circles now occur nearer the large end of the shell. Again, in the vicinity of $n=10$ to 12 the generator begins to deviate from a nearly straight line into a reverse curve. This transition is reflected on the frequency plots of figure 5.65(c) where the slope of the Ω^*-n curve abruptly changes. This indicates that the new mode shape formed during this transition has a slightly lower energy level than the corresponding inextensional modes.

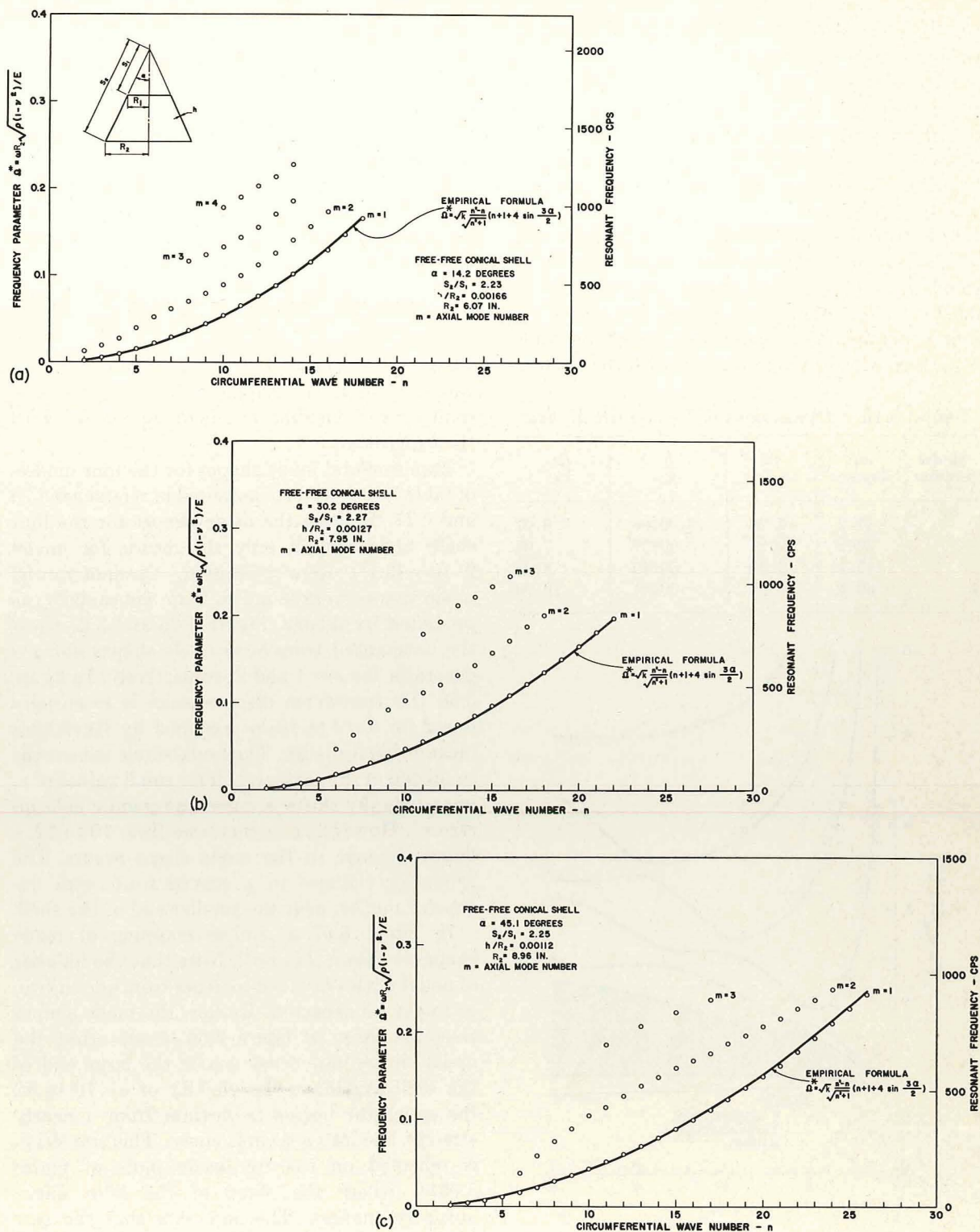


FIGURE 5.65.—Experimentally determined frequencies for free-free conical shells. (After ref. 5.77)

(a) Model 1, $\alpha = 14.2^\circ$. (b) Model 2, $\alpha = 30.2^\circ$. (c) Model 3, $\alpha = 45.1^\circ$. (d) Model 4, $\alpha = 60.5^\circ$.

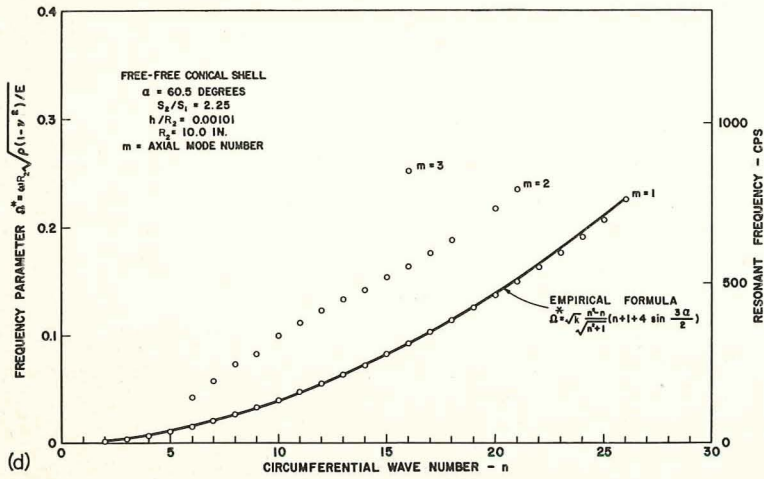
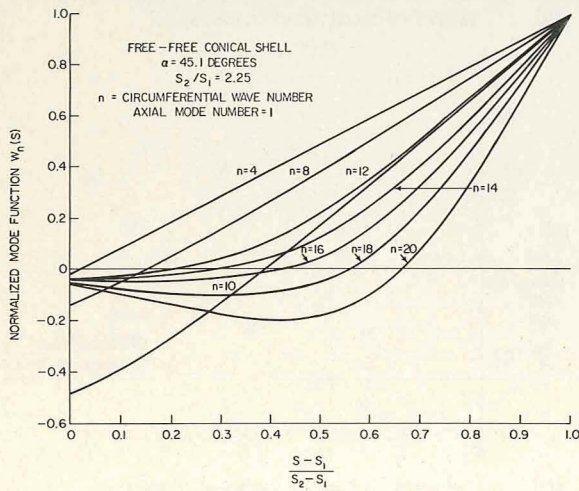
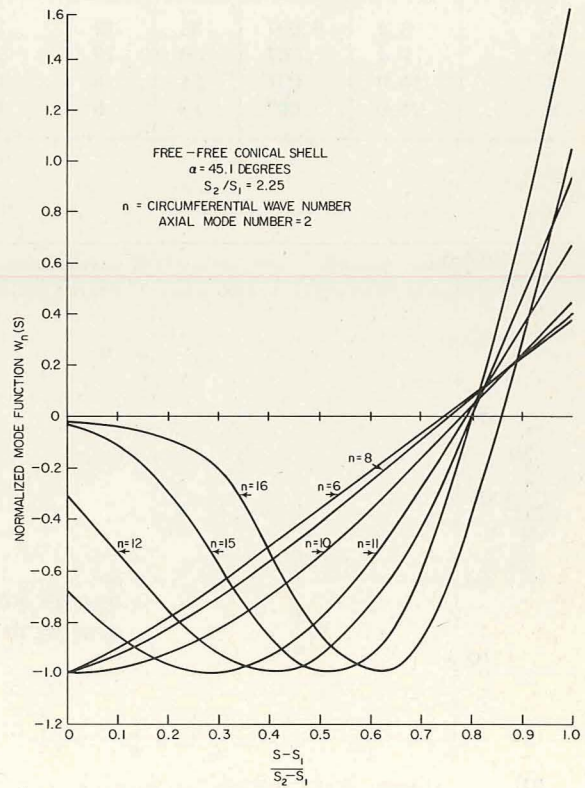


FIGURE 5.65.—Concluded.

FIGURE 5.66.—Normalized mode shapes for the transverse displacements of a free-free conical shell; $m=1$. (After refs. 5.76 and 5.77)FIGURE 5.67.—Normalized mode shapes for the transverse displacements of a free-free conical shell; $m=2$. (After refs. 5.76 and 5.77)

In 1964 Watkins and Clary (refs. 5.64 and 5.65) presented the results of an experimental investigation on free-free conical shells which were the subject of considerable subsequent discussion by other writers. Tests were conducted on four stainless steel models, described in table 5.14, made with 5/32 in. overlapped, spotwelded, longitudinal seams. They found that at higher frequencies there were a greater number of circumferential waves at the larger end than at the smaller end. The difference in the number of waves increases as the frequencies increased and also as the apex angle α increased. The difference ranged from one to five waves for the frequency range covered in the investigation, as shown in figure 5.68.

TABLE 5.14.—Dimensions of Four Different Shell Models (see figs. 5.1 and 5.2)

Model number	α , degrees	h , in.	l , in.	R_1 , in.	R_2 , in.
1	3.2	0.007	36	12	14
2	7.4	.007	30	10	14
3	14.0	.007	24	8	14
4	24.0	.007	18	6	14

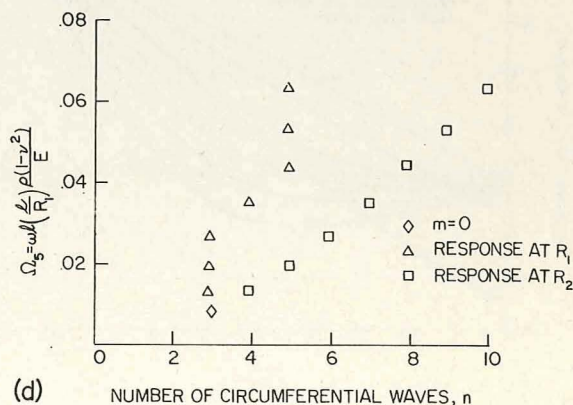
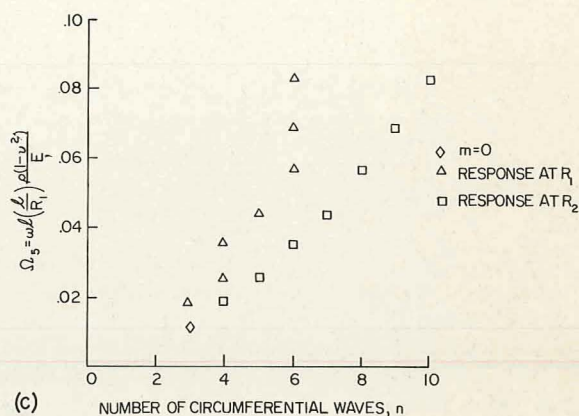
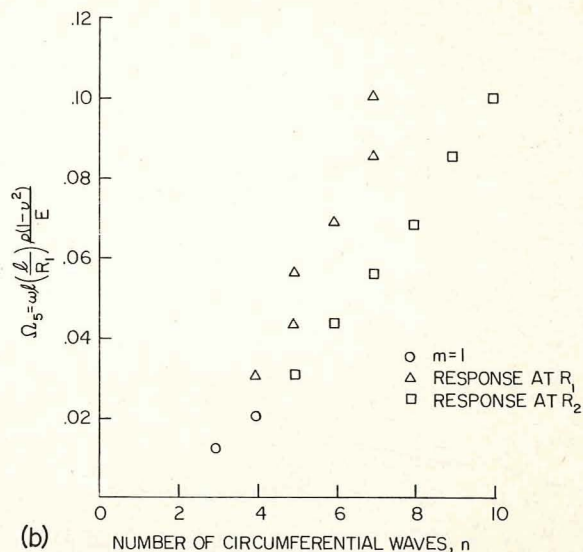
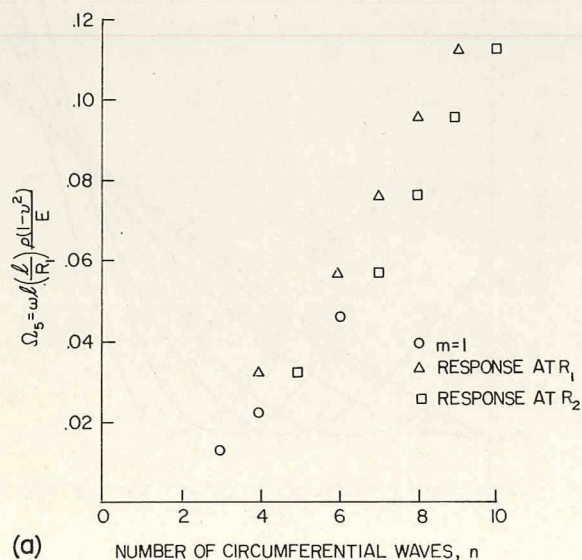
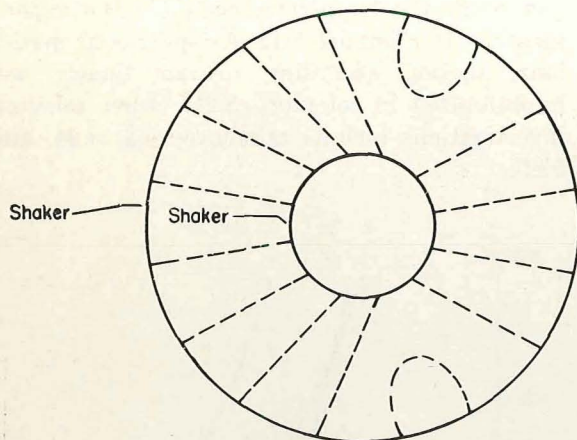


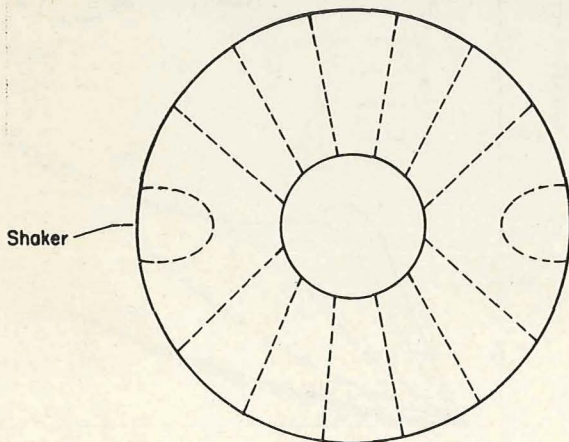
FIGURE 5.68.—Experimental frequencies for free-free conical shells. (After ref. 5.64) (a) Model 1, $\alpha=3.2^\circ$. (b) Model 2, $\alpha=7.4^\circ$. (c) Model 3, $\alpha=14.0^\circ$. (d) Model 4, $\alpha=24.0^\circ$.

Figure 5.69 shows typical nodal patterns observed for model 3 with six and eight circumferential waves at the smaller and larger ends, respectively. Two shakers tended to excite asymmetrical nodal patterns, while a nodal pattern from a single shaker tended to be symmetric, as shown.

The behavior observed by Watkins and Clary was discussed by Hu (ref. 5.78) and by Koval (ref. 5.79). Hu thought that the difference in circumferential wave number at the two ends was due to the location of the shakers. Koval



(a) Asymmetrical nodal pattern.



(b) Symmetrical nodal pattern.

FIGURE 5.69.—Typical nodal patterns as viewed along the longitudinal axis for model 3. (After ref. 5.64)

suggested the anomaly might be the result of dynamic asymmetries due to the lap joint method of model fabrication. This problem received further study by Mixson (refs. 5.80, 5.81, and 5.82) who tested five additional shell models, three having butt-welded seams and two having lapped seams. He found that the location of the shaker did indeed cause mixed modes in some cases, but that the effect of seams was even more important. The method of suspension was also found to be significant in determining coupling between the modes having different circumferential wave numbers.

Naumann (ref. 5.83) analyzed the free-free case using the Ritz method with power series in the meridional direction to approximate the mode shapes. Results were obtained for shells made of aluminum 0.0635 cm thick and having $\alpha = 60^\circ$ and $R_1/R_2 = 1/8$. These are depicted in figure 5.70, where the inextensional frequency is also shown. Corresponding mode shapes for the

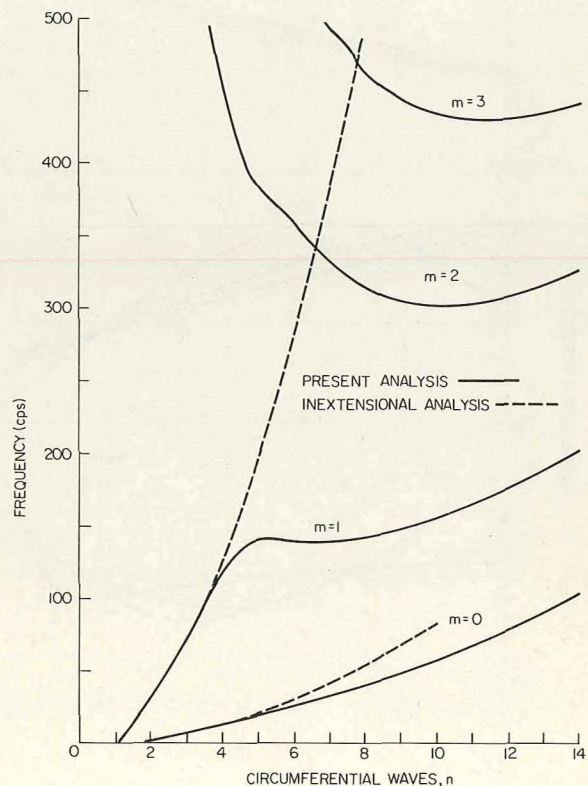


FIGURE 5.70.—Frequencies for free-free conical shells; $\alpha = 60^\circ$, $R_1/R_2 = 1/8$. (After ref. 5.83)

transverse deflection are displayed in figure 5.71. Frequencies for other R_1/R_2 ratios are shown in figure 5.72. In reference 5.83 extensive numerical results were obtained for the experimental models of references 5.64, 5.65, 5.76, 5.77, 5.80, 5.81, and 5.82 and the agreement obtained with the experimental results given in the above references is remarkably good.

Another comprehensive study of the free vibrations of free-free conical shells was made by Krause (ref. 5.84). Analytical investigations were made using the Galerkin procedure with meridional variations in the displacement functions taken as algebraic polynomials. Extensive comparisons were made with references 5.64 and 5.77. Of particular interest is the study made of the difference in circumferential wave number at the two ends found experimentally by Watkins and Clary (ref. 5.64) and discussed above. Reference 5.84 shows that two analytical curves

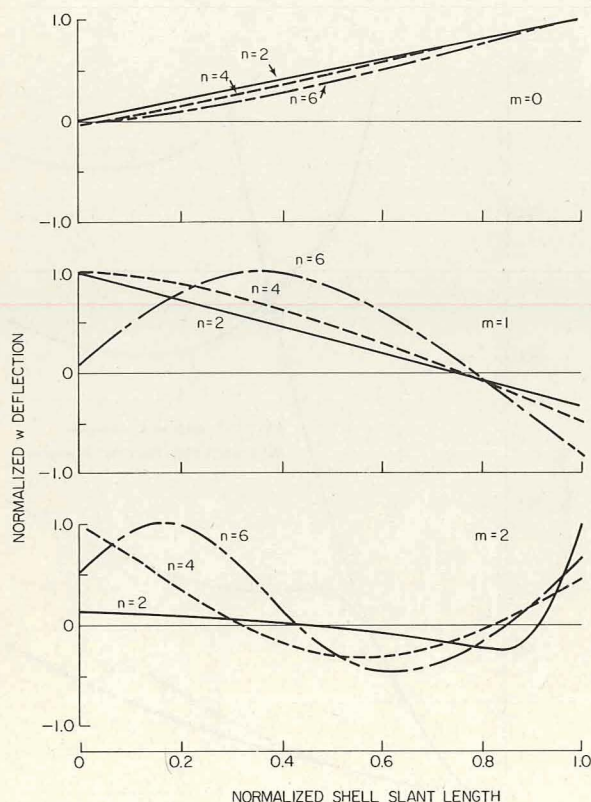


FIGURE 5.71.—Mode shapes for transverse displacements of free-free conical shells; $\alpha=60^\circ$, $R_1/R_2=1/8$. (After ref. 5.83)

giving reasonably close agreement with the experimental results of reference 5.64 were obtained; however, one curve corresponded to modes having $m=1$ and the other to modes having $m=2$. This is seen, for example, in figure 5.73 which corresponds to model 3 ($\alpha=14.0^\circ$) (compare with fig. 5.68(c)). Thus, at a given frequency two modes can be excited having different values of m and n and it is hypothesized that the experimental results of reference 5.64 represent the coupling of two such modes.

Other numerical results for the free vibrations of free-free conical shells were obtained by the finite element method in reference 5.66, using membrane theory in reference 5.58, and experimentally in reference 5.15. Axisymmetric meridional motion according to bar theory was hypothesized in reference 5.21. Other relevant investigations include references 5.3, 5.24, and 5.85.

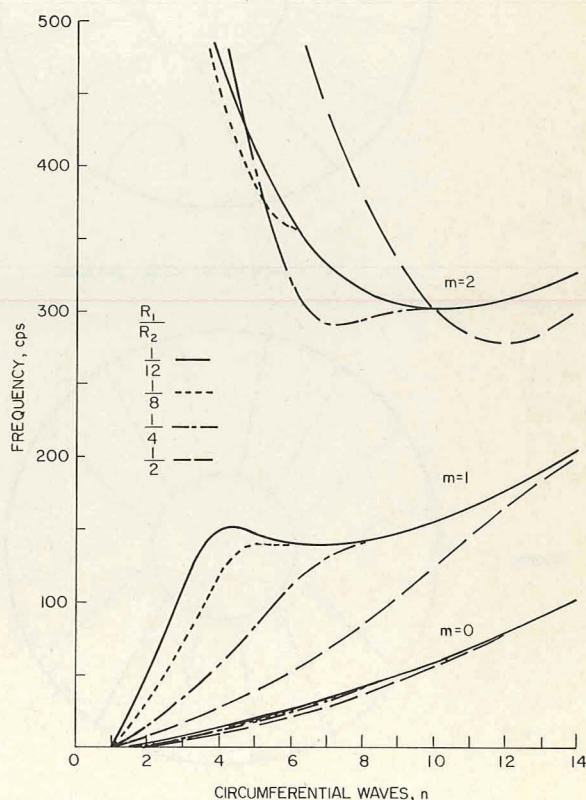


FIGURE 5.72.—Effect of length ratio R_1/R_2 upon the frequencies of free-free conical shells; $\alpha=60^\circ$. (After ref. 5.83)

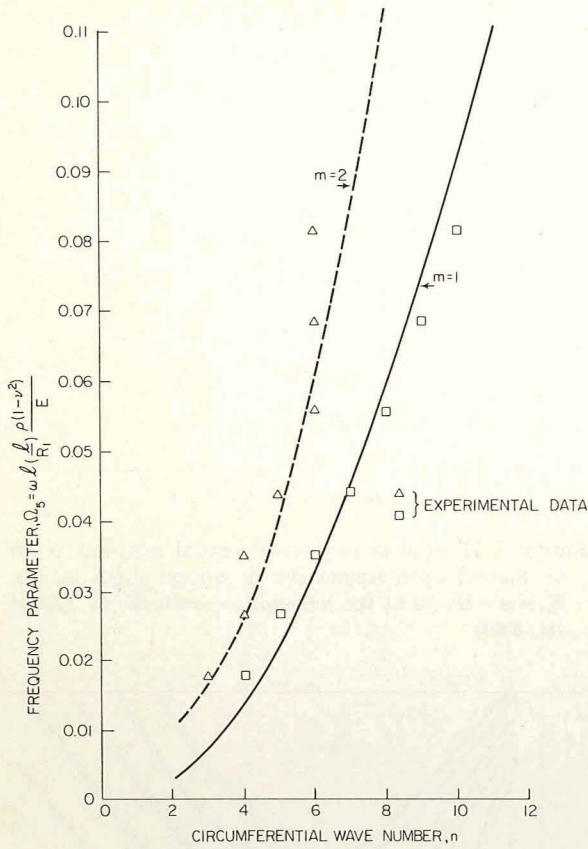


FIGURE 5.73.—Comparison of analytical and experimental data for free-free conical shells; $\alpha = 14.0^\circ$. (After ref. 5.84)

5.3.7 Other Edge Conditions

A study of the effect of various types of edge constraints upon the free vibration frequencies of frustums of conical shells was made by Weingarten and Gelman (ref. 5.69). The Sanders shell theory was used and sinusoidal variation of the displacement functions was assumed in the circumferential direction, as in equation (5.14). The resulting set of ordinary differential equations in u_n , v_n , and w_n was then cast into a finite difference format. Numerical studies were made on shells having boundaries which are either completely free or have various degrees of edge constraint as indicated in the five cases below:

1. $N_s = v = w = M_s = 0$ (SD)
2. $u = v = w = M_s = 0$
3. $N_s = S_{s\theta} = w = M_s = 0$

4. $u = S_{s\theta} = w = M_s = 0$

5. $u = v = w = \partial w / \partial s = 0$ (clamped)

Variation of frequencies with circumferential wave number n is shown in figure 5.74 for shells having the same boundary conditions at each end. The numbers on the curves correspond to the cases listed above. In figure 5.75 frequencies are shown for shells having the *large end free* and the other boundary supported according to one of the five conditions listed. A similar plot is made in figure 5.76 for those cases having the *small end free*. The dimensions of the shell used for the theoretical study were not given in reference 5.69; however, comparison of the 1-1 (SD-SD) curve with a corresponding curve in reference 5.31 indicates that the shell had a thickness of $h = 0.040$ in., the material was steel, and the other dimensions were: $\alpha = 20^\circ$, $R_1 = 2$ in., $s_2 - s_1 = 8\text{--}3/8$ in.

The effect of circumferential restraint $v = 0$ upon the free vibrations of conical shells was studied by Seide (ref. 5.49) and Cohen (ref. 5.51). In reference 5.49 the Donnell equations were used, neglecting the effects of tangential inertia. Solution functions for the displacements were taken as trigonometric terms in the meridional direction, and the Galerkin procedure was used. Results were obtained for two shells having $h = 0.020$ in. and 0.040 in. The shells were made of steel and the other dimensions were: $\alpha = 20^\circ$, $R_1 = 2.13$ in., and $R_2 = 4.86$ in. Figure 5.77 shows

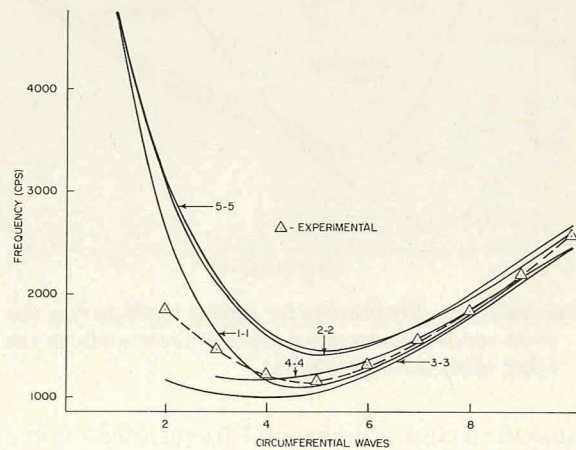


FIGURE 5.74.—Frequencies for conical shells having various types of symmetric edge constraints. (After ref. 5.69)

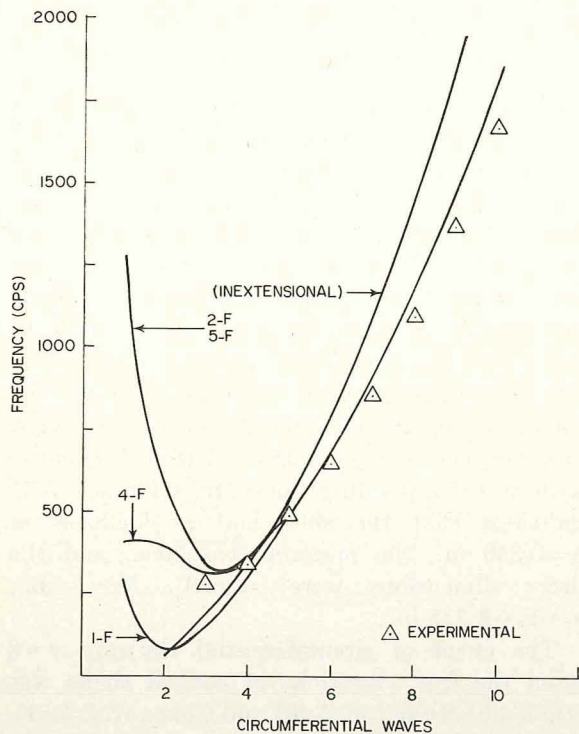


FIGURE 5.75.—Frequencies for conical shells having the *large* end free and various types of constraints on the other edge. (After ref. 5.69)

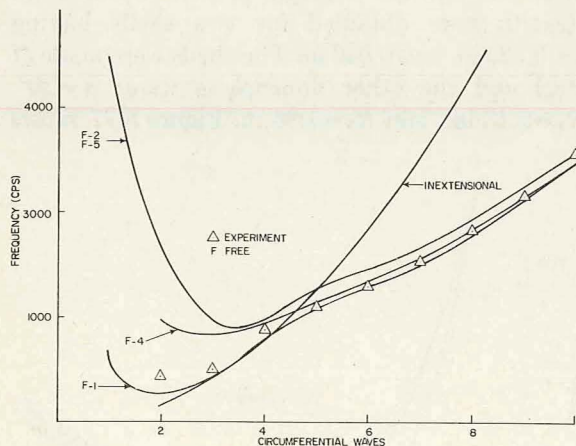


FIGURE 5.76.—Frequencies for conical shells having the *small* end free and various types of constraints on the other edge. (After ref. 5.69)

analytical and experimental frequencies for the 0.020 in. thick shell having two types of boundary conditions—either $S_{\theta\theta}=0$ or $v=0$ —on both ends of the shell. The other boundary conditions are

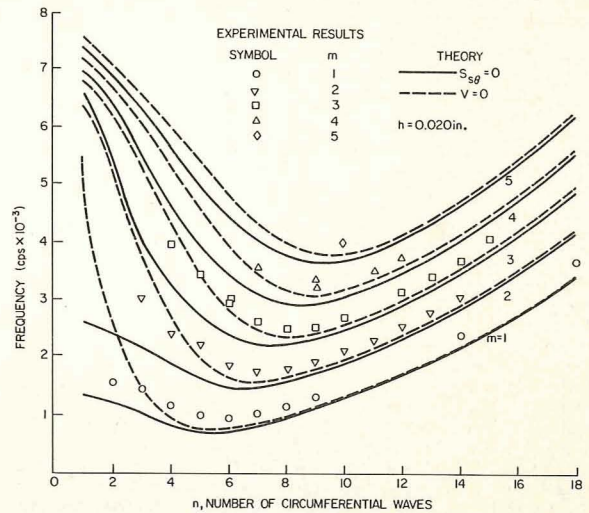


FIGURE 5.77.—Effect of circumferential restraint ($v=0$ or $S_{\theta\theta}=0$) upon frequencies of conical shells having $N_s=w=M_s=0$ at the boundaries; $h=0.020$ in. (After ref. 5.49)

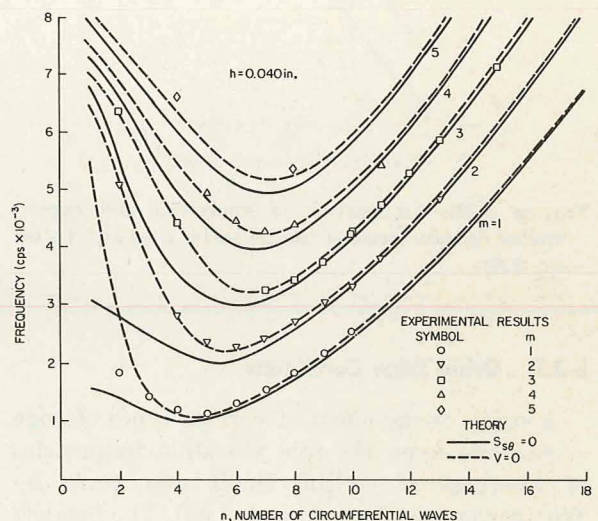


FIGURE 5.78.—Effect of circumferential restraint ($v=0$ or $S_{\theta\theta}=0$) upon frequencies of conical shells having $N_s=w=M_s=0$ at the boundaries; $h=0.040$ in. (After ref. 5.49)

$N_s=w=M_s=0$ for both cases. Figure 5.78 is the corresponding set of curves for $h=0.040$ in. The circumferential restraint is very important. When n is equal to 2, for instance, the frequency for $S_{\theta\theta}=0$ is about half of the frequency for $v=0$. For $n=1$, the ratio of the two is only about one-to-four. The normal displacement mode shapes

for small values of n are considerably different, as can be seen from the curves of figure 5.79.

Cohen (ref. 5.51) also obtained numerical results for Seide's shell model having $h=0.040$ in. (described in the preceding paragraph). Results for frequencies and mode shapes of the first three modes arising for $n=1$ and 2 are shown in figures 5.80 and 5.81, respectively, for the case when $S_{s\theta}=0$ on the edges. In table 5.15 the frequencies are compared for the cases when either $S_{s\theta}=0$ or $\nu=0$. The differences are attributed to two factors:

(1) The Donnell-Mushtari shell equations, which give poor results for $n=1$ and 2 (cf., chapter 2), were used in reference 5.49.

(2) Tangential inertia, which is very important for $n=1$ (cf., chapter 2), was neglected in reference 5.49.

A comparison of the effects of various types of boundary conditions was also made by Kolman (ref. 5.25). The Novozhilov shell equations were used and solved by the finite difference method. Frequencies were obtained for three shells having $\alpha=30^\circ$, 45° , and 60° and all having $s_2/s_1=5$, $\bar{R}=(R_1+R_2)/2=0.01h$, $\nu=0.3$, and having the following types of edge conditions:

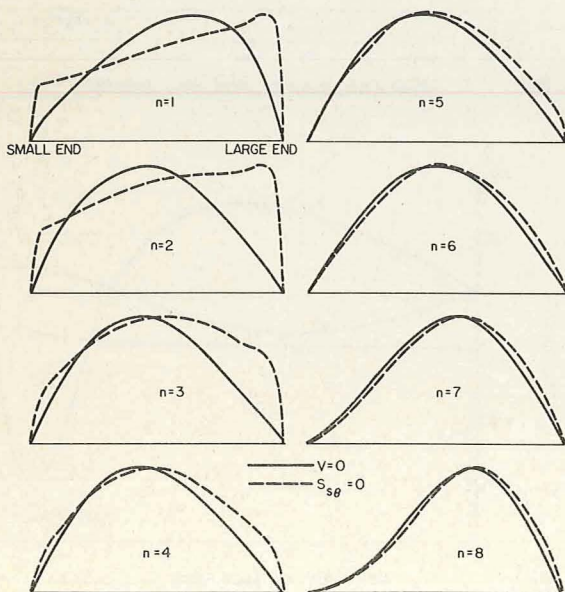


FIGURE 5.79.—Effects of circumferential restraint ($\nu=0$) upon the normal displacement mode shapes of a conical shell. (After ref. 5.49)

TABLE 5.15.—Comparison of Frequencies for Conical Shells With and Without Circumferential Restraint; $h=0.040$ in.

Boundary condition	n	Frequency, cps		Difference, %
		Ref. 5.51	Ref. 5.49	
$S_{s\theta}=0$	1	1091	1555	42.5
		1364	3077	125.6
		6212	6781	9.2
	2	1279	1424	11.3
		2442	2830	15.9
		5259	5566	5.8
$\nu=0$	1	4624	5495	18.8
		4934	6465	31.0
		6494	7032	8.3
	2	2433	2744	12.8
		5096	5344	4.9
		6178	6295	1.9

$$(1) \quad u=v=w=\frac{\partial w}{\partial s}=0 \quad \text{at} \quad s=s_1, s_2$$

$$(2) \quad u=v=w=M_s=0 \quad \text{at} \quad s=s_1$$

$$u=v=w=\frac{\partial w}{\partial s}=0 \quad \text{at} \quad s=s_2$$

$$(3) \quad u=v=w=M_s=0 \quad \text{at} \quad s=s_1, s_2$$

$$(4) \quad u=v=w=M_s=0 \quad \text{at} \quad s=s_1$$

$$N_s=v=w=M_s=0 \quad \text{at} \quad s=s_2$$

$$(5) \quad u=v=w=M_s=0 \quad \text{at} \quad s=s_1$$

$$N_s=S_{s\theta}=w=M_s=0 \quad \text{at} \quad s=s_2$$

Minimum frequency parameters

$$\Omega_8 = \omega s_2 \sqrt{\frac{\rho(1-\nu^2)}{E}}$$

and the values of n at which they occur (in parentheses) are displayed in table 5.16. The effects of lessening constraint as one moves from cases one to five is clearly seen in the table.

In reference 5.3 a general procedure is exhibited which accommodates conical shells having arbitrary boundary conditions. A characteristic equation is obtained by the Ritz method and is explicitly presented. However, the coefficients of the characteristic determinant include 17 integrals involving the products of displacement

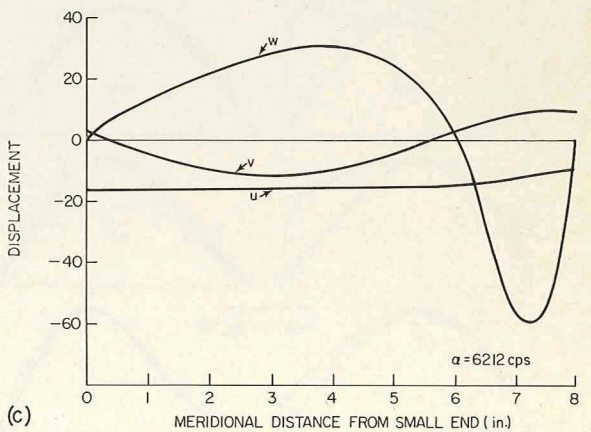
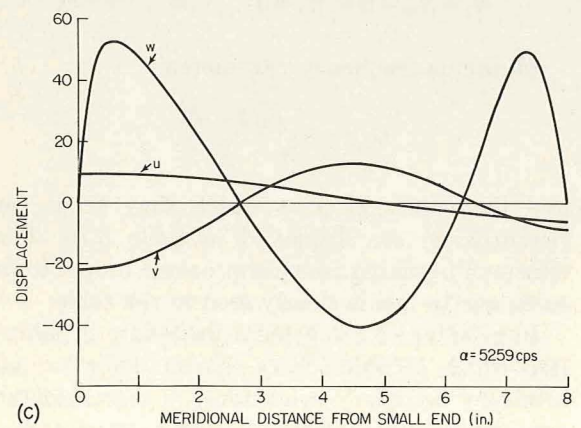
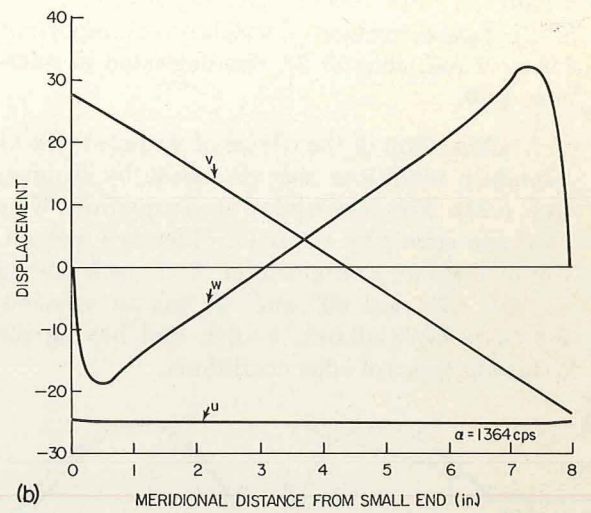
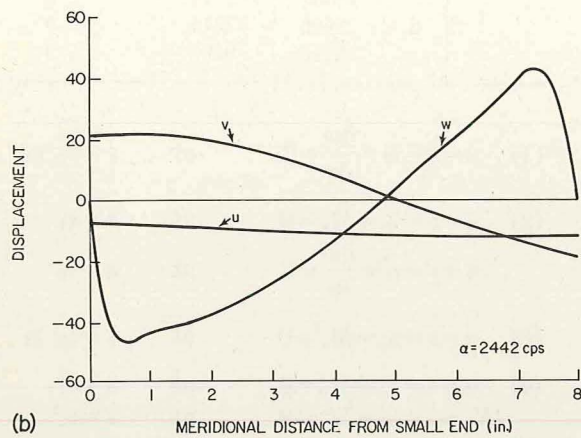
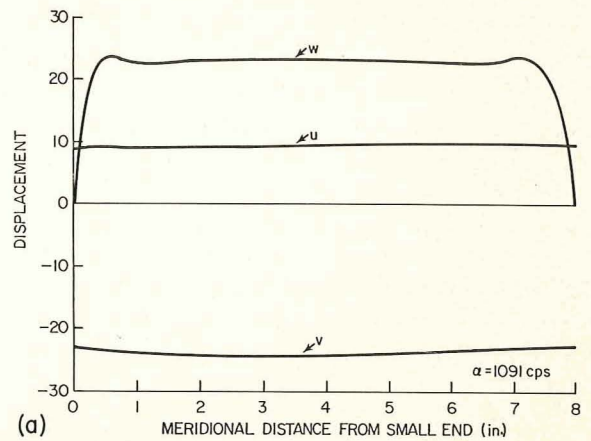
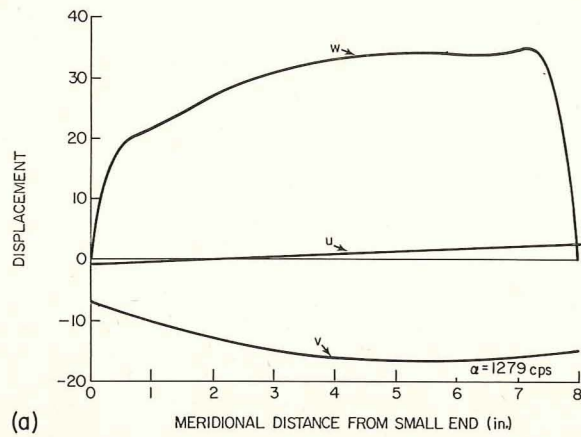


FIGURE 5.80.—Frequencies and mode shapes for conical shells having $N_s = S_{s\theta} = w = M_s = 0$ at both ends; $n=1$. (After ref. 5.51) (a) $m=1$. (b) $m=2$. (c) $m=3$.

FIGURE 5.81.—Frequencies and mode shapes for conical shells having $N_s = S_{s\theta} = w = M_s = 0$ at both ends; $n=2$. (After ref. 5.51) (a) $m=1$. (b) $m=2$. (c) $m=3$.

TABLE 5.16.—Frequency Parameters $\Omega_s = \omega s_2 \sqrt{\rho(1-\nu^2)/E}$ and the Values at Which They Occur (in Parentheses) for Conical Shells Having Various Boundary Conditions

α	Type of boundary conditions				
	1	2	3	4	5
60°	0.2829 (5)	0.2821 (5)	0.2744 (5)	0.2334 (5)	0.1850 (4)
45°	.3542 (5)	.3536 (5)	.3494 (5)	.2790 (5)	.2280 (4)
30°	.4092 (5)	.4091 (5)	.4071 (5)	.3347 (4)	.2613 (4)

functions and their derivatives. No tabular values of the integrals are available, thus the results given are of limited usefulness.

The "method of parallel springs" (see sec. 5.2.1) was outlined in reference 5.5 for conical shells having arbitrary boundary conditions. A method based upon power series displacement functions is discussed in reference 5.86.

Conical shells having elastic supports or rigid attached masses at an end are investigated in references 5.58, 5.71, 5.87, 5.88, and 5.89. Other literature dealing with conical shells having edge conditions not discussed in an earlier section includes references 5.27, 5.90, and 5.91.

5.4 OPEN CONICAL SHELLS

An open conical shell is depicted in figure 5.82. Strangely, no references have been found which deal explicitly with the free vibrations of such shells.

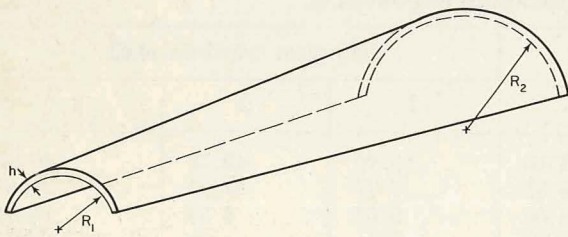


FIGURE 5.82.—Open conical shell.

However, useful information for open conical shells having lateral edges supported by shear diaphragms can be gleaned from the results of the previous sections in the same manner as for open circular cylindrical shells (see secs. 2.8.1 and 2.8.2 for details).

5.5 ANISOTROPY

As in the case of circular cylindrical shells, no free vibration results are available for conical shells composed of materials having properties which possess general anisotropy. Rather, the few results which are available are for the special case of orthotropic materials.

The equations of motion for orthotropic circular conical shells are derived in the same manner as those for orthotropic circular cylindrical shells (see sec. 3.1.1). That is, the orthotropic force and moment resultant equations (3.4) through (3.7) are used with the equations of motion and generalized strain-displacement equations from chapter 1, where the shell coordinates α and β are replaced by s and θ for conical shells, respectively, and where A , B , R_α , and R_β are given by equations (5.1). The resulting sets of equations for the various shell theories are quite lengthy and will not be repeated here. The detailed equations of motion of a Donnell-Mushtari type shell theory can be found, for example, in references 5.92, 5.93, and 5.94. The orthotropic form of the Novozhilov equations of motion in terms of displacements is found in detail in reference 5.95.

Weingarten (ref. 5.93 and 5.96) used the Donnell-Mushtari theory, displacement functions in the form of power series, and the Galerkin method to investigate conical shells which satisfy the boundary conditions

$$w = M_s = 0 \quad (5.62)$$

at $s = s_1$, s_2 , but the usual shear diaphragm boundary conditions of $v = N_s = 0$ are replaced by elastic support conditions. Numerical results for frequency parameters were obtained for shells having orthotropic elastic moduli ratios of $E_\theta/E_s = 0.02$ and 50. Comparison was also made with an "equivalent" cylindrical shell (i.e.,

one having a radius R equal to the average radius $(R_1 + R_2)/2$ of the conical shell) as seen in table 5.17. The parameters of the shell described by table 5.17 are: $\alpha = 20^\circ$, $R_1 = 2.13$ in., $s_2 - s_1 = 8$ in., $h = 0.02$ in., and $\nu_\theta = 0$. Note that the frequency parameter $12\omega^2\rho(1 - \nu_s\nu_\theta)/h^2E_s$ has dimensions. Table 5.17 shows that the *minimum* frequency predictions of the equivalent cylindrical shell for both values of E_θ/E_s are in good agreement with those of the conical shell, but that at either low or high values of n the cylindrical representation is inadequate. Extensive results are also given in references 5.93 and 5.96 for ring-stiffened conical shells and experimental data are compared with those computed from "equivalent orthotropic" analyses.

Bacon and Bert (ref. 5.39) showed the effect of changing the ratio of orthotropic constants E_θ/E_s upon the minimum frequencies of SD-SD shells. The Ritz method was used with trigonometric functions assumed for the displacements. Values of the frequency parameter $2\omega^2s_1^2\rho(1 - \nu_s\nu_\theta)/E_s$ versus E_θ/E_s are shown in figure 5.83 for shells having: $\alpha = 20^\circ$, $s_2/s_1 = 2.2840$, $l/\bar{R} = 2.1490$ ($\bar{R} = (R_1 + R_2)/2$), $h/\bar{R} = 0.00466$, and $\nu_s/(1 - \nu_s\nu_\theta) = 0.3$. The analysis included shear deformation and rotary inertia effects, but these are negligible for the h/\bar{R} ratio under consideration.

Other works giving some attention to orthotropic SD-SD shells include references 5.38, 5.52, and 5.97.

Conical shells having circumferential stiffeners (rings) and longitudinal stiffeners (stringers) were

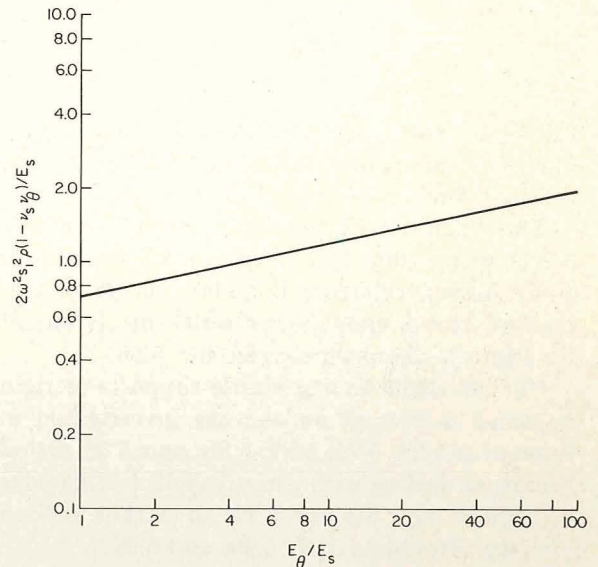


FIGURE 5.83.—Effect of changing E_θ/E_s upon the minimum frequency parameters of an orthotropic, SD-SD, conical shell (dimensions in text). (After ref. 5.39)

TABLE 5.17.—Frequency Parameters $12\omega^2\rho(1 - \nu_s\nu_\theta)/h^2E_s$ for Orthotropic Conical and Equivalent Cylindrical Shells (Dimensions Given in Text)

$\frac{E_\theta}{E_s}$	n	Number of meridional half-waves, m					
		Conical shell			Equivalent cylindrical shell		
		1	2	3	1	2	3
0.02	0	29.18	38.05	48.15	43.46	43.78	45.37
	3	7.26	18.83	28.35	7.77	21.22	31.40
	6	1.88	7.61	15.56	2.02	8.38	17.01
	9	1.61	5.07	10.85	1.41	4.86	11.00
	12	2.76	6.42	11.78	2.57	4.87	9.71
	15	4.95	10.07	17.10	5.60	7.47	11.76
	18	8.59	15.97	25.84	11.25	13.04	17.21
50	0	26,540.51	53,454.28	59,419.53	108,679.74	108,572.32	108,564.04
	3	108.64	849.98	2,563.52	121.24	1,020.16	3,087.68
	6	303.64	648.28	1,102.63	344.72	442.34	746.68
	9	996.97	1,543.22	2,144.33	1,705.07	1,736.59	1,833.89
	12	2,633.27	3,520.09	4,415.69	5,384.51	5,402.42	5,464.43
	15	5,855.81	7,311.60	8,726.67	13,143.70	13,156.38	13,217.88

analyzed by Crenwelge and Muster (ref. 5.98) using an "equivalent orthotropic" shell model. A variant of simple support boundary conditions given by

$$u = S_{s\theta} = w = M_s = 0 \quad \text{at} \quad s = s_1, s_2 \quad (5.63)$$

was used in the analysis. Numerical results were obtained for three aluminum shells having $\alpha = 10^\circ$, $R_1 = 3.42$ in., $R_2 = 5.25$ in., $s_2 - s_1 = 10.50$ in., $h = 0.10$ in., and various combinations of integral rings and stringers. These results will not be repeated here because of the detail required to describe the determination of the equivalent orthotropic constants from the dimensions of the shell, rings, and stringers. Comparison of frequencies with those obtained from experiment and those obtained by an analysis which treats the stiffeners as discrete elements is also made in reference 5.98.

The clamped-clamped orthotropic conical shell is investigated in reference 5.97. The solution of the problem having boundary conditions $u = v = w = M_s = 0$ is described in reference 5.99, but no numerical results are obtained. Orthotropic conical shells having elastic support conditions are discussed in reference 5.100. Other investigations dealing with the free vibrations of orthotropic conical shells include references 5.3, 5.20, and 5.101.

5.6 LARGE DISPLACEMENTS

The effect of large displacements is to add nonlinear terms to the relationships between the membrane strains and the displacements, as was seen in equations (3.49) for circular cylindrical shells. For circular conical shells, equations (3.49) are generalized to (refs. 5.102 and 5.103)

$$\left. \begin{aligned} \epsilon_s &= \frac{\partial u}{\partial s} + \frac{1}{2} \left(\frac{\partial w}{\partial s} \right)^2 \\ \epsilon_\theta &= \frac{1}{B} \frac{\partial v}{\partial \theta} + \frac{u}{B} \frac{\partial B}{\partial s} + \frac{w}{R_\theta} + \frac{1}{2} \left(\frac{1}{B} \frac{\partial w}{\partial \theta} \right)^2 \\ \gamma_{s\theta} &= \frac{1}{B} \frac{\partial u}{\partial \theta} + B \frac{\partial}{\partial s} \left(\frac{v}{B} \right) + \frac{1}{B} \frac{\partial w}{\partial s} \frac{\partial w}{\partial \theta} \end{aligned} \right\} \quad (5.64)$$

where B and R_θ are the middle surface parameters given in equations (5.1).

However, in contrast with the special case of cylindrical shells, very little consideration has

been given to the nonlinear, large amplitude vibrations of conical shells. Sun and Lu (refs. 5.102 and 5.103) investigated *postbuckling* vibrations and found that for the boundary conditions used ($u = v = w = M_s = 0$ at $s = s_1, s_2$) the nonlinear effect was always of the hardening type. Large amplitude free vibrations are also discussed in references 5.104 and 5.105.

5.7 INITIAL STRESS

For an understanding of how initial stresses affect the free vibrations of conical shells, review section 3.4 which deals with circular cylindrical shells. Most of the discussion in that section is also relevant to the more general case of conical shells.

As in the case of cylindrical shells (see sec. 3.4.1), the equations of motion for conical shells can be adjusted to account for initial stresses by the addition of simple terms. For example, for a Donnell-Mushtari type theory, equations (5.2a) and (5.2b) remain unchanged, while equation (5.2c) has the terms

$$\begin{aligned} & -\frac{1}{Eh} \left[N_s^i \frac{\partial^2 w}{\partial s^2} + 2N_{s\theta}^i \left(\frac{1}{s \sin \alpha} \frac{\partial^2 w}{\partial s \partial \theta} \right. \right. \\ & \quad \left. \left. - \frac{1}{s^2 \sin \alpha} \frac{\partial w}{\partial \theta} \right) \right. \\ & \quad \left. + N_\theta^i \left(\frac{1}{s^2 \sin^2 \alpha} \frac{\partial^2 w}{\partial \theta^2} + \frac{1}{s} \frac{\partial w}{\partial s} \right) \right] \quad (5.65) \end{aligned}$$

(cf., refs. 5.92, 5.96, 5.106, and 5.107) added to its left-hand side in the case of *uniform* initial force resultants N_s^i , N_θ^i , and $N_{s\theta}^i$. The term (eq. (5.65)) simplifies to the same form as that given by equation (3.103) in the case of a cylindrical shell (i.e., $s \sin \alpha = R$, $s \rightarrow \infty$).

Weingarten (ref. 5.106) investigated the case of the conical shell frustum subjected to internal and external pressures. In the case of an internal pressure p_0 the static initial stress field was given in reference 5.106 by (correcting an apparent misprint)

$$\left. \begin{aligned} \sigma_s^i &= \frac{p_0}{2} \frac{\bar{R}}{h} \frac{s}{s_1} \tan \alpha \\ \sigma_\theta^i &= p_0 \frac{\bar{R}}{h} \frac{s}{s_1} \tan \alpha \end{aligned} \right\} \quad (5.66)$$

where $\bar{R} = (R_1 + R_2)/2$, the mean radius, and

$N_s^i = \sigma_s^i h$, $N_\theta^i = \sigma_\theta^i h$. However, it must be pointed out that the stress distributions given by equations (5.66) are not those usually accepted as the solution for uniform pressure from membrane theory; namely (cf., ref. 5.108, p. 97)

$$\left. \begin{aligned} \sigma_s^i &= \frac{p_0}{2} \frac{s}{h} \tan \alpha + \frac{c_1}{s} \\ \sigma_\theta^i &= \frac{p_0 s}{h} \tan \alpha \end{aligned} \right\} \quad (5.67)$$

where c_1 is an arbitrary constant determining the distribution of the axial end thrust between the boundaries at $s = s_1$ and $s = s_2$.

In reference 5.106 the Galerkin method was used with displacement functions in the form of algebraic polynomials to solve the free vibration problem for conical shells having $w = M_s = 0$ at $x = s_1, s_2$. The remaining two boundary conditions involve elastic restraints. A Donnell-Mushtari type of shell theory was used (i.e., eq. 5.65). Numerical results were obtained for an aluminum conical shell having the following dimensions: $\alpha = 20^\circ$, $R_1 = 2.144$ in., $l = 8.00$ in., and $h = 0.020$ in. (see figs. 5.1 and 5.2). Experimental data were also obtained. These are compared in table 5.18 for values of $p_0/p_{cr} = 0, -0.446$, and $+0.446$, where p_{cr} is the critical pressure for buckling. Because p_{cr} corresponds to external pressure, it is a negative number, and occurs for a circumferential wave number n of 6 for this particular shell. Thus, negative values of p_0/p_{cr} correspond to internal pressures, and positive values correspond to external pressures. In table 5.18 results are presented for mode shapes having 1, 2, and 3 meridional half-waves m . In some places in the table, two experimental values listed in reference 5.106 have been replaced by a single average value. The lack of agreement between theoretical and experimental frequencies in table 5.18 is attributed in reference 5.106 to

(1) The end conditions of the experiment are more rigid than those used in the theoretical analysis.

(2) The typically poor analytical results arise from a Donnell-Mushtari type shell theory for $n \leq 3$.

However, the second argument would seem spurious for the l/R ratio being considered (see the

comparison of theories for cylindrical shells in sec. 2.3.1).

The numerical results for $m = 1$ are also plotted in figure 5.84. Experimental data are shown by discrete points in the figure. As the internal pressure increases, the circumferential wave number n at which the minimum frequency occurs is decreased, as was observed for cylindrical shells (see sec. 3.4.3).

A comparison of analytical mode shapes for $m = 1$ and $n = 3, 6$, and 15 is shown in figure 5.85. At large values of n , the shell hardly vibrates in the vicinity of its small end. The effects of changing the pressure parameter p_0/p_{cr} are also observed from figure 5.85. A comparison of experimental and analytical mode shapes for $m = 1$ and $n = 3$ and 14 is made in figure 5.86.

Goldberg, Bogdanoff, and Alsbaugh (refs. 5.109 and 5.110) demonstrated their general numerical integration computer program on the problem of the clamped-clamped conical shell subjected to pressure. Unfortunately, these ref-

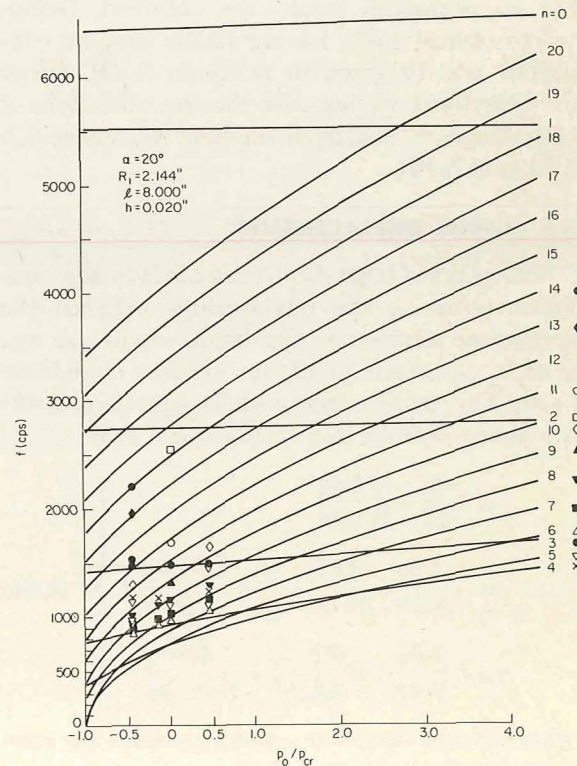


FIGURE 5.84.—Variation of frequency (cps) with pressure parameter p_0/p_{cr} for a conical shell. (After ref. 5.106)

TABLE 5.18.—*Theoretical and Experimental Frequencies (cps) for Conical Shells Subjected to Internal or External Initial Pressure*

$\frac{p_0}{p_{cr}}$	n	$m=1$		$m=2$		$m=3$	
		Theor.	Exper.	Theor.	Exper.	Theor.	Exper.
-0.446	2	2730	5323	3100	6175
	3	1441	1501	3807	5289
	4	862	1163	2685	2708	4259
	5	609	944	1973	2180	3394	2996
	6	569	840	1575	1825	2766	2930
	7	651	880	1430	1658	2377	2584
	8	771	985	1470	1708	2215	2452
	9	912	1130	1594	1761	2245	2438
	10	1075	1301	1749	1927	2379	2344
	11	1260	1931	2121	2556	2601
	12	1466	2140	2344	2766	2883
	13	1692	1949	2375	3008	3197
	14	1937	2204	2634	3281
	15	2203	2918	3584
	16	2487	3226	3919
	17	2791	3558	4284
	18	3113	3913	4681
0	2	2733	1551	5335	6175
	3	1459	1486	3816	3047	5306
	4	924	1182	2705	2407	4277	3980
	5	740	1001	2020	2195	3423	3472
	6	759	964	1661	1862	2818	2969
	7	868	1032	1561	1740	2461	2635
	8	1004	1160	1629	1781	2336	2514
	9	1157	1317	1776	1915	2395	2543
	10	1330	1946	2086	2548	2694
	11	1523	1689	2142	2293	2740	2790
	12	1735	2462	2424	2963	3078
	13	1966	2607	3216
	14	2216	2875	2497
	14	2486	3166	3805
	16	2773	3479	4138
	17	3080	3813	4496
	18	3405	4169	4878
+0.446	2	2745	5335	6204
	3	1488	1489	3830	5314
	4	988	1227	2736	4298
	5	851	1082	2073	2233	3461
	6	904	1060	1745	1932	2876	3000
	7	1033	1148	1675	1822	2542	2692
	8	1183	1290	1767	1863	2439	2580
	9	1348	1461	1924	2009	2515
	10	1531	1650	2106	2198	2682	2793
	11	1731	2312	2423	2885
	12	1950	2540	3118
	13	2186	2793	3379	2930
	14	2441	3067	3669	3210
	15	2713	3363	3987
	16	3003	3680	4333
	17	3312	4021	4709
	18	3628	4383	5114

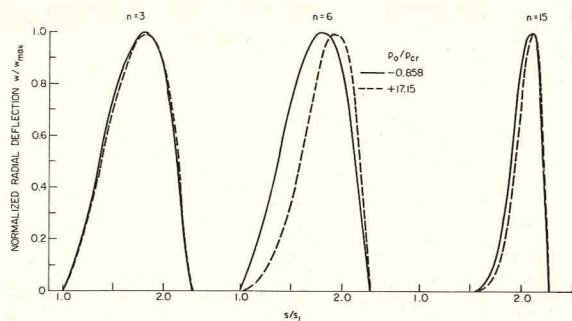


FIGURE 5.85.—Effect of internal pressure and wave number n upon mode shapes of a conical shell. (After ref. 5.106)

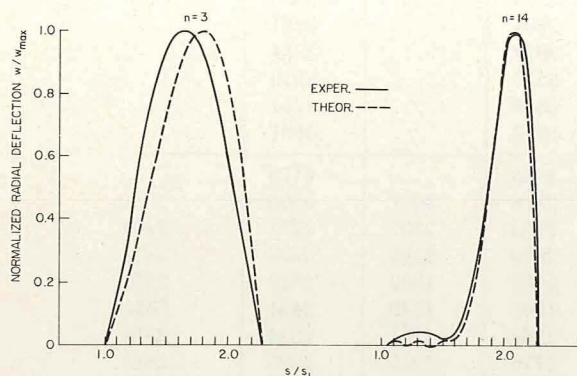


FIGURE 5.86.—Comparison of theoretical and experimental mode shapes for a pressurized conical shell; $p_0/p_{cr} = -0.446$. (After ref. 5.106)

erences do not state whether the pressure is internal or external. Nevertheless, mode shapes corresponding to $n=2$ are reproduced in figure 5.87 for a shell having

$$R_1 = 5 \text{ in.}, R_2 = 10 \text{ in.}, l = 8.66 \text{ in.}$$

$$\alpha = 30^\circ, \rho = 0.00762 \text{ slugs/in}^3$$

$$h = 0.2 \text{ in.}, E = 30 \times 10^6 \text{ psi, and } \nu = 0.3$$

The corresponding frequency is $f = 718.4 \text{ cps}$.

The free vibration of conical shells subjected to initial pressure is also discussed in reference 5.23.

In the case of *torsional loading* the static prestress varies according to

$$\tau_{s\theta}^i = \frac{N_{s\theta}^i}{h} = \frac{T^i}{2\pi h R^2} = \frac{T^i}{2\pi h s^2 \sin^2 \alpha} \quad (5.68)$$

where T^i is the initial torque; that is, the prestress varies with inversely proportionality to the meridional distance s measured from the vertex.

Weingarten (ref. 5.107) obtained theoretical and experimental frequencies for a conical shell

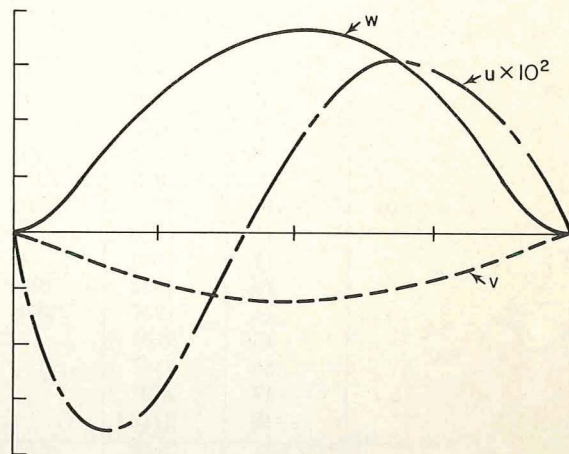


FIGURE 5.87.—Mode shapes for a clamped-clamped, pressurized conical shell. (After refs. 5.109 and 5.110)

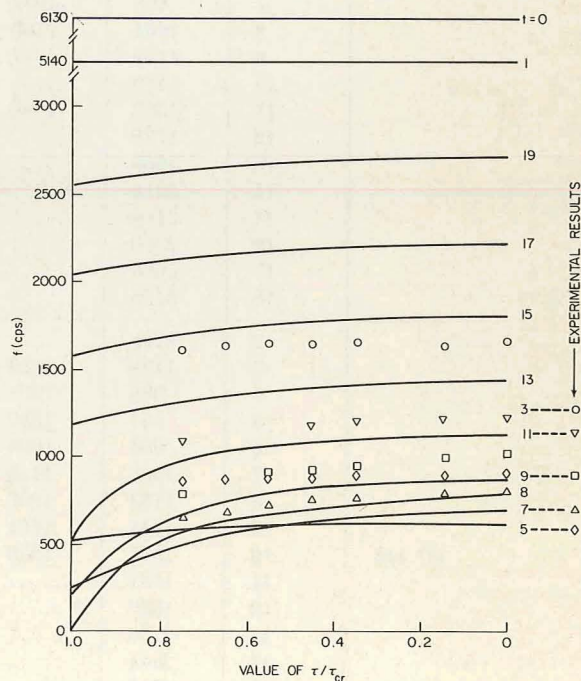


FIGURE 5.88.—Theoretical and experimental frequencies for a conical shell subjected to torsional prestress. (After ref. 5.107)

subjected to torsional prestress. The Galerkin procedure and the same boundary conditions described earlier in this section (ref. 5.106) were used. Calculations were made for an aluminum shell having the following dimensions: $\alpha = 20^\circ$, $R_1 = 2.14$ in., $s_2 - s_1 = 8.76$ in., and $h = 0.016$ in. Experimental data were also obtained. The results are shown in figure 5.88. The node lines (lines of $w = 0$) lie in a helical pattern, as for cylindrical shells loaded in torsion (see sec. 3.4.5).

Free vibrations of shallow conical shells subjected to initial stress are examined in reference 5.105. Other works dealing with conical shells under initial stress include references 5.4, 5.86, and 5.111.

5.8 OTHER EFFECTS

5.8.1 Effects of Surrounding Media

Very little has been written about the effects of surrounding media, such as air and water, upon the free vibration frequencies and mode shapes of conical shells. In reference 5.112 conical shells having small apex angle α and partially filled with a liquid are treated by thin-walled beam theory. In reference 5.113 a method of analysis based on the membrane theory of shells is formulated for conical shells partially filled with a fluid, but no numerical results are given.

5.8.2 Shear Deformation and Rotary Inertia

The effects of shear deformation and rotary inertia on cylindrical shells were discussed in section 3.5.2; most of the discussion applies to conical shells as well. However, some additional work on conical shells has been done.

Garnet and Kempner (refs. 5.36 and 5.114) analyzed the axisymmetric response by means of a Ritz procedure. Comparison was made between two classical shell theories and two shear deformation theories. One type of formulation used was that of Love and others whereby the change of arc length through the thickness is ignored in integrating the force and moment resultant equations (see sec. 1.5). Another type used was that of Naghdi (ref. 5.115) (see also the derivation of Flügge, Byrne, Lur'ye in sec. 1.5) whereby the arc length change is included. Displacement functions were taken in the form of trigonometric series, as in equations (3.127), to satisfy shear diaphragm boundary conditions at both ends of the shell.

Comparison of lowest axisymmetric frequency parameters $\Omega_0 = \omega s_1 \sqrt{\rho(1-\nu^2)/E}$ according to the four theory formulations described above is made in table 5.19 for shells having various values of α , h/\bar{R} , and l/\bar{R} (where \bar{R} is the average radius, $(R_1 + R_2)/2$). The effects of shear deformation

TABLE 5.19.—Comparison of Axisymmetric Frequency Parameters $\omega s_1 \sqrt{\rho(1-\nu^2)/E}$ for Conical Shells Having Shear Diaphragm End Conditions

α	$\frac{h}{\bar{R}}$	$\frac{l}{\bar{R}}$	Shear deformation and rotary inertia			
			Included		Neglected	
			Naghdi formulation	Love formulation	Naghdi formulation	Love formulation
5°	0.05	0.25	26.188	26.233	27.736	27.785
		.375	15.261	15.296	15.548	15.584
		.50	12.282	12.370	12.363	12.388
10°	.15	.30	19.792	19.862	26.224	26.340
		.50	9.393	9.454	10.405	10.479
		1.0	5.286	5.314	5.329	5.360
15°	.20	.375	10.572	10.630	14.171	14.273
		1.0	3.450	3.478	3.509	3.541
20°	.10	.375	5.012	5.031	5.429	5.451
		.50	3.453	3.469	3.563	3.580

and rotary inertia are significant even for the thinnest shell used ($h/\bar{R}=0.05$), although virtually no difference occurs between the frequencies arising from the Naghdi and Love type formulations, whether shear deformation and rotary are included or not. However, note that all the shells described in table 5.19 are relatively short ($l/\bar{R} \leq 1$). The effects of shear deformation and rotary inertia were found in reference 5.36 to be significant only for the relatively short shells. This factor is particularly evident in the table for the shell having $\alpha=10^\circ$, $h/\bar{R}=0.15$, and l/\bar{R} of only 0.30. As further found in reference 5.36 the effect of rotary inertia by itself is insignificant for axisymmetric motions.

The ratio of the frequency obtained when shear deformation is neglected (ω_0) to that when it is included (ω) as a function of the semivertex angle α is depicted in figure 5.89 for a shell having $h/\bar{R}=0.20$ and $l/\bar{R}=0.50$. The ratio decreases as

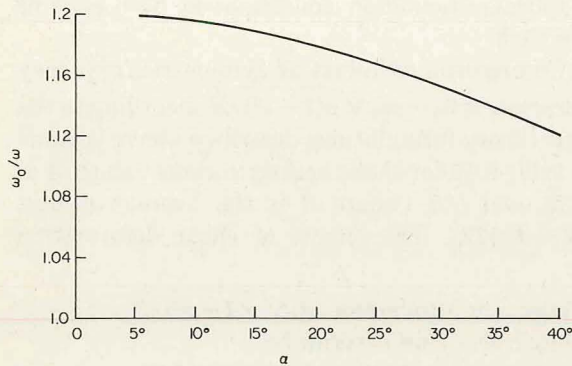


FIGURE 5.89.—Ratio of frequencies without and with shear deformation; $h/\bar{R}=0.20$, $l/\bar{R}=0.50$. (After ref. 5.36)

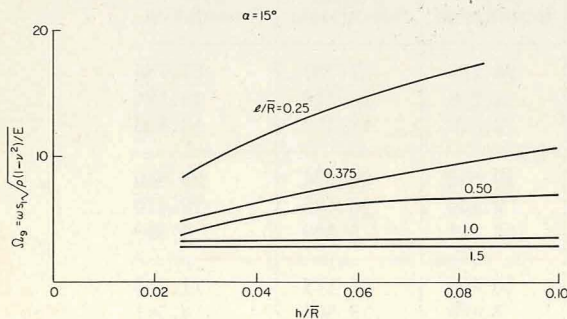


FIGURE 5.90.—Influence of thickness parameter h/\bar{R} upon the frequency parameter (shear deformation included). (After ref. 5.36)

α increases. The influence of the thickness parameter h/\bar{R} upon the frequency parameter Ω_s when shear deformation is included is shown in figure 5.90.

Hu (ref. 5.29) developed a special type of transverse shear theory for conical shells wherein the transverse shear deformation in the circumferential direction alone is neglected. This has the significant effect of reducing the order of the equations of motion from ten to eight. Numerical results obtained by Lindholm and Hu (refs. 5.27 and 5.28) using this theory have already been given in section 5.3.3 because the shells analyzed were *not* short; that is, the effects of shear deformation were small in the numerical examples chosen.

Jain (ref. 5.20) derived a theory for conical shells which included the effects of transverse normal stress, as well as shear deformation and rotary inertia. Only axisymmetric motions were considered. Results were obtained for conical shells supported by shear diaphragms at both ends. A variational procedure was followed using displacement functions which varied sinusoidally in the meridional s direction. Numerical results are listed in table 5.20 for $\alpha=10^\circ$ and 15° ; $l/\bar{R}=0.25$, 0.50 , and 1.00 ; $h/\bar{R}=0.05$ to 0.30 ; and $\nu=0.3$. Frequency parameters

$$\Omega_{10} = \omega s_1 \sqrt{\frac{\rho(1+\nu)(1-2\nu)}{E(1-\nu)}}$$

are given for shear deformation theories with and without the added transverse normal stress effects. The effects of transverse normal stress are significant, especially for thick ($h/\bar{R}=0.30$), short ($l/\bar{R}=0.25$) shells. Also, for short shells the number of terms in the displacement functions required for adequate numerical convergence is small for small l/\bar{R} , a single term being quite adequate for parameter ranges used in the table.

In reference 5.20 the axisymmetric *torsional* frequencies of clamped-clamped conical shells were also investigated, with and without shear deformation and rotary inertia effects being considered. The frequency *differences* obtained between the two cases were found to be negligible.

The effects of shear deformation and rotary inertia considerations upon the free vibrations of conical shells were also discussed in references 5.39 and 5.116.

TABLE 5.20.—Comparison of Frequency Parameters $\omega s_1 \sqrt{\rho(1+\nu)(1-2\nu)/E(1-\nu)}$ for Axisymmetric Vibrations Including Shear Deformation; Transverse Normal Stress Either Neglected or Included

α	$\frac{l}{\bar{R}}$	$\frac{h}{\bar{R}}$	Number of terms	Transverse normal stress	
				Neglected	Included
10°	0.25	0.05	1	12.766	12.449
			2	12.775	12.444
		.10	1	20.758	20.049
			2	20.758	20.046
		.15	1	26.011	24.765
			2	26.010	24.763
		.20	1	29.371	27.640
			2	29.371	27.638
		.25	1	31.576	29.453
			2	31.576	29.452
		.30	1	33.073	30.646
			2	33.073	30.645
	.50	.05	1	5.970	5.527
			2	5.969	5.516
		.10	1	7.635	7.241
			2	7.634	7.233
		.15	1	9.407	8.981
			2	9.407	8.974
		.20	1	10.973	10.459
			2	10.972	10.454
		.25	1	12.271	11.645
			2	12.271	11.640
		.30	1	13.323	12.578
			2	13.323	12.574
	1.00	.05	1	4.999	4.525
			2	4.997	4.505
		.10	1	5.123	4.658
			2	5.122	4.639
		.15	1	5.312	4.856
			2	5.311	4.838
		.20	1	5.545	5.096
			2	5.543	5.097
		.25	1	5.801	5.354
			2	5.800	5.338
		.30	1	6.064	5.613
			2	6.063	5.598

TABLE 5.20.—*Comparison of Frequency Parameters $\omega s_1 \sqrt{\rho(1+\nu)(1-2\nu)/E(1-\nu)}$ for Axisymmetric Vibrations Including Shear Deformation; Transverse Normal Stress Either Neglected or Included—Concluded*

α	$\frac{l}{\bar{R}}$	$\frac{h}{\bar{R}}$	Number of terms	Transverse normal stress	
				Neglected	Included
15°	.25	0.05	1	8.203	7.991
		.10	1	13.341	12.891
		.15	1	16.761	15.970
		.20	1	18.967	17.863
		.25	1	20.422	19.064
		.30	1	21.415	19.857
	.50	.05	1	3.844	3.556
		.10	1	4.878	4.622
		.15	1	5.992	5.719
		.20	1	6.986	6.660
		.25	1	7.816	7.420
		.30	1	8.493	8.021
	1.00	.05	1	3.161	2.861
		.10	1	3.234	2.940
		.15	1	3.346	3.057
		.20	1	3.484	3.200
		.25	1	3.638	3.355
		.30	1	3.797	3.512

5.8.3 Nonhomogeneity

For a discussion of the meaning of nonhomogeneity in shells and how it arises, refer to section 3.5.3.

An excellent collection of papers dealing with the free vibrations of sandwich conical shells has been written by Bert, Bacon, Ray, Egle, Siu, Soder, Azar, and Wilkins (refs. 5.39, and 5.117 through 5.123). Shells supported at both ends by shear diaphragms were considered in references 5.39, 5.118, and 5.120 through 5.123. Free-free shells were treated in references 5.117, 5.119,

5.120, and 5.123, and clamped-clamped shells in references 5.120 and 5.123. Because of the extremely large number of parameters which must be used to define a sandwich shell, particularly when the face sheets are not isotropic, the numerous results in the above references will not be reproduced here.

Reference 5.71 deals with conical shells having orthotropic material properties which vary in the meridional direction. Other investigations into the free vibrations of nonhomogeneous conical shells include references 5.104, 5.124, and 5.125.

REFERENCES

- 5.1. HU, W. C. L.: A Survey of the Literature on the Vibrations of Thin Shells. Tech. Rept. No. 1, Contract NASr-94(06), SwRI Proj. No. 02-1504, Southwest Research Institute, June 1964.
- 5.2. HUNG, F. C.; ET AL.: Dynamics of Shell-Like Lifting Bodies. Part I—The Analytical Investigation. Tech. Rept. AFFDL-TR-65-17, part I, Air Force Flight Dynamics Lab., Res. and Tech. Div., Air Force Systems Command, Wright-Patterson AFB, June 1965.
- 5.3. GONTKEVICH, V. S.: Natural Vibrations of Plates and Shells. A. P. Filipov, Ed., Nauk Dumka (Kiev), 1964. (Transl. by Lockheed Missiles and Space Co.)
- 5.4. KARIMBAEV, T. D.: Effect of Static Loads on the Natural Oscillations of Conical Shells. All-Union Conf. on the Theory of Shells and Plates, 6th, Baku, Azerbaidzhan SSR, Transactions, Sept. 1966, pp. 457-462. (In Russian.)
- 5.5. TANG, C. T.: The Vibration Modes and Eigenfrequencies of Circular Conical (and Cylindrical) Shells. *Scientia Sinica*, vol. 13, no. 8, Aug. 1964, pp. 1189-1210.
- 5.6. TRAPYEZIN, I. I.: Small Vibrations of a Thin Circular Conical Shell. *Raschety na Prochnost*, vol. 2, 1958, pp. 334-341. (In Russian.)
- 5.7. KOL'MAN, E. R.: Axisymmetric Configurations of Oscillations of a Thin Conical Shell. *Raschety na Rasch. na Prochn. i Zhestk.*, Mashgiz, Moscow, 1965, pp. 49-60. (In Russian.) (English Transl. by Lockheed Missiles and Space Co.)
- 5.8. FLÜGGE, W.: *Stresses in Shells*. Springer-Verlag (Berlin), 1962.
- 5.9. PFLUEGER, A.: Stabilität dünner Kegelschale. *Ingenieur-Archiv*, vol. 8, no. 3, 1937, pp. 151-172.
- 5.10. FEDERHOFER, K.: Eigenschwingungen der Kegelschale. *Ingenieur-Archiv*, vol. 9, 1938, pp. 288-308. NASA TT F-8261, Nov. 1962.
- 5.11. DREHER, J. F.: Axisymmetric Vibration of Thin Conical Shells. Ph.D. Dissertation, The Ohio State Univ., 1966.
- 5.12. DREHER, J. F.; AND LEISSA, A. W.: Axisymmetric Vibration of Thin Conical Shells. Proc. 4th Southwestern Conf. on Theoretical and Appl. Mech. (New Orleans, La.), Feb. 29-Mar. 1, 1968, pp. 163-181.
- 5.13. FEDERHOFER, K.: Ueber die Eigenschwingungen der Zylinder-Kegel-Und Kugelschalen. Proc. 5th Int. Cong. for Appl. Mech. (Cambridge, Mass.), 1938, pp. 719-723.
- 5.14. KALNINS, A.: Free Vibration of Rotationally Symmetric Shells. *J. Acoust. Soc. Amer.*, vol. 36, no. 7, July 1964, pp. 1355-1365.
- 5.15. MILLER, D. K.; AND HART, F. D.: The Density of Eigenvalues in Thin Circular Conical Shells. NASA CR-1497, Mar. 1970.
- 5.16. BORDONI, P. G.: Asymmetric Vibrations of Cones. *J. Acoust. Soc. Amer.*, vol. 19, no. 1, Jan. 1947, pp. 146-155.
- 5.17. McLACHLAN, N. W.: *Loudspeakers*. Clarendon Press (England), 1934, p. 318.
- 5.18. DeSILVA, C. N.; AND TERSTEEG, G. E.: Axisymmetric Vibrations of Thin Elastic Shells. *J. Acoust. Soc. Amer.*, vol. 36, no. 4, Apr. 1964, pp. 666-672.
- 5.19. GARNET, H.; GOLDBERG, M. A.; AND SALERNO, V. L.: Torsional Vibrations of Shells of Revolution. *J. Appl. Mech.*, vol. 28, no. 4, Dec. 1961, pp. 571-573.
- 5.20. JAIN, R. K.: Elastic Problems in Shells. Ph.D. Dissertation, Univ. of Roorkee, India, 1966.
- 5.21. KEEFFE, R. E.: Natural Frequencies of Meridional Vibration in Thin Conical Shells. *AIAA J.*, vol. 2, no. 10, Oct. 1964, pp. 1825-1827.
- 5.22. WHEELER, P. W.; AND SHULMAN, Y.: On the Vibrations of Conical Shell Frustums. Proc. 10th Midwestern Mechanics Conf., Aug. 1967, pp. 801-817.
- 5.23. AGENOSOV, L. G.; AND SACHENKOV, A. V.: Stability and Free Oscillations of Thin Cylindrical and Conical Shells of a Circular Cross-Section With Various Boundary Conditions. Investigations on the Theory of Plates and Shells, *Sbornik II, Kazan'*, Izd-vo Kazan'. Univ., 1964, pp. 111-126. (In Russian.)
- 5.24. HARTUNG, R. F.; AND LODEN, W. A.: Axisymmetric Vibration of Conical Shells. *J. Spacecraft and Rockets*, vol. 7, no. 10, Oct. 1970, pp. 1153-1159.
- 5.25. KOL'MAN, E. R.: Influence of the Boundary Conditions on the Free Vibrations Frequency and Modes of a Conical Shell. *Izv. VUZ, Mashinost.*, No. 3, 1966, pp. 178-183. (Transl. by Lockheed Missiles and Space Co.)
- 5.26. SAUNDERS, H.; WISNIEWSKI, E. J.; AND PASLAY, P. R.: Vibrations of Conical Shells. *J. Acoust. Soc. Amer.*, vol. 32, no. 6, June 1960, pp. 765-772.
- 5.27. LINDHOLM, U. S.; AND HU, W. C. L.: Nonsymmetric Transverse Vibrations of Truncated Conical Shells. Tech. Rept. No. 3, Contract NASr-94(06), SwRI Proj. No. 02-1504, Southwest Research Institute, Mar. 1965.
- 5.28. LINDHOLM, U. S.; AND HU, W. C. L.: Non-Symmetric Transverse Vibrations of Truncated Conical Shells. *Int. J. Mech. Sci.*, vol. 8, 1966, pp. 561-579. (Also AIAA Symposium on Structural Dynamics and Aeroelasticity (Boston, Mass.), 1965, pp. 389-399.)
- 5.29. HU, W. C. L.: Free Vibrations of Conical Shells. NASA TN D-2666, Contract No. NASr-94(06), Southwest Research Institute, 1965.
- 5.30. HERRMANN, G.; AND MIRSKY, I.: On Vibrations of Conical Shells. *J. Aerospace Sci.*, vol. 25, July 1958, pp. 451-458.
- 5.31. WEINGARTEN, V. I.: Free Vibrations of Conical Shells. Paper 440, J. Eng. Mech. Div., Proc. Amer. Soc. Civil Engrs., vol. 91, EM4, Aug. 1965, pp. 69-87.

- 5.32. GRIGOLYUK, E. I.: Small Oscillations of Thin Elastic Shells. *Izv. Akad. Nauk SSR, O.T.D.*, no. 6, 1956, pp. 35-44. NASA TT F-25.
- 5.33. GODZEVICH, V. G.: Free Oscillations of Circular Conical Shells. Theory of Shells and Plates, Proc. of the 4th All-Union Conf., Yerevan, Armenian SSR, Oct. 24-31, 1962. Yerevan, Izdatel'stvo Akademii Nauk Armianskoi SSR, 1964, pp. 378-382. (In Russian.)
- 5.34. COOPER, R. M.; AND DiGIACOMO, A. F.: Blast Loading Tests of Conical Shells. Rept. No. TDR-469(5250-30)-3, Ballistic Systems and Space Systems Div., Air Force Systems Command, Los Angeles Air Force Station, Nov. 1964.
- 5.35. MEYEROVICH, I. I.: Approximate Method for the Determination of the Natural Oscillation Frequencies of Cylindrical, Conic and Toroidal Shells. *Prochnost' i Dinamika Aviatsonnykh Dvigatelay*, Izd. Mashinosts., Moscow, 1965, pp. 148-172. NASA TT F-10,377.
- 5.36. GARNET, H.; AND KEMPNER, J.: Axisymmetric Free Vibrations of Conical Shells. *J. Appl. Mech.*, vol. 31, no. 3, Sept. 1964, pp. 458-466.
- 5.37. SHULMAN, Y.: Vibration and Flutter of Cylindrical and Conical Shells. Contract No. AF49-(638)-219, OSR Tech. Rept. No. 59-776, ASRL Tech. Rept. No. 74-2, Office of Scientific Research, U.S. Air Force, June 1959.
- 5.38. AHMED, N.: Lowest Axisymmetric Body Modes of Vibration of the Apollo Vehicle. Rept. No. WR 66-16, NASA Contract NAS 9-4305, Wyle Lab., Mar. 1966.
- 5.39. BACON, M. D.; AND BERT, C. W.: Unsymmetric Free Vibrations of Orthotropic Sandwich Shells of Revolution. *AIAA J.*, vol. 5, no. 3, Mar. 1967, pp. 413-417.
- 5.40. TRAPYEZIN, I. I.: Vibrations of a Thin Circular Conical Shell. *Raschety na Prochnost*, vol. 4, 1959, pp. 367-373. (In Russian.)
- 5.41. VEIGEL', I.; MYANNIL', A.; AND ORG, E.: The Small Steady Axisymmetrical Vibrations of a Conical Shell of Revolution. *Izv. Akad. Nauk Eston. SSR*, vol. 9, Ser. Tekh. i Fizz.-Mat. Nauk, no. 1, 1960, pp. 16-25. (In Russian.)
- 5.42. KORNECKI, A.: Dynamic Stability of Truncated Conical Shells Under Pulsating Pressure. *Israel J. of Technology*, vol. 4, no. 1, 1966, pp. 110-120.
- 5.43. BRESLAVSKII, V. E.: Certain Basic Instances of Free Vibrations of Conical Shells. *Trudy Kar'kovskogo Vysohego aviatsonnozhinernogo uchilishcha*, vol. 27, 1954, pp. 107-123. (In Russian.)
- 5.44. POVERUS, L. YU.; AND RYAYAMET, R. K.: Small Nonaxisymmetrical Eigen Vibrations of Elastic Thin Conical and Cylindrical Shells. *Trudy Tallinsk, Politekh. In-Ta*, vol. 19, 1958, pp. 31-64. (In Russian.)
- 5.45. BLUHM, J. I.; AND NEAL, D. M.: Rotationally Symmetric, Transient Response of a Small-Angle Truncated Conical Shell Owing to a Moving Pressure Front. *J. Acoust. Soc. Amer.*, vol. 38, no. 4, Oct. 1965, pp. 608-613.
- 5.46. BLUHM, J. I.: The Rotationally Symmetric Motion of a Small Angle Truncated Conical Shell Due to a Constant Velocity Pressure Front. Part I—Analysis. Tech. Rept. ARMA TR 63-28 (AD 425 702), U.S. Army Materials Agency, Dec. 1963.
- 5.47. BLUHM, J. I.; AND NEAL, D. M.: The Rotationally Symmetric Motion of a Small-Angle Truncated Conical Shell Due to a Constant Velocity Pressure Front. Part II—Numerical Results. Tech. Rept. 65-09 (AD 616 605), U.S. Army Materials Agency, Apr. 1965.
- 5.48. MALKINA, R. L.; AND GODZEVICH, V. G.: Free Oscillations of Shells of Zero Curvature. *Aviatsonnaya Tekhnika*, no. 1, 1963, pp. 48-57. (In Russian.)
- 5.49. SEIDE, P.: On the Free Vibrations of Simply Supported Truncated Conical Shells. Rept. No. TDR-269(4560-40)-2, Contract No. AF 04(695)-269, Aerospace Corp., Feb. 1964.
- 5.50. SEIDE, P.: On the Free Vibrations of Simply Supported Truncated Conical Shells. *Israel J. of Technology*, vol. 3, no. 1, 1965, pp. 50-61.
- 5.51. COHEN, G. A.: Computer Analysis of Axisymmetric Free Vibrations of Ring-Stiffened Orthotropic Shells of Revolution. *AIAA J.*, vol. 3, no. 12, Dec. 1965, pp. 2305-2312.
- 5.52. TRAPYEZIN, I. I.: Critical Load and Natural Vibrations of a Structurally Orthotropic Conical Shell, Closed at the Top, Loaded by Uniform Hydrostatic Pressure. *Trudy Moskovskogo Aviatsonnogo Instituta*, No. 130, 1960, pp. 5-18. (In Russian.)
- 5.53. NIMURA, T.; MATSUI, E.; SHIBAYAMA, K.; AND KIDO, K.: Studies on the Cone Type Dynamic Loudspeaker (II). S.C.I. Rept. RITU, B-(Elect. Comm.), vol. 3, no. 1, 1951.
- 5.54. KAGAWA, Y.; SHIBAYAMA, K.; KIDO, K.; NIMURA, T.; AND MIKAME, T.: Analysis of the Axisymmetric Vibration of a Conical Shell. The Record of Electrical and Communication Engineering Conversazione, Tohoku Univ., vol. 31, no. 1, Mar. 1962.
- 5.55. GOLDBERG, J. E.: Axisymmetric Oscillations of Conical Shells. Proc. 9th Inter. Cong. of Appl. Mech., Brussels, 1956, pp. 333-343.
- 5.56. GOLDBERG, J. E.; BOGDANOFF, J. L.; AND MARCUS, L.: On the Calculation of the Axisymmetric Modes and Frequencies of Conical Shells. *J. Acoust. Soc. Amer.*, vol. 32, no. 6, June 1960, pp. 738-742.
- 5.57. GOLDBERG, J. E.; AND BOGDANOFF, J. L.: Static and Dynamic Analysis of Nonuniform Conical Shells Under Symmetrical and Unsymmetrical Conditions. Sixth Symposium on Ballistic Missiles and Aerospace Technology. Academic Press (New York), 1961, pp. 219-238.
- 5.58. KAGAWA, Y.: On the Axisymmetrical Vibrations of Conical Shells. Scientific Report No. 6, Contract AF 49(638)-1290 (AFOSR-65-1422, AD 627 963), Polytechnic Inst. of Brooklyn, June 1965.

- 5.59. RAMAKRISHNA, B. S.: Transient Response of Speakers and Vibrations of Conical Shells. Ph.D. Dissertation, Ill. Institute of Technology, 1949.
- 5.60. PARTRIDGE, G. R.: Modes of Vibrations of a Loud-speaker Cone. Ph.D. Dissertation, Univ. of New Haven, 1950.
- 5.61. PLATUS, D. H.: Conical Shell Vibrations. NASA TN D-2767, Apr. 1965.
- 5.62. ANON.: Study on Bell-Mode Vibrations of Conical Nozzles. Rept. No. 0060-01-2 (quarterly) Contract No. NASr-111, Aerojet-General Corp., Sept. 1962.
- 5.63. ANON.: Study on Bell-Mode Vibrations of Conical Nozzles. Final Rept. No. 2581, Contract No. NASr-111, NASA CR 50692, Aerojet-General Corp., May 1963.
- 5.64. WATKINS, J. D.; AND CLARY, R. R.: Vibrational Characteristics of Some Thin-Walled Cylindrical and Conical Frustum Shells. NASA TN D-2729, Mar. 1965.
- 5.65. WATKINS, J. D.; AND CLARY, R. R.: Vibrational Characteristics of Thin-Wall Conical Frustum Shells. AIAA J., vol. 2, no. 10, Oct. 1964, pp. 1815-1816.
- 5.66. ADELMAN, H. M.; CATHERINES, D. S.; AND WALTON, W. C., JR.: A Method for Computation of Vibration Modes and Frequencies of Orthotropic Thin Shells of Revolution Having General Meridional Curvature. NASA TN D-4972, Jan. 1969.
- 5.67. WOODMAN, N. J.; AND SEVERN, R. T.: A Double-Curvature Shell Finite-Element and Its Use in the Dynamic Analysis of Cooling Towers and Other Shell Structures. Symposium on Structural Dynamics, Mar. 23-25, 1970, Loughborough Univ. of Tech., England, pp. A.5.1-A.5.18.
- 5.68. ABDULLA, K. M.; AND GALLETLY, G. D.: Free Vibration of Cones, Cylinders and Cone-Cylinder Combinations. Symposium on Structural Dynamics, Mar. 23-25, 1970, Loughborough Univ. of Tech., England, pp. B.2.1-B.2.20.
- 5.69. WEINGARTEN, V. I.; AND GELMAN, A. P.: Free Vibrations of Cantilevered Conical Shells. Paper 5661, J. of Eng. Mech. Div., Proc. Amer. Soc. Civil Engrs., EM6, Dec. 1967, pp. 127-138.
- 5.70. CARTER, R. L.; ROBINSON, A. R.; AND SCHNOBRICH, W. C.: Free and Forced Vibrations of Hyperboloidal Shells of Revolution. Civil Engineering Studies, Structural Research Series No. 334, Univ. of Ill., Feb. 1968.
- 5.71. NEWTON, R. A.: Free Vibrations of Rocket Nozzles. AIAA J., vol. 4, no. 7, July 1966, pp. 1303-1305.
- 5.72. STRUTT, M. J. O.: Eigenschwingungen der Kegelschale. Annalen der Physik, vol. 17, 1933, pp. 729-735.
- 5.73. RAYLEIGH, LORD: On the Infinitesimal Bending of Surfaces of Revolution. London Math. Soc. Proc., vol. 13, Nov. 1881, p. 4.
- 5.74. VAN URK, A. T.; AND HUT, G. B.: Measurement of Radial Vibrations of Aluminum Conical Shells. Annalen der Physik, vol. 17, 1933, pp. 915-920. (In German.)
- 5.75. RAYLEIGH, LORD: On the Bending and Vibration of Thin Elastic Shells, Especially of Cylindrical Form. Roy. Soc. (London), Dec. 1888, pp. 105-123.
- 5.76. HU, W. C. L.; GORMLEY, J. F.; AND LINDHOLM, U. S.: An Experimental Study and Inextensional Analysis of Vibrations of Free-Free Conical Shells. Int. J. Mech. Sci., vol. 9, no. 3, Mar. 1967, pp. 123-135.
- 5.77. HU, W. C. L.; GORMLEY, J. F.; AND LINDHOLM, U. S.: Flexural Vibrations of Conical Shells With Free Edges. NASA CR-384, Mar. 1966.
- 5.78. HU, W. C. L.: Comments on "Vibrational Characteristics of Thin-Wall Conical Frustum Shells." AIAA J., vol. 3, no. 6, June 1965, p. 1213.
- 5.79. KOVAL, L. R.: Note on the Vibrational Characteristics of Thin-Walled Shells. AIAA J., vol. 4, no. 3, Mar. 1966, pp. 571-572.
- 5.80. MIXSON, J. S.: Models of Vibration of Conical Frustum Shells With Free Ends. Proc. AIAA West Coast Aerospace Sciences Meeting (Los Angeles, Calif.), June 27-29, 1966.
- 5.81. MIXSON, J. S.: Modes of Vibration of Conical Frustum Shells With Free Ends. J. Spacecraft and Rockets, vol. 4, no. 3, Mar. 1967, pp. 414-416.
- 5.82. MIXSON, J. S.: Experimental Modes of Vibration of 14° Conical-Frustum Shells With Free Ends. NASA TN D-4428, Apr. 1968.
- 5.83. NAUMANN, E. C.: On the Prediction of the Vibratory Behavior of Free-Free Truncated Conical Shells. NASA TN D-4772, Sept. 1968.
- 5.84. KRAUSE, F. A.: Natural Frequencies and Mode Shapes of the Truncated Conical Shell With Free Edges. Rept. No. SAMSO-TR-68-37 (AD 665 828), U.S. Air Force, Jan. 1968.
- 5.85. HU, W. C. L.: Comments on "Axisymmetric Vibrations of Thin Elastic Shells." J. Acoust. Soc. Amer., vol. 38, no. 2, Aug. 1965, pp. 365-366.
- 5.86. KARNAUKHOV, V. G.: Analytical Solutions of Problems on the Free Oscillations and Stability of Conical Shells. Prikl. Mekh., vol. 9, no. 3, 1963, pp. 259-263. (In Ukrainian.)
- 5.87. ALDOSHINA, I. A.: Investigation of the Oscillations of a Conical Shell. Issledovaniia Po Uprugosti i Plaslichnosti, Sbornik 3, Izdatel'stvo Leningradskogo Universiteta, 1964, pp. 107-113. (In Russian.)
- 5.88. HOLMES, W. T.: Axisymmetric Vibrations of a Conical Shell Supporting a Mass. J. Acoust. Soc. Amer., vol. 34, no. 4, April 1962, pp. 458-461.
- 5.89. KANA, D. D.; AND HU, W. C. L.: Transmission Characteristics of Conical and Cylindrical Shells Under Lateral Excitation. J. Acoust. Soc. Amer., vol. 44, no. 6, June 1968, pp. 1647-1657.
- 5.90. KOPLIK, B.: Dynamics and Vibrations of Homogeneous and Layered Plates and Shells, Including Those of Sandwich Construction. AFOSR-67-2368, Contract AF 49(638)-1290 (AD 661 567),

- Final Sci. Rept., Dept. of Mech. Engineering, Polytechnic Inst. of Brooklyn, Sept. 1967.
- 5.91. LU, S. Y.; AND SUN, C. L.: Vibrations of Thin Conical Shells Subjected to Sudden Heating. *J. Aircraft*, vol. 4, no. 1, Jan./Feb. 1967, pp. 11-15.
 - 5.92. SINGER, J.; AND FERSHT-SCHER, R.: Buckling of Orthotropic Conical Shells Under External Pressure. TAE Rept. 22, Technion Research and Development Foundation (Israel), 1962.
 - 5.93. WEINGARTEN, V. I.: Free Vibrations of Ring-Stiffened Conical Shells. *AIAA J.*, vol. 3, no. 8, Aug. 1965, pp. 1475-1481.
 - 5.94. SAKHAROV, I. E.: Equations of Vibrations of Orthotropic Shallow Spherical and Conical Shells. *Izv. Akad. Nauk SSSR, Otd. Tekh. Nauk, Mekh. i Mashinostr.*, vol. 5, 1960, pp. 154-156. (In Russian.)
 - 5.95. GODZEVICH, V. G.: Free Oscillations of Circular Orthotropic Conical Shells. *Izv. Uchebn. Zavodov, Seriya, Aviatsionnaya Tekhnika*, no. 4, 1963, pp. 55-62. (In Russian.)
 - 5.96. WEINGARTEN, V. I.: Free Vibration of Ring Stiffened Conical Shells. Ph.D. Dissertation, Dept. of Engineering, Univ. of Calif., 1964.
 - 5.97. KARNAUKHOV, V. G.: Nonsymmetric Oscillations of Conical Shells. *Prikl. Mekh.*, vol. 1, no. 11, 1965, pp. 12-19. (In Russian.)
 - 5.98. GRENWELGE, O. E., JR.; AND MUSTER, D.: Free Vibrations of Ring-and-Stringer-Stiffened Conical Shells. *J. Acoust. Soc. Amer.*, vol. 46, no. 1, part 2, July 1969, pp. 176-185.
 - 5.99. MARTIN, R. E.: Free Vibrations of Anisotropic Conical Shells. *AIAA J.*, vol. 7, no. 5, May 1969, pp. 960-962.
 - 5.100. KUTNIKOVA, V. P.; AND SAKHAROV, I. E.: Natural Frequencies of Vibration of Orthotropic Shallow Conical Shells. *Izv. Akad. Nauk SSR, Otd. Tekh. Nauk, Mekh. i Mash.* no. 4, July/Aug. 1961, pp. 183-186. (In Russian.)
 - 5.101. NATUSHKIN, V. F.; AND KIRICHENKO, A. N.: Stability and Natural Vibrations of Truncated Structurally Orthotropic Conical Shells. *Aviatsionnaya Tekhnika*, vol. 9, no. 1, 1966, pp. 73-79. (In Russian.)
 - 5.102. SUN, C. L.; AND LU, S. Y.: Nonlinear Dynamic Behavior of Heated Conical and Cylindrical Shells. *Nuclear Engineering and Design*, vol. 7, 1968, pp. 113-122.
 - 5.103. SUN, C. L.: Dynamic Behavior of Heated Cylindrical and Conical Shells. Dissertation, Univ. of Florida, 1967.
 - 5.104. BAGDASARIAN, G. E.; AND GNUNI, V. Ts.: Resonance in Forced Nonlinear Oscillations of Laminar Anisotropic Shells. *Izvestiya Akademii Nauk Armyanskoy SSR, Seriya Fiziko-Matematicheskikh Nauk*, vol. 41, no. 1, 1961, pp. 41-49. (English transl.: FTD-TT-61-313/1+2, Foreign Technology Div., Wright-Patterson AFB, Jan. 1962.)
 - 5.105. GRIGOLYUK, E. I.: Nonlinear Vibrations and Stability of Shallow Rods and Shells. *Izv. AN SSSR, OTN*, no. 3, 1955, pp. 33-68. (In Russian.)
 - 5.106. WEINGARTEN, V. I.: The Effect of Internal or External Pressure on the Free Vibrations of Conical Shells. *Int. J. Mech. Sci.*, vol. 8, no. 2, Feb. 1966, pp. 115-124.
 - 5.107. WEINGARTEN, V. I.: Vibration of Conical Shells Subjected to Torsion. Paper 5783, *J. of Eng. Mech. Div., Proc. Amer. Soc. Civil Engrs.*, vol. 94, EM1, Feb. 1968, pp. 47-56.
 - 5.108. KRAUS, H.: *Thin Elastic Shells*. John Wiley & Sons, Inc. (New York), 1967.
 - 5.109. GOLDBERG, J. E.; BOGDANOFF, J. L.; AND ALSPAUGH, D. W.: On the Calculation of the Modes and Frequencies of Vibration of Pressurized Conical Shells. *Proc. AIAA 5th Annual Structures and Materials Conf.*, 1964, pp. 243-249.
 - 5.110. GOLDBERG, J. E.; BOGDANOFF, J. L.; AND ALSPAUGH, D. W.: Modes and Frequencies of Pressurized Conical Shells. *J. Aircraft*, vol. 1, no. 6, 1964, pp. 372-374.
 - 5.111. SALNIKOV, G. M.: Stability and Oscillations of a Conical Shell Under Combined Loads. *Aviatsionnaya Tekhnika*, vol. 9, no. 4, 1966, pp. 57-62.
 - 5.112. DOKUCHAEV, L. V.: On the Equations of Elastic Vibrations of a Cavity Partially Filled With Fluid. *Izv. AN SSR, OTN, Mekhanika*, no. 3, 1965, pp. 149-153. (English Transl. by Lockheed Missiles and Space Co.)
 - 5.113. SHKLIARCHUK, F. N.: Variational Methods for Calculating Axisymmetrical Oscillations of Shells of Revolution Partially Filled With a Fluid. *All-Union Conf. on the Theory of Shells and Plates*, 6th, Baku. Azerbaidzhan SSR, Sept. 15-20, 1966, transactions, pp. 835-840. (In Russian.)
 - 5.114. GARNET, H.: Free Vibrations of Conical Shells of Moderate Thickness. Ph.D. Dissertation, Polytechnic Institute of Brooklyn, 1962.
 - 5.115. NAGHDI, P. M.: On the Theory of Thin Elastic Shells. *Quart. Appl. Math.*, vol. 14, no. 4, Jan. 1957, pp. 369-380.
 - 5.116. CHOU, P. C.; AND MORTIMER, R. W.: Axisymmetric Motions of Nearly-Flat Shells of Revolution. *Proc. AIAA/ASME 8th Structures, Structural Dynamics, and Materials Conf.*, Mar. 1967, pp. 695-705.
 - 5.117. BERT, C. W.; AND RAY, J. D.: Vibrations of Orthotropic Sandwich Conical Shells With Free Edges. *Int. J. Mech. Sci.*, vol. 11, no. 9, Sept. 1969, pp. 767-779.
 - 5.118. RAY, I. E.; BERT, C. W.; AND EGLE, D. M.: The Application of the Kennedy-Pancu Method to Experimental Vibration Studies of Complex Shell Structures. *Shock and Vibration Bulletin* 39, pt. 3, Jan. 1969, pp. 107-115.
 - 5.119. SIU, C. C.; AND BERT, C. W.: Free Vibrational Analysis of Sandwich Conical Shells With Free Edges. *J. Acoust. Soc. Amer.*, vol. 47, no. 3, pt. 2, Mar. 1970, pp. 943-945.
 - 5.120. WILKINS, D. J., JR.; BERT, C. W.; AND EGLE,

- D. M.: Free Vibrations of Orthotropic Sandwich Conical Shells With Various Boundary Conditions. *J. Sound Vib.*, vol. 13, no. 2, Oct. 1970, pp. 211-228.
- 5.121. EGGLE, D. M.; AND SODER, K. E., JR.: A Theoretical Analysis of the Free Vibration of Discretely Stiffened Cylindrical Shells With Arbitrary End Conditions. NASA CR-1316, 1969.
- 5.122. AZAR, J. J.: Axisymmetric Free Vibrations of Sandwich Shells of Revolution. Ph.D. Dissertation, Univ. of Oklahoma, 1965.
- 5.123. WILKINS, D. J., JR.: Free Vibrations of Orthotropic Sandwich Conical Shells With Various Boundary Conditions. Ph.D. Dissertation, Univ. of Oklahoma, 1969.
- 5.124. GUTIN, N. L.: The Free Vibrations of a Conical Sandwich Shell. V sb. Issled. po Teorii Platin i Obolochek., no. 2, Kazan', Kazansk. Un-t, 1964, pp. 64-103. (In Russian.)
- 5.125. STEPANYUK, V. V.; AND BABICH, D. V.: Vibrations and Stability of a Conical Triple-Layered Shell With Fluid Flow in the Middle Layer. Issledovaniya po Prikladnoy Gidrodinamike, Izd-vo Naukova Dumka, Kiev, 1965, pp. 15-19. (English transl.: FTD-HT-23-554-67, Transl. Div., Foreign Tech. Div., Wright-Patterson AFB.)

Page intentionally left blank

Spherical and Other Shells

The circular cylindrical and conical shells considered in chapters 2, 3, and 5 are special cases of a class of shells called "shells of revolution."

A shell of revolution is characterized by a middle surface generated by the rotation of a line segment about an axis. If the line segment is straight a conical surface is generated. If, further, the straight line segment is parallel to the axis, the surface is circular cylindrical. As in chapters 2, 3, and 5 the term "closed" is used when the generator rotates one full revolution about the axis *and* if the proper continuity conditions are satisfied along the junction line. When the generator rotates less than one full revolution, an open shell results.

In addition to the circular cylindrical and conical shells already discussed, many other shells of revolution exist which have practical application; e.g., spherical, ellipsoidal (or spheroidal), paraboloidal, toroidal, hyperboloidal, and ogival.

The literature of free vibrations of spherical shells is vast, whereas for other shells of revolution, relatively few results are available in the literature. However, a number of methods of analysis have been developed for general, closed shells of revolution and the necessary computer programs have been written and are available. These methods are largely of three types: (1) finite difference, (2) finite element, or (3) numerical integration. The methods can accommodate thickness variation in the meridional direction in a routine manner and are often generalized to include complicating effects of the type discussed in chapter 3. However, the methods are either not applicable or involve a great deal more computational time in the case of open shells of revolution, or if the axisymmetric geometry of the problem is otherwise disturbed.

A surface of revolution is further characterized by the fact that all cross sections perpendicular to its axis are circles. One generalization, therefore, is that class of surfaces for which an axis exists so that all perpendicular planes have curves of the same form (although not necessarily circles) at their intersections with the surface. The noncircular cylindrical shell described in chapter 4 (for which there were few results) is a special case for which the curves of the intersecting planes have the same size, as well as the same form. Elliptical conical shells (for which virtually no free vibration results exists) or *general* ellipsoidal shells (having elliptical intersection curves with respect to *two* perpendicular axes) are other examples. Finally, other shells of practical value exist (e.g., hyperbolic paraboloid) for which little or no investigation of free vibrational behavior has been reported.

The literature dealing with free vibrations of spherical shells is second in size only to that for circular cylindrical shells. The large amount written is probably because of two of the same reasons which apply for circular cylindrical shells:

(1) The relative mathematical simplicity of the equations of motion because of constant radii of curvature, $R_1 = R_2 = R$, and constant Lamé parameters $A = B = R$.

(2) The widespread practical usage of this type of shell.

In the remainder of this chapter bibliographies are given for the free vibrations of spherical and other shells. The amount of investigation that has been carried out for the various curvatures is quite clear from the length of the bibliographies. No attempt has been made to summarize numerical results as in the previous chapters.

6.1 SPHERICAL SHELLS

- ADVANI, S. H.; AND LEE, Y. C.: Free Vibrations of Fluid-Filled Spherical Shells. *J. Sound Vib.*, vol. 12, no. 4, 1970, pp. 453-462.
- ANDERSON, G. L.: On Gegenbauer Transforms and Forced Torsional Vibrations of Thin Spherical Shells. *J. Sound Vib.*, vol. 12, no. 3, 1970, pp. 265-275.
- ANISIMOV, A. M.: Axially Symmetrical Oscillations of a Spherical Shell Filled With Fluid. English Transl. of *Izv. Vissikh Vchebnykh Zavedeniy MViSSO SSSR, Seriya Aviatsionnaya Tekhnika*, no. 2, 1963, Kazan', pp. 28-33.
- ARCHER, R. R.: On the Influence of Uniform Stress States on the Natural Frequencies of Spherical Shells. *J. Appl. Mech.*, vol. 29, no. 3, Sept. 1962, pp. 502-505.
- ARCHER, R. R.; AND FAMILI, J.: On the Vibration and Stability of Finitely Deformed Shallow Spherical Shells. *J. Appl. Mech.*, vol. 32, no. 1, Mar. 1965, pp. 116-120.
- ARCHER, R. R.; AND LANGE, C. G.: Nonlinear Dynamic Behavior of Shallow Spherical Shells. *AIAA J.*, vol. 3, no. 12, Dec. 1965, pp. 2313-2317.
- AUSTIN, A. L.: Thermally Induced Vibrations of Concentric Thin Spherical Shells. Contract No. w-7405-eng-48, Lawrence Radiation Lab., Univ. of Calif., Jan. 1964.
- AVERY, J. P.: Investigation of Dynamic Behavior of Thin Spherical Shells. NASA Res. Grant NGR-03-001-013, N66-15480, Ariz. State Univ., Dec. 1965.
- AVERY, J. P.: A Green's Function Approach to the Vibration of Thin Spherical Shell Segments. NASA CR-602, Sept. 1966.
- AVERY, J. P.: Investigation of Dynamic Behavior of Thin Spherical Shells. NASA Res. Grant NGR-03-001-013, N67-19091, Ariz. State Univ., Feb. 1967.
- BAGDASARIAN, G. E.; AND GNUNI, V. Ts.: Resonance in Forced Nonlinear Oscillations of Laminar Anisotropic Shells. *Izv. Akad. Nauk Arm. SSR, Seriya Fiziko-Matematicheskikh Nauk*, vol. 41, no. 1, 1961, pp. 41-49. (English transl.: FTD-TT-61-313/1+2 (AD 270 785), Foreign Technology Div., Wright-Patterson AFB, Jan. 1962.)
- BAKER, W. E.: The Elastic-Plastic Response of Thin Shells to Internal Blast Loading. Rept. No. 1194, Ballistic Research Laboratories, Feb. 1959.
- BAKER, W. E.: The Axisymmetric Modes of Vibration of Thin Spherical Shell. Rept. No. 1122 (AD 253 596), Ballistic Research Laboratories, Dec. 1960.
- BAKER, W. E.: Axisymmetric Modes of Vibration of Thin Spherical Shell. *J. Acoust. Soc. Amer.*, vol. 33, no. 12, Dec. 1961, pp. 1749-1758.
- BAKER, W. E.; HU, W. C. L.; AND JACKSON, T. R.: Elastic Response of Thin Spherical Shells to Axisymmetric Transient Loading. Tech. Rept. No. 1, Proj. No. 02-1635(IR), Southwest Research Institute, Aug. 1965.
- BAKER, W. E.; HU, W. C. L.; AND JACKSON, T. R.: Elastic Response of Thin Spherical Shells to Axisymmetric Transient Loading. Proc. 5th U.S. Nat. Cong. Appl. Mech. (Minneapolis, Minn.), 1966, p. 102.
- BALABUKH, L. I.; AND MOLCHANOV, A. G.: Axisymmetric Oscillations of a Spherical Shell Partially Filled With Liquid. *Inzhenernyi Zhurnal-Mekhanika Tverdogo Tela*, Sept.-Oct. 1967, pp. 56-61. (In Russian.)
- BALAKIREV, I. G.: Axisymmetric Oscillations of a Shallow Spherical Shell Containing a Liquid. *Inzhenernyi Zhurnal, Mekhanika Tverdogo Tela*, Sept.-Oct. 1967, pp. 116-123. (In Russian.)
- BERGASSOLI, A.; CANAC, F.; AND VOGEL, TH.: Sur La Transmission du Son par des Hublots Sphériques. *Acustica*, vol. 4, 1954, pp. 403-406.
- BERT, C. W.; AND EGGLE, D. M.: Dynamics of Composite, Sandwich, and Stiffened Shell-Type Structures. *J. Spacecraft and Rockets*, vol. 6, no. 12, Dec. 1969, pp. 1345-1361.
- BOLOTIN, V. V.: The Edge Effect in the Oscillations of Elastic Shells. *Appl. Math. Mech.*, vol. 24, no. 5, 1960, pp. 1257-1272.
- BOLOTIN, V. V.: On the Density of the Distribution of Natural Frequencies of Thin Elastic Shells. *Appl. Math. Mech.*, vol. 27, no. 2, 1963, pp. 538-543.
- BOLOTIN, V. V.: The Density of Eigenvalues in Vibration Problems of Elastic Plates and Shells. *Proc. Vibr. Problems (Warsaw)*, vol. 4, no. 6, 1965, pp. 341-351.
- CHAKRAVORTY, J. G.: Vibrations of Spherically Aeolotropic Shell. *Bull. Calcutta Math. Soc.*, vol. 47, no. 4, Dec. 1955, pp. 235-238.
- CHOW, H. Y.; AND POPOV, E. P.: Finite Element Solution of Axisymmetrical Dynamic Problems of Shells of Revolution. NASA CR-76100, Apr. 1966.
- CHREE, C.: Forced Vibrations in Isotropic Elastic Solid Spheres and Spherical Shells. *Camb. Phil. Soc. Trans.*, vol. 14, 1889.
- CINELLI, G.: Dynamic Vibrations and Stresses in Elastic Cylinders and Spheres. *J. Appl. Mech.*, vol. 33, no. 4, Dec. 1966, pp. 825-830.
- COALE, C. W.: Axisymmetric Vibrations of a Cylindrical-Hemispherical Tank Partially Filled With a Liquid. AIAA Paper No. 67-75, AIAA 5th Aerospace Sciences Meeting (New York), Jan. 23-26, 1967.
- COALE, C. W.; AND NAGANO, M.: Axisymmetric Modes of an Elastic Cylindrical-Hemispherical Tank Partially Filled With a Liquid. AIAA Symposium on Structural Dynamics and Aeroelasticity (Boston, Mass.), 1965, pp. 169-176.
- COHEN, G. A.: Computer Analysis of Asymmetric Free Vibrations of Ring-Stiffened Orthotropic Shells of Revolution. *AIAA J.*, vol. 3, no. 12, Dec. 1965, pp. 2305-2312.
- CONNOR, J., JR.: Nonlinear Transverse Axisymmetric Vibrations of Shallow Spherical Shells. NASA TN-D1510, 1962, pp. 623-642.
- CULKOWSKI, P. M.; AND REISMANN, H.: The Spherical Sandwich Shell Under Axisymmetric Static and Dynamic Loadings. *J. Sound Vib.*, vol. 14, no. 2, Jan. 1971, pp. 229-240.
- DAVIDS, N.; AND DAWSON, D. E.: Zero Order Spherical Harmonic Stress Distributions. *J. Math. and Phys.*, vol. 40, April 1961, pp. 46-54.

- DESILVA, C. N.; AND TERSTEEG, G. E.: Axisymmetric Vibrations of Thin Elastic Shells. *J. Acoust. Soc. Amer.*, vol. 36, no. 4, Apr. 1964, pp. 666-672.
- EASON, G.: On the Vibration of Anisotropic Cylinders and Spheres. *Appl. Sci. Res.*, sec. A, vol. 12, no. 1, 1963, pp. 81-85.
- ENGIN, A. E.: Vibrations of Fluid-Filled Spherical Shells. *J. Acoust. Soc. Amer.*, vol. 46, no. 1, pt. 2, July 1969, pp. 186-190.
- ENGIN, A. E.; AND LIU, Y. K.: Axisymmetric Response of a Fluid Filled Spherical Shell in Free Vibrations. *J. Biomechanics*, vol. 3, no. 1, Jan. 1970, pp. 11-22.
- EVENSEN, D. A.; AND FULTON, R. E.: Some Studies on the Nonlinear Dynamic Response of Shell-Type Structures. Rept. No. NASA TMX 56843, NASA Langley Research Center, Oct. 1965.
- EVERSMAN, W.: Some Free Vibration and Dynamic Response Problems Associated With Centrifugally Stabilized Disk and Shell Structures. NASA CR 77014, Aug. 1966.
- EVERSMAN, W.: Some Free Vibration and Dynamic Response Problems Associated With Centrifugally Stabilized Disk and Shell Structures. NASA CR 82525, Feb. 1967.
- EVERSMAN, W.: Some Equilibrium and Free Vibration Problems Associated With Centrifugally Stabilized Disk and Shell Structures. Final Rept., NASA Grant NGR 17-003-004, Feb. 1968.
- FEDERHOFER, K.: Über die Eigenschwingungen der geschlossenen Kugelschale bei gleichförmigem Oberflächenrucke. *ZAMM*, Band 15, Heft 1/2, Feb. 1935, pp. 26-31.
- FEDERHOFER, K.: Zur Berechnung der Eigenschwingungen der Kugelschale. *Sitzber. Akad. Wiss. Wien*, vol. 146, 1937, pp. 57-69.
- FEDERHOFER, K.: Über die Eigenschwingungen der Zylinder-Kegel-Und Kugelschalen. *Proc. 5th Int. Cong. for Appl. Mech.* (Cambridge, Mass.), 1938, pp. 719-723.
- FEIT, D.; AND JUNGER, M. C.: High Frequency Response of an Elastic Spherical Shell. *J. Appl. Mech.*, vol. 36, no. 4, Dec. 1969, pp. 859-864.
- GHOSH, P. R.: Vibrations of Nonhomogeneous Spherically Aeolotropic Spherical Shell. *Indian J. Phys.*, vol. 43, no. 5, 1968, pp. 296-304.
- GOLDENVEIZER, A. L.; AND LUR'YE, A. I.: On the Mathematical Theory of the Equilibrium of Elastic Shells. *Prikl. Mat. Mekh.*, vol. 11, 1947, pp. 565-592. (In Russian.)
- GONTKEVICH, V. S.: Natural Vibrations of Plates and Shells. A. P. Filipov, Ed., *Nauk Dumka* (Kiev), 1964. (Transl. by Lockheed Missiles and Space Co.)
- GONTKEVICH, V. S.: Natural Vibrations of Spherical Shells. *Issled. po Teorii Sooruzh.*, no. 13, 1964, pp. 77-83. (In Russian.) (English transl.: N66-16399, Lockheed Missiles and Space Co.)
- GONTKEVICH, V. S.: Natural Vibrations of Shells in a Liquid. Published: Kiev, *Naukova Dumka*, 1964. (In Russian.)
- GORMELY, J. F.; AND HU, W. C. L.: Nonsymmetric Modes and Frequencies of Complete Spherical Shells. Tech. Rept. No. 8, Contract NASr-94(06), SwRI Proj. 02-1504, Southwest Research Institute, Apr. 1967.
- GRIGOLIUK, E. I.: Nonlinear Vibrations and Stability of Shallow Rods and Shells. *Izv. Akad. Nauk SSSR, OTN*, no. 3, 1955, pp. 33-68.
- GRIGOREV, E. T.: Axisymmetric Oscillations of a Shell Containing Liquid. *Prikl. Mekh.*, 1966, pp. 39-49. (In Russian.)
- GROSSMAN, P. L.; AND KOPLIK, B.: On Nonlinear Equations of Isotropic Elastic Spherical Shells. Contract AF 49(638)-1290 (AFOSR-67-2254, AD 661 568), Air Force Office of Scientific Research, Sept. 1967.
- GROSSMAN, P. L.; KOPLIK, B.; AND YU, Y. Y.: Nonlinear Vibrations of Shallow Spherical Shells. *J. Appl. Mech.*, vol. 36, no. 3, Sept. 1969, pp. 451-458.
- GUPTA, A. P.: Elastic Vibrations of Beams, Plates, and Shells. Ph.D. Dissertation, University of Rookee, India, Dec. 1967.
- HAYEK, S.: Vibration of a Spherical Shell in an Acoustic Medium. *J. Acoust. Soc. Amer.*, vol. 40, no. 2, Aug. 1966, pp. 342-348.
- HENG, G. Z.; AND SOLECKI, R.: Free and Forced Finite-Amplitude Oscillations of an Elastic Thick-Walled Hollow Sphere Made of Incompressible Material. *Archiwum Mechaniki Stosowanej*, vol. 15, no. 3, 1963, pp. 427-433.
- HOPPMANN, W. H., II: Forced Vibrations of Elastic Orthotropic Spherical Shells. Contract No. DA 30-115-509-ORD-912 (AD 237 083), Dept. of the Army-Ordnance Corps, May 1960.
- HOPPMANN, W. H., II: Frequencies of Vibration of Shallow Spherical Shells. *J. Appl. Mech.*, vol. 28, no. 2, June 1961, pp. 305-307.
- HOPPMANN, W. H., II: Extensional Vibrations of Segment of Elastic Orthotropic Spherical Shell. *Proc. 4th U.S. Nat. Congr. Appl. Mech.* (Berkeley, Calif.), vol. 1, June 1962, pp. 215-218.
- HOPPMANN, W. H., II; AND BAKER, W. E.: Extensional Vibrations of Elastic Orthotropic Spherical Shells. *J. Appl. Mech.*, vol. 28, no. 2, June 1961, pp. 229-237.
- HOPPMANN, W. H., II; AND BARONET, C. N.: A Study of the Vibrations of Shallow Spherical Shells. Rept. No. 1188 (AD 401 669), Ballistic Research Laboratories, Jan. 1963.
- HOPPMANN, W. H., II; AND BARONET, C. N.: A Study of the Vibrations of Shallow Spherical Shells. *J. Appl. Mech.*, vol. 30, no. 3, Sept. 1963, pp. 329-334.
- HOPPMANN, W. H., II; AND MILLER, C. E.: Flexural Vibration of Shallow Orthotropic Spherical Shells. *J. Acoust. Soc. Amer.*, vol. 34, no. 8, Aug. 1962, pp. 1067-1072.
- HU, W. C. L.: A Survey of the Literature on the Vibrations of Thin Shells. Tech. Rept. No. 1, Contract NASr-94(06), Southwest Research Inst., June 1964.
- HU, W. C. L.: Comments on "Axisymmetric Vibrations of Thin Elastic Shells." *J. Acoust. Soc. Amer.*, vol. 38, no. 2, Aug. 1965, pp. 365-366.
- HWANG, C.: Extensional Vibration of Axisymmetrical Shells. *AIAA J.*, vol. 3, no. 1, Jan. 1965, pp. 23-26.

- HWANG, C.: Some Experiments on the Vibrations of a Hemispherical Shell. *J. Appl. Mech.*, vol. 33, no. 4, Dec. 1966, pp. 817-824.
- HWANG, C.: Vibration of Ring-Stiffened and Mass-Attached Hemispherical Shells. *J. Appl. Mech.*, vol. 36, no. 2, June 1969, pp. 318-320.
- JAHANSHAHI, A.: Equations of Motion of Spherical Shells. *J. Acoust. Soc. Amer.*, vol. 38, no. 5, Nov. 1965, pp. 883-885.
- JAIN, R. K.: Elastic Problems in Shells. Ph.D. Dissertation, Univ. of Roorkee, India, 1966.
- JENNINGS, R. L.: The Elastic Response of Spherical Shells to Blast Waves. Ph.D. Dissertation, Univ. of Ill., 1964.
- JOHNSON, M. W.: On the Dynamics of Shallow Elastic Membranes. Contract No. DA-11-022-ORD-2059 (AD 231 350), Mathematics Research Center, U.S. Army, Univ. of Wisc., Dec. 1959.
- JOHNSON, M. W.; AND REISSNER, E.: On Inextensional Deformations of Shallow Elastic Shells. *J. Math. Phys.*, vol. 34, no. 4, Jan. 1956, pp. 335-346.
- JOHNSON, M. W.; AND REISSNER, E.: On Transverse Vibrations of Shallow Spherical Shells. *Quart. Appl. Math.*, vol. 15, no. 4, Jan. 1958, pp. 367-380.
- JULLIEN, Y.: Sur les Phenomenes de Transition et Rotation dans les Modes de Vibration des Enveloppes minces en Excitation Forcee. *Proc. Conf. on Acoustics of Solid Media (Nadbitka)*, 1964, pp. 73-82.
- JULLIEN, Y.: Flexion des Plaques et Coques Elastiques. From a series of course lecture at the Univ. of Sherbrooke, Aout, France, 1966.
- JULLIEN, Y.: Vibrations aléatoires de calottes sphériques élastiques. *J. de Mécanique*, vol. 5, no. 4, Dec. 1966, pp. 419-438.
- JULLIEN, Y.; AND VIVOLI, J.: Sur les Vibrations de Calottes Sphériques dont l'Angle d'ouverture n'est pas necessairement petit. Centre National de la Recherche Scientifique, Centre de Recherches Physiques, Note No. 778 bis., 1964.
- JULLIEN, Y.; AND VIVOLI, J.: Sur les Lingnes Nodales des Calottes Sphériques. Centre de Recherches Physiques, CNRS, Note No. 778, Réunion de la Société Française de Physique de l'acoustique aux hypersons, Royat 16-18, Sept. 1964.
- JUNGER, M. C.: Vibrations of Elastic Shells in a Fluid Medium and the Associated Radiation of Sound. *J. Appl. Mech.*, vol. 19, no. 4, Dec. 1952, pp. 439-445.
- JUNGER, M. C.: Nonmodal Solution of Spherical Shells With Cutouts Excited by High-Frequency Axisymmetric Forces. *J. Appl. Mech.*, vol. 37, no. 4, Dec. 1970, pp. 977-983.
- JUNGER, M. C.; AND FEIT, D.: High-Frequency Response of Point-Excited Submerged, Spherical Shells. *J. Acoust. Soc. Amer.*, vol. 45, no. 3, March 1969, pp. 630-636.
- KALNINS, A.: On Vibrations of Shallow Spherical Shells. *J. Acoust. Soc. Amer.*, vol. 33, no. 8, Aug. 1961, pp. 1102-1107.
- KALNINS, A.: Free Nonsymmetric Vibrations of Shallow Spherical Shells. *Proc. 4th U.S. Nat. Cong. Appl. Mech.*, Univ. of Calif., Berkeley, 1962, pp. 225-233.
- KALNINS, A.: Effect of Bending on Vibrations of Spherical Shells. *J. Acoust. Soc. Amer.*, vol. 36, no. 1, Jan. 1964, pp. 74-81.
- KALNINS, A.: Free Vibration of Rotationally Symmetric Shells. *J. Acoust. Soc. Amer.*, vol. 36, no. 7, July 1964, pp. 1355-1365.
- KALNINS, A.: Comments on the "Analysis of Free Vibration of Rotationally Symmetric Shells." *AIAA J.*, vol. 4, no. 8, Aug. 1966, pp. 1497-1499.
- KALNINS, A.: Analysis of Thin Elastic Shells With Attached Systems. *AIAA 5th Aerospace Sciences Meeting* (New York), Jan. 23-26, 1967.
- KALNINS, A.: A Discussion of "Some Experiments on the Vibration of a Hemispherical Shell." *J. Appl. Mech.*, vol. 34, no. 3, Sept. 1967, pp. 792-793.
- KALNINS, A.; AND KRAUS, H.: Effect of Transverse Shear and Rotary Inertia on Vibration of Spherical Shells. *Proc. 5th U.S. Nat. Cong. Appl. Mech.* (Minneapolis), 1966, p. 134.
- KALNINS, A.; AND NAGHDI, P. M.: Axisymmetric Vibrations of Shallow Elastic Spherical Shells. *Tech. Rept. No. 6, Series No. 131, Issue No. 6, Contract Nonr-22269 (AD 230 120)*, Inst. of Eng. Res., Univ. of Calif., Nov. 1959.
- KALNINS, A.; AND NAGHDI, P. M.: Axisymmetric Vibrations of Shallow Elastic Spherical Shells. *J. Acoust. Soc. Amer.*, vol. 32, no. 3, March 1960, pp. 342-347.
- KALNINS, A.; AND NAGHDI, P. M.: Propagation of Axisymmetric Waves in an Unlimited Elastic Shell. *J. Appl. Mech.*, vol. 27, no. 4, Dec. 1960, pp. 690-695.
- KHACHATRYAN, A. A.: Stability and Oscillations of the Transversally Isotropic Spherical Shell. *Academy of Sciences of the Armenian SSR-Physical Mathematical Science Series*, vol. 13, no. 4, 1960, pp. 19-28. (In Russian.)
- KLEIN, S.; AND SYLVESTER, R. J.: The Linear Elastic Dynamic Analysis of Shells of Revolution by the Matrix Displacement Method. *AFFDL-TR-66-80*, Aerospace Corp., Dec. 1965, pp. 299-328.
- KOBYCHKIN, V. S.; SHMAKOV, V. P.; AND IABLOKOV, V. A.: Axisymmetric Oscillations of a Hemispherical Shell Partially Filled With Liquid. *Inzhenernyi Zhurnal, Mekh. Tverdogo Tela*, Sept.-Oct. 1968, pp. 46-54. (In Russian.)
- KOPLIK, B.: Axisymmetric Vibrations of Homogeneous and Sandwich Shallow Spherical Shells. Ph.D. Dissertation, Polytechnic Institute of Brooklyn, 1966.
- KOPLIK, B.: Dynamics and Vibrations of Homogeneous and Layered Plates and Shells, Including Those of Sandwich Construction. Contract AF 49(638)-1290, Final Sci. Rept., AFOSR-67-2368 (AD 661 569), Air Force Office of Scientific Research, Sept. 1967.
- KOPLIK, B.; AND YU, Y. Y.: Torsional Vibrations of Homogeneous and Sandwich Spherical Caps and Circular Plates. Contract AF 49(638)-1290, Sci. Rept. No. 9 (AD 659 491), Air Force Office of Scientific Research, July 1967.
- KOPLIK, B.; AND YU, Y. Y.: Axisymmetric Vibrations of Homogeneous and Sandwich Spherical Caps. *J. Appl. Mech.*, vol. 34, no. 3, Sept. 1967, pp. 667-673.

- KOPLIK, B.; AND YU, Y. Y.: Approximate Solutions for Frequencies of Axisymmetric Vibrations of Spherical Caps. *J. Appl. Mech.*, vol. 34, no. 3, Sept. 1967, pp. 785-789.
- KOVAL, L. R.; AND BHUTA, P. G.: Axisymmetric Dynamic Response of Shallow Spherical Shells. Rept. No. EM 13-21, TRW Space Tech. Lab., Thompson Ramo Wooldridge, Inc., Oct. 1963.
- KOVAL, L. R.; AND BHUTA, P. G.: Dynamic Response of Shallow Spherical Shells. Rept. No. EM 13-21, 6121-7532-RU000, TRW Space Tech. Lab., Thompson Ramo Wooldridge, Inc., Oct. 1963.
- KOVAL, L. R.; AND BHUTA, P. G.: Orthogonality Condition for the Exact Linearized Equations of Shallow Spherical Shells. *J. Appl. Mech.*, vol. 31, no. 3, Sept. 1964, pp. 548-550.
- KRAUS, H.: Interim Technical Report on Dynamic Thermal and Pressure Stresses in Thin Spherical Shell. Contract No. DA-31-124-ARO(D)-146 (AD 604 542), Pratt and Whitney Aircraft, Apr. 1964.
- KRAUS, H.: Thermally Induced Vibrations of Thin Non-Shallow Spherical Shells. Paper 65-409, AIAA Second Annual Meeting (San Francisco), July 26-29, 1965.
- KRAUS, H.; AND KALNINS, A.: Transient Vibration of Thin Elastic Shells. *J. Acoust. Soc. Amer.*, vol. 38, no. 6, Dec. 1965, pp. 994-1002.
- KRISHNA, B.: On Vibrations of Elastic Spherical Shells. *University of Roorkee Research Journal*, vol. 7, nos. 1 and 2, 1964, pp. 9-23.
- KRISHNA, B.; AND JAIN, P. C.: Torsional and Thickness Shear Vibrations of Spherical Shells. *University of Roorkee Research Journal*, vol. 9, no. 4, 1967, pp. 23-34.
- LAMB, H.: On the Vibrations of a Spherical Shell. *Proc. London Math. Soc.*, vol. 14, 1882, pp. 50-56.
- LEE, T. H.: Vibration of Shallow Spherical Shells With Concentrated Mass. *J. Appl. Mech.*, vol. 33, no. 4, Dec. 1966, pp. 938-939.
- LISOWSKI, A.: Investigation of Shell Vibration and Stability by Means of Model Tests. *Rozprawy Inz.*, vol. 6, no. 1, 1958, pp. 25-91. (In Polish.)
- LISOWSKI, A.: Knickung und Schwingungen von Schalen im Lichte der Modellprüfung. *Der Bauingenieur*, 35(1960) Heft 3, pp. 86-89.
- LIZAREV, A. D.: Lowest Frequencies of the Natural Axisymmetric Oscillations of Nonshallow Spherical Shells. *Inzhenernyi Zhurnal-Mekhanika Tverdogo Tela*, May-June 1967, pp. 66-72. (In Russian.)
- LOCK, M. H.; OKUBO, S.; AND WHITTIER, J. S.: Experiments on the Snapping of a Shallow Dome Under a Step Pressure Load. Rept. No. SSD-TR-67-117, (AD 655 057), U.S. Air Force, June 1967.
- LOCK, M. H.; WHITTIER, J. S.; AND MALCOM, H. A.: Transverse Vibrations of a Shallow Spherical Dome. Rept. No. SSD-TR-67-113 (AD 655 056), U.S. Air Force, June 1967.
- LOCK, M. H.; WHITTIER, J. S.; AND MALCOM, H. A.: Transverse Vibrations of a Shallow Spherical Dome. *J. Appl. Mech.*, vol. 35, no. 2, June 1968, pp. 402-403.
- LONG, C. F.: Vibration of a Radially Loaded Spherical Shell. *J. Eng. Mech. Div., Proc. ASCE, EM 2*, Apr. 1966, pp. 235-250.
- LOVE, A. E. H.: The Small Vibrations and Deformations of a Thin Elastic Shell. *Phil. Trans. Roy. Soc. (London)*, ser. A, 179, 1888, pp. 491-546.
- LUZHIN, O. V.: Problem of Free Vibrations of Thin Spherical Shells. *Stroit. Mekh. i Raschet Sooruzh.*, no. 3, 1961, pp. 32-36. (In Russian.)
- LUZHIN, O. V.: Axisymmetric Vibrations of Spherical Domes Under Different Boundary Conditions. *Issledovaniya Po Teorii Sooruzhenii*, no. 11, 1962, pp. 35-53. (In Russian.)
- LUZHIN, O. V.: Some Problems of Shell Dynamics. *Theory of Shells and Plates; Proc. of the 4th All-Union Conf., Yerevan, Armenian SSR, Oct. 24-31, 1962*, pp. 652-658. (In Russian.)
- LYAMSHEV, L. M.: Theory of Sound Radiation by Thin Elastic Shells and Plates. *Akusticheskii Zhurnal*, vol. 5, no. 4, Oct.-Dec. 1959, pp. 420-427. (In Russian.)
- MALKINA, R. L.: Application of the Method of Asymptotic Integration to Problems of Shell Vibrations. *Teoriya Obolochek i Plastin, Erevan Akad Arm SSR*, 1964, pp. 668-673. (In Russian.)
- MALKINA, R. L.: Free Oscillations of a Spherical Dome. *Aviatsionnaia Tekh.*, no. 1, 1964, pp. 67-74. (In Russian.)
- MALKINA, R. L.: Application of the Method of Asymptotic Integration to the Problems of Oscillations of Near-Spherical Shells of Revolution. *Aviatsionnaia Tekh.*, vol. 7, no. 2, 1964, pp. 47-56. (In Russian.)
- MANASYAN, A. A.: Vibrations of a Spherical Shell Under the Action of a Concentrated Force. *Theory of Shells and Plates, Proc. of the 4th All-Union Conf., Yerevan, Armenian SSR, 1962*, pp. 674-679. (In Russian.)
- MAURO, A.: Una soluzione completa del problema delle vibrazioni libere di volte sottili ribassate su pianta rettangolare. *Technica Italiana*, vol. 32, no. 3, Mar. 1967, pp. 145-161.
- MCDONALD, C.: A Numerical Analysis of the Dynamic Response of Thin Elastic Spherical Shells. Ph.D. Dissertation, Univ. of Ill., 1959.
- MCIVOR, I. K.; AND SONSTEGARD, D. A.: The Axisymmetric Response of a Closed Spherical Shell to a Nearly Uniform Radial Impulse. *J. Acoust. Soc. Amer.*, vol. 40, no. 6, Dec. 1966, pp. 1540-1547.
- MEDICK, M. A.: On the Initial Response of Thin Elastic Shells to Localized Transient Forces. Tech. Rept. No. RAD-TR-61-6, Contract AF04(647)-258, Avco Corp., Apr. 1961.
- MEDICK, M. A.: Initial Response of an Elastic Spherical Shell Upon Impact With a Compressible Fluid. *Proc. 4th U.S. Nat. Cong. Appl. Mech. (Berkeley, Calif.)*, June 18-21, 1962, pp. 285-292.
- MORTELL, M. P.: Waves on a Spherical Shell. *J. Acoust. Soc. Amer.*, vol. 45, no. 1, Jan. 1969, pp. 144-149.
- MUKHERJEE, J.: Stresses due to Vibration of Spherical Shells of Anisotropic Materials. *AIAA J.*, vol. 6, no. 8, Aug. 1968, pp. 1563-1565.

- NAGHDI, P. M.: On the General Problem of Elastokinetics in the Theory of Shallow Shells. Proc. of the IUTAM Symp. on Theory of Thin Elastic Shells, North Holland Publishing Co. (Amsterdam, Holland), 1960, pp. 301-330.
- NAGHDI, P. M.; AND KALNINS, A.: On Vibrations of Elastic Spherical Shells. Contract Nonr-222(69), Proj. NR-064-436, Tech. Rept. No. 13 (AD 251 800), Office of Naval Research, Jan. 1961.
- NAGHDI, P. M.; AND KALNINS, A.: On Vibrations of Elastic Spherical Shells. J. Appl. Mech., vol. 29, no. 1, Mar. 1962, pp. 65-72.
- NAGHDI, P. M.; AND ORTHWEIN, W. C.: On Axisymmetric Vibrations of Thin Shallow Viscoelastic Spherical Shells. Proj. No. 1750-17500-717, Contract No. AF 18(603)-47, Air Force Office of Scientific Research, Jan. 1959.
- NAGHDI, P. M.; AND ORTHWEIN, W. C.: Response of Shallow Viscoelastic Spherical Shells to Time Dependent Axisymmetric Loads. Quart. Appl. Math., vol. 18, July 1960, pp. 107-121.
- NAVARATNA, D. R.: Natural Vibrations of Deep Spherical Shells. AIAA J., vol. 4, no. 11, Nov. 1966, pp. 2056-2058.
- OGBALOV, P. M.: Problems in Dynamics and Stability of Shells. Izdate'stvo Moskovskozo Universtiteta, 1963. (In Russian.)
- OKUBO, S.; AND WHITTIER, J. S.: A Note on Buckling and Vibrations of an Externally Pressurized Shallow Spherical Shell. J. Appl. Mech., vol. 34, no. 4, Dec. 1967, pp. 1032-1034.
- ONIAHVILI, O. D.: Certain Dynamic Problems of the Theory of Shells. Academy of Sciences of the Georgian SSR, Construction Institute. (Transl. and Publ. by M. D. Friedman, Inc., Foreign Tech. Transl., West Newton, Mass., 1959.)
- ÖRY, H.; HORNUNG, E.; AND FAHLBUSCH, G.: A Simplified Matrix Method for the Dynamic Examination of Different Shells of Revolution. Symposium on Structural Dynamics and Aeroelasticity, AIAA (Boston), 1965, pp. 365-388.
- PANDALAI, K. A. V.; AND DYM, C. L.: On the Equations for Axisymmetric Deformation of Shallow Shells of Revolution. Contract No. AF 49(638)1276 (AD 635 095), Air Force Office of Scientific Research, Apr. 1966.
- PENZES, L. E.: Free Vibrations of Thin Orthotropic Oblate Spheroidal Shells. J. Acoust. Soc. Amer., vol. 45, no. 2, Feb. 1969, pp. 500-505.
- PENZES, L. E.; AND BURGIN, G. H.: Free Vibrations of Thin Isotropic Oblate Spheroidal Shells. Rept. No. GD/C-BTD65-113, Convair Div., General Dynamics, July 1965.
- PESENNIKOVA, N. K.; AND SAKHAROV, I. E.: Natural Vibration Frequencies of Fundamental Tone of Spherical Shells. Izv. Akad. Nauk SSSR, OTD Tekh. Nauk, Mekh. i Mash. (2), 1961, pp. 168-172. (In Russian.)
- PILKEY, W. D.: Mechanically and/or Thermally Generated Dynamic Response of Thick Spherical and Cylindrical Shells With Variable Material Properties. J. Sound Vib., vol. 6, no. 1, 1967, pp. 105-109.
- POZHALOSTIN, A. A.: On the Analysis of the Natural Vibrations Frequencies of a Shallow Spherical Shell. Izv. Vyssh. Uchebn. Zaved., Mashinostro (Moscow), no. 10, 1965, pp. 30-34. (In Russian.)
- PRASAD, C.: On Vibrations of Spherical Shells. J. Acoust. Soc. Amer., vol. 36, no. 3, Mar. 1964, pp. 489-494.
- PRASAD, C.; AND JAIN, R. K.: On Axisymmetric Vibrations of Thick Spherical Shells. (Private communication.) Univ. of Roorkee, Roorkee, India.
- RAMAKRISHNAN, C. V.; AND SHAH, A. H.: Vibration of an Aeolotropic Spherical Shell. J. Acoust. Soc. Amer., vol. 47, no. 5, part 2, May 1970, pp. 1366-1374.
- RAND, R.; AND DIMAGGIO, F.: Vibrations of Fluid-Filled Spherical and Spheroidal Shells. J. Acoust. Soc. Amer., vol. 42, no. 6, Dec. 1967, pp. 1278-1286.
- RAYLEIGH, LORD: On the Bending and Vibration of Thin Elastic Shells, Especially of Cylindrical Form. Phil. Trans. Roy. Soc. (London), Dec. 1888, pp. 105-123.
- REISMANN, H.; AND CULKOWSKI, P. M.: Forced Motion of Shallow Spherical Shells. Durham ARO-D Proj. No. 5637-E*, Tech. Rept. No. 21 (AD 650 221), U.S. Army Research Office, Apr. 1967.
- REISMANN, H.; AND CULKOWSKI, P. M.: Forced Axisymmetric Motion of Shallow Spherical Shells. J. Eng. Mech. Div., Proc. ASCE, vol. 94, Apr. 1968, pp. 653-670.
- REISSNER, E.: On Vibrations of Shallow Spherical Shells. J. Appl. Phys., vol. 17 no. 12, Dec. 1946, pp. 1038-1042.
- REISSNER, E.: On Transverse Vibrations of Thin, Shallow Elastic Shells. Quart. Appl. Math., vol. 13, no. 2, July 1955, pp. 169-176.
- REISSNER, E.: On Axisymmetric Vibrations of Shallow Spherical Shells. Quart. Appl. Math., vol. 13, no. 3, Oct. 1955, pp. 279-290.
- REISSNER, E.: Contributions to the Theory of Thin Elastic Shells. 9th Congr. Intern. Mecan. Appl., Univ. of Bruxelles, 1957, vol. 6, pp. 290-296.
- ROSS, E. W., JR.: Membrane Natural Frequencies for Axisymmetric Vibration of Deep Spherical Caps. Tech. Rept. AMRA TR 63-23 (AD 428 442), U.S. Army Materials Research Agency, Dec. 1963.
- ROSS, E. W., JR.: Natural Frequencies and Mode Shapes for Axisymmetric Vibration of Deep Spherical Caps. Tech. Rept. AMRA TR 64-38 (AD 457 109), U.S. Army Materials Research Agency, Nov. 1964.
- ROSS, E. W., JR.: Membrane Natural Frequencies for Spherical Caps. J. Appl. Mech., vol. 32, no. 2, June 1965, pp. 432-434.
- ROSS, E. W., JR.: Natural Frequencies and Mode Shapes for Axisymmetric Vibration of Deep Spherical Shells. J. Appl. Mech., vol. 32, no. 3, Sept. 1965, pp. 553-561.
- ROSS, E. W., JR.: Comment on "Computer Analysis of Asymmetric Free Vibrations of Ring-Stiffened Orthotropic Shells of Revolution." AIAA J., vol. 4, no. 7, July 1966, pp. 1310-1312.
- ROSS, E. W., JR.: On Membrane Frequencies for Spherical Shell Vibrations. Tech. Rept. 67-74-OSD (AD 651 475), U.S. Army Natick Laboratories, May 1967.

- ROSS, E. W., JR.: On Inextensional Vibrations of Thin Shells. Tech. Rept. 68-14-OSD (AD 658 672), U.S. Army Natick Laboratories, July 1967.
- ROSS, E. W., JR.: Membrane Frequencies for Spherical Shell Vibrations. AIAA J., vol. 6, no. 5, May 1968, pp. 803-808.
- ROSS, E. W., JR.: On Inextensional Vibrations of Thin Shells. J. Appl. Mech., vol. 35, no. 3, Sept. 1968, pp. 516-523.
- ROSS, E. W., JR.; AND MATTHEWS, W. T.: Frequencies and Mode Shapes for Axisymmetric Vibration of Shells. J. Appl. Mech., vol. 34, no. 1, Mar. 1967, pp. 73-80.
- SACHENKOV, A. V.: Determination of the Frequencies of Free Oscillations of Shallow Spherical Shells and Plane Plates by Analogy with Membrane Oscillation. Prikl. Mekh., vol. 1, no. 1, 1965, pp. 104-108. (In Russian.)
- SAKHAROV, I. E.: Equations of Vibrations of Orthotropic Shallow Spherical and Conical Shells. Izv. Akad. Nauk SSSR, OTD Tekh. Nauk, Mekh. i Mash. vol. 5, 1960, pp. 154-156. (In Russian.)
- SAMOILOV, E. A.: Dynamic Calculation of Spherical Shells on Digital Computers. Prochnost' i Ustoichivost' Elementov Tonkostennykh Konstruktsii, no. 2, 1967, pp. 234-247. (In Russian.)
- SAMOILOV, E. A.; AND PAVLOV, B. S.: Vibrations of a Hemispherical Shell Filled With a Fluid. Aviatsonnaia Tekhnika, vol. 7, no. 3, 1964, pp. 79-86. (In Russian.)
- SAMOILOV, E. A.; AND PAVLOV, B. S.: Oscillations of a Hemispherical Shell Filled With a Fluid. Aviatsonnaia Tekhnika, vol. 9, no. 1, 1966, pp. 38-46. (In Russian.)
- SAUNDERS, H.; AND PASLAY, P. R.: Inextensional Vibrations of a Sphere-Cone Shell Combination. J. Acoust. Soc. Amer., vol. 31, no. 5, May 1959, pp. 579-583.
- SEIDE, P.: Radial Vibrations of Spherical Shells. J. Appl. Mech., vol. 37, no. 2, June 1970, pp. 528-530.
- SEN, N.: On a Type of Vibration of an Elastic Spherical Shell. Phil. Mag., 6th series, vol. 42, pp. 185-193.
- SHAH, A. H.; RAMKRISHNAN, C. V.; AND DATTA, S. K.: Three-Dimensional and Shell-Theory Analysis of Elastic Waves in a Hollow Sphere, Parts 1 and 2. J. Appl. Mech., vol. 36, no. 3, Sept. 1969, pp. 431-444.
- SHIRAIISHI, N.; AND DIMAGGIO, F. L.: Perturbation Solution for Axisymmetric Vibrations of Prolated Spherical Shells. J. Acoust. Soc. Amer., vol. 34, no. 11, Nov. 1962, pp. 1725-1731.
- SHKLYARCHUK, F. N.: About an Approximate Method of Calculating Axially Symmetrical Oscillations of Shells of Rotation With Liquid Filling. Izv. Akad. Nauk SSSR, Mekh., no. 6, 1965, pp. 123-129. (In Russian.) (English Transl.: FTD-HT-66-527, Foreign Technology Div., Wright-Patterson AFB.)
- SHMAKOV, V. P.: Method of Integrating the Equations of the Axisymmetric Oscillations of a Spherical Shell. Inzhenernyi Zhurnal-Mekh. Tver. Tela, Mar.-Apr. 1966, pp. 154-159. (In Russian.)
- SILBINGER, A.: Free and Forced Vibrations of a Spherical Shell. Rept. U-106-48, Contract Nonr-2739(00) (AD 251 628), Cambridge Acoustical Associates, Inc., Dec. 1960.
- SILBINGER, A.: Nonaxisymmetric Modes of Vibration of Thin Spherical Shells. J. Acoust. Soc. Amer., vol. 34, no. 6, June 1962, p. 862.
- SONG, Q. G.: An Approximate Solution for Symmetric Vibration in Spherical Shells. Acta Mech. Sinica, vol. 7, no. 4, Dec. 1964, pp. 335-341. (In Chinese.) (English Transl.: FTD-HT-23-550-67, Foreign Technology Div., Wright-Patterson AFB, 1967.)
- SONSTEGARD, D. A.: Effects of a Surrounding Fluid on the Free, Axisymmetric Vibrations of Thin Elastic Spherical Shells. J. Acoust. Soc. Amer., vol. 45, no. 2, Feb. 1969, pp. 506-510.
- SUVERNEV, V. G.: Natural Vibrations of Spherical Sandwich Shells With Freely Supported and Fixed Edges. Rasch. Elementov Aviat. Konstr., no. 3, MASHGIZ, 1965, pp. 219-225. N66 33788.
- SUVERNEV, V. G.: Small Natural Oscillations of Triple-Layer Shells of Rotation. FTD-TT-65-1874/1+2+4 (AD 639 556), Foreign Technology Div., Wright-Patterson AFB, June 1966.
- TASI, J.: Effect of Mass Loss on the Transient Response of a Shallow Spherical Sandwich Shell. AIAA J., vol. 2, no. 1, Jan. 1964, pp. 58-63.
- TOVSTIK, P. E.: Regular Integrals of the Equations of Axisymmetrical Oscillations of a Dome. Issledovaniia Po Uprugosti i Plastichnosti, no. 4, Leningrad, 1965, pp. 117-133. (In Russian.)
- TOVSTIK, P. E.: Free Vibrations of a Thin Spherical Dome. Akad. Nauk SSSR, Izv. Mekh., Nov.-Dec. 1965, pp. 111-113. (In Russian.)
- VLASOV, V. Z.: Theory of Space Vibration of Thin-Walled, Bars and Shells as well as Aerodynamic Stability of Suspension Bridges. 9th Congres. Intern. Mecan. Appl., Univ. of Bruxelles, 1957, pp. 519-526.
- VAN FO FY, G. A.: Vibrations of a Shallow Spherical Segment. Prikl. Mekh., vol. 7, no. 1, 1961, pp. 105-107. (In Ukrainian.)
- VAN FO FY, G. A.; AND BUIVOL, V. N.: Oscillations of Shallow Spherical Shells. Theory of Shells and Plates, Proc. of the 4th All-Union Conf., Yerevan, Armenian, SSR, 1962, pp. 309-312. (In Russian.)
- WANG, C. C.: On the Radial Oscillations of a Spherical Thin Shell in the Finite Elasticity Theory. Quart. Appl. Math., vol. 23, no. 3, Oct. 1965, pp. 270-274.
- WANG, J. T. S.; STADLER, W.; AND LIN, C.: The Axisymmetric Response of Cylindrical and Hemispherical Shells to Time-Dependent Loading. NASA CR-572, Sept. 1966.
- WANG, J. T. S.; LIN, C. W.; AND STADLER, W.: Axisymmetric Dynamic Response of Spherical and Cylindrical Shells. American Astronaut. Soc. Southeastern Symposium on Missiles and Aerospace Vehicles Sciences (Huntsville, Alabama), Dec. 5-7, 1966.
- WEBSTER, J. J.: Free Vibrations of Shells of Revolution Using Ring Finite Elements. Int. J. Mech. Sci., vol. 9, no. 8, Aug. 1967, pp. 559-570.

- WILKINSON, J. P.: Natural Frequencies of Closed Spherical Shells. *J. Acoust. Soc. Amer.*, vol. 38, no. 2, Aug. 1965, pp. 367-368.
- WILKINSON, J. P.: Transient Response of Thin Elastic Shells. *J. Acoust. Soc. Amer.*, vol. 39, no. 5, part 1, May 1966, pp. 895-898.
- WILKINSON, J. P.: Natural Frequencies of Closed Spherical Sandwich Shells. *J. Acoust. Soc. Amer.*, vol. 40, no. 4, Oct. 1966, pp. 801-806.
- WILKINSON, J. P.: The Oscillations of a Sandwich Sphere. *J. Appl. Mech.*, vol. 36, no. 2, June 1969, pp. 307-309.
- WILKINSON, J. P.; AND KALNINS, A.: On Nonsymmetric Dynamic Problems of Elastic Spherical Shells. *J. Appl. Mech.*, vol. 32, no. 3, Sept. 1965, pp. 525-532.
- WILKINSON, J. P.; AND KALNINS, A.: Deformation of Open Spherical Shells Under Arbitrarily Located Concentrated Loads. *J. Appl. Mech.*, vol. 33, no. 2, June 1966, pp. 305-312.
- WITMER, E. A.; BALMER, H. A.; LEECH, J. W.; AND PIAN, T. H. H.: Large Dynamic Deformations of Beams, Rings, Plates, and Shells. *AIAA J.*, vol. 1, no. 8, Aug. 1963, pp. 1848-1857.
- YU, Y. Y.; AND KOPLIK, B.: Torsional Vibrations of Homogeneous and Sandwich Spherical Caps and Circular Plates. *J. Appl. Mech.*, vol. 34, no. 3, Sept. 1967, pp. 787-789.
- ZARGHAMEE, M. S.; AND ROBINSON, A. R.: Free and Forced Vibrations of Spherical Shells. Contract Nonr-1834(03) (AD 620 906), July 1965.
- ZARGHAMEE, M. S.; AND ROBINSON, A. R.: A Numerical Method for Analysis of Free Vibration of Spherical Shells. *AIAA J.*, vol. 5, no. 7, July 1967, pp. 1256-1261.
- ZIMIN, V. I.: On the Dynamic Calculation of Axisymmetrically Loaded Shells of Revolution. *Aviatsionnaia Tekhnika*, no. 3, 1960, pp. 34-42. (In Russian.)
- Int. *J. Solids Structures*, vol. 6, no. 3, Mar. 1970, pp. 333-351.
- HWANG, C.: Extensional Vibration of Axisymmetrical Shells. *AIAA J.*, vol. 3, no. 1, Jan. 1965, pp. 23-26.
- NEMERGUT, P. J.; AND BRAND, R. S.: Axisymmetric Vibrations of Prolate Spheroidal Shells. *J. Acoust. Soc. Amer.*, vol. 38, no. 2, Apr. 1965, pp. 262-265.
- PENZES, L. E.: Free Vibrations of Thin Oblate Spheroidal Shells. *J. Acoust. Soc. Amer.*, vol. 45, no. 2, Feb. 1969, pp. 500-505.
- PENZES, L. E.; AND BURGIN, G.: Free Vibrations of Thin Isotropic Oblate Spheroidal Shells. Rept. No. CD/C-BTD65-113, Convair Div., General Dynamics, July 1965.
- PENZES, L. E.; AND BURGIN, G.: Free Vibrations of Thin Isotropic Oblate-Spheroidal Shells. *J. Acoust. Soc. Amer.*, vol. 39, no. 1, Jan. 1966, pp. 8-13.
- RAND, R. H.: Torsional Vibrations of Elastic Prolate Spheroids. *J. Acoust. Soc. Amer.*, vol. 44, no. 3, Sept. 1968, pp. 749-751.
- RAND, R.; AND DiMAGGIO, F.: Vibrations of Fluid-Filled Spherical and Spheroidal Shells. *J. Acoust. Soc. Amer.*, vol. 42, no. 6, Dec. 1967, pp. 1278-1286.
- ROSS, E. W., JR.; AND MATTHEWS, W. T.: Frequencies and Mode Shapes for Axisymmetric Vibration of Shells. Tech. Rept. AMRA TR 66-04, U.S. Army Materials Research Agency, Feb. 1966.
- ROSS, E. W., JR.; AND MATTHEWS, W. T.: Frequencies and Mode Shapes for Axisymmetric Vibration of Shells. *J. Appl. Mech.*, vol. 34, no. 1, Mar. 1967, pp. 73-80.
- SHIRAIISHI, N.; AND DiMAGGIO, F. L.: Perturbation Solution for the Axisymmetric Vibrations of Prolate Spheroidal Shells. *J. Acoust. Soc. Amer.*, vol. 34, no. 11, Nov. 1962, pp. 1725-1731.
- SILBINGER, A.; AND DiMAGGIO, F. L.: Extensional Axisymmetric Second Class Vibrations of a Prolate Spheroidal Shell. Contract Nonr 266(67) Proj. 385-414, Tech. Rept. No. 3, Office of Naval Research, 1961.
- YEN, T.; AND DiMAGGIO, F.: Forced Vibrations of Submerged Spheroidal Shells. *J. Acoust. Soc. Amer.*, vol. 41, no. 3, Mar. 1967, pp. 618-626.

6.2 ELLIPSOIDAL (OR SPHEROIDAL) SHELLS

- DiMAGGIO, F.; AND RAND, R.: Axisymmetric Vibrations of Prolate Spheroidal Shells. *J. Acoust. Soc. Amer.*, vol. 40, no. 1, July 1966, pp. 179-186.
- DiMAGGIO, F. L.; AND SILBINGER, A.: Free Extensional Torsional Vibrations of a Prolate Spheroidal Shell. Contract Nonr 266(67), Proj. 385 414, Tech. Rept. No. 2, Office of Naval Research, Mar. 1960.
- DiMAGGIO, F. L.; AND SILBINGER, A.: Free Extensional Torsional Vibrations of a Prolate Spheroidal Shell. *J. Acoust. Soc. Amer.*, vol. 33, no. 1, Jan. 1961, pp. 56-58.
- GONTKEVICH, V. S.: Natural Vibrations of Shells in a Liquid. Published: Kiev, Naukova Dumka, 1964. (In Russian.)
- HAYEK, S.; AND DiMAGGIO, F. L.: Axisymmetric Vibrations of Submerged Spheroidal Shells. Contract Nonr 266(67) Proj. 385-414, Tech. Rept. No. 4, Office of Naval Research, Jan. 1965.
- HAYEK, S.; AND DiMAGGIO, F. L.: Complex Natural Frequencies of Vibrating Submerged Spheroidal Shells.

6.3 PARABOLOIDAL SHELLS

- BACON, M. D.; AND BERT, C. W.: Unsymmetric Free Vibrations of Orthotropic Sandwich Shells of Revolution. *AIAA J.*, vol. 5, no. 3, Mar. 1967, pp. 413-417.
- CRAIG, R. R., JR.: Analysis of Reinforced Concrete Thin Shells—A Preliminary Study. Tech. Note N-750 (AD 624 197), U.S. Naval Civil Engineering Lab., Oct. 1965.
- HOPPMANN, W. H., II; COHEN, M. I.; AND KUNUKKASERIL, V. X.: Elastic Vibrations of Paraboloidal Shells of Revolution. *J. Acoust. Soc. Amer.*, vol. 36, no. 2, Feb. 1964, pp. 349-353.
- JOHNSON, M. W.; AND REISSNER, E.: On Inextensional Deformations of Shallow Elastic Shells. *J. Math. Phys.*, vol. 34, no. 4, 1956, pp. 335-346.

- KALNINS, A.: Free Vibration of Rotationally Symmetric Shells. *J. Acoust. Soc. Amer.*, vol. 36, no. 7, July 1964, pp. 1355-1365.
- LIN, Y. K.; AND LEE, F. A.: Vibrations of Thin Paraboloidal Shells of Revolution. *J. Appl. Mech.*, vol. 27, no. 4, Dec. 1960, pp. 743-746.
- REISSNER, E.: On Transverse Vibrations of Thin, Shallow Elastic Shells. *Quart. Appl. Math.*, vol. 13, no. 2, 1955, pp. 169-176.
- WANG, J. T. S.; AND LIN, C. W.: On the Differential Equations of the Axisymmetric Vibration of Paraboloidal Shells of Revolution. NASA CR-932, Nov. 1967.

6.4 TOROIDAL SHELLS

- BUDIANSKY, B.; AND LIEPINS, A. A.: Vibration and Stability of Prestressed Shells: General Theory and the Membrane Torus. Presented at the Conference on Shell Theory and Analysis (Palo Alto, Calif.), 1963.
- FLÜGGE, W.; AND SOBEL, L. H.: Stability of Shells of Revolution: General Theory and Application to the Torus. NASA Rept. N65-27912, Stanford Univ., 1965.
- JORDAN, P. F.: Vibration and Buckling of Pressurized Torus Shells. Paper 66-445, AIAA 4th Aerospace Sciences Meeting (Los Angeles, Calif.), June 1966.
- JORDAN, P. F.: Vibration Test of a Pressurized Torus Shell. Paper 67-73, AIAA 5th Aerospace Sciences Meeting, New York, N.Y., Jan. 23-26, 1967. (Also NASA CR-884, Oct. 1967.)
- LIEPINS, A. A.: Free Vibrations of the Prestressed Toroidal Membrane. Rept. No. 474, Synatech Corp., May 22, 1964.
- LIEPINS, A. A.: Flexural Vibrations of the Prestressed Toroidal Shell. NASA CR-296, Sept. 1965.
- LIEPINS, A. A.: Free Vibrations of the Prestressed Toroidal Membrane. *AIAA J.*, vol. 3, no. 1, Oct. 1965, pp. 1924-1933.
- LIEPINS, A. A.: Vibration Study of a Pressurized Torus Shell. Part II—Development and Applications of Analysis. NASA CR-885, Oct. 1967.
- MCGILL, D. J.: Axisymmetric Free Oscillations of Thick Toroidal Shells. Ph.D. Dissertation, Univ. of Kansas, June 1966.
- MCGILL, D. J.; AND LENZEN, K. H.: Polar Axisymmetric Free Oscillations of Thick Hollowed Tori. *SIAM J. Appl. Math.*, vol. 15, no. 3, May 1967, pp. 678-692.
- MCGILL, D. J.; AND LENZEN, K. H.: Circumferential Axisymmetric Free Oscillations of Thick Hollowed Tori. *Int. J. Solids Structures*, vol. 3, no. 5, Sept. 1967, pp. 771-780.
- MEYEROVICH, I. I.: Approximate Method for the Determination of the Natural Oscillation Frequencies of Cylindrical, Conic and Toroidal Shells. NASA TT F-10,377, Nov. 1966.
- SANDERS, J. L., JR.; AND LIEPINS, A. A.: The Circular Torus Membrane Under Internal Pressure. Contract No. AF 49(638)-1096 (AD 607 990), Dynatech Corp., May 1962.
- SUMNER, I. E.: Preliminary Experimental Investigation of Frequencies and Forces Resulting From Liquid Slushing in Toroidal Tanks. NASA TN D-1709, June 1963.

6.5 OTHER SHELLS OF REVOLUTION

- ADELMAN, H. M.; CATHERINES, D. S.; AND WALTON, W. C., JR.: A Method for Computation of Vibration Modes and Frequencies of Orthotropic Thin Shells of Revolution Having General Meridional Curvature. NASA TN D-4972, Jan. 1969.
- ADELMAN, H. M.; CATHERINES, D. S.; AND WALTON, W. C., JR.: A Geometrically Exact Finite Element for Thin Shells of Revolution. AIAA 7th Aerospace Sciences Meeting (New York), Jan. 20-22, 1969.
- AKSEL'RAD, E. L.: Periodic Solutions of the Axisymmetric Problem in Shell Theory. *Inzhenernyi Zhurnal-Mekhanika Tverdogo Tela*, Mar.-Apr. 1966, pp. 77-83. (In Russian.)
- ALEKSANDROVICH, L. I.; AND LAMPER, R. E.: Natural Oscillations of an Elastic Axisymmetric Vessel of Arbitrary Contour. All-Union Conf. on the Theory of Shells and Plates, 6th, Baku, Azerbaidzhan SSR, Sept. 15-20, 1966, transactions, pp. 25-27. (In Russian.)
- AMBARTSUMYAN, S. A.; AND DURGAR'YAN, S. M.: Oscillation of an Orthotropic Tapered Shell in a Variable Temperature Field. *AN ARMSSR. Doklady*, vol. 38, no. 2, 1964, pp. 87-92. (In Russian.)
- BACON, M. D.; AND BERT, C. W.: Unsymmetric Free Vibrations of Orthotropic Sandwich Shells of Revolution. *AIAA J.*, vol. 5, no. 3, Mar. 1967, pp. 413-417.
- BIRGER, I. A.; PROKOPEV, V. I.; AND SHEKHTMAN, I. V.: Use of Matrix Integral Equations to Calculate Critical Loads and Natural Frequencies of Oscillation of Shells of Revolution. All-Union Conf. on the Theory of Shells and Plates, 6th, Baku, Azerbaidzhan SSR, Sept. 1966, transactions, pp. 155-160. (In Russian.)
- BOGNER, F. K.; AND ARCHER, R. R.: On the Orthogonality Condition of Axisymmetric Vibration Modes for Shells of Revolution. *J. Appl. Mech.*, vol. 32, no. 2, June 1965, pp. 447-448.
- BURMISTROV, E. F.: Nonlinear Transverse Vibrations of Orthotropic Shells of Revolution. *Inzh. Sb.*, vol. 26, 1958, pp. 5-20. (In Russian.)
- BUSHNELL, D.: Analysis of Buckling and Vibration of Ring-Stiffened, Segmented Shells of Revolution. *Int. J. Solids Structures*, vol. 6, no. 1, Jan. 1970, pp. 157-181.
- CHOW, H. Y.; AND POPOV, E. P.: Finite Element Solution of Axisymmetrical Dynamic Problems of Shells of Revolution. NASA CR-76100, Apr. 1966.
- COHEN, G. A.: Computer Analysis of Asymmetric Free Vibrations of Ring-Stiffened Orthotropic Shells of Revolution. *AIAA J.*, vol. 3, no. 12, Dec. 1965, pp. 2305-2312.
- COOPER, P. A.: Vibration and Buckling of Prestressed Shells of Revolution. NASA TN D-3831, 1967.

- COOPER, P. A.: Vibration of Stressed Shells of Double Curvature. Ph.D. Dissertation, Virginia Polytechnic Institute, June 1968.
- DUDDECK, H.: Bending Theory of Universal Shells of Revolution With Slightly Varying Shell Curvatures. *Ingenieur-Archiv*, vol. 33, no. 5, 1964, pp. 279-300. (In German.)
- GARNET, H.; GOLDBERG, M. A.; AND SALERNO, V. L.: Torsional Vibrations of Shells of Revolution. *J. Appl. Mech.*, vol. 28, no. 4, Dec. 1961, pp. 571-573.
- GONTKEVICH, V. S.: Natural Vibrations of Plates and Shells. A. P. Filipov, Ed., *Nauk Dumka* (Kiev), 1964. (Transl. by Lockheed Missiles and Space Co.)
- GRIGOLYUK, E. I.: Nonlinear Vibrations and Stability of Shallow Rods and Shells. *Izv. AN SSSR, OTN*, no. 3, 1955, pp. 33-68. (In Russian.)
- HU, W. C. L.: A Survey of the Literature on the Vibrations of Thin Shells. Southwest Research Inst., Tech. Rept. No. 1, Contract NASr-94(06), June 1964.
- KALNINS, A.: On Free and Forced Vibration of Rotationally Symmetric Layered Shells. *J. Appl. Mech.*, vol. 32, no. 4, Dec. 1965, pp. 941-943.
- KALNINS, A.: Analysis of Thin Elastic Shells With Attached Systems. AIAA 5th Aerospace Sciences Meeting (New York), Jan. 23-26, 1967.
- KLEIN, S.; AND SYLVESTER, R. J.: The Linear Elastic Dynamic Analysis of Shells of Revolution by the Matrix Displacement Method. AFFDL-TR-66-80, Aerospace Corp., Dec. 1965, pp. 299-328.
- LEISSA, A. W.: On the Nonlinear Strain-Curvature-Displacement Relationships for Thin Elastic Shells. *J. Aerospace Sci.*, vol. 29, Nov. 1962, pp. 1381-1382.
- PSHENICHNOV, G. I.: Small Free Vibrations of Elastic Shells of Revolution. *Inzhenernyi Zhurnal*, vol. 5, no. 4, 1965, pp. 685-690. (In Russian.)
- PSHENICHONOV, G. I.: Free and Forced Axisymmetrical Oscillations of Thin Elastic Shells of Revolution. All-Union Conf. on the Theory of Shells and Plates, 6th, Baku, Azerbaidzhan SSR, Sept. 1966, transactions, pp. 641-645. (In Russian.)
- RAPOPORT, L. D.; AND IASIN, E. M.: Determination of the Frequencies of the Natural Oscillations of Corrugated Circular Cylindrical Shells. *Prochnost' i Dinamika Aviatsionnykh Dvigateli*, no. 2, Moscow, Izdatel'stvo Mashinostroenie, 1965, pp. 129-147.
- RAYLEIGH, LORD: On Bells. *Phil. Mag. and J. Sci.*, Series 5, vol. 29, no. 176, Jan. 1890, pp. 1-17.
- ROSS, E. W., JR.: Asymptotic Analysis of the Axisymmetric Vibration of Shells. Tech. Rept. AMRA TR 65-08 (AD 616 604), U.S. Army Materials Research Agency, Apr. 1965.
- ROSS, E. W., JR.: Asymptotic Analysis of the Axisymmetric Vibration of Shells. *J. Appl. Mech.*, vol. 33, no. 1, Mar. 1966, pp. 85-92.
- ROSS, E. W., JR.: Transition Solutions for Axisymmetric Shell Vibrations. *J. Math. Phys.*, vol. 45, Dec. 1966, pp. 335-355.
- ROSS, E. W., JR.: Approximations in Nonsymmetric Shell Vibrations. Tech. Rept. AMRA TR 67-08 (AD 652 255), U.S. Army Material Research Agency, Apr. 1967.
- ROSS, E. W., JR.; AND MATTHEWS, W. T.: Frequencies and Mode Shapes for Axisymmetric Vibration of Shells. Tech. Rept. AMRA TR 66-04, U.S. Army Materials Research Agency, Feb. 1966.
- SHKLYARCHUK, F. N.: Variational Methods for Calculating Axisymmetrical Oscillations of Shells of Revolution Partially Filled With a Fluid. All-Union Conf. on the Theory of Shells and Plates, 6th, Baku, Azerbaidzhan SSR, Sept. 15-20, 1966, transactions, pp. 835-840. (In Russian.)
- SIMMONDS, J. G.: A Discussion of "On the Orthogonality Condition of Axisymmetric Vibration Modes for Shells of Revolution." *J. Appl. Mech.*, vol. 32, no. 4, Dec. 1965, p. 954.
- SUVERNEV, V. G.: Some Oscillation Problems of Three-Layer Shells. All-Union Conf. on the Theory of Shells and Plates, 6th, Baku, Azerbaidzhan SSR, Sept. 15-20, 1966, transactions, pp. 707-709. (In Russian.)
- TOVSTIK, P. E.: Integrals of Equations of the Axisymmetrical Oscillations of a Shell of Revolution. *Issledovaniia Po Uprugosti i Plastichnosti*, no. 4, 1965, pp. 107-116. (In Russian.)
- TOVSTIK, P. E.: Oscillation Frequency Spectrum of Shells of Revolution With a Great Number of Waves Along a Parallel. All-Union Conf. on the Theory of Shells and Plates, 6th, Baku, Azerbaidzhan SSR, Sept. 1966, transactions, pp. 746-752. (In Russian.)
- TOVSTIK, P. E.: Problem of Axisymmetrical Oscillations of a Shell of Revolution in the Case of a Double Reversal Point. *Leningradskii Universitet, Vestnik, Matematika, Mekhanika, Astronomiia*, vol. 22, Jan. 1967, pp. 118-124. (In Russian.)
- WEBSTER, J. J.: Free Vibrations of Shells of Revolution Using Ring Finite Elements. *Int. J. Mech. Sci.*, vol. 9, no. 8, Aug. 1967, pp. 559-570.

6.6 OTHERS

- CARTER, R. L.; ROBINSON, A. R.; AND SCHNOBRICH, W. C.: Free and Forced Vibrations of Hyperboloidal Shells of Revolution. Civil Engineering Studies, Structural Research Series No. 334, Univ. of Illinois, Feb. 1968.
- ANON.: Report of the Committee of Inquiry into Collapse of Cooling Towers at Ferrybridge Monday 1 Nov. 1965. Central Electricity Generating Board, London, England.
- DESILVA, C. N.; AND TERSTEEG, G. E.: Axisymmetric Vibrations of Thin Elastic Shells. *J. Acoust. Soc. Amer.*, vol. 36, no. 4, Apr. 1964, pp. 666-672.
- LISOWSKI, A.: Investigation of Shell Vibration and Stability by Means of Model Tests. *Rozprawy Inz.*, vol. 6, no. 1, 1958, pp. 25-91. (In Polish.)
- NEAL, B. G.: Natural Frequencies of Cooling Towers. *J. Strain Analysis*, vol. 2, no. 2, 1967, pp. 127-133.
- STRUTT, M. J. O.: Eigenschwingungen einer Kezelschale. *Annalen der Physik*. 5 Folge, Band 17, Heft 7, Aug. 1933, pp. 729-735.

Solution of the Three Dimensional Equations of Motion for Cylinders

A.1 EQUATIONS OF MOTION

The three dimensional equations of motion in terms of circular cylindrical coordinates are readily available in standard textbooks on the theory of elasticity (cf., ref. A.1, p. 306 and ref. A.2, p. 184). Neglecting couple stresses, they are given by

$$\left. \begin{aligned} \frac{\partial \sigma_x}{\partial x} + \frac{1}{r} \frac{\partial \tau_{x\theta}}{\partial \theta} + \frac{\partial \tau_{xr}}{\partial r} + \frac{\tau_{xr}}{r} &= \rho \frac{\partial^2 u}{\partial t^2} \\ \frac{\partial \tau_{x\theta}}{\partial x} + \frac{1}{r} \frac{\partial \sigma_\theta}{\partial \theta} + \frac{\partial \tau_{\theta r}}{\partial r} + \frac{2\tau_{\theta r}}{r} &= \rho \frac{\partial^2 v}{\partial t^2} \\ \frac{\partial \tau_{rx}}{\partial x} + \frac{1}{r} \frac{\partial \tau_{r\theta}}{\partial \theta} + \frac{\partial \sigma_r}{\partial r} + \frac{\sigma_r - \sigma_\theta}{r} &= \rho \frac{\partial^2 w}{\partial t^2} \end{aligned} \right\} \quad (\text{A.1})$$

where the stresses are defined as in figure A.1 and the displacements u , v , and w are in the x , θ , and r directions to be consistent with circular cylindrical shell coordinates, except that the shell coordinate z (see sec. 1.2) measured from the middle surface is now replaced by the radial coordinate r , measured from the axis of the cylinder (see fig. A.2). The strain displacement equations (1.35) in cylindrical coordinates are

$$\left. \begin{aligned} e_x &= \frac{\partial u}{\partial x}, \quad e_\theta = \frac{1}{r} \frac{\partial v}{\partial \theta} + \frac{w}{r}, \quad e_r = \frac{\partial w}{\partial r} \\ \gamma_{x\theta} &= \gamma_{\theta x} = \frac{\partial v}{\partial x} + \frac{1}{r} \frac{\partial u}{\partial \theta} \\ \gamma_{xr} &= \gamma_{rx} = \frac{\partial w}{\partial x} + \frac{\partial u}{\partial r} \\ \gamma_{\theta r} &= \gamma_{r\theta} = \frac{1}{r} \frac{\partial w}{\partial \theta} + \frac{\partial v}{\partial r} - \frac{v}{r} \end{aligned} \right\} \quad (\text{A.2})$$

Using the three dimensional form of Hooke's law for isotropic materials (eqs. (1.69), with α , β , and

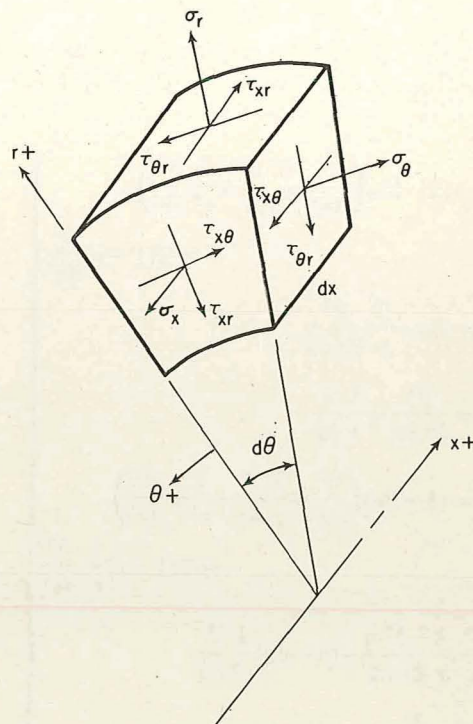


FIGURE A.1.—Positive stress convention in circular cylindrical coordinates.

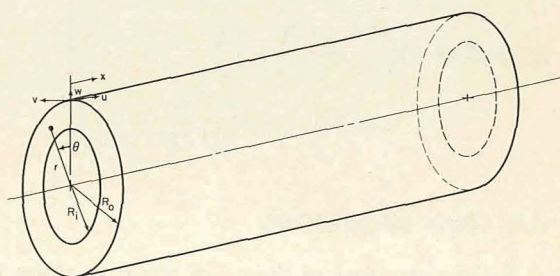


FIGURE A.2.—Circular cylinder and corresponding coordinates.

z replaced by x , θ , and r , respectively), and substituting equations (A.2) into equations (A.1) yield the equations of motion in terms of displacements (refs. A.3 and A.4):

$$\left. \begin{aligned} L_{11}u + L_{12}v + L_{13}w &= \delta^2 \frac{\partial^2 u}{\partial t^2} \\ L_{21}u + L_{22}v + L_{23}w &= \delta^2 \frac{\partial^2 v}{\partial t^2} \\ L_{31}u + L_{32}v + L_{33}w &= \delta^2 \frac{\partial^2 w}{\partial t^2} \end{aligned} \right\} \quad (\text{A.3})$$

where u , v , w are the displacements in the x , θ , r directions, respectively, $\delta^2 = 2(1+\nu)(1-2\nu)\rho/E$, and

$$\left. \begin{aligned} L_{11} &= (1-2\nu) \left(\frac{\partial^2}{\partial r^2} + \frac{1}{r} \frac{\partial}{\partial r} + \frac{1}{r^2} \frac{\partial^2}{\partial \theta^2} \right) \\ &\quad + 2(1-\nu) \frac{\partial^2}{\partial x^2} \\ L_{12} &= L_{21} = \frac{1}{r} \frac{\partial^2}{\partial \theta \partial x} \\ L_{13} &= \frac{\partial^2}{\partial r \partial x} + \frac{1}{r} \frac{\partial}{\partial x} \\ L_{22} &= (1-2\nu) \left(\frac{\partial^2}{\partial r^2} + \frac{1}{r} \frac{\partial}{\partial r} - \frac{1}{r^2} + \frac{\partial^2}{\partial x^2} \right) \\ &\quad + 2(1-\nu) \frac{1}{r^2} \frac{\partial^2}{\partial \theta^2} \\ L_{23} &= \frac{1}{r} \frac{\partial^2}{\partial r \partial \theta} + (3-4\nu) \frac{1}{r^2} \frac{\partial}{\partial \theta} \\ L_{31} &= \frac{\partial^2}{\partial r \partial x} \\ L_{32} &= \frac{1}{r} \frac{\partial^2}{\partial r \partial \theta} - (3-4\nu) \frac{1}{r^2} \frac{\partial}{\partial \theta} \\ L_{33} &= 2(1-\nu) \left(\frac{\partial^2}{\partial r^2} + \frac{1}{r} \frac{\partial}{\partial r} - \frac{1}{r^2} \right) \\ &\quad + (1-2\nu) \left(\frac{1}{r^2} \frac{\partial^2}{\partial \theta^2} + \frac{\partial^2}{\partial x^2} \right) \end{aligned} \right\} \quad (\text{A.4})$$

A.2 END CONDITIONS

Using the classical theory of shells solution for a circular cylindrical shell supported by shear diaphragms at both ends as a guide, and choosing

$$\left. \begin{aligned} u &= U(r, \theta) \cos \lambda x \cos \omega t \\ v &= V(r, \theta) \sin \lambda x \cos \omega t \\ w &= W(r, \theta) \sin \lambda x \cos \omega t \end{aligned} \right\} \quad (\text{A.5})$$

where $\lambda = m\pi/l$, the boundary conditions

$$\sigma_x = v = w = 0 \quad \text{at} \quad x = 0, l \quad (\text{A.6})$$

are found to be exactly satisfied.

A.3 DISPLACEMENT POTENTIAL FUNCTIONS

Mirsky (ref. A.5) suggested the use of displacement potentials Φ and Ψ in order to continue the solution of the equations of motion. The functions Φ and Ψ are related to $U(r, \theta)$, $V(r, \theta)$ and $W(r, \theta)$ by the following expressions

$$\left. \begin{aligned} U(r, \theta) &= C\Phi \\ V(r, \theta) &= \frac{1}{r} \frac{\partial \Phi}{\partial \theta} - \frac{\partial \Psi}{\partial r} \\ W(r, \theta) &= \frac{\partial \Phi}{\partial r} + \frac{1}{r} \frac{\partial \Psi}{\partial \theta} \end{aligned} \right\} \quad (\text{A.7})$$

where C is an arbitrary constant to be determined later in the analysis.

A.4 SOLUTION OF THE EQUATIONS OF MOTION

Substituting equations (A.5) and (A.7) into equations (A.3) one obtains

$$\lambda \nabla^2 \Phi + [(1-2\nu)\nabla^2 - 2(1-\nu)\lambda^2 + \delta^2\omega^2]C\Phi = 0 \quad (\text{A.8})$$

$$\begin{aligned} \frac{1}{r} \frac{\partial}{\partial \theta} [2(1-\nu)\nabla^2 - (1-2\nu)\lambda^2 + \delta^2\omega^2 - \lambda C] \Phi \\ - \frac{\partial}{\partial r} [(1-2\nu)\nabla^2 - (1-2\nu)\lambda^2 + \delta^2\omega^2] \Psi = 0 \end{aligned} \quad (\text{A.9})$$

$$\begin{aligned} \frac{\partial}{\partial r} [2(1-\nu)\nabla^2 - (1-2\nu)\lambda^2 + \delta^2\omega^2 - \lambda C] \Phi \\ + \frac{1}{r} \frac{\partial}{\partial \theta} [(1-2\nu)\nabla^2 \\ - (1-2\nu)\lambda^2 + \delta^2\omega^2] \Psi = 0 \end{aligned} \quad (\text{A.10})$$

where

$$\nabla^2 = \frac{\partial^2}{\partial r^2} + \frac{1}{r} \frac{\partial}{\partial r} + \frac{1}{r^2} \frac{\partial^2}{\partial \theta^2}$$

Uncoupling these equations yields

$$\nabla^2 \left[\nabla^2 - \lambda^2 + \frac{\delta^2 \omega^2}{2(1-\nu)} \right] \left[\nabla^2 - \lambda^2 + \frac{\delta^2 \omega^2}{(1-2\nu)} \right] \Phi = 0 \quad (\text{A.11})$$

$$\nabla^2 \left[\nabla^2 - \lambda^2 + \frac{\delta^2 \omega^2}{(1-2\nu)} \right] \Psi = 0 \quad (\text{A.12})$$

$$\lambda \left[-\lambda^2 + \frac{\delta^2 \omega^2}{2(1-\nu)} \right] C\Phi + \nabla^2 \left\{ (1-2\nu) \left[\nabla^2 - \frac{(1-2\nu)}{2(1-\nu)} \lambda^2 + \delta^2 \omega^2 \right] \right\} \Phi = 0 \quad (\text{A.13})$$

At this stage the shell will be assumed to be closed; thus

$$\Phi(r, \theta) = f(r) \cos n\theta \quad (\text{A.14})$$

$$\Psi(r, \theta) = g(r) \sin n\theta \quad (\text{A.15})$$

Substitution of equations (A.14) and (A.15) into equations (A.11) and (A.12), one obtains the differential equations governing $f(r)$ and $g(r)$:

$$\bar{\nabla}^2 \left[\bar{\nabla}^2 - \lambda^2 + \frac{\delta^2 \omega^2}{2(1-\nu)} \right] \left[\bar{\nabla}^2 - \lambda^2 + \frac{\delta^2 \omega^2}{(1-2\nu)} \right] f(r) = 0 \quad (\text{A.16})$$

$$\bar{\nabla}^2 \left[\bar{\nabla}^2 - \lambda^2 + \frac{\delta^2 \omega^2}{(1-2\nu)} \right] g(r) = 0 \quad (\text{A.17})$$

where $\bar{\nabla}^2 = (\partial^2/\partial r^2 + \partial/r \partial r - n^2/r^2)$. The solution of equation (A.16)

$$f(r) = f_1(r) + f_2(r) + f_3(r) \quad (\text{A.18})$$

where $f_1(r)$, $f_2(r)$, $f_3(r)$ are solutions of the following differential equations

$$(\bar{\nabla}^2 + p_1^2) f_1(r) = 0 \quad (\text{A.19})$$

$$(\bar{\nabla}^2 + p_2^2) f_2(r) = 0 \quad (\text{A.20})$$

$$\bar{\nabla}^2 f_3(r) = 0 \quad (\text{A.21})$$

and

$$p_1^2 = -\lambda^2 + \delta^2 \omega^2 / 2(1-\nu)$$

$$p_2^2 = -\lambda^2 + \delta^2 \omega^2 / (1-2\nu)$$

are always real. The solution of equation (A.17) is

$$g(r) = g_1(r) + g_2(r) \quad (\text{A.22})$$

where $g_1(r)$ and $g_2(r)$ are solutions of

$$(\bar{\nabla}^2 + p_2^2) g_1(r) = 0 \quad (\text{A.23})$$

$$\bar{\nabla}^2 g_2(r) = 0 \quad (\text{A.24})$$

Upon substitution of $f_3(r) \cos n\theta$ and $g_2(r) \sin n\theta$ for $\Phi(r, \theta)$ and $\Psi(r, \theta)$, respectively, in equations (A.9), (A.10), and (A.13) one finds that

$$u = v = w = 0$$

Thus one can discard $f_3(r)$ in equation (A.18) and $g_2(r)$ in equation (A.22), since these functions do not contribute to the displacements. Hence, equations (A.18) and (A.22) becomes

$$f(r) = f_1(r) + f_2(r) \quad (\text{A.25})$$

$$g(r) = g_1(r) \quad (\text{A.26})$$

Equations (A.19), (A.20), and (A.23) are standard forms of Bessel's equation, which can be written as

$$\left(\frac{\partial^2}{\partial r^2} + \frac{1}{r} \frac{\partial}{\partial r} + p^2 - \frac{n^2}{r^2} \right) V(r) = 0 \quad (\text{A.27})$$

Solution of equation (A.27) depends on the sign of p^2 . If one adopts the notation of Gazis (ref. A.6), the general solution may be written as

$$V(r) = A_n Z_n(qr) + B_n \bar{Z}_n(qr) \quad (\text{A.28})$$

where A_n and B_n are constants of integration, $q^2 = |p^2|$

$$Z_n(qr) = \begin{cases} J_n(qr) & \text{if } p^2 > 0 \\ I_n(qr) & \text{if } p^2 < 0 \end{cases} \quad (\text{A.29})$$

$$\bar{Z}_n(qr) = \begin{cases} Y_n(qr) & \text{if } p^2 > 0 \\ K_n(qr) & \text{if } p^2 < 0 \end{cases} \quad (\text{A.30})$$

J_n and Y_n are the Bessel functions of the first and second kinds, respectively, and I_n and K_n are the modified Bessel functions of the first and second kinds, respectively. Using equations (A.29) and (A.30), one obtains the following expressions for Φ , Ψ and $C\Phi$

$$\Phi = [A_{mn} Z_n(q_1 r) + B_{mn} \bar{Z}_n(q_1 r) + C_{mn} Z_n(q_2 r) + D_{mn} \bar{Z}_n(q_2 r)] \cos n\theta \quad (\text{A.31})$$

$$\Psi = [E_{mn} Z_n(q_1 r) + F_{mn} \bar{Z}_n(q_2 r)] \sin n\theta \quad (\text{A.32})$$

$$C\Phi = \left\{ \lambda A_{mn} Z_n(q_1 r) + \lambda B_{mn} \bar{Z}_n(q_1 r) - \frac{p_2^2}{\lambda} [C_{mn} Z_n(q_2 r) + D_{mn} \bar{Z}_n(q_2 r)] \right\} \cos n\theta \quad (\text{A.33})$$

where A_{mn}, \dots, F_{mn} are undetermined coefficients, and where $q_1^2 = |p_1^2|$ and $q_2^2 = |p_2^2|$.

The proper selection of Z_n and \bar{Z}_n for different intervals of the frequency to be used in equations (A.31), (A.32), and (A.33) appear in table A.1 (ref. A.7).

Substituting equations (A.31), (A.32), and (A.33) into equations (A.5) and (A.7), one obtains for the displacements

$$u = \left[\lambda A_{mn} Z_n(q_1 r) + \lambda B_{mn} \bar{Z}_n(q_1 r) - \frac{p_2^2}{\lambda} C_{mn} Z_n(q_2 r) - \frac{p_2^2}{\lambda} D_{mn} \bar{Z}_n(q_2 r) \right] \cos \lambda x \cos n\theta \cos \omega t \quad (\text{A.34})$$

$$v = - \left[\frac{n}{r} A_{mn} Z_n(q_1 r) + \frac{n}{r} B_{mn} \bar{Z}_n(q_1 r) + \frac{n}{r} C_{mn} Z_n(q_2 r) + \frac{n}{r} D_{mn} \bar{Z}_n(q_2 r) + E_{mn} \frac{dZ_n(q_2 r)}{dr} + F_{mn} \frac{d\bar{Z}_n(q_2 r)}{dr} \right] \sin \lambda x \sin n\theta \cos \omega t \quad (\text{A.35})$$

$$w = \left[A_{mn} \frac{dZ_n(q_1 r)}{dr} + B_{mn} \frac{d\bar{Z}_n(q_1 r)}{dr} + C_{mn} \frac{dZ_n(q_2 r)}{dr} + D_{mn} \frac{d\bar{Z}_n(q_2 r)}{dr} + \frac{n}{r} E_{mn} Z_n(q_2 r) + \frac{n}{r} F_{mn} \bar{Z}_n(q_2 r) \right] \sin \lambda x \cos n\theta \cos \omega t \quad (\text{A.36})$$

A.5 EXPRESSIONS FOR STRESSES

The stresses are expressed in terms of the functions $Z_n(q_1 r)$, $\bar{Z}_n(q_1 r)$, $Z_n(q_2 r)$, and $\bar{Z}_n(q_2 r)$ by substitution of equations (A.34), (A.35), and (A.36) into the displacement-strain and stress-strain relationships, equations (A.2) and (1.69). The stresses are

$$\begin{aligned} \sigma_r = \frac{E}{(1+\nu)r^2} & \left\{ \left[\frac{1}{2} [2n(n-1) + (\lambda^2 - p_2^2)r^2] Z_n(q_1 r) + \zeta q_1 r Z_{n+1}(q_1 r) \right] A_{mn} + \left[\frac{1}{2} [2n(n-1) \right. \right. \\ & + (\lambda^2 - p_2^2)r^2 \bar{Z}_n(q_1 r)] + q_1 r \bar{Z}_{n+1}(q_1 r) \left. \right] B_{mn} + \{ [n(n-1) - p_2^2 r^2] Z_n(q_2 r) + \zeta q_2 r Z_{n+1}(q_2 r) \} C_{mn} \\ & + \{ [n(n-1) - p_2^2 r^2] \bar{Z}_n(q_2 r) + q_2 r \bar{Z}_{n+1}(q_2 r) \} D_{mn} + [n(n-1) Z_n(q_2 r) - \zeta n q_2 r Z_{n+1}(q_2 r)] E_{mn} \\ & \left. + [n(n-1) \bar{Z}_n(q_2 r) - n q_2 r \bar{Z}_{n+1}(q_2 r)] F_{mn} \right\} \sin \lambda x \cos n\theta \cos \omega t \quad (\text{A.37}) \end{aligned}$$

$$\begin{aligned} \tau_{r\theta} = \frac{E}{(1+\nu)r^2} & \left\{ [-n(n-1) Z_n(q_1 r) + \zeta n q_1 r Z_{n+1}(q_1 r)] A_{mn} + [-n(n-1) \bar{Z}_n(q_1 r) + n q_1 r \bar{Z}_{n+1}(q_1 r)] B_{mn} \right. \\ & + [-n(n-1) Z_n(q_2 r) + \zeta n q_2 r Z_{n+1}(q_2 r)] C_{mn} + [-n(n-1) \bar{Z}_n(q_2 r) + n q_2 r \bar{Z}_{n+1}(q_2 r)] D_{mn} \\ & + \left[- \left(n^2 - n - \frac{p_2^2 r^2}{2} \right) Z_n(q_2 r) - \zeta q_2 r Z_{n+1}(q_2 r) \right] E_{mn} + \left[- \left(n^2 - n - \frac{p_2^2 r^2}{2} \right) \bar{Z}_n(q_2 r) \right. \\ & \left. \left. - q_2 r \bar{Z}_{n+1}(q_2 r) \right] F_{mn} \right\} \sin \lambda x \sin n\theta \cos \omega t \quad (\text{A.38}) \end{aligned}$$

$$\begin{aligned} \tau_{rz} = \frac{E}{(1+\nu)r^2} & \left\{ \lambda r [n Z_n(q_1 r) - \zeta q_1 r Z_{n+1}(q_1 r)] A_{mn} + \lambda r [n \bar{Z}_n(q_1 r) - q_1 r \bar{Z}_{n+1}(q_1 r)] B_{mn} \right. \\ & + \frac{r}{2\lambda} (\lambda^2 - p_2^2) [n Z_n(q_2 r) - \zeta q_2 r Z_{n+1}(q_2 r)] C_{mn} + \frac{r}{2\lambda} (\lambda^2 - p_2^2) [n \bar{Z}_n(q_2 r) - q_2 r \bar{Z}_{n+1}(q_2 r)] D_{mn} \\ & \left. + \frac{\lambda r}{2} n Z_n(q_2 r) E_{mn} + \frac{\lambda r}{2} n \bar{Z}_n(q_2 r) F_{mn} \right\} \cos \lambda x \cos n\theta \cos \omega t \quad (\text{A.39}) \end{aligned}$$

TABLE A.1.—*Bessel Functions To Be Used With Frequency Intervals*

Interval	Function			
	$Z_n(q_1 r)$	$\bar{Z}_n(q_1 r)$	$Z_n(q_2 r)$	$\bar{Z}_n(q_2 r)$
$\omega > a$	$J_n(q_1 r)$	$Y_n(q_1 r)$	$J_n(q_2 r)$	$Y_n(q_2 r)$
$a > \omega > b$	$I_n(q_1 r)$	$K_n(q_1 r)$	$J_n(q_2 r)$	$Y_n(q_2 r)$
$\omega < b$	$I_n(q_1 r)$	$K_n(q_1 r)$	$I_n(q_2 r)$	$K_n(q_2 r)$

$$a = \lambda \{ E / [\rho h (1 + \nu) (1 - 2\nu)] \}^{1/2}$$

$$b = \lambda \{ E / [2\rho h (1 + \nu)] \}^{1/2}$$

$$\sigma_x = -\frac{E}{(1+\nu)r^2} \left\{ \left[\frac{\nu}{(1-2\nu)} p_1^2 r^2 + \frac{(1-\nu)}{(1-2\nu)} \lambda^2 r^2 \right] Z_n(q_1 r) A_{mn} + \left[\frac{\nu}{(1-2\nu)} p_1^2 r^2 + \frac{(1-\nu)}{(1-2\nu)} \lambda^2 r^2 \right] \bar{Z}_n(q_1 r) B_{mn} - p_2^2 r^2 C_{mn} - p_2^2 r^2 D_{mn} \right\} \sin \lambda x \cos n\theta \cos \omega t \quad (\text{A.40})$$

$$\tau_{x\theta} = -\frac{E}{(1+\nu)r^2} \left[n\lambda r Z_n(q_1 r) A_{mn} + n\lambda r \bar{Z}_n(q_1 r) B_{mn} + \frac{1}{2} \left(-\frac{np_2^2 r}{\lambda} + n\lambda r \right) Z_n(q_2 r) C_{mn} + \frac{1}{2} \left(-\frac{np_2^2 r}{\lambda} + n\lambda r \right) \bar{Z}_n(q_2 r) D_{mn} + \frac{1}{2} (n\lambda r Z_n(q_2 r) - \zeta q_2 \lambda r^2 Z_{n+1}(q_2 r)) E_{mn} + \frac{1}{2} (n\lambda r \bar{Z}_n(q_2 r) - \zeta q_2 \lambda r^2 \bar{Z}_{n+1}(q_2 r)) F_{mn} \right] \cos \lambda x \sin n\theta \cos \omega t \quad (\text{A.41})$$

$$\sigma_\theta = \frac{E}{(1+\nu)r^2} \left\{ \left[\left[-n(n-1) - \frac{\nu}{(1-2\nu)} (\lambda^2 r^2 + p_1^2 r^2) \right] Z_n(q_1 r) - \zeta q_1 r Z_{n+1}(q_1 r) \right] A_{mn} + \left[\left[-n(n-1) - \frac{\nu}{(1-2\nu)} (\lambda^2 r^2 + p_1^2 r^2) \right] \bar{Z}_n(q_1 r) - q_1 r \bar{Z}_{n+1}(q_1 r) \right] B_{mn} + [-n(n-1) Z_n(q_2 r) - \zeta q_2 r Z_{n+1}(q_2 r)] C_{mn} + [-n(n-1) \bar{Z}_n(q_2 r) - q_2 r \bar{Z}_{n+1}(q_2 r)] D_{mn} + [-n(n-1) Z_n(q_2 r) + \zeta n q_2 r Z_{n+1}(q_2 r)] E_{mn} + [-n(n-1) \bar{Z}_n(q_2 r) + n q_2 r Z_{n+1}(q_2 r)] F_{mn} \right\} \sin \lambda x \cos n\theta \cos \omega t \quad (\text{A.42})$$

In equations (A.37) through (A.42) the parameter ζ was introduced to account for the differences in the differentiation formulas between the different kinds of Bessel functions. The value of ζ is 1 when J and Y functions are used and -1 when I and K functions are used.

A.6 FREQUENCY EQUATION

For free vibration, the stresses must vanish on the cylindrical boundaries $r = R_i, R_0$ (see fig. A.2). That is

$$\sigma_r = \tau_{r\theta} = \tau_{\theta x} = 0 \quad \text{at} \quad r = R_i, R_0 \quad (\text{A.43})$$

Substituting equations (A.37), (A.38), and (A.39) into equations (A.43) yields six homogeneous equations in the unknown coefficients, A_{mn}, \dots, F_{mn} . For a nontrivial solution, the determinant of the coefficient matrix is set equal to zero, yielding (ref. A.8)

$$|a_{ij}| = 0 \quad (i, j = 1, \dots, 6) \quad (\text{A.44})$$

where

$$a_{11} = \frac{1}{2} [2n(n-1) + (\lambda^2 - p_2^2) R_0^2] Z_n(q_1 R_0) + \zeta q_1 R_0 Z_{n+1}(q_1 R_0)$$

$$a_{12} = \frac{1}{2} [2n(n-1) + (\lambda^2 - p_2^2) R_0^2] \bar{Z}_n(q_1 R_0) + q_1 R_0 \bar{Z}_{n+1}(q_1 R_0)$$

$$a_{13} = [n(n-1) - p_2^2 R_0^2] Z_n(q_2 R_0) + \zeta q_2 R_0 Z_{n+1}(q_2 R_0)$$

$$a_{14} = [n(n-1) - p_2^2 R_0^2] \bar{Z}_n(q_2 R_0) + q_2 R_0 \bar{Z}_{n+1}(q_2 R_0)$$

$$a_{15} = n(n-1) Z_n(q_2 R_0) - \zeta n q_2 R_0 Z_{n+1}(q_2 R_0)$$

$$a_{16} = n(n-1) \bar{Z}_n(q_2 R_0) - n q_2 R_0 \bar{Z}_{n+1}(q_2 R_0)$$

$$a_{21} = -n(n-1) Z_n(q_1 R_0) + \zeta n q_1 R_0 Z_{n+1}(q_1 R_0)$$

$$a_{22} = -n(n-1) \bar{Z}_n(q_1 R_0) + n q_1 R_0 \bar{Z}_{n+1}(q_1 R_0)$$

$$a_{23} = -n(n-1) Z_n(q_2 R_0) + \zeta n q_2 R_0 Z_{n+1}(q_2 R_0)$$

$$a_{24} = -n(n-1) \bar{Z}_n(q_2 R_0) + n q_2 R_0 \bar{Z}_{n+1}(q_2 R_0)$$

$$a_{25} = -\left(n^2 - n - \frac{p_2^2 R_0^2}{2} \right) Z_n(q_2 R_0) - \zeta q_2 R_0 Z_{n+1}(q_2 R_0)$$

$$a_{26} = -\left(n^2 - n - \frac{p_2^2 R_0^2}{2} \right) \bar{Z}_n(q_2 R_0) - q_2 R_0 \bar{Z}_{n+1}(q_2 R_0)$$

$$a_{31} = \lambda R_0 [n Z_n(q_1 R_0) - \zeta q_1 R_0 Z_{n+1}(q_1 R_0)]$$

$$a_{32} = \lambda R_0 [n \bar{Z}_n(q_1 R_0) - q_1 R_0 \bar{Z}_{n+1}(q_1 R_0)]$$

$$a_{33} = \frac{R_0}{2\lambda} (\lambda^2 - p_2^2) [n Z_n(q_2 R_0) - \zeta q_2 R_0 Z_{n+1}(q_2 R_0)]$$

$$a_{34} = \frac{R_0}{2\lambda} (\lambda^2 - p_2^2) [n \bar{Z}_n(q_2 R_0) - q_2 R_0 \bar{Z}_{n+1}(q_2 R_0)]$$

$$a_{35} = \frac{\lambda R_0}{2} n Z_n(q_2 R_0)$$

$$a_{36} = \frac{\lambda R_0}{2} n \bar{Z}_n(q_2 R_0)$$

The remaining three rows of the determinant are obtained from the first three by substituting R_i for R_0 . The free vibration frequencies ω are the roots of equation (A.44).

Other investigations which are useful in studying the three-dimensional vibrations of circular cylinders include reference A.9.

REFERENCES

- A.1. TIMOSHENKO, S.; AND GOODIER, J. N.: *Theory of Elasticity*. Second ed., McGraw-Hill Book Co., Inc., 1951.
- A.2. SOKOLNIKOFF, I. S.: *Mathematical Theory of Elasticity*. Second ed., McGraw-Hill Book Co., Inc., 1956.
- A.3. FLÜGGE, W.; AND KELKAR, V. S.: The Problem of an Elastic Circular Cylinder. *Int. J. Solids Struct.*, vol. 4, no. 4, Apr. 1968, pp. 397-420.
- A.4. GREENSPON, J. E.: *Vibrations of Thick Shells in Vacuum and in an Acoustic Medium, Part I: Vibrations of Thick Shells in Vacuum*. Tech. Rept. No. 1, Proj. No. NR 385-412, Contract No. Nonr-2733(00), Office of Naval Research, Feb. 1959.
- A.5. MIRSKY, I.: *Wave Propagation in Transversely Isotropic Circular Cylinders. Part I—Theory*. *J. Acoust. Soc. Amer.*, vol. 37, no. 6, June 1965, pp. 1016-1021.
- A.6. GAZIS, D. C.: *Three-Dimensional Investigation of the Propagation of Waves in Hollow Circular Cylinders. Part I—Analytical Foundation*. *J. Acoust. Soc. Amer.*, vol. 31, no. 5, May 1959, pp. 568-573.
- A.7. ARMENAKAS, A. E.; GAZIS, D. G.; AND HERRMANN, G.: *Free Vibrations of Circular Cylindrical Shells*. Pergamon Press (New York), 1969.
- A.8. KADI, A. S.: *A Study and Comparison of the Equations of Thin Shell Theories*. Ph.D. Dissertation, The Ohio State Univ., 1970.
- A.9. MIRSKY, I.: *Three-Dimensional and Shell-Theory Analysis for Axisymmetric Vibrations of Orthotropic Shells*. *J. Acoust. Soc. Amer.*, vol. 39, no. 3, March 1966, pp. 549-555. (Also Dept. of Army Proj. No. 20010501B700, U.S. Army Research Office—Durham Proj. No. DA-31-124-ARO-D-250 (AD 459 477).)

Author Index

- Abdulla, K. M., 113, 369
 Abramson, H. N., 48, 225, 291
 Adelman, H. M., 47, 87, 88, 112, 199, 369, 382, 411
 Advani, S. H., 404
 Agamirov, V. L., 47, 248
 Agenosov, L. G., 248, 345, 359, 369, 392
 Ahmed, N., 359, 388
 Aksel'rad, E. L., 411
 Aldoshina, I. A., 387
 Aleksandrovich, L. I., 411
 Allwood, R. J., 121, 151
 Al-Najafi, A. M. J., 297
 Alspaugh, D. W., 390
 Ambartsumyan, S. A., 299, 411
 Anderson, G. L., 404
 Anisimov, A. M., 291, 404
 Archer, R. R., 404, 411
 Armenakas, A. E., 35, 47, 48, 67, 81, 100, 232, 238, 243, 245, 253, 257, 258, 294, 416
 Arnold, R. N., 35, 48, 67, 73, 82, 87, 88, 95, 99, 108, 125, 134, 147, 264
 Aron, H., 2
 Asher, G. W., 291
 Austin, A. L., 404
 Avery, J. P., 404
 Azar, J. J., 396

 Babich, D. V., 291, 396
 Bacon, M. D., 359, 388, 394, 396, 410, 411
 Bagdasarian, G. E., 291, 389, 396, 404
 Baker, E. H., 299, 301, 307
 Baker, J. L., 307
 Baker, W. E., 404
 Balabukh, L. I., 19, 404
 Balakirev, Iu. G., 404
 Ball, R. E., 299, 301
 Ballentine, J. R., 170
 Balmer, H. A., 410
 Baron, M. L., 69, 146, 243, 290, 291
 Barsuk, R. P., 291
 Basset, A. B., 2
 Beal, T. R., 291
 Beam, R. M., 291
 Bell, F. L., 88
 Bergassoli, A., 404
 Berglund, J. W., 87
 Bernstein, M., 187, 198, 211
 Berry, J. G., 1, 2, 8, 15, 35, 291
 Bert, C. W., 307, 359, 388, 394, 396, 404, 410, 411
 Bhuta, P. G., 291, 407
 Bieniek, M. P., 299
 Bienzeno, C. B., 33, 40, 44
 Bijlaard, P. P., 35
 Birger, I. A., 411
 Bleich, H. H., 47, 48, 69, 146, 149, 209, 243, 290, 291
 Bluhm, J. I., 359
 Blum, R. E., 119
 Bogdanoff, J. L., 359, 390
 Bogner, F. K., 411
 Bolotin, V. V., 62, 88, 166, 404
 Bonnet, O., 5
 Bordoni, P. G., 343
 Boyd, D. E., 182, 321, 328
 Bozich, W. F., 48, 63, 81, 235, 248
 Brand, R. S., 410
 Brebbia, C., 182
 Breslavskii, V. E., 48, 265, 291, 359
 Britvec, S. J., 147
 Brogan, F., 88, 148, 151
 Brogan, W. L., 241
 Brusilovski, A. D., 48, 87
 Bryan, G. H., 248
 Bublik, B. N., 47
 Bubnov, I. G., 88
 Buckens, F., 289
 Budiansky, B., 1, 411
 Buivol, V. N., 409
 Bukharinov, G. N., 150
 Burgin, G. H., 408, 410
 Burmistrov, E. F., 411
 Bushnell, D., 289, 307, 411
 Butler, D. J., 290
 Byrne, R., 1, 8, 16, 35

 Canac, F., 404
 Carter, R. L., 412
 Catherines, D. S., 47, 87, 88, 112, 199, 369, 382, 411
 Chakravorthy, J. G., 404
 Chen, R., 162, 175
 Chien, W. Z., 2
 Chou, P. C., 294, 394
 Chow, H. Y., 404, 411
 Chree, C., 404
 Chu, H. N., 219, 220, 222, 224, 228, 299, 307
 Chu, W. H., 47, 48, 291
 Chulkov, P. P., 299
 Cinelli, G., 404
 Clary, R. R., 87, 88, 95, 115, 134, 209, 211, 217, 368, 380
 Clausen, W. E., 88, 218
 Coale, C. W., 291, 404
 Cohen, G. A., 359, 383, 404, 411
 Cohen, J. W., 2, 13

- Cohen, M. I., 410
 Connor, J., Jr., 404
 Cooper, P. A., 47, 48, 115, 265, 411
 Cooper, R. M., 293, 358
 Cottis, M. G., 261
 Coupury, G., 35, 47, 48, 131, 241, 261
 Craig, R. R., Jr., 291, 410
 Cranch, E. T., 44, 48, 83, 87, 88, 92, 145, 151, 272
 Crouzet-Pascal, J., 298, 299
 Culkowski, P. M., 404, 408
 Cummings, B. E., 220, 221, 227, 230, 231

 Darevski, V. M., 151
 Das, Y. C., 191
 Datta, S. K., 409
 Davids, N., 404
 Dawson, D. E., 404
 Deb Nath, J. M., 183, 265
 DeSilva, C. N., 87, 134, 344, 345, 405, 412
 Diet, W. K., 209
 DiGiacomo, A. F., 358
 DiGiovanni, P. R., 48, 186, 188, 194, 252
 DiMaggio, F. L., 69, 146, 408, 409, 410
 Dong, S. B., 195, 299, 307
 Dmitriev, Yu. V., 307
 Dokuchaev, L. V., 393
 Donnell, L. H., 1, 11, 15, 35
 Dowell, E. H., 222
 Dreher, J. F., 333, 334, 342, 359
 Duddeck, H., 412
 Dugundji, J., 48, 88, 117, 121, 186, 188, 190, 194, 211, 252
 Dungar, R., 174
 Durgar'yan, S. M., 411
 Dym, C. L., 265, 408

 Eason, G., 405
 Egle, D. M., 47, 48, 207, 307, 396, 404
 Elsbernd, G. F., 95
 Engin, A. E., 405
 Epstein, P. S., 2, 35, 134
 Eulitz, W. R., 291
 Evensen, D. A., 219, 220, 221, 222, 223, 405
 Eversman, W., 405

 Fahlbusch, G., 265, 408
 Federhofer, K., 48, 88, 219, 241, 333, 335, 337, 372, 373, 405
 Feit, D., 405, 406
 Felgar, R., 95
 Fersht-Scher, R., 387
 Filippov, A. P., 47, 82, 146
 Finkel'shteyn, R. M., 47, 48, 86, 87, 100, 115, 145, 239, 261, 262
 Flügge, W., 1, 8, 16, 35, 40, 44, 48, 83, 85, 233, 333, 411, 414
 Fontenot, L. L., 291
 Forsberg, K., 47, 48, 62, 72, 74, 75, 83, 87, 88, 89, 90, 98, 106, 115, 134, 138, 140, 148, 149, 151
 Foxwell, J. H., 290
 Franken, P. A., 48

 Franklin, R. E., 290
 Freese, C. E., 121
 Freudenthal, A. M., 299
 Fulton, R. E., 119, 220, 223, 405
 Fung, Y. C., 48, 49, 151, 234, 244, 254, 256, 261

 Galerkin, B. G., 35, 88, 183
 Galimov, K. Z., 220
 Galletly, G. D., 48, 113, 208, 369
 Garnet, H., 47, 298, 299, 344, 359, 393, 412
 Gavrillov, Yu. V., 88
 Gazis, D. C., 415, 416
 Geers, T. L., 48, 74, 198, 208
 Gelman, A. P., 369, 372, 383
 Gere, J. M., 234
 Ghosh, P. R., 405
 Glaser, R. F., 291
 Gnuni, V. Ts., 291, 389, 396, 404
 Godzevich, V. G., 355, 359, 387
 Goldberg, J. E., 359, 390
 Goldberg, M. A., 47, 344, 412
 Goldenveizer, A. L., 1, 2, 4, 8, 17, 19, 35, 405
 Gontkevich, V. S., 82, 85, 87, 88, 95, 99, 117, 121, 129, 162, 165, 210, 218, 278, 290, 329, 332, 339, 344, 359, 382, 385, 389, 405, 410, 412
 Gonzales, R., 291
 Goodier, J. N., 38, 48, 151, 413
 Goree, J. G., 291
 Gormley, J. F., 48, 203, 373, 377, 405
 Gottenberg, W. G., 134, 259
 Grammel, R., 33, 40, 44
 Greenspon, J. E., 48, 209, 248, 265, 290, 298, 299, 414
 Grenwelge, O. E., Jr., 389
 Grigolyuk, E. I., 162, 231, 299, 355, 389, 393, 405, 412
 Grigorev, E. T., 405
 Grinsted, B., 134
 Grossman, P. L., 405
 Grützmacher, M., 48, 81, 124, 125, 131
 Guist, L. R., 291
 Gupta, A. P., 405
 Gutin, N. L., 396

 Habip, L. M., 307
 Haft, E. E., 87
 Hahne, H. V., 290
 Hart, F. D., 48, 62, 341, 355, 382
 Hartung, R. F., 345, 359, 363, 382
 Hayek, S., 405, 410
 Haywood, J. H., 2
 Heckl, M., 6, 48, 62
 Heinrichsbauer, F. J., 205, 209
 Heki, K., 121, 163
 Heng, G. Z., 405
 Herr, R. W., 166, 174, 261, 263, 291
 Herrmann, G., 35, 47, 48, 100, 232, 239, 245, 247, 248, 257, 259, 289, 290, 293, 294, 296, 299, 301, 304, 307, 322, 352, 416
 Hess, R. W., 166, 174
 Higgs, J., 121
 Hildebrand, F. B., 2, 7, 294

- Holmes, W. T., 387
 Hopper, A. T., 88, 218
 Hoppmann, W. H., II., 47, 48, 197, 209, 405, 410
 Hornung, E., 265, 408
 Houghton, D. S., 1, 35
 Hsu, T. M., 299
 Hu, W. C. L., 2, 48, 83, 125, 150, 198, 203, 208, 298, 332, 347, 373, 376, 377, 381, 382, 387, 394, 404, 405, 412
 Hughes, W. G., 290
 Hulbert, L. E., 88, 218
 Hung, F. C., 332
 Hut, G. B., 372
 Hwang, C., 405, 406, 410
- Iablokov, V. A., 406
 Iasin, E. M., 412
 Il'gamov, M. A., 48, 299
 Il'gamov, M. I., 299
 Il'ina, A. M., 48
 Ishizaki, H., 47
 Ivanyuta, E. I., 47, 48, 86, 87, 100, 115, 145, 239, 261, 262
- Jackson, T. R., 404
 Jahanshahi, A., 406
 Jain, P. C., 407
 Jain, R. K., 344, 389, 394, 406, 408
 John, F., 1
 Johns, D. J., 1, 35, 120, 121, 151, 209
 Johnson, M. W., 406, 410
 Jones, J. P., 298, 299, 300
 Jordan, P. F., 411
 Joseph, J. A., 2
 Jullien, Y., 406
 Junger, M. C., 48, 87, 290, 405, 406
- Kabulov, V. K., 307
 Kadi, A. S., 2, 13, 28, 49, 220, 231, 417
 Kagawa, Y., 298, 304, 359, 363, 382, 387
 Kallenbach, W., 48, 81, 124, 125, 131
 Kalnin, V. S., 229
 Kalnins, A., 2, 338, 359, 363, 406, 407, 408, 410, 411, 412
 Kamalov, A. Z., 48
 Kan, S. N., 307
 Kana, D. D., 48, 150, 225, 291, 387
 Kantorovich, L. V., 88
 Kao, G. C., 291
 Kaplan, A., 48, 151, 234, 244, 254, 256
 Kaplan, I. I., 209
 Karimaev, T. D., 332, 393
 Karlsson, T., 301
 Karnaukhov, V. G., 387, 388, 393
 Keeffe, R. E., 299, 344, 363, 382
 Kelkar, V. S., 414
 Kempner, J., 321, 359, 393
 Kennard, E. H., 35
 Kessel, P. G., 287
 Khachatryan, A. A., 406
 Kholod, L. I., 307
 Kido, K., 359, 369
- Kil'chevskyy, M. O., 291
 Kil'dibekov, I. G., 231, 261
 Kinn, E. Ia., 48, 88
 Kislevskaya, L. M., 162, 209
 Klein, S., 406, 412
 Klosner, J. M., 1, 2, 87, 321, 326
 Knowles, J. K., 2
 Kobychkin, V. S., 406
 Koiter, W. T., 1, 2
 Kol'man, E. R., 333, 339, 340, 345, 359, 369, 385
 Kololikhina, Z. V., 290
 Kondrashov, N. S., 88, 101, 113, 133, 137, 307
 Koplik, B., 307, 387, 405, 406, 407, 410
 Korbut, B. A., 48
 Kornecki, A., 83, 359
 Koval, L. R., 44, 48, 81, 83, 87, 88, 92, 112, 115, 145, 151, 247, 262, 272, 291, 292, 381, 407
 Kozarov, M., 209
 Kraus, H., 2, 4, 7, 13, 21, 25, 87, 95, 98, 104, 105, 125, 321, 390, 406, 407
 Krause, F. A., 382
 Kreyszig, E., 2, 3
 Krishna, B., 407
 Krylov, V. I., 88
 Kukudzhinov, S. N., 248, 278
 Kunukasseril, V. X., 307, 410
 Kurshin, L. M., 299
 Kurt, C. E., 183, 321, 328
 Kutnikova, V. P., 389
- Lamb, H., 2, 5, 407
 Lamper, R. E., 411
 Leadbetter, S. A., 87, 88, 95, 115, 134, 209, 211, 217
 Lee, F. A., 411
 Lee, T. H., 407
 Lee, T. N., 291
 Lee, Y. C., 404
 Leech, J. W., 410
 Leissa, A. W., 28, 88, 94, 100, 126, 173, 185, 218, 219, 220, 231, 292, 333, 334, 342, 412
 Lenzen, K. H., 411
 Leroy, J., 291
 Levine, H. S., 1, 2
 Lianis, G., 291
 Liber, T., 261, 291
 Librescu, L., 299, 307
 Liepins, A. A., 411
 Lin, C. W., 87, 88, 409, 411
 Lin, T. C., 293, 294
 Lin, Y. K., 411
 Lindholm, U. S., 48, 203, 225, 291, 347, 373, 377, 387, 394
 Lipovski, D. E., 261
 Lisowski, A., 48, 174, 407, 412
 Liu, Y. K., 405
 Livanov, K. K., 48, 261, 290
 Lizarev, A. D., 407
 Lock, M. H., 149, 407
 Loden, W. A., 345, 359, 363, 382
 Long, C. F., 407

- Love, A. E. H., 1, 6, 8, 15, 18, 35, 37, 121, 124, 125, 407
 Lu, S. Y., 229, 387, 389
 Lur'ye, A. I., 1, 2, 16, 35, 405
 Luzhin, O. V., 407
 Lyamshev, L. M., 407
 Lyons, W. C., 35, 47, 87, 100, 248, 290

 Mahoney, J. B., 299
 Malcom, H. A., 407
 Malkina, R. L., 48, 162, 328, 359, 407
 Manasyan, A. A., 407
 Marcus, L., 359
 Marguerre, K., 27
 Martin, R. E., 389
 Matsui, E., 359, 369
 Matthews, W. T., 409, 410, 412
 Mauro, A., 162, 407
 Mayers, J., 220, 221, 225
 Mayes, W. H., 166, 174
 Mazurkiewicz, Z., 289, 329
 McCallum, H., 47
 McCormick, J. M., 290
 McDonald, C., 407
 McElman, J. A., 186, 202, 203, 265, 307
 McFadden, J. A., 296
 McGill, D. J., 411
 McIvor, I. K., 38, 48, 151, 298, 407
 McLachlan, N. W., 343, 359
 Mead, D. J., 299
 Medick, M. A., 407
 Medige, J., 48, 293, 296
 Mel'nikova, L. M., 48, 87
 Men'shov, A. L., 48
 Meyerovich, I. I., 47, 48, 87, 88, 121, 134, 358, 411
 Michalopoulos, C. D., 47
 Mikame, T., 359
 Mikulas, M. M., 186, 202, 203, 265, 307
 Miles, J. W., 291
 Miller, D. K., 48, 62, 341, 355, 382
 Miller, P. R., 35, 48, 209
 Mindlin, R. D., 290
 Mirsky, I., 35, 293, 294, 298, 304, 322, 352, 414, 418
 Miserentino, R., 148, 240, 264
 Mishenkov, G. V., 231
 Mixson, J. S., 47, 48, 261, 263, 291, 381
 Mizoguchi, K., 47, 294, 298
 Mnev, Ye. M., 291
 Modi, V. J., 265, 306
 Molchanov, A. G., 404
 Morgan, G. W., 293, 294
 Morley, L. S. D., 35, 47, 92
 Mortell, M. P., 407
 Mortimer, R. W., 394
 Movisian, L. A., 209
 Mugnier, D., 35, 234, 261, 291, 307
 Mukherjee, J., 407
 Mushtari, Kh. M., 1, 11, 15, 220, 299
 Muster, D., 47, 291, 389
 Myannil', A., 359

 Nachbar, W., 241
 Nagano, M., 291, 404
 Naghdi, P. M., 1, 2, 6, 8, 15, 35, 292, 393, 406, 408
 Natushkin, V. F., 291, 389
 Naumann, E. C., 47, 48, 87, 88, 100, 117, 125, 130, 198, 210, 211, 217, 381
 Navaratna, D. R., 408
 Neal, B. G., 412
 Neal, D. M., 359
 Nellesen, E., 48, 81, 124, 125, 131
 Nelson, H. C., 187, 198, 211
 Nemat-Nasser, S., 162
 Nemergut, P. J., 410
 Neubert, V. H., 48, 87, 88, 134, 209
 Newton, R. A., 369, 387, 396
 Nigul, U. K., 1
 Nikolai, E. L., 290
 Nikulin, M. V., 235, 239, 242, 261, 264, 274, 279
 Nimura, T., 359, 369
 Nolar, F., 298, 299
 Novozhilov, V. V., 1, 2, 8, 17, 18, 19, 21, 35
 Nowacki, W., 162, 289
 Nowinski, J. L., 220, 221, 222, 228

 Ogibalov, P. M., 125, 408
 Okubo, S., 407, 408
 Olson, M. D., 220, 222, 225, 261
 Ong, C. C., 289
 Oniashvili, O. D., 162, 219, 220, 289, 329, 408
 Org, E., 359
 Orthwein, W. C., 408
 Öry, H., 265, 408
 Osgood, W. A., 2

 Padlog, J., 48, 298
 Padovan, J., 307
 Palladino, J. L., 48, 87, 88, 134
 Palmer, J. H., 291
 Palmer, P. J., 162, 174
 Pandalai, K. A. V., 321, 327, 408
 Park, A. C., 323
 Parthan, S., 209
 Partridge, G. R., 363
 Paslay, P. R., 291, 346, 363, 364, 409
 Patel, J. S., 209
 Pavlov, B. S., 409
 Pawlik, P. S., 38, 48, 298
 Payton, R. G., 299, 301
 Pearson, C. M., 291
 Penzes, L. E., 200, 215, 408, 410
 Pesennikova, N. K., 408
 Petrenko, M. P., 291
 Petrov, V. I., 48
 Petyt, M., 183, 265
 Pflueger, A., 333
 Phillips, H. B., 10
 Pian, T. H. H., 410
 Pifko, A., 299
 Pilkey, W. D., 408
 Pister, K. S., 299

- Platus, D. H., 121, 125, 363
 Plumblee, H. E., 170
 Pohle, F. V., 321, 326
 Poplawski, B., 241
 Popov, E. P., 404, 411
 Poverus, L. Yu., 359
 Pozhalostin, A. A., 291, 408
 Prasad, C., 408
 Pretlove, A. J., 299
 Prokópév, V. I., 265, 279, 411
 Prusakov, A. P., 307
 Pshenichorov, G. I., 412

 Rabinovich, B. I., 291
 Rakhimov, I. S., 261, 291
 Ramakrishna, B. S., 363
 Ramakrishnan, C. V., 408, 409
 Rand, R., 408, 410
 Rand, R. H., 410
 Rapoport, L. D., 48, 87, 88, 115, 121, 124, 134, 291, 412
 Ray, I. E., 396
 Ray, J. D., 396
 Rayleigh, Lord, 37, 74, 88, 124, 290, 292, 372, 373, 408, 412
 Rehfield, L., 221
 Reismann, H., 38, 48, 85, 293, 296, 298, 404, 408
 Reissner, E., 1, 2, 7, 8, 15, 25, 28, 35, 80, 81, 219, 220, 229, 234, 248, 261, 289, 291, 294, 406, 408, 410, 411
 Ren, N., 307
 Resnick, B. S., 48, 88, 117, 121, 190, 209, 211
 Ritz, W., 87
 Robinson, A. R., 410, 412
 Rosato, F. J., 48, 87
 Ross, E. W., Jr., 408, 409, 410, 412
 Rucker, C. E., 166, 170
 Russell, J. E., 35, 47, 87, 248, 290
 Ryayamet, R. K., 359

 Sachenkov, A. V., 248, 345, 359, 369, 392, 409
 Sakharov, I. E., 387, 389, 408, 409
 Saleme, E., 261, 291
 Salerno, V. L., 299, 344, 412
 Salnikov, G. M., 393
 Samoilov, E. A., 409
 Sampath, S. G., 232, 286
 Sanders, J. L., Jr., 1, 9, 13, 15, 35, 115, 232, 411
 Sathyamoorthy, M., 321, 327
 Saunders, H., 346, 364, 409
 Schjelderup, H. C., 299
 Schlack, A. L., Jr., 287
 Schnell, W., 205, 209
 Schnobrich, W. C., 412
 Schroeter, D., 35, 234, 261, 291, 307
 Sechler, E. E., 48, 151, 234, 244, 254, 256
 Seggelke, P., 261, 284
 Seide, P., 359, 383, 409
 Sen, N., 409
 Servin, H., 125, 252, 261
 Severn, R. T., 174, 369

 Sewall, J. L., 47, 48, 87, 88, 95, 100, 115, 117, 125, 130, 134, 160, 198, 207, 209, 210, 211, 217
 Shah, A. H., 408, 409
 Sharinov, I. L., 151
 Sharman, C. B., 120, 151
 Shashkov, I. E., 48, 291
 Shaw, J., 48, 239, 247, 259
 Shekhtman, Iu. V., 411
 Sheng, J., 48
 Shibayama, K., 359, 369
 Shiraishi, N., 409, 410
 Shkenev, Yu. S., 121, 229, 265, 291
 Shklyarchuk, F. N., 291, 393, 409, 412
 Shmakov, V. P., 291, 406, 409
 Shul'man, S. G., 291
 Shulman, Y., 48, 345, 359, 369
 Shveiko, Iu. Iu., 48
 Silbiger, A., 409, 410
 Simmonds, J. G., 2, 83, 142, 412
 Singer, J., 387, 389
 Siu, C. C., 396
 Skalak, R., 291
 Slepov, B. I., 322, 323
 Smirnov, M. M., 150
 Smith, B. L., 48, 85, 87
 Smith, P. W., Jr., 48
 Smith, S., 88, 151
 Sobel, L. H., 411
 Soder, J. E., Jr., 396
 Sokolnikoff, I. S., 7, 23
 Solecki, R., 405
 Song, Q. G., 409
 Sonstegard, D. A., 407, 409
 Southwell, R. V., 101, 137
 Stadler, W., 87, 88, 162, 409
 Stearman, R. O., 149
 Stein, M., 203, 265
 Stepanov, A. P., 291
 Stepanyuk, V. V., 396
 Stern, M., 125, 265
 Strutt, M. J. O., 369, 373, 412
 Sumner, I. E., 411
 Sun, C. L., 229, 387, 389
 Suvernev, V. G., 305, 307, 409, 412
 Suwalski, L., 289
 Sylvester, R. J., 406, 412
 Synge, J. L., 2
 Szechenyi, E., 265

 Tahbildar, U., 183
 Tang, C. T., 47, 88, 332, 339, 387
 Tang, S. C., 294
 Tans, S., 48
 Tasi, J., 215, 409
 Tatge, R. B., 291
 Taylor, P. R., 174
 Taylor, R. L., 299
 Tersteeg, C. E., 87, 134, 344, 345, 405, 412
 Thomas, G. B., 2, 7, 294

- Timoshenko, S. P., 1, 8, 15, 35, 234, 292, 413
Tobias, S. A., 151
Tokarenko, V. M., 261
Tolok, V. A., 47
Tottenham, H., 183
Tovstik, P. E., 409, 412
Trapyezin, I. I., 333, 359, 388
Treftz, E., 2
- Van Fo Fy, G. A., 409
Van Urk, A. T., 372
Veigel', I., 359
Ventres, C. S., 222
Visarian, V., 209
Vivoli, J., 406
Vlasov, V. Z., 1, 2, 8, 15, 16, 27, 35, 158, 162, 248, 289, 294, 409
Vogel, Th., 404
Volmir, A. S., 47, 231, 248, 261
Voss, H. M., 48, 234, 261
Vosteen, L. F., 148, 240, 264
Vronay, D. F., 48, 85
- Wah, T., 48, 83, 198, 203, 208
Walsh, E. K., 291
Walton, W. C., Jr., 47, 88, 112, 199, 369, 382, 411
Wang, C. C., 409
Wang, J. T. S., 87, 88, 162, 299, 409, 411
Warburton, G. B., 35, 48, 67, 73, 81, 82, 83, 87, 88, 94, 95, 98, 99, 108, 113, 121, 125, 134, 147, 162, 264, 290, 297
Washizu, K., 232
Watkins, J. D., 134, 368, 380
- Watts, G. A., 48, 88, 265
Weatherburn, C. E., 4, 5
Webster, J. J., 47, 48, 162, 170, 409, 412
Weingarten, V. I., 48, 87, 88, 94, 118, 121, 124, 183, 209, 279, 306, 307, 354, 368, 369, 372, 383, 387, 389
Wernick, R. J., 291
Wheeler, P. W., 345, 369
White, J. C., 307
Whittier, J. S., 298, 299, 300, 407, 408
Wieckowski, J., 162, 176
Wilkins, D. J., Jr., 396
Wilkinson, J. P., 410
Wisniewski, E. J., 346, 364
Wilson, L. B., 2
Windholz, W. M., 299
Witmer, E. A., 410
Woodman, N. J., 369
Wrenn, B. G., 220, 221, 225
- Yamane, J. R., 47
Yao, J. C., 209
Yen, T., 410
Young, D., 95
Young, R., 47
Yu, Y. Y., 35, 44, 48, 80, 83, 87, 90, 115, 145, 149, 294, 298, 307, 405, 406, 407, 410
- Zapatowski, B., 187, 198, 211
Zarghamee, M. S., 410
Zdel', Yu. U., 291
Zimm, V. I., 410

Subject Index

- Beam bending mode, 66
- Beam-type behavior, 141
- Boundary conditions
 - clamped, 87
 - elastic supports, 146
 - essential, 88
 - fixed, 87
 - free, 117, 124
 - freely supported, 43
 - general, 26-27
 - generalized force, 88
 - geometric, 87
 - natural, 88
 - Sanders' equations, 27
 - shear diaphragm, 43
 - simply supported, 43
- Characteristic determinant, 44
- Characteristic equation, 44
- Circular cylindrical, 31-175
 - added mass, 149-151
 - anisotropy, 185
 - arbitrary boundary conditions, 131
 - beam-like vibrations, 141
 - clamped-clamped (*see also* Clamped-clamped, circular cylindrical), 87-113
 - clamped-free (*see also* Clamped-free, circular cylindrical), 117-121
 - clamped-shear diaphragm (*see also* Clamped-shear diaphragm, circular cylindrical), 113-116
 - closed, shear diaphragms (*see also* Shear diaphragms, circular cylindrical), 43-83
 - comparison with elliptical cylindrical, 322-323
 - comparison with oval cylindrical, 326-327
 - complicating effects (*see also* Complicating effects, circular cylindrical), 185-308
 - cutouts, 151-156
 - deep, 158
 - edges not necessarily clamped, SD, or free, 136-146
 - effect of boundary conditions, 138-140
 - eighth order equations, 32-34
 - elastic supports, 146-149
 - extensional equations, 37
 - filled with fluids, 291
 - fixed (*see* clamped-clamped)
 - free-free, 124-136
 - freely supported (*see* shear diaphragms)
 - fully fixed (*see* clamped-clamped)
 - gyroscopic forces, 289
 - helical edges (turbine blade), 176
 - inextensional theory, 74, 124
- Circular cylindrical—*Continued*
 - infinite length, 37, 43
 - infinite length, circumferential prestress, 245-247
 - infinite length, large displacements, 221, 223
 - infinite length, shear deformation and rotary inertia, 294
 - initial stress (*see also* Initial stress, circular cylindrical), 231-289
 - large displacements (*see also* Large displacements, circular cylindrical), 219, 231
 - membrane equations, 37
 - momentless theory (*see* shallow)
 - noncircular boundaries, 151
 - nonlinear equations (*see also* large displacements), 220
 - open, 157-176
 - open, large deflections, 229-231
 - open, orthotropic, 218
 - open, prestressed, 289
 - orthotropic (*see also* Orthotropic, circular cylindrical), 185-218
 - prestress (*see under* initial stress)
 - shallow, 158
 - shear deformation and rotary inertia, 291-294
 - shear diaphragm (SD)-free (*see also* Free-free, axisymmetric modes), 121-124
 - SD-free, boundary conditions, 121
 - SD-free, stiffened, 215, 216
 - SD-free, uniform circumferential pressure, 248
 - shear diaphragms supported (SD-SD) (*see also* Shear diaphragms, circular cylindrical), 43-83
 - simply supported (*see under* Shear diaphragms)
 - stiffened SD-SD, 195-209
 - technical theory (*see* shallow)
 - three-dimensional equations, solution, 413-418
 - thermal prestress, 289
- Clamped base, cone, complete (*see also* Complete cone), 335-340
- Clamped base, cone, frustum, 345-347
- Clamped-clamped, circular cylindrical, 87-113
 - antisymmetric modes, 88
 - beam functions, 94
 - bounds for frequencies, 88, 101
 - combined uniform prestress, 262-265, 278-279
 - comparison with SD-SD, 90, 91
 - dynamic edge effect method, 88
 - equivalent wavelength, 99
 - experimental results, 88
 - finite differences, 88
 - finite elements, 88
 - frequency formulas, 92, 101

- Clamped-clamped, circular cylindrical—*Continued*
 - modal characteristics, 106–112
 - parallel springs method, 88
 - series method, 88
 - Southwell method, 88
 - stiffened, 210–215
 - strain energy distribution, 104
 - symmetric modes, 88
 - uniform axial prestress, 239, 240
 - uniform circumferential prestress, 247, 248
- Clamped-free, circular cylindrical, 117–121
 - boundary conditions, 117
 - frequency envelopes, 121
 - imperfect clamping, 119
 - mode shape, 118
 - stiffened, 215–217
 - Yu's assumption, 118
- Clamped-free, elliptical cylindrical, 323–325
- Clamped-shear diaphragm, circular cylindrical, 113–116
 - comparison with SD-SD, 114
 - frequency formulas, 114, 115
 - modal characteristics, 115, 116
 - stiffened, 215, 216
 - uniform torsional prestress, 278
- Complete cone, 331, 334–344
 - clamped base, 335–340
 - free base, 342–344
 - shear diaphragm base, 340–342
- Complicating effects, circular cylindrical, 185–308
 - anisotropy, 185
 - initial stress, 231–289
 - moving fluid field, 291
 - nonhomogeneous, 298–308
 - nonhomogeneous, prestressed, 307
 - orthotropy, 185–218
 - prestress (*see* initial stress)
 - prestressed, nonhomogeneous, 307
 - shear deformation and rotary inertia, 291–298
 - smeared out orthotropy, 195–218
 - stiffened, 195–218
 - surrounding media, 290, 291
- Conical, 331–396
 - added mass, 387
 - anisotropy, 387
 - arbitrary boundary conditions, 387
 - circumferential restraint, 384, 385
 - complete (*see also* Complete cone), 331, 334–344
 - elastic supports, 387
 - equations of motion, 332–334
 - frustum (*see also* Frustum of a cone), 344–387
 - large displacements, 389
 - nodal circles, 347
 - nonhomogeneous, 396
 - open, 331, 387
 - orthotropic, 387–389
 - prestressed, 389–393
 - shear deformation and rotary inertia, 393–396
 - stiffened, 388, 389
 - surrounding media, 393
 - surveys on, 332
- Elliptical cylindrical, 322–326
- Frustum of a cone, 331, 344–387
 - attached masses, 387
 - clamped-clamped, 344, 345
 - clamped-free, 359–369
 - clamped-shear diaphragm, 345–347
 - elastic supports, 387
 - free-free, 373–383
 - free large end, 383
 - free small end, 383
 - other edge conditions, 383–387
 - prestressed, 389–392
 - shear diaphragm (SD)-free, 369–373
 - SD-SD, 347–359
- Fully fixed (*see* clamped)
- Fundamental frequency, 62
- Gaussian curvature, 5
- Generalized displacements, 9
- Generalized forces, 9, 10
- Generalized resultants, 10
- Generator, 331
- Hamilton's principle, 36
- Hooke's law, 14
- Inertial terms, 26
- Inextensional theory, 74, 124
- Infinitely long, circular cylindrical (*see under* Circular cylindrical)
- Infinitely long, oval cylindrical, 327
- Initial stress, circular cylindrical, 231–289
 - comparison of different prestresses, 243
 - equations of motion, 232–234
 - nonhomogeneous, 307
 - nonhomogeneous, fluid filled, 291
 - nonuniform prestress, 279–289
 - open shells, 289
 - orthotropic, 253–255
 - shear deformation effect, 294
 - uniform axial, 234–241
 - uniform axial, circumferential and erosional, 278–279
 - uniform circumferential, 241–248
 - uniform torsional, 265–278
- Kirchhoff's hypothesis, 6
- Lamb's equations, 5
- Large deflections, oval, orthotropic, 327
- Large displacements, circular cylindrical, 219–231
 - comparison with flat plate, 228
 - equations of motion, 220, 221
 - frequency formulas, 221, 222, 224, 227
 - infinitely long, 221–223
 - open shells, 229–231
 - shear diaphragms supported, 223–228
- Layered, 298
- Love's assumptions, 6

- Love's first approximation, 6
 Love's postulates, 1, 6-7
- Middle surface, 1
 Modal density, 62
 Moment resultants, 13, 20
 Momentless theory (*see* Shallow shell)
 Moments, 13
- Nodal circles, cones, 247
 Normal curvature, 3
- Open, circular cylindrical, 157-176
 added mass, 175-176
 boundary conditions, 157
 helical edges, 176
 modal characteristics, 164
 shear diaphragms, all edges, 158-162
 shear diaphragms, ends, 165
 shear diaphragms, lateral edges, 162
 Open, noncircular cylindrical, 328, 329
 Orthotropic (*see also* Smeared out orthotropy and Stiffened)
 Orthotropic, circular cylindrical, 185-218
 axial prestress, 240
 clamped-clamped, 211
 clamped-free, 215
 clamped-shear diaphragm, 215
 combined uniform prestress, 278
 equations of motion, 186-191
 free-free, 217
 frequency envelopes, 197
 internal pressure, 253-255
 open shells, 218
 pressurized membrane, 265
 shear deformation and rotary inertia, 294
 shear diaphragms supported, 191-209
 smeared out orthotropy, 195-218
 stress-strain equations, 185
 Orthotropic, elliptical cylindrical, 325
 Orthotropic, oval cylindrical, 327
 Oval cylindrical, 326-328
 comparison with circular cylindrical, 326-327
 infinitely long, 327, 328
 orthotropic, large deflections, 327
- Parallel springs method, 88, 339
 Plane curve, 3
 Plane strain concept, 38
- Quadratic forms, 3
- Ring modes, cone, 376
- Sandwich (*see also* Nonhomogeneous and Layered), 298
 Sandwich cone, 396
 Sandwich elliptical shell, 326
 Shallow shell, 1, 27, 158
 Shear diaphragm (SD), 43
- SD base, cone, complete, 340-342
 SD base, cone, frustum, 347-373
 SD-SD, circular cylindrical, 43-83
 axisymmetric motion, 66-67
 beam like vibrations, 83
 characteristic determinant, 44
 characteristic equation, modifying constants, 44-46
 comparison of theories, 43-61
 comparison with clamped-clamped, 90, 91
 exact solutions, 48
 experimental results, 48
 frequency formulas, 39, 44, 75, 86
 inextensional theory, 74
 large deflections, 223-228
 modal density, 43
 neglect of tangential inertia, 74-80
 nodal patterns, 47
 nonhomogeneous, 300-308
 orthotropic, 185-218
 Poisson's ratio, variation with, 67-71
 prestressed, bending moment, 285
 prestressed, combined uniform, 255-261, 279
 prestressed, internal pressure, 248-253
 prestressed, nonuniform, 279-286
 prestressed, uniform axial, 235-239
 prestressed, uniform circumferential, 241-245, 247
 prestressed, uniform torsional, 273-275
 shear deformation and rotary inertia, 294-298
 simplified theories, 48, 80-83
 stiffened, 195-209
 strain energy, 73
 Yu's assumption, 80
 SD-SD, elliptical cylindrical, 324
 Shell of revolution, 403
 Smeared out orthotropy, 186
 Stiffened (*see also* Orthotropic), 186
 Strain-displacement equations, 7-13
 Strain energy, 17
 Stress couples, 13
 Stress resultants, 13
- Theories, comparison (*see under* Various theories, comparison)
 Theory of surfaces, 2-5
 coordinate system, 2
 derivatives of basic vectors, 4
 first fundamental quantities, 3
 Gauss characteristic equation, 4
 Gauss derivative formulas, 4
 normal curvature, 3
 principal coordinates, 4
 principal curvature, 4
 second quadratic form, 3
 Thin shell theory, 1-28
 arbitrary curvature, 2
 beam like vibrations, 83
 first approximation of Love, 6, 7
 fundamental equations, 1-23
 generalized displacements, 9
 generalized forces, 10

Thin shell theory—*Continued*

generalized resultants, 10

Thin shells, definition, 6

Three-dimensional equations of motion, 413

Various theories, comparison

change in twist, middle surface, 12

circular cylindrical, equations of motion, 32-34

circular cylindrical, infinite length, 40

circular cylindrical, SD-SD, 43-61, 73

Various theories, comparison—*Continued*circular cylindrical, other, 98, 112-113, 126, 204, 209,
295-297

conical, SD-SD, 393-396

curvature change, middle surface, 12

force resultants, 20

moment resultants, 21

strains at a point, 11

Yu's assumption, 80

FIRST CLASS MAIL

POSTAGE AND FEES PAID
NATIONAL AERONAUTICS AND
SPACE ADMINISTRATION
451



POSTMASTER : If Undeliverable (Section 158
Postal Manual) Do Not Return

"The aeronautical and space activities of the United States shall be conducted so as to contribute . . . to the expansion of human knowledge of phenomena in the atmosphere and space. The Administration shall provide for the widest practicable and appropriate dissemination of information concerning its activities and the results thereof."

—NATIONAL AERONAUTICS AND SPACE ACT OF 1958

NASA SCIENTIFIC AND TECHNICAL PUBLICATIONS

TECHNICAL REPORTS: Scientific and technical information considered important, complete, and a lasting contribution to existing knowledge.

TECHNICAL NOTES: Information less broad in scope but nevertheless of importance as a contribution to existing knowledge.

TECHNICAL MEMORANDUMS: Information receiving limited distribution because of preliminary data, security classification, or other reasons. Also includes conference proceedings with either limited or unlimited distribution.

CONTRACTOR REPORTS: Scientific and technical information generated under a NASA contract or grant and considered an important contribution to existing knowledge.

TECHNICAL TRANSLATIONS: Information published in a foreign language considered to merit NASA distribution in English.

SPECIAL PUBLICATIONS: Information derived from or of value to NASA activities. Publications include final reports of major projects, monographs, data compilations, handbooks, sourcebooks, and special bibliographies.

TECHNOLOGY UTILIZATION PUBLICATIONS: Information on technology used by NASA that may be of particular interest in commercial and other non-aerospace applications. Publications include Tech Briefs, Technology Utilization Reports and Technology Surveys.

Details on the availability of these publications may be obtained from:

SCIENTIFIC AND TECHNICAL INFORMATION OFFICE

NATIONAL AERONAUTICS AND SPACE ADMINISTRATION
Washington, D.C. 20546